Hydrogen-Transfer-Mediated C–C bond Formation with Oxygen-Containing Compounds

Chen-Chen Li

Thesis submitted to McGill University

In partial fulfillment of the requirement for the degree of

Doctor of Philosophy

Department of Chemistry

McGill University, Montréal

July 2021

Abstract

Chen-Chen Li *Supervisor: Prof. Dr. Chao-Jun Li*

McGill University

C–C bond formation is a cornerstone of organic chemistry that enables the transformation of simple molecules into complex molecules. In addition, most natural organic compounds contain oxygen, including alcohols and carbonyl compounds. Thus, it is highly desirable to develop C–C bond formation methods with alcohols or carbonyl compounds.

The Grignard reaction is one of the most powerful methods for forming C–C bonds and it is widely used in synthetic chemistry, especially in early-stage synthesis. However, the use of stoichiometric amounts of metal elements and the instability of organometallic reagents limit its application in late-stage functionalization. Thus, it is necessary to provide an alternative carbanion equivalent for Grignard-type reactions that avoids the use of haloalkanes and stoichiometric amounts of metal.

Several years ago, we were inspired by the Wolff–Kishner reduction and developed hydrazones as carbanion equivalents to complete a series of C–C bond formation reactions. Such a novel carbanion equivalent not only avoids the requirement for stoichiometric amounts of metal and alkyl halides but is also air and moisture stable. Among the C–C bond formation reactions, the ruthenium-catalyzed Grignard-type reaction was the first reaction we discovered. By taking advantage of the ruthenium catalytic system, some unique derivative transformations could be realized. Particularly, the hydrogen transfer strategy was utilized to allow alcohol to act as a surrogate for the carbonyl group. This technique enabled a direct C–C bond formation from alcohol, which is hard to realize through classic methods.

In addition, controlling the chemoselectivity of 1,2-addition and olefination products in Grignard-type reactions with hydrazones was a significant challenge during our initial study. The selectivity of 1,2-addition products could only be realized by aromatic aldehyde hydrazones, while the aliphatic aldehyde hydrazones favored olefination. Thus, we designed an electron-rich and bulky PCP-type tridentate ligand for the ruthenium catalytic system to enable aliphatic aldehyde hydrazones to realize 1,2-addition with ketones. With this development, the range of suitable substrates for Grignard-type reactions has been extended to include aliphatic aldehyde hydrazones.

Finally, by using hydrazones as carbanion equivalents, we eliminated the need to use stoichiometric amounts of metal and haloalkanes; however, precious metals, such as ruthenium, are still required to catalyze the reaction, which somewhat limits its application in late-stage pharmaceutical synthesis.

In this study, we developed well-defined iron-bisphosphine complexes for nucleophilic addition reactions of hydrazones with aldehydes, ketones, imines, and Michael acceptors. A key advantage is that this reaction could occur at room temperature with a broad range of substrates. This development in iron catalysts provides an alternative to the previous ruthenium catalytic system and opens new avenues for the synthetic application of Grignard-type reactions with hydrazones.

Résumé

La formation de liaisons C–C est la pierre angulaire de la chimie organique en permettant la transformation de molécules simples en molécules complexes. En outre, les composés contenant de l'oxygène, notamment les alcools et les composés carbonylés, constituent la plupart des composés organiques naturels. Ainsi, le développement de méthodes de formation de liaisons C–C avec des alcools ou des composés carbonylés est hautement souhaitable.

La réaction de Grignard est l'une des méthodes puissantes de formation de liaisons C–C et est largement appliquée en chimie de synthèse, en particulier dans les premiers stades.. Cependant, l'utilisation de quantités stœchiométriques d'éléments métalliques et l'instabilité des réactifs organométalliques limitent son application dans les fonctionnalisations tardives. Il est donc nécessaire de fournir un équivalent alternatif de carbanion pour les réactions de type Grignard afin d'éviter l'utilisation d'haloalcanes et de quantités stoechiométriques de métal.

Dans cette optique, il y a plusieurs années, inspirés par la réduction de Wolff-Kishner, nous avons développé les hydrazones en tant qu'équivalents de carbanion pour compléter une série de réactions de formation de liaison C–C. Ce nouvel équivalent carbanion permet non seulement d'éviter l'utilisation de quantités stoechiométriques d'halogénures métalliques et alkyliques, mais il est également stable à l'air et à l'humidité. Parmi ces réactions de formation de liaisons C–C, la réaction de type Grignard catalysée par le ruthénium a été la première réaction que nous avons découverte. En tirant parti du système catalytique du ruthénium, certaines transformations dérivées uniques ont pu être réalisées. En particulier, l'utilisation de la stratégie de transfert d'hydrogène pour permettre à l'alcool d'être le substitut des carbonyles a permis la formation d'une liaison C–C directe à partir de l'alcool, ce qui est difficile à réaliser par les méthodes classiques.

De plus, dans une réaction de type Grignard avec des hydrazones, le contrôle de la chimiosélectivité de l'addition-1,2 et du produit d'oléfination était un défi important lors de notre étude initiale. La sélectivité du produit d'addition-1,2ne pouvait être réalisée que par les hydrazones d'aldéhydes aromatiques, alors que les hydrazones d'aldéhydes aliphatiques favorisaient l'oléfination. Dans ce projet, nous avons conçu un ligand tridenté de type PCP, riche en électrons et possédant un encombrement stérique pour le système catalytique au ruthénium afin de permettre aux aldéhyde hydrazones aliphatiques de réaliser l'addition-1,2avec des cétones. Ce développement a étendu les substrats possibles de la réaction de type Grignard avec les hydrazones.

Enfin, l'utilisation d'hydrazones comme équivalents de carbanion permet d'éviter l'utilisation de quantités stoechiométriques de métal et d'haloalcane ; cependant, elle nécessite toujours un métal précieux, le ruthénium, pour être catalysée, ce qui limite quelque peu son application dans la synthèse pharmaceutique de stade avancé. Ici, nous avons développé des complexes fer-bisphosphine bien définis pour une réaction d'addition de l'hydrazone avec des aldéhydes, des cétones, des imines et des accepteurs de Michael. La réaction a pu être conduite à température ambiante avec un large éventail de différents produits. Un tel développement des catalyseurs à base de fer fournit une alternative au système catalytique précédent basé sur le ruthénium et ouvre de nouvelles opportunités d'application synthétique pour les réactions de type Grignard avec les hydrazones.

'The synthesis of substances occurring in Nature, perhaps in greater measure than activities in any other area of organic chemistry, provides a measure of the conditions and powers of science.'

by Robert Burns Woodward

for my beloved fiancée, Siyi Luo, my dear parents, Yibo Li and Yuedong Li and my great family and friends.

Acknowledgement

First of all, I am grateful to my PhD supervisor, Prof. Dr. Chao-Jun Li, who not only guided every detail of my research but also gave me a symbolic model for conducting the research. Prof. Li helped me transform from a student to a researcher and doctoral candidate well as helping me complete the project step by step. The most significant thing Prof. Li taught me was how to set up a big picture for every research project, which helped me answer both 'How does this happen?' and 'Why do we study this?' Such a valuable experience will greatly benefit me in my future research. Every time I faced difficulties in my research, Prof. Li told me how to properly solve the problem with great patience. Prof. Li's guidance was like getting a cable car to the top of a mountain.

Second, I would like to thank the other faculty members at McGill University, especially Prof. Jean-Philip Lumb, Prof. Bruce Arndtsen, Prof. James Gleason, and Prof. Nicolas Moitessier, for their valuable courses; Prof. Youla Tsantrizos and Prof. Audrey Moores for their guidance and advice on my yearly reviews; Dr. Robin Stein, Dr. Alexander Wahba, and Dr. Nadim Saadé for their help with the characterization of my experimental data; and Mr. Michel Daoust, Mr. Mathieu Behard, Ms. Chantal Marrotte, and Dr. Laura Pavelka for helping with my daily affairs and TA duties. As well, I would like to express my gratitude to Prof. Youla Tsantrizos for her help and guidance in my collaboration projects and for recommending me for postdoc positions.

Third, I would like to express my gratitude to my group members. Without their help, I would not have finished my PhD career so smoothly and wonderfully. I would first like to thank Dr. Inna Perepichka, our lab research associate. Her daily care of our lab affairs and everyone in our lab has created such a supportive environment for my five years of research. Next, I would like to thank three of our alumni, Dr. Xi-Jie Dai, Haining Wang, and Dr. Zhong-Zhen Zhou, whose help at the very beginning of my PhD career set the foundations for all of my PhD research. I am also grateful to my close friends in our lab, Dr. Zihang Qiu and Mr. Jianbin Li. Discussing research and daily life with them made me continually enthusiastic about my research. I would also like to thank Dr. Dianhu Zhu, Dr. Leiyang Lv, Dr. Jian Gao, Dr. Jian Kan, Dr. Zhang-Pei Chen, Dr. Dawei Cao, Mr. Yunen Cen, and Mr. Malcolm Sim for their help with my research project. Also, I would like to thank Dr. Zoe Hearne, Ms. Yiram Kim, Ms. Daliah Farajat, Mr. Durbis Castillo Pazos, and Mr.

Sosthene Ung for assisting me with the revision of my thesis and previously published research papers.

Next, I would like to send my gratitude to my undergraduate professors, including my undergraduate supervisors, Prof. Shang-Dong Yang and Yong-Qiang Tu; my inorganic chemistry teacher, Prof. Yu Tang; and my organic chemistry teacher, Prof. Xin-Ping Hui. Their enlightenment created the man capable of writing this PhD thesis.

Then, I will thank my dear parents, Ms. Yibo Li and Mr. Yuedong Li. Although they are one thousand miles away, their continuous support and love have enabled me to complete my doctoral degree.

Finally, I am truly grateful to my fiancée, Ms. Siyi Luo. Meeting her was one of the luckiest things to happen to me during my PhD. Her love and support in every aspect of daily life has motivated me to overcome one difficulty after another. I hope that this thesis can also bless her with a great time in her PhD study!

Contributions and Publications

Research works:

(1) ***Li, C.-C.***; Wang, H.; Sim, M. M.; Qiu, Z.; Chen, Z.-P.; Khaliullin, R. Z.; Li, C.-J., Empowering alcohols as carbonyl surrogates for Grignard-type reactions. *Nat. Commun.* **2020,** *11*, 6022.

This work was discovered and developed by myself under guidance of Prof. C.-J. Li and with assistance of my colleagues listed above. Particularly, the DFT calculation part was done with assistance of Dr. Haining Wang, Mr. Malcolm Sim. and Prof. Rustam Z. Khaliullin. In this thesis, Chapter 4, Section 4.3 mainly discusses this work in details.

(2) ***Li, C.-C.***; Kan, J.; Qiu, Z.; Li, J.; Lv, L.; Li, C.-J., Synergistic relay reactions to achieve redox-neutral α-alkylations of olefinic alcohols with ruthenium(II) Catalysis. *Angew. Chem. Int. Ed.* **2020,** *59*, 4544–4549.

This work was discovered and developed by myself under guidance of Prof. C.-J. Li and with assistance of my colleagues listed above. In this thesis, Chapter 4, Section 4.2 and Chapter 5, Section 5.3 mainly discuss this work in details.

(3) ***Li. C.-C.***; Dai, X.-J.; Wang, H.; Zhu, D.; Gao, J.; Li, C.-J., Iron-catalyzed nucleophilic addition reaction of organic carbanion equivalents *via* hydrazones. *Org. Lett.* **2018,** *20,* 3801-3805.

This work was discovered and developed by myself under guidance of Prof. C.-J. Li and with assistance of my colleagues listed above. In this thesis, Chapter 6 mainly discusses this work in details.

The following published research works were not mainly discovered and developed by me, but I contributed more or less:

(4) Cao, D.; ***Li, C.-C.***; Zeng, H.; Peng, Y.; Li, C.-J., C(sp^3)−C(sp^3) bond formation *via* nickel-catalyzed deoxygenative homo-coupling of aldehydes/ketones mediated by hydrazine. *Nat. Commun*, **2021**, *12*, 3729.

(5) Qiu, Z.; Pham, H. D. M.; Li, J.; ***Li, C.-C.***; Castillo-Pazos, D. J.; Khaliullin, R. Z.; Li, C.-J., Light-enabled metal-free pinacol coupling by hydrazine. *Chem. Sci.* **2019**, *10*, 10937–10943.

(6) Qiu, Z.; Lv, L.; Li, J.; ***Li, C.-C.***; Li, C.-J., Direct conversion of phenols into primary anilines with hydrazine catalyzed by palladium. *Chem. Sci.* **2019,** *10*, 4775–4781.

(7) Zhu, D.; Lv, L.; ***Li, C.-C.***; Ung, S.; Gao, J.; Li, C.-J., *Umpolung* of carbonyl groups as alkyl organometallic reagent surrogates for palladium-catalyzed allylic alkylation. *Angew. Chem. Int. Ed.* **2018,** *57*, 16520–16524.

(8) Lv, L.; Zhu, D.; Tang, J.; Qiu, Z.; ***Li, C.-C.***; Gao, J.; Li, C.-J., Cross-coupling of phenol derivatives with *umpolung* aldehydes catalyzed by nickel. *ACS Catal.* **2018,** *8*, 4622–4627.

(9) Tang, J.; Lv, L.; Dai, X.-J.; ***Li, C.-C.***; Li, L.; Li, C.-J., Nickel-catalyzed cross-coupling of aldehydes with aryl halides *via* hydrazone intermediates. *Chem. Commun.* **2018,** *54*, 1750–1753.

Review:

(10) Dai, X.-J.;† ***Li, C.-C.***;† Li, C.-J. Carbonyl *umpolung* as organometallic reagent surrogates. *Chem. Soc. Rev.* **2021,** *50*, 10733-10742. (†: These authors contributed equally)

This review was written by Dr. Xi-Jie Dai and me who contributed equally under the supervision of Prof. C.-J. Li. Chapter 2 in this thesis was written based on this review.

Content

List of Tables

List of Figures

List of Schemes

List of Abbreviations

AAD	Acceptorless alcohol dehydrogenation
Ac	acetyl
Ar	aromatic group
BINAP	2,2′-bis(diphenylphosphino)-1,1′-binaphthyl
bipy	2,2’-bipyridine
Bn	benzyl
Boc	*tert*-butyloxycarbonyl
B_2pin_2	bispnacolatodiboron
Bu	butyl
Bz	benzoyl
COD (cod)	1,5-cyclooctadiene
Cp	cyclopentadiene
Cp*	pentamethylcyclopentadiene
Cy	cyclohexyl
DCE	1,2-dichloroethane
dcypb	1,2-bis(dicyclophosphino)butane
dcype	1,2-bis(dicyclophosphino)ethane
dcypf	1,2-bis(dicyclophosphino)ferrocene
depe	bis(diethylphosphino)ethane
DFT	Density Functional Theory
DIPEA	diisopropylethylamine
DMAP	4-(dimethylamino)pyridine
DME	dimethoxyethane
DMF	*N*,*N*-dimethylformamide
dmpe	bis(dimethylphosphino)ethane
DMSO	dimethylsulfoxide
d.r.	diastereomeric ratio
dppb	bis(diphenylphosphino)butane
dppe	bis(diphenylphosphino)ethane
dppf	bis(diphenylphosphino)ferrocene
dppp	bis(diphenylphosphino)propane

E	elecrophile
EDG	electron-donating group
ee	enantiomeric excess
en	ethylenediamine
e.r.	enantiomeric ratio
es	enantiospecificity
Et	ethyl
EtOAc	ethyl acetate
EWG	electron-withdrawing group
FG	functional group
Het	heteroatom (atoms other than carbon in organic compounds)
IMes	1,3-bis(2,4,6-trimethylphenyl)-1,3-dihydro-2*H*-imidazol-2-ylidene
IPr	1,3-bis(2,6-diisoproylphenyl)-1,3-dihydro-2*H*-imidazol-2-ylidene
i	iso
m	*meta*
Me	metyl
2-Me-THF	2-methyltetrahydrofuran
NHC	*N*-heterocyclic carbene
NMO	*N*-methylmorpholine *N*-oxide
NMR	nuclear-magnetic resonance
Nu	nucleophile
o	*ortho*
[O]	oxidant
Oct	octyl
p	*para*
Ph	phenyl
PhMe	toluene
Pr	propyl
R.T. (rt)	room temperature
SIMes	1,3-bis(2,4,6-trimethylphenyl)-4,5-dihydroimidazol-2-ylidene
SIPr	1,3-bis(2, 6-diisopropylphenyl)-4,5-dihydroimidazol-2-ylidene
t	*tert*

TEMPH	(2,2,6,6-tetramethylpiperidin-1-yl)hydroxide
TEMPO	(2,2,6,6-tetramethylpiperidin-1-yl)oxyl
Tf	trifluoromethanesulfonyl
TFA	trifluoroacetic acid
THF	tetrahydrofuran
TLC	thin-layer chromatography
Ts	4-toluenesulfonyl
TS	transition state
UV	ultraviolate

Chapter 1. Application of Transition Metal-Catalyzed Hydrogen Transfer Strategy in Functionalization of Alcohols.

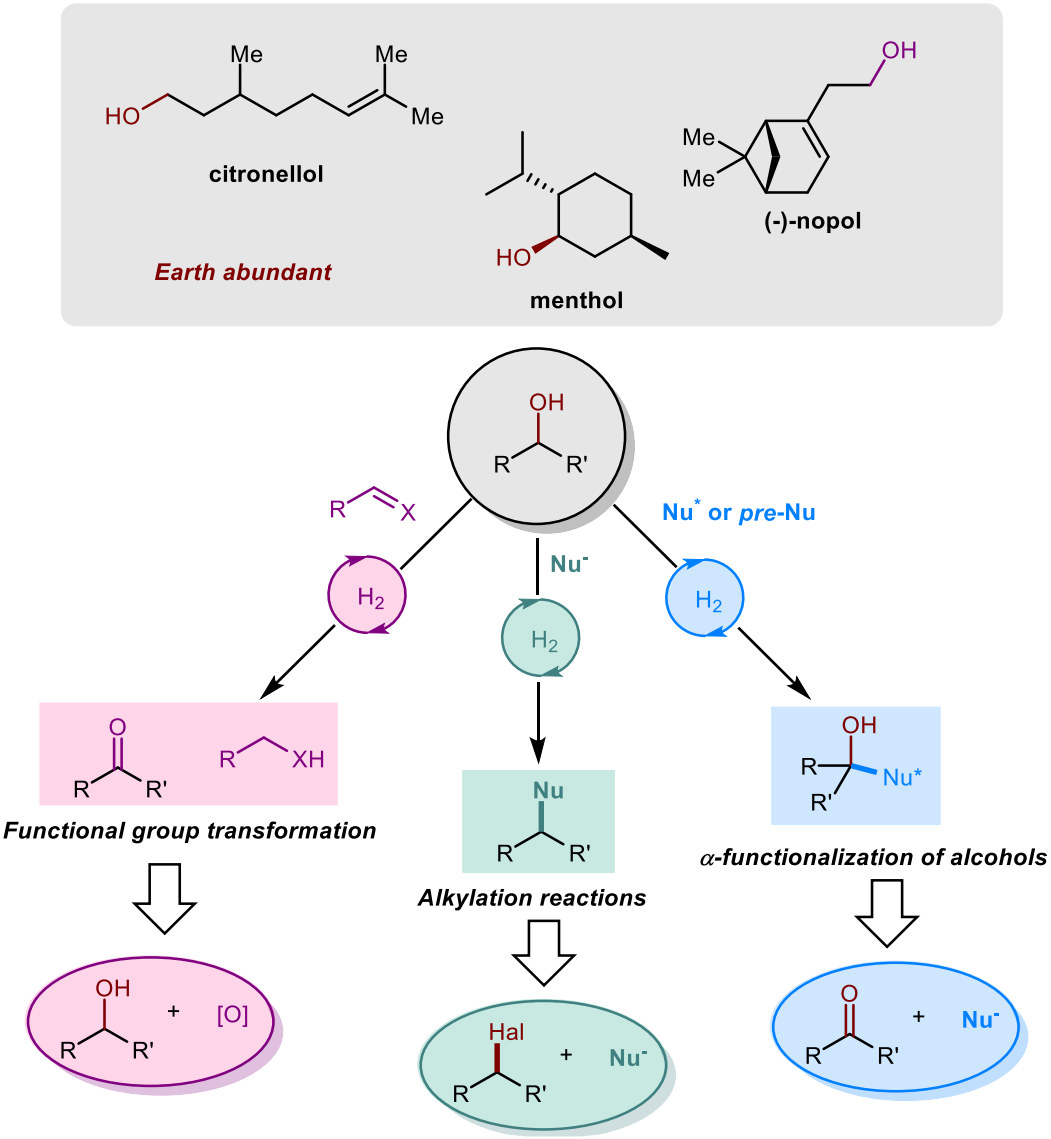

Figure 1.1 Various functionalization of alcohols via hydrogen transfer strategy

1.1 Introduction

The hydrogen atom, as the simplest element in chemistry, plays a vital role in various organic transformations. As transition metal catalysis is made increasingly essential for organic synthesis, hydrogen transfer reactions have now attracted increased attention, which is because the transformation of a hydride in organic reactions is not only the most atom economical and efficient but also the easiest way to conduct study and exercise control. For example, two of the most common functional groups in organic chemistry, hydroxyl and carbonyl, can be converted into each other *via* a transition-metal-catalyzed hydrogen-transfer process. Alcohol functional groups are present in most natural organic compounds and are higher in abundance than aldehydes/ketones. In general, alcohols are less reactive than carbonyls (aldehydes and ketones), especially in the formation of C–C or C–Het (e.g., C–N, C–B) bond. Recently, a novel hydrogen transfer strategy has been proposed to circumvent the low reactivity of alcohols by enabling alcohols to directly complete several vital functionalizations through the high reactivity of carbonyls, which however was difficult to achieve in the past with alcohol itself for classic methods. The development of hydrogen-transfer-mediated alcohol functionalization consists mainly of three aspects. The first one is to carry out one-pot intra- or intermolecular functional group transformation. The second one is to facilitate the reaction with alkyl halides using an alkylation reagent for various analogies of C–C or C–Het bond formation. The last one is to achieve various alcohol α-functionalization reactions through a carbonyl surrogate. In the following part, the discussion will be conducted from these three perspectives.

1.2 Dehydrogenation of alcohols

1.2.1 Low-valent-metal-catalyzed aerobic oxidation of alcohols

The oxidation (dehydrogenation) of alcohols provides the most efficient means to convert alcohols into carbonyls.[1] Throughout the history of organic chemistry, there have been plenty of efficient methods developed for the oxidation of alcohols, such as the nonmetal oxidation including Swern Oxidation,[2,3] Dess–Martin Oxidation,[4] Oppenaur Oxidation,[5–7] and NaClO/NMO oxidation[8] or the oxidation with such high-valent-metal oxidants as Cr(VI)[9] and Fe(VI).[10] Although these methods are crucial for organic synthesis, their limitations are also self-evident. Firstly, more than a stoichiometric amount of oxidants is usually required, which can cause unnecessary waste. Secondly, the functional group involved in these methods shows quite limited tolerance. Lastly,

the oxidants used in these methods are either toxic or difficult to obtain. As organometallic chemistry has played an increasingly significant role since the late stage of the last century, some low-valent transition metals such as ruthenium (II),[11] palladium (II),[12] and iridium (III)[13] have been identified as efficient in the hydrogen-transfer process. On this basis, the aerobic oxidation involving these low-valent metal-catalyzed dehydrogenations was proposed. Ruthenium (II)-catalyzed aerobic oxidation plays a particularly significant role because of its capability to achieve the *β*-hydride elimination of alcohols.[14–18]

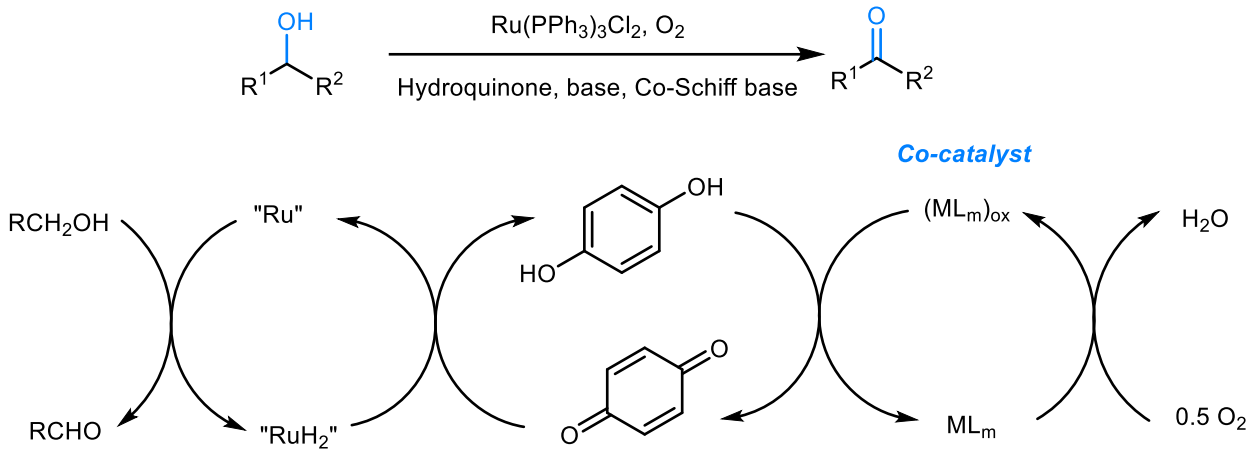

Scheme 1.1 General mechanism of ruthenium (II)-catalyzed aerobic oxidation

The general mechanism followed by ruthenium-catalyzed aerobic oxidation of alcohols is detailed in Scheme 1.1. The ruthenium (II) complex is first subjected to oxidative addition with the alcohol, which is followed by *β*-hydride elimination to generate the corresponding aldehyde and ruthenium–hydride complex. Subsequently, the co-oxidant (e.g., quinone) is used to oxidize the ruthenium–hydride complex to regenerate ruthenium (II), thus initiating a new cycle. Meanwhile, the generated hydroquinone is re-oxidized by O_2 for the second cycle. In the initial stage of development for this method, the oxidation of hydroquinone required the involvement of a cobalt Schiff base complex as the cocatalyst.[14] However, in 1998, Hanyu *et al.* proposed to use $PhCF_3$ as a solvent, thus enabling this process to take place quantitatively in the absence of cobalt cocatalyst (Scheme 1.2).[19] The success achieved in this work is potentially attributed to the higher solubility of $PhCF_3$ to O_2 gas, which promotes the interaction with hydroquinone without the involvement of any cocatalyst.

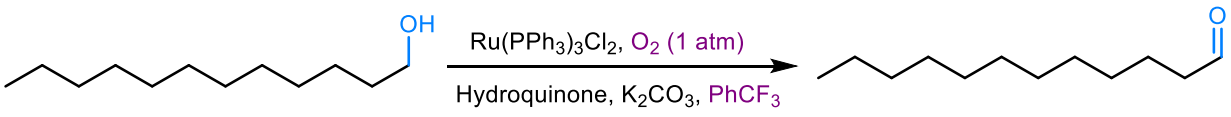

Scheme 1.2 Cobalt-catalyst free aerobic oxidation of alcohol with ruthenium (II) catalysis

In addition to quinone, TEMPO appears to be a more efficient co-oxidant in the ruthenium complex catalytic cycle, which is far more conducive to the oxidization of TEMPH by O_2 gas. Furthermore, the involvement of TEMPO also contributes to maintaining selectivity for the oxidation of primary alcohols because of its inability shown in further oxidizing aldehydes to the corresponding carboxylic acids. Differently, it was showed in some experiments that the addition of TEMPO could hinder the full oxidation of aldehydes to acids relative to control reactions without any catalysts used. The mechanism of TEMPO-assisted ruthenium (II)-catalyzed aerobic oxidation is similar to that of the hydroquinone version (Scheme 1.3).[18] In this case, however, only 4% co-oxidant was required, far lower than the 10% in the hydroquinone case.

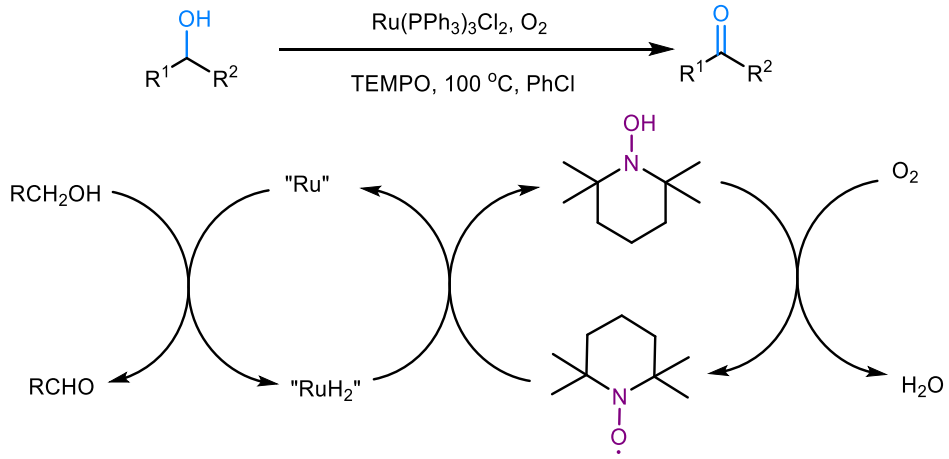

Scheme 1.3 Mechanism of Ru(II)-catalyzed aerobic oxidation with TEMPO as cocatalyst

Aside from ruthenium, copper complexes represent another efficient catalysts suitable for the aerobic oxidation of alcohols with the assistance of TEMPO. The mechanism of oxidation was put forward as a *β*–hydrogen trap by TEMPO *via* a five-membered ring transition state (Scheme 1.4).[20] This shows difference from ruthenium complexes because copper (II) complexes are not as effective as ruthenium (II) in the process of *β*–hydride elimination. For this reason, the copper-catalyzed dehydrogenation of alcohol is supposed to rely on the use of TEMPO, an excellent

hydrogen acceptor, together with its kinetically favored five-membered ring conformation. Besides, the disadvantage in *β*–hydride elimination over ruthenium means that the copper catalytic system could efficiently oxidize activated alcohols (e.g. *α*-aryl alcohols) only in its first development.[21] Moreover, the high conformational requirement makes more sterically hindered secondary alcohols not as efficient as primary ones. In order to address these problems, it was discovered in a subsequent study that the reactivity of oxidation could be increased significantly with the addition of catalytic amounts of *N*-methylimidazole, thus achieving nearly quantitative yields for the oxidation of aliphatic alcohols.[22, 23] Furthermore, the use of certain polar solvents such as fluorobenzene could also improve the solubility of inorganic base, thus leading to a decrease in base requirement from 2 equiv. to a catalytic amount.[22]

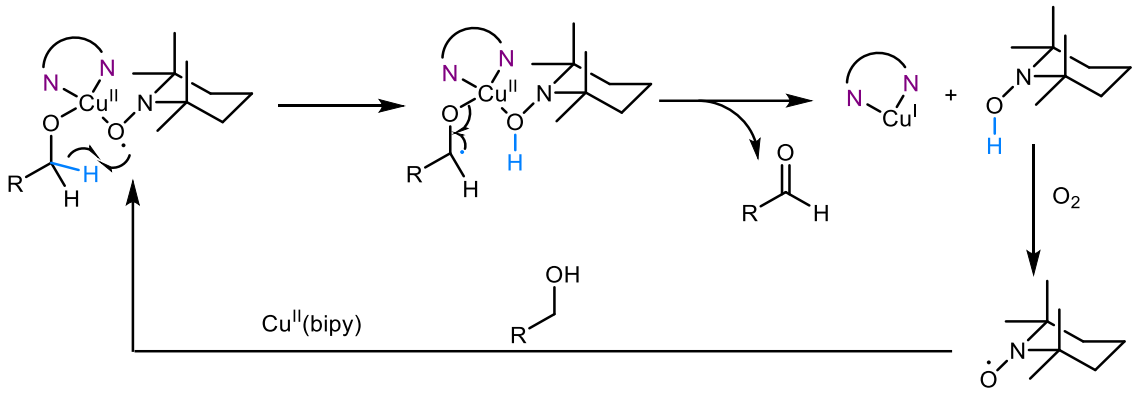

Scheme 1.4 Mechanism of copper-catalyzed aerobic oxidation of alcohols

The palladium (II) complexes are the effective catalysts suitable for the *β*–hydride elimination process as well. Therefore, Pd(II) catalysts are applied as another series of efficient catalysts for aerobic oxidation. Similar to the ruthenium system, the mechanism of palladium-catalyzed oxidation starts with the coordination of alcohol to the Pd (II) center, which is followed by a *β*–hydride elimination to generate the corresponding carbonyls, thus resulting in the Pd(II)–H species. Subsequently, the obtained Pd(II)–H will undergo reductive elimination to generate Pd(0), which can be immediately reoxidized by O_2 (Scheme 1.5).[24] Although the involvement of co-oxidant is not required in this case, the addition of catalytic amounts of TEMPO remains necessary in many other cases to prevent the overoxidation of aldehydes (Scheme 1.6).[25, 26]

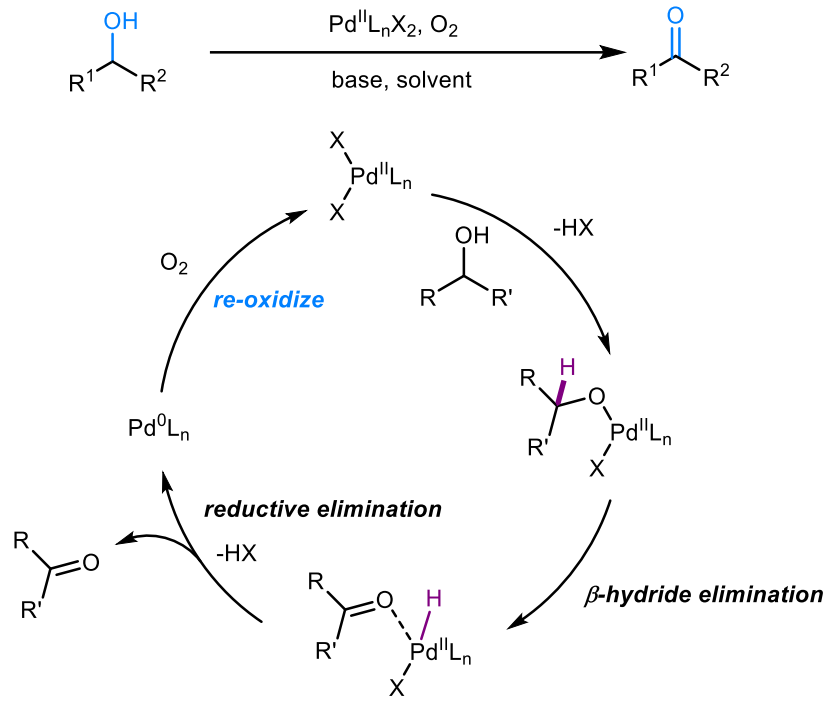

Scheme 1.5 Mechanism of palladium-catalyzed aerobic oxidation of alcohols

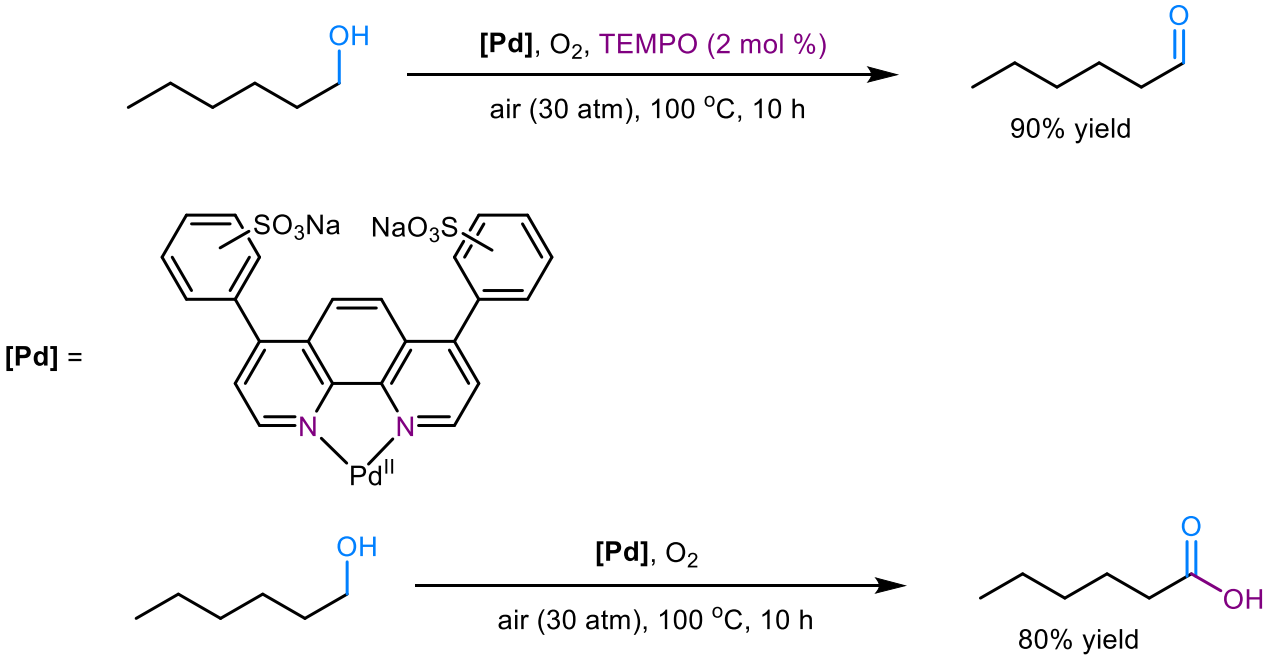

Scheme 1.6 Role of TEMPO in palladium-catalyzed alcohol oxidation

1.2.2 Anaerobic oxidation of alcohols *via* hydrogen transfer

Apart from oxygen gas, such double bond-containing organic compounds as carbonyls or alkenes can also be applied as hydride acceptors. Furthermore, the involvement of alkenes or carbonyls could, to some degree, can help address the limitations of oxygen gas, including overoxidation and the low tolerance of functional group. The mechanism followed by this process is illustrated in Scheme 1.7. First of all, the transition metal will coordinate with alcohols before *β*–hydride elimination. Subsequently, the obtained metal hydride species will coordinate with the double bond system, which is followed by insertion. This process is effective in transferring the hydride from the *α*-position of alcohols to another organic compound, thus forming a new C–C bond, which demonstrates the significant concept raised in this chapter, that is, 'hydrogen transfer.'

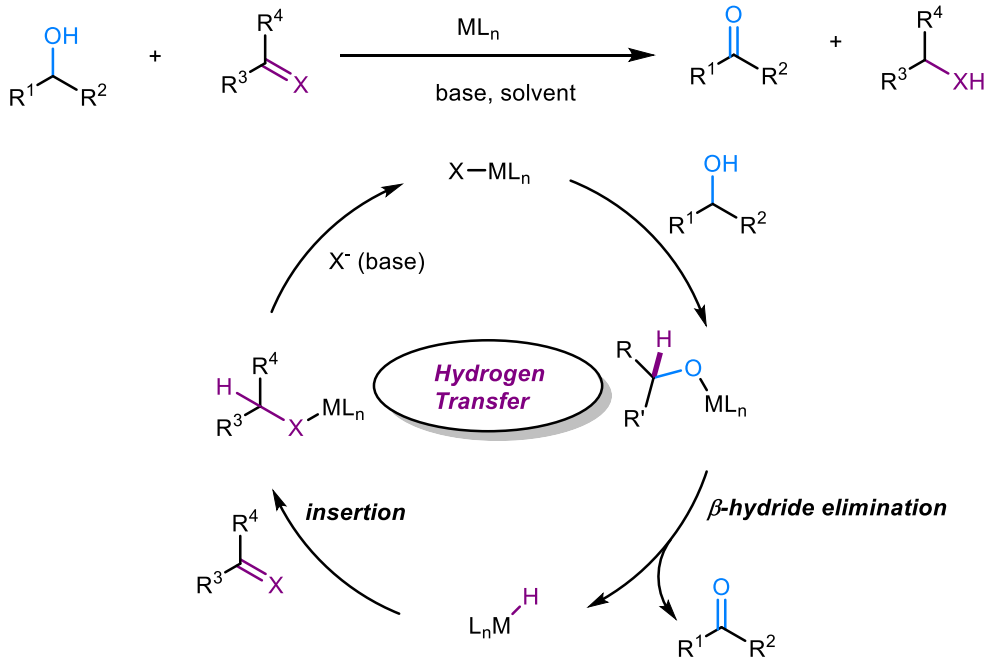

Scheme 1.7 General mechanism for hydrogen-transfer-mediated anaerobic oxidation of alcohols

The most widely known hydrogen-transfer-mediated alcohol oxidation is Oppenauer oxidation,[27] which is mediated by a strong Lewis Acid, $AlCl_3$. With the development of late-transition metal catalysis, the ruthenium (II) complex,[28] which was previously demonstrated as ideal for alcohol dehydrogenation, has also been identified as conducive to the oxidation of hydrogen-transfer-mediated alcohol. In 1992, Bäckvall *et al.* proposed the ruthenium-catalyzed Oppenauer-type oxidation of alcohols.[16] In this reaction, acetone was treated as a hydride acceptor, and oxidation

could occur only to secondary alcohols. Subsequently, in 1996, a further study was conducted on this chemistry,[29] which led to the discovery of Shvo's catalyst (Scheme 1.8),[30] a well-defined ruthenium catalyst that can be applied for hydrogenation reactions. Exhibiting a stronger reactivity than the previously discussed $Ru(PPh_3)_3Cl_2$, it could fit a broader substrate scope. The higher efficiency shown by Shvo's catalyst in hydrogenation/dehydrogenation reaction is attributed mainly to the active proton present on the Cp ring, which enables the induction of a favorable cyclic transition state for hydrogenation/dehydrogenation at the time of interaction with carbonyl or alcohol substrates (Scheme 1.8). What is also noteworthy with this discovery is that a trace amount of water can increase the efficiency of the oxidation process to a significant extent. As for the substrates, the simplest secondary alcohols demonstrated the highest efficiency for this reaction. This catalytic system, however, is unsuitable for certain sensitive functional groups containing such substrates as alkyl halides, amines, or carbonates. Notably, the double bond in linear allylic alcohols would be reduced to a single bond in the final product.

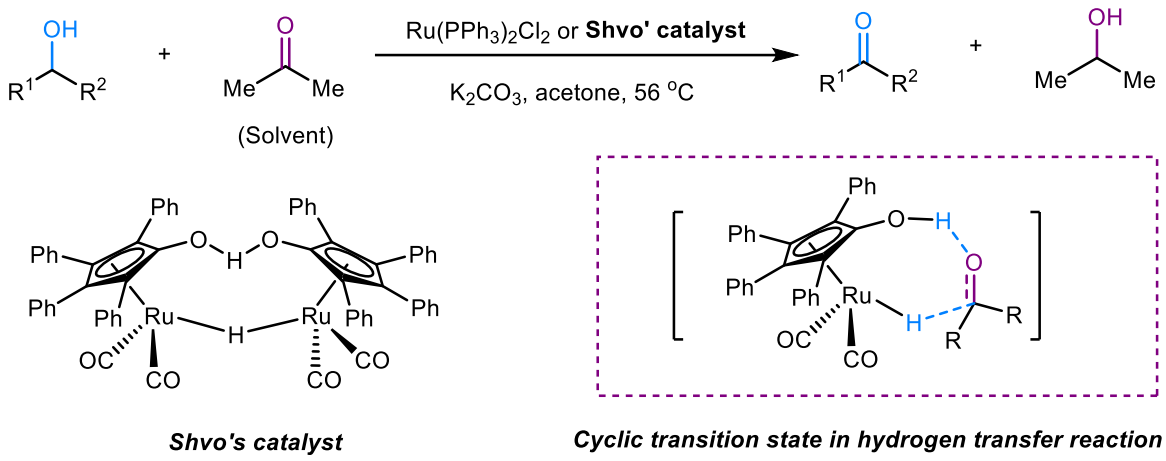

Scheme 1.8 Ru(II)-catalyzed Oppenauer-type oxidation

Inspired by the outstanding capability displayed by the Shvo's catalyst in hydrogen transfer reactions, an analogue using iron instead of ruthenium was developed by the Casey group in 2007[31, 32]. Then, it was applied to the hydrogen-transfer oxidation of alcohols.[33] Compared with the previously-developed ruthenium system, more functional groups could be effectively tolerated, such as halogen atoms and cyclopropyl groups. Moreover, there was neither reduction nor isomerization of the double bond observed for double-bond-containing substrates. These advantages result from the comparatively less intense interaction of the iron complex with C–X

bonds and π-systems (Scheme 1.9). Notably, a success was achieved in adopting the iron catalytic system for some primary alcohols with conjugate systems, which showed poor reactivity in classic Oppenauer-type oxidation. In spite of this, a limitation on this iron catalyst lies in its sensitivity to air, which requires the storage and use under inert conditions. To solve this problem, Funk *et al.* developed an air-stable iron complex in 2010 for the transformation of this type (Scheme 1.9).[34]

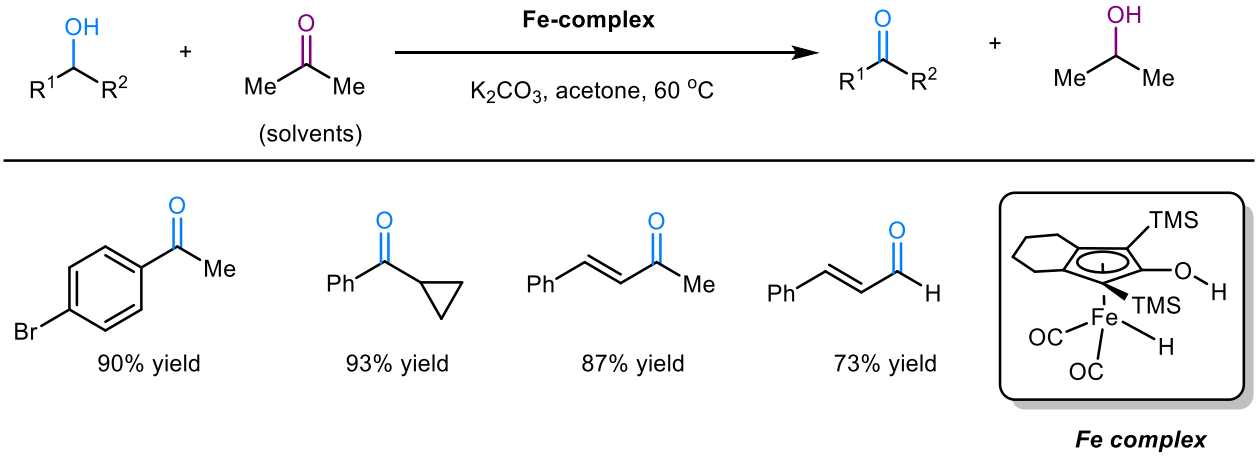

Scheme 1.9 Iron-catalyzed Oppenauer-type oxidation

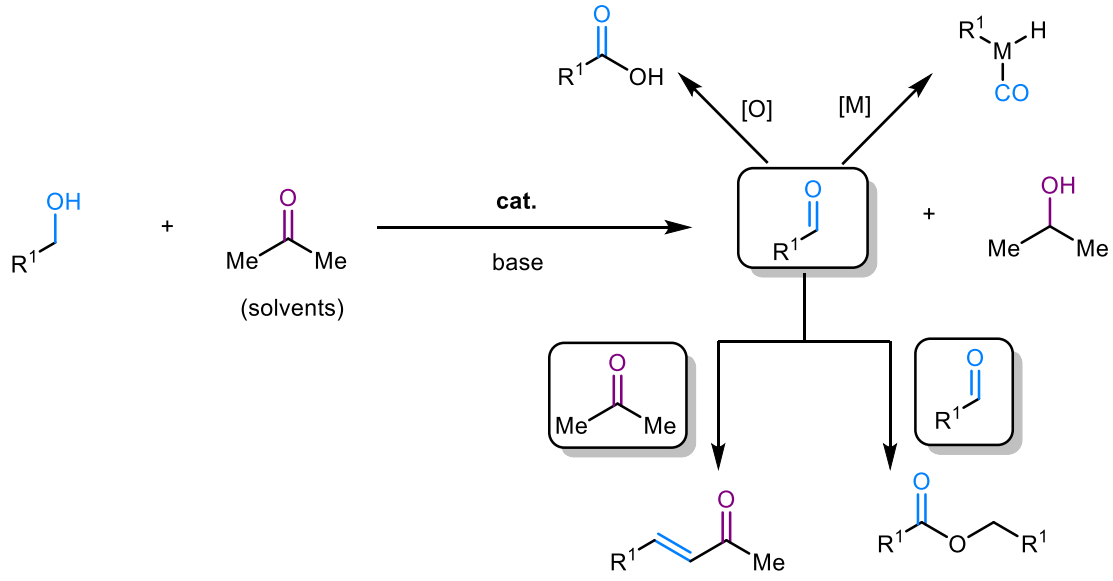

Scheme 1.10 Potential side reactions of primary alcohol oxidation

Although ruthenium- and iron-catalyzed hydrogen-transfer oxidation of alcohols provides an effective alternative solution to classic Oppenauer oxidation, they remain incapable to achieve

efficiency in primary alcohol oxidation. In fact, the oxidation of primary alcohols is a long-standing challenge facing alcohol oxidations for a number of reasons. Firstly, the aldehyde itself is not as stable as ketones thermodynamically and is even more susceptible to further oxidation. Secondly, the aldehyde is highly reactive and can cause various side reactions with hydrogen acceptors such as aldol condensations. Lastly, the aldehyde C–H bond can be immediately activated to interact with transition metal complexes, thus leading to CO de-insertion (Scheme 1.10). Therefore, in the initial stage of development for Oppenauer-type oxidation, there were few reports on the efficient oxidation of primary alcohols, even though plenty of transition metal catalysts had been developed.

In 2003, however, Hiroi *et al.* developed a well-defined iridium complex to drive the Oppenauer-type oxidation of primary alcohols in an efficient way. The iridium (III) complex can be used to break the previously discussed limitations with primary alcohols due to its comparatively lower Lewis acidity and neutral nature, which hinders the occurrence of side reactions involving aldehydes. This method has shown a broad substrate scope and the tolerance of various sensitive functional groups such as halides, double bonds, and thioethers. Among the substrates, benzyl alcohol and derivatives exhibited higher reactivity than the linear aliphatic alcohols (Scheme 1.11).[35]

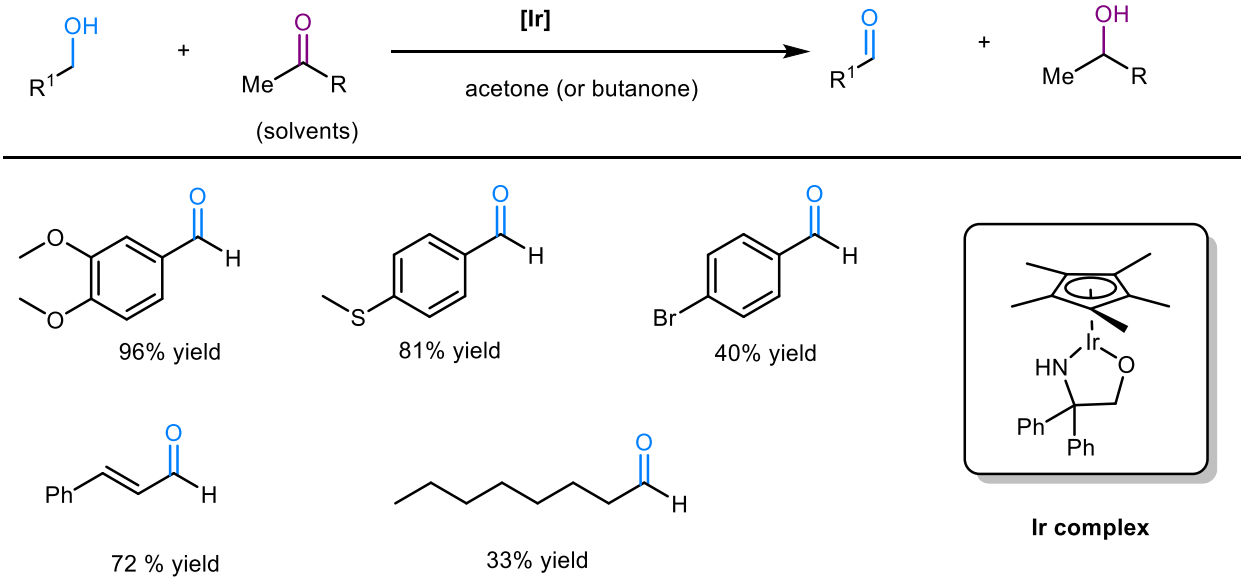

Scheme 1.11 Iridium-catalyzed Oppenauer oxidation of primary alcohols

In addition to ketones (C=O double bond), C=C double bonds are also applicable as hydride acceptor. Due to to the more demanding conditions for hydrogenation of alkenes as required by homogeneous catalysis, however, the transfer dehydrogenation of alcohols with alkene was reported mostly by heterogeneous catalysts[36] such as Pd/C,[37] Cu/La_2O_3,[38] and nanoparticle Ni.[39] To promote this transformation both thermodynamically and kinetically, it is necessary for the alkene taken as a hydride acceptor to be less sterically hindered and reactive. The most-used ones include ethylene, styrene, and cyclohexene.[36–38] In this case, which is similar to the Oppenauer-type oxidation, primary alcohols play a far less efficient role than secondary ones. In contrast, the Cu/La_2O_3 system,[38] developed in 2010, could enable the oxidation of aliphatic primary alcohols with alkene to achieve moderate-to-high yield.

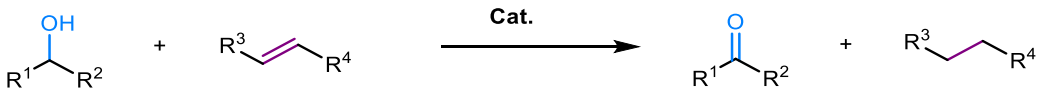

Scheme 1.12 Transfer dehydrogenation of alcohols with alkenes

The homogeneous transfer dehydrogenation of alcohols with alkenes, as previously discussed, has been comparatively less reported. Furthermore, it is worth noting that such a transformation was most performed as the methodology adopted for the hydrogenation of alkenes rather than for the oxidation of alcohols, which might result from the substrate limitation of alcohols and the higher driving force for alkene reduction compared to alcohol oxidation. The iridium complexes were demonstrated as one of the most efficient catalytic systems suitable for this type of transformation. For instance, in 2001, Ishii *et al.* revealed that iridium (I) catalysts could be efficient in enabling hydrogen transfer from alcohols to both activated and unactivated alkenes.[40] Then, in 2014, Ding *et al.* developed a well-defined bisbenzothienyl iridium (III) complex, which was shown to be efficient in the transfer dehydrogenation of alcohols with styrene as assisted by phosphine compounds.[41]

1.2.3 Acceptorless dehydrogenation of alcohols

Despite the development of numerous oxidants and hydride acceptors for the oxidation of alcohols, the conversion of alcohols into carbonyls could also be achieved through an acceptorless pathway *via* transition metal-catalyzed dehydrogenation. In addition to reacting with hydride acceptors, metal–hydride species can also be protonated to generate hydrogen gas. Under the classic catalytic

systems as mentioned above, however, this process is not kinetically or thermodynamically facilitated to a sufficient extent. Thus, it is necessary to develop a new catalytic system for this process to take place efficiently with the acceptorless dehydrogenation of alcohols.

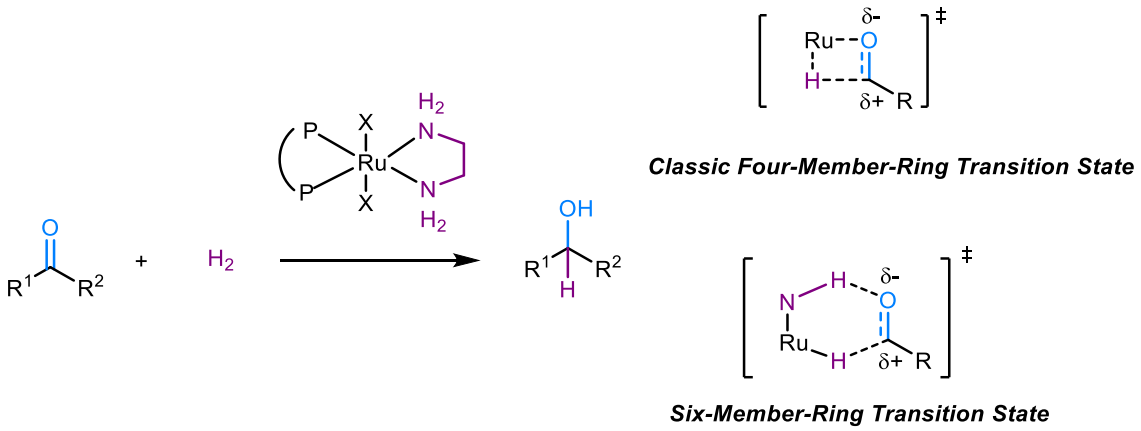

Scheme 1.13 Transition state in Noyori-type hydrogenation with ruthenium–diphosphine–diamine complex

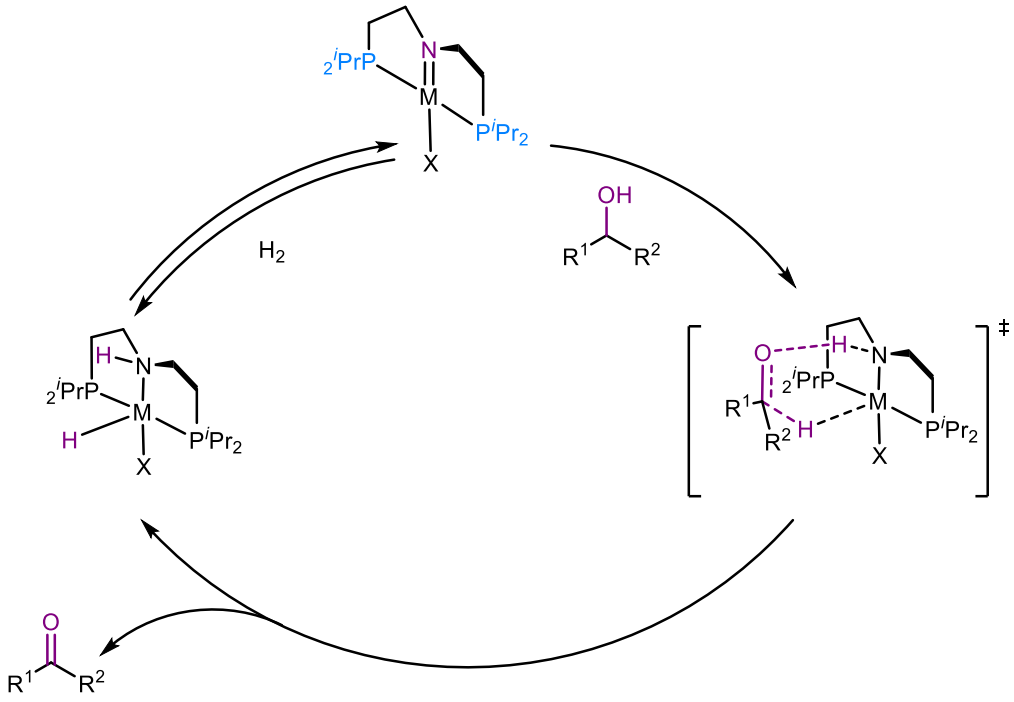

Scheme 1.14 Mechanism of PNP–pincer complex catalyzed acceptorless alcohol dehydrogenation (AAD)

At the beginning of this century, when the asymmetric hydrogenation reaction was studied, Noyori *et al.* made a discovery that the combination of phosphine ligands and amine ligands could lead to a significant improvement of efficiency for hydride insertion.[42] From a mechanistic perspective, this phenomenon is attributed to the introduction of nitrogen into the complex to act as an internal base and a hydrogen bond provider simultaneously. In this case, a favorable six-membered ring transition state could be formed when the metal–hydride species develops during hydrogenation, which facilitates the hydrogenation process kinetically (Scheme 1.13).[42] Inspired by this, our consideration is given to the reverse case where the dehydrogenation of alcohols could also be a kinetically facilitated process under the catalysis of a metal–phosphine–amine complex. Although this helps break the previously discussed kinetic limitations, the occurrence of a hydrogen gas generation process remained hindered by its anti-thermodynamic nature. Conversely, the success achieved in the acceptorless dehydrogenation of alcohols is contributed to by the hydrogen gas released from the reaction system, which makes this process irreversible to some degree.[43] Furthermore, Noyori's catalyst was used to develop a metal–PNP pincer complex that is more stable and widely used (Scheme 1.14) for this transformation.[44–48] The advantages of the PNP pincer complex[49] over **MP_2N_2** type complex are detailed as follows. Firstly, the tridentate ligand structure improves stability for the complex, especially at high temperatures.[49] Secondly, the rigid structure is conducive to stabilizing intermediates and transition states. Lastly, space can be made available by occupying only three coordinating sites for substrate interaction. According to these principles, in 2011, Beller *et al.* achieved a success in releasing H_2 in the dehydrogenation of alcohols with an aliphatic ruthenium–PNP complex.[50] According to the mechanism proposed for this reaction, the nitrogen group present on the complex serves as both an internal base and proton provider (Scheme 1.14). Other than ruthenium, Mn,[51] Fe,[52] and Co[53] bearing the same type of PNP pincer ligand also proved efficient in promoting acceptorless dehydrogenation of alcohols.

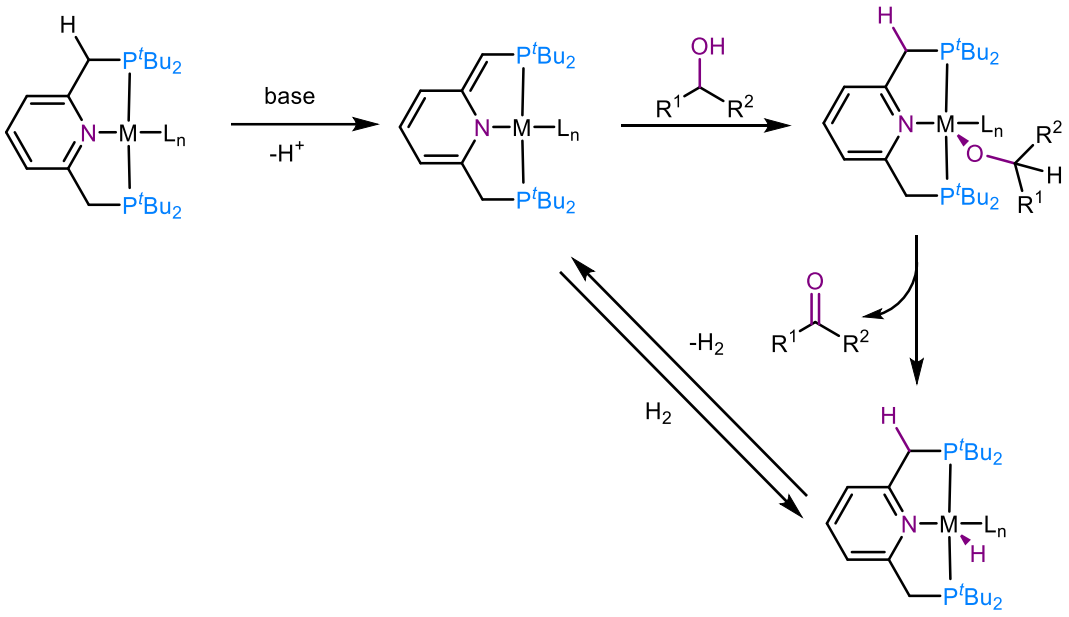

Scheme 1.15 Mechanism of alcohol dehydrogenation with $PN_{pyridine}P$ type pincer complex

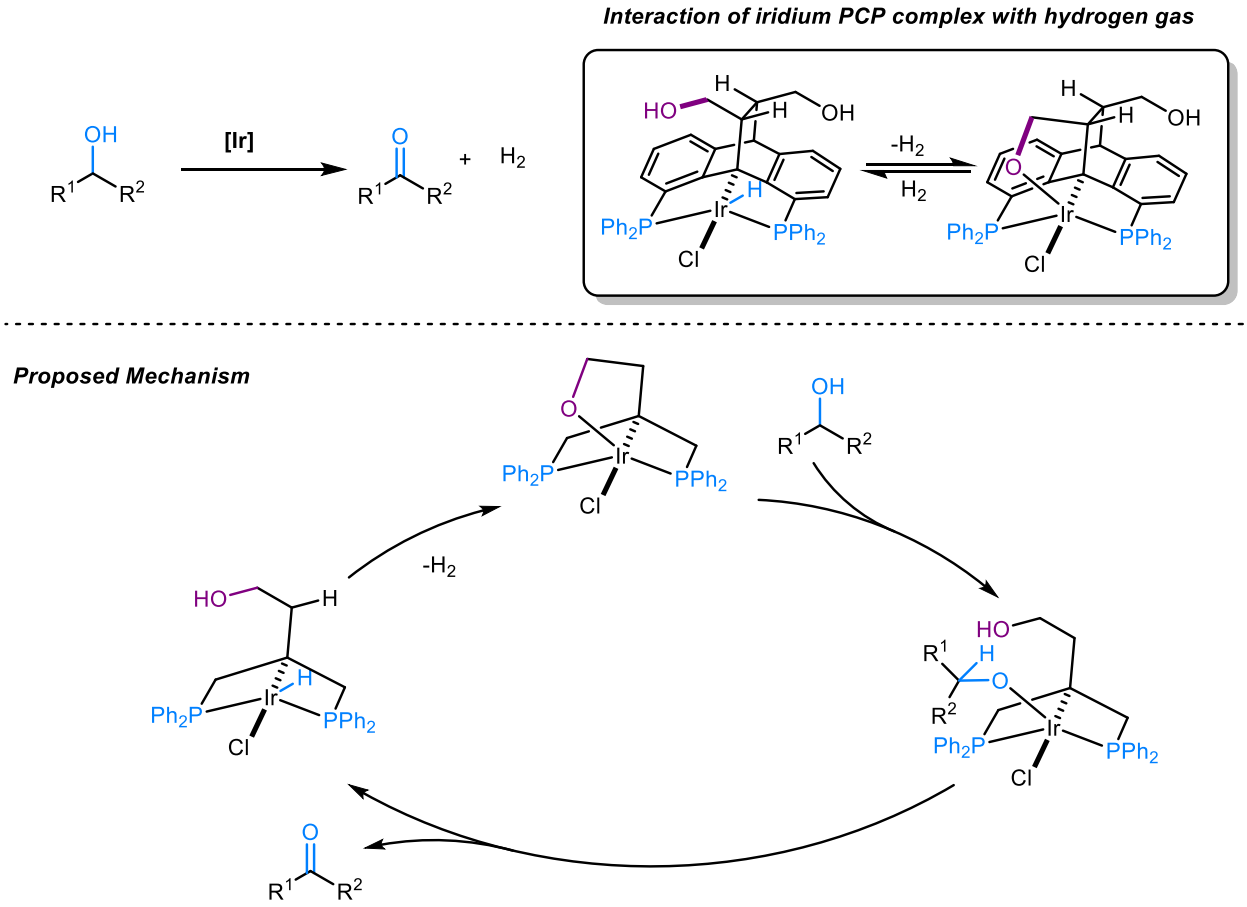

Scheme 1.16 Iridium–PCP-catalyzed AAD reaction utilizing M–L interaction strategy

Apart from aliphatic PNP ligands, Milstein *et al.* developed another type of PNP pincer ligand with pyridine as the central atom, which was demonstrated as another effective tool for hydrogen transfer reactions.[54] Since the nitrogen atom ceases to contain any active proton in the $PN_{pyridine}P$ type pincer complex, the proton transfer will instead occur on the side arm of the ligand as shown in Scheme 1.15. Given this unique property, the $PN_{pyridine}P$ type pincer complex could also be taken as an ideal catalyst for AAD.[50]

Further with the discovery of unique properties possessed by PNP pincer complexes in the catalysis of AAD, scientists then made attempt to modify the PNP ligand by replacing the center nitrogen with carbon (now PCP). This is aimed to further increase the electron density, which plays a crucial role in the hydride insertion and de-insertion process.[55] For instance, Gelman *et al.* took advantage of metal–ligand interaction to develop an iridium–PCP complex for AAD reaction in 2011.[56] More specifically, a hydroxyalkyl group is connected to the center carbon on this PCP ligand, which could act as a proton provider to interact with the M–H generated during the catalytic cycle (Scheme 1.16). As illustrated in the scheme, the hydroxyl group would substitute the M–H bond while neutralizing the hydride, so as to generate hydrogen gas and *O*-coordinating species. In this process, both H_2 release and the five-membered ring intermediate formation provide the driving forces required for an efficient AAD reaction. With the catalysis of the iridium–PCP complex involved, both primary and secondary alcohols could be dehydrogenated efficiently under mild conditions.

In addition to Gelman's iridium–PCP complex, different metal–ligand interactions were also introduced into other catalytic systems for AAD reactions. So far, the *N*-heterocyclic carbene (NHC) complexes have been widely known for their high electron density and excellent capability as electron donor, which enables the immediate oxidative addition and insertion/de-insertion reactions. Thus, the combination of phosphine and NHC is regarded as another effective solution to the alcohol dehydrogenation process.[57] In 2017, Song *et al.* found out that a bidentate-phosphine-substituted protic NHC–ruthenium complex was highly efficient for AAD reaction.[58] Distinct from other NHC, only one arm of the benzimidazole was substituted in this complex, with the other bearing a free proton. Such a design is conducive to the H_2 release process by enabling the proton–hydride interaction between N–H and M–H (Scheme 1.17).[57, 58] Under this catalytic system, a large proportion of the secondary alcohols could be dehydrogenated at moderate to high

yields. However, primary alcohols showed a significantly lower level of efficiency. For this reason, the reaction must be conducted under 140 °C. However, only a catalytic amount (1–2 mol %) of base was required with the assistance of free N–H on the ligand. It is noteworthy that the cyclopentadienyl ligand can be used to increase electron density for the ruthenium complex, which is commonly used for the purpose of hydrogen-transfer catalysis.

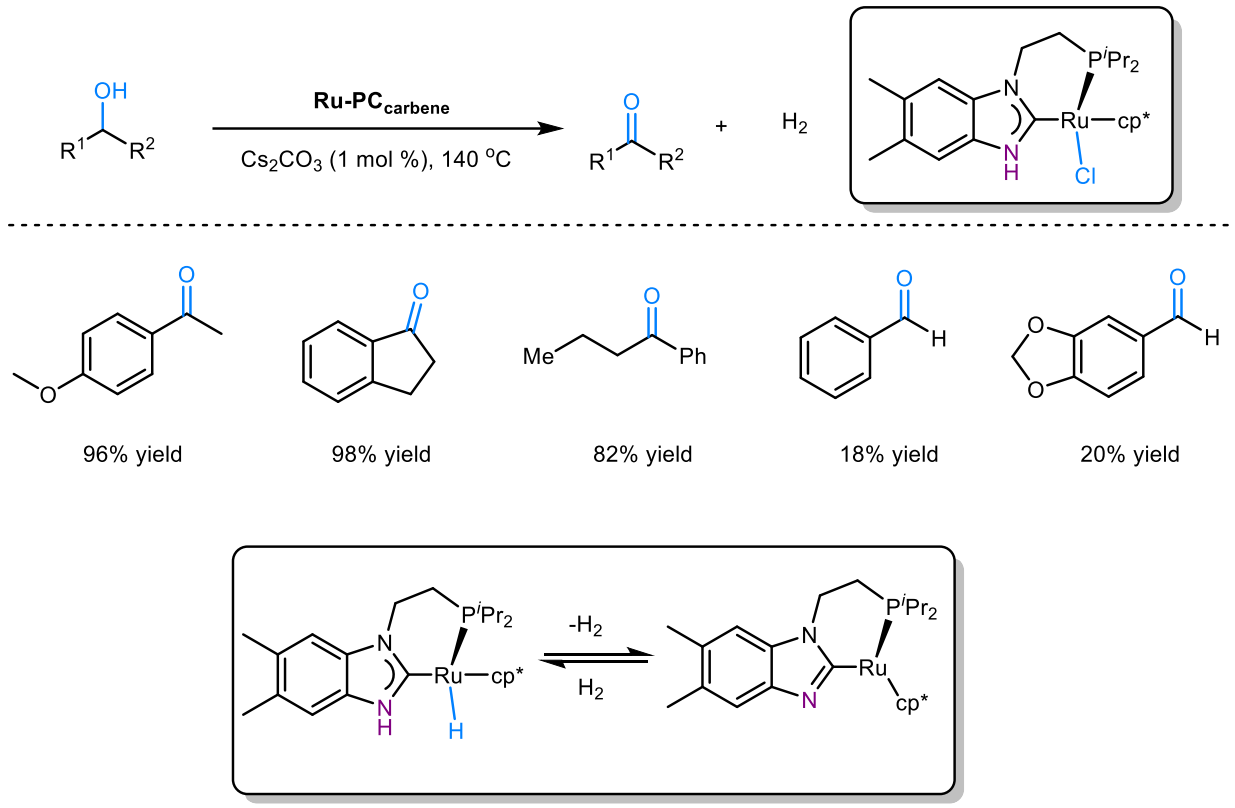

Scheme 1.17 AAD reaction with ruthenium protic NHC complex catalysis

The lactam (hydroxylpyridine)-type complex provides another typical example of an AAD reaction with a metal–ligand interaction strategy applied by taking advantage of the aromatization/de-aromatization process. Back in 2007, Yamaguchi *et al.* developed several iridium–Cp* complexes with mono-dentate 2-hydroxylpyridine or bidentate *α*, *α'*-bipyridonate (bpyO) as ligands, which was also demonstrated as highly efficient for AAD reactions (Scheme 1.18).

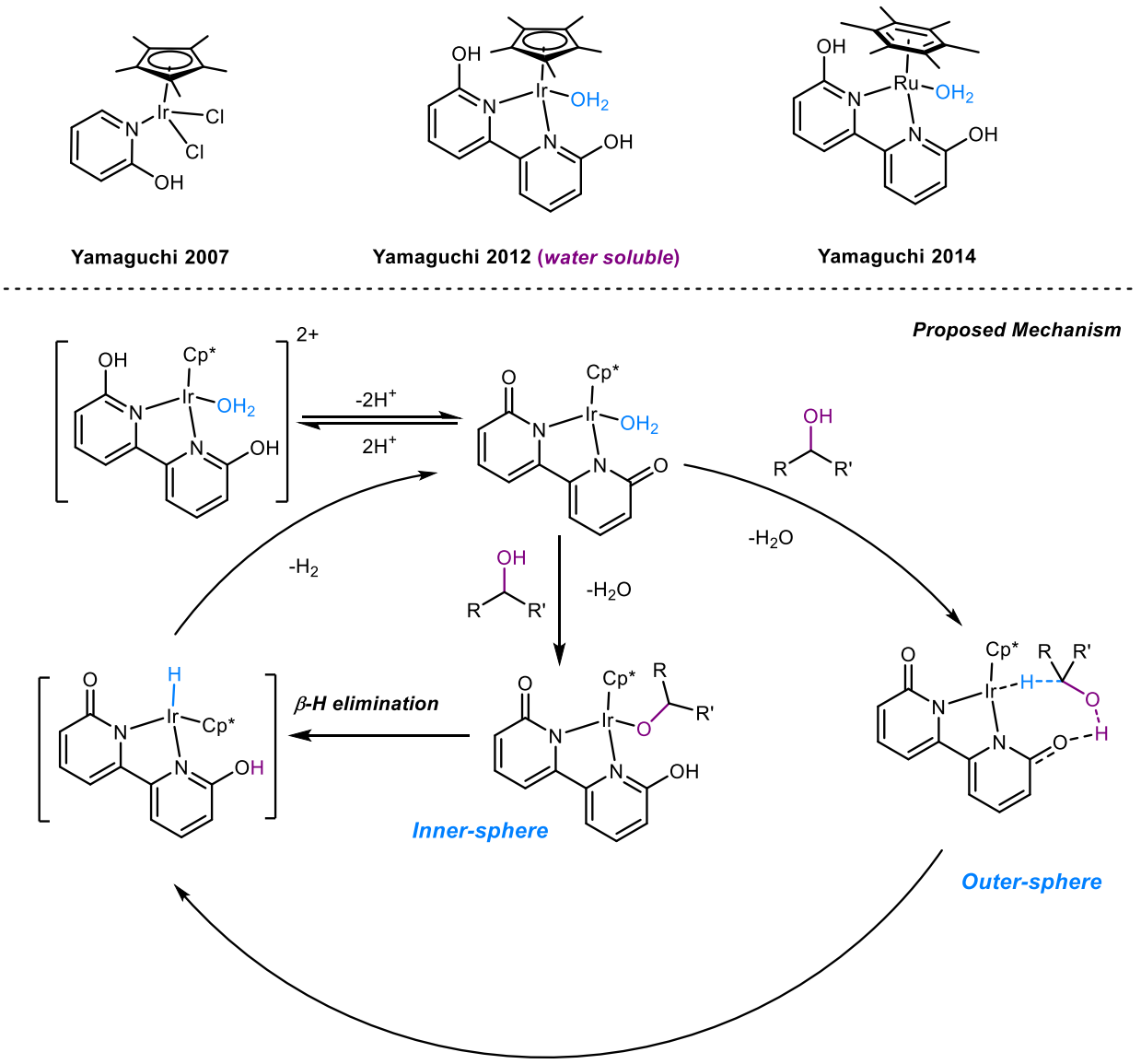

Scheme 1.18 Lactam-type complex as catalyst for AAD reaction and its mechanism

In 2007, Yamaguchi *et al.* developed the first iridium–hydroxylpyridine complex for application in the AAD reaction, with an extremely high level of efficiency reached for a broad range of secondary alcohols.[59] The reaction was allowed to take place in toluene at reflux temperature. Further with this discovery, they developed another bidentate *α*, *α'*-bipyridonate (bpyO)–iridium complex in 2012 to further enhance efficiency for this type of reaction by enabling this reaction to occur at room temperature and in the aqueous phase.[60] Moreover, aryl-conjugated primary alcohols could also be dehydrogenated with an extremely high yield produced. Subsequently, in order to reveal the mechanism of the iridium–hydroxylpyridine-catalyzed AAD reaction, DFT calculations

were performed to propose that the dehydrogenation step could involve a *β*-hydride elimination (inner-sphere) process, or an assisted seven-member-ring transition state (outer-sphere) process, as shown in Scheme 1.18. Additionally, this was also relied on to predict the (bpyO)-complex with ruthenium (II) and rhodium (I) centers, where both of them proved effective for the AAD reaction.[61]

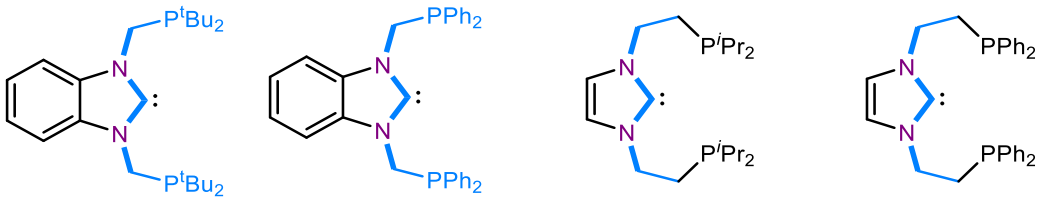

Scheme 1.19 Examples of common PCP pincer ligand

From the above discussion about various AAD reactions, it can be known that the key point is to design the complexes that are conducive to the internal proton and hydride transfer. In some cases, however, some complexes could still be efficient in enabling the acceptorless dehydrogenation process to occur, even in the absence of a proton acceptor. For instance, a new type of $PC_{carbene}P$ pincer ligand has been developed in recent years and shown as efficient in AAD reactions (Scheme 1.19).[62–64] Compared with PNP complexes and other AAD catalysts, the $PC_{carbene}P$ complex exhibits a significantly higher level of electron density, which makes it a much better electron donor due to the center carbene. Thus, despite the lack of internal proton transfer site, the $PC_{carbene}P$ complex could still complete oxidant-free dehydrogenation and hydrogen-transfer of alcohols in an efficient way.

1.3 Redox-neutral isomerization of allylic alcohols

In the previous section, a discussion has been conducted about the most efficient way of converting alcohols into carbonyls through the introduction of external hydride acceptors or the generation of hydrogen gas. In some cases, however, the internal functional groups present in some unique types of alcohol substrates could also facilitate such a transformation. As a classic example in this case, Allyl alcohol contains two close functional groups, which are OH and C=C double bond. As discussed above, C=C double bond could act as a hydride acceptor to drive the dehydrogenation of alcohols. In allylic alcohols, the internal double bond could still enable this process to take place

efficiently or even more rapidly. Most importantly, both of them are not as reactive as carbonyls in most organic reactions, whereas the inactive OH and C=C are capable of conversion into active carbonyls. Therefore, allylic alcohol isomerization attracted widespread interest for study, which is followed by several useful applications.

1.3.1 Isomerization of allylic alcohols *via* 1,4 hydride insertion pathways

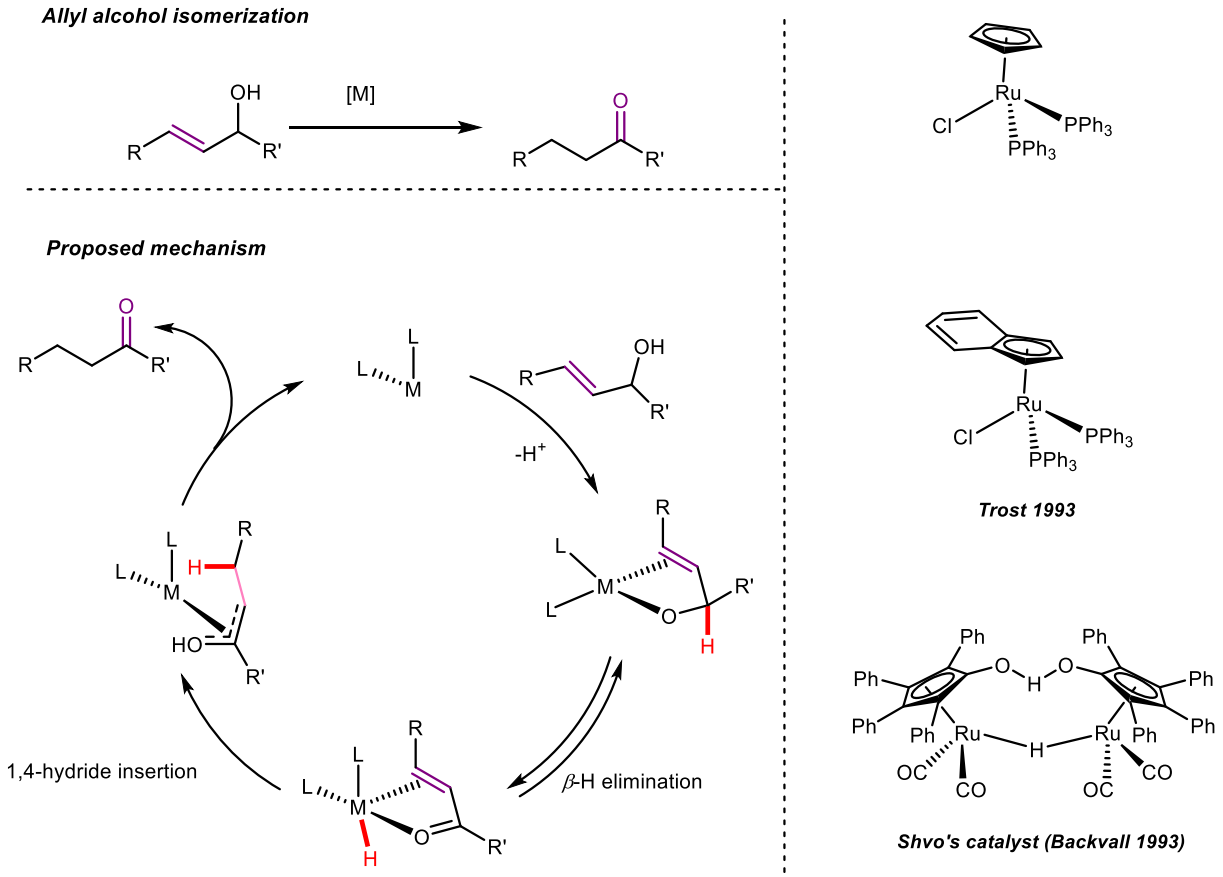

Scheme 1.20 Mechanism of allylic alcohol isomerization *via* 1,4-hydride insertion

The most common and recognized mechanism of allylic alcohol isomerization is a 1,4-hydride insertion. As shown in Scheme 1.20, the alcohol first coordinates with the catalyst along with the adjacent double bond to form a chelating intermediate. Then, *β*-hydride elimination occurs to generate the conjugated carbonyl intermediate with a metal–hydride species. Finally, facilitated by both conformation and electronic matching, metal hydride is subjected to the nucleophilic addition to double bond, thus forming the saturated carbonyl and completing the isomerization process.[65, 66]

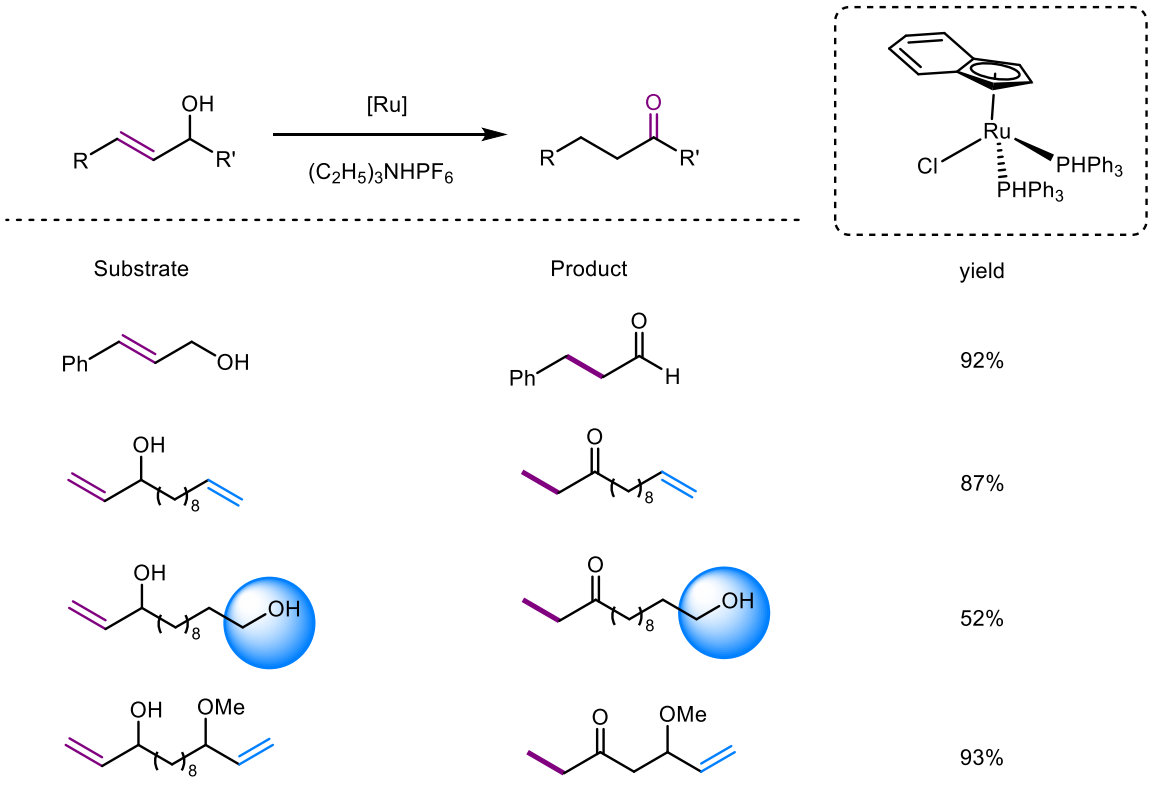

Scheme 1.21 Chemoselective allylic alcohol isomerization with ruthenium–Cp complex

Such a process could be catalyzed using a wide variety of ruthenium–phosphine complexes, among which the cyclopentadienyl–ruthenium complex has been identified as most efficient. The Cp ligand shows such advantages as the high electron density that enables dehydrogenation and flexible η^3–η^5 tautomerization, which is conducive to releasing more coordination sites for allylic alcohol to form the chelating intermediate.[65] In 1993, Trost *et al.* achieved success in enabling the isomerization of allylic alcohols through the use of a Cp–ruthenium phosphine complex. The reaction showed tolerance to a broad range of primary and secondary allylic alcohols while achieving high chemoselectivity where simple alcohols and separate double bonds would not react (Scheme 1.21). Furthermore, protected allylic alcohols neither showed reactivity nor made difference to the efficiency of normal allyl isomerization. Subsequently, the mechanism of this transformation was also studied, with the isotropic experiment conducted to demonstrate the 1,4-hydride insertion process.[65]

In the meantime, Backvall *et al.* found out that the Shvo's catalyst was also capable to catalyze the allylic alcohol isomerization efficiently. Through a comparison performed in reactivity between

the Shvo's catalyst and other common ruthenium–phosphine catalysts, it was discovered that the demand catalyst loading of the Shvo's catalyst was only one-fifth that of others. It was also found out in this study that the base played a vital role in the isomerization process, which might assist the coordination of alcohols while accelerating the process of proton transfer.[67]

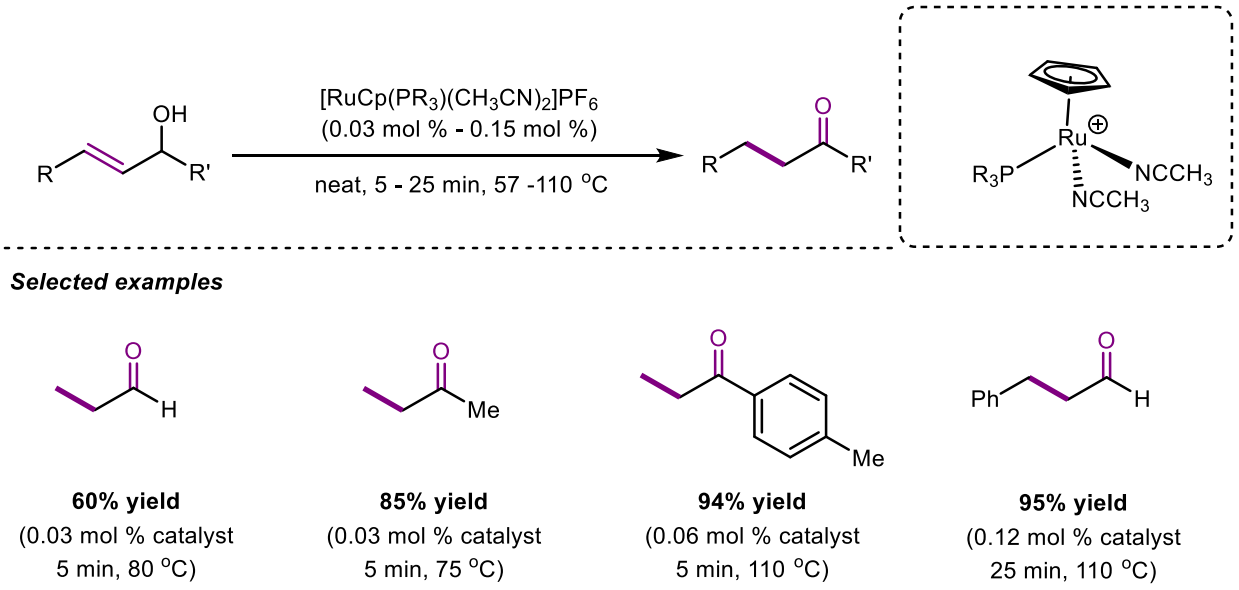

Scheme 1.22 Cationic ruthenium–nitrile complex for redox allylic alcohol isomerization

In order to further improve the efficiency and applicability of ruthenium-catalyzed allylic alcohol isomerization, there were a number of in-depth studies conducted subsequently on the adaptation of ruthenium catalysts. In 1999, Kirchner *et al.* developed a series of $[Ru(PR_3)(CH_3CN)_2]PF_6$-type complexes, which led to a significant increase in the efficiency of allylic alcohol isomerization (Scheme 1.22).[68] According to their results, the catalyst loading was as low as 0.03 mol % relative to the level of around 5 mol % in Trost and Backvall's system.[65, 67] In addition, with these type of complexes used for most of the substrates, the redox isomerization process takes less than 10 min to complete rather than the 5–8 h required for the traditional Ru–Cp or Ru–phosphine systems. As indicated by Kirchner *et al.*, the key influencing factor for improved efficiency is the comparatively labile structure of such weakly coordinating cationic complexes, which could accelerate the coordination of the complex with substrates to a significant degree. The nitrile ligand adapted here could be released with extremely ease during the reaction, thus providing an empty coordination site for OH and the double bond. From the perspective of substrate scope, C1 or C3 disubstituted

bulky allylic alcohols would not be converted, and primary allylic alcohols usually show a lower efficiency, which requires harsher conditions than the secondary ones. These trends are consistent with what was reported by Trost and Backvall.

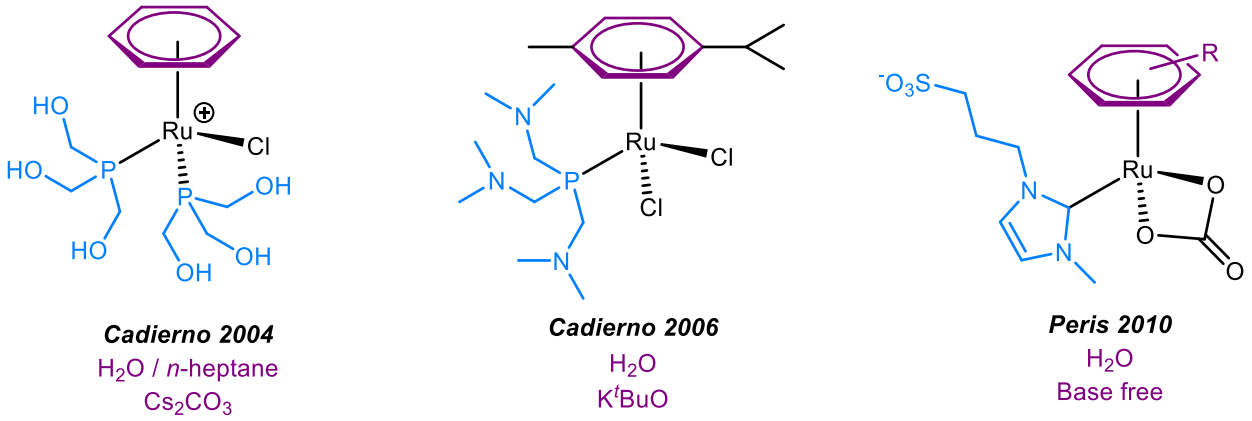

Scheme 1.23 Water-soluble ruthenium catalysts for redox isomerization of allylic alcohol in aqueous phases

For synthetically useful transformation, in addition to the reaction efficiency, the usage of green solvent is another reason to study the redox isomerization of allylic alcohols. Since the end of the last century, the organic chemistry in the aqueous phase has attracted attention from chemists for its outstanding advantages in both green chemistry and atom economy over traditional organic-phase reactions.[69, 70] Allyl alcohol, as an ideal hydrotropic compound, is a desirable substrate suitable for transformation in the aqueous phase. Thus, to achieve the isomerization of allylic alcohols in the aqueous phase would be more crucial for its application in synthetic chemistry. The allylic alcohol isomerization in aqueous phase was first developed by our group in 1998 with the air and water-stable $Ru(PPh_3)_3Cl_2$ as the catalyst. In that study, it was demonstrated that both allylic and homoallylic alcohols could be efficiently isomerized with Ru catalysis in water. (This work will be further discussed in detail in Section 1.3.4).[71] Then in 2004, Cadierno *et al.* developed a water-soluble ruthenium complex and achieved allylic alcohol isomerization in two phases (H_2O/heptane).[72] The design of ruthenium complex involved the introduction of a multi-hydroxyl-substituted phosphine ligand ($P(CH_2OH)_3$), which not only maintained the sufficient level of electron density but also made the whole complex more hydrotropic. Based on this design, a similar ruthenium complex was developed two years later, with the phosphine ligand adapted to

the amine-substituted one to achieve the transformation in the complete aqueous phase.[73] Subsequently, such a strategy intended to adapt phosphine ligands to hydrotropic systems was also adopted by other groups to develop various ruthenium catalysts for redox isomerization in the aqueous phase.[74–76] In addition to ruthenium–phosphine complexes, Peris developed a water-soluble ruthenium–NHC complex in 2010 to achieve the allylic alcohol isomerization in the aqueous phase under base-free conditions. Peris showed innovation in applying the structure of NHC through the introduction of a sulfonic acid group onto one of the arms. Not only did this design make the whole structure hydrotropic, it also made the structure an internal base, thus removing the need for extra bases.[77]

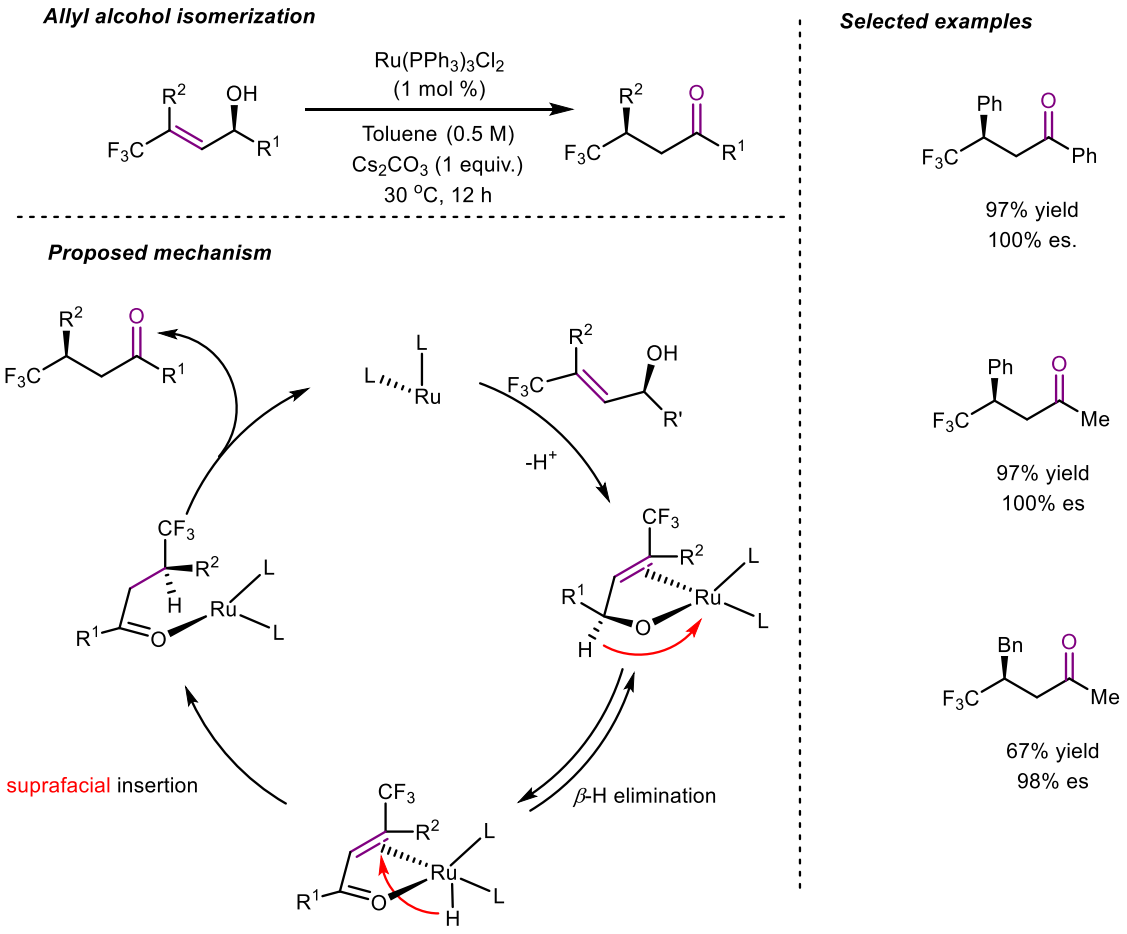

Scheme 1.24 Chirality transfer isomerization of trifluoromethyl-substituted allylic alcohols

With the 1,4-hydride insertion process in place, not only can the redox isomerization of allylic alcohols be performed to construct carbonyl compounds in one pot, it can also create new

stereogenic centers. For instance, a new chiral center at C3 could be efficiently introduced *via* chirality transfer after the isomerization by taking an allylic alcohol with a chiral center at the C1 position. In 2012, Cahard *et al.* achieved a success in the enantioselective isomerization of 3-trifluoromethyl allylic alcohols through such a strategy. The reaction showed an excellent enantiospecificity (es), whereas it could achieve nearly 100% es for most substrates.[78] A mechanism proposed to account for this ideal enantiospecificity is the suprafacial 1,3-hydride shift process as shown in Scheme 1.24.

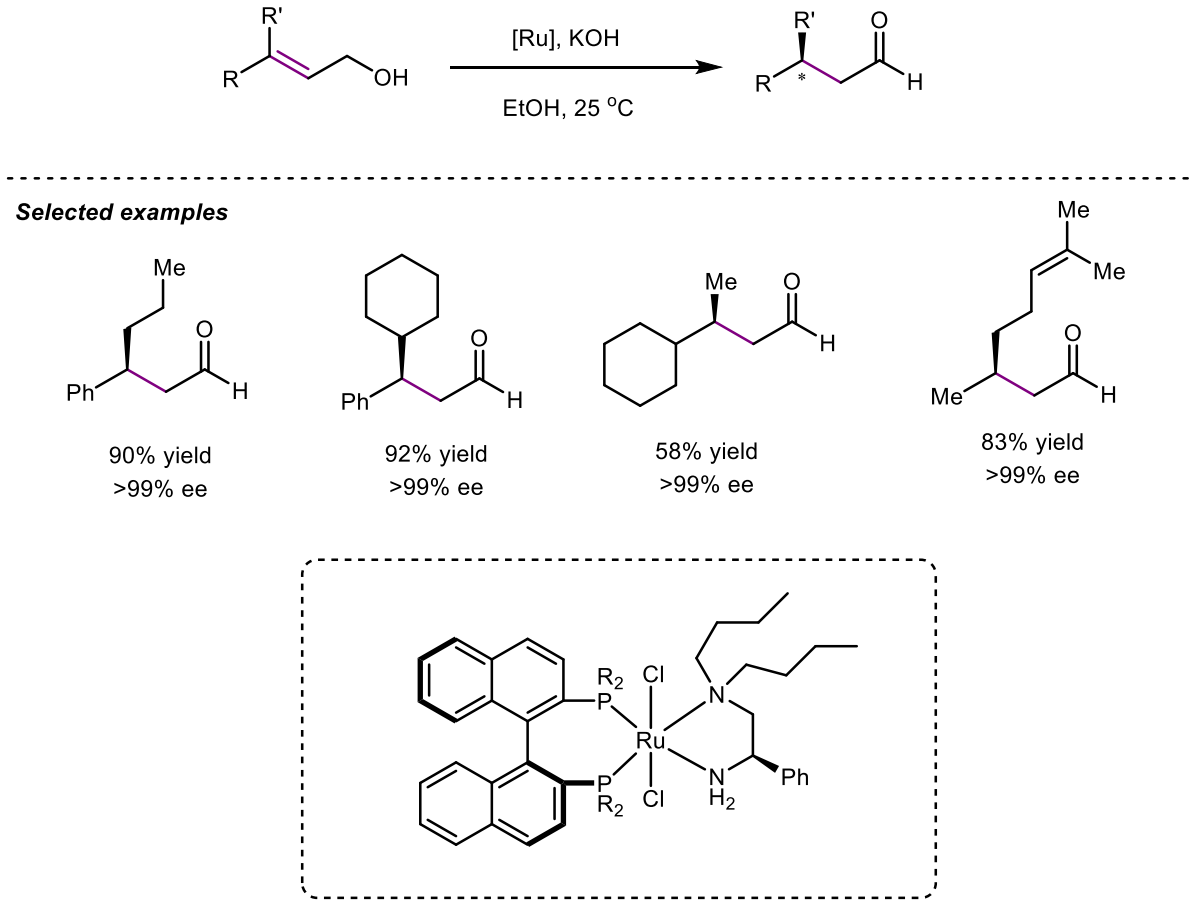

Scheme 1.25 Enantioselective allylic alcohol isomerization catalyzed by chiral ruthenium–BINAP complexes

Apart from chirality transfer, the asymmetric catalysis in allylic alcohol isomerization was also suggested, especially for 3,3-disubstituted primary allylic alcohols.[79] Since the ruthenium-catalyzed allylic alcohol isomerization undergoes a hydride de-insertion/insertion process, Noyori-type chiral ruthenium–aminophosphine complexes were most commonly used for enantioselective

isomerization. For example, Okuma *et al.* applied the chiral ruthenium–binap–diamine complex to achieve the enantioselective isomerization of various 3,3-disubstituted primary allylic alcohols in an efficient way. In the study, it was also revealed that the chirality was most affected by the BINAP ligand, which is because high enantioselectivity remains achievable even in the absence of diamine ligands. In the meantime, it was indicated that strong diamine ligands would result in low efficiency for catalysis as they would inhibit the coordination of ruthenium complex with substrates.[80]

1.3.2 Isomerization of allylic alcohols *via* C–H activation pathway

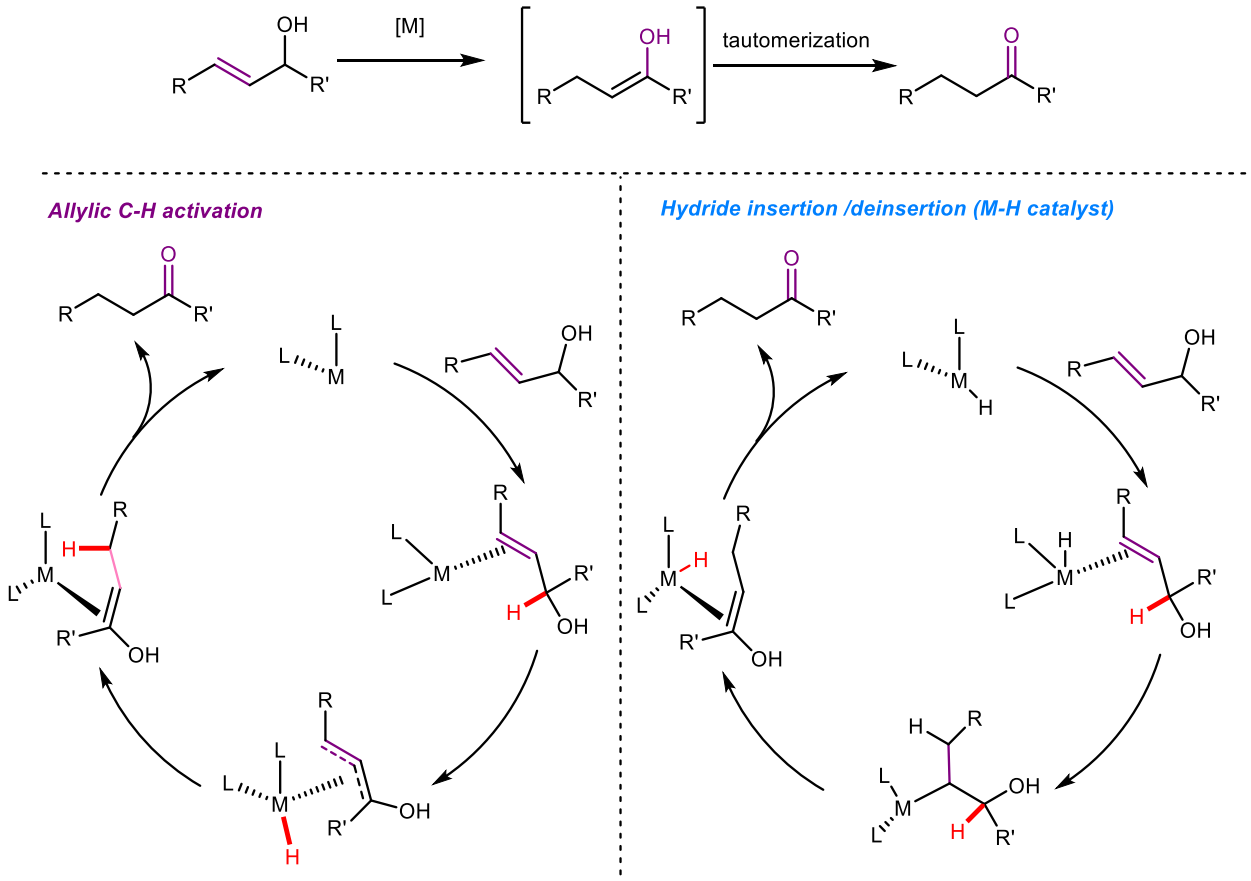

Scheme 1.26 Allylic alcohol isomerization *via* allylic C–H bond activation pathway

Aside from ruthenium (II), other precious metals such as Rh,[81] Ir,[82] and Pd[83] or low-valent non-noble metals like Ni[84, 85] or Fe[86] could also act as catalysts for the redox isomerization of allylic alcohols. However, a large majority of those catalysts tend to drive the isomerization through an allyl C–H activation pathway without any interaction with the OH group, which is because those

metals are relatively softer than ruthenium and more likely to have coordination and interaction with non-polar C=C double bonds or C–H bonds, rather than polar C–O or O-H bonds. Due to those catalysts, the allylic alcohol would first coordinate with the metal center, and the C–H bond at the allyl position would be activated to generate an M–H intermediate. Then, olefin isomerization would be completed to generate enol intermediate after the 1,3-hydride shift. Finally, the thus-formed enol would tautomerize to the corresponding carbonyl (Scheme 1.26).[74, 79] In addition, there are some circumstances where this process is promoted by a metal–hydride precursor. Consequently, the 1,3-hydride shift would occur stepwise. As for the metal hydride, it would first perform an insertion to the double bond after the coordination. Then, the intermediate would conduct a β-hydride elimination at α-position of the OH to generate a new double bond, thus leading to enol intermediate. Eventually, tautomerization would occur to generate the desired carbonyl products.

The most significant difference between the allyl C–H activation process and the hydrogen-borrowing 1,4-hydride insertion process lies in the presence of enol intermediate. Although this difference cannot be clearly observed or even detected in the presence of free allylic alcohols, the enol ether would be quantitatively generated in some allylic ethers, which however is unachievable through the 1,4-hydride insertion pathway. Thus, the control experiment of allylic alcohol ether could help clearly distinguish between these two mechanisms. Furthermore, such a transformation could also provide an efficient solution to the synthesis of enol ethers, which are not easily accessible using classic methods. In 1978, Baudry *et al.* achieve the isomerization of various allyl ethers to enol ethers with nearly quantitative yield and an ideal *E*-selectivity through the use of iridium catalysts. Regarding the scope, however, only translinear primary allylic alcohol ethers could work efficiently, while both secondary and cis allyl ethers showed no reactivity.[87]

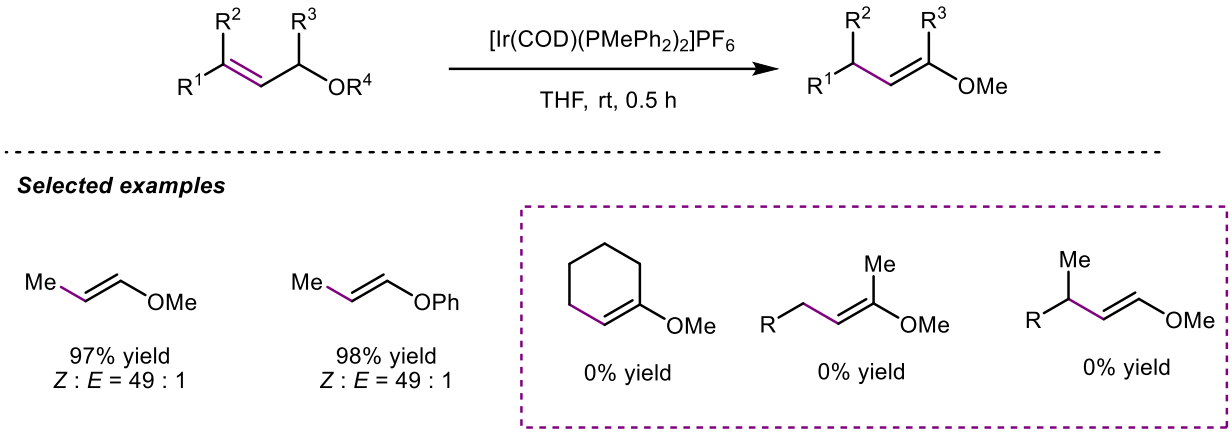

Scheme 1.27 Iridium-catalyzed isomerization of allyl ether

These results suggest a clear difference in selectivity between the iridium-catalyzed allylic alcohol isomerization and the ruthenium-catalyzed one. As discussed above, ruthenium-catalyzed allylic alcohol isomerization produces the best outcome with secondary allylic alcohols, whereas it shows a comparatively low efficiency for primary ones because the formation of aldehydes is hindered thermodynamically. As a result, the formed aldehyde undergoes various side reactions such as decarbonylation and self-condensations.[88] However, in the aforementioned iridium-catalyzed allylic C–H activation case, the intermediates formed are enols rather than aldehydes, which prevents potential side reactions. From another perspective, the restriction of steric hinderance causes a significant reduction in the reactivity of secondary or multi-substituted allylic alcohols. Thus, iridium-catalysts could even contribute to the isomerization of primary allylic alcohols, which provides an ideal alternative for the ruthenium-catalyzed system.[82]

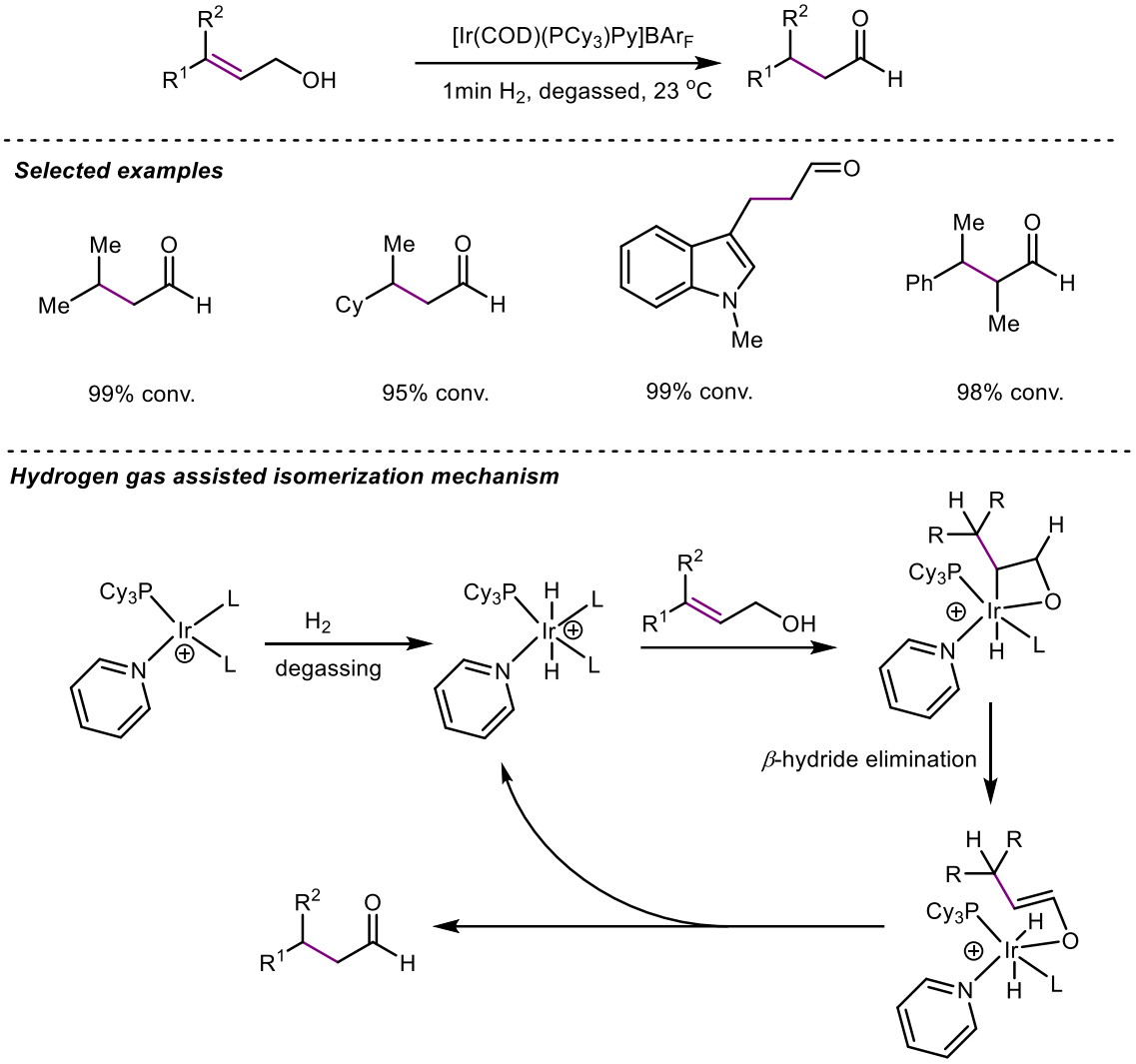

Scheme 1.28 H_2-assisted iridium-catalyzed isomerization of primary allylic alcohols

In 2009, Mazet *et al.* adopted an iridium–phosphine complex to achieve the isomerization of primary allylic alcohols. A highlight of this work is the effectiveness of some bulky and highly substituted primary alcohols, which proved inactive in some previous reports.[89] The key strategy applied to address previous challenges is the the activation of hydrogen gas. Through literature review, it was discovered that iridium–phosphine complexes could be efficient in catalyzing the hydrogenation of bulky alkenes.[90] Therefore, the use of iridium hydride was considered to initiate isomerization through hydrogenation/dehydrogenation instead of direct allylic C–H activation (Scheme 1.28). In addition, different kinds of iridium complexes were tested to find out that iridium–bisphosphine and iridium–NHC showed low or even no reactivity for isomerization due

to the overly strong coordination and the significant steric effect, which suppressed the coordination of iridium–bisphosphine and iridium–NHC with allylic alcohol substrates. Also, it is notable that the completion of this reaction does not require the involvement of base, which is another mechanistic difference between iridium- and ruthenium-catalyzed allylic alcohol isomerizations. Then, the same strategy was adopted to achieve the enantioselective[91] and diastereoselective[92] isomerization of primary allylic alcohol.

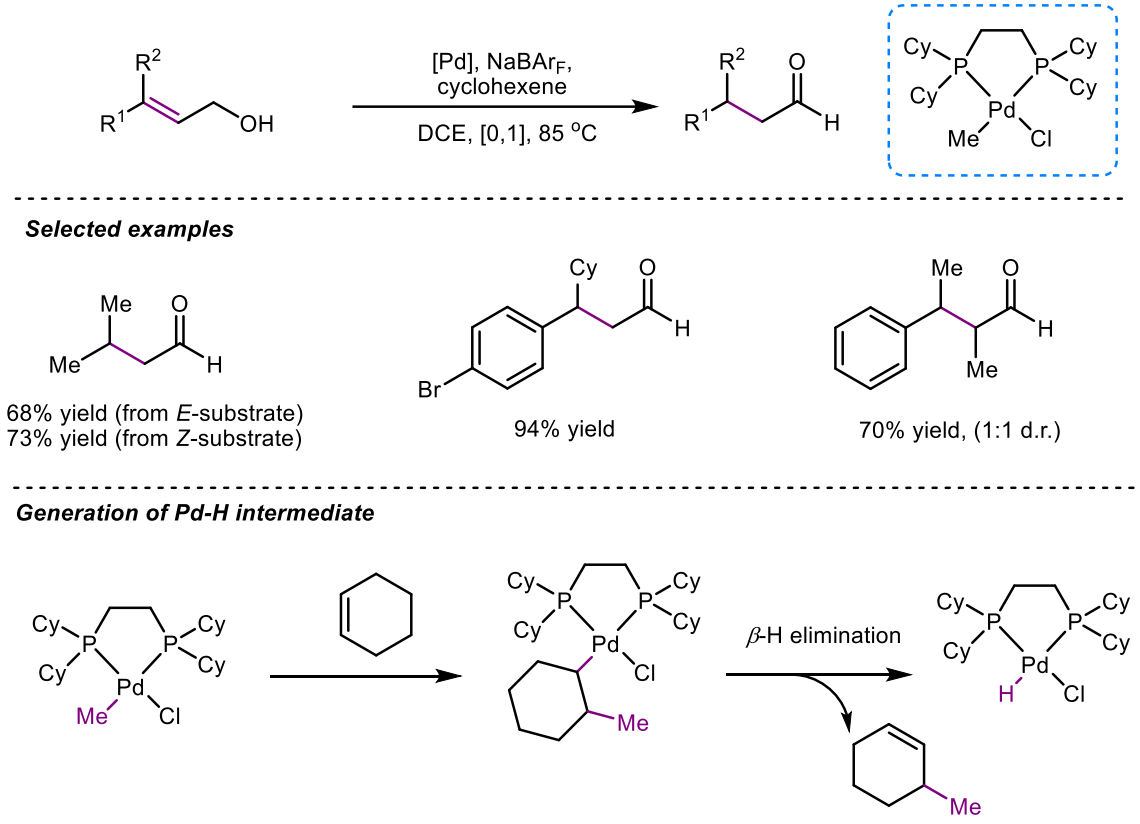

Scheme 1.29 Pd–H-catalyzed isomerization of allylic alcohol

In addition to iridium, palladium is another effective catalyst for C=C double bond hydrogenation and C–H activation. Thus, the palladium complex represents another potential catalyst for the isomerization of primary allylic alcohol. In 2014, Mazet *et al.* developed an analogous palladium catalyst to achieve the large-scale isomerization of primary allylic alcohol (Scheme 1.29).[83] Inspired by the iridium catalysis, they continued applying the strategy of the M–H intermediate. As palladium (II) is not as reactive as iridium (I) to H_2 and has a better capability of insertion/de-insertion, however, they designed a Pd–alkyl complex as the catalyst precursor and applied

cyclohexene as a hydride source to generate the Pd–H intermediate. DFT calculations were also performed to support the insertion/de-insertion process for 1,3-hydride shift. Moreover, attempt was made to adapt the dcype (dicyclohexylphosphinoethane) ligand into a chiral bisphosphine ligand, which led to the success in asymmetric isomerization.

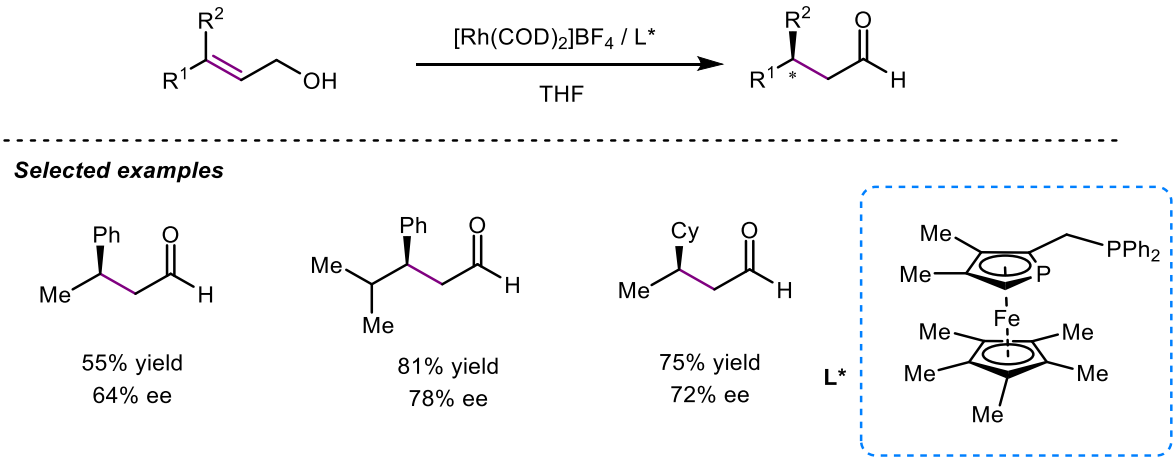

Scheme 1.30 Rhodium-catalyzed asymmetric isomerization of primary allylic alcohols

Though the isomerization of rhodium-catalyzed allylic alcohol is less reported than the palladium or iridium analogues, it is more readily used and studied in the isomerization of allylamines.[93–95] Different from Ru, Ir, and Pd, the isomerization of rhodium-catalyzed allylic alcohol does not have its symbolic mechanism whereby either 1,4-hydride insertion or allyl C–H activation is achievable. Thus, both primary allylic alcohols and secondary allylic alcohols could be isomerized efficiently in the presence of rhodium catalysis. For example, in 2000, Fu *et al.* proposed the asymmetric isomerization of primary alcohols with rhodium catalysis.[96] The chiral ligand used by them was a chiral phosphaferrocene ligand. Despite no discussion about the possible mechanism, the allylic C–H activation pathway appears to be a more rational mechanism based on the trend of the substrate scope, which is because it occurred in the iridium-catalytic system. Paradoxically, the asymmetric isomerization of secondary allylic alcohols was also suggested with rhodium catalysis. For instance, in 2017, Zhao *et al.* reported a secondary isomerization of allylic alcohol under the chiral rhodium–BINAP complexes. In their study, the most significant difference to that of Fu *et al.* is that a base is required for the reaction, which suggests a dehydrogenation/1,4-hydride insertion progress as proposed after their mechanistic studies.[81]

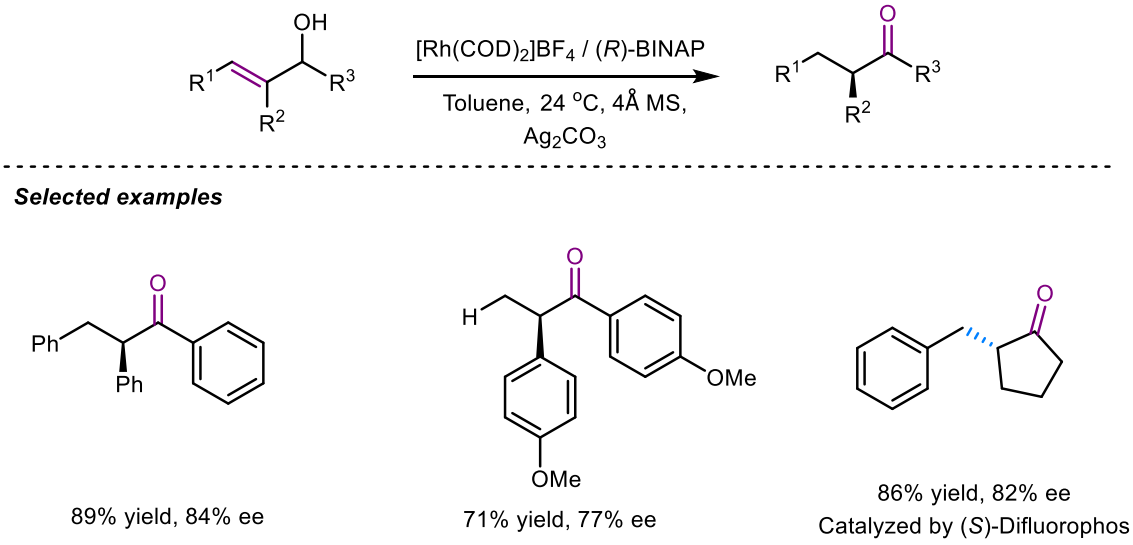

Scheme 1.31 Rhodium-catalyzed asymmetric isomerization of secondary allylic alcohols

Aside from the precious metal catalysts, the isomerization of allylic alcohol could also be catalyzed using such inexpensive metals as Ni and Fe.[85, 86] Given few reports and the lack of novelty in the reaction mechanism, they will be excluded from discussion herein.

1.3.3 Tandem reactions concerning allylic alcohol isomerization

Carbonyl compounds are the significant intermediates required for some synthetic transformations. In contrast, carbonyl compounds are difficult to store in some cases and tend to react with other internal functional groups. Thus, the one-pot reaction with carbonyls as intermediates is one of the popular areas of research for synthetic chemists. As discussed above, the isomerization of allylic alcohols provides an effective solution to generating carbonyls. Thus, it is also considered sensible to make allylic alcohol isomerization and corresponding carbonyl reactions occur in the same pot. The tandem allylic alcohol isomerization/aldol reaction is one of the most symbolic cases.

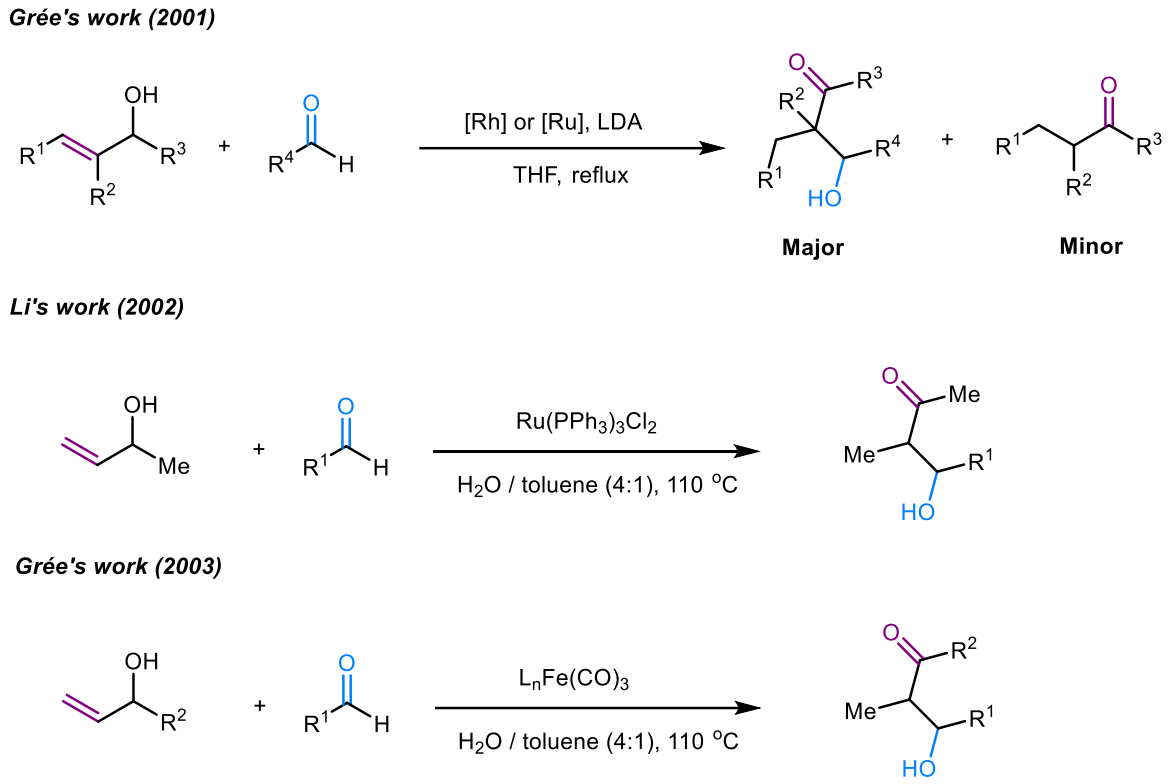

Scheme 1.32 Tandem allylic alcohol isomerization/aldol reaction

In 2001, Grée *et al.* proposed the ruthenium-/rhodium-catalyzed tandem allylic alcohol isomerization/aldol reaction. Given the fact that transition metal catalysts could promote the isomerization of lithium allylic alcohol salt,[97] they achieved innovation in developing the pre-catalyst with a catalytic amount of ruthenium/rhodium catalysts and 1 equiv. of lithium base (BuLi or LDA), which led to a success in facilitating the tandem reaction. In this transformation, however, it is worth noting that even though the yield of the final product reaches a reasonable level, there remain a significant amount of starting materials stuck at the isomerization step without any further progress. One year after the report of Grée *et al.*, our group managed to achieve this transformation in aqueous phase through the $Ru(PPh_3)_3Cl_2$ system. Notably, a discovery was made in the work of Li that the mixture of toluene and water as solvent would improve efficiency for this transformation.[98] Based on these findings, Kanai *et al.* developed a rhodium–dppf catalyst in 2012 to complete this process with a high efficiency. At the same time, the allylic alcohol was also adapted into allyloxyborane for the same transformation (Scheme 1.33).[99] In addition to precious metal catalysis, tandem allylic alcohol isomerization / aldol reaction could also be achieved using

such non-noble metal complexes as the iron-carbonyl complex developed by Grée *et al.* in 2003 (Scheme 1.32).[100]

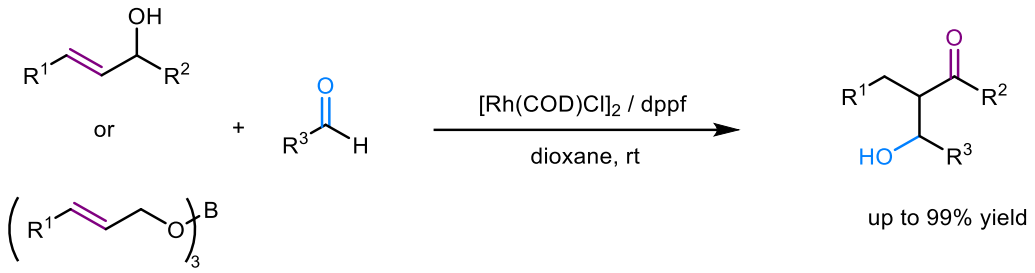

Scheme 1.33 Rhodium-catalyzed tandem isomerization/aldol reaction with allylic alcohol or allyloxyborane

As for the tandem aldol reaction, allylic alcohol serves as the nucleophile taking advantage of the enol intermediate upon isomerization. In comparison, the use of allylic alcohol as an electrophile in the tandem reaction has drawn limited attention for report. In 2020, our group developed a tandem allylic alcohol isomerization/Grignard-type reaction using allylic alcohol as a carbonyl surrogate, taking advantage of the novel nonmetal carbanion equivalent, hydrazone.[88] This work will be discussed in detail in Chapter 4.

1.3.4 Isomerization of homoallylic alcohol and other olefinic alcohols

The discussion about the isomerization of allylic alcohols leads to a question about whether the homoallylic alcohol or the alcohol with olefins at remote positions can isomerize into the corresponding carbonyls. It is widely known that a remote olefin could be continuously isomerized on a long chain *via* multiple instances of 'M–H insertion, de-insertion, insertion,' which is known as 'chain walking.'[101–103] Since the 'chain walking' is reversible, it is difficult to gain control of this process without applying a strong driving force. For olefinic alcohols, the olefins could principally isomerize multiple times to the enol position. At this stage, the enol would tautomerize to a carbonyl immediately, thus providing a strong driving force for the whole process. Thus, the isomerization of linear olefinic alcohols is considered plausible and has been studied by different research groups.

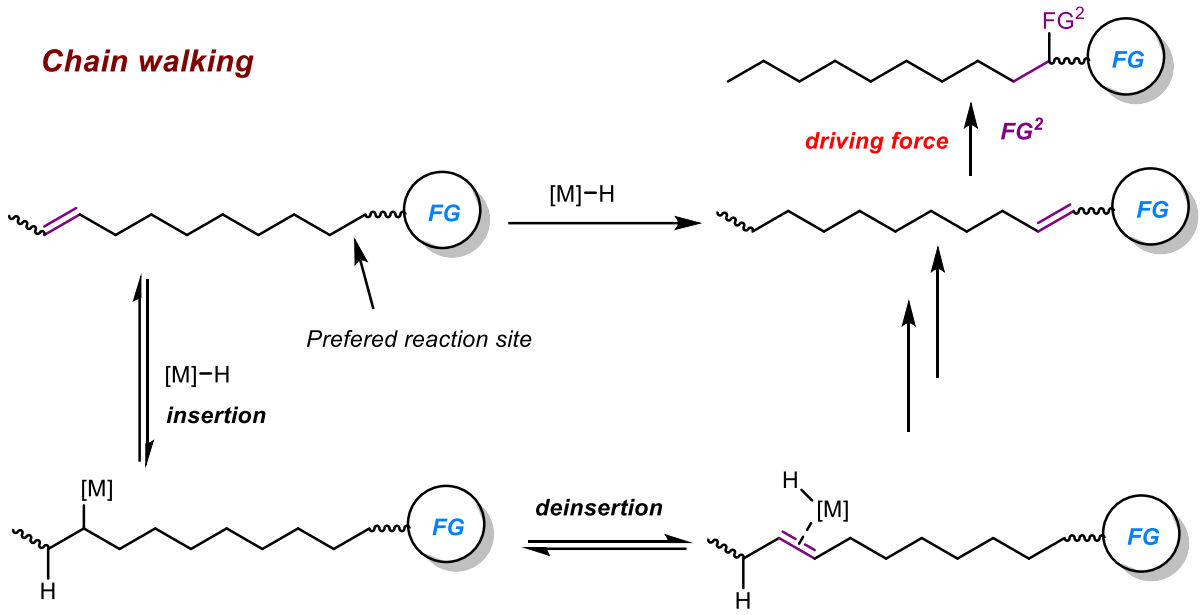

Scheme 1.34 The concept of 'chain walking'

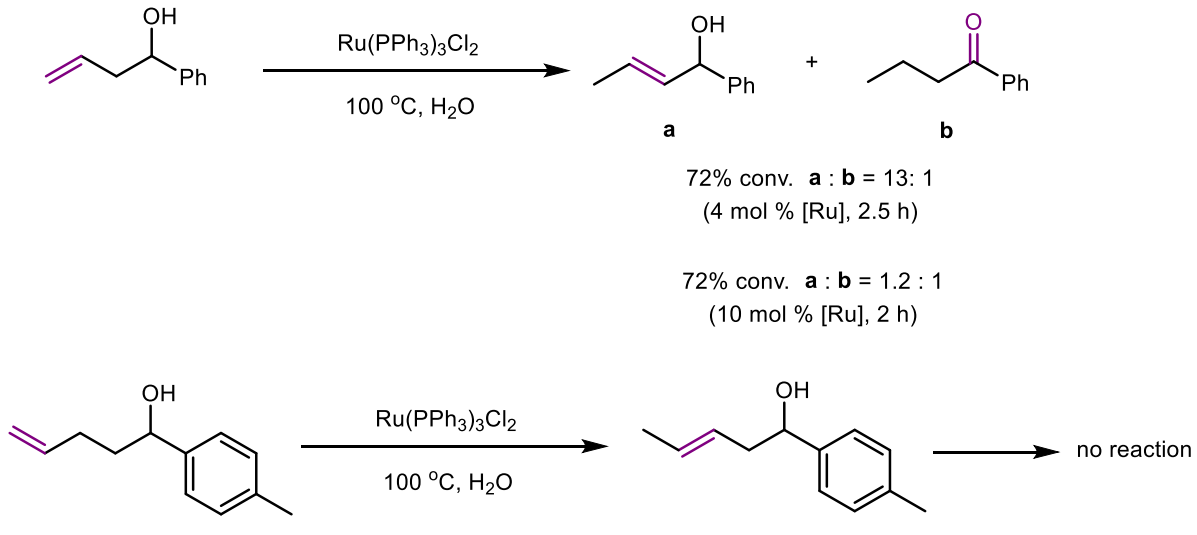

Scheme 1.35 Ruthenium-catalyzed isomerization of homoallylic alcohols

In 1998, it was discovered by our group that a ruthenium phosphine complex can convert homoallylic alcohols into carbonyls.[71] In the same study, however, it was also found out that the efficiency of isomerization into the carbonyl is comparatively low. Most of the substrates stopped at the first isomerization from the homoallylic alcohol to the allylic alcohol, which might be attributed to the efficiency of insertion/de-insertion of the Ru–H to C=C double bonds. Also,

regarding the ruthenium-catalyzed isomerization of allylic alcohols, the 1,4-hydride insertion mechanism leads to a comparatively low efficiency for *C3*-substituted allylic alcohol. In the presence of longer-chained alkenyl alcohols, the efficiency of isomerization can be further reduced. With the increase in catalyst loading, however, the efficiency of isomerization to the carbonyl improves significantly.

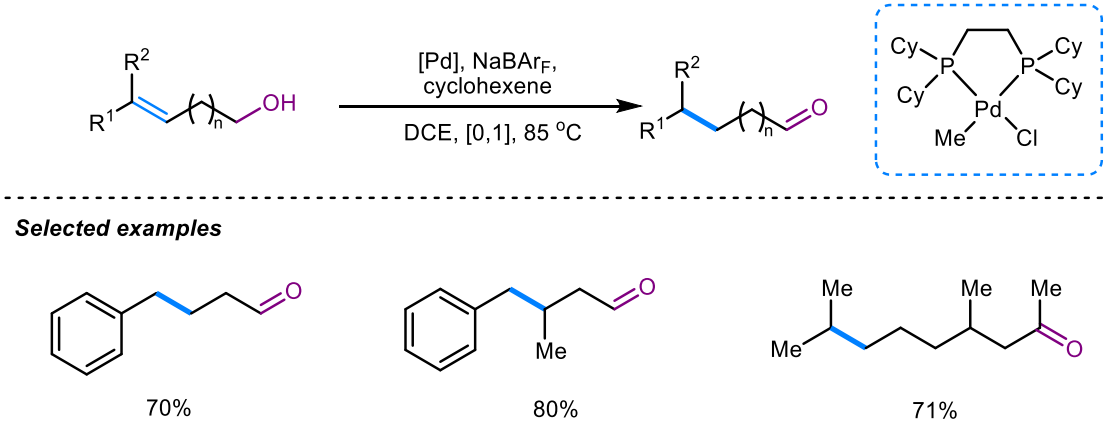

Scheme 1.36 Palladium-catalyzed isomerization of olefinic alcohols

In comparison with ruthenium, palladium catalysts tend to show higher efficiency in the chain walking process. Thus, a much higher efficiency can be achieved for the palladium-catalyzed isomerization of homoallylic alcohols and longer olefinic alcohols. In 2014, Mazet achieved the efficient isomerization of various long-chain olefinic alcohols to corresponding carbonyls using a Pd–H catalyst.[83] Under the same reaction conditions as in the isomerization of allylic alcohols, the carbonyl products were obtained at almost the same efficiency even for some bulky and complex substrates.

In some cases, the isomerization of homoallylic alcohols or bishomoallylic alcohols to carbonyls could be completed through a one-step hydrogen transfer instead of chain walking. With regard to the ruthenium-catalyzed allylic alcohol isomerization as initially discussed, the transformation from allylic alcohol to the carbonyl undergoes the dehydrogenation of alcohol first and then the hydride insertion to the double bond, which circumvents the step of 'olefin isomerization.' For homoallylic alcohols or even bishomoallylic alcohols, such an alcohol dehydrogenation/hydride insertion could also occur efficiently if conformation allows. For instance, Zhao *et al.* Found out in 2018 that the enantioselective isomerization to carbonyls could be completed *via* the previously

discussed mechanism under the catalysis of Rh for *C3*-substituted homoallylic alcohols (Scheme 1.37). Furthermore, the reaction shows tolerance to a wide range of secondary homoallylic alcohols. It is clearly showed in this study that the whole reaction undergoes only the hydride delivery from α-position to δ-position without the isomerization of olefins. In addition, it is also indicated that bishomoallylic alcohol could also be enantioselectively isomerized to carbonyl but requires the olefin isomerization to homoallylic alcohol. Then, hydrogen transfer occurs to generate carbonyl.[104]

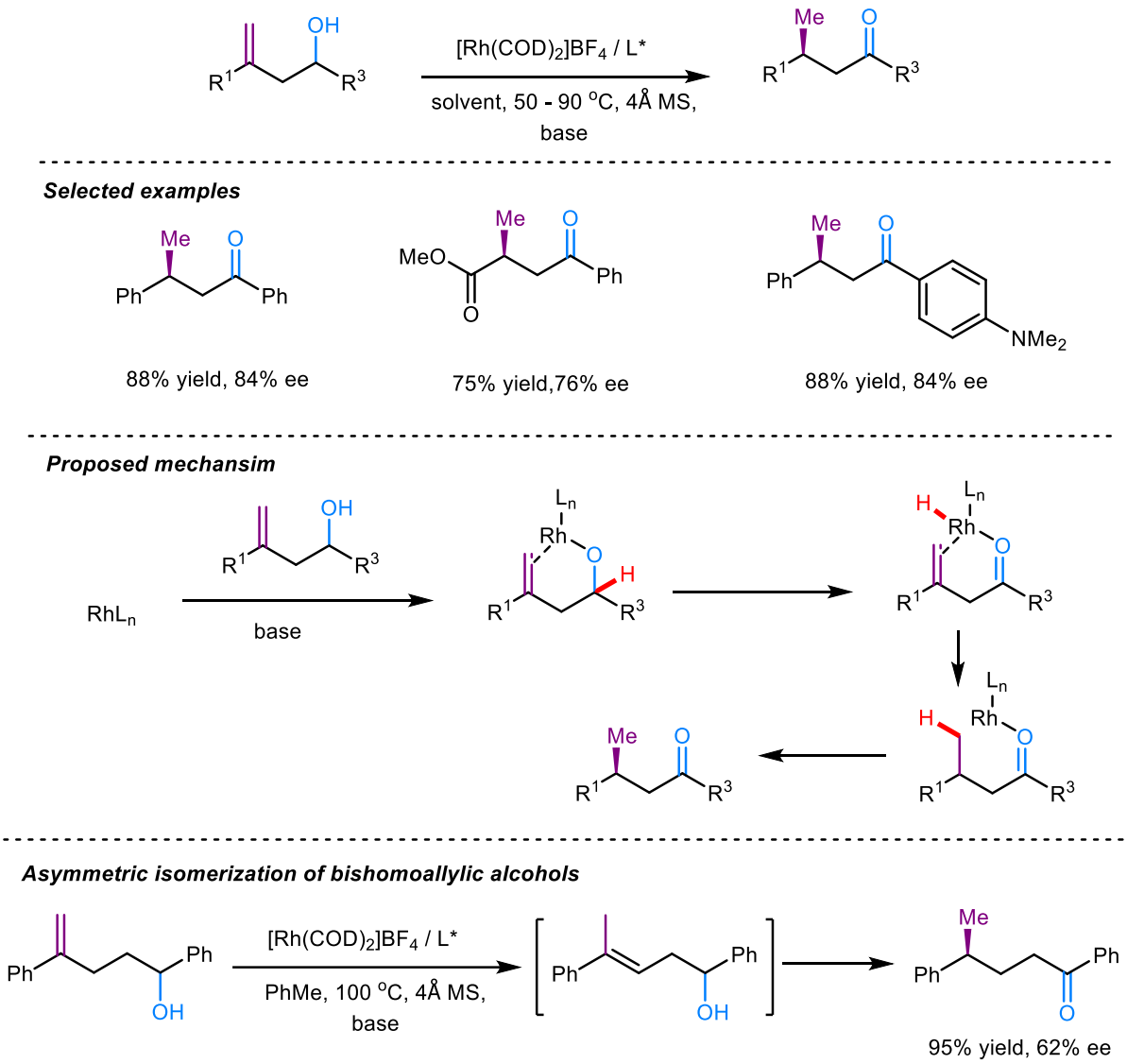

Scheme 1.37 Rhodium-catalyzed asymmetric isomerization of homoallylic and bishomoallylic alcohols

1.4 Hydrogen-transfer-mediated C–Het bond formation from alcohols

C–Het bond construction plays a crucial role in organic chemistry because it is the most common and direct way to introduce new functional groups. On the one hand, in classic organic reactions, nucleophilic addition to carbonyl is one of the most significant methods of introducing C–Het bond.[105] On the other hand, various alcohols could be transformed to carbonyls *via* hydrogen-transfer process under the catalysis of transition metals. Inspired by these facts, various C–Het bond formation reaction directly from alcohols *via* carbonyl intermediates was developed. In this section, we will discuss those C–Het bond formations from alcohols mediated by hydrogen transfers.

1.4.1 Redox amination of alcohols

Nitrogen is widely present in natural products and other biologically relevant compounds. Plenty of vital biological molecules contains nitrogen-based functional groups such as amino acids, nucleosides, and ureas. Thus, C–N bond formation is one of the most studied areas in organic methodology. Reductive amination of carbonyl is one of the most efficient ways to introduce C–N bond, especially for the generation of primary or secondary amines where carbonyl will first condense with an amine or ammonia to generate imine, followed by the reduction of imine to amines by additional reducing reagents.[105–108] According to this process, we could consider that if we make the alcohol dehydrogenation and reductive amination in one pot, no additional reductant would be needed because the alcohol itself could serve as a reductant *via* hydrogen transfer to make the whole process occur in a redox-neutral pathway (Scheme 1.38). Because such a process experiences a dehydrogenation of alcohol at the first step and a hydrogenation at the second step, we also call this process a 'borrowing hydrogen' process.[109, 110]

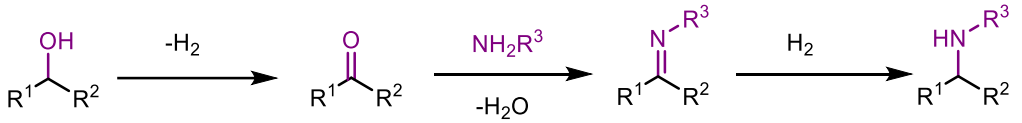

Scheme 1.38 General process of redox amination of alcohols

Redox amination was first discovered in 1932, when Ni served as the heterogeneous catalyst to assist hydrogen transfer.[111] Later, several catalysts were developed for redox amination, but most of them were heterogeneous catalysts. Besides heterogeneous catalysis, the first homogeneous

catalysis of alcohol amination was developed by Grigg *et al.* They took advantage of transition-metal catalysts (Ru, Rh, and Ir), previously developed for hydrogen transfer reactions, to successfully realize the redox amination of alcohols.[112] However, the reaction condition in their report was comparatively harsh, which required a reflux solvent and extremely long reaction time. Furthermore, only limited substrate examples were shown.

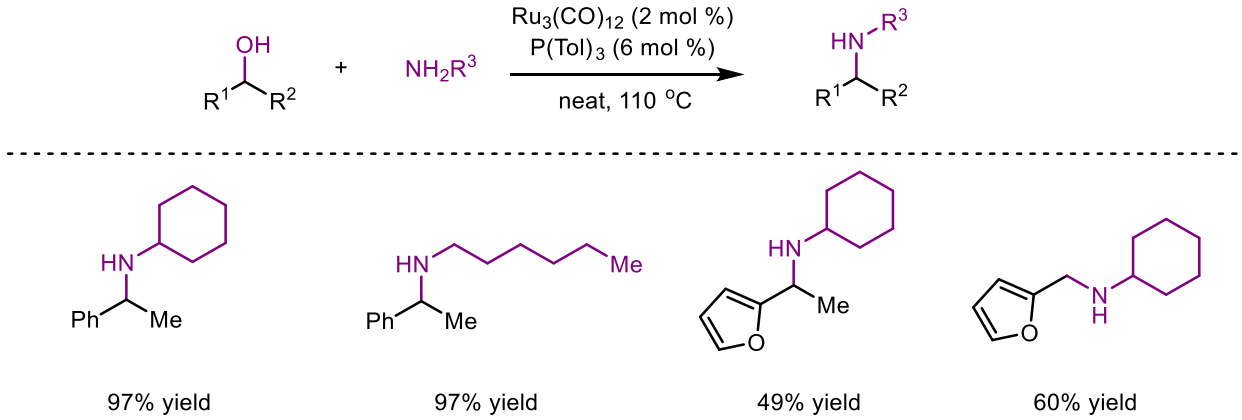

Scheme 1.39 $Ru_3(CO)_{12}$-catalyzed redox amination of alcohols

Later, several groups performed further modification of catalysts to increase the efficiency and expand the substrate scope of alcohol amination. For example, in 2006, Beller *et al.* found the combination of $Ru_3(CO)_3$ and phosphine ligands could effectively drive the redox amination of various alcohols (Scheme 1.39).[113] The reaction was conducted under neat condition with access amount of alcohols (5 times to amine substrates). Various primary alcohols and secondary alcohols were well suited. For the amine part, alkyl-substituted amines could be well tolerated. However, they did not test the reactivity of anilines.

One year later, Williams *et al.* used a more commercially available [Ru(*p*-cymene)Cl_2]$_2$ as a pre-catalyst to realize the redox amination of alcohols.[114] Compared with Beller's reaction system, other than the catalyst, the greatest improvement was the use of base and molecular thieves. Base accelerates the hydrogen-transfer process, and the molecular thieves drive the amine condensation by removing H_2O generated in this step. From the substrate scope, we can clearly see that both alkylamine and anilines could complete the redox amination efficiently. Besides this, some substrates with a heteroaromatic system could also achieve a moderate-to-high yield of desired products. Other than single alcohols, they also tried diols and found that a primary aniline could

undergo double-redox amination process with alcohols and successfully realize the cyclization to form piperidine.

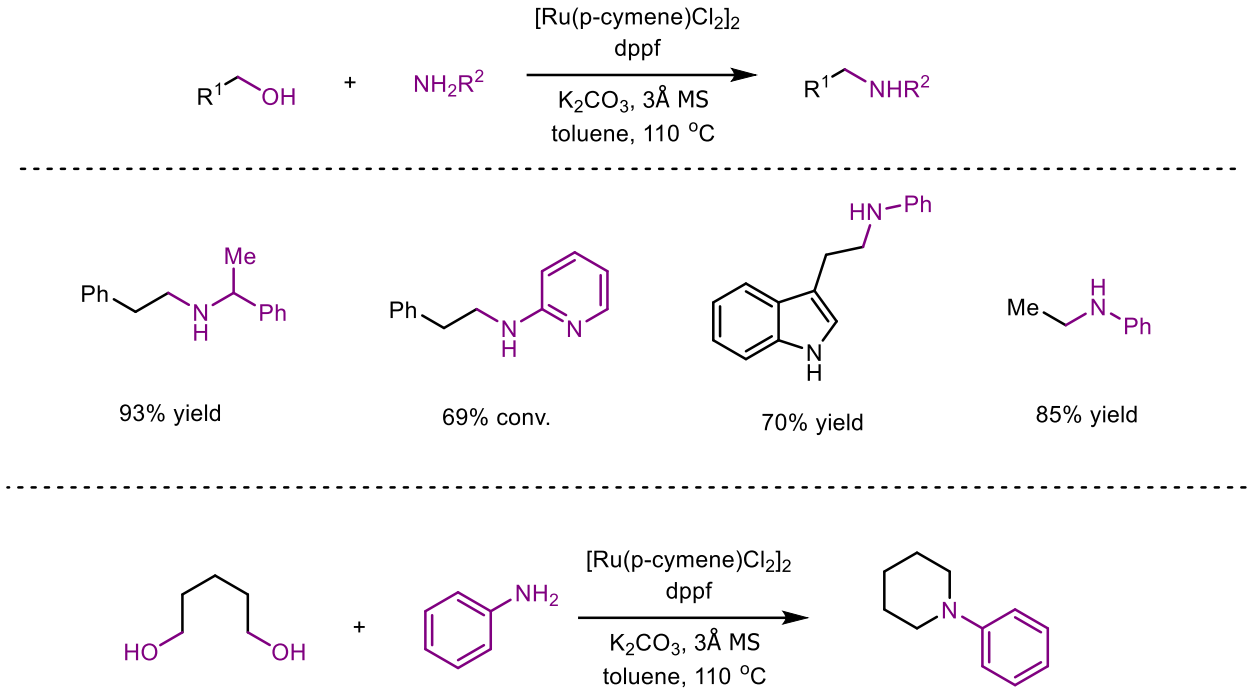

Scheme 1.40 Ru(II)-catalyzed redox amination of alcohols

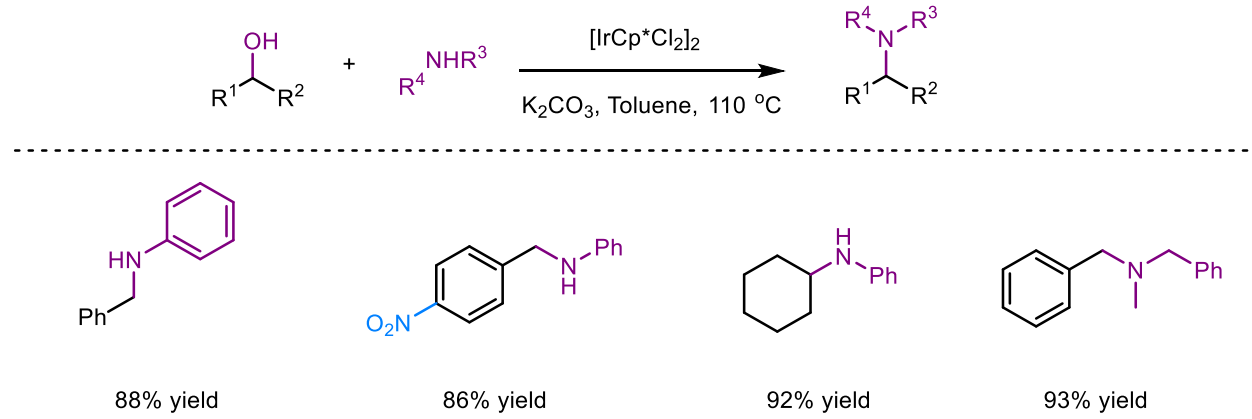

Scheme 1.41 Iridium–Cp*-catalyzed redox amination of alcohols

Other than ruthenium catalysts, iridium–Cp* complex is another potential homogeneous catalyst for alcohol redox amination. In 2003, Yamaguchi *et al.* used $[Cp^*IrCl_2]_2$ to enable the redox amination of various primary and secondary alcohols. Thanks to the stronger ability of hydrogen

transfer, iridium catalyst has a higher efficiency than its ruthenium counterpart in the redox amination process, where it has a much better functional group tolerance even to some sensitive functional groups such as nitro group. In addition, both primary and secondary amines and anilines could effectively complete the alkylation with alcohols.[115] Later, they also applied this catalytic system to complete the cyclization to *N*-cyclic ring with diols.[116]

In the homogeneous redox amination reactions, one of the largest challenges is the reaction with small molecules including the methylation of amines with methanol and amination of alcohols with ammonia, which were mostly developed as heterogeneous catalysis. As is known, both methylation reaction and primary amine generation are critical in the synthetic chemistry and pharmaceutical industries. Thus, developing homogeneous-catalyzed small molecule redox amination is highly desirable. The challenge of homogeneous catalysis in small molecules mainly lies in their uncontrollable reactivity and the difficulty of being trapped owing to their low boiling points. For instance, for the dehydrogenation of methanol, either methanol or formaldehyde (the dehydrogenation product of methanol) has an extremely low boiling point and can highly easily escape from the reaction systems, which largely limits its reaction efficiency. However, there are still several reports about the efficient methylation of amines with methanol. For example, in 2015, Seayad *et al.* developed a ruthenium-catalyzed *N*-methylation of amines. In this work, they used the methanol directly as a solvent, which solved the problem of insufficient methylation source. Under the ruthenium catalysts, various amines, anilines, and amides could be methylated. Notably, for the methylation of primary alkylamines, dimethylation would occur, whereas for anilines and amides, the methylation could be controlled at the mono-methylated product. Additionally, a competing experiment showed that by controlling the reaction temperature, the methylation would selectively occur on the amide side instead of anilines.[117]

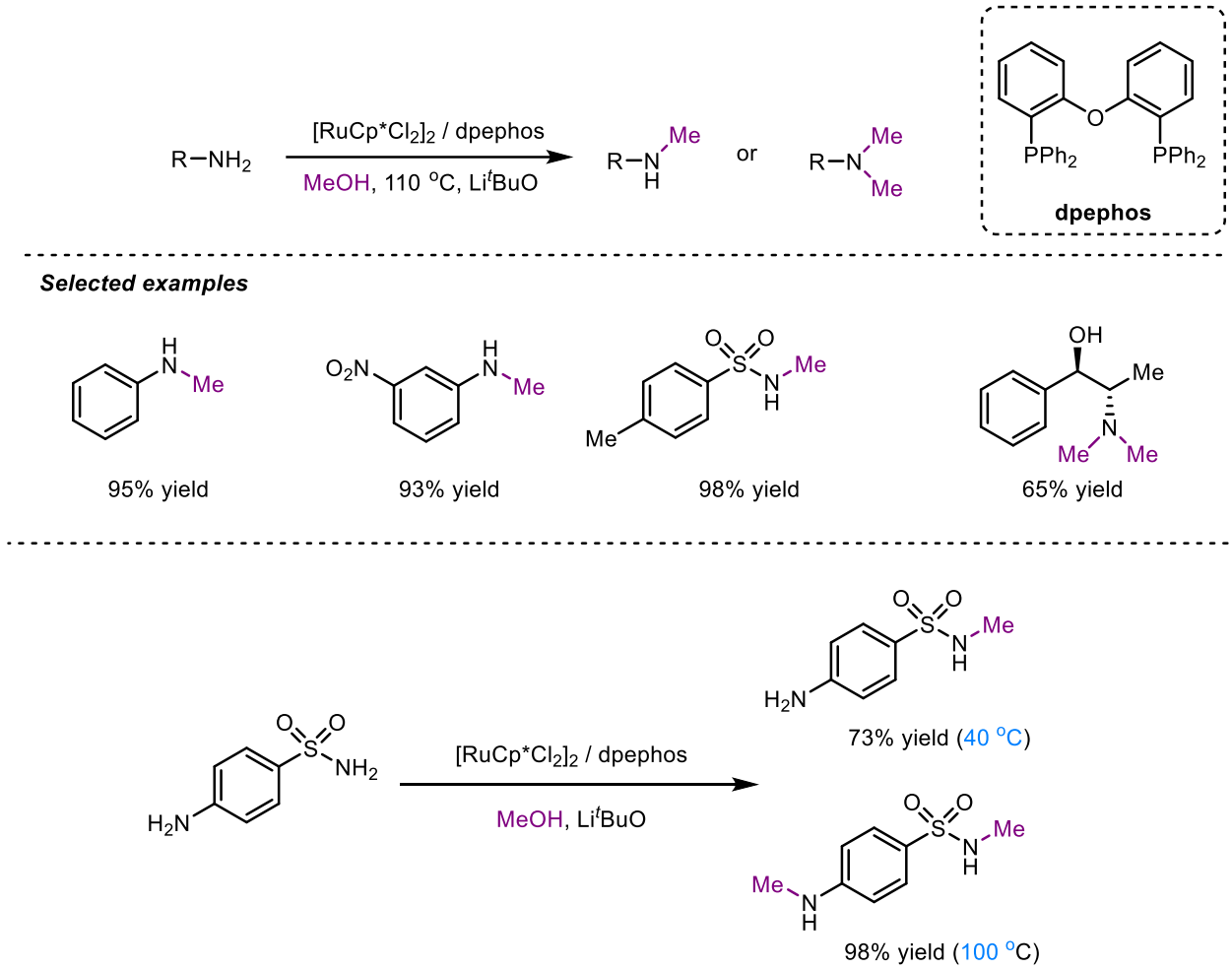

Scheme 1.42 Ruthenium-catalyzed methylation of amine with methanol

Apart from methylation of amines, the amination of alcohols with ammonia was another major challenge. There are two main challenges for this transformation: 1. Ammonia is in the gas phase at or above room temperature, meaning it could not be used as a solvent; 2. The primary amine generated has a stronger nucleophilicity to perform another alkylation with alcohols, so it struggles to stay at the primary amine level. In 2008, Milstein used Ru–PNP pincer complex to first realize the primary amine synthesis by redox amination of alcohol with ammonia.[118] In this work, they set up the reaction under high-pressure NH_3 atmosphere (7.5 atm). Although the reaction could be conducted under mild conditions and achieve a comparatively high efficiency, it has some unavoidable side reactions such as generation of imine from the condensation of primary amine product with the carbonyl compounds (from dehydrogenation of alcohols). In addition, under the Ru–PNP catalytic system, only primary alcohol could work efficiently.

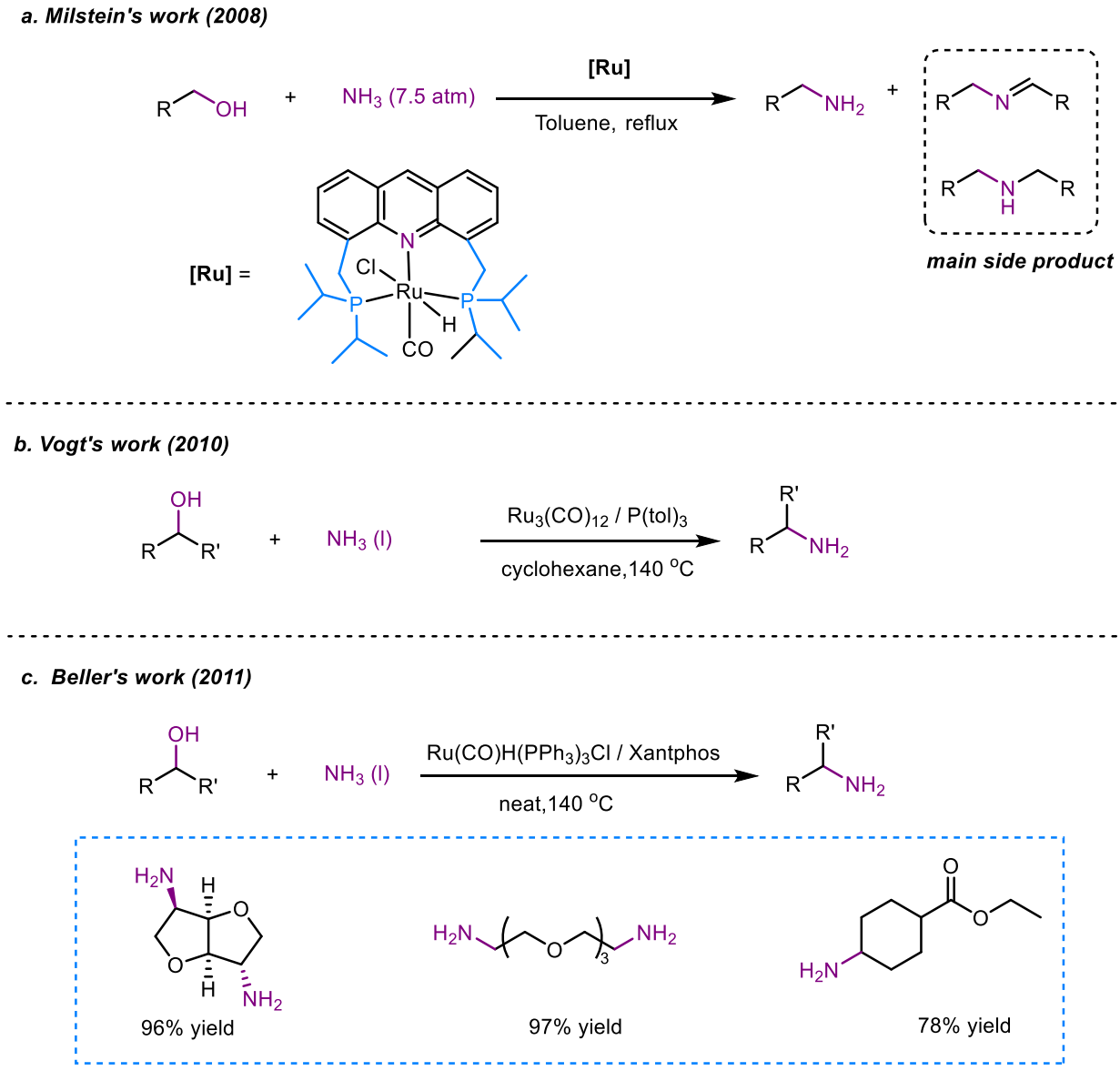

Scheme 1.43 Ruthenium-catalyzed amination of alcohols with ammonia

The amination of secondary alcohols was realized by Vogt *et al.*, taking advantage of Beller's $Ru_3(CO)_{12}$ system.[119] However, they still could not avoid the formation of secondary amines or imines as side products. In addition, only simple-structured alcohols were tested in that system. Later, Beller *et al.* found a more efficient $Ru(CO)H(PPh_3)_3Cl$ to enable some more complicated alcohols, including diols, to be aminated by ammonia with nearly quantitative yield.[120]

1.4.2 One-pot azine or hydrazone synthesis from alcohols

Other than amines, hydrazones and azines are another significant series of compounds in organic chemistry. The classic methods of hydrazone/azine synthesis are mainly focused on the direct condensation of hydrazine with carbonyls.[105] Thus, it is also plausible to synthesize hydrazones and azines, starting directly from alcohol *via* the transition metal-catalyzed hydrogen-transfer process. In 2013, the concept of hydrogen-transfer-mediated hydrazone formation from alcohol was put forward by our group by studying the reaction of iridium-catalyzed direct deoxygenation from alcohols.[121] The new strategy of alcohol deoxygenation is initiated from the dehydrogenation of alcohol to aldehyde followed by the condensation of aldehyde with hydrazine to give hydrazone. Finally, the hydrazone would conduct a Wolff–Kishner reduction with the assistance of base to generate alkane product. Overviewing the whole process, the reaction formally realizes the alcohol deoxygenation (Scheme 1.44). Later, in 2016, a ruthenium catalytic system was developed to make this process more efficient and tolerate a broader range of substrates.[122]

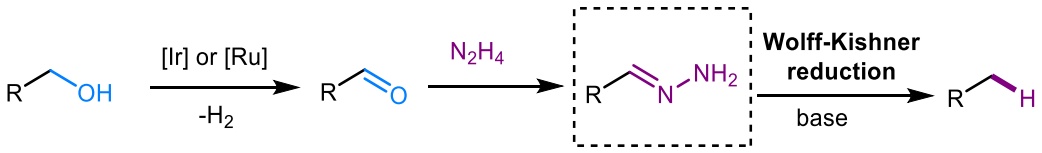

Scheme 1.44 Deoxygenation of alcohols through the hydrazone intermediate

Inspired by this concept, in 2016, Milstein *et al.* used a ruthenium–PNP complex to accomplish the one-pot synthesis of azines from alcohols.[123] The greatest challenge for this transformation is to prevent the hydrazone by-product and its ability to undergo Wolff–Kishner reduction. In their study, they applied excess amount of alcohols (3.5 equivalent to hydrazine) to guarantee sufficient aldehydes to condense with hydrazines. Moreover, in this transformation, only a catalytic amount of base could be used because an excess amount of base would possibly cause Wolff–Kishner reduction at the hydrazone level. The substrate test showed that only primary alcohols could be successfully condensed to azine, whereas benzyl alcohol derivatives worked better than the aliphatic alcohols.

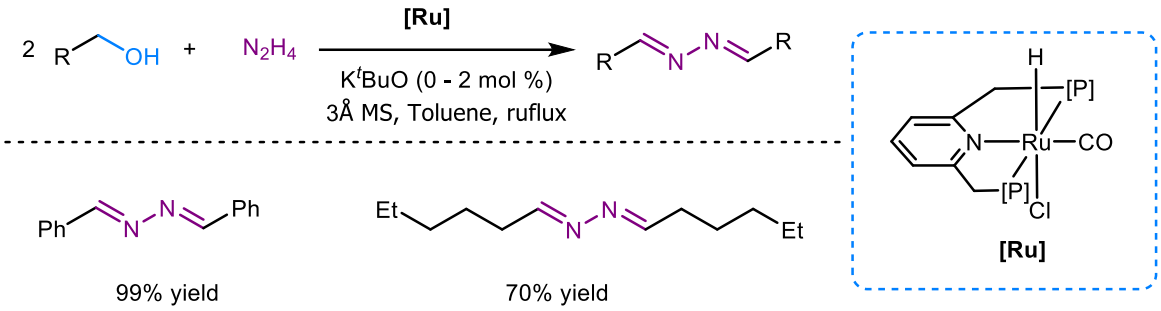

Scheme 1.45 Ruthenium-catalyzed azine formation from alcohols

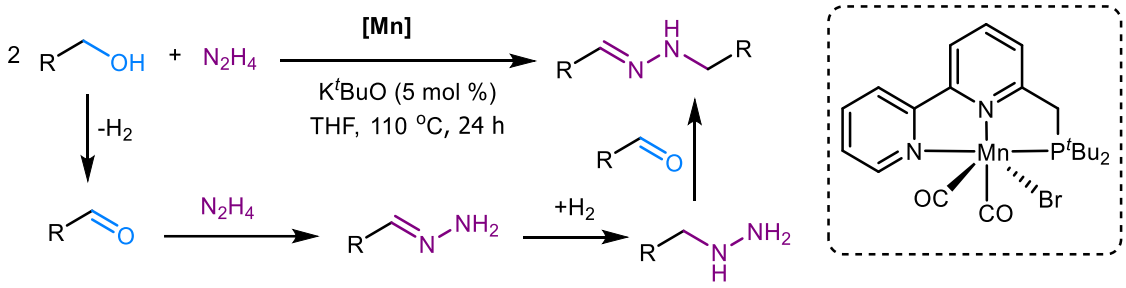

Scheme 1.46 Mn-catalyzed one-pot synthesis of alkyl-substituted hydrazone

Later, in 2018, they used a manganese–pincer complex to study the same transformation and found it reactive as well. However, there is one interesting difference from the ruthenium-catalyzed case. They discovered that under the Mn catalyst, after the first dehydrogenative condensation of alcohol to hydrazone, the M–H would hydrogenate back to the hydrazone to give alkyl-substituted hydrazine. Then, the alkyl hydrazine continuously condensed with another alcohol to give the alkyl-substituted hydrazone instead of azine.[124] This might be because of the stronger hydrogenation ability of Mn-complex to C=N double bond compared with ruthenium. Such a transformation provides a one-pot pathway to synthesize alkyl-substituted hydrazones. In contrast, in the classic synthesis, the alkyl-substituted hydrazines usually involve multiple steps.

1.4.3 Hydrogen-transfer-mediated C–B bond formation of alcohols

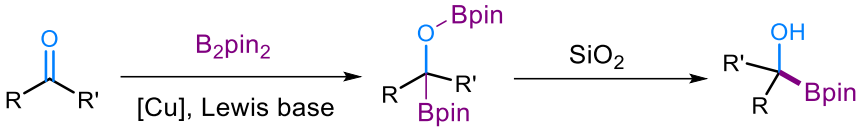

Scheme 1.47 C–B bond formation from carbonyl compounds

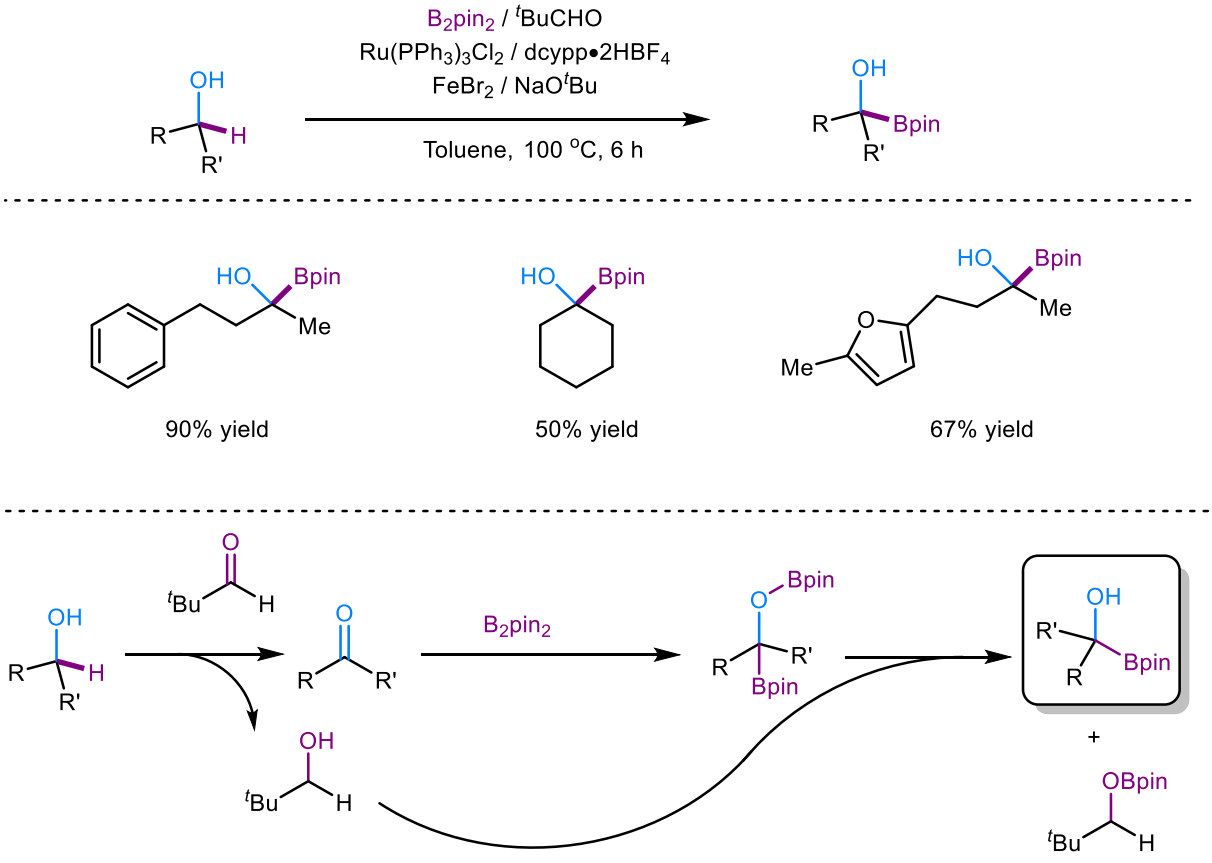

Scheme 1.48 Ruthenium-catalyzed direct C–B bond formation from alcohols

Other than C–N bond, there are also other C–X bond formation reactions from carbonyls. However, the applications of those reactions in C–X bond formation are quite limited. Thus, the study of other types of C–X bond formation from alcohol *via* hydrogen transfer is highly rare. Nonetheless, C–B bond formation is one of the examples. As we know, boron-containing compounds are quite useful in organic synthesis.[125] Thus, C–B bond formation is another highly popular topic in methodology. One of the methods of introducing C–B bond is the simultaneous addition of di-

boron reagent to carbonyls as shown in Scheme 1.47.[126] Such a process could efficiently generate *α*-hydroxyl boronic compounds.

Taking advantage of this transformation, alcohol was able to complete the C–B bond formation in one pot *via* hydrogen-transfer process. In 2019, Liu *et al.* developed a ruthenium-catalyzed direct C–B bond formation of alcohols to form synthetically useful *α*-hydroxyl boronic compounds. The reaction was initiated with the transfer dehydrogenation of alcohols to carbonyls and followed by diboration/hydrolysis to realize the *α*-borylation process. The design of such a transformation has several challenges such as 1) the proton/boron exchange on OH might block the dehydrogenation process; 2) the diboration might directly occur on the hydride acceptor instead of starting material; 3) *α*-hydroxyl–Bpin might further dehydrogenate to form unstable acylboron species. In regard to those challenges, Liu *et al.* chose the secondary alcohols as starting materials, which kinetically blocked the possible O–B formation during the reaction. At the same time, they chose a bulky ^{t}BuCHO as hydride acceptor, which would conduct diboration much slower than the ketones generated from secondary alcohols. Finally, the thus-formed tertiary boronic alcohol would not undergo dehydrogenation owing to the lack of *α*-hydrogen. Such a transformation could tolerate a broad range of secondary alcohols including the substrates with some heteroaromatic systems. Moreover, the *α*-boric alcohol would efficiently conduct further functionalization on both the OH and boron side because the introduction of C–B bond at *α*-position would largely activate the reactivity of the OH group.[127]

1.5 C–C bond formation *via* hydrogen transfer from substrates to products

C–C bond construction is fundamental in organic synthesis to build up a complex molecule from a simple and small one. Throughout the history of organic chemistry, the discovery of C–C bond formation has been a challenging and popular research area. As is known, carbonyl compound is a crucial component in several condensation reactions such as aldol reaction, Wittig reaction, and Knoevenagel condensation.[105] That said, alcohols struggle to complete C–C formation in classic organic transformation. Thus, empowering earth-abundant alcohols to complete various C–C bond formations is an ideal target for organic chemists. At this stage, hydrogen transfer strategy transpires to be the key step for realizing this meaningful goal. As per what we discussed in the alcohol amination reactions, the borrowing hydrogen process could also be well applied in the alcohol-involved C–C bond formations.[128] As shown in Scheme 1.49, alcohol first undergoes

dehydrogenation with the assistance of transition metal catalyst to form the corresponding carbonyls together with metal hydride. Next, the thus-formed carbonyl would condense with nucleophiles to generate an unsaturated bond, which is followed by the insertion of M–H species to complete the formation of new C–C bond. Such a transformation not only enables alcohol as starting material but also provides a series of novel C–C single-bond formation methods, which was hard to realize using classic methods. In the following part, we will discuss several symbolic examples of borrowing hydrogen in C–C bond formation from alcohols.

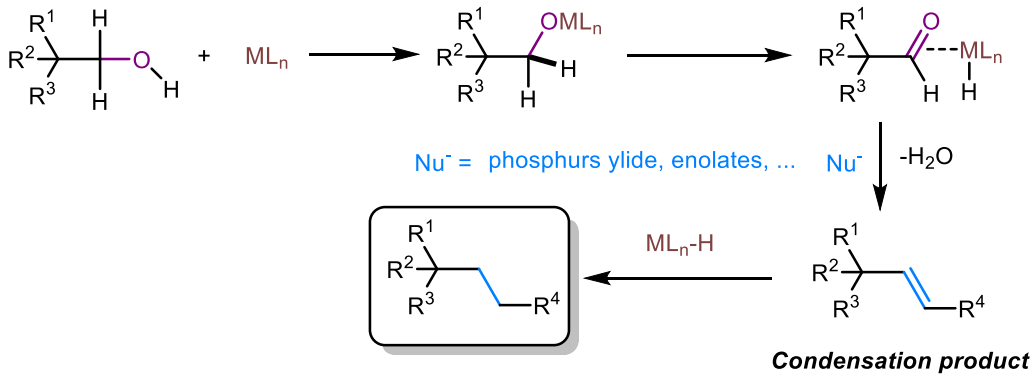

Scheme 1.49 C–C bond formation with alcohols *via* borrowing hydrogen

1.5.1 C–C bond formation of alcohols *via* aldol condensation

1.5.1.1 α-alkylation of ketones with alcohols

Aldol reaction is the earliest developed and one of the most used C–C bond formation methods.[105] The product of aldol reaction is *β*-hydroxyketone or *α*, *β*-unsaturated ketone (E1cB elimination product of *β*-hydroxyketone), whereas the latter product is a perfect hydride acceptor. Thus, aldol condensation is a perfect medium to complete saturated C–C bond formation of alcohol through the borrowing hydrogen process. With such a transformation, we can formally realize the *α*-alkylation of carbonyl compounds (Scheme 1.50).

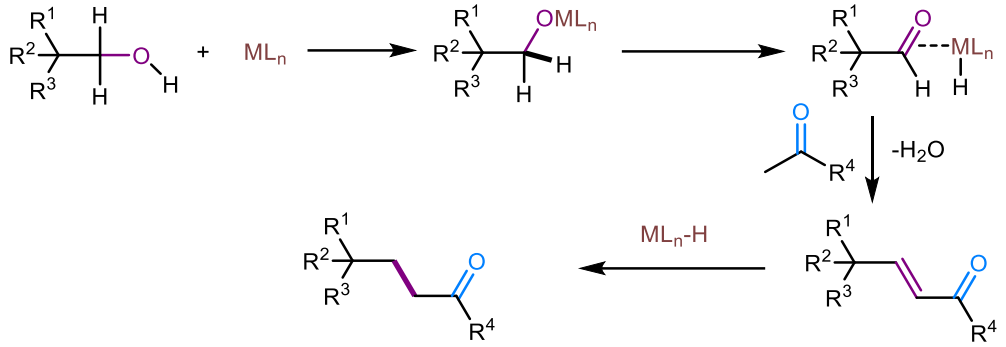

Scheme 1.50 Mechanism of C–C bond formation of alcohols *via* aldol condensation

Such an *α*-alkylation of ketone with alcohols was first discovered by accident in 2001 by Shim *et al. via* ruthenium catalysis when they were designing the reaction of direct transfer hydrogenation of ketones. However, owing to the requirement of excess amount of alcohol, the reaction would not stop at the alkylation of ketone but was followed up by another hydrogenation of the carbonyl to alcohols. Such an accidental discovery also raised the challenge of the borrowing-hydrogen aldol reaction with alcohols in that the direct hydrogen transfer between alcohols and ketones might be a potential side reaction. However, with the assistance of base, ketone would first form enolate, which accelerates the aldol condensation but deactivates the hydrogenation, and, in this case, the aldol condensation would be much faster than hydrogenation of ketone.[129]

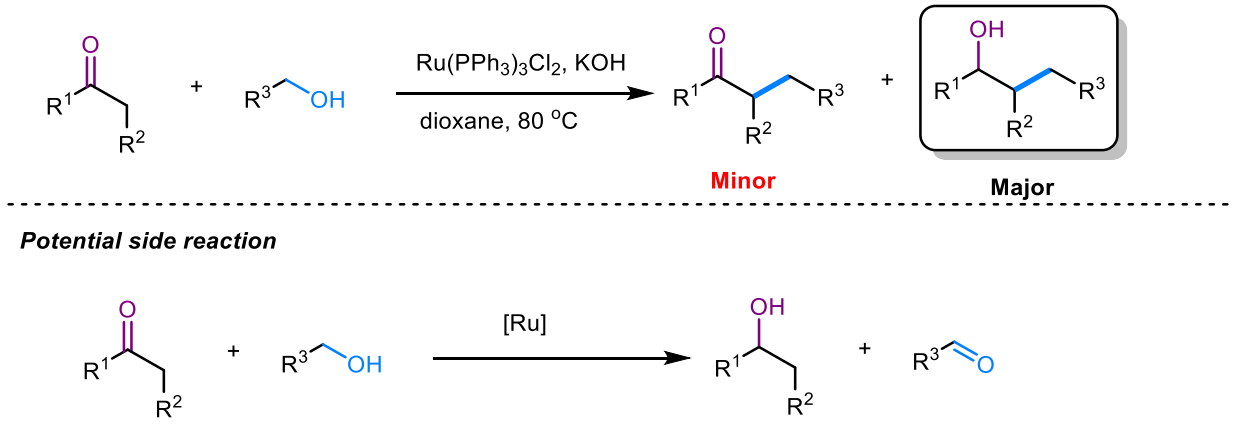

Scheme 1.51 Ruthenium-catalyzed reductive alkylation of ketones with alcohols

Taking advantage of this discovery, the same group later realized the redox-neutral *α*-alkylation of ketones with primary alcohols without the final hydrogenation of carbonyls. The adaptation

they performed in this case was to introduce 1-dodecene as a hydride acceptor and, at the same time, decrease the amount of alcohol from 3 equivalent to 1 equivalent. The reaction could achieve a good regioselectivity where the less-hindered side was preferred to be alkylated.[130]

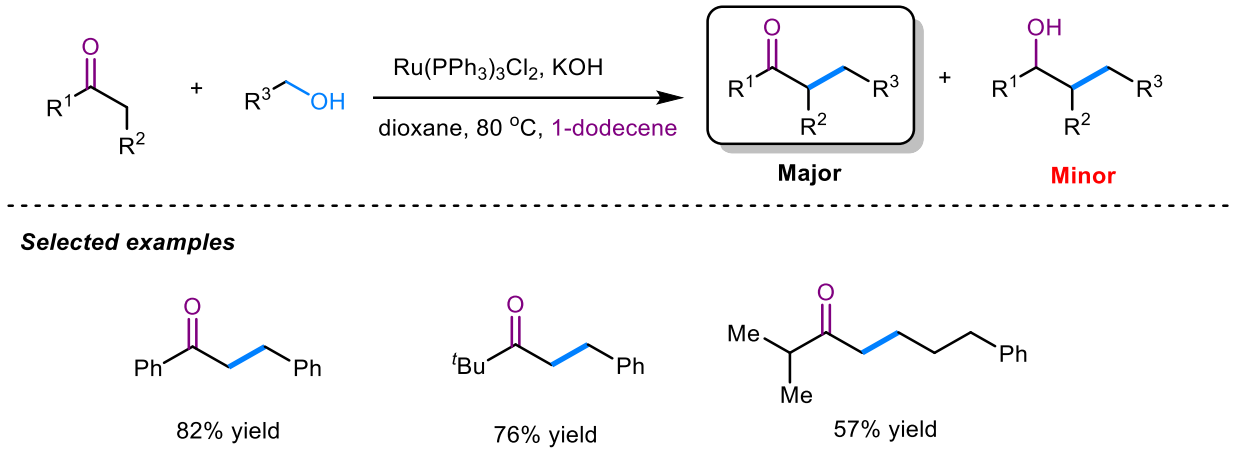

Scheme 1.52 The first case of alkylation of ketones with alcohols under ruthenium catalysis

Later, many further studies were conducted on this type of transformation. Moreover, even without the hydride acceptors, the product could be controlled at the ketone level (without hydrogenation) by limiting the amount of alcohols around 1 equivalent. In addition, other than the ruthenium catalysis, the hydrogen-transfer alkylation of ketone with alcohol could also be catalyzed by other transition metal catalysts including iridium, palladium, and rhodium.[131–134] Despite the adaptation of various catalysts, the alkylation reagent had thus far mostly been focused on primary alcohols, and the regioselectivity in different reaction systems was similar. In particular, with such a strategy of α-alkylation of ketones, the methanol was again considered as a methylation reagent for α-methylation of ketones. In 2014, Obora *et al.* successfully used iridium complex to realize the methylation of various ketones with methanol. Similar to the methylation of amine as we discussed previously, the methylation of ketone also used methanol as solvent to guarantee the sufficient methyl source. Different from other alkylations, the methylation could occur twice on methyl ketones and even complete the three-component reaction to realize the alkylation and methylation at the same time (Scheme 1.53). Another thing to be noted is that under the iridium catalyst, the over-hydrogenation of the ketone product would occur extremely rarely, even with the huge excess amount of methanol.[135]

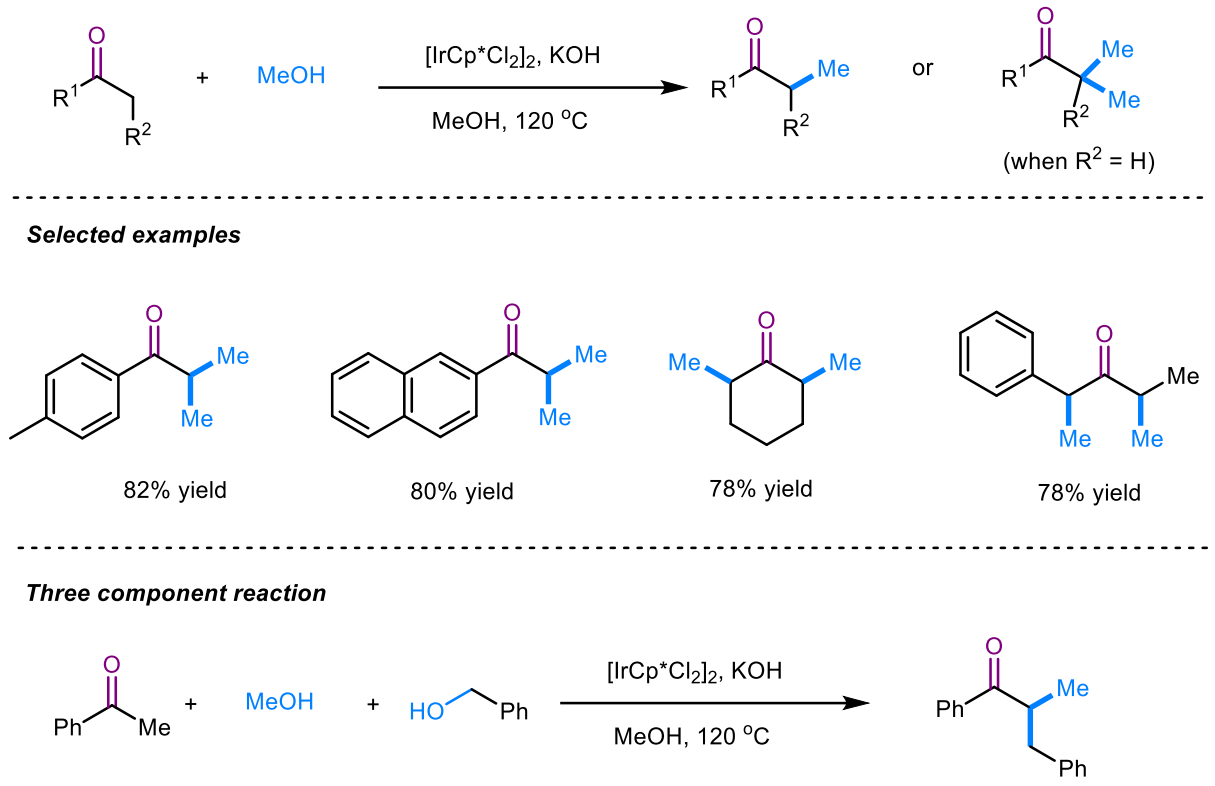

Scheme 1.53 Iridium-catalyzed methylation of ketones with methanol

α-alkylation of ketone with secondary alcohols was comparatively much less reported. The main barriers to the success of secondary alcohols in this transformation are 1) the possibility of self-condensation instead of cross C–C coupling; 2) the difficulty of controlling the selectivity. However, during recent years, the exploration of secondary alcohol for hydrogen-borrowing aldol reaction has become increasingly popular and has further extended its application potential in synthetic chemistry. For instance, in 2017, Donohoe *et al.* used iridium(III) complex to successfully realize the *α*-alkylation of ketone with various secondary alcohols.[136] During the exploration they discovered that if continuously using acetophenone as the model substrate (the most ideal substrate in *α*-alkylation of ketone with primary alcohols), the reaction would only give the desired product in an extremely low yield owing to the insufficient specificity of cross-condensation. As such, they modified the model substrate to a bulky aryl-substituted ketone to prevent its ability to self-condense, and, at the same time, to prevent the self-condensation of alcohol, they limited the catalyst loading to maintain the oxidation of alcohol to ketone at a low level. At this stage, a high yield of desired product was achieved (Scheme 1.54). Other than iridium catalysis, later on, several nonnoble metal catalysts were developed for *α*-alkylation of ketones

with secondary alcohols.[137, 138] Moreover, the asymmetric version of this transformation was also reported.[139]

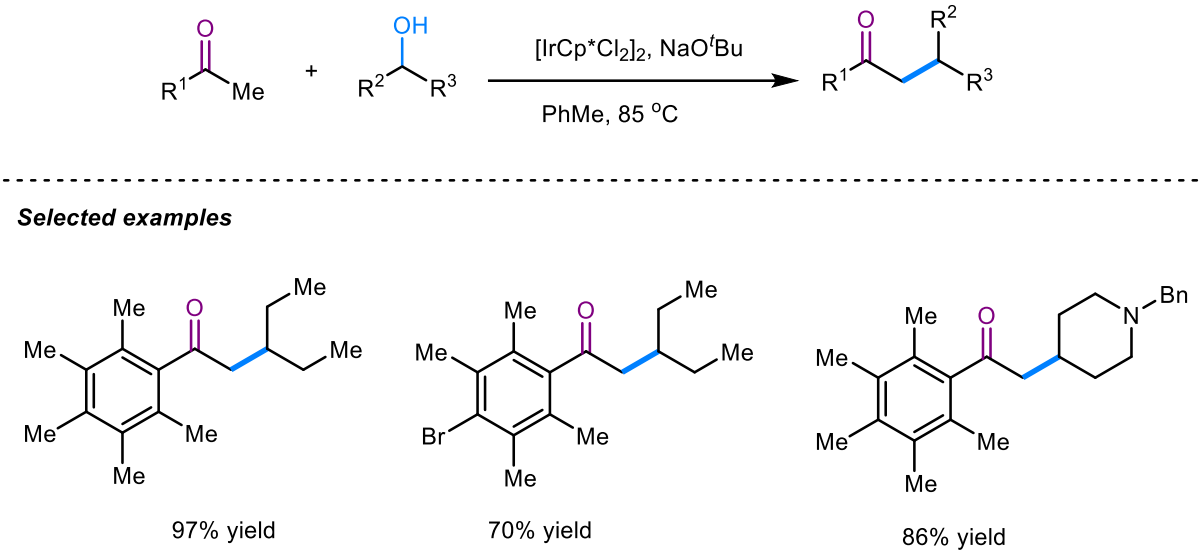

Scheme 1.54 *α*-alkylation of ketones with secondary alcohols

1.5.1.2 β-alkylation of secondary alcohol with primary (secondary) alcohol

The application of the borrowing-hydrogen strategy in aldol reaction could result in not only the *α*-alkylation of ketones but also the C–C bond formation between primary alcohol and secondary alcohol. In the reaction of *α*-alkylation of ketones, the hydrogen transfer only occurs between the electrophile and the product. However, in the C–C bond formation between two alcohols, both components experience a hydrogen transfer with the final product. Referring to the ketone alkylation reaction, it could be proposed that secondary alcohol in this case would serve as the nucleophile, while the primary alcohol serves as the electrophile (Scheme 1.55). Generally, the reaction is initiated by the dehydrogenation of both alcohols to generate ketone and aldehyde. Then, with the assistance of base, the ketone will form enolate to complete the aldol condensation with the aldehyde. Finally, the hydrogenation occurs on both C=C double bond and C=O double bond to give the final product, which formally realizes the *β*-alkylation of secondary alcohols.

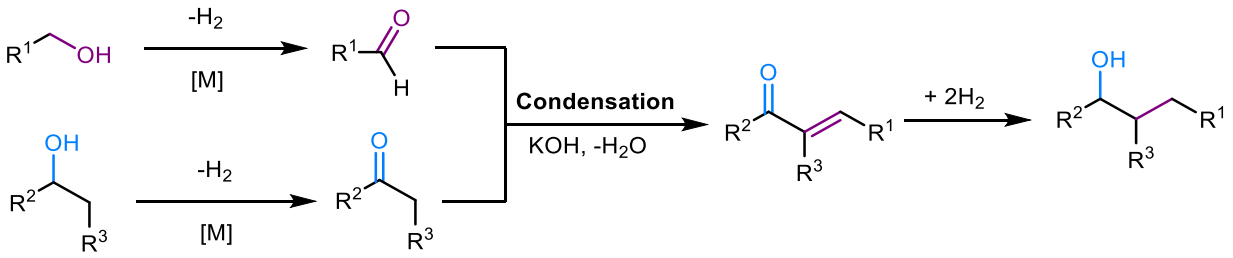

Scheme 1.55 General mechanism of C–C coupling between primary and secondary alcohols

The first discovery of such type of transformation was in 2003 by Shim with a ruthenium–phosphine system. Upon optimization of reaction conditions, they found that the additional hydride acceptor, 1-dodecene was still necessary to maintain the high efficiency, like what they did in the ketone alkylation.[130] The reaction was conducted in dioxane at 80 °C and could tolerate a broad range of primary and secondary alcohols. However, they did not conduct the study on substrates with some sensitive functional groups and even a heteroaromatic system.

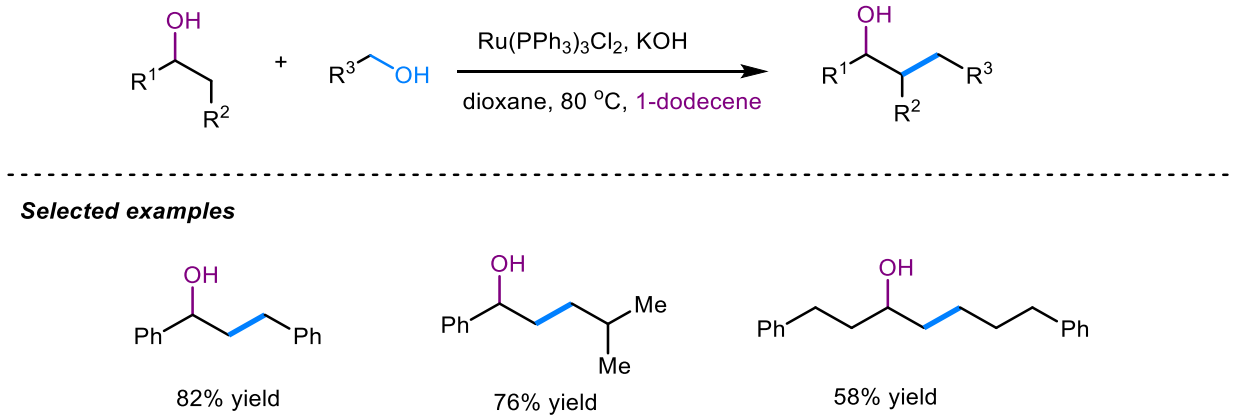

Scheme 1.56 The first case of *β*-alkylation of secondary alcohols with primary alcohols by Ru catalysis

Inspired by this work and referring to the ketone alkylation, different kinds of catalysts were also developed for this type of transformation, such as Ru,[140–142] Ir,[143, 144] Fe,[145] and Mn[146]. The key to the high efficiency of this type of transformation is the utilization of the reactivity difference of ketone and aldehyde in aldol condensation, where ketone is favored to form enolate to undertake a nucleophilic attack with aldehydes. Such a property restricts every single step of hydrogen-borrowing aldol condensation, causing it to occur sequentially. Taking advantage of this, the C–C

bond formation could even be extended to the reaction between two different secondary alcohols. In 2019, Gunanathan *et al.* successfully realized the efficient cross-coupling of two secondary alcohols under the catalysis of the Ru–MACHO catalyst. In their study, they chose a 1-aryl-1-ethanol and a complete aliphatic alcohol as two coupling partners. The reason for this choice was that the methyl–aryl ketone could more easily be used to form the enolate, which made it react specifically with the aliphatic ketones without self-condensation (Scheme 1.57).[147] Notably, in this reaction, the product was ketone instead of alcohol, which was different from the normal alcohol coupling *via* aldol condensation. This may be ascribed to the strong dehydrogenation ability of Ru–MACHO, which caused the hydride to be directly released as hydrogen gas instead of reducing the carbonyl back to alcohol.

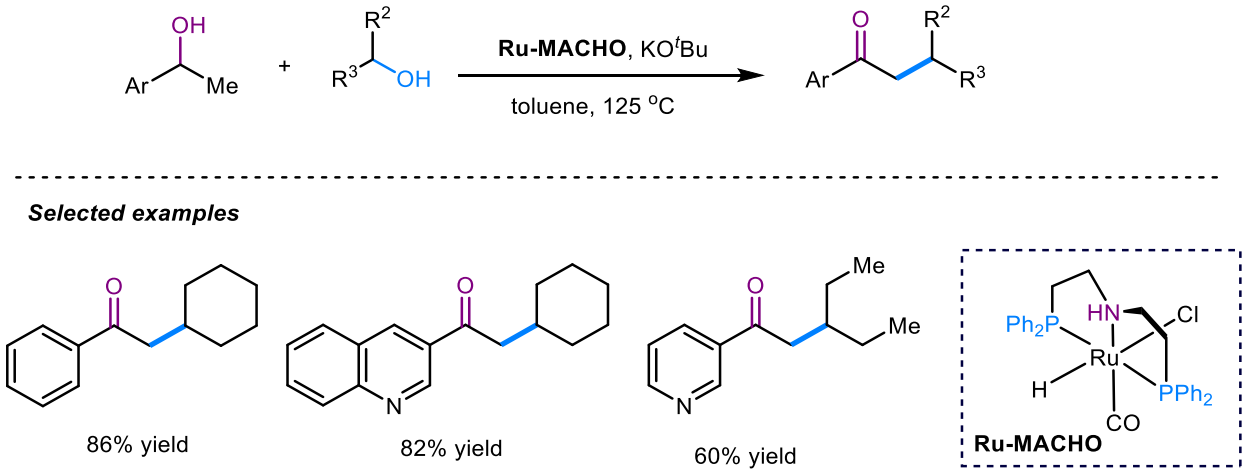

Scheme 1.57 Cross-coupling of secondary alcohols *via* hydrogen-transfer aldol condensation

1.5.2 C–C bond formation of alcohols *via* Knoevenagel condensation

The hydrogen transfer strategy applied in aldol reaction could also be extended to other Knoevenagel-type condensations[148] where alcohol serves as an alkylation reagent. As is known, alkylation of acidic C–H bond is one of the most common methods to introduce C–C bond. However, in the classic organic reactions, the alkylation of acidic C–H bond is always *via* the substitution of alkyl halides. As the concept of atom economy and green chemistry has received more and more attention, the development of organic reaction avoiding alkyl halides has become a research trend for organic chemists. The hydrogen-transfer-mediated Knoevenagel condensation perfectly enables alcohol as the alkylation reagent instead of alkyl halides with H_2O as the only

waste. Thus, this type of transformation has been studied by many research groups, especially during the 21st century. In this section, we will discuss some significant cases.

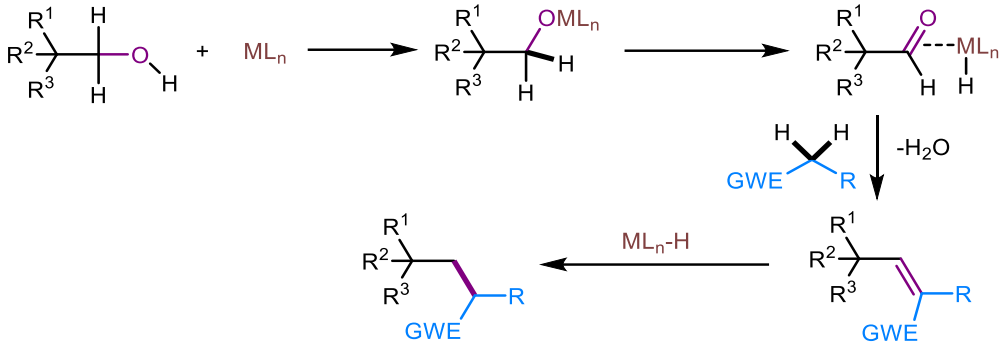

Scheme 1.58 C–C bond formation of alcohols *via* Knoevenagel condensation

1.5.2.1 α-alkylation of nitriles with alcohols

Nitrile is one of the classic substrates for Knoevenagel condensation, which contains protic C–H bonds at *α*-position. The alkylation of nitrile, meanwhile, is a crucial method of constructing C–C bond, especially for the synthesis of nitrogen-containing compounds.[105] Thus, enabling alcohol as an alkylation reagent for alkylation of nitrile is feasible and of great significance.

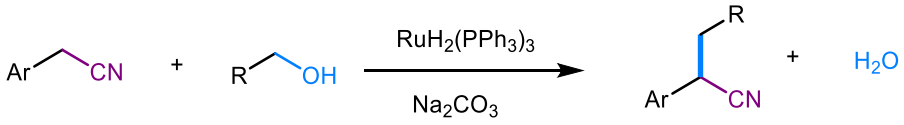

Scheme 1.59 *α*-alkylation of benzyl nitrile with alcohols

The first report on alkylation of nitrile by alcohol was in 1981 by Grigg *et al.*[149] In this work, they used benzyl nitrile as the substrate and screened different kinds of transition metal catalysts including Ru, Rh, and Ir. Among them, they found that Ru–H complex catalyzed this reaction with the highest efficiency. For the alcohols, they found various primary alcohols such as methanol, ethanol, and benzyl alcohol to be all effective. Furthermore, they found that, when introducing a chlorine atom at the *para*-position of the phenyl group on nitrile, it would largely accelerate the reaction process by increasing the acidity of ***α***-proton of nitrile. After this discovery, many other catalytic systems were developed for this type of transformation.[131, 150, 151] Among these works, the nitrile was mostly focused on the benzyl nitriles and its derivatives, and for the alcohols, both

primary and secondary alcohols could serve as efficient alkylation reagents. Such a facile strategy for nitrile alkylation also inspired many groups to consider its potential synthetic values. For instance, in 2011, Cossy *et al.* applied this transformation in an intramolecular reaction to successfully realize the construction of a six-membered ring (Scheme 1.60).[152]

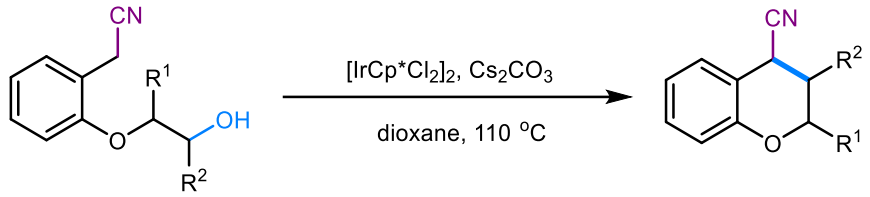

Scheme 1.60 Iridium-catalyzed intramolecular alkylation of benzyl nitrile with alcohol

In addition to benzyl nitrile, other types of nitriles, including ketonitrile, though limited, were also proved efficient for this type of transformation. As we know, the key to making the Knoevenagel condensation efficient is to activate the C–H bond by increasing its acidity. As for benzyl nitrile, the aromatic system would largely activate the adjacent C–H bond to make it more reactive. Similarly, in the ketonitrile, the carbonyl as a strong electron-withdrawing group adjacent to α–C–H bond would even activate it to a higher degree. In 2006, Williams *et al.* used ruthenium catalyst to successfully realize the alkylation of various β-ketonitriles with primary alcohols. The reaction had a broad substrate scope including some heteroaromatic substrates.[153]

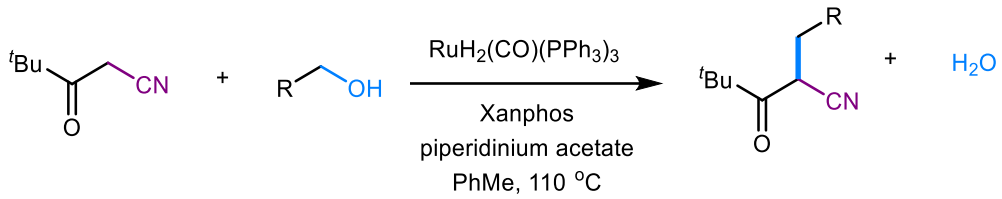

Scheme 1.61 Ruthenium-catalyzed alkylation of ketonitrile with alcohols

Other than activated nitrile compounds, the simplest acetonitrile was also proved effective for α-alkylation with alcohols by Cossy *et al.* in 2011, with the assistance of Ir catalysis (Scheme 1.62).[154] Because acetonitrile is comparatively less reactive than benzyl nitrile and ketonitriles in Knoevenagel condensation, the reaction condition for alkylation of acetonitrile was comparatively harsher than for the latter two. As we can see, 180 °C was required with the assistance of a

microwave in this case. Another highlight of this work is that the alkylation of nitrile could be controlled at the single alkylation level because the second alkylation would be much less reactive owing to both the electronic effect and the steric effect.

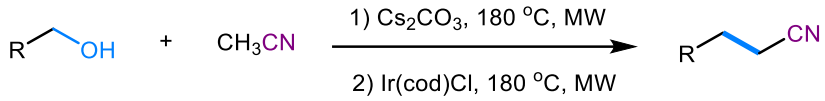

Scheme 1.62 Alkylation of acetonitrile with alcohols

1.5.2.2 α-alkylation of carboxylic acid derivatives with alcohols

Carboxylic acid derivatives are another series of compounds containing acidic C–H bond. Thus, they could also realize the *α*-alkylation with alcohols through the borrowing hydrogen–Knoevenagel condensation process (Scheme 1.63).

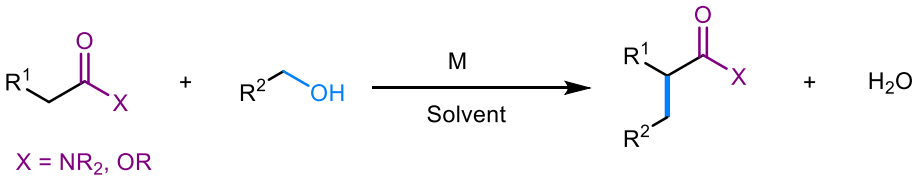

Scheme 1.63 *α*-alkylation of carboxylic acid derivatives with alcohols

Amide compounds are of great significance in both biological and pharmaceutical areas.[105] The alkylation of amide is of great synthetic value to build up amide-containing compounds. Previously, the alkylation of amides was limited to the substitution with alkyl halides *via* enolate process. However, there are two main disadvantages of using this method: 1) the use of alkyl halides would cause pollution and waste, which contravenes the spirit of the atom economy and green chemistry; 2) a strong base such as LDA or the even stronger BuLi should be used owing to the insufficient acidity of *α*-C–H of amides. Thus, developing the hydrogen-borrowing alkylation of amides is highly desirable.

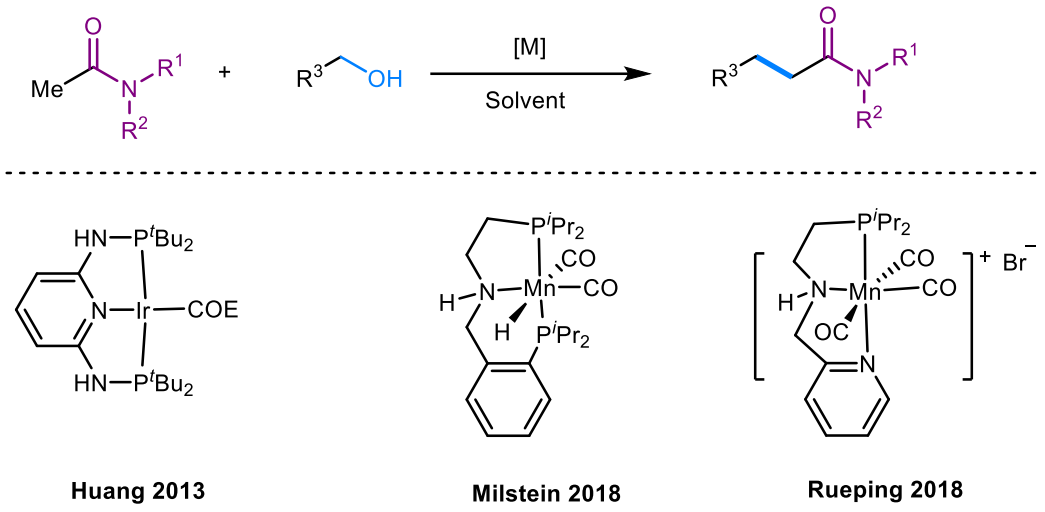

Scheme 1.64 *α*-alkylation of acetamides with alcohols

In 2013, Huang *et al.* developed an iridium-catalyzed *α*-alkylation of various acetamides. The reaction could tolerate both secondary and tertiary amides. For the alcohol part, both aryl- and alkyl-substituted primary alcohols could efficiently be alkylated on amides (Scheme 1.64).[155] Inspired by this work, the alkylation of acetamides was later reported by Rueping and Milstein with manganese catalysis.[156, 157]

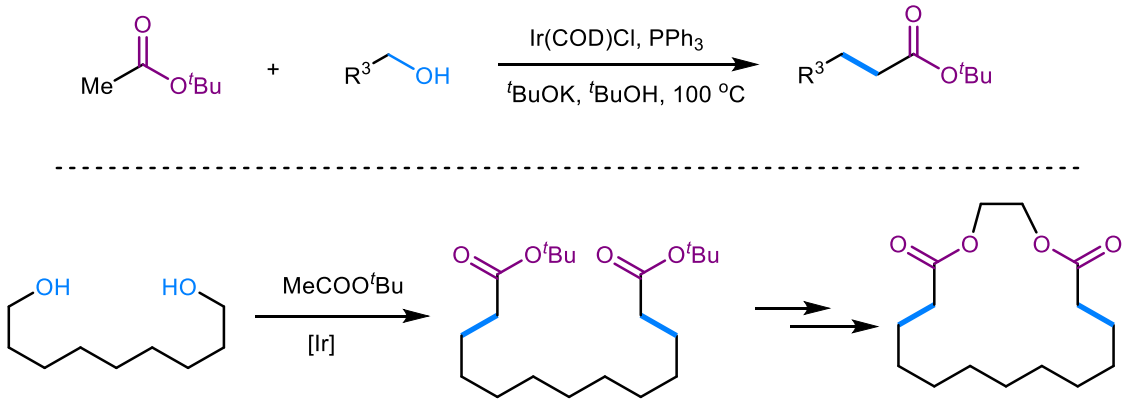

Scheme 1.65 *α*-alkylation of *tert*-butyl acetate with alcohols

Esters share similar properties as amides, making them even more reactive than amides in *α*-functionalization reactions. Thus, *α*-alkylation of esters with alcohols is also feasible. In 2010, Ishii *et al.* realized the *α*-alkylation of *tert*-butyl acetate with various primary alcohols with the catalysis

of iridium phosphine complex. The reaction experienced a similar process with the amide alkylation. Other than simple primary alcohols, the reaction could also occur efficiently with diols, for which they conducted double alkylation with two *tert*-butyl acetate molecules. Such a transformation could provide a crucial method of synthesizing a macrocyclic compound.[158]

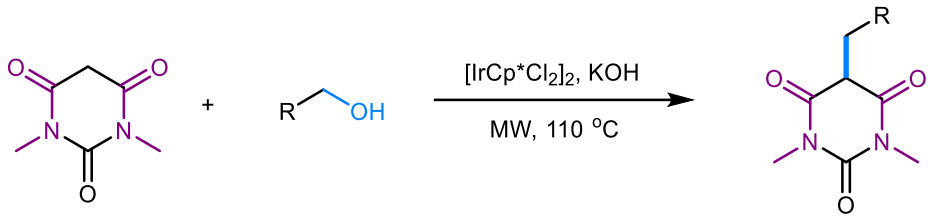

Scheme 1.66 Alkylation of barbituric acid with alcohols

Compared with simple esters or amides, 1,3-dicarbonyl compounds are principally more reactive in Knoevenagel condensation owing to the higher acidity of adjacent C–H bond, which is similar to the nitrile case we discussed in the previous section. The alkylation of barbituric acid is an example, which was developed by Grigg.[159] The reaction has high efficiency with benzyl alcohol and its derivatives as alkylation reagent. In addition, thanks to the high reactivity of barbituric acid, the reaction only took 10 min to complete with the assistance of a microwave.

1.5.2.3 Alkylation of o-methyl N-heteroaromatics with alcohols

Among the acidic proton containing compounds, *o*-Me-substituted *N*-heteroaromatic is a specific one. Owing to the strong electron-withdrawing ability of nitrogen atoms on *N*-heteroarenes, the C–H on the adjacent methyl group would have a comparatively strong acidity that is able to undergo Knoevenagel condensation. Thus, the alkylation of alcohol is also able to occur on *o*-Me-substituted *N*-heteroaromatics.

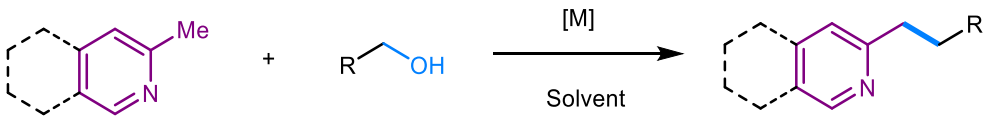

Scheme 1.67 Alkylation of *o*-methyl *N*-heteroaromatics with alcohols

In 2010, Kempe *et al.* reported an iridium-catalyzed alkylation of various methyl *N*-heteroaromatics with alcohols. The reaction worked efficiently with both benzyl alcohols and

aliphatic alcohols. Additionally, various monocyclic *N*-heteroaromatics were proved reactive, including some amine-substituted ones. Such a transformation provides great potential for certain biomolecule and drug molecule modifications because many of heteroaromatic structures could be found in biomolecules such as pyrimidines.[160]

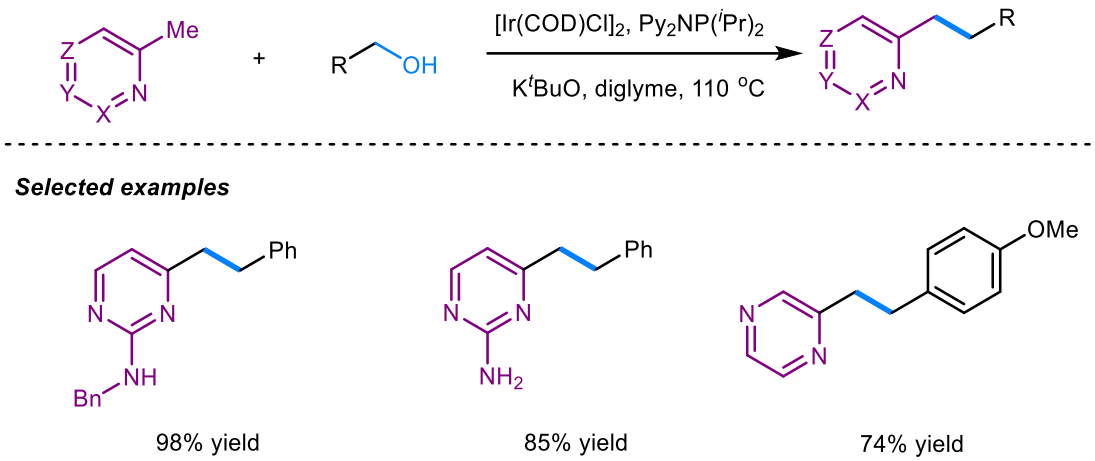

Scheme 1.68 Alkylation of methyl monocyclic *N*-heteroaromatics with alcohols

Other than the monocyclic *N*-heteroaromatics, methyl bicyclic *N*-heteroaromatics could also complete the same alkylation reaction. For instance, in 2012, Obora *et al.* developed another iridium catalytic system to successfully realize the alkylation of methyl quinoline with various primary alcohols.[161]

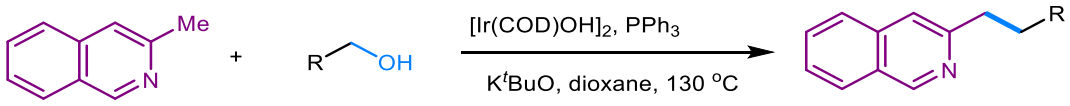

Scheme 1.69 Alkylation of 2-methyl-quinoline with alcohols

1.5.3 C–C bond formation of alcohols *via* Wittig reaction

Wittig reaction, known as one of the most famous olefination protocols, is another powerful method of constructing C–C bond. Its high efficiency, broad functional group tolerance, and mild reaction condition have even driven Wittig reaction to become one of the organic reactions winning *Nobel Prize*.[162] Combined with hydrogen transfer strategy, alcohols could indirectly participate in Wittig reaction as an aldehyde surrogate to form C–C bond and complete the alkylation of

phosphorus ylide, which is similar to the hydrogen-transfer-mediated aldol reaction and Knoevenagel reaction.

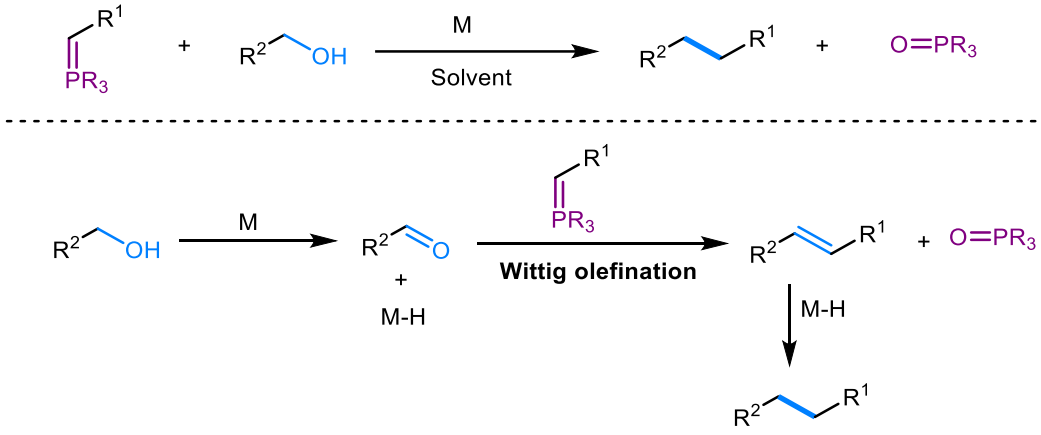

Scheme 1.70 C–C bond formation of alcohols *via* Wittig reaction

The hydrogen-transfer-cascaded Wittig reaction of alcohols was first developed by Williams *et al.* in 2002.[163] They initiated their study of this reaction by Horner–Wadsworth–Emmons (HWE) reaction with benzyl alcohol as a carbonyl surrogate. After testing different kinds of homogeneous and heterogeneous catalysts, they found the $[Ir(COD)Cl]_2$/dppp (diphenylphosphinopropane) system to be of the highest efficiency. However, even in this case, they found the reaction efficiency was still not high enough, with a significant amount of starting materials and unhydrogenated olefins left over. They explained this with the chelation of carbonyl and *β*-P=O bond on HWE reagent to deactivate the whole process. Based on this, they adapted the HWE reagent to the stabilized Wittig reagent and found the efficiency of reaction was largely increased. The electron-withdrawing groups on the ylide could be esters, amides, or cyano groups. For the alcohols, primary and secondary alcohols were both tested effective, and the former were with higher efficiency. However, it should be noted that only *α*-aryl-substituted alcohols were shown in the substrate scopes, perhaps because of their greater performance in the dehydrogenation process. In this study, they also examined the nonstabilized and semi-stabilized phosphorus ylides under the same catalytic system. However, the desired product was generated at an extremely low yield owing to the over-reactivity of ylides and the insufficient reactivity for the hydrogenation of unactivated olefins.

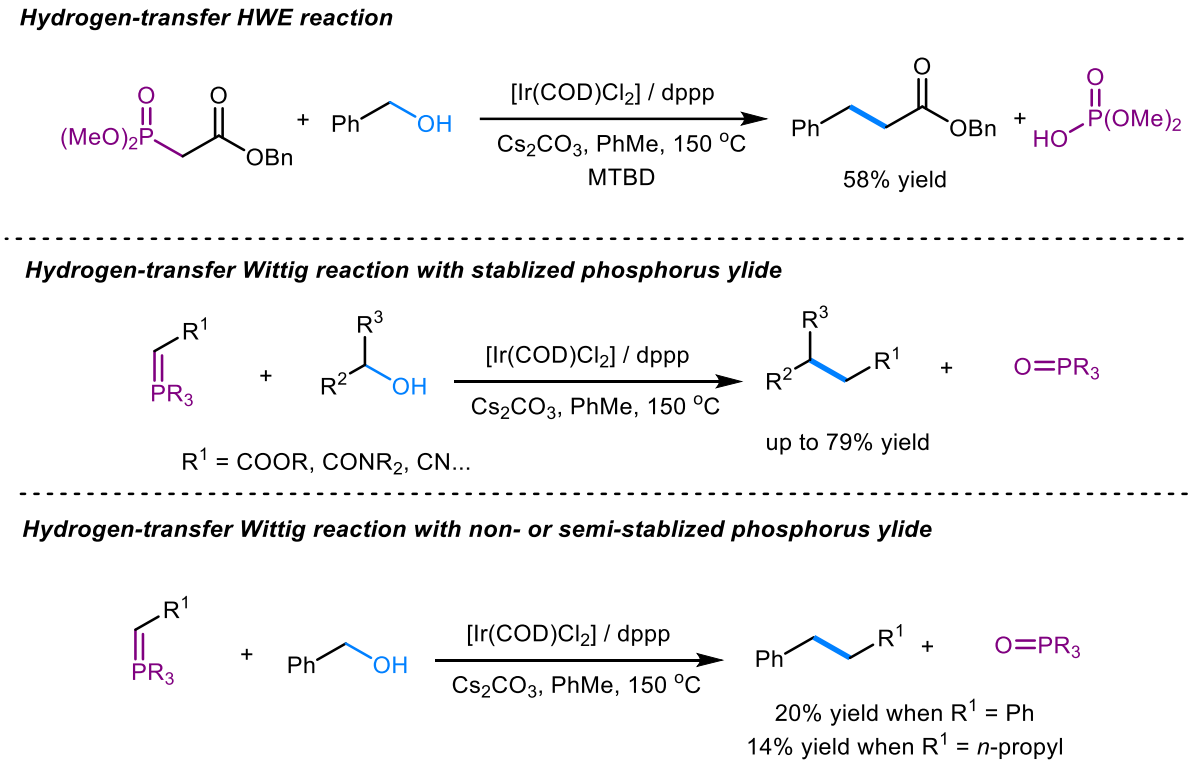

Scheme 1.71 Reactivity of different phosphorus ylides in hydrogen-transfer Wittig reaction with alcohols

Later in 2004, they found the Ru–NHC complex could also catalyze this transformation under a milder reaction condition and with a higher efficiency for convertion.[164] Other than ruthenium, this reaction was later proved to be efficient under non-noble metal catalysis. For instance, in 2021, Werner successfully utilized Mn–pincer complex, which is commonly used in hydrogen transfer reactions, to efficiently drive the hydrogen-transfer Wittig reaction with alcohols. Interestingly, in this work, when different Mn-catalysts were used, the results were different. According to their results, the Mn–PNP ligand would lead to the alkane product, while the Mn–PNN ligand would lead to the alkene product. This result was probably caused by the insufficient reactivity of Mn–PNN on hydrogenation.[165] However, such a trend was only for primary alcohols and primary ylides. For secondary alcohols and ylides, the selectivity was instead controlled by the amount of base (Scheme 1.72).

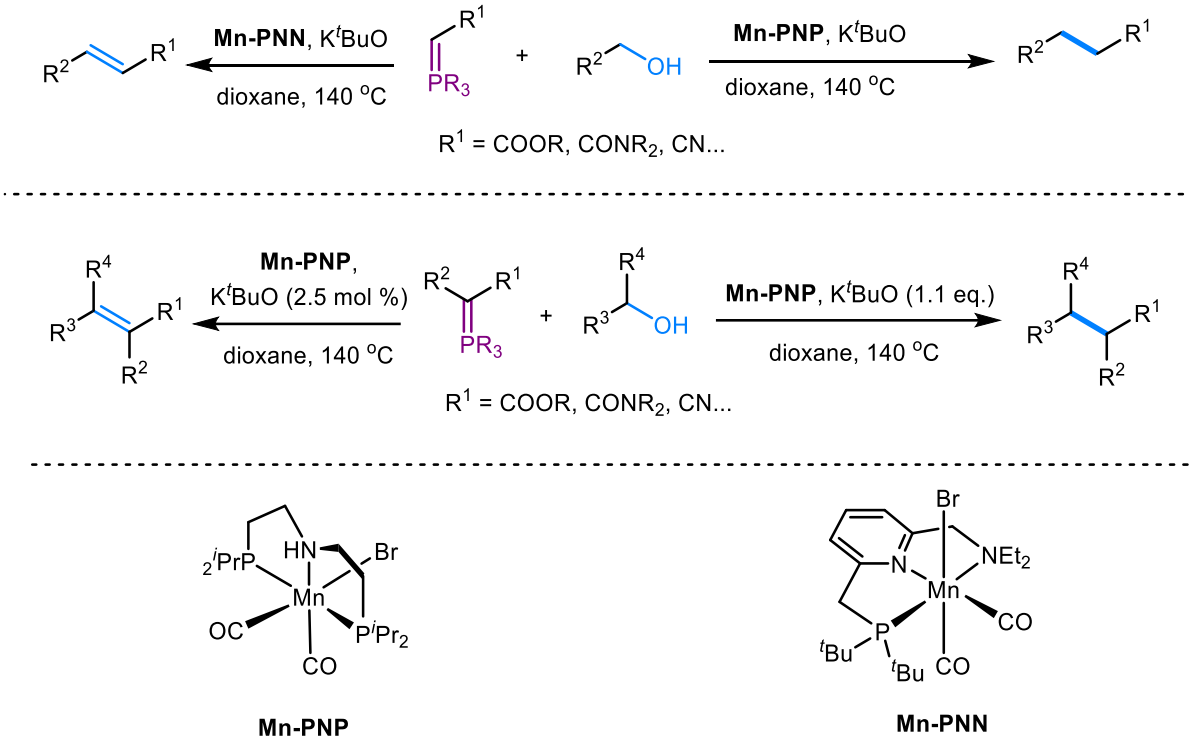

Scheme 1.72 Different selectivities of product controlled by catalyst in hydrogen-transfer Wittig reaction with alcohols

Apart from the catalyst modification, the extension of hydrogen-transfer Wittig reaction to nonstabilized or semi-stabilized ylides was another major challenge in this chemistry. As we discussed previously in Scheme 1.71, the challenges in nonstabilized ylides were mainly concluded as two points: 1). The over reactive ylide is easy to decompose, especially with the presence of alcohol; 2). The olefins after Wittig condensation would be unactivated alkenes, which require more effort to hydrogenate than their activated counterparts. Thus, the key to solving these two problems is to increase the efficiency of both dehydrogenation of alcohols and hydrogenation of alkenes. However, over the past 20 years, progress in this area has been somewhat limited. In 2009, Yus *et al.* used heterogeneous Ni catalyst to partially solve this challenge by enabling semi-stabilized ylide (phenyl-substituted ylide) to undergo hydrogen-transfer Wittig reaction with alcohols.[166] However, the product they obtained was alkene instead of alkane, indicating the final hydrogenation step could still not efficiently occur. Similarly, in 2015, Milstein used homogeneous ruthenium–pincer complex to attain the same results with a breakthrough of extending the scope of ylides from semi-stabilized to nonstabilized (Scheme 1.73).[167]

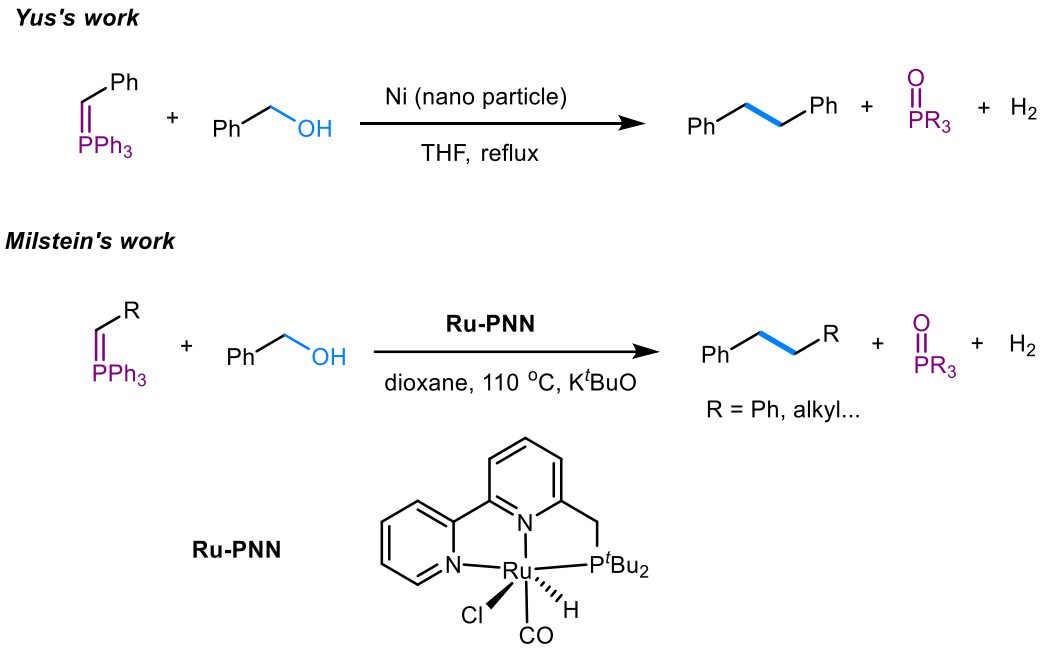

Scheme 1.73 Hydrogen-transfer Wittig reaction with semi- and nonstabilized ylides

1.5.4 Other type of C–C bond formation of alcohols *via* 'borrowing hydrogen' strategy

The main use of the 'borrowing hydrogen' strategy of enabling C–C bond formation of alcohol is to temporarily oxidize it to more reactive carbonyl and utilize the condensation of carbonyls with other carbon nucleophiles to generate C=C double bond, which is reduced back to a single bond. In these transformations, the C–C bond formation usually occurs directly on the C–O site. However, in some cases, the temporary dehydrogenation of alcohols to form carbonyls is only to borrow the strong electron-withdrawing ability of carbonyl instead of its own reactivity. In this case, after the reaction, the hydride would be added back to the carbonyl to return the original OH group to the substrates. This kind of example is comparatively rare and not as systematic as what we discussed in the previous part.

The most significant application of this strategy is the nucleophilic addition of allylic alcohols, which was reported in 2005 by Williams *et al.* As is known, allylic alcohol itself is not an especially good electrophile, especially on the alkene side. This is because the alkene in allylic alcohol is an unactivated alkene, which has a comparatively high electron density and is inactive in nucleophilic addition. However, with a dehydrogenation on the alcohol side, the electron-donating hydroxymethyl group would transpire to be an electron-withdrawing carbonyl group, which makes

the adjacent alkenes electron-deficient. In this case, the nucleophile would easily implement a Michael addition to the temporarily formed *α*, *β*-unsaturated ketone (aldehyde). Finally, the hydride would return to the carbonyl to give the original alcohol back, which would formally complete a nucleophilic addition of allylic alcohol on the alkene side. William *et al.* used this strategy to enable different kinds of stabilized nucleophiles to complete the addition reaction (Scheme 1.74). Notably, the catalyst they used in this reaction was main-group Lewis acid instead of transition metal catalyst. The adaptation here was to prevent the potential allylic alcohol isomerization by-product.[168]

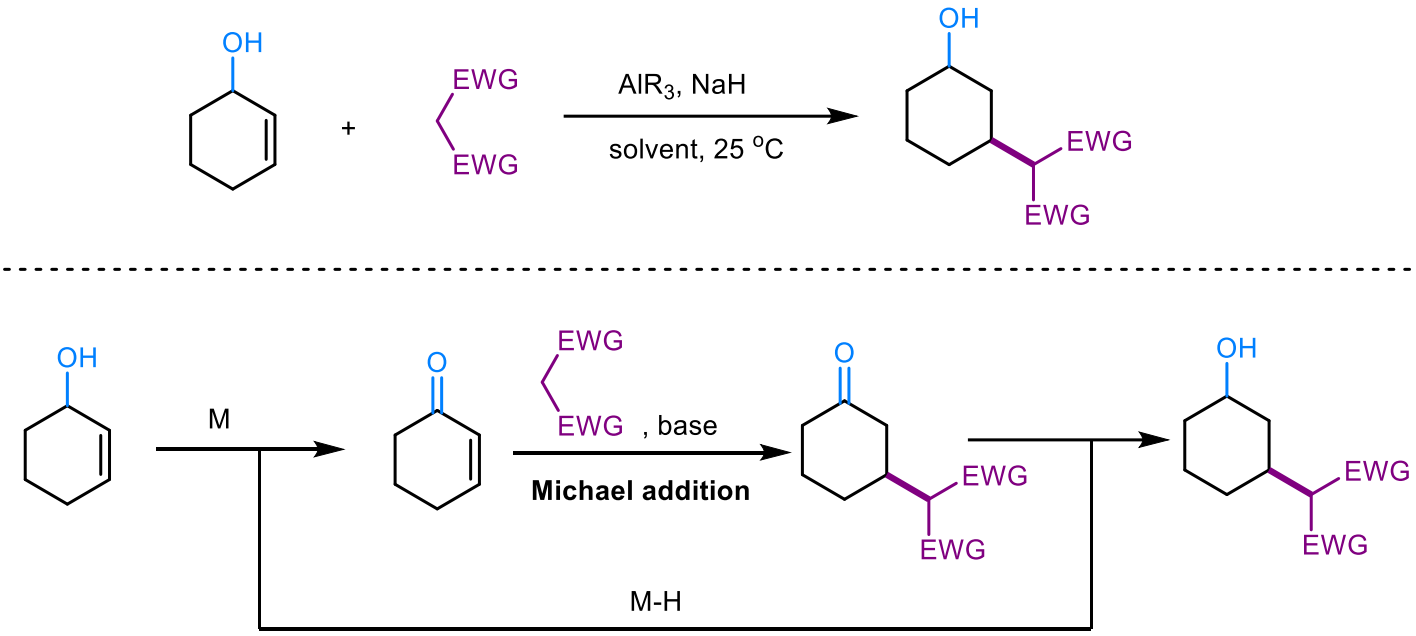

Scheme 1.74 Hydrogen-borrowing Michael addition of allylic alcohols

1.6 C–C bond formation *via* hydrogen transfer between reactants

In the preceding section, we discussed the 'borrowing hydrogen' strategy in the C–C bond formation of alcohols. The core of this strategy is to 'borrow' the reactivity of carbonyl to conduct various C–C bond formation reactions. The hydride, in this case, is borrowed from alcohol and returned to the final product. During the whole process, another component of C–C bond formation usually does not participate in the hydrogen-transfer process. At the same time, the original reactivity of this component does not change. Thus, utilizing such a strategy would require the component other than alcohols (usually nucleophile) to have sufficient reactivity on its own. Such

a fact leads us to consider whether we could make even more use of hydrogen transfer by letting it occur directly between alcohols and another inert coupling partner to make both of them reactive and complete C–C bond formation reaction (Figure 1.2).

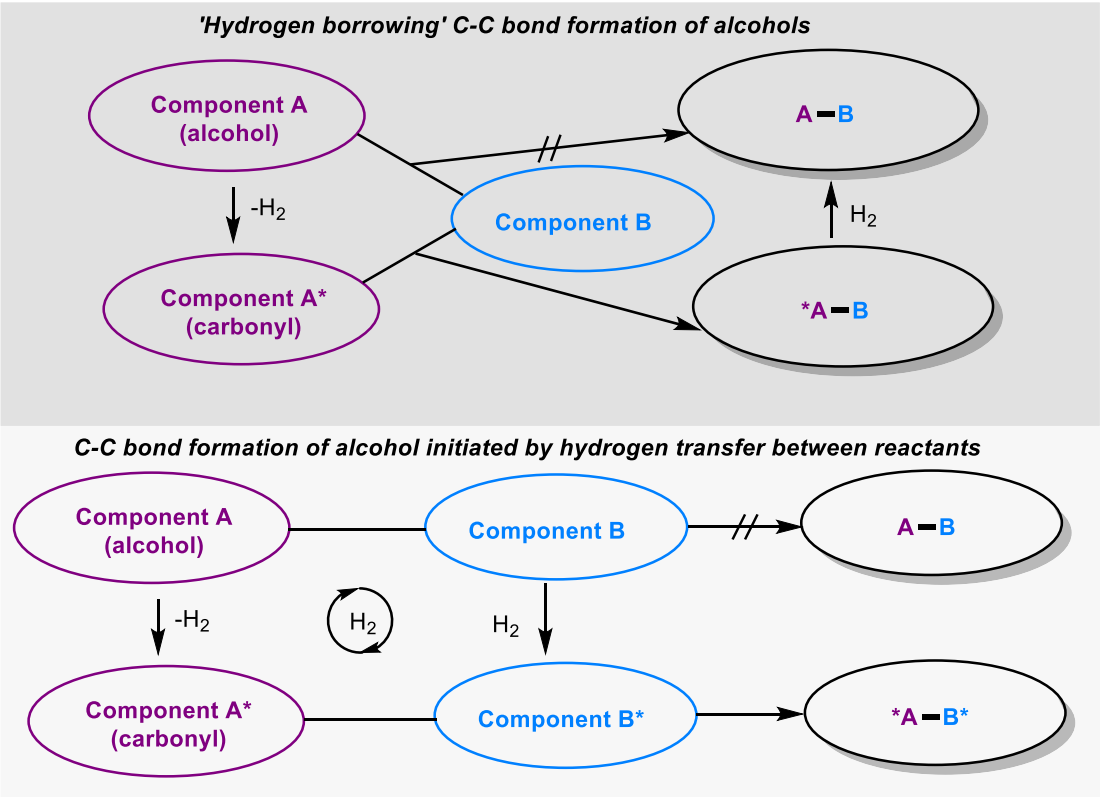

Figure 1.2 Conceptual icon comparing two different types of hydrogen-transfer C–C bond formation reactions

The most symbolic application of this strategy is the α-alkylation of alcohol with alkene and its derivatives.[169–171] Alcohol and alkene (unactivated) are originally two nonreactive components. The direct mixture of these two compounds would never cause any elementary reaction, even with alcohol being transformed to carbonyls (as in the borrowing-hydrogen process discussed in the previous section). However, if we conduct dehydrogenation of alcohol and follow it with the hydrogenation of alkene with transition metal, we will generate a carbonyl together with an M–alkyl complex, which could easily complete a nucleophilic addition reaction to form C–C bond. That is to say, the hydrogen transfer between alcohol and alkene transformed both components from inert to activated ones and enabled them to perfectly follow up C–C bond formation. In this

section, we will discuss such a novel type of C–C bond formation reaction, which occurs on the basis of hydrogen transfer between two reactants.

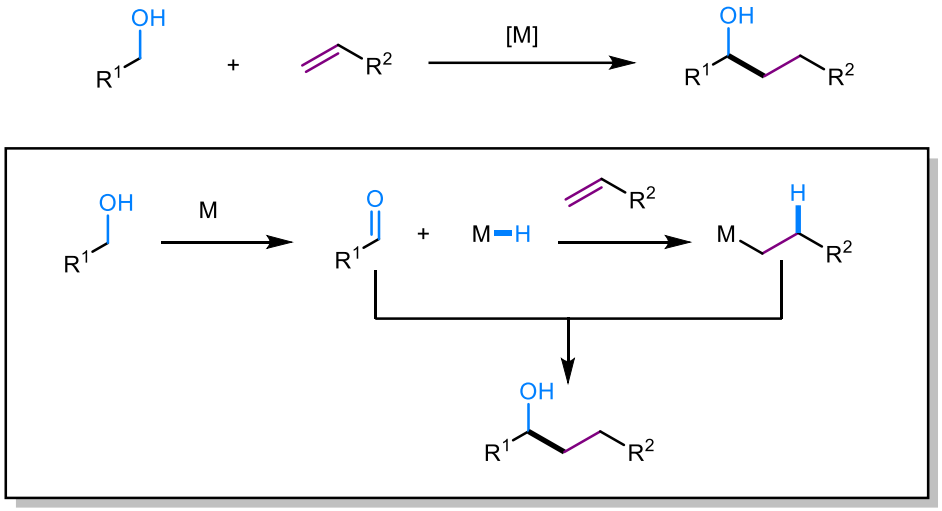

Scheme 1.75 *α*-alkylation of alcohol with alkene and its derivatives

1.6.1 *α*-allylation of alcohol with allene

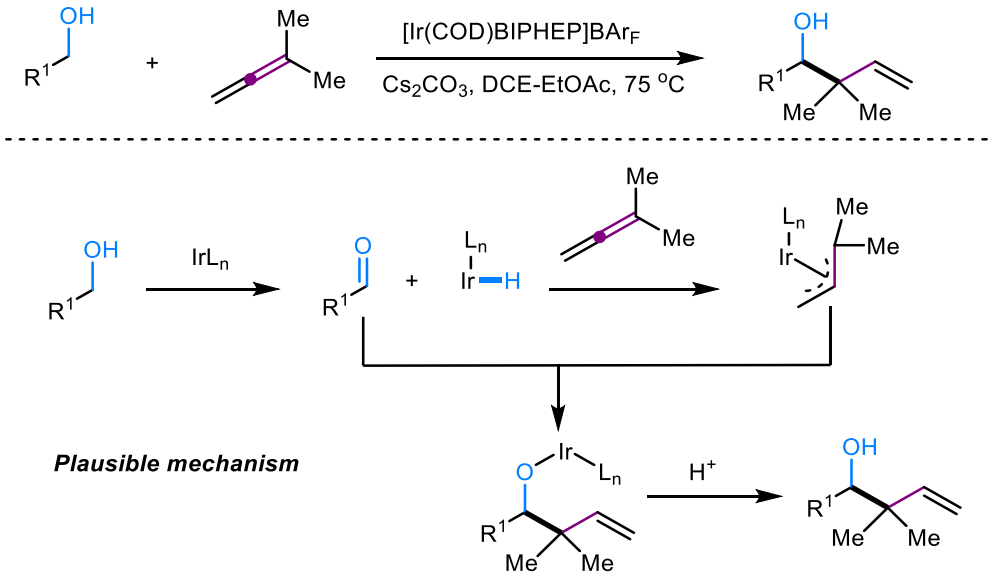

Scheme 1.76 Iridium-catalyzed *α*-allylation of alcohol with allenes

Allene is a highly commonly used alkene derivative in synthetic chemistry with an extremely strong ability to accept hydride insertion to serve as an allylation reagent.[172] Thus, allene could

serve as a perfect substrate for hydrogen-transfer-mediated α-alkylation of alcohol as discussed earlier. In 2007, the α-allylation of alcohol with allene was first reported by Krische *et al.* under iridium catalysis. In this case, they used 1,1-dimethyl-substituted allene as model substrate and let it react with various benzyl alcohol derivatives with a high efficiency and perfect branch selectivities. *Via* in-depth study, they found that the whole process was a redox-neutral process without observation of over-reduction or over-oxidation. The mechanistic study also proved that the hydrogen-transfer process occurred between alcohol and allene before allylation (Scheme 1.76).[173] Later, in 2009, they adapted the iridium catalyst with chiral ligands to realize the asymmetric version of this reaction.[174]

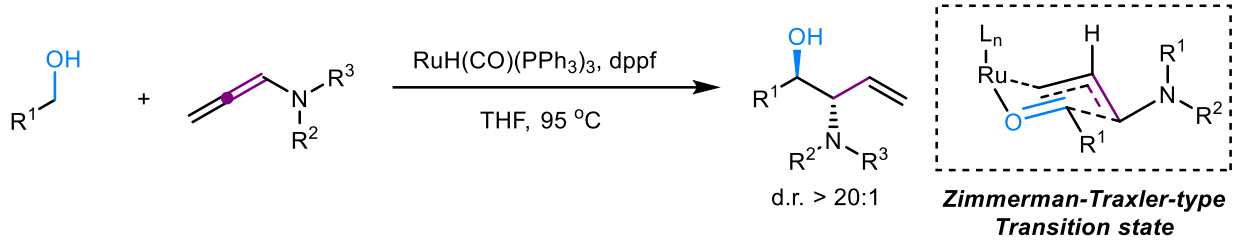

Scheme 1.77 α-allylation of alcohol with allenamides to generate α-amino alcohols

With the success of alkyl allene in allylation of alcohols, Krische *et al.* then turned their attention to some functional groups containing allenes, such as allenamide. In 2010, they used ruthenium catalysts to realize the highly efficient allylation of primary alcohols with allenamides to generate various α-amino alcohol products. Notably, this reaction has an extremely high diastereoselectivity (mostly > 20:1 d.r.). To explain this selectivity, they also advanced a Zimmerman–Traxler-type six-membered ring transition state as shown in Scheme 1.77. The asymmetric version of this reaction was also realized by the same authors in 2019 by chiral iridium complexes, which largely increased the synthetic value of this reaction to attain access to synthesis of numerous drugs and biomolecules containing α-amino alcohol structures.[175]

1.6.2 α-alkylation of alcohol with conjugated alkenes

Besides allenes, dienes (enynes) are another series of activated unsaturated systems, which are also experts in hydrogen transfer reactions. Thus, the reaction concerning α-alkylation of alcohol with dienes and enynes was also well studied, mainly by Krische *et al.*

1.6.2.1 α-alkylation of alcohol with dienes

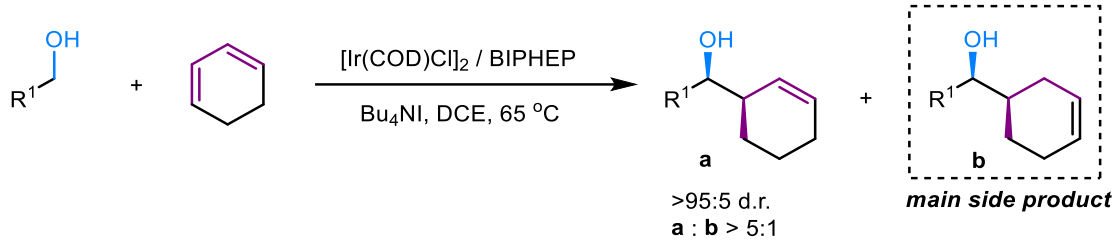

Scheme 1.78 *α*-alkylation of alcohol with cyclohexadiene with Ir-catalysis

The first report of *α*-alkylation of alcohol with dienes was in 2008, shortly after the discovery of allylation reaction with allenes. Inspired by the success of allene, Krische *et al.* used the same iridium catalytic system to initiate the study with cyclohexadiene as model substrate. However, they found that the reaction has extremely poor diastereoselectivity, and a significant amount of regioisomers was observed. To solve this problem, they added a catalytic amount of Bu_4NI and found it significantly increased the diastereoselectivity and minimized the regioisomers. With such a modification, they successfully enabled various primary alcohols to efficiently complete *α*-alkylation with cyclohexadiene (Scheme 1.78).[176]

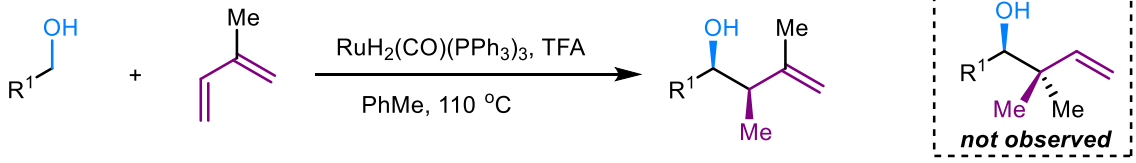

Scheme 1.79 Regioselective *α*-alkylation of alcohol with isoprene and derivatives

After their success with cyclohexadiene, they tried to extend the dienes to acyclic ones. In the same year, they used ruthenium catalytic system to realize such a transformation with isoprene and its derivatives. In this work they found that the alkylation has extremely high branch selectivity. However, probably because of the high steric hindrance, the alkylation tended to occur on the less substituted alkene site.[177, 178] Interestingly, later in 2010, they adapted the alcohol to a less bulky ethanol to run the same reaction and found the regioselectivity was totally converted. In this case, the alkylation occurred on the more substituted site even with highly bulky substituents such as

aromatic ring. However, the regioselectivity was not as good with some linear alkyl substituents (Scheme 1.80).[179]

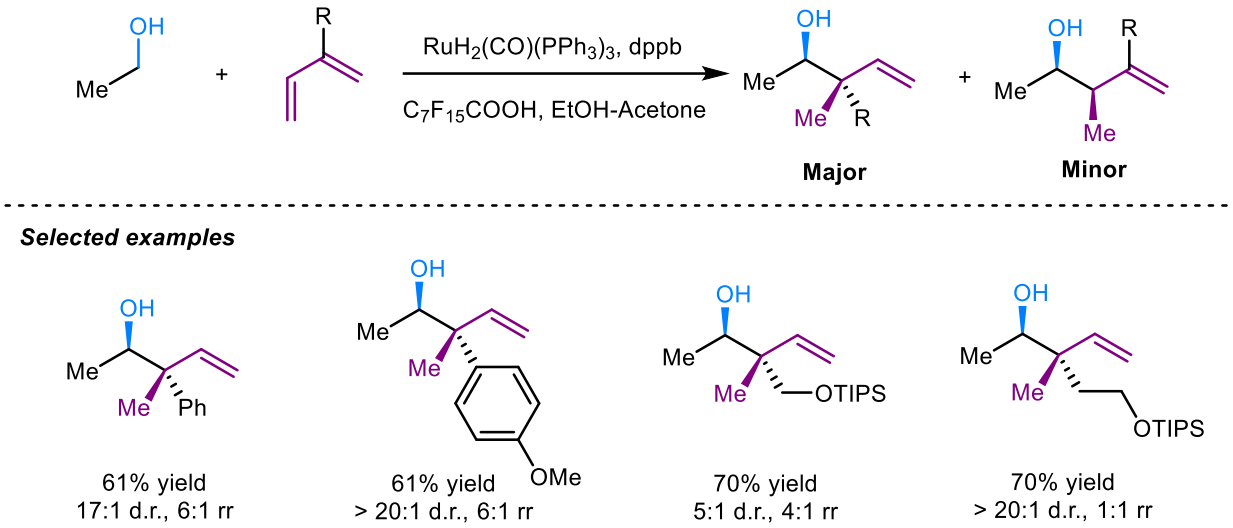

Scheme 1.80 Regioselective *α*-alkylation of ethanol with 2-substituted dienes

Taking advantage of the regioselectivity of diene with ethanol, the asymmetric version of this reaction was developed in 2016 by iridium catalysts, which enabled an introduction of a quaternary chiral carbon center (Scheme 1.81). In this study, they used methanol instead of ethanol as a starting material to avoid multiple chiral centers and found methanol has similar reactivity and regioselectivity as ethanol.[180]

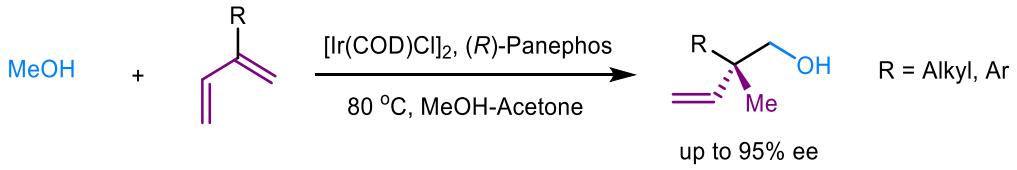

Scheme 1.81 Asymmetric *α*-alkylation of ethanol with 2-substituted dienes

1.6.2.2 α-alkylation of alcohol with enynes

As another conjugated unsaturated system, enyne has similar properties and reactivity as dienes. The *α*-alkylation of alcohol with enyne was first developed in 2008, when Krische *et al.* utilized ruthenium catalytic system, which they used in the diene alkylation, to efficiently complete the alkylation of alcohol with enyne. Owing to the comparatively higher reactivity of alkene than

alkyne in the enyne system,[181] the alkylation would specifically occur on the alkene side to attain the branched product. However, the alkylation of enyne did not achieve as high a diastereoselectivity as the diene system. This might have contributed to the linear structure of alkyne, which had a quite limited influence on the conformation.[182]

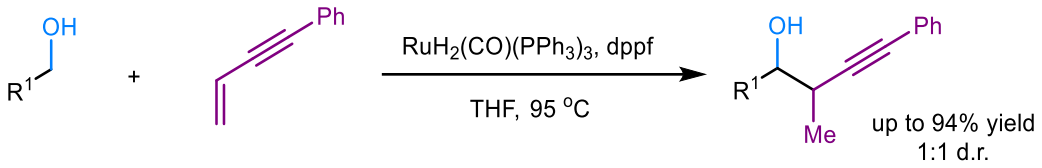

Scheme 1.82 *α*-alkylation of alcohol with enynes under Ru-catalysis

To solve the problem of diastereoselectivity and achieve enantioselectivity, in 2012, they studied this reaction under a chiral-iridium catalytic system and adapted the substituent of enyne from the phenyl group to a tertiary carbon group. Fortunately, in this case, they realized both high enantioselectivity and diastereoselectivity for this transformation.[183]

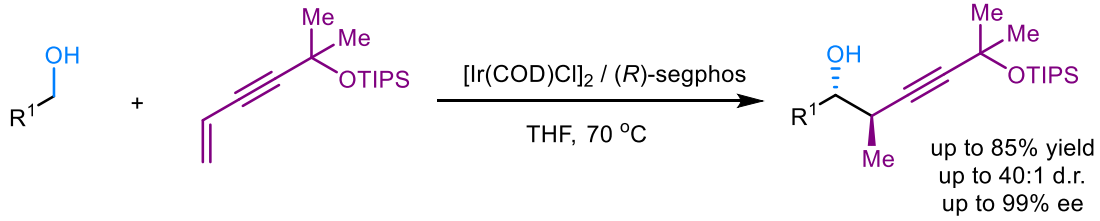

Scheme 1.83 Diastereo- and enantioselective *α*-alkylation of alcohol with enynes

1.6.3 *α*-alkylation of alcohol with alkynes

Alkyne, as a nonconjugated unsaturated compound, has a comparatively lower reactivity than dienes, enynes, and even, in some cases, alkenes. However, owing to its rich π-electron and *sp*-hybridized carbon, the alkyne would sometimes more easily be activated than alkenes, especially with some specific catalysts such as Ru,[184, 185] Cu[186]. Taking advantage of hydrogen-transfer C–C bond formation strategy, the direct *α*-vinylation of alcohols to form synthetic-useful allylic alcohol[187, 188] could be realized by a simple alkyne.

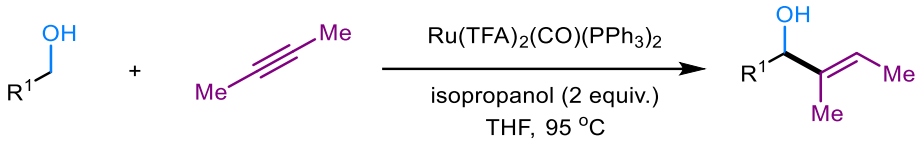

Scheme 1.84 *α*-vinylation of alcohol with alkynes under Ru-catalysis

In 2009, Krische *et al.* discovered that with a special ruthenium catalyst, $Ru(TFA)_2CO(PPh_3)_3$, the alkynes could be successfully activated even in nonconjugated systems. Taking advantage of this discovery, they successfully realized the vinylation of alcohol with alkyne under the catalysis of $Ru(TFA)_2CO(PPh_3)_3$ (Scheme 1.84). The reaction has a (*Z*)-selectivity on the final product, which suggest a cis-hydrogenation process in hydrogen transfer. Another thing to be noted is that unlike the alkylation with conjugated unsaturated systems, the alcohol alkylation with alkyne requires isopropanol as a hydride source to accelerate the hydrogenation step.[189]

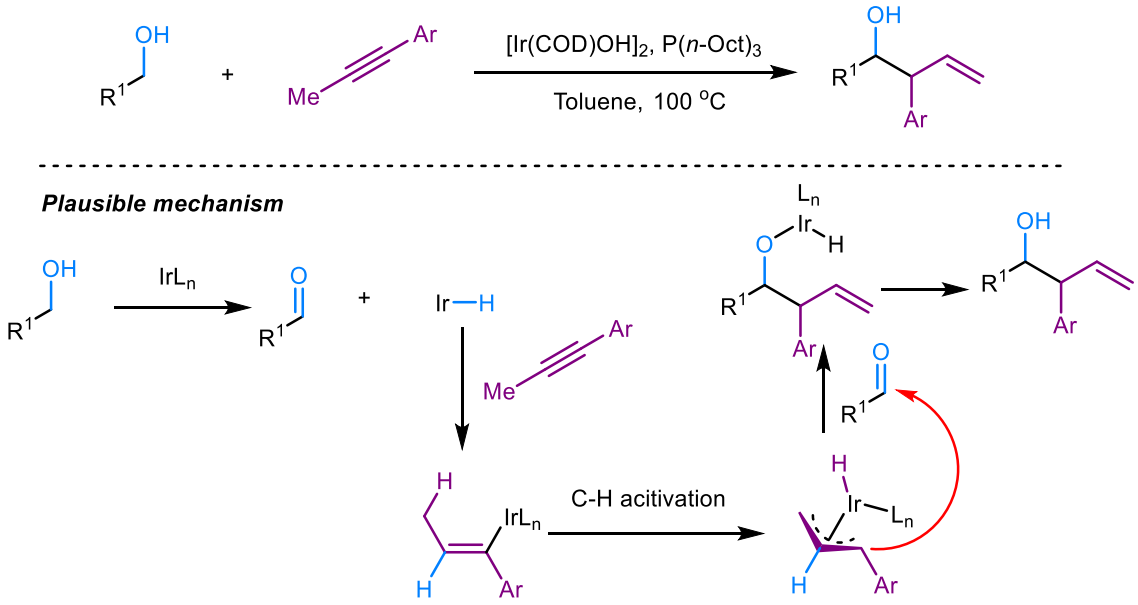

Scheme 1.85 *α*-allylation of alcohol with methyl alkynes under iridium catalysis

Other than the simple hydrogen-transfer vinylation, the reaction of alcohol with alkyne could have some other unique results under different catalytic systems. For instance, Ishii *et al.* used iridium catalysts for the hydrogen-transfer alkylation of alcohol with alkynes (Scheme 1.85). However, the product they attained was homoallylic alcohols instead of allylic alcohols. Based on this

unusual discovery, they proposed an explanatory mechanism that, after the hydrogen transfer from alcohol to alkynes, the iridium would perform another allylic C–H bond activation[190] to form an allyl-π coordination intermediate. Then, the allyl group would conduct a nucleophilic attack on carbonyls with branch selectivity to generate the final homoallylic alcohol product.[191]

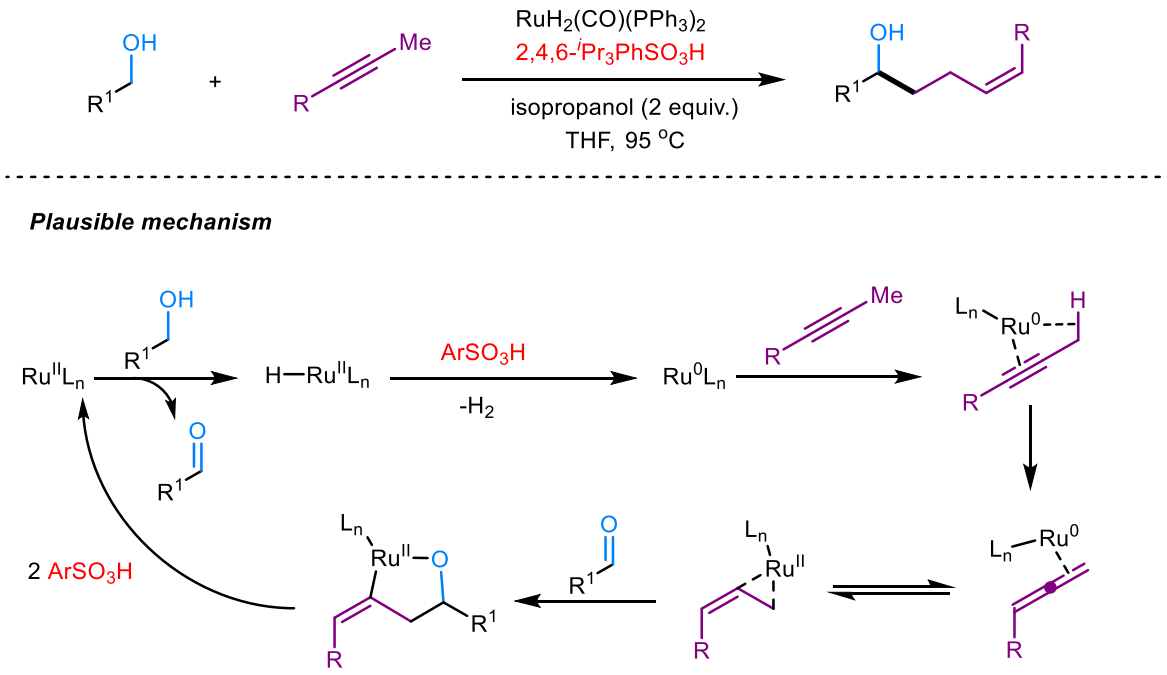

Scheme 1.86 *α*-allylation of alcohol with methyl alkynes with linear selectivity under Ru-catalysis

Such a unique type of alcohol *α*-allylation with alkyne could also be realized by ruthenium catalysis. In 2014, Krische *et al.* found the alkyne was able to tautomerize to allene under the catalysis of Ru(0) in-situ generated from Ru–H and Brønsted acid (Scheme 1.86). Then, the *α*-allylation occurs *via* hydrogen transfer between alcohol and allene. However, owing to the existence of Ru(0) in the reaction system, the allylation of allene had a linear selectivity instead of a branched one. Later, they found that if bulky chiral ligand was added to the reaction system, the regioselectivity of this reaction would return to branched-selective together with a high enantioselectivity.[192]

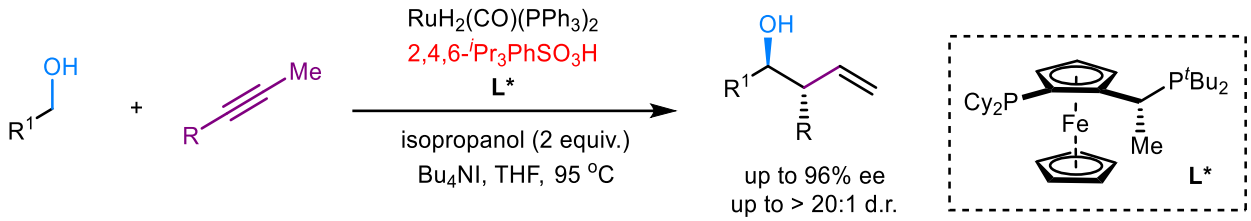

Scheme 1.87 Asymmetric branched-selective *α*-allylation of alcohol with methyl alkynes under Ru catalysis

1.6.4 *α*-alkylation of alcohol with unactivated alkenes

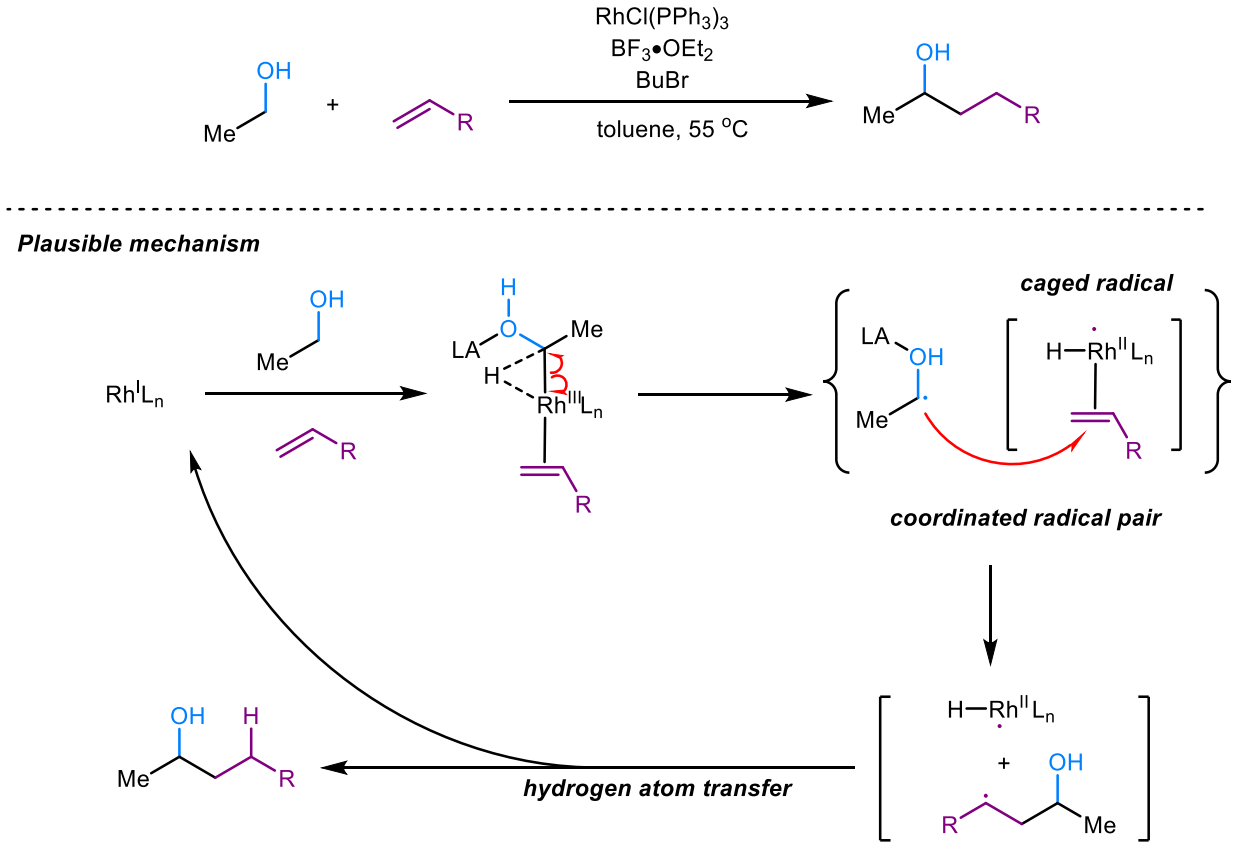

Scheme 1.88 Rhodium catalyzed direct *α*-alkylation of alcohol

Having discussed various types of unsaturated system, we can now turn to the simplest but most unreactive one: unactivated alkenes. In homogeneous catalysis, unactivated alkene is not a particularly efficient hydride acceptor. This is because alkene is a nonpolar compound and has comparatively high electron density on π-system. Thus, it is not a good electrophile most of the time. This property blocked its reactivity to accept the attack from hydride (considered as a

nucleophile).[181] Thus, to make alkenes successfully 'hydrogenated' to M–alkyl complex for C–C bond formation, some special approach for alkene activation was required. If, strictly speaking, in homogeneous catalysis, few reports have seen a realization of the alkylation of alcohol with unactivated alkenes *via* direct hydrogen-transfer process. However, if utilizing some indirect means of activating alkenes other than hydrogen transfer, such a transformation could still be realized.

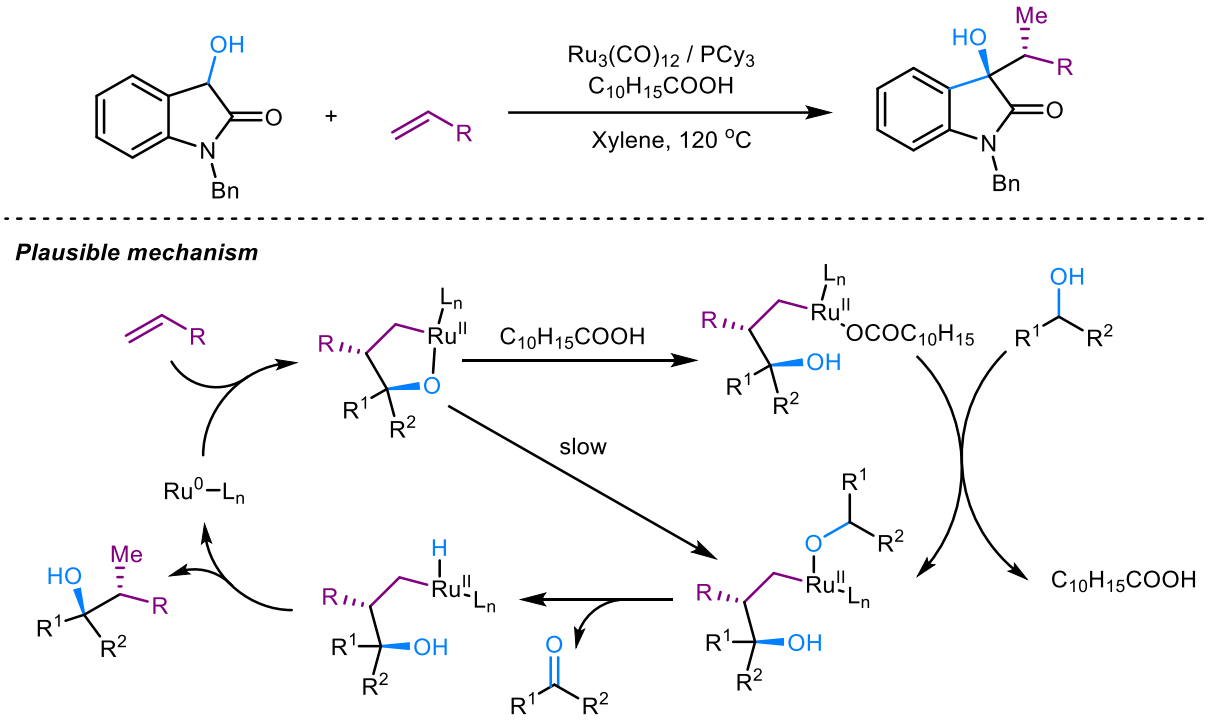

Scheme 1.89 *α*-alkylation of alcohol with unactivated alkenes

For instance, in 2005, Tu *et al.* developed a rhodium-catalyzed direct *α*-alkylation of alcohol with alkenes. According to their mechanistic study, such a transformation experiences a radical process instead of hydride transfer. As is shown in Scheme 1.88, the rhodium(I) catalyst coordinates alkene and at the same time activates the *α*-C–H bond of alcohol to form a alkyl–Rh–H intermediate. Then, the homo cleavage of C–Rh bond leads the formation of a radical pair which includes C-radical and rhodium-radical. Then, the so-formed C-radical is able to attack the alkene which is under activation of rhodium-radical. Finally, with a hydrogen-atom-transfer process from rhodium to the alkyl, the alkylation product forms.[193]The key of the high efficiency of this transformation is that the formation of radical pair provides an ideal kinetic for the 1-hydroxyl alkyl radical to

attack the alkenes smoothly which avoid the potential side reactions such as homo-coupling of 1-hydroxyl alkyl radical and the polymerization of alkenes.

Another symbolic example was developed in 2013 by Krische *et al.* as they utilized Ru(0) catalysis to realize the direct α-alkylation of alcohols with unactivated alkene. As is known, the Ru(0) is a low valent transition metal, which has an extremely high electron density to serve as a good π-donor.[194] Thus, the coordination of alkene with Ru(0) is highly strong with the existence of strong back-bonding from Ru-center. This would make the alkene sufficiently reactive to form C–C bond with carbonyls *via* a five-membered ring metalacyclic intermediate. Finally, with the hydrogenolysis of acid, the alkylation product forms (Scheme 1.89). Overviewing the whole process, the hydrogen transfer does not occur directly between alcohol and alkene. Instead, it occurs between alcohol and ruthenium catalysts with the cycle of Ru^0/Ru^{II} to formally realize the 'hydrogen-transfer' α-alkylation of alcohol with simple alkenes.[195]

1.7 Conclusion and outlook

Hydrogen transfer is a highly powerful protocol in organic chemistry that can transform a functional group to another in the most efficient and atom-economic manner. Taking advantage of hydrogen transfer, the earth-abundant but comparatively unreactive alcohols could be transformed to highly reactive carbonyls. In addition, the strategy of hydrogen transfer between alcohols and reactants or intermediates can enable alcohols to utilize the high reactivity of carbonyls to complete various C–heteroatom or C–C bond formations, which are unable to complete by previous methods. The high atom economy, low waste production, and easy accessibility of starting materials give these hydrogen-transfer C–X or C–C bond formations with alcohols a huge advantage over the classic means of realizing these transformations with alkyl halides.

Despite these advantages, the hydrogen-transfer-mediated alcohol functionalization still has several unignorable problems which limited its application in the synthesis and industry such as: 1) The substrate scope is comparatively limited, and the functional group tolerance has not been widely studied, especially for the various hydrogen-transfer-mediated C–C bond formations of alcohol; 2) The regioselectivity of alcohols has rarely been studied for these transformations (e.g., primary alcohol vs. secondary alcohol); 3) The condition of these reactions is usually harsh, especially for high temperature or refluxing solvents. Considering these factors, hydrogen-transfer-mediated functionalization of alcohols is worthy of further development. In future study

of this area, it would be highly desirable to focus on the following directions: 1) to study the substrate scope for these reactions more deeply and broadly, including the study of these reactions in late-stage functionalization; 2) to develop more powerful homogeneous catalysts with higher efficiency of hydrogen transfer and higher selectivity of reaction sites; 3) to move the hydrogen transfer strategy to more challenging C–C or C–Het bond formations with alcohols, for example by utilizing some more inert unsaturated systems such as aromatic systems.

References

(1). Tojo, G.; Fernandez, M. I., *Oxidation of Alcohols to Aldehydes and Ketones: A Guide to Current Common Practice*. Springer Science & Business Media: New York, 2006.
(2). Omura, K.; Swern, D., Oxidation of alcohols by 'activated' dimethyl sulfoxide. A preparative, steric and mechanistic study. *Tetrahedron* **1978,** *34*, 1651–1660.
(3). Tidwell, T. T., Oxidation of alcohols by activated dimethyl sulfoxide and related reactions: An update. *Synthesis* **1990,** *1990*, 857–870.
(4). Dess, D. B.; Martin, J. C., Readily accessible 12-I-5 oxidant for the conversion of primary and secondary alcohols to aldehydes and ketones. *J. Org. Chem.* **1983,** *48*, 4155–4156.
(5). Oppenauer, R., Dehydration of secondary alcohols to ketones. I. Preparation of sterol ketones and sex hormones. *Recl. Trav. Chim. Pays-Bas* **1937,** *56*, 137–144.
(6). Yager, B. J.; Hancock, C. K., Equilibrium and kinetic studies of the Meerwein–Ponndorf–Verley-Oppenauer (mpvo) reaction1. *J. Org. Chem.* **1965,** *30*, 1174–1179.
(7). Djerassi, C., The oppenauer oxidation. In *Org. React.*, John Wiley & Sons, Inc.: New York, 2004.
(8). Stevens, R. V.; Chapman, K. T.; Weller, H. N., Convenient and inexpensive procedure for oxidation of secondary alcohols to ketones. *J. Org. Chem.* **1980,** *45*, 2030–2032.
(9). Corey, E. J.; Suggs, J. W., Pyridinium chlorochromate. An efficient reagent for oxidation of primary and secondary alcohols to carbonyl compounds. *Tetrahedron Lett.* **1975,** *16*, 2647–2650.
(10). Sharma, V. K., Ferrate(VI) and ferrate(V) oxidation of organic compounds: Kinetics and mechanism. *Coord. Chem. Rev.* **2013,** *257*, 495–510.
(11). Moran, J.; Krische, M. J., Formation of C–C bonds *via* ruthenium-catalyzed transfer hydrogenation. *Pure Appl. Chem.* **2012,** *84*, 1729–1739.
(12). Muzart, J., Pd-catalyzed hydrogen-transfer reactions from alcohols to C=C, C=O, and C=N bonds. *Eur. J. Org. Chem.* **2015,** *2015*, 5693–5707.
(13). Saidi, O.; Williams, J. M. J., Iridium-catalyzed hydrogen transfer reactions. In *Iridium Catalysis*, Andersson, P. G., Ed. Springer: Berlin, 2011; pp 77–106.
(14). Bäckvall, J.-E.; Chowdhury, R. L.; Karlsson, U., Ruthenium-catalysed aerobic oxidation of alcohols *via* multistep electron transfer. *J. Chem. Soc., Chem, Commun.* **1991**, 473–475.

(15). Chowdhury, R. L.; Bäckvall, J.-E., Efficient ruthenium-catalysed transfer hydrogenation of ketones by propan-2-ol. *J. Chem. Soc., Chem, Commun.* **1991**, 1063–1064.
(16). Wang, G. Z.; Bäckvall, J.-E., Ruthenium-catalysed oxidation of alcohols by acetone. *J. Chem. Soc., Chem, Commun.* **1992**, 337–339.
(17). Wang, G.-Z.; Andreasson, U.; Bäckvall, J.-E., Aerobic oxidation of secondary alcohols *via* ruthenium-catalysed hydrogen transfer involving a new triple catalytic system. *J. Chem. Soc., Chem, Commun.* **1994**, 1037–1038.
(18). Dijksman, A.; W. C. E. Arends, I.; A. Sheldon, R., Efficient ruthenium–TEMPO-catalysed aerobic oxidation of aliphatic alcohols into aldehydes and ketones. *Chem. Commun.* **1999**, 1591–1592.
(19). Hanyu, A.; Takezawa, E.; Sakaguchi, S.; Ishii, Y., Selective aerobic oxidation of primary alcohols catalyzed by a $Ru(PPh_3)_3Cl_2$/hydroquinone system. *Tetrahedron Lett.* **1998,** *39*, 5557–5560.
(20). Dijksman, A.; Arends, I. W. C. E.; Sheldon, R. A., Cu(II)–nitroxyl radicals as catalytic galactose oxidase mimics. *Org. Biomol. Chem.* **2003,** *1*, 3232–3237.
(21). Semmelhack, M. F.; Schmid, C. R.; Cortes, D. A.; Chou, C. S., Oxidation of alcohols to aldehydes with oxygen and cupric ion, mediated by nitrosonium ion. *J. Am. Chem. Soc.* **1984,** *106*, 3374–3376.
(22). Markó, I. E.; Gautier, A.; Chellé-Regnaut, I.; Giles, P. R.; Tsukazaki, M.; Urch, C. J.; Brown, S. M., Efficient and practical catalytic oxidation of alcohols using molecular oxygen. *J. Org. Chem.* **1998,** *63*, 7576–7577.
(23). Markó, I. E.; Gautier, A.; Dumeunier, R.; Doda, K.; Philippart, F.; Brown, S. M.; Urch, C. J., Efficient, copper-catalyzed, aerobic oxidation of primary alcohols. *Angew. Chem. Int. Ed.* **2004,** *43*, 1588–1591.
(24). Parmeggiani, C.; Cardona, F., Transition metal based catalysts in the aerobic oxidation of alcohols. *Green Chem.* **2012,** *14*, 547–564.
(25). Brink, G.-J. t.; Arends, I. W. C. E.; Sheldon, R. A., Green, catalytic oxidation of alcohols in water. **2000,** *287*, 1636–1639.
(26). ten Brink, G.-J.; Arends, I. W. C. E.; Sheldon, R. A., Catalytic conversions in water. Part 21: Mechanistic investigations on the palladium-catalysed aerobic oxidation of alcohols in water†. *Adv. Synth. Catal.* **2002,** *344*, 355–369.
(27). Djerassi, C., The Oppenauer oxidation. In *Org. React.*, pp 207–272.
(28). Bruneau, C.; Dixneuf, P. H., *Ruthenium Catalysts and Fine Chemistry*. Springer: Berlin, 2004; Vol. 11.
(29). Almeida, M. L. S.; Beller, M.; Wang, G.-Z.; Bäckvall, J.-E., Ruthenium(II)-catalyzed Oppenauer-type oxidation of secondary alcohols. *Chem. Eur. J.* **1996,** *2*, 1533–1536.

(30). Blum, Y.; Czarkie, D.; Rahamim, Y.; Shvo, Y., (cyclopentadienone)ruthenium carbonyl complexes — a new class of homogeneous hydrogenation catalysts. *Organometallics* **1985,** *4*, 1459–1461.
(31). Casey, C. P.; Guan, H., An efficient and chemoselective iron catalyst for the hydrogenation of ketones. *J. Am. Chem. Soc.* **2007,** *129*, 5816–5817.
(32). Casey, C. P.; Guan, H., Cyclopentadienone iron alcohol complexes: Synthesis, reactivity, and implications for the mechanism of iron-catalyzed hydrogenation of aldehydes. *J. Am. Chem. Soc.* **2009,** *131*, 2499–2507.
(33). Coleman, M. G.; Brown, A. N.; Bolton, B. A.; Guan, H., Iron-catalyzed Oppenauer-type oxidation of alcohols. *Adv. Synth. Catal.* **2010,** *352*, 967–970.
(34). Moyer, S. A.; Funk, T. W., Air-stable iron catalyst for the Oppenauer-type oxidation of alcohols. *Tetrahedron Lett.* **2010,** *51*, 5430–5433.
(35). Suzuki, T.; Morita, K.; Tsuchida, M.; Hiroi, K., Iridium-catalyzed Oppenauer oxidations of primary alcohols using acetone or 2-butanone as oxidant. *J. Org. Chem.* **2003,** *68*, 1601–1602.
(36). Matsumoto, T.; Ueno, M.; Wang, N.; Kobayashi, S., Recent advances in immobilized metal catalysts for environmentally benign oxidation of alcohols. *Chem. Asian J.* **2008,** *3*, 196–214.
(37). Hayashi, M.; Yamada, K.; Nakayama, S.-z.; Hayashi, H.; Yamazaki, S., Environmentally benign oxidation using a palladium catalyst system. *Green Chem.* **2000,** *2*, 257–260.
(38). Shi, R.; Wang, F.; Tana; Li, Y.; Huang, X.; Shen, W., A highly efficient Cu/La_2O_3 catalyst for transfer dehydrogenation of primary aliphatic alcohols. *Green Chem.* **2010,** *12*, 108–113.
(39). Alonso, F.; Riente, P.; Yus, M., Nickel nanoparticles in hydrogen transfer reactions. *Acc. Chem. Res.* **2011,** *44*, 379–391.
(40). Sakaguchi, S.; Yamaga, T.; Ishii, Y., Iridium-catalyzed transfer hydrogenation of *α,β*-unsaturated and saturated carbonyl compounds with 2-propanol. *J. Org. Chem.* **2001,** *66*, 4710–4712.
(41). Zhao, K.; Wang, D.; Wang, H.; Zhu, Z.; Ding, Y., Phosphine-assisted bisbenzothienyl iridium(III) complexes: Synthesis, structures and photophysical properties. *Inorg. Chem. Commun.* **2014,** *47*, 131–133.
(42). Sandoval, C. A.; Ohkuma, T.; Muñiz, K.; Noyori, R., Mechanism of asymmetric hydrogenation of ketones catalyzed by BINAP/1,2-diamine−ruthenium(II) complexes. *J. Am. Chem. Soc.* **2003,** *125*, 13490–13503.
(43). Gunanathan, C.; Milstein, D., Applications of acceptorless dehydrogenation and related transformations in chemical synthesis. *Science* **2013,** *341*, 1229712.
(44). Askevold, B.; Khusniyarov, M. M.; Herdtweck, E.; Meyer, K.; Schneider, S., A square-planar ruthenium(II) complex with a low-spin configuration. *Angew. Chem. Int. Ed.* **2010,** *49*, 7566–7569.

(45). Friedrich, A.; Drees, M.; Käss, M.; Herdtweck, E.; Schneider, S., Ruthenium complexes with cooperative PNP-pincer amine, amido, imine, and enamido ligands: Facile ligand backbone functionalization processes. *Inorg. Chem.* **2010,** *49*, 5482–5494.
(46). Bertoli, M.; Choualeb, A.; Lough, A. J.; Moore, B.; Spasyuk, D.; Gusev, D. G., Osmium and ruthenium catalysts for dehydrogenation of alcohols. *Organometallics* **2011,** *30*, 3479–3482.
(47). Rozenel, S. S.; Arnold, J., Bimetallic ruthenium–PNP-pincer complex as a platform to model proposed intermediates in dinitrogen reduction to ammonia. *Inorg. Chem.* **2012,** *51*, 9730–9739.
(48). Fillman, K. L.; Bielinski, E. A.; Schmeier, T. J.; Nesvet, J. C.; Woodruff, T. M.; Pan, C. J.; Takase, M. K.; Hazari, N.; Neidig, M. L., Flexible binding of PNP pincer ligands to monomeric iron complexes. *Inorg. Chem.* **2014,** *53*, 6066–6072.
(49). Dupont, J.; Consorti, C. S.; Spencer, J., Chapter 1 — Organometallic pincer-type complexes: Recent applications in synthesis and catalysis. In *The Chemistry of Pincer Compounds*, Morales-Morales, D.; Jensen, C. M., Eds. Elsevier Science B.V.: Amsterdam, 2007; pp 1–24.
(50). Nielsen, M.; Kammer, A.; Cozzula, D.; Junge, H.; Gladiali, S.; Beller, M., Efficient hydrogen production from alcohols under mild reaction conditions. *Angew. Chem. Int. Ed.* **2011,** *50*, 9593–9597.
(51). Garbe, M.; Junge, K.; Beller, M., Homogeneous catalysis by manganese-based pincer complexes. *Eur. J. Org. Chem.* **2017,** *2017*, 4344–4362.
(52). Chakraborty, S.; Lagaditis, P. O.; Förster, M.; Bielinski, E. A.; Hazari, N.; Holthausen, M. C.; Jones, W. D.; Schneider, S., Well-defined iron catalysts for the acceptorless reversible dehydrogenation–hydrogenation of alcohols and ketones. *ACS Catal.* **2014,** *4*, 3994–4003.
(53). Xu, S.; Alhthlol, L. M.; Paudel, K.; Reinheimer, E.; Tyer, D. L.; Taylor, D. K.; Smith, A. M.; Holzmann, J.; Lozano, E.; Ding, K., Tripodal N,P-mixed-donor ligands and their cobalt complexes: Efficient catalysts for acceptorless dehydrogenation of secondary alcohols. *Inorg. Chem.* **2018,** *57*, 2394–2397.
(54). Milstein, D., Discovery of environmentally benign catalytic reactions of alcohols catalyzed by pyridine-based pincer Ru complexes, based on metal–ligand cooperation. *Top. Catal.* **2010,** *53*, 915–923.
(55). Hartwig, J. F., *Organotransition Metal Chemistry: From Bonding to Catalysis*. University Science Books: Sausalito, 2010.
(56). Musa, S.; Shaposhnikov, I.; Cohen, S.; Gelman, D., Ligand–metal cooperation in PCP pincer complexes: Rational design and catalytic activity in acceptorless dehydrogenation of alcohols. *Angew. Chem. Int. Ed.* **2011,** *50*, 3533–3537.

(57). Cepa, S.; Schulte to Brinke, C.; Roelfes, F.; Hahn, F. E., Hydrogen activation by an iridium(III) complex bearing a bidentate protic NH, NR–NHC^phosphine ligand. *Organometallics* **2015,** *34*, 5454–5460.
(58). Chang, W.; Gong, X.; Wang, S.; Xiao, L.-P.; Song, G., Acceptorless dehydrogenation and dehydrogenative coupling of alcohols catalysed by protic nhc ruthenium complexes. *Org. Biomol. Chem.* **2017,** *15*, 3466–3471.
(59). Fujita, K.-i.; Tanino, N.; Yamaguchi, R., Ligand-promoted dehydrogenation of alcohols catalyzed by Cp*Ir complexes. A new catalytic system for oxidant-free oxidation of alcohols. *Org. Lett.* **2007,** *9*, 109–111.
(60). Kawahara, R.; Fujita, K.-i.; Yamaguchi, R., Dehydrogenative oxidation of alcohols in aqueous media using water-soluble and reusable Cp*Ir catalysts bearing a functional bipyridine ligand. *J. Am. Chem. Soc.* **2012,** *134*, 3643–3646.
(61). Zeng, G.; Sakaki, S.; Fujita, K.-i.; Sano, H.; Yamaguchi, R., Efficient catalyst for acceptorless alcohol dehydrogenation: Interplay of theoretical and experimental studies. *ACS Catal.* **2014,** *4*, 1010–1020.
(62). Eizawa, A.; Arashiba, K.; Tanaka, H.; Kuriyama, S.; Matsuo, Y.; Nakajima, K.; Yoshizawa, K.; Nishibayashi, Y., Remarkable catalytic activity of dinitrogen-bridged dimolybdenum complexes bearing NHC-based PCP-pincer ligands toward nitrogen fixation. *Nat. Commun*, **2017,** *8*, 14874.
(63). Eizawa, A.; Nishimura, S.; Arashiba, K.; Nakajima, K.; Nishibayashi, Y., Synthesis of ruthenium complexes bearing PCP-type pincer ligands and their application to direct synthesis of imines from amines and benzyl alcohol. *Organometallics* **2018**.
(64). Matoba, K.; Eizawa, A.; Nishimura, S.; Arashiba, K.; Nakajima, K.; Nishibayashi, Y., Practical synthesis of a PCP-type pincer ligand and its metal complexes-. *Synthesis* **2018,** *50*, 1015–1019.
(65). Trost, B. M.; Kulawiec, R. J., Chemoselectivity in the ruthenium-catalyzed redox isomerization of allyl alcohols. *J. Am. Chem. Soc.* **1993,** *115*, 2027–2036.
(66). Trost, B. M.; Livingston, R. C., Two-metal catalyst system for redox isomerization of propargyl alcohols to enals and enones. *J. Am. Chem. Soc.* **1995,** *117*, 9586–9587.
(67). Bäckvall, J.-E.; Andreasson, U., Ruthenium-catalyzed isomerization of allylic alcohols to saturated ketones. *Tetrahedron Lett.* **1993,** *34*, 5459–5462.
(68). Slugovc, C.; Rüba, E.; Schmid, R.; Kirchner, K., Improved efficiency of the ruthenium-catalyzed redox isomerization of allyl alcohols. *Organometallics* **1999,** *18*, 4230–4233.
(69). Li, C.-J., Organic reactions in aqueous media with a focus on carbon−carbon bond formations: A decade update. *Chem. Rev.* **2005,** *105*, 3095–3166.
(70). Li, C. J., Organic reactions in aqueous media — with a focus on carbon-carbon bond formation. *Chem. Rev.* **1993,** *93*, 2023–2035.

(71). Wang, D.; Chen, D.; Haberman, J. X.; Li, C.-J., Ruthenium-catalyzed isomerization of homoallylic alcohols in water. *Tetrahedron* **1998,** *54*, 5129–5142.
(72). Cadierno, V.; Crochet, P.; García-Garrido, S. E.; Gimeno, J., Water-soluble ruthenium(II) catalysts [$RuCl_2(\eta^6$-arene){$P(CH_2OH)_3$}] for isomerization of allylic alcohols and alkyne hydration. *Dalton Trans.* **2004**, 3635–3641.
(73). Crochet, P.; Díez, J.; Fernández-Zúmel, M. A.; Gimeno, J., Catalytic isomerization of allylic alcohols by (η^6-*p*-cymene)–ruthenium(II) complexes in organic and aqueous media: New recyclable and highly efficient catalysts in water containing ammonium-functionalized ligands. *Adv. Synth. Catal.* **2006,** *348*, 93–100.
(74). Lorenzo-Luis, P.; Romerosa, A.; Serrano-Ruiz, M., Catalytic isomerization of allylic alcohols in water. *ACS Catal.* **2012,** *2*, 1079–1086.
(75). Campos-Malpartida, T.; Fekete, M.; Joó, F.; Kathó, Á.; Romerosa, A.; Saoud, M.; Wojtków, W., Redox isomerisation of allylic alcohols catalysed by water-soluble ruthenium complexes in aqueous systems. *J. Organomet. Chem.* **2008,** *693*, 468–474.
(76). Servin, P.; Laurent, R.; Gonsalvi, L.; Tristany, M.; Peruzzini, M.; Majoral, J.-P.; Caminade, A.-M., Grafting of water-soluble phosphines to dendrimers and their use in catalysis: Positive dendritic effects in aqueous media. *Dalton Trans.* **2009**, 4432–4434.
(77). Azua, A.; Sanz, S.; Peris, E., Sulfonate-functionalized NHC-based ruthenium catalysts for the isomerization of allylic alcohols in water. Recyclability studies. *Organometallics* **2010,** *29*, 3661–3664.
(78). Bizet, V.; Pannecoucke, X.; Renaud, J.-L.; Cahard, D., Ruthenium-catalyzed redox isomerization of trifluoromethylated allylic alcohols: Mechanistic evidence for an enantiospecific pathway. *Angew. Chem. Int. Ed.* **2012,** *51*, 6467–6470.
(79). Cahard, D.; Gaillard, S.; Renaud, J.-L., Asymmetric isomerization of allylic alcohols. *Tetrahedron Lett.* **2015,** *56*, 6159–6169.
(80). Arai, N.; Sato, K.; Azuma, K.; Ohkuma, T., Enantioselective isomerization of primary allylic alcohols into chiral aldehydes with the Tol-BINAP/dbapen/ruthenium(II) catalyst. *Angew. Chem. Int. Ed.* **2013,** *52*, 7500–7504.
(81). Liu, T.-L.; Ng, T. W.; Zhao, Y., Rhodium-catalyzed enantioselective isomerization of secondary allylic alcohols. *J. Am. Chem. Soc.* **2017,** *139*, 3643–3646.
(82). Li, H.; Mazet, C., Iridium-catalyzed selective isomerization of primary allylic alcohols. *Acc. Chem. Res.* **2016,** *49*, 1232–1241.
(83). Larionov, E.; Lin, L.; Guénée, L.; Mazet, C., Scope and mechanism in palladium-catalyzed isomerizations of highly substituted allylic, homoallylic, and alkenyl alcohols. *J. Am. Chem. Soc.* **2014,** *136*, 16882–16894.
(84). Bricout, H.; Monflier, E.; Carpentier, J.-F.; Mortreux, A., Homogeneous and biphasic nickel-catalyzed isomerization of allylic alcohols. *Eur. J. Inorg. Chem.* **1998,** *1998*, 1739–1744.

(85). Wang, X.; Liu, F.; Yan, Z.; Qiang, Q.; Huang, W.; Rong, Z.-Q., Redox-neutral nickel-catalyzed cross-coupling reactions of (homo)allylic alcohols and aryltriflates. *ACS Catal.* **2021**, 7319–7326.
(86). Damico, R.; Logan, T., Isomerization of unsaturated alcohols with iron pentacarbonyl. Preparation of ketones and aldehydes. *J. Org. Chem.* **1967,** *32*, 2356–2358.
(87). Baudry, D.; Ephritikhine, M.; Felkin, H., Isomerisation of allyl ethers catalysed by the cationic iridium complex [Ir(cyclo-octa-1,5-diene)($PMePh_2$)$_2$]PF_6. A highly stereoselective route to trans-propenyl ethers. *J. Chem. Soc., Chem, Commun.* **1978**, 694–695.
(88). Li, C.-C.; Kan, J.; Qiu, Z.; Li, J.; Lv, L.; Li, C.-J., Synergistic relay reactions to achieve redox-neutral *α*-alkylations of olefinic alcohols with ruthenium(II) catalysis. *Angew. Chem. Int. Ed.* **2020,** *59*, 4544–4549.
(89). Mantilli, L.; Mazet, C., Iridium-catalyzed isomerization of primary allylic alcohols under mild reaction conditions. *Tetrahedron Lett.* **2009,** *50*, 4141–4144.
(90). Crabtree, R., Iridium compounds in catalysis. *Acc. Chem. Res.* **1979,** *12*, 331–337.
(91). Mantilli, L.; Gérard, D.; Torche, S.; Besnard, C.; Mazet, C., Iridium-catalyzed asymmetric isomerization of primary allylic alcohols. *Angew. Chem. Int. Ed.* **2009,** *48*, 5143–5147.
(92). Li, H.; Mazet, C., Steric parameters in the Ir-catalyzed regio- and diastereoselective isomerization of primary allylic alcohols. *Org. Lett.* **2013,** *15*, 6170–6173.
(93). Nova, A.; Ujaque, G.; Albéniz, A. C.; Espinet, P., Mechanism of the rhodium-catalyzed asymmetric isomerization of allylamines to enamines. *Chem. Eur. J.* **2008,** *14*, 3323–3329.
(94). Otsuka, S.; Tani, K., Catalytic asymmetric hydrogen migration of allylamines. *Synthesis* **1991,** *1991*, 665–680.
(95). Mao, L.-L.; Li, C.-C.; Yang, Q.; Cheng, M.-X.; Yang, S.-D., One-pot synthesis of *α*-aminophosphonates *via* a cascade sequence of allylamine isomerization/hydrophosphonylation. *Chem. Commun.* **2017,** *53*, 4473–4476.
(96). Tanaka, K.; Qiao, S.; Tobisu, M.; Lo, M. M. C.; Fu, G. C., Enantioselective isomerization of allylic alcohols catalyzed by a rhodium/phosphaferrocene complex. *J. Am. Chem. Soc.* **2000,** *122*, 9870–9871.
(97). Motherwell, W. B.; Sandham, D. A., Observations on a nickel-catalyzed isomerization of allylic lithium alkoxides. *Tetrahedron Lett.* **1992,** *33*, 6187–6190.
(98). Wang, M.; Li, C.-J., Aldol reaction *via* in situ olefin migration in water. *Tetrahedron Lett.* **2002,** *43*, 3589–3591.
(99). Lin, L.; Yamamoto, K.; Matsunaga, S.; Kanai, M., Rhodium-catalyzed cross-aldol reaction: In situ aldehyde-enolate formation from allyloxyboranes and primary allylic alcohols. *Angew. Chem. Int. Ed.* **2012,** *51*, 10275–10279.

(100). Uma, R.; Gouault, N.; Crévisy, C.; Grée, R., Development of new iron catalysts for the tandem isomerization–aldol condensation of allylic alcohols. *Tetrahedron Lett.* **2003,** *44*, 6187–6190.
(101). Juliá-Hernández, F.; Moragas, T.; Cornella, J.; Martin, R., Remote carboxylation of halogenated aliphatic hydrocarbons with carbon dioxide. *Nature* **2017,** *545*, 84.
(102). Sommer, H.; Juliá-Hernández, F.; Martin, R.; Marek, I., Walking metals for remote functionalization. *ACS Cent. Sci.* **2018,** *4*, 153–165.
(103). Guan, Z.; Cotts, P. M.; McCord, E. F.; McLain, S. J., Chain walking: A new strategy to control polymer topology. *Science* **1999,** *283*, 2059.
(104). Huang, R.-Z.; Lau, K. K.; Li, Z.; Liu, T.-L.; Zhao, Y., Rhodium-catalyzed enantioconvergent isomerization of homoallylic and bishomoallylic secondary alcohols. *J. Am. Chem. Soc.* **2018,** *140*, 14647–14654.
(105). Carey, F. A.; Sundberg, R. J., *Advanced Organic Chemistry: Part B: Reaction and Synthesis*. Springer Science & Business Media: New York, 2007.
(106). Abdel-Magid, A. F.; Maryanoff, C. A.; Carson, K. G., Reductive amination of aldehydes and ketones by using sodium triacetoxyborohydride. *Tetrahedron Lett.* **1990,** *31*, 5595–5598.
(107). Abdel-Magid, A. F.; Carson, K. G.; Harris, B. D.; Maryanoff, C. A.; Shah, R. D., Reductive amination of aldehydes and ketones with sodium triacetoxyborohydride. Studies on direct and indirect reductive amination procedures1. *J. Org. Chem.* **1996,** *61*, 3849–3862.
(108). Abdel-Magid, A. F.; Mehrman, S. J., A review on the use of sodium triacetoxyborohydride in the reductive amination of ketones and aldehydes. *Org. Pro. Res. Dev.* **2006,** *10*, 971–1031.
(109). Edwards, M. G.; Jazzar, R. F. R.; Paine, B. M.; Shermer, D. J.; Whittlesey, M. K.; Williams, J. M. J.; Edney, D. D., Borrowing hydrogen: A catalytic route to C–C bond formation from alcohols. *Chem. Commun.* **2004**, 90–91.
(110). Hamid, M. H. S. A.; Slatford, P. A.; Williams, J. M. J., Borrowing hydrogen in the activation of alcohols. *Adv. Synth. Catal.* **2007,** *349*, 1555–1575.
(111). Winans, C. F.; Adkins, H., The alkylation of amines as catalyzed by nickel. *J. Am. Chem. Soc.* **1932,** *54*, 306–312.
(112). Grigg, R.; Mitchell, T. R. B.; Sutthivaiyakit, S.; Tongpenyai, N., Transition metal-catalysed *N*-alkylation of amines by alcohols. *J. Chem. Soc., Chem, Commun.* **1981**, 611–612.
(113). Tillack, A.; Hollmann, D.; Michalik, D.; Beller, M., A novel ruthenium-catalyzed amination of primary and secondary alcohols. *Tetrahedron Lett.* **2006,** *47*, 8881–8885.
(114). Hamid, M. H. S. A.; Williams, J. M. J., Ruthenium catalysed *N*-alkylation of amines with alcohols. *Chem. Commun.* **2007**, 725–727.
(115). Fujita, K.-i.; Li, Z.; Ozeki, N.; Yamaguchi, R., *N*-alkylation of amines with alcohols catalyzed by a Cp*Ir complex. *Tetrahedron Lett.* **2003,** *44*, 2687–2690.

(116). Fujita, K.-i.; Fujii, T.; Yamaguchi, R., Cp*Ir complex-catalyzed *N*-heterocyclization of primary amines with diols: A new catalytic system for environmentally benign synthesis of cyclic amines. *Org. Lett.* **2004,** *6*, 3525–3528.
(117). Dang, T. T.; Ramalingam, B.; Seayad, A. M., Efficient ruthenium-catalyzed *N*-methylation of amines using methanol. *ACS Catal.* **2015,** *5*, 4082–4088.
(118). Gunanathan, C.; Milstein, D., Selective synthesis of primary amines directly from alcohols and ammonia. *Angew. Chem. Int. Ed.* **2008,** *47*, 8661–8664.
(119). Pingen, D.; Müller, C.; Vogt, D., Direct amination of secondary alcohols using ammonia. *Angew. Chem. Int. Ed.* **2010,** *49*, 8130–8133.
(120). Imm, S.; Bähn, S.; Zhang, M.; Neubert, L.; Neumann, H.; Klasovsky, F.; Pfeffer, J.; Haas, T.; Beller, M., Improved ruthenium-catalyzed amination of alcohols with ammonia: Synthesis of diamines and amino esters. *Angew. Chem. Int. Ed.* **2011,** *50*, 7599–7603.
(121). Huang, J.-L.; Dai, X.-J.; Li, C.-J., Iridium-catalyzed direct dehydroxylation of alcohols. *Eur. J. Org. Chem.* **2013,** *2013*, 6496–6500.
(122). Dai, X.-J.; Li, C.-J., En route to a practical primary alcohol deoxygenation. *J. Am. Chem. Soc.* **2016,** *138*, 5433–5440.
(123). Bauer, J. O.; Leitus, G.; Ben-David, Y.; Milstein, D., Direct synthesis of symmetrical azines from alcohols and hydrazine catalyzed by a ruthenium–pincer complex: Effect of hydrogen bonding. *ACS Catal.* **2016,** *6*, 8415–8419.
(124). Das, U. K.; Ben-David, Y.; Diskin-Posner, Y.; Milstein, D., *N*-substituted hydrazones by manganese-catalyzed coupling of alcohols with hydrazine: Borrowing hydrogen and acceptorless dehydrogenation in one system. *Angew. Chem. Int. Ed.* **2018,** *57*, 2179–2182.
(125). Miyaura, N., Organoboron compounds. In *Cross-Coupling Reactions: A practical guide*, Miyaura, N., Ed. Springer: Berlin, 2002; pp 11–59.
(126). McIntosh, M. L.; Moore, C. M.; Clark, T. B., Copper-catalyzed diboration of ketones: Facile synthesis of tertiary *α*-hydroxyboronate esters. *Org. Lett.* **2010,** *12*, 1996–1999.
(127). Zhu, Q.; He, Z.; Wang, L.; Hu, Y.; Xia, C.; Liu, C., *α*-C–H borylation of secondary alcohols *via* ru/fe relay catalysis: Building a platform for alcoholic C–H/C–O functionalizations. *Chem. Commun.* **2019,** *55*, 11884–11887.
(128). Hamid, M. H. S. A.; Slatford, P. A.; Williams, J. M. J., Borrowing hydrogen in the activation of alcohols. **2007,** *349*, 1555–1575.
(129). Cho, C. S.; Kim, B. T.; Kim, T.-J.; Shim, S. C., An unusual type of ruthenium-catalyzed transfer hydrogenation of ketones with alcohols accompanied by C−C coupling. *J. Org. Chem.* **2001,** *66*, 9020–9022.
(130). Cho, C. S.; Kim, B. T.; Kim, T.-J.; Chul Shim, S., Ruthenium-catalyzed regioselective *α*-alkylation of ketones with primary alcohols. *Tetrahedron Lett.* **2002,** *43*, 7987–7989.

(131). Obora, Y., Recent advances in *α*-alkylation reactions using alcohols with hydrogen borrowing methodologies. *ACS Catal.* **2014,** *4*, 3972–3981.
(132). Genç, S.; Günnaz, S.; Çetinkaya, B.; Gülcemal, S.; Gülcemal, D., Iridium(I)-catalyzed alkylation reactions to form *α*-alkylated ketones. *J. Org. Chem.* **2018,** *83*, 2875–2881.
(133). Martínez, R.; Brand, G. J.; Ramón, D. J.; Yus, M., $[Ru(DMSO)_4]Cl_2$ catalyzes the *α*-alkylation of ketones by alcohols. *Tetrahedron Lett.* **2005,** *46*, 3683–3686.
(134). Taguchi, K.; Nakagawa, H.; Hirabayashi, T.; Sakaguchi, S.; Ishii, Y., An efficient direct *α*-alkylation of ketones with primary alcohols catalyzed by $[Ir(cod)Cl]_2/PPh_3$/KOH system without solvent. *J. Am. Chem. Soc.* **2004,** *126*, 72–73.
(135). Ogawa, S.; Obora, Y., Iridium-catalyzed selective *α*-methylation of ketones with methanol. *Chem. Commun.* **2014,** *50*, 2491–2493.
(136). Akhtar, W. M.; Cheong, C. B.; Frost, J. R.; Christensen, K. E.; Stevenson, N. G.; Donohoe, T. J., Hydrogen borrowing catalysis with secondary alcohols: A new route for the generation of *β*-branched carbonyl compounds. *J. Am. Chem. Soc.* **2017,** *139*, 2577–2580.
(137). Chakraborty, P.; Gangwar, M. K.; Emayavaramban, B.; Manoury, E.; Poli, R.; Sundararaju, B., *α*-alkylation of ketones with secondary alcohols catalyzed by well-defined Cp^*Co^{III}-complexes. *ChemSusChem* **2019,** *12*, 3463–3467.
(138). Bettoni, L.; Gaillard, S.; Renaud, J.-L., Iron-catalyzed *α*-alkylation of ketones with secondary alcohols: Access to *β*-disubstituted carbonyl compounds. *Org. Lett.* **2020,** *22*, 2064–2069.
(139). Cheang, D. M. J.; Armstrong, R. J.; Akhtar, W. M.; Donohoe, T. J., Enantioconvergent alkylation of ketones with racemic secondary alcohols *via* hydrogen borrowing catalysis. *Chem. Commun.* **2020,** *56*, 3543–3546.
(140). Martínez, R.; Ramón, D. J.; Yus, M., $RuCl_2(DMSO)_4$ catalyzes the *β*-alkylation of secondary alcohols with primary alcohols through a hydrogen autotransfer process. *Tetrahedron* **2006,** *62*, 8982–8987.
(141). Cheung, H. W.; Lee, T. Y.; Lui, H. Y.; Yeung, C. H.; Lau, C. P., Ruthenium-catalyzed *β*-alkylation of secondary alcohols with primary alcohols. *Adv. Synth. Catal.* **2008,** *350*, 2975–2983.
(142). Wang, Q.; Wu, K.; Yu, Z., Ruthenium(III)-catalyzed *β*-alkylation of secondary alcohols with primary alcohols. *Organometallics* **2016,** *35*, 1251–1256.
(143). Fujita, K.-i.; Asai, C.; Yamaguchi, T.; Hanasaka, F.; Yamaguchi, R., Direct *β*-alkylation of secondary alcohols with primary alcohols catalyzed by a Cp*Ir complex. *Org. Lett.* **2005,** *7*, 4017–4019.
(144). Pontes da Costa, A.; Viciano, M.; Sanaú, M.; Merino, S.; Tejeda, J.; Peris, E.; Royo, B., First Cp*-functionalized *N*-heterocyclic carbene and its coordination to iridium. Study of the catalytic properties. *Organometallics* **2008,** *27*, 1305–1309.

(145). Yang, J.; Liu, X.; Meng, D.-L.; Chen, H.-Y.; Zong, Z.-H.; Feng, T.-T.; Sun, K., Efficient iron-catalyzed direct *β*-alkylation of secondary alcohols with primary alcohols. *Adv. Synth. Catal.* **2012,** *354*, 328–334.
(146). Chakraborty, S.; Daw, P.; Ben David, Y.; Milstein, D., Manganese-catalyzed *α*-alkylation of ketones, esters, and amides using alcohols. *ACS Catal.* **2018**, 10300–10305.
(147). Thiyagarajan, S.; Gunanathan, C., Catalytic cross-coupling of secondary alcohols. *J. Am. Chem. Soc.* **2019,** *141*, 3822–3827.
(148). Knoevenagel, E., Condensation von malonsäure mit aromatischen aldehyden durch ammoniak und amine. *Chem. Ber.* **1898,** *31*, 2596–2619.
(149). Grigg, R.; Mitchell, T. R. B.; Sutthivaiyakit, S.; Tongpenyai, N., Oxidation of alcohols by transition metal complexes part V. Selective catalytic monoalkylation of arylacetonitriles by alcohols. *Tetrahedron Lett.* **1981,** *22*, 4107–4110.
(150). Thiyagarajan, S.; Gunanathan, C., Ruthenium-catalyzed *α*-olefination of nitriles using secondary alcohols. *ACS Catal.* **2018,** *8*, 2473–2478.
(151). Thiyagarajan, S.; Gunanathan, C., Facile ruthenium(II)-catalyzed *α*-alkylation of arylmethyl nitriles using alcohols enabled by metal–ligand cooperation. *ACS Catal.* **2017,** *7*, 5483–5490.
(152). Anxionnat, B.; Gomez Pardo, D.; Ricci, G.; Cossy, J., First intramolecular alkylation of nitriles with primary and secondary alcohols catalyzed by iridium complexes. *Eur. J. Org. Chem.* **2012,** *2012*, 4453–4456.
(153). Slatford, P. A.; Whittlesey, M. K.; Williams, J. M. J., C–C bond formation from alcohols using a xantphos ruthenium complex. *Tetrahedron Lett.* **2006,** *47*, 6787–6789.
(154). Anxionnat, B.; Gomez Pardo, D.; Ricci, G.; Cossy, J., Monoalkylation of acetonitrile by primary alcohols catalyzed by iridium complexes. *Org. Lett.* **2011,** *13*, 4084–4087.
(155). Guo, L.; Liu, Y.; Yao, W.; Leng, X.; Huang, Z., Iridium-catalyzed selective *α*-alkylation of unactivated amides with primary alcohols. *Org. Lett.* **2013,** *15*, 1144–1147.
(156). Chakraborty, S.; Daw, P.; Ben David, Y.; Milstein, D., Manganese-catalyzed *α*-alkylation of ketones, esters, and amides using alcohols. *ACS Catal.* **2018,** *8*, 10300–10305.
(157). Jang, Y. K.; Krückel, T.; Rueping, M.; El-Sepelgy, O., Sustainable alkylation of unactivated esters and amides with alcohols enabled by manganese catalysis. *Org. Lett.* **2018,** *20*, 7779–7783.
(158). Iuchi, Y.; Obora, Y.; Ishii, Y., Iridium-catalyzed *α*-alkylation of acetates with primary alcohols and diols. *J. Am. Chem. Soc.* **2010,** *132*, 2536–2537.
(159). Löfberg, C.; Grigg, R.; Keep, A.; Derrick, A.; Sridharan, V.; Kilner, C., Sequential one-pot bimetallic Ir(III)/Pd(0) catalysed mono-/bis-alkylation and spirocyclisation processes of 1,3-dimethylbarbituric acid and allenes. *Chem. Commun.* **2006**, 5000–5002.

(160). Blank, B.; Kempe, R., Catalytic alkylation of methyl-*N*-heteroaromatics with alcohols. *J. Am. Chem. Soc.* **2010,** *132*, 924–925.
(161). Obora, Y.; Ogawa, S.; Yamamoto, N., Iridium-catalyzed alkylation of methylquinolines with alcohols. *J. Org. Chem.* **2012,** *77*, 9429–9433.
(162). Maercker, A., The wittig reaction. In *Org. React.*, pp 270–490.
(163). Edwards, M. G.; Williams, J. M. J., Catalytic electronic activation: Indirect 'Wittig' reaction of alcohols. *Angew. Chem. Int. Ed.* **2002,** *41*, 4740–4743.
(164). Edwards, M. G.; Jazzar, R. F. R.; Paine, B. M.; Shermer, D. J.; Whittlesey, M. K.; Williams, J. M. J.; Edney, D. D., Borrowing hydrogen: A catalytic route to C–C bond formation from alcohols. *Chem. Commun.* **2004**, 90–91.
(165). Liu, X.; Werner, T., Selective construction of C−C and C=C bonds by manganese catalyzed coupling of alcohols with phosphorus ylides. *Adv. Synth. Catal.* **2021,** *363*, 1096–1104.
(166). Alonso, F.; Riente, P.; Yus, M., One-pot synthesis of stilbenes from alcohols through a wittig-type olefination reaction promoted by nickel nanoparticles. *Synlett* **2009,** *2009*, 1579–1582.
(167). Khaskin, E.; Milstein, D., Catalytic, oxidant-free, direct olefination of alcohols using Wittig reagents. *Chem. Commun.* **2015,** *51*, 9002–9005.
(168). Black, P. J.; Edwards, M. G.; Williams, J. M. J., Catalytic electronic activation as a tool for the addition of stabilised nucleophiles to allylic alcohols. *Tetrahedron* **2005,** *61*, 1363–1374.
(169). Bower, J. F.; Kim, I. S.; Patman, R. L.; Krische, M. J., Catalytic carbonyl addition through transfer hydrogenation: A departure from preformed organometallic reagents. *Angew. Chem. Int. Ed.* **2009,** *48*, 34–46.
(170). Nguyen, K. D.; Park, B. Y.; Luong, T.; Sato, H.; Garza, V. J.; Krische, M. J., Metal-catalyzed reductive coupling of olefin-derived nucleophiles: Reinventing carbonyl addition. *Science* **2016,** *354*, aah5133.
(171). Doerksen, R. S.; Meyer, C. C.; Krische, M. J., Feedstock reagents in metal-catalyzed carbonyl reductive coupling: Minimizing preactivation for efficiency in target-oriented synthesis. *Angew. Chem. Int. Ed.* **2019,** *58*, 14055–14064.
(172). Muñoz, M. P., Silver and platinum-catalysed addition of O–H and N–H bonds to allenes. *Chem. Soc. Rev.* **2014,** *43*, 3164–3183.
(173). Bower, J. F.; Skucas, E.; Patman, R. L.; Krische, M. J., Catalytic C−C coupling *via* transfer hydrogenation: Reverse prenylation, crotylation, and allylation from the alcohol or aldehyde oxidation level. *J. Am. Chem. Soc.* **2007,** *129*, 15134–15135.
(174). Han, S. B.; Kim, I. S.; Han, H.; Krische, M. J., Enantioselective carbonyl reverse prenylation from the alcohol or aldehyde oxidation level employing 1,1-dimethylallene as the prenyl donor. *J. Am. Chem. Soc.* **2009,** *131*, 6916–6917.

(175). Spielmann, K.; Xiang, M.; Schwartz, L. A.; Krische, M. J., Direct conversion of primary alcohols to 1,2-amino alcohols: Enantioselective iridium-catalyzed carbonyl reductive coupling of phthalimido–allene *via* hydrogen auto-transfer. *J. Am. Chem. Soc.* **2019,** *141*, 14136–14141.
(176). Bower, J. F.; Patman, R. L.; Krische, M. J., Iridium-catalyzed C−C coupling *via* transfer hydrogenation: Carbonyl addition from the alcohol or aldehyde oxidation level employing 1,3-cyclohexadiene. *Org. Lett.* **2008,** *10*, 1033–1035.
(177). Shibahara, F.; Bower, J. F.; Krische, M. J., Ruthenium-catalyzed C−C bond forming transfer hydrogenation: Carbonyl allylation from the alcohol or aldehyde oxidation level employing acyclic 1,3-dienes as surrogates to preformed allyl metal reagents. *J. Am. Chem. Soc.* **2008,** *130*, 6338–6339.
(178). Shibahara, F.; Bower, J. F.; Krische, M. J., Diene hydroacylation from the alcohol or aldehyde oxidation level *via* ruthenium-catalyzed C−C bond-forming transfer hydrogenation: Synthesis of *β,γ*-unsaturated ketones. *J. Am. Chem. Soc.* **2008,** *130*, 14120–14122.
(179). Han, H.; Krische, M. J., Direct ruthenium-catalyzed C−C coupling of ethanol: Diene hydro-hydroxyethylation to form all-carbon quaternary centers. *Org. Lett.* **2010,** *12*, 2844–2846.
(180). Nguyen, K. D.; Herkommer, D.; Krische, M. J., Enantioselective formation of all-carbon quaternary centers *via* C–H functionalization of methanol: Iridium-catalyzed diene hydrohydroxymethylation. *J. Am. Chem. Soc.* **2016,** *138*, 14210–14213.
(181). Carey, F. A.; Sundberg, R. J., *Advanced Organic Chemistry: Part A: Structure and Mechanisms*. Springer Science & Business Media: New York, 2007.
(182). Patman, R. L.; Williams, V. M.; Bower, J. F.; Krische, M. J., Carbonyl propargylation from the alcohol or aldehyde oxidation level employing 1,3-enynes as surrogates to preformed allenylmetal reagents: A ruthenium-catalyzed C−C bond-forming transfer hydrogenation. *Angew. Chem. Int. Ed.* **2008,** *47*, 5220–5223.
(183). Geary, L. M.; Woo, S. K.; Leung, J. C.; Krische, M. J., Diastereo- and enantioselective iridium-catalyzed carbonyl propargylation from the alcohol or aldehyde oxidation level: 1,3-enynes as allenylmetal equivalents. *Angew. Chem. Int. Ed.* **2012,** *51*, 2972–2976.
(184). Duarah, G.; Kaishap, P. P.; Begum, T.; Gogoi, S., Recent advances in ruthenium(II)-catalyzed C−H bond activation and alkyne annulation reactions. *Adv. Synth. Catal.* **2019,** *361*, 654–672.
(185). Shek, H.-L.; Yeung, C.-F.; Chung, L.-H.; Wong, C.-Y., A focused review on the unconventional alkyne activations by ruthenium(II) and osmium(II) complexes supported by 1,2-bis(diphenylphosphino)methane (dppm). *Polyhedron* **2021,** *197*, 115023.
(186). Shah, S.; Das, B. G.; Singh, V. K., Recent advancement in copper-catalyzed asymmetric reactions of alkynes. *Tetrahedron* **2021**, 132238.
(187). Katsuki, T.; Martin, V., Asymmetric epoxidation of allylic alcohols: The katsuki–sharpless epoxidation reaction. In *Org. React.*, pp 1–299.

(188). Li, J. J., Tsuji-trost reaction. In *Name Reactions*, Springer: New York, 2021; pp 543–546.
(189). Patman, R. L.; Chaulagain, M. R.; Williams, V. M.; Krische, M. J., Direct vinylation of alcohols or aldehydes employing alkynes as vinyl donors: A ruthenium catalyzed C−C bond-forming transfer hydrogenation. *J. Am. Chem. Soc.* **2009,** *131*, 2066–2067.
(190). Cheng, Q.; Tu, H.-F.; Zheng, C.; Qu, J.-P.; Helmchen, G.; You, S.-L., Iridium-catalyzed asymmetric allylic substitution reactions. *Chem. Rev.* **2019,** *119*, 1855–1969.
(191). Obora, Y.; Hatanaka, S.; Ishii, Y., Iridium-catalyzed coupling reaction of primary alcohols with 1-aryl-1-propynes leading to secondary homoallylic alcohols. *Org. Lett.* **2009,** *11*, 3510–3513.
(192). Liang, T.; Nguyen, K. D.; Zhang, W.; Krische, M. J., Enantioselective ruthenium-catalyzed carbonyl allylation *via* alkyne–alcohol C–C bond-forming transfer hydrogenation: Allene hydrometalation vs oxidative coupling. *J. Am. Chem. Soc.* **2015,** *137*, 3161–3164.
(193). Shi, L.; Tu, Y.-Q.; Wang, M.; Zhang, F.-M.; Fan, C.-A.; Zhao, Y.-M.; Xia, W.-J., A reaction for sp^3–sp^3 C−C bond formation *via* cooperation of lewis acid-promoted/Rh-catalyzed C−H bond activation. *J. Am. Chem. Soc.* **2005,** *127*, 10836–10837.
(194). Hartwig, J. F.; Collman, J. P., *Organotransition Metal Chemistry: From Bonding to Catalysis*. University Science Books: Sausalito, 2010; Vol. 1.
(195). Yamaguchi, E.; Mowat, J.; Luong, T.; Krische, M. J., Regio- and diastereoselective C–C coupling of α-olefins and styrenes to 3-hydroxy-2-oxindoles by Ru-catalyzed hydrohydroxyalkylation. *Angew. Chem. Int. Ed.* **2013,** *52*, 8428–8431.

Chapter 2. *Umpolung* of Carbonyl Compounds as Alkyl Organometallic Reagent Surrogates

2.1 Introduction

Among modern synthetic techniques, organometallic compounds (i.e., chemical complexes containing at least one metal–carbon bond) are the most widely exploited chemical reagents by organic chemists to forge carbon–carbon bonds.[1–3] The partial negative charge of carbon atoms from these compounds provides an exclusive pattern of reactivity, commonly referred to as carbanion character or nucleophilic.[4] Because of the bond polarity, tunable reactivity and selectivity, organometallic complexes find broad and diverse applications in academic and industrial chemical syntheses.[5–7] Classical stoichiometric examples include organolithium,[8, 9] organomagnesium (i.e., Grignard reagents)[10–12] and organoaluminium,[13–15] which are often employed as alkylating agents in nucleophilic addition reactions to carbonyl derivatives. Alternatively, metal–metal exchange of the reactive organometallic compounds with zinc,[16] copper,[17–22] tin,[23, 24] silicon[25–27] and titanium[28] reduces basicity, increases selectivity and functional group compatibility, and thus enables other classes of organic reactions. Organocopper complexes, for example, are versatile nucleophilic reagents for either conjugate addition or substitution reactions, depending on the constitution of cuprate species and electrophilic substrates.[18–22] More importantly, they can catalyze these reactions in an stereoselective manner.[29, 30] Beyond addition and substitution reactions, past decades have witnessed the extensive uptake of organometallic compounds (e.g., organoboron, -magnesium, -copper, -zinc, -tin, -lithium, and -silicon) as nucleophilic partners in metal-catalyzed (e.g, copper, palladium, nickel, iron, cobalt, etc.) cross-coupling reactions.[31–37] With the aid of metal catalysts and ligands, these coupling reactions impart precise control over the product distribution in terms of chemo-, regio- and stereochemistry. As a result, cross-coupling reactions exert a profound impact on the modern production of agrochemicals and pharmaceuticals. Despite organometallic reagents prevail as vital carbon-based nucleophiles, there are three main constraints or considerations when applying them to different classes of chemical reactions: 1) the preparations of the highly active organometallic species are non-trivial due to the stringent exclusion of oxygen and moisture, and safety precautions for handling cryogenic conditions; 2) high reactivity is associated with low functional group tolerance

and poor chemoselectivity, which further limits functional groups that can present in the feedstock chemical precursors. Although efforts on reducing reactivity were made *via* either metal–metal or metal–halogen exchange,[38–40] the presynthesis of highly active organometallic complexes or solution titration (titration to ensure the correct molar concentration of organometallic reagents) was often required (i.e., added operational complexity); 3) a strong dependence on petroleum-derived feedstock chemicals (e.g., organohalides and unsaturated hydrocarbons) and metal as stoichiometric precursors to produce metallic carbanion equivalents,[41–43] which are commercially accessible but may not be sustainable in the long-term.[44, 45]

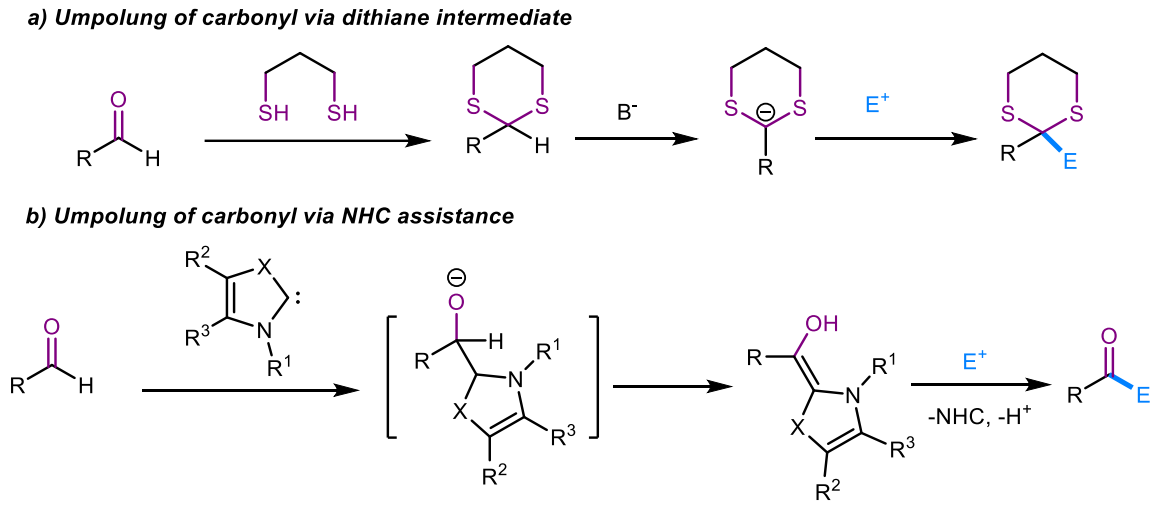

Scheme 2.1 Symbolic examples of *umpolung* carbonyl chemistry

The inversion of innate polarity of organic functional groups, coined as '*umpolung*' in the late 1970s, is a key conceptual advancement in the chemical bond-forming strategy.[46, 47] As is shown in the seminal work by Seebach and Corey, the *umpolung* of electrophilic aldehydes as acyl anion equivalents *via* stoichiometric dithiane chemistry, where a negative charge is placed on the carbon atom of a carbonyl group.[48] As a result, aldehydes become nucleophilic and prone to attack other electrophiles. More recently, the *N*-cyclic carbene (NHC) chemistry offered catalytic access to acyl anion equivalents as an elegant avenue (Scheme 2.1).[49–51] Carbanion intermediates derived from carbonyl groups at a lower oxidation state than acyl anions, or alkyl (deoxy-acyl) anions, are synthetically important yet much less explored in the modern era. The Wolff–Kishner (WK) reduction generates such anionic alkyl species, which are protonated and converted to methylene products.[52, 53] The *umpolung* of carbonyl compounds as alkyl anion equivalents is achieved by a

sequential hydrazone formation, deprotonation-tautomerization and N_2 extrusion process. While being a powerful synthetic method, the WK reduction and its related modifications have found rare applications beyond the deoxygenation chemistry in organic synthesis.[54] The alkyl carbanion equivalents obtained from this carbonyl *umpolung* process, in principle, can react with other electrophiles, and therefore construct chemical bonds other than carbon–hydrogen bond.[55–59]

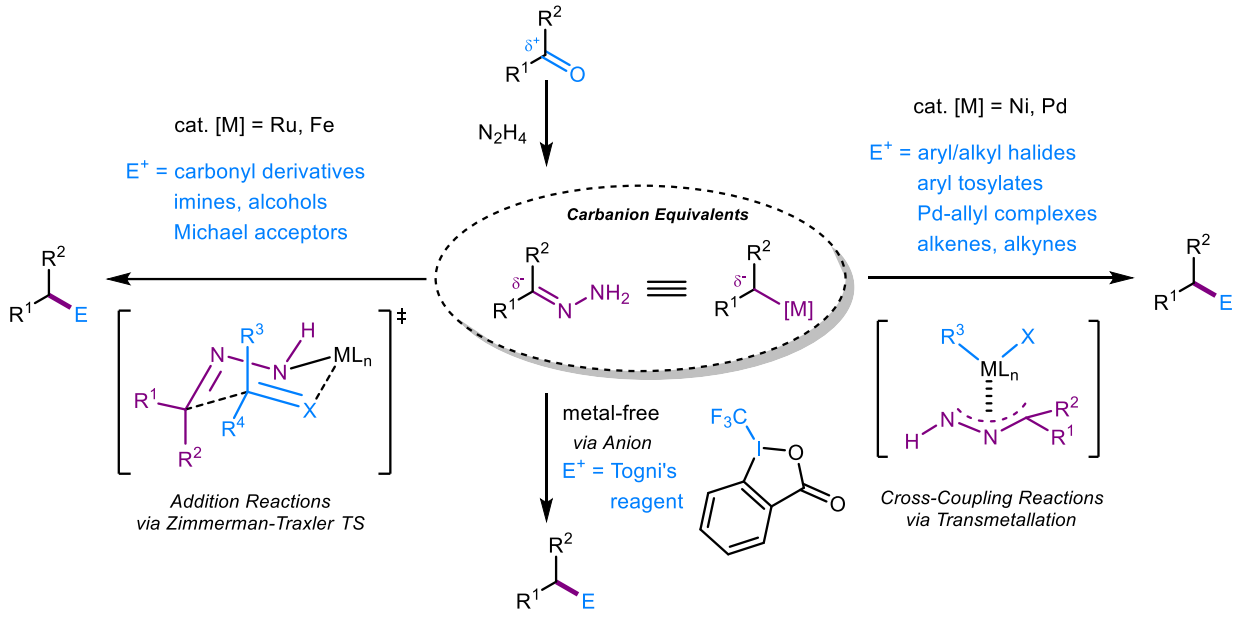

Figure 2.1 Three different mechanisms of C–C bond formation of hydrazones

Concurrent to sustainable chemical syntheses — a long-term research objective in our laboratory, we recently discovered an efficient ruthenium-based catalytic system that promotes 1,2-carbonyl addition reaction between carbonyl-derived hydrazones and carbonyl compounds. By engineering base, catalyst, auxiliary ligand and reaction conditions, the synthetic utility of such carbonyl-derived hydrazones has been rapidly expanded to a variety of carbon–carbon bond-forming processes, where carbonyl compounds are masked as catalytic alkyl organometallic pronucleophiles. This Account summaries the relevant conceptual and research development in our research group. Importantly, we think that all carbon–carbon bond-forming reactions shown in the Account undergo through three distinctive reaction mechanisms, which are tied to the choice of metals and electrophiles. Therefore, discussions are classified based on these three general mechanisms: (1) *via* the Zimmerman–Traxler transition state (TS) and denitrogenation process, (2) *via* the denitrogenation and transmetallation process, and (3) *via* the anionic process (Figure 2.1).

2.2 C–C bond formation *via* Zimmerman–Traxler TS and denitrogenation

2.2.1 Additions to carbonyl compounds

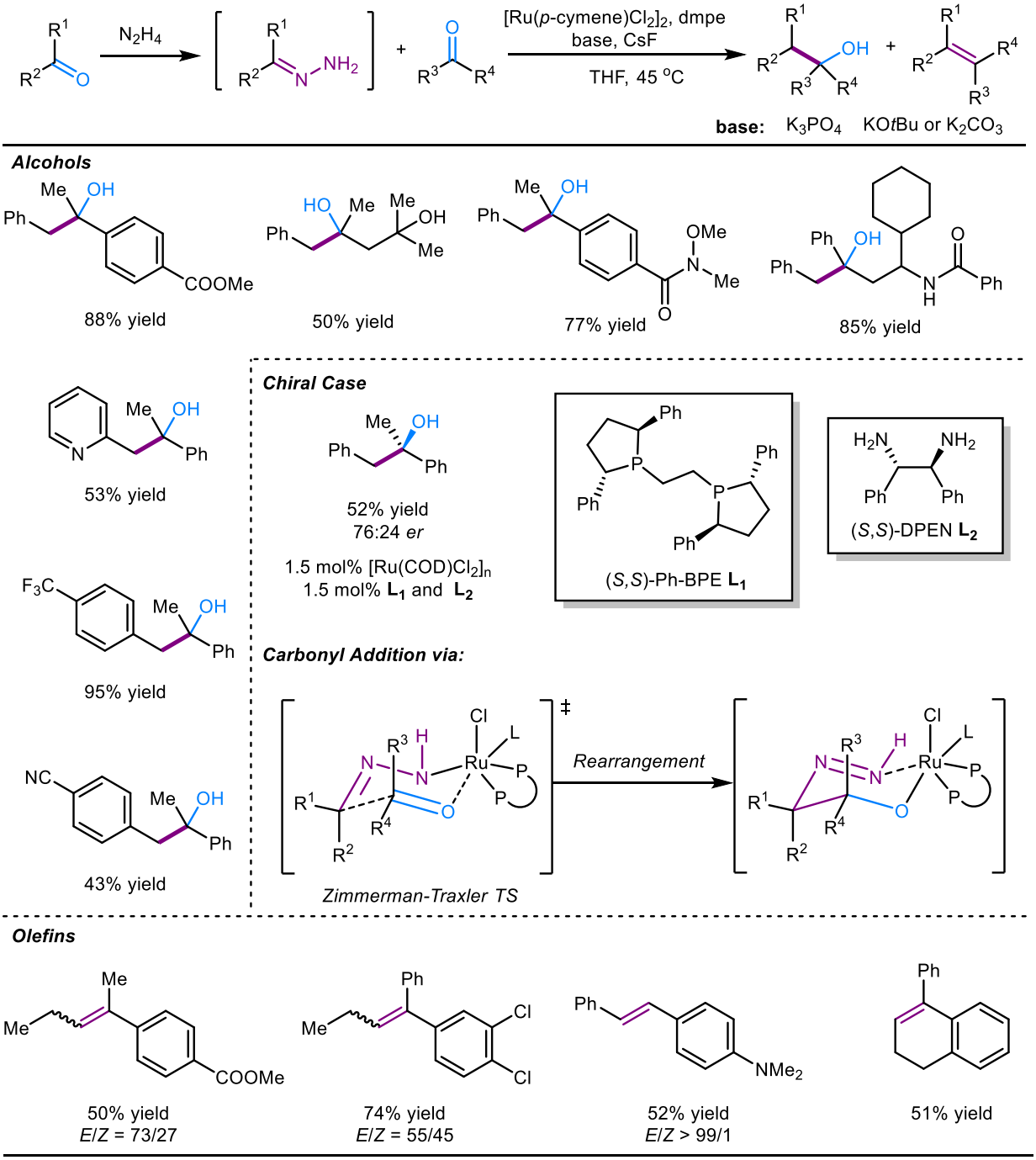

Scheme 2.2 *Umpolung* of carbonyl compounds for additions to carbonyl compounds

Inspired by the design of using hydrazone as carbanion equivalent, we began evaluating aldehydes and ketones, the most commonly used electrophiles, in attempts to trap the hydrazone-derived alkyl anions (Scheme 2.2).[60] To favor the desired carbon–carbon bond-forming pathway, the employment of an electron-rich bidentate phosphine ligand dmpe and a mild base K_3PO_4 proved quite crucial. Despite a less apparent mechanistic rationale, the addition of CsF to the reaction mixture enabled a fast reaction kinetics and an improved reaction conversion. Due to the mild reaction conditions, valuable classes of secondary and tertiary alcohols are readily accessible with very high chemoselectivity and good tolerance for polar functional groups. Contrary to aldehydes bearing *α*-aryl and heteraryl substituents, which are generally good pronucleophiles in this chemistry, ketones were less prone to the metal ligation and exhibited poor reactivity and slow kinetics even at 80 °C. Importantly, this ruthenium-catalyzed addition reaction of carbonyl-derived nucleophiles to carbonyl compounds showed a great potential for the catalyst control over stereoselectivity. A modest enantioselectivity was achieved when chiral bisphosphine and diamine ligands replaced the racemic dmpe. Inspired by aldol type C–C bond formation and the indispensable role of ruthenium catalyst, we proposed that the most plausible reaction mechanism of this catalytic carbon–carbon bond-forming process involved the generation of a coordinately unsaturated ruthenium-bound hydrazone, its metalation with the carbonyl compound *via* the Zimmerman–Traxler six-membered ring transition state,[61] and the subsequent rearrangement, denitrogenation and protonation. After extensive screening, we found that two carbonyl compounds can not only form alcohols, but also generate olefins.[62] The divergence of these different reaction pathways is primarily controlled by (1) carbonyl substrates (i.e., pronucleophiles) and (2) basicity of base. While aromatic aldehydes and a weak inorganic base prefer the formation of alcohols, aliphatic aldehydes and a strong base favor the olefination reaction. Specifically, by switching to KO^tBu, aliphatic aldehyde-derived hydrazones can react with aromatic aldehydes or ketones to generate *di*- or *tri*-substituted olefins — olefination *via* a formally reductive carbonyl cross-coupling reaction. This divergent olefination pathway is presumably due to the formation of a less stabilized carbanionic intermediate (i.e., sp^3 alkyl vs sp^2 aryl substituent at the *α*-position of the anions) and its propensity to undergo E1cB-type elimination mediated by a strong base. Recently, Milstein *et al.* reported an elegant Mn-catalyzed olefination approach, in which alcohols act as alternative precursors to carbonyl compounds.[63] The study of chemoselectivity in C–C bond formation of hydrazones with carbonyls will be discussed in details in Chapter 5.

2.2.2 Additions to aryl imines

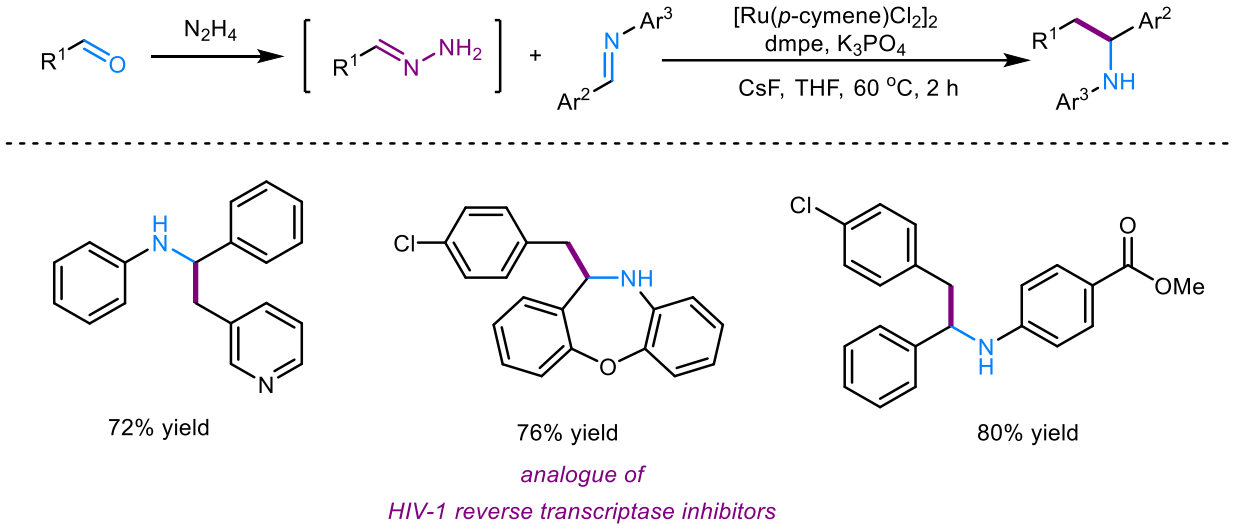

Scheme 2.3 *Umpolung* of carbonyl compounds for additions to aryl imines

Following our initial findings of the nucleophilic addition reaction to form carbon–carbon bonds together with the inspiration of possible Zimmerman–Traxler six-membered ring transition state, we naturally considered whether other polarized π-system could be utilized as *C*-electrophiles, such as imines (Scheme 2.3). We recognized that less electrophilic imines could be challenging partners than ketones and aldehydes for the development of an analogues 1,2-addition reaction. In fact, slightly higher amounts of K_3PO_4 and CsF, as well as an elevated temperature were necessary in the imine addition to achieve the comparable reactivity seen in the carbonyl addition reaction.[64] Unlike ketimines and *N*-alkyl aldimines, which were unreactive imine electrophiles, *N*-aryl aldimines were viable electrophilic partners to react with aldehyde-derived alkyl carbanion equivalents, delivering a library of secondary aniline analogs that are difficult to attain otherwise. Consistent with the carbonyl addition and the olefination chemistry, the imine addition reaction tolerates functional groups including cyano, amide and ester. This method was successfully applied to the gram-scale alkylation of the dibenzoxazepine bearing a *cis* imine functional group, a common *aza*-heterocyclic scaffold shared among bioactive medicinal agents such as antidepressants, antipsychotics and HIV-1 reverse transcriptase inhibitors.[65, 66]

2.2.3 Additions to carbon dioxide

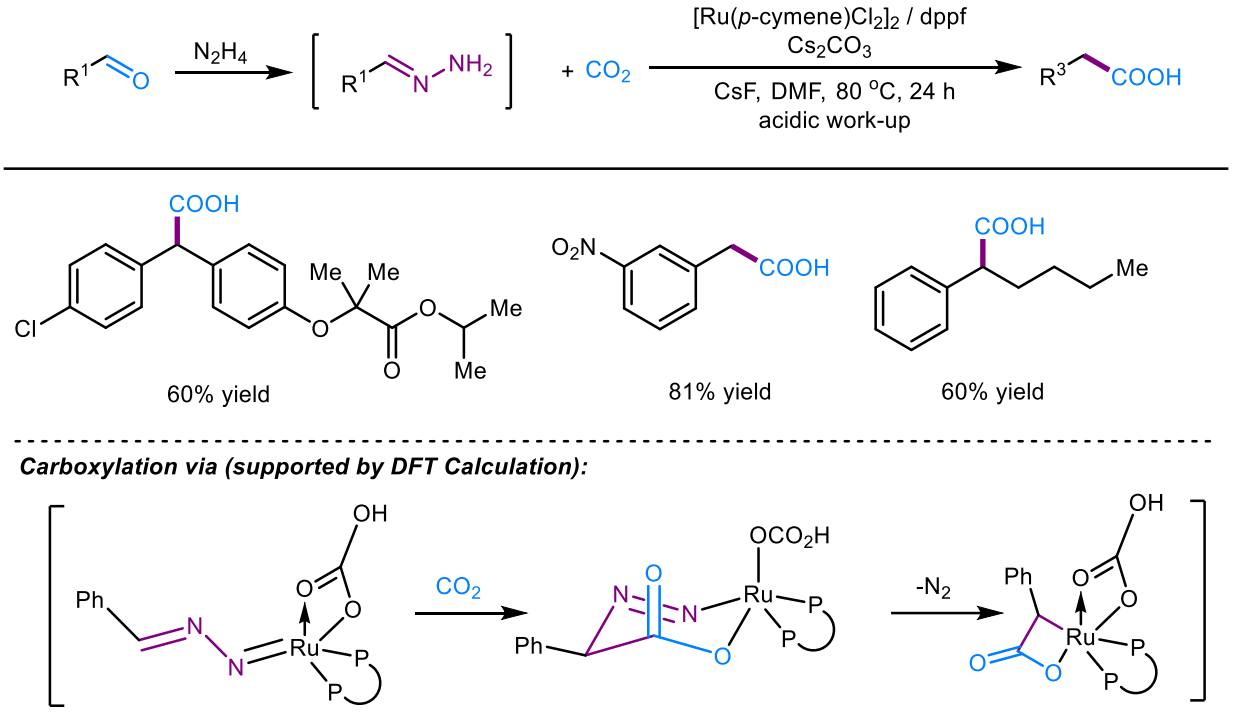

Scheme 2.4 *Umpolung* of carbonyl compounds for additions to carbon dioxide

During our studies on this novel carbonyl *umpolung* chemistry, it is quite evident that ketones are much less reactive than aldehydes as pronucleophiles to generate catalytic alkyl carbanions. Although the exact reason has not been fully elucidated, one of the mitigation strategies could be the employment of carbonyl derivatives that are innately more electrophilic than aldehydes. We thus envisioned that carbon dioxide may serve this purpose by intercepting the low reactive ketone-derived carbanionic species. Indeed, the Ru-catalyzed carboxylation of hydrazones occurred efficiently by replacement of air-sensitive bisphosphine ligand dmpe with relatively more air-stable dppf (Scheme 2.4).[67] In addition to aromatic and heteroaromatic aldehydes, we demonstrated that a variety of aromatic ketones can be used as feasible pronucleophiles to react with CO_2. Consequently, rapid structural diversification of the corresponding aryl acetic acids enabled synthesis of multiple valuable bioactive molecules, including Felbinac and Adiphenine.[68] In parallel with above synthetic applications, DFT calculations uncovered the catalytic cycle of this new carboxylation reaction, consisting of a key Ru-nitrenoid intermediate to undergo intermolecular [4+2] cycloaddition.

2.2.4 Additions to Michael acceptors

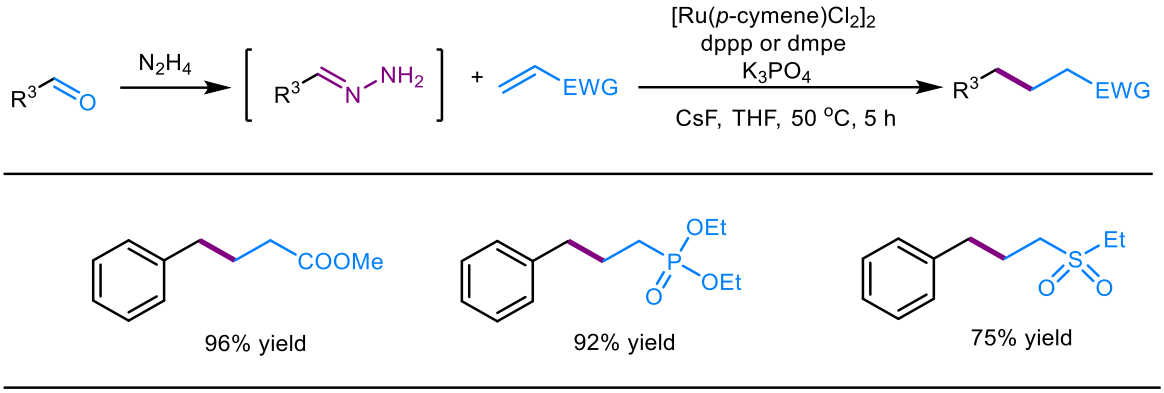

Scheme 2.5 *Umpolung* of carbonyl compounds for additions to Michael acceptors

Another important class of C–C bond forming strategy features the conjugate addition reaction of carbon nucleophiles to electron-deficient olefins, where the exclusive 1,4-regioselectivity is often achieved by the presence of 'soft' metal catalysts such as copper, rhodium and among others.[29, 30, 69–71] By analogy to the polarized C=X bonds in carbonyl derivatives, we contemplated that the electron-deficient olefins bearing the polarized C–C double bonds could be as equally reactive when intercepting the Ru-ligated hydrazone complex.[60] Capitalizing on the 'soft' nature of the homogenous ruthenium(II) catalysis (Scheme 2.5),[72] the conjugate addition reaction of aldehyde-derived hydrazones to a wide range of electron-deficient olefins took place under mild conditions.[73] Ligand selection influenced much the reaction outcomes. As an example, 1,3-bis(diphenylphosphino)propane (dppp) was a more efficient spectator ligand for the most electron-deficient aromatic aldehyde pronucleophiles, whereas dmpe provided higher yields with those electron-rich counterparts. Viable electron-withdrawing substituents of the *α*,*β*-unsaturated olefins included esters, ketones, sulfones, phosphonates and amides. The complete 1,4-regioselectivity was observed in the cases of the acyclic enone and 2-cycolpentenone.

2.2.5 Iron-catalyzed addition reaction

In retrospect, it would have been difficult to predict that the ruthenium-based catalyst we developed for a selective alcohol deoxygenation process could accommodate such a diverse array of *C*-electrophiles in the nucleophilic addition reactions. More fortuitously, we learned that the precious ruthenium metal is not the only catalyst capable of promoting the carbon–carbon bond-

forming processes. In a subsequent study, we found that an earth abundant metal — iron, with dmpe bound, is a much more robust catalyst than the ruthenium complex for most of the addition-type transformations at room temperature (Scheme 2.6). In particular, the higher efficiency was observed in the carbonyl addition reactions.[74] We were encouraged by these positive results attainable from a non-precious metal source. They prompted us to explore alternative metal catalysts which might have ligated carbonyl-derived hydrazones and electrophiles differently in types of chemical reactions beyond the addition reactions. (This section is going to be discussed in detail in Chapter 6).

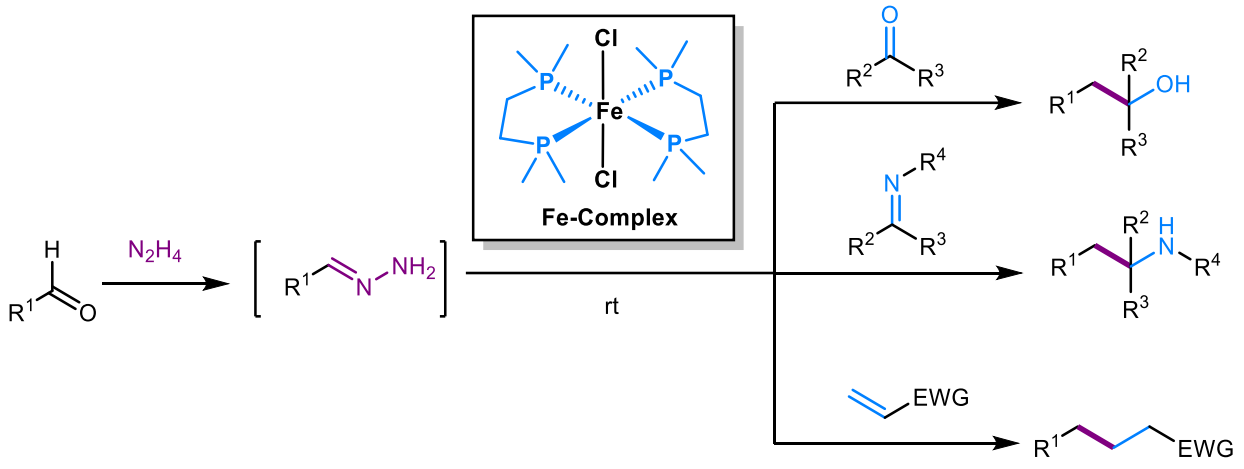

Scheme 2.6 *Umpolung* of carbonyl compounds for the addition reactions with iron catalysis

2.2.6 Cascade reactions

The strategy of *umpolung* carbonyl as organometallic reagent surrogate is not only providing a method of various C–C bond formation reaction, but also identifying the advantages over the traditional carbanion reagent. It is known that most of organometallic reagents are sensitive to air, water and sometimes transition metal catalysts.[75–82] Moreover, they usually has poor functional group tolerance especially acidic protons. Consequently, the utilization of organometallic reagent in one-pot reaction is quite limited. *Umpolung* carbonyls, however, have a much stronger acidic proton tolerance. Thus, we turned to study the possible cascade reaction of hydrazones taking advantage of transition metal catalytic system.

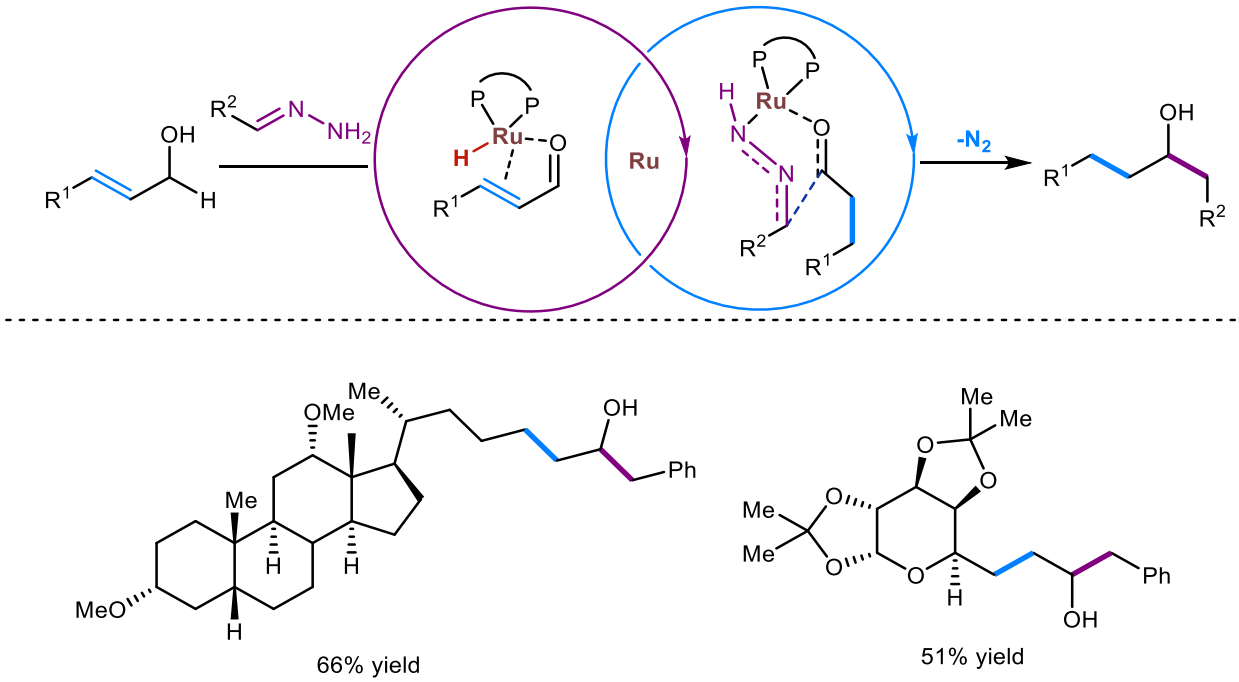

Scheme 2.7 *Umpolung* of carbonyl compounds for the cascade redox reaction

Since our initial study of such an *umpolung* carbonyl chemistry was under ruthenium system, we first considered the possible cascade reaction bound ruthenium catalysis. Recently, the concept of 'chain walking' arouse the interest of chemists for its being an efficient way to realize remote functionalization.[83–86] Ruthenium catalyst, serving as one of the most common catalysts in olefin isomerization reaction, seems to be a potential catalyst for 'chain walking' reaction.[87–93] As such, we considered to utilize this strategy together with the C–C bond formation ability of hydrazones to realize some unique transformations.

The α-alkylation of alcohol is one of the successful cases. As is known, aldehydes/ketones, though very synthetically useful, are sometimes hard to access and with poor functional group tolerance, especially in late-stage functionalization.[82] Alcohol, to the opposite, is not only easily accessible in nature, but also much more stable than carbonyls. Thus, empowering alcohol as carbonyl surrogate would be appealing for synthetic chemistry. In the late 20th century, Trost *et al* had shown that with ruthenium catalysts, allylic alcohols could undergo isomerization to form carbonyls.[87–90] Inspired by this, we investigated using allylic alcohol as carbonyl surrogate to C–C bonds with hydrazone, directly on the α-position of allylic alcohols *via* a tandem isomerization/nucleophilic addition process. Fortunately, our study shows that with bulky and electron-rich bidentate

phosphine ligand, such a transformation could occur smoothly under very mild conditions (Scheme 2.7).[94] Substrate wise, both primary and secondary allylic alcohols were effective. Homoallylic and alcohols possessing olefins at longer range could also efficiently achieve such a transformation, albeit with both a higher temperature and higher catalyst loading. However, the hydrazone wise, the Ru–bisphosphine system was only effective with aromatic aldehyde hydrazones; whereas the Ru–PCP pincer complex as catalyst could overcome this limitation and was effective for aliphatic aldehyde hydrazones.

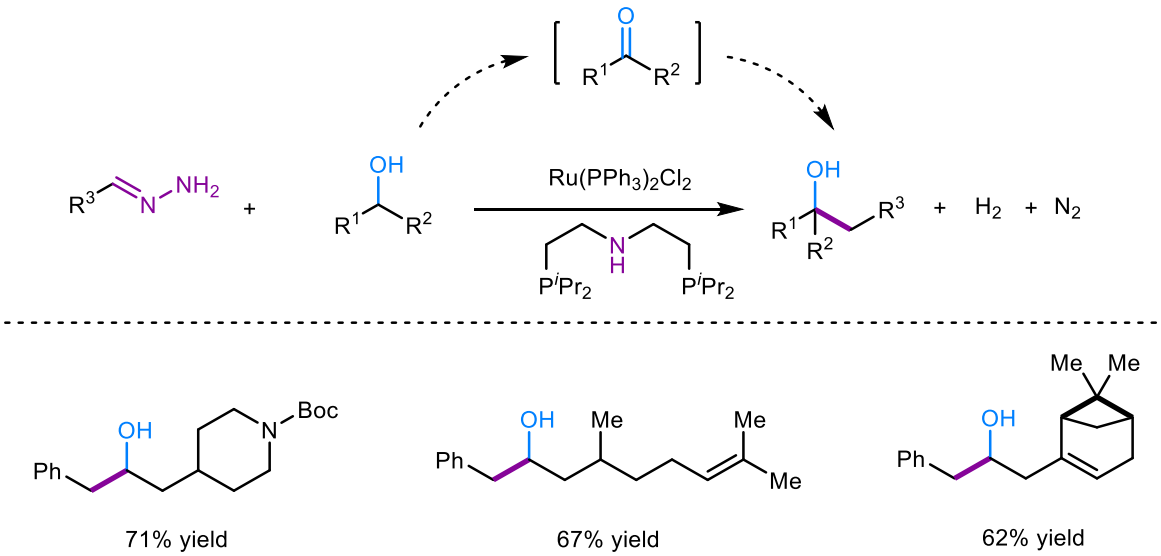

Scheme 2.8 Grignard-type reaction with alcohol as carbonyl surrogate

Other than olefinic alcohols, we then studied whether the simple alcohol can still serve as carbonyl surrogate to undergo *α*-alkylation directly (Scheme 2.8). We initially tested the ruthenium–bisphosphine system as used in the reaction of olefinic alcohols. However, despite the trace amount of product being observed, the starting material mostly remains unchanged. We attributed this low reactivity a kinetic problem associated with oxidation of alcohol to carbonyl step. According to Noyori-type hydrogenation / dehydrogenation, the introduction of amine ligand in Ru–phosphine system could greatly accelerate the hydrogenation / dehydrogenation process tributed to the six-membered ring transition state.[95–97] Inspired by this, we found that, by using the Ru–PNP complex, various alcohols allowed the *α*-alkylation with hydrazones in moderate to high yield, with various sensitive functional groups being tolerated. Thus, we successfully enabled alcohols as carbonyl

surrogate for C–C bond formation, very hard to realize by classical organometallic chemistry. (This section is going to be discussed in detail in Chapter 4.)

2.3 C–C bond formation *via* denitrogenation and transmetallation

Given an increasingly significant role that cross-coupling reactions play in contemporary organic chemistry and drug discovery, our next target was to enable this catalytic process of carbonyl *umpolung* in these reactions. In contrast to the polarized π bonds that electrophiles contain in the addition reactions, however, most electrophilic cross-coupling partners typically share the polarized σ bonds. As a result, the involvement of a Zimmerman–Traxler chair-like transition state is unlikely in the coupling reaction. In fact, the attempt to employ ruthenium complex in the cross-coupling reactions proved unsuccessful. Instead, common metal catalysts of choice in the field, such as palladium and nickel complexes, provided us with highly successful results.[98]

2.3.1 Cross-couplings with aryl halides

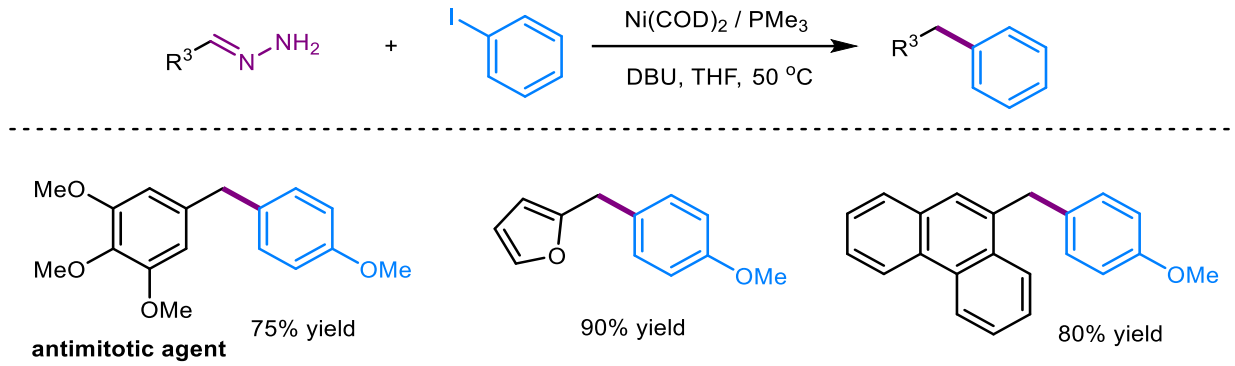

Scheme 2.9 *Umpolung* of carbonyl compounds for the cross-coupling reaction with aryl halides

Aryl iodides, for their higher reactivity, were first examined as the electrophilic coupling partners (Scheme 2.9).[99] After extensive catalyst screenings, we found that bis(cyclooctadiene)nickel could serve as an efficient precatalyst for the cross-coupling reaction between hydrazones and aryl iodides. Coupled with this nickel(0) complex, the electron-rich non-bulky monodentate phosphine ligand PMe_3 and the soluble organic base DBU were required to achieve the desirable catalytic turnovers in THF at 50 °C. Such mild reaction conditions encompassed a broad array of pronucleophilic hydrazone substrates as well as extended the coupling reactions to less reactive aryl bromides and aryl chlorides, albeit in a prolonged reaction time.[98]

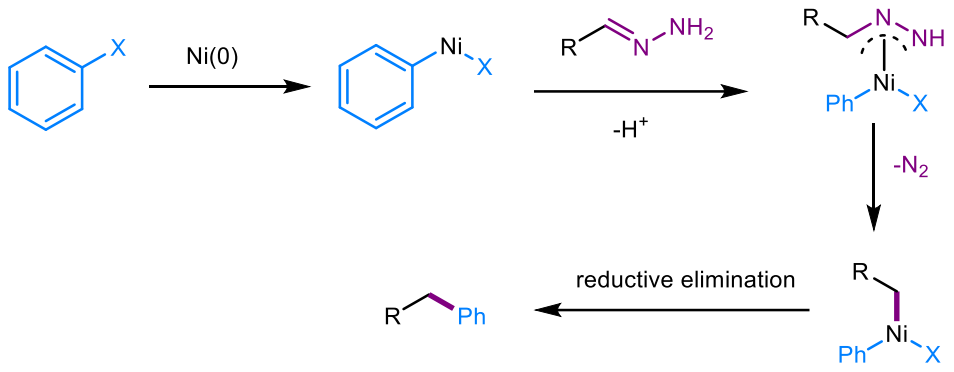

Scheme 2.10 Tentative mechanism for the cross-coupling reaction with aryl halides

While lacking of the experimental evidence to elucidate the reaction pathway, we thought that the metalation of hydrazone might have occurred in a different manner than that from the addition reactions, where the Zimmerman–Traxler transition state stemmed from hydrazone and the π electrophile tends to be the most plausible intermediate prior to the formation of a new carbon–carbon bond (Scheme 2.10). Specifically, the base-mediated exclusion of nitrogen from the Ni metal center could have happened proceeding the ligation of the oxidative Ni(II) complex with hydrazone *via* a four-member-ring *aza*-metallacycle. Subsequent to the transmetalation of the alkyl group from hydrazone to the Ni(II) complex, the reductive elimination would have delivered the alkyl–aryl coupling products. Despite the elusive mechanistic insights, the success of implementing carbonyl-derived hydrazones in the cross-coupling reaction implied that they are feasible nucleophilic alkyl coupling partners.

2.3.2 Cross-couplings with phenol derivatives

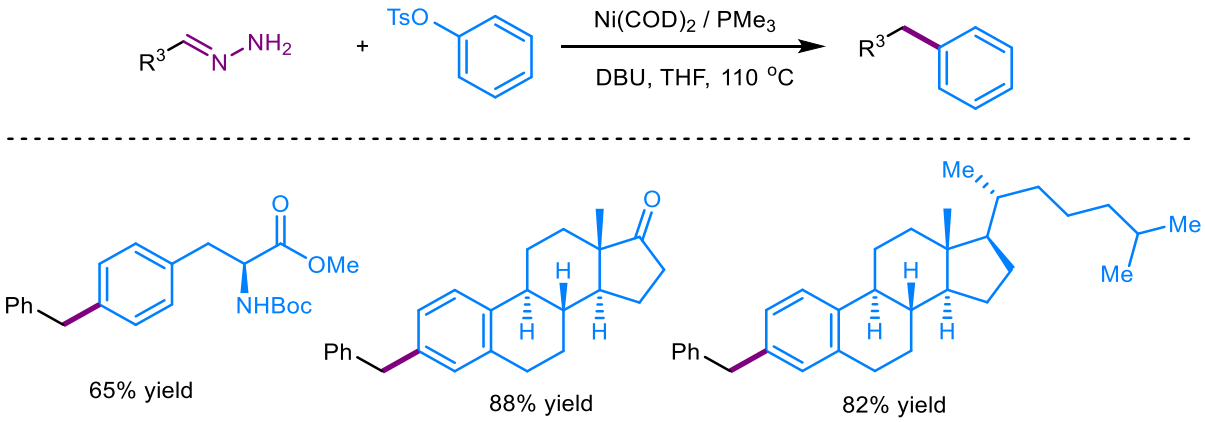

Scheme 2.11 *Umpolung* of carbonyl compounds for the cross-coupling reaction with phenol derivatives

As the alternative sp^2 cross-coupling partners, phenol derivatives represent more naturally abundant and less chemically hazardous aryl sources than aryl halides (Scheme 2.11).[100] Thus, developing greener aryl/alkyl equivalents from alcohol and phenol derivatives in the coupling reactions has gained much of academic interest over years.[101–103] We considered expanding the substrate scope to phenol derivatives by nickel catalysis based on two assumptions: 1) being a first-row transition metal, nickel is harder than the second-row metals such as palladium or ruthenium, and hence has stronger affinity to the oxygen atom;[98] 2) nickel-catalyzed C–O activation reactions have been extensively studied in recent years.[104, 105] Utilizing the same nickel-based catalyst that was developed for the aryl halide coupling, several phenol derivatives including tosyl phenols showed comparable reactivity as aryl electrophiles at an elevated reaction temperature (i.e., 110 °C).[106] This coupling reaction features broad functional group tolerance with esters, amines, amides, carbamates, heterocycles, and is even compatible with an excessive amount of water. In addition, it displays excellent chemoselectivity, where the only viable coupling electrophiles are sp^2 aryl or alkenyl tosylates but not sp^3 alkyl counterparts.

2.3.3 Cross-couplings with alkenes

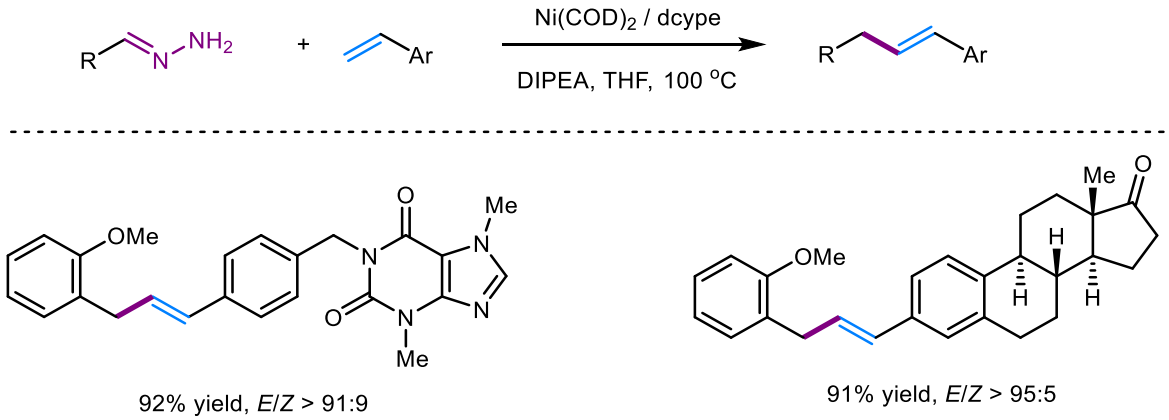

Scheme 2.12 *Umpolung* of carbonyl compounds for Heck-type cross-coupling reaction with olefins

Vinylation is another significant and challenging field in C (sp^3)–C(sp^3) coupling. Due to the instability of vinyl halides, the research of vinylation was much less than arylation in cross

coupling field. Inspired by our previous work on nucleophilic addition of hydrazone to activated olefins (Michael type addition), we wondered the possibility of reacting hydrazone with simple olefins to complete the olefin alkylation *via* an addition/*β*-hydride elimination (Heck-type) process (Scheme 2.12).[107] Fortunately, under nickel (0) system, such a transformation can be efficiently achieved without an extra oxidant. According to our proposed mechanism, nickel complex first assists the addition of hydrazone substrate to olefin *via* a Zimmerman–Traxler transition state as we discussed in nucleophilic addition part. After the C–C bond formation, *β*-hydride elimination of nickel together with the de-nitrogen occurred to give the Heck type coupling product. This transformation is suitable mostly for aryl-conjugated olefins and has a very good functional group tolerance. Even some complex molecules could efficiently complete such a coupling under the Ni(0) catalytic system. Moreover, under this system, other than aromatic aldehyde hydrazones, aliphatic ones can also serve as an efficient substrate but with lower reaction efficiency.

2.3.4 Cross-couplings with alkyl halides

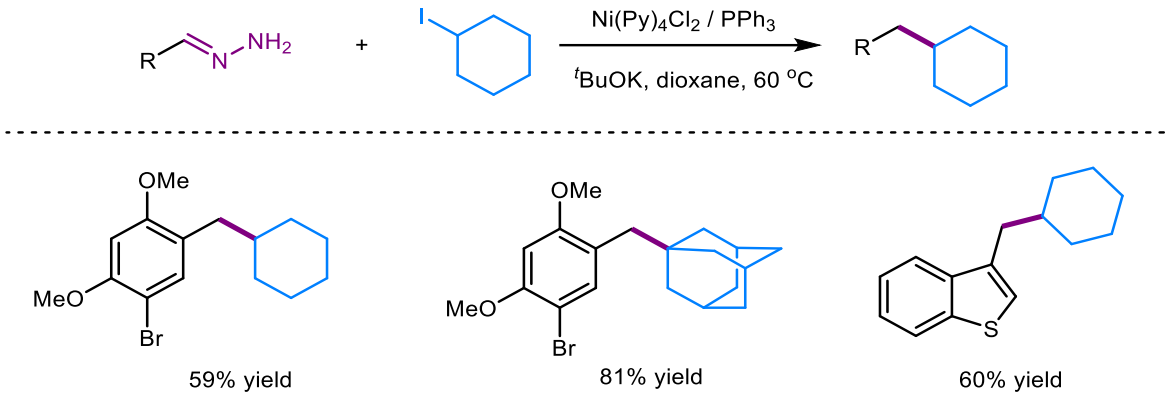

Scheme 2.13 *Umpolung* of carbonyl compounds for the cross-coupling reaction with alkyl halides

Unlike aryl–alkyl and vinyl–alkyl (sp^2–sp^3) coupling reactions, alkyl–alkyl (sp^3–sp^3) coupling reactions are generally more challenging to perform due to the *β*-hydride elimination of alkyl halides as an unproductive pathway (Scheme 2.13).[108] One elegant solution to circumvent this off-cycle issue is the use of nickel catalysis, which enables the reaction to undergo a single electron transfer (SET) rather than an ionic process.[109] Inspired by the relevant literature precedent and the initial success in sp^2–sp^3 coupling reactions with various aryl sources, we further interrogated alkyl halides as the sp^3 electrophiles in the coupling reaction with hydrazones.[110] In this case, $Ni(Py)_4Cl_2$

was slightly more efficient than $Ni(COD)_2$ as a precatalyst to initiate the catalytic cycle. Control experiments in the presence of radical inhibitors such as TEMPO or BHT implied the involvement of a SET process in the reaction. While *prim*-, *sec*-, *tert*-alkyl iodides or bromides were robust alkyl coupling partners, benzyl halides were not because of the outcompeting *N*-alkylation process (i.e., reacting with the terminus nitrogen of hydrazone). Concurrently, Zhang *et al.* reported a similar Ni-catalyzed alkyl–alkyl reductive coupling reaction of aldehydes and secondary alkyl bromides.[111]

2.3.5 Cross-couplings with Pd–allyl complexes

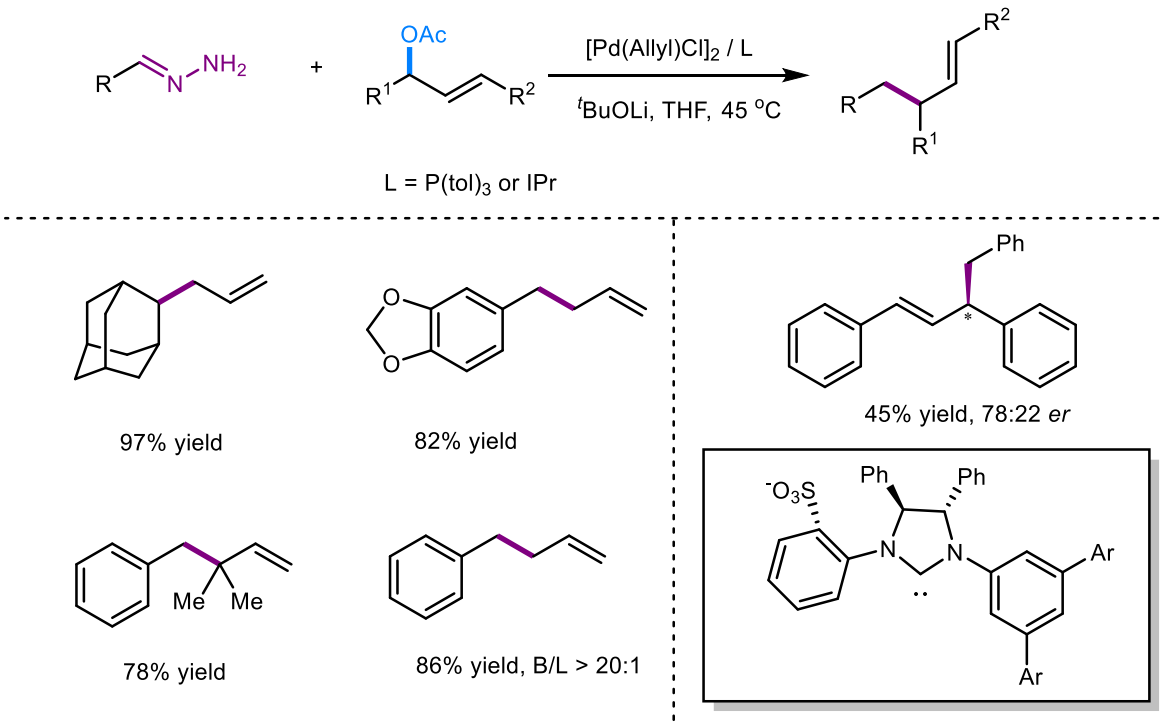

Scheme 2.14 *Umpolung* of carbonyl compounds for the allylation reaction

Other than coupling with alkyl halides, another powerful sp^3–sp^3 bond-forming method is Tsuji–Trost reaction which has found numerous applications in medicinal chemistry and natural product synthesis since its discovery.[112] The allylic alkylation reaction features the *in-situ* generation of a palladium-ligated π-allyl complex which is subject to the nucleophilic attack.[113–117] Considering the tremendous progress made in this allylation reaction over years, the development of nonstabilized nucleophiles has remained rather limited. In a continuing effort to expand the new

umpolung chemistry, we questioned if palladium could selectively catalyze the C–allylation reaction of carbonyl-derived hydrazones and π-allyl complex (Scheme 2.14). Specifically, a key challenge was how to control the regioselectivity such that allylation would occur at *ipso*-carbon of hydrazones, not at their *N*-terminus. By optimizing palladium precatalysts, ligands and bases, we learned that the strong basicity favors *C*-allylation over *N*-monoallylation or *N*-diallylation in the product distribution, as weak bases are inefficient to mediate the denitrogenation process.[118] Intriguingly, aliphatic aldehydes or ketones previously failed to act as efficient pronucleophiles in other types of reactions (i.e., addition and cross-coupling reactions) were extremely robust nucleophilic partners in this allylation chemistry when 1,3-bis(2,6-diisopropylphenyl)imidazolium chloride was employed as a NHC ligand precursor. The regioselectivity continued in the allyl acetate substrates, with the ratio of branched/linear substitution higher than 5:1. Similar to the enantioselective 1,2-carbonyl addition reaction,[60] the asymmetric allylation of hydrazones was made possible by using a chiral sulfonate-bearing NHC ligand precursor, albeit with a 78:22 enantiomeric ratio.

2.3.6 Alkylation/hydroalkylation reactions

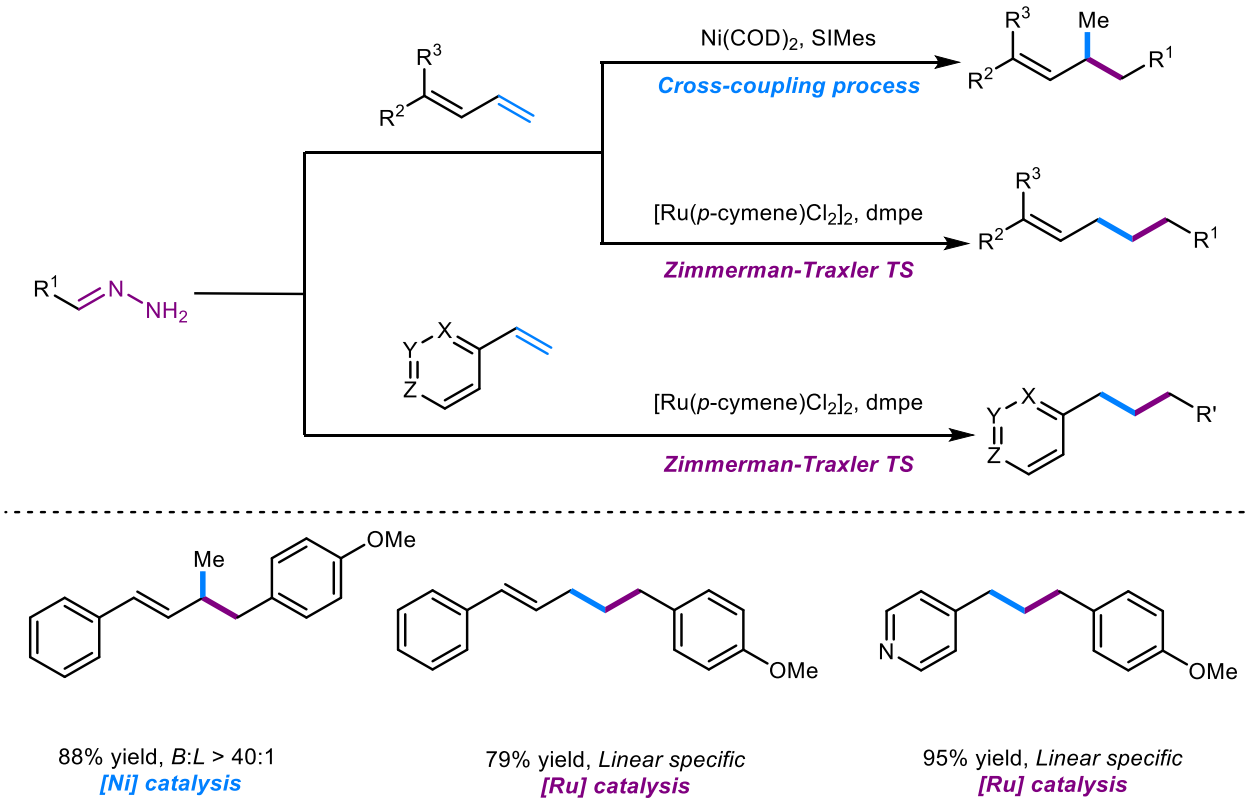

Scheme 2.15 *Umpolung* of carbonyl compounds for the hydroalkylation reaction of conjugated olefins

Conjugated double bond (non-polar) can also realize the C–C bond formation with hydrazones such as dienes (Scheme 2.15).[119] The success of this transformation contributed to the unique ability of Ni(0)–NHC to do the oxidative addition with N–H bond on hydrazone, which serves as the initiation step. Then, the so-formed Ni(II)–H species tends to complete the insertion with diene. Finally, a similar reductive elimination and dinitrogen process enables the completion of such a reductive Heck-coupling process. This hydroalkylation process can be applied to a wide range of dienes with very specific site selectivity including several complex molecules.

The Ni-catalyzed hydroalkylation protocol was successfully applied to various dienes with excellent branched regioselectivity. On the other hand, the linear hydroalkylated products were exclusively obtained when the ruthenium complex was employed in this chemistry.[120, 121] The opposite regioselectivity observed by nickel and ruthenium catalysis highlighted the two distinctive reaction pathways. Enynes and aryl olefins are also suitable substrates for the hydroalkylation chemistry. Aryl substituents were limited to electron deficient heterocyclic species such as pyridine, quinolines or thioazoles.[121] A complete switchable regioselectivity under two different catalysts was an unexpected yet interesting finding in these studies (Scheme 2.15).

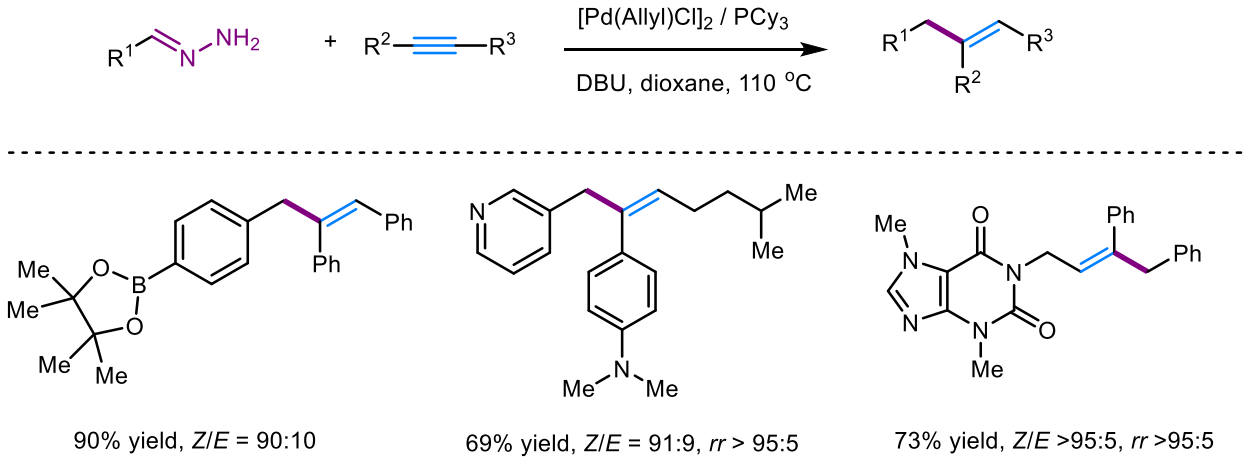

Scheme 2.16 *Umpolung* of carbonyl compounds for the hydroalkylation reaction of alkynes

Hydroalkylation of unsaturated bond is one of the critical methods to construct C–C bond. Previously, we have discussed the hydroalkylation of activated double bond with nickel catalysis.

However, so far, hydroalkylation of non-conjugated multiple bonds was not effective under Ni(0) system. Thus, palladium system, being more interactive with π bonds,[98] was then considered to extend the hydroalkylation to broader unsaturated bond system. Alkyne was investigated successfully by us with palladium–phosphine catalysis (Scheme 2.16). Such a reaction provided an efficient method for the direct construction of alkenes from alkyne efficiently under mild conditions. More importantly, such a method effectively form (***Z***)-olefin, which is more synthetically challenging and useful.[122]

Methylenecyclopropanes can also serve as an electrophile to complete the alkylation with hydrazones under palladium carbene system (Scheme 2.17).[123] The mechanism of this reaction is somewhat similar to the reaction of hydrazone allylation reaction where palladium first activated methylenecyclopropane to form palladium–allyl-π complex. Then, the carbon side of hydrazone do the nucleophilic attack to generate the alkylation product. With such a transformation, various terminal alkenes could be generated, which turns out to be significant synthetic intermediates.

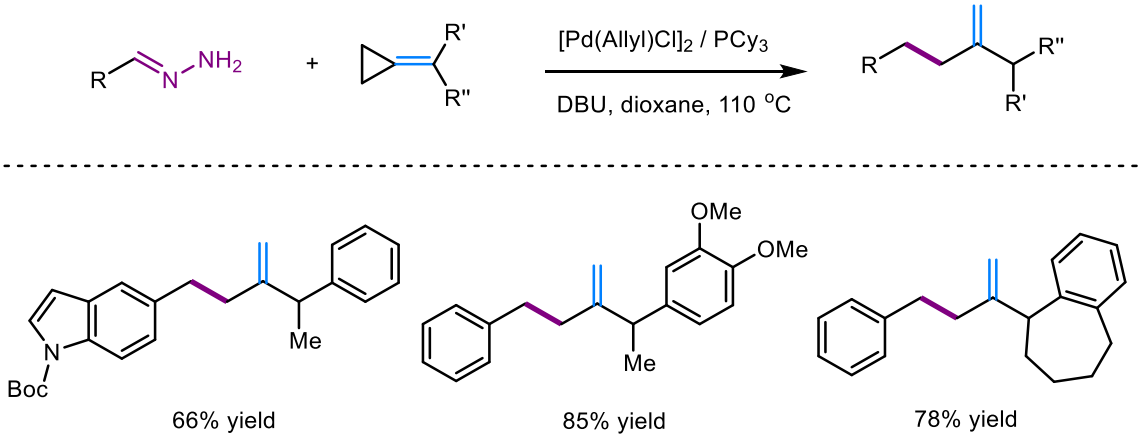

Scheme 2.17 *Umpolung* of carbonyl compounds for the hydroalkylation reaction of methylenecyclopropenes

The last example in hydroalkylation is our recent study on *gem*-difluorocyclopropane ring opening by palladium catalysis (Scheme 2.18).[124] Conventionally, palladium-catalyzed ring-opening couplings of *gem*-difluorocyclopropanes with nucleophiles typically favor the *β*-fluoroalkene scaffolds (linear regioselectivity). For example, Fu *et al.* reported the first Pd-catalyzed *gem*-difluorocyclopropane activation with high regio- and stereoselectivity.[125] Utilizing hydrazones as pronucleophiles, we achieved a switch in regioselectivity from the linear *β*-fluoroalkene to the

branched α-fluoroalkene. The exclusive regioselectivity is presumably ascribed to the formation of bis(η^1-allyl) species **G** which undergoes a regioselective 3,3'-reductive elimination to afford the intermediate **H** (Scheme 2.18). The current method provides a direct incorporation of α-fluoroalkene motifs into pharmaceutically relevant molecules that may be of interest to medicinal chemists.

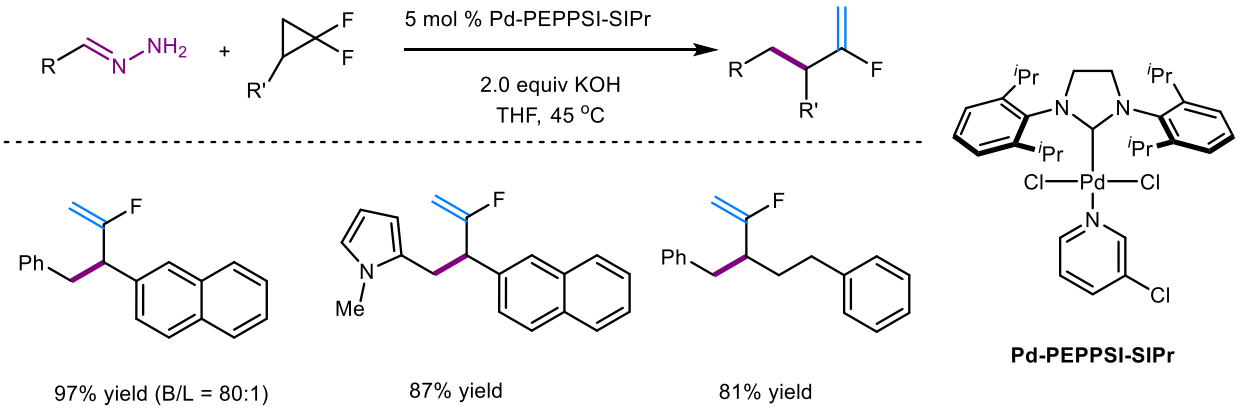

Plausible Mechanism

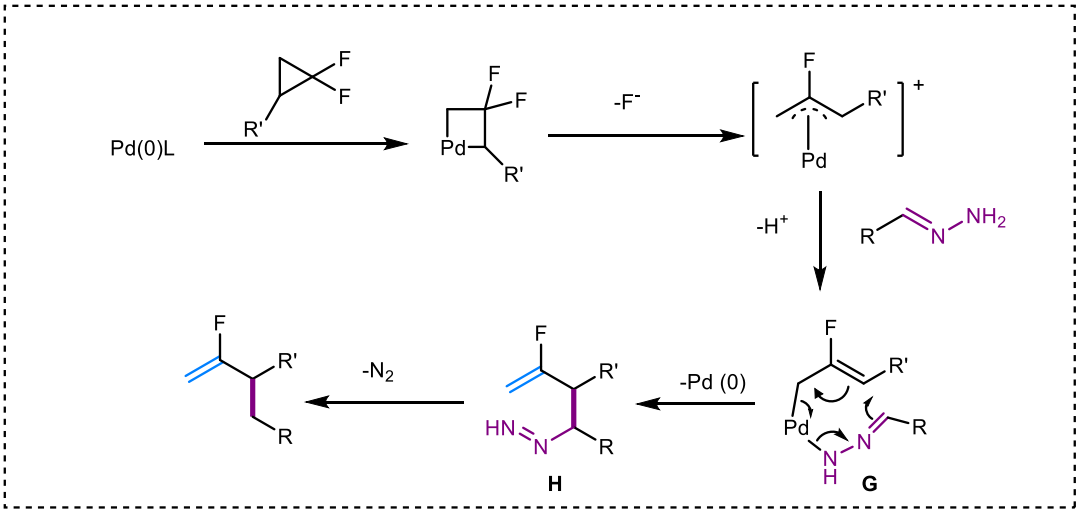

Scheme 2.18 Carbonyl *Umpolung* for the hydroalkylation reaction of *gem*-difluorocyclopropanes

2.4 C–C bond formation *via* anionic process

Transition metal-free transformation has become a hot field since several years ago due to its environmentally friendliness and the practical demand in pharmaceutical industry. In the early

1980s, Baldwin *et al.* pioneered a few metal-mediated carbon–carbon bond-forming processes between substituted hydrazones and *C*-electrophiles.[56–59] Synthesis of sterically encumbered hydrazones, stoichiometric lithium salts as well as strongly basic and cryogenic reaction conditions, nonetheless, limit much of its synthetic utility. However, inspired by Baldwin's discovery, we pondered the possibility of non-substituted hydrazone serving as a 'real carbanion' to react with some electrophiles without the assistance of transition metals. Thus, Togni reagent[126] is one of our successful cases. Due to its strong electrophilicity and efficient trifluoromethylation ability, it reacted with hydrazones under metal-free conditions to give a trifluoromethylation product (Scheme 2.19).[127] By studying the substrate scope, we found that in this case, electron deficient hydrazones have a comparatively higher efficiency. In addition, polarized solvent such as DMSO were also required. Mechanistic study showed that no radical intermediate is involved in such a transformation which suggest a nucleophilic-attack mechanism. Apart from trifluoromethylation, we are still investigating other potential electrophiles to complete the metal-free alkylation with hydrazones, including some electrophiles other than carbocation synthons. On top of this, the trifluoromethylation work also proved the fact that hydrazones could serve as a carbanion equivalent even under transition metal-free pathway.

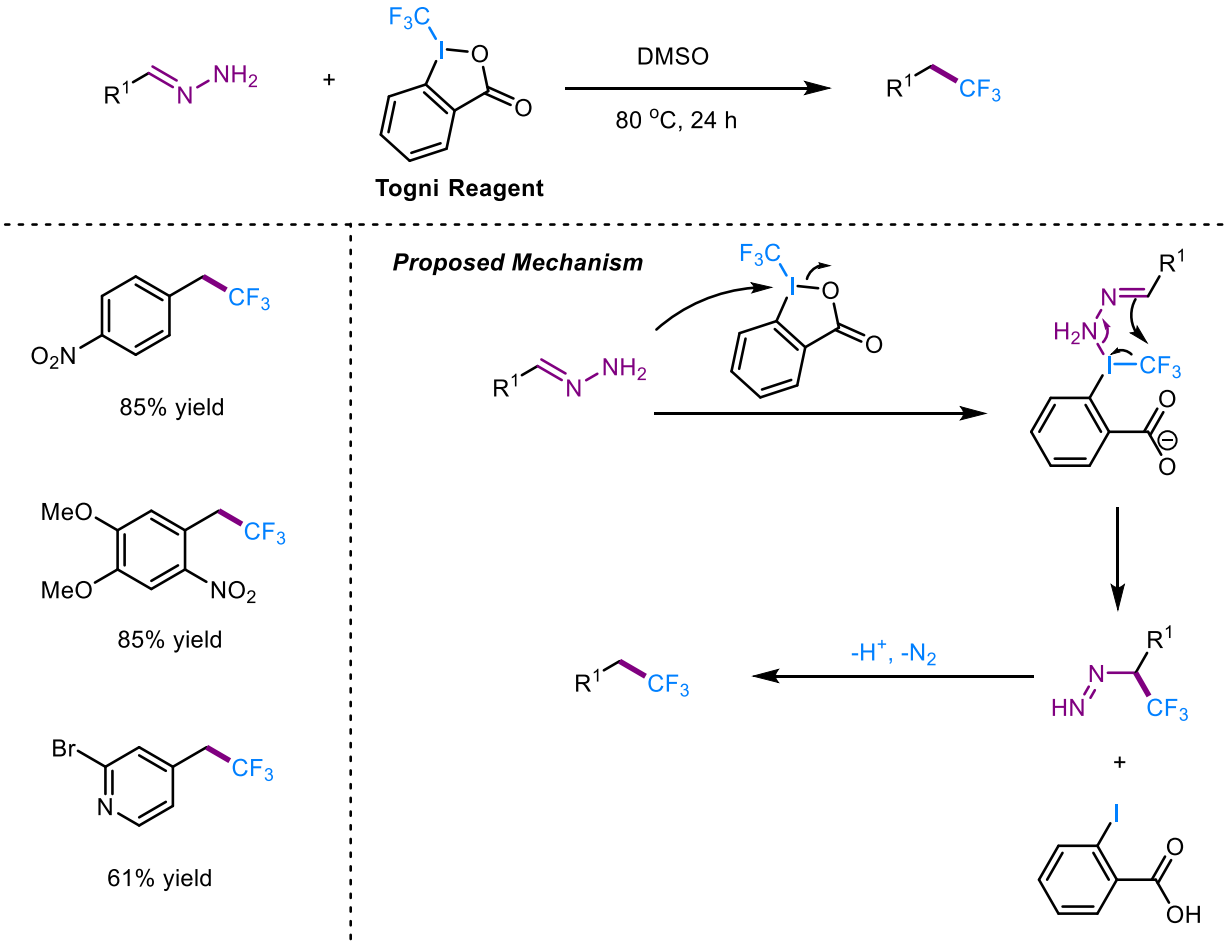

Scheme 2.19 *Umpolung* of carbonyl compounds for the trifluoromethylation with Togni reagent

2.5 Conclusion and outlook

The *umpolung* of carbonyl compounds as catalytic organometallic reagent surrogates *via* hydrazones uncovers new avenues for the carbon–carbon bond formation. To capitalize on the innate anionic character of sp^2 carbon in the hydrazone, exercising a prudent selection of metal and electrophiles is important. While addition reactions *via* the Zimmerman–Traxler TS occur with ruthenium or iron and polarized π-acceptors, cross-coupling reactions *via* the transmetallation process predominate in the presence of nickel or palladium and common cross-coupling electrophilic partners. These two diverging catalytic reaction paradigms are distinctive when compared to the traditional anionic alkylation pathway of hydrazones either through *N*- or *C*-terminus, with stoichiometric amounts of metal or metal-free. Furthermore, utilizing carbonyl compounds as feedstock chemical precursors of catalytic alkyl carbanion equivalents not only

overcomes the stoichiometry constraint on the traditional organometallic reagents, but also exhibits broad functional group tolerance and excellent chemo- and regioselectivity, complementary to the recent development of unsaturated hydrocarbons (e.g., olefins, alkynes, enynes, etc.) as latent catalytic carbanion precursors.

Like all emerging research advancement in synthetic chemistry, there are challenges and opportunities remained in this *umpolung* chemistry. Firstly, moderate enantioselectivity. The current chemistry struggled to deliver high enantioselectivity in either the addition or the cross-coupling reactions, even though exploitation of commercially available chiral ligands provided us with a few encouraging hits. Secondly, mechanistic deconvolution. Improvement of mechanistic understandings can perhaps be achieved by characterizing the active metal species or running kinetic NMR studies at varying temperatures. Thirdly, broadening substrate scope. Ketones and aliphatic aldehydes were challenging substrates, particularly seen in the addition reactions due to the steric hindrance or the competing background reaction (e.g., azine formation). Lastly, formation beyond carbon–carbon bond. Electrophiles other than carbon-based ones may offer alternative means to construct C–Het bonds.

References

(1). Corey, E. J. C., Xue Ming, *The Logic of Chemical Synthesis*. John Wiley & Sons: New York, 1989.
(2). Kobayashi, S.; Sugiura, M.; Schneider, U.; Matsubara, R.; Fossey, J.; Yamashita, Y., C–C bond formation through addition of C–M to CO, CN, and CN bonds. In *Comprehensive Organometallic Chemistry III*, Crabtree, R. H., Ed. Elsevier: Oxford, 2007; pp 403–491.
(3). Schlosser, M., *Organometallics in Synthesis: 3rd Manual*. John Wiley & Sons: Chichester, 2013.
(4). Stowell, J. C., *Carbanions in Organic Synthesis*. John Wiley & Sons: New York, 1979.
(5). Snieckus, V., Directed ortho metalation. Tertiary amide and *o*-carbamate directors in synthetic strategies for polysubstituted aromatics. *Chem. Rev.* **1990,** *90*, 879–933.
(6). Noyori, R.; Kitamura, M., Enantioselective addition of organometallic reagents to carbonyl compounds: Chirality transfer, multiplication, and amplification. *Angew. Chem. Int. Ed.* **1991,** *30*, 49–69.
(7). Wu, G.; Huang, M., Organolithium reagents in pharmaceutical asymmetric processes. *Chem. Rev.* **2006,** *106*, 2596–2616.
(8). Rappoport, Z.; Marek, I., *The Chemistry of Organolithium Compounds*. John Wiley & Sons: New York, 2004.

(9). Reich, H. J., Role of organolithium aggregates and mixed aggregates in organolithium mechanisms. *Chem. Rev.* **2013,** *113*, 7130–7178.
(10). Kharasch, M. S.; Reinmuth, O., *Grignard Reactions of Nonmetallic Substances*. Prentice-Hall: New York, 1954.
(11). Wakefield, B. J., *Organomagnesium Methods in Organic Chemistry*. Academic Press: London, 1995.
(12). Silverman, G. S.; Rakita, P. E., *Handbook of Grignard Reagents*. Marcel Dekker, Inc.: Monticello, 1996.
(13). Yamamoto, H.; Nozaki, H., Selective reactions with organoaluminum compounds. *Angew. Chem. Int. Ed.* **1978,** *17*, 169–175.
(14). Maruoka, K.; Yamamoto, H., Selective reactions using organoaluminum reagents. *Angew. Chem. Int. Ed.* **1985,** *24*, 668–682.
(15). Negishi, E.-I.; Kondakov, D. Y., An odyssey from stoichiometric carbotitanation of alkynes to zirconium-catalysed enantioselective carboalumination of alkenes. *Chem. Soc. Rev.* **1996,** *25*, 417–426.
(16). Pu, L.; Yu, H.-B., Catalytic asymmetric organozinc additions to carbonyl compounds. *Chem. Rev.* **2001,** *101*, 757–824.
(17). Shibasaki, M.; Kanai, M., Asymmetric synthesis of tertiary alcohols and α-tertiary amines *via* Cu-catalyzed C−C bond formation to ketones and ketimines. *Chem. Rev.* **2008,** *108*, 2853–2873.
(18). Krause, N.; Gerold, A., Regio- and stereoselective syntheses with organocopper reagents. *Angew. Chem. Int. Ed.* **1997,** *36*, 186–204.
(19). Posner, G. H., *Synthesis Using Organocopper Reagents*. John Wiley & Sons: New York, 1980.
(20). Lipshutz, B. H.; Sengupta, S., Organocopper reagents: Substitution, conjugate addition, carbo/metallocupration, and other reactions. *Org. React.* **1992,** *41*, 135–631.
(21). Lipshutz, B. H., Applications of higher-order mixed organocuprates to organic synthesis. *Synthesis* **1987**, 325–341.
(22). Lipshutz, B. H.; Wilhelm, R. S.; Kozlowski, J. A., The chemistry of higher order organocuprates. *Tetrahedron* **1984,** *40*, 5005–5038.
(23). Pereyre, M.; Quintard, J.-P.; Rahm, A., *Tin in Organic Synthesis*. Butterworth-Heinemann: Toronto, 1987.
(24). Abel, E. W.; Stone, F. G. A.; Wilkinson, G., *Comprehensive Organometallic Chemistry II: A Review of the Literature 1982–1994*. Elsevier: Oxford, 1995.
(25). Chan, T.; Fleming, I., Electrophilic substitution of organosilicon compounds- applications to organic synthesis. *Synthesis* **1979**, 761–786.

(26). Chan, T. H.; Wang, D., Chiral organosilicon compounds in asymmetric synthesis. *Chem. Rev.* **1992,** *92*, 995–1006.
(27). Marciniec, B., *Hydrosilylation: A Comprehensive Review on Recent Advances*. Springer Science: Berlin, 2009.
(28). Duthaler, R. O.; Hafner, A., Chiral titanium complexes for enantioselective addition of nucleophiles to carbonyl groups. *Chem. Rev.* **1992,** *92*, 807–832.
(29). Alexakis, A.; Bäckvall, J. E.; Krause, N.; Pàmies, O.; Diéguez, M., Enantioselective copper-catalyzed conjugate addition and allylic substitution reactions. *Chem. Rev.* **2008,** *108*, 2796–2823.
(30). Rossiter, B. E.; Swingle, N. M., Asymmetric conjugate addition. *Chem. Rev.* **1992,** *92*, 771–806.
(31). Nakao, Y.; Hiyama, T., Silicon-based cross-coupling reaction: An environmentally benign version. *Chem. Soc. Rev.* **2011,** *40*, 4893–4901.
(32). Diederich, F.; Stang, P. J., *Metal-Catalyzed Cross-Coupling Reactions*. Wiley-VCH: New York, 1998.
(33). Miyaura, N.; Suzuki, A., Palladium-catalyzed cross-coupling reactions of organoboron compounds. *Chem. Rev.* **1995,** *95*, 2457–2483.
(34). Stille, J. K., The palladium-catalyzed cross-coupling reactions of organotin reagents with organic electrophiles. *Angew. Chem. Int. Ed.* **1986,** *25*, 508–524.
(35). Beletskaya, I. P.; Cheprakov, A. V., Copper in cross-coupling reactions: The post-ullmann chemistry. *Coord. Chem. Rev.* **2004,** *248*, 2337–2364.
(36). Cahiez, G.; Moyeux, A., Cobalt-catalyzed cross-coupling reactions. *Chem. Rev.* **2010,** *110*, 1435–1462.
(37). Kumada, M., Nickel and palladium complex catalyzed cross-coupling reactions of organometallic reagents with organic halides. *Pure Appl. Chem.* **1980,** *52*, 669–679.
(38). Knochel, P.; Singer, R. D., Preparation and reactions of polyfunctional organozinc reagents in organic synthesis. *Chem. Rev.* **1993,** *93*, 2117–2188.
(39). Krasovskiy, A.; Knochel, P., A licl-mediated br/mg exchange reaction for the preparation of functionalized aryl-and heteroarylmagnesium compounds from organic bromides. *Angew. Chem. Int. Ed.* **2004,** *43*, 3333–3336.
(40). Knochel, P.; Dohle, W.; Gommermann, N.; Kneisel, F. F.; Kopp, F.; Korn, T.; Sapountzis, I.; Vu, V. A., Highly functionalized organomagnesium reagents prepared through halogen–metal exchange. *Angew. Chem. Int. Ed.* **2003,** *42*, 4302–4320.
(41). Jackson, E. P.; Malik, H. A.; Sormunen, G. J.; Baxter, R. D.; Liu, P.; Wang, H.; Shareef, A.-R.; Montgomery, J., Mechanistic basis for regioselection and regiodivergence in nickel-catalyzed reductive couplings. *Acc. Chem. Res.* **2015,** *48*, 1736–1745.

(42). Kim, S. W.; Zhang, W.; Krische, M. J., Catalytic enantioselective carbonyl allylation and propargylation *via* alcohol-mediated hydrogen transfer: Merging the chemistry of grignard and sabatier. *Acc. Chem. Res.* **2017,** *50*, 2371–2380.
(43). Liu, R. Y.; Buchwald, S. L., CuH-catalyzed olefin functionalization: From hydroamination to carbonyl addition. *Acc. Chem. Res.* **2020,** *53*, 1229–1243.
(44). Anastas, P. T.; Warner, J. C., Green chemistry: Theory and practice. In *Green chemistry: Theory and Practice*, Oxford University Press: New York, 1998.
(45). Li, C. J.; Trost, B. M., Green chemistry for chemical synthesis. *P. Natl. Acad. Sci. USA* **2008,** *105*, 13197–13202.
(46). Gröbel, B.-T.; Seebach, D., *Umpolung* of the reactivity of carbonyl compounds through sulfur-containing reagents. *Synthesis* **1977**, 357–402.
(47). Seebach, D., Methods of reactivity *umpolung*. *Angew. Chem. Int. Ed.* **1979,** *18*, 239–258.
(48). Seebach, D.; Corey, E. J., Generation and synthetic applications of 2-lithio-1,3-dithianes. *J. Org. Chem.* **1975,** *40*, 231–237.
(49). Nair, V.; Vellalath, S.; Babu, B. P., Recent advances in carbon–carbon bond-forming reactions involving homoenolates generated by NHC catalysis. *Chem. Soc. Rev.* **2008,** *37*, 2691–2698.
(50). Bugaut, X.; Glorius, F., Organocatalytic *umpolung*: *N*-heterocyclic carbenes and beyond. *Chem. Soc. Rev.* **2012,** *41*, 3511–3522.
(51). Flanigan, D. M.; Romanov-Michailidis, F.; White, N. A.; Rovis, T., Organocatalytic reactions enabled by *N*-heterocyclic carbenes. *Chem. Rev.* **2015,** *115*, 9307–9387.
(52). Kishner, N., Wolff–Kishner reduction; huang–minlon modification. *J. Russ. Phys. Chem. Soc.* **1911,** *43*, 582–595.
(53). Wolff, L., Chemischen institut der universität jena: Methode zum ersatz des sauerstoffatoms der ketone und aldehyde durch wasserstoff. *Lieb. Ann. Chem.* **1912,** *394*, 86–108.
(54). Lewis, D. E., Chapter 7 — deoxygenation in modern synthesis. In *The Wolff – Kishner Reduction and Related Reactions: Discovery and Development*, Lewis, D. E., Ed. Elsevier Amsterdam, 2019; pp 191–217.
(55). Dai, X.-J.; Li, C.-J., En route to a practical primary alcohol deoxygenation. *J. Am. Chem. Soc.* **2016,** *138*, 5433–5440.
(56). Baldwin, J. E.; Adlington, R. M.; Bottaro, J. C.; Kolhe, J. N.; Newington, I. M.; Perry, M. W. D., Azo anions in synthesis. *Tetrahedron* **1986,** *42*, 4235–4246.
(57). Baldwin, J. E.; Bottaro, J. C.; Kolhe, J. N.; Adlington, R. M., Azo anions in synthesis. Use of trityl- and diphenyl-4-pyridylmethyl-hydrazones for reductive c-c bond formation from aldehydes and ketones. *J. Chem. Soc., Chem. Commun.* **1984**, 22–23.

(58). Baldwin, J. E.; Adlington, R. M.; Bottaro, J. C.; Jain, A. U.; Kolhe, J. N.; Perry, M. W. D.; Newington, I. M., Michael additions of hydrazones for carbon–carbon bond formation. *J. Chem. Soc., Chem. Commun.* **1984**, 1095–1096.
(59). Adlington, R. M.; Baldwin, J. E.; Bottaro, J. C.; Perry, M. W. D., Azo anions in synthesis. T-butylhydrazones as acyl-anion equivalents. *J. Chem. Soc., Chem. Commun.* **1983**, 1040–1041.
(60). Wang, H.; Dai, X.-J.; Li, C.-J., Aldehydes as alkyl carbanion equivalents for additions to carbonyl compounds. *Nat. Chem.* **2017,** *9*, 374–378.
(61). Zimmerman, H. E.; Traxler, M. D., The stereochemistry of the ivanov and reformatsky reactions. I. *J. Am. Chem. Soc.* **1957,** *79*, 1920–1923.
(62). Wei, W.; Dai, X.-J.; Wang, H.; Li, C.; Yang, X.; Li, C.-J., Ruthenium(II)-catalyzed olefination *via* carbonyl reductive cross-coupling. *Chem. Sci.* **2017,** *8*, 8193–8197.
(63). Das, U. K.; Chakraborty, S.; Diskin-Posner, Y.; Milstein, D., Direct conversion of alcohols into alkenes by dehydrogenative coupling with hydrazine/hydrazone catalyzed by manganese. *Angew. Chem. Int. Ed.* **2018,** *57*, 13444–13448.
(64). Chen, N.; Dai, X. J.; Wang, H.; Li, C. J., *Umpolung* addition of aldehydes to aryl imines. *Angew. Chem. Int. Ed.* **2017,** *56*, 6260–6263.
(65). Klunder, J. M.; Hargrave, K. D.; West, M.; Cullen, E.; Pal, K.; Behnke, M. L.; Kapadia, S. R.; McNeil, D. W.; Wu, J. C.; Chow, G. C.; Adams, J., Novel non-nucleoside inhibitors of HIV-1 reverse transcriptase. 2. Tricyclic pyridobenzoxazepinones and dibenzoxazepinones. *J. Med. Chem.* **1992,** *35*, 1887–1897.
(66). Gijsen, H. J. M.; Berthelot, D.; Zaja, M.; Brône, B.; Geuens, I.; Mercken, M., Analogues of morphanthridine and the tear gas dibenz[*b*,*f*][1,4]oxazepine (CR) as extremely potent activators of the human transient receptor potential ankyrin 1 (TRPA1) channel. *J. Med. Chem.* **2010,** *53*, 7011–7020.
(67). Yan, S.-S.; Zhu, L.; Ye, J.-H.; Zhang, Z.; Huang, H.; Zeng, H.; Li, C.-J.; Lan, Y.; Yu, D.-G., Ruthenium-catalyzed *umpolung* carboxylation of hydrazones with CO_2. *Chem. Sci.* **2018,** *9*, 4873–4878.
(68). Spitzmaul, G.; Gumilar, F.; Dilger, J. P.; Bouzat, C., The local anaesthetics proadifen and adiphenine inhibit nicotinic receptors by different molecular mechanisms. *Br. J. Pharmacol.* **2009,** *157*, 804–17.
(69). Christoffers, J.; Koripelly, G.; Rosiak, A.; Rössle, M., Recent advances in metal-catalyzed asymmetric conjugate additions. *Synthesis* **2007**, 1279–1300.
(70). Krause, N.; Hoffmann-Röder, A., Recent advances in catalytic enantioselective michael additions. *Synthesis* **2001**, 171–196.
(71). Hayashi, T.; Yamasaki, K., Rhodium-catalyzed asymmetric 1,4-addition and its related asymmetric reactions. *Chem. Rev.* **2003,** *103*, 2829–2844.

(72). Bruneau, C.; Dixneuf, P. H., *Ruthenium Catalysts and Fine Chemistry*. Springer: Berlin, 2004; Vol. 11.
(73). Dai, X. J.; Wang, H.; Li, C. J., Carbonyls as latent alkyl carbanions for conjugate additions. *Angew. Chem. Int. Ed.* **2017,** *56*, 6302–6306.
(74). Li, C.-C.; Dai, X.-J.; Wang, H.; Zhu, D.; Gao, J.; Li, C.-J., Iron-catalyzed nucleophilic addition reaction of organic carbanion equivalents *via* hydrazones. *Org. Lett.* **2018,** *20*, 3801–3805.
(75). Grignard, V., Sur quelques nouvelles combinaisons organometalliques du magnésium et leur application à des synthèses d'alcools et d'hydrocarbures. *Compt. Rend.* **1900,** *130*, 1322.
(76). Gilman, H.; Jones, R. G.; Woods, L., The preparation of methylcopper and some observations on the decomposition of organocopper compounds. *J. Org. Chem.* **1952,** *17*, 1630–1634.
(77). Shirley, D. A., The synthesis of ketones from acid halides and organometallic compounds of magnesium, zinc, and cadmium. *Org. React.* **1954,** *8*, 28.
(78). Larock, R. C., Organomercurials in organic synthesis. *Tetrahedron* **1982,** *38*, 1713–1754.
(79). Knochel, P.; Jones, P., *Organozinc Reagents: A Practical Approach*. Oxford University Press: 1999.
(80). Rappoport, Z.; Marek, I., *The Chemistry of Organolithium Compounds*. John Wiley & Sons: Chichester, U.K., 2006.
(81). Hall, D. G., *Boronic Acids: Preparation, Applications in Organic Synthesis and Medicine*. Wiley-VCH: Weinheim, 2005.
(82). Smith, M. B.; March, J., *March's Advanced Organic Chemistry: Reactions, Mechanisms, and Structure*. Wiley: New York, 2007.
(83). Sorimachi, K.; Terada, M., Relay catalysis by a metal-complex/brønsted acid binary system in a tandem isomerization/carbon−carbon bond forming sequence. *J. Am. Chem. Soc.* **2008,** *130*, 14452–14453.
(84). Scheuermann, M. L.; Johnson, E. J.; Chirik, P. J., Alkene isomerization–hydroboration promoted by phosphine-ligated cobalt catalysts. *Org. Lett.* **2015,** *17*, 2716–2719.
(85). Vasseur, A.; Bruffaerts, J.; Marek, I., Remote functionalization through alkene isomerization. *Nat. Chem.* **2016,** *8*, 209–219.
(86). Sommer, H.; Juliá-Hernández, F.; Martin, R.; Marek, I., Walking metals for remote functionalization. *ACS Cent. Sci.* **2018,** *4*, 153–165.
(87). Bäckvall, J.-E.; Andreasson, U., Ruthenium-catalyzed isomerization of allylic alcohols to saturated ketones. *Tetrahedron Lett.* **1993,** *34*, 5459–5462.
(88). Trost, B. M.; Kulawiec, R. J., Chemoselectivity in the ruthenium-catalyzed redox isomerization of allyl alcohols. *J. Am. Chem. Soc.* **1993,** *115*, 2027–2036.

(89). Trost, B. M.; Livingston, R. C., Two-metal catalyst system for redox isomerization of propargyl alcohols to enals and enones. *J. Am. Chem. Soc.* **1995,** *117*, 9586–9587.
(90). Wang, D.; Chen, D.; Haberman, J. X.; Li, C.-J., Ruthenium-catalyzed isomerization of homoallylic alcohols in water. *Tetrahedron* **1998,** *54*, 5129–5142.
(91). Cadierno, V.; Francos, J.; Gimeno, J.; Nebra, N., Ruthenium-catalyzed reduction of allylic alcohols: An efficient isomerization/transfer hydrogenation tandem process. *Chem. Commun.* **2007**, 2536–2538.
(92). Cadierno, V.; Crochet, P.; Francos, J.; García-Garrido, S. E.; Gimeno, J.; Nebra, N., Ruthenium-catalyzed redox isomerization/transfer hydrogenation in organic and aqueous media: A one-pot tandem process for the reduction of allylic alcohols. *Green Chem.* **2009,** *11*, 1992–2000.
(93). Bizet, V.; Pannecoucke, X.; Renaud, J.-L.; Cahard, D., Ruthenium-catalyzed redox isomerization of trifluoromethylated allylic alcohols: Mechanistic evidence for an enantiospecific pathway. *Angew. Chem. Int. Ed.* **2012,** *51*, 6467–6470.
(94). Li, C.-C.; Kan, J.; Qiu, Z.; Li, J.; Lv, L.; Li, C.-J., Synergistic relay reactions to achieve redox-neutral *α*-alkylations of olefinic alcohols with ruthenium(II) catalysis. *Angew. Chem. Int. Ed.* **2020,** *59*, 4544–4549.
(95). Muthaiah, S.; Hong, S. H., Acceptorless and base-free dehydrogenation of alcohols and amines using ruthenium–hydride complexes. *Adv. Synth. Catal.* **2012,** *354*, 3045–3053.
(96). Gunanathan, C.; Milstein, D., Applications of acceptorless dehydrogenation and related transformations in chemical synthesis. *Science* **2013,** *341*, 1229712.
(97). Chang, W.; Gong, X.; Wang, S.; Xiao, L.-P.; Song, G., Acceptorless dehydrogenation and dehydrogenative coupling of alcohols catalysed by protic nhc ruthenium complexes. *Org. Biomol. Chem.* **2017,** *15*, 3466–3471.
(98). Hartwig, J. F.; Collman, J. P., *Organotransition Metal Chemistry: From Bonding to Catalysis*. University Science Books Sausalito, CA: 2010; Vol. 1.
(99). Tang, J.; Lv, L.; Dai, X.-J.; Li, C.-C.; Li, L.; Li, C.-J., Nickel-catalyzed cross-coupling of aldehydes with aryl halides *via* hydrazone intermediates. *Chem. Commun.* **2018,** *54*, 1750–1753.
(100). Carey, F. A.; Sundberg, R. J., *Advanced Organic Chemistry Part B: Reactions and Synthesis*. 5th ed.; Springer: New York, 2007.
(101). Jana, R.; Pathak, T. P.; Sigman, M. S., Advances in transition metal (Pd, Ni, Fe)-catalyzed cross-coupling reactions using alkyl–organometallics as reaction partners. *Chem. Rev.* **2011,** *111*, 1417–1492.
(102). So, C. M.; Kwong, F. Y., Palladium-catalyzed cross-coupling reactions of aryl mesylates. *Chem. Soc. Rev.* **2011,** *40*, 4963–4972.

(103). Zeng, H.; Qiu, Z.; Domínguez-Huerta, A.; Hearne, Z.; Chen, Z.; Li, C.-J., An adventure in sustainable cross-coupling of phenols and derivatives *via* carbon–oxygen bond cleavage. *ACS Catal.* **2017,** *7*, 510–519.
(104). Guo, L.; Hsiao, C.-C.; Yue, H.; Liu, X.; Rueping, M., Nickel-catalyzed Csp^2–Csp^3 cross-coupling *via* C–O bond activation. *ACS Catal.* **2016,** *6*, 4438–4442.
(105). Yue, H.; Guo, L.; Lee, S.-C.; Liu, X.; Rueping, M., Selective reductive removal of ester and amide groups from arenes and heteroarenes through nickel-catalyzed C−O and C−N bond activation. *Angew. Chem. Int. Ed.* **2017,** *56*, 3972–3976.
(106). Lv, L.; Zhu, D.; Tang, J.; Qiu, Z.; Li, C.-C.; Gao, J.; Li, C.-J., Cross-coupling of phenol derivatives with *umpolung* aldehydes catalyzed by nickel. *ACS Catal.* **2018,** *8*, 4622–4627.
(107). Lv, L.; Zhu, D.; Li, C.-J., Direct dehydrogenative alkyl Heck-couplings of vinylarenes with *umpolung* aldehydes catalyzed by nickel. *Nat. Commun,* **2019,** *10,* 715.
(108). Choi, J.; Fu, G. C., Transition metal-catalyzed alkyl–alkyl bond formation: Another dimension in cross-coupling chemistry. *Science* **2017,** *356*, eaaf7230.
(109). Wang, X.; Dai, Y.; Gong, H., Nickel-catalyzed reductive couplings. *Top Curr. Chem. (Z).* **2016,** *374*, 43–72.
(110). Zhu, D.; Lv, L.; Qiu, Z.; Li, C.-J., Nickel-catalyzed cross-coupling of *umpolung* carbonyls and alkyl halides. *J. Org. Chem.* **2019,** *84*, 6312–6322.
(111). Zhu, C.; Zhang, J., Nickel-catalyzed alkyl–alkyl cross-coupling reactions of non-activated secondary alkyl bromides with aldehydes as alkyl carbanion equivalents. *Chem. Commun.* **2019,** *55*, 2793–2796.
(112). Rössler, S. L.; Petrone, D. A.; Carreira, E. M., Iridium-catalyzed asymmetric synthesis of functionally rich molecules enabled by (phosphoramidite,olefin) ligands. *Acc. Chem. Res.* **2019,** *52*, 2657-2672.
(113). Lu, Z.; Ma, S., Metal-catalyzed enantioselective allylation in asymmetric synthesis. *Angew. Chem. Int. Ed.* **2008,** *47*, 258–297.
(114). Vulovic, B.; Bihelovic, F.; Matovic, R.; Saicic, R. N., Organocatalyzed tsuji–trost reaction: A new method for the closure of five- and six-membered rings. *Tetrahedron* **2009,** *65*, 10485–10494.
(115). Trost, B. M.; Fraisse, P. L.; Ball, Z. T., A stereospecific ruthenium-catalyzed allylic alkylation. *Angew. Chem. Int. Ed.* **2002,** *41*, 1059–1061.
(116). Tsuji, J., The Tsuji–Trost reaction and related carbon–carbon bond formation reactions: Overview of the palladium–catalyzed carbon–corbon bond formation *via* π-allylpalladium and propargylpalladium intermediates. In *Handbook of Organopalladium Chemistry for Organic Synthesis*, Negishi, E., Ed. Wiley: New York, 2002; Vol. 2, pp 1669–1687.

(117). Rossler, S. L.; Petrone, D. A.; Carreira, E. M., Iridium-catalyzed asymmetric synthesis of functionally rich molecules enabled by (phosphoramidite, olefin) ligands. *Acc. Chem. Res.* **2019,** *52*, 2657–2672.
(118). Zhu, D.; Lv, L.; Li, C.-C.; Ung, S.; Gao, J.; Li, C.-J., *Umpolung* of carbonyl groups as alkyl organometallic reagent surrogates for palladium-catalyzed allylic alkylation. *Angew. Chem. Int. Ed.* **2018,** *57*, 16520–16524.
(119). Lv, L.; Zhu, D.; Qiu, Z.; Li, J.; Li, C.-J., Nickel-catalyzed regioselective hydrobenzylation of 1,3-dienes with hydrazones. *ACS Catal.* **2019,** *9*, 9199–9205.
(120). Lv, L.; Yu, L.; Qiu, Z.; Li, C.-J., Switch in selectivity for formal hydroalkylation of 1,3-dienes and enynes with simple hydrazones. *Angew. Chem. Int. Ed.* **2020,** *59*, 6466–6472.
(121). Lv, L.; Li, C.-J., Ruthenium catalyzed *β*-selective alkylation of vinylpyridines with aldehydes/ketones *via* N_2H_4 mediated deoxygenative couplings. *Chem. Sci.* **2021,** *12*, 2870–2875.
(122). Yu, L.; Lv, L.; Qiu, Z.; Chen, Z.; Tan, Z.; Liang, Y.-F.; Li, C.-J., Palladium-catalyzed formal hydroalkylation of aryl-substituted alkynes with hydrazones. *Angew. Chem. Int. Ed.* **2020,** *59*, 14009–14013.
(123). Yao, J.; Chen, Z.; Yu, L.; Lv, L.; Cao, D.; Li, C.-J., Palladium-catalyzed hydroalkylation of methylenecyclopropanes with simple hydrazones. *Chem. Sci.* **2020**.
(124). Lv, L.; Li, C.-J., Palladium-catalyzed defluorinative alkylation of *gem*-difluorocyclopropanes: Switching regioselectivity *via* simple hydrazones. *Angew. Chem. Int. Ed.* **2021,** *60*, 13098–13104.
(125). Xu, J.; Ahmed, E.-A.; Xiao, B.; Lu, Q.-Q.; Wang, Y.-L.; Yu, C.-G.; Fu, Y., Pd-catalyzed regioselective activation of *gem*-difluorinated cyclopropanes: A highly efficient approach to 2-fluorinated allylic scaffolds. *Angew. Chem. Int. Ed.* **2015,** *54*, 8231–8235.
(126). Charpentier, J.; Früh, N.; Togni, A., Electrophilic trifluoromethylation by use of hypervalent iodine reagents. *Chem. Rev.* **2015,** *115*, 650–682.
(127). Zeng, H.; Luo, Z.; Han, X.; Li, C.-J., Metal-free construction of the C(sp^3)–CF_3 bond: Trifluoromethylation of hydrazones with togni's reagent under mild conditions. *Org. Lett.* **2019,** *21*, 5948–5951.

Chapter 3. The General Design and Outline of My PhD Research

3.1 Introduction

Grignard reaction plays a significant role in organic chemistry as one of the most crucial tools for constructing C–C bond, which is widely applied in synthetic chemistry especially in the early-stage synthesis. In the last century, various robust organometallic reagents were developed to carry out Grignard-type reactions. However, there are still limitations with classic Grignard-type reactions: (a) The organometallic reagents are mostly from alkyl halides and require stoichiometric amounts of metal elements to participate; (b) Some of the organometallic reagents are sensitive to air and water, and they have poor functional group tolerance as well. Thus, providing an alternative carbanion equivalent for Grignard-type reactions, which avoid the usage of haloalkanes and stoichiometric amounts of metal, is highly desirable. With these regards, several years ago, inspired by the Wolff–Kishner reduction, our group developed the use of hydrazone as a carbanion equivalent to complete a series of C–C bond formation reactions, and among which ruthenium-catalyzed Grignard-type reaction was the very first reaction that we discovered. This new carbanion equivalent not only avoids the usage of stoichiometric amounts of metal and alkyl halides but is also air- and moisture-stable. In addition, taking advantage of the transition metal catalytic system, some unique derivative transformations could be realized:

Firstly, aldehydes/ketones, though powerful substrates for various organic reactions, are sometimes hard to access and store, especially for some complex molecules. In most cases, carbonyls come from the oxidation of alcohols, the latter as ones of the most abundant organic compounds. Ruthenium–phosphine complexes used in the hydrazone chemistry are powerful catalysts for dehydrogenation/hydrogenation of alcohols/carbonyls. This fact inspired us to consider whether we could take advantage of the ruthenium catalytic system to enable various alcohols as carbonyl surrogates for Grignard-type reactions to formally realize the direct C–H alkylation of alcohols.

Secondly, as discussed in the last chapter, the reaction between hydrazones and carbonyls could be more than Grignard-type reaction, but also olefination reaction. Previous studies from our group showed the selectivity of Grignard-type addition and olefination depends mostly on the structure

of the substrates, where aliphatic aldehyde hydrazones usually lead to olefination products and aromatic ones lead to nucleophilic addition products. However, in a realistic setting, the opposite selectivity would also highly useful. Thus, enabling the unusual selectivity of reaction of hydrazones with carbonyls by adjusting the catalytic system is also attractive.

Thirdly, while using hydrazones as carbanion equivalents does avoid the usage of stoichiometric amounts of metal and haloalkanes, it still requires a precious metal, ruthenium, to catalyze. This somewhat limits its application in late-stage pharmaceutical synthesis. Thus, developing earth-abundant metal catalysts for this kind of transformation is also highly desirable.

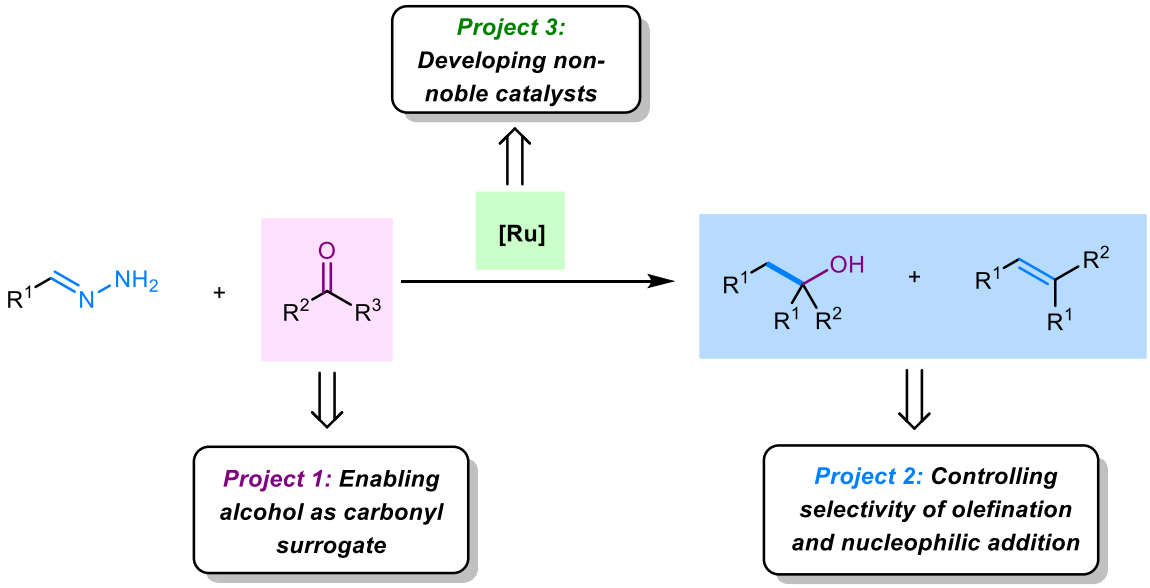

Scheme 3.1 General design of my PhD research

Thus, my PhD research work was mainly focused on the derivative reactions of Grignard-type reactions with hydrazone. It was divided into three directions: (a) The use of hydrogen transfer strategies to empower various alcohols as carbonyl surrogates for Grignard-type reactions with hydrazones, (b) The study of the chemo-selectivity in hydrazone reaction with carbonyls and the development of new catalytic system to realize the unusual selectivity, (c) The conversion of non-noble transition metal complex to catalysts for various addition reactions with hydrazone.

3.2 Empowering alcohol as carbonyl surrogate for Grignard reaction with hydrazone

Hydrogen transfer strategy is a powerful protocol to bridge the earth-abundant alcohols to reactive carbonyls as discussed in the first chapter. In addition, the ruthenium catalytic system is one of the most used catalytic systems in hydrogen transfer reactions.[1] Thus, in ruthenium-catalyzed Grignard reaction with hydrazone, it was potentially a suitable candidate to utilize the hydrogen transfer strategy to enable alcohols as carbonyl surrogates for 1,2-addition reactions.

3.2.1 Empowering olefinic alcohol as carbonyl surrogate

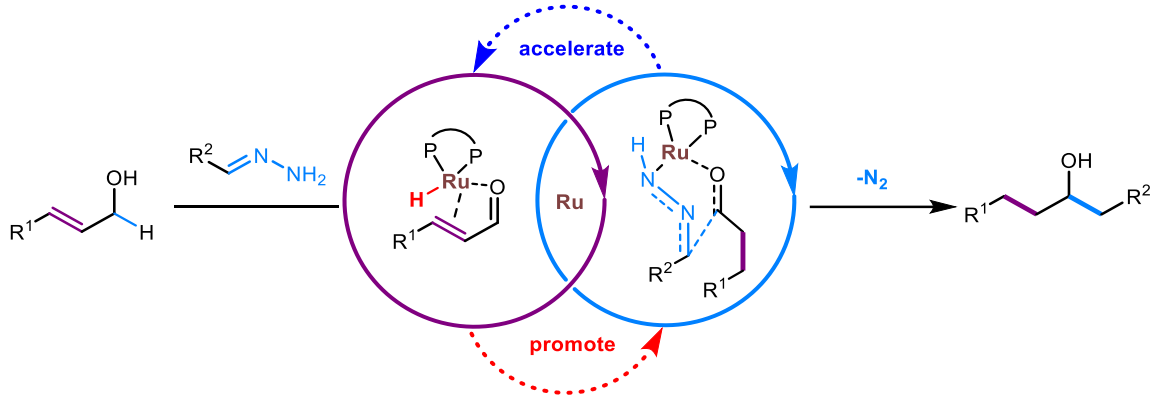

Scheme 3.2 Empowering olefinic alcohols as carbonyl surrogate

To achieve the goal of empowering alcohols as carbonyl surrogates for Grignard reaction, we first started from the reaction with olefinic alcohols taking advantage of olefin isomerization.[2, 3] We discovered a ruthenium-catalyzed redox neutral α-alkylation of unsaturated alcohols based on a synergistic relay process involving olefin isomerization (chain walking) and *umpolung* hydrazone addition, which thanks to the interaction between the two rather inefficient individual reaction steps to enable an efficient overall process. This transformation displays the compatibility of hydrazone type 'carbanions' and active protons in a one-pot reaction. At the same time, it achieves the first Grignard-type nucleophilic addition using olefinic alcohols as latent carbonyl groups, providing a higher yield of the corresponding secondary alcohol than the classical hydrazone addition to aldehydes does. A broad scope of unsaturated alcohols and hydrazones, including some complex molecules, were tested effective for this reaction. This demonstrates the versatility of this

approach and its suitability as an alternative efficient method for the generation of secondary and tertiary alcohols.[4]

3.2.2 Empowering saturated alcohol as carbonyl surrogate for Grignard-type reaction

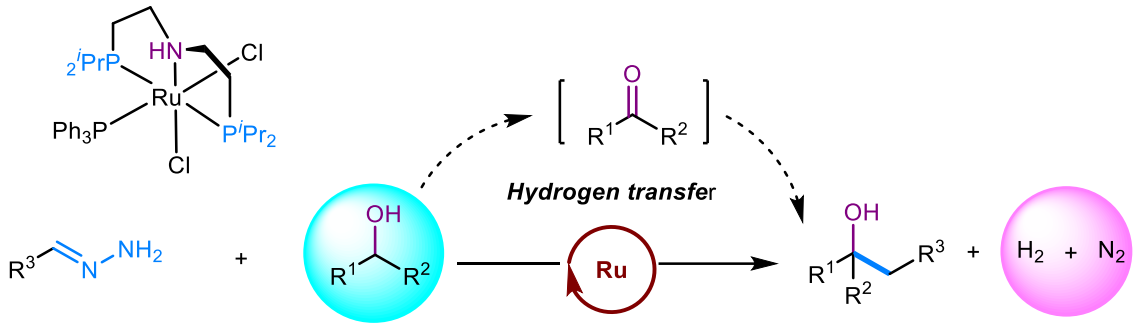

Scheme 3.3 Empowering saturated alcohols as carbonyl surrogates for Grignard-type reactions

We then extended the alcohols to saturated alcohols with a ruthenium(II) PNP–pincer complex as catalyst. In this transformation, since there is no hydrogen acceptor in the substrate molecules, a new catalytic system needed to be developed to turn over metal hydride species. Taking advantage of the Noyori-type hydrogenation/dehydrogenation,[5] we discovered that Ru–PNP type complexes can greatly help the dehydrogenation process. The reaction conditions are mild and can tolerate a broad range of substrates. No oxidant is involved during the entire transformation, with only H_2 and N_2 being generated as byproducts. This reaction opens a new avenue for Grignard-type reactions by enabling the use of naturally abundant alcohols as starting materials without the need for pre-synthesized carbonyls.[6]

3.3 Chemoselectivity study on the hydrazone reaction with carbonyls

The reaction of hydrazone with carbonyls under ruthenium catalysts could lead to Grignard-type addition or olefination. The selectivity between these two pathways is originally substrate-dependent where aromatic aldehyde hydrazones lead to the addition products and aliphatic aldehyde hydrazones lead to the olefination products. Based on the mechanistic study of our original work,[7, 8] the selectivity determining step is possibly the step after the C–C bond formation and the lost of nitrogen gas, where direct protonation results in alcohol products (1,2-addition product) and the E1cB elimination leads to olefination products (Scheme 3.4).[7, 8] We proposed that the adaptation of catalysts by electron density and Lewis acidity could, in some cases, make the

original selectivity inverted. In this project, we successfully designed a Ru–PCP pincer complex to realize the 1,2-addition reactions with less favored aliphatic aldehyde hydrazones.[4]

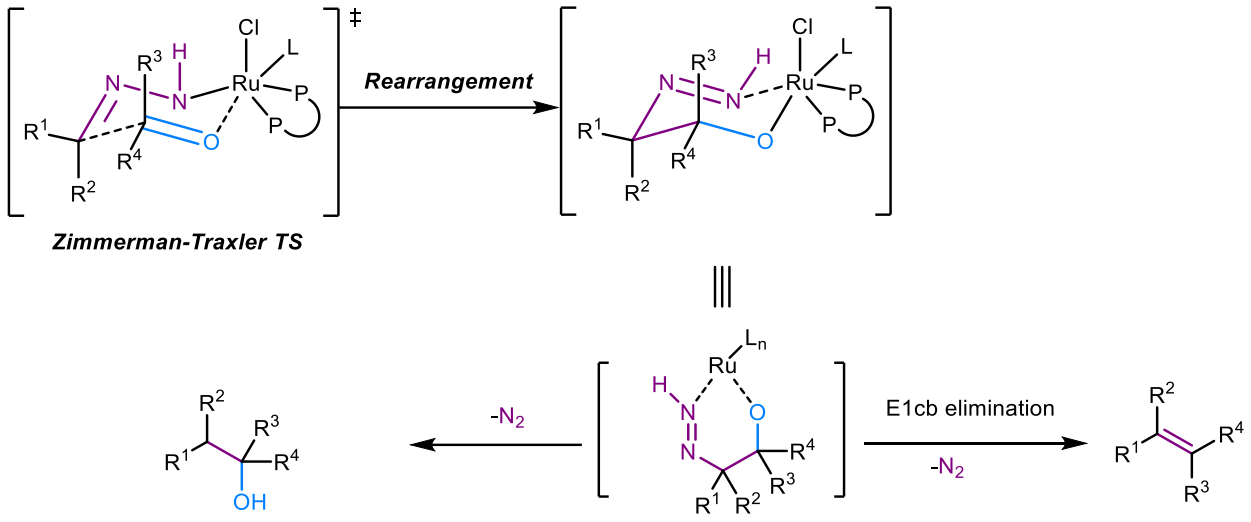

Scheme 3.4 Chemoselectivity in Ru-catalyzed C–C bond formation of hydrazone with carbonyls

3.4 Iron-catalyzed various nucleophilic addition reactions *via* hydrazones

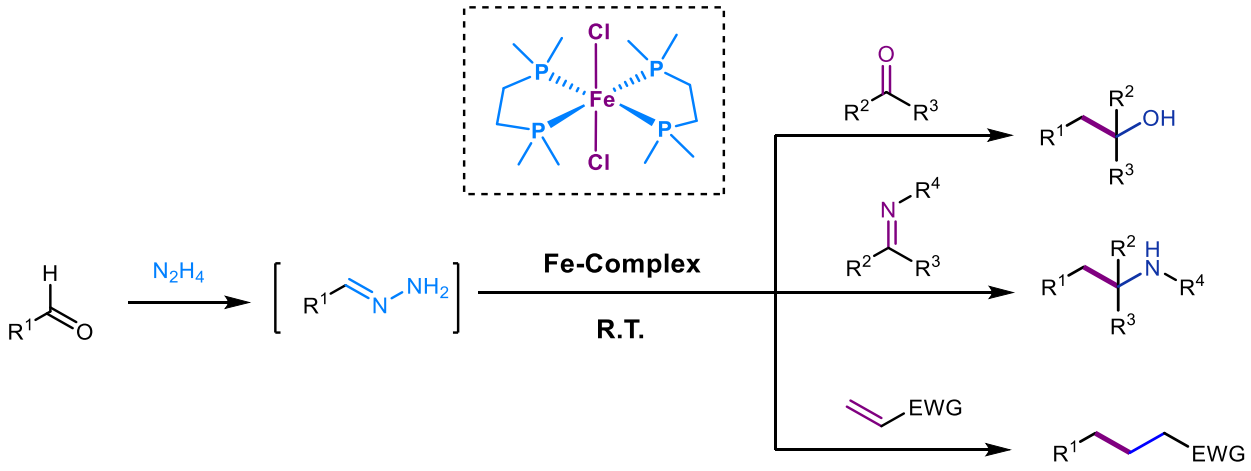

Scheme 3.5 Iron-catalyzed various nucleophilic addition reactions *via* hydrazones

In the same group as ruthenium, earth-abundant and well-defined iron complexes were found to be cheap and effective catalysts for a series of '*umpolung*' nucleophilic additions of hydrazones.

The new catalytic system maintains the broad substrate scope of an earlier expensive ruthenium system and attains chemoselectivity of different kinds of carbonyl groups. Furthermore, the iron catalyst enables this reaction at ambient temperature.[9]

References

(1). Samec, J. S. M.; Bäckvall, J.-E.; Andersson, P. G.; Brandt, P., Mechanistic aspects of transition metal-catalyzed hydrogen transfer reactions. *Chem. Soc. Rev.* **2006,** *35*, 237–248.
(2). Bäckvall, J.-E.; Andreasson, U., Ruthenium-catalyzed isomerization of allylic alcohols to saturated ketones. *Tetrahedron Lett.* **1993,** *34*, 5459–5462.
(3). Trost, B. M.; Kulawiec, R. J., Chemoselectivity in the ruthenium-catalyzed redox isomerization of allyl alcohols. *J. Am. Chem. Soc.* **1993,** *115*, 2027–2036.
(4). Li, C.-C.; Kan, J.; Qiu, Z.; Li, J.; Lv, L.; Li, C.-J., Synergistic relay reactions to achieve redox-neutral α-alkylations of olefinic alcohols with ruthenium(II) catalysis. *Angew. Chem. Int. Ed.* **2020,** *59*, 4544–4549.
(5). Sandoval, C. A.; Ohkuma, T.; Muñiz, K.; Noyori, R., Mechanism of asymmetric hydrogenation of ketones catalyzed by BINAP/1,2-diamine−ruthenium(II) complexes. *J. Am. Chem. Soc.* **2003,** *125*, 13490–13503.
(6). Li, C.-C.; Wang, H.; Sim, M. M.; Qiu, Z.; Chen, Z.-P.; Khaliullin, R. Z.; Li, C.-J., Empowering alcohols as carbonyl surrogates for grignard-type reactions. *Nat. Commun,* **2020,** *11*, 6022.
(7). Wang, H.; Dai, X.-J.; Li, C.-J., Aldehydes as alkyl carbanion equivalents for additions to carbonyl compounds. *Nat. Chem.* **2017,** *9*, 374–378.
(8). Wei, W.; Dai, X.-J.; Wang, H.; Li, C.; Yang, X.; Li, C.-J., Ruthenium(II)-catalyzed olefination *via* carbonyl reductive cross-coupling. *Chem. Sci.* **2017,** *8*, 8193–8197.
(9). Li, C.-C.; Dai, X.-J.; Wang, H.; Zhu, D.; Gao, J.; Li, C.-J., Iron-catalyzed nucleophilic addition reaction of organic carbanion equivalents *via* hydrazones. *Org. Lett.* **2018,** *20*, 3801–3805.

Chapter 4. Empowering Alcohols as Carbonyl Surrogates for Grignard-Type Reactions

4.1 Introduction

In tandem with the significant advancements of biological and pharmaceutical technologies, the role of organic chemists has evolved beyond the discovery of new chemical transformations. Developments such as rapid and direct late-stage functionalizations of large molecules have shown great potentials, with increased significance of organic reactions.[1] The Grignard reaction is a fundamental transformation in chemical synthesis and has been continuously developed over the past century. Its importance is attributed to the reaction's versatility and capacity to form C–C bonds, leading to the formation of secondary and tertiary alcohols.[2–7] A key limitation of this reaction, however, is its instability and broad reactivity. In addition, classical synthetic methods used to transform carbonyl compounds often requires the participation of oxidants, many of which are hazardous and have poor functional group tolerance.[7] Insofar, the Grignard reaction has typically been limited to early-stage construction instead of the direct late-stage modification of complex molecules or natural products.

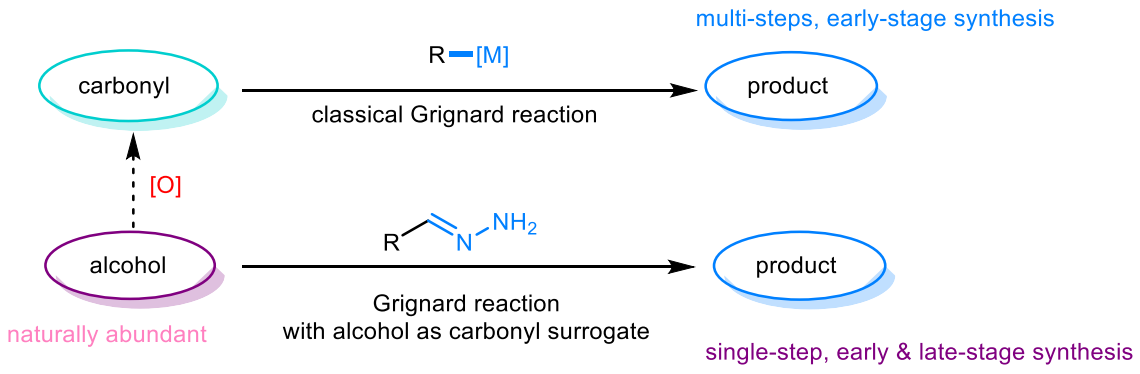

Scheme 4.1 Classical Grignard reaction and Grignard reaction with alcohol as carbonyl surrogate

In contrast, alcohols are among the most naturally abundant functional groups, which are commonly found in biomass and natural products. The direct transformation of alcohols into C–C bonds has been a long pursuit of synthetic chemists.[8–11] This type of transformation would be an especially vital tool for the late-stage functionalization of alcohol-containing natural products and

pharmaceuticals. Furthermore, this type of transformation will contribute greatly to the future sustainability of chemical syntheses by minimizing the number of steps required (Scheme 4.1). Motivated by these potential benefits, we contemplated the possibility of using alcohols as surrogates of aldehydes and ketones for the Grignard-type reaction *via* the in situ formal 'dehydrogenation' of alcohol catalyzed by transition metals.[8] Early extensive studies have shown that ruthenium(II) and other transition-metal complexes are efficient catalysts for the aerobic oxidation of alcohol to carbonyl,[12–16] which indicates the potential for hydroxyl groups to act as carbonyl surrogates. This strategy, however, has been limited to the hydrogen-borrowing aldol reactions, Michael addition[11, 17–21] and reductive amination.[22] The use of alcohols as carbonyl surrogates for a Grignard-type reaction has never been successfully demonstrated. Thus, in this chapter, we are going to discuss using various alcohols as carbonyl surrogates for Grignard reaction.

4.2 Empowering olefinic alcohol as carbonyl surrogate

4.2.1 Background

Relay strategy was widely used in the organic methodology development and total synthesis.[23–27] The utility of relay reactions simplifies the synthetic steps and avoids the separation of unstable intermediates to a certain extent.[28–30] Moreover, a relay of two originally inefficient catalytic cycles in one-pot could sometimes enables generation of the target product in an efficient way compared to stepwise process. Taking advantage of this, several unique types of transformations could be designed, which are not possible to easily achieve *via* classical methods.[23, 24] Sp^3 carbon–carbon bond formation is fundamental in organic synthesis since it is a direct way to build up the skeleton of a complex molecule. Thus, C–C bond formation has been an everlasting research topic in organic chemistry. Our group recently developed a C–C bond formation reaction using aldehydes as carbanion equivalents to undergo ruthenium(II)-complex catalyzed Grignard nucleophilic addition to carbonyls.[31–33] This newly developed 'carbanion' reagent not only avoids the usage of stoichiometric amounts of metals and alkyl halides, but also is more stable to air and water. In addition, it can tolerate various sensitive functional groups such as acidic protons, esters, halogens, etc. In order to uncover the unique reactivities of this new type of carbanion, we put our efforts into two aspects: 1) apply this new 'carbanion' towards other electrophiles beyond aldehydes;[34–40] and 2) explore unprecedented transformations concerning sp^3 C–C bond formation by combining

carbanion addition with some other Ru-catalyzed reaction. Herein we report the development of a novel, redox-neutral *α*-alkylation of allylic alcohols *via* a synergistic relay reactions of allylic isomerization/carbanion addition catalyzed by ruthenium (II) complex.[41–43]

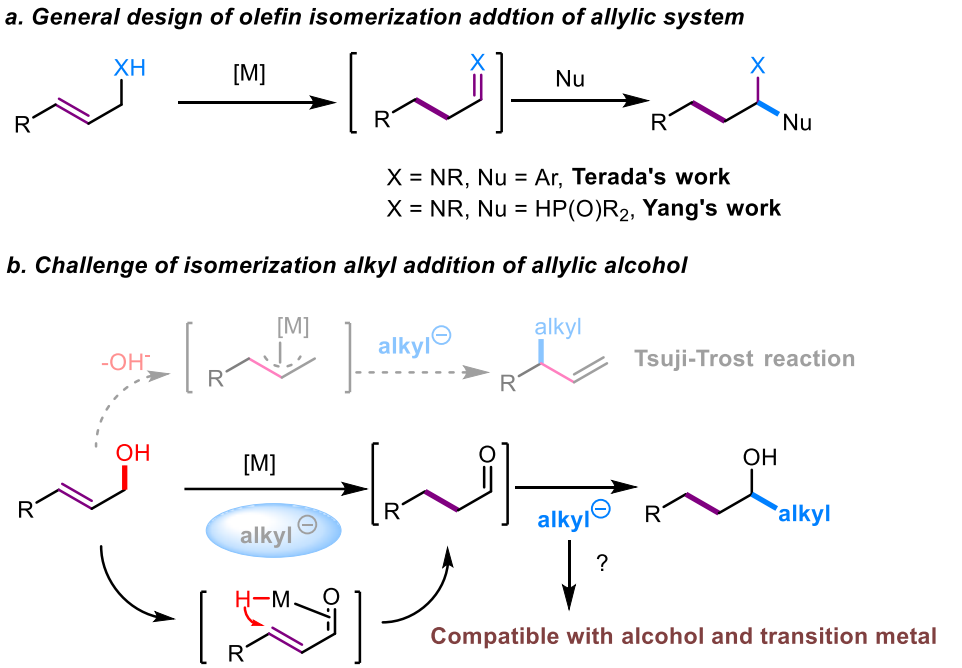

Scheme 4.2 *α*-Alkylation of allylic alcohol *via* olefin isomerization/addition strategy

Redox isomerization of allylic systems is a unique transformation in the field of organometallic chemistry, and has been well studied since the middle of the 20th century.[44–49] The advantage of this transformation lies in its ability to translocate a non-polar C=C double bond to a polar C=X (X = O, N, etc) double bond within a molecule without the assistance of extra oxidant or reductant. Correspondingly, cascade reactions using an olefin isomerization strategy such as remote functionalization enable a host of unique transformations to take place, which opens up new avenues for organic synthesis and other related fields.[50–59] In 2008, Terada *et al.* reported a

transition-metal and Brønsted acid binary catalyzed tandem olefin isomerization and addition of an allyl amine. This work utilized an allyl amine as an imine precursor to facilitate an aryl addition.[51] Later, in 2017, Yang *et al.* applied the same strategy onto phosphine chemistry and successfully realized the formation of α-aminophosphonates.[50] These successful works suggest that the strategy of using an allylic system as a C=X precursor is feasible. At the end of the last century, ruthenium-catalyzed isomerization of allylic alcohols was developed and with this transformation, various allylic alcohols were later on successfully transformed to the corresponding carbonyls.[46, 47, 60–66] However, to the best of our knowledge, the relay of allylic alcohols isomerization/carbanion addition has not been succeeded up to now. The biggest problem for this transformation is the incompatibility of classic carbanion reagents and acidic proton on allylic alcohol. The special tolerance of '*umpolung*' aldehyde 'carbanion' towards acidic proton and the similar ruthenium(II) catalyst in both reactions inspired us to test the feasibility of relaying the isomerization of allylic alcohol and the *umpolung* aldehyde addition to carbonyl to realize a redox-neutral α-alkylation of allylic alcohols.

However, the design of this relay reaction bears several challenges (Scheme 4.2, b). First of all, according to the previous literature,[46, 47, 60–66] the isomerization of allylic alcohol usually requires a high temperature (> 100 ^{o}C) and synchronized reaction time. Nevertheless, under high temperature, the hydrazone intermediate would easily undergo Wolff–Kishner reduction instead of forming C–C bond. Additionally, from previous mechanistic studies, the hydrazone carbanion has the possibility to undergo a 1,4-addition instead of a 1,2-addition, since the isomerization of allylic alcohol could potentially form an α, β-unsaturated aldehyde (ketone) intermediate. Furthermore, unlike allyl amines, allylic alcohols have the possibility to undergo Tsuji–Trost reaction as well in the presence of transition metal catalyst (allylic alkylation with OH as a leaving group),[67–75] which raised the challenge of attaining a certain chemoselectivity for allylic alcohols.

4.2.2 Results and discussions

4.2.2.1 Exploration of reaction conditions

After the analysis of the allylic alcohol isomerization literatures and our recently developed hydrazone chemistry,[31–40, 76, 77] a ruthenium (II)–phosphine system was initially chosen to start our study. Nevertheless, several factors were then taken into consideration:1) To make the metal complex favor the π-coordination, insertion and de-insertion process, an electron-rich metal center

should be created,[78] and thus we initially chose electron-rich phosphine ligands; 2) To ensure the olefin isomerization and the hydrazone transformation occur simultaneously, more flexible coordinating sites should be provided, which implies the importance of the ratio of metals and ligands in the catalytic process; and 3) Base is a necessary component for the transformation of hydrazone chemistry. Last but not the least, the leaving ability of -OH group is probably attenuated in basic system, which is capable of inhibiting side Tsuji–Trost reactions. Thus, a suitable base should also be chosen.

Table 4.1 Examination of reaction conditions

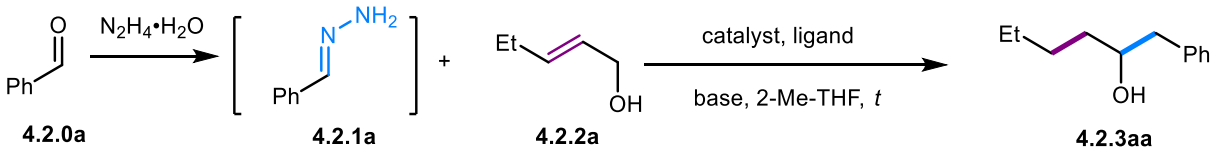

4.2.0a **4.2.1a** **4.2.2a** **4.2.3aa**

entry	catalyst	ligand	base	*t* (°C)	yield (%)
1	$Ru(PPh_3)_4Cl_2$	dmpe	K_3PO_4	80	0
2	$Ru(PPh_3)_4Cl_2$	dppe	K_3PO_4	80	0
3	$Ru(PPh_3)_4Cl_2$	dppb	K_3PO_4	80	0
4	$Ru(PPh_3)_4Cl_2$	dppf	K_3PO_4	80	trace
5	$Ru(PPh_3)_4Cl_2$	PCy_3	K_3PO_4	80	0
6	$Ru(PPh_3)_4Cl_2$	dcype	K_3PO_4	80	trace
7	$Ru(PPh_3)_4Cl_2$	dcypb	K_3PO_4	80	68
8	$Ru(PPh_3)_4Cl_2$	dcypb	K_2CO_3	80	68
9	$Ru(PPh_3)_4Cl_2$	dcypb	KOH	80	44
10	$Ru(PPh_3)_4Cl_2$	dcypb	^tBuOK	80	18
11	**Grubbs I**	dcypb	K_3PO_4	80	35
12	$Ru(PPh_3)_3Cl_2$	dcypb	K_3PO_4	80	69
13	$Ru(PPh_3)_3Cl_2$	dcypb	K_3PO_4	40	77
14	**$Ru(PPh_3)_3Cl_2$**	**dcypf**	**K_3PO_4**	**40**	**78**

Main byproduct observed:

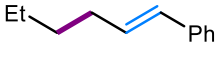

from olefination process of hydrazone and aldehyde

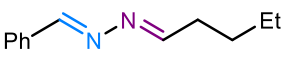

from condensation of free hydrazones and aldehdyes

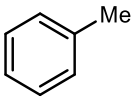

from Wolff-Kishner reduction of hydrazones

4.2.1a (0.25 mmol), **4.2.2a** (0.2 mmol), catalyst (3 mol %), ligand (3 mol %), base (1.1 equiv), solvent (0.2 mL) under N_2 atmosphere. ^{1}H NMR yield was determined using mesitylene as an internal standard. 'Trace' amount of product was noted when the desired product was not clearly detected.

With the considerations above, we used 2-pentene-1-ol and benzaldehyde hydrazone as the model substrates with $Ru(PPh_3)_4Cl_2$ as catalyst, K_3PO_4 as base, 2-Me-THF as solvent and examined several electron-rich phosphine ligands at 80 °C (Table 4.1, entries 1–6). Unfortunately, no or trace amounts of the desired product was observed with some non-bulky or electron poor bi-dentate and mono-dentate phosphine ligands. For our propose, apart from electronic effect, the failure of these ligands lies in the formation of M(bisphosphine)$_2$ type stable complex which blocks the necessary free-coordinating site. To solve this problem, we turned to bulkier electron-rich bidentate phosphine ligands with larger bite angle, such as bis-(dicyclohexylphosphino)-butane (dcypb), which would disfavor the formation of ML_2 and provide more free-coordinating site.[79, 80] To our satisfaction, the desired product was observed in moderate yield with the presence of dcypb (Table 4.1, entry 7). Another key factor for the success of this cascade reaction is to synchronize the rate of the hydrazone transformation and the rate of the olefin isomerization. As shown in our previous work, the initiation of the hydrazone transformation involves base. Generally, a stronger base tends to initiate the hydrazone transformation faster and easier than a weaker one.[31–34, 76] As the olefin isomerization process is likely the slower step, controlling the rate of the hydrazone transformation might favor this reaction. The examination of different bases confirmed this hypothesis (Table 4.1, entries 7–10). Regarding the catalyst, a ruthenium triphenylphosphine complex seemed to be the proper choice, among which $Ru(PPh_3)_3Cl_2$ worked the best. Some other types of ruthenium precursors, such as the Grubbs catalysts, could also gave the desired products, but with much lower efficiency (Table 4.1, entry 7, entries 10–12). We then analyzed the type of side products formed in order to improve the yield of final product. Wolff–Kishner reduction[81–87] (self-reduction of hydrazones) and alkene formation (from the dehydrative condensation of hydrazone and allylic alcohol) turned out to be two main side reactions. From both thermodynamic and kinetic points of view, lowering the temperature might reduce the formation of these byproducts. To our delight, decreasing the temperature to 40 °C increased the yield (77%) indeed (Table 4.1, entry 13). Additionally, another bidentate phosphine ligand, bis-(dicyclohexylphosphino)-ferrocene, which

shares a similar bite angle but bears richer electron density, worked also slightly better at 40 °C (Table 4.1, entry 14).[88]

4.2.2.2 Exploration of substrate scope

Table 4.2 Substrate scope of allylic alcohols

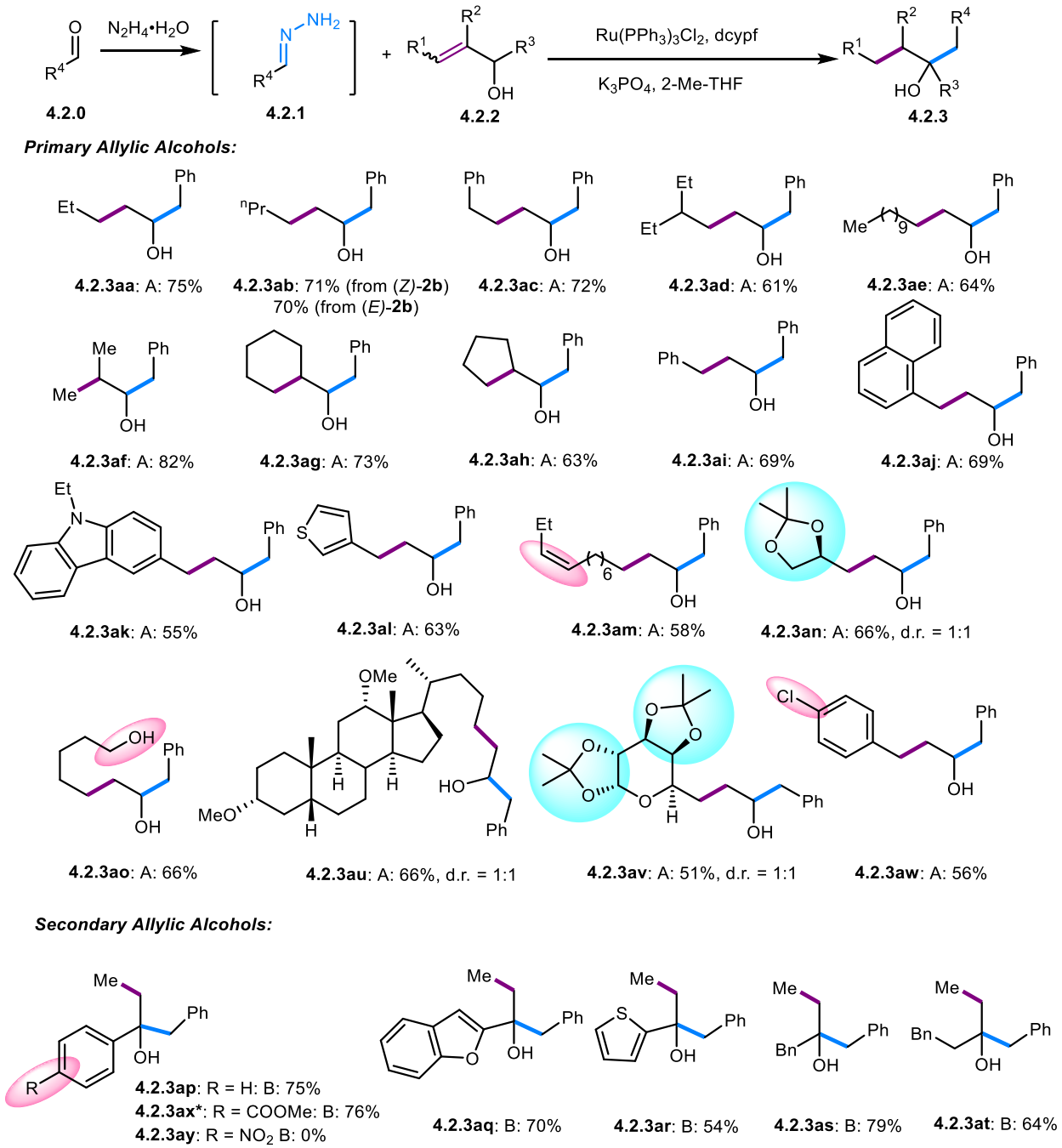

General reaction conditions A: **1a** (0.25 mmol), **2a** (0.2 mmol), catalyst (3 mol %), ligand (3 mol %), base (1.1 equiv), solvent (0.2 mL) under N_2 atmosphere under 40 °C. General reaction conditions B: **1a** (0.8 mmol), **2a** (0.2 mmol), catalyst (3 mol %), ligand (3 mol %), base (1.1 equiv), solvent (0.2 mL) under N_2 atmosphere under 70 °C. Yield of isolated product was reported otherwise noted.*catalyst (5 mol %) and ligand (5 mol %) was used.

A broad scope of allylic alcohols was then evaluated (Table 4.2). Alkyl substituted allylic alcohols were proved to undergo the isomerization/addition process in moderate to high yields, including the ones with substituents on the *β*-position (**4.2.3aa**–**4.2.3ae**) and *γ*-position (**4.2.3af**–**4.2.3ah**). The configuration of the double bond has little influence on the reaction process, which gives the desired product in similar yields (**4.2.3ab**). By replacing with bulkier or longer chain substituents, the yield was slightly reduced (**4.2.3ad**–**4.2.3ae**). Aryl (**4.2.3ai**–**4.2.3al**) and heteroaryl (**4.2.3ak**–**4.2.3al**) substituted allylic alcohols could also be transformed to the final products smoothly, albeit with slightly lower yields. Apart from these simple and non-functional group-containing structures, those with reactive functional groups also proceeded smoothly. For instance, when catalyzing substrates that bear multiple double bonds, only the double bond closest to -OH was reactive and prone to isomerize and undergo further transformation while the further ones remained unchanged (**4.2.3am**). Besides, some oxygen-containing compounds also showed comparatively high reactivity (**4.2.3an**). More importantly, this method can tolerate active protons (**4.2.3ao**). As mentioned at the beginning, one of the biggest problems of carbanion chemistry is the intolerance of the active proton which presents a potential challenge to the isomerization/carbanion addition process. The success of the multi-OH substrate further sheds light on the advantages of *umpolung* hydrazones as alkyl carbanion surrogates.

Secondary allylic alcohols were then examined for expanding the scope of this process. Initial testing of secondary allylic alcohols under the standard conditions gave us a very poor and disappointing result with only trace amounts of the desired product being observed. However, the isomerization intermediate (ketone) was observed in a significant amount while the hydrazone counterpart was completely consumed, mainly to form the Wolff–Kishner reduction product. This result suggests that for secondary allylic alcohols, both the isomerization and the nucleophilic addition processes of hydrazone might be much slower than for primary allylic alcohols. As a result, Wolff–Kishner reduction was faster than the isomerization/addition process. Under this

circumstance, we increased both the hydrazone substrates to 4 equivalent and temperature a bit in order to: 1) maintain a high concentration of hydrazone to accelerate the process of hydrazone addition even towards the end of the reaction; and 2) shorten the time to minimize the Wolff–Kishner reduction for the hydrazone. Fortunately, with all these efforts, a moderate to high yield of the desired product was realized for various secondary allylic alcohols (**4.2.3ap**–**4.2.3at**).

Considering it may have potential in synthetic applications, we then studied the reaction on selected complex molecules. Thanks to the broad functional group tolerance, several types of allylic alcohols bearing complex structures, including some steroids (**4.2.3au**) and protected sugars (**4.2.3av**), could also undergo this reaction. These results showed a promising application of this reaction in late-stage functionalizations.

Table 4.3 Substrate scope of hydrazones

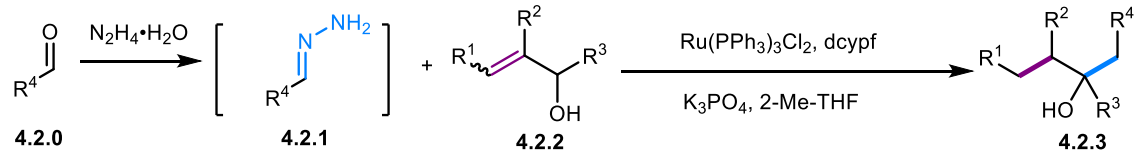

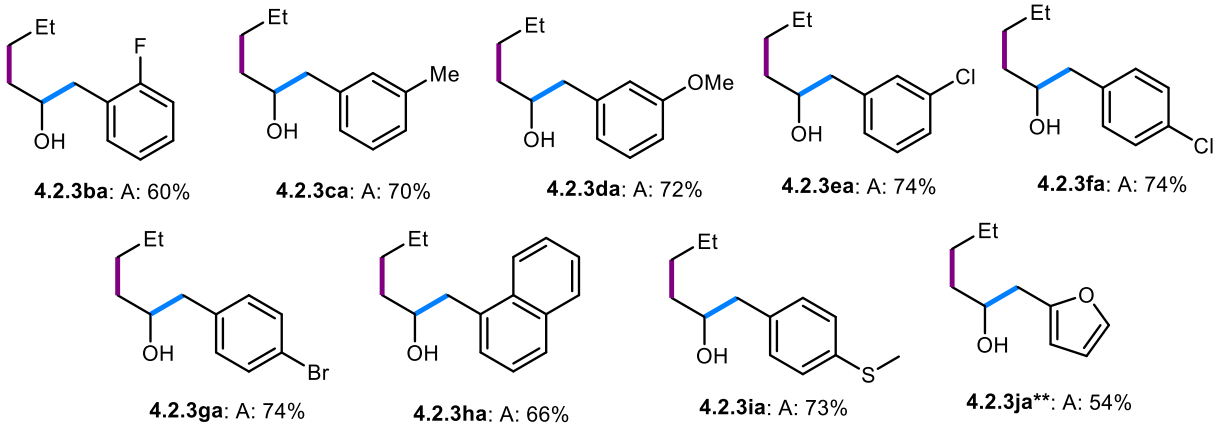

General reaction conditions A: **1a** (0.25 mmol), **2a** (0.2 mmol), catalyst (3 mol %), ligand (3 mol %), base (1.1 equiv), solvent (0.2 mL) under N_2 atmosphere under 40 °C. General reaction conditions B: **1a** (0.8 mmol), **2a** (0.2 mmol), catalyst (3 mol %), ligand (3 mol %), base (1.1 equiv), solvent (0.2 mL) under N_2 atmosphere under 70 °C. Yield of isolated product was reported otherwise noted. **This product is volatile, and the yield of this product was determined by ^{1}HNMR with mesitylene as standard (this reaction requires 0.375 equiv **1a**).

Apart from allylic alcohols, the scope of nucleophiles was also tested (Table 4.3). Aromatic aldehyde hydrazones including some heterocycles were the first series of candidates being tested. Among these substrates, having substituents at the *ortho*-position to some extent lowered the reactivity due to the presence of steric effect. Thus, with a small fluoro substituent, the reaction gave the desired product in slightly higher yield (**4.2.3ba**). All *meta*-substituted benzaldehyde hydrazones tested can tolerate this reaction regardless of the electronic nature of the substituent (**4.2.3ca**–**4.2.3ea**). With *para*-substituted aldehyde hydrazones, most of the substrates also gave good results (**4.2.3fa**–**4.2.3ga**, **4.2.3ia**). In addition to substituted benzaldehyde hydrazones, hydrazones bearing other aromatic rings could also act as proper substrates. Notably, heterocyclic substrates, can also proceed by increasing the equivalents of hydrazone substrate (**4.2.3ja**).

Table 4.4 Reactivity with remote-unsaturated alcohols

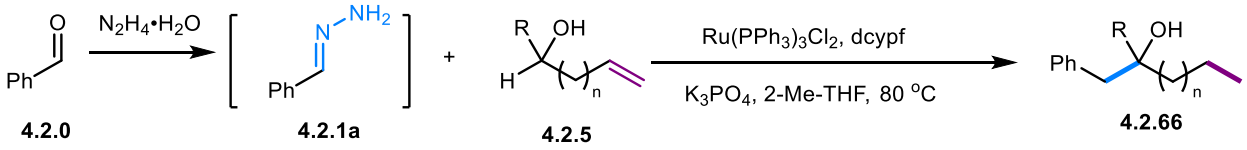

4.2.0 4.2.1a 4.2.5 4.2.66

substrate	n	product	yield (%)
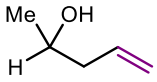 4.2.5a	1	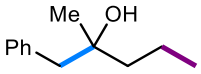 4.2.6aa	76
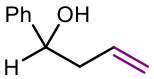 4.2.5b	1	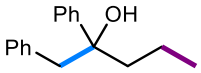 4.2.6ab	80
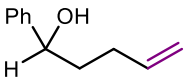 4.2.5c	2	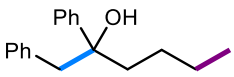 4.2.6ac	72

General reaction conditions: **1a** (0.8 mmol), **2a** (0.2 mmol), catalyst (5 mol %), ligand (5 mol %), base (1.1 equiv), solvent (0.2 mL) under N_2 atmosphere. Yield of isolated product was reported.

After the successful exploration of reactivity of allylic alcohol, we tuned our attention to alcohols bearing olefins at a longer range (Table 4.4). As 'chain-walking' is a powerful strategy to realize remote functionalization, we tested the possibility of longer chain olefinic alcohols to undergo this

synergistic relay reaction. We used 4-pentene-2-ol as a testing substrate for homoallylic-type alcohols. Delightfully, under the standard reaction conditions with 5 mol % catalyst at 80 °C. the relay chain-walking and nucleophilic addition proceeded efficiently (**4.2.6aa**). Such an efficiency could also be observed with other substituted homoallylic alcohols (**4.2.6ab**) and even longer-chain unsaturated alcohols (**4.2.6ac**).

4.2.2.3 Mechanistic study

To verify the synergistic enhancement nature of the cascade reaction, as is shown in Scheme 4, we performed the isomerization and nucleophilic addition of hydrazone independently. The results clearly showed that neither of them could happen efficiently under the standard conditions. The inefficiency of 1,2-addition is likely due to several side reactions of aldehydes such as azine condensation and aldol condensation while the inefficiency of allylic isomerization lies in its huge energy barrier. However, in the cascade reaction, the aldehyde (electrophile) was generated *in-situ via* the relay of allylic alcohol isomerization so that low concentration of aldehyde would largely inhibit the side reactions. Moreover, as the two catalytic cycles share the same catalytic system, the ruthenium aldehyde adduct would directly go through the next C–C formation cycle. On the other hand, the quick consumption of aldehyde intermediate to form C–C bond would accelerate the allylic alcohol isomerization.

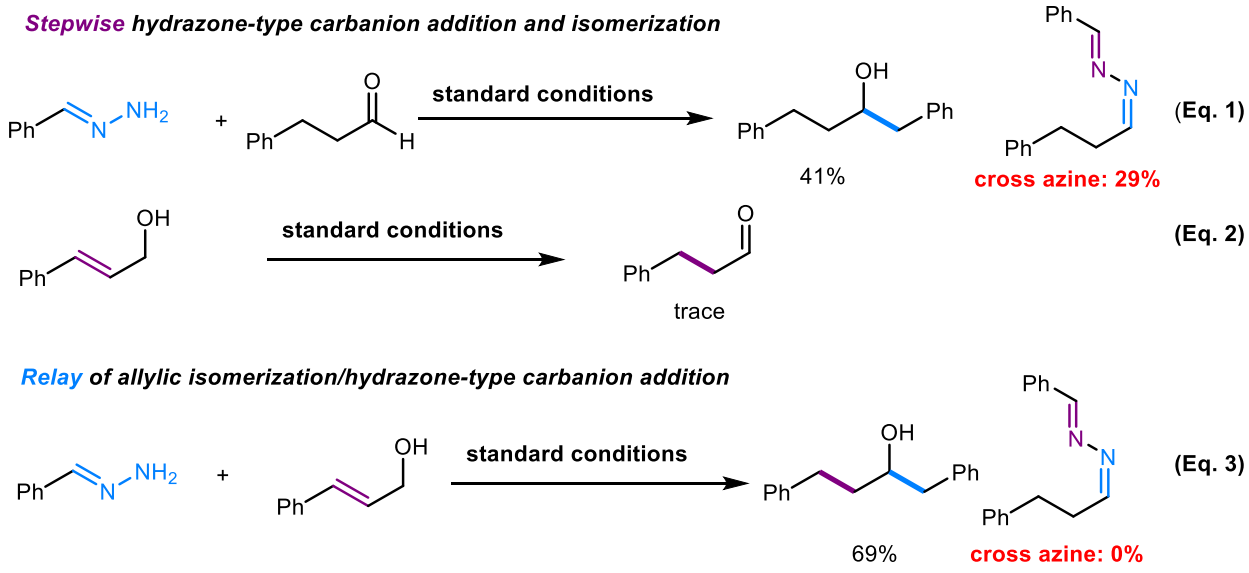

Scheme 4.3 Comparison of efficiency of relay reactions and the corresponding separate reactions

In order to gain a better understanding of the reaction, several mechanistic experiments were conducted (Scheme 4.4). First, when secondary allylic alcohol were reacting with 1.25 equivalent of hydrazones, we obtained both ketones and 1,2 carbonyl addition products, indicating carbonyl intermediate formation which largely supports the proposed isomerization/nucleophilic addition process (Scheme 4.4, Eq. 4). Then, the absence of either olefin isomerization or C–C bond formation product from methyl-protected allylic alcohols is consistent with the hypothesis that the formation of reactive carbonyl intermediate could be the driving force of the isomerization step (Eq. 5). Finally, from the isotopic labelling experiment with α-deuterated allylic alcohol (Eq. 6), nearly quantitative 1,3-deuteride shift product was obtained. This result, together with carbonyl capture experiment (Eq. 4) and alcohol protection experiment (Eq. 5), strongly suggests β-hydride elimination / 1,4 hydride insertion for the isomerization step.

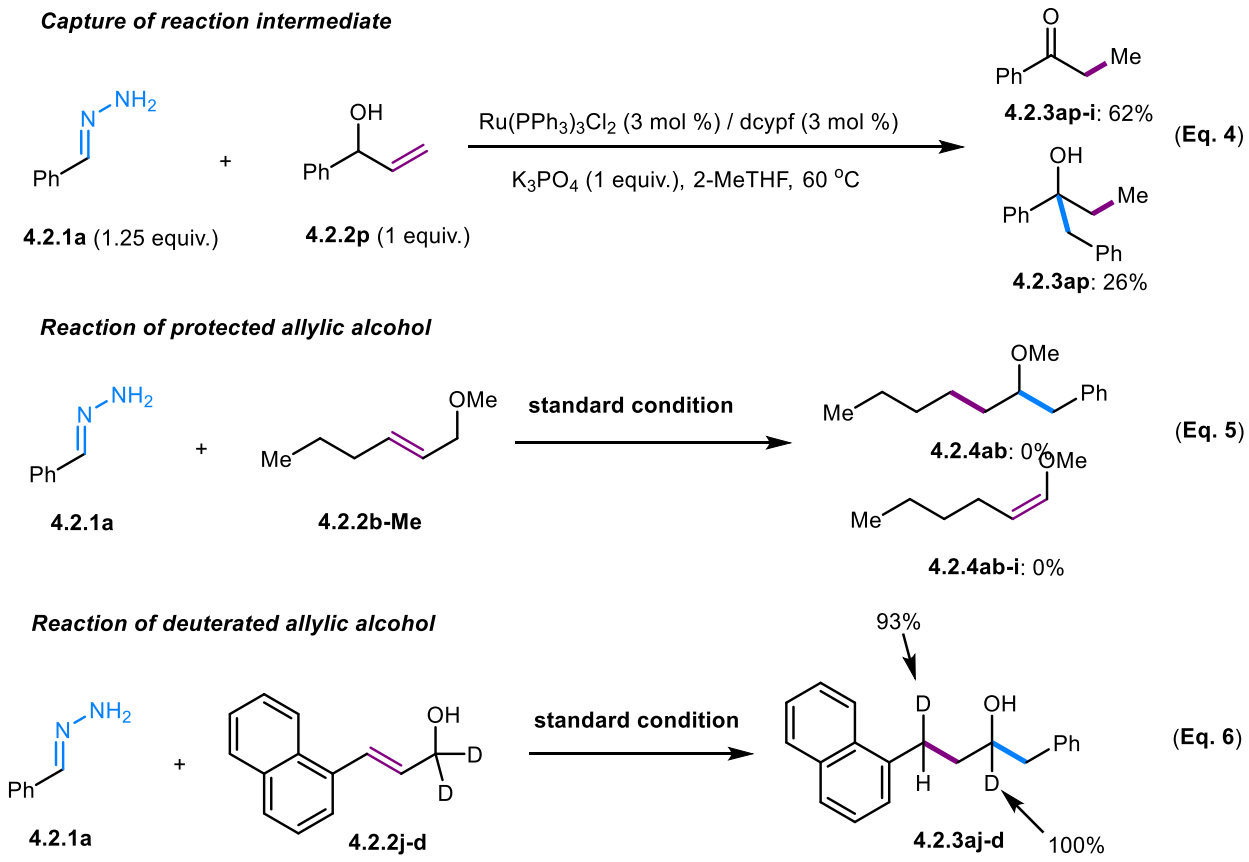

Scheme 4.4 Mechanistic study of relay allyl isomerization/carbanion addition

Based on the experimental data and analyses above, a tentative mechanism for the reaction is proposed involving a ruthenium-catalyzed olefin isomerization cycle and hydrazone addition cycle

(Scheme 4.5). For the isomerization, the reaction likely proceeds *via* a *β*-H elimination-hydride insertion according to the corresponding experiments (Scheme 4.4) and previous literatures.[46, 89, 90] The ruthenium complex **4.2.A** coordinates with allylic alcohol to form complex **4.2.B**. Then, a *β*-hydride elimination occurs to generate a ruthenium hydride complex **4.2.C**. At this stage, the so-formed Ru–H undergoes a 1,4-hydride insertion to the unsaturated carbonyl to complete the olefin isomerization and generate complex **4.2.D**. With the formation of **4.2.D**, hydrazone addition takes place *via* a six-membered ring transition state as we reported before to give the desired product as is shown in Scheme 4.5.

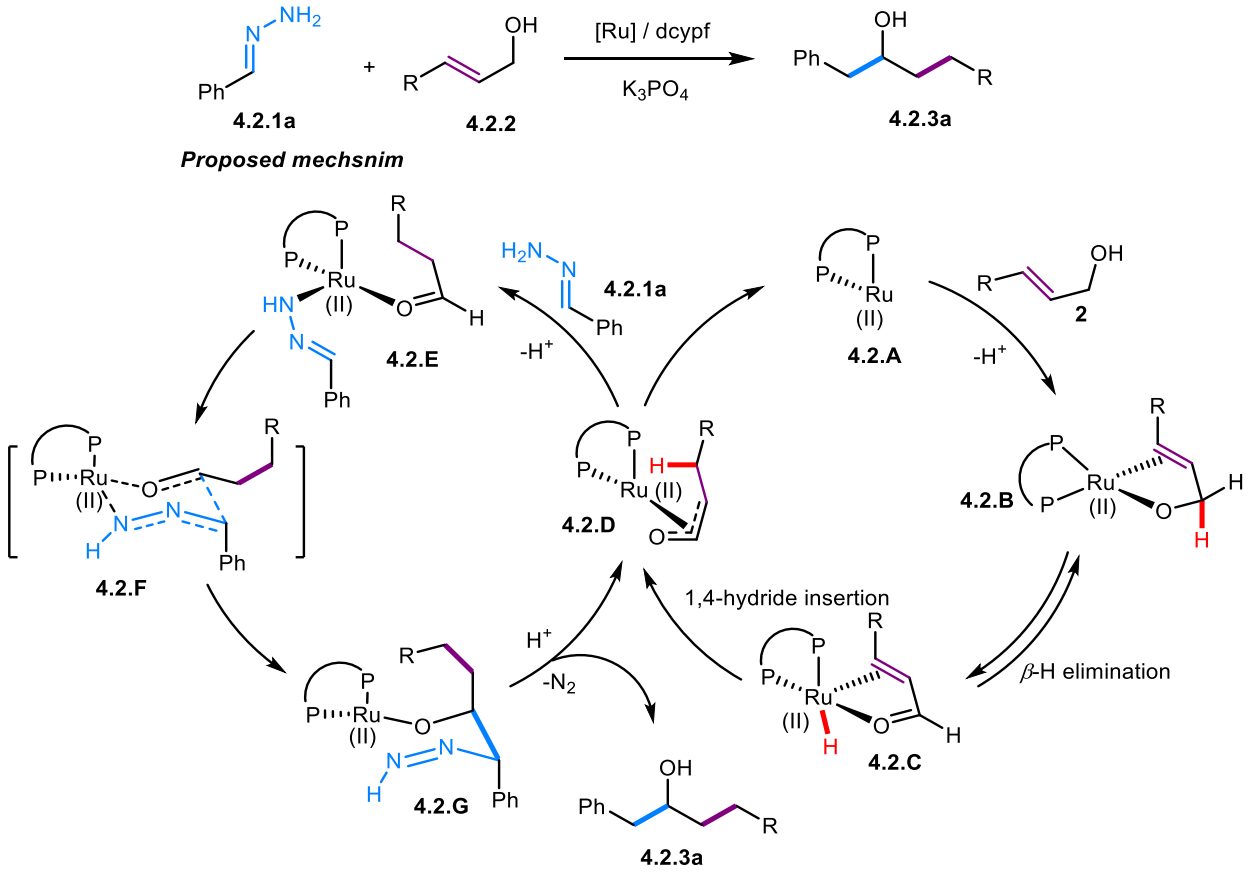

Scheme 4.5 Proposed mechanism for relay nucleophilic addition of hydrazones

4.2.3 Conclusion

In conclusion, a relay of allylic alcohols isomerization and Grignard-type nucleophilic addition of *umpolung* hydrazone was developed by utilizing Ru(II) catalytic system. This reaction allows the chemoselective redox isomerization process to occur with nucleophilic addition of ‘carbanion’ in

one-pot, and can tolerate various functional groups (e.g. -OH, -Halo, etc). At the same time, this synergistic 'relay' of reactivity makes two originally inefficient reactions proceed in high efficiency and excellent yield. This work not only explored the utility of allylic alcohol as carbonyl surrogate to undergo C–C formation but also further demonstrated the advantage of using *umpolung* hydrazone as a carbanion equivalent. The potential of late-stage functionalization by this method was also demonstrated on complex molecules. Further investigations and more in-depth mechanistic study are still undergoing in our laboratory.

4.2.4 Experimental section

4.2.4.1 General experimental information

Reaction Setup: All reactions were carried out in flame-dried V-shaped microwave reaction vials which were covered by aluminum seals with PTFE-faced silicone septa, under an atmosphere of nitrogen unless otherwise stated. All reaction temperatures corresponded to oil bath temperatures. All air and moisture-sensitive catalysts, ligands, and reagents were stored and charged in MBRAUN UNIlab Pro Glove Box Workstation unless otherwise stated.

Purifications: All work-up and purification procedures were carried out with reagent-grade solvents. Analytical thin-layer chromatography (TLC) was performed using E. Merck silica gel 60 F254 pre-coated plates (0.25 mm). Flash column chromatography was performed with E. Merck silica gel P60 (40–63 μm particle size, 230–400 mesh) (SiO_2). Unless otherwise specified, 'SiO_2' refers to P60 grade silica gel. Visualization was accomplished with UV light and/or iodine (I_2) or Vanillin solution. Retention factor (R_f) values reported were measured using a 10 × 2 cm TLC plate in a developing chamber containing the solvent system (10 mL) described. Automated flash column chromatography was performed on Biotage Isolera™ Spektra Systems with ACI™.

Solvents: 2-methyl-tetrahydrofuran (2-Me-THF), ordered from Sigma Aldrich without any purification. Solvents for filtration, transfers and chromatography, were dichloromethane (CH_2Cl_2) (ACS grade, amylene stabilized), acetone (ACS grade), ethyl acetate (EtOAc) (Fisher, ACS grade), hexane (Fisher, ACS grade), pentane (ACS grade), methanol (ACS grade).

Chemicals: In the model study, benzaldehyde (Aldrich) were distilled prior to use. Other chemicals that are commercially available and used without further purification: 2-pentene-1-ol (Aldrich), $Ru(PPh_3)_4Cl_2$ (Aldrich), $Ru(PPh_3)_3Cl_2$ (Aldrich), **Grubbs I** catalyst (Aldrich), [Ru(*p*-cymene)$_2Cl_2$] (Aldrich & Aspira), dmpe (Aspira), dppe (Aldrich), dppf (Aldrich), PCy_3 (Aldrich),

dcype (Aldrich), dcypb (Aldrich), dcypf (Aldrich & Aspira), potassium phosphate (Aldrich), potassium carbonate (Aldrich), potassium *t*-butoxide (Aldrich), hydrazine hydrate (Reagent Grade, 64–65% wt, Aldrich), mesitylene (Aldrich), 1,3,5-trimethoxylbenzene (Aldrich), anhydrous sodium sulfate. All liquid carbonyls were distilled, and solid ones were recrystallized prior to use. The ligand **PCP-1** was prepared according to previous literature.[91]

NMR Spectroscopy: Nuclear magnetic resonance (^{1}H and ^{13}C NMR) spectra were recorded on a Bruker AV500 equipped with a 60-position Sample Xpress sample changer (^{1}H, 500 MHz; ^{13}C, 125 MHz), a Varian MERCURY plus-500 spectrometer (^{1}H, 500 MHz; ^{13}C, 125 MHz) or Bruker AV400 spectrometer (^{1}H, 400 MHz; ^{13}C, 100 MHz). Chemical shifts for both ^{1}H NMR and ^{13}C NMR spectra are expressed in parts per million (ppm) units downfield from TMS, with the solvent residue peak as the chemical shift standard ($CDCl_3$: δ 7.28 ppm in ^{1}H NMR; δ 77.00 ppm in ^{13}C NMR). Data are reported as following: chemical shift, multiplicity (s = singlet, d = doublet, dd = doublet of doublets, t = triplet, td = triplet of doublets, q = quartet, quin = quintet, sep = septet, m = multiplet, br = broad singlet), coupling constants *J* (Hz), and integration.

Mass Spectrometry: Mass spectrometry (MS) was performed by the McGill Chemistry Department Mass Spectrometry Facility. High resolution mass spectra were recorded using electrospray ionization (ESI+) and/or atmospheric pressure chemical ionization APCI (+/-), performed either on 'Exactive Plus Orbitrap' a ThermoScientific high resolution accurate mass (HR/AM) FT mass spectrometer, or a Bruker Daltonics Maxis Impact quadrupole-time of flight (QTOF) mass spectrometer.

Characterization of Products: For the products, we report NMR spectra, R_f value of TLC and HRMS data.

4.2.4.2 Experimental procedures

4.2.4.2.1 Preparation of hydrazone or hydrazone solution

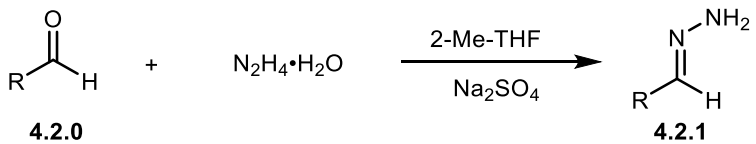

4.2.0 **4.2.1**

Procedure A: For Table 4.1, Table 4.2 Conditions A, Table 4.3: 2-Me-THF (4 mL) was added first into a small bottle with a stir bar. Then, hydrazine monohydrate (0.35 mL, 7 mmol) was added

into the bottle. After that, **4.2.0** (5 mmol)* was added dropwise into the stirred solution and the mixture was stirred for 5 min. Next, proper amount of anhydrous Na_2SO_4 was added to remove water. After stirring for another 3h, the so-formed solution was ready to use.

* Specifically, for **4.2.3ja** substrate, **4.2.0j** (7.5 mmol) was added.

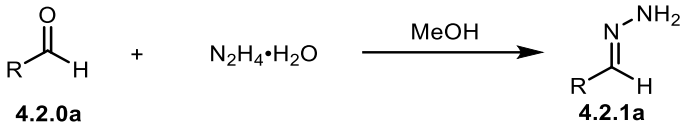

4.2.0a **4.2.1a**

Procedure B: For Table 4.2 Conditions B, Table 4.4 MeOH (5 mL) was added first into a small bottle with a stir bar. Then, hydrazine monohydrate (0.75 mL, 15 mmol) was added into the bottle. After that, **4.2.0a** (1.00 mL, 10.0 mmol) was added dropwise into the stirred solution and the mixture was stirred for 5 min. After stirring for 3 h, the so-formed solution was concentrated by vacuum to dryness. Next, the crude hydrazone was frozen-dried under vacuum for three times to remove excess amount of hydrazine hydrate. The so formed hydrazone was directly used without further purification.

4.2.4.2.2 Preparation of allylic alcohol substrates

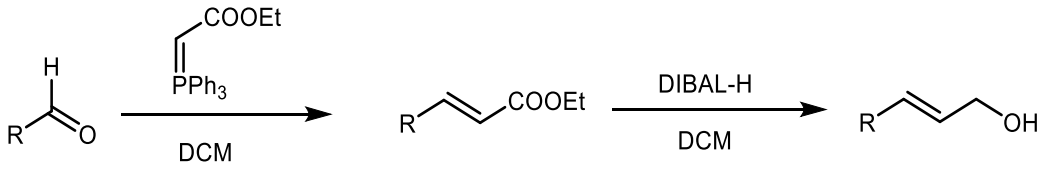

General procedure for primary allylic alcohols:[50] preparation of primary allylic alcohols was according to the previous literatures. Aldehydes (1 equiv) and ylide (1 equiv) was mixed and dissolved by proper amount of DCM (0.2 M solution). The mixture was stirred overnight at room temperature and then solvent was evaporated to give the product. Pure unsaturated ester was collected by column chromatography on silica gel. The so-formed unsaturated ester was dissolved in dry DCM and charged with Ar. The solution was cooled to -78 ^oC before DIBAL-H (1M in hexane, 2.2 equiv) was added dropwise and the reaction was last for 1.5 h at this temperature. After completion, 20% NaOH aqueous solution was added to quench the reaction and the mixture was allowed to cool to room temperature and stirred for further 10 min. Then, the organic layer was separated, and aqueous layer was extracted with DCM twice. The combined organic layer was

dried over Na_2SO_4 and the solvent was evaporated to give the desired allylic alcohol which can be directly used without any further purifications.

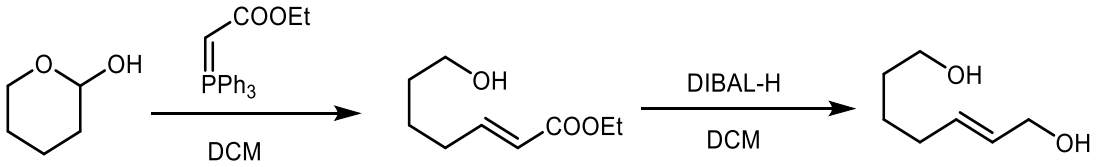

Procedure for multi-OH containing allylic alcohol (4.2.2o):[92] dihydropyran hydrate (1 equiv) and ylide (1 equiv) was mixed and dissolved by proper amount of DCM (0.2 M solution). The mixture was stirred for 2d and then solvent was evaporated to give the crude product, unsaturated ester. Pure unsaturated ester was collected by column chromatography on silica gel. The so-formed unsaturated ester was dissolved in dry DCM and charged with Ar. The solution was cooled to -78 ^oC before DIBAL-H (1M in hexane, 3.5 equiv) was added dropwise and the reaction was kept for 2.5 h at this temperature. After completion, 20% NaOH aqueous solution was added to quench the reaction and the mixture was allowed to cool to room temperature and stirred for further 10 min. Then, the organic layer was separated, and aqueous layer was extracted with DCM twice. The combined organic layer was dried over Na_2SO_4 and the solvent was evaporated to give the desired allylic alcohol **2o** which can be directly used without any further purifications.

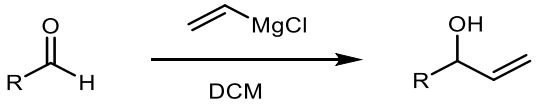

General procedure for secondary allylic alcohols:[93, 94] preparation of secondary allylic alcohols was from the corresponding aldehydes and vinyl Grignard reagents. Aldehydes (1 equiv) was dissolved in dry THF and charged with Ar. Then, the solution was cooled down to 0 ^oC before vinyl magnesium chloride solution (1.0 M in THF, 1.2 equiv) was added dropwise. After addition, the mixture was allowed to warm to room temperature and stirred for 6 h. Then, the mixture was cooled to 0 ^oC again and saturated NH_4Cl solution was added to quench the reaction. The so-formed mixture was stirred for further 10 min and the mixture was warmed to room temperature. The organic layer was separated and aqueous layer was extracted by EtOAc twice. The combined organic layer was dried by Na_2SO_4 and solvent was evaporated under vacuum. The crude product was purified by column chromatography.

4.2.4.2.3 General procedure for Scheme 2–7

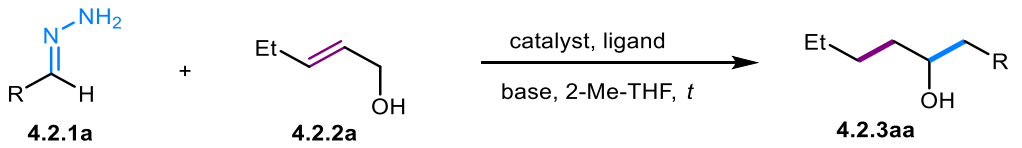

General procedure for reaction condition exploration: catalyst (0.006 mmol), ligand (0.006 mmol) and base (0.22 mmol) were added into a V-shaped reaction tube with a stir bar in the glovebox. Then, the reaction tube was sealed and moved out of the glovebox. After that, **4.2.1a** solution (prepared through ***Procedure A*** , 0.22 mL, 0.25 mmol) was added first and followed by the addition of **4.2.2a** (20 μL, 0.2 mmol). The mixture was stirred for 24h. Then, 1,3,5-trimethoxylbenzene (11.2 mg, 0.067 mmol) was added in the mixture as standard. Then, the solution was filtered by celite and concentrated to dryness. The crude mixture was diluted by $CDCl_3$ to run the ^1H NMR test to determine the ^1H NMR yield.

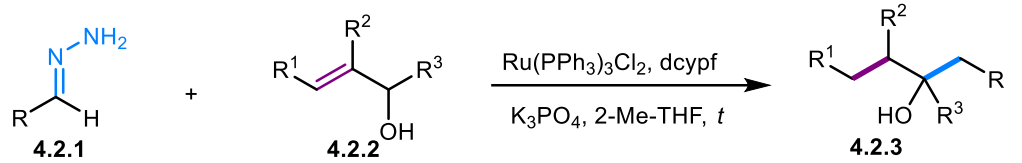

General procedure for Table 4.2 Condition A, Table 4.3 (When 2 is liquid): $Ru(PPh_3)_3Cl_2$ (0.006 mmol), dcypf (0.006 mmol) and K_3PO_4 (0.22 mmol) were added into a V-shaped reaction tube with a stir bar in the glovebox. Then, the reaction tube was sealed and moved out of the glovebox. After that, **4.2.1** solution (prepared through ***Procedure A***, 0.22 mL, 0.25 mmol) was added first and followed by the addition of **4.2.2** (0.2 mmol). The mixture was stirred under 40 °C for 24h. The reaction mixture was filtered through a celite plug with 2-3 mL CH_2Cl_2. The solvent was removed by rotary evaporator and the residue was purified by column chromatography on silica gel (using hexane and ethyl acetate as eluent) to give the pure product.

General procedure for Table 4.2 Condition A (When 2 is solid): $Ru(PPh_3)_3Cl_2$ (0.006 mmol), dcypf (0.006 mmol), K_3PO_4 (0.22 mmol) and **4.2.2** (0.2 mmol) were added into a V-shaped reaction tube with a stir bar in the glovebox. Then, the reaction tube was sealed and moved out of the glovebox. After that, **4.2.1** solution (prepared through ***Procedure A*** , 0.22 mL, 0.25 mmol) was added. The mixture was stirred under 40 °C for 24h. The reaction mixture was filtered through a celite plug with 2-3 mL CH_2Cl_2. The solvent was removed by rotary evaporator and the residue

was purified by column chromatography on silica gel (using hexane and ethyl acetate as eluent) to give the pure product.

General procedure for Table 4.2 Condition B: $Ru(PPh_3)_3Cl_2$ (0.006 mmol), dcypf (0.006 mmol) and K_3PO_4 (0.22 mmol) were added into a V-shaped reaction tube with a stir bar in the glovebox. Then, the reaction tube was sealed and moved out of the glovebox. After that, pure **4.2.1a** (prepared through ***Procedure B***, 96 μL, 0.8 mmol) was added first and followed by the addition of **4.2.2** (0.2 mmol). The mixture was stirred under 70 ^oC for 24h. The reaction mixture was filtered through a celite plug with 2-3 mL CH_2Cl_2. The solvent was removed by rotary evaporator and the residue was purified by column chromatography on silica gel (using hexane and ethyl acetate as eluent) to give the pure product.

General procedure for Table 4.4: $Ru(PPh_3)_3Cl_2$ (0.01 mmol), dcypf (0.01 mmol) and K_3PO_4 (0.22 mmol) were added into a V-shaped reaction tube with a stir bar in the glovebox. Then, the reaction tube was sealed and moved out of the glovebox. After that, pure **4.2.1a** (prepared through ***Procedure B***, 96 μL, 0.8 mmol) was added first and followed by the addition of **4.2.2** (0.2 mmol). The mixture was stirred under 80 ^oC for 24h. The reaction mixture was filtered through a celite plug with 2-3 mL CH_2Cl_2. The solvent was removed by rotary evaporator and the residue was purified by column chromatography on silica gel (using hexane and ethyl acetate as eluent) to give the pure product.

General procedure for control experiment and mechanistic study experiment: $Ru(PPh_3)_3Cl_2$ (0.006 mmol), dcypf (0.006 mmol) and K_3PO_4 (0.22 mmol) were added into a V-shaped reaction tube with a stir bar in the glovebox. Then, the reaction tube was sealed and moved out of the glovebox. After that, **4.2.1a** solution (if applicable, prepared through ***Procedure A*** , 0.22 mL, 0.25 mmol) was added first and followed by the addition of **4.2.2** (0.2 mmol). The mixture was stirred for 24h. Then, 1,3,5-trimethoxylbenzene (11.2 mg, 0.067 mmol) was added in the mixture as standard. Then, the solution was filtered by celite and concentrated to dryness. The crude mixture was diluted by $CDCl_3$ to run the ^1H NMR test to determine the ^1H NMR yield.

4.2.4.2.5 Procedure of isotope labeling experiment

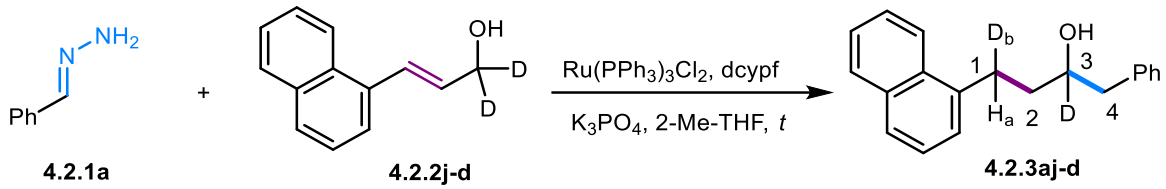

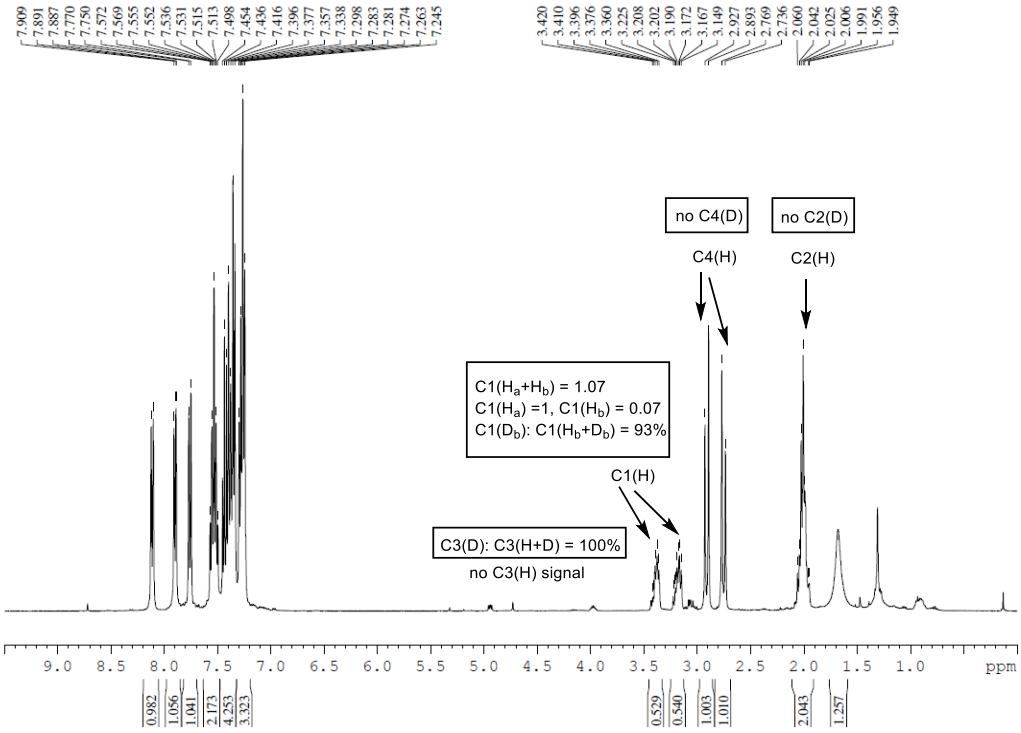

Procedure: $Ru(PPh_3)_3Cl_2$ (0.006 mmol), dcypf (0.006 mmol), K_3PO_4 (0.22 mmol) and **4.2.2j-d** (0.2 mmol) were added into a V-shaped reaction tube with a stir bar in the glovebox. Then, the reaction tube was sealed and moved out of the glovebox. After that, **4.2.1a** solution (prepared through ***Procedure A***, 0.22 mL, 0.25 mmol) was added. The mixture was stirred under 40 ^oC for 24h. The reaction mixture was filtered through a celite plug with 2-3 mL CH_2Cl_2. The solvent was removed by rotary evaporator and the residue was purified by column chromatography on silica gel (using hexane and ethyl acetate as eluent) to give the pure product.

4.2.4.3 Spectroscopic data of products

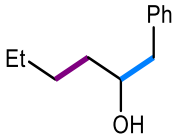

4.2.3aa

(Generated following corresponding general procedure and isolated by column chromatography on silica gel with hexane: EtOAc = 96:4 as eluent, light brown oil, 26 mg, yield: 75%): **^{1}H NMR** (500 MHz, $CDCl_3$) δ 7.39 – 7.31 (m, 2H), 7.30 – 7.22 (m, 3H), 3.84 (tt, *J* = 8.7, 4.5 Hz, 1H), 2.86 (dd, *J* = 13.6, 4.2 Hz, 1H), 2.68 (dd, *J* = 13.6, 8.4 Hz, 1H), 1.69 – 1.46 (m, 4H), 1.46 – 1.29 (m, 3H), 0.95 (t, *J* = 7.2 Hz, 3H). **^{13}C NMR** (126 MHz, $CDCl_3$) δ 138.6, 129.4, 128.5, 126.4, 72.7, 44.0, 36.5, 27.9, 22.7, 14.0. **TLC**: R_f 0.45 (5:1 hexane/EtOAc) [Phosphomolybdic acid]. **HRMS:** (ESI, *m*/*z*): calcd. for $C_{12}H_{18}ONa[M+Na]^+$ 201.1250, found: 201.1250.

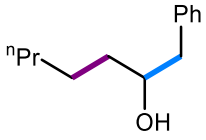

4.2.3ab

(Generated following corresponding general procedure and isolated by column chromatography on silica gel with hexane: EtOAc = 96:4 as eluent, light brown oil, 27 mg, yield: 70% from (*Z*)-allylic alcohol and 27 mg, yield: 71% from (*E*)-allylic alcohol): **^{1}H NMR** (500 MHz, $CDCl_3$) δ 7.38 – 7.31 (m, 2H), 7.31 – 7.13 (m, 3H), 3.92 – 3.76 (m, 1H), 2.86 (dd, *J* = 13.6, 4.2 Hz, 1H), 2.68 (dd, *J* = 13.6, 8.4 Hz, 1H), 1.62 – 1.45 (m, 4H), 1.48 – 1.22 (m, 5H), 0.93 (t, *J* = 6.9 Hz, 3H). **^{13}C NMR** (126 MHz, $CDCl_3$) δ 138.6, 129.4, 128.5, 126.4, 72.7, 44.0, 36.8, 31.8, 25.4, 22.6, 14.0. **TLC**: R_f 0.45 (5:1 hexane/EtOAc) [Phosphomolybdic acid]. **HRMS:** (ESI, *m*/*z*): calcd. for $C_{13}H_{20}ONa[M+Na]^+$ 215.1406, found: 215.1409.

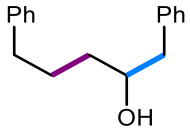

4.2.3ac

(Generated following corresponding general procedure and isolated by column chromatography on silica gel with hexane: EtOAc = 95:5 as eluent, light brown oil, 34.5 mg, yield: 72%): **^{1}H NMR** (500 MHz, $CDCl_3$) δ 7.45 – 7.17 (m, 10H), 3.94 – 3.80 (m, 1H), 2.86 (dd, *J* = 13.5, 4.2 Hz, 1H),

2.76 – 2.62 (m, 3H), 1.97 – 1.83 (m, 1H), 1.82 – 1.69 (m, 1H), 1.68 – 1.52 (m, 3H). **^{13}C NMR** (126 MHz, $CDCl_3$) δ 142.3, 138.5, 129.4, 128.5, 128.4, 128.3, 126.4, 125.7, 72.5, 44.0, 36.3, 35.8, 27.6. **TLC**: R_f 0.33 (5:1 hexane/EtOAc) [Phosphomolybdic acid]. **HRMS:** (ESI, *m*/*z*): calcd. for $C_{17}H_{20}ONa[M+Na]^+$ 263.1406, found: 263.1407.

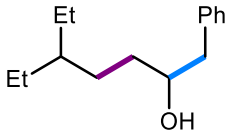

4.2.3ad

(Generated following corresponding general procedure and isolated by column chromatography on silica gel with hexane: EtOAc = 96:4 as eluent, light brown oil, 27 mg, yield: 61%): **^{1}H NMR** (500 MHz, $CDCl_3$) δ 7.38 – 7.31 (m, 2H), 7.31 – 7.18 (m, 3H), 3.89 – 3.74 (m, 1H), 2.88 (dd, *J* = 13.6, 4.1 Hz, 1H), 2.67 (dd, *J* = 13.6, 8.5 Hz, 1H), 1.67 – 1.41 (m, 4H), 1.42 – 1.27 (m, 5H), 1.27 – 1.18 (m, 1H), 0.88 (t, *J* = 7.4 Hz, 6H). **^{13}C NMR** (126 MHz, $CDCl_3$) δ 138.6, 129.4, 128.5, 126.4, 73.1, 44.0, 40.4, 34.0, 28.6, 25.4, 25.3, 10.9, 10.8. **TLC**: R_f 0.48 (5:1 hexane/EtOAc) [Phosphomolybdic acid]. **HRMS:** (ESI, *m*/*z*): calcd. for $C_{15}H_{24}ONa[M+Na]^+$ 243.1719, found: 243.1721.

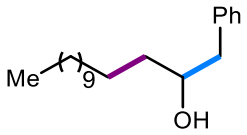

4.2.3ae

(Generated following corresponding general procedure and isolated by column chromatography on silica gel with hexane: EtOAc = 95:5 as eluent, white solid, 37 mg, yield: 64%): **^{1}H NMR** (500 MHz, $CDCl_3$) δ 7.38 – 7.31 (m, 2H), 7.31 – 7.14 (m, 3H), 3.93 – 3.77 (m, 1H), 2.86 (dd, *J* = 13.6, 4.2 Hz, 1H), 2.67 (dd, *J* = 13.6, 8.4 Hz, 1H), 1.62 – 1.47 (t, *J* = 12.6 Hz, 4H), 1.46 – 1.15 (m, 19H), 0.92 (t, *J* = 6.9 Hz, 3H). **^{13}C NMR** (126 MHz, $CDCl_3$) δ 138.6, 129.4, 128.5, 126.4, 72.7, 44.0, 36.8, 31.9, 29.7, 29.6, 29.6, 29.6, 29.3, 25.8, 22.7, 14.1. **TLC**: R_f 0.52 (5:1 hexane/EtOAc) [Phosphomolybdic acid]. **HRMS:** (ESI, *m*/*z*): calcd. for $C_{20}H_{34}ONa[M+Na]^+$ 313.2502, found: 313.2502.

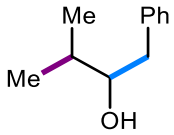

4.2.3af

(Generated following corresponding general procedure and isolated by column chromatography on silica gel with hexane: EtOAc = 96:4 as eluent, colorless oil, 26 mg, yield: 82%): **^{1}H NMR** (500 MHz, $CDCl_3$) δ 7.40 – 7.31 (m, 2H), 7.31 – 7.20 (m, 3H), 3.62 (ddd, *J* = 9.1, 5.1, 3.6 Hz, 1H), 2.89 (dd, *J* = 13.6, 3.5 Hz, 1H), 2.63 (dd, *J* = 13.6, 9.4 Hz, 1H), 1.84 – 1.73 (m, 1H), 1.49 (s, 1H), 1.03 (d, *J* = 6.8 Hz, 6H). **^{13}C NMR** (126 MHz, $CDCl_3$) δ 139.1, 129.3, 128.6, 126.4, 77.5, 40.8, 33.1, 18.9, 17.4. **TLC**: R_f 0.39 (5:1 hexane/EtOAc) [Phosphomolybdic acid]. **HRMS:** (ESI, *m*/*z*): calcd. for $C_{11}H_{16}ONa[M+Na]^+$ 187.1093, found: 187.1096.

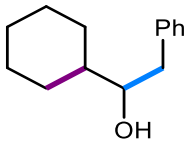

4.2.3ag

(Generated following corresponding general procedure and isolated by column chromatography on silica gel with hexane: EtOAc = 96:4 as eluent, light brown oil, 30 mg, yield: 73%): **^{1}H NMR** (500 MHz, $CDCl_3$) δ 7.45 – 7.33 (m, 2H), 7.30 – 7.22 (m, 3H), 3.61 (ddd, *J* = 9.2, 5.4, 3.5 Hz, 1H), 2.91 (dd, *J* = 13.6, 3.4 Hz, 1H), 2.63 (dd, *J* = 13.6, 9.5 Hz, 1H), 1.95 (d, *J* = 12.6 Hz, 1H), 1.89 – 1.76 (m, 3H), 1.76 – 1.68 (m, 1H), 1.58 – 1.40 (m, 2H), 1.39 – 1.04 (m, 5H). **^{13}C NMR** (126 MHz, $CDCl_3$) δ 139.2, 129.4, 128.5, 126.3, 76.9, 43.2, 40.8, 29.3, 28.0, 26.5, 26.3, 26.1. **TLC**: R_f 0.42 (5:1 hexane/EtOAc) [Phosphomolybdic acid]. **HRMS:** (ESI, *m*/*z*): calcd. for $C_{14}H_{20}ONa[M+Na]^+$ 227.1406, found: 227.1407.

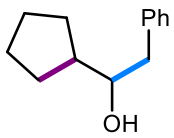

4.2.3ah

(Generated following corresponding general procedure and isolated by column chromatography on silica gel with hexane: EtOAc = 95:5 as eluent, light brown oil, 24 mg, yield: 63%): **^{1}H NMR** (500 MHz, $CDCl_3$) δ 7.44 – 7.32 (m, 2H), 7.30 – 7.22 (m, 3H), 3.66 (ddd, *J* = 8.9, 7.5, 3.5 Hz, 1H),

2.94 (dd, *J* = 13.7, 3.4 Hz, 1H), 2.64 (dd, *J* = 13.7, 9.0 Hz, 1H), 2.03 – 1.92 (m, 1H), 1.92 – 1.75 (m, 2H), 1.74 – 1.55 (m, 5H), 1.53 – 1.43 (m, 1H), 1.41 – 1.27 (m, 1H). **^{13}C NMR** (126 MHz, $CDCl_3$) δ 138.9, 129.4, 128.5, 126.3, 76.6, 45.6, 42.8, 29.3, 28.6, 25.8, 25.7. **TLC**: R_f 0.38 (5:1 hexane/EtOAc) [Phosphomolybdic acid]. **HRMS:** (ESI, *m*/*z*): calcd. for $C_{13}H_{18}ONa[M+Na]^+$ 213.1250, found: 213.1250.

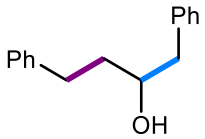

4.2.3ai

(Generated following corresponding general procedure and isolated by column chromatography on silica gel with hexane: EtOAc = 95:5 as eluent, colorless oil, 31 mg, yield: 69%): **^{1}H NMR** (500 MHz, $CDCl_3$) δ 7.45 – 7.16 (m, 10H), 3.89 (tt, *J* = 8.4, 4.3 Hz, 1H), 2.98 – 2.84 (m, 2H), 2.81 – 2.69 (m, 2H), 1.99 – 1.79 (m, 2H), 1.62 (s, 1H). **^{13}C NMR** (126 MHz, $CDCl_3$) δ 142.0, 138.3, 129.4, 128.6, 128.4, 128.4, 126.5, 125.8, 71.9, 44.1, 38.4, 32.1. **TLC**: R_f 0.31 (5:1 hexane/EtOAc) [Phosphomolybdic acid]. **HRMS:** (ESI, *m*/*z*): calcd. for $C_{16}H_{18}ONa[M+Na]^+$ 249.1250, found: 249.1250.

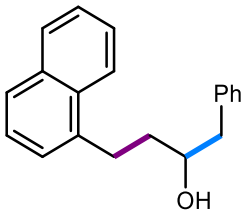

4.2.3aj

(Generated following corresponding general procedure and isolated by column chromatography on silica gel with hexane: EtOAc = 93:7 as eluent, light brown oil, 37 mg, yield: 69%): **^{1}H NMR** (500 MHz, $CDCl_3$) δ 8.12 (d, *J* = 8.2 Hz, 1H), 7.91 (d, *J* = 7.8 Hz, 1H), 7.77 (d, *J* = 8.0 Hz, 1H), 7.64 – 7.49 (m, 2H), 7.48 – 7.32 (m, 4H), 7.33 – 7.19 (m, 3H), 4.02 – 3.94 (m, 1H), 3.49 – 3.32 (m, 1H), 3.28 – 3.12 (m, 1H), 2.92 (dd, *J* = 13.6, 4.0 Hz, 1H), 2.76 (dd, *J* = 13.5, 8.6 Hz, 1H), 2.14 – 1.90 (m, 2H), 1.71 (s, 1H). **^{13}C NMR** (126 MHz, $CDCl_3$) δ 138.3, 138.2, 133.9, 131.8, 129.4, 128.7, 128.6, 126.6, 126.5, 126.0, 125.8, 125.5, 125.4, 123.8, 72.2, 44.2, 37.8, 29.2. **TLC**: R_f 0.26 (5:1 hexane/EtOAc) [Phosphomolybdic acid]. **HRMS:** (ESI, *m*/*z*): calcd. for $C_{20}H_{20}ONa[M+Na]^+$ 299.1406, found: 299.1408.

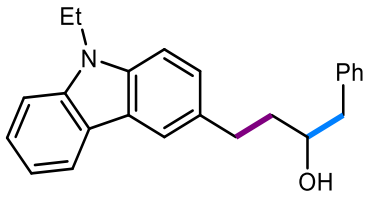

4.2.3ak

(Generated following corresponding general procedure and isolated by column chromatography on silica gel with hexane: EtOAc = 90:10 as eluent, light brown oil, 38 mg, yield: 55%): **^{1}H NMR** (500 MHz, $CDCl_3$) δ 8.13 (d, *J* = 7.7 Hz, 1H), 7.98 (s, 1H), 7.55 – 7.47 (m, 1H), 7.44 (d, *J* = 8.1 Hz, 1H), 7.40 – 7.32 (m, 4H), 7.32 – 7.23 (m, 4H), 4.39 (q, *J* = 7.2 Hz, 2H), 4.00 – 3.91 (m, 1H), 3.14 – 3.03 (m, 1H), 3.03 – 2.89 (m, 2H), 2.77 (dd, *J* = 13.6, 8.4 Hz, 1H), 2.10 – 1.91 (m, 2H), 1.66 (s, 1H), 1.47 (t, *J* = 7.2 Hz, 3H). **^{13}C NMR** (126 MHz, $CDCl_3$) δ 140.1, 138.5, 138.4, 132.3, 129.4, 128.5, 126.4, 126.3, 125.4, 123.0, 122.7, 120.3, 119.8, 118.5, 108.3, 108.3, 72.0, 44.2, 39.3, 37.5, 32.1, 13.8. **TLC**: R_f 0.52 (2:1 hexane/EtOAc) [Phosphomolybdic acid]. **HRMS:** (ESI, *m*/*z*): calcd. for $C_{24}H_{26}ON[M+H]^+$ 344.2009, found: 344.2005.

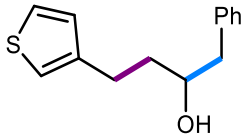

4.2.3al

(Generated following corresponding general procedure and isolated by column chromatography on silica gel with hexane: EtOAc = 94:6 as eluent, light brown oil, 28 mg, yield: 61%): **^{1}H NMR** (500 MHz, $CDCl_3$) δ 7.41 – 7.18 (m, 6H), 6.98 (br, 2H), 3.97 – 3.77 (m, 1H), 2.97 – 2.84 (m, 2H), 2.84 – 2.64 (m, 2H), 1.99 – 1.78 (m, 2H), 1.62 (s, 1H). **^{13}C NMR** (126 MHz, $CDCl_3$) δ 142.2, 138.3, 129.4, 128.6, 128.2, 126.5, 125.4, 120.1, 71.9, 44.1, 37.4, 26.5. **TLC**: R_f 0.32 (5:1 hexane/EtOAc) [Phosphomolybdic acid]. **HRMS:** (ESI, *m*/*z*): calcd. for $C_{14}H_{16}ONa[M+Na]^+$ 255.0814, found: 255.0810.

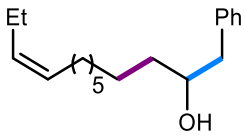

4.2.3am

(Generated following corresponding general procedure and isolated by column chromatography on silica gel with hexane: EtOAc = 96:4 as eluent, light brown oil, 32 mg, yield: 58%): **^{1}H NMR** (500 MHz, $CDCl_3$) δ 7.37 – 7.31 (m, 2H), 7.31 – 7.17 (m, 3H), 5.49 – 5.30 (m, 2H), 3.92 – 3.76 (m, 1H), 2.86 (dd, *J* = 13.6, 4.2 Hz, 1H), 2.67 (dd, *J* = 13.6, 8.4 Hz, 1H), 2.16 – 1.96 (m, 4H), 1.65 – 1.45 (m, 4H), 1.45 – 1.20 (m, 9H), 0.99 (t, *J* = 7.5 Hz, 3H). **^{13}C NMR** (126 MHz, $CDCl_3$) δ 138.6, 131.5, 129.4, 129.3, 128.5, 126.4, 72.6, 44.0, 36.8, 29.7, 29.6, 29.5, 29.2, 27.0, 25.7, 20.5, 14.4. **TLC**: R_f 0.48 (5:1 hexane/EtOAc) [Phosphomolybdic acid]. **HRMS:** (ESI, *m*/*z*): calcd. for $C_{19}H_{30}ONa[M+Na]^+$ 297.2189, found: 297.2186.

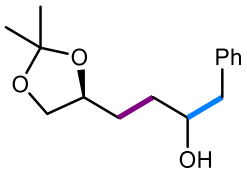

4.2.3an

(Generated following corresponding general procedure and isolated by column chromatography on silica gel with hexane: EtOAc = 88:12 as eluent, light brown oil, 33 mg, yield: 66%, d.r. = 1: 1): Combined **^{1}H NMR** (500 MHz, $CDCl_3$) δ 7.37 – 7.30 (m, 2H), 7.29 – 7.20 (m, 3H), 4.19 – 3.99 (m, 2H), 3.94 – 3.80 (m, 1H), 3.55 (td, *J* = 7.6, 3.1 Hz, 1H), 2.84 (ddd, *J* = 12.8, 7.9, 4.7 Hz, 1H), 2.78 – 2.64 (m, 1H), 2.36 (s, 0.5H), 2.00 (s, 0.5H), 1.85 – 1.48 (m, 4H), 1.44 (s, 3H), 1.38 (s, 3H). **^{13}C NMR** (126 MHz, $CDCl_3$) δ 138.6, 138.4, 129.4, 128.5, 128.5, 126.4, 126.4, 109.0, 108.9, 76.1, 76.1, 72.5, 72.2, 69.4, 69.4, 44.1, 44.0, 33.1, 33.0, 30.1, 29.7, 26.9, 26.9, 25.7. **TLC**: R_f 0.14 (5:1 hexane/EtOAc) [Phosphomolybdic acid]. **HRMS:** (ESI, *m*/*z*): calcd. for $C_{16}H_{22}O_3Na[M+Na]^+$ 273.1461, found: 273.1456.

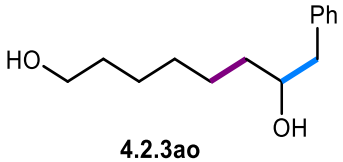

4.2.3ao

(Generated following corresponding general procedure and isolated by column chromatography on silica gel with hexane: EtOAc = 60:40 as eluent, light brown oil, 29 mg, yield: 66%): **^{1}H NMR** (500 MHz, $CDCl_3$) δ 7.36 – 7.30 (m, 2H), 7.28 – 7.20 (m, 3H), 3.83 (tt, *J* = 8.6, 4.4 Hz, 1H), 3.64 (t, *J* = 6.6 Hz, 2H), 2.84 (dd, *J* = 13.5, 4.3 Hz, 1H), 2.67 (dd, *J* = 13.5, 8.4 Hz, 1H), 1.85 – 1.67 (s, *J* = 32.2 Hz, 2H), 1.64 – 1.48 (m, 5H), 1.45 – 1.31 (m, 5H). **^{13}C NMR** (126 MHz, $CDCl_3$) δ 138.6,

129.4, 128.5, 126.4, 72.6, 62.9, 44.0, 36.6, 32.6, 29.3, 25.6. **TLC**: R_f 0.14 (2:1 hexane/EtOAc) [Phosphomolybdic acid]. **HRMS:** (ESI, *m*/*z*): calcd. for $C_{14}H_{22}ONa[M+Na]^+$ 245.1512, found: 245.1510.

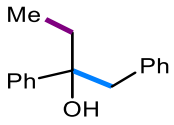

4.2.3ap

(Generated following corresponding general procedure and isolated by column chromatography on silica gel with hexane: EtOAc = 97:3 as eluent, colorless oil, 34 mg, yield: 75%): **^{1}H NMR** (500 MHz, $CDCl_3$) δ 7.46 – 7.33 (m, 4H), 7.33 – 7.16 (m, 4H), 7.05 – 6.98 (m, 2H), 3.21 (d, *J* = 13.3 Hz, 1H), 3.10 (d, *J* = 13.3 Hz, 1H), 2.04 (dq, *J* = 14.8, 7.5 Hz, 1H), 1.96 – 1.80 (m, 2H), 0.81 (t, *J* = 7.45, 3H). **^{13}C NMR** (126 MHz, $CDCl_3$) δ 145.4, 136.4, 130.6, 128.0, 127.9, 126.6, 126.4, 125.5, 76.9, 49.4, 34.4, 7.8. **TLC**: R_f 0.54 (5:1 hexane/EtOAc) [Phosphomolybdic acid]. **HRMS:** (ESI, *m*/*z*): calcd. for $C_{16}H_{18}ONa[M+Na]^+$ 249.1250, found: 249.1247.

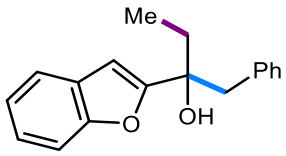

4.2.3aq

(Generated following corresponding general procedure and isolated by column chromatography on silica gel with hexane: EtOAc = 96:4 as eluent, colorless oil, 37 mg, yield: 70%): **^{1}H NMR** (500 MHz, $CDCl_3$) δ 7.62 – 7.47 (m, 2H), 7.40 – 7.12 (m, 5H), 7.08 – 6.96 (m, 2H), 6.49 (d, *J* = 0.6 Hz, 1H), 3.44 (d, *J* = 13.5 Hz, 1H), 3.11 (d, *J* = 13.5 Hz, 1H), 2.16 – 2.06 (m, 2H), 1.95 (dq, *J* = 14.6, 7.3 Hz, 1H), 0.94 (t, *J* = 7.4 Hz, 3H). **^{13}C NMR** (126 MHz, $CDCl_3$) δ 160.7, 154.7, 135.8, 130.3, 128.4, 128.2, 126.8, 123.6, 122.6, 120.8, 111.1, 103.6, 75.3, 46.4, 32.8, 8.0. **TLC**: R_f 0.49 (5:1 hexane/EtOAc) [Phosphomolybdic acid]. **HRMS:** (ESI, *m*/*z*): calcd. for $C_{18}H_{18}O_2Na[M+Na]^+$ 289.1199, found: 289.1196.

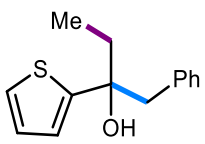

4.2.3ar

(Generated following corresponding general procedure and isolated by column chromatography on silica gel with hexane: EtOAc = 96:4 as eluent, colorless oil, 25 mg, yield: 54%): **^{1}H NMR** (500 MHz, $CDCl_3$) δ 7.32 – 7.18 (m, 4H), 7.11 – 7.02 (m, 2H), 6.98 (dd, *J* = 5.0, 3.5 Hz, 1H), 6.80 (dd, *J* = 3.5, 1.2 Hz, 1H), 3.22 (d, *J* = 13.4 Hz, 1H), 3.13 (d, *J* = 13.4 Hz, 1H), 2.09 (s, 1H), 2.01 – 1.84 (m, 2H), 0.92 (t, *J* = 7.4 Hz, 3H). **^{13}C NMR** (126 MHz, $CDCl_3$) δ 151.2, 136.1, 130.6, 128.1, 126.8, 126.6, 123.7, 123.0, 76.7, 49.7, 35.5, 8.0. **TLC**: R_f 0.51 (5:1 hexane/EtOAc) [Phosphomolybdic acid]. **HRMS:** (ESI, *m*/*z*): calcd. for $C_{14}H_{16}ONaS[M+Na]^+$ 255.0814, found: 255.0811.

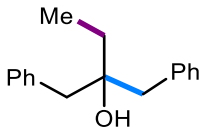

4.2.3as

(Generated following corresponding general procedure and isolated by column chromatography on silica gel with hexane: EtOAc = 96:4 as eluent, colorless oil, 38 mg, yield: 79%): **^{1}H NMR** (500 MHz, $CDCl_3$) δ 7.41 – 7.32 (m, 4H), 7.32 – 7.25 (m, 6H), 2.85 (s, 4H), 1.47 – 1.29 (m, 3H), 1.06 (t, *J* = 7.5 Hz, 3H). **^{13}C NMR** (126 MHz, $CDCl_3$) δ 137.4, 130.7, 128.1, 126.4, 74.5, 44.9, 30.6, 8.4. **TLC**: R_f 0.54 (5:1 hexane/EtOAc) [Phosphomolybdic acid]. **HRMS:** (ESI, *m*/*z*): calcd. for $C_{17}H_{20}ONa[M+Na]^+$ 263.1406, found: 263.1402.

.

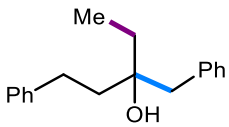

4.2.3at

(Generated following corresponding general procedure and isolated by column chromatography on silica gel with hexane: EtOAc = 96:4 as eluent, colorless oil, 32 mg, yield: 64%): **^{1}H NMR** (500 MHz, $CDCl_3$) δ 7.47 – 7.05 (m, 10H), 2.87 (s, 2H), 2.75 (t, *J* = 8.6 Hz, 2H), 1.89 – 1.72 (m, 2H), 1.71 – 1.50 (m, 2H), 1.35 (s, 1H), 1.04 (t, *J* = 7.3 Hz, 3H). **^{13}C NMR** (126 MHz, $CDCl_3$) δ 142.5, 137.2, 130.6, 128.4, 128.3, 128.3, 126.5, 125.7, 74.3, 45.1, 40.1, 31.0, 30.0, 8.2. **TLC**: R_f 0.46 (5:1 hexane/EtOAc) [Phosphomolybdic acid]. **HRMS:** (ESI, *m*/*z*): calcd. for $C_{18}H_{22}ONa[M+Na]^+$ 277.1563, found: 277.1559..

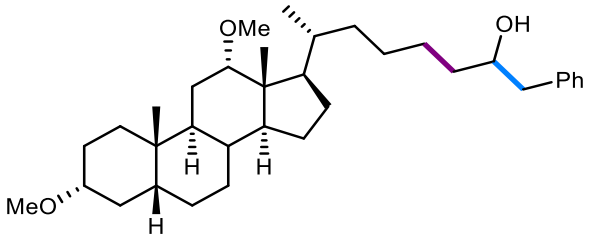

4.2.3au

(Generated following corresponding general procedure and isolated by column chromatography on silica gel with hexane: EtOAc = 93:7 as eluent, colorless oil, 68 mg, yield: 66%, d.r. = 1:1): Combined **^{1}H NMR** (500 MHz, $CDCl_3$) δ 7.36 – 7.30 (m, 2H), 7.27 – 7.21 (m, 3H), 3.92 – 3.75 (m, 1H), 3.41 (s, 1H), 3.35 (s, 3H), 3.27 (s, 3H), 3.21 – 3.11 (m, 1H), 2.84 (dd, *J* = 13.5, 4.0 Hz, 1H), 2.67 (dd, *J* = 13.3, 8.4 Hz, 1H), 1.98 – 1.65 (m, 9H), 1.64 – 1.49 (m, 5H), 1.47 – 0.81 (m, 23H), 0.68 (s, 3H). **^{13}C NMR** (126 MHz, $CDCl_3$) δ 138.6, 129.4, 128.4, 126.3, 82.3, 80.4, 72.7, 72.6, 55.6, 55.4, 48.8, 46.7, 46.2, 44.0, 42.0, 36.9, 36.8, 36.0, 35.8, 35.7, 35.4, 35.3, 34.4, 33.5, 32.5, 27.5, 27.3, 26.7, 26.2, 26.1, 26.1, 26.0, 23.6, 23.2, 21.9, 17.7, 12.7. **TLC**: R_f 0.27 (5:1 hexane/EtOAc) [Phosphomolybdic acid]. **HRMS:** (ESI, *m*/*z*): calcd. for $C_{35}H_{56}O_3Na[M+Na]^+$ 547.4122, found: 547.4128.

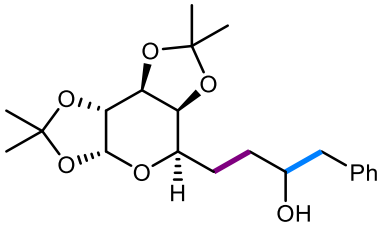

4.2.3av

(Generated following corresponding general procedure and isolated by column chromatography on silica gel with hexane: EtOAc = 88:12 as eluent, light brown oil, 38.5 mg, yield: 51%, d.r. = 1:1): Combined **^{1}H NMR** (500 MHz, $CDCl_3$) δ 7.35 – 7.30 (m, 2H), 7.27 – 7.21 (m, 3H), 5.56 (d, *J* = 5.1 Hz, 1H), 4.60 (dt, *J* = 7.9, 2.2 Hz, 1H), 4.32 (ddd, *J* = 5.1, 2.3, 0.8 Hz, 1H), 4.15 (td, *J* = 7.9, 1.8 Hz, 1H), 3.96 – 3.84 (m, 1H), 3.84 – 3.72 (m, 1H), 2.85 (ddd, *J* = 13.6, 4.3, 2.4 Hz, 1H), 2.76 – 2.66 (m, 1H), 2.04 – 1.62 (m, 5H), 1.53 (d, *J* = 4.5 Hz, 3H), 1.48 (s, 3H), 1.38 – 1.31 (m, 6H). **^{13}C NMR** (126 MHz, $CDCl_3$) δ 138.7, 138.7, 129.4, 129.4, 128.5, 128.4, 126.3, 109.0, 109.0, 108.4, 108.3, 96.5, 96.5, 72.9, 72.9, 72.5, 72.1, 70.9, 70.8, 70.5, 70.5, 67.8, 67.3, 44.0, 43.9, 33.3,

32.9, 26.6, 26.4, 26.0, 24.9, 24.4, 24.3. **TLC**: R_f 0.38 (2:1 hexane/EtOAc) [Phosphomolybdic acid]. **HRMS:** (ESI, *m*/*z*): calcd. for $C_{19}H_{32}O_6Na[M+Na]^+$ 379.2115, found: 379.2108

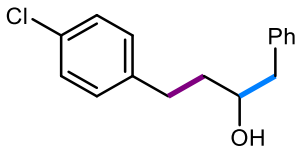

4.2.3aw

(Generated following corresponding general procedure and isolated by column chromatography on silica gel with hexane: EtOAc = 95:5 as eluent, light brown oil, 29 mg, yield: 56%): **^{1}H NMR** (500 MHz, $CDCl_3$) δ 7.39 – 7.32 (m, 2H), 7.32 – 7.20 (m, 5H), 7.21 – 7.10 (m, 2H), 3.84 (tt, *J* = 8.4, 4.4 Hz, 1H), 2.94 – 2.80 (m, 2H), 2.78 – 2.65 (m, 2H), 1.93 – 1.75 (m, 2H), 1.61 (s, 1H). **^{13}C NMR** (126 MHz, $CDCl_3$) δ 140.4, 138.1, 131.5, 129.8, 129.4, 128.6, 128.4, 126.6, 71.7, 44.2, 38.2, 31.4. **TLC**: R_f 0.33 (5:1 hexane/EtOAc) [Phosphomolybdic acid]. **HRMS:** (ESI, *m*/*z*): calcd. for $C_{16}H_{17}OClNa[M+Na]^+$ 283.0860, found: 283.0864.

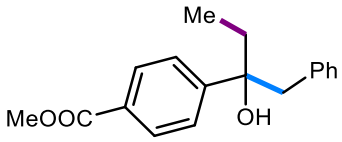

4.2.3ax

(Generated following corresponding general procedure and isolated by column chromatography on silica gel with hexane: EtOAc = 93:7 as eluent, colorless oil, 43 mg, yield: 76%): **^{1}H NMR** (500 MHz, $CDCl_3$) δ 8.04 – 7.99 (m, 2H), 7.45 – 7.41 (m, 2H), 7.25 – 7.18 (m, 3H), 6.99 – 6.93 (m, 2H), 3.94 (s, 3H), 3.18 (d, *J* = 13.4 Hz, 1H), 3.08 (d, *J* = 13.4 Hz, 1H), 2.08 – 1.98 (m, 1H), 1.94 – 1.82 (m, 2H), 0.77 (t, *J* = 7.4 Hz, 3H). **^{13}C NMR** (126 MHz, $CDCl_3$) δ 167.1, 150.9, 135.9, 130.6, 129.3, 128.3, 128.2, 126.8, 125.7, 77.1, 76.7, 52.0, 49.3, 34.6, 7.7. **TLC**: R_f 0.38 (5:1 hexane/EtOAc) [Phosphomolybdic acid]. **HRMS:** (ESI, *m*/*z*): calcd. for $C_{18}H_{20}O_3Na[M+Na]^+$ 307.1305, found: 307.1299.

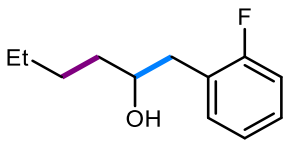

4.2.3ba

(Generated following corresponding general procedure and isolated by column chromatography on silica gel with hexane: EtOAc = 96:4 as eluent, colorless oil, 24 mg, yield: 60%): **^{1}H NMR** (500 MHz, $CDCl_3$) δ 7.34 – 7.18 (m, 2H), 7.17 – 6.97 (m, 2H), 3.95 – 3.78 (m, 1H), 2.92 (dd, *J* = 13.7, 3.7 Hz, 1H), 2.71 (dd, *J* = 13.6, 8.2 Hz, 1H), 1.66 – 1.44 (m, 4H), 1.45 – 1.27 (m, 3H), 0.94 (t, *J* = 7.2 Hz, 3H). **^{13}C NMR** (126 MHz, $CDCl_3$) δ 161.3 (d, *J* = 244.4 Hz), 131.79 (d, *J* = 5.0 Hz), 128.13 (d, *J* = 8.1 Hz), 125.66 (d, *J* = 15.8 Hz), 123.97 (d, *J* = 3.5 Hz), 115.3 (d, *J* = 22.9 Hz), 71.7, 37.2, 36.7, 27.8, 22.6, 14.0. **^{19}F NMR** (471 MHz, $CDCl_3$) δ -117.75. **TLC**: R_f 0.46 (5:1 hexane/EtOAc) [Phosphomolybdic acid]. **HRMS:** (ESI, *m*/*z*): calcd. for $C_{12}H_{17}OFNa[M+Na]^+$ 219.1156, found: 219.1152.

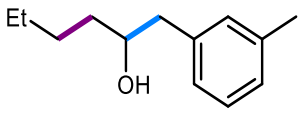

4.2.3ca

(Generated following corresponding general procedure and isolated by column chromatography on silica gel with hexane: EtOAc = 96:4 as eluent, light brown oil, 27 mg, yield: 70%): **^{1}H NMR** (500 MHz, $CDCl_3$) δ 7.23 (t, *J* = 7.4 Hz, 1H), 7.13 – 7.00 (m, 3H), 3.88 – 3.78 (m, 1H), 2.83 (dd, *J* = 13.5, 4.1 Hz, 1H), 2.63 (dd, *J* = 13.5, 8.6 Hz, 1H), 2.37 (s, 3H), 1.62 – 1.46 (m, 4H), 1.45 – 1.29 (m, 3H), 0.95 (t, *J* = 7.2 Hz, 3H). **^{13}C NMR** (126 MHz, $CDCl_3$) δ 138.5, 138.1, 130.2, 128.4, 127.2, 126.4, 72.6, 44.0, 36.5, 27.9, 22.7, 21.4, 14.0. **TLC**: R_f 0.48 (5:1 hexane/EtOAc) [Phosphomolybdic acid]. **HRMS:** (ESI, *m*/*z*): calcd. for $C_{13}H_{20}O_2Na[M+Na]^+$ 215.1406, found: 215.1402.

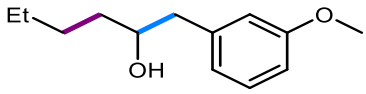

4.2.3da

(Generated following corresponding general procedure and isolated by column chromatography on silica gel with hexane: EtOAc = 94:6 as eluent, light brown oil, 30 mg, yield: 72%): **^{1}H NMR** (500 MHz, $CDCl_3$) δ 7.28 – 7.22 (m, 1H), 6.91 – 6.71 (m, 3H), 3.89 – 3.74 (m, 4H), 2.83 (dd, *J* = 13.5, 4.1 Hz, 1H), 2.64 (dd, *J* = 13.5, 8.5 Hz, 1H), 1.69 – 1.44 (m, 4H), 1.45 – 1.29 (m, 3H), 0.94 (t, *J* = 7.2 Hz, 3H). **^{13}C NMR** (126 MHz, $CDCl_3$) δ 159.7, 140.2, 129.5, 121.7, 115.1, 111.7, 72.6,

55.1, 44.1, 36.5, 27.9, 22.7, 14.0. **TLC**: R_f 0.34 (5:1 hexane/EtOAc) [Phosphomolybdic acid]. **HRMS:** (ESI, *m*/*z*): calcd. for $C_{13}H_{20}O_2Na[M+Na]^+$ 231.1356, found: 231.1351.

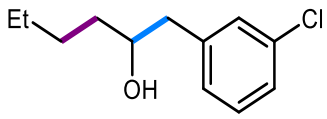

4.2.3ea

(Generated following corresponding general procedure and isolated by column chromatography on silica gel with hexane: EtOAc = 96:4 as eluent, light brown oil, 31 mg, yield: 74%): **^{1}H NMR** (500 MHz, $CDCl_3$) δ 7.28 – 7.21 (m, 3H), 7.12 (dt, *J* = 6.8, 1.6 Hz, 1H), 3.83 (tt, *J* = 8.7, 4.5 Hz, 1H), 2.82 (dd, *J* = 13.7, 4.2 Hz, 1H), 2.65 (dd, *J* = 13.7, 8.4 Hz, 1H), 1.63 – 1.44 (m, 4H), 1.45 – 1.30 (m, 3H), 0.94 (t, *J* = 7.2 Hz, 3H). **^{13}C NMR** (126 MHz, $CDCl_3$) δ 140.8, 134.2, 129.7, 129.5, 127.6, 126.6, 72.4, 43.6, 36.6, 27.8, 22.6, 14.0. **TLC**: R_f 0.46 (5:1 hexane/EtOAc) [Phosphomolybdic acid]. **HRMS:** (ESI, *m*/*z*): calcd. for $C_{12}H_{17}OClNa[M+Na]^+$ 235.0860, found: 235.0857.

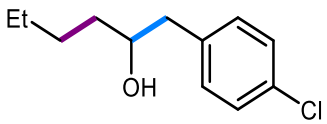

4.2.3fa

(Generated following corresponding general procedure and isolated by column chromatography on silica gel with hexane: EtOAc = 96:4 as eluent, white solid, 31 mg, yield: 74%): **^{1}H NMR** (500 MHz, $CDCl_3$) δ 7.30 (d, *J* = 8.3 Hz, 2H), 7.17 (d, *J* = 8.3 Hz, 2H), 3.80 (tt, *J* = 8.7, 4.5 Hz, 1H), 2.81 (dd, *J* = 13.7, 4.2 Hz, 1H), 2.65 (dd, *J* = 13.7, 8.3 Hz, 1H), 1.65 – 1.43 (m, 4H), 1.42 – 1.29 (m, 3H), 0.94 (t, *J* = 7.1 Hz, 3H). **^{13}C NMR** (126 MHz, $CDCl_3$) δ 137.2, 132.2, 130.7, 128.6, 72.5, 43.2, 36.5, 27.8, 22.6, 14.0. **TLC**: R_f 0.45 (5:1 hexane/EtOAc) [Phosphomolybdic acid]. **HRMS:** (ESI, *m*/*z*): calcd. for $C_{12}H_{17}OClNa[M+Na]^+$ 235.0860, found: 235.0858.

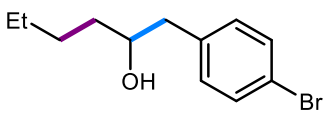

4.2.3ga

(Generated following corresponding general procedure and isolated by column chromatography on silica gel with hexane: EtOAc = 96:4 as eluent, white solid, 38 mg, yield: 74%): **^{1}H NMR** (500

MHz, $CDCl_3$) δ 7.45 (d, *J* = 8.3 Hz, 2H), 7.12 (d, *J* = 8.4 Hz, 2H), 3.80 (tt, *J* = 8.7, 4.5 Hz, 1H), 2.79 (dd, *J* = 13.7, 4.3 Hz, 1H), 2.63 (dd, *J* = 13.7, 8.3 Hz, 1H), 1.64 – 1.43 (m, 4H), 1.42 – 1.30 (m, 3H), 0.93 (t, *J* = 7.2 Hz, 3H). **^{13}C NMR** (126 MHz, $CDCl_3$) δ 137.7, 131.5, 131.1, 120.2, 72.5, 43.3, 36.5, 27.8, 22.6, 14.0. **TLC**: R_f 0.47 (5:1 hexane/EtOAc) [Phosphomolybdic acid]. **HRMS:** (ESI, *m*/*z*): calcd. for $C_{12}H_{17}OBrNa[M+Na]^+$ 279.0355, found: 279.0349.

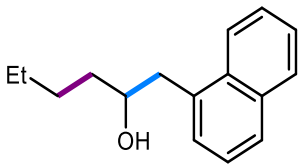

4.2.3ha

(Generated following corresponding general procedure and isolated by column chromatography on silica gel with hexane: EtOAc = 95:5 as eluent, colorless oil, 30 mg, yield: 70%): **^{1}H NMR** (500 MHz, $CDCl_3$) δ 8.08 (d, *J* = 8.3 Hz, 1H), 7.95 – 7.88 (m, 1H), 7.79 (d, *J* = 8.0 Hz, 1H), 7.59 – 7.49 (m, 2H), 7.49 – 7.36 (m, 2H), 4.06 – 3.92 (m, 1H), 3.39 (dd, *J* = 13.9, 4.0 Hz, 1H), 3.08 (dd, *J* = 13.9, 8.7 Hz, 1H), 1.73 – 1.51 (m, 4H), 1.52 – 1.33 (m, 3H), 0.97 (t, *J* = 7.2 Hz, 3H). **^{13}C NMR** (126 MHz, $CDCl_3$) δ 134.8, 134.0, 132.2, 128.8, 127.6, 127.3, 125.9, 125.6, 125.4, 123.8, 71.9, 41.2, 37.0, 28.0, 22.8, 14.1. **TLC**: R_f 0.43 (5:1 hexane/EtOAc) [Phosphomolybdic acid]. **HRMS:** (ESI, *m*/*z*): calcd. for $C_{16}H_{20}ONa[M+Na]^+$ 251.1406, found: 251.1402.

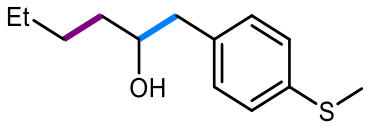

4.2.3ia

(Generated following corresponding general procedure and isolated by column chromatography on silica gel with hexane: EtOAc = 95:5 as eluent, colorless oil, 33 mg, yield: 73%): **^{1}H NMR** (500 MHz, $CDCl_3$) δ 7.24 (d, *J* = 8.2 Hz, 2H), 7.17 (d, *J* = 8.2 Hz, 2H), 3.80 (tt, *J* = 8.7, 4.5 Hz, 1H), 2.81 (dd, *J* = 13.6, 4.2 Hz, 1H), 2.63 (dd, *J* = 13.6, 8.3 Hz, 1H), 2.50 (s, 3H), 1.63 – 1.44 (m, 4H), 1.44 – 1.29 (m, 3H), 0.94 (t, *J* = 7.1 Hz, 3H). **^{13}C NMR** (126 MHz, $CDCl_3$) δ 136.1, 135.6, 129.9, 127.0, 72.6, 43.4, 36.5, 27.9, 22.7, 16.1, 14.0. **TLC**: R_f 0.38 (5:1 hexane/EtOAc) [Phosphomolybdic acid]. **HRMS:** (ESI, *m*/*z*): calcd. for $C_{13}H_{20}ONaS[M+Na]^+$ 247.1127, found: 247.1123.

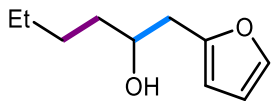

4.2.3ja

(Generated following corresponding general procedure and isolated by column chromatography on silica gel with hexane: EtOAc = 96:4 as eluent, colorless volatile oil, yield was determined by ^{1}H NMR with mesitylene as standard before isolation. Following reported the NMR spectrum data of pure product): **^{1}H NMR** (500 MHz, $CDCl_3$) δ 7.37 (dd, *J* = 1.8, 0.7 Hz, 1H), 6.34 (dd, *J* = 3.1, 1.9 Hz, 1H), 6.13 (dd, *J* = 3.1, 0.6 Hz, 1H), 3.94 – 3.87 (m, 1H), 2.87 (dd, *J* = 15.0, 4.1 Hz, 1H), 2.74 (dd, *J* = 15.0, 8.0 Hz, 1H), 1.81 (br, 1H), 1.59 – 1.42 (m, 3H), 1.42 – 1.29 (m, 3H), 0.93 (t, *J* = 7.2 Hz, 3H). **^{13}C NMR** (126 MHz, $CDCl_3$) δ 152.9, 141.6, 110.3, 107.0, 70.5, 36.4, 36.1, 27.8, 22.6, 14.0. **TLC**: R_f 0.33 (5:1 hexane/EtOAc) [Phosphomolybdic acid]. **HRMS:** (ESI, *m*/*z*): calcd. for $C_{10}H_{16}O_2Na[M+Na]^+$ 191.1042, found: 191.1040.

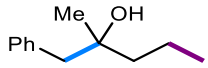

4.2.6aa

(Generated following corresponding general procedure and isolated by column chromatography on silica gel with hexane: EtOAc = 96:4 as eluent, 27 mg, colorless oil, yield: 76%): **^{1}H NMR** (500 MHz, $CDCl_3$) δ 7.37 – 7.31 (m, 2H), 7.31 – 7.21 (m, 3H), 2.78 (dd, *J* = 28.69, 13.33 Hz, 2H), 1.53 – 1.43 (m, 5H), 1.17 (s, 3H), 0.99 – 0.94 (m, 3H). **^{13}C NMR** (126 MHz, $CDCl_3$) δ 137.6, 130.5, 128.1, 126.4, 72.5, 48.0, 44.1, 26.5, 17.2, 14.6. **TLC**: R_f 0.43 (5:1 hexane/EtOAc) [Phosphomolybdic acid]. **HRMS:** (ESI, *m*/*z*): calcd. for $C_{12}H_{18}ONa[M+Na]^+$ 201.1250, found: 201.1246.

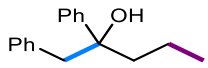

4.2.6ab

(Generated following corresponding general procedure and isolated by column chromatography on silica gel with hexane: EtOAc = 97:3 as eluent, 38 mg, colorless oil, yield: 80%): **^{1}H NMR** (500 MHz, $CDCl_3$) δ 7.40 – 7.31 (m, 4H), 7.30 – 7.19 (m, 4H), 7.02 – 6.96 (m, 2H), 3.19 (d, *J* = 13.39 Hz, 1H), 3.08 (d, *J* = 13.39 Hz, 1H), 2.02 – 1.91 (m, 1H), 1.90 – 1.74 (m, 2H), 1.43 – 1.29 (m, 1H), 1.15 – 1.02 (m, 1H), 0.88 (t, *J* = 7.25 Hz, 3H). **^{13}C NMR** (126 MHz, $CDCl_3$) δ145.8,

135.4, 130.7, 128.0, 127.9, 126.6, 126.3, 125.4, 76.7, 49.7, 44.3, 16.8, 14.4. **TLC**: R_f 0.57 (5:1 hexane/EtOAc) [Phosphomolybdic acid]. **HRMS:** (ESI, *m*/*z*): calcd. for $C_{17}H_{20}ONa[M+Na]^+$ 263.1406, found: 263.1397.

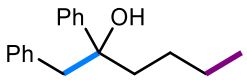

4.2.6ac

Generated following corresponding general procedure and isolated by column chromatography on silica gel with hexane: EtOAc = 97:3 as eluent, 36.5 mg, colorless oil, yield: 72%): **^{1}H NMR** (500 MHz, $CDCl_3$) δ 7.41 – 7.31 (m, 4H), 7.31 – 7.18 (m, 4H), 7.03 – 6.93 (m, 2H), 3.19 (d, *J* = 13.3 Hz, 1H), 3.08 (d, *J* = 13.3 Hz, 1H), 2.00 (ddd, *J* = 13.9, 11.7, 4.6 Hz, 1H), 1.89 – 1.74 (m, 2H), 1.40 – 1.20 (m, 3H), 1.11 – 0.99 (m, 1H), 0.86 (t, *J* = 7.2 Hz, 3H). **^{13}C NMR** (126 MHz, $CDCl_3$) δ 145.8, 136.4, 130.6, 128.0, 127.9, 126.6, 126.3, 125.4, 76.7, 49.7, 41.8, 25.7, 23.0, 14.0. **TLC**: R_f 0.60 (5:1 hexane/EtOAc) [Phosphomolybdic acid]. **HRMS:** (ESI, *m*/*z*): calcd. for $C_{18}H_{22}ONa[M+Na]^+$ 277.1563, found: 277.1563.

4.3 Empowering simple alcohol as carbonyl surrogate

4.3.1 Background

After the success of olefinic alcohols in serving as carbonyl surrogates for Grignard-type reaction, our attention turned to saturated alcohols to make such a strategy more widely applicable. Compared with olefinic alcohols, saturated alcohols could not be transformed directly to carbonyls *via* a redox-neutral pathway. Thus, A key step of this surrogate strategy was the in situ catalytic generation of carbonyls from alcohols through their 'dehydrogenation'. Based on previous studies from our group[33, 95] and others,[96] *β*-hydride elimination of alcohols could be efficiently catalyzed by Ru(II)-complexes with or without stoichiometric amounts of oxidants (hydride acceptors). The former has often been conducted under milder conditions, while the latter usually requires high temperatures with the use of special catalysts.[97–104]

Table 4.5 Investigation of oxidants and hydride acceptors[a]

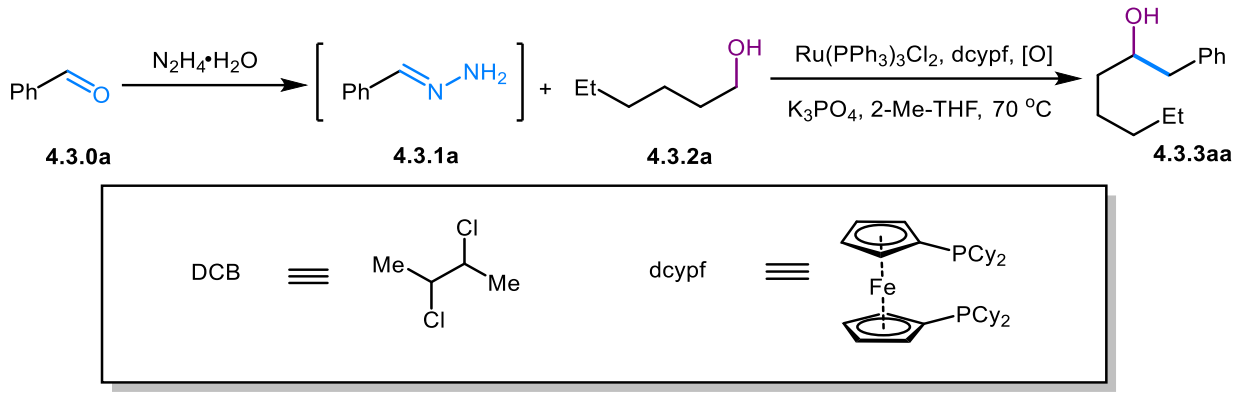

entry	oxidant	result	entry	oxidant	result
1	none	9%	5	isoprene	0
2[b]	air	trace	6	Ag_2O	trace
3[c]	O_2	0	7	CuO	15%
4	NCS	0	8	DCB	21%

[a] Reaction conditions: **4.3.1a** (0.25 mmol), **4.3.2a** (0.2 mmol), $Ru(PPh_3)_3Cl_2$ (3 mol %), dcypf (3 mol %), K_3PO_4 (1.1 equiv), oxidant (2.0 equiv), solvent (0.2 mL) at 70 °C under N_2 atmosphere. ^1H NMR yield was determined using mesitylene as an internal standard. A 'trace' amount of product was noted when the desired product was not clearly detected. [b] The reaction was performed under air. [c] Oxygen balloon was used to provide O_2 gas during the reaction.

4.3.2 Results and discussions

4.3.2.1 Exploration of the hydride-acceptor system

Thus, our investigation started by seeking a proper hydride acceptor. On the basis of our previous work,[33] a ruthenium(II)–bisphosphine system was first explored by varying the type of oxidants (hydride acceptors) used (Table 4.5). We observed a 9% yield of the desired product in the absence of a hydride acceptor (Table 4.5, entry 1). Under such conditions, however, most of the alcohols remained unchanged while the hydrazone substrate had mostly undergone the competing Wolff–Kishner reduction, which led to an overall low efficiency for the Grignard-type C–C bond formation. Inspired by the aerobic oxidation of alcohols, we then tested the reaction under air and O_2 atmospheres, respectively; however, even lower yields were obtained in both cases (Table 4.5, entries 2 and 3). In the cases of NCS, isoprene and silver oxide as oxidants, no generation of the desired product was observed (Table 4.5, entries 4–6). These results indicated that either the ruthenium(II) catalyst or the hydrazone substrate was incompatible with strong oxidants. For this

reason, weaker oxidants such as copper oxide and DCB (2,3-dichlorobutane) were then tested. As expected, the product yield showed a notable increase. The conversion efficiencies of the reactants, however, were still relatively low (Table 4.5, entries 7 and 8). Nevertheless, these results suggested that weak oxidants can be tolerated in this Ru(II)–bisphosphine system, albeit not significantly promoting the oxidation.

Table 4.6 Investigation of reaction conditions under oxidant free system[a]

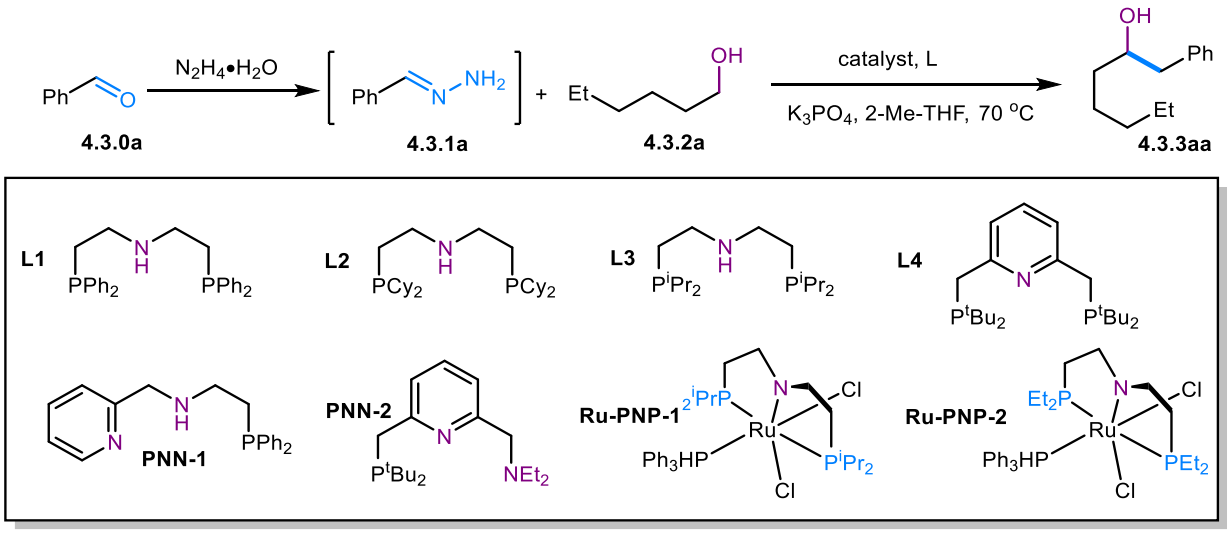

entry	catalyst	ligand	K_3PO_4 (equiv)	solvent (mL)	yield
1	$Ru(dppf)(en)Cl_2$	-	2	0.2	22
2	$Ru(PPh_3)_3Cl_2$	**L1**	2	0.2	40
3	$Ru(PPh_3)_3Cl_2$	**L2**	2	0.2	66
4	$Ru(PPh_3)_3Cl_2$	**L3**	2	0.2	73
5	$Ru(PPh_3)_3Cl_2$	**L3**	1.5	0.2	66
6	$Ru(PPh_3)_3Cl_2$	**L3**	2	0.3	71
7	$Ru(PPh_3)_3Cl_2$	**L3**	2.5	0.3	64
8	$Ru(PPh_3)_3Cl_2$	**L3**	2	0.5	70
9[b]	$Ru(PPh_3)_3Cl_2$	**L3**	2	0.5	74
10[b]	Ru(**PNN-1**)$(PPh_3)Cl_2$	-	2	0.5	36
11[b]	$Ru(PPh_3)_3Cl_2$	**L4**	2	0.5	32
12[b]	Ru(**PNN-2**)$H(CO)Cl_2$	-	2	0.5	17
13[b]	**Ru-PNP-1**	-	2	0.5	73
14[b]	**Ru-PNP-2**	-	2	0.5	74

[a] Reaction conditions: **4.3.1a** (0.7 mmol), **4.3.2a** (0.2 mmol), $Ru(PPh_3)_3Cl_2$ (5 mol %), ligand (5 mol %), K_3PO_4, 2-Me-THF at 70 °C under N_2 atmosphere. See Supplementary Information (SI) for details. ^1H NMR yield was determined using 1,3,5-trimethoxylbenzene as an internal standard. A

'trace' amount of product was noted when the desired product was not clearly detected. [b] **4.3.1a** (0.6 mmol) was used.

4.3.2.2 Exploration of oxidant-free system

The results above led us to consider an oxidant-free strategy in order to increase the efficiency of alcohol dehydrogenation which will in turn allow the subsequent 1,2-addition of hydrazone by modifying the catalytic system. Upon carefully analyzing the results with the Ru(II)–dcypf system, we attributed the main reason for the low efficiency to the inefficient kinetics of the dehydrogenation process. The extensive researches on Noyori-type reactions have shown that a mixture of phosphine and amine ligands could accelerate the hydrogenation and dehydrogenation processes due to the favored six-membered ring transition state.[105] Furthermore, most reported reactions concerning acceptorless dehydrogenation of alcohols require P–N type ligands.[102]These studies inspired us to investigate alternative catalytic systems other than Ru(II)–bisphosphine.

We started by using a well-defined Noyori-type ruthenium complex, Ru(dppf)(en)Cl_2. In addition, we increased the hydrazone substrate equivalence to 3.5 in order to minimize the Wolff–Kishner reduction of the hydrazone. This initial attempt, however, only increased the yield slightly (Table 4.6, entry 1). We reasoned that since Ru(dppf)(en)Cl_2 is a stable complex with a limited number of empty coordination sites, it cannot drive the whole cascade process to proceed efficiently. To solve this problem, PNP–pincer type ligands[19, 106–109]were then considered because: 1) with a tridentate structure, they can form more stable complexes with the metal center in order to stabilize the intermediates in the catalytic cycle, and 2) by occupying only three coordination sites, more space could be provided for the substrates and intermediates in order to facilitate the catalytic process. To our delight, the use of PNP–pincer type ligands indeed significantly increased the reactivity, among which bis[(2-diisopropylphosphino]ethyl)amine (**L3**) provided the best result (Table 4.6, entry 4).

Although the yield was increased, there were still some notable side products being generated when using **L3** as a ligand. One of the side products was the olefination product (**4.3.3aa-s1**) and the other was the hydrogen-borrowing hydrazination product (**4.3.3aa-s2**). Additionally, the Wolff–Kishner reduction also consumed all the remaining hydrazone before the complete conversion of the alcohol. We therefore carried out further optimizations in order to reduce the generation of these side products (Table 4.6, entries 5–9). The results showed that, by diluting the

solution to 0.5 mL, the side reactions (i.e. the WK reduction and hydrogen-borrowing hydrazination) were significantly reduced without impeding the reactivity of the desired reaction. Furthermore, the dilution also enabled the alcohol to be fully consumed in the presence of a smaller amount of hydrazone. Under the optimized conditions, different pincer ligands such as PNN-type and $PN_{pyridine}P$-type ligands were investigated, however, none of them gave better results compared to **L3** (Table 4.6, entries 10–12). Furthermore, pre-synthesizing the ruthenium complex with **L3** gave almost the same results as the one generated in situ (Table 4.6, entry 13). In addition, we also tested a less bulky PNP ligand, bis[(2-diethylphosphino]ethyl)amine (**L-Et**), and produced a well-defined complex (**Ru-PNP-2**) to run the reaction (Table 4.6, entry 14). The result with this complex was similar to the Ru-**L3** system. Later substrate scope studies also showed that both catalytic systems worked efficiently for primary alcohols. Thus, due to the fact that **L-Et** was less available, **L3** was used as the optimized ligand in most of our later studies. The use of a less bulky pincer ligand, however, did increase the yield for bulkier secondary alcohols, which will be discussed later.

4.3.2.3 Investigation of the substrate scope

With the optimized reaction conditions in hand, the substrate scope investigation (Table 4.7) was started for the alcohol partners in which simple alcohols were tested first. The results showed that the linear aliphatic alcohols examined all underwent the reaction smoothly. Notably, longer aliphatic chains led to lower yields (**4.3.3aa–4.3.3ac**); however, the overall yields were generally high. Aliphatic alcohols substituted with methylthio (**4.3.3ae**) and -NBoc (**4.3.3ah**) were also compatible with this process and provided moderate to high yields of the desired products. Similar results were obtained for heterocyclic substituted alcohols (**4.3.3ad–4.3.3ai**). In order to investigate the potential application of this reaction for pharmaceutical or agricultural industries, we demonstrated that the fluorine-containing alcohol also underwent the Grignard-type reaction and provided a moderate yield (**4.3.3hj**). A noteworthy finding was that small molecular alcohols such as ethanol could also participate in this C–C bond formation process at an elevated temperature (**4.3.3hk**). Benzyl alcohol and its derivatives were also effective substrates for this reaction; however, they generated more olefination products (**4.3.3am–4.3.3ao**). Increased steric effects suppressed this reaction as shown by the use of α-substituted alcohols (**4.3.3ap–4.3.3ar**) with the exception of α-cyclobutyl alcohol (**4.3.3ap**). A likely explanation was that the highly strained and small cyclobutyl group reduced the steric bulk around the metal center, generating the

product in a relatively higher yield. In order to better illustrate the potential application of this reaction for total synthesis and late-stage functionalization, certain substrates containing sensitive functional groups were investigated. Substrates bearing amides and esters were well tolerated (**4.3.3ax**, **4.3.3az**), while the ones bearing more reactive functional group such as carbonate (**4.3.3ay**) demonstrated a lower yield. Nitriles and nitro-containing substrates were not competible, possibly due to their strong coordinating or oxidation ability.

Table 4.7 Substrate scope of alcohols

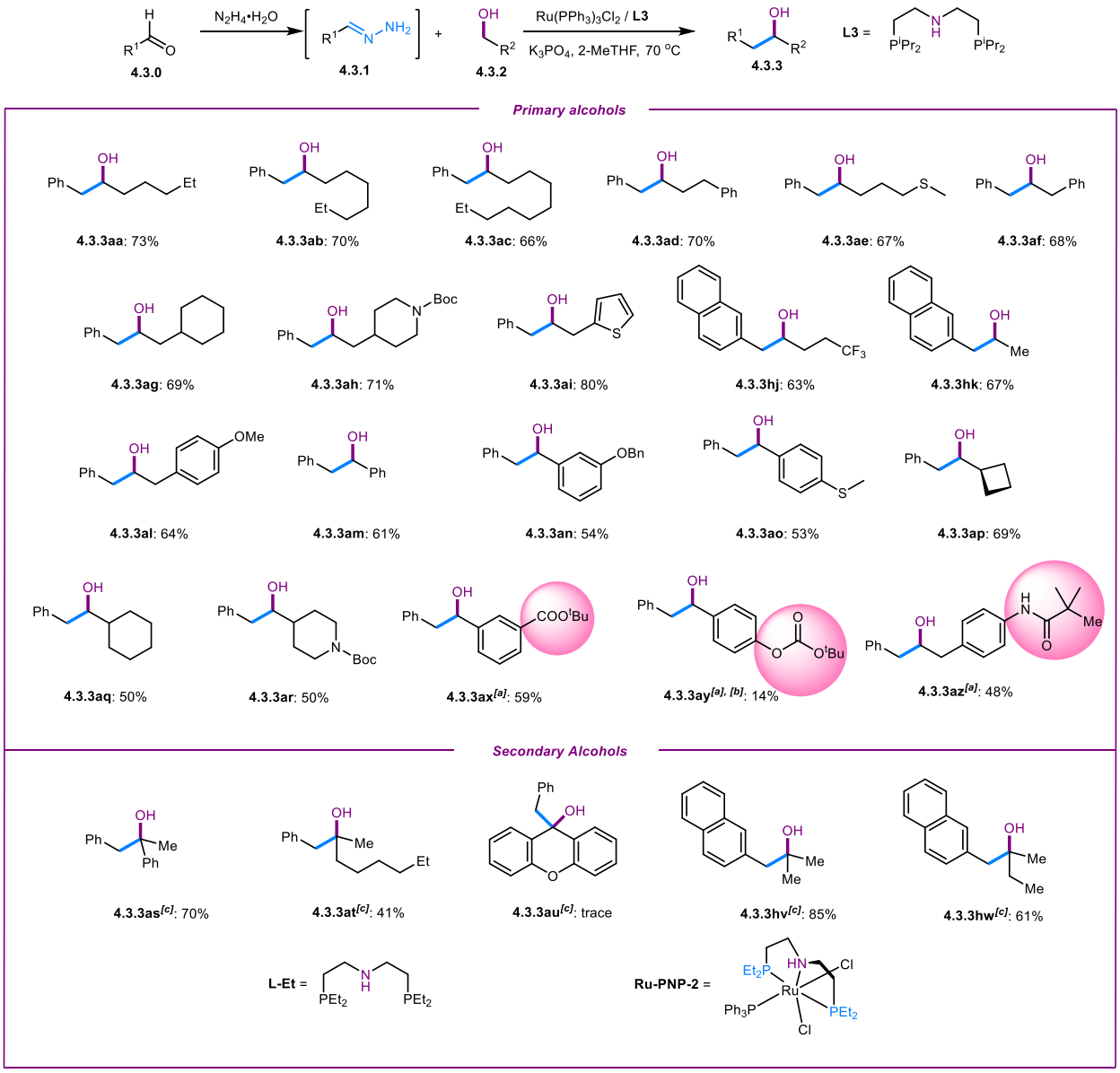

Reaction conditions: **4.3.1** (0.6 mmol), **4.3.2** (0.2 mmol), $Ru(PPh_3)_3Cl_2$ (5 mol %), ligand (5 mol %), K_3PO_4 (2 equiv), 2-Me-THF at 70 °C under N_2 atmosphere for 24h. Yield of isolated product was reported otherwise noted. [a] **Ru-PNP-1** was used as catalyst. [b] ^1H NMR yield was determined using mesitylene as an internal standard. [c] The reaction was conducted at 100 °C, 1a (0.8 mmol), **Ru-PNP-2** was used as catalyst.

Additionally, we noticed that the reaction with secondary alcohols both required harsher conditions and produced the corresponding products in relatively lower yields. The result further confirmed the significant steric effect of this reaction. To overcome this challenge, we switched the ligand from PNP **L3** to the less bulky **L-Et**. To our delight, when conducting the reaction under the catalysis of the ruthenium(II)–**L-Et** complex (**Ru-PNP-2**), the tested secondary alcohols (**4.3.3as**–**4.3.3hw**) reacted as efficiently as the primary ones, with the exception of **4.3.3au** due to its very high steric hindrance.

Table 4.8 Substrate scope of hydrazones

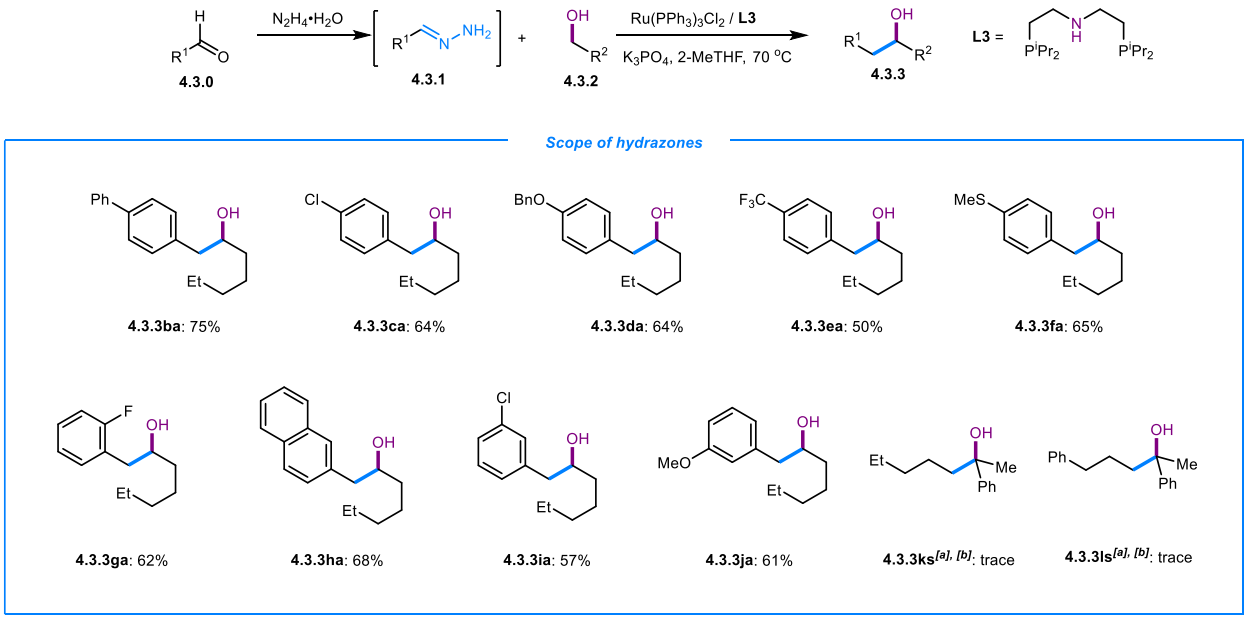

Reaction conditions: **4.3.1** (0.6 mmol), **4.3.2** (0.2 mmol), $Ru(PPh_3)_3Cl_2$ (5 mol %), ligand (5 mol %), K_3PO_4 (2 equiv), 2-Me-THF at 70 °C under N_2 atmosphere for 24h. Yield of isolated product was reported otherwise noted. [a] ^1H NMR yield was determined using mesitylene as an internal standard. [b] The reaction was conducted at 100 °C, **4.3.1** (0.8 mmol), **Ru-PNP-2** was used as catalyst.

Subsequently, we decided to vary the hydrazones (Table 4.8). *Para*-substituted benzaldehyde hydrazones were explored first, all of which produced the desired products in moderate to high yields. The CF_3 substituted hydrazone demonstrated the lowest yield due to the competing and rapid WK reduction in the presence of the strong electron-withdrawing effects of CF_3 (**4.3.3ba**–**4.3.3ea**). Similarly, most *o*- and *m*-substituted benzaldehyde hydrazones proceeded smoothly and produced the desired products in moderate yields. Notably, certain hydrazones with low solubility in the reaction solvent, such as naphthaldehyde hydrazone (**4.3.3ha**), *p*-phenylbenzaldehyde hydrazone (**4.3.3ba**) and *p*-benzyloxylbenzaldehyde hydrazone (**4.3.3da**), were still able to undergo this transformation smoothly. Aliphatic aldehyde hydrazones proved to be reactive as well, albeit less efficiently (**4.3.3ks**–**4.3.3ls**).

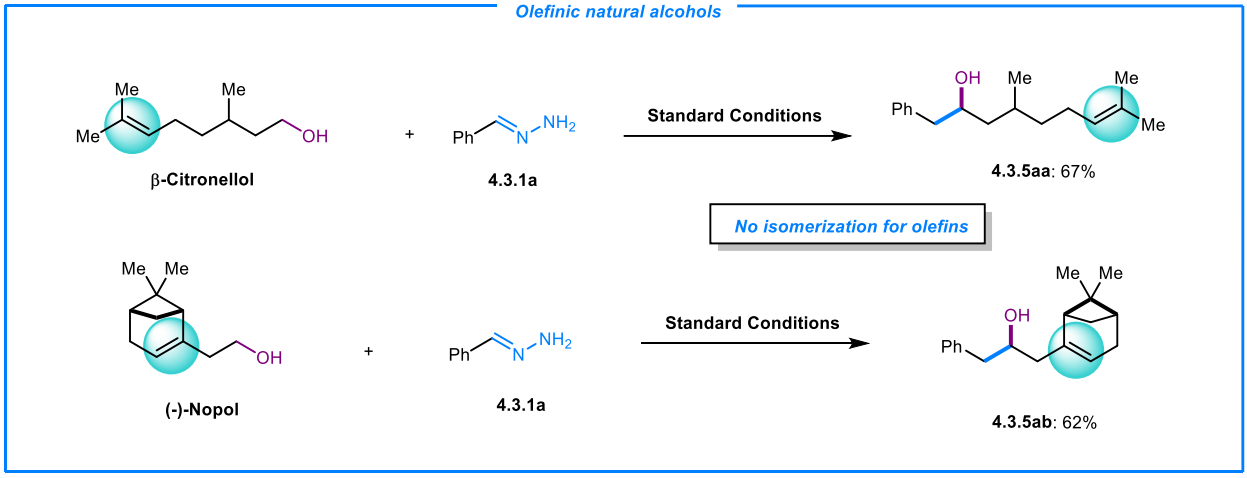

Scheme 4.6 Grignard-type reaction of hydrazone with natural alcohols

Standard reaction conditions: **4.3.1a** (0.6 mmol), alcohols (0.2 mmol), $Ru(PPh_3)_3Cl_2$ (5 mol %), ligand (5 mol %), K_3PO_4 (2 equiv.), 2-Me-THF at 70 °C under N_2 atmosphere for 24h.

To further evaluate the application potential of this transformation, some naturally occurring complex alcohols, such as *β*-Citronellol and (-)-Nopol (**4.3.5aa**–**4.3.5ab**), were examined (Scheme 4.6). Both of them provided the desired Grignard-type reaction products in good yields. More importantly, the *π*-bonds in these natural products were unaffected during the reaction process. The olefin isomerization product as reported in our earlier studies[95] was not observed. A possible reason for the complimentary reactivity could be that in the PNP–Ru(II) system, the H_2 gas release proceeded much faster than the hydride insertion process. These results demonstrated a great

synthetic value for C–C bond construction using olefinic natural alcohols, in which the chemoselective Grignard-type reaction of alcohols over olefin transformations could be realized.

4.3.2.4 Mechanistic studies

4.3.2.4.1 DFT study for the dehydrogenation step

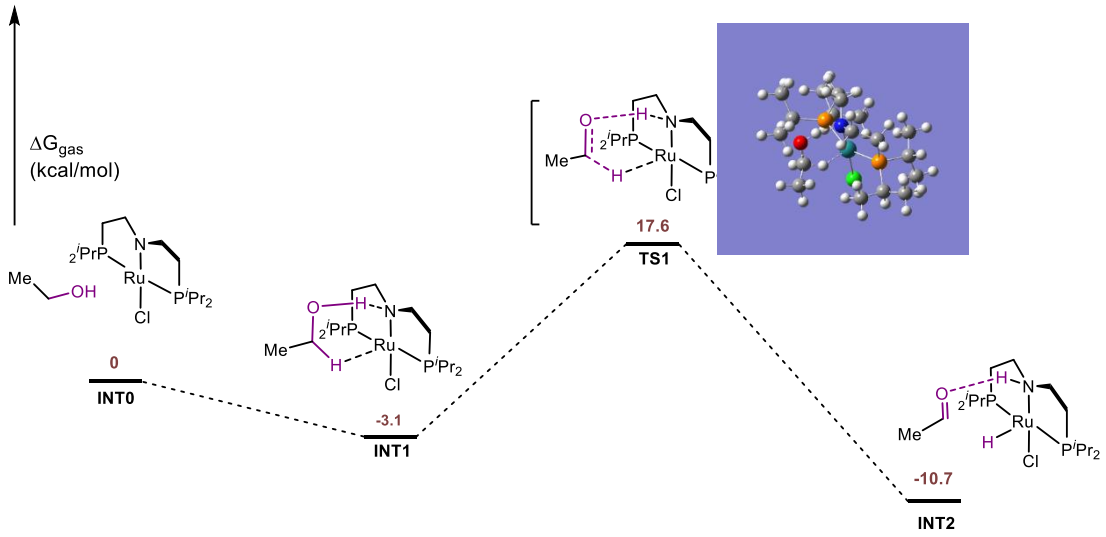

Figure 4.1 Energy diagram of the dehydrogenation step based on DFT calculation

Since the first step (dehydrogenation) is the key step of this dehydrogenative Grignard reaction, we mainly did the calculation for the first step. The result shows that the six-membered ring transition state that we proposed is reasonable in this case (Figure 4.1). Furthermore, we also predicted a four-member-ring transition state which corresponds to the classic *β*-hydride elimination process. The preliminary calculation shows that the free energy of transition state is 54.3 kcal/mol higher than the six-membered ring one and the intermediate does not show a perfect match with transition state possibly due to the geometry mismatch (thus we did not show on the diagram), which suggested that the six-membered ring transition state is a more favorable transition state in this case. For the 1,2-addition step, we already did several studies in previous work done by us and others.[33, 110]

4.3.2.4.2 Proposed mechanism

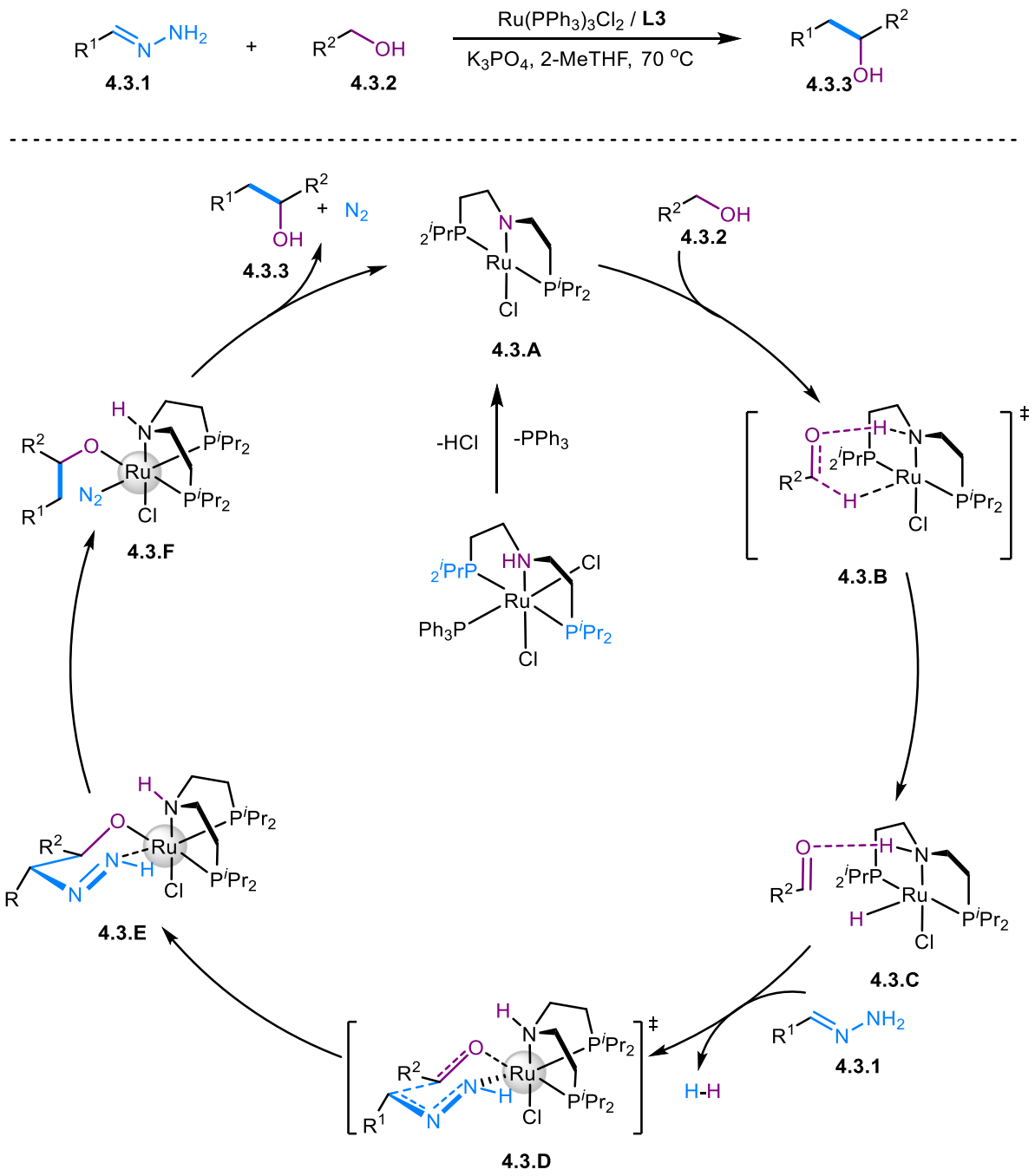

Scheme 4.7 Tentative mechanism for alcohol surrogated Grignard reaction

A tentative mechanism for this alcohol surrogated Grignard-type reaction is proposed in Scheme 4.7 based on previous literature[19, 33, 95, 99, 105–107, 111, 112] as well as experimental results. The ruthenium(II) catalyst first coordinates with the PNP–pincer ligand **L3** to form complex **4.3.A** with the assistance of a base in order to form a highly reactive square planar complex.[106] The alcohol then interacts with complex **4.3.A** to undergo a *β*-hydride elimination *via* a Noyori-type six-membered ring transition state **4.3.B** and produces the intermediate **4.3.C**.[105] This process is also supported by the Density Functional Theory (DFT) calculations. Next, the hydrazone substrate coordinates with the ruthenium center which interacts with a hydride and hydrogen gas is released.[111] Concurrently, the 1,2-addition process *via* a Zimmerman–Traxler chair-like transition state **4.3.D** is completed as we proposed previously.[33] Finally, after the C–C bond formation and the release of N_2 gas, the desired product is formed with the regeneration of the catalyst for the next cycle.

4.3.3 Conclusion

In conclusion, an oxidant-free Ru(II)–PNP catalyzed Grignard-type reaction with alcohol as a carbonyl surrogate was successfully demonstrated. This reaction takes advantage of both the kinetically favored dehydrogenation process provided by a phosphine–amine ligand and the thermodynamic driving force of the 1,2-addition to carbonyls by hydrazone with Ru(II) catalysis. The development of this transformation marks an evolution in the Grignard-type reaction, wherein direct construction of C–C bonds are possible from various naturally abundant alcohols, with a tolerance for sensitive functional groups and further expanding Grignard-type reactions from an early-stage constructions to late-stage modifications. Future work includes a more in-depth investigation of the application potentials as well as mechanistic studies for this alcohol-surrogated Grignard-type reaction.

4.3.4 Experimental section

4.3.4.1 General experimental information

Reaction Setup: All reactions were carried out in flame-dried V-shaped microwave reaction vials which were covered by aluminum seals with PTFE-faced silicone septa, under an atmosphere of nitrogen unless otherwise stated. All reaction temperatures corresponded to oil bath temperatures. All air and moisture-sensitive catalysts, ligands, and reagents were stored and charged in MBRAUN UNIlab Pro Glove Box Workstation unless otherwise stated.

Purifications: All work-up and purification procedures were carried out with reagent-grade solvents. Analytical thin-layer chromatography (TLC) was performed using E. Merck silica gel 60 F254 pre-coated plates (0.25 mm). Flash column chromatography was performed with E. Merck silica gel P60 (40–63 μm particle size, 230–400 mesh) (SiO_2). Unless otherwise specified, 'SiO_2' refers to P60 grade silica gel. Visualization was accomplished with UV light and/or iodine (I_2) or Vanillin solution. Retention factor (R_f) values reported were measured using a 10 × 2 cm TLC plate in a developing chamber containing the solvent system (10 mL) described. Automated flash column chromatography was performed on Biotage Isolera™ Spektra Systems with ACI™.

Solvents: 2-methyl-tetrahydrofuran (2-Me-THF), ordered from Sigma Aldrich without any purification. Solvents for filtration, transfers and chromatography, were dichloromethane (CH_2Cl_2) (ACS grade, amylene stabilized), acetone (ACS grade), ethyl acetate (EtOAc) (Fisher, ACS grade), hexane (Fisher, ACS grade), pentane (ACS grade), methanol (ACS grade).

Chemicals: In the model study, benzaldehyde (Aldrich) were distilled prior to use. Other chemicals that are commercially available and used without further purification: 2-penten-1-ol (Aldrich), $Ru(PPh_3)_4Cl_2$ (Aldrich), $Ru(PPh_3)_3Cl_2$ (Aldrich), dcypf (Aspira), potassium phosphate (Aldrich), hydrazine hydrate (Reagent Grade, 64–65% wt, Aldrich), mesitylene (Aldrich), 1,3,5-trimethoxylbenzene (Aldrich), anhydrous sodium sulfate. All liquid carbonyls were distilled, and solid ones were recrystallized prior to use. The **PNP** pincer ligands (**L1**, **L2**, **L3**) were purchased from Aldrich. All the alcohol substrates are commercially available (Aldrich, Oakwood & Combi Block)

NMR Spectroscopy: Nuclear magnetic resonance (^1H and ^{13}C NMR) spectra were recorded on a Bruker AV500 equipped with a 60-position Sample Xpress sample changer (^1H, 500 MHz; ^{13}C, 125 MHz), a Varian MERCURY plus-500 spectrometer (^1H, 500 MHz; ^{13}C, 125 MHz) or Bruker AV400 spectrometer (^1H, 400 MHz; ^{13}C, 100 MHz). Chemical shifts for both ^1H NMR and ^{13}C NMR spectra are expressed in parts per million (ppm) units downfield from TMS, with the solvent residue peak as the chemical shift standard ($CDCl_3$: δ 7.28 ppm in ^1H NMR; δ 77.00 ppm in ^{13}C NMR). Data are reported as following: chemical shift, multiplicity (s = singlet, d = doublet, dd = doublet of doublets, t = triplet, td = triplet of doublets, q = quartet, quin = quintet, sep = septet, m = multiplet), coupling constants *J* (Hz), and integration.

Mass Spectrometry: Mass spectrometry (MS) was performed by the McGill Chemistry Department Mass Spectrometry Facility. High resolution mass spectra were recorded using electrospray ionization (ESI+) and/or atmospheric pressure chemical ionization APCI (+/-), performed either on 'Exactive Plus Orbitrap' a ThermoScientific high resolution accurate mass (HR/AM) FT mass spectrometer, or a Bruker Daltonics Maxis Impact quadrupole-time of flight (QTOF) mass spectrometer.

Characterization of Products: For the products, most of which are known compounds, we report the physical states, NMR spectra and HRMS data.

DFT calculation: All the calculations were carried out at the B3LYP/6-31G(d,p) level (LANL2DZ for Ru), using the Gaussian 16, Rev A.03 suite of programs.[114] Harmonic frequencies were calculated at the same level to characterize the stationary points and to determine the zeropoint energies (ZPE). Intrinsic reaction coordinate (IRC) studies were performed in ambiguous cases to confirm the relation of the transition states with the corresponding minima.

4.3.4.2 Experimental procedures

4.3.4.2.1 Preparation of hydrazone or hydrazone solution

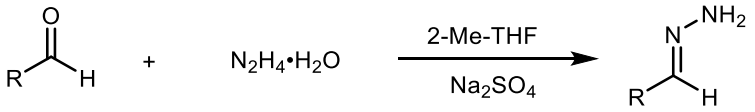

4.3.0 **4.3.1**

Procedure A: For Table 4.5: 2-Me-THF (4 mL) was added first into a small bottle with a stir bar. Then, hydrazine monohydrate (0.35 mL, 7 mmol) was added into the bottle. After that, **0** (5 mmol)* was added dropwise into the stirred solution and the mixture was stirred for 5 min. Next, proper amount of anhydrous Na_2SO_4 was added to remove water. After stirring for another 3h, the so-formed solution was ready to use.

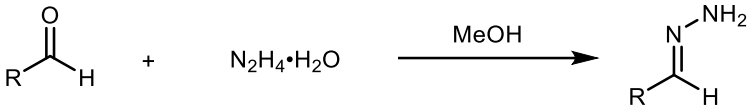

4.3.0 **4.3.1**

Procedure B: For Table 4.6–4.8, Scheme 4.6: MeOH (5 mL) was added first into a small bottle with a stir bar. Then, hydrazine monohydrate (0.75 mL, 15 mmol) was added into the bottle. After that, **0** (10.0 mmol) was added dropwise into the stirred solution and the mixture was stirred for 5

min. After stirring for 3 h, ***a.*** if the solution is a homogeneity, the so-formed solution was concentrated by vacuum to dryness. Next, the crude hydrazone was frozen dried under vacuum for three times to remove excess amount of hydrazine hydrate. The so formed hydrazone was directly used without further purification. ***b.*** if precipitates formed from the solution, the solid was filtered and washed with small potion of MeOH and then dried under vacuum, after which the hydrazone can be used directly without further purifications.

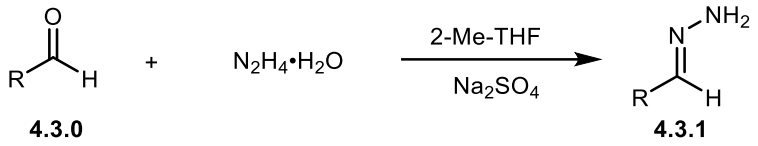

4.3.0 **4.3.1**

Procedure C: For Table 4.7, 4.3.3ks, 4.3.3ls: 2-Me-THF (5 mL) was added first into a small bottle with a stir bar. Then, hydrazine monohydrate (0.4 mL, 8 mmol) was added into the bottle. After that, **0** (6 mmol) was added dropwise into the stirred solution and the mixture was stirred for 5 min. Next, proper amount of anhydrous Na_2SO_4 was added to remove water. After stirring for another 3h, the so-formed solution was ready to use.

4.3.4.2.2 General procedure for reactions

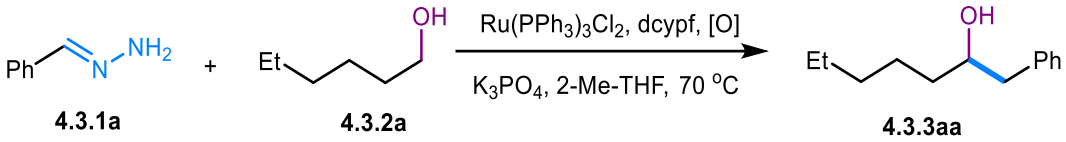

4.3.1a **4.3.2a** **4.3.3aa**

General procedure for Table 4.5: $Ru(PPh_3)_2Cl_2$ (0.01 mmol), dcypf (0.01 mmol), K_3PO_4 (0.22 mmol), oxidant (0.4 mmol, 2 equiv)* were added into a V-shaped reaction tube with a stir bar in the glovebox. Then, the reaction tube was sealed and moved out of the glovebox. After that, **4.3.1a** solution (prepared through ***Procedure A*** , 0.22 mL, 0.25 mmol) was added first and followed by the addition of **4.3.2a** (25.0 μL, 0.2 mmol). The mixture was stirred for 24h. Then, 1,3,5-trimethoxylbenzene (11.2 mg, 0.067 mmol) was added in the mixture as standard. Then, the solution was filtered by celite and concentrated to dryness. The crude mixture was diluted by $CDCl_3$ to run the ^1H NMR test to determine the ^1H NMR yield.

*For entry 2, the reaction tube was sealed before exposed to air for 5 min. For entry 3, after removing reaction tube out of the glovebox, it was charged with O_2 *via* 3 times vacuum-refill by oxygen balloon.

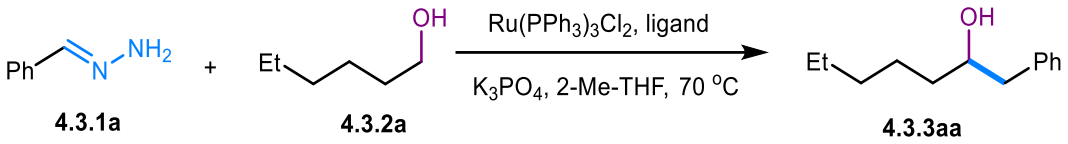

General procedure for Table 4.6: $Ru(PPh_3)_2Cl_2$ (0.01 mmol), ligand (0.01 mmol), K_3PO_4 (0.4 mmol) were added into a V-shaped reaction tube with a stir bar in the glovebox. Then, the reaction tube was sealed and moved out of the glovebox. After that, 0.5 mL 2-Me-THF was added and followed by the addition of corresponding amount of **4.3.1a** (prepared through ***Procedure B***) and **4.3.2a** (25.0 μL, 0.2 mmol). The mixture was stirred for 24h under N_2 at 70 °C. After completion, the solution was filtered by celite and concentrated to dryness. Then, 1,3,5-trimethoxylbenzene (11.2 mg, 0.067 mmol) was added in the mixture as standard. The crude mixture was diluted by $CDCl_3$ to run the ^1H NMR test to determine the ^1H NMR yield.

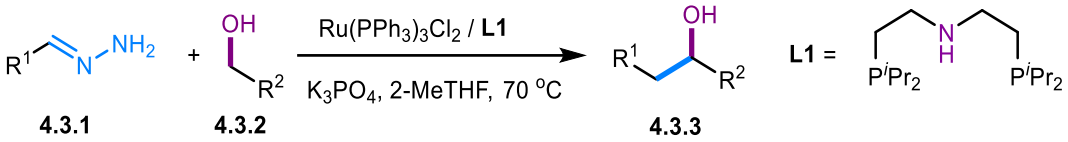

General procedure for Table 4.7–4.8, Scheme 4.6: $Ru(PPh_3)_3Cl_2$ (0.01 mmol), **L1** (0.01 mmol) and K_3PO_4 (0.4 mmol) and solid substrates were added into a V-shaped reaction tube with a stir bar in the glovebox. Then, the reaction tube was sealed and moved out of the glovebox. After that, 0.5 mL 2-Me-THF was added first followed by the addition of liquid substrates. The mixture was stirred under 70 °C for 24h. The reaction mixture was filtered through a celite plug with 2-3 mL CH_2Cl_2. The solvent was removed by a rotary evaporator and the residue was purified by column chromatography on silica gel (using hexane and ethyl acetate as eluent) to give the pure product.

General procedure for Table 4.7, 4.3.3as–4.3.3hv and 4.3.3hw: **Ru-PNP-2** (0.01 mmol), and K_3PO_4 (0.4 mmol) and solid substrates were added into a V-shaped reaction tube with a stir bar in the glovebox. Then, the reaction tube was sealed and moved out of the glovebox. After that, 0.5 mL 2-Me-THF was added first followed by the addition of liquid substrates. The mixture was stirred under 100 °C for 24h. The reaction mixture was filtered through a celite plug with 2-3 mL CH_2Cl_2. The solvent was removed by a rotary evaporator and the residue was purified by column chromatography on silica gel (using hexane and ethyl acetate as eluent) to give the pure product.

General procedure for Table 4.7 4.3.3ax–4.3.3az: **Ru-PNP-1** (0.01 mmol), K_3PO_4 (0.4 mmol) and solid alcohol (0.2 mmol, if applicable) were added into a V-shaped reaction tube with a stir bar in the glovebox. Then, the reaction tube was sealed and moved out of the glovebox. After that, 0.5 mL 2-Me-THF was added first followed by the addition of **4.3.1a** (0.6 mmol, 3 equiv.) and liquid alcohols (0.2 mmol, if applicable). The mixture was stirred under 70 ^oC for 24h. The reaction mixture was filtered through a celite plug with 2-3 mL CH_2Cl_2. The solvent was removed by a rotary evaporator and the residue was purified by column chromatography on silica gel (using hexane and ethyl acetate as eluent) to give the pure product. Specifically, for **4.3.3ay,** the mixture was diluted with $CDCl_3$ and run the ^1H NMR test to determine trace amount of desired product.

Procedure for Table 4.8 (4.3.3ks, 4.3.3ls): $Ru(PPh_3)_3Cl_2$ (0.01 mmol), **L3** (0.006 mmol) and K_3PO_4 (0.4 mmol) were added into a V-shaped reaction tube with a stir bar in the glovebox. Then, the reaction tube was sealed and moved out of the glovebox. After that, **4.3.1** solution (prepared through ***Procedure B***, 0.55 mL, 0.6 mmol) was added. The mixture was stirred at 100 ^oC for 24h. The reaction mixture was filtered through a celite plug with 2-3 mL CH_2Cl_2. The solvent was removed by a rotary evaporator and the residue was added mesitylene as internal standard. The mixture was diluted with $CDCl_3$ and run the ^1H NMR test to determine trace amount of desired product based on the standard spectrum from literature.[2, 3]

4.3.4.2.3 Synthesis of active species

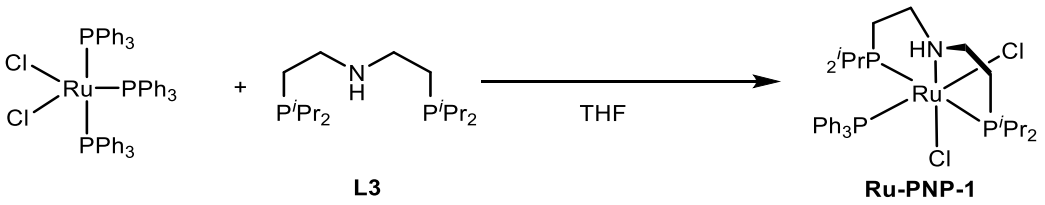

Preparation of Ru-PNP-1: To a solution of $Ru(PPh_3)_3Cl_2$ (958 mg, 1 mmol) in THF (8 mL) was dropwise added bis(2-(diisopropylphosphino)ethyl)amine (3.5 mL, 10 w% in THF, 1 mmol). The mixture was stirred at room temperature for 2h. Then, most of THF was evaporated by rotavapor followed by the addition of pentane (25 mL) while stirring. At this period, solid was precipitated. It was placed at 4 ^oC for 1h. Then, the solid was collected by filtration which was washed by ether and dried under vacuum to give **Ru-PNP-1** as a light brown solid. The characterization was reported by previous literature.[113]

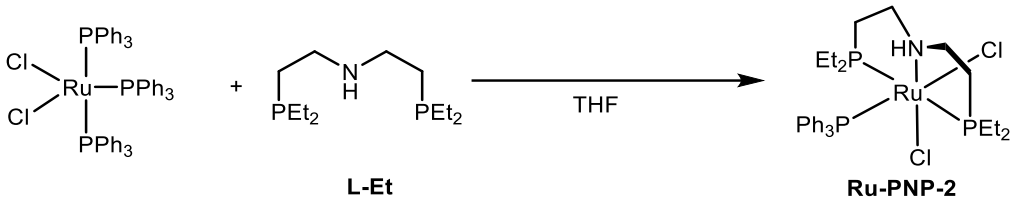

L-Et **Ru-PNP-2**

Preparation of Ru-PNP-2: To a solution of $Ru(PPh_3)_3Cl_2$ (958 mg, 1 mmol) in THF (8 mL) was dropwise added bis(2-(diethylphosphino)ethyl)amine (250 mg, 1 mmol). The mixture was stirred at room temperature for 2h. Then, most of THF was evaporated by rotavapor followed by the addition of pentane (25 mL) while stirring. At this period, solid was precipitated. It was placed at 4 ^oC for 1h. Then, the solid was collected by filtration which was washed by ether and dried under vacuum to give **Ru-PNP-2** as a green to yellow solid.

^{1}H NMR (500 MHz, C_6D_6) δ 8.32 –8.10 (m, 6H), 7.13 – 7.00 (m, 9H), 3.83 – 3.61 (m, 1H), 2.96 – 2.79 (m, 2H), 2.31 – 2.13 (m, 2H), 2.00 – 1.82 (m, 4H), 1.73 – 1.57 (m, 2H), 1.52 – 1.31 (m, 4H), 1.04 – 0.86 (m, 8H), 0.82 (p, *J* = 7.1 Hz, 6H). **^{13}C NMR** (126 MHz, C_6D_6) δ 143.6 (d, *J* = 36.5 Hz), 136.1 (d, *J* = 9.5 Hz), 129.1, 127.7 (d, *J* = 8.5 Hz), 48.9, 26.3, 14.4 (t, *J* = 10.8 Hz), 13.4 (t, *J* = 10.3 Hz), 9.5, 9.0. **^{31}P NMR** (203 MHz, C_6D_6) δ 42.7 (t, *J* = 28.1 Hz), 33.7 (d, *J* = 28.0 Hz). **HRMS:** (APCI, *m*/*z*): calcd. for $C_{30}H_{44}ClNP_3Ru[M\text{-}Cl]^+$ 648.1410, found: 648.1413.

^{1}HNMR spectrum

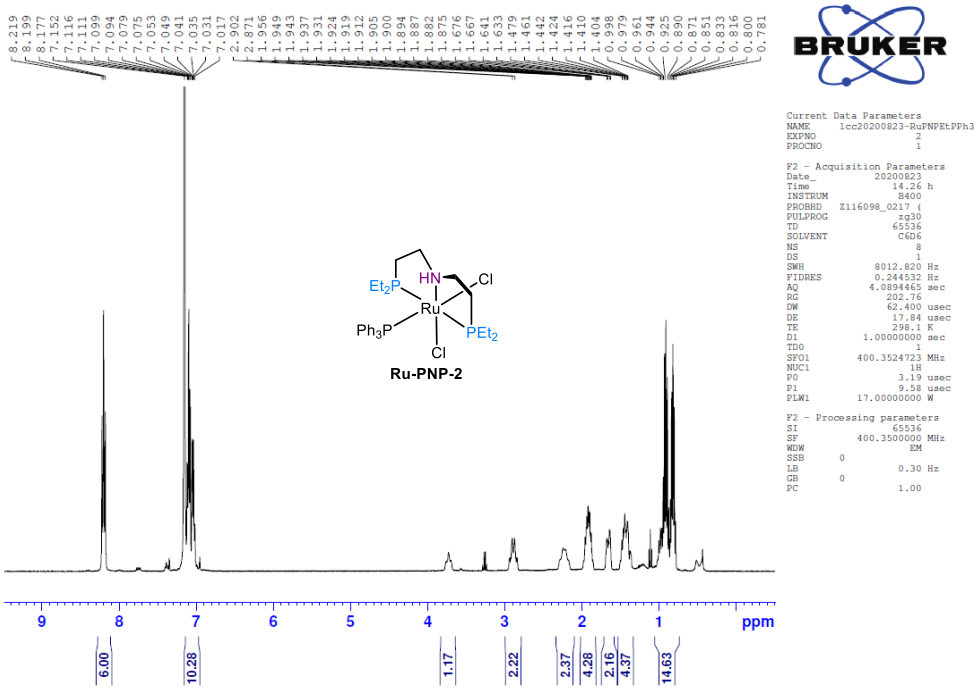

^{13}C NMR spectrum

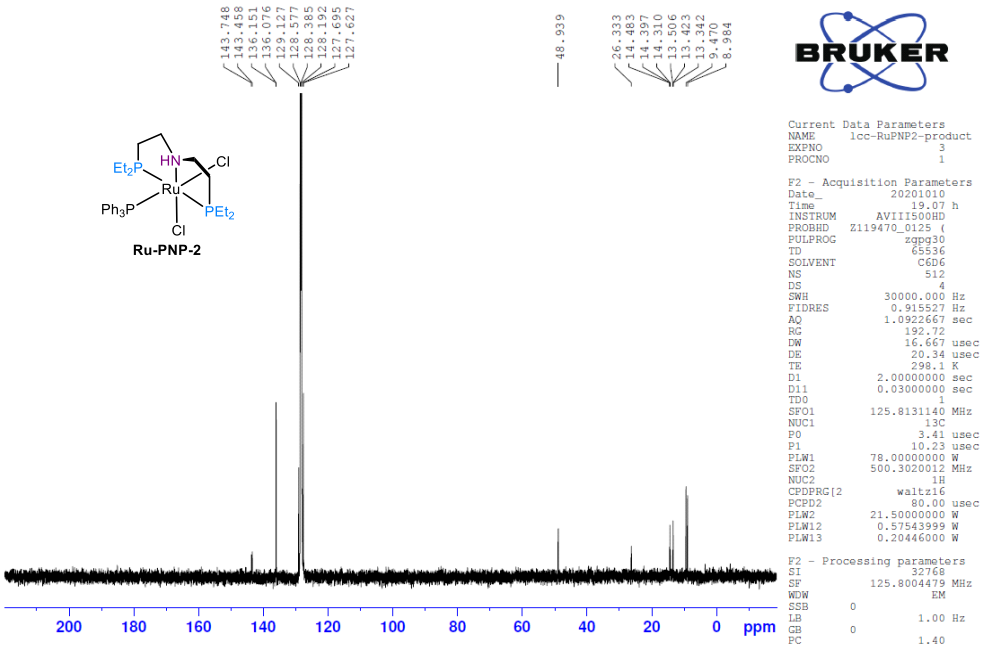

^{31}PNMR spectrum

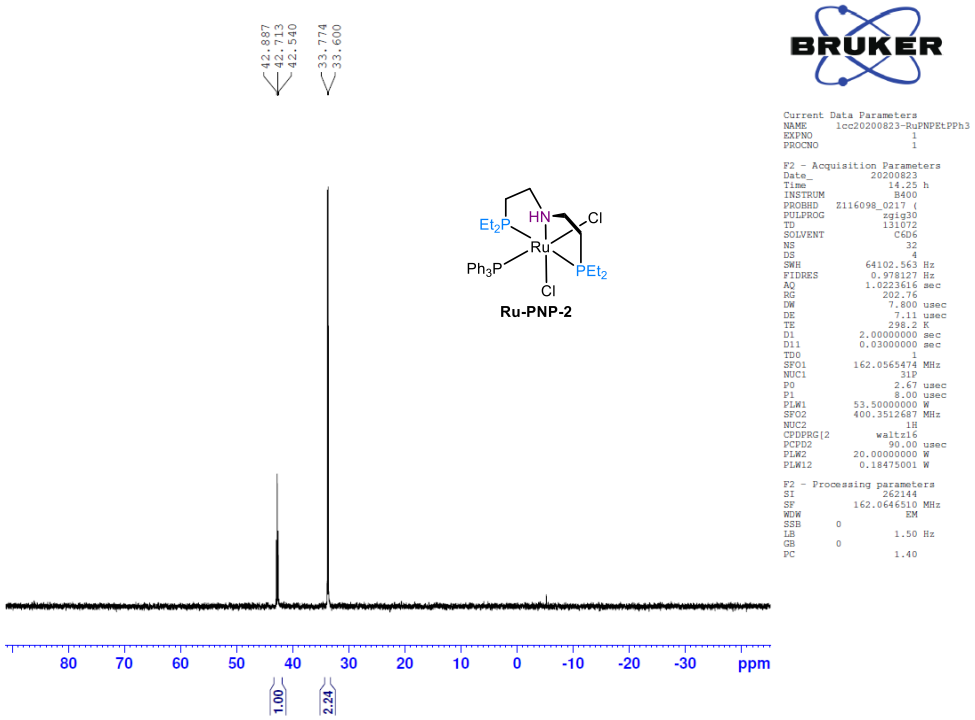

4.3.4.3 Spectroscopic data of products

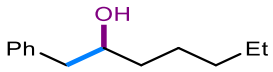

4.3.3aa

(Generated following the corresponding general procedure and isolated by column chromatography on silica gel with hexane: EtOAc = 95:5 as eluent, light brown oil, 28 mg, yield: 73%): **^{1}H NMR** (500 MHz, $CDCl_3$) δ 7.38 – 7.31 (m, 2H), 7.31 – 7.16 (m, 3H), 3.90 – 3.79 (m, 1H), 2.86 (dd, *J* = 13.6, 4.2 Hz, 1H), 2.68 (dd, *J* = 13.5, 8.4 Hz, 1H), 1.73 – 1.46 (m, 4H), 1.46 – 1.21 (m, 5H), 0.93 (t, *J* = 6.9 Hz, 3H). **^{13}C NMR** (126 MHz, $CDCl_3$) δ 138.6, 129.4, 128.5, 126.4, 72.7, 44.0, 36.8, 31.8, 25.4, 22.6, 14.0. **HRMS:** (ESI, *m/z*): calcd. for $C_{13}H_{20}ONa[M+Na]^+$ 215.1406, found: 215.1404.

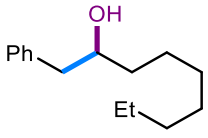

4.3.3ab

(Generated following the corresponding general procedure and isolated by column chromatography on silica gel with hexane: EtOAc = 95:5 as eluent, light brown oil, 31.5 mg, yield: 70%) **^{1}H NMR** (500 MHz, $CDCl_3$) δ 7.38 – 7.31 (m, 2H), 7.31 – 7.16 (m, 3H), 3.90 – 3.79 (m, 1H), 2.86 (dd, *J* = 13.6, 4.2 Hz, 1H), 2.67 (dd, *J* = 13.6, 8.4 Hz, 1H), 1.70 – 1.46 (m, 4H), 1.46 – 1.18 (m, 9H), 1.00 – 0.84 (m, 3H). **^{13}C NMR** (126 MHz, $CDCl_3$) δ 138.6, 129.4, 128.5, 126.4, 72.7, 44.0, 36.8, 31.8, 29.6, 29.3, 25.7, 22.6, 14.1. **HRMS:** (ESI, *m*/*z*): calcd. for $C_{15}H_{24}ONa[M+Na]^+$ 243.1719, found: 243.1717.

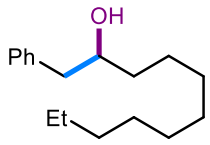

4.3.3ac

(Generated following the corresponding general procedure and isolated by column chromatography on silica gel with hexane: EtOAc = 95:5 as eluent, light brown oil, 33 mg, yield: 66%) **^{1}H NMR** (500 MHz, $CDCl_3$) δ 7.41 – 7.30 (t, *J* = 7.4 Hz, 2H), 7.30 – 7.18 (m, 3H), 3.90 – 3.79 (m, 1H), 2.86 (dd, *J* = 13.5, 4.2 Hz, 1H), 2.67 (dd, *J* = 13.5, 8.4 Hz, 1H), 1.68 – 1.46 (m, 4H), 1.45 – 1.16 (m, 13H), 0.92 (t, *J* = 6.9 Hz, 3H). **^{13}C NMR** (126 MHz, $CDCl_3$) δ 138.6, 129.4, 128.5, 126.4, 72.7, 44.0, 36.8, 31.9, 29.6, 29.6, 29.6, 29.3, 25.7, 22.7, 14.1. **HRMS:** (ESI, *m*/*z*): calcd. for $C_{17}H_{28}ONa[M+Na]^+$ 271.2032, found: 271.2038.

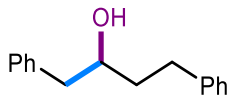

4.3.3ad

(Generated following the corresponding general procedure and isolated by column chromatography on silica gel with hexane: EtOAc = 94:6 as eluent, colorless oil, 31 mg, yield: 70%) **^{1}H NMR** (500 MHz, $CDCl_3$) δ 7.43 – 7.18 (m, 10H), 3.94 – 3.83 (m, 1H), 2.97 – 2.84 (m, 2H), 2.83 – 2.68 (m, 2H), 1.97 – 1.80 (m, 2H), 1.60 (s, 1H). **^{13}C NMR** (126 MHz, $CDCl_3$) δ 142.0, 138.3, 129.4, 128.6, 128.4, 128.4, 126.5, 125.8, 71.9, 44.1, 38.4, 32.1. **HRMS:** (ESI, *m*/*z*): calcd. for $C_{16}H_{18}ONa[M+Na]^+$ 249.1250, found: 249.1247.

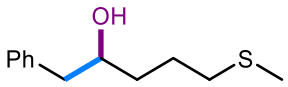

4.3.3ae

(Generated following the corresponding general procedure and isolated by column chromatography on silica gel with hexane: EtOAc = 93:7 as eluent, white solid, 28 mg, yield: 67%) **^{1}H NMR** (500 MHz, $CDCl_3$) δ 7.40 – 7.30 (m, 2H), 7.30 – 7.18 (m, 3H), 3.93 – 3.82 (m, 1H), 2.86 (dd, *J* = 13.7, 4.3 Hz, 1H), 2.69 (dd, *J* = 13.2, 8.5 Hz, 1H), 2.55 (t, *J* = 7.0 Hz, 2H), 2.13 (s, 3H), 1.92 – 1.80 (m, 1H), 1.78 – 1.54 (m, 4H). **^{13}C NMR** (126 MHz, $CDCl_3$) δ 138.3, 129.4, 128.6, 126.5, 72.2, 44.2, 35.8, 34.2, 25.3, 15.5. **HRMS:** (ESI, *m*/*z*): calcd. for $C_{12}H_{18}OSNa[M+Na]^+$ 233.0971, found: 233.0967.

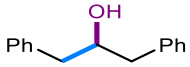

4.3.3af

(Generated following the corresponding general procedure and isolated by column chromatography on silica gel with hexane: EtOAc = 94:6 as eluent, colorless oil, 29 mg, yield: 68%) **^{1}H NMR** (500 MHz, $CDCl_3$) δ 7.41 – 7.31 (m, 4H), 7.31 – 7.20 (m, 6H), 4.15 – 4.05 (m, 1H), 2.90 (dd, *J* = 13.5, 4.7 Hz, 2H), 2.80 (dd, *J* = 13.5, 8.2 Hz, 2H), 1.71 (s, 1H). **^{13}C NMR** (126 MHz, $CDCl_3$) δ 138.4, 129.4, 128.5, 126.5, 73.5, 43.3. **HRMS:** (ESI, *m*/*z*): calcd. for $C_{15}H_{16}ONa[M+Na]^+$ 235.1093, found: 235.1092.

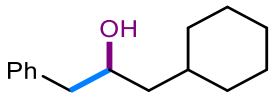

4.3.3ag

(Generated following the corresponding general procedure and isolated by column chromatography on silica gel with hexane: EtOAc = 94:6 as eluent, colorless oil, 30 mg, yield: 69%) **^{1}H NMR** (500 MHz, $CDCl_3$) δ 7.42 – 7.30 (m, 2H), 7.30 – 7.18 (m, 3H), 4.00 – 3.92 (m, 1H), 2.84 (dd, *J* = 13.6, 4.2 Hz, 1H), 2.66 (dd, *J* = 13.6, 8.4 Hz, 1H), 1.88 – 1.78 (m, 1H), 1.78 – 1.64 (m, 4H), 1.64 – 1.43 (m, 3H), 1.43 – 1.11 (m, 4H), 1.05 – 0.82 (m, 2H). **^{13}C NMR** (126 MHz, $CDCl_3$) δ 138.6, 129.4, 128.5, 126.4, 70.0, 44.7, 44.6, 34.1, 32.8, 26.6, 26.3, 26.2. **HRMS:** (ESI, *m*/*z*): calcd. for $C_{15}H_{22}ONa[M+Na]^+$ 241.1563, found: 241.1556.

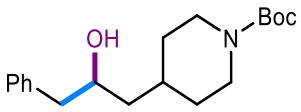

4.3.3ah

(Generated following the corresponding general procedure and isolated by column chromatography on silica gel with hexane: EtOAc = 80:20 as eluent, colorless oil, 45 mg, yield: 71%) **^{1}H NMR** (500 MHz, $CDCl_3$) δ 7.39 – 7.30 (m, 2H), 7.30 – 7.16 (m, 3H), 4.08 (s, 2H), 4.00 – 3.84 (m, 1H), 2.82 (dd, *J* = 13.5, 4.2 Hz, 1H), 2.77 – 2.62 (m, 3H), 1.90 – 1.56 (m, 4H), 1.56 – 1.31 (m, 11H), 1.24 – 0.96 (m, 3H). **^{13}C NMR** (126 MHz, $CDCl_3$) δ 154.8, 138.2, 129.3, 128.6, 126.5, 79.2, 69.7, 44.8, 43.5, 32.9, 32.5, 28.4. **HRMS:** (ESI, *m*/*z*): calcd. for $C_{19}H_{29}O_3NNa[M+Na]^+$ 342.2040, found: 342.2041.

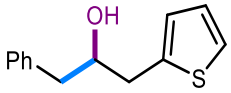

4.3.3ai

(Generated following the corresponding general procedure and isolated by column chromatography on silica gel with hexane: EtOAc = 94:6 as eluent, colorless oil, 35 mg, yield: 80%) **^{1}H NMR** (500 MHz, $CDCl_3$) δ 7.44 – 7.32 (m, 2H), 7.32 – 7.24 (m, 3H), 7.24 – 7.18 (m, 1H), 7.05 – 6.97 (m, 1H), 6.97 – 6.87 (m, 1H), 4.18 – 4.02 (m, 1H), 3.11 (dd, *J* = 14.7, 4.4 Hz, 1H), 3.01 (dd, *J* = 14.7, 7.8 Hz, 1H), 2.92 (dd, *J* = 13.6, 4.8 Hz, 1H), 2.80 (dd, *J* = 13.6, 8.0 Hz, 1H), 1.92 (s, 1H). **^{13}C NMR** (126 MHz, $CDCl_3$) δ 140.4, 138.1, 129.4, 128.5, 126.9, 126.5, 126.0, 124.2, 73.2, 43.0, 37.2. **HRMS:** (ESI, *m*/*z*): calcd. for $C_{13}H_{14}OSNa[M+Na]^+$ 241.0658, found: 241.0650.

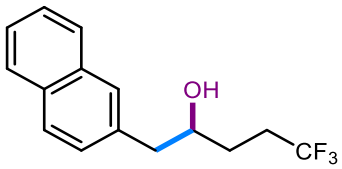

4.3.3hj

(Generated following the corresponding general procedure and isolated by column chromatography on silica gel with hexane: EtOAc = 93:7 as eluent, white solid, 32 mg, yield: 63%) **^{1}H NMR** (500 MHz, $CDCl_3$) δ 8.00 – 7.79 (m, 3H), 7.69 (s, 1H), 7.59 – 7.44 (m, 2H), 7.40 – 7.31

(m, 1H), 4.02 – 3.87 (m, 1H), 3.02 (dd, *J* = 13.6, 4.1 Hz, 1H), 2.86 (dd, *J* = 13.6, 8.7 Hz, 1H), 2.51 – 2.34 (m, 1H), 2.31 – 2.13 (m, 1H), 1.97 – 1.85 (m, 1H), 1.85 – 1.72 (m, 1H), 1.67 (s, 1H). **^{13}C NMR** (126 MHz, $CDCl_3$) δ 135.1, 133.6, 132.4, 130.7, 128.5, 128.0, 127.7, 127.5, 127.5, 127.4 (q, *J* = 276.6 Hz), 126.3, 125.8, 71.1, 44.3, 30.4 (q, *J* = 28.9 Hz), 29.0 (q, *J* = 2.7 Hz). **^{19}F NMR** (471 MHz, $CDCl_3$) δ -66.3. **HRMS:** (ESI, *m*/*z*): calcd. for $C_{15}H_{15}OF_3Na[M+Na]^+$ 291.0967, found: 291.0972.

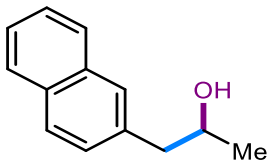

4.3.3hk

(Generated following the corresponding general procedure and isolated by column chromatography on silica gel with hexane: EtOAc = 90:10 as eluent, white solid, 24 mg, yield: 67%) **^{1}H NMR** (500 MHz, $CDCl_3$) δ 7.95 – 7.77 (m, 3H), 7.70 (s, 1H), 7.56 – 7.44 (m, 2H), 7.43 – 7.33 (m, 1H), 4.20 – 4.08 (m, 1H), 2.98 (dd, *J* = 13.5, 4.8 Hz, 1H), 2.89 (dd, *J* = 13.5, 8.0 Hz, 1H), 1.67 (s, 1H), 1.32 (d, *J* =6.3 Hz, 3H). **^{13}C NMR** (126 MHz, $CDCl_3$) δ 136.0, 133.5, 132,2, 128.1, 127.8, 127.7, 127.6, 127.5, 126.1, 125.5, 68.7, 45.9, 22.8. **HRMS:** (ESI, *m*/*z*): calcd. for $C_{13}H_{14}ONa[M+Na]^+$ 209.0937, found: 209.0935.

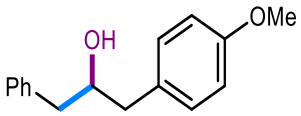

4.3.3al

(Generated following the corresponding general procedure and isolated by column chromatography on silica gel with hexane: EtOAc = 92:8 as eluent, colorless oil, 30 mg, yield: 64%) **^{1}H NMR** (500 MHz, $CDCl_3$) δ 7.40 – 7.31 (m, 2H), 7.31 – 7.22 (m, 3H), 7.22 – 7.13 (m, 2H), 6.94 – 6.84 (m, 2H), 6.97 – 6.87 (m, 1H), 4.11 – 3.99 (m, 1H), 3.82 (s, 3H), 2.94 – 2.68 (m, 4H), 1.68 (s, 1H). **^{13}C NMR** (126 MHz, $CDCl_3$) δ 158.3, 138.5, 130.3, 129.4, 128.5, 126.4, 113.9, 73.6, 55.2, 43.3, 42.4. **HRMS:** (ESI, *m*/*z*): calcd. for $C_{16}H_{18}O_2Na[M+Na]^+$ 265.1199, found: 265.1197.

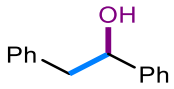

4.3.3am

(Generated following the corresponding general procedure and isolated by column chromatography on silica gel with hexane: EtOAc = 95:5 as eluent, white solid, 24 mg, yield: 61%)[2] **^{1}H NMR** (500 MHz, $CDCl_3$) δ 7.42 – 7.37 (m, 4H), 7.37 – 7.30 (m, 3H), 7.30 – 7.26 (m, 1H), 7.26 – 7.20 (m, 2H), 4.93 (dd, *J* = 8.5, 4.9 Hz, 1H), 3.11 – 2.99 (m, 2H), 2.02 (s, 1H). **^{13}C NMR** (126 MHz, $CDCl_3$) δ 143.8, 138.0, 129.5, 128.5, 128.4, 127.6, 126.6, 125.9, 75.3, 46.1. **HRMS:** (ESI, *m*/*z*): calcd. for $C_{14}H_{14}ONa[M+Na]^+$ 221.0937, found: 221.0942.

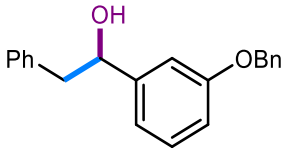

4.3.3an

(Generated following the corresponding general procedure and isolated by column chromatography on silica gel with hexane: EtOAc = 92:8 as eluent, white solid, 33 mg, yield: 54%) **^{1}H NMR** (500 MHz, $CDCl_3$) δ 7.56 – 7.41 (m, 4H), 7.41 – 7.18 (m, 7H), 7.11 – 7.04 (m, 1H), 7.04 – 6.89 (m, 2H), 5.09 (s, 2H), 4.91 (dd, *J* = 8.5, 4.8 Hz, 1H), 3.11 – 2.98 (m, 2H), 2.07 (s, 1H). **^{13}C NMR** (126 MHz, $CDCl_3$) δ 158.9, 145.5, 138.0, 137.0, 129.5, 129.4, 128.5, 128.5, 127.9, 127.5, 126.6, 118.5, 114.0, 112.3, 75.2, 69.9, 46.0. **HRMS:** (ESI, *m*/*z*): calcd. for $C_{21}H_{20}O_2Na[M+Na]^+$ 327.1356, found: 327.1360.

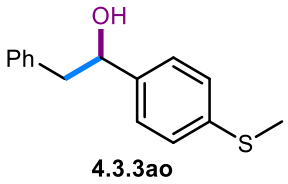

4.3.3ao

(Generated following the corresponding general procedure and isolated by column chromatography on silica gel with hexane: EtOAc = 93:7 as eluent, white solid, 26 mg, yield: 53%) **^{1}H NMR** (500 MHz, $CDCl_3$) δ 7.36 – 7.24 (m, 7H), 7.24 – 7.19 (m, 2H), 4.88 (dd, *J* = 8.1, 5.1 Hz, 1H), 3.09 – 2.95 (m, 2H), 2.51 (s, 3H), 2.01 (s, 1H). **^{13}C NMR** (126 MHz, $CDCl_3$) δ 140.7, 137.8, 137.5, 129.5, 128.5, 126.6, 126.4, 74.9, 45.9, 15.9. **HRMS:** (ESI, *m*/*z*): calcd. for $C_{15}H_{16}OSNa[M+Na]^+$ 267.0814, found: 267.0813.

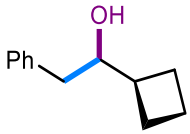

4.3.3ap

(Generated following the corresponding general procedure and isolated by column chromatography on silica gel with hexane: EtOAc = 95:5 as eluent, colorless oil, 24 mg, yield: 69%): **^{1}H NMR** (500 MHz, $CDCl_3$) δ 7.39 – 7.31 (m, 2H), 7.31 – 7.18 (m, 3H), 3.83 – 3.70 (m, 1H), 2.79 (dd, *J* = 13.7, 3.9 Hz, 1H), 2.56 (dd, *J* = 13.7, 8.4 Hz, 1H), 2.48 – 2.34 (m, 1H), 2.12 – 1.90 (m, 4H), 1.90 – 1.79 (m, 2H), 1.58 (s, 1H). **^{13}C NMR** (126 MHz, $CDCl_3$) δ 138.6, 129.4, 128.4, 126.3, 76.4, 40.9, 40.7, 24.4, 24.2, 17.8. **HRMS:** (ESI, *m*/*z*): calcd. for $C_{12}H_{16}ONa[M+Na]^+$ 199.1093, found: 199.1095.

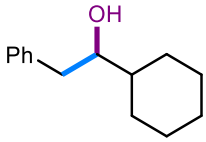

4.3.3aq

(Generated following the corresponding general procedure and isolated by column chromatography on silica gel with hexane: EtOAc = 95:5 as eluent, colorless oil, 21 mg, yield: 50%)[1] **^{1}H NMR** (500 MHz, $CDCl_3$) δ 7.44 – 7.31 (m, 2H), 7.31 – 7.16 (m, 3H), 3.65 – 3.56 (m, 1H), 2.91 (dd, *J* = 13.6, 3.4 Hz, 1H), 2.56 (dd, *J* = 13.6, 9.6 Hz, 1H), 2.00 – 1.90 (m, 1H), 1.88 – 1.75 (m, 3H), 1.75 – 1.65 (m, 1H), 1.60 – 1.37 (m, 2H), 1.37 – 1.03 (m, 5H). **^{13}C NMR** (126 MHz, $CDCl_3$) δ 139.2, 129.4, 128.5, 126.3, 76.9, 43.2, 40.8, 29.3, 28.0, 26.5, 26.3, 26.1. **HRMS:** (ESI, *m*/*z*): calcd. for $C_{14}H_{20}ONa[M+Na]^+$ 227.1406, found: 227.1415.

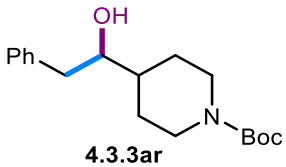

4.3.3ar

(Generated following the corresponding general procedure and isolated by column chromatography on silica gel with hexane: EtOAc = 82:18 as eluent, white solid, 31 mg, yield: 50%): **^{1}H NMR** (500 MHz, $CDCl_3$) δ 7.38 – 7.30 (m, 2H), 7.30 – 7.18 (m, 3H), 4.19 (s, 2H), 3.68 – 3.56 (m, 1H), 2.91 (dd, *J* = 13.5, 3.3 Hz, 1H), 2.80 – 2.54 (m, 3H), 1.97 – 1.85 (m, 1H), 1.80 – 1.54 (m, 3H), 1.54 – 1.21 (m, 12H). **^{13}C NMR** (126 MHz, $CDCl_3$) δ 154.8, 138.5, 129.3, 128.6,

126.5, 79.3, 75.9, 43.5, 41.6, 40.8, 28.4. **HRMS:** (ESI, *m*/*z*): calcd. for $C_{18}H_{27}O_3NNa[M+Na]^+$ 328.1883, found: 328.1887.

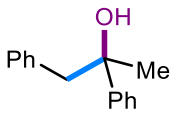

4.3.3as

(Generated following the corresponding general procedure and isolated by column chromatography on silica gel with hexane: EtOAc = 96:4 as eluent, colorless oil, 23 mg, yield: 54%)[2] **^{1}H NMR** (500 MHz, $CDCl_3$) δ 7.47 – 7.41 (m, 2H), 7.41 – 7.33 (m, 2H), 7.33 – 7.19 (m, 4H), 7.08 – 6.98 (m, 2H), 3.17 (d, *J* = 13.4 Hz, 1H), 3.06 (d, *J* = 13.4 Hz, 1H), 1.90 (s, 1H), 1.60 (s, 3H). **^{13}C NMR** (126 MHz, $CDCl_3$) δ 147.5, 136.7, 130.6, 128.0, 126.6, 124.9, 74.4, 50.5, 29.4. **HRMS:** (ESI, *m*/*z*): calcd. for $C_{15}H_{16}ONa[M+Na]^+$ 235.1093, found: 235.1096.

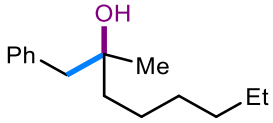

4.3.3at

(Generated following the corresponding general procedure and isolated by column chromatography on silica gel with hexane: EtOAc = 96:4 as eluent, colorless oil, 10 mg, yield: 23%) **^{1}H NMR** (500 MHz, $CDCl_3$) δ 7.37 – 7.30 (m, 2H), 7.30 – 7.19 (m, 3H), 2.78 (dd, *J* = 29.4, 13.3 Hz, 2H), 1.55 – 1.40 (m, 4H), 1.40 – 1.24 (m, 7H), 1.16 (s, 3H), 0.92 (t, *J* = 6.9 Hz, 3H). **^{13}C NMR** (126 MHz, $CDCl_3$) δ 137.6, 130.5, 128.2, 126.4, 72.5, 48.0, 41.9, 31.9, 29.8, 26.5, 24.0, 22.6, 14.1. **HRMS:** (ESI, *m*/*z*): calcd. for $C_{15}H_{24}ONa[M+Na]^+$ 243.1719, found: 243.1728.

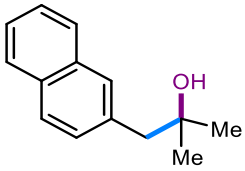

4.3.3hv

(Generated following the corresponding general procedure and isolated by column chromatography on silica gel with hexane: EtOAc = 95:5 as eluent, white solid, 34 mg, yield: 85%) **^{1}H NMR** (500 MHz, $CDCl_3$) δ 7.91 – 7.78 (m, 3H), 7.71 (s, 1H), 7.56 – 7.45 (m, 2H), 7.41 (dd, *J* = 8.4, 1.8 Hz, 1H), 2.97 (s, 2H), 1.56 (s, 1H), 1.31 (s, 6H). **^{13}C NMR** (126 MHz, $CDCl_3$) δ 135.4,

133.3, 132.2, 129.0, 128.8, 127.6, 127.6, 126.0, 125.4, 70.9, 49.8, 29.2. **HRMS:** (ESI, *m/z*): calcd. for $C_{14}H_{16}ONa[M+Na]^+$ 223.1093, found: 223.1094.

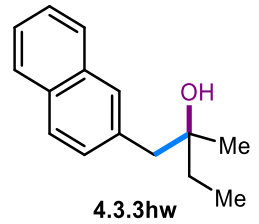

4.3.3hw

.

(Generated following the corresponding general procedure and isolated by column chromatography on silica gel with hexane: EtOAc = 95:5 as eluent, white solid, 26 mg, yield: 61%) **^{1}H NMR** (500 MHz, $CDCl_3$) δ 7.92 – 7.77 (m, 3H), 7.71 (s, 1H), 7.57 – 7.45 (m, 2H), 7.41 (dd, *J* = 8.4, 1.8 Hz, 1H), 2.95 (q, *J* = 13.3 Hz, 2H), 1.59 (q, *J* = 7.5 Hz, 2H), 1.47 (s, 1H), 1.21 (s, 3H), 1.04 (t, *J* = 7.5 Hz, 3H). **^{13}C NMR** (126 MHz, $CDCl_3$) δ 135.3, 133.3, 132.2, 129.1, 128.9, 127.6, 126.0, 125.4, 72.9, 47.6, 34.3, 26.0, 8.3. **HRMS:** (ESI, *m/z*): calcd. for $C_{15}H_{18}ONa[M+Na]^+$ 237.1250, found: 237.1254.

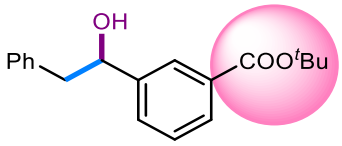

4.3.3ax

(Generated following the corresponding general procedure and isolated by column chromatography on silica gel with hexane: EtOAc = 90:10 as eluent, colorless oil, 35 mg, yield: 59%) **^{1}H NMR** (500 MHz, $CDCl_3$) δ 8.00 (s, 1H), 7.93 (d, *J* = 7.7 Hz, 1H), 7.53 (d, *J* = 7.6 Hz, 1H), 7.41 (t, *J* = 7.7 Hz, 1H), 7.37 – 7.14 (m, 5H), 4.97 (dd, *J* = 8.7, 4.7 Hz, 1H), 3.16 – 2.89 (m, 2H), 2.16 (s, 1H), 1.63 (s, 9H). **^{13}C NMR** (126 MHz, $CDCl_3$) δ 165.7, 144.0, 137.7, 132.1, 129.9, 129.5, 128.6, 128.5, 128.2, 126.8, 126.7, 81.1, 74.9, 46.0, 28.2. **HRMS:** (ESI, *m/z*): calcd. for $C_{19}H_{22}O_3Na[M+Na]^+$ 321.1461, found: 321.1470.

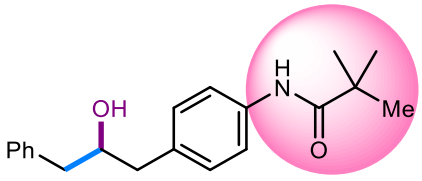

4.3.3az

(Generated following the corresponding general procedure and isolated by column chromatography on silica gel with hexane: EtOAc = 65:35 as eluent, white solid, 30 mg, yield: 48%) **^{1}H NMR** (500 MHz, $CDCl_3$) δ 7.56 – 7.45 (m, 2H), 7.44 – 7.30 (m, 3H), 7.31 – 7.13 (m, 5H), 4.12 – 3.98 (m, 1H), 2.85 (ddd, *J* = 14.2, 9.7, 4.7 Hz, 2H), 2.81 – 2.65 (m, 2H), 1.73 (s, 1H), 1.34 (s, 9H). **^{13}C NMR** (126 MHz, $CDCl_3$) δ 176.5, 138.4, 136.4, 134.2, 129.8, 129.4, 128.5, 126.4, 120.2, 73.5, 43.2, 42.7, 39.5, 27.6. **HRMS:** (ESI, *m*/*z*): calcd. for $C_{20}H_{25}O_2NNa[M+Na]^+$ 334.1777, found: 334.1775.

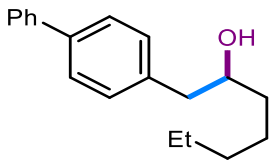

4.3.3ba

(Generated following the corresponding general procedure and isolated by column chromatography on silica gel with hexane: EtOAc = 94:6 as eluent, white solid, 40 mg, yield: 75%): **^{1}H NMR** (500 MHz, $CDCl_3$) δ 7.70 – 7.56 (m, 4H), 7.54 – 7.43 (m, 2H), 7.42 – 7.29 (m, 3H), 4.00 – 3.77 (m, 1H), 2.91 (dd, *J* = 13.6, 4.2 Hz, 1H), 2.73 (dd, *J* = 13.6, 8.4 Hz, 1H), 1.73 – 1.50 (m, 4H), 1.50 – 1.19 (m, 5H), 0.95 (t, *J* = 6.9 Hz, 3H). **^{13}C NMR** (126 MHz, $CDCl_3$) δ 140.9, 139.3, 137.7, 129.8, 128.7, 127.2, 127.1, 127.0, 72.7, 43.6, 36.9, 31.8, 25.4, 22.6, 14.0. **HRMS:** (ESI, *m*/*z*): calcd. for $C_{19}H_{24}ONa[M+Na]^+$ 291.1719, found: 291.1730.

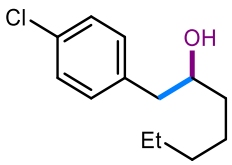

4.3.3ca

(Generated following the corresponding general procedure and isolated by column chromatography on silica gel with hexane: EtOAc = 94:6 as eluent, white solid, 29 mg, yield: 64%): **^{1}H NMR** (500 MHz, $CDCl_3$) δ 7.37 – 7.25 (m, 2H), 7.21 – 7.12 (m, 2H), 3.88 – 3.72 (m, 1H), 2.81 (dd, *J* = 13.7, 4.3 Hz, 1H), 2.65 (dd, *J* = 13.7, 8.3 Hz, 1H), 1.67 – 1.44 (m, 4H), 1.44 – 1.21 (m, 5H), 0.92 (t, *J* = 6.9 Hz, 3H). **^{13}C NMR** (126 MHz, $CDCl_3$) δ 137.2, 132.2, 130.7, 128.6, 72.5, 43.3, 36.8, 31.8, 25.4, 22.6, 14.0. **HRMS:** (ESI, *m*/*z*): calcd. for $C_{13}H_{19}OClNa[M+Na]^+$ 249.1017, found: 249.1019.

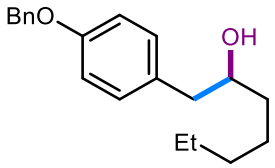

4.3.3da

(Generated following the corresponding general procedure and isolated by column chromatography on silica gel with hexane: EtOAc = 94:6 as eluent, white solid, 38 mg, yield: 64%): **^{1}H NMR** (500 MHz, $CDCl_3$) δ 7.54 – 7.32 (m, 5H), 7.17 (d, *J* = 8.5 Hz, 2H), 6.97 (d, *J* = 8.5 Hz, 2H), 5.09 (s, 1H), 3.88 – 3.74 (m, 1H), 2.81 (dd, *J* = 13.7, 4.2 Hz, 1H), 2.62 (dd, *J* = 13.7, 8.4 Hz, 1H), 1.71 – 1.46 (m, 4H), 1.46 – 1.23 (m, 5H), 0.94 (t, *J* = 6.9 Hz, 3H). **^{13}C NMR** (126 MHz, $CDCl_3$) δ 157.5, 137.1, 130.9, 130.3, 128.5, 127.9, 127.4, 114.9, 72.7, 70.0, 43.1, 36.7, 31.8, 25.4, 22.6, 14.0. **HRMS:** (ESI, *m*/*z*): calcd. for $C_{20}H_{26}O_2Na[M+Na]^+$ 321.1825, found: 321.1825.

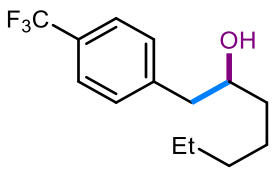

4.3.3ea

(Generated following the corresponding general procedure and isolated by column chromatography on silica gel with hexane: EtOAc = 94:6 as eluent, colorless oil, 26 mg, yield: 50%): **^{1}H NMR** (500 MHz, $CDCl_3$) δ 7.59 (d, *J* = 8.0 Hz, 2H), 7.36 (d, *J* = 8.0 Hz, 2H), 3.95 – 3.78 (m, 1H), 2.89 (dd, *J* = 13.6, 4.1 Hz, 1H), 2.75 (dd, *J* = 13.6, 8.3 Hz, 1H), 1.67 – 1.46 (m, 4H), 1.46 – 1.22 (m, 5H), 0.92 (t, *J* = 6.9 Hz, 3H). **^{13}C NMR** (126 MHz, $CDCl_3$) δ 143.0, 129.7, 128.7 (q, *J* = 32.4 Hz), 125.3 (q, *J* = 3.2 Hz), 124.3 (q, *J* = 271.2 Hz), 72.5, 43.7, 37.0, 31.8, 25.3, 22.6, 14.0. **^{19}F NMR** (471 MHz, $CDCl_3$) δ -62.4. **HRMS:** (ESI, *m*/*z*): calcd. for $C_{14}H_{19}OF_3Na[M+Na]^+$ 283.1280, found: 283.1277.

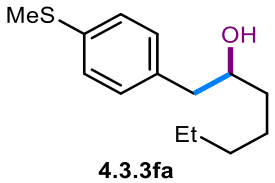

4.3.3fa

(Generated following the corresponding general procedure and isolated by column chromatography on silica gel with hexane: EtOAc = 93:7 as eluent, colorless oil, 31 mg, yield:

65%): **^{1}H NMR** (500 MHz, $CDCl_3$) δ 7.24 (d, *J* = 8.2 Hz, 2H), 7.16 (d, *J* = 8.2 Hz, 2H), 3.87 – 3.75 (m, 1H), 2.81 (dd, *J* = 13.6, 4.3 Hz, 1H), 2.63 (dd, *J* = 13.6, 8.3 Hz, 1H), 2.50 (s, 3H), 1.63 – 1.44 (m, 4H), 1.44 – 1.20 (m, 5H), 0.92 (t, *J* = 6.9 Hz, 3H). **^{13}C NMR** (126 MHz, $CDCl_3$) δ 136.1, 135.6, 129.9, 127.0, 72.6, 43.4, 36.8, 31.8, 25.4, 22.6, 16.1, 14.0. **HRMS:** (ESI, *m*/*z*): calcd. for $C_{14}H_{22}OSNa[M+Na]^+$ 261.1284, found: 261.1284.

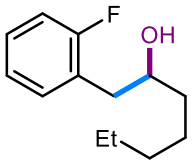

4.3.3ga

(Generated following the corresponding general procedure and isolated by column chromatography on silica gel with hexane: EtOAc = 95:5 as eluent, colorless oil, 26 mg, yield: 62%): **^{1}H NMR** (500 MHz, $CDCl_3$) δ 7.33 – 7.16 (m, 2H), 7.16 – 6.97 (m, 2H), 3.96 – 3.80 (m, 1H), 2.92 (dd, *J* = 13.8, 4.4 Hz, 1H), 2.71 (dd, *J* = 13.8, 8.2 Hz, 1H), 2.50 (s, 3H), 1.66 – 1.46 (m, 4H), 1.46 – 1.22 (m, 5H), 0.92 (t, *J* = 6.9 Hz, 3H). **^{13}C NMR** (126 MHz, $CDCl_3$) δ 161.4 (d, *J* = 244.7 Hz), 131.8 (d, *J* = 4.7 Hz), 128.2 (d, *J* = 8.1 Hz), 125.7 (d, *J* = 15.6 Hz), 124.0 (d, *J* = 3.5 Hz), 115.4 (d, *J* = 22.4 Hz), 71.7, 37.2, 37.0, 31.8, 25.4, 22.6, 14.1. **^{19}F NMR** (471 MHz, $CDCl_3$) δ -117.7. **HRMS:** (ESI, *m*/*z*): calcd. for $C_{13}H_{19}OFNa[M+Na]^+$ 233.1312, found: 233.1315.

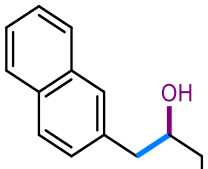

4.3.3ha

(Generated following the corresponding general procedure and isolated by column chromatography on silica gel with hexane: EtOAc = 94:6 as eluent, white solid, 33 mg, yield: 68%): **^{1}H NMR** (500 MHz, $CDCl_3$) δ 7.92 – 7.77 (m, 1H), 7.71 (s, 1H), 7.55 – 7.44 (m, 2H), 7.43 – 7.34 (m, 1H), 4.01 – 3.87 (m, 1H), 3.03 (dd, *J* = 13.6, 4.2 Hz, 1H), 2.85 (dd, *J* = 13.6, 8.4 Hz, 1H), 1.72 – 1.50 (m, 4H), 1.50 – 1.24 (m, 5H), 0.94 (t, *J* = 6.9 Hz, 3H). **^{13}C NMR** (126 MHz, $CDCl_3$) δ 136.2, 133.5, 132.2, 128.1, 127.8, 127.8, 127.6, 127.5, 126.0, 125.4, 72.6, 44.2, 36.9, 31.8, 25.4, 22.6, 14.0. **HRMS:** (ESI, *m*/*z*): calcd. for $C_{17}H_{22}ONa[M+Na]^+$ 265.1563, found: 265.1564.

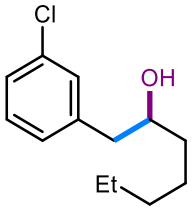

4.3.3ia

(Generated following the corresponding general procedure and isolated by column chromatography on silica gel with hexane: EtOAc = 94:6 as eluent, white solid, 26 mg, yield: 57%): **^{1}H NMR** (500 MHz, $CDCl_3$) δ 7.33 – 7.19 (m, 3H), 7.17 – 7.08 (m, 1H), 3.89 – 3.75 (m, 1H), 2.81 (dd, *J* = 13.7, 4.2 Hz, 1H), 2.65 (dd, *J* = 13.6, 8.4 Hz, 1H), 1.63 – 1.45 (m, 4H), 1.45 – 1.23 (m, 5H), 0.92 (t, *J* = 6.9 Hz, 3H). **^{13}C NMR** (126 MHz, $CDCl_3$) δ 140.8, 134.2, 129.7, 129.5, 127.6, 126.6, 72.5, 43.6, 36.9, 31.8, 25.4, 22.6, 14.0. **HRMS:** (ESI, *m*/*z*): calcd. for $C_{13}H_{19}OClNa[M+Na]^+$ 249.1017, found: 249.1020.

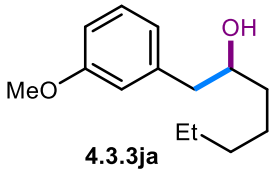

4.3.3ja

(Generated following the corresponding general procedure and isolated by column chromatography on silica gel with hexane: EtOAc = 92:8 as eluent, colorless oil, 27 mg, yield: 61%): **^{1}H NMR** (500 MHz, $CDCl_3$) δ 7.32 – 7.20 (m, 1H), 6.90 – 6.71 (m, 3H), 3.89 – 3.76 (m, 4H), 2.83 (dd, *J* = 13.5, 4.2 Hz, 1H), 2.64 (dd, *J* = 13.5, 8.5 Hz, 1H), 1.72 – 1.46 (m, 4H), 1.46 – 1.21 (m, 5H), 0.92 (t, *J* = 6.9 Hz, 3H). **^{13}C NMR** (126 MHz, $CDCl_3$) δ 159.7, 140.2, 129.5, 121.7, 115.1, 111.7, 72.6, 55.1, 44.1, 36.8, 31.8, 25.4, 22.6, 14.0. **HRMS:** (ESI, *m*/*z*): calcd. for $C_{14}H_{22}O_2Na[M+Na]^+$ 245.1512, found: 245.1521.

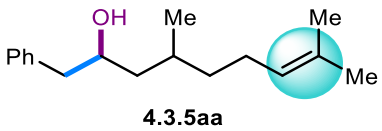

4.3.5aa

(Generated following the corresponding general procedure and isolated by column chromatography on silica gel with hexane: EtOAc = 95:5 as eluent, colorless oil, 33 mg, yield: 67%, mixture of two diastereomers, d.r. = 1:1) **^{1}H NMR** (500 MHz, $CDCl_3$) δ 7.43 – 7.31 (m, 2H), 7.31 – 7.15 (m, 3H), 5.23 – 5.05 (m, 1H), 4.02 – 3.88 (m, 1H), 2.94 – 2.77 (m, 1H), 2.77 – 2.58

(m, 1H), 2.13 – 1.90 (m, 2H), 1.80 – 1.12 (m, 12H), 1.06 – 0.81 (m, 3H). **^{13}C NMR** (126 MHz, $CDCl_3$) δ 138.6, 138.6, 131.2, 131.2, 129.4, 128.5, 126.4, 126.4, 124.7, 70.7, 70.3, 44.8, 44.3, 44.2, 44.2, 37.9, 36.6, 29.3, 28.9, 25.7, 25.5, 25.3, 20.2, 19.1, 17.6. **HRMS:** (ESI, *m*/*z*): calcd. for $C_{17}H_{26}ONa[M+Na]^+$ 269.1876, found: 269.1875.

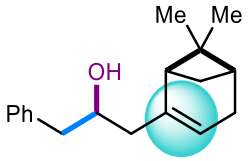

4.3.5ab

(Generated following the corresponding general procedure and isolated by column chromatography on silica gel with hexane: EtOAc = 95:5 as eluent, colorless oil, 32 mg, yield: 62%, mixture of two diastereomers, d.r. = 1:1) **^{1}H NMR** (500 MHz, $CDCl_3$) δ 7.41 – 7.30 (m, 2H), 7.30 – 7.16 (m, 3H), 5.48 – 5.34 (m, 1H), 3.93 – 3.78 (m, 1H), 2.88 – 2.73 (m, 2H), 2.48 – 2.38 (m, 1H), 2.38 – 2.11 (m, 5H), 2.11 – 2.00 (m, 1H), 1.92 – 1.74 (m, 1H), 1.30 (d, *J* = 2.6 Hz, 3H), 1.24 – 1.11 (m, 1H), 0.89 (d, *J* = 2.2 Hz, 3H). **^{13}C NMR** (126 MHz, $CDCl_3$) δ 145.3, 145.0, 138.8, 138.8, 129.4, 128.4, 128.3, 126.3, 120.3, 120.0, 69.8, 69.6, 45.9, 45.6, 45.0, 44.7, 43.4, 43.4, 40.7, 40.6, 38.0, 37.7, 32.0, 31.7, 31.4, 31.4, 26.2, 26.2, 21.3, 21.2. **HRMS:** (ESI, *m*/*z*): calcd. for $C_{18}H_{24}ONa[M+Na]^+$ 279.1719, found: 279.1728.

References

(1). Cernak, T.; Dykstra, K. D.; Tyagarajan, S.; Vachal, P.; Krska, S. W., The medicinal chemist's toolbox for late stage functionalization of drug-like molecules. *Chem. Soc. Rev.* 2016, *45*, 546–576.
(2). Grignard, V., Sur quelques nouvelles combinaisons organometalliques du magnésium et leur application à des synthèses d'alcools et d'hydrocarbures. *Compt. Rend.* 1900, *130*, 1322.
(3). Shirley, D. A., The synthesis of ketones from acid halides and organometallic compounds of magnesium, zinc, and cadmium. *Org. React.* 1954, *8*, 28.
(4). Larock, R. C., Organomercurials in organic synthesis. *Tetrahedron* 1982, *38*, 1713–1754.
(5). Knochel, P.; Jones, P., *Organozinc Reagents: A Practical Approach*. Oxford University Press: Oxford, 1999.
(6). Rappoport, Z.; Marek, I., *The Chemistry of Organolithium Compounds, Volume 1, 2 Volume Set*. John Wiley & Sons: Chichester, 2004.
(7). Smith, M. B.; March, J., *March's Advanced Organic Chemistry: Reactions, Mechanisms, and Structure*. Wiley: New York, 2007.

(8). Bower, J. F.; Kim, I. S.; Patman, R. L.; Krische, M. J., Catalytic carbonyl addition through transfer hydrogenation: A departure from preformed organometallic reagents. *Angew. Chem. Int. Ed.* 2009, *48*, 34–46.
(9). Nguyen, K. D.; Park, B. Y.; Luong, T.; Sato, H.; Garza, V. J.; Krische, M. J., Metal-catalyzed reductive coupling of olefin-derived nucleophiles: Reinventing carbonyl addition. *Science* 2016, *354*, aah5133.
(10). Doerksen, R. S.; Meyer, C. C.; Krische, M. J., Feedstock reagents in metal-catalyzed carbonyl reductive coupling: Minimizing preactivation for efficiency in target-oriented synthesis. *Angew. Chem. Int. Ed.* 2019, *58*, 14055–14064.
(11). Obora, Y., Recent advances in α-alkylation reactions using alcohols with hydrogen borrowing methodologies. *ACS Catal.* 2014, *4*, 3972-3981.
(12). Bäckvall, J.-E.; Chowdhury, R. L.; Karlsson, U., Ruthenium-catalysed aerobic oxidation of alcohols *via* multistep electron transfer. *J. Chem. Soc., Chem, Commun.* 1991, 473–475.
(13). Chowdhury, R. L.; Bäckvall, J.-E., Efficient ruthenium-catalysed transfer hydrogenation of ketones by propan-2-ol. *J. Chem. Soc., Chem, Commun.* 1991, 1063–1064.
(14). Wang, G. Z.; Bäckvall, J.-E., Ruthenium-catalysed oxidation of alcohols by acetone. *J. Chem. Soc., Chem, Commun.* 1992, 337-339.
(15). Wang, G.-Z.; Andreasson, U.; Bäckvall, J.-E., Aerobic oxidation of secondary alcohols *via* ruthenium-catalysed hydrogen transfer involving a new triple catalytic system. *J. Chem. Soc., Chem, Commun.* 1994, 1037–1038.
(16). Dijksman, A.; W. C. E. Arends, I.; A. Sheldon, R., Efficient ruthenium–TEMPO-catalysed aerobic oxidation of aliphatic alcohols into aldehydes and ketones. *Chem. Commun.* 1999, 1591–1592.
(17). Edwards, M. G.; Jazzar, R. F. R.; Paine, B. M.; Shermer, D. J.; Whittlesey, M. K.; Williams, J. M. J.; Edney, D. D., Borrowing hydrogen: A catalytic route to C–C bond formation from alcohols. *Chem. Commun.* 2004, 90–91.
(18). Nixon, T. D.; Whittlesey, M. K.; Williams, J. M. J., Transition metal catalysed reactions of alcohols using borrowing hydrogen methodology. *Dalton Trans.* 2009, 753–762.
(19). Bertoli, M.; Choualeb, A.; Lough, A. J.; Moore, B.; Spasyuk, D.; Gusev, D. G., Osmium and ruthenium catalysts for dehydrogenation of alcohols. *Organometallics* 2011, *30*, 3479-3482.
(20). Kulkarni, N. V.; Brennessel, W. W.; Jones, W. D., Catalytic upgrading of ethanol to *n*-butanol *via* manganese-mediated guerbet reaction. *ACS Catal.* 2017, 997–1002.
(21). Chakraborty, S.; Daw, P.; Ben David, Y.; Milstein, D., Manganese-catalyzed α-alkylation of ketones, esters, and amides using alcohols. *ACS Catal.* 2018, 10300–10305.
(22). Yang, F.-L.; Wang, Y.-H.; Ni, Y.-F.; Gao, X.; Song, B.; Zhu, X.; Hao, X.-Q., An efficient homogenized ruthenium(II) pincer complex for *N*-monoalkylation of amines with alcohols. *Eur. J. Org. Chem.* 2017, *2017*, 3481-3486.

(23). Hoye, T. R.; Jeffrey, C. S.; Tennakoon, M. A.; Wang, J.; Zhao, H., Relay ring-closing metathesis (RRCM): A strategy for directing metal movement throughout olefin metathesis sequences. *J. Am. Chem. Soc.* 2004, *126*, 10210–10211.
(24). Wallace, D. J., Relay ring-closing metathesis — a strategy for achieving reactivity and selectivity in metathesis chemistry. *Angew. Chem. Int. Ed.* 2005, *44*, 1912–1915.
(25). Vora, H. U.; Rovis, T., Nucleophilic carbene and hoat relay catalysis in an amide bond coupling: An orthogonal peptide bond forming reaction. *J. Am. Chem. Soc.* 2007, *129*, 13796–13797.
(26). Hoye, T. R.; Jeon, J.; Kopel, L. C.; Ryba, T. D.; Tennakoon, M. A.; Wang, Y., Total synthesis of peloruside a through kinetic lactonization and relay ring-closing metathesis cyclization reactions. *Angew. Chem. Int. Ed.* 2010, *49*, 6151–6155.
(27). Dong, G.; Teo, P.; Wickens, Z. K.; Grubbs, R. H., Primary alcohols from terminal olefins: Formal anti-markovnikov hydration *via* triple relay catalysis. *Science* 2011, *333*, 1609–1612.
(28). Nicolaou, K. C.; Edmonds, D. J.; Bulger, P. G., Cascade reactions in total synthesis. *Angew. Chem. Int. Ed.* 2006, *45*, 7134–7186.
(29). Li, C.-J., Cross-dehydrogenative coupling (CDC): Exploring C−C bond formations beyond functional group transformations. *Acc. Chem. Res.* 2009, *42*, 335-344.
(30). Grondal, C.; Jeanty, M.; Enders, D., Organocatalytic cascade reactions as a new tool in total synthesis. *Nat. Chem.* 2010, *2*, 167.
(31). Chen, N.; Dai, X.-J.; Wang, H.; Li, C.-J., *Umpolung* addition of aldehydes to aryl imines. *Angew. Chem. Int. Ed.* 2017, *56*, 6260–6263.
(32). Dai, X.-J.; Wang, H.; Li, C.-J., Carbonyls as latent alkyl carbanions for conjugate additions. *Angew. Chem. Int. Ed.* 2017, *56*, 6302–6306.
(33). Wang, H.; Dai, X.-J.; Li, C.-J., Aldehydes as alkyl carbanion equivalents for additions to carbonyl compounds. *Nat. Chem.* 2017, *9*, 374-378.
(34). Wei, W.; Dai, X.-J.; Wang, H.; Li, C.; Yang, X.; Li, C.-J., Ruthenium(II)-catalyzed olefination *via* carbonyl reductive cross-coupling. *Chem. Sci.* 2017, *8*, 8193–8197.
(35). Lv, L.; Qiu, Z.; Li, J.; Liu, M.; Li, C.-J., N_2H_4 as traceless mediator for homo- and cross-aryl coupling. *Nat. Commun*, 2018, *9*, 4739.
(36). Lv, L.; Zhu, D.; Tang, J.; Qiu, Z.; Li, C.-C.; Gao, J.; Li, C.-J., Cross-coupling of phenol derivatives with *umpolung* aldehydes catalyzed by nickel. *ACS Catal.* 2018, *8*, 4622–4627.
(37). Tang, J.; Lv, L.; Dai, X.-J.; Li, C.-C.; Li, L.; Li, C.-J., Nickel-catalyzed cross-coupling of aldehydes with aryl halides *via* hydrazone intermediates. *Chem. Commun.* 2018, *54*, 1750–1753.
(38). Zhu, D.; Lv, L.; Li, C.-C.; Ung, S.; Gao, J.; Li, C.-J., *Umpolung* of carbonyl groups as alkyl organometallic reagent surrogates for palladium-catalyzed allylic alkylation. *Angew. Chem. Int. Ed.* 2018, *57*, 16520–16524.

(39). Lv, L.; Zhu, D.; Li, C.-J., Direct dehydrogenative alkyl heck-couplings of vinylarenes with *umpolung* aldehydes catalyzed by nickel. *Nat. Commun,* 2019, *10*, 715.
(40). Zhu, C.; Zhang, J., Nickel-catalyzed alkyl–alkyl cross-coupling reactions of non-activated secondary alkyl bromides with aldehydes as alkyl carbanion equivalents. *Chem. Commun.* 2019, *55*, 2793–2796.
(41). Bruneau, C.; Dixneuf, P. H., *Ruthenium Catalysts and Fine Chemistry*. Springer: Berlin, 2004; Vol. 11.
(42). Allard, J.; Curbet, I.; Chollet, G.; Tripoteau, F.; Sambou, S.; Caijo, F.; Raoul, Y.; Crévisy, C.; Baslé, O.; Mauduit, M., Bleaching earths as powerful additives for Ru-catalyzed self-metathesis of non-refined methyl oleate at pilot scale. *Chem. Eur. J.* 2017, *23*, 12729–12734.
(43). Dumas, A.; Tarrieu, R.; Vives, T.; Roisnel, T.; Dorcet, V.; Baslé, O.; Mauduit, M., A versatile and highly *Z*-selective olefin metathesis ruthenium catalyst based on a readily accessible n-heterocyclic carbene. *ACS Catal.* 2018, *8*, 3257-3262.
(44). Sasson, Y.; Rempel, G. L., Homogeneous rearrangement of unsaturated carbinols to saturated ketones catalyzed by ruthenium complexes. *Tetrahedron Lett.* 1974, *15*, 4133–4136.
(45). Seijiro, M.; Takashi, O.; Koichiro, O.; Kazuhiko, T.; Hitosi, N., Isomerization of allylic alcohols catalyzed by vanadium or molybdenum complexes. *Bull. Chem. Soc. Jpn.* 1985, *58*, 844–849.
(46). Trost, B. M.; Kulawiec, R. J., Chemoselectivity in the ruthenium-catalyzed redox isomerization of allyl alcohols. *J. Am. Chem. Soc.* 1993, *115*, 2027–2036.
(47). Trost, B. M.; Livingston, R. C., Two-metal catalyst system for redox isomerization of propargyl alcohols to enals and enones. *J. Am. Chem. Soc.* 1995, *117*, 9586–9587.
(48). Crochet, P.; Fernández-Zúmel, M. A.; Gimeno, J.; Scheele, M., Efficient redox isomerization of allylic alcohols under mild conditions catalyzed by arene−ruthenium(ii) complexes. *Organometallics* 2006, *25*, 4846–4849.
(49). Goetz, R. W.; Orchin, M., The isomerization of allyl alcohols with cobalt hydrocarbonyl. *J. Am. Chem. Soc.* 1963, *85*, 1549–1550.
(50). Mao, L.-L.; Li, C.-C.; Yang, Q.; Cheng, M.-X.; Yang, S.-D., One-pot synthesis of *α*-aminophosphonates *via* a cascade sequence of allylamine isomerization/hydrophosphonylation. *Chem. Commun.* 2017, *53*, 4473–4476.
(51). Sorimachi, K.; Terada, M., Relay catalysis by a metal-complex/brønsted acid binary system in a tandem isomerization/carbon−carbon bond forming sequence. *J. Am. Chem. Soc.* 2008, *130*, 14452–14453.
(52). Scheuermann, M. L.; Johnson, E. J.; Chirik, P. J., Alkene isomerization–hydroboration promoted by phosphine-ligated cobalt catalysts. *Org. Lett.* 2015, *17*, 2716–2719.
(53). Vasseur, A.; Bruffaerts, J.; Marek, I., Remote functionalization through alkene isomerization. *Nat. Chem.* 2016, *8*, 209.

(54). Uma, R.; Davies, M.; Crévisy, C.; Grée, R., A tandem allylic alcohol isomerization–aldol condensation catalyzed by Rh and Ru complexes. *Tetrahedron Lett.* 2001, *42*, 3069-3072.
(55). Zhang, S.-Y.; Zhang, F.-M.; Tu, Y.-Q., Direct sp^3 α-C–H activation and functionalization of alcohol and ether. *Chem. Soc. Rev.* 2011, *40*, 1937–1949.
(56). Allen, J. R.; Bahamonde, A.; Furukawa, Y.; Sigman, M. S., Enantioselective *N*-alkylation of indoles *via* an intermolecular aza-Wacker-type reaction. *J. Am. Chem. Soc.* 2019, *141*, 8670–8674.
(57). Sommer, H.; Juliá-Hernández, F.; Martin, R.; Marek, I., Walking metals for remote functionalization. *ACS Cent. Sci.* 2018, *4*, 153–165.
(58). Sun, S.-Z.; Börjesson, M.; Martin-Montero, R.; Martin, R., Site-selective Ni-catalyzed reductive coupling of α-haloboranes with unactivated olefins. *J. Am. Chem. Soc.* 2018, *140*, 12765–12769.
(59). Juliá-Hernández, F.; Moragas, T.; Cornella, J.; Martin, R., Remote carboxylation of halogenated aliphatic hydrocarbons with carbon dioxide. *Nature* 2017, *545*, 84.
(60). Bäckvall, J.-E.; Andreasson, U., Ruthenium-catalyzed isomerization of allylic alcohols to saturated ketones. *Tetrahedron Lett.* 1993, *34*, 5459–5462.
(61). Wang, D.; Chen, D.; Haberman, J. X.; Li, C.-J., Ruthenium-catalyzed isomerization of homoallylic alcohols in water. *Tetrahedron* 1998, *54*, 5129–5142.
(62). Finnegan, D.; Seigal, B. A.; Snapper, M. L., Preparation of aliphatic ketones through a ruthenium-catalyzed tandem cross-metathesis/allylic alcohol isomerization. *Org. Lett.* 2006, *8*, 2603–2606.
(63). Cadierno, V.; Francos, J.; Gimeno, J.; Nebra, N., Ruthenium-catalyzed reduction of allylic alcohols: An efficient isomerization/transfer hydrogenation tandem process. *Chem. Commun.* 2007, 2536–2538.
(64). Cadierno, V.; Crochet, P.; Francos, J.; García-Garrido, S. E.; Gimeno, J.; Nebra, N., Ruthenium-catalyzed redox isomerization/transfer hydrogenation in organic and aqueous media: A one-pot tandem process for the reduction of allylic alcohols. *Green Chem.* 2009, *11*, 1992–2000.
(65). Bizet, V.; Pannecoucke, X.; Renaud, J.-L.; Cahard, D., Ruthenium-catalyzed redox isomerization of trifluoromethylated allylic alcohols: Mechanistic evidence for an enantiospecific pathway. *Angew. Chem. Int. Ed.* 2012, *51*, 6467–6470.
(66). Lorenzo-Luis, P.; Romerosa, A.; Serrano-Ruiz, M., Catalytic isomerization of allylic alcohols in water. *ACS Catal.* 2012, *2*, 1079–1086.
(67). Trost, B. M.; Fraisse, P. L.; Ball, Z. T., A stereospecific ruthenium-catalyzed allylic alkylation. *Angew. Chem. Int. Ed.* 2002, *41*, 1059–1061.
(68). Kayaki, Y.; Koda, T.; Ikariya, T., Halide-free dehydrative allylation using allylic alcohols promoted by a palladium−triphenyl phosphite catalyst. *J. Org. Chem.* 2004, *69*, 2595–2597.

(69). Kinoshita, H.; Shinokubo, H.; Oshima, K., Water enables direct use of allyl alcohol for tsuji−trost reaction without activators. *Org. Lett.* 2004, *6*, 4085–4088.
(70). Usui, I.; Schmidt, S.; Breit, B., Dual palladium- and proline-catalyzed allylic alkylation of enolizable ketones and aldehydes with allylic alcohols. *Org. Lett.* 2009, *11*, 1453–1456.
(71). Hamilton, J. Y.; Hauser, N.; Sarlah, D.; Carreira, E. M., Iridium-catalyzed enantioselective allyl–allylsilane cross-coupling. *Angew. Chem. Int. Ed.* 2014, *53*, 10759–10762.
(72). Krautwald, S.; Schafroth, M. A.; Sarlah, D.; Carreira, E. M., Stereodivergent *α*-allylation of linear aldehydes with dual iridium and amine catalysis. *J. Am. Chem. Soc.* 2014, *136*, 3020-3023.
(73). Sandmeier, T.; Krautwald, S.; Zipfel, H. F.; Carreira, E. M., Stereodivergent dual catalytic *α*-allylation of protected *α*-amino- and *α*-hydroxyacetaldehydes. *Angew. Chem. Int. Ed.* 2015, *54*, 14363–14367.
(74). Rössler, S. L.; Krautwald, S.; Carreira, E. M., Study of intermediates in iridium–(phosphoramidite,olefin)-catalyzed enantioselective allylic substitution. *J. Am. Chem. Soc.* 2017, *139*, 3603-3606.
(75). Rössler, S. L.; Petrone, D. A.; Carreira, E. M., Iridium-catalyzed asymmetric synthesis of functionally rich molecules enabled by (phosphoramidite,olefin) ligands. *Acc. Chem. Res.* 2019.
(76). Li, C.-C.; Dai, X.-J.; Wang, H.; Zhu, D.; Gao, J.; Li, C.-J., Iron-catalyzed nucleophilic addition reaction of organic carbanion equivalents *via* hydrazones. *Org. Lett.* 2018, *20*, 3801-3805.
(77). Dai, X.-J.; Li, C.-J., En route to a practical primary alcohol deoxygenation. *J. Am. Chem. Soc.* 2016, *138*, 5433–5440.
(78). Hartwig, J. F.; Collman, J. P., *Organotransition Metal Chemistry: From Bonding to Catalysis*. University Science Books: Sausalito, 2010; Vol. 1.
(79). Jung, C. W.; Garrou, P. E.; Hoffman, P. R.; Caulton, K. G., Reexamination of the reactions of $Ph_2P(CH_2)_nPPh_2$ (n = 1–4) with $RuCl_2(PPh_3)_3$. *Inorg. Chem.* 1984, *23*, 726–729.
(80). Baratta, W.; Herdtweck, E.; Siega, K.; Toniutti, M.; Rigo, P., 2-(aminomethyl)pyridine−phosphine ruthenium(II) complexes: Novel highly active transfer hydrogenation catalysts. *Organometallics* 2005, *24*, 1660–1669.
(81). Kishner, N., Wolff–kishner reduction; huang–minlon modification. *J. Russ. Phys. Chem. Soc.* 1911, *43*, 582–595.
(82). Wolff, L., Chemischen institut der universität jena: Methode zum ersatz des sauerstoffatoms der ketone und aldehyde durch wasserstoff. *Justus Liebigs Annal. Chem.* 1912, *394*, 86–108.
(83). Wolff, L., Chemischen institut der universität jena: Methode zum ersatz des sauerstoffatoms der ketone und aldehyde durch wasserstoff. *Eur. J. Org. Chem.* 1912, *394*, 86–108.

(84). Herr, C. H.; Whitmore, F. C.; Schiessler, R. W., The Wolff–Kishner reaction at atmospheric pressure. *J. Am. Chem. Soc.* 1945, *67*, 2061–2063.
(85). Wharton, P.; Bohlen, D., Communications — hydrazine reduction of *α, β*-epoxy ketones to allylic alcohols. *J. Org. Chem.* 1961, *26*, 3615-3616.
(86). Caglioti, L.; Magi, M., The reaction of tosylhydrazones with lithium aluminium hydride. *Tetrahedron* 1963, *19*, 1127–1131.
(87). Szmant, H. H.; Harmuth, C. M., The Wolff–Kishner reaction of hydrazones. *J. Am. Chem. Soc.* 1964, *86*, 2909–2914.
(88). Dierkes, P.; W. N. M. van Leeuwen, P., The bite angle makes the difference: A practical ligand parameter for diphosphine ligands. *J. Chem. Soc., Dalton Trans.* 1999, 1519–1530.
(89). McGrath, D. V.; Grubbs, R. H., The mechanism of aqueous ruthenium(II)-catalyzed olefin isomerization. *Organometallics* 1994, *13*, 224–235.
(90). Davies, S. G., *Organotransition Metal Chemistry: Applications to Organic Synthesis: Applications to Organic Synthesis*. Elsevier: Exeter, 2013; Vol. 2.
(91). Matoba, K.; Eizawa, A.; Nishimura, S.; Arashiba, K.; Nakajima, K.; Nishibayashi, Y., Practical synthesis of a PCP–type pincer ligand and its metal complexes-. *Synthesis* 2018, *50*, 1015–1019.
(92). Grünenfelder, C. E.; Kisunzu, J. K.; Wennemers, H., Peptide-catalyzed stereoselective conjugate addition reactions of aldehydes to maleimide. *Angew. Chem. Int. Ed.* 2016, *55*, 8571–8574.
(93). Grassi, D.; Alexakis, A., Improvements and applications of the transition metal-free asymmetric allylic alkylation using grignard reagents and magnesium alanates. *Adv. Synth. Catal.* 2015, *357*, 3171-3186.
(94). Luo, S.; Zhang, N.; Wang, Z.; Yan, H., Enantioselective addition of selenosulfonates to *α,β*-unsaturated ketones. *Org. Biomol. Chem.* 2018, *16*, 2893–2901.
(95). Li, C.-C.; Kan, J.; Qiu, Z.; Li, J.; Lv, L.; Li, C.-J., Synergistic relay reactions to achieve redox-neutral *α*-alkylations of olefinic alcohols with ruthenium(II) catalysis. *Angew. Chem. Int. Ed.* 2020, *59*, 4544–4549.
(96). Dobereiner, G. E.; Crabtree, R. H., Dehydrogenation as a substrate-activating strategy in homogeneous transition-metal catalysis. *Chem. Rev.* 2010, *110*, 681–703.
(97). Friedrich, A.; Schneider, S., Acceptorless dehydrogenation of alcohols: Perspectives for synthesis and H_2 storage. 2009, *1*, 72–73.
(98). Musa, S.; Shaposhnikov, I.; Cohen, S.; Gelman, D., Ligand–metal cooperation in pcp pincer complexes: Rational design and catalytic activity in acceptorless dehydrogenation of alcohols. *Angew. Chem. Int. Ed.* 2011, *50*, 3533-3537.

(99). Nielsen, M.; Kammer, A.; Cozzula, D.; Junge, H.; Gladiali, S.; Beller, M., Efficient hydrogen production from alcohols under mild reaction conditions. *Angew. Chem. Int. Ed.* 2011, *50*, 9593–9597.
(100). Kawahara, R.; Fujita, K.-i.; Yamaguchi, R., Dehydrogenative oxidation of alcohols in aqueous media using water-soluble and reusable Cp*Ir catalysts bearing a functional bipyridine ligand. *J. Am. Chem. Soc.* 2012, *134*, 3643-3646.
(101). Muthaiah, S.; Hong, S. H., Acceptorless and base-free dehydrogenation of alcohols and amines using ruthenium–hydride complexes. *Adv. Synth. Catal.* 2012, *354*, 3045-3053.
(102). Pandey, P.; Dutta, I.; Bera, J. K., Acceptorless alcohol dehydrogenation: A mechanistic perspective. *Proc. Natl. Acad. Sci., India, Sect. A Phys. Sci.* 2016, *86*, 561–579.
(103). Chang, W.; Gong, X.; Wang, S.; Xiao, L.-P.; Song, G., Acceptorless dehydrogenation and dehydrogenative coupling of alcohols catalysed by protic nhc ruthenium complexes. *Org. Biomol. Chem.* 2017, *15*, 3466-3471.
(104). Garbe, M.; Junge, K.; Beller, M., Homogeneous catalysis by manganese-based pincer complexes. *Eur. J. Org. Chem.* 2017, *2017*, 4344–4362.
(105). Sandoval, C. A.; Ohkuma, T.; Muñiz, K.; Noyori, R., Mechanism of asymmetric hydrogenation of ketones catalyzed by binap/1,2-diamine−ruthenium(II) complexes. *J. Am. Chem. Soc.* 2003, *125*, 13490–13503.
(106). Askevold, B.; Khusniyarov, M. M.; Herdtweck, E.; Meyer, K.; Schneider, S., A square-planar ruthenium(II) complex with a low-spin configuration. *Angew. Chem. Int. Ed.* 2010, *49*, 7566–7569.
(107). Friedrich, A.; Drees, M.; Käss, M.; Herdtweck, E.; Schneider, S., Ruthenium complexes with cooperative PNP-pincer amine, amido, imine, and enamido ligands: Facile ligand backbone functionalization processes. *Inorg. Chem.* 2010, *49*, 5482–5494.
(108). Rozenel, S. S.; Arnold, J., Bimetallic ruthenium–PNP pincer complex as a platform to model proposed intermediates in dinitrogen reduction to ammonia. *Inorg. Chem.* 2012, *51*, 9730–9739.
(109). Fillman, K. L.; Bielinski, E. A.; Schmeier, T. J.; Nesvet, J. C.; Woodruff, T. M.; Pan, C. J.; Takase, M. K.; Hazari, N.; Neidig, M. L., Flexible binding of PNP pincer ligands to monomeric iron complexes. *Inorg. Chem.* 2014, *53*, 6066–6072.
(110). Yan, S.-S.; Zhu, L.; Ye, J.-H.; Zhang, Z.; Huang, H.; Zeng, H.; Li, C.-J.; Lan, Y.; Yu, D.-G., Ruthenium-catalyzed *umpolung* carboxylation of hydrazones with CO_2. *Chem. Sci.* 2018, *9*, 4873–4878.
(111). Garbe, M.; Junge, K.; Walker, S.; Wei, Z.; Jiao, H.; Spannenberg, A.; Bachmann, S.; Scalone, M.; Beller, M., Manganese(I)-catalyzed enantioselective hydrogenation of ketones using a defined chiral pnp pincer ligand. *Angew. Chem. Int. Ed.* 2017, *56*, 11237–11241.

(112). Das, U. K.; Chakraborty, S.; Diskin-Posner, Y.; Milstein, D., Direct conversion of alcohols into alkenes by dehydrogenative coupling with hydrazine/hydrazone catalyzed by manganese. *Angew. Chem. Int. Ed.* 2018, *57*, 13444–13448.
(113). Abdur-Rashid, K.; Graham, T.; Tsang, C.-W.; Chen, X.; Guo, R.; Jia, W.; Amoroso, D.; Sui-Seng, C. Method for the production of hydrogen from ammonia borane. U.S. Patent No. 8,518,368. 2013.
(114). M. J. Frisch, G. W. Trucks, H. B. Schlegel, G. E. Scuseria, M. A. Robb, J. R. Cheeseman, G. Scalmani, V. Barone, G. A. Petersson, H. Nakatsuji, X. Li, M. Caricato, A. V. Marenich, J. Bloino, B. G. Janesko, R. Gomperts, B. Mennucci, H. P. Hratchian, J. V. Ortiz, A. F. Izmaylov, J. L. Sonnenberg, D. Williams-Young, F. Ding, F. Lipparini, F. Egidi, J. Goings, B. Peng, A. Petrone, T. Henderson, D. Ranasinghe, V. G. Zakrzewski, J. Gao, N. Rega, G. Zheng, W. Liang, M. Hada, M. Ehara, K. Toyota, R. Fukuda, J. Hasegawa, M. Ishida, T. Nakajima, Y. Honda, O. Kitao, H. Nakai, T. Vreven, K. Throssell, J. A. Montgomery, Jr., J. E. Peralta, F. Ogliaro, M. J. Bearpark, J. J. Heyd, E. N. Brothers, K. N. Kudin, V. N. Staroverov, T. A. Keith, R. Kobayashi, J. Normand, K. Raghavachari, A. P. Rendell, J. C. Burant, S. S. Iyengar, J. Tomasi, M. Cossi, J. M. Millam, M. Klene, C. Adamo, R. Cammi, J. W. Ochterski, R. L. Martin, K. Morokuma, O. Farkas, J. B. Foresman, and D. J. Fox, Gaussian, Inc., Wallingford CT, 2016.

Chapter 5. Switching Chemoselectivity in the Interaction of Hydrazones and Carbonyls

5.1 Introduction

While we have discussed numerous advantages of hydrazones as carbanion equivalents to react with carbonyls over classic organometallic reagents, there remains a prominent challenge in this transformation. The C–C bond formation of hydrazone with carbonyl, as we previously studied, plausibly experiences a Zimmerman–Traxler type six-membered ring transition state.[1] After the C–C bond formation, the reaction can go through two alternative pathways: 1) The azo intermediate decomposes and the so-formed carbanion is directly protonated to give 1,2-addition product like the Grignard reaction; 2) The azo intermediate decomposes and the so-formed carbanion undergoes a E1cB elimination to generate C=C double bond like the Wittig reaction.[2] However, based on our initial studies, the selectivity between 1,2-addition and olefination mostly depends on the substrate that we chose. For instance, aromatic aldehyde hydrazones favor 1,2-addition product and the aliphatic ones favor olefination product.[1, 3]

However, in synthetic chemistry, both 1,2-addition and olefination reactions are widely used C–C bond formation methodologies. In many cases, the selectivity of either 1,2-addition or olefination in the C–C bond formation of hydrazone with carbonyls is highly desirable. Thus, we made our efforts to realize and control both selectivities above for the hydrazone addition to carbonyls.

5.2 Results and discussions

5.2.1 In-depth understanding the selectivity

Our initial research was focused on the analysis of the selectivity in our previous studies.[1, 3] By reviewing the substrate scope of 1,2-addition and olefination, we discovered that the most significant difference in selectivity is reflected in the different hydrazone substrates (Scheme 5.1) where aromatic aldehyde hydrazones always favor 1,2-addition product, while aliphatic aldehyde hydrazones favor olefination product.

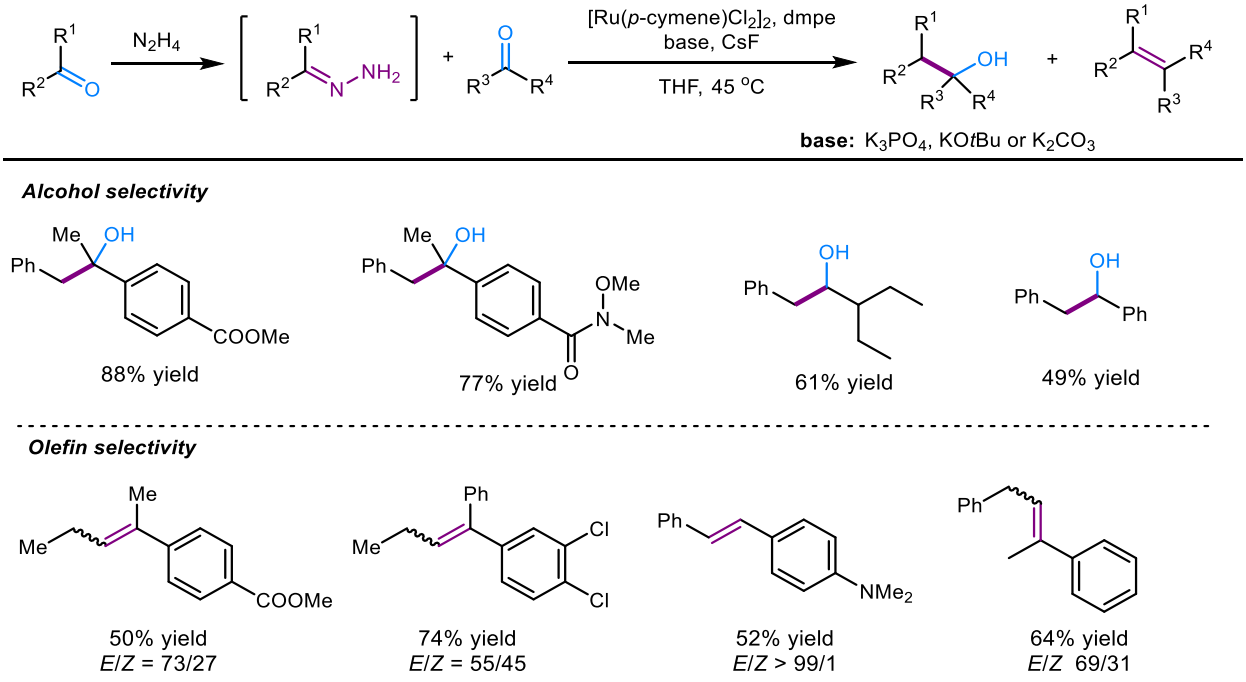

Scheme 5.1 Chemoselectivity in C–C bond formation of hydrazone and carbonyls in Ru–bisphosphine system

Besides the hydrazone substrate, we also found that the choice of electrophiles would, though at a lower level, influence the selectivity. For instance, 1) with the aromatic aldehyde hydrazone, we found that the 1,2-addition to aldehyde and diaryl ketones has a poorer selectivity than to aliphatic or mono-aromatic ketones (with the latter one, 1,2-addition was close to 100% selectivity). 2) Among the aldehydes, the 1,2-addition selectivity to aliphatic aldehydes is higher than the aromatic one. From these observations, we concluded that nucleophiles with conjugated systems favor 1,2-addition reaction while electrophiles with conjugated systems favor olefination reactions.

To gain more insight on this trend, we also conducted some control experiments based on our later-developed alcohol-surrogated Grignard reactions.[4] As is shown in Scheme 5.2, when benzaldehyde hydrazone was chosen as the nucleophile, we found a 73: 22 ratio of 1,2-addition and olefination product with aliphatic alcohols (aliphatic aldehyde surrogate) (**Eq 1**) and a 66: 34 ratio with benzyl alcohols (aromatic aldehyde surrogate) (**Eq 2**). When the benzyl alcohol was chosen as electrophile, the reaction with aliphatic hydrazone yielded a 7:33 ratio of 1,2-addition and olefination (**Eq 3**) which is much lower than the one with benzaldehyde hydrazone (66:34) (**Eq 2**). In addition, we noticed that the conversion of aliphatic aldehyde hydrazone reaction with carbonyl

was much lower than the aromatic one. These control experiments further confirmed the trend of chemoselectivity that we initially proposed and also suggest that such a trend would not be influenced even in cascade reactions.

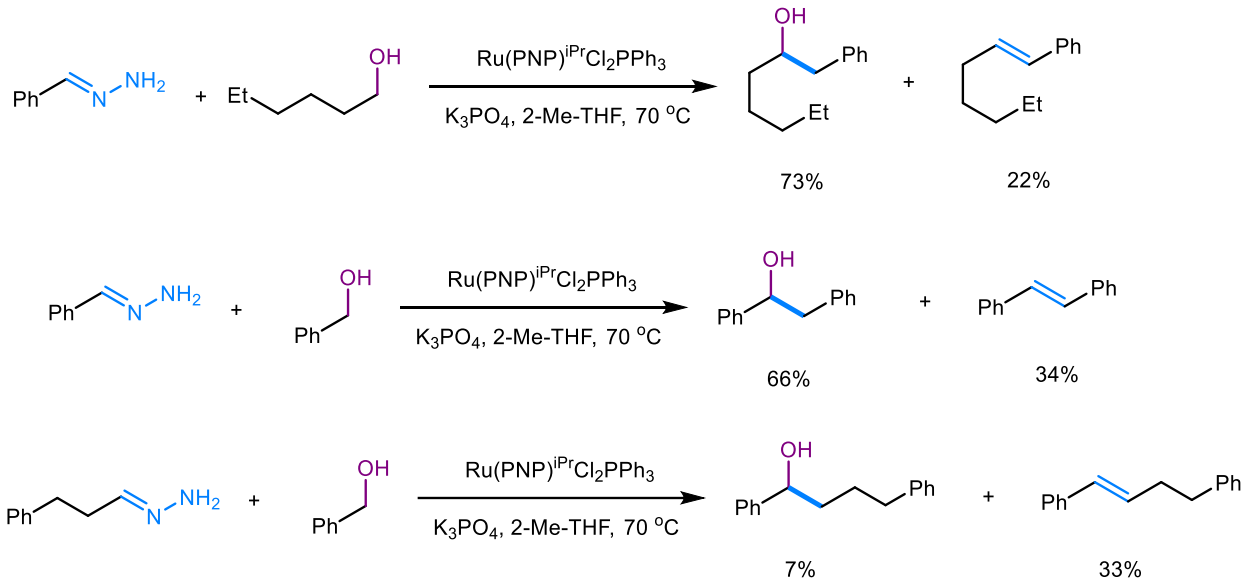

Scheme 5.2 Control experiment for chemoselectivity in alcohol surrogated Grignard reaction

5.2.2 Analysis from proposed mechanism

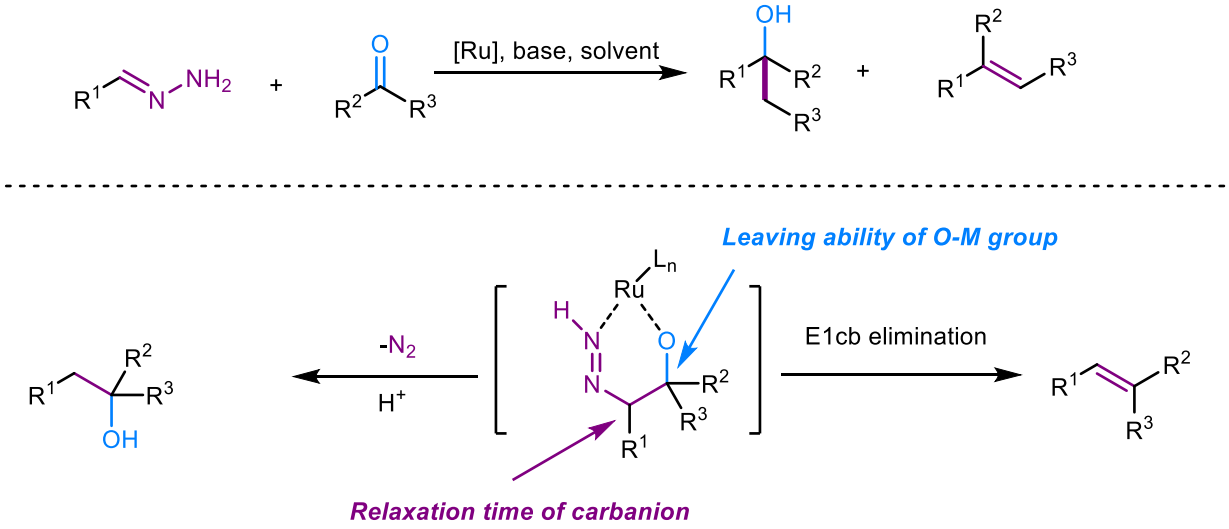

Scheme 5.3 Mechanistic explanation for the chemoselectivity

We then turned to analyze the selectivity from the mechanistic aspect. As shown in Scheme 5.3, after the decomposition of azo to give a carbanion intermediate, the direct protonation gives a 1,2-addition product while the E1cB elimination process gives an olefin product. To analyze these two processes from the basic knowledge of organic transformations,[5] we proposed two factors that might affect the selectivity: 1) A longer lifetime of the carbanion intermediate after the decomposition of azo would favor an intermolecular protonation process, while a shorter lifetime would favor intramolecular E1cB elimination; 2) O–M group with a better leaving ability would favor E1cB process, while the one with a lower leaving ability would favor protonation.[5] This explanation also corresponds to our experimental results: carbanion intermediates generated from hydrazones bearing a conjugated system is stabilized, which guarantees longer lifetime of carbanion itself to abstract a proton. Carbanions from aliphatic aldehyde hydrazones are non-stabilized, which would favor intramolecular E1cB elimination. Moreover, from the aspect of electrophiles, aromatic substituents would make the leaving of O–M much easier, which would favor E1cB elimination and lead to an improved olefination selectivity.

5.2.3 Switching selectivity by modifying metal catalyst

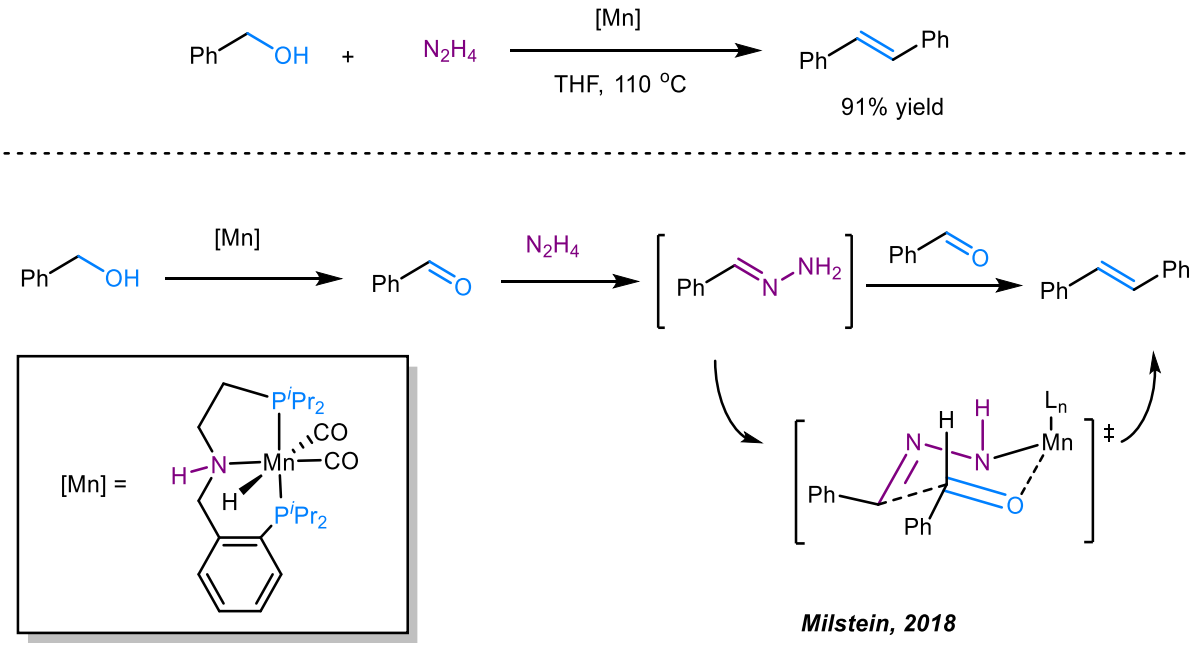

Scheme 5.4 Direct transformation from alcohols to alkenes under Mn-catalysis *via* hydrazone intermediate

With the mechanistic analysis in hand, we considered the possibility to switch the selectivity of hydrazone reaction with carbonyls. In 2018, Milstein *et al.* developed a direct conversion of primary alcohols to alkenes with hydrazine (Scheme 5.4).[6] This transformation first undergoes a hydrogen transfer by manganese catalysts to generate the aldehyde from the alcohol. Then, the so formed aldehyde partially condenses with the hydrazine to give a hydrazone intermediate. Finally, the hydrazone reacts with the remaining aldehyde to undergo C–C bond formation and results in an alkene product at the end. According to their mechanistic study, the C–C bond formation of hydrazone and carbonyl experiences a similar Zimmerman–Traxler transition state. However, we noticed that with the benzyl alcohol as the substrate (equivalent to benzaldehyde hydrazone to react with benzaldehyde), the yield of olefination product was 91%. Although they did not show the yield of corresponding 1,2-addition product (alcohol product), the 91% yield for olefination indicates a greater than 10: 1 selectivity between olefination and 1,2-addition, in contrast to the 1:2 ratio in the ruthenium–bisphosphine system (Scheme 5.2). Such a significant difference of selectivity under Mn catalysis is possibly due to two reasons: 1) As manganese is a comparatively stronger Lewis acid, it usually bears a stronger coordination with oxygen atoms. In addition, the carbonyl ligand on manganese complex would decrease its electron density and increase the Lewis acidity of the catalyst. These all make Mn–O a better leaving group,[7] which largely benefits the E1cB elimination and results in selectivity of alkene. 2) The higher temperature of this manganese catalytic system (110 ^{o}C) compared with the ruthenium one (70 ^{o}C) would thermodynamically favor the E1cB elimination due to an entropy-increasing process.[5]

Inspired by the success of switching selectivity from 1,2-addition to olefination by Milstein's group, we further thought about whether it is also possible to realize the switching selectivity from olefination to 1,2-addition. As in our initially developed Grignard-type reaction with hydrazone, the only effective substates are aromatic aldehyde hydrazones and for aliphatic ones, olefination is a favorable pathway. However, in general, aliphatic Grignard reagents are more widely used ones.[8] Thus, to better enable hydrazone as an equivalent Grignard reagent, an efficient 1,2-addition selectivity of aliphatic aldehyde to react with carbonyls is highly desirable. With this regard, we considered to adapt our original ruthenium catalysts to realize this switching selectivity. In our initial study, we discovered that the C–C bond formation of hydrazone with carbonyl is favored by using electron-rich bis-phosphine ligands such as dmpe, aiming to increase the nucleophilicity of hydrazone intermediate.[1] Based on these, we hypothesized that ruthenium catalysts with an

electron-richer ligand might enhance 1,2-addition selectivity of aliphatic aldehyde hydrazone to carbonyl compounds due to two reasons: 1) the electron-richer ruthenium catalyst would have a weaker Lewis acidity and poorer coordination with alkyl oxide groups, which will disfavor the E1cB elimination process; 2) the higher electron density of the catalyst could lead to higher reactivity, which potentially enables the reaction to be conducted under lower temperature to disfavor elimination.

Table 5.1 Exploration of ligands for Grignard-type reaction with aliphatic aldehyde hydrazone

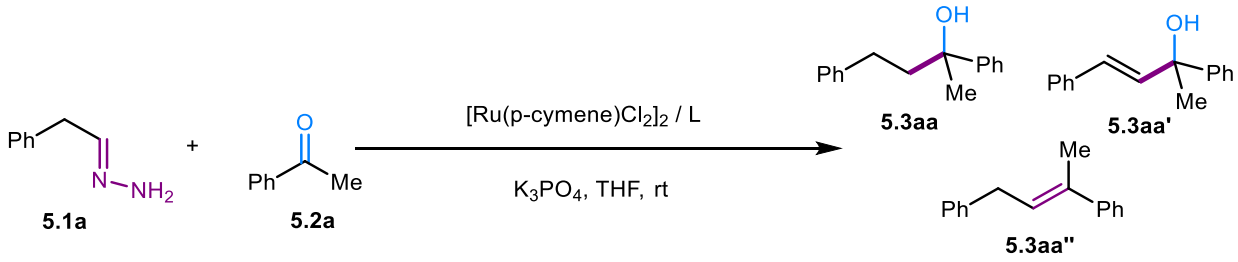

entry	L	5.3aa (%)	5.3aa' (%)	5.3aa'' (%)
1	**PCP**	63	21	0
2	IMes	trace	0	0
3	SIMes	trace	0	0
4	dmpe	0	0	trace

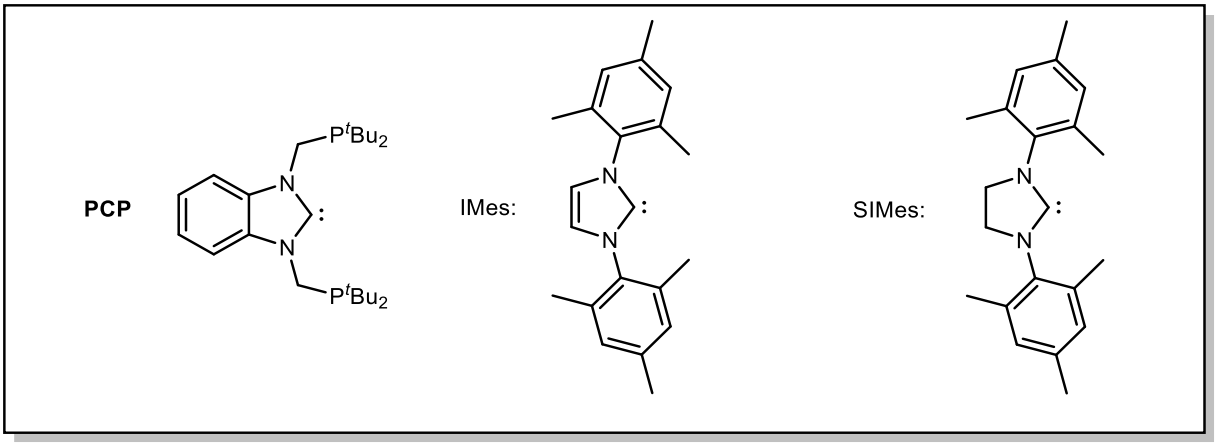

Reaction conditions: [Ru(*p*-cymene)Cl_2]$_2$ (0.003 mmol), **L** (0.006 mmol), **5.1a** (0.25 mmol) and **5.2a** (0.2 mmol), K_3PO_4 (0.2 mmol), THF (0.2 mL) under N_2 atmosphere at room temperature. ^{1}H NMR yield was determined using 1,3,5-trimethoxybenzene as an internal standard.

Table 5.2 Exploration of base for Grignard-type reaction with aliphatic aldehyde hydrazone

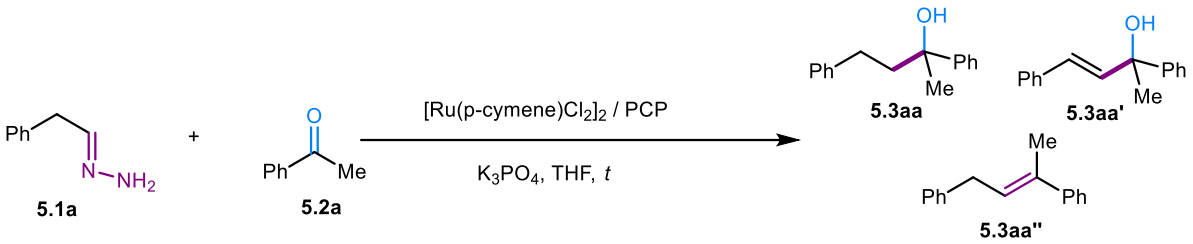

entry	base	5.3aa (%)	5.3aa' (%)	5.3aa'' (%)
1	K_3PO_4	63	21	trace
2*	K_3PO_4	32	12	0
3	K_2CO_3	0	0	0
4	K^{t}BuO	30	16	trace
5	Cs_2CO_3	53	22	trace

Reaction conditions: [Ru(*p*-cymene)Cl_2]$_2$ (0.003 mmol), **PCP** (0.006 mmol), **5.1a** (0.25 mmol) and **5.2a** (0.2 mmol), base (0.2 mmol), THF (0.2 mL) under N_2 atmosphere at room temperature. ^{1}H NMR yield was determined using 1,3,5-trimethoxybenzene as an internal standard. *0.1 mmol K_3PO_4 was used.

NHC (*N*-heterocyclic carbene), being a very good σ-donor and π-donor, is a widely used electron-rich ligand in metal complex which has an even higher electron density than aliphatic phosphine ligands.[7] On top of this, in our study of Pd-catalyzed allylation reaction with hydrazone as discussed in Chapter 2, NHC ligand significantly increased the efficiency of allylation with aliphatic aldehyde hydrazone (which is comparatively unreactive under Pd–phosphine system).[9] Thus, we considered whether NHC ligand could also increase the efficiency and selectivity of aliphatic aldehyde hydrazone in Grignard-type reaction. We initiated our exploration by screening different kinds of NHC ligands (Table 5.1, entry 1–3), and compared them with bisphosphine ligand (Table 5.1, entry 4). We found that phenyl acetaldehyde hydrazone was unreactive at room temperature with common monodentate NHC ligands such as IMes (Table 5.1, entry 2) and SIMes (Table 5.1, entry 3) or bisphosphine ligand (Table 5.1, entry 4). We delightfully discovered that with a special PCP pincer-type ligand (ligand with two phosphine groups on the arm and NHC at the center), the 1,2-addition proceeded efficiently at room temperature with a moderate yield (63%)

(Table 5.1, entry 1). No olefination product was observed under this Ru–PCP catalytic system, which means that the selectivity of 1,2-addition over olefination with aliphatic aldehyde hydrazone was successfully achieved. It is important to note, however, with such a Ru–PCP system, we observed a significant amount of Shapiro-type 1,2-addition product[10] , where hydrazone serves as a vinyl carbanion equivalent instead of alkyl carbanion equivalent. This is possibly due to the unforeseeable *β*-hydride elimination by Ru–PCP catalyst after the C–C bond formation.

Table 5.3 Exploration of reaction temperature

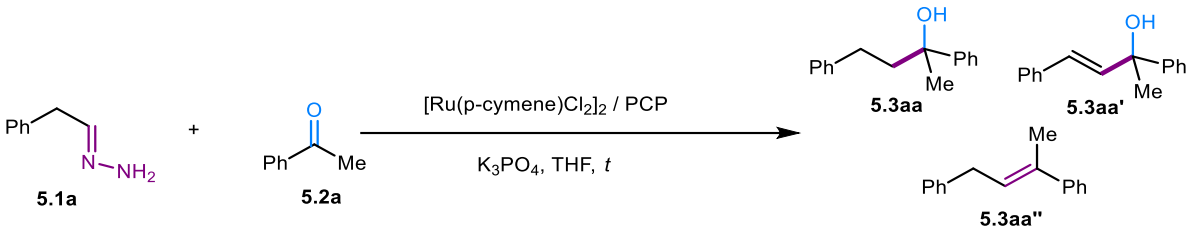

entry	*t* (°C)	5.3aa (%)	5.3aa' (%)	5.3aa'' (%)
1	22	63	21	trace
2	4	30	20	trace
3	40	30	11	8

Reaction conditions: [Ru(*p*-cymene)Cl_2]$_2$ (0.003 mmol), **PCP** (0.006 mmol), **5.1a** (0.25 mmol) and **5.2a** (0.2 mmol), K_3PO_4 (0.2 mmol), THF (0.2 mL) under N_2 atmosphere. ^{1}H NMR yield was determined using 1,3,5-trimethoxybenzene as an internal standard.

With this initial discovery, we adopted the Ru–PCP system to test different kinds of base and found K_3PO_4 to be the most effective one (Table 5.2). At the same time, different temperatures were also examined (Table 5.3); and the results suggest that the reaction has the highest efficiency for 1,2-addition reaction at room temperature, whereas with higher or lower temperature, the reaction has a poorer conversion. In addition, we noticed that higher temperature increases the selectivity of olefination product and the lower temperature results in a higher ratio of the Shapiro-type 1,2-addition product.

With the optimized conditions in hand, different kinds of aliphatic aldehyde hydrazones were tested for the Grignard-type 1,2-addition with carbonyls (Table 5.4). We showed that the linear aliphatic aldehyde hydrazones could efficiently undergo 1,2-addition with acetophenone with a

moderate to high yield (**5.3aa**–**5.3ab**, **5.3ad**). However, *α*-substituted hydrazones do not react efficiently, which is possibly due to the steric hindrance (**5.3ac**, **5.3af**). Cinnamaldehyde is not reactive in this case, plausibly owing to the chelation of ruthenium catalyst by C=C double bond and hydrazone, which deactivated the whole catalytic cycle (**5.3ae**).

Table 5.4 Grignard-type 1,2-addition with various aliphatic aldehyde hydrazones

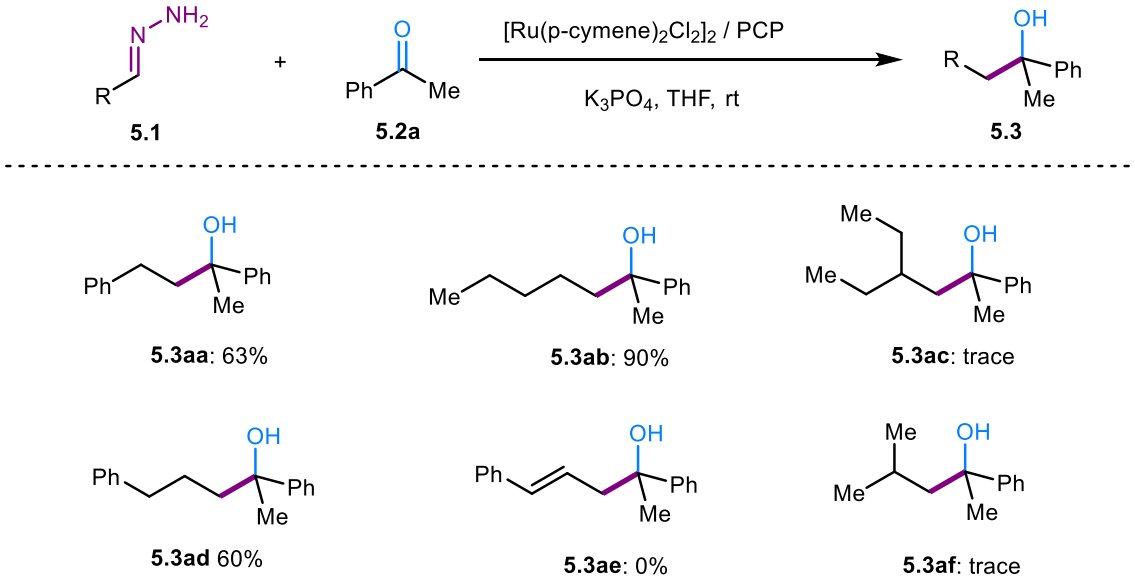

Reaction conditions: [Ru(*p*-cymene)Cl_2]$_2$ (0.003 mmol), **PCP** (0.006 mmol), **5.1** (0.25 mmol) and **5.2a** (0.2 mmol), K_3PO_4 (0.2 mmol), THF (0.2 mL) under N_2 atmosphere at room temperature. ^{1}H NMR yield was determined using 1,3,5-trimethoxybenzene as an internal standard.

After this initial test of substrate scope, we further discovered that the ruthenium–PCP catalytic system could also efficiently catalyze the tandem allylic alcohol isomerization / 1,2-addition as discussed in Section 4.2. In addition, under the original ruthenium-bisphosphine reaction system. Such a synergistic tandem reaction was not effective for aliphatic aldehyde hydrazones due to its poor selectivity of 1,2-addition over olefination and its insufficient conversion itself to drive the reaction to occur smoothly. Comparatively, with the ruthenium–PCP catalytic system, such a transformation achieves a much higher conversion and an almost perfect selectivity for 1,2-addition with aliphatic aldehyde hydrazone, even at room temperature.[11] As is shown in Table 5.5, different kinds of aliphatic aldehyde hydrazones were proved effective in this transformation (**5.6aa**–**5.6ga**). The main side product for this transformation is still the Shapiro-type 1,2-addition

product. Shorter-chained hydrazone and hydrazone with a conjugated system at α-position have a comparatively higher ratio of this side product (**5.6ca**–**5.6da**, **5.5ga**), which is possibly due to the comparatively higher thermo-stability of the corresponding alkenes.[5] In contrast, with the long-chain hydrazone bearing β-substituent, such a side product could be hardly observed, probably due to the inhibition for β-hydride elimination by the steric hindrance (**5.6ea**–**5.6fa**). In any case, all these side products could be efficiently transformed back to the desired product with the workup by H_2 under a catalytic amount of Pd/C.

Table 5.5 Scope of aliphatic aldehyde hydrazone in redox

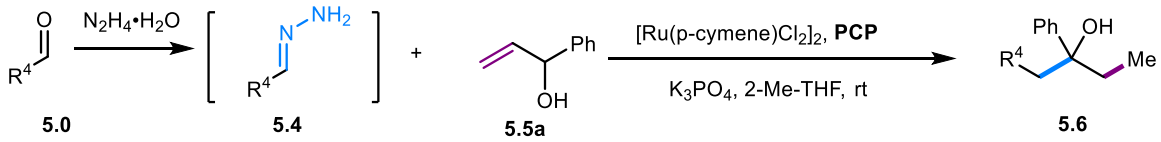

product entry	aldehydes	normal products (A)	vinyl-type products (B)	yield (A+B) (%)	A:B[a]	A:B[b]
5.6aa	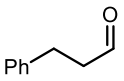	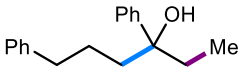	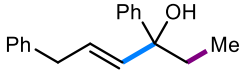	64%	>10:1	>20:1
5.6ba	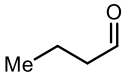	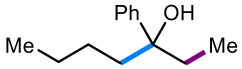	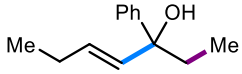	63%	>10:1	>20:1
5.6ca[c]		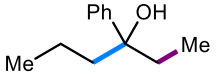	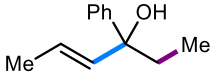	70%	4:1	>20:1
5.6da[c]		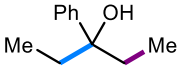	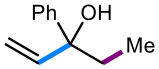	67%	2.2:1	>20:1
5.6ea	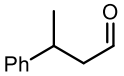	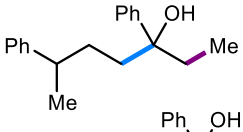	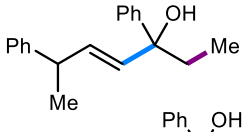	55%	>20:1	–
5.5fa	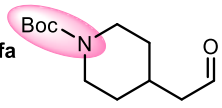	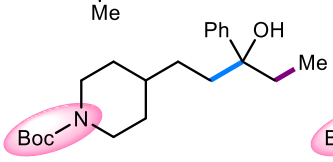	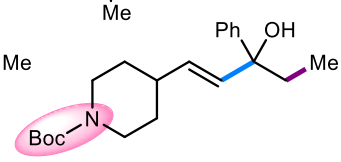	50%	>20:1	–
5.6ga	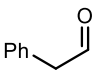	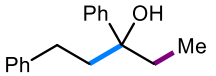	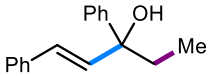	71%	5:1	>20:1

General reaction conditions: **5.4** (0.3 mmol), **5.5a** (0.2 mmol), catalyst (2.5 mol%), ligand (5 mol%), base (1.1 equiv), solvent (0.3 mL) under N_2 atmosphere. Yields of isolated products are given unless otherwise noted. [a] The ratio of major product A and minor product B after initial separation by

column chromatography without further workup. [b] The ratio of major product A and minor product B after a further transformation with Pd/ C and H_2 gas. [c] These products are volatile. The yields were determined by ^{1}H NMR analysis with mesitylene as an internal standard.

5.3 Conclusion

In conclusion, our control experiments and mechanistic analyses demonstrated that the key factor influencing the chemoselectivity of 1,2-addition and olefination is the competition between protonation and E1cB elimination after the C–C bond formation. This is mainly determined by 1) the stability of carbanion intermediate after C–C bond formation and decomposition of the azo intermediate; 2) the leaving ability of metal-oxide group on the initial carbonyl-C. Based on these analyses and previous successful cases, we developed a novel ruthenium–PCP catalytic system to enable an unusual selectivity for aliphatic aldehyde hydrazones to efficiently undergo Grignard-type 1,2-addition at room temperature. Furthermore, such a catalytic system enables the aliphatic aldehyde hydrazones to efficiently complete the synergistic tandem allylic alcohol isomerization / Grignard-type 1,2-addition reaction. This catalytic system greatly increases the hydrazone scope for the reaction under the original Ru–bisphosphine system. Our development further enables Grignard-type reactions with hydrazone as carbanion equivalent to be applicable in the broader field of synthetic chemistry.

5.4 Experimental section

5.4.1 General experimental information

Reaction Setup: All reactions were carried out in flame-dried V-shaped microwave reaction vials which were covered by aluminum seals with PTFE-faced silicone septa, under an atmosphere of nitrogen unless otherwise stated. All reaction temperatures corresponded to oil bath temperatures. All air and moisture-sensitive catalysts, ligands, and reagents were stored and charged in MBRAUN UNIlab Pro Glove Box Workstation unless otherwise stated.

Purifications: All work-up and purification procedures were carried out with reagent-grade solvents. Analytical thin-layer chromatography (TLC) was performed using E. Merck silica gel 60 F254 pre-coated plates (0.25 mm). Flash column chromatography was performed with E. Merck silica gel P60 (40–63 μm particle size, 230–400 mesh) (SiO_2). Unless otherwise specified, 'SiO_2' refers to P60 grade silica gel. Visualization was accomplished with UV light and/or iodine (I_2) or

Vanillin solution. Retention factor (R_f) values reported were measured using a 10 × 2 cm TLC plate in a developing chamber containing the solvent system (10 mL) described. Automated flash column chromatography was performed on Biotage Isolera™ Spektra Systems with ACI™.

Solvents: 2-methyl-tetrahydrofuran (2-Me-THF) was ordered from Sigma Aldrich without any purification. Solvents for filtration, transfers and chromatography, were dichloromethane (CH_2Cl_2) (ACS grade, amylene stabilized), acetone (ACS grade), ethyl acetate (EtOAc) (Fisher, ACS grade), hexane (Fisher, ACS grade), pentane (ACS grade), methanol (ACS grade).

Chemicals: In the model study, benzaldehyde (Aldrich) was distilled prior to use. Other chemicals that are commercially available and are used without further purification: 2-pentene-1-ol (Aldrich), $Ru(PPh_3)_4Cl_2$ (Aldrich), $Ru(PPh_3)_3Cl_2$ (Aldrich), **Grubbs I** catalyst (Aldrich), [Ru(*p*-cymene)$_2Cl_2$] (Aldrich & Aspira), dmpe (Aspira), dppe (Aldrich), dppf (Aldrich), PCy_3 (Aldrich), dcype (Aldrich), dcypb (Aldrich), dcypf (Aldrich & Aspira), potassium phosphate (Aldrich), potassium carbonate (Aldrich), potassium *t*-butoxide (Aldrich), hydrazine hydrate (Reagent Grade, 64–65% wt, Aldrich), mesitylene (Aldrich), 1,3,5-trimethoxylbenzene (Aldrich), anhydrous sodium sulfate, acetophenone (Aldrich). All liquid carbonyls were distilled, and solid ones were recrystallized prior to use. The ligand **PCP** was prepared according to previous literature.[12] The commercially unavailable starting material was synthesized following the procedure shown in Section 4.2.4.

NMR Spectroscopy: Nuclear magnetic resonance (^{1}H and ^{13}C NMR) spectra were recorded on a Bruker AV500 equipped with a 60-position Sample Xpress sample changer (^{1}H, 500 MHz; ^{13}C, 125 MHz), a Varian MERCURY plus-500 spectrometer (^{1}H, 500 MHz; ^{13}C, 125 MHz) or Bruker AV400 spectrometer (^{1}H, 400 MHz; ^{13}C, 100 MHz). Chemical shifts for both ^{1}H NMR and ^{13}C NMR spectra are expressed in parts per million (ppm) units downfield from TMS, with the solvent residue peak as the chemical shift standard ($CDCl_3$: δ 7.28 ppm in ^{1}H NMR; δ 77.00 ppm in ^{13}C NMR). Data are reported as following: chemical shift, multiplicity (s = singlet, d = doublet, dd = doublet of doublets, t = triplet, td = triplet of doublets, q = quartet, quin = quintet, sep = septet, m = multiplet, br = broad singlet), coupling constants *J* (Hz), and integration.

Mass Spectrometry: Mass spectrometry (MS) was performed by the McGill Chemistry Department Mass Spectrometry Facility. High resolution mass spectra were recorded using electrospray ionization (ESI+) and/or atmospheric pressure chemical ionization APCI (+/-), performed either on 'Exactive Plus Orbitrap' a ThermoScientific high resolution accurate mass

(HR/AM) FT mass spectrometer, or a Bruker Daltonics Maxis Impact quadrupole-time of flight (QTOF) mass spectrometer.

Characterization of Products: For the products, we report NMR spectra, R_f value of TLC and HRMS data.

5.4.2 Experimental procedures

5.4.2.1 Preparation of hydrazone or hydrazone solution

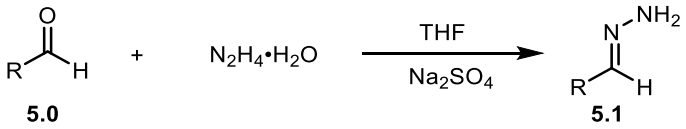

5.0 **5.1**

Procedure A: For Table 5.1–5.4: THF (4 mL) was added first into a small bottle with a stir bar. Then, hydrazine monohydrate (0.35 mL, 7 mmol) was added into the bottle. After that, **5.0** (5 mmol) was added dropwise into the stirred solution and the mixture was stirred for 5 min. Next, proper amount of anhydrous Na_2SO_4 was added to remove water. After stirring for another 3 h, the so-formed solution was ready to use.

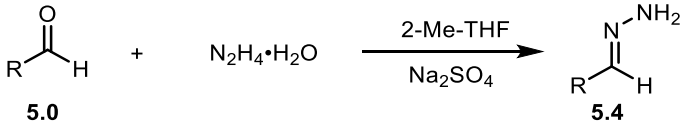

5.0 **5.4**

Procedure B: For Table 5.5: 2-Me-THF (4 mL) was added first into a small bottle with a stir bar. Then, hydrazine monohydrate (0.35 mL, 7 mmol) was added into the bottle. After that, **5.0** (5 mmol) was added dropwise into the stirred solution and the mixture was stirred for 5 min. Next, proper amount of anhydrous Na_2SO_4 was added to remove water. After stirring for another 3 h, the so-formed solution was ready to use.

5.4.2.2 General procedure for Table 5.1–5.5

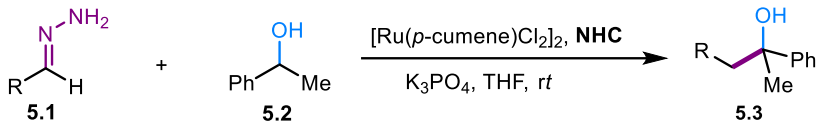

5.1 **5.2** **5.3**

General procedure for Table 5.1–5.4: $[Ru(p\text{-cymene})Cl_2]_2$ (0.003 mmol), **NHC** (0.006 mmol) and ^{t}BuOK (3 mg) were added into a V-shaped reaction tube with a stir bar in the glovebox. Then, 0.1 mL THF was added before the reaction tube was sealed and stirred in the glovebox for 1h before

base was added. The mixture was sealed again and moved out of the glovebox.* Then, **5.1** solution (prepared through ***Procedure A***, 0.22 mL, 0.25 mmol) and **5.2a** (0.2 mmol) were added in sequence. The reaction mixture was stitted for 24 h. Then, 1,3,5-trimethoxylbenzene (11.2 mg, 0.067 mmol) was added in the mixture as standard. Then, the solution was filtered by celite and concentrated to dryness. The crude mixture was diluted by $CDCl_3$ to run the ^1H NMR test to determine the ^1H NMR yield.

*For Table 5.1, entry 4, $[Ru(p\text{-cymene})Cl_2]_2$ (0.003 mmol), dmpe (0.006 mmol) were added into a V-shaped reaction tube with a stir bar in the glovebox. Then, **5.1** solution (prepared through ***Procedure A***, 0.22 mL, 0.25 mmol) and **5.2a** (0.2 mmol) were added in sequence. The reaction mixture was stirred for 24 h. Then, 1,3,5-trimethoxylbenzene (11.2 mg, 0.067 mmol) was added in the mixture as standard. Then, the solution was filtered by celite and concentrated to dryness. The crude mixture was diluted by $CDCl_3$ to run the ^1H NMR test to determine the ^1H NMR yield.

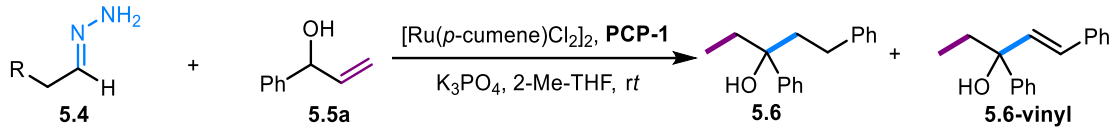

General procedure for Table 5.5: $[Ru(p\text{-cymene})Cl_2]_2$ (0.005 mmol), **PCP** (0.01 mmol) and ^{t}BuOK (5 mg) were added into a V-shaped reaction tube with a stir bar in the glovebox. Then, 0.1 mL 2-Me-THF was added before the reaction tube was sealed and stirred in the glovebox for 1h before K_3PO_4 (0.22 mmol) was added. The mixture was sealed again and moved out of the glovebox. Then, **5.4** solution (prepared through ***Procedure B***, 0.22 mL, 0.25 mmol) and **5.5a** (0.2 mmol) were added in sequence. The mixture was stirred under rt for 24h. The reaction mixture was filtered through a celite plug with 2-3 mL CH_2Cl_2. The solvent was removed by rotary evaporator and the residue was purified by column chromatography on silica gel (using hexane and ethyl acetate as eluent) to give the mixture of desired product **5.6** and vinylation product **5.6-vinyl**. If **5.6**: **5.6-vinyl** > 20:1, the product was identified as pure product and directly collected to do the related structure characterization. If **5.6**: **5.6-vinyl** < 20:1 (determined by ^{1}HNMR), the mixture was collected in a 25 mL round-bottom flask with a stir bar before 2 mg Pd/C (10% Pd) was added. Then, the flask was charged with H_2 balloon and MeOH (4 mL) was added. It was stirred for 2h under rt and the mixture was filtered through a celite plug again with 2-3 mL CH_2Cl_2. The solvent was removed to give the pure product **5.6**.

5.4.3 Spectroscopic data of products

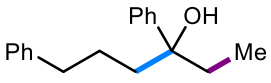

5.6aa

(Generated following corresponding general procedure and isolated by column chromatography on silica gel with hexane: EtOAc = 97:3 as eluent to give mixture of **5.6aa** and corresponding vinylation product in 32 mg. Then, working up with Pd/C and H_2 and give the pure desired product in 32 mg, colorless oil, yield: 64%): **^{1}H NMR** (500 MHz, $CDCl_3$) δ 7.40 – 7.33 (m, 4H), 7.33 – 7.23 (m, 3H), 7.22 – 7.17 (m, 1H), 7.17 – 7.11 (m, 2H), 2.67 – 2.52 (m, 2H), 1.96 – 1.79 (m, 4H),, 1.74 – 1.62 (m, 2H), 1.50 – 1.39 (m, 1H), 0.78 (t, *J* = 7.57 Hz, 3H). **^{13}C NMR** (126 MHz, $CDCl_3$) δ 145.8, 142.2, 128.3, 128.2, 128.0, 126.3, 125.7, 125.3, 77.1, 42.1, 36.1, 35.4, 25.2, 7.7. **TLC**: R_f 0.46 (5:1 hexane/EtOAc) [Phosphomolybdic acid]. **HRMS:** (ESI, *m*/*z*): calcd. for $C_{18}H_{22}ONa[M+Na]^+$ 277.1563, found: 277.1567.

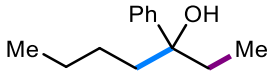

5.6ba

(Generated following corresponding general procedure and isolated by column chromatography on silica gel with hexane: EtOAc = 97:3 as eluent to give mixture of **5.6ba** and corresponding vinylation product in 24 mg. Then, working up with Pd/C and H_2 and give the pure desired product in 24 mg, colorless oil, yield: 63%): **^{1}H NMR** (500 MHz, $CDCl_3$) δ 7.43 – 7.33 (m, 4H), 7.28 – 7.22 (m, 1H), 1.95 – 1.59 (m, 5H), 1.36 – 1.19 (m, 3H), 1.13 – 1.00 (m, 1H), 0.86 (t, *J* = 6.99 Hz, 3H), 0.78 (t, *J* = 7.44 Hz, 3H). **^{13}C NMR** (126 MHz, $CDCl_3$) δ 146.1, 128.0, 126.2, 125.4, 77.2, 42.3, 35.4, 25.7, 23.1, 14.0, 7.8. **TLC**: R_f 0.51 (5:1 hexane/EtOAc) [Phosphomolybdic acid]. **HRMS:** (ESI, *m*/*z*): calcd. for $C_{13}H_{20}ONa[M+Na]^+$ 215.1406, found: 215.1400.

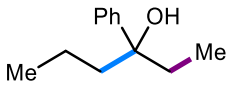

5.6ca

(Generated following corresponding general procedure and isolated by column chromatography on silica gel with hexane: EtOAc = 97:3 as eluent to give mixture of **5.6ca** and corresponding vinylation product. Then, working up with Pd/C and H_2 and give the pure desired product, colorless

volatile oil and yield was determined by ^{1}H NMR with mesitylene as standard before isolation. Following reported the NMR spectrum data of pure product): **^{1}H NMR** (500 MHz, $CDCl_3$) δ 7.43 – 7.32 (m, 4H), 7.28 – 7.21 (m, 1H), 1.96 – 1.57 (m, 5H), 1.39 – 1.22 (m, 1H), 1.16 – 1.03 (m, 1H), 0.88 (t, *J* = 7.35 Hz, 3H), 0.78 (t, *J* = 7.44 Hz, 3H). **^{13}C NMR** (126 MHz, $CDCl_3$) δ 146.1, 128.0, 126.2, 125.3, 77.3, 44.9, 35.3, 16.8, 14.4, 7.8. **TLC**: R_f 0.49 (5:1 hexane/EtOAc) [Phosphomolybdic acid]. **HRMS:** (ESI, *m*/*z*): calcd. for $C_{12}H_{18}ONa[M+Na]^+$ 201.1250, found: 201.1255.

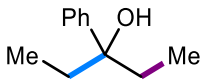

5.6da

(Generated following corresponding general procedure and isolated by column chromatography on silica gel with hexane: EtOAc = 97:3 as eluent to give mixture of **5.6da** and corresponding vinylation product. Then, working up with Pd/C and H_2 and give the pure desired product, colorless volatile oil and yield was determined by ^{1}H NMR with mesitylene as standard before isolation. Following reported the NMR spectrum data of pure product): **^{1}H NMR** (500 MHz, $CDCl_3$) δ 7.43 – 7.33 (m, 4H), 7.28 – 7.22 (m, 1H), 1.96 – 1.74 (m, 5H), 0.79 (t, *J* = 7.42 Hz, 6H). **^{13}C NMR** (126 MHz, $CDCl_3$) δ 145.7, 128.0, 126.2, 125.5, 77.4, 34.9, 7.8. **TLC**: R_f 0.43 (5:1 hexane/EtOAc) [Phosphomolybdic acid]. **HRMS:** (ESI, *m*/*z*): calcd. for $C_{11}H_{16}ONa[M+Na]^+$ 187.1093, found: 187.1085.

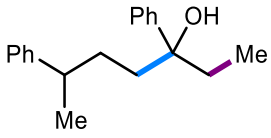

5.6ea

(Generated following corresponding general procedure and isolated by column chromatography on silica gel with hexane: EtOAc = 96:4 as eluent, colorless oil, 29 mg, yield: 55%, d.r. = 1:1): **^{1}H NMR** (500 MHz, $CDCl_3$) δ 7.42 – 7.24 (m, 7H), 7.24 – 7.19 (m, 1H), 7.19 – 7.14 (m, 1H), 7.14 – 7.06 (m, 1H), 2.69 – 2.56 (m, 1H), 1.92 – 1.55 (m, 6H), 1.46 – 1.34 (m, 1H), 1.21 (dd, *J* = 7.0, 0.9 Hz, 3H), 0.73 (td, *J* = 7.4, 4.9 Hz, 3H). **^{13}C NMR** (126 MHz, $CDCl_3$) δ 147.3, 147.2, 145.8, 145.7, 128.3, 128.3, 128.0, 128.0, 128.0, 127.2, 127.0, 126.9, 126.2, 125.8, 125.3, 125.3, 77.17, 77.02, 40.6, 40.3, 40.3, 40.2, 35.6, 35.4, 31.8, 31.6, 22.9, 22.4, 7.7. **TLC**: R_f 0.46 (5:1 hexane/EtOAc)

[Phosphomolybdic acid]. **HRMS:** (ESI, *m*/*z*): calcd. for $C_{19}H_{24}ONa[M+Na]^+$ 291.1719, found: 291.1712.

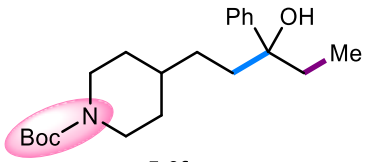

5.6fa

(Generated following corresponding general procedure and isolated by column chromatography on silica gel with hexane: EtOAc = 89:11 as eluent, colorless oil, 34.5 mg, yield: 50%): **^{1}H NMR** (500 MHz, $CDCl_3$) δ 7.41 – 7.31 (m, 4H), 7.28 – 7.20 (m, 1H), 4.04 (s, 2H), 2.71 – 2.56 (m, 2H), 1.94 – 1.73 (m, 5H), 1.60 (d, *J* = 12.9 Hz, 2H), 1.45 (s, 9H), 1.35 – 1.19 (m, 3H), 1.09 – 0.96 (m, 3H), 0.77 (t, *J* = 7.4 Hz, 3H). **^{13}C NMR** (126 MHz, $CDCl_3$) δ 154.8, 145.8, 128.0, 126.3, 125.3, 79.1, 77.04, 76.7, 44.0, 39.5, 36.3, 35.4, 32.1, 32.0, 30.0, 28.4, 7.7. **TLC**: R_f 0.13 (5:1 hexane/EtOAc) [Phosphomolybdic acid]. **HRMS:** (ESI, *m*/*z*): calcd. for $C_{21}H_{33}NO_3Na[M+Na]^+$ 370.2353, found: 370.2362.

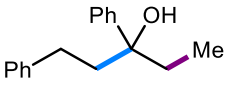

5.6ga

(Generated following corresponding general procedure and isolated by column chromatography on silica gel with hexane: EtOAc = 96:4 as eluent to give mixture of **5.6ga** and corresponding vinylation product in 33 mg. Then, working up with Pd/C and H_2 and give the pure desired product in 33 mg, colorless oil, yield: 71%): **^{1}H NMR** (500 MHz, $CDCl_3$) δ 7.52 – 7.38 (m, 4H), 7.35 – 7.25 (m, 3H), 7.23 – 7.12 (m, 3H), 2.72 – 2.62 (m, 1H), 2.45 – 2.36 (m, 1H), 2.24 – 2.11 (m, 2H), 2.02 – 1.86 (m, 2H), 1.78 (br, 1H), 1.50 – 1.39 (m, 1H), 0.82 (t, *J* = 7.46 Hz, 3H). **^{13}C NMR** (126 MHz, $CDCl_3$) δ 145.5, 142.4, 128.3, 128.3, 128.1, 126.4, 125.7, 125.3, 77.2, 44.5, 35.7, 30.0, 7.7. **TLC**: R_f 0.49 (5:1 hexane/EtOAc) [Phosphomolybdic acid]. **HRMS:** (ESI, *m*/*z*): calcd. for $C_{17}H_{20}ONa[M+Na]^+$ 263.1406, found: 263.1407.

References

(1). Wang, H.; Dai, X.-J.; Li, C.-J., Aldehydes as alkyl carbanion equivalents for additions to carbonyl compounds. *Nat. Chem.* **2017,** *9*, 374-378.

(2). Maercker, A., The wittig reaction. In *Org. React.*, pp 270–490.
(3). Wei, W.; Dai, X.-J.; Wang, H.; Li, C.; Yang, X.; Li, C.-J., Ruthenium(II)-catalyzed olefination *via* carbonyl reductive cross-coupling. *Chem. Sci.* **2017,** *8*, 8193–8197.
(4). Li, C.-C.; Wang, H.; Sim, M. M.; Qiu, Z.; Chen, Z.-P.; Khaliullin, R. Z.; Li, C.-J., Empowering alcohols as carbonyl surrogates for grignard-type reactions. *Nat. Commun,* **2020,** *11*, 6022.
(5). Carey, F. A.; Sundberg, R. J., *Advanced Organic Chemistry: Part A: Structure and Mechanisms*. Springer Science & Business Media: New York, 2007.
(6). Das, U. K.; Chakraborty, S.; Diskin-Posner, Y.; Milstein, D., Direct conversion of alcohols into alkenes by dehydrogenative coupling with hydrazine/hydrazone catalyzed by manganese. *Angew. Chem. Int. Ed.* **2018,** *57*, 13444–13448.
(7). Hartwig, J. F.; Collman, J. P., *Organotransition Metal Chemistry: From Bonding to Catalysis*. University Science Books: Sausalito, 2010; Vol. 1.
(8). Knochel, P.; Skotnitzki, J., The grignard reaction. *Synfacts* **2020,** *16*, 0946.
(9). Zhu, D.; Lv, L.; Li, C.-C.; Ung, S.; Gao, J.; Li, C.-J., *Umpolung* of carbonyl groups as alkyl organometallic reagent surrogates for palladium-catalyzed allylic alkylation. *Angew. Chem. Int. Ed.* **2018,** *57*, 16520–16524.
(10). Adlington, R. M.; Barrett, A. G. M., Recent applications of the shapiro reaction. *Acc. Chem. Res.* **1983,** *16*, 55–59.
(11). Li, C.-C.; Kan, J.; Qiu, Z.; Li, J.; Lv, L.; Li, C.-J., Synergistic relay reactions to achieve redox-neutral α-alkylations of olefinic alcohols with ruthenium(II) catalysis. *Angew. Chem. Int. Ed.* **2020,** *59*, 4544–4549.
(12). Matoba, K.; Eizawa, A.; Nishimura, S.; Arashiba, K.; Nakajima, K.; Nishibayashi, Y., Practical synthesis of a PCP-type pincer ligand and its metal complexes-. *Synthesis* **2018,** *50*, 1015–1019.

Chapter 6. Iron-Catalyzed Nucleophilic Addition Reactions of Hydrazone to Polar Unsaturated Bonds

6.1 Introduction

Carbon-skeleton-construction is the basis of organic synthesis and the core for forming various organic molecules, among which the nucleophilic reactions of carbanion and its equivalents play a vital role.[1] For instance, by the nucleophilic addition of carbanion to carbonyl compounds, imines or Michael acceptors, secondary or tertiary alcohols and amines as well as long carbon-chains can be generated readily. Initiated by the classical organozinc reagents and the Grignard reaction,[2] there has been continued development of unstabilized organometallic reagents as free-carbanion equivalents during the past century, with many metals or metalloids being explored.[3–8] However, most of these reagents require stoichiometric amounts of metals or metalloids which are dangerous (e.g. lithium reagents[5]), toxic (e.g. Hg and Sn reagents[6, 7]) and wasteful. As a result, the development of a non-metal or catalytic-amount-of-metal based carbanion reagents is highly desirable.

Inspired by the classical Wolff-Kishner reduction,[9–14] we recently found that hydrazones, readily generated *in situ* from aldehydes and hydrazine, can serve as an alkyl carbanion equivalent[15–17] to undergo nucleophilic additions.[18] To date, a series of such hydrazone reactions including carbonyl addition,[19] imine addition[20] and conjugate addition have been realized with ruthenium catalysts.[21] In those reactions, the hydrazone was established as an organic carbanion equivalent based on just catalytic amounts of metal catalyst rather than stoichiometric amounts of metals. Nevertheless, as noted earlier,[19] the requirement for ruthenium as a catalyst, a scarce and precious metal, is still expensive and unsustainable. Thus, a major effort was made to develop an earth-abundant metal-catalyzed organic carbanion equivalent addition reaction to make the carbanion chemistry safer, less wasteful and more sustainable.

Iron, an inexpensive and earth-abundant metal, is one of the ideal catalysts for organic reactions. So far, a considerable number of iron-catalyzed organic reactions have been studied by chemists such as free radical reactions, cross coupling reactions, C–H functionalizations, Lewis acid-catalyzed reactions, etc.[22–25] Up to now, however, iron-based Grignard-type reaction has rarely

been reported and limited to stoichiometric transformations.[22, 23, 25–36] Early in 1961, an iron–bisphosphine complex and several derivatives were reported to be stable.[37] Further studies showed that such iron–bisphosphine complexes could coordinate and interact with hydrazine derivatives with the help of a base.[38–44] Thus, we hypothesized that an iron catalyst bound to phosphine ligands might also catalyze the nucleophilic addition of hydrazones to carbonyl compounds, imine or Michael acceptors. Also, it is worth-noting that most earlier studies[41–44] on related iron–bisphospine complexes were limited to stoichiometric transformations of the complex themselves and such complexes have rarely been used to catalyze organic reactions.

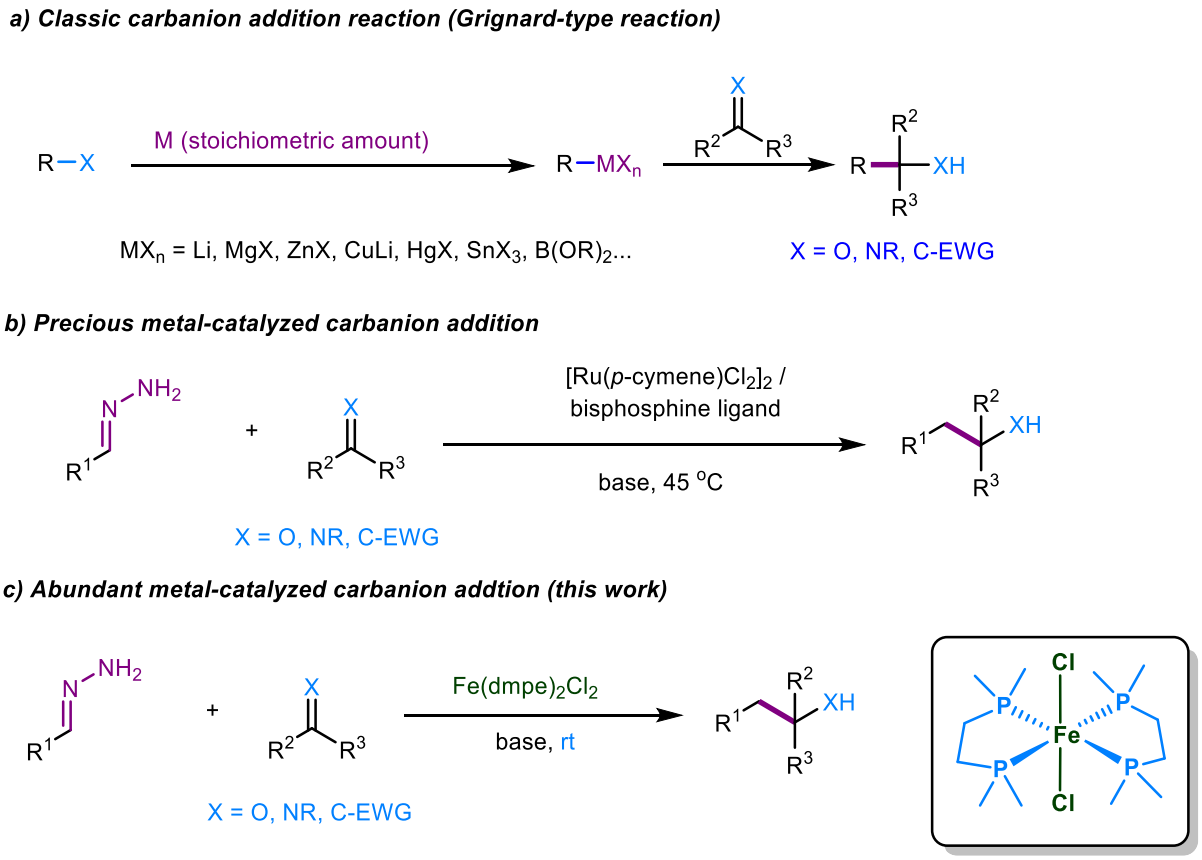

Scheme 6.1 Development of carbanion chemistry

On the other hand, key challenges were envisioned in our hypothesis: First, iron is a first-row transition metal which is a comparatively harder Lewis acid and more likely to coordinate with harder ligands such as water, hydroxide anion, and nitrogen-containing compounds[45–49] Thus, hydrolysis and hydrozinolysis may proceed in the reaction system and should be taken into

consideration. Second, iron has two stable oxidation states, iron(II) and iron(III), that can easily interchange.[50–52] This means that it may undergo single electron transfer in the reaction system and influence the main transformation. Nevertheless, herein, we report earth-abundant iron–phosphine complexes as cheap, highly effective and sustainable catalysts for a series of *umpolung* nucleophilic additions of hydrazone, proceeding at room temperature with a broad substrate scope.

6.2 Results and discussions

6.2.1 Investigation of reaction conditions

Table 6.1 Initial investigation of reaction conditions

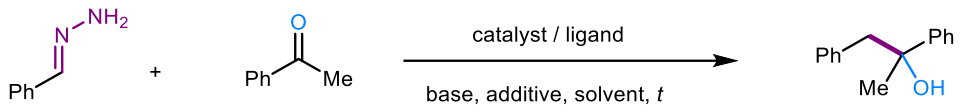

6.1a **6.2a** **6.3aa**

entry	catalyst	ligand	base	additive	solvent	*t* (°C)	3aa (%)
1	$FeSO_4$	dmpe	K_3PO_4	-	THF	100	0
2	FeF_2	dmpe	K_3PO_4	-	THF	100	trace
3	$FeCl_2$	dmpe	K_3PO_4	-	THF	100	trace
4	$FeCl_3$	dmpe	K_3PO_4	-	THF	100	8
5	$Fe(acac)_3$	dmpe	K_3PO_4	-	THF	100	0
6	$FeCl_3$	dppe	K_3PO_4	-	THF	100	0
7	$FeCl_3$	dppp	K_3PO_4	-	THF	100	0
8	$FeCl_3$	dppf	K_3PO_4	-	THF	100	0
9	$FeCl_3$	BINAP	K_3PO_4	-	THF	100	0

General reaction conditions: **6.1a** (0.25 mmol), **6.2a** (0.2 mmol), [Fe] catalyst (5 mol %), ligand (5 mol %), base (50 mol %), additive (50 mol %), solvent (0.2 mL) under N_2 atmosphere. ^{1}H NMR yield was determined using 1,3,5-trimethoxybenzene as an internal standard.

We initiated our research by selecting different iron salts together with the ligand 1,2-bis(dimethylphosphino)ethane (dmpe), K_3PO_4 as base and THF as solvent at 100 °C. Fortunately, we successfully obtained trace amounts of the desired product with FeF_2, $FeCl_3$ and $FeCl_2$ as catalysts, of which $FeCl_3$ gives the best yield of 8% (Table 6.1, entries 1–5). With $FeCl_3$, we then tested different ligands and found that the desired product could only be formed when dmpe was used as the ligand (Table 6.1, entry 4, entries 6–9). However, further explorations showed that the

yield with the $FeCl_3$-catalyst system was extremely low and dark particles would always form at the end of the reaction. Based on chemical properties of iron, we reasoned that $FeCl_3$ may undergo hydrolysis under such a high temperature and the catalyst easily deactivates during the reaction process.

Table 6.2 Investigation of reaction conditions with well-defined iron-complex

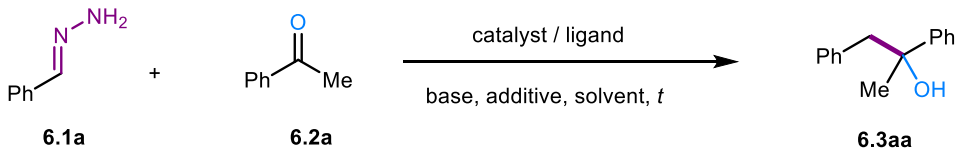

6.1a **6.2a** **6.3aa**

entry	catalyst	ligand	base	additive	solvent	*t* (°C)	yield (%)[b]
1	**Fe 1**	-	K_3PO_4	-	THF	100	15
2	**Fe 1**	-	K_3PO_4	-	THF	60	trace
3	**Fe 1**	-	K_3PO_4	-	THF	rt	20
4	**Fe 1**	-	K_3PO_4	CsF	THF	rt	72
5	**Fe 1**	-	KO^tBu	CsF	THF	rt	56
6	**Fe 1**	-	K_2CO_3	CsF	THF	rt	8
7	**Fe 1**	-	DABCO	CsF	THF	rt	0
8*	**Fe 1**	-	K_3PO_4	CsF	THF	rt	90
9*	**Fe 1**	-	K_3PO_4	CsF	DMSO	rt	89
10*	**Fe 1**	-	K_3PO_4	CsF	dioxane	rt	trace
11*	**Fe 1**	-	K_3PO_4	CsF	DCM	rt	0
12**	**Fe 1**	-	K_3PO_4	CsF	THF	rt	97
13**	**Fe 2**	**-**	**K_3PO_4**	**CsF**	**THF**	**rt**	**99**

Fe 1: $[Fe(dmpe)_2Cl_2]^+[FeCl_4]^-$ **Fe 2**: $Fe(dmpe)_2Cl_2$ dmpe = 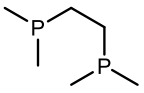

General reaction conditions: **6.1a** (0.25 mmol), **6.2a** (0.2 mmol), [Fe] catalyst (5 mol %), ligand (5 mol %), base (50 mol %), additive (50 mol %), solvent (0.2 mL) under N_2 atmosphere. ^1H NMR yield was determined using 1,3,5-trimethoxybenzene as an internal standard. *20 mg 4 Å molecule sieve was added in the reaction system. ****6.1a** solution was treated with 4 Å molecule sieves beforehand.

To avoid this problem, we pre-mixed $FeCl_3$ and dmpe (1:1) to form a stable complex $[Fe(dmpe)_2Cl_2]^+[FeCl_4]^-$to catalyze the reaction. Unfortunately, only a slight improvement of the

yield was observed (Table 6.2, entry 1). We then suspected that the reaction temperature may play a significant role in this catalytic process. To further alleviate the hydrolysis problem, we tested the model reaction at different temperatures (Table 6.2, entries 1-3). To our surprise, the reaction gave an even better yield of 20% at room temperature (compared with 15% at 100 ^{o}C). In our previous ruthenium work, the addition of CsF was found to be beneficial to the reaction which either serves as a water-removing reagent or assist the ligand exchange of the catalytic cycle. Accordingly, we found that adding 50% of CsF to the reaction system, the yield of the target product indeed increased to 72% (Table 6.2, entries 4). The test of a variety of bases showed that K_3PO_4 provided the best yield of 72% (Table 6.2, entries 4–7). Up to then, although the yield was relatively high, significant quantities of both starting materials remained, which suggested the deactivation of the catalyst during the reaction process. According to the procedure of preparing hydrazone solution (see supporting information), a trace amount of water may remain in the reaction system and destroy the iron catalyst slowly. To test this hypothesis, we added some 4Å molecular sieves directly to the reaction system under the optimized conditions. Indeed, the yield was increased to 90% and the starting materials were nearly consumed (Table 6.2, entry 8). We also tested a series of solvents and found that the reaction worked well in THF and DMSO (Table 6.2, entries 8–11). To simplify the reaction system, we further considered whether the 4Å molecule sieves could be used to pre-treat the hydrazone solution before running the reaction. By doing this, the yield of the product was further increased to 97% (Table 6.2, entry 12).

Having reached these conditions (Table 6.2, entry 12), we turned to different substrates. However, we discovered that aliphatic ketones have low reactivity under this catalyst system and large amounts of side products were generated. One of the key side products was azine, which was formed by the condensation of hydrazones and ketones or hydrolyzed hydrazones. As Fe(III) has a stronger Lewis acidity due to a high positive charge, we asserted that Fe(III) may also assist azine formation while catalyzing the main reaction. Also, Fe(III) could oxidize the dmpe (sensitive to oxidant) and lower down the catalysis efficiency. To avoid these problems, we considered preparing Fe(II) dmpe complex, which may have lower Lewis acidity, to catalyze this reaction. As we expected, using $Fe(dmpe)_2Cl_2$, a stable neutral complex generated by the literature procedure, instead of $[Fe(dmpe)_2Cl_2]^+[FeCl_4]^-$ as catalyst gave nearly quantitative yield of the desired product under the same conditions (Table 6.2, entry 13).

6.2.2 Investigation of substrate scope

6.2.2.1 Substrate scope of 1,2-addition to carbonyls

Table 6.3 Substrate scope of 1,2-addition of hydrazones to carbonyls

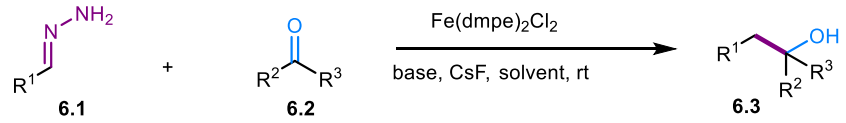

6.1 + **6.2** → **6.3**

Scope of carbonyls

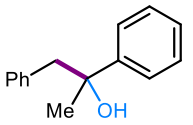

6.3aa: A: 99%

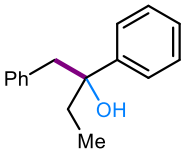

6.3ba: A: 97%

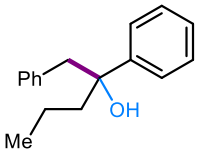

6.3ca: A: 93%

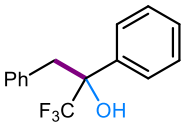

6.3da: A: 91%

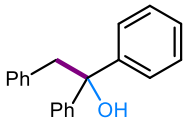

6.3ea: A: 50%

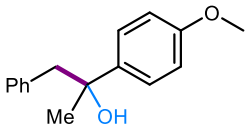

6.3fa: A: 90%

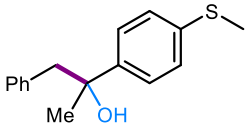

6.3ga: A: 85%

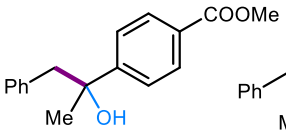

6.3ha: A: 75%

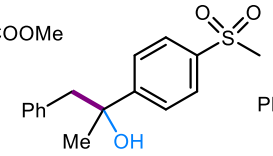

6.3ia: A: 82%

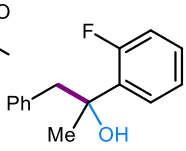

6.3ja: A: 87%

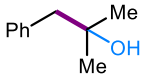

6.3ka*: A: 80%

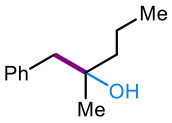

6.3la: A: 75%

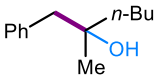

6.3ma: A: 52%

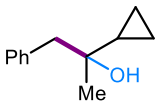

6.3na: A: 88%

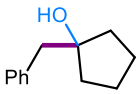

6.3oa: A: 69%

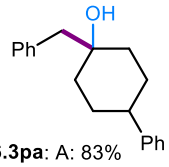

6.3pa: A: 83%

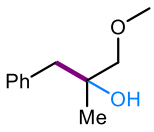

6.3qa: A: 83%

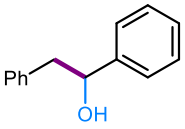

6.3ra: C: 32%

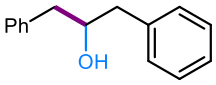

6.3sa: C: 61%

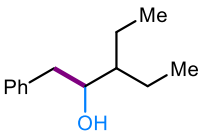

6.3xa: C: 37%

Scope of hydrazones

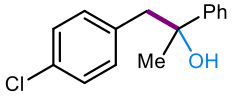

6.3ab: A: 99%

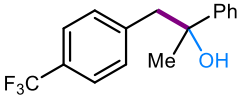

6.3ac: A: 99%

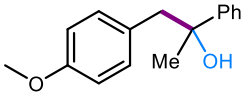

6.3ad: B: 56%

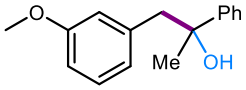

6.3ae: A: 83%

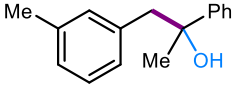

6.3af: A: 87%

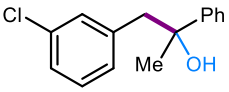

6.3ag: A: 99%

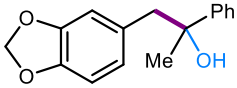

6.3ah: B: 70%

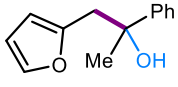

6.3ai: A: 65%

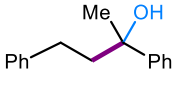

6.3aj: A: 0%

Reaction conditions: **6.1** (0.25 mmol), **6.2** (0.2 mmol), $Fe(dmpe)_2Cl_2$ (5 mol %), base (50 mol %), CsF (50 mol %), solvent (0.2 mL), rt under N_2. Condition A: base: K_3PO_4, solvent: THF. Condition B: base: K_3PO_4, solvent: DMSO. Condition C: base: ^{t}BuOK, solvent: THF. Yield of isolated product is reported unless noted. *These products are volatile. ^{1}H NMR yield was determined using 1,3,5-trimethylbenzene as standard.

With the newly optimized conditions in hand, the substrate scopes of both electrophiles and hydrazones were tested again, and this time, things were much better (Table 6.3). First, different types of carbonyl compounds were studied. For acetophenone derivatives, most have high reactivities. Non-bulky alkyl–aryl ketones reacted very well, with a slight decrease in yield for longer alkyl chains **6.3aa**–**6.3ca**. When we changed the alkyl to trifluoromethyl, a very strong electron-withdrawing group, the reaction also gave an extremely high yield (**6.3da**). However, benzophenone has a much lower reactivity maybe due to the increased steric effect (**6.3ea**). Acetophenones bearing either electron-donating or electron-withdrawing groups gave good yields of the desired products **6.3fa**–**6.3ja**. As previously mentioned, iron can also serve as an efficient Lewis acid to catalyze the nucleophilic (both *C*- and *N*-) addition to carbonyl compounds, and a main side reaction for aliphatic ketone substrates was the nucleophilic attack by nitrogen on hydrazone to form azine. For linear aliphatic ketones, the shorter the aliphatic chain, the less side products **6.3ka**–**6.3ma**. For cyclic ketones, both cyclopentanone and cyclohexanone, as well as some derivatives, can give good yields of the final products **6.3oa**–**6.3pa**. Ketone substrates containing functional group such as methoxy or cyclopropyl, also gave good, and sometimes better, yields than the simple alkyl ketones (**6.3na**, **6.3qa**). Aldehydes, being much more reactive than ketones, also worked in this reaction. However, due to their high reactivity, competing azine formation was difficult to prevent. Under the standard conditions, less than 50% yield of the desired product was obtained. To improve the yield, we considered two possible solutions: to use a stronger base, such as ^{t}BuOK, or to use DMSO as the solvent (since the azine product was always harder to form in DMSO).[15] After testing these two ideas, we found that using ^{t}BuOK as the base and running the reaction in THF gave the desired product in higher yields for aldehydes (**6.3ra**–**6.3sa,** 6.**3xa**).

Next, we tested different kinds of hydrazones as nucleophiles in this reaction and found that the scope of hydrazone was relatively limited. Only aromatic aldehyde hydrazones worked well in this reaction. Hydrazones with electron-withdrawing groups on the *para* position generally had high

reactivity and all gave quantitative yield (**6.3ab**–**6.3ac**). In contrast, when electron-donating groups were in the *para*-position, the hydrazone did not react well in THF. However, the result was better in DMSO (**6.3ad**, **6.3ah**). Substituents at the *meta* position did not influence the reaction significantly (**6.3ae**–**6.3ag**). Apart from these, other types of aromatic hydrazones also gave high yields of the desired products (**6.3ai**).

6.2.2.2 Substrate scope of Michael acceptors

In addition to carbonyl 1,2-additions, the iron–phosphine complex also catalyzes Michael addition of hydrazones to activated alkenes(**6.3ta**–**6.3wa**). To our delight, in contrast to our previously reported ruthenium-catalyzed conjugate addition, Michael acceptors lacking an oxygen coordinating group such as acrylonitrile also work in this reaction system. This may greatly broaden the scope of conjugate addition of hydrazones.

Table 6.4 Substrate scope of Michael addition of hydrazones

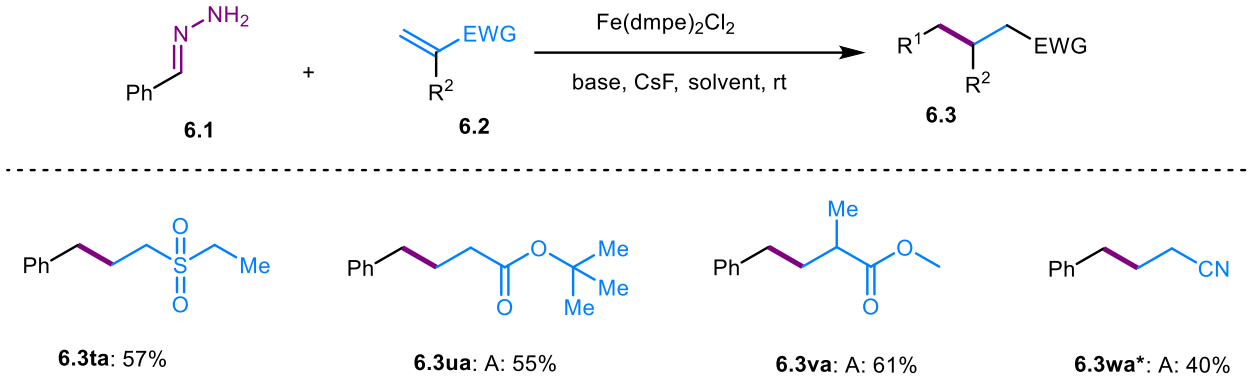

Reaction conditions: **6.1** (0.2 mmol), **6.2** (0.3 mmol), $Fe(dmpe)_2Cl_2$ (5 mol %), base (50 mol %), CsF (50 mol %), solvent (0.2 mL), rt under N_2. Yield of isolated product is reported unless noted. *These products are volatile. ^{1}H NMR yield was determined using 1,3,5-trimethylbenzene as standard.

6.2.2.3 Substrate scope of aromatic imines

Aromatic imines, a comparatively weaker electrophile, can also undergo similar nucleophilic addition with hydrazone (Table 6.5); Their reactivity, however, is much lower than carbonyl compounds and the substrate scope is narrower than those. Generally, imines with electron-deficient aromatic substituents favor the reaction (**6.4aa**–**6.4ca**) with various aromatic aldehyde hydrazones (**6.4aa**–**6.4ac**, **6.4ba**, **6.4bb**). With electron-rich aromatic rings as substituents, the

imine showed low or no reactivity (**6.4da**–**6.4ea**). On the other hand, a strong electron-withdrawing group other than an aromatic ring on imine nitrogen failed to generate the target product (**6.4fa**), and the azine byproduct was formed almost quantitatively.

Table 6.5 Substrate scope of aromatic imine addition of hydrazones

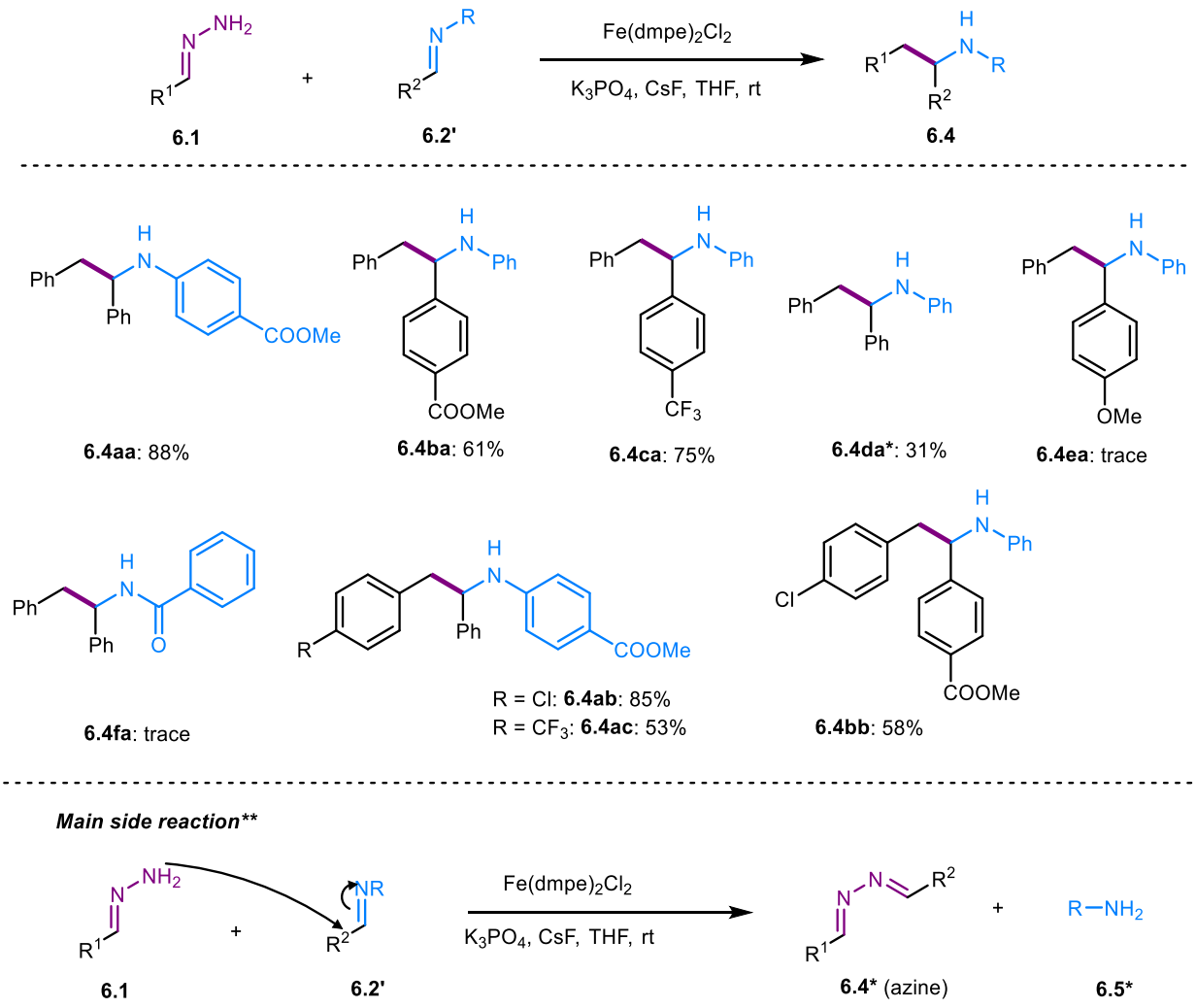

Reaction conditions: **6.1** (0.25 mmol), **6.2'** (0.2 mmol), $Fe(dmpe)_2Cl_2$ (5 mol %), K_3PO_4 (50 mol %), CsF (50 mol %), solvent (0.2 mL), rt under N_2. Yield of isolated product is reported unless noted. *These products cannot be isolated efficiently because of similar polarity to by-product and the low yield. ^{1}H NMR yield was determined using 1,3,5-trimethylbenzene as an internal standard based on the previous literature.[20] **The side reaction was observed by the standard ^{1}H NMR peaks of side product **6.4*** and **6.5***.

6.2.3 Chemoselectivity study

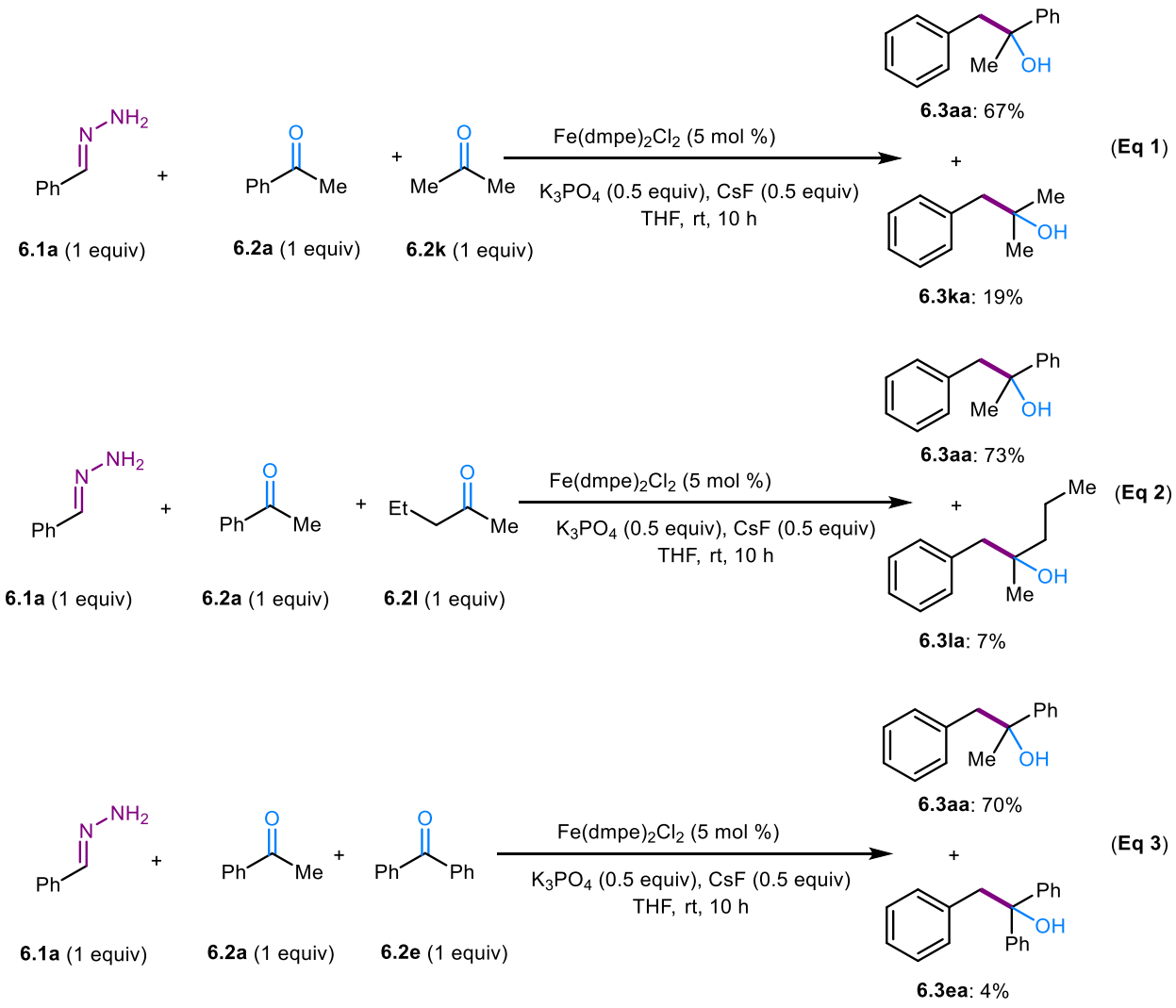

Scheme 6.2 Chemoselectivity study of 1,2-addition of hydrazone with carbonyls

To study the chemoselectivity of this reaction, we designed a competing experiment shown in Scheme 4. Using a 1:1 mixture of acetophenone and acetone, the nucleophilic addition of acetophenone was much more favored than acetone, suggesting higher reactivity of acetophenone derivatives than aliphatic ketones for such reactions (Eq. 1). Replacing acetone with a long-chain aliphatic ketone increased the product ratio in favor of the acetophenone addition product (Eq. 2). The reactivity of benzophenone is also much lower than acetophenone probably due to its high steric effect as previously mentioned (Eq. 3). Based on these analyses, we concluded that

acetophenone derivatives are more reactive for this transformation than other kinds of ketone substrates.

6.2.4 Mechanistic study

Table 6.6 Control experiments for catalysts and additives

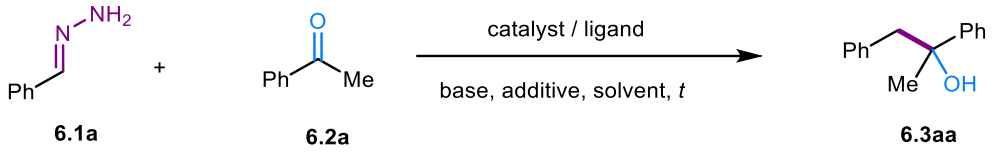

6.1a **6.2a** **6.3aa**

entry	catalyst	ligand	base	additive	solvent	*t* (°C)	yield (%)
1	$Fe(dmpe)_2Cl_2$	-	K_3PO_4	-	THF	rt	95
2	$Fe(dmpe)_2Cl_2$	-	K_3PO_4	CsF	THF	rt	99
3	$Fe(dmpe)_2Br_2$	-	K_3PO_4	-	THF	rt	40
4	$Fe(dmpe)_2Br_2$	-	K_3PO_4	CsF	THF	rt	90
5	$Fe(dmpe)_2Cl_2$	-	K_3PO_4	NaF	THF	rt	93
6	$Fe(dmpe)_2Cl_2$	-	K_3PO_4	KF	THF	rt	99
7	$Fe(dmpe)_2Cl_2$	-	K_3PO_4	MgF_2	THF	rt	81
8	$Fe(dmpe)_2Cl_2$	-	K_3PO_4	CsCl	THF	rt	93
9	FeF_2	dmpe	K_3PO_4	-	THF	rt	0

General reaction conditions: **6.1a** (0.25 mmol), **6.2a** (0.2 mmol), [Fe] catalyst (5 mol %), ligand (5 mol %), base (50 mol %), additive (50 mol %), solvent (0.2 mL) under N_2. **1a** solution was treated by 4Å molecular sieves beforehand. ^{1}H NMR yield was determined using 1,3,5-trimethoxybenzene as the internal standard.

To further understand the reaction and explore the role of each component in the reaction system, we performed several control experiments (Table 6.6). The following results were observed: (a) the halide ion has a strong influence on the reaction (Table 6.6, entries 1 and 3) with $Fe(dmpe)_2Br_2$ showing low catalytic activity possibly due to the low ligand exchange rate of bromide anions with hydrazone (anions) on [Fe] than chloride anions; (b) the addition of CsF helped both $Fe(dmpe)_2Cl_2$ and $Fe(dmpe)_2Br_2$ systems, exerting a more prominent effect on the latter (Table 6.6, entries 2 and 4); (c) examining different fluoride salts (Table 6.6, entries 5–7) showed that a higher Lewis acidity of the cation tended to decrease the product yield, with the most Lewis acidic MgF_2 giving only

81% of the corresponding product, possibly by increasing the rate of the hydrazone hydrolysis or other side reactions.

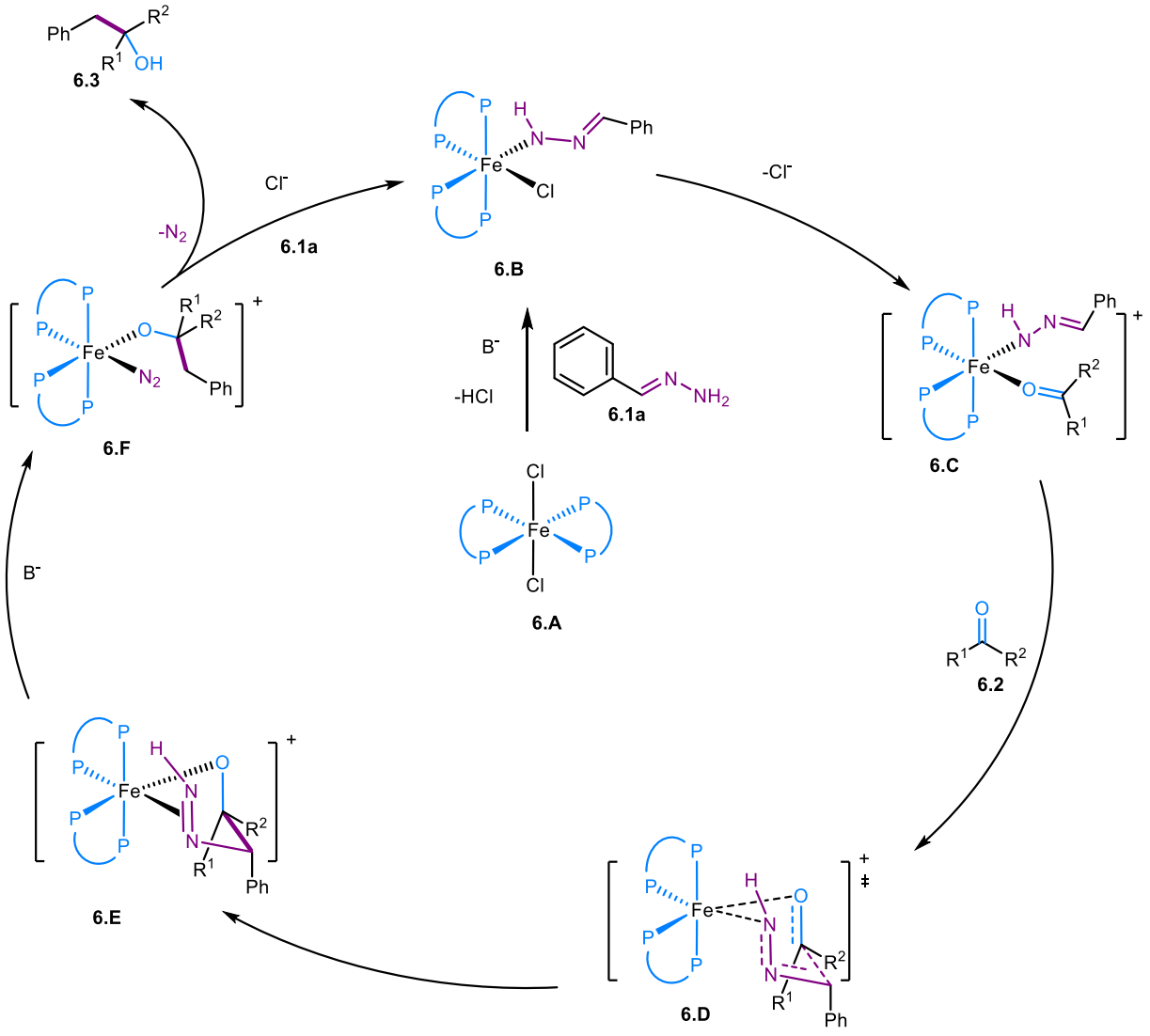

Scheme 6.3 Plausible mechanism for iron-catalyzed hydrazone addition

Based on analysis of the above experimental results in combination with the literature studies[39, 42–44], a tentative mechanism was proposed for this reaction as is shown in Scheme 5. Using the carbonyl addition reaction as an example, a ligand exchange initially occurs between the iron-phosphine complex **6.A** and hydrazone to form iron–amido complex **6.B** in the presence of base. This is followed by a ligand dissociation of chloride anion to generate a cationic iron complex **6.C**.[39] By activating the incoming carbonyl compounds, this more Lewis acidic cationic complex

6.C facilitates the C–C bond formation, presumably *via* a similar six-membered ring transition state **6.D** proposed earlier.[19] Finally, protonation of iron–oxygen bond gives rise to the corresponding alcohols, with concomitant exclusion of N_2 and regeneration of active catalyst **6.B**. As H_2O will adversely influence the reaction by coordinating with iron to form iron–hydroxide or iron–oxide complexes, especially under the basic conditions,[48] fluoride anion might compete with H_2O or OH^- to coordinate with iron, thus inhibiting the hydrolysis process and facilitating the reaction.

6.3 Conclusion

In conclusion, we have successfully utilized earth–abundant and well–defined iron complexes to catalyze the nucleophilic addition of hydrazones to a broad scope of carbonyl compounds, imines and Michael acceptors at room temperature, which not only marks the first abundant metal–catalyzed nucleophilic reaction of organic carbanion equivalent, but also opens a new chapter in the field of iron catalysis. In addition, chemoselectivity of different kinds of carbonyl groups can be realized. The mechanism and the applications of this reaction and this catalytic system are under further investigation.

6.4 Experimental section

6.4.1 General experimental information

Reaction Setup: All reactions were carried out in flame-dried V-shaped microwave reaction vials which were covered by aluminum seals with PTFE-faced silicone septa, under an atmosphere of nitrogen unless otherwise stated. All reaction temperatures corresponded to oil bath temperatures. All air and moisture-sensitive catalysts, ligands, and reagents were stored and charged in MBRAUN UNIlab Pro Glove Box Workstation unless otherwise stated.

Purifications: All work-up and purification procedures were carried out with reagent-grade solvents. Analytical thin-layer chromatography (TLC) was performed using E. Merck silica gel 60 F254 pre-coated plates (0.25 mm). Flash column chromatography was performed with E. Merck silica gel P60 (40–63 μm particle size, 230–400 mesh) (SiO_2). Unless otherwise specified, 'SiO_2' refers to P60 grade silica gel. Visualization was accomplished with UV light and/or iodine (I_2) or Vanillin solution. Retention factor (R_f) values reported were measured using a 10 × 2 cm TLC

plate in a developing chamber containing the solvent system (10 mL) described. Automated flash column chromatography was performed on Biotage Isolera™ Spektra Systems with ACI™.

Solvents: tetrahydrofuran (THF), dimethyl sulfoxide (DMSO) and toluene were taken directly from the Pure Solvent MD-7 purification system (Innovative Technology). Solvents for filtration, transfers and chromatography, were dichloromethane (CH_2Cl_2) (ACS grade, amylene stabilized), acetone (ACS grade), ethyl acetate (EtOAc) (Fisher, ACS grade), hexane (Fisher, ACS grade), pentane (ACS grade), methanol (ACS grade).

Chemicals: In the model study, benzaldehyde (Aldrich) and acetophenone (Aldrich) were distilled prior to use. Other chemicals that are commercially available and were used without further purification: $FeCl_3$ (Aldrich), $FeCl_2$ (Aldrich), dppe (Strem), dmpe (Aldrich & Aspira), dppp (Aldrich), dppf (Aldrich), BINAP (Aldrich), potassium *tert*-butoxide (Aldrich), potassium phosphate (Aldrich), potassium carbonate (Aldrich), DABCO (Aldrich), cesium fluoride (Aldrich & Aspira), hydrazine hydrate (Reagent Grade, 64–65% wt, Aldrich), mesitylene (Aldrich), 1,3,5-trimethoxylbenzene (Aldrich), anhydrous sodium sulfate. All liquid carbonyls were distilled, and solid ones were recrystallized prior to use. $Fe(dmpe)_2Cl_2$ and $[Fe(dmpe)_2Cl_2]^+[FeCl_4]^-$ was prepared following the literature procedure.[37] The aromatic imine substrates (substrates in Scheme 3) were synthesized following the previous literatures.[53, 54]

NMR Spectroscopy: Nuclear magnetic resonance (^1H and ^{13}C NMR) spectra were recorded on a Bruker AV500 equipped with a 60-position Sample Xpress sample changer (^1H, 500 MHz; ^{13}C, 125 MHz), a Varian MERCURY plus-500 spectrometer (^1H, 500 MHz; ^{13}C, 125 MHz) or Bruker AV400 spectrometer (^1H, 400 MHz; ^{13}C, 100 MHz). Chemical shifts for both ^1H NMR and ^{13}C NMR spectra are expressed in parts per million (ppm) units downfield from TMS, with the solvent residue peak as the chemical shift standard ($CDCl_3$: δ 7.28 ppm in ^1H NMR; δ 77.00 ppm in ^{13}C NMR). Data are reported as following: chemical shift, multiplicity (s = singlet, d = doublet, dd = doublet of doublets, t = triplet, td = triplet of doublets, q = quartet, quin = quintet, sep = septet, m = multiplet, br = broad singlet), coupling constants *J* (Hz), and integration.

Mass Spectrometry: Mass spectrometry (MS) was performed by the McGill Chemistry Department Mass Spectrometry Facility. High resolution mass spectra were recorded using electrospray ionization (ESI+) and/or atmospheric pressure chemical ionization APCI (+/-), performed either on 'Exactive Plus Orbitrap' a ThermoScientific high resolution accurate mass

(HR/AM) FT mass spectrometer, or a Bruker Daltonics Maxis Impact quadrupole-time of flight (QTOF) mass spectrometer.

Characterization of Products: The following products were newly synthesized compounds in this article: **6.3ga**, **6.3ia**, **6.3pa**, and for these products, we report NMR spectra and HRMS data. The rest are known compounds which were noted with references in spectroscopic data section and we only reported the NMR data.

6.4.2 Experimental procedures

6.4.2.1 Preparation of hydrazone solution

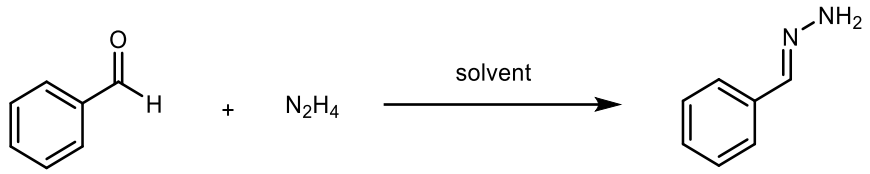

6.0a **6.1a**

Procedure A: For Table 6.1, Table 6.2 (entries 1–11): Solvent (2 mL) was added first in a small bottle with a stir bar. Then, the hydrazine monohydrate (0.17 mL, 3.5 mmol) was added into the bottle. After that, **6.0a** (0.25 mL, 2.5 mmol) was added dropwise into the stirred solution and the mixture was stirred for 5 min. Next, proper amount of anhydrous Na_2SO_4 was added to remove water. Finally, after stirring for another 3h, the so-formed solution was ready to use.

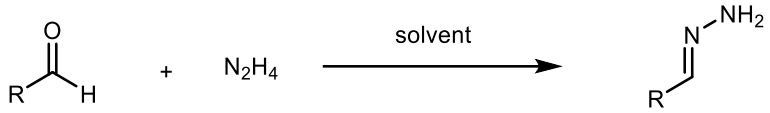

6.0 **6.1**

Procedure B: For Table 6.2, entries 12–13, Table 6.3, Table 6.4: Solvent (2 mL) was added first in a small bottle with a stir bar. Then, hydrazine monohydrate (0.17 mL, 3.5 mmol) was added into the bottle. After that, **0** (0.25 mL, 2.5 mmol) was added dropwise into the stirred solution and the mixture was stirred for 5 min. Next, proper amount of anhydrous Na_2SO_4 was added to remove water. After stirring for another 3h, the so-formed solution was transferred to another same sized bottle with proper amount of activated 4Å molecular sieve to further remove water. Finally, the solution was kept for 2 more hours before it can be used.

Procedure C: For Table 6.4: Solvent (5 mL) was added first in a small bottle with a stir bar. Then, hydrazine monohydrate (0.68 mL, 14 mmol) was added into the bottle. After that, **6.0a** (1.00 mL, 10.0 mmol) was added dropwise into the stirred solution and the mixture was stirred for 5 min. Next, proper amount of anhydrous Na_2SO_4 was added to remove water. After stirring for another 3 h, the so-formed solution was transferred to a capacity bottle (10 mL) and diluted to 10 mL, and then transferred the solution into another bottle with proper amount of activated 4Å molecular sieve to further remove water. Finally, the solution was kept for 2 more hours before it can be used as accurate 1M hydrazone solution.

6.4.2.2 General procedure for Table 6.3–6.5

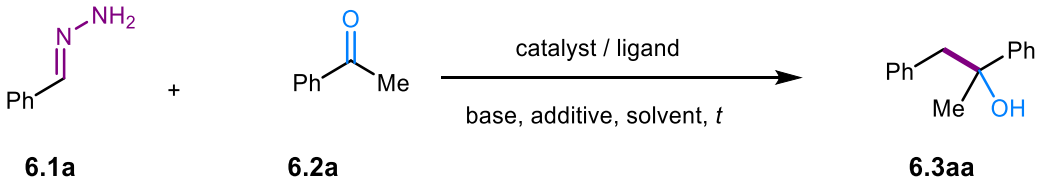

6.1a **6.2a** **6.3aa**

General procedure for reaction condition exploration: catalyst (0.01 mmol) and base (0.1 mmol) were added into a V-shaped reaction tube with a stir bar. Then, the ligand (0.01 mmol) and additive (0.1 mmol) were added in the glovebox (filled by N_2). After that, **6.1a** solution (prepared through ***Procedure A*** or ***Procedure B***, 0.22 mL, 0.25 mmol) was added first and followed by the addition of **2a** (24 μL, 0.2 mmol). The mixture was stirred for 24h. Then, 1,3,5-trimethoxylbenzene (11.2 mg, 0.067 mmol) was added in the mixture as standard. Then, one drop of solution was diluted by $CDCl_3$ to run the ^1H NMR test to determine the ^1H NMR yield.

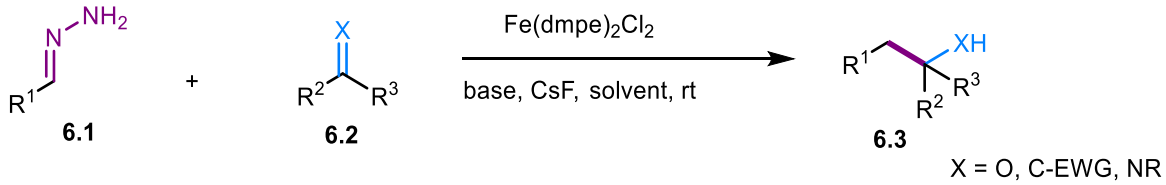

6.1 **6.2** **6.3**

General procedure for Table 6.3, Table 6.5, Condition A(1): $Fe(dmpe)_2Cl_2$ (0.01 mmol) and K_3PO_4 (0.1 mmol) were added into a V-shaped reaction tube with a stir bar. Then, CsF (0.1 mmol) was added in the glovebox (filled by N_2). After that, **6.1** solution (prepared through ***Procedure B***, 0.22 mL THF solution, 0.25 mmol) was added first and followed with the addition of **6.2** (0.2 mmol) (if **6.2** was a solid, it was added before entering the glovebox). The mixture was stirred for

24 h. Then, for ^{1}H NMR yield, 1,3,5-trimethylbenzene (9.3 μL, 0.067 mmol) was added in the mixture as standard. Then, one drop of solution was diluted by $CDCl_3$ to do the ^{1}H NMR test to determine the ^{1}H NMR yield. For separation of product, the reaction mixture was filtered through a silica plug with 2-3 mL EtOAc. The solvent was removed by rotary evaporator and the residue was purified by column chromatography (using hexane and ethyl acetate as eluent) to give the pure product.

General procedure for Table 6.4, Condition A(2): $Fe(dmpe)_2Cl_2$ (0.01 mmol) and K_3PO_4 (0.1 mmol) were added into a V-shaped reaction tube with a stir bar. Then, CsF (0.1 mmol) was added in the glovebox (filled by N_2). After that, **6.1** solution (prepared through ***Procedure C***, 0.2 mL THF solution, 0.2 mmol) was added first and followed by the addition of **2** (0.2 mmol) (if **6.2** was a solid, it was added before entering the glovebox). The mixture was stirred for 24 h. Then, for ^{1}H NMR yield, 1,3,5-trimethylbenzene (9.3 μL, 0.067 mmol) was added in the mixture as standard. Then, one drop of solution was diluted by $CDCl_3$ to do the ^{1}H NMR test to determine the ^{1}H NMR yield. For product separation, the reaction mixture was filtered through a silica plug with 2-3 mL EtOAc. The solvent was removed by rotary evaporator and the residue was purified by column chromatography (using hexane and ethyl acetate as eluent) to give the pure product.

General procedure for Table 6.3, Condition B: $Fe(dmpe)_2Cl_2$ (0.01 mmol) and K_3PO_4 (0.1 mmol) were added into a V-shaped reaction tube with a stir bar. Then, CsF (0.1 mmol) was added in the glovebox (filled by N_2). After that, **6.1** solution (prepared through ***Procedure B***, 0.22 mL DMSO solution, 0.25 mmol) was added first and followed by the addition of **2** (0.2 mmol) (if **6.2** was a solid, it was added before entering the glovebox). The mixture was stirred for 24 h. Then, for ^{1}H NMR yield, 1,3,5-trimethylbenzene (9.3 μL, 0.067 mmol) was added in the mixture as standard. Then, one drop of solution was diluted by $CDCl_3$ to do the ^{1}H NMR test to determine the ^{1}H NMR yield. For separating the product, the reaction mixture was filtered through a silica plug with 2-3 mL EtOAc. The solvent was removed by rotary evaporator and the residue was purified by column chromatography (using hexane and ethyl acetate as eluent) to give the pure product.

General procedure for Table 6.3, Condition C: $Fe(dmpe)_2Cl_2$ (0.01 mmol) and ^{t}BuOK (0.1 mmol) were added into a V-shaped reaction tube with a stir bar. Then, CsF (0.1 mmol) was added in the glovebox (filled by N_2). After that, **6.1** solution (prepared through ***Procedure B***, 0.22 mL THF solution, 0.25 mmol) was added first and the mixture was stirred for 5 min. Then, **6.2** (0.2 mmol)

was added. The mixture was stirred for 12 h. Afterwards, for ^{1}H NMR yield, 1,3,5-trimethylbenzene (9.3 µL, 0.067 mmol) was added in the mixture as standard. Then, one drop of solution was diluted by $CDCl_3$ to run the ^{1}H NMR test to determine the ^{1}H NMR yield. For product separation, the reaction mixture was filtered through a silica plug with 2-3 mL EtOAc. The solvent was removed by rotary evaporator and the residue was purified by column chromatography (using hexane and ethyl acetate as eluent) to give the pure product.

6.4.2.3 Procedure for competing reaction to test chemoselectivity

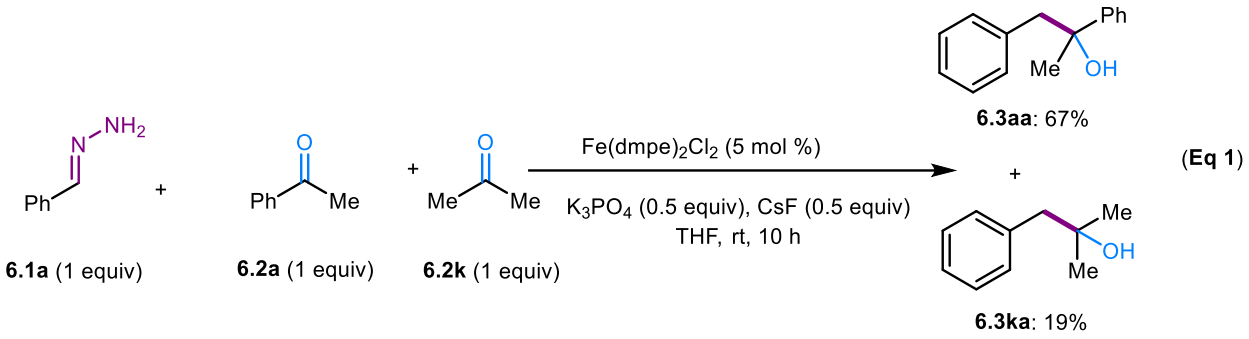

6.1a (1 equiv) **6.2a** (1 equiv) **6.2k** (1 equiv)

6.3aa: 67%

6.3ka: 19%

(**Eq 1**)

(**Eq 1**): $Fe(dmpe)_2Cl_2$ (0.01 mmol) and K_3PO_4 (0.1 mmol) were added into a V-shaped reaction tube with a stir bar. Then, CsF (0.1 mmol) was added in the glovebox (filled by N_2). After that, **6.1** solution (prepared through ***Procedure C***, 0.2 mL THF solution, 0.2 mmol) was added first and followed by the addition of the mixture of **6.2a** (0.2 mmol) and **6.2k** (0.2 mmol). The mixture was stirred for 10 h. Then, 1,3,5-trimethylbenzene (9.3 µL, 0.067 mmol) was added in the mixture as standard. Then, one drop of solution was diluted by $CDCl_3$ to do the ^{1}H NMR with 67% for **6.3aa** and 19% for **6.3ka**.

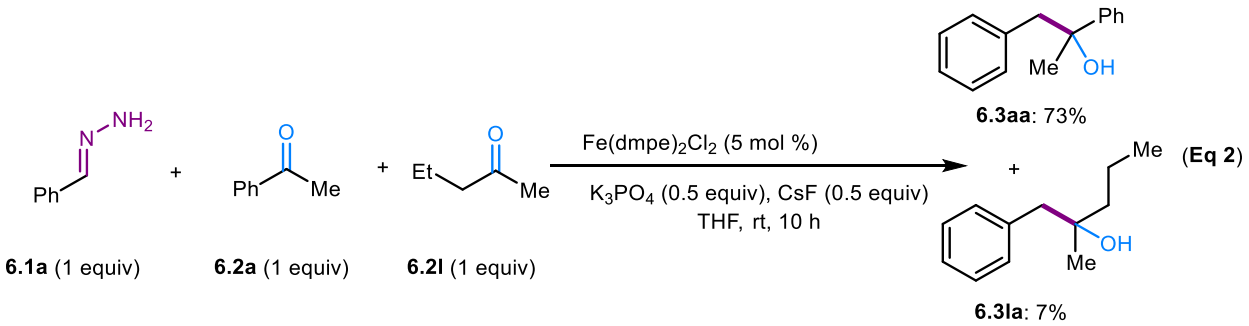

6.1a (1 equiv) **6.2a** (1 equiv) **6.2l** (1 equiv)

6.3aa: 73%

6.3la: 7%

(**Eq 2**)

(**Eq 2**): $Fe(dmpe)_2Cl_2$ (0.01 mmol) and K_3PO_4 (0.1 mmol) were added into a V-shaped reaction tube with a stir bar. Then, CsF (0.1 mmol) was added in the glovebox (filled by N_2). After that, **6.1** solution (prepared through ***Procedure C***, 0.2 mL THF solution, 0.2 mmol) was added first and

followed by the addition of the mixture of **6.2a** (0.2 mmol) and **6.2l** (0.2 mmol). The mixture was stirred for 10 h. Then, 1,3,5-trimethylbenzene (9.3 μL, 0.067 mmol) was added in the mixture as standard. Then, one drop of solution was diluted by $CDCl_3$ to do the ^1H NMR with 73% for **6.3aa** and 7% for **6.3la**.

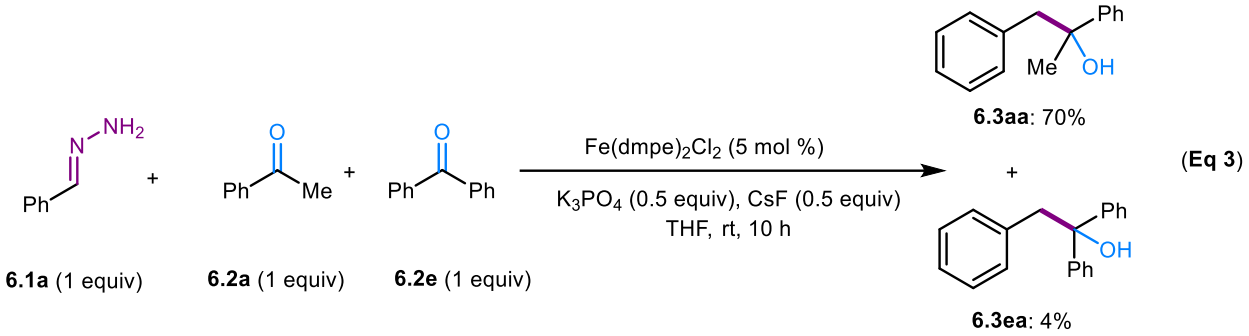

(**Eq 3**): $Fe(dmpe)_2Cl_2$ (0.01 mmol) and K_3PO_4 (0.1 mmol), **6.2e** (0.2 mmol) were added into a V-shaped reaction tube with a stir bar. Then, CsF (0.1 mmol) was added in the glovebox (filled by N_2). After that, **6.1** solution (prepared through ***Procedure C***, 0.2 mL THF solution, 0.2 mmol) was added first and followed by the addition of **6.2a** (0.2 mmol). The mixture was stirred for 10 h. Then, 1,3,5-trimethylbenzene (9.3 μL, 0.067 mmol) was added in the mixture as standard. Then, one drop of solution was diluted by $CDCl_3$ to do the ^1H NMR with 70% for **6.3aa** and 4% for **6.3la**.

6.4.3 Spectroscopic data of products

Note: references of the characterization data of known compounds are marked before our NMR experimental data.

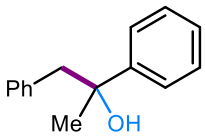

6.3aa

(Generated following ***Condition A(1)*** and isolated by column chromatography on silica gel with hexane: EtOAc = 96:4 as eluent, colorless oil, 43 mg, yield: 99%) [19]: **^{1}H NMR** (500 MHz, $CDCl_3$) δ 7.47 (s, 2H), 7.39 (t, *J* = 7.6 Hz, 2H), 7.35 – 7.22 (m, 4H), 7.11 – 7.02 (m, 2H), 3.20 (d, *J* = 13.3 Hz, 1H), 3.09 (d, *J* = 13.3 Hz, 1H), 1.99 (s, 1H), 1.63 (s, 3H). **^{13}C NMR** (126 MHz, $CDCl_3$) δ 147.5, 136.7, 130.5, 128.0, 126.6, 126.6, 124.9, 74.4, 50.4, 29.3.

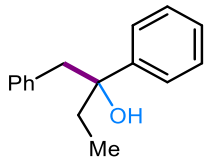

6.3ba

(Generated following ***Condition A(1)*** and isolated by column chromatography with hexane: EtOAc = 96:4 as eluent, colorless oil, 44 mg, yield: 97%) [19]:**^{1}H NMR** (500 MHz, $CDCl_3$) δ 7.46 – 7.33 (m, 4H), 7.33 – 7.16 (m, 4H), 7.01 (dd, *J* = 6.6, 2.9 Hz, 2H), 3.21 (d, *J* = 13.3 Hz, 1H), 3.10 (d, *J* = 13.3 Hz, 1H), 2.04 (dq, *J* = 14.8, 7.5 Hz, 1H), 1.96 – 1.80 (m, 2H), 0.89 – 0.74 (m, 3H). **^{13}C NMR** (126 MHz, $CDCl_3$) δ 145.4, 136.4, 130.6, 128.0, 127.9, 126.6, 126.4, 125.6, 76.9, 49.4, 34.5, 7.8.

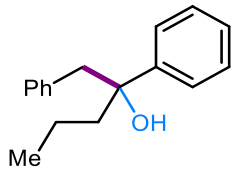

6.3ca

(Generated following ***Condition A(1)*** and isolated by column chromatography on silica gel with hexane: EtOAc = 96:4 as eluent, colorless oil, 45 mg, yield: 93%): **^{1}H NMR** (500 MHz, $CDCl_3$) δ 7.44 – 7.31 (m, 4H), 7.31 – 7.14 (m, 4H), 7.07 – 6.90 (m, 2H), 3.19 (d, *J* = 13.3 Hz, 1H), 3.09 (d, *J* = 13.3 Hz, 1H), 1.97 (ddd, *J* = 13.8, 12.1, 4.5 Hz, 1H), 1.89 – 1.73 (m, 2H), 1.48 – 1.27 (m, 1H), 1.17 – 0.99 (m, 1H), 0.88 (t, *J* = 7.4 Hz, 3H). **^{13}C NMR** (126 MHz, $CDCl_3$) δ 145.8, 136.4, 130.6, 128.0, 127.9, 126.6, 126.3, 125.4, 49.7, 44.3, 16.8, 14.4. **HRMS:** (ESI, *m*/*z*): calcd. for $C_{17}H_{20}ONa[M+Na]^+$ 263.1406, found: 263.1407.

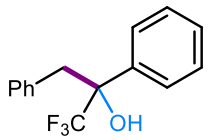

6.3da

(Generated following ***Condition A(1)*** and isolated by column chromatography on silica gel with hexane: EtOAc = 80:20 as eluent, colorless oil, 48 mg, yield: 91%) [19]: **^{1}H NMR** (500 MHz, $CDCl_3$) δ 7.70 – 7.50 (m, 2H), 7.50 – 7.33 (m, 3H), 7.33 – 7.15 (m, 3H), 7.15 – 6.90 (m, 2H), 3.60 – 3.37 (m, 2H), 2.50 (s, 1H). **^{13}C NMR** (126 MHz, $CDCl_3$) δ 137.0, 133.0, 130.7, 128.5, 128.4, 128.2,

127.5, 126.4, 125.5 (q, J = 284.8 Hz), 77.0 (q, J = 27.7 Hz), 41.8. **^{19}F NMR** (471 MHz, $CDCl_3$) δ -78.3.

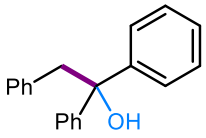

6.3ea

(Generated following ***Condition A(1)*** and isolated by column chromatography on silica gel with hexane: EtOAc = 90:10 as eluent, white solid, 28 mg, yield: 50%) [19]: **^{1}H NMR** (500 MHz, $CDCl_3$) δ 7.59 – 7.43 (m, 4H), 7.35 (dd, J = 8.5, 6.9 Hz, 4H), 7.31 – 7.25 (m, 2H), 7.25 – 7.16 (m, 3H), 7.00 – 6.91 (m, 2H), 3.70 (s, 2H), 2.37 (s, 1H). **^{13}C NMR** (126 MHz, $CDCl_3$) δ 146.5, 135.7, 130.8, 128.0, 128.0, 126.8, 126.7, 126.1, 77.8, 47.9.

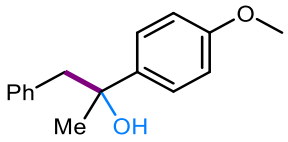

6.3fa

(Generated following ***Condition A(1)*** and isolated by column chromatography on silica gel with hexane: EtOAc = 92:8 as eluent, colorless oil, 44 mg, yield: 91%) [19]: **^{1}H NMR** (500 MHz, $CDCl_3$) δ 7.36 – 7.31 (m, 2H), 7.27 – 7.20 (m, 3H), 7.02 (dd, J = 7.3, 2.4 Hz, 2H), 6.91 – 6.85 (m, 2H), 3.84 (s, 3H), 3.13 (d, J = 13.3 Hz, 1H), 3.03 (d, J = 13.3 Hz, 1H), 1.83 (s, 1H), 1.57 (s, 3H). **^{13}C NMR** (126 MHz, $CDCl_3$) δ 158.3, 139.7, 136.9, 130.6, 128.0, 126.6, 126.2, 113.3, 74.2, 55.2, 50.6, 29.4.

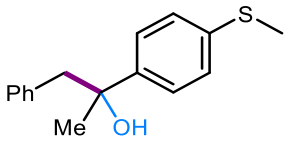

6.3ga

(Generated following ***Condition A(1)*** and isolated by column chromatography on silica gel with hexane: EtOAc = 95:5 as eluent, white solid, 44 mg, yield: 85%): **^{1}H NMR** (500 MHz, $CDCl_3$) δ 7.41 – 7.32 (m, 2H), 7.32 – 7.18 (m, 5H), 7.10 – 6.99 (m, 2H), 3.14 (d, J = 13.3 Hz, 1H), 3.04 (d, J = 13.3 Hz, 1H), 2.52 (s, 3H), 1.90 (s, 1H), 1.57 (s, 3H). **^{13}C NMR** (126 MHz, $CDCl_3$) δ 144.6,

136.6, 136.4, 130.6, 128.0, 126.6, 126.3, 125.6, 74.2, 50.4, 29.4, 15.9. **HRMS:** (ESI, *m*/*z*): calcd. for $C_{16}H_{18}OSNa[M+Na]^+$ 281.0971, found: 281.0970.

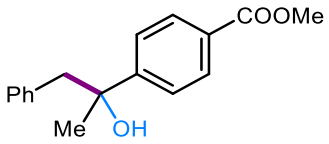

6.3ha

(Generated following ***Condition A(1)*** and isolated by column chromatography on silica gel with hexane: EtOAc = 90:10 as eluent, colorless oil, 40 mg, yield: 75%) [19]: **^{1}H NMR** (500 MHz, $CDCl_3$) δ 8.09 – 7.94 (m, 2H), 7.56 – 7.42 (m, 2H), 7.30 – 7.18 (m, 3H), 6.99 (dd, *J* = 6.6, 3.0 Hz, 2H), 3.94 (s, 3H), 3.16 (d, *J* = 13.4 Hz, 1H), 3.06 (d, *J* = 13.4 Hz, 1H), 2.02 (s, 1H), 1.61 (s, 3H). **^{13}C NMR** (126 MHz, $CDCl_3$) δ 167.0, 152.7, 136.1, 130.5, 129.4, 128.5, 128.1, 126.8, 125.1, 77.2, 74.5, 52.0, 50.2, 29.4.

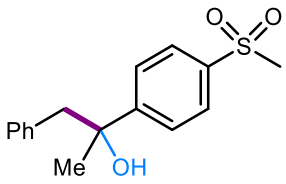

6.3ia

(Generated following ***Condition A(1)*** and isolated by column chromatography on silica gel with hexane: EtOAc = 60:40 as eluent, white solid, 48 mg, yield: 82%): **^{1}H NMR** (500 MHz, $CDCl_3$) δ 7.98 – 7.83 (m, 1H), 7.72 – 7.58 (m, 1H), 7.34 – 7.19 (m, 2H), 7.09 – 6.95 (m, 1H), 3.19 – 3.00 (m, 3H), 1.60 (s, 2H). **^{13}C NMR** (126 MHz, $CDCl_3$) δ 154.0, 138.6, 135.7, 130.4, 128.2, 127.1, 126.9, 126.1, 74.3, 50.2, 44.5, 29.3. **HRMS:** (ESI, *m*/*z*): calcd. for $C_{16}H_{18}O_3SNa[M+Na]^+$ 313.0869, found: 313.0865.

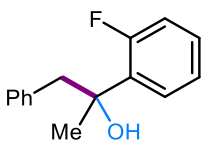

6.3ja

(Generated following ***Condition A(1)*** and isolated by column chromatography on silica gel with hexane: EtOAc = 96:4 as eluent, colorless oil, 40 mg, yield: 87%) [19]: **^{1}H NMR** (500 MHz, $CDCl_3$) δ 7.37 (m, 1H), 7.32 – 7.17 (m, 4H), 7.08 (m, 4H), 3.38 (d, *J* = 13.4 Hz, 1H), 3.16 (d, *J* = 13.4 Hz, 1H), 2.15 (s, 1H), 1.69 (s, 3H). **^{13}C NMR** (126 MHz, $CDCl_3$) δ 159.5 (d, *J* = 244 Hz), 136.5, 133.9 (d, *J* = 12.6 Hz), 130.4, 128.7 (d, *J* = 8.82 Hz), 128.1, 127.4 (d, *J* = 5.04), 126.7, 123.9 (d, *J* = 2.52 Hz), 115.8 (d, *J* = 23.9 Hz), 73.5 (d, *J* = 5.04 Hz), 48.0 (d, *J* = 3.78), 28.2 (d, *J* = 3.78). **^{19}F NMR** (471 MHz, $CDCl_3$) δ -112.8.

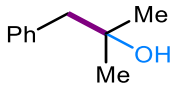

6.3ka

(Generated following ***Condition A(1)***, volatile colorless oil. Yield calculation was based on ^{1}H NMR. Isolation of pure product for NMR was based on column chromatography on silica gel with hexane: EtOAc = 90:10 as eluent)[19]: **^{1}H NMR** (500 MHz, Chloroform-d) δ 7.34 (dd, *J* = 8.0, 6.6 Hz, 2H), 7.31 – 7.17 (m, 3H), 2.80 (s, 2H), 1.42 (s, 1H), 1.26 (s, 6H). **^{13}C NMR** (126 MHz, $CDCl_3$) δ 137.7, 130.4, 128.2, 126.5, 70.7, 49.7, 29.2.

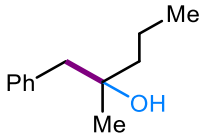

6.3la

(Generated following ***Condition A(1)*** and isolated by column chromatography on silica gel with hexane: EtOAc = 96:4 as eluent, colorless oil, 26 mg, yield: 75%) [55]: **^{1}H NMR** (500 MHz, $CDCl_3$) δ 7.39 – 7.31 (m, 2H), 7.31 – 7.19 (m, 3H), 2.88 – 2.69 (m, 2H), 1.54 – 1.41 (m, 4H), 1.35 (s, 1H), 1.17 (s, 3H), 1.02 – 0.92 (m, 3H). **^{13}C NMR** (126 MHz, $CDCl_3$) δ 137.6, 130.5, 128.1, 126.4, 72.5, 48.0, 44.2, 26.5, 17.2, 14.6.

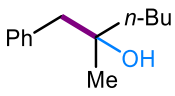

6.3ma

(Generated following ***Condition A(1)*** and isolated by column chromatography on silica gel with hexane: EtOAc = 96:4 as eluent, colorless oil, 20 mg, yield: 52%) [56]: **^{1}H NMR** (500 MHz, $CDCl_3$)

δ 7.39 – 7.30 (m, 1H), 7.30 – 7.16 (m, 2H), 2.87 – 2.71 (m, 1H), 1.54 – 1.26 (m, 4H), 1.17 (s, 2H), 0.95 (t, *J* = 7.2 Hz, 2H). **^{13}C NMR** (126 MHz, $CDCl_3$) δ 137.6, 130.5, 128.1, 126.4, 72.5, 47.9, 41.6, 26.5, 26.2, 23.2, 14.1.

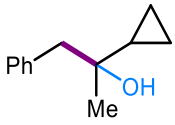

6.3na

(Generated following ***Condition A(1)*** and isolated by column chromatography on silica gel with hexane: EtOAc = 96:4 as eluent, colorless oil, 31 mg, yield: 88%) [19]: **^{1}H NMR** (500 MHz, $CDCl_3$) δ 7.39 – 7.19 (m, 5H), 2.97 – 2.78 (m, 2H), 1.19 (s, 1H), 1.13 (s, 3H), 0.99 – 0.88 (m, 1H), 0.49 – 0.28 (m, 4H). **^{13}C NMR** (126 MHz, $CDCl_3$) δ 137.5, 130.6, 128.0, 126.3, 71.0, 49.1, 25.9, 20.8, 0.75, 0.72.

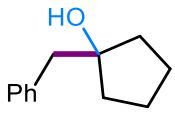

6.3oa

(Generated following ***Condition A(1)*** and isolated by column chromatography on silica gel with hexane: EtOAc = 92:8 as eluent, colorless oil, 24 mg, yield: 69%) [57]: **^{1}H NMR** (500 MHz, $CDCl_3$) δ 7.39 – 7.31 (m, 2H), 7.31 – 7.21 (m, 3H), 2.91 (s, 2H), 1.84 (tdd, *J* = 8.8, 6.5, 3.7 Hz, 2H), 1.77 – 1.64 (m, 4H), 1.64 – 1.53 (m, 2H), 1.33 (s, 1H). **^{13}C NMR** (126 MHz, $CDCl_3$) δ 138.3, 130.1, 128.2, 126.4, 82.1, 47.0, 39.3, 23.5.

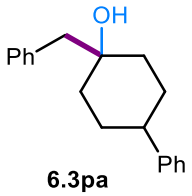

6.3pa

(Generated following ***Condition A(1)*** and isolated by column chromatography on silica gel with hexane: EtOAc = 92:8 as eluent, white solid, 44 mg, yield: 83%): **^{1}H NMR** (500 MHz, $CDCl_3$) δ 7.43 – 7.26 (m, 9H), 7.26 – 7.18 (m, 1H), 2.84 (s, 2H), 2.51 (tt, *J* = 12.2, 3.7 Hz, 1H), 1.88 (qd, *J* = 13.4, 12.8, 3.8 Hz, 2H), 1.82 – 1.70 (m, 4H), 1.63 (td, *J* = 14.3, 13.7, 4.3 Hz, 2H), 1.29 (s, 1H).

^{13}C NMR (126 MHz, $CDCl_3$) δ 147.2, 136.9, 130.6, 128.3, 128.2, 126.8, 126.5, 125.9, 70.2, 50.4, 44.0, 37.3, 29.2. **HRMS:** (ESI, *m*/*z*): calcd. for $C_{19}H_{22}ONa[M+Na]^+$ 289.1563, found: 289.1562.

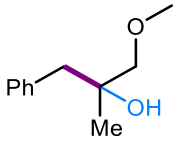

6.3qa

(Generated following ***Condition A(1)*** and isolated by column chromatography on silica gel with hexane: EtOAc = 90:10 as eluent, colorless oil, 30 mg, yield: 83%) [19]: **^{1}H NMR** (500 MHz, $CDCl_3$) δ 7.35 – 7.29 (m, 2H), 7.29 – 7.20 (m, 3H), 3.43 (s, 3H), 3.24 (d, *J* = 8.9 Hz, 1H), 3.18 (d, *J* = 8.9 Hz, 1H), 2.85 (s, 2H), 2.28 (s, 1H), 1.16 (s, 3H). **^{13}C NMR** (126 MHz, $CDCl_3$) δ 137.4, 130.4, 128.1, 126.3, 78.7, 72.3, 59.1, 45.1, 23.7.

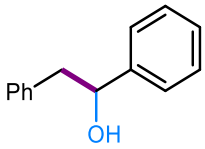

6.3ra

(Generated following ***Condition C*** and isolated by column chromatography on silica gel with hexane: EtOAc = 95:5 as eluent, colorless oil, 13 mg, yield: 32%) [19]: **^{1}H NMR** (500 MHz, $CDCl_3$) δ 7.41 – 7.30 (m, 6H), 7.34 – 7.20 (m, 3H), 4.93 (dd, *J* = 8.5, 4.8 Hz, 1H), 3.08 (dd, *J* = 13.7, 4.9 Hz, 1H), 3.02 (dd, *J* = 13.6, 8.4 Hz, 1H), 1.99 (s, 1H). **^{13}C NMR** (126 MHz, $CDCl_3$) δ 143.8, 138.0, 129.5, 128.5, 128.4, 127.6, 126.6, 125.9, 77.2, 75.3, 46.1.

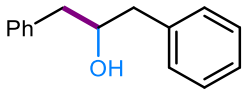

6.3sa

(Generated following ***Condition C*** and isolated by column chromatography on silica gel with hexane: EtOAc = 95:5 as eluent, colorless oil, 26 mg, yield: 61%) [58]: **^{1}H NMR** (500 MHz, $CDCl_3$) δ 7.35 (t, *J* = 7.6 Hz, 4H), 7.28 (dd, *J* = 7.6, 5.2 Hz, 6H), 4.17 – 4.03 (m, 1H), 2.90 (dd, *J* = 13.7, 4.6 Hz, 2H), 2.80 (dd, *J* = 13.7, 8.2 Hz, 2H), 1.70 (s, 1H). **^{13}C NMR** (126 MHz, $CDCl_3$) δ 138.4, 129.4, 128.5, 126.5, 73.6, 43.3.

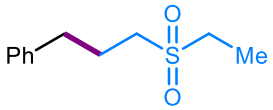

6.3ta

(Generated following ***Condition A(2)*** and isolated by column chromatography on silica gel with hexane: EtOAc = 85:15 as eluent, colorless oil, 24 mg, 57%) [21]: **^{1}H NMR** (500 MHz, $CDCl_3$) δ 7.33 (t, *J* = 7.5 Hz, 2H), 7.29 – 7.10 (m, 3H), 3.04 – 2.87 (m, 4H), 2.81 (t, *J* = 7.4 Hz, 2H), 2.28 – 2.11 (m, 2H), 1.38 (t, *J* = 7.5 Hz, 3H). **^{13}C NMR** (126 MHz, $CDCl_3$) δ 139.8, 128.6, 128.4, 126.5, 50.9, 47.1, 34.2, 23.4, 6.5.

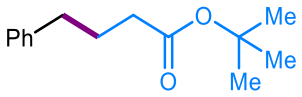

6.3ua

(Generated following ***Condition A(2)*** and isolated by column chromatography on silica gel with hexane: EtOAc = 97:3 as eluent, colorless oil, 24 mg, yield: 55%) [21]: **^{1}H NMR** (500 MHz, $CDCl_3$) δ 7.36 – 7.26 (m, 2H), 7.26 – 7.14 (m, 3H), 2.67 (t, *J* = 7.5 Hz, 2H), 2.27 (t, *J* = 7.5 Hz, 2H), 2.01 – 1.89 (m, 2H), 1.48 (s, 9H). **^{13}C NMR** (126 MHz, $CDCl_3$) δ 172.9, 141.6, 128.5, 128.3, 125.9, 80.1, 35.1, 34.9, 28.1, 26.8.

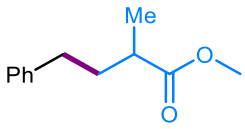

6.3va

(Generated following ***Condition A(2)*** and isolated by column chromatography on silica gel with hexane: EtOAc = 97:3 as eluent, colorless oil, 24 mg, yield: 61%) [21]: **^{1}H NMR** (500 MHz, $CDCl_3$) δ 7.36 – 7.26 (m, 2H), 7.26 – 7.16 (m, 3H), 3.71 (s, 3H), 2.65 (t, *J* = 8.0 Hz, 2H), 2.57 – 2.45 (m, 1H), 2.11 – 1.99 (m, 1H), 1.82 – 1.69 (m, 1H), 1.22 (d, *J* = 7.0 Hz, 3H). **^{13}C NMR** (126 MHz, $CDCl_3$) δ 177.0, 141.6, 128.4, 128.3, 125.9, 51.5, 38.9, 35.4, 33.5, 17.1.

6.3wa

(Generated following ***Condition A(2)***, volatile colorless to slight yellow oil, reported yield was determined by ^{1}H NMR. Isolation of pure product for NMR was based on Preparative Thin Layer Chromatography on silica gel with hexane: EtOAc = 5:1 as developing agent)[59]: **^{1}H NMR** (500 MHz, $CDCl_3$) δ 7.40 – 7.30 (m, 2H), 7.28 – 7.24 (m, 1H), 7.24 – 7.14 (m, 2H), 2.81 (t, *J* = 7.5 Hz, 2H), 2.35 (t, *J* = 7.1 Hz, 2H), 2.01 (p, *J* = 7.2 Hz, 2H). **^{13}C NMR** (126 MHz, $CDCl_3$) δ 139.7, 128.7, 128.4, 126.5, 119.5, 34.37, 26.9, 16.4.

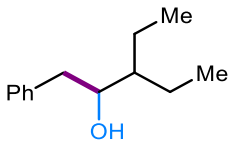

6.3xa

(Generated following ***Condition C*** and isolated by column chromatography on silica gel with hexane: EtOAc = 96:4 as eluent, colorless oil, 14 mg, yield: 37%) [19]: **^{1}H NMR** (500 MHz, $CDCl_3$) δ 7.38 – 7.30 (m, 2H), 7.30 – 7.16 (m, 3H), 3.86 (dt, *J* = 8.1, 3.8 Hz, 1H), 2.86 (dd, *J* = 13.6, 3.2 Hz, 1H), 2.65 (dd, *J* = 13.6, 9.7 Hz, 1H), 1.67 – 1.30 (m, 6H), 0.97 (q, *J* = 7.5 Hz, 6H). **^{13}C NMR** (126 MHz, $CDCl_3$) δ 139.4, 129.3, 128.6, 126.4, 74.1, 46.3, 40.6, 22.1, 21.4, 11.8, 11.7.

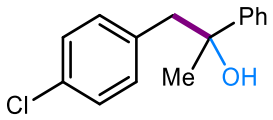

6.3ab

(Generated following ***Condition A(1)*** and isolated by column chromatography on silica gel with hexane: EtOAc = 96:4 as eluent, colorless oil, 50 mg, yield: 99%) [19]: **^{1}H NMR** (500 MHz, $CDCl_3$) δ 7.47 – 7.32 (m, 4H), 7.32 – 7.25 (m, 1H), 7.24 – 7.15 (m, 2H), 6.99 – 6.87 (m, 2H), 3.12 (d, *J* = 13.4 Hz, 1H), 3.02 (d, *J* = 13.4 Hz, 1H), 1.87 (s, 1H), 1.60 (s, 3H). **^{13}C NMR** (126 MHz, $CDCl_3$) δ 147.1, 135.3, 132.5, 131.8, 128.1, 128.0, 126.8, 124.9, 74.4, 49.8, 29.3.

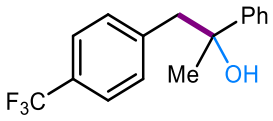

6.3ac

(Generated following ***Condition A(1)*** and isolated by column chromatography on silica gel with hexane: EtOAc = 96:4 as eluent, colorless oil, 58 mg, yield: 99%) [19]: **^{1}H NMR** (500 MHz, $CDCl_3$)

δ 7.49 (d, *J* = 8.0 Hz, 2H), 7.45 – 7.33 (m, 4H), 7.33 – 7.24 (m, 1H), 7.13 (d, *J* = 7.9 Hz, 2H), 3.19 (d, *J* = 13.3 Hz, 1H), 3.11 (d, *J* = 13.3 Hz, 1H), 1.85 (s, 1H), 1.62 (s, 3H). **^{13}C NMR** (126 MHz, $CDCl_3$) δ 147.0, 141.1, 130.8, 128.8 (q, *J* = 32.8 Hz), 128.2, 126.9, 124.9, 124.7 (q, *J* = 3.78 Hz), 124.3 (q, *J* = 272 Hz), 74.5, 50.2, 29.4. **^{19}F NMR** (471 MHz, $CDCl_3$) δ -62.4.

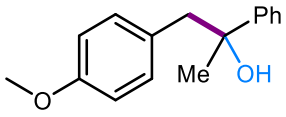

6.3ad

(Generated following ***Condition B*** and isolated by column chromatography on silica gel with hexane: EtOAc = 92:8 as eluent, colorless oil, 27 mg, yield: 56%) [19]: **^{1}H NMR** (500 MHz, $CDCl_3$) δ 7.47 – 7.39 (m, 2H), 7.36 (dd, *J* = 8.5, 6.9 Hz, 2H), 7.32 – 7.23 (m, 1H), 6.93 (d, *J* = 8.6 Hz, 2H), 6.79 (d, *J* = 8.6 Hz, 2H), 3.79 (s, 3H), 3.11 (d, *J* = 13.5 Hz, 1H), 3.00 (d, *J* = 13.5 Hz, 1H), 1.92 (s, 1H), 1.59 (s, 3H). **^{13}C NMR** (126 MHz, $CDCl_3$) δ 158.4, 147.6, 131.5, 128.6, 128.0, 126.6, 125.0, 113.5, 74.4, 55.1, 49.6, 29.3.

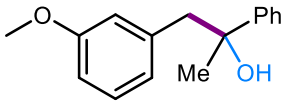

6.3ae

(Generated following ***Condition A(1)*** and isolated by column chromatography on silica gel with hexane: EtOAc = 92:8 as eluent, colorless oil, 40 mg, yield: 83%): **^{1}H NMR** (500 MHz, $CDCl_3$) δ 7.50 – 7.41 (m, 2H), 7.37 (dd, *J* = 8.6, 6.9 Hz, 2H), 7.33 – 7.24 (m, 1H), 7.18 (t, *J* = 7.9 Hz, 1H), 6.79 (ddd, *J* = 8.2, 2.6, 0.9 Hz, 1H), 6.66 (dt, *J* = 7.5, 1.2 Hz, 1H), 6.50 (dd, *J* = 2.7, 1.5 Hz, 1H), 3.69 (s, 3H), 3.16 (d, *J* = 13.3 Hz, 1H), 3.04 (d, *J* = 13.3 Hz, 1H), 2.01 (s, 1H), 1.62 (s, 3H). **^{13}C NMR** (126 MHz, $CDCl_3$) δ 159.2, 147.5, 138.1, 128.9, 128.0, 126.6, 125.0, 122.9, 115.8, 112.5, 74.4, 55.0, 50.5, 29.4. **HRMS:** (ESI, *m*/*z*): calcd. for $C_{16}H_{18}O_2Na[M+Na]^+$ 265.1199, found: 265.1206.

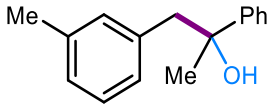

6.3af

(Generated following ***Condition A(1)*** and isolated by column chromatography on silica gel with hexane: EtOAc = 96:4 as eluent, colorless oil, 39 mg, yield: 87%) [60]: **^{1}H NMR** (500 MHz, $CDCl_3$) δ 7.50 – 7.41 (m, 2H), 7.37 (dd, *J* = 8.4, 6.9 Hz, 2H), 7.33 – 7.25 (m, 1H), 7.15 (t, *J* = 7.5 Hz, 1H), 7.07 (d, *J* = 7.5 Hz, 1H), 6.87 (s, 1H), 6.83 (d, *J* = 7.5 Hz, 1H), 3.14 (d, *J* = 13.3 Hz, 1H), 3.03 (d, *J* = 13.3 Hz, 1H), 2.32 (s, 3H), 1.95 (s, 1H), 1.60 (s, 3H). **^{13}C NMR** (126 MHz, $CDCl_3$) δ 147.7, 137.6, 136.5, 131.4, 128.0, 127.9, 127.6, 127.4, 126.6, 124.9, 74.3, 50.4, 29.3, 21.3.

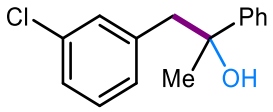

6.3ag

(Generated following ***Condition A(1)*** and isolated by column chromatography on silica gel with hexane: EtOAc = 96:4 as eluent, colorless oil, 50 mg, yield: 99%) [19]: **^{1}H NMR** (500 MHz, $CDCl_3$) δ 7.45 – 7.40 (m, 2H), 7.37 (dd, *J* = 8.5, 6.8 Hz, 2H), 7.33 – 7.26 (m, 1H), 7.22 (ddd, *J* = 8.0, 2.1, 1.2 Hz, 1H), 7.16 (t, *J* = 7.7 Hz, 1H), 7.05 (t, *J* = 1.9 Hz, 1H), 6.89 (dt, *J* = 7.6, 1.5 Hz, 1H), 3.11 (d, *J* = 13.4 Hz, 1H), 3.02 (d, *J* = 13.3 Hz, 1H), 1.89 (s, 1H), 1.60 (s, 3H). **^{13}C NMR** (126 MHz, $CDCl_3$) δ 147.1, 138.9, 133.7, 130.6, 129.1, 128.7, 128.1, 126.8, 126.7, 124.9, 74.4, 50.1, 29.2.

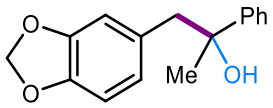

6.3ah

(Generated following ***Condition B*** and isolated by column chromatography on silica gel with hexane: EtOAc = 92:8 as eluent, colorless oil, 36 mg, yield: 70%) [19]: **^{1}H NMR** (500 MHz, $CDCl_3$) δ 7.43 (d, *J* = 7.7 Hz, 2H), 7.36 (t, *J* = 7.6 Hz, 2H), 7.28 (t, *J* = 7.3 Hz, 1H), 6.70 (d, *J* = 7.8 Hz, 1H), 6.57 – 6.41 (m, 2H), 5.92 (s, 2H), 3.08 (d, *J* = 13.5 Hz, 1H), 2.97 (d, *J* = 13.5 Hz, 1H), 1.96 (s, 1H), 1.59 (s, 3H). **^{13}C NMR** (126 MHz, $CDCl_3$) δ 147.5, 147.2, 146.3, 130.3, 128.0, 126.6, 124.9, 123.6, 110.8, 107.8, 100.8, 74.3, 50.1, 29.3.

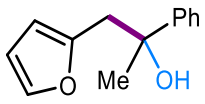

6.3ai

(Generated following ***Condition A(1)*** and isolated by column chromatography on silica gel with hexane: EtOAc = 90:10 as eluent, yellow oil, 25 mg, yield: 70%)[19]: **^{1}H NMR** (500 MHz, $CDCl_3$) δ 7.54 – 7.43 (m, 2H), 7.42 – 7.31 (m, 3H), 7.31 – 7.22 (m, 1H), 6.29 (dd, *J* = 3.2, 1.9 Hz, 1H), 5.99 (d, *J* = 3.1 Hz, 1H), 3.17 (q, *J* = 14.9 Hz, 2H), 2.42 (s, 1H), 1.59 (s, 3H). **^{13}C NMR** (126 MHz, $CDCl_3$) δ 151.9, 147.2, 141.7, 128.1, 126.7, 124.7, 110.3, 108.2, 74.1, 42.7, 29.5.

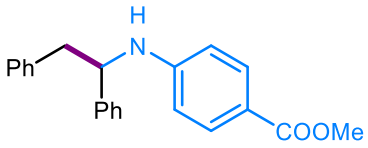

6.4aa

(Generated following ***Condition A(1)*** and isolated by column chromatography on silica gel with hexane: EtOAc = 100:0 →90:10 as eluent, colorless oil, 58 mg, yield: 88%): **^{1}H NMR** (500 MHz, $CDCl_3$) δ 7.87 – 7.76 (m, 2H), 7.43 – 7.23 (m, 8H), 7.20 – 7.08 (m, 2H), 6.55 – 6.43 (m, 2H), 4.75 – 4.68 (m, 2H), 3.85 (s, 3H), 3.21 (dd, *J* = 14.0, 5.8 Hz, 1H), 3.11 (dd, *J* = 14.0, 7.9 Hz, 1H). **^{13}C NMR** (126 MHz, $CDCl_3$) δ 167.1, 150.8, 142.24, 137.1, 131.2, 129.1, 128.6, 128.5, 127.3, 126.8, 126.3, 118.5, 112.4, 58.6, 51.4, 44.7. **HRMS:** (ESI, *m/z*): calcd. for $C_{22}H_{21}O_2NNa[M+Na]^+$ 354.1464, found: 354.1462.

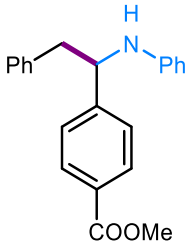

6.4ba

(Generated following ***Condition A(1)*** and isolated by column chromatography on silica gel with hexane: EtOAc = 100:0 →90:10 as eluent, colorless oil, 40 mg, yield: 61%) **^{1}H NMR** (500 MHz, $CDCl_3$) δ 8.02 (d, *J* = 8.3 Hz, 2H), 7.43 (d, *J* = 8.2 Hz, 2H), 7.36 – 7.22 (m, 3H), 7.21 – 7.03 (m, 4H), 6.69 (t, *J* = 7.3 Hz, 1H), 6.47 (d, *J* = 7.7 Hz, 2H), 4.68 (dd, *J* = 7.6, 6.3 Hz, 1H), 4.21 (br, 1H), 3.94 (s, 3H), 3.16 (dd, *J* = 13.9, 5.9 Hz, 1H), 3.08 (dd, *J* = 13.9, 8.0 Hz, 1H). **^{13}C NMR** (126 MHz, $CDCl_3$) δ 166.9, 148.9, 146.8, 137.0, 129.9, 129.2, 129.0, 128.6, 126.9, 126.5, 117.8, 113.6, 59.1, 52.0, 44.8. **HRMS:** (ESI, *m/z*): calcd. for $C_{22}H_{21}O_2NNa[M+Na]^+$ 354.1464, found: 354.1468.

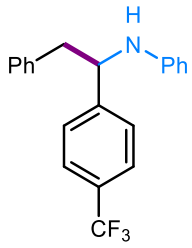

6.4ca

(Generated following ***Condition A(1)*** and isolated by column chromatography on silica gel with hexane: EtOAc = 100:0 →96:4 as eluent, colorless oil, 50 mg, yield: 75%) **^{1}H NMR** (500 MHz, $CDCl_3$) δ 7.62 (d, *J* = 8.1 Hz, 2H), 7.49 (d, *J* = 8.0 Hz, 2H), 7.32 (ddd, *J* = 16.5, 11.9, 4.4 Hz, 3H), 7.24 – 7.02 (m, 4H), 6.72 (t, *J* = 7.3 Hz, 1H), 6.48 (d, *J* = 7.9 Hz, 2H), 4.70 (t, *J* = 6.9 Hz, 1H), 4.21 (s, 1H), 3.18 (dd, *J* = 14.0, 5.7 Hz, 1H), 3.08 (dd, *J* = 13.9, 8.2 Hz, 1H). **^{13}C NMR** (126 MHz, $CDCl_3$) δ 147.7, 146.8, 136.9, 129.3 (q, *J* = 32.2 Hz), 129.1, 129.1, 128.7, 127.0, 126.8, 125.6 (q, *J* = 3.6 Hz), 124.2 (q, *J* = 271.9), 117.9, 113.6, 58.9, 45.0. **^{19}F NMR** (471 MHz, $CDCl_3$) δ -62.2. **HRMS:** (ESI, *m*/*z*): calcd. for $C_{21}H_{19}NF_3[M+H]^+$ 342.1464, found: 342.1459.

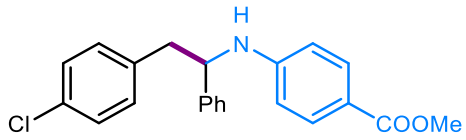

6.4ab

(Generated following ***Condition A(1)*** and isolated by column chromatography on silica gel with hexane: EtOAc = 100:0 →90:10 as eluent, colorless oil, 63 mg, yield: 85%) **^{1}H NMR** (500 MHz, $CDCl_3$) δ 7.80 (d, *J* = 8.8 Hz, 2H), 7.36 – 7.30 (m, 2H), 7.30 – 7.19 (m, 5H), 7.02 (d, *J* = 8.3 Hz, 2H), 6.49 (d, *J* = 8.8 Hz, 2H), 4.72 – 4.53 (m, 2H), 3.84 (s, 3H), 3.20 – 3.01 (m, 2H). **^{13}C NMR** (126 MHz, $CDCl_3$) δ 167.1, 150.6, 141.7, 135.5, 132.6, 131.3, 130.5, 128.7, 128.6, 127.4, 126.3, 118.8, 112.4, 58.5, 51.4, 43.8. **HRMS:** (ESI, *m*/*z*): calcd. for $C_{22}H_{20}O_2NClNa[M+Na]^+$ 388.1075, found: 388.1078.

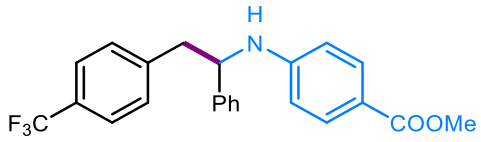

6.4ac

(Generated following ***Condition A(1)*** and isolated by column chromatography on silica gel with hexane: EtOAc = 100:0 →90:10 as eluent, colorless oil, 42 mg, yield: 53%) **^{1}H NMR** (500 MHz, $CDCl_3$) δ 7.80 (d, *J* = 8.8 Hz, 2H), 7.54 (d, *J* = 8.1 Hz, 2H), 7.39 – 7.32 (m, 2H), 7.32 – 7.24 (m, 3H), 7.21 (d, *J* = 8.0 Hz, 2H), 6.49 (d, *J* = 8.8 Hz, 2H), 4.74 (t, *J* = 6.8 Hz, 1H), 4.58 (br, 1H), 3.83 (s, 3H), 3.27 – 3.13 (m, 2H). **^{13}C NMR** (126 MHz, $CDCl_3$) δ 167.1, 150.5, 141.6, 141.3, 131.4, 129.5, 129.2 (q, *J* = 32.7 Hz), 128.8, 127.6, 126.3, 125.4 (q, *J* = 3.7 Hz), 124.1 (q, *J* = 272.9), 119.0, 112.4, 58.4, 51.5, 44.2. **^{19}F NMR** (471 MHz, $CDCl_3$) δ -62.4. **HRMS:** (ESI, *m*/*z*): calcd. for $C_{23}H_{20}O_2NF_3Na[M+Na]^+$ 422.1338, found: 422.1337.

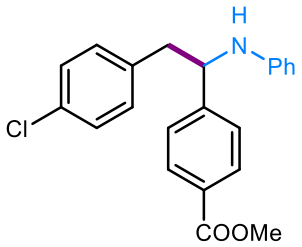

6.4bb

(Generated following ***Condition A(1)*** and isolated by column chromatography on silica gel with hexane: EtOAc = 100:0 →90:10 as eluent, colorless oil, 42 mg, yield: 58%) **^{1}H NMR** (500 MHz, $CDCl_3$) δ 8.00 (d, *J* = 8.2 Hz, 2H), 7.38 (d, *J* = 8.2 Hz, 2H), 7.26 (d, *J* = 8.3 Hz, 2H), 7.09 (t, *J* = 7.9 Hz, 2H), 7.02 (d, *J* = 8.3 Hz, 2H), 6.69 (t, *J* = 7.3 Hz, 1H), 6.48 (d, *J* = 7.9 Hz, 2H), 4.65 (t, *J* = 6.9 Hz, 1H), 4.18 (br, 1H), 3.95 (d, *J* = 22.5 Hz, 3H), 3.18 – 3.00 (m, 2H). **^{13}C NMR** (126 MHz, $CDCl_3$) δ 166.9, 148.3, 146.6, 135.4, 132.7, 130.5, 130.0, 129.2, 129.1, 128.7, 126.5, 118.0, 113.6, 59.0, 52.0, 43.9. **HRMS:** (ESI, *m*/*z*): calcd. for $C_{22}H_{20}O_2NClNa[M+Na]^+$ 388.1075, found: 388.1072.

References

(1). Shirley, D. A., The synthesis of ketones from acid halides and organometallic compounds of magnesium, zinc, and cadmium. *Org. React.* **1954,** *8*, 28.
(2). Grignard, V., Sur quelques nouvelles combinaisons organometalliques du magnésium et leur application à des synthèses d'alcools et d'hydrocarbures. *Compt. Rend.* **1900,** *130*, 1322.
(3). Gilman, H.; Jones, R. G.; Woods, L., The preparation of methylcopper and some observations on the decomposition of organocopper compounds. *J. Org. Chem.* **1952,** *17*, 1630–1634.

(4). Knochel, P.; Jones, P., *Organozinc Reagents: A Practical Approach*. Oxford University Press: Oxford, 1999.
(5). Rappoport, Z.; Marek, I., *The Chemistry of Organolithium Compounds, Volume 1, 2 Volume set*. John Wiley & Sons: New York, 2004.
(6). Van Der Kerk, G.; Luijten, J., Tetraethyltin. *Org. Syn.*, 86–86.
(7). Larock, R. C., Organomercurials in organic synthesis. *Tetrahedron* **1982,** *38*, 1713–1754.
(8). Hall, D. G., *Boronic Acids: Preparation, Applications in Organic Synthesis and Medicine*. John Wiley & Sons: New York, 2006.
(9). Kishner, N., Wolff–Kishner reduction; huang–minlon modification. *J. Russ. Phys. Chem. Soc.* **1911,** *43*, 582–595.
(10). Wolff, L., Chemischen institut der universität jena: Methode zum ersatz des sauerstoffatoms der ketone und aldehyde durch wasserstoff. *Eur. J. Org. Chem.* **1912,** *394*, 86–108.
(11). Herr, C. H.; Whitmore, F. C.; Schiessler, R. W., The Wolff–Kishner reaction at atmospheric pressure. *J. Am. Chem. Soc.* **1945,** *67*, 2061–2063.
(12). Wharton, P.; Bohlen, D., Communications — hydrazine reduction of α, β-epoxy ketones to allylic alcohols. *J. Org. Chem.* **1961,** *26*, 3615-3616.
(13). Caglioti, L.; Magi, M., The reaction of tosylhydrazones with lithium aluminium hydride. *Tetrahedron* **1963,** *19*, 1127–1131.
(14). Szmant, H. H.; Harmuth, C. M., The Wolff–Kishner reaction of hydrazones. *J. Am. Chem. Soc.* **1964,** *86*, 2909–2914.
(15). Baldwin, J. E.; Bottaro, J. C.; Kolhe, J. N.; Adlington, R. M., Azo anions in synthesis. Use of trityl-and diphenyl-4-pyridylmethyl-hydrazones for reductive C–C bond formation from aldehydes and ketones. *J. Chem. Soc., Chem, Commun.* **1984**, 22–23.
(16). Baldwin, J. E.; Adlington, R. M.; Bottaro, J. C.; Kolhe, J. N.; Newington, I. M.; Perry, M. W., Azo anions in synthesis: Use of trityl-and diphenyl-4-pyridylmethylhydrazones for reductive cc bond formation. *Tetrahedron* **1986,** *42*, 4235–4246.
(17). Dai, X.-J.; Li, C.-J., En route to a practical primary alcohol deoxygenation. *J. Am. Chem. Soc.* **2016,** *138*, 5433–5440.
(18). Little, R. D.; Masjedizadeh, M. R.; Wallquist, O.; McLoughlin, J. I., The intramolecularmichael reaction. *Org. React.* **2004**, *47*, 315
(19). Wang, H.; Dai, X.-J.; Li, C.-J., Aldehydes as alkyl carbanion equivalents for additions to carbonyl compounds. *Nat. Chem.* **2017,** *9*, 374-378.
(20). Chen, N.; Dai, X.-J.; Wang, H.; Li, C.-J., *Umpolung* addition of aldehydes to aryl imines. *Angew. Chem. Int. Ed.* **2017,** *56*, 6260–6263.
(21). Dai, X.-J.; Wang, H.; Li, C.-J., Carbonyls as latent alkyl carbanions for conjugate additions. *Angew. Chem. Int. Ed.* **2017,** *56*, 6302–6306.

(22). Bauer, I.; Knölker, H.-J., Iron catalysis in organic synthesis. *Chem. Rev.* **2015,** *115*, 3170-3387.
(23). Sun, C.-L.; Li, B.-J.; Shi, Z.-J., Direct C−H transformation *via* iron catalysis. *Chem. Rev.* **2011,** *111*, 1293–1314.
(24). Ludwig, J. R.; Zimmerman, P. M.; Gianino, J. B.; Schindler, C. S., Iron(III)-catalysed carbonyl–olefin metathesis. *Nature* **2016,** *533*, 374-379.
(25). Zhong, Y.; Han, W., Iron-catalyzed carbonylative suzuki reactions under atmospheric pressure of carbon monoxide. *Chem. Commun.* **2014,** *50*, 3874-3877.
(26). Fürstner, A.; Leitner, A.; Méndez, M.; Krause, H., Iron-catalyzed cross-coupling reactions. *J. Am. Chem. Soc.* **2002,** *124*, 13856–13863.
(27). Nakamura, M.; Matsuo, K.; Ito, S.; Nakamura, E., Iron-catalyzed cross-coupling of primary and secondary alkyl halides with aryl grignard reagents. *J. Am. Chem. Soc.* **2004,** *126*, 3686-3687.
(28). Alois, F.; Rubén, M., Advances in iron catalyzed cross coupling reactions. *Chem. Lett.* **2005,** *34*, 624–629.
(29). Sapountzis, I.; Lin, W.; Kofink, C. C.; Despotopoulou, C.; Knochel, P., Iron-catalyzed aryl–aryl cross-couplings with magnesium-derived copper reagents. *Angew. Chem. Int. Ed.* **2005,** *44*, 1654–1658.
(30). Guérinot, A.; Reymond, S.; Cossy, J., Iron-catalyzed cross-coupling of alkyl halides with alkenyl grignard reagents. *Angew. Chem. Int. Ed.* **2007,** *46*, 6521–6524.
(31). Hatakeyama, T.; Nakamura, M., Iron-catalyzed selective biaryl coupling: Remarkable suppression of homocoupling by the fluoride anion. *J. Am. Chem. Soc.* **2007,** *129*, 9844–9845.
(32). Fürstner, A.; Martin, R.; Krause, H.; Seidel, G.; Goddard, R.; Lehmann, C. W., Preparation, structure, and reactivity of nonstabilized organoiron compounds. Implications for iron-catalyzed cross coupling reactions. *J. Am. Chem. Soc.* **2008,** *130*, 8773–8787.
(33). Norinder, J.; Matsumoto, A.; Yoshikai, N.; Nakamura, E., Iron-catalyzed direct arylation through directed C−H bond activation. *J. Am. Chem. Soc.* **2008,** *130*, 5858–5859.
(34). Sherry, B. D.; Fürstner, A., The promise and challenge of iron-catalyzed cross coupling. *Acc. Chem. Res.* **2008,** *41*, 1500–1511.
(35). Zhao, D.; Shi, Z.; Glorius, F., Indole synthesis by rhodium(III)-catalyzed hydrazine-directed c□h activation: Redox-neutral and traceless by N–N bond cleavage. *Angew. Chem. Int. Ed.* **2013,** *52*, 12426–12429.
(36). Shang, R.; Ilies, L.; Asako, S.; Nakamura, E., Iron-catalyzed C(sp^2)–H bond functionalization with organoboron compounds. *J. Am. Chem. Soc.* **2014,** *136*, 14349–14352.
(37). Chatt, J.; Hayter, R. G., 1079. Some hydrido-complexes of iron(II). *J. Chem. Soc.* **1961**, 5507–5511.

(38). Field, L. D.; Guest, R. W.; Vuong, K. Q.; Dalgarno, S. J.; Jensen, P., Iron(0) and ruthenium(0) complexes of dinitrogen. *Inorg. Chem.* **2009,** *48*, 2246–2253.
(39). Field, L. D.; Li, H. L.; Dalgarno, S. J.; McIntosh, R. D., Side-on bound complexes of phenyl- and methyl-diazene. *Inorg. Chem.* **2012,** *51*, 3733-3742.
(40). Field, L. D.; Li, H. L.; Dalgarno, S. J.; McIntosh, R. D., Base-induced dehydrogenation of ruthenium hydrazine complexes. *Inorg. Chem.* **2013,** *52*, 1570–1583.
(41). Pasternack, R. F.; Huber, P. R.; Boyd, P.; Engasser, G.; Francesconi, L.; Gibbs, E.; Fasella, P.; Cerio Venturo, G.; Hinds, L. d., Aggregation of *meso*-substituted water-soluble porphyrins. *J. Am. Chem. Soc.* **1972,** *94*, 4511–4517.
(42). Whittlesey, M. K.; Mawby, R. J.; Osman, R.; Perutz, R. N.; Field, L. D.; Wilkinson, M. P.; George, M. W., Transient and matrix photochemistry of $Fe(dmpe)_2H_2$ (dmpe = me2pch2ch2me2): Dynamics of C–H and H–H activation. *J. Am. Chem. Soc.* **1993,** *115*, 8627–8637.
(43). Field, L. D.; Li, H. L.; Magill, A. M., Base-mediated conversion of hydrazine to diazene and dinitrogen at an iron center. *Inorg. Chem.* **2009,** *48*, 5–7.
(44). Hazari, N., Homogeneous iron complexes for the conversion of dinitrogen into ammonia and hydrazine. *Chem. Soc. Rev.* **2010,** *39*, 4044–4056.
(45). Koerner von Gustorf, E. A.; Grevels, F.-W.; Fischler, I., *The Organic Chemistry of Iron*. Academic Press: New York, 1978.
(46). Silver, J., *Chemistry of iron*. Blackie Academic & Professional: London; New York, 1993.
(47). Symons, M. C. R.; Gutteridge, J. M. C., *Free Radicals and Iron : Chemistry, Biology, and Medicine*. Oxford University Press: Oxford; New York, 1998.
(48). Miessler, G. L.; Tarr, D. A., *Inorganic Chemistry*. Pearson Education: Upper Saddle River, N.J., 2004.
(49). Bauer, I.; Knölker, H.-J., Iron complexes in organic chemistry. In *Iron Catalysis in Organic Chemistry*, Wiley-VCH Verlag GmbH & Co. KGaA: Berlin, 2008; pp 1–27.
(50). Mashuta, M. S.; Webb, R. J.; McCusker, J. K.; Schmitt, E. A.; Oberhausen, K. J.; Richardson, J. F.; Buchanan, R. M.; Hendrickson, D. N., Electron transfer in iron (II iron (III) model complexes of iron–oxo proteins. *J. Am. Chem. Soc.* **1992,** *114*, 3815-3827.
(51). Feng, W.; Nansheng, D., Photochemistry of hydrolytic iron (III) species and photoinduced degradation of organic compounds. A minireview. *Chemosphere* **2000,** *41*, 1137–1147.
(52). Williams, A. G. B.; Scherer, M. M., Spectroscopic evidence for Fe(II)−Fe(III) electron transfer at the iron oxide−water interface. *Environ. Sci. Tech.* **2004,** *38*, 4782–4790.
(53). Cowen, B. J.; Saunders, L. B.; Miller, S. J., Pyridylalanine (pal)-peptide catalyzed enantioselective allenoate additions to *N*-acyl imines. *J. Am. Chem. Soc.* **2009,** *131*, 6105–6107.
(54). Fava, E.; Millet, A.; Nakajima, M.; Loescher, S.; Rueping, M., Reductive *umpolung* of carbonyl derivatives with visible-light photoredox catalysis: Direct access to vicinal diamines

and amino alcohols *via* α-amino radicals and ketyl radicals. *Angew. Chem. Int. Ed.* **2016,** *55*, 6776–6779.
(55). Rodríguez, A.; Albert, J.; Ariza, X.; Garcia, J.; Granell, J.; Farràs, J.; La Mela, A.; Nicolás, E., Catalytic C–H activation of phenylethylamines or benzylamines and their annulation with allenes. *J. Org. Chem.* **2014,** *79*, 9578–9585.
(56). Billaud, C.; Goddard, J.-P.; Le Gall, T.; Mioskowski, C., Preparation of alcohols from sulfones and trialkylboranes. *Tetrahedron Lett.* **2003,** *44*, 4451–4454.
(57). Zhou, L.; Liu, X.; Ji, J.; Zhang, Y.; Wu, W.; Liu, Y.; Lin, L.; Feng, X., Regio- and enantioselective baeyer–villiger oxidation: Kinetic resolution of racemic 2-substituted cyclopentanones. *Org. Lett.* **2014,** *16*, 3938-3941.
(58). Surzhko, V.; Roisnel, T.; Le Grel, B.; Le Grel, P.; Lalli, C.; Argouarch, G., Synthesis of picolinohydrazides and their evaluation as ligands in the zinc-catalyzed hydrosilylation of ketones. *Tetrahedron Lett.* **2017,** *58*, 1343–1347.
(59). Ray, R.; Chandra, S.; Yadav, V.; Mondal, P.; Maiti, D.; Lahiri, G. K., Ligand controlled switchable selectivity in ruthenium catalyzed aerobic oxidation of primary amines. *Chem. Commun.* **2017,** *53*, 4006–4009.
(60). Su, Y.; Sun, X.; Wu, G.; Jiao, N., Catalyst-controlled highly selective coupling and oxygenation of olefins: A direct approach to alcohols, ketones, and diketones. *Angew. Chem. Int. Ed.* **2013,** *52*, 9808–9812.

Chapter 7. Summary and Outlook of My PhD Research

7.1 Summary of my PhD research

The core design of my PhD research was based on the aim of enabling greener oxygen-containing compounds (alcohols and carbonyls) to complete C–C bond formation, which provides an alternative to classic C–C bond formations with halogenated compounds and stoichiometric toxic metals. In such a design, hydrogen transfer strategy played a vital role. The main projects I completed were derived from a Grignard-type reaction with hydrazone as a carbanion equivalent, which could be concluded from three dimensions: (a) my research enabled saturated and unsaturated alcohols to be carbonyl surrogates for Grignard reactions taking advantage of ruthenium catalytic system, (b) I was able to switch chemoselectivity of C–C bond formation of hydrazones with carbonyls, and (c) I developed an alternative non-noble iron catalyst for hydrazone-involved Grignard-type reactions. These three completed projects opened three plausible research fields regarding hydrazone-involved C–C bond formation reactions.

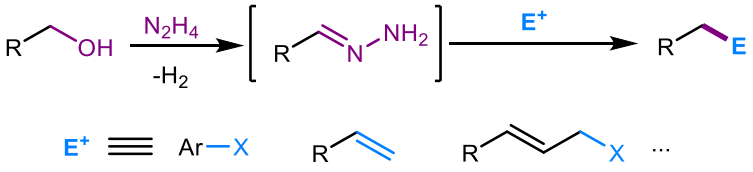

Scheme 7.1 General design of various hydrazone-involved C–C bond formations with alcohols

7.2 Outlook

My first project detailed that a hydrogen transfer strategy could enable alcohol as a carbonyl surrogate for Grignard-type reactions. This suggests that hydrazone-involved C–C bond formation has a strong compatibility with the hydrogen transfer of alcohols. We determined that we could then consider alcohol for other hydrazone-involved transformations, more than the electrophile of Grignard-type reactions. When taking advantage of hydrogen transfer, alcohol could serve as a precursor of hydrazone by dehydrogenation and condensation with free hydrazines. With this realization, alcohols could complete several hydrazone-involved C–C bond formations as developed in our group[1] such as Michael addition,[2] palladium-catalyzed allylation,[3] nickel-catalyzed cross-coupling reactions[4, 5] or hydroalkylation reactions.[6, 7] However, the biggest

challenge to realize these transformations is to find a catalytic system that can tolerate the highly reductive hydrazine, which might deactivate the metal catalysts. Through reviewing the literature and conducting experiments, we discovered that comparatively stable metal–pincer complexes have a great tolerance with hydrazines and can complete the alcohol dehydrogenation/hydrazine condensation process. For instance, Milstein *et al.* utilized Mn–PNP[8] and Ru–PNP[9] to achieve the direct generation of azines and alkyl hydrazines with alcohols and free hydrazines, as discussed in Section 1.4.2. Inspired by this, we had put our efforts into developing various alcohol-surrogated hydrazone-involved C–C bond formations by adapting the original catalytic system to pincer-type complexes to test their hydrazine tolerance. These transformations could further extend the usage of earth-abundant alcohols in C–C bond formations, which could benefit synthetic and industrial chemistry.

Regarding my second project, despite the fact that aliphatic aldehyde hydrazones could realize the selectivity of a Grignard reaction when facing carbonyl compounds, there are still some challenges to be solved: (a) the structure of aliphatic aldehyde hydrazone was still comparatively restricted where *α*-substituted hydrazones could not be tolerated, (b) study of this reaction at late-stage functionalization was still limited, and (c) an efficient asymmetric version of a hydrazone-involved Grignard reaction was not realized. To solve these challenges, first, we adapted PCP ligand with a smaller substituent such as methyl or ethyl instead of *tert*-butyl to better suit for bulky substrates. Secondly, to realize the asymmetric version, the adaptation of phosphine into a chiral center could be feasible according to the success in a significant enantioselectivity in our initial study.[10]

Regarding my third project, non-noble iron catalysts were also proved effective for nucleophilic addition with hydrazones.[11] However, in our initial study, we discovered that in this type of transformation, such an iron catalytic system still has its limitations. For instance, the effective iron catalyst for this transformation is limited to the well-defined Fe–dmpe complexes, and it has a comparatively narrower substrate scope than the ruthenium-catalyzed complex. In addition, iron-complexes cascade the hydrogen transfer/C–C bond formation of hydrazone with alcohols could not be realized. Such a limitation is because iron has a comparatively smaller atomic radius compared with ruthenium, which restricts its space for tolerating bulky substrates or ligands. Iron, as a comparatively harder acid, has a comparatively poorer coordination ability with phosphine ligands, which makes the catalyst itself less stable.[12–14] As such, at the next stage, we plan to focus

on developing a more stable iron complex with some chelating ligands, such as tridentate or tetradentate phosphine ligands and PCP or PNP type pincer ligands. This could enable the iron catalysts to have a broader substrate scope and a higher efficiency in various hydrazone-involved Grignard-type reactions, including the hydrogen-transfer-mediated reactions.

References

(1). Li, C.-J.; Huang, J.; Dai, X.-J.; Wang, H.; Chen, N.; Wei, W.; Zeng, H.; Tang, J.; Li, C.; Zhu, D.; Lv, L., An old dog with new tricks: Enjoin Wolff–Kishner reduction for alcohol deoxygenation and c–c bond formations. *Synlett* **2019,** *30*, 1508–1524.
(2). Dai, X.-J.; Wang, H.; Li, C.-J., Carbonyls as latent alkyl carbanions for conjugate additions. *Angew. Chem. Int. Ed.* **2017,** *56*, 6302–6306.
(3). Zhu, D.; Lv, L.; Li, C.-C.; Ung, S.; Gao, J.; Li, C.-J., *Umpolung* of carbonyl groups as alkyl organometallic reagent surrogates for palladium-catalyzed allylic alkylation. *Angew. Chem. Int. Ed.* **2018,** *57*, 16520–16524.
(4). Lv, L.; Zhu, D.; Tang, J.; Qiu, Z.; Li, C.-C.; Gao, J.; Li, C.-J., Cross-coupling of phenol derivatives with *umpolung* aldehydes catalyzed by nickel. *ACS Catal.* **2018,** *8*, 4622–4627.
(5). Tang, J.; Lv, L.; Dai, X.-J.; Li, C.-C.; Li, L.; Li, C.-J., Nickel-catalyzed cross-coupling of aldehydes with aryl halides *via* hydrazone intermediates. *Chem. Commun.* **2018,** *54*, 1750–1753.
(6). Lv, L.; Zhu, D.; Qiu, Z.; Li, J.; Li, C.-J., Nickel-catalyzed regioselective hydrobenzylation of 1,3-dienes with hydrazones. *ACS Catal.* **2019,** *9*, 9199–9205.
(7). Lv, L.; Yu, L.; Qiu, Z.; Li, C.-J., Switch in selectivity for formal hydroalkylation of 1,3-dienes and enynes with simple hydrazones. *Angew. Chem. Int. Ed.* **2020,** *59*, 6466–6472.
(8). Das, U. K.; Ben-David, Y.; Diskin-Posner, Y.; Milstein, D., *N*-substituted hydrazones by manganese-catalyzed coupling of alcohols with hydrazine: Borrowing hydrogen and acceptorless dehydrogenation in one system. *Angew. Chem. Int. Ed.* **2018,** *57*, 2179–2182.
(9). Bauer, J. O.; Leitus, G.; Ben-David, Y.; Milstein, D., Direct synthesis of symmetrical azines from alcohols and hydrazine catalyzed by a ruthenium pincer complex: Effect of hydrogen bonding. *ACS Catal.* **2016,** *6*, 8415–8419.
(10). Wang, H.; Dai, X.-J.; Li, C.-J., Aldehydes as alkyl carbanion equivalents for additions to carbonyl compounds. *Nat. Chem.* **2017,** *9*, 374-378.
(11). Li, C.-C.; Dai, X.-J.; Wang, H.; Zhu, D.; Gao, J.; Li, C.-J., Iron-catalyzed nucleophilic addition reaction of organic carbanion equivalents *via* hydrazones. *Org. Lett.* **2018,** *20*, 3801-3805.
(12). Koerner von Gustorf, E. A.; Grevels, F.-W.; Fischler, I., *The Organic Chemistry of Iron*. Academic Press: New York, 1978.
(13). Silver, J., *Chemistry of Iron*. Blackie Academic & Professional: London; New York, 1993.

(14). Miessler, G. L.; Tarr, D. A., *Inorganic Chemistry*. Pearson Education: Upper Saddle River, 2004.

Chapter 8. Significant Contributions to Fundamental Knowledge

The two main transformations discussed in this thesis are (a) ruthenium- or iron-catalyzed Grignard-type reactions with *umpolung* aldehyde as a carbanion equivalent and (b) ruthenium-catalyzed hydrogen transfer reactions. In a Grignard reaction with *umpolung* aldehyde (hydrazone) as a carbanion equivalent, ruthenium serves as both a Lewis acid to activate the carbonyl compounds and a catalyst for hydrazone to attack the carbonyl nucleophilically *via* an enolate-like pathway, which is similar to a metal-catalyzed aldol reaction. Our proposed mechanism was based on the Zimmerman–Traxler transition state, which was originally put forward to explain aldol reactions. However, the mechanism for this newly developed transformation still requires further study. In addition, after the C–C bond formation, such a transformation has two options: to be directly protonated to generate 1,2-addition product or to undergo E1cB elimination to generate alkenes. Such a selectivity is also similar to aldol condensations. In Chapter 5, we discussed adjusting a metal catalyst to control 1,2-addition selectivity by increasing the electron density of ruthenium complexes to lower the temperature and decrease the leaving ability of Ru–O to disfavor E1cB elimination process and realize the opposite selectivity.

Another significant transformation in this thesis was the ruthenium-catalyzed hydrogen transfer with alcohols, which is principally enabled by β-H elimination from ruthenium–alkoxyl complexes and hydride insertion to unsaturated bonds, as concluded in Chapter 1. Such processes have a strong compatibility with *umpolung* aldehyde transformations. In Chapter 4, we discussed the utilization of the hydrogen transfer strategy to enable various alcohols to serve as a carbonyl surrogate for a hydrazone-involved Grignard reaction. With allylic alcohols, the hydrogen transfer occurs on the alcohols and C=C double bonds, which enables allylic alcohols to be transformed into carbonyls in a redox-neutral fashion to further undergo a 1,2-addition reaction with hydrazones. With saturated alcohols, a ruthenium–PNP pincer complex was used to enable various alcohols to undergo the acceptorless dehydrogenation process and generate carbonyl intermediate with the release of H_2 gas. Based on the reactions, we concluded that the key to using hydrogen transfer into hydrazone addition reaction is that the hydrazone-involved Grignard reaction is an efficient irreversible reaction without any potential side reaction with the metal–hydride

intermediate. This makes it compatible with the hydrogen transfer process and allows it to serve as a driving force for the comparatively slow step of the dehydrogenation of alcohols to carbonyls. Moreover, as an efficient catalyst both for hydrogen transfer reactions and hydrazone-involved Grignard reactions, the ruthenium–phosphine complex serves as a vital bridge to connect these two transformations.

Finally, regarding the discovery of several advantages of the ruthenium–phosphine complex in the success of various hydrazone-involved C–C bond formation reactions, in Chapter 6, we discussed the development of non-noble iron complexes as an alternative to ruthenium catalysts to undergo such a transformation. Iron shares several significant properties with ruthenium but still differs when catalyzing hydrazone that are involved in C–C bond formation reactions. Because iron is a harder metal than ruthenium, it is less effective in hydrogen transfer reactions. Furthermore, its smaller atomic size makes substituents more sterically hindered, which leads to a narrower substrate scope than ruthenium. However, as a non-noble metal, the further development of an iron catalytic system to provide an alternative for or even replace the ruthenium catalytic system in such transformations is of great significance.

Appendix

I. NMR spectra of products in Chapter 4

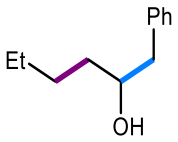

4.2.3aa

^{1}H NMR

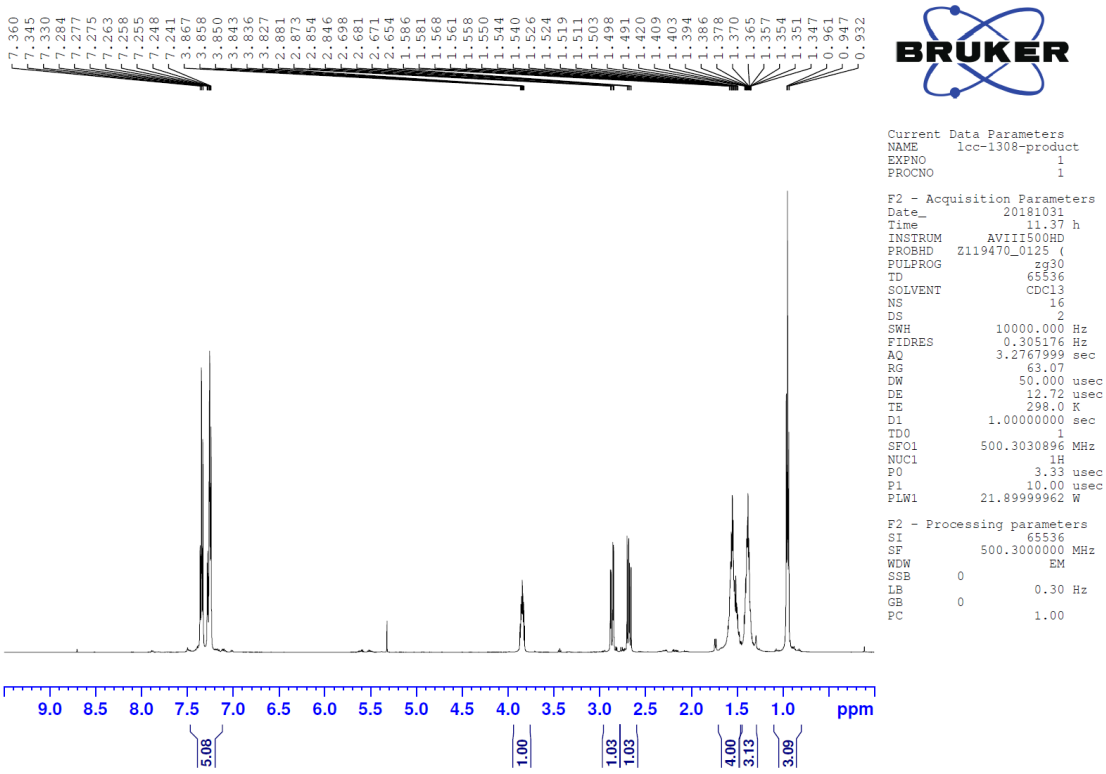

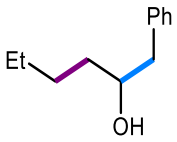

4.2.3aa

^{13}C NMR

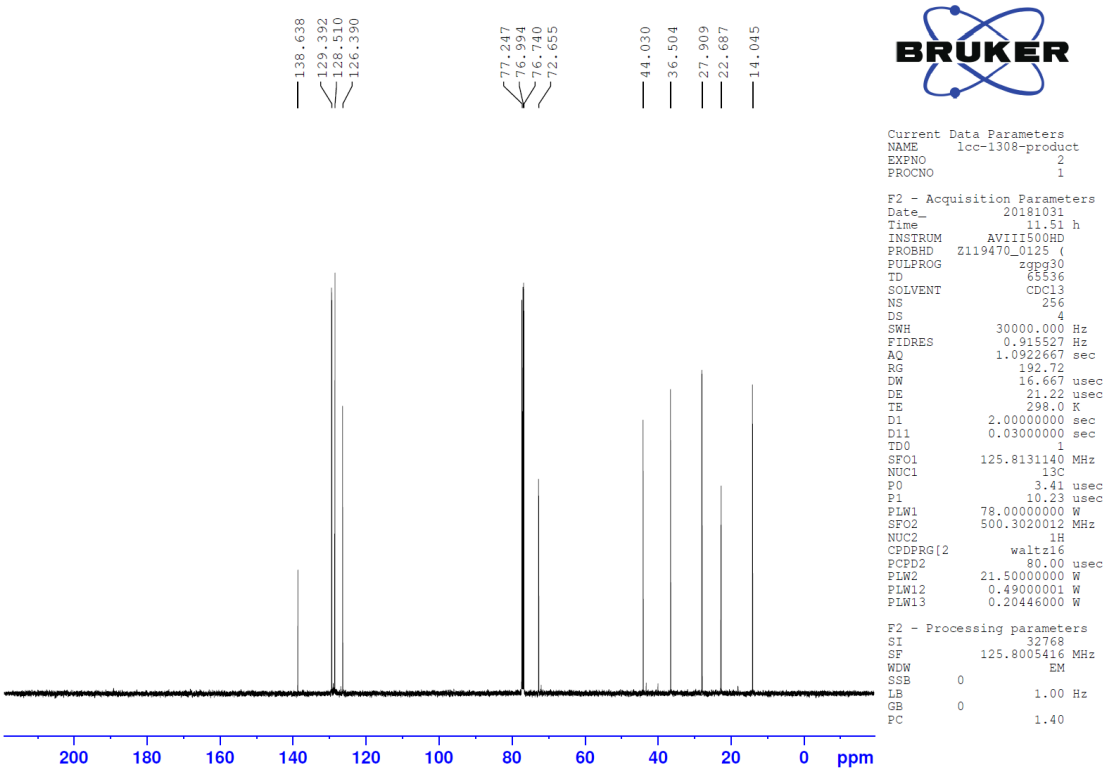

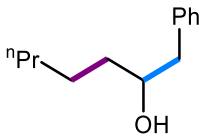
Ph
nPr
OH

4.2.3ab

^{1}H NMR

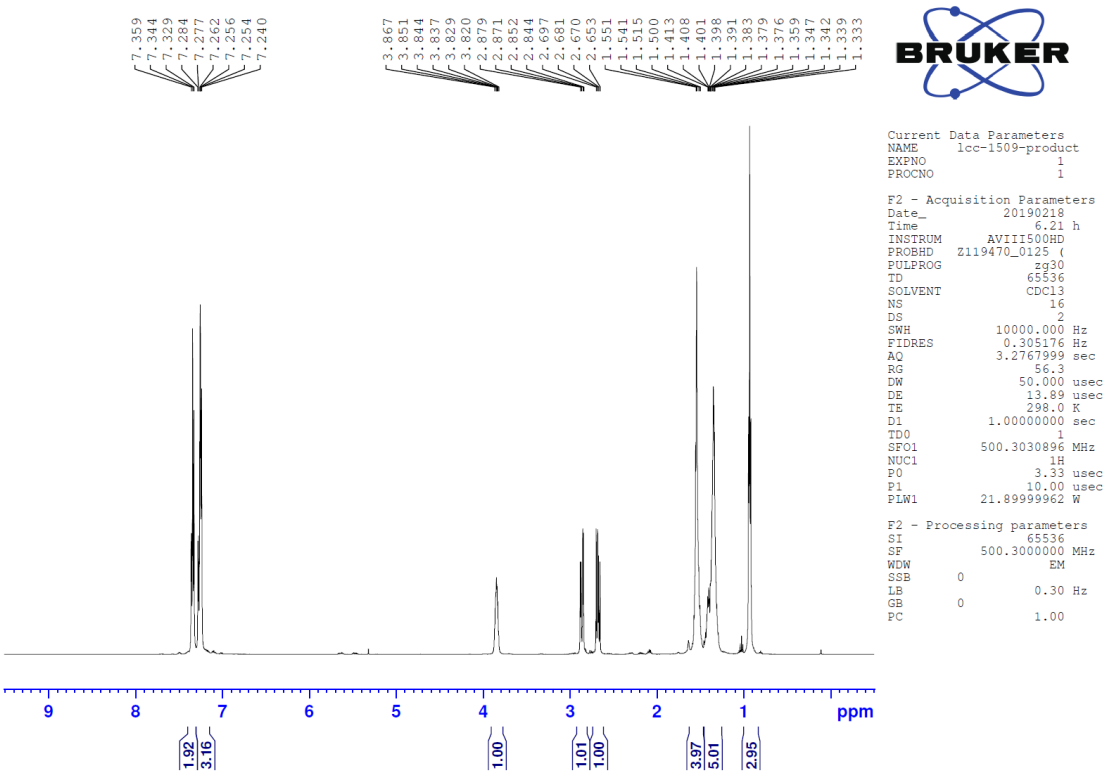
7.359
7.344
7.329
7.284
7.277
7.262
7.256
7.254
7.240
3.867
3.851
3.844
3.837
3.829
3.820
2.879
2.871
2.852
2.844
2.697
2.681
2.670
2.653
1.551
1.541
1.515
1.500
1.413
1.408
1.401
1.398
1.391
1.383
1.379
1.376
1.359
1.347
1.342
1.339
1.333
BRUKER
Current Data Parameters
NAME lcc-1509-product
EXPNO 1
PROCNO 1
F2 - Acquisition Parameters
Date_ 20190218
Time 6.21 h
INSTRUM AVIII500HD
PROBHD Z119470_0125 (
PULPROG zg30
TD 65536
SOLVENT CDCl3
NS 16
DS 2
SWH 10000.000 Hz
FIDRES 0.305176 Hz
AQ 3.2767999 sec
RG 56.3
DW 50.000 usec
DE 13.89 usec
TE 298.0 K
D1 1.00000000 sec
TD0 1
SFO1 500.3030896 MHz
NUC1 1H
P0 3.33 usec
P1 10.00 usec
PLW1 21.89999962 W
F2 - Processing parameters
SI 65536
SF 500.3000000 MHz
WDW EM
SSB 0
LB 0.30 Hz
GB 0
PC 1.00
9
8
7
6
5
4
3
2
1
ppm
1.92
3.16
1.00
1.01
1.00
3.97
5.01
2.95

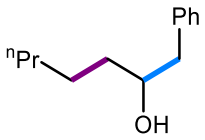

4.2.3ab

^{13}C NMR

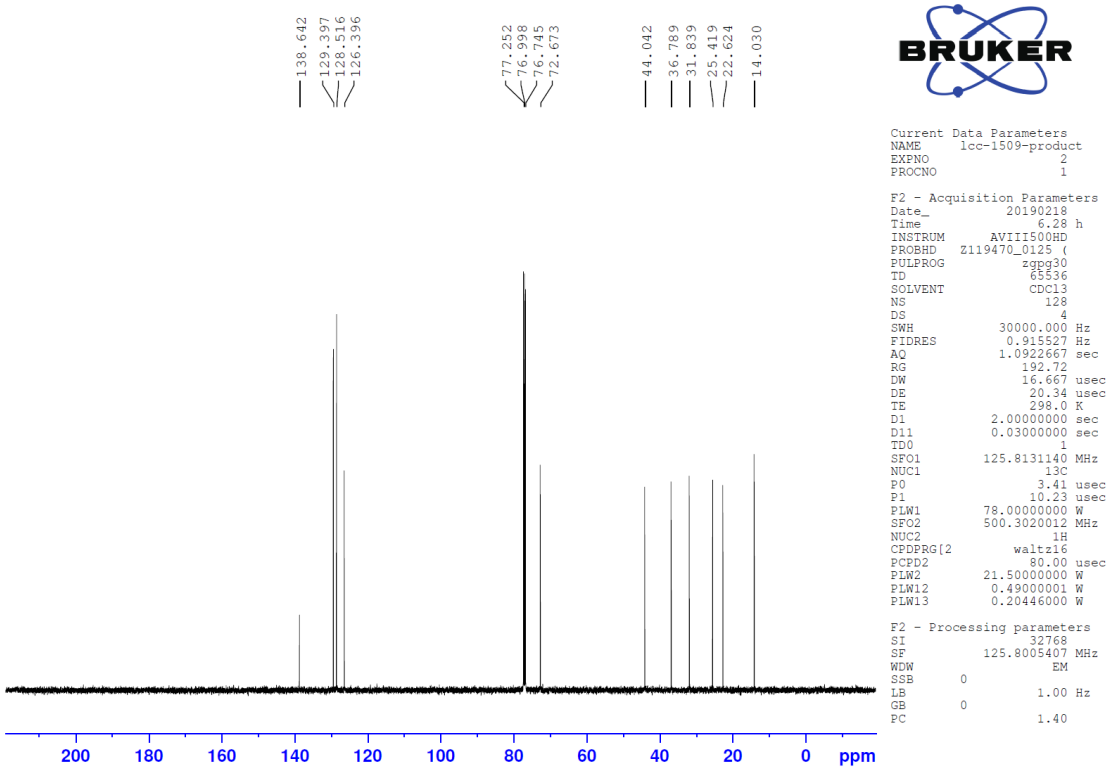


```
Current Data Parameters
NAME      lcc-1509-product
EXPNO                    2
PROCNO                   1

F2 - Acquisition Parameters
Date_              20190218
Time                   6.28 h
INSTRUM       AVIII500HD
PROBHD    Z119470_0125 (
PULPROG            zgpg30
TD                  65536
SOLVENT             CDCl3
NS                    128
DS                      4
SWH             30000.000 Hz
FIDRES              0.915527 Hz
AQ                1.0922667 sec
RG                    192.72
DW                   16.667 usec
DE                    20.34 usec
TE                    298.0 K
D1              2.00000000 sec
D11             0.03000000 sec
TD0                     1
SFO1          125.8131140 MHz
NUC1                   13C
P0                    3.41 usec
P1                   10.23 usec
PLW1          78.00000000 W
SFO2          500.3020012 MHz
NUC2                   1H
CPDPRG[2          waltz16
PCPD2                80.00 usec
PLW2          21.50000000 W
PLW12          0.49000001 W
PLW13          0.20446000 W

F2 - Processing parameters
SI                   32768
SF            125.8005407 MHz
WDW                    EM
SSB       0
LB                    1.00 Hz
GB        0
PC                    1.40
```

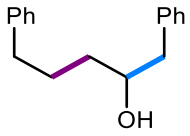
Ph
Ph
OH

4.2.3ac

^{1}H NMR

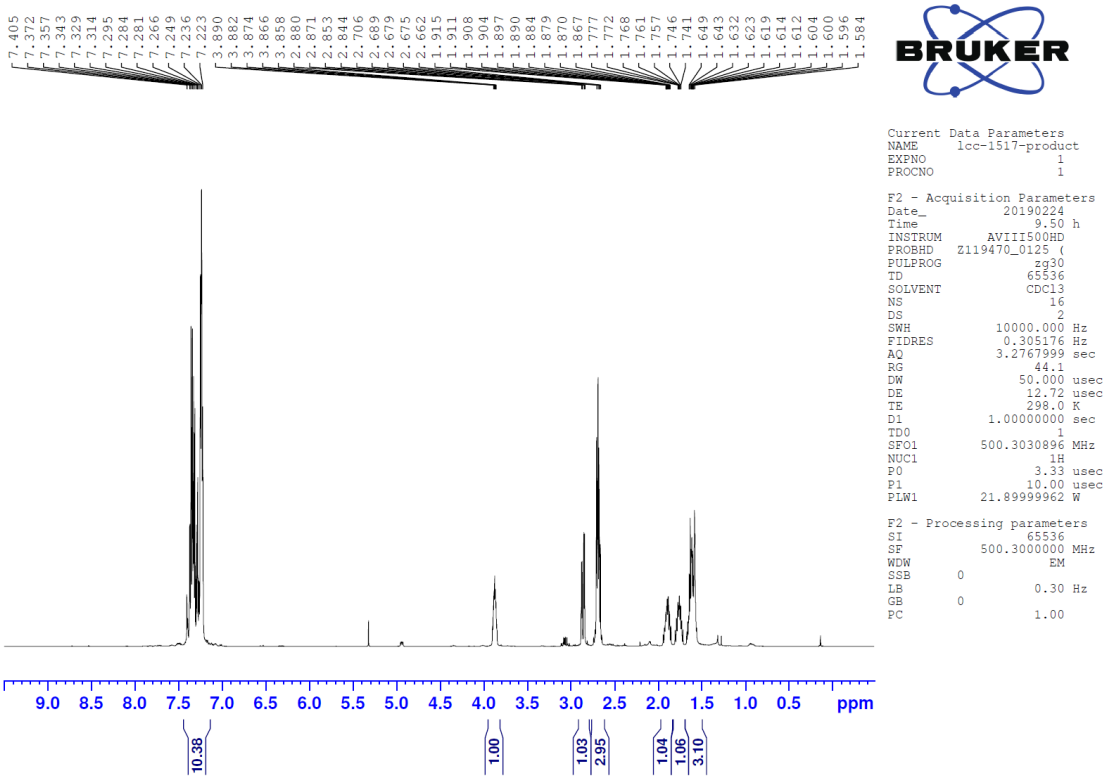
7.405
7.372
7.357
7.343
7.329
7.314
7.295
7.284
7.281
7.266
7.249
7.236
7.223
3.890
3.882
3.874
3.866
3.858
3.880
2.871
2.853
2.844
2.706
2.689
2.679
2.675
2.662
1.915
1.911
1.908
1.904
1.897
1.890
1.884
1.879
1.870
1.867
1.777
1.772
1.768
1.761
1.757
1.746
1.741
1.649
1.643
1.632
1.623
1.619
1.614
1.612
1.604
1.600
1.596
1.584
BRUKER
Current Data Parameters
NAME lcc-1517-product
EXPNO 1
PROCNO 1
F2 - Acquisition Parameters
Date_ 20190224
Time 9.50 h
INSTRUM AVIII500HD
PROBHD Z119470_0125 (
PULPROG zg30
TD 65536
SOLVENT CDCl3
NS 16
DS 2
SWH 10000.000 Hz
FIDRES 0.305176 Hz
AQ 3.2767999 sec
RG 44.1
DW 50.000 usec
DE 12.72 usec
TE 298.0 K
D1 1.00000000 sec
TD0 1
SFO1 500.3030896 MHz
NUC1 1H
P0 3.33 usec
P1 10.00 usec
PLW1 21.89999962 W
F2 - Processing parameters
SI 65536
SF 500.3000000 MHz
WDW EM
SSB 0
LB 0.30 Hz
GB 0
PC 1.00
9.0 8.5 8.0 7.5 7.0 6.5 6.0 5.5 5.0 4.5 4.0 3.5 3.0 2.5 2.0 1.5 1.0 0.5 ppm
10.38
1.00
1.03
2.95
1.04
1.06
3.10

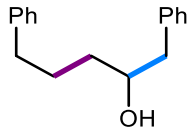

4.2.3ac

^{13}C NMR

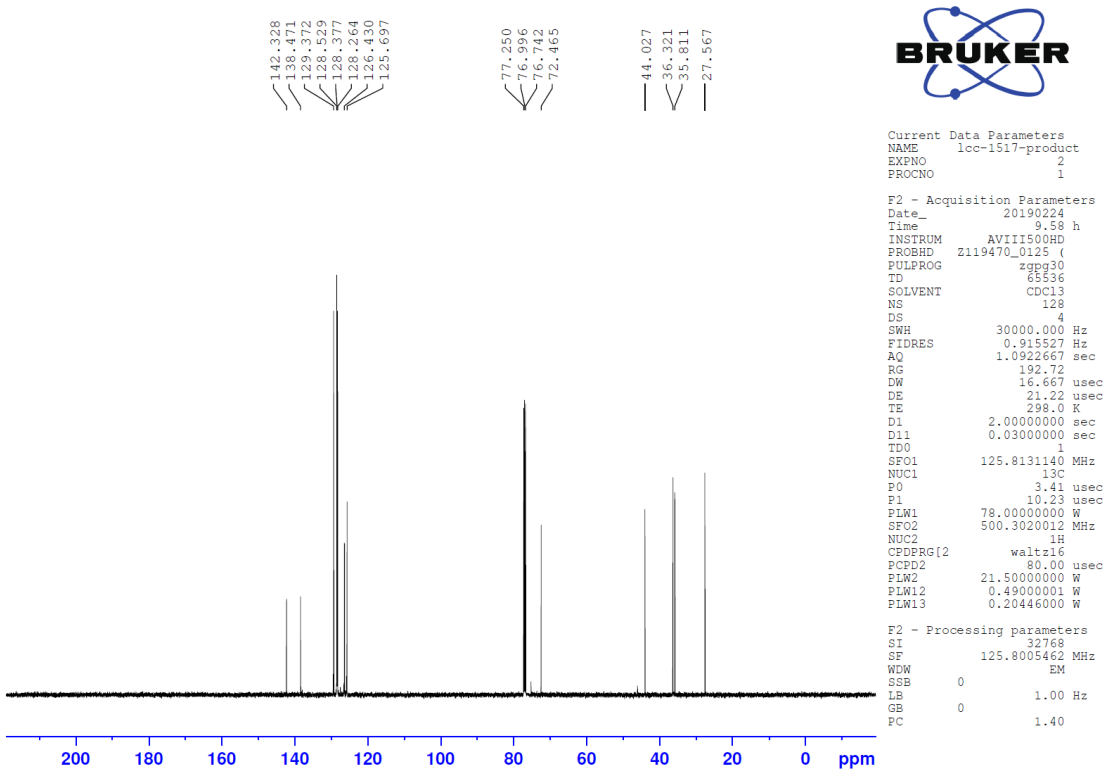


```
Current Data Parameters
NAME      lcc-1517-product
EXPNO                    2
PROCNO                   1

F2 - Acquisition Parameters
Date_           20190224
Time                9.58 h
INSTRUM       AVIII500HD
PROBHD    Z119470_0125 (
PULPROG          zgpg30
TD                65536
SOLVENT           CDCl3
NS                  128
DS                    4
SWH           30000.000 Hz
FIDRES         0.915527 Hz
AQ             1.0922667 sec
RG                192.72
DW                16.667 usec
DE                21.22 usec
TE                298.0 K
D1            2.00000000 sec
D11           0.03000000 sec
TD0                   1
SFO1         125.8131140 MHz
NUC1                 13C
P0                  3.41 usec
P1                 10.23 usec
PLW1         78.00000000 W
SFO2         500.3020012 MHz
NUC2                 1H
CPDPRG[2         waltz16
PCPD2               80.00 usec
PLW2         21.50000000 W
PLW12         0.49000001 W
PLW13         0.20446000 W

F2 - Processing parameters
SI                32768
SF           125.8005462 MHz
WDW                  EM
SSB       0
LB                 1.00 Hz
GB        0
PC                 1.40
```

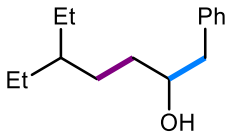
Et
Ph
Et
OH

4.2.3ad

^{1}H NMR

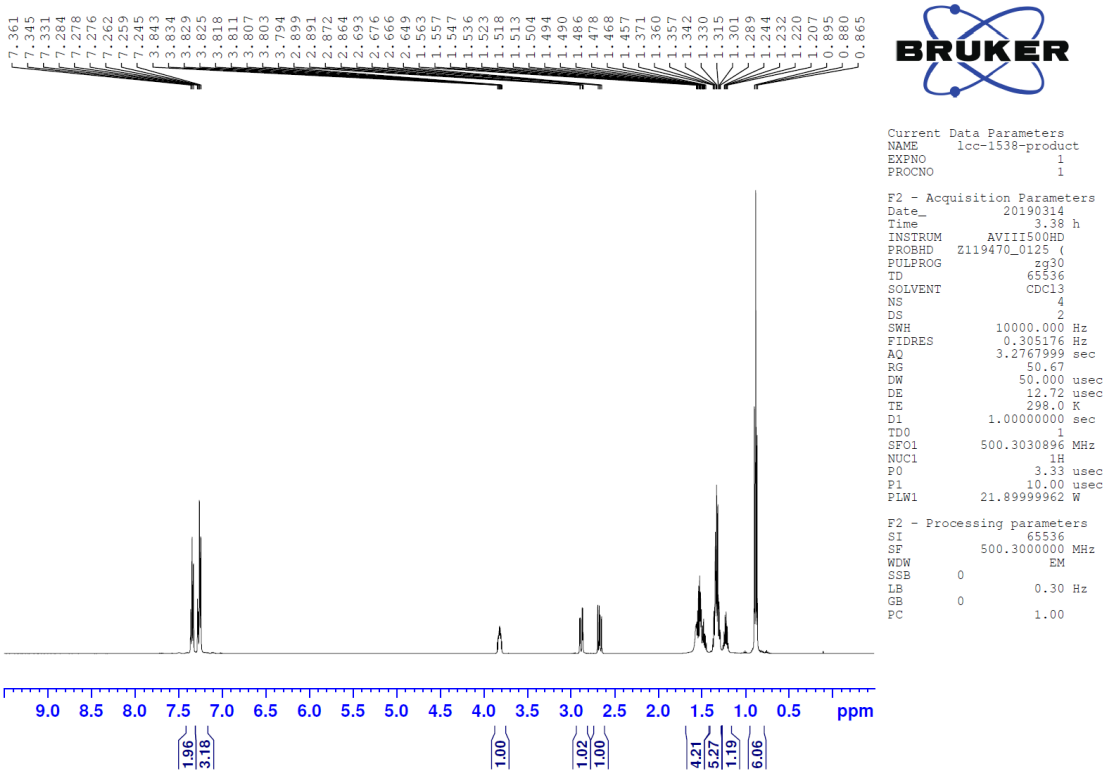
7.361
7.345
7.331
7.284
7.278
7.276
7.262
7.259
7.245
3.843
3.834
3.829
3.825
3.818
3.811
3.807
3.803
3.794
2.899
2.891
2.872
2.864
2.693
2.676
2.666
2.649
1.563
1.557
1.547
1.536
1.523
1.518
1.513
1.504
1.494
1.490
1.486
1.478
1.468
1.457
1.371
1.360
1.357
1.342
1.330
1.315
1.301
1.289
1.244
1.232
1.220
1.207
0.895
0.880
0.865
BRUKER
Current Data Parameters
NAME lcc-1538-product
EXPNO 1
PROCNO 1
F2 - Acquisition Parameters
Date_ 20190314
Time 3.38 h
INSTRUM AVIII500HD
PROBHD Z119470_0125 (
PULPROG zg30
TD 65536
SOLVENT CDCl3
NS 4
DS 2
SWH 10000.000 Hz
FIDRES 0.305176 Hz
AQ 3.2767999 sec
RG 50.67
DW 50.000 usec
DE 12.72 usec
TE 298.0 K
D1 1.00000000 sec
TD0 1
SFO1 500.3030896 MHz
NUC1 1H
P0 3.33 usec
P1 10.00 usec
PLW1 21.89999962 W
F2 - Processing parameters
SI 65536
SF 500.3000000 MHz
WDW EM
SSB 0
LB 0.30 Hz
GB 0
PC 1.00
9.0 8.5 8.0 7.5 7.0 6.5 6.0 5.5 5.0 4.5 4.0 3.5 3.0 2.5 2.0 1.5 1.0 0.5 ppm
1.96
3.18
1.00
1.02
1.00
4.21
5.27
1.19
6.06

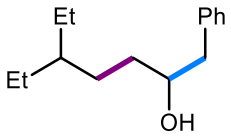

4.2.3ad

^{13}C NMR

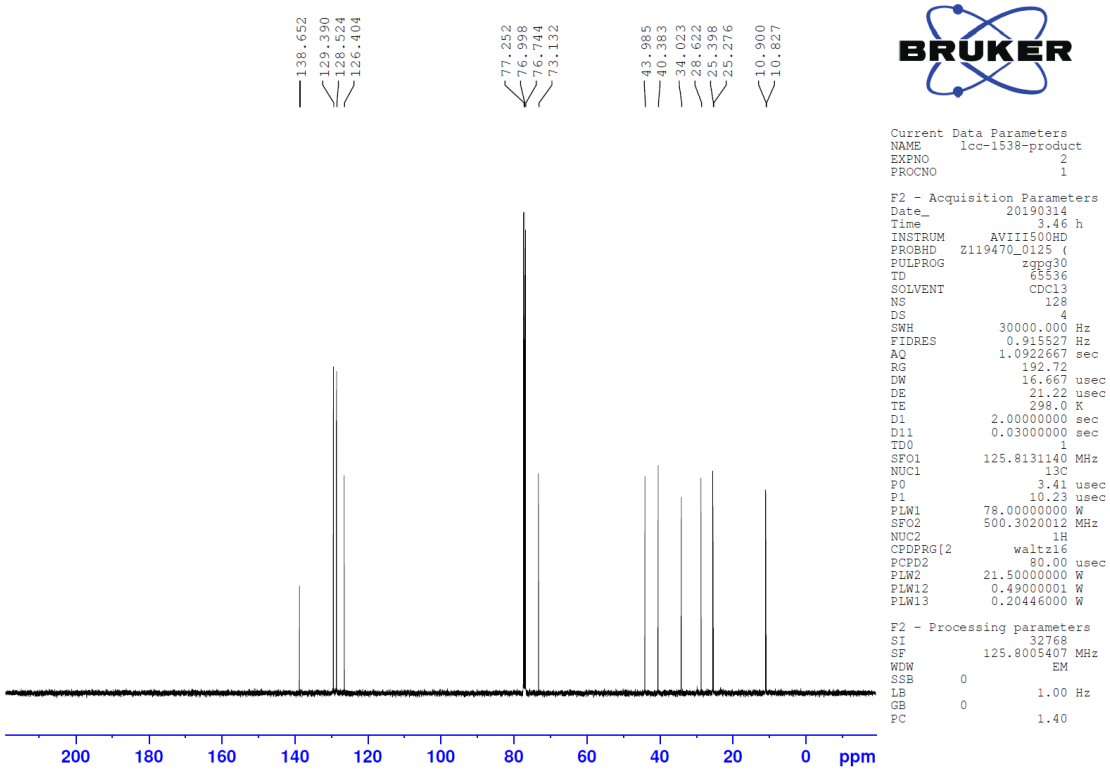


```
Current Data Parameters
NAME      lcc-1538-product
EXPNO                    2
PROCNO                   1

F2 - Acquisition Parameters
Date_           20190314
Time                3.46 h
INSTRUM       AVIII500HD
PROBHD    Z119470_0125 (
PULPROG          zgpg30
TD                65536
SOLVENT           CDCl3
NS                  128
DS                    4
SWH           30000.000 Hz
FIDRES            0.915527 Hz
AQ              1.0922667 sec
RG                192.72
DW                16.667 usec
DE                21.22 usec
TE                298.0 K
D1             2.00000000 sec
D11            0.03000000 sec
TD0                   1
SFO1          125.8131140 MHz
NUC1                 13C
P0                  3.41 usec
P1                 10.23 usec
PLW1          78.00000000 W
SFO2          500.3020012 MHz
NUC2                  1H
CPDPRG[2          waltz16
PCPD2              80.00 usec
PLW2          21.50000000 W
PLW12          0.49000001 W
PLW13          0.20446000 W

F2 - Processing parameters
SI                32768
SF            125.8005407 MHz
WDW                  EM
SSB       0
LB                1.00 Hz
GB        0
PC                1.40
```

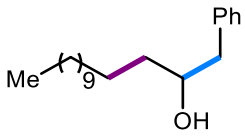
Ph
Me
9
OH

4.2.3ae

^{1}H NMR

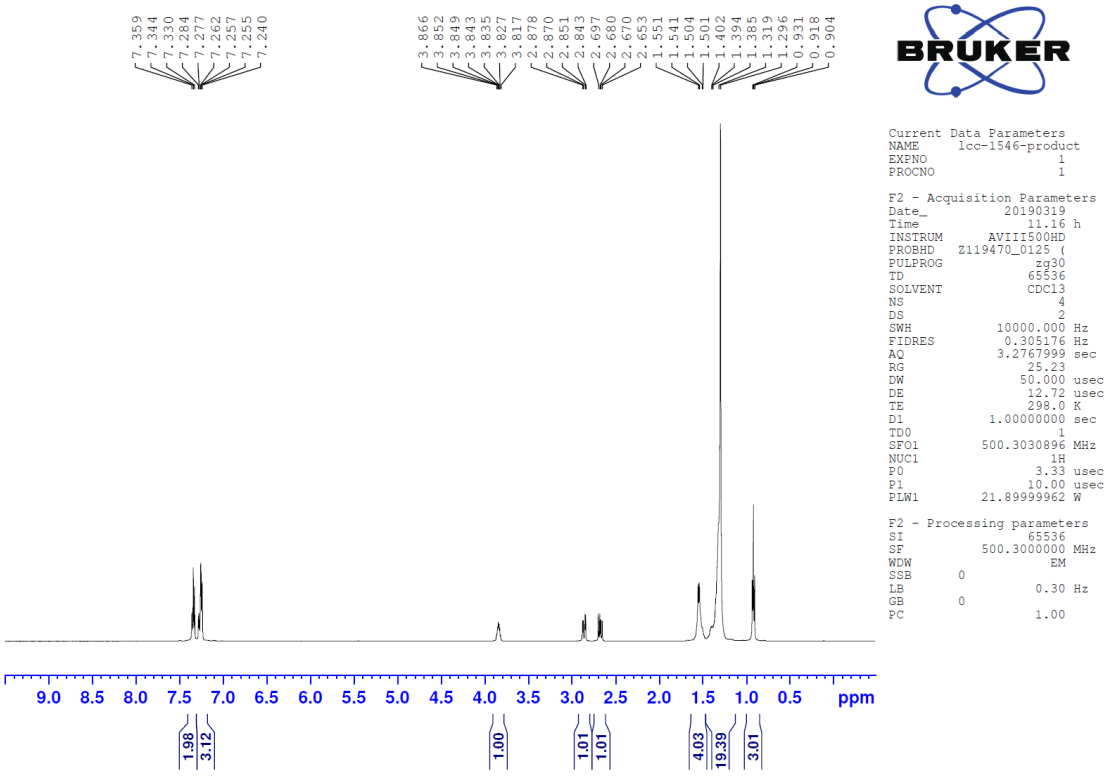
7.359
7.344
7.330
7.284
7.277
7.262
7.257
7.255
7.240
3.866
3.852
3.849
3.843
3.835
3.827
3.817
2.878
2.870
2.851
2.843
2.697
2.680
2.670
2.653
1.551
1.541
1.504
1.501
1.402
1.394
1.385
1.319
1.296
0.931
0.918
0.904
BRUKER
Current Data Parameters
NAME lcc-1546-product
EXPNO 1
PROCNO 1
F2 - Acquisition Parameters
Date_ 20190319
Time 11.16 h
INSTRUM AVIII500HD
PROBHD Z119470_0125 (
PULPROG zg30
TD 65536
SOLVENT CDCl3
NS 4
DS 2
SWH 10000.000 Hz
FIDRES 0.305176 Hz
AQ 3.2767999 sec
RG 25.23
DW 50.000 usec
DE 12.72 usec
TE 298.0 K
D1 1.00000000 sec
TD0 1
SFO1 500.3030896 MHz
NUC1 1H
P0 3.33 usec
P1 10.00 usec
PLW1 21.89999962 W
F2 - Processing parameters
SI 65536
SF 500.3000000 MHz
WDW EM
SSB 0
LB 0.30 Hz
GB 0
PC 1.00
9.0 8.5 8.0 7.5 7.0 6.5 6.0 5.5 5.0 4.5 4.0 3.5 3.0 2.5 2.0 1.5 1.0 0.5 ppm
1.98
3.12
1.00
1.01
1.01
4.03
19.39
3.01

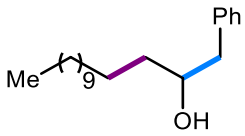

4.2.3ae

^{13}C NMR

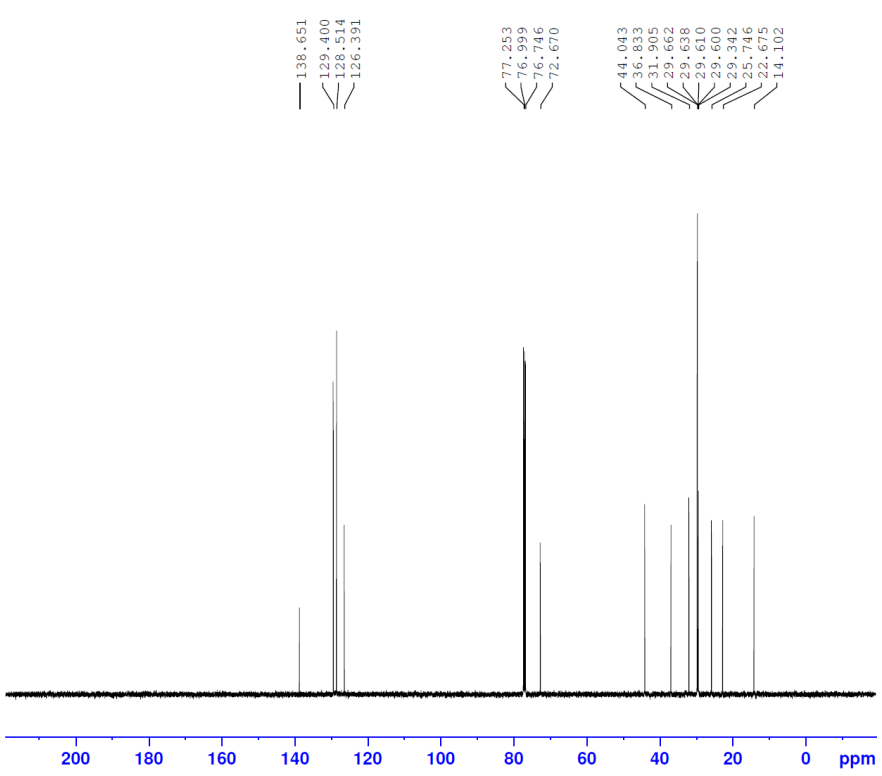


```
Current Data Parameters
NAME      lcc-1546-product
EXPNO                    2
PROCNO                   1

F2 - Acquisition Parameters
Date_             20190319
Time                11.24 h
INSTRUM       AVIII500HD
PROBHD    Z119470_0125 (
PULPROG             zgpg30
TD                   65536
SOLVENT              CDCl3
NS                     128
DS                       4
SWH              30000.000 Hz
FIDRES           0.915527 Hz
AQ               1.0922667 sec
RG                  192.72
DW                  16.667 usec
DE                   21.22 usec
TE                   298.0 K
D1              2.00000000 sec
D11             0.03000000 sec
TD0                      1
SFO1         125.8131140 MHz
NUC1                   13C
P0                    3.41 usec
P1                   10.23 usec
PLW1         78.00000000 W
SFO2         500.3020012 MHz
NUC2                   1H
CPDPRG[2           waltz16
PCPD2                80.00 usec
PLW2         21.50000000 W
PLW12         0.49000001 W
PLW13         0.20446000 W

F2 - Processing parameters
SI                   32768
SF           125.8005407 MHz
WDW                     EM
SSB       0
LB                    1.00 Hz
GB        0
PC                    1.40
```

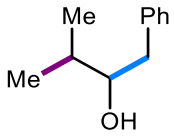
Me
Ph
Me
OH

4.2.3af

^{1}H NMR

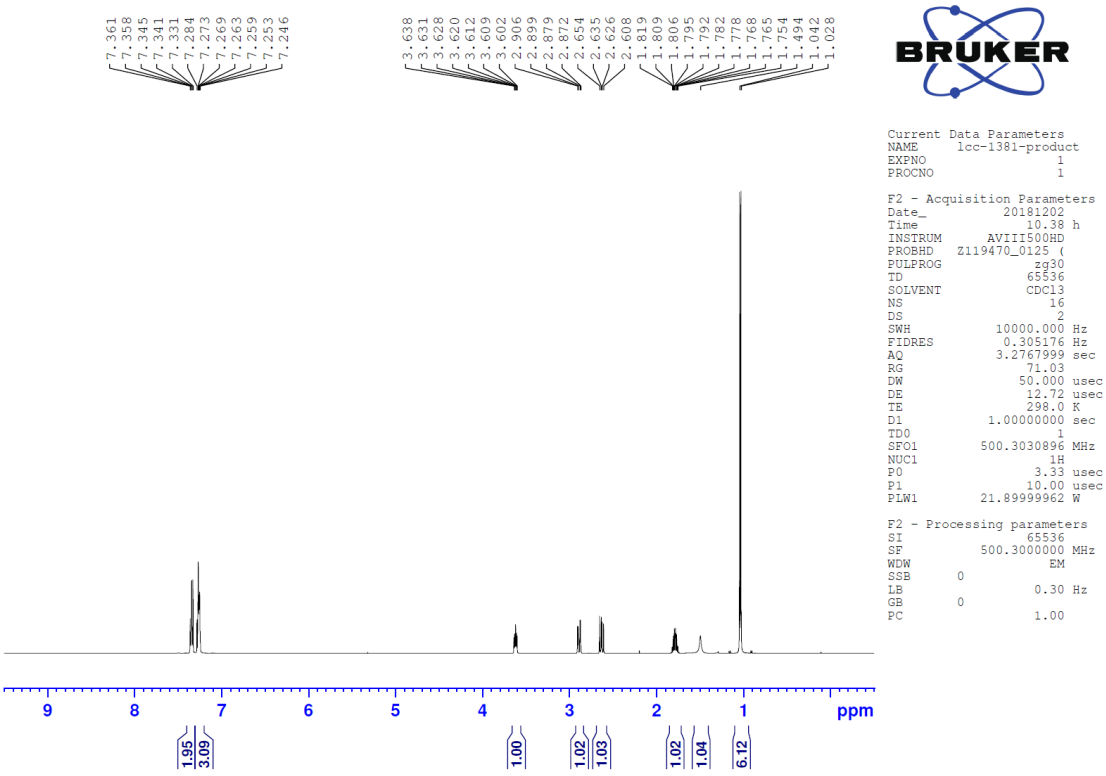
7.361
7.358
7.345
7.341
7.331
7.284
7.273
7.269
7.263
7.259
7.253
7.246
3.638
3.631
3.628
3.620
3.612
3.609
3.602
2.906
2.899
2.879
2.872
2.654
2.635
2.626
2.608
1.819
1.809
1.806
1.795
1.792
1.782
1.778
1.768
1.765
1.754
1.494
1.042
1.028
BRUKER
Current Data Parameters
NAME lcc-1381-product
EXPNO 1
PROCNO 1
F2 - Acquisition Parameters
Date_ 20181202
Time 10.38 h
INSTRUM AVIII500HD
PROBHD Z119470_0125 (
PULPROG zg30
TD 65536
SOLVENT CDCl3
NS 16
DS 2
SWH 10000.000 Hz
FIDRES 0.305176 Hz
AQ 3.2767999 sec
RG 71.03
DW 50.000 usec
DE 12.72 usec
TE 298.0 K
D1 1.00000000 sec
TD0 1
SFO1 500.3030896 MHz
NUC1 1H
P0 3.33 usec
P1 10.00 usec
PLW1 21.89999962 W
F2 - Processing parameters
SI 65536
SF 500.3000000 MHz
WDW EM
SSB 0
LB 0.30 Hz
GB 0
PC 1.00
9
8
7
6
5
4
3
2
1
ppm
1.95
3.09
1.00
1.02
1.03
1.02
1.04
6.12

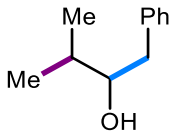

4.2.3af

^{13}C NMR

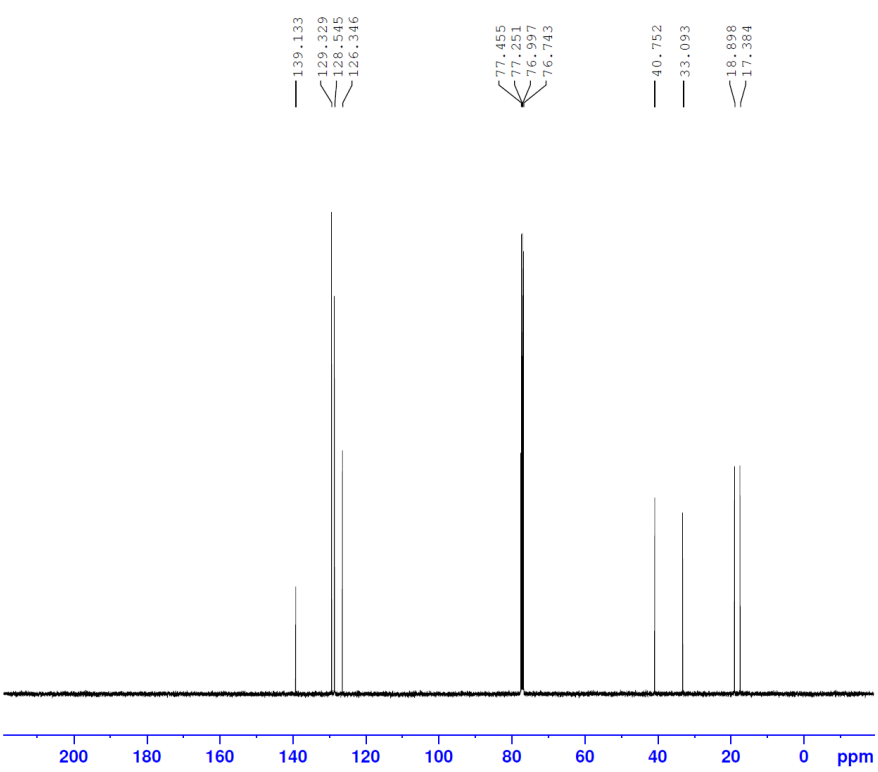

BRUKER

```
Current Data Parameters
NAME      lcc-1381-product
EXPNO                    2
PROCNO                   1

F2 - Acquisition Parameters
Date_           20181202
Time              10.53 h
INSTRUM       AVIII500HD
PROBHD   Z119470_0125 (
PULPROG           zgpg30
TD                65536
SOLVENT           CDCl3
NS                  256
DS                    4
SWH           30000.000 Hz
FIDRES            0.915527 Hz
AQ             1.0922667 sec
RG                192.72
DW                16.667 usec
DE                21.22 usec
TE                298.0 K
D1             2.00000000 sec
D11            0.03000000 sec
TD0                   1
SFO1         125.8131140 MHz
NUC1                 13C
P0                  3.41 usec
P1                 10.23 usec
PLW1         78.00000000 W
SFO2         500.3020012 MHz
NUC2                 1H
CPDPRG[2         waltz16
PCPD2              80.00 usec
PLW2         21.50000000 W
PLW12         0.49000001 W
PLW13         0.20446000 W

F2 - Processing parameters
SI                32768
SF           125.8005407 MHz
WDW                  EM
SSB       0
LB                1.00 Hz
GB        0
PC                1.40
```

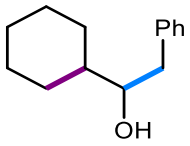
Ph
OH

4.2.3ag

^{1}H NMR

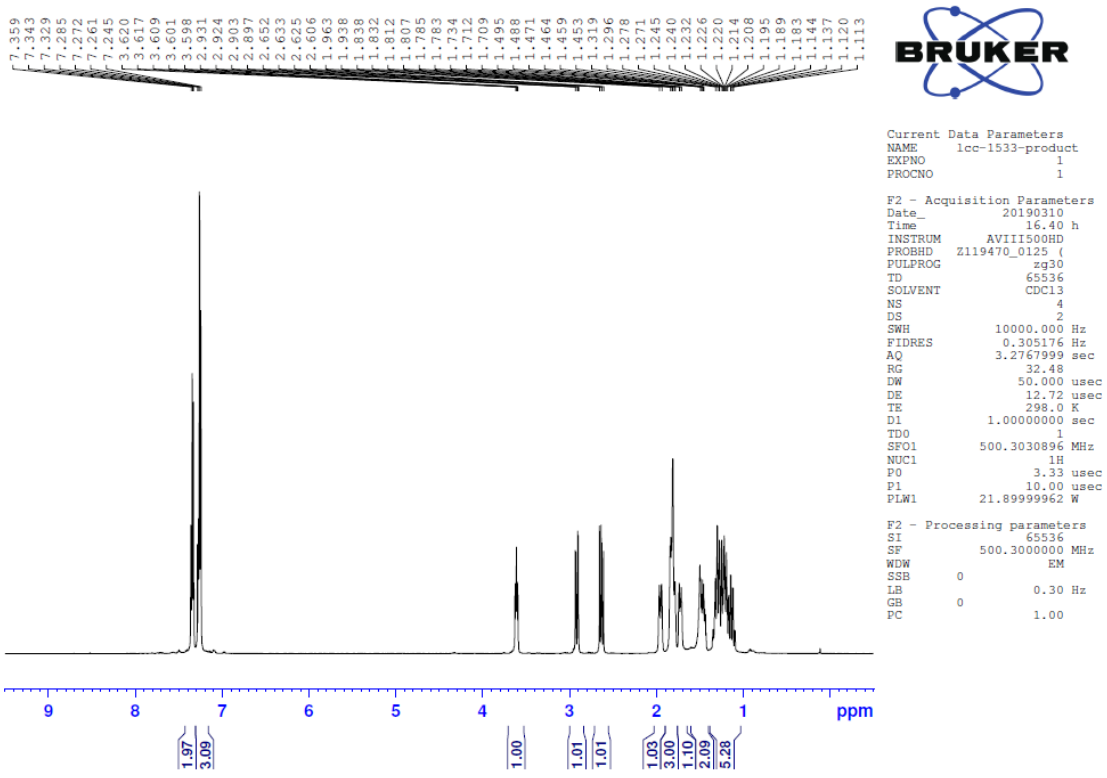
7.359
7.343
7.329
7.285
7.272
7.261
7.245
3.620
3.617
3.609
3.601
3.598
2.931
2.924
2.903
2.897
2.652
2.633
2.625
2.606
1.963
1.938
1.838
1.832
1.812
1.807
1.785
1.783
1.734
1.712
1.709
1.495
1.488
1.471
1.464
1.459
1.453
1.319
1.296
1.278
1.271
1.245
1.240
1.232
1.226
1.220
1.214
1.208
1.195
1.189
1.183
1.144
1.137
1.120
1.113
BRUKER
Current Data Parameters
NAME 1cc-1533-product
EXPNO 1
PROCNO 1
F2 - Acquisition Parameters
Date_ 20190310
Time 16.40 h
INSTRUM AVIII500HD
PROBHD Z119470_0125 (
PULPROG zg30
TD 65536
SOLVENT CDCl3
NS 4
DS 2
SWH 10000.000 Hz
FIDRES 0.305176 Hz
AQ 3.2767999 sec
RG 32.48
DW 50.000 usec
DE 12.72 usec
TE 298.0 K
D1 1.00000000 sec
TD0 1
SFO1 500.3030896 MHz
NUC1 1H
P0 3.33 usec
P1 10.00 usec
PLW1 21.89999962 W
F2 - Processing parameters
SI 65536
SF 500.3000000 MHz
WDW EM
SSB 0
LB 0.30 Hz
GB 0
PC 1.00
9
8
7
6
5
4
3
2
1
ppm
1.97
3.09
1.00
1.01
1.01
1.03
3.00
1.10
2.09
5.28

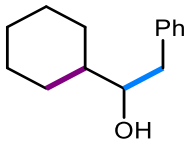

4.2.3ag

^{13}C NMR

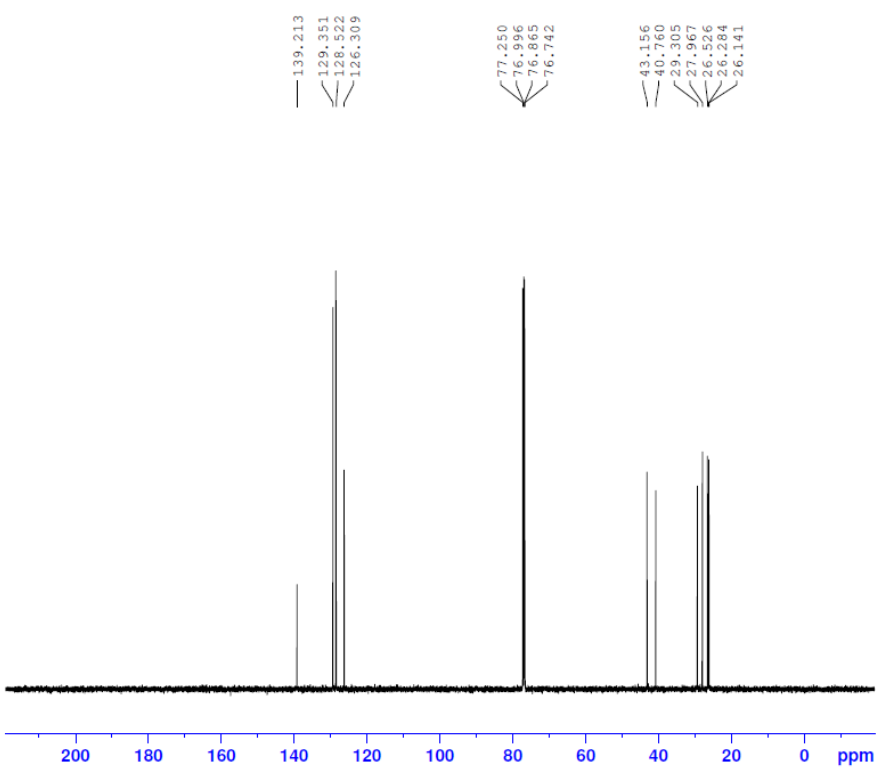

BRUKER

```
Current Data Parameters
NAME      1cc-1533-product
EXPNO                    2
PROCNO                   1

F2 - Acquisition Parameters
Date_           20190310
Time              16.48 h
INSTRUM       AVIII500HD
PROBHD    Z119470_0125 (
PULPROG          zgpg30
TD                65536
SOLVENT           CDCl3
NS                  128
DS                    4
SWH           30000.000 Hz
FIDRES         0.915527 Hz
AQ             1.0922667 sec
RG                192.72
DW                16.667 usec
DE                21.22 usec
TE                298.0 K
D1             2.00000000 sec
D11            0.03000000 sec
TD0                   1
SFO1         125.8131140 MHz
NUC1                 13C
P0                  3.41 usec
P1                 10.23 usec
PLW1         78.00000000 W
SFO2         500.3020012 MHz
NUC2                 1H
CPDPRG[2         waltz16
PCPD2              80.00 usec
PLW2         21.50000000 W
PLW12         0.49000001 W
PLW13         0.20446000 W

F2 - Processing parameters
SI                32768
SF           125.8005425 MHz
WDW                  EM
SSB       0
LB                 1.00 Hz
GB        0
PC                 1.40
```

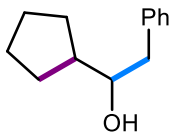
Ph
OH

4.2.3ah

^{1}H NMR

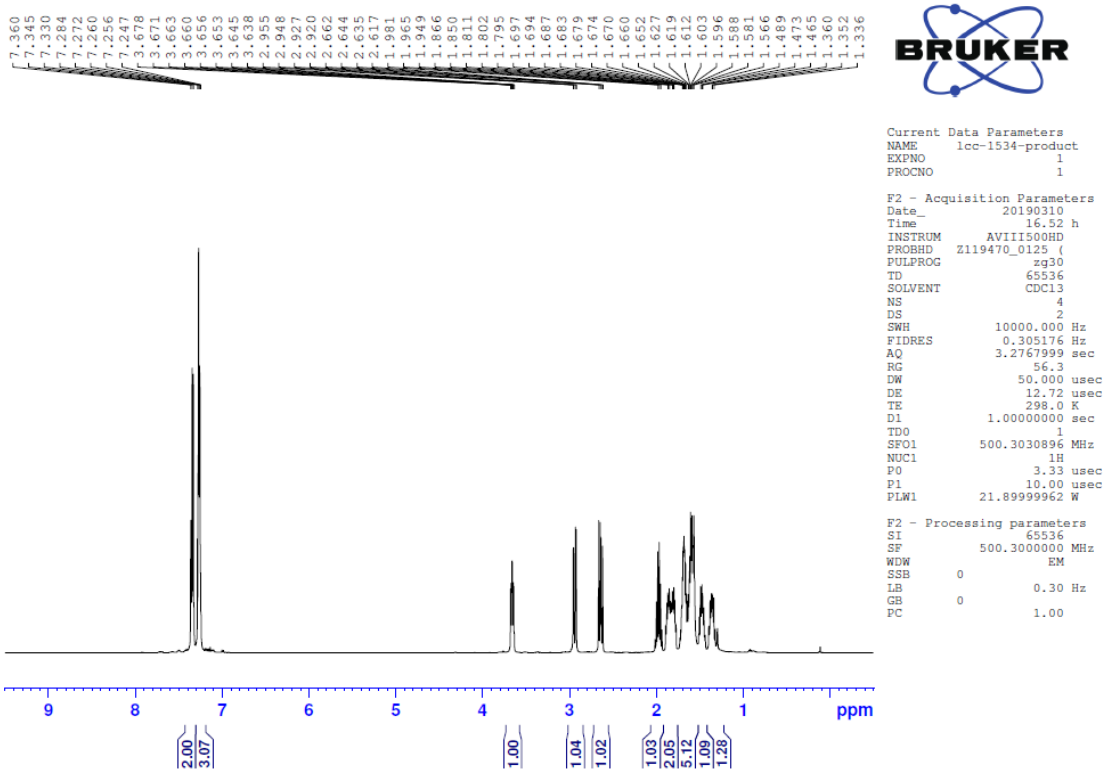
7.360
7.345
7.330
7.284
7.272
7.260
7.256
7.247
3.678
3.671
3.663
3.660
3.656
3.653
3.645
3.638
2.955
2.948
2.927
2.920
2.662
2.644
2.635
2.617
1.981
1.965
1.949
1.866
1.850
1.811
1.802
1.795
1.697
1.694
1.687
1.683
1.679
1.674
1.670
1.660
1.652
1.627
1.619
1.612
1.603
1.596
1.588
1.581
1.566
1.489
1.473
1.465
1.360
1.352
1.336
BRUKER
Current Data Parameters
NAME 1cc-1534-product
EXPNO 1
PROCNO 1
F2 - Acquisition Parameters
Date_ 20190310
Time 16.52 h
INSTRUM AVIII500HD
PROBHD Z119470_0125 (
PULPROG zg30
TD 65536
SOLVENT CDCl3
NS 4
DS 2
SWH 10000.000 Hz
FIDRES 0.305176 Hz
AQ 3.2767999 sec
RG 56.3
DW 50.000 usec
DE 12.72 usec
TE 298.0 K
D1 1.00000000 sec
TD0 1
SFO1 500.3030896 MHz
NUC1 1H
P0 3.33 usec
P1 10.00 usec
PLW1 21.89999962 W
F2 - Processing parameters
SI 65536
SF 500.3000000 MHz
WDW EM
SSB 0
LB 0.30 Hz
GB 0
PC 1.00
9
8
7
6
5
4
3
2
1
ppm
2.00
3.07
1.00
1.04
1.02
1.03
2.05
5.12
1.09
1.28

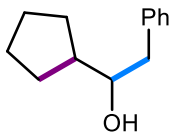

4.2.3ah

^{13}C NMR

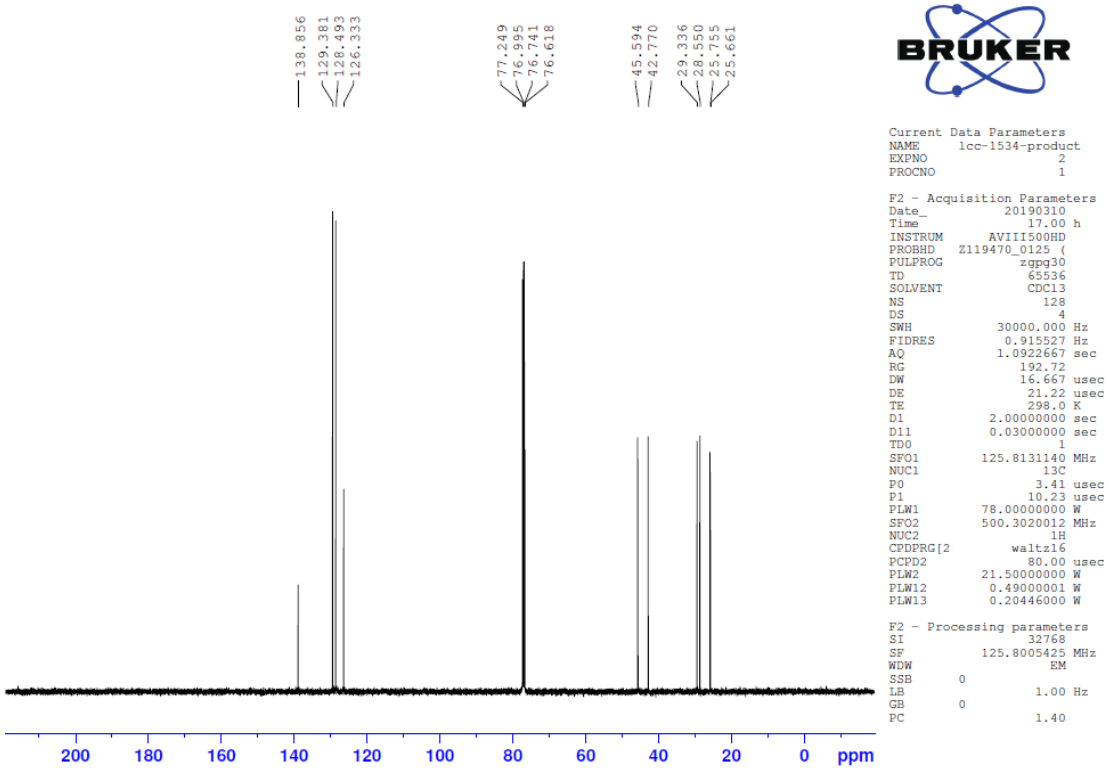


```
Current Data Parameters
NAME      1cc-1534-product
EXPNO                    2
PROCNO                   1

F2 - Acquisition Parameters
Date_           20190310
Time              17.00 h
INSTRUM       AVIII500HD
PROBHD    Z119470_0125 (
PULPROG           zgpg30
TD                65536
SOLVENT           CDCl3
NS                  128
DS                    4
SWH           30000.000 Hz
FIDRES         0.915527 Hz
AQ             1.0922667 sec
RG                192.72
DW                16.667 usec
DE                21.22 usec
TE                298.0 K
D1             2.00000000 sec
D11            0.03000000 sec
TD0                   1
SFO1         125.8131140 MHz
NUC1                 13C
P0                 3.41 usec
P1                10.23 usec
PLW1         78.00000000 W
SFO2         500.3020012 MHz
NUC2                 1H
CPDPRG[2         waltz16
PCPD2              80.00 usec
PLW2         21.50000000 W
PLW12         0.49000001 W
PLW13         0.20446000 W

F2 - Processing parameters
SI                32768
SF           125.8005425 MHz
WDW                  EM
SSB       0
LB                1.00 Hz
GB        0
PC                1.40
```

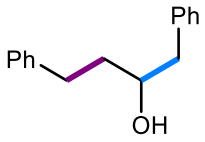
Ph
Ph
OH

4.2.3ai

^{1}H NMR

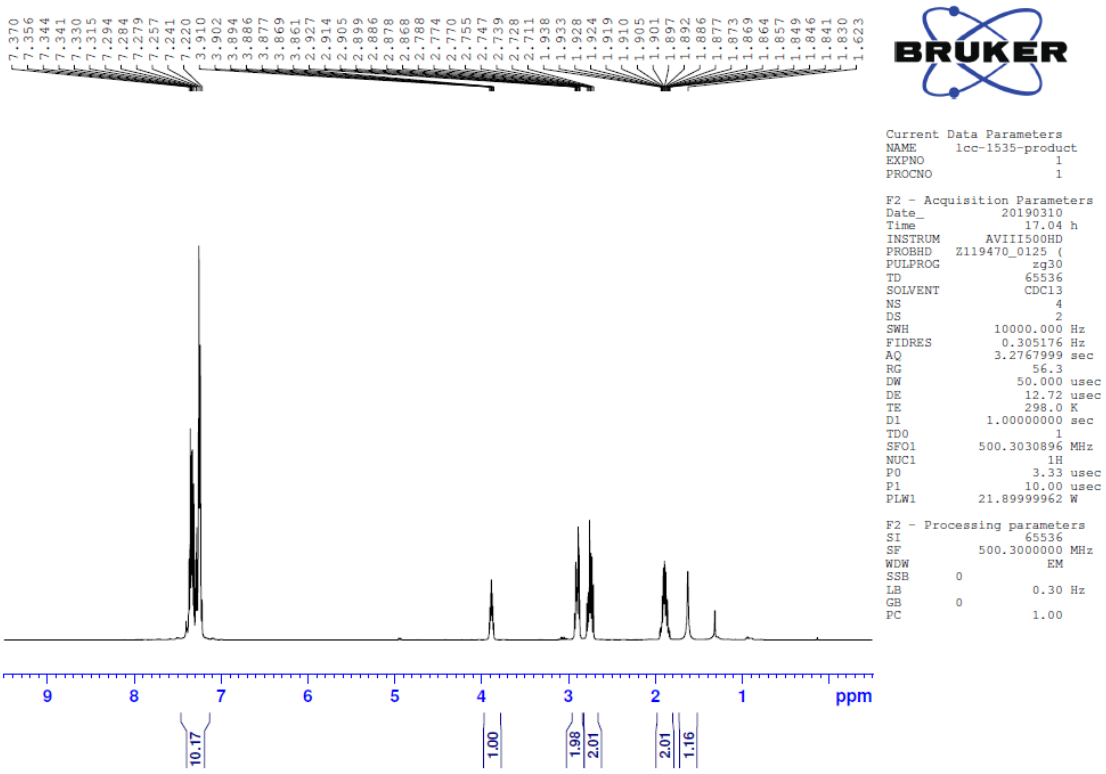
7.370
7.356
7.344
7.341
7.330
7.315
7.294
7.284
7.279
7.257
7.241
7.220
3.910
3.902
3.894
3.886
3.877
3.869
3.861
2.927
2.914
2.905
2.899
2.886
2.878
2.868
2.788
2.774
2.770
2.755
2.747
2.739
2.728
2.711
1.938
1.933
1.928
1.924
1.919
1.910
1.905
1.901
1.897
1.892
1.886
1.877
1.873
1.869
1.864
1.857
1.849
1.846
1.841
1.830
1.623
BRUKER
Current Data Parameters
NAME 1cc-1535-product
EXPNO 1
PROCNO 1
F2 - Acquisition Parameters
Date_ 20190310
Time 17.04 h
INSTRUM AVIII500HD
PROBHD Z119470_0125 (
PULPROG zg30
TD 65536
SOLVENT CDCl3
NS 4
DS 2
SWH 10000.000 Hz
FIDRES 0.305176 Hz
AQ 3.2767999 sec
RG 56.3
DW 50.000 usec
DE 12.72 usec
TE 298.0 K
D1 1.00000000 sec
TD0 1
SFO1 500.3030896 MHz
NUC1 1H
P0 3.33 usec
P1 10.00 usec
PLW1 21.89999962 W
F2 - Processing parameters
SI 65536
SF 500.3000000 MHz
WDW EM
SSB 0
LB 0.30 Hz
GB 0
PC 1.00
9
8
7
6
5
4
3
2
1
ppm
10.17
1.00
1.98
2.01
2.01
1.16

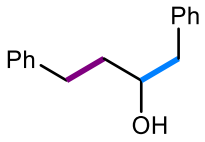

4.2.3ai

^{13}C NMR

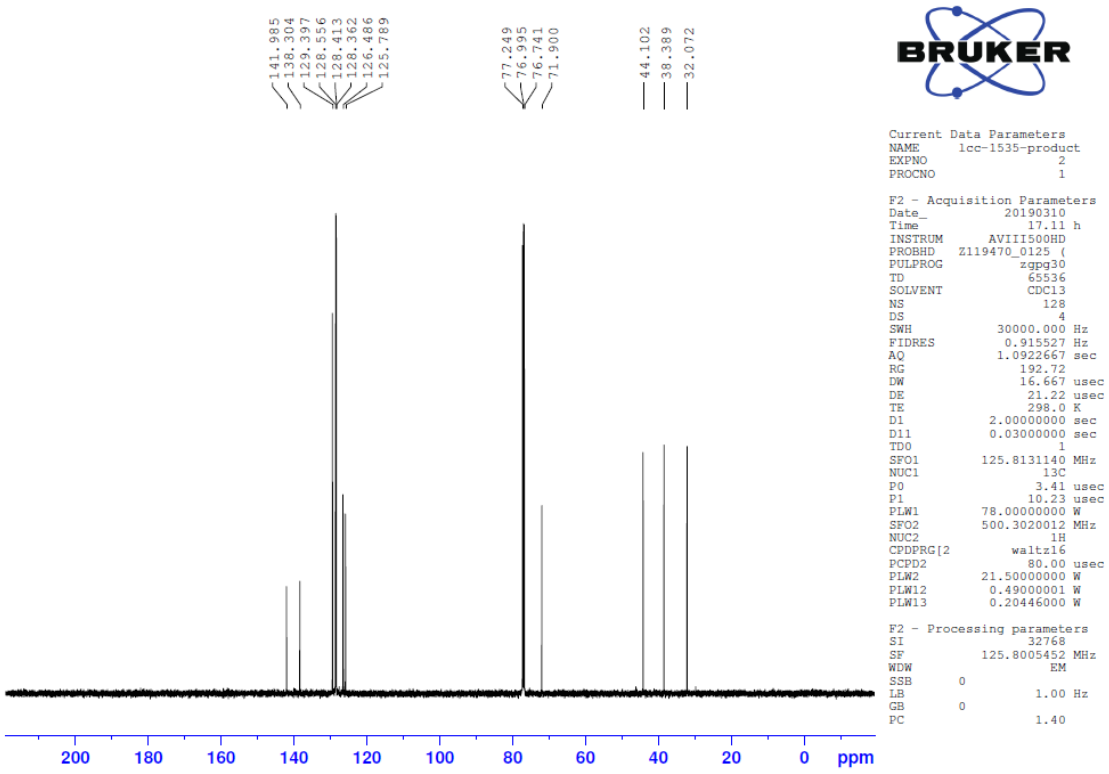


```
Current Data Parameters
NAME      1cc-1535-product
EXPNO                    2
PROCNO                   1

F2 - Acquisition Parameters
Date_           20190310
Time              17.11 h
INSTRUM       AVIII500HD
PROBHD    Z119470_0125 (
PULPROG          zgpg30
TD                65536
SOLVENT           CDCl3
NS                  128
DS                    4
SWH           30000.000 Hz
FIDRES         0.915527 Hz
AQ             1.0922667 sec
RG                192.72
DW                16.667 usec
DE                21.22 usec
TE                298.0 K
D1             2.00000000 sec
D11            0.03000000 sec
TD0                   1
SFO1         125.8131140 MHz
NUC1                 13C
P0                  3.41 usec
P1                 10.23 usec
PLW1          78.00000000 W
SFO2         500.3020012 MHz
NUC2                  1H
CPDPRG[2          waltz16
PCPD2              80.00 usec
PLW2          21.50000000 W
PLW12          0.49000001 W
PLW13          0.20446000 W

F2 - Processing parameters
SI                32768
SF           125.8005452 MHz
WDW                  EM
SSB       0
LB                 1.00 Hz
GB        0
PC                 1.40
```

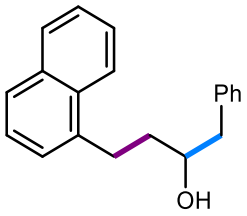
Ph
OH

4.2.3aj

^{1}H NMR

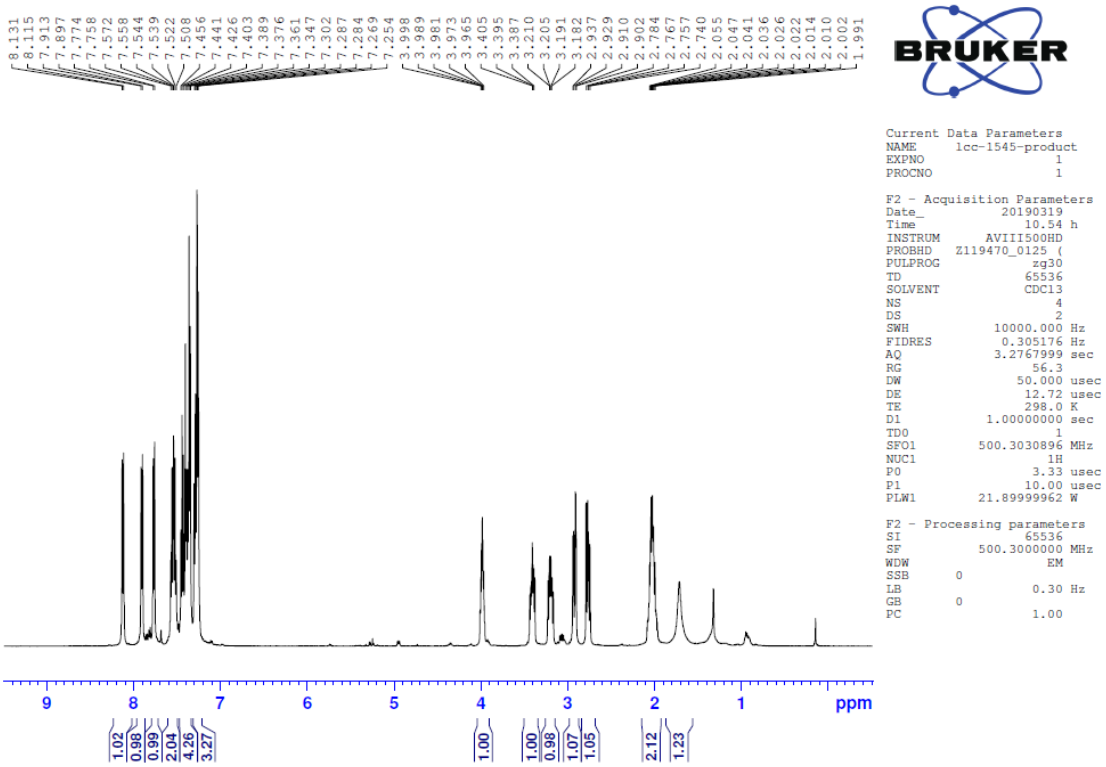
8.131
8.115
7.913
7.897
7.774
7.758
7.572
7.558
7.544
7.539
7.522
7.508
7.456
7.441
7.426
7.403
7.389
7.376
7.361
7.347
7.302
7.287
7.284
7.269
7.254
3.998
3.989
3.981
3.973
3.965
3.405
3.395
3.387
3.210
3.205
3.191
3.182
2.937
2.929
2.910
2.902
2.784
2.767
2.757
2.740
2.055
2.047
2.041
2.036
2.026
2.022
2.014
2.010
2.002
1.991
BRUKER
Current Data Parameters
NAME 1cc-1545-product
EXPNO 1
PROCNO 1
F2 - Acquisition Parameters
Date_ 20190319
Time 10.54 h
INSTRUM AVIII500HD
PROBHD Z119470_0125 (
PULPROG zg30
TD 65536
SOLVENT CDCl3
NS 4
DS 2
SWH 10000.000 Hz
FIDRES 0.305176 Hz
AQ 3.2767999 sec
RG 56.3
DW 50.000 usec
DE 12.72 usec
TE 298.0 K
D1 1.00000000 sec
TD0 1
SFO1 500.3030896 MHz
NUC1 1H
P0 3.33 usec
P1 10.00 usec
PLW1 21.89999962 W
F2 - Processing parameters
SI 65536
SF 500.3000000 MHz
WDW EM
SSB 0
LB 0.30 Hz
GB 0
PC 1.00
9
8
7
6
5
4
3
2
1
ppm
1.02
0.98
0.99
2.04
4.26
3.27
1.00
1.00
0.98
1.07
1.05
2.12
1.23

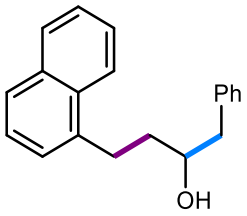

4.2.3aj

^{13}C NMR

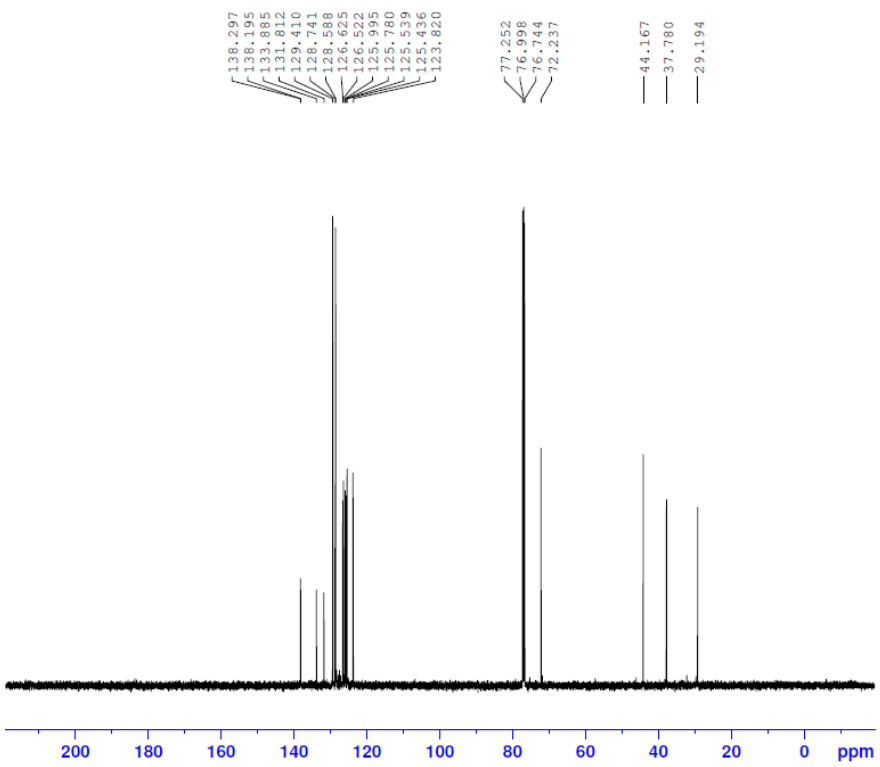


```
Current Data Parameters
NAME      1cc-1545-product
EXPNO                    2
PROCNO                   1

F2 - Acquisition Parameters
Date_             20190319
Time                11.12 h
INSTRUM         AVIII500HD
PROBHD    Z119470_0125 (
PULPROG            zgpg30
TD                  65536
SOLVENT             CDCl3
NS                    128
DS                      4
SWH             30000.000 Hz
FIDRES              0.915527 Hz
AQ                1.0922667 sec
RG                  192.72
DW                  16.667 usec
DE                  21.22 usec
TE                  298.0 K
D1              2.00000000 sec
D11             0.03000000 sec
TD0                     1
SFO1          125.8131140 MHz
NUC1                   13C
P0                    3.41 usec
P1                   10.23 usec
PLW1          78.00000000 W
SFO2          500.3020012 MHz
NUC2                   1H
CPDPRG[2           waltz16
PCPD2                80.00 usec
PLW2          21.50000000 W
PLW12          0.49000001 W
PLW13          0.20446000 W

F2 - Processing parameters
SI                   32768
SF            125.8005453 MHz
WDW                     EM
SSB         0
LB                    1.00 Hz
GB          0
PC                    1.40
```

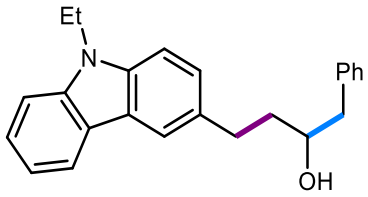
Et
N
Ph
OH

4.2.3ak

^{1}H NMR

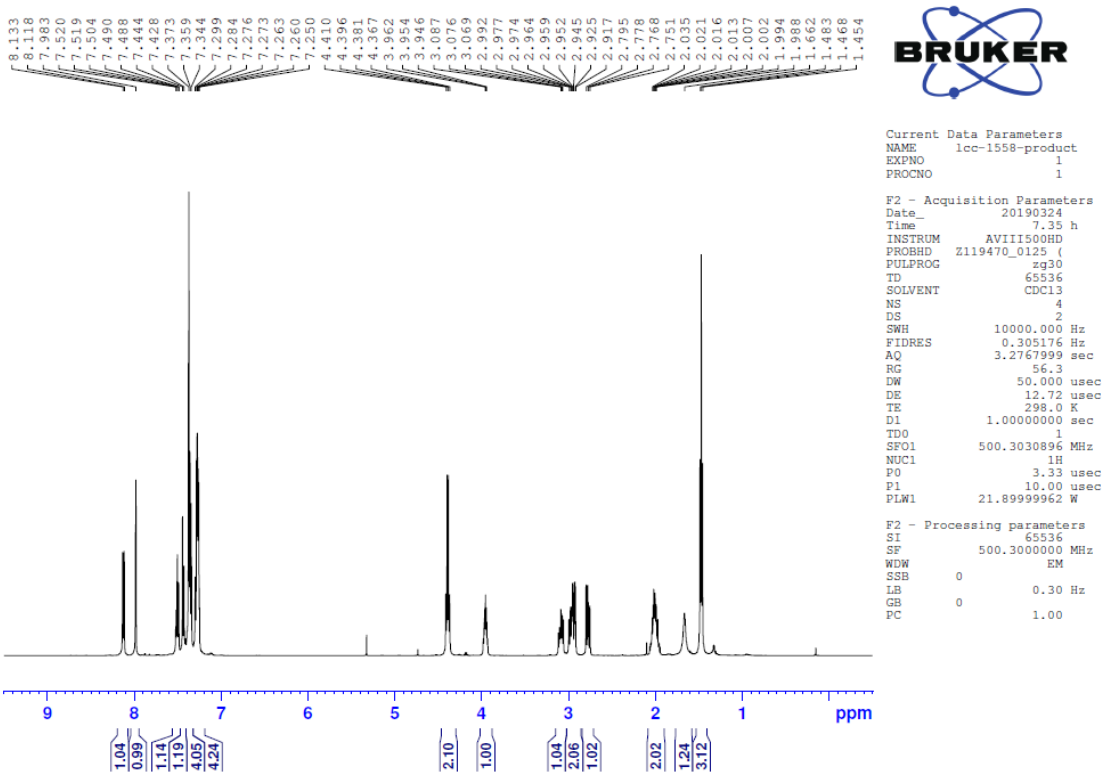
8.133
8.118
7.983
7.520
7.519
7.504
7.490
7.488
7.444
7.428
7.373
7.359
7.344
7.299
7.284
7.276
7.273
7.263
7.260
7.250
4.410
4.396
4.381
4.367
3.962
3.954
3.946
3.087
3.076
3.069
2.992
2.977
2.974
2.964
2.959
2.952
2.945
2.925
2.917
2.795
2.778
2.768
2.751
2.035
2.021
2.016
2.013
2.007
2.002
1.994
1.988
1.662
1.483
1.468
1.454
BRUKER
Current Data Parameters
NAME 1cc-1558-product
EXPNO 1
PROCNO 1
F2 - Acquisition Parameters
Date_ 20190324
Time 7.35 h
INSTRUM AVIII500HD
PROBHD Z119470_0125 (
PULPROG zg30
TD 65536
SOLVENT CDCl3
NS 4
DS 2
SWH 10000.000 Hz
FIDRES 0.305176 Hz
AQ 3.2767999 sec
RG 56.3
DW 50.000 usec
DE 12.72 usec
TE 298.0 K
D1 1.00000000 sec
TD0 1
SFO1 500.3030896 MHz
NUC1 1H
P0 3.33 usec
P1 10.00 usec
PLW1 21.89999962 W
F2 - Processing parameters
SI 65536
SF 500.3000000 MHz
WDW EM
SSB 0
LB 0.30 Hz
GB 0
PC 1.00
9
8
7
6
5
4
3
2
1
ppm
1.04
0.99
1.14
1.19
4.05
4.24
2.10
1.00
1.04
2.06
1.02
2.02
1.24
3.12

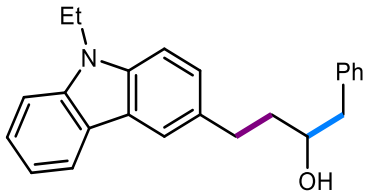

4.2.3ak

^{13}C NMR

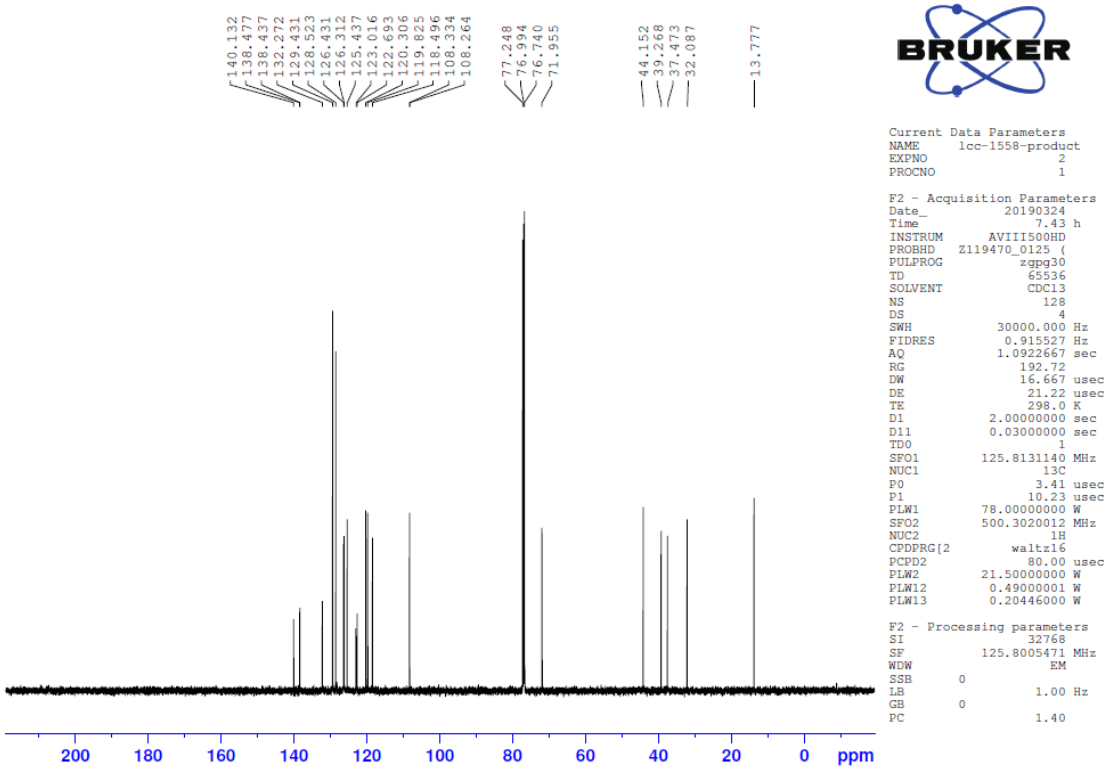

BRUKER

```
Current Data Parameters
NAME      1cc-1558-product
EXPNO                    2
PROCNO                   1

F2 - Acquisition Parameters
Date_           20190324
Time                7.43 h
INSTRUM       AVIII500HD
PROBHD    Z119470_0125 (
PULPROG           zgpg30
TD                65536
SOLVENT           CDCl3
NS                  128
DS                    4
SWH           30000.000 Hz
FIDRES            0.915527 Hz
AQ                1.0922667 sec
RG                  192.72
DW                  16.667 usec
DE                  21.22 usec
TE                  298.0 K
D1              2.00000000 sec
D11             0.03000000 sec
TD0                   1
SFO1          125.8131140 MHz
NUC1                 13C
P0                  3.41 usec
P1                 10.23 usec
PLW1          78.00000000 W
SFO2          500.3020012 MHz
NUC2                 1H
CPDPRG[2          waltz16
PCPD2               80.00 usec
PLW2          21.50000000 W
PLW12          0.49000001 W
PLW13          0.20446000 W

F2 - Processing parameters
SI                  32768
SF            125.8005471 MHz
WDW                    EM
SSB       0
LB                  1.00 Hz
GB        0
PC                  1.40
```

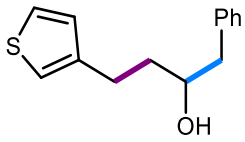
Ph
S
OH

4.2.3al

^{1}H NMR

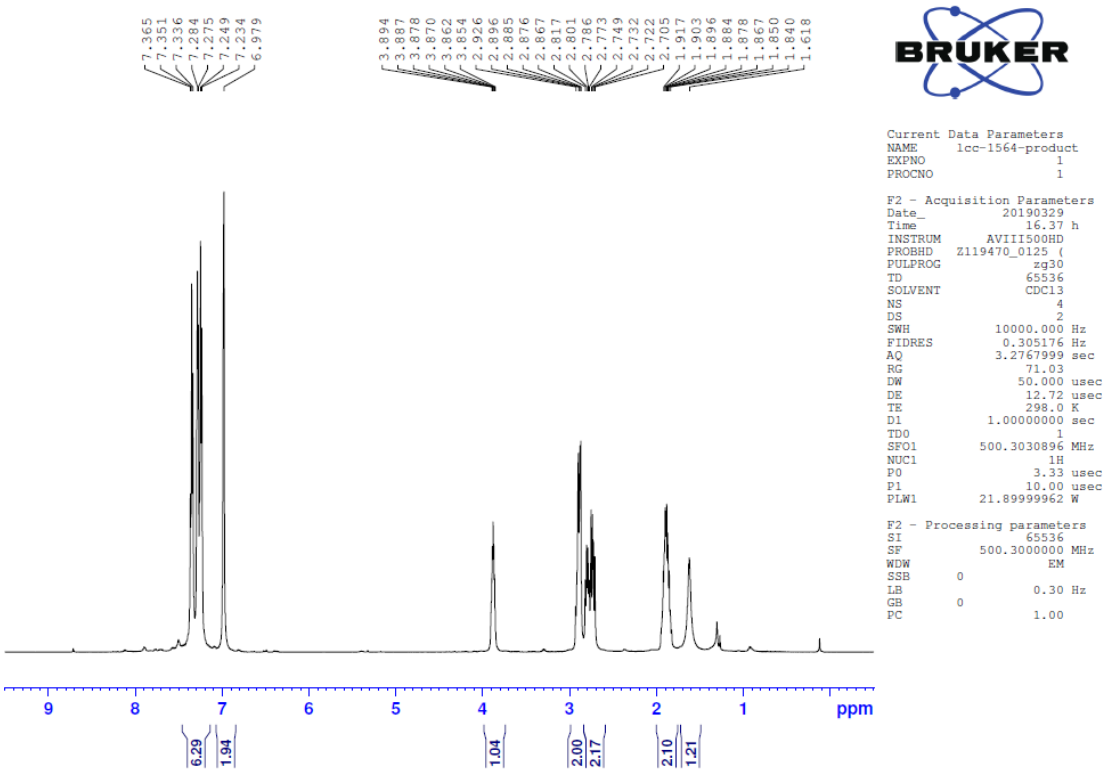
7.365
7.351
7.336
7.284
7.275
7.249
7.234
6.979
3.894
3.887
3.878
3.870
3.862
3.854
2.926
2.896
2.885
2.876
2.867
2.817
2.801
2.786
2.773
2.749
2.732
2.722
2.705
1.917
1.903
1.896
1.884
1.878
1.867
1.850
1.840
1.618
BRUKER
Current Data Parameters
NAME 1cc-1564-product
EXPNO 1
PROCNO 1
F2 - Acquisition Parameters
Date_ 20190329
Time 16.37 h
INSTRUM AVIII500HD
PROBHD Z119470_0125 (
PULPROG zg30
TD 65536
SOLVENT CDCl3
NS 4
DS 2
SWH 10000.000 Hz
FIDRES 0.305176 Hz
AQ 3.2767999 sec
RG 71.03
DW 50.000 usec
DE 12.72 usec
TE 298.0 K
D1 1.00000000 sec
TD0 1
SFO1 500.3030896 MHz
NUC1 1H
P0 3.33 usec
P1 10.00 usec
PLW1 21.89999962 W
F2 - Processing parameters
SI 65536
SF 500.3000000 MHz
WDW EM
SSB 0
LB 0.30 Hz
GB 0
PC 1.00
9
8
7
6
5
4
3
2
1
ppm
6.29
1.94
1.04
2.00
2.17
2.10
1.21

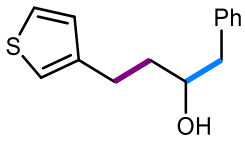

4.2.3al

^{13}C NMR

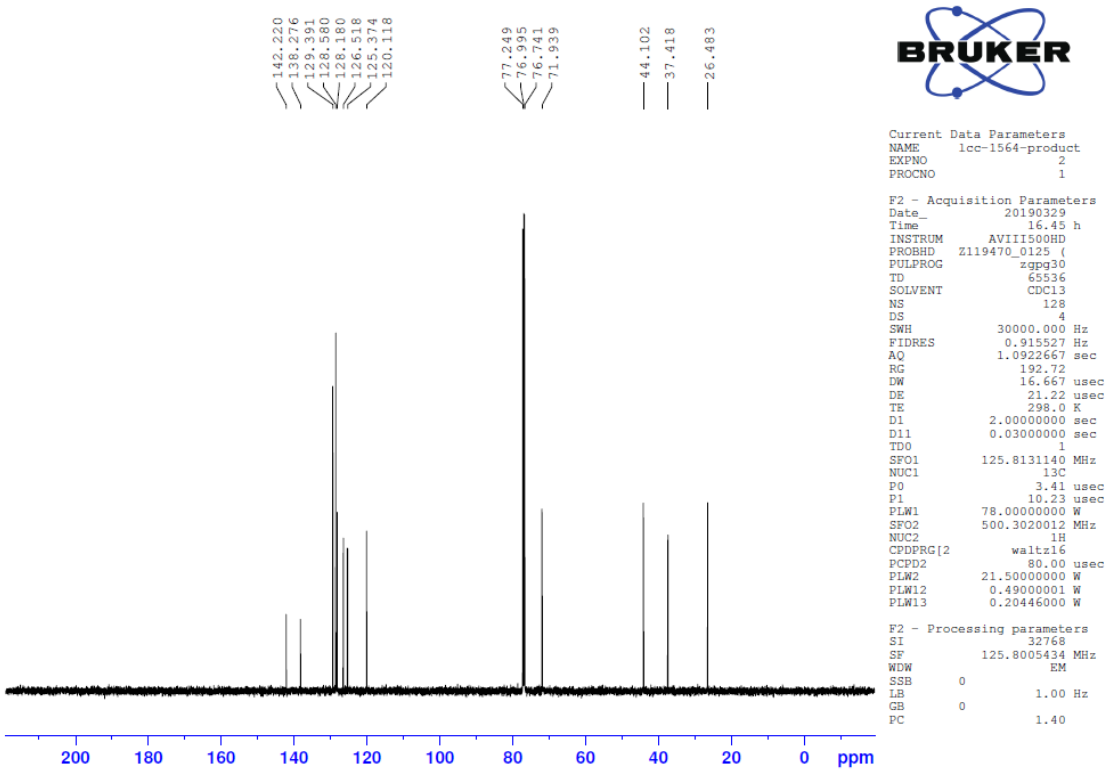


```
Current Data Parameters
NAME      1cc-1564-product
EXPNO                    2
PROCNO                   1

F2 - Acquisition Parameters
Date_             20190329
Time                16.45 h
INSTRUM       AVIII500HD
PROBHD    Z119470_0125 (
PULPROG            zgpg30
TD                  65536
SOLVENT             CDCl3
NS                    128
DS                      4
SWH             30000.000 Hz
FIDRES          0.915527 Hz
AQ              1.0922667 sec
RG                 192.72
DW                 16.667 usec
DE                 21.22 usec
TE                 298.0 K
D1              2.00000000 sec
D11             0.03000000 sec
TD0                     1
SFO1         125.8131140 MHz
NUC1                  13C
P0                   3.41 usec
P1                  10.23 usec
PLW1         78.00000000 W
SFO2         500.3020012 MHz
NUC2                   1H
CPDPRG[2          waltz16
PCPD2               80.00 usec
PLW2         21.50000000 W
PLW12         0.49000001 W
PLW13         0.20446000 W

F2 - Processing parameters
SI                  32768
SF           125.8005434 MHz
WDW                    EM
SSB       0
LB                   1.00 Hz
GB        0
PC                   1.40
```

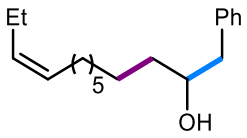
Et
Ph
5
OH

4.2.3am

^{1}H NMR

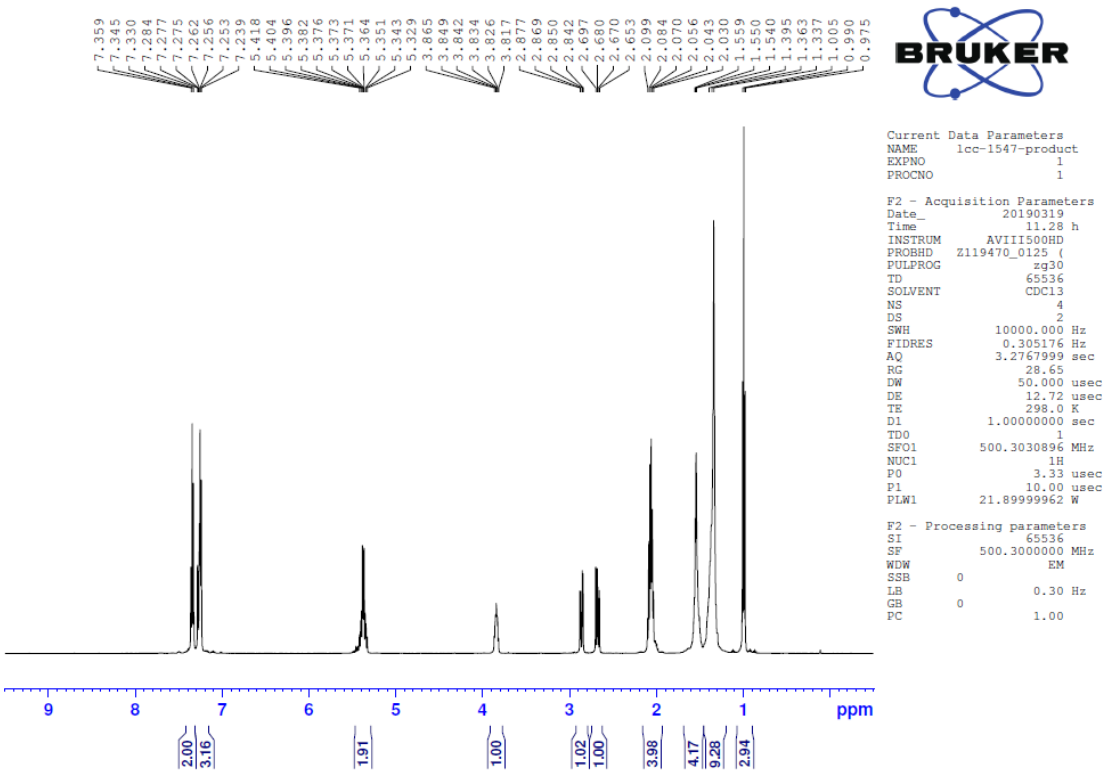
7.359
7.345
7.330
7.284
7.277
7.275
7.262
7.256
7.253
7.239
5.418
5.404
5.396
5.382
5.376
5.373
5.371
5.364
5.351
5.343
5.329
3.865
3.849
3.842
3.834
3.826
3.817
2.877
2.869
2.850
2.842
2.697
2.680
2.670
2.653
2.099
2.084
2.070
2.056
2.043
2.030
1.559
1.550
1.540
1.395
1.363
1.337
1.005
0.990
0.975
BRUKER
Current Data Parameters
NAME 1cc-1547-product
EXPNO 1
PROCNO 1
F2 - Acquisition Parameters
Date_ 20190319
Time 11.28 h
INSTRUM AVIII500HD
PROBHD Z119470_0125 (
PULPROG zg30
TD 65536
SOLVENT CDCl3
NS 4
DS 2
SWH 10000.000 Hz
FIDRES 0.305176 Hz
AQ 3.2767999 sec
RG 28.65
DW 50.000 usec
DE 12.72 usec
TE 298.0 K
D1 1.00000000 sec
TD0 1
SFO1 500.3030896 MHz
NUC1 1H
P0 3.33 usec
P1 10.00 usec
PLW1 21.89999962 W
F2 - Processing parameters
SI 65536
SF 500.3000000 MHz
WDW EM
SSB 0
LB 0.30 Hz
GB 0
PC 1.00
9
8
7
6
5
4
3
2
1
ppm
2.00
3.16
1.91
1.00
1.02
1.00
3.98
4.17
9.28
2.94

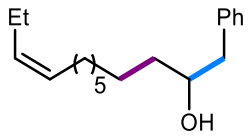

4.2.3am

^{13}C NMR

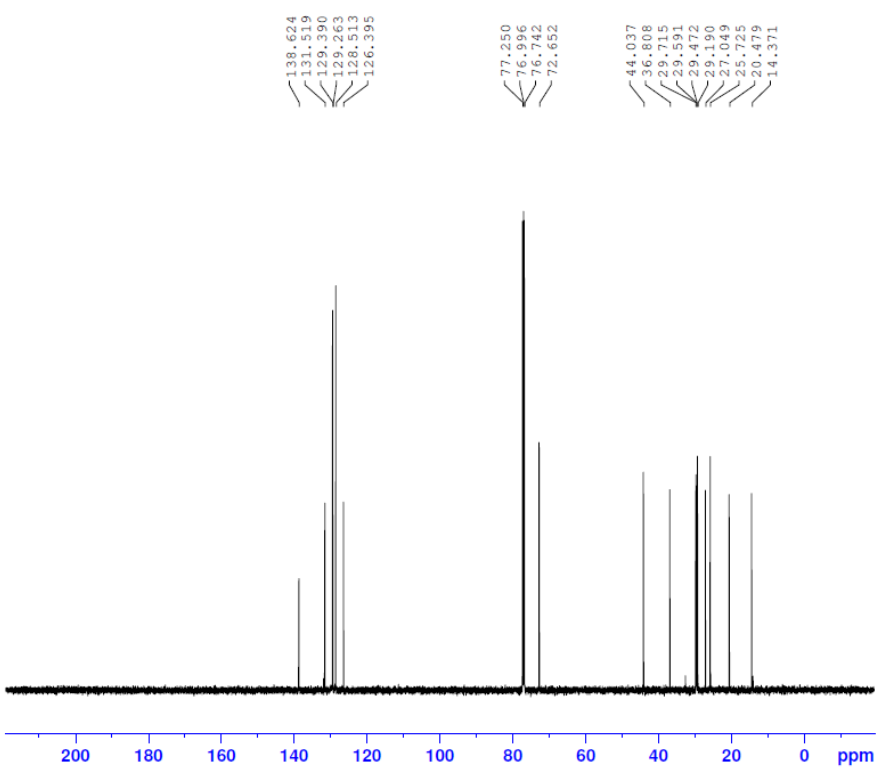


```
Current Data Parameters
NAME      1cc-1547-product
EXPNO                    2
PROCNO                   1

F2 - Acquisition Parameters
Date_             20190319
Time                11.35 h
INSTRUM       AVIII500HD
PROBHD    Z119470_0125 (
PULPROG             zgpg30
TD                   65536
SOLVENT              CDCl3
NS                     128
DS                       4
SWH              30000.000 Hz
FIDRES           0.915527 Hz
AQ               1.0922667 sec
RG                  192.72
DW                  16.667 usec
DE                  21.22 usec
TE                  298.0 K
D1             2.00000000 sec
D11            0.03000000 sec
TD0                      1
SFO1          125.8131140 MHz
NUC1                   13C
P0                   3.41 usec
P1                  10.23 usec
PLW1          78.00000000 W
SFO2          500.3020012 MHz
NUC2                   1H
CPDPRG[2          waltz16
PCPD2               80.00 usec
PLW2          21.50000000 W
PLW12          0.49000001 W
PLW13          0.20446000 W

F2 - Processing parameters
SI                   32768
SF            125.8005416 MHz
WDW                     EM
SSB         0
LB                    1.00 Hz
GB          0
PC                    1.40
```

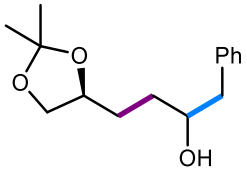
O
O
Ph
OH

4.2.3an

^{1}H NMR

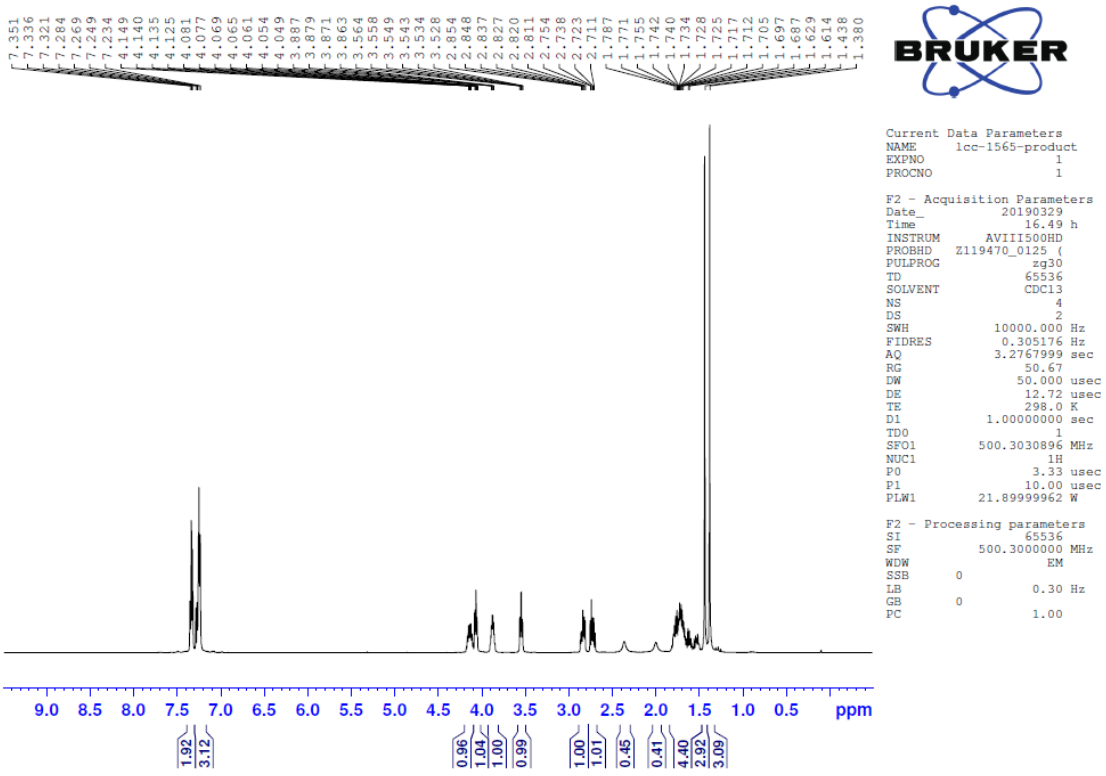
7.351
7.336
7.321
7.284
7.269
7.249
7.234
4.149
4.140
4.135
4.125
4.081
4.077
4.069
4.065
4.061
4.054
4.049
3.887
3.879
3.871
3.863
3.564
3.558
3.549
3.543
3.534
3.528
2.854
2.848
2.837
2.827
2.820
2.811
2.754
2.738
2.723
2.711
1.787
1.771
1.755
1.742
1.740
1.734
1.728
1.725
1.717
1.712
1.705
1.697
1.687
1.629
1.614
1.438
1.380
BRUKER
Current Data Parameters
NAME lcc-1565-product
EXPNO 1
PROCNO 1
F2 - Acquisition Parameters
Date_ 20190329
Time 16.49 h
INSTRUM AVIII500HD
PROBHD Z119470_0125 (
PULPROG zg30
TD 65536
SOLVENT CDCl3
NS 4
DS 2
SWH 10000.000 Hz
FIDRES 0.305176 Hz
AQ 3.2767999 sec
RG 50.67
DW 50.000 usec
DE 12.72 usec
TE 298.0 K
D1 1.00000000 sec
TD0 1
SFO1 500.3030896 MHz
NUC1 1H
P0 3.33 usec
P1 10.00 usec
PLW1 21.89999962 W
F2 - Processing parameters
SI 65536
SF 500.3000000 MHz
WDW EM
SSB 0
LB 0.30 Hz
GB 0
PC 1.00
9.0 8.5 8.0 7.5 7.0 6.5 6.0 5.5 5.0 4.5 4.0 3.5 3.0 2.5 2.0 1.5 1.0 0.5 ppm
1.92
3.12
0.96
1.04
1.00
0.99
1.00
1.01
0.45
0.41
4.40
2.92
3.09

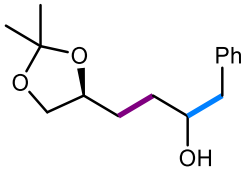

4.2.3an

^{13}C NMR

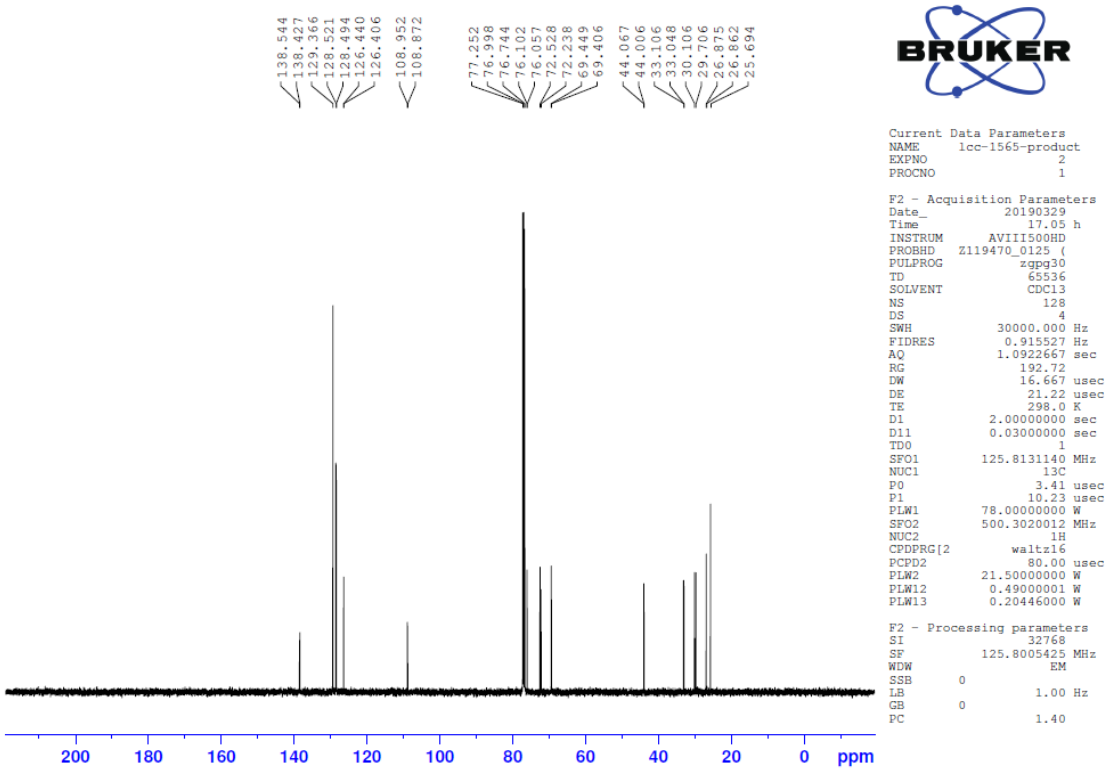

BRUKER

```
Current Data Parameters
NAME      lcc-1565-product
EXPNO                    2
PROCNO                   1

F2 - Acquisition Parameters
Date_             20190329
Time                17.05 h
INSTRUM       AVIII500HD
PROBHD    Z119470_0125 (
PULPROG            zgpg30
TD                  65536
SOLVENT             CDCl3
NS                    128
DS                      4
SWH             30000.000 Hz
FIDRES              0.915527 Hz
AQ                1.0922667 sec
RG                   192.72
DW                  16.667 usec
DE                  21.22 usec
TE                  298.0 K
D1              2.00000000 sec
D11             0.03000000 sec
TD0                     1
SFO1           125.8131140 MHz
NUC1                   13C
P0                   3.41 usec
P1                  10.23 usec
PLW1           78.00000000 W
SFO2           500.3020012 MHz
NUC2                   1H
CPDPRG[2          waltz16
PCPD2               80.00 usec
PLW2           21.50000000 W
PLW12           0.49000001 W
PLW13           0.20446000 W

F2 - Processing parameters
SI                   32768
SF             125.8005425 MHz
WDW                     EM
SSB       0
LB                   1.00 Hz
GB        0
PC                   1.40
```

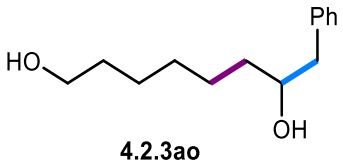
Ph
HO
OH

4.2.3ao

^{1}H NMR

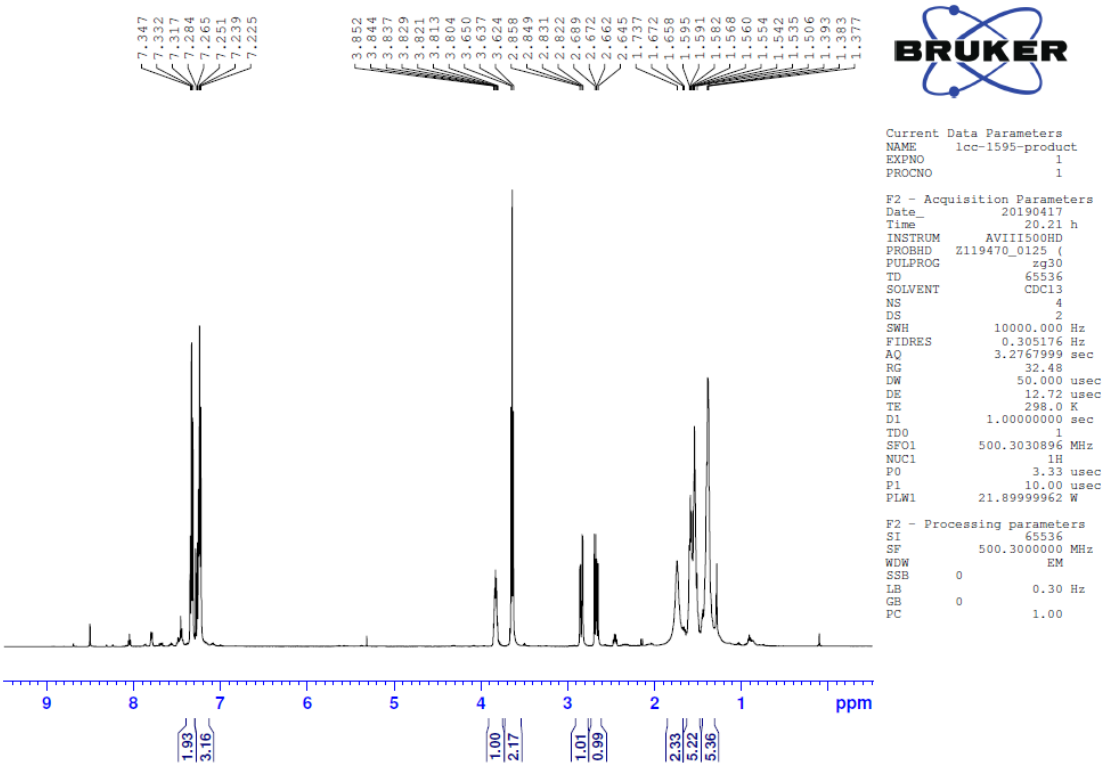
7.347
7.332
7.317
7.284
7.265
7.251
7.239
7.225
3.852
3.844
3.837
3.829
3.821
3.813
3.804
3.650
3.637
3.624
2.858
2.849
2.831
2.822
2.689
2.672
2.662
2.645
1.737
1.672
1.658
1.595
1.591
1.582
1.568
1.560
1.554
1.542
1.535
1.506
1.393
1.383
1.377
BRUKER
Current Data Parameters
NAME 1cc-1595-product
EXPNO 1
PROCNO 1
F2 - Acquisition Parameters
Date_ 20190417
Time 20.21 h
INSTRUM AVIII500HD
PROBHD Z119470_0125 (
PULPROG zg30
TD 65536
SOLVENT CDCl3
NS 4
DS 2
SWH 10000.000 Hz
FIDRES 0.305176 Hz
AQ 3.2767999 sec
RG 32.48
DW 50.000 usec
DE 12.72 usec
TE 298.0 K
D1 1.00000000 sec
TD0 1
SFO1 500.3030896 MHz
NUC1 1H
P0 3.33 usec
P1 10.00 usec
PLW1 21.89999962 W
F2 - Processing parameters
SI 65536
SF 500.3000000 MHz
WDW EM
SSB 0
LB 0.30 Hz
GB 0
PC 1.00
9
8
7
6
5
4
3
2
1
ppm
1.93
3.16
1.00
2.17
1.01
0.99
2.33
5.22
5.36

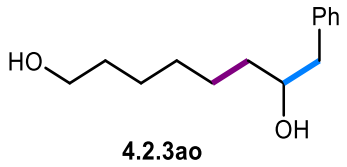

4.2.3ao

^{13}C NMR

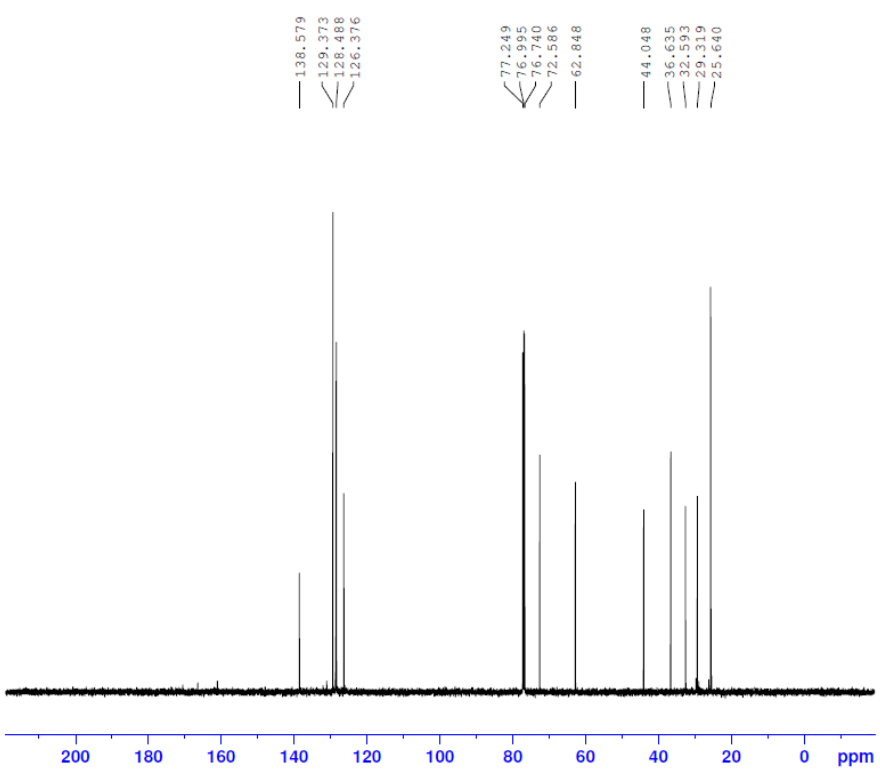


```
Current Data Parameters
NAME      1cc-1595-product
EXPNO                    2
PROCNO                   1

F2 - Acquisition Parameters
Date_           20190418
Time                2.27 h
INSTRUM       AVIII500HD
PROBHD    Z119470_0125 (
PULPROG           zgpg30
TD                 65536
SOLVENT            CDCl3
NS                   128
DS                     4
SWH            30000.000 Hz
FIDRES             0.915527 Hz
AQ                 1.0922667 sec
RG                   192.72
DW                  16.667 usec
DE                  21.22 usec
TE                  298.0 K
D1               2.00000000 sec
D11              0.03000000 sec
TD0                    1
SFO1         125.8131140 MHz
NUC1                  13C
P0                   3.41 usec
P1                  10.23 usec
PLW1         78.00000000 W
SFO2         500.3020012 MHz
NUC2                   1H
CPDPRG[2          waltz16
PCPD2               80.00 usec
PLW2         21.50000000 W
PLW12         0.49000001 W
PLW13         0.20446000 W

F2 - Processing parameters
SI                 32768
SF           125.8005434 MHz
WDW                   EM
SSB       0
LB                  1.00 Hz
GB        0
PC                  1.40
```

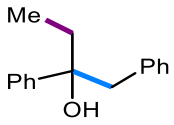

4.2.3ap

^{1}H NMR

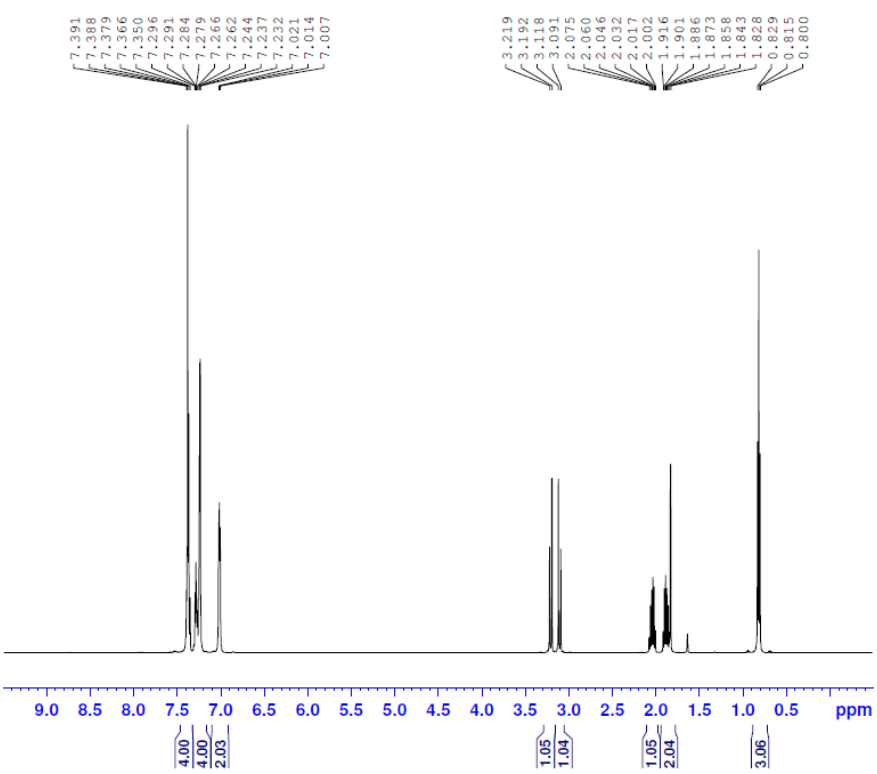


```
Current Data Parameters
NAME      1cc-491-product-H
EXPNO                   1
PROCNO                  1

F2 - Acquisition Parameters
Date_           20170603
Time              20.20 h
INSTRUM       AVIII500HD
PROBHD    Z119470_0125 (
PULPROG             zg30
TD                 65536
SOLVENT            CDCl3
NS                    16
DS                     2
SWH            10000.000 Hz
FIDRES         0.305176 Hz
AQ             3.2767999 sec
RG                 25.23
DW                50.000 usec
DE                13.50 usec
TE                298.3 K
D1             1.00000000 sec
TD0                    1
SFO1         500.3030896 MHz
NUC1                  1H
P1                10.00 usec
PLW1         21.89999962 W

F2 - Processing parameters
SI                 65536
SF           500.3000000 MHz
WDW                   EM
SSB       0
LB                 0.30 Hz
GB        0
PC                 1.00
```

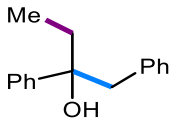

4.2.3ap

^{13}C NMR

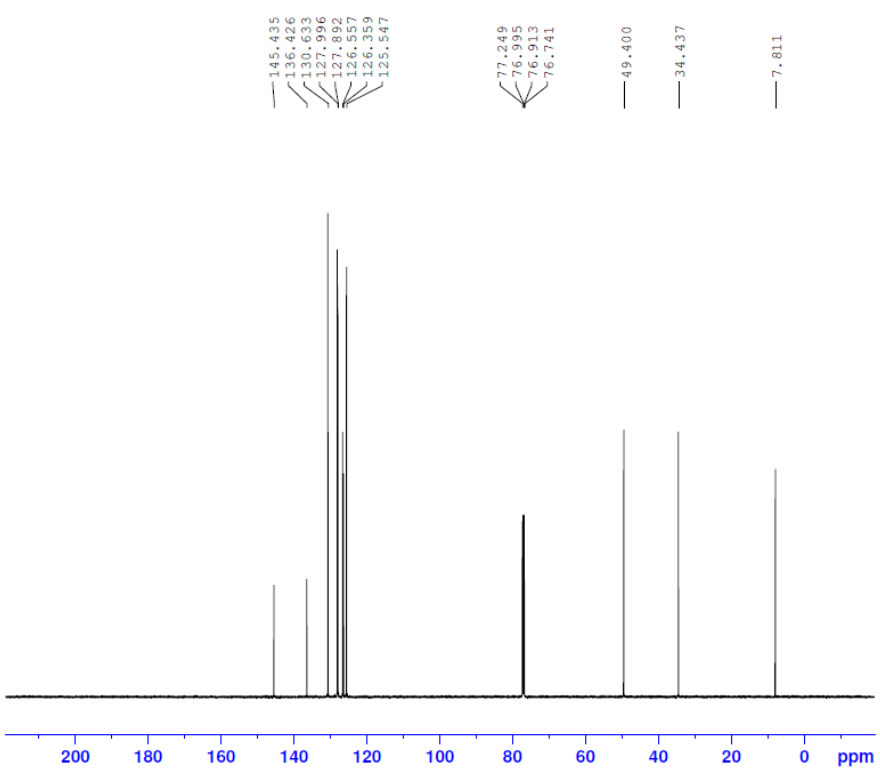


```
Current Data Parameters
NAME      1cc-491-product-C
EXPNO                     1
PROCNO                    1

F2 - Acquisition Parameters
Date_           20170603
Time              20.48 h
INSTRUM       AVIII500HD
PROBHD    Z119470_0125 (
PULPROG          zgpg30
TD                65536
SOLVENT           CDCl3
NS                  512
DS                    4
SWH           30000.000 Hz
FIDRES        0.915527 Hz
AQ            1.0922667 sec
RG               192.72
DW               16.667 usec
DE               22.02 usec
TE               298.3 K
D1            2.00000000 sec
D11           0.03000000 sec
TD0                   1
SFO1        125.8131140 MHz
NUC1                13C
P1                10.23 usec
PLW1         78.00000000 W
SFO2        500.3020012 MHz
NUC2                1H
CPDPRG[2         waltz16
PCPD2             80.00 usec
PLW2         21.50000000 W
PLW12         0.40648001 W
PLW13         0.20446000 W

F2 - Processing parameters
SI                32768
SF          125.8005462 MHz
WDW                  EM
SSB       0
LB                1.00 Hz
GB        0
PC                1.40
```

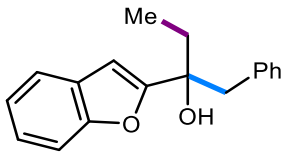
Me
Ph
O
OH

4.2.3aq

^{1}H NMR

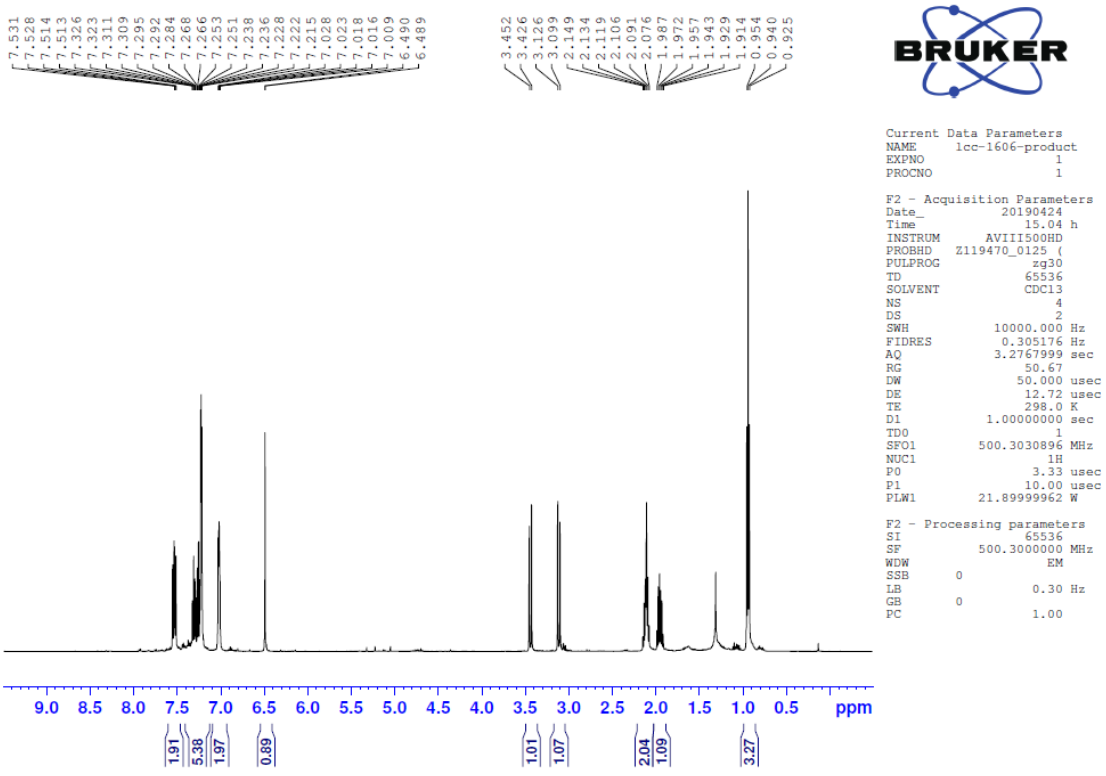
7.531
7.528
7.514
7.513
7.326
7.323
7.311
7.309
7.295
7.292
7.284
7.268
7.266
7.253
7.251
7.238
7.236
7.228
7.222
7.215
7.028
7.023
7.018
7.016
7.009
6.490
6.489
3.452
3.426
3.126
3.099
2.149
2.134
2.119
2.106
2.091
2.076
1.987
1.972
1.957
1.943
1.929
1.914
0.954
0.940
0.925
BRUKER
Current Data Parameters
NAME 1cc-1606-product
EXPNO 1
PROCNO 1
F2 - Acquisition Parameters
Date_ 20190424
Time 15.04 h
INSTRUM AVIII500HD
PROBHD Z119470_0125 (
PULPROG zg30
TD 65536
SOLVENT CDCl3
NS 4
DS 2
SWH 10000.000 Hz
FIDRES 0.305176 Hz
AQ 3.2767999 sec
RG 50.67
DW 50.000 usec
DE 12.72 usec
TE 298.0 K
D1 1.00000000 sec
TD0 1
SFO1 500.3030896 MHz
NUC1 1H
P0 3.33 usec
P1 10.00 usec
PLW1 21.89999962 W
F2 - Processing parameters
SI 65536
SF 500.3000000 MHz
WDW EM
SSB 0
LB 0.30 Hz
GB 0
PC 1.00
9.0 8.5 8.0 7.5 7.0 6.5 6.0 5.5 5.0 4.5 4.0 3.5 3.0 2.5 2.0 1.5 1.0 0.5 ppm
1.91
5.38
1.97
0.89
1.01
1.07
2.04
1.09
3.27

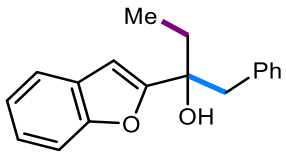

4.2.3aq

^{13}C NMR

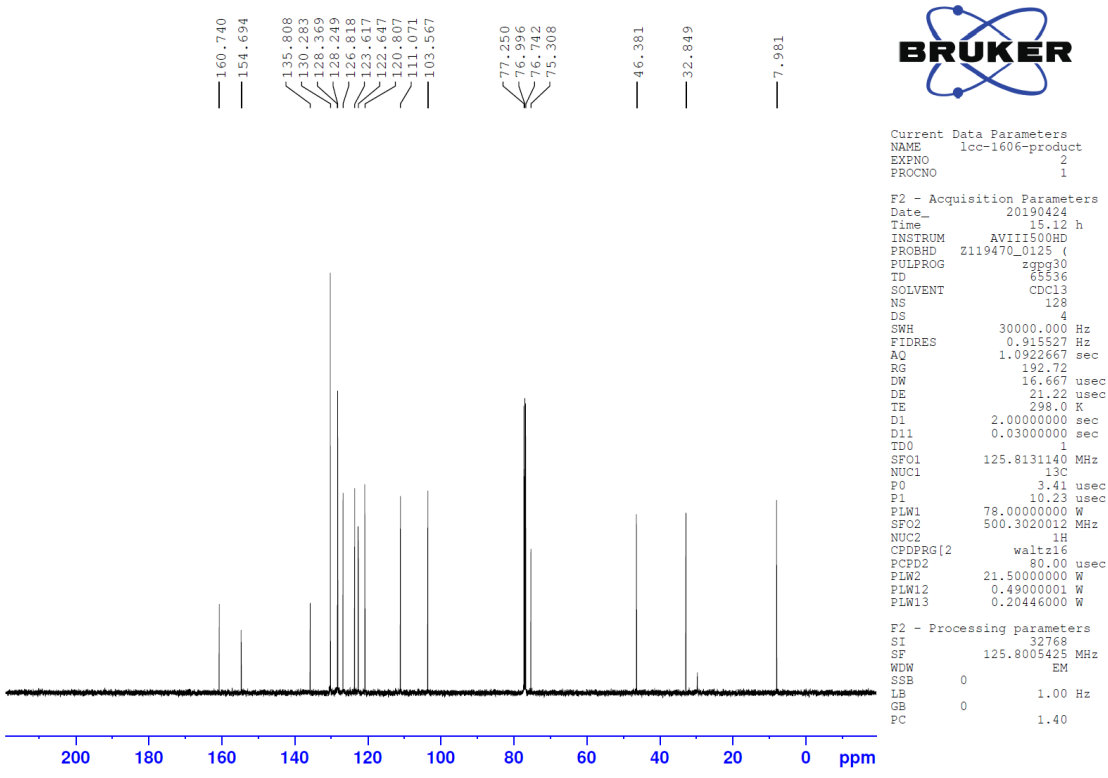

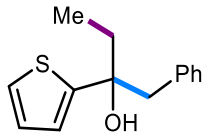
Me
S
Ph
OH

4.2.3ar

^{1}H NMR

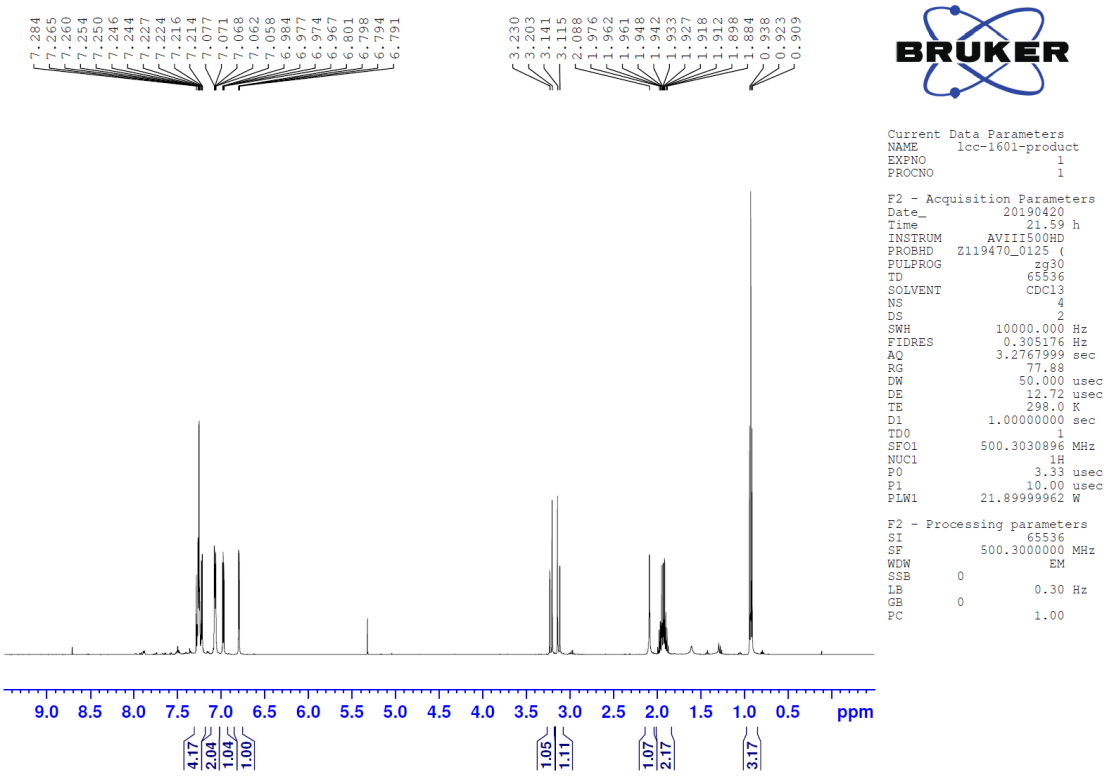
7.284
7.265
7.260
7.254
7.250
7.246
7.244
7.227
7.224
7.216
7.214
7.077
7.071
7.068
7.062
7.058
6.984
6.977
6.974
6.967
6.801
6.798
6.794
6.791
3.230
3.203
3.141
3.115
2.088
1.976
1.962
1.961
1.948
1.942
1.933
1.927
1.918
1.912
1.898
1.884
0.938
0.923
0.909
BRUKER
Current Data Parameters
NAME lcc-1601-product
EXPNO 1
PROCNO 1
F2 - Acquisition Parameters
Date_ 20190420
Time 21.59 h
INSTRUM AVIII500HD
PROBHD Z119470_0125 (
PULPROG zg30
TD 65536
SOLVENT CDCl3
NS 4
DS 2
SWH 10000.000 Hz
FIDRES 0.305176 Hz
AQ 3.2767999 sec
RG 77.88
DW 50.000 usec
DE 12.72 usec
TE 298.0 K
D1 1.00000000 sec
TD0 1
SFO1 500.3030896 MHz
NUC1 1H
P0 3.33 usec
P1 10.00 usec
PLW1 21.89999962 W
F2 - Processing parameters
SI 65536
SF 500.3000000 MHz
WDW EM
SSB 0
LB 0.30 Hz
GB 0
PC 1.00
9.0 8.5 8.0 7.5 7.0 6.5 6.0 5.5 5.0 4.5 4.0 3.5 3.0 2.5 2.0 1.5 1.0 0.5 ppm
4.17
2.04
1.04
1.00
1.05
1.11
1.07
2.17
3.17

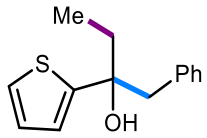

4.2.3ar

^{13}C NMR

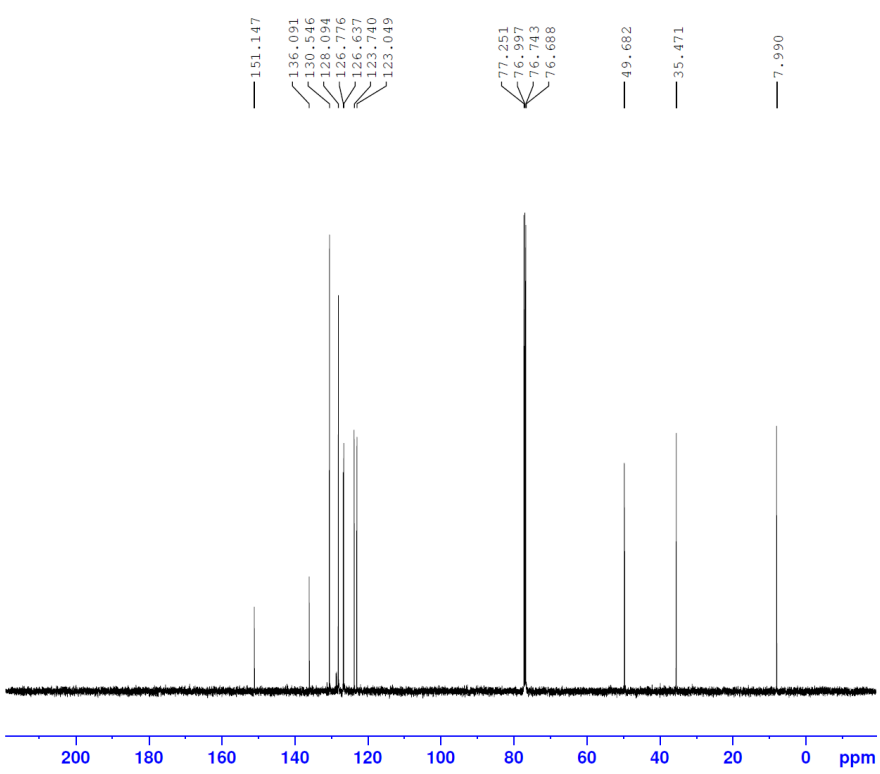


```
Current Data Parameters
NAME      lcc-1601-product
EXPNO                    2
PROCNO                   1

F2 - Acquisition Parameters
Date_           20190420
Time              22.07 h
INSTRUM      AVIII500HD
PROBHD   Z119470_0125 (
PULPROG          zgpg30
TD                65536
SOLVENT           CDCl3
NS                  128
DS                    4
SWH           30000.000 Hz
FIDRES          0.915527 Hz
AQ             1.0922667 sec
RG                192.72
DW                16.667 usec
DE                21.22 usec
TE                298.0 K
D1            2.00000000 sec
D11           0.03000000 sec
TD0                   1
SFO1        125.8131140 MHz
NUC1                13C
P0                 3.41 usec
P1                10.23 usec
PLW1         78.00000000 W
SFO2        500.3020012 MHz
NUC2                1H
CPDPRG[2        waltz16
PCPD2             80.00 usec
PLW2         21.50000000 W
PLW12         0.49000001 W
PLW13         0.20446000 W

F2 - Processing parameters
SI                32768
SF          125.8005407 MHz
WDW                  EM
SSB       0
LB                1.00 Hz
GB        0
PC                1.40
```

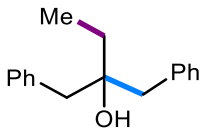
Me
Ph
Ph
OH

4.2.3as

^{1}H NMR

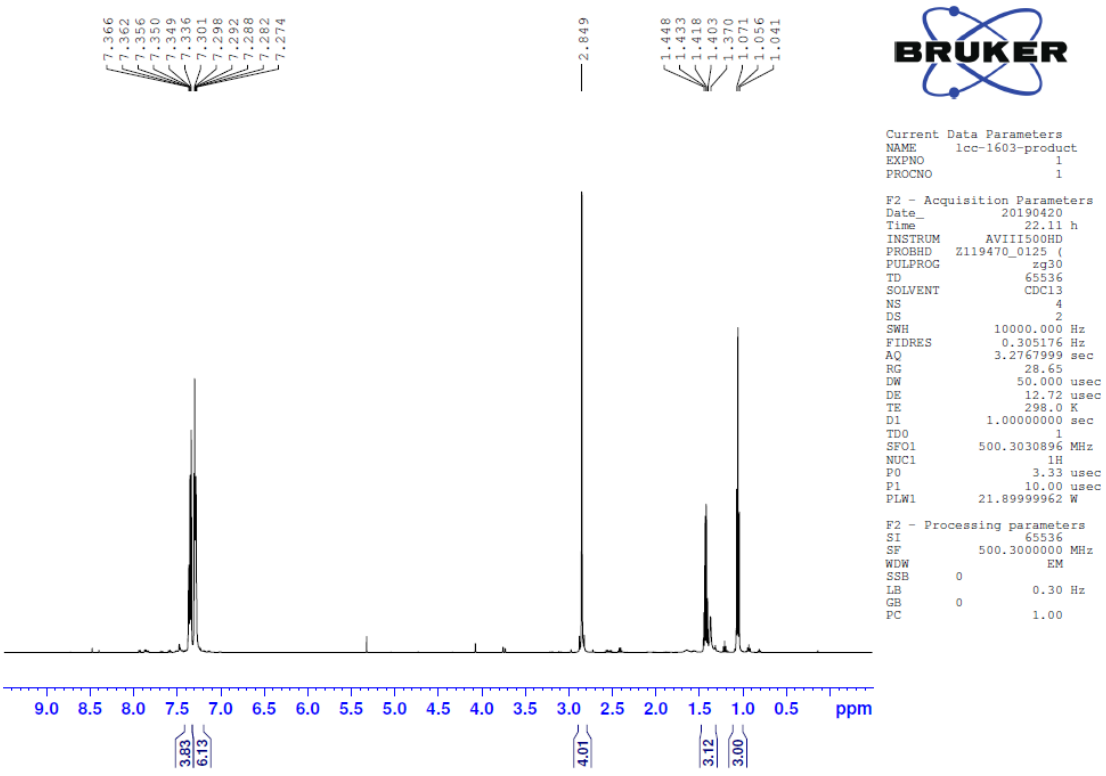
7.366
7.362
7.356
7.350
7.349
7.336
7.301
7.298
7.292
7.288
7.282
7.274
2.849
1.448
1.433
1.418
1.403
1.370
1.071
1.056
1.041
BRUKER
Current Data Parameters
NAME 1cc-1603-product
EXPNO 1
PROCNO 1
F2 - Acquisition Parameters
Date_ 20190420
Time 22.11 h
INSTRUM AVIII500HD
PROBHD Z119470_0125 (
PULPROG zg30
TD 65536
SOLVENT CDCl3
NS 4
DS 2
SWH 10000.000 Hz
FIDRES 0.305176 Hz
AQ 3.2767999 sec
RG 28.65
DW 50.000 usec
DE 12.72 usec
TE 298.0 K
D1 1.00000000 sec
TD0 1
SFO1 500.3030896 MHz
NUC1 1H
P0 3.33 usec
P1 10.00 usec
PLW1 21.89999962 W
F2 - Processing parameters
SI 65536
SF 500.3000000 MHz
WDW EM
SSB 0
LB 0.30 Hz
GB 0
PC 1.00
9.0 8.5 8.0 7.5 7.0 6.5 6.0 5.5 5.0 4.5 4.0 3.5 3.0 2.5 2.0 1.5 1.0 0.5 ppm
3.83
6.13
4.01
3.12
3.00

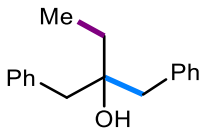

4.2.3as

^{13}C NMR

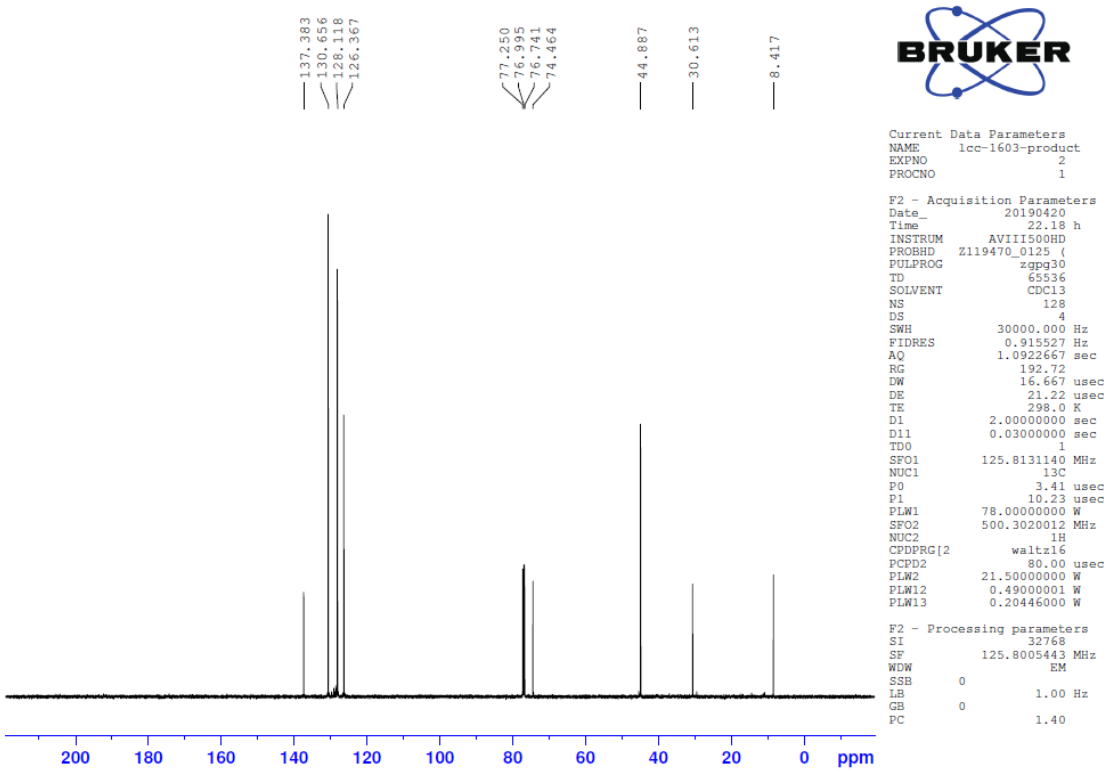


```
Current Data Parameters
NAME      1cc-1603-product
EXPNO                    2
PROCNO                   1

F2 - Acquisition Parameters
Date_             20190420
Time                22.18 h
INSTRUM       AVIII500HD
PROBHD    Z119470_0125 (
PULPROG            zgpg30
TD                  65536
SOLVENT             CDCl3
NS                    128
DS                      4
SWH             30000.000 Hz
FIDRES          0.915527 Hz
AQ              1.0922667 sec
RG                 192.72
DW                 16.667 usec
DE                 21.22 usec
TE                 298.0 K
D1              2.00000000 sec
D11             0.03000000 sec
TD0                     1
SFO1         125.8131140 MHz
NUC1                  13C
P0                  3.41 usec
P1                 10.23 usec
PLW1         78.00000000 W
SFO2         500.3020012 MHz
NUC2                   1H
CPDPRG[2         waltz16
PCPD2              80.00 usec
PLW2         21.50000000 W
PLW12         0.49000001 W
PLW13         0.20446000 W

F2 - Processing parameters
SI                  32768
SF           125.8005443 MHz
WDW                    EM
SSB       0
LB                  1.00 Hz
GB        0
PC                  1.40
```

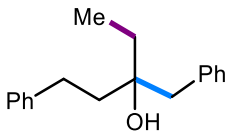

4.2.3at

^{1}H NMR

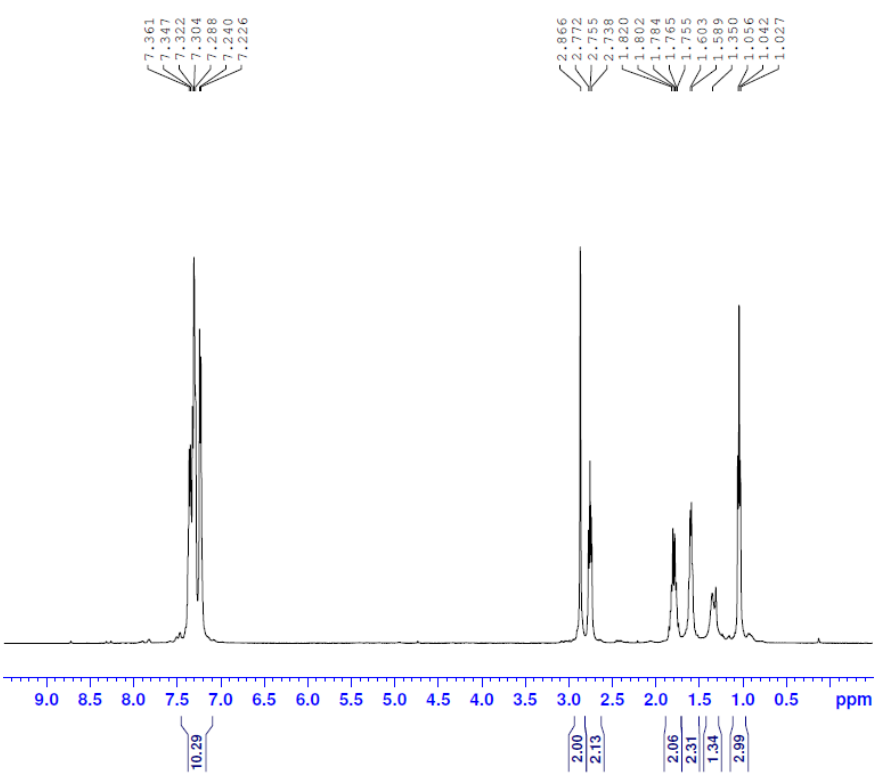


```
Current Data Parameters
NAME      1cc-1612-product
EXPNO                   1
PROCNO                  1

F2 - Acquisition Parameters
Date_           20190428
Time              15.43 h
INSTRUM       AVIII500HD
PROBHD    Z119470_0125 (
PULPROG             zg30
TD                 65536
SOLVENT            CDCl3
NS                     4
DS                     2
SWH           10000.000 Hz
FIDRES            0.305176 Hz
AQ                3.2767999 sec
RG                    56.3
DW                50.000 usec
DE                12.72 usec
TE                298.0 K
D1             1.00000000 sec
TD0                    1
SFO1          500.3030896 MHz
NUC1                  1H
P0                 3.33 usec
P1                10.00 usec
PLW1          21.89999962 W

F2 - Processing parameters
SI                 65536
SF            500.3000000 MHz
WDW                   EM
SSB       0
LB                 0.30 Hz
GB        0
PC                 1.00
```

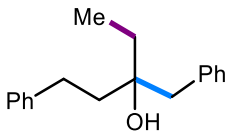

4.2.3at

^{13}C NMR

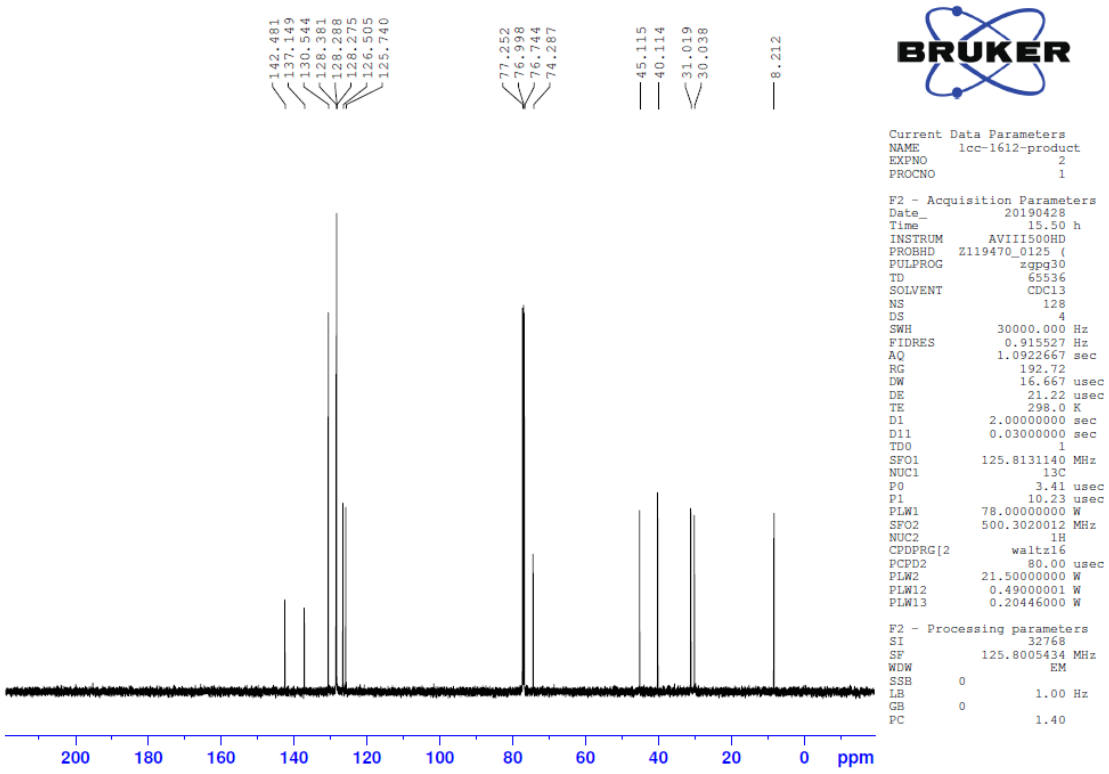

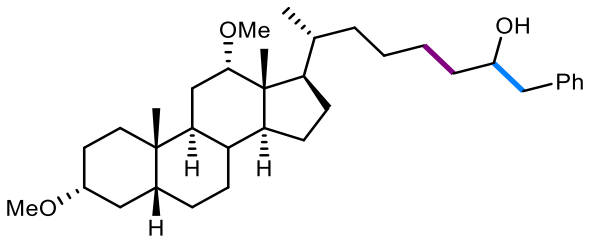
OMe
OH
Ph
H
H
MeO
H

4.2.3au

^{1}H NMR

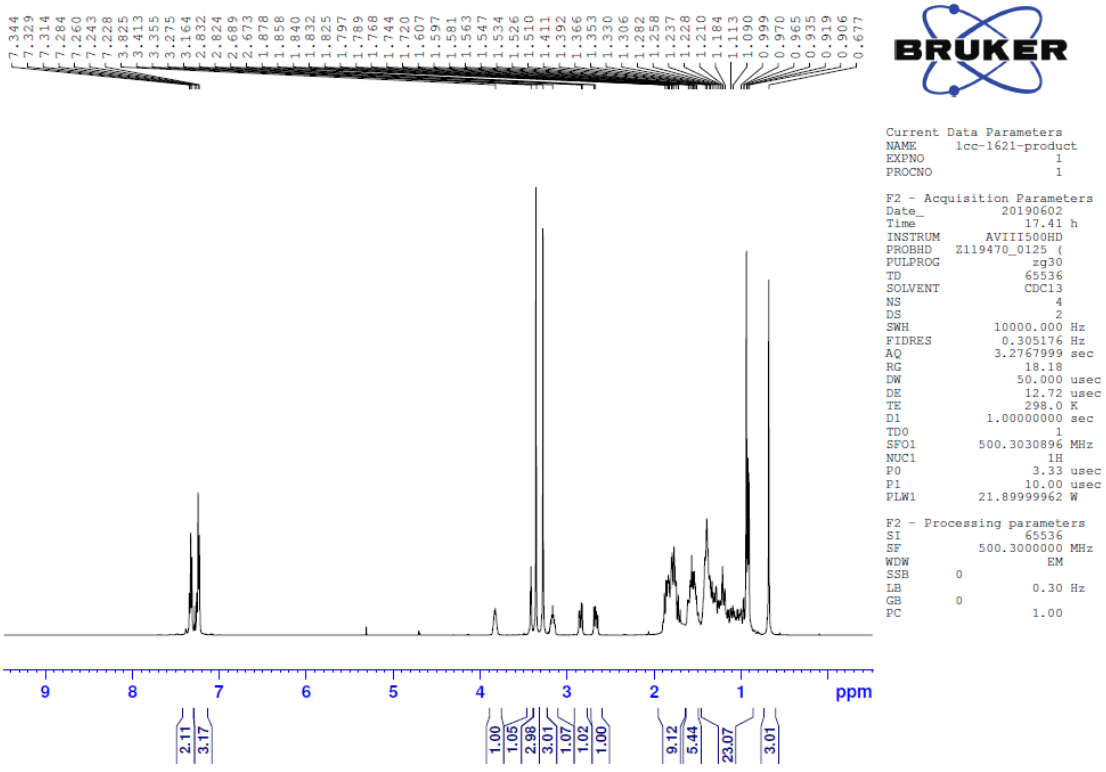
7.344
7.329
7.314
7.284
7.260
7.243
7.228
3.825
3.413
3.355
3.275
3.164
2.832
2.824
2.689
2.673
1.878
1.858
1.840
1.832
1.825
1.797
1.789
1.768
1.744
1.720
1.607
1.597
1.581
1.563
1.547
1.534
1.526
1.510
1.411
1.392
1.366
1.353
1.330
1.306
1.282
1.258
1.237
1.228
1.210
1.184
1.113
1.090
0.999
0.970
0.965
0.935
0.919
0.906
0.677
BRUKER
Current Data Parameters
NAME 1cc-1621-product
EXPNO 1
PROCNO 1
F2 - Acquisition Parameters
Date_ 20190602
Time 17.41 h
INSTRUM AVIII500HD
PROBHD Z119470_0125 (
PULPROG zg30
TD 65536
SOLVENT CDCl3
NS 4
DS 2
SWH 10000.000 Hz
FIDRES 0.305176 Hz
AQ 3.2767999 sec
RG 18.18
DW 50.000 usec
DE 12.72 usec
TE 298.0 K
D1 1.00000000 sec
TD0 1
SFO1 500.3030896 MHz
NUC1 1H
P0 3.33 usec
P1 10.00 usec
PLW1 21.89999962 W
F2 - Processing parameters
SI 65536
SF 500.3000000 MHz
WDW EM
SSB 0
LB 0.30 Hz
GB 0
PC 1.00
9
8
7
6
5
4
3
2
1
ppm
2.11
3.17
1.00
1.05
2.98
3.01
1.07
1.02
1.00
9.12
5.44
23.07
3.01

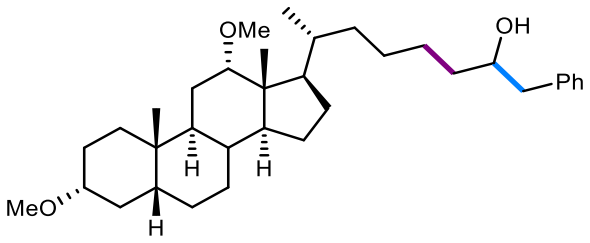

4.2.3au

^{13}C NMR

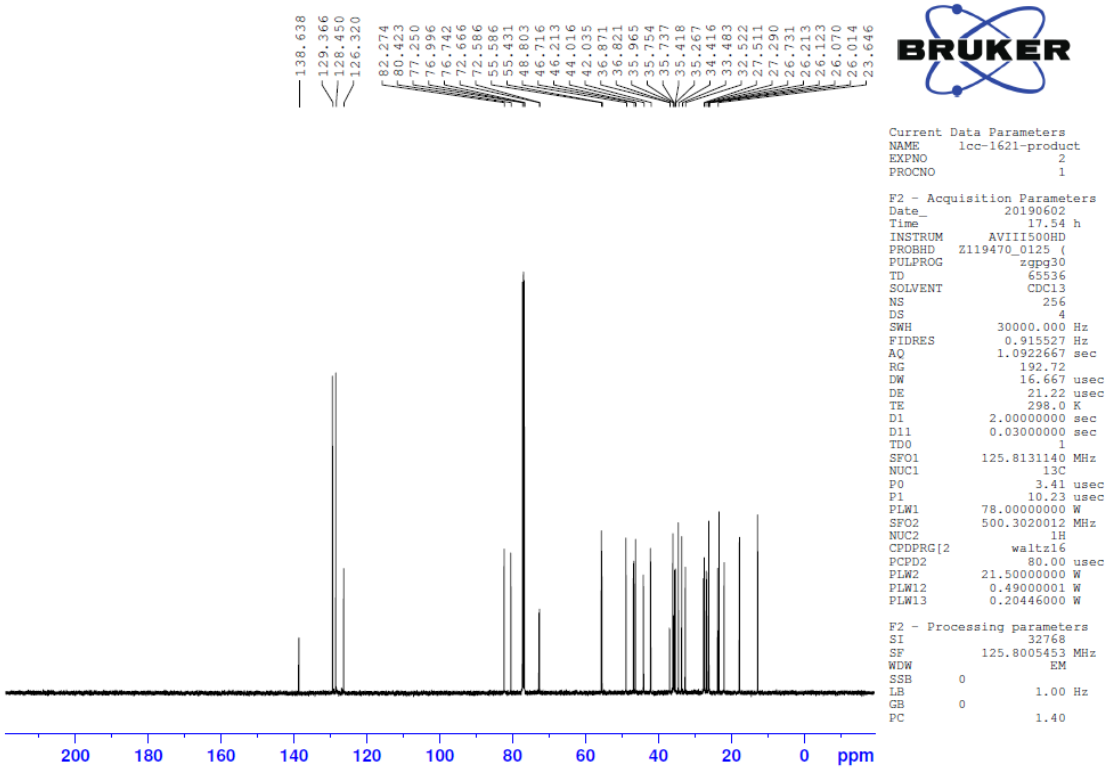

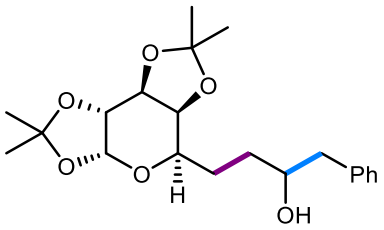
O
O
O
O
O
H
OH
Ph

4.2.3av

^{1}H NMR

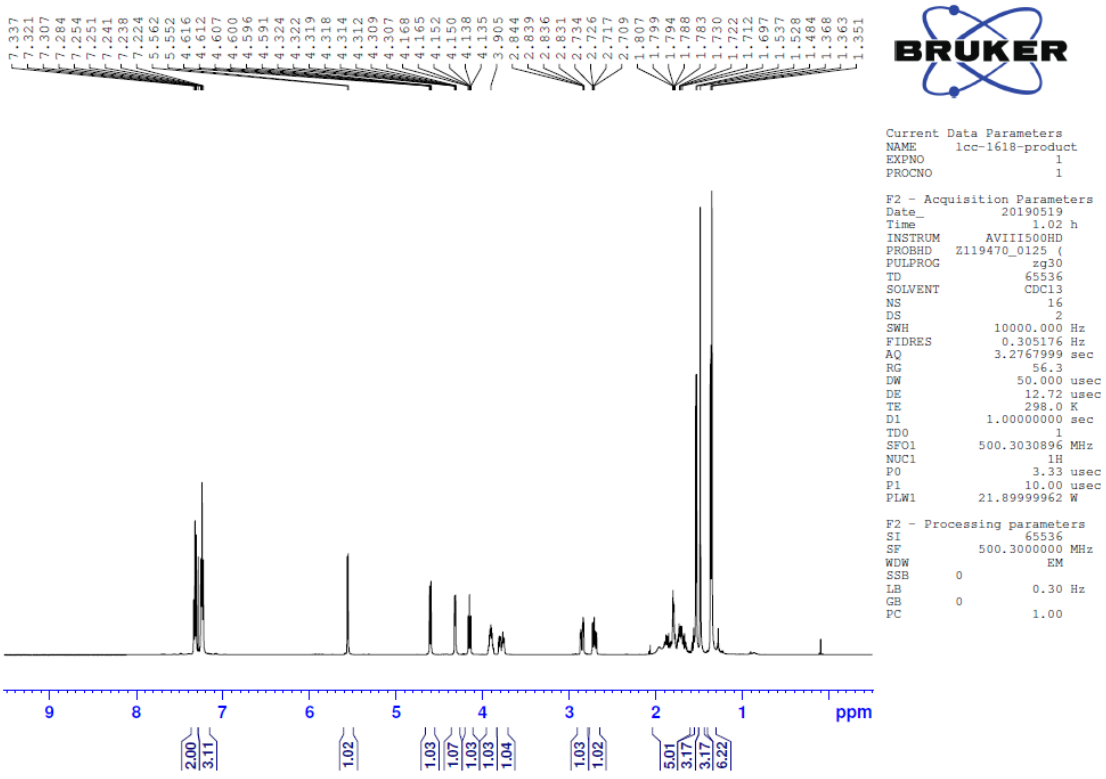
7.337
7.321
7.307
7.284
7.254
7.251
7.241
7.238
7.224
5.562
5.552
4.616
4.612
4.607
4.600
4.596
4.591
4.324
4.322
4.319
4.318
4.314
4.312
4.309
4.307
4.168
4.165
4.152
4.150
4.138
4.135
3.905
2.844
2.839
2.836
2.831
2.734
2.726
2.717
2.709
1.807
1.799
1.794
1.788
1.783
1.730
1.722
1.712
1.697
1.537
1.528
1.484
1.368
1.363
1.351
BRUKER
Current Data Parameters
NAME 1cc-1618-product
EXPNO 1
PROCNO 1
F2 - Acquisition Parameters
Date_ 20190519
Time 1.02 h
INSTRUM AVIII500HD
PROBHD Z119470_0125 (
PULPROG zg30
TD 65536
SOLVENT CDCl3
NS 16
DS 2
SWH 10000.000 Hz
FIDRES 0.305176 Hz
AQ 3.2767999 sec
RG 56.3
DW 50.000 usec
DE 12.72 usec
TE 298.0 K
D1 1.00000000 sec
TD0 1
SFO1 500.3030896 MHz
NUC1 1H
P0 3.33 usec
P1 10.00 usec
PLW1 21.89999962 W
F2 - Processing parameters
SI 65536
SF 500.3000000 MHz
WDW EM
SSB 0
LB 0.30 Hz
GB 0
PC 1.00
9
8
7
6
5
4
3
2
1
ppm
2.00
3.11
1.02
1.03
1.07
1.03
1.03
1.04
1.03
1.02
5.01
3.17
3.17
6.22

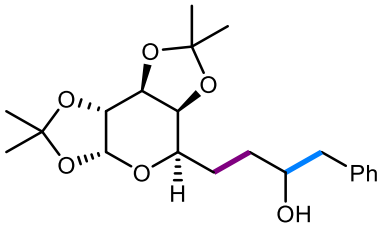

4.2.3av

^{13}C NMR

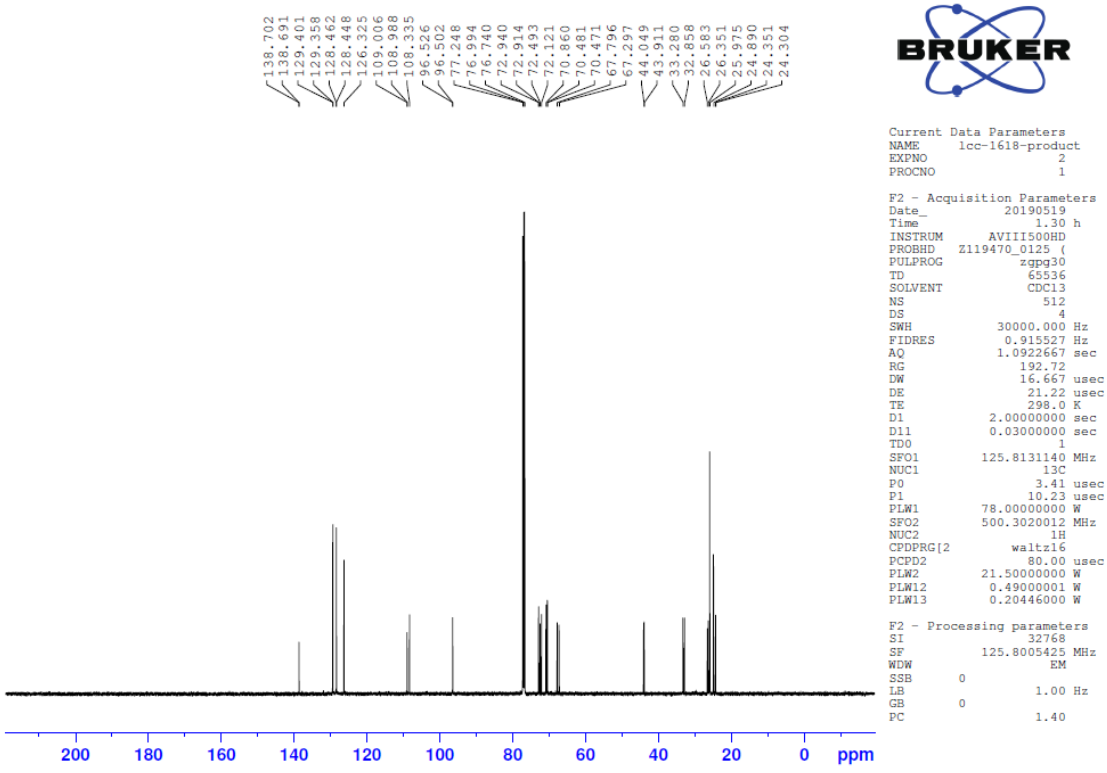

BRUKER

```
Current Data Parameters
NAME      1cc-1618-product
EXPNO                    2
PROCNO                   1

F2 - Acquisition Parameters
Date_              20190519
Time                   1.30 h
INSTRUM       AVIII500HD
PROBHD    Z119470_0125 (
PULPROG             zgpg30
TD                   65536
SOLVENT              CDCl3
NS                     512
DS                       4
SWH              30000.000 Hz
FIDRES               0.915527 Hz
AQ                1.0922667 sec
RG                   192.72
DW                  16.667 usec
DE                  21.22 usec
TE                   298.0 K
D1               2.00000000 sec
D11              0.03000000 sec
TD0                      1
SFO1           125.8131140 MHz
NUC1                   13C
P0                    3.41 usec
P1                   10.23 usec
PLW1            78.00000000 W
SFO2           500.3020012 MHz
NUC2                   1H
CPDPRG[2           waltz16
PCPD2                80.00 usec
PLW2            21.50000000 W
PLW12            0.49000001 W
PLW13            0.20446000 W

F2 - Processing parameters
SI                   32768
SF             125.8005425 MHz
WDW                    EM
SSB       0
LB                    1.00 Hz
GB        0
PC                    1.40
```

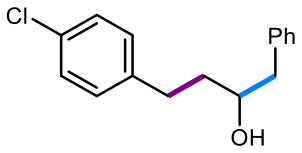
Cl
Ph
OH

4.2.3aw

^{1}H NMR

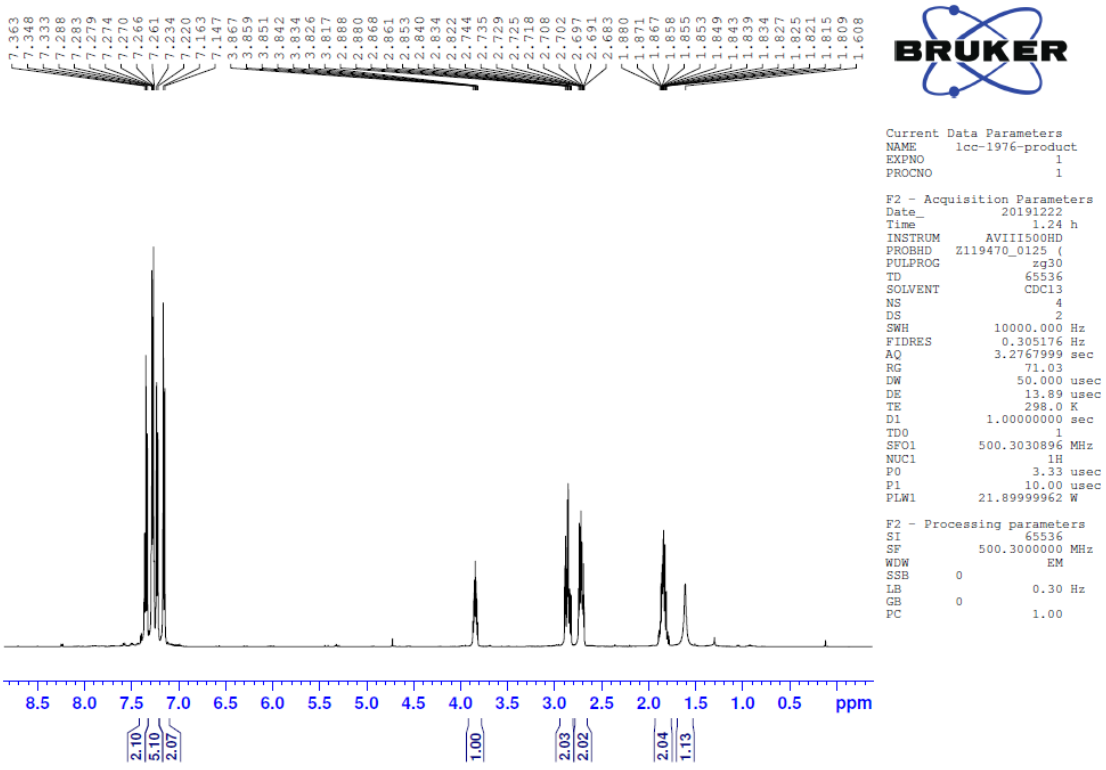
7.363
7.348
7.333
7.288
7.283
7.279
7.274
7.270
7.266
7.261
7.234
7.220
7.163
7.147
3.867
3.859
3.851
3.842
3.834
3.826
3.817
2.888
2.880
2.868
2.861
2.853
2.840
2.834
2.822
2.744
2.735
2.729
2.725
2.718
2.708
2.702
2.697
2.691
2.683
1.880
1.871
1.867
1.858
1.855
1.853
1.849
1.843
1.839
1.834
1.827
1.825
1.821
1.815
1.809
1.608
BRUKER
Current Data Parameters
NAME 1cc-1976-product
EXPNO 1
PROCNO 1
F2 - Acquisition Parameters
Date_ 20191222
Time 1.24 h
INSTRUM AVIII500HD
PROBHD Z119470_0125 (
PULPROG zg30
TD 65536
SOLVENT CDCl3
NS 4
DS 2
SWH 10000.000 Hz
FIDRES 0.305176 Hz
AQ 3.2767999 sec
RG 71.03
DW 50.000 usec
DE 13.89 usec
TE 298.0 K
D1 1.00000000 sec
TD0 1
SFO1 500.3030896 MHz
NUC1 1H
P0 3.33 usec
P1 10.00 usec
PLW1 21.89999962 W
F2 - Processing parameters
SI 65536
SF 500.3000000 MHz
WDW EM
SSB 0
LB 0.30 Hz
GB 0
PC 1.00
8.5 8.0 7.5 7.0 6.5 6.0 5.5 5.0 4.5 4.0 3.5 3.0 2.5 2.0 1.5 1.0 0.5 ppm
2.10
5.10
2.07
1.00
2.03
2.02
2.04
1.13

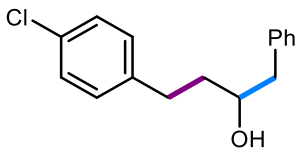

4.2.3aw

^{13}C NMR

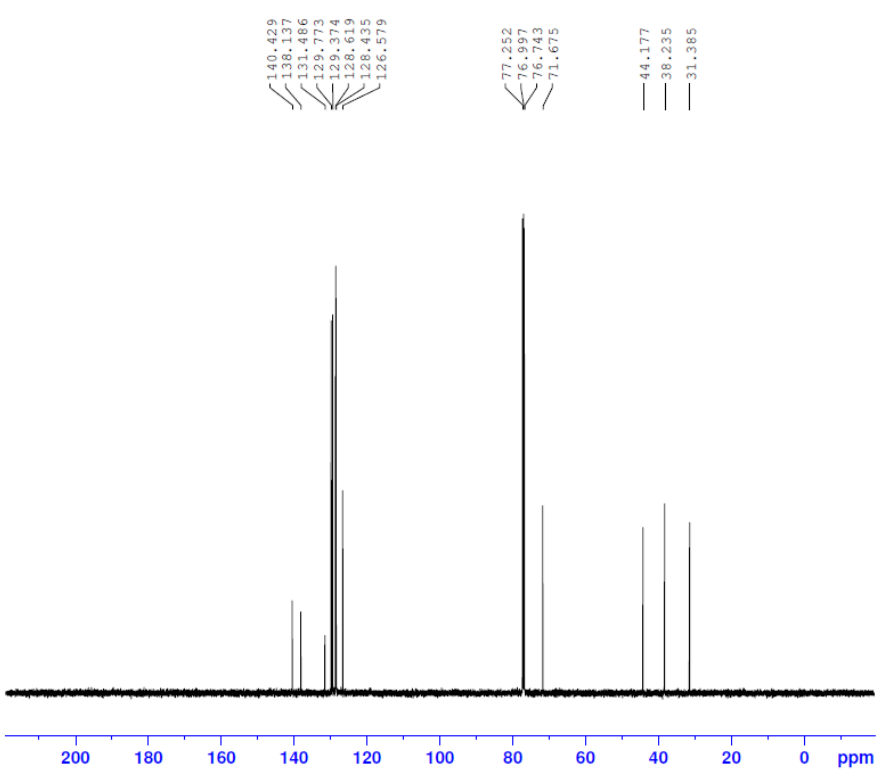

BRUKER

```
Current Data Parameters
NAME      1cc-1976-product
EXPNO                    2
PROCNO                   1

F2 - Acquisition Parameters
Date_             20191222
Time                  1.31 h
INSTRUM       AVIII500HD
PROBHD    Z119470_0125 (
PULPROG             zgpg30
TD                   65536
SOLVENT              CDCl3
NS                     128
DS                       4
SWH              30000.000 Hz
FIDRES           0.915527 Hz
AQ               1.0922667 sec
RG                  192.72
DW                 16.667 usec
DE                 20.34 usec
TE                 298.0 K
D1              2.00000000 sec
D11             0.03000000 sec
TD0                      1
SFO1           125.8131140 MHz
NUC1                   13C
P0                  3.41 usec
P1                 10.23 usec
PLW1           78.00000000 W
SFO2           500.3020012 MHz
NUC2                   1H
CPDPRG[2           waltz16
PCPD2              80.00 usec
PLW2           21.50000000 W
PLW12           0.49000001 W
PLW13           0.20446000 W

F2 - Processing parameters
SI                   32768
SF            125.8005425 MHz
WDW                     EM
SSB       0
LB                    1.00 Hz
GB        0
PC                    1.40
```

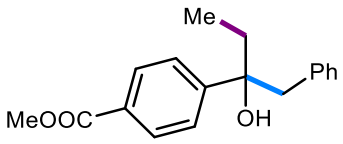
Me
Ph
MeOOC
OH

4.2.3ax

^{1}H NMR

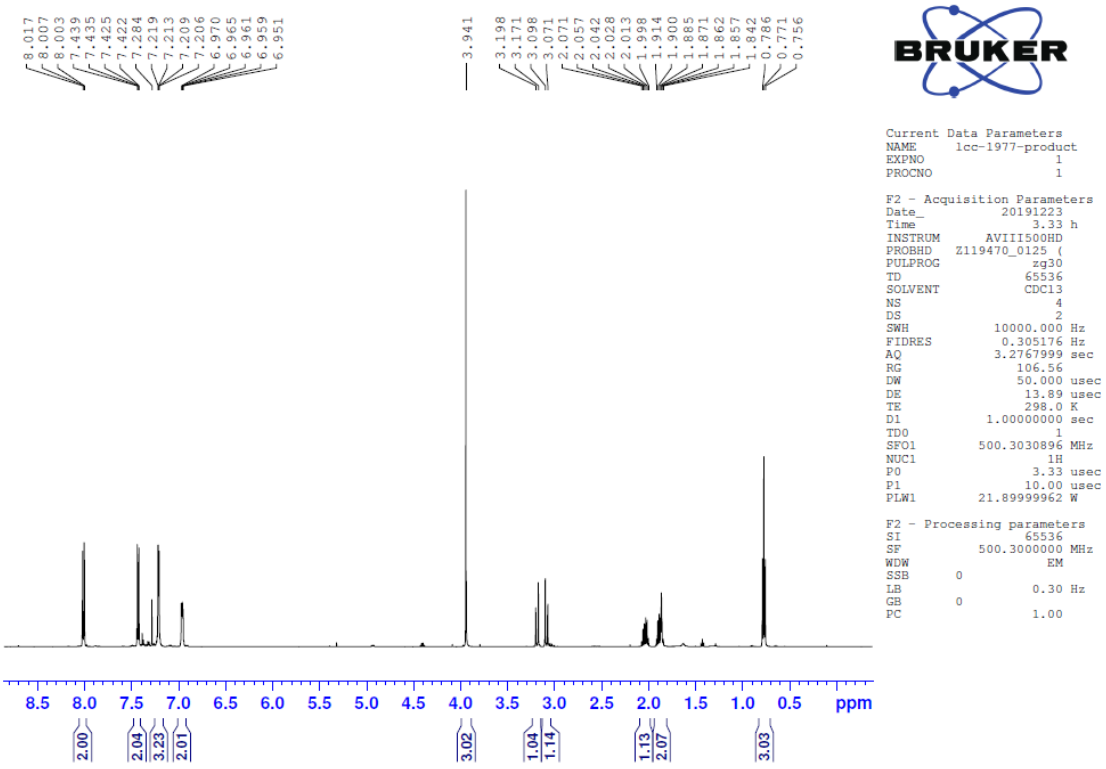
8.017
8.007
8.003
7.439
7.435
7.425
7.422
7.284
7.219
7.213
7.209
7.206
6.970
6.965
6.961
6.959
6.951
3.941
3.198
3.171
3.098
3.071
2.071
2.057
2.042
2.028
2.013
1.998
1.914
1.900
1.885
1.871
1.862
1.857
1.842
0.786
0.771
0.756
BRUKER
Current Data Parameters
NAME lcc-1977-product
EXPNO 1
PROCNO 1
F2 - Acquisition Parameters
Date_ 20191223
Time 3.33 h
INSTRUM AVIII500HD
PROBHD Z119470_0125 (
PULPROG zg30
TD 65536
SOLVENT CDCl3
NS 4
DS 2
SWH 10000.000 Hz
FIDRES 0.305176 Hz
AQ 3.2767999 sec
RG 106.56
DW 50.000 usec
DE 13.89 usec
TE 298.0 K
D1 1.00000000 sec
TD0 1
SFO1 500.3030896 MHz
NUC1 1H
P0 3.33 usec
P1 10.00 usec
PLW1 21.89999962 W
F2 - Processing parameters
SI 65536
SF 500.3000000 MHz
WDW EM
SSB 0
LB 0.30 Hz
GB 0
PC 1.00
8.5 8.0 7.5 7.0 6.5 6.0 5.5 5.0 4.5 4.0 3.5 3.0 2.5 2.0 1.5 1.0 0.5 ppm
2.00
2.04
3.23
2.01
3.02
1.04
1.14
1.13
2.07
3.03

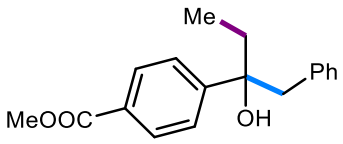

4.2.3ax

^{13}C NMR

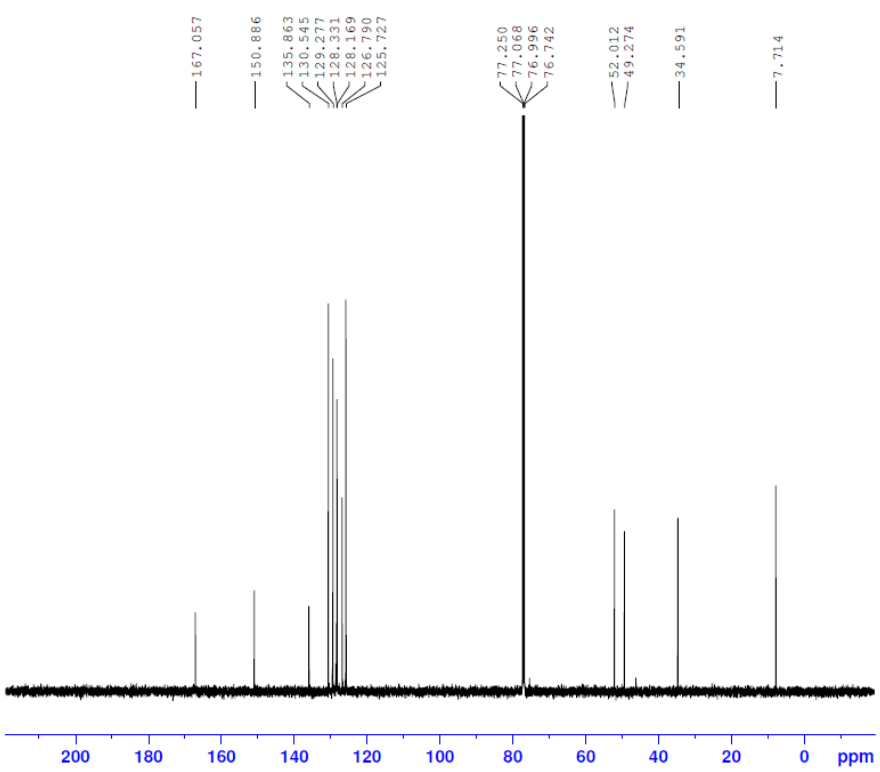


```
Current Data Parameters
NAME      lcc-1977-product
EXPNO                    2
PROCNO                   1

F2 - Acquisition Parameters
Date_             20191223
Time                 3.40 h
INSTRUM       AVIII500HD
PROBHD    Z119470_0125 (
PULPROG           zgpg30
TD                65536
SOLVENT           CDCl3
NS                  128
DS                    4
SWH           30000.000 Hz
FIDRES            0.915527 Hz
AQ                1.0922667 sec
RG                  192.72
DW                 16.667 usec
DE                 20.34 usec
TE                 298.0 K
D1             2.00000000 sec
D11            0.03000000 sec
TD0                    1
SFO1          125.8131140 MHz
NUC1                  13C
P0                  3.41 usec
P1                 10.23 usec
PLW1          78.00000000 W
SFO2          500.3020012 MHz
NUC2                   1H
CPDPRG[2          waltz16
PCPD2              80.00 usec
PLW2          21.50000000 W
PLW12          0.49000001 W
PLW13          0.20446000 W

F2 - Processing parameters
SI                   32768
SF            125.8005407 MHz
WDW                     EM
SSB       0
LB                  1.00 Hz
GB        0
PC                  1.40
```

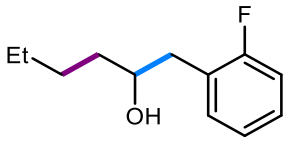
F
Et
OH

4.2.3ba

^{1}H NMR

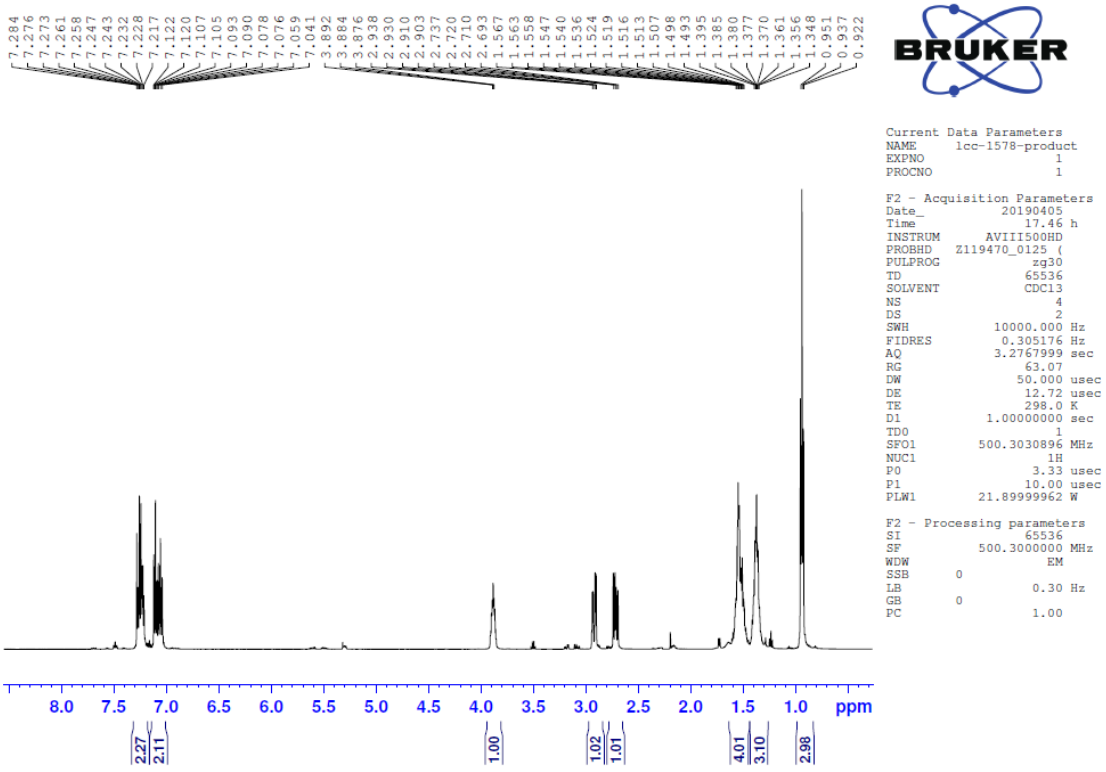
7.284
7.276
7.273
7.261
7.258
7.247
7.243
7.232
7.228
7.217
7.122
7.120
7.107
7.105
7.093
7.090
7.078
7.076
7.059
7.041
3.892
3.884
3.876
2.938
2.930
2.910
2.903
2.737
2.720
2.710
2.693
1.567
1.563
1.558
1.547
1.540
1.536
1.524
1.519
1.516
1.513
1.507
1.498
1.493
1.395
1.385
1.380
1.377
1.370
1.361
1.356
1.348
0.951
0.937
0.922
BRUKER
Current Data Parameters
NAME 1cc-1578-product
EXPNO 1
PROCNO 1
F2 - Acquisition Parameters
Date_ 20190405
Time 17.46 h
INSTRUM AVIII500HD
PROBHD Z119470_0125 (
PULPROG zg30
TD 65536
SOLVENT CDCl3
NS 4
DS 2
SWH 10000.000 Hz
FIDRES 0.305176 Hz
AQ 3.2767999 sec
RG 63.07
DW 50.000 usec
DE 12.72 usec
TE 298.0 K
D1 1.00000000 sec
TD0 1
SFO1 500.3030896 MHz
NUC1 1H
P0 3.33 usec
P1 10.00 usec
PLW1 21.89999962 W
F2 - Processing parameters
SI 65536
SF 500.3000000 MHz
WDW EM
SSB 0
LB 0.30 Hz
GB 0
PC 1.00
8.0 7.5 7.0 6.5 6.0 5.5 5.0 4.5 4.0 3.5 3.0 2.5 2.0 1.5 1.0 ppm
2.27
2.11
1.00
1.02
1.01
4.01
3.10
2.98

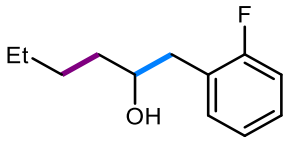

4.2.3ba

^{13}C NMR

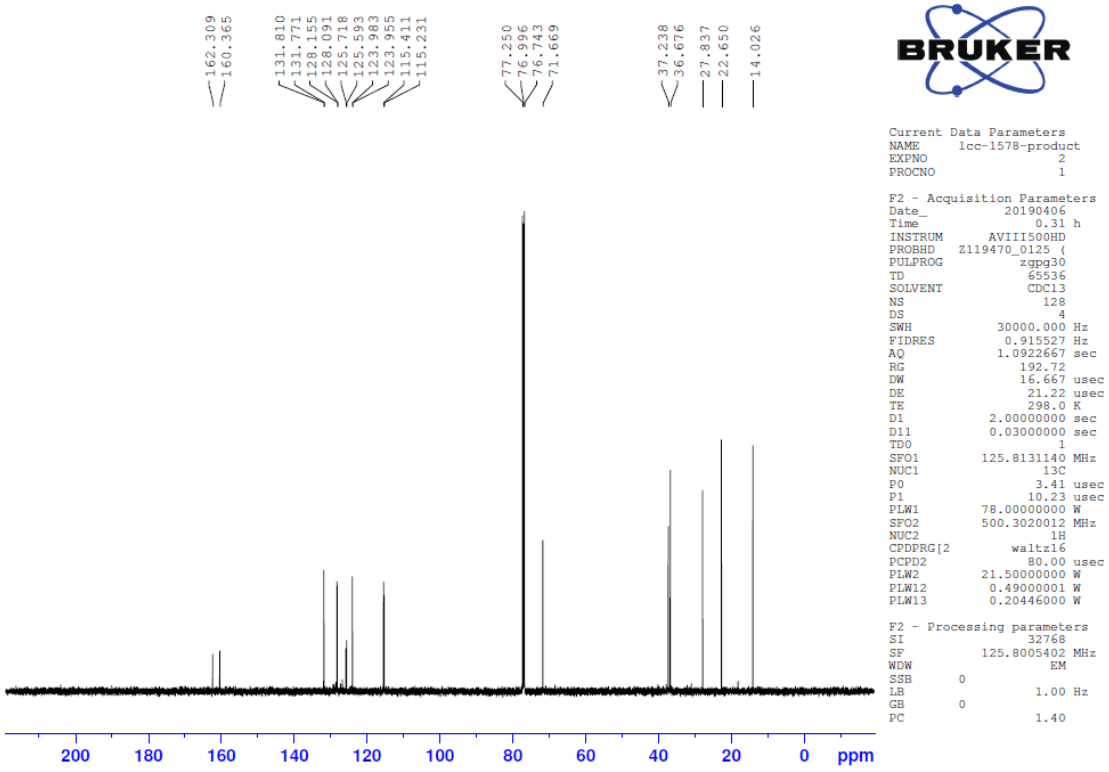


```
Current Data Parameters
NAME      1cc-1578-product
EXPNO                    2
PROCNO                   1

F2 - Acquisition Parameters
Date_             20190406
Time                  0.31 h
INSTRUM         AVIII500HD
PROBHD    Z119470_0125 (
PULPROG             zgpg30
TD                   65536
SOLVENT              CDCl3
NS                     128
DS                       4
SWH              30000.000 Hz
FIDRES           0.915527 Hz
AQ               1.0922667 sec
RG                  192.72
DW                 16.667 usec
DE                  21.22 usec
TE                  298.0 K
D1              2.00000000 sec
D11             0.03000000 sec
TD0                      1
SFO1           125.8131140 MHz
NUC1                   13C
P0                   3.41 usec
P1                  10.23 usec
PLW1           78.00000000 W
SFO2           500.3020012 MHz
NUC2                   1H
CPDPRG[2           waltz16
PCPD2               80.00 usec
PLW2           21.50000000 W
PLW12           0.49000001 W
PLW13           0.20446000 W

F2 - Processing parameters
SI                   32768
SF             125.8005402 MHz
WDW                     EM
SSB         0
LB                    1.00 Hz
GB          0
PC                    1.40
```

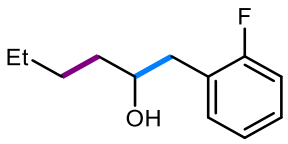

4.2.3ba

^{19}F NMR

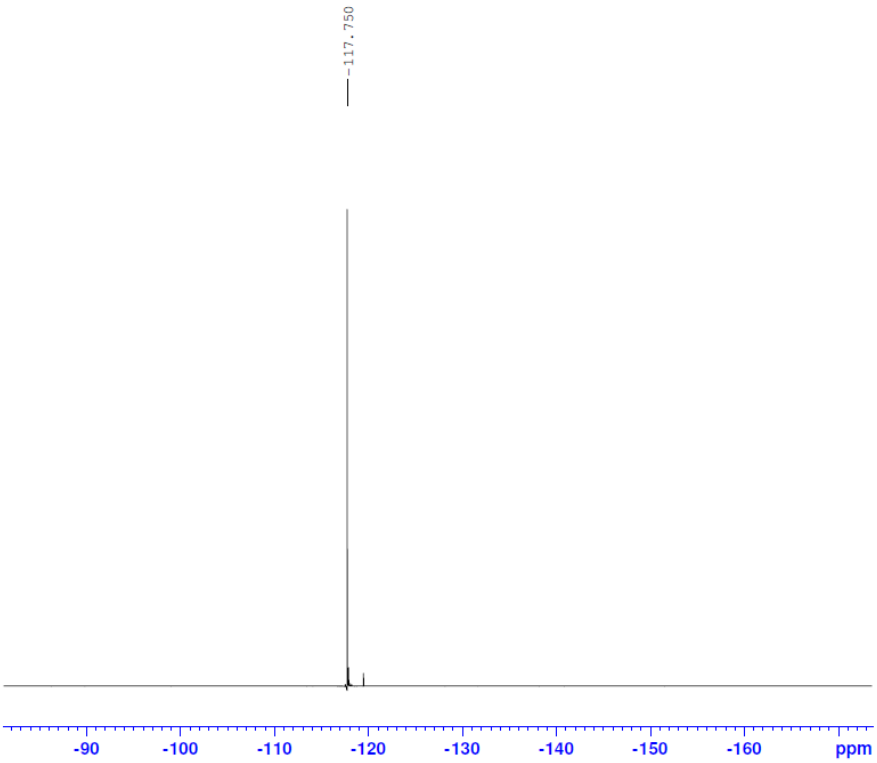


```
Current Data Parameters
NAME      1cc-1578-product
EXPNO                   3
PROCNO                  1

F2 - Acquisition Parameters
Date_           20190406
Time                5.22 h
INSTRUM       AVIII500HD
PROBHD    Z119470_0125 (
PULPROG   zgbsfhigqn.baseopt
TD                 131072
SOLVENT             CDCl3
NS                     16
DS                      4
SWH           111111.109 Hz
FIDRES          1.695421 Hz
AQ              0.5898240 sec
RG                 192.72
DW                  4.500 usec
DE                 35.33 usec
TE                 298.0 K
D1            1.00000000 sec
D11           0.03000000 sec
D12           0.00002000 sec
TD0                     1
SFO1         470.7052618 MHz
NUC1                  19F
P1                  15.00 usec
P2                  30.00 usec
PLW1         39.50000000 W
SFO2         500.3025015 MHz
NUC2                  1H
CPDPRG[2         waltz16
PCPD2               80.00 usec
PLW2         21.50000000 W
PLW12         0.49000001 W

F2 - Processing parameters
SI                  65536
SF           470.7523370 MHz
WDW                    EM
SSB       0
LB                  0.30 Hz
GB        0
PC                  1.00
```

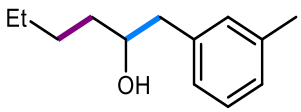
Et
OH

4.2.3ca

^{1}H NMR

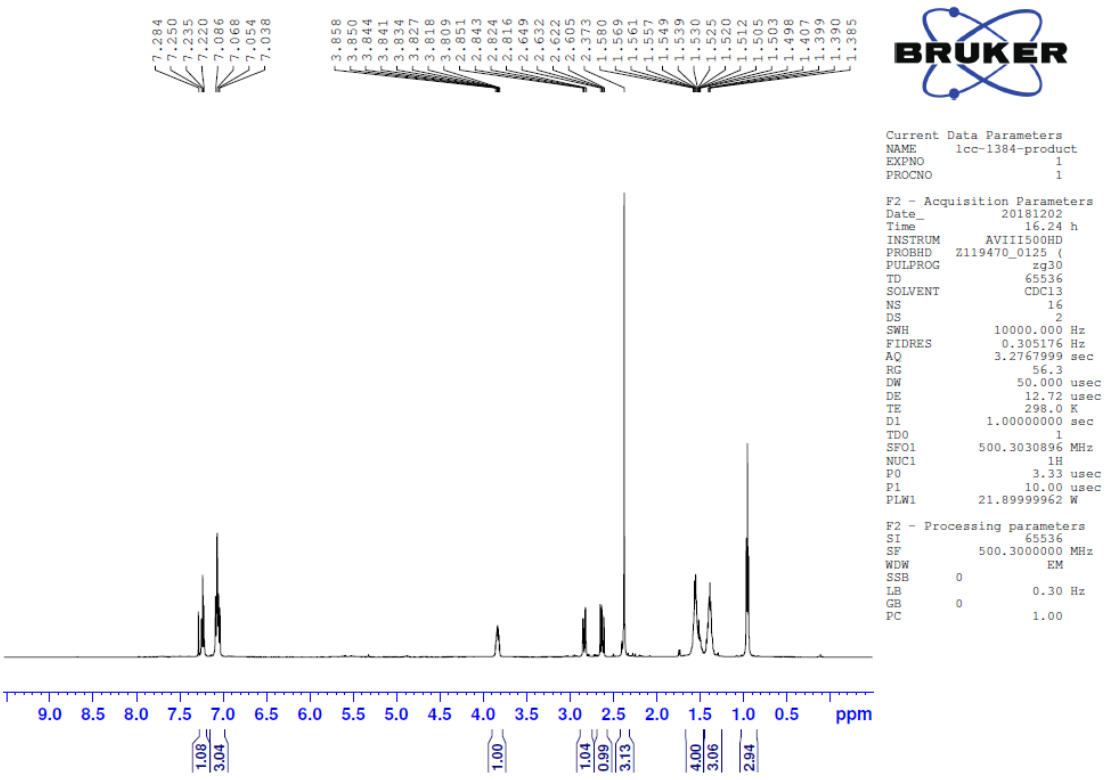
7.284
7.250
7.235
7.220
7.086
7.068
7.054
7.038
3.858
3.850
3.844
3.841
3.834
3.827
3.818
3.809
2.851
2.843
2.824
2.816
2.649
2.632
2.622
2.605
2.373
1.580
1.569
1.561
1.557
1.549
1.539
1.530
1.525
1.520
1.512
1.505
1.503
1.498
1.407
1.399
1.390
1.385
BRUKER
Current Data Parameters
NAME 1cc-1384-product
EXPNO 1
PROCNO 1
F2 - Acquisition Parameters
Date_ 20181202
Time 16.24 h
INSTRUM AVIII500HD
PROBHD Z119470_0125 (
PULPROG zg30
TD 65536
SOLVENT CDCl3
NS 16
DS 2
SWH 10000.000 Hz
FIDRES 0.305176 Hz
AQ 3.2767999 sec
RG 56.3
DW 50.000 usec
DE 12.72 usec
TE 298.0 K
D1 1.00000000 sec
TD0 1
SFO1 500.3030896 MHz
NUC1 1H
P0 3.33 usec
P1 10.00 usec
PLW1 21.89999962 W
F2 - Processing parameters
SI 65536
SF 500.3000000 MHz
WDW EM
SSB 0
LB 0.30 Hz
GB 0
PC 1.00
9.0 8.5 8.0 7.5 7.0 6.5 6.0 5.5 5.0 4.5 4.0 3.5 3.0 2.5 2.0 1.5 1.0 0.5 ppm
1.08
3.04
1.00
1.04
0.99
3.13
4.00
3.06
2.94

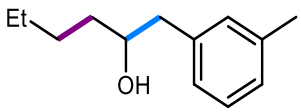

4.2.3ca

^{13}C NMR

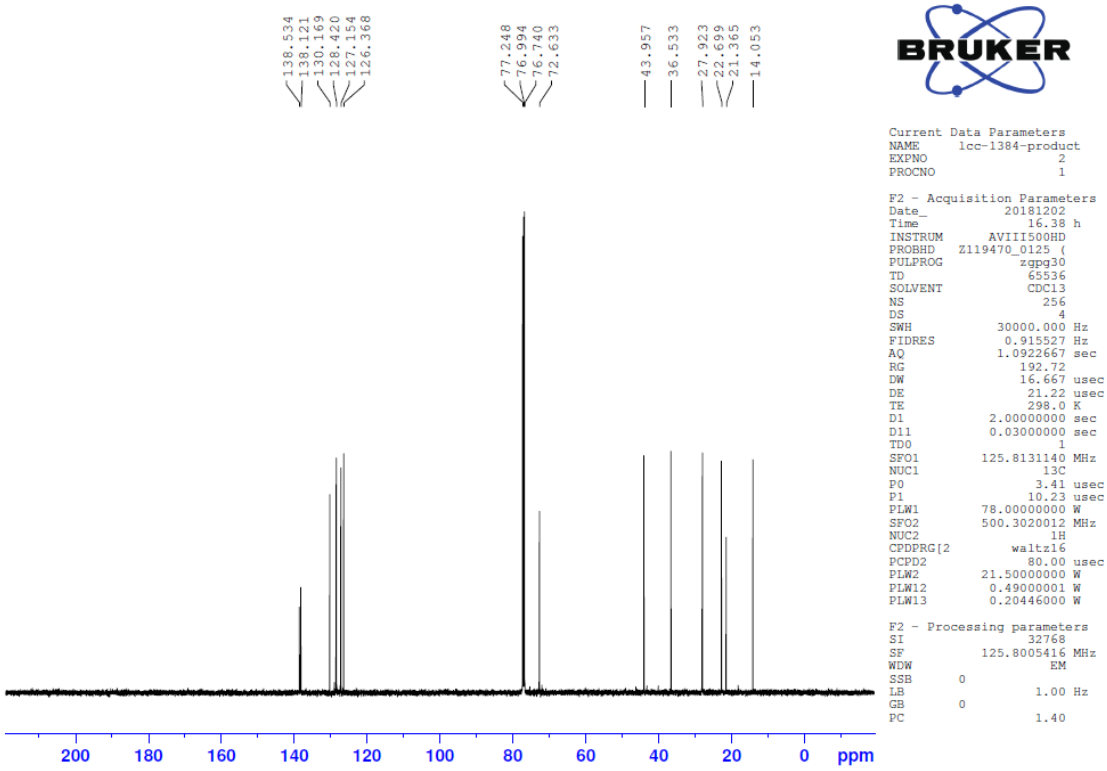


```
Current Data Parameters
NAME      1cc-1384-product
EXPNO                    2
PROCNO                   1

F2 - Acquisition Parameters
Date_             20181202
Time                16.38 h
INSTRUM       AVIII500HD
PROBHD    Z119470_0125 (
PULPROG            zgpg30
TD                  65536
SOLVENT             CDCl3
NS                    256
DS                      4
SWH             30000.000 Hz
FIDRES              0.915527 Hz
AQ                1.0922667 sec
RG                  192.72
DW                  16.667 usec
DE                  21.22 usec
TE                  298.0 K
D1              2.00000000 sec
D11             0.03000000 sec
TD0                     1
SFO1          125.8131140 MHz
NUC1                  13C
P0                   3.41 usec
P1                  10.23 usec
PLW1          78.00000000 W
SFO2          500.3020012 MHz
NUC2                  1H
CPDPRG[2          waltz16
PCPD2               80.00 usec
PLW2          21.50000000 W
PLW12          0.49000001 W
PLW13          0.20446000 W

F2 - Processing parameters
SI                   32768
SF            125.8005416 MHz
WDW                     EM
SSB       0
LB                    1.00 Hz
GB        0
PC                    1.40
```

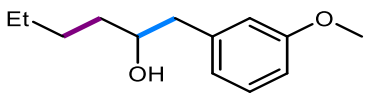
Et
O
OH

4.2.3da

^{1}H NMR

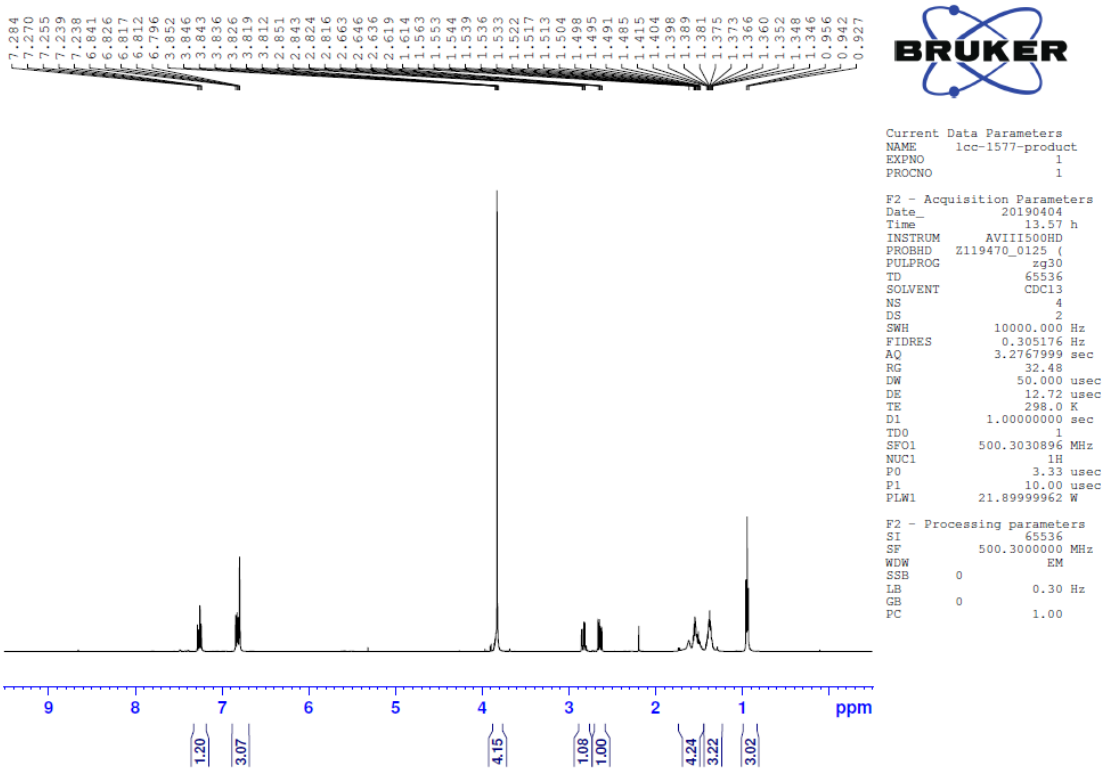
7.284
7.270
7.255
7.239
7.238
6.841
6.826
6.817
6.812
6.796
3.852
3.846
3.843
3.836
3.826
3.819
3.812
3.851
2.843
2.824
2.816
2.663
2.646
2.636
2.619
1.614
1.563
1.553
1.544
1.539
1.536
1.533
1.522
1.517
1.513
1.504
1.498
1.495
1.491
1.485
1.415
1.404
1.398
1.389
1.381
1.375
1.373
1.366
1.360
1.352
1.348
1.346
0.956
0.942
0.927
BRUKER
Current Data Parameters
NAME 1cc-1577-product
EXPNO 1
PROCNO 1
F2 - Acquisition Parameters
Date_ 20190404
Time 13.57 h
INSTRUM AVIII500HD
PROBHD Z119470_0125 (
PULPROG zg30
TD 65536
SOLVENT CDCl3
NS 4
DS 2
SWH 10000.000 Hz
FIDRES 0.305176 Hz
AQ 3.2767999 sec
RG 32.48
DW 50.000 usec
DE 12.72 usec
TE 298.0 K
D1 1.00000000 sec
TD0 1
SFO1 500.3030896 MHz
NUC1 1H
P0 3.33 usec
P1 10.00 usec
PLW1 21.89999962 W
F2 - Processing parameters
SI 65536
SF 500.3000000 MHz
WDW EM
SSB 0
LB 0.30 Hz
GB 0
PC 1.00
9
8
7
6
5
4
3
2
1
ppm
1.20
3.07
4.15
1.08
1.00
4.24
3.22
3.02

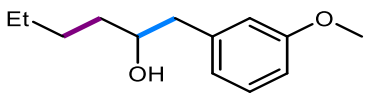

4.2.3da

^{13}C NMR

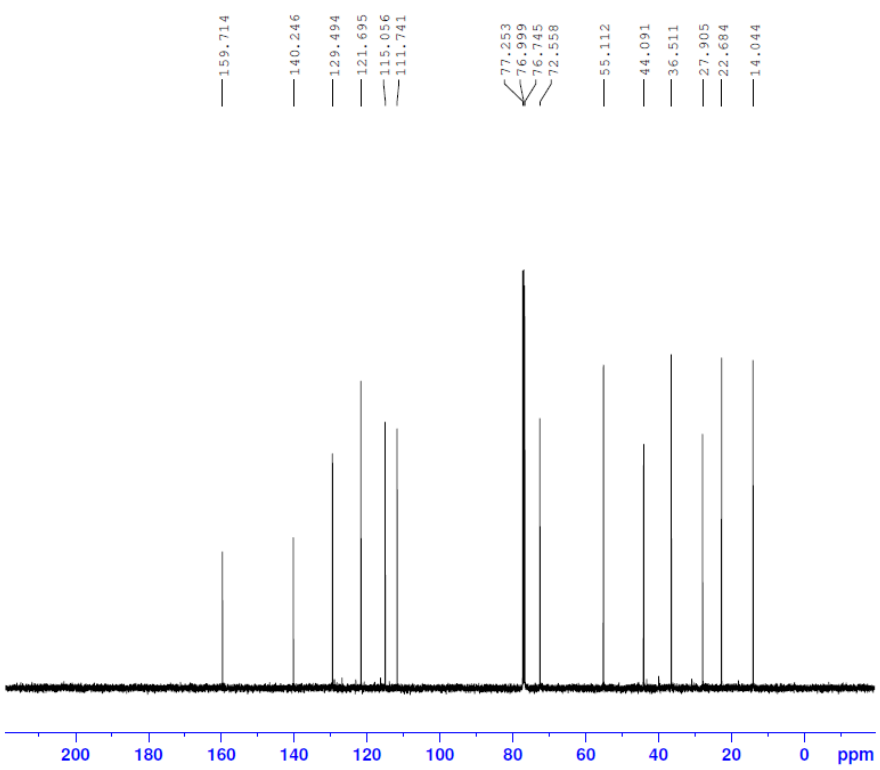

BRUKER

```
Current Data Parameters
NAME      1cc-1577-product
EXPNO                    2
PROCNO                   1

F2 - Acquisition Parameters
Date_              20190404
Time                 14.05 h
INSTRUM         AVIII500HD
PROBHD    Z119470_0125 (
PULPROG            zgpg30
TD                  65536
SOLVENT             CDCl3
NS                    128
DS                      4
SWH             30000.000 Hz
FIDRES          0.915527 Hz
AQ              1.0922667 sec
RG                 192.72
DW                16.667 usec
DE                21.22 usec
TE                298.0 K
D1              2.00000000 sec
D11             0.03000000 sec
TD0                     1
SFO1          125.8131140 MHz
NUC1                   13C
P0                  3.41 usec
P1                 10.23 usec
PLW1          78.00000000 W
SFO2          500.3020012 MHz
NUC2                   1H
CPDPRG[2          waltz16
PCPD2              80.00 usec
PLW2          21.50000000 W
PLW12          0.49000001 W
PLW13          0.20446000 W

F2 - Processing parameters
SI                  32768
SF            125.8005416 MHz
WDW                    EM
SSB       0
LB                  1.00 Hz
GB        0
PC                  1.40
```

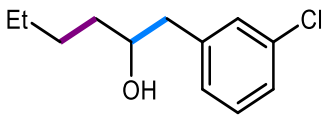
Et
Cl
OH

4.2.3ea

^{1}H NMR

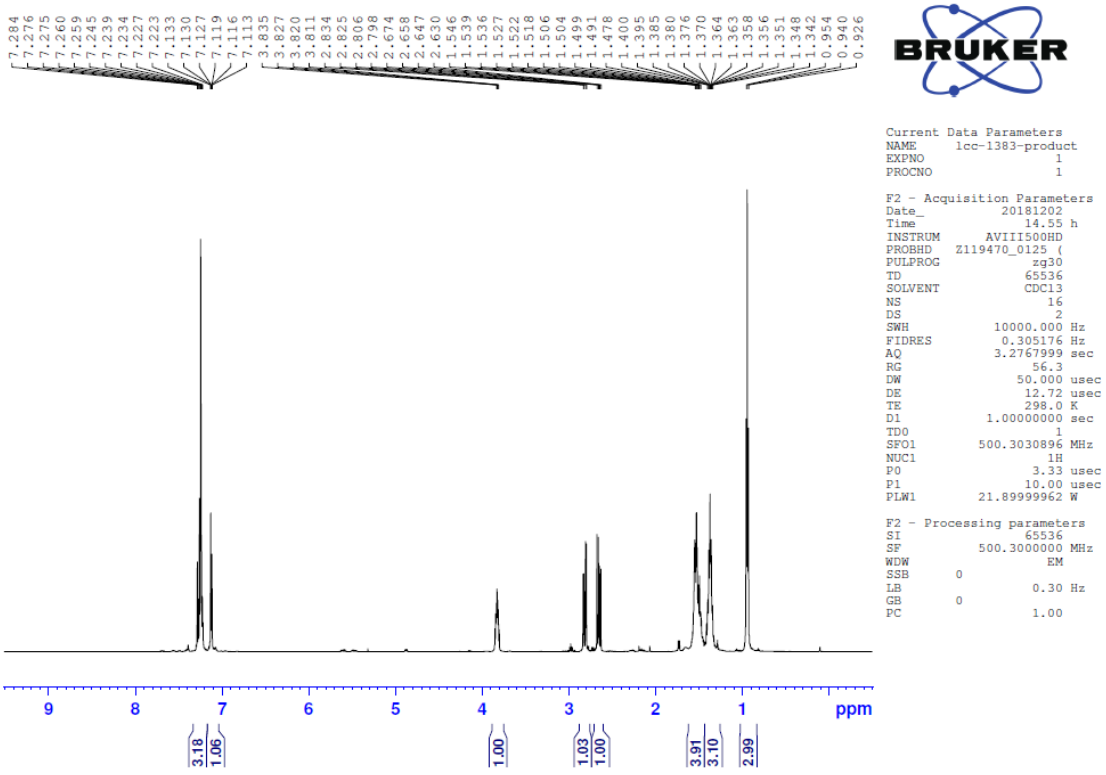
7.284
7.276
7.275
7.260
7.259
7.245
7.239
7.234
7.227
7.223
7.133
7.130
7.127
7.119
7.116
7.113
3.835
3.827
3.820
3.811
2.834
2.825
2.806
2.798
2.674
2.658
2.647
2.630
1.546
1.539
1.536
1.527
1.522
1.518
1.506
1.504
1.499
1.491
1.478
1.400
1.395
1.385
1.380
1.376
1.370
1.364
1.363
1.358
1.356
1.351
1.348
1.342
0.954
0.940
0.926
BRUKER
Current Data Parameters
NAME 1cc-1383-product
EXPNO 1
PROCNO 1
F2 - Acquisition Parameters
Date_ 20181202
Time 14.55 h
INSTRUM AVIII500HD
PROBHD Z119470_0125 (
PULPROG zg30
TD 65536
SOLVENT CDCl3
NS 16
DS 2
SWH 10000.000 Hz
FIDRES 0.305176 Hz
AQ 3.2767999 sec
RG 56.3
DW 50.000 usec
DE 12.72 usec
TE 298.0 K
D1 1.00000000 sec
TD0 1
SFO1 500.3030896 MHz
NUC1 1H
P0 3.33 usec
P1 10.00 usec
PLW1 21.89999962 W
F2 - Processing parameters
SI 65536
SF 500.3000000 MHz
WDW EM
SSB 0
LB 0.30 Hz
GB 0
PC 1.00
9
8
7
6
5
4
3
2
1
ppm
3.18
1.06
1.00
1.03
1.00
3.91
3.10
2.99

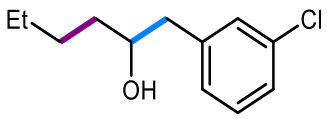

4.2.3ea

^{13}C NMR

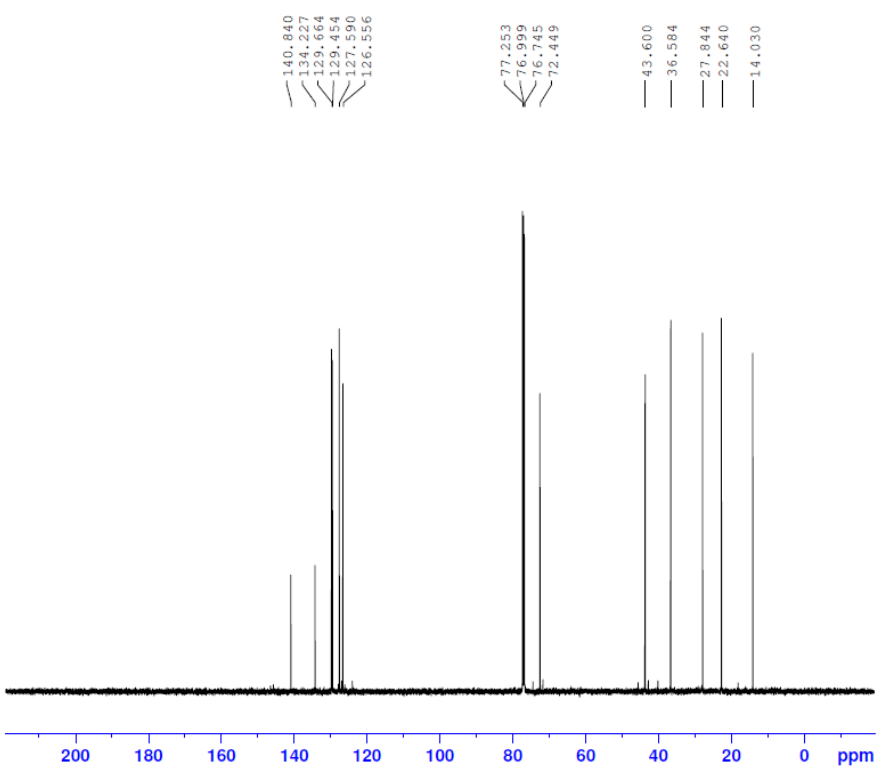

BRUKER

```
Current Data Parameters
NAME      1cc-1383-product
EXPNO                    2
PROCNO                   1

F2 - Acquisition Parameters
Date_             20181202
Time                16.19 h
INSTRUM       AVIII500HD
PROBHD    Z119470_0125 (
PULPROG            zgpg30
TD                  65536
SOLVENT             CDCl3
NS                    256
DS                      4
SWH             30000.000 Hz
FIDRES              0.915527 Hz
AQ                1.0922667 sec
RG                  192.72
DW                  16.667 usec
DE                  21.22 usec
TE                  298.0 K
D1              2.00000000 sec
D11             0.03000000 sec
TD0                     1
SFO1          125.8131140 MHz
NUC1                  13C
P0                   3.41 usec
P1                  10.23 usec
PLW1          78.00000000 W
SFO2          500.3020012 MHz
NUC2                  1H
CPDPRG[2          waltz16
PCPD2               80.00 usec
PLW2          21.50000000 W
PLW12          0.49000001 W
PLW13          0.20446000 W

F2 - Processing parameters
SI                   32768
SF            125.8005407 MHz
WDW                     EM
SSB       0
LB                    1.00 Hz
GB        0
PC                    1.40
```

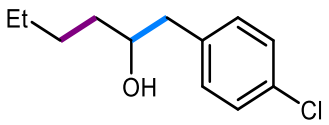
Et
OH
Cl

4.2.3fa

^{1}H NMR

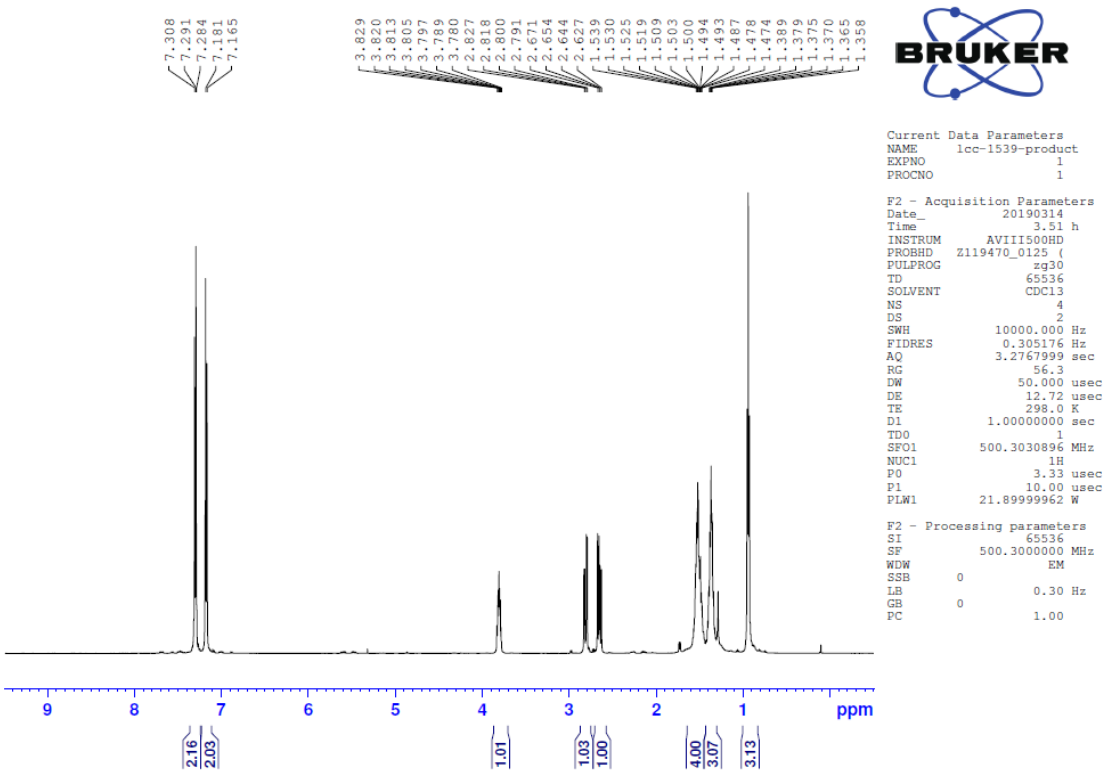
7.308
7.291
7.284
7.181
7.165
3.829
3.820
3.813
3.805
3.797
3.789
3.780
2.827
2.818
2.800
2.791
2.671
2.654
2.644
2.627
1.539
1.530
1.525
1.519
1.509
1.503
1.500
1.494
1.493
1.487
1.478
1.474
1.389
1.379
1.375
1.370
1.365
1.358
BRUKER
Current Data Parameters
NAME 1cc-1539-product
EXPNO 1
PROCNO 1
F2 - Acquisition Parameters
Date_ 20190314
Time 3.51 h
INSTRUM AVIII500HD
PROBHD Z119470_0125 (
PULPROG zg30
TD 65536
SOLVENT CDCl3
NS 4
DS 2
SWH 10000.000 Hz
FIDRES 0.305176 Hz
AQ 3.2767999 sec
RG 56.3
DW 50.000 usec
DE 12.72 usec
TE 298.0 K
D1 1.00000000 sec
TD0 1
SFO1 500.3030896 MHz
NUC1 1H
P0 3.33 usec
P1 10.00 usec
PLW1 21.89999962 W
F2 - Processing parameters
SI 65536
SF 500.3000000 MHz
WDW EM
SSB 0
LB 0.30 Hz
GB 0
PC 1.00
9
8
7
6
5
4
3
2
1
ppm
2.16
2.03
1.01
1.03
1.00
4.00
3.07
3.13

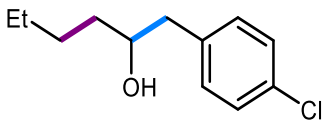

4.2.3fa

^{13}C NMR

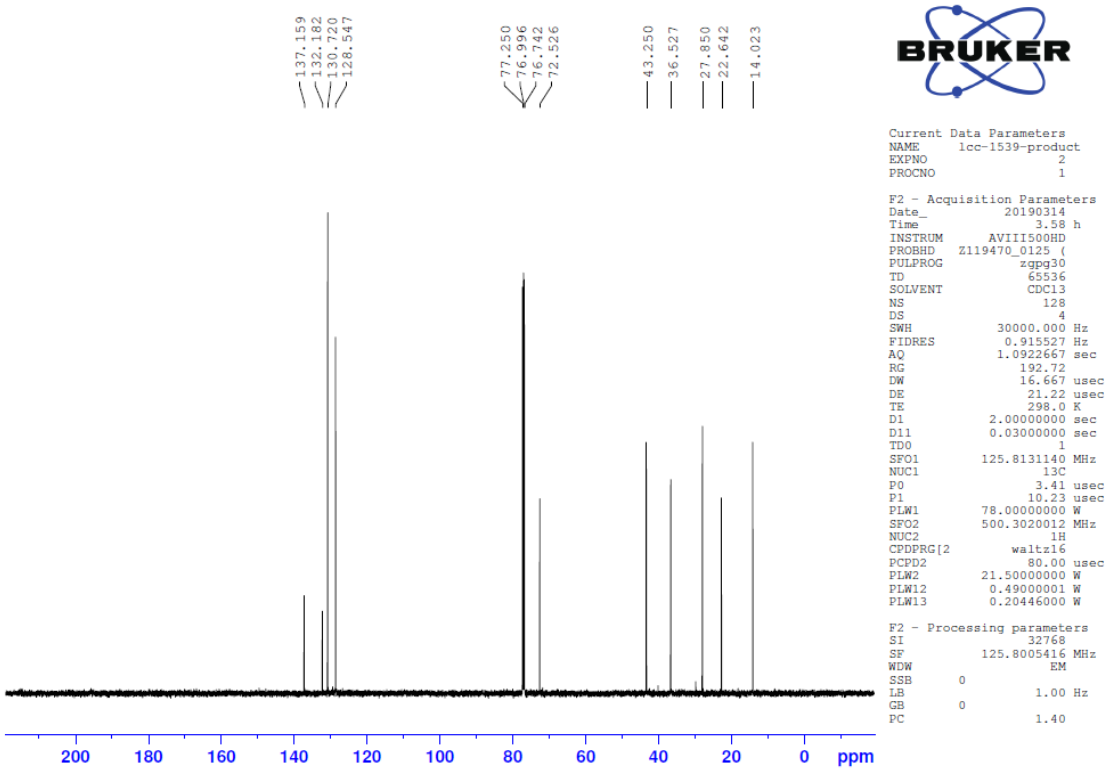

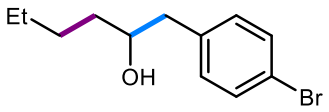
Et
OH
Br

4.2.3ga

^{1}H NMR

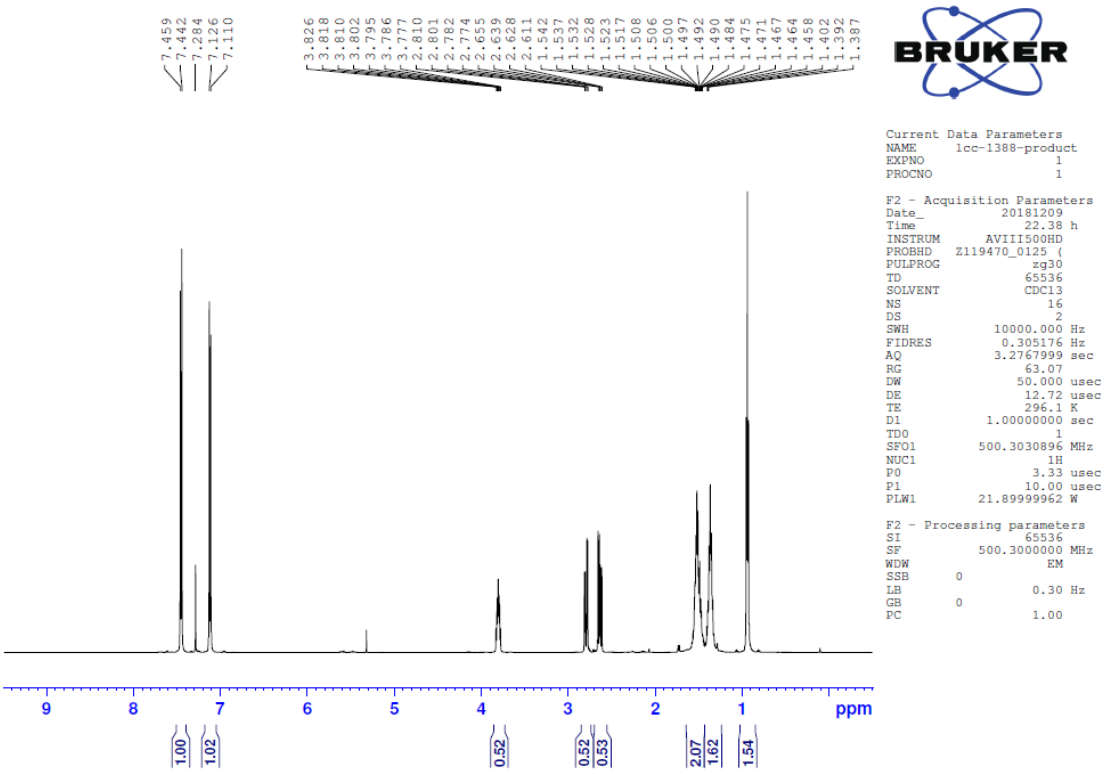
7.459
7.442
7.284
7.126
7.110
3.826
3.818
3.810
3.802
3.795
3.786
3.777
2.810
2.801
2.782
2.774
2.655
2.639
2.628
2.611
1.542
1.537
1.532
1.528
1.523
1.517
1.508
1.506
1.500
1.497
1.492
1.490
1.484
1.475
1.471
1.467
1.464
1.458
1.402
1.392
1.387
BRUKER
Current Data Parameters
NAME lcc-1388-product
EXPNO 1
PROCNO 1
F2 - Acquisition Parameters
Date_ 20181209
Time 22.38 h
INSTRUM AVIII500HD
PROBHD Z119470_0125 (
PULPROG zg30
TD 65536
SOLVENT CDCl3
NS 16
DS 2
SWH 10000.000 Hz
FIDRES 0.305176 Hz
AQ 3.2767999 sec
RG 63.07
DW 50.000 usec
DE 12.72 usec
TE 296.1 K
D1 1.00000000 sec
TD0 1
SFO1 500.3030896 MHz
NUC1 1H
P0 3.33 usec
P1 10.00 usec
PLW1 21.89999962 W
F2 - Processing parameters
SI 65536
SF 500.3000000 MHz
WDW EM
SSB 0
LB 0.30 Hz
GB 0
PC 1.00
9
8
7
6
5
4
3
2
1
ppm
1.00
1.02
0.52
0.52
0.53
2.07
1.62
1.54

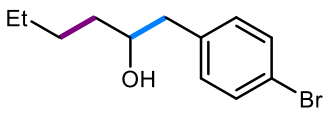

4.2.3ga

^{13}C NMR

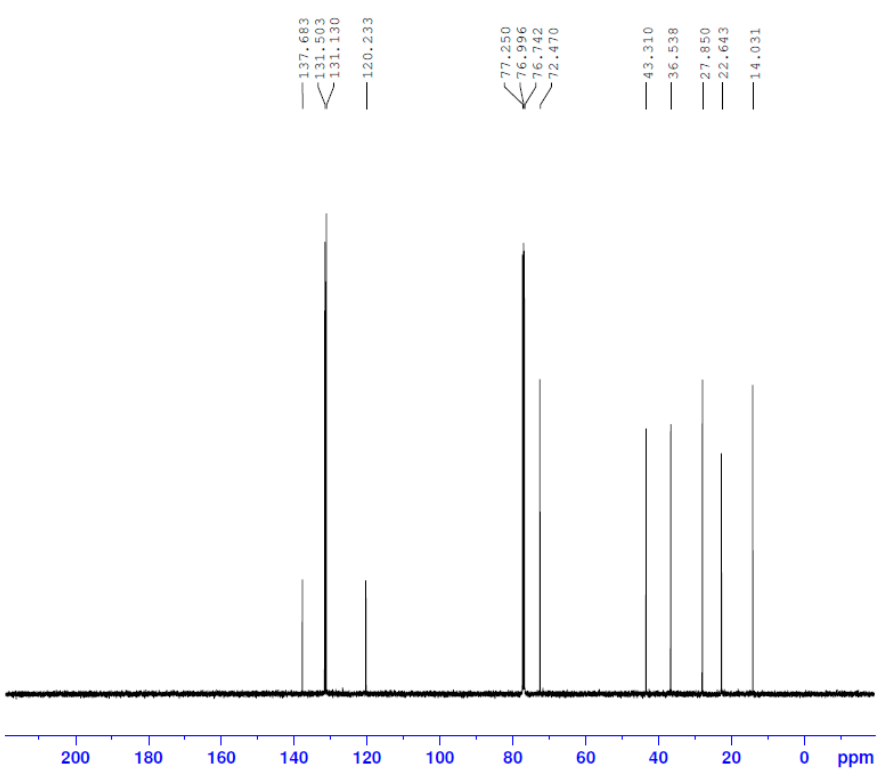

BRUKER

```
Current Data Parameters
NAME      lcc-1388-product
EXPNO                    2
PROCNO                   1

F2 - Acquisition Parameters
Date_             20181209
Time                22.52 h
INSTRUM       AVIII500HD
PROBHD    Z119470_0125 (
PULPROG             zgpg30
TD                   65536
SOLVENT              CDCl3
NS                     256
DS                       4
SWH              30000.000 Hz
FIDRES           0.915527 Hz
AQ               1.0922667 sec
RG                  192.72
DW                 16.667 usec
DE                 21.22 usec
TE                 297.0 K
D1             2.00000000 sec
D11            0.03000000 sec
TD0                      1
SFO1          125.8131140 MHz
NUC1                  13C
P0                  3.41 usec
P1                 10.23 usec
PLW1          78.00000000 W
SFO2          500.3020012 MHz
NUC2                   1H
CPDPRG[2          waltz16
PCPD2              80.00 usec
PLW2          21.50000000 W
PLW12          0.49000001 W
PLW13          0.20446000 W

F2 - Processing parameters
SI                   32768
SF            125.8005416 MHz
WDW                     EM
SSB       0
LB                  1.00 Hz
GB        0
PC                  1.40
```

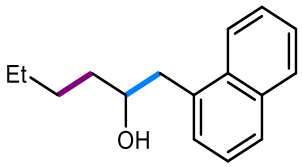
Et
OH

4.2.3ha

^{1}H NMR

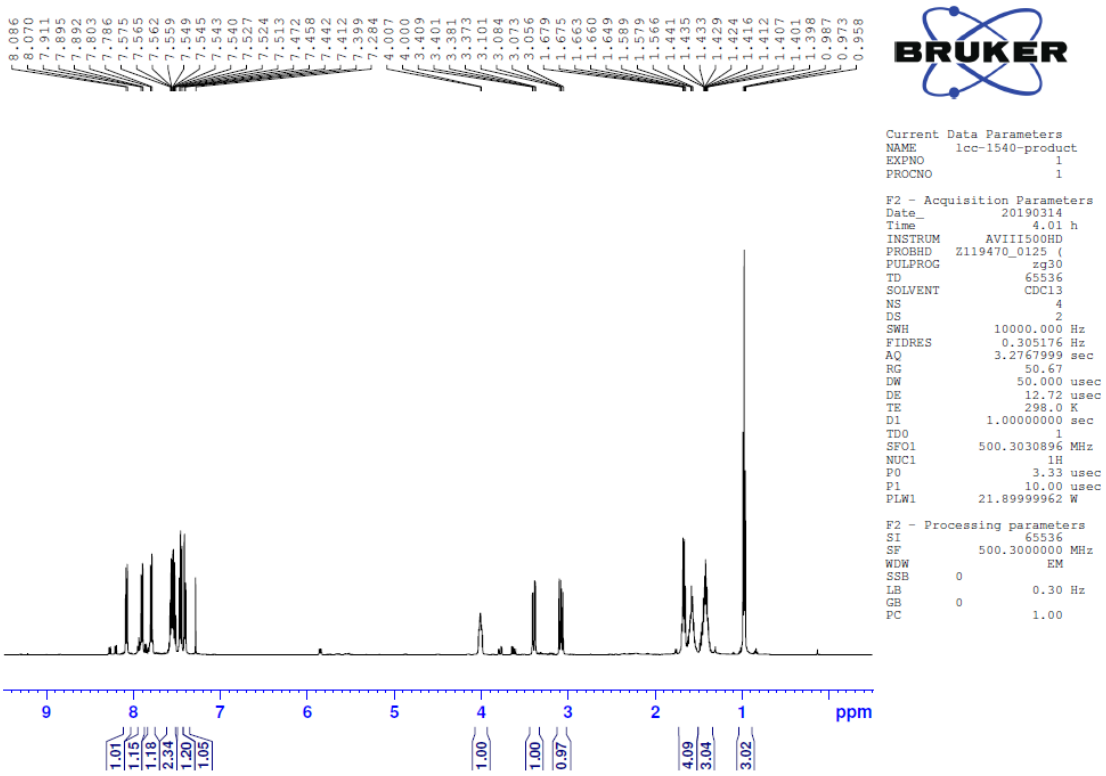
8.086
8.070
7.911
7.895
7.892
7.803
7.786
7.575
7.565
7.562
7.559
7.549
7.545
7.543
7.540
7.527
7.524
7.513
7.472
7.458
7.442
7.412
7.399
7.284
4.007
4.000
3.409
3.401
3.381
3.373
3.101
3.084
3.073
3.056
1.679
1.675
1.663
1.660
1.649
1.589
1.579
1.566
1.441
1.435
1.433
1.429
1.424
1.416
1.412
1.407
1.401
1.398
0.987
0.973
0.958
BRUKER
Current Data Parameters
NAME 1cc-1540-product
EXPNO 1
PROCNO 1
F2 - Acquisition Parameters
Date_ 20190314
Time 4.01 h
INSTRUM AVIII500HD
PROBHD Z119470_0125 (
PULPROG zg30
TD 65536
SOLVENT CDCl3
NS 4
DS 2
SWH 10000.000 Hz
FIDRES 0.305176 Hz
AQ 3.2767999 sec
RG 50.67
DW 50.000 usec
DE 12.72 usec
TE 298.0 K
D1 1.00000000 sec
TD0 1
SFO1 500.3030896 MHz
NUC1 1H
P0 3.33 usec
P1 10.00 usec
PLW1 21.89999962 W
F2 - Processing parameters
SI 65536
SF 500.3000000 MHz
WDW EM
SSB 0
LB 0.30 Hz
GB 0
PC 1.00
9
8
7
6
5
4
3
2
1
ppm
1.01
1.15
1.18
2.34
1.20
1.05
1.00
1.00
0.97
4.09
3.04
3.02

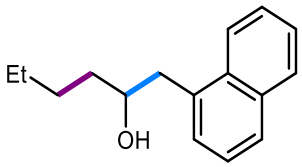

4.2.3ha

^{13}C NMR

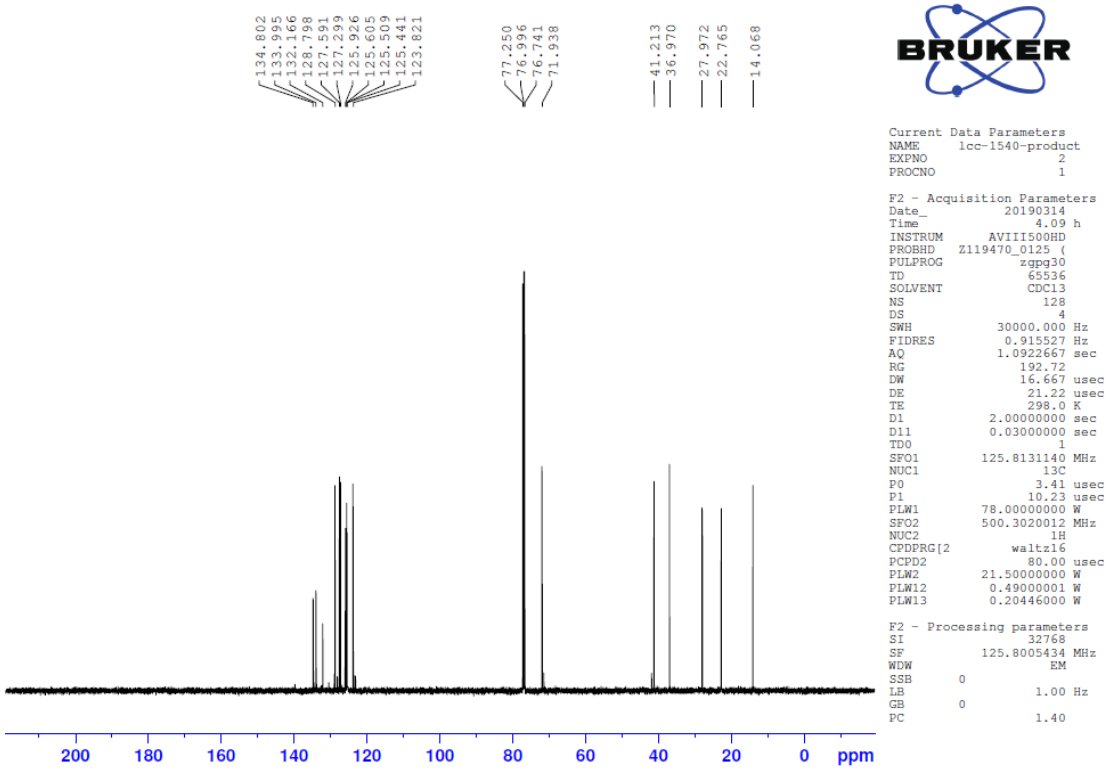


```
Current Data Parameters
NAME      1cc-1540-product
EXPNO                    2
PROCNO                   1

F2 - Acquisition Parameters
Date_           20190314
Time                4.09 h
INSTRUM       AVIII500HD
PROBHD    Z119470_0125 (
PULPROG           zgpg30
TD                 65536
SOLVENT            CDCl3
NS                   128
DS                     4
SWH            30000.000 Hz
FIDRES             0.915527 Hz
AQ                 1.0922667 sec
RG                   192.72
DW                  16.667 usec
DE                  21.22 usec
TE                  298.0 K
D1              2.00000000 sec
D11             0.03000000 sec
TD0                    1
SFO1          125.8131140 MHz
NUC1                  13C
P0                   3.41 usec
P1                  10.23 usec
PLW1          78.00000000 W
SFO2          500.3020012 MHz
NUC2                   1H
CPDPRG[2          waltz16
PCPD2               80.00 usec
PLW2          21.50000000 W
PLW12          0.49000001 W
PLW13          0.20446000 W

F2 - Processing parameters
SI                 32768
SF            125.8005434 MHz
WDW                   EM
SSB       0
LB                  1.00 Hz
GB        0
PC                  1.40
```

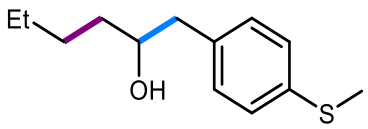
Et
OH
S

4.2.3ia

^{1}H NMR

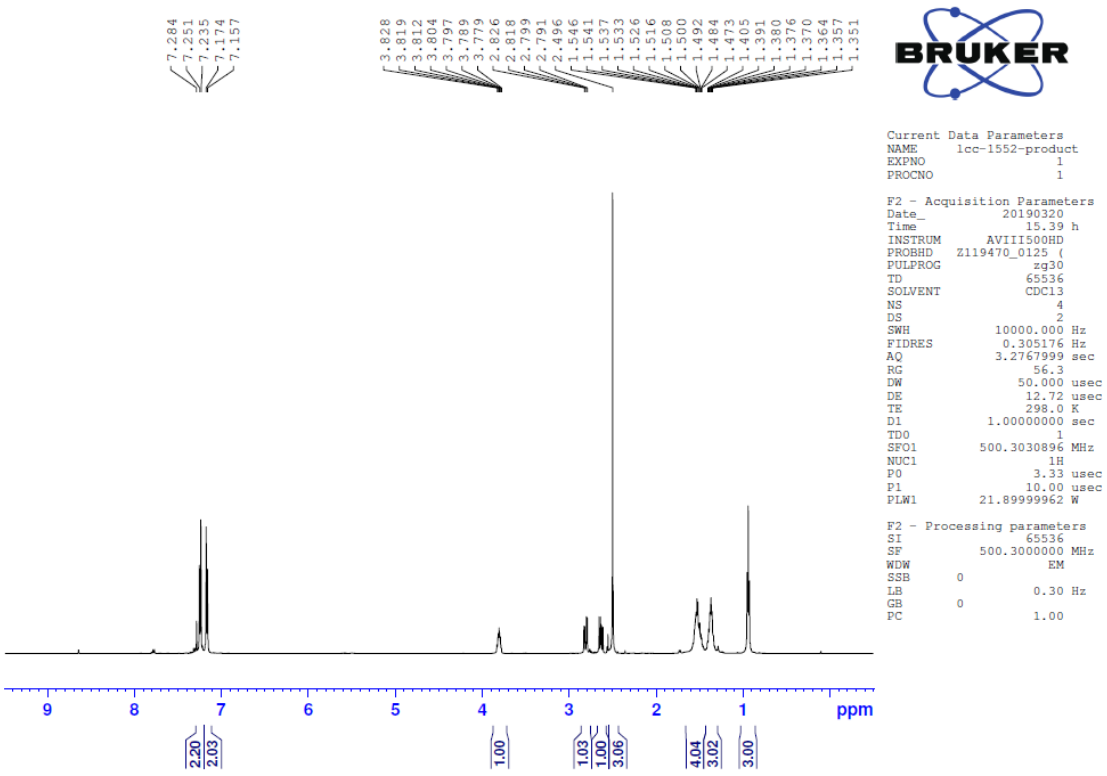
7.284
7.251
7.235
7.174
7.157
3.828
3.819
3.812
3.804
3.797
3.789
3.779
2.826
2.818
2.799
2.791
2.496
1.546
1.541
1.537
1.533
1.526
1.516
1.508
1.500
1.492
1.484
1.473
1.405
1.391
1.380
1.376
1.370
1.364
1.357
1.351
BRUKER
Current Data Parameters
NAME 1cc-1552-product
EXPNO 1
PROCNO 1
F2 - Acquisition Parameters
Date_ 20190320
Time 15.39 h
INSTRUM AVIII500HD
PROBHD Z119470_0125 (
PULPROG zg30
TD 65536
SOLVENT CDC13
NS 4
DS 2
SWH 10000.000 Hz
FIDRES 0.305176 Hz
AQ 3.2767999 sec
RG 56.3
DW 50.000 usec
DE 12.72 usec
TE 298.0 K
D1 1.00000000 sec
TD0 1
SFO1 500.3030896 MHz
NUC1 1H
P0 3.33 usec
P1 10.00 usec
PLW1 21.89999962 W
F2 - Processing parameters
SI 65536
SF 500.3000000 MHz
WDW EM
SSB 0
LB 0.30 Hz
GB 0
PC 1.00
9
8
7
6
5
4
3
2
1
ppm
2.20
2.03
1.00
1.03
1.00
3.06
4.04
3.02
3.00

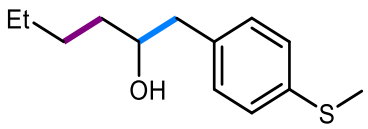

4.2.3ia

^{13}C NMR

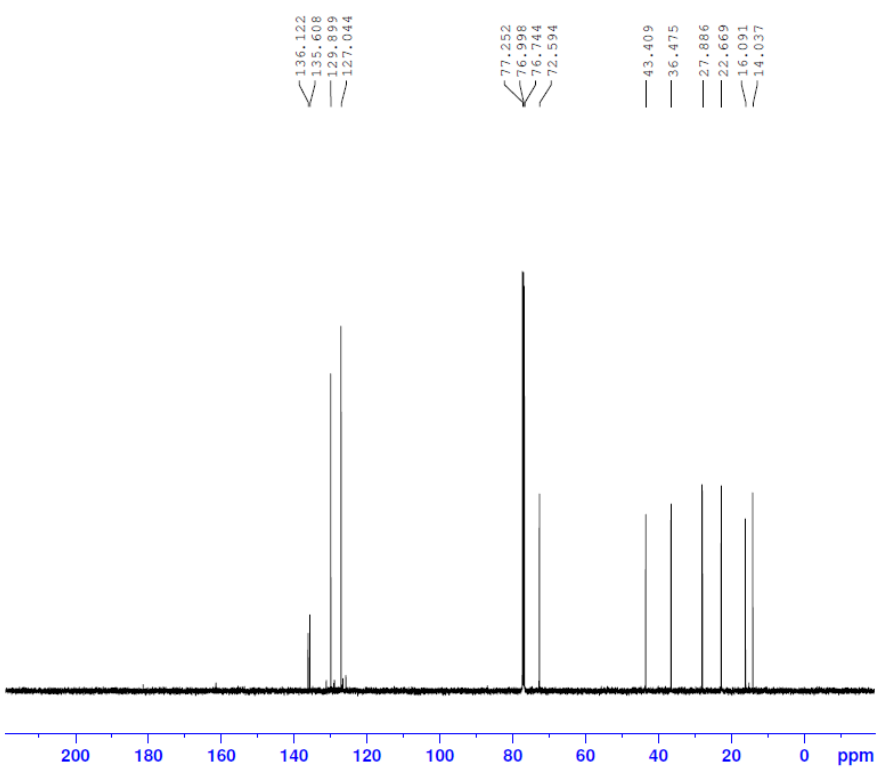


```
Current Data Parameters
NAME      1cc-1552-product
EXPNO                    2
PROCNO                   1

F2 - Acquisition Parameters
Date_           20190320
Time              15.47 h
INSTRUM       AVIII500HD
PROBHD    Z119470_0125 (
PULPROG           zgpg30
TD                65536
SOLVENT           CDCl3
NS                  128
DS                    4
SWH           30000.000 Hz
FIDRES         0.915527 Hz
AQ             1.0922667 sec
RG                192.72
DW                16.667 usec
DE                21.22 usec
TE                298.0 K
D1           2.00000000 sec
D11          0.03000000 sec
TD0                   1
SFO1         125.8131140 MHz
NUC1                 13C
P0                 3.41 usec
P1                10.23 usec
PLW1         78.00000000 W
SFO2         500.3020012 MHz
NUC2                 1H
CPDPRG[2         waltz16
PCPD2             80.00 usec
PLW2         21.50000000 W
PLW12         0.49000001 W
PLW13         0.20446000 W

F2 - Processing parameters
SI                32768
SF           125.8005425 MHz
WDW                  EM
SSB       0
LB                 1.00 Hz
GB        0
PC                 1.40
```

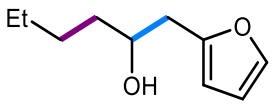
Et
O
OH

4.2.3ja

^{1}H NMR

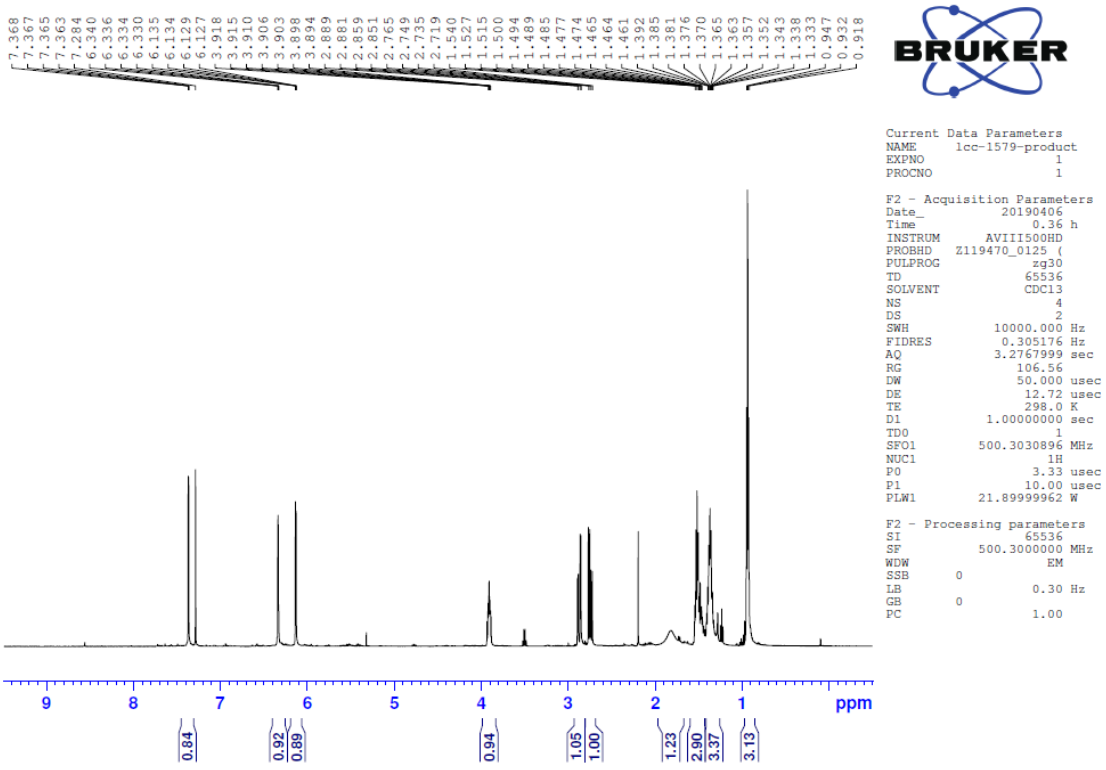
7.368
7.367
7.365
7.363
7.284
6.340
6.336
6.334
6.330
6.135
6.134
6.129
6.127
3.918
3.915
3.910
3.906
3.903
3.898
3.894
2.889
2.881
2.859
2.851
2.765
2.749
2.735
2.719
1.540
1.527
1.515
1.500
1.494
1.489
1.485
1.477
1.474
1.465
1.464
1.461
1.392
1.385
1.381
1.376
1.370
1.365
1.363
1.357
1.352
1.343
1.338
1.333
0.947
0.932
0.918
BRUKER
Current Data Parameters
NAME 1cc-1579-product
EXPNO 1
PROCNO 1
F2 - Acquisition Parameters
Date_ 20190406
Time 0.36 h
INSTRUM AVIII500HD
PROBHD Z119470_0125 (
PULPROG zg30
TD 65536
SOLVENT CDCl3
NS 4
DS 2
SWH 10000.000 Hz
FIDRES 0.305176 Hz
AQ 3.2767999 sec
RG 106.56
DW 50.000 usec
DE 12.72 usec
TE 298.0 K
D1 1.00000000 sec
TD0 1
SFO1 500.3030896 MHz
NUC1 1H
P0 3.33 usec
P1 10.00 usec
PLW1 21.89999962 W
F2 - Processing parameters
SI 65536
SF 500.3000000 MHz
WDW EM
SSB 0
LB 0.30 Hz
GB 0
PC 1.00
9
8
7
6
5
4
3
2
1
ppm
0.84
0.92
0.89
0.94
1.05
1.00
1.23
2.90
3.37
3.13

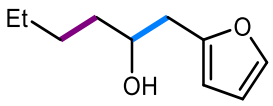

4.2.3ja

^{13}C NMR

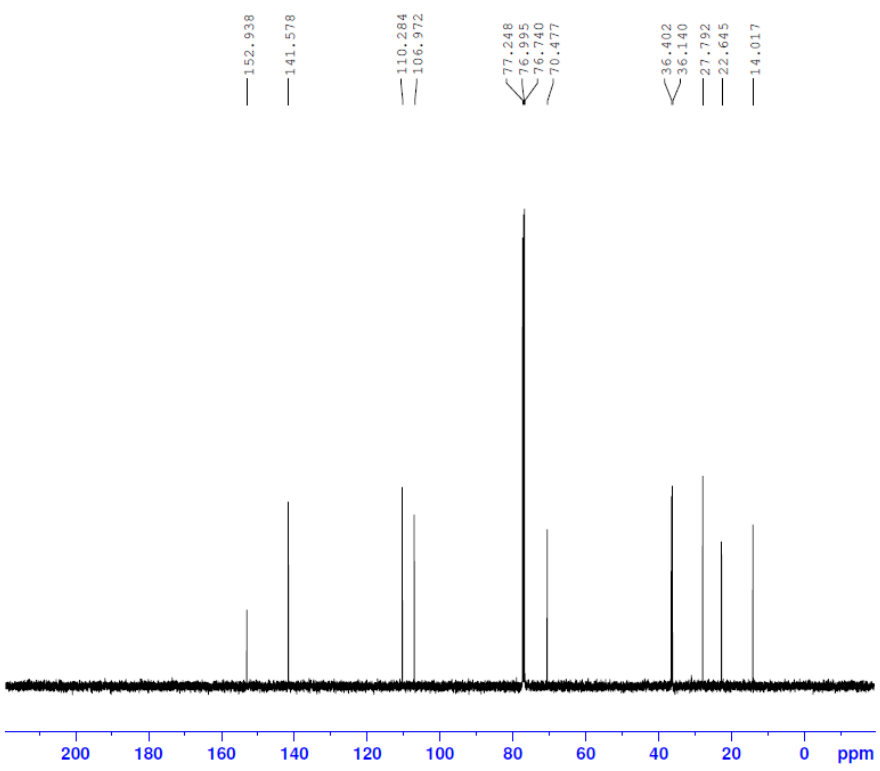


```
Current Data Parameters
NAME      1cc-1579-product
EXPNO                    2
PROCNO                   1

F2 - Acquisition Parameters
Date_           20190406
Time                0.43 h
INSTRUM       AVIII500HD
PROBHD    Z119470_0125 (
PULPROG           zgpg30
TD                 65536
SOLVENT            CDCl3
NS                   128
DS                     4
SWH            30000.000 Hz
FIDRES             0.915527 Hz
AQ                 1.0922667 sec
RG                   192.72
DW                  16.667 usec
DE                  21.22 usec
TE                  298.0 K
D1              2.00000000 sec
D11             0.03000000 sec
TD0                    1
SFO1          125.8131140 MHz
NUC1                  13C
P0                   3.41 usec
P1                  10.23 usec
PLW1          78.00000000 W
SFO2          500.3020012 MHz
NUC2                   1H
CPDPRG[2           waltz16
PCPD2               80.00 usec
PLW2          21.50000000 W
PLW12          0.49000001 W
PLW13          0.20446000 W

F2 - Processing parameters
SI                  32768
SF            125.8005379 MHz
WDW                    EM
SSB       0
LB                   1.00 Hz
GB        0
PC                   1.40
```

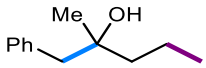
Me
OH
Ph

4.2.6aa

^{1}H NMR

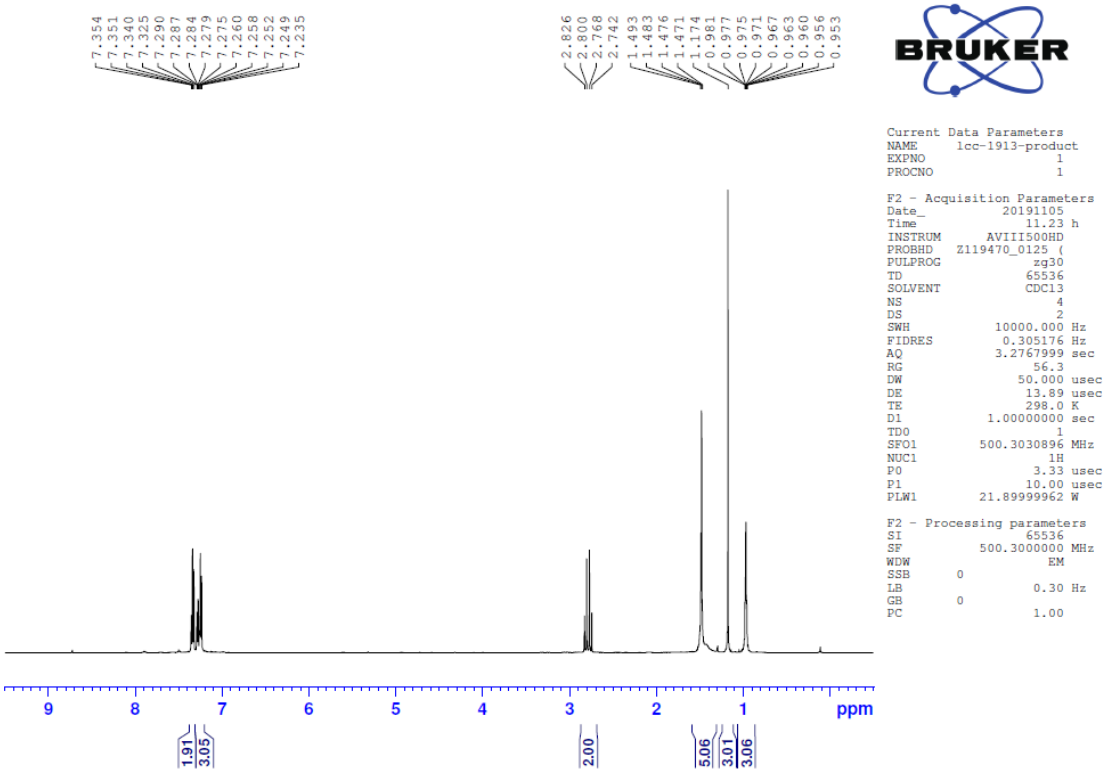
7.354
7.351
7.340
7.325
7.290
7.287
7.284
7.279
7.275
7.260
7.258
7.252
7.249
7.235
2.826
2.800
2.768
2.742
1.493
1.483
1.476
1.471
1.174
0.981
0.977
0.975
0.971
0.967
0.963
0.960
0.956
0.953
BRUKER
Current Data Parameters
NAME lcc-1913-product
EXPNO 1
PROCNO 1
F2 - Acquisition Parameters
Date_ 20191105
Time 11.23 h
INSTRUM AVIII500HD
PROBHD Z119470_0125 (
PULPROG zg30
TD 65536
SOLVENT CDCl3
NS 4
DS 2
SWH 10000.000 Hz
FIDRES 0.305176 Hz
AQ 3.2767999 sec
RG 56.3
DW 50.000 usec
DE 13.89 usec
TE 298.0 K
D1 1.00000000 sec
TD0 1
SFO1 500.3030896 MHz
NUC1 1H
P0 3.33 usec
P1 10.00 usec
PLW1 21.89999962 W
F2 - Processing parameters
SI 65536
SF 500.3000000 MHz
WDW EM
SSB 0
LB 0.30 Hz
GB 0
PC 1.00
9
8
7
6
5
4
3
2
1
ppm
1.91
3.05
2.00
5.06
3.01
3.06

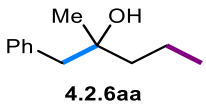

4.2.6aa

^{13}C NMR

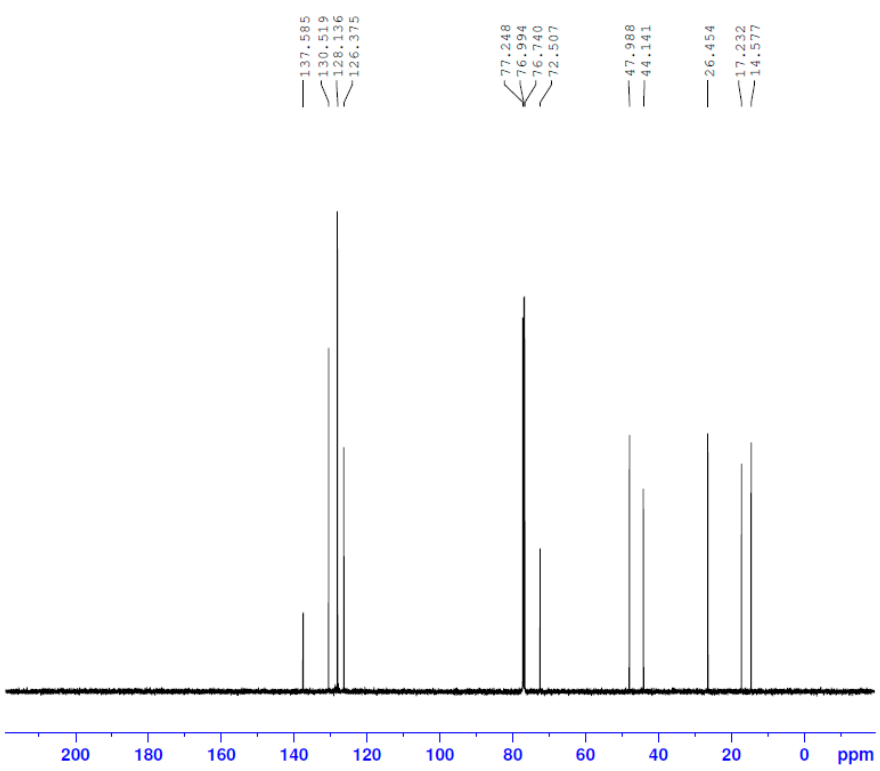


```
Current Data Parameters
NAME      1cc-1913-product
EXPNO                    2
PROCNO                   1

F2 - Acquisition Parameters
Date_           20191105
Time              11.31 h
INSTRUM       AVIII500HD
PROBHD    Z119470_0125 (
PULPROG           zgpg30
TD                65536
SOLVENT           CDCl3
NS                  128
DS                    4
SWH           30000.000 Hz
FIDRES        0.915527 Hz
AQ            1.0922667 sec
RG               192.72
DW               16.667 usec
DE                20.34 usec
TE                298.0 K
D1            2.00000000 sec
D11           0.03000000 sec
TD0                   1
SFO1         125.8131140 MHz
NUC1                 13C
P0                3.41 usec
P1               10.23 usec
PLW1         78.00000000 W
SFO2         500.3020012 MHz
NUC2                 1H
CPDPRG[2         waltz16
PCPD2             80.00 usec
PLW2         21.50000000 W
PLW12         0.49000001 W
PLW13         0.20446000 W

F2 - Processing parameters
SI                32768
SF           125.8005425 MHz
WDW                  EM
SSB       0
LB                1.00 Hz
GB        0
PC                1.40
```

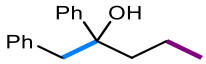
Ph
OH
Ph

4.2.6ab

^{1}H NMR

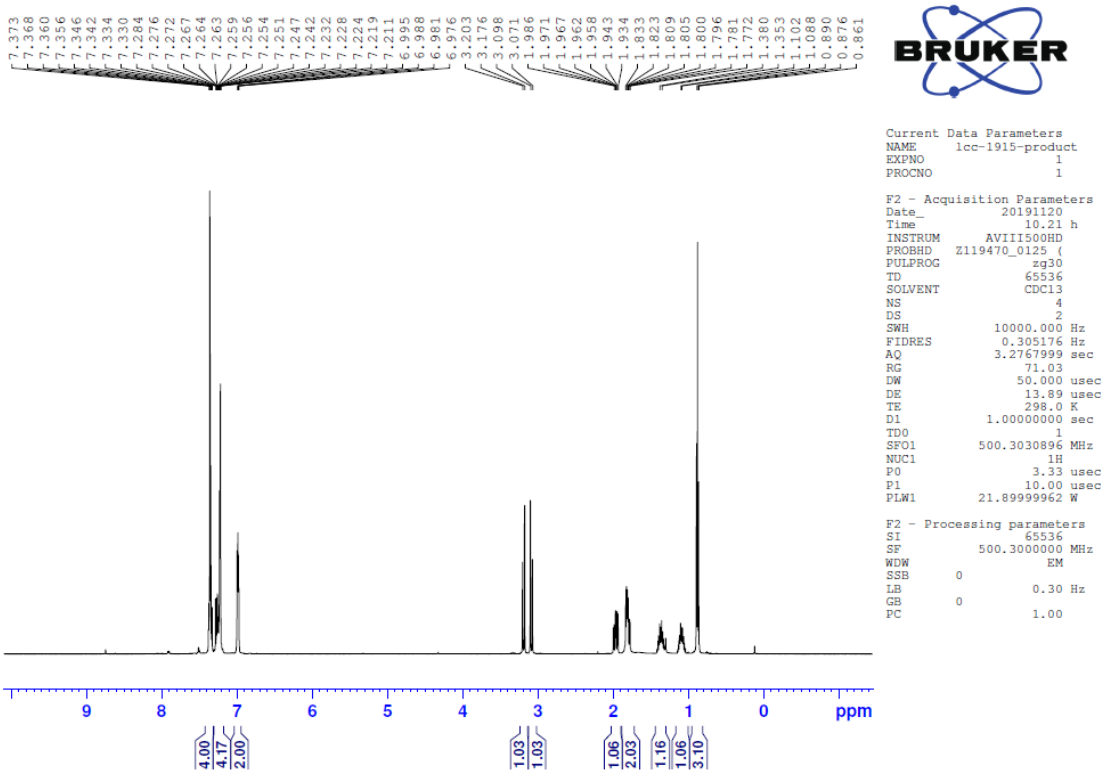
7.373
7.368
7.360
7.356
7.346
7.342
7.334
7.330
7.284
7.276
7.272
7.267
7.264
7.263
7.259
7.256
7.254
7.251
7.247
7.242
7.232
7.228
7.224
7.219
7.211
6.995
6.988
6.981
6.976
3.203
3.176
3.098
3.071
1.986
1.971
1.967
1.962
1.958
1.943
1.934
1.833
1.823
1.809
1.805
1.800
1.796
1.781
1.772
1.380
1.353
1.102
1.088
0.890
0.876
0.861
BRUKER
Current Data Parameters
NAME 1cc-1915-product
EXPNO 1
PROCNO 1
F2 - Acquisition Parameters
Date_ 20191120
Time 10.21 h
INSTRUM AVIII500HD
PROBHD Z119470_0125 (
PULPROG zg30
TD 65536
SOLVENT CDCl3
NS 4
DS 2
SWH 10000.000 Hz
FIDRES 0.305176 Hz
AQ 3.2767999 sec
RG 71.03
DW 50.000 usec
DE 13.89 usec
TE 298.0 K
D1 1.00000000 sec
TD0 1
SFO1 500.3030896 MHz
NUC1 1H
P0 3.33 usec
P1 10.00 usec
PLW1 21.89999962 W
F2 - Processing parameters
SI 65536
SF 500.3000000 MHz
WDW EM
SSB 0
LB 0.30 Hz
GB 0
PC 1.00
9
8
7
6
5
4
3
2
1
0
ppm
4.00
4.17
2.00
1.03
1.03
1.06
2.03
1.16
1.06
3.10

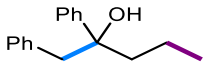

4.2.6ab

^{13}C NMR

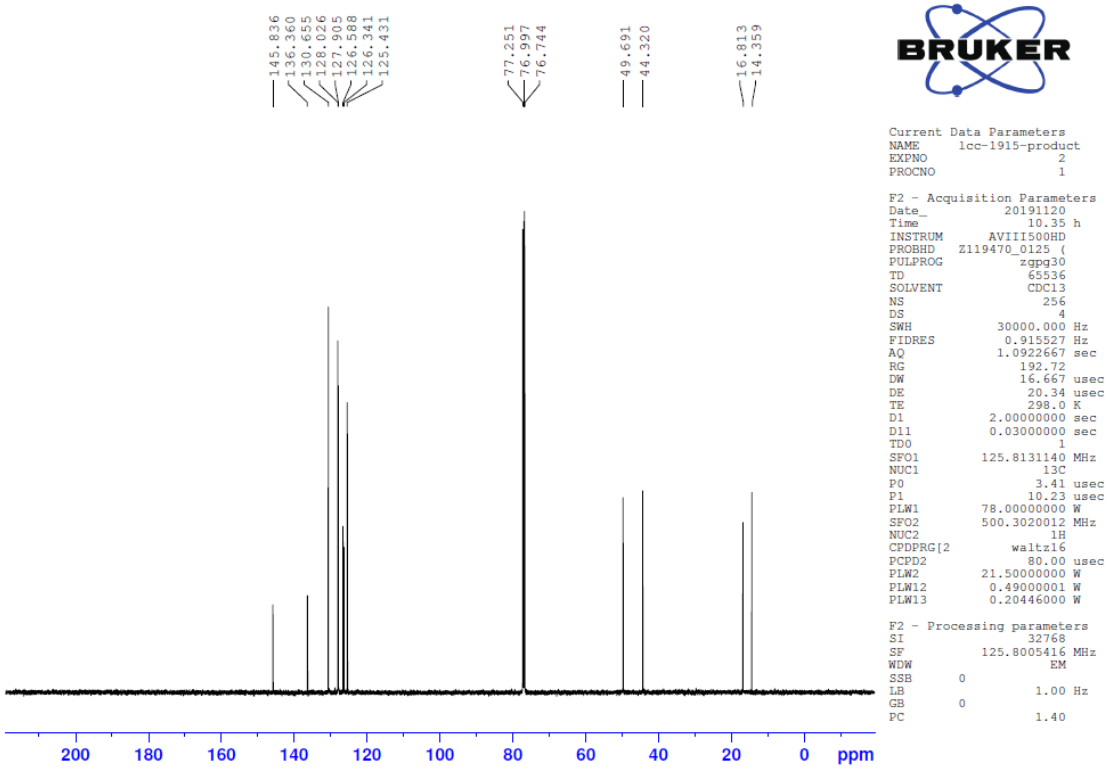


```
Current Data Parameters
NAME      1cc-1915-product
EXPNO                    2
PROCNO                   1

F2 - Acquisition Parameters
Date_           20191120
Time              10.35 h
INSTRUM       AVIII500HD
PROBHD    Z119470_0125 (
PULPROG          zgpg30
TD                65536
SOLVENT           CDCl3
NS                  256
DS                    4
SWH           30000.000 Hz
FIDRES            0.915527 Hz
AQ                1.0922667 sec
RG                  192.72
DW                 16.667 usec
DE                 20.34 usec
TE                298.0 K
D1             2.00000000 sec
D11            0.03000000 sec
TD0                   1
SFO1         125.8131140 MHz
NUC1                 13C
P0                  3.41 usec
P1                 10.23 usec
PLW1          78.00000000 W
SFO2         500.3020012 MHz
NUC2                 1H
CPDPRG[2          waltz16
PCPD2              80.00 usec
PLW2          21.50000000 W
PLW12          0.49000001 W
PLW13          0.20446000 W

F2 - Processing parameters
SI                  32768
SF           125.8005416 MHz
WDW                    EM
SSB       0
LB                  1.00 Hz
GB        0
PC                  1.40
```

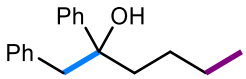
Ph
OH
Ph

4.2.6ac

^{1}H NMR

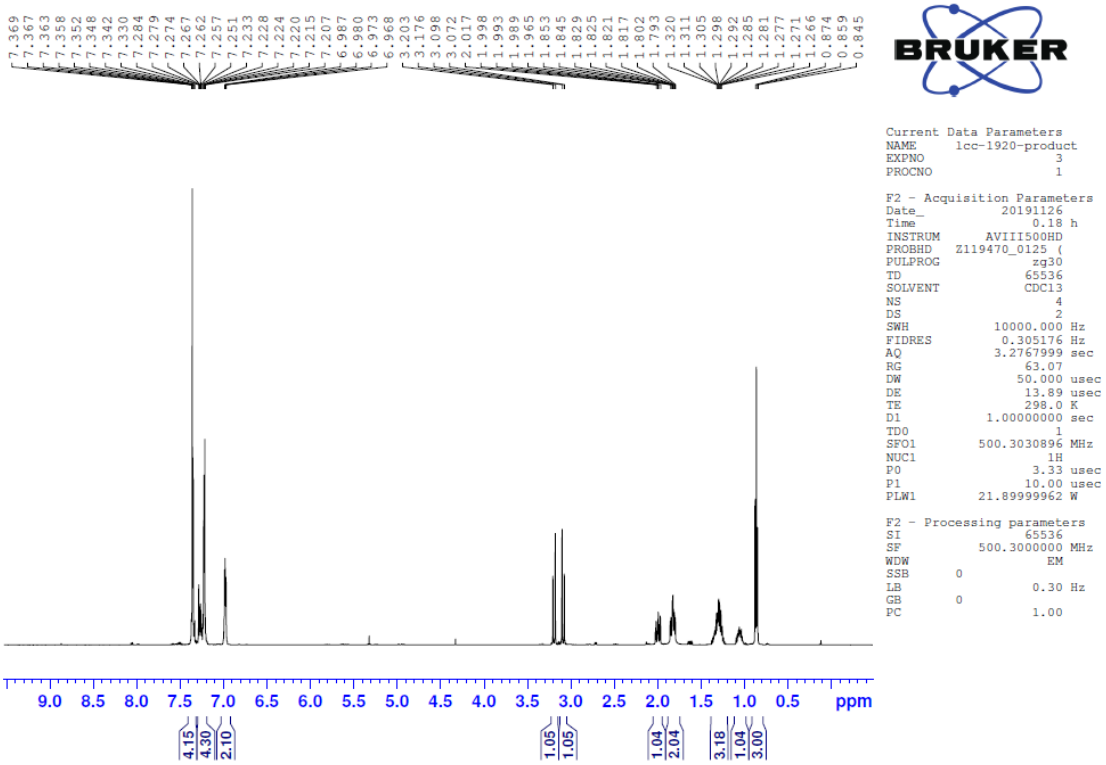
7.369
7.367
7.363
7.358
7.352
7.348
7.342
7.330
7.284
7.279
7.274
7.267
7.262
7.257
7.251
7.233
7.228
7.224
7.220
7.215
7.207
6.987
6.980
6.973
6.968
3.203
3.176
3.098
3.072
2.017
1.998
1.993
1.989
1.965
1.853
1.845
1.829
1.825
1.821
1.817
1.802
1.793
1.320
1.311
1.305
1.298
1.292
1.285
1.281
1.277
1.271
1.266
0.874
0.859
0.845
BRUKER
Current Data Parameters
NAME 1cc-1920-product
EXPNO 3
PROCNO 1
F2 - Acquisition Parameters
Date_ 20191126
Time 0.18 h
INSTRUM AVIII500HD
PROBHD Z119470_0125 (
PULPROG zg30
TD 65536
SOLVENT CDCl3
NS 4
DS 2
SWH 10000.000 Hz
FIDRES 0.305176 Hz
AQ 3.2767999 sec
RG 63.07
DW 50.000 usec
DE 13.89 usec
TE 298.0 K
D1 1.00000000 sec
TD0 1
SFO1 500.3030896 MHz
NUC1 1H
P0 3.33 usec
P1 10.00 usec
PLW1 21.89999962 W
F2 - Processing parameters
SI 65536
SF 500.3000000 MHz
WDW EM
SSB 0
LB 0.30 Hz
GB 0
PC 1.00
9.0 8.5 8.0 7.5 7.0 6.5 6.0 5.5 5.0 4.5 4.0 3.5 3.0 2.5 2.0 1.5 1.0 0.5 ppm
4.15
4.30
2.10
1.05
1.05
1.04
2.04
3.18
1.04
3.00

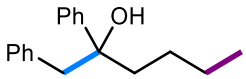

4.2.6ac

^{13}C NMR

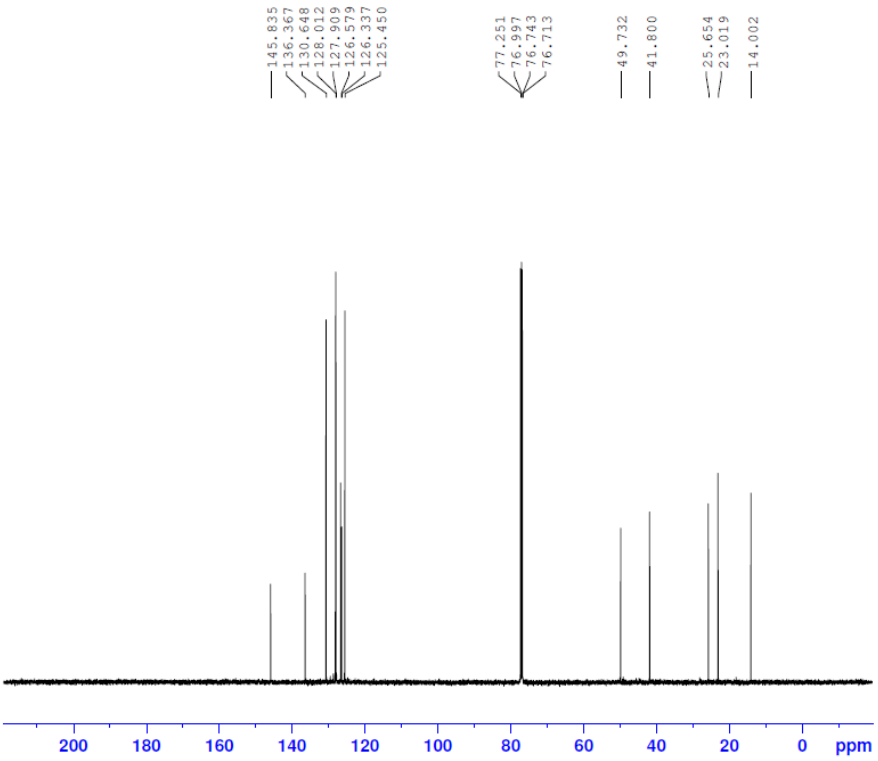


```
Current Data Parameters
NAME      1cc-1920-product
EXPNO                    4
PROCNO                   1

F2 - Acquisition Parameters
Date_           20191126
Time                0.32 h
INSTRUM       AVIII500HD
PROBHD    Z119470_0125 (
PULPROG             zgpg30
TD                   65536
SOLVENT              CDCl3
NS                     256
DS                       4
SWH             30000.000 Hz
FIDRES              0.915527 Hz
AQ                1.0922667 sec
RG                   192.72
DW                  16.667 usec
DE                  20.34 usec
TE                  298.0 K
D1              2.00000000 sec
D11             0.03000000 sec
TD0                      1
SFO1          125.8131140 MHz
NUC1                   13C
P0                   3.41 usec
P1                  10.23 usec
PLW1          78.00000000 W
SFO2          500.3020012 MHz
NUC2                   1H
CPDPRG[2           waltz16
PCPD2                80.00 usec
PLW2          21.50000000 W
PLW12          0.49000001 W
PLW13          0.20446000 W

F2 - Processing parameters
SI                   32768
SF            125.8005416 MHz
WDW                     EM
SSB       0
LB                    1.00 Hz
GB        0
PC                    1.40
```

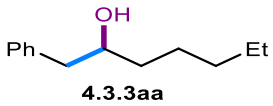
OH
Ph
Et

4.3.3aa

^{1}H NMR

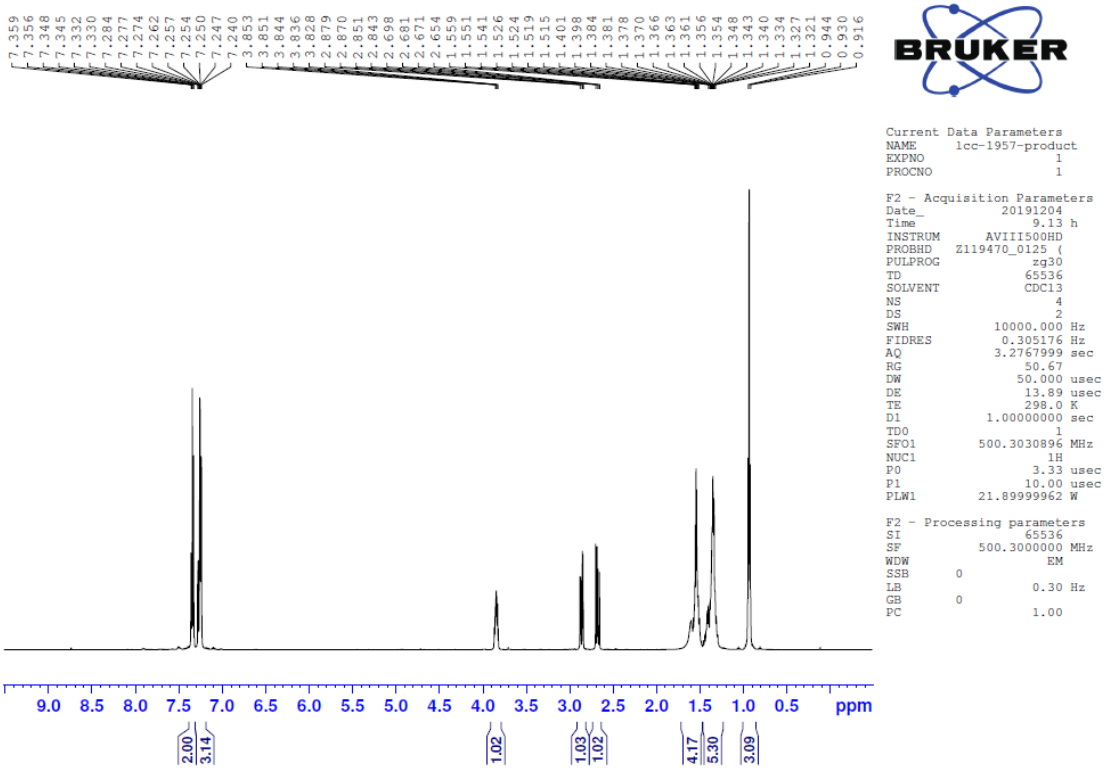
7.359
7.356
7.348
7.345
7.332
7.330
7.284
7.277
7.274
7.262
7.257
7.254
7.250
7.247
7.240
3.853
3.851
3.844
3.836
3.828
2.879
2.870
2.851
2.843
2.698
2.681
2.671
2.654
1.559
1.551
1.541
1.526
1.524
1.519
1.515
1.401
1.398
1.384
1.381
1.378
1.370
1.366
1.363
1.361
1.356
1.354
1.348
1.343
1.340
1.334
1.327
1.321
0.944
0.930
0.916
BRUKER
Current Data Parameters
NAME 1cc-1957-product
EXPNO 1
PROCNO 1
F2 - Acquisition Parameters
Date_ 20191204
Time 9.13 h
INSTRUM AVIII500HD
PROBHD Z119470_0125 (
PULPROG zg30
TD 65536
SOLVENT CDCl3
NS 4
DS 2
SWH 10000.000 Hz
FIDRES 0.305176 Hz
AQ 3.2767999 sec
RG 50.67
DW 50.000 usec
DE 13.89 usec
TE 298.0 K
D1 1.00000000 sec
TD0 1
SFO1 500.3030896 MHz
NUC1 1H
P0 3.33 usec
P1 10.00 usec
PLW1 21.89999962 W
F2 - Processing parameters
SI 65536
SF 500.3000000 MHz
WDW EM
SSB 0
LB 0.30 Hz
GB 0
PC 1.00
9.0 8.5 8.0 7.5 7.0 6.5 6.0 5.5 5.0 4.5 4.0 3.5 3.0 2.5 2.0 1.5 1.0 0.5 ppm
2.00
3.14
1.02
1.03
1.02
4.17
5.30
3.09

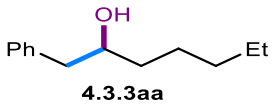

4.3.3aa

^{13}C NMR

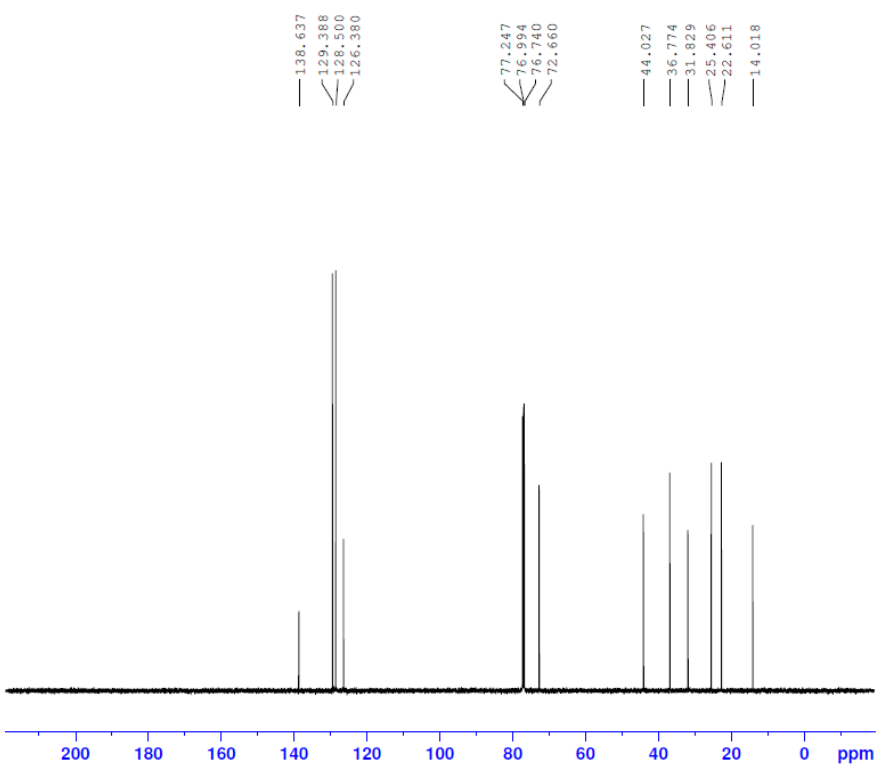


```
Current Data Parameters
NAME      1cc-1957-product
EXPNO                    2
PROCNO                   1

F2 - Acquisition Parameters
Date_           20191204
Time                9.21 h
INSTRUM       AVIII500HD
PROBHD    Z119470_0125 (
PULPROG          zgpg30
TD                65536
SOLVENT           CDCl3
NS                  128
DS                    4
SWH           30000.000 Hz
FIDRES            0.915527 Hz
AQ                1.0922667 sec
RG                  192.72
DW                  16.667 usec
DE                  20.34 usec
TE                 298.0 K
D1              2.00000000 sec
D11             0.03000000 sec
TD0                   1
SFO1          125.8131140 MHz
NUC1                 13C
P0                  3.41 usec
P1                 10.23 usec
PLW1          78.00000000 W
SFO2          500.3020012 MHz
NUC2                 1H
CPDPRG[2          waltz16
PCPD2               80.00 usec
PLW2          21.50000000 W
PLW12          0.49000001 W
PLW13          0.20446000 W

F2 - Processing parameters
SI                  32768
SF            125.8005425 MHz
WDW                    EM
SSB       0
LB                  1.00 Hz
GB        0
PC                  1.40
```

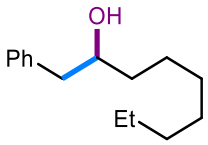
OH
Ph
Et

4.3.3ab

^{1}H NMR

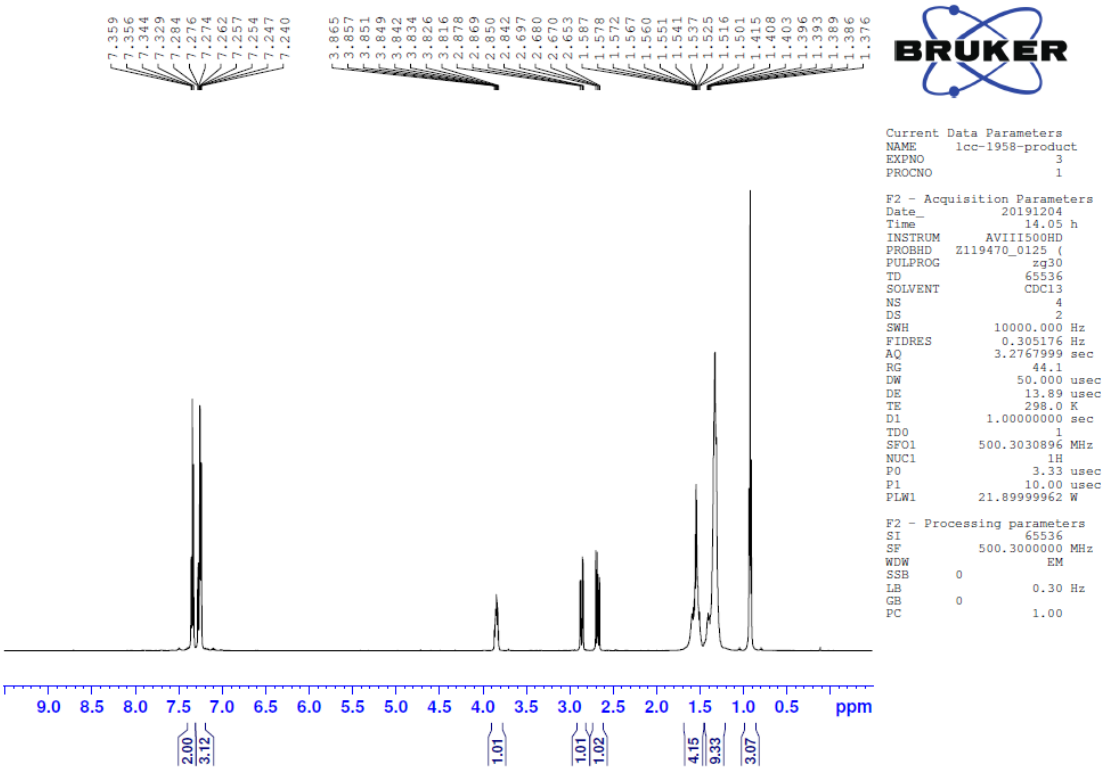
7.359
7.356
7.344
7.329
7.284
7.276
7.274
7.262
7.257
7.254
7.247
7.240
3.865
3.857
3.851
3.849
3.842
3.834
3.826
3.816
2.878
2.869
2.850
2.842
2.697
2.680
2.670
2.653
1.587
1.578
1.572
1.567
1.560
1.551
1.541
1.537
1.525
1.516
1.501
1.415
1.408
1.403
1.396
1.393
1.389
1.386
1.376
BRUKER
Current Data Parameters
NAME lcc-1958-product
EXPNO 3
PROCNO 1
F2 - Acquisition Parameters
Date_ 20191204
Time 14.05 h
INSTRUM AVIII500HD
PROBHD Z119470_0125 (
PULPROG zg30
TD 65536
SOLVENT CDCl3
NS 4
DS 2
SWH 10000.000 Hz
FIDRES 0.305176 Hz
AQ 3.2767999 sec
RG 44.1
DW 50.000 usec
DE 13.89 usec
TE 298.0 K
D1 1.00000000 sec
TD0 1
SFO1 500.3030896 MHz
NUC1 1H
P0 3.33 usec
P1 10.00 usec
PLW1 21.89999962 W
F2 - Processing parameters
SI 65536
SF 500.3000000 MHz
WDW EM
SSB 0
LB 0.30 Hz
GB 0
PC 1.00
9.0 8.5 8.0 7.5 7.0 6.5 6.0 5.5 5.0 4.5 4.0 3.5 3.0 2.5 2.0 1.5 1.0 0.5 ppm
2.00
3.12
1.01
1.01
1.02
4.15
9.33
3.07

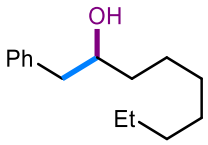

4.3.3ab

^{13}C NMR

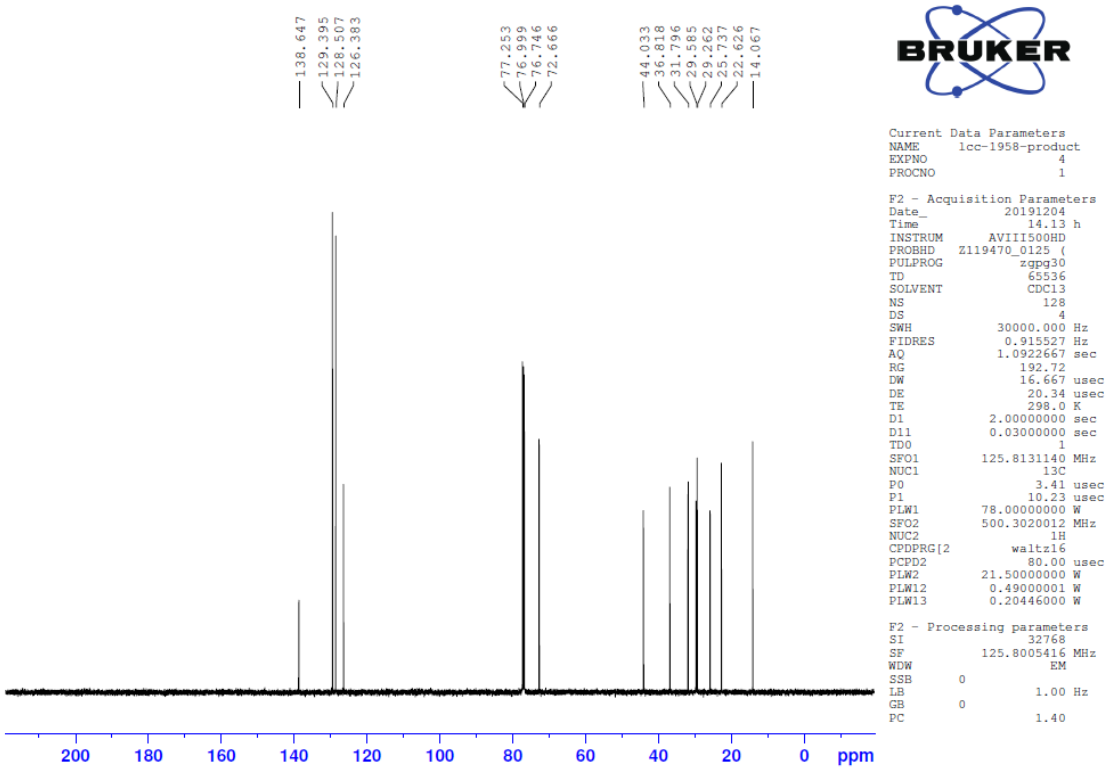


```
Current Data Parameters
NAME      1cc-1958-product
EXPNO                    4
PROCNO                   1

F2 - Acquisition Parameters
Date_           20191204
Time              14.13 h
INSTRUM       AVIII500HD
PROBHD    Z119470_0125 (
PULPROG          zgpg30
TD                65536
SOLVENT           CDCl3
NS                  128
DS                    4
SWH           30000.000 Hz
FIDRES            0.915527 Hz
AQ              1.0922667 sec
RG                192.72
DW                16.667 usec
DE                20.34 usec
TE                298.0 K
D1              2.00000000 sec
D11             0.03000000 sec
TD0                   1
SFO1          125.8131140 MHz
NUC1                 13C
P0                  3.41 usec
P1                 10.23 usec
PLW1          78.00000000 W
SFO2          500.3020012 MHz
NUC2                 1H
CPDPRG[2          waltz16
PCPD2               80.00 usec
PLW2          21.50000000 W
PLW12          0.49000001 W
PLW13          0.20446000 W

F2 - Processing parameters
SI                32768
SF          125.8005416 MHz
WDW                  EM
SSB       0
LB                1.00 Hz
GB        0
PC                1.40
```

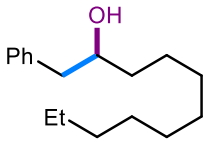
OH
Ph
Et

4.3.3ac

^{1}H NMR

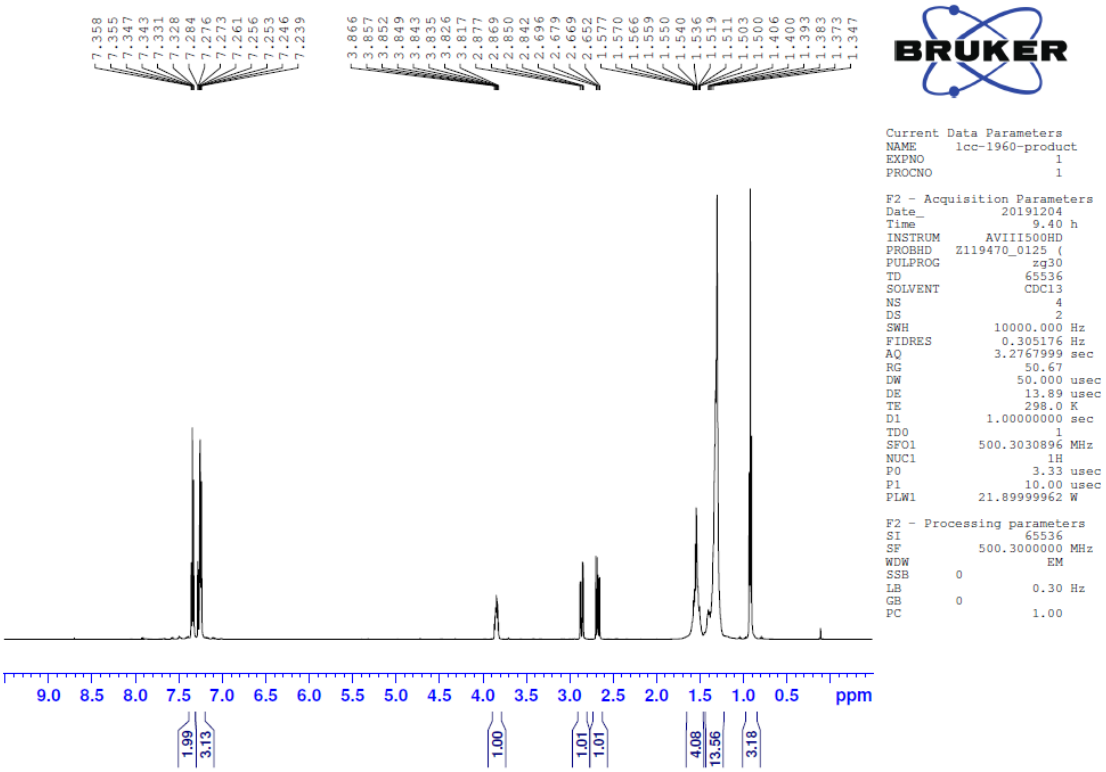
7.358
7.355
7.347
7.343
7.331
7.328
7.284
7.276
7.273
7.261
7.256
7.253
7.246
7.239
3.866
3.857
3.852
3.849
3.843
3.835
3.826
3.817
2.877
2.869
2.850
2.842
2.696
2.679
2.669
2.652
1.577
1.570
1.566
1.559
1.550
1.540
1.536
1.519
1.511
1.503
1.500
1.406
1.400
1.393
1.383
1.373
1.347
BRUKER
Current Data Parameters
NAME lcc-1960-product
EXPNO 1
PROCNO 1
F2 - Acquisition Parameters
Date_ 20191204
Time 9.40 h
INSTRUM AVIII500HD
PROBHD Z119470_0125 (
PULPROG zg30
TD 65536
SOLVENT CDCl3
NS 4
DS 2
SWH 10000.000 Hz
FIDRES 0.305176 Hz
AQ 3.2767999 sec
RG 50.67
DW 50.000 usec
DE 13.89 usec
TE 298.0 K
D1 1.00000000 sec
TD0 1
SFO1 500.3030896 MHz
NUC1 1H
P0 3.33 usec
P1 10.00 usec
PLW1 21.89999962 W
F2 - Processing parameters
SI 65536
SF 500.3000000 MHz
WDW EM
SSB 0
LB 0.30 Hz
GB 0
PC 1.00
9.0 8.5 8.0 7.5 7.0 6.5 6.0 5.5 5.0 4.5 4.0 3.5 3.0 2.5 2.0 1.5 1.0 0.5 ppm
1.99
3.13
1.00
1.01
1.01
4.08
13.56
3.18

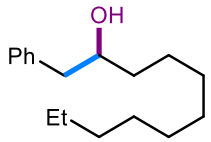

4.3.3ac

^{13}C NMR

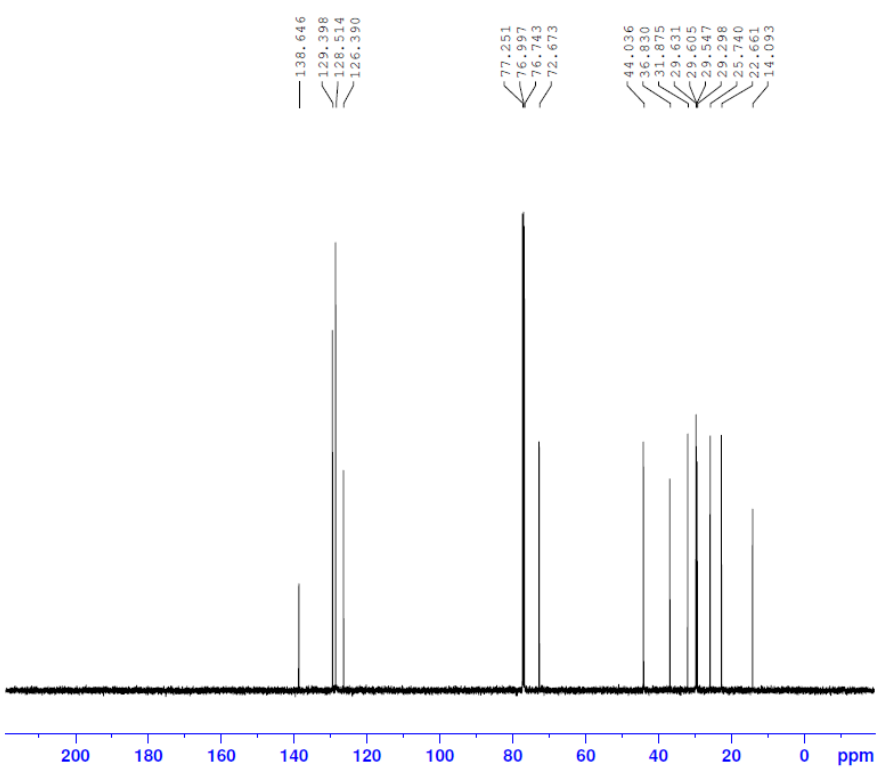

BRUKER

```
Current Data Parameters
NAME      1cc-1960-product
EXPNO                    2
PROCNO                   1

F2 - Acquisition Parameters
Date_           20191204
Time                9.47 h
INSTRUM       AVIII500HD
PROBHD    Z119470_0125 (
PULPROG           zgpg30
TD                65536
SOLVENT           CDCl3
NS                  128
DS                    4
SWH           30000.000 Hz
FIDRES            0.915527 Hz
AQ              1.0922667 sec
RG                192.72
DW                16.667 usec
DE                20.34 usec
TE                298.0 K
D1              2.00000000 sec
D11             0.03000000 sec
TD0                   1
SFO1          125.8131140 MHz
NUC1                 13C
P0                  3.41 usec
P1                 10.23 usec
PLW1          78.00000000 W
SFO2          500.3020012 MHz
NUC2                 1H
CPDPRG[2          waltz16
PCPD2               80.00 usec
PLW2          21.50000000 W
PLW12          0.49000001 W
PLW13          0.20446000 W

F2 - Processing parameters
SI                  32768
SF            125.8005407 MHz
WDW                   EM
SSB       0
LB                  1.00 Hz
GB        0
PC                  1.40
```

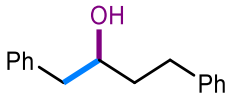
OH
Ph
Ph

4.3.3ad

^{1}H NMR

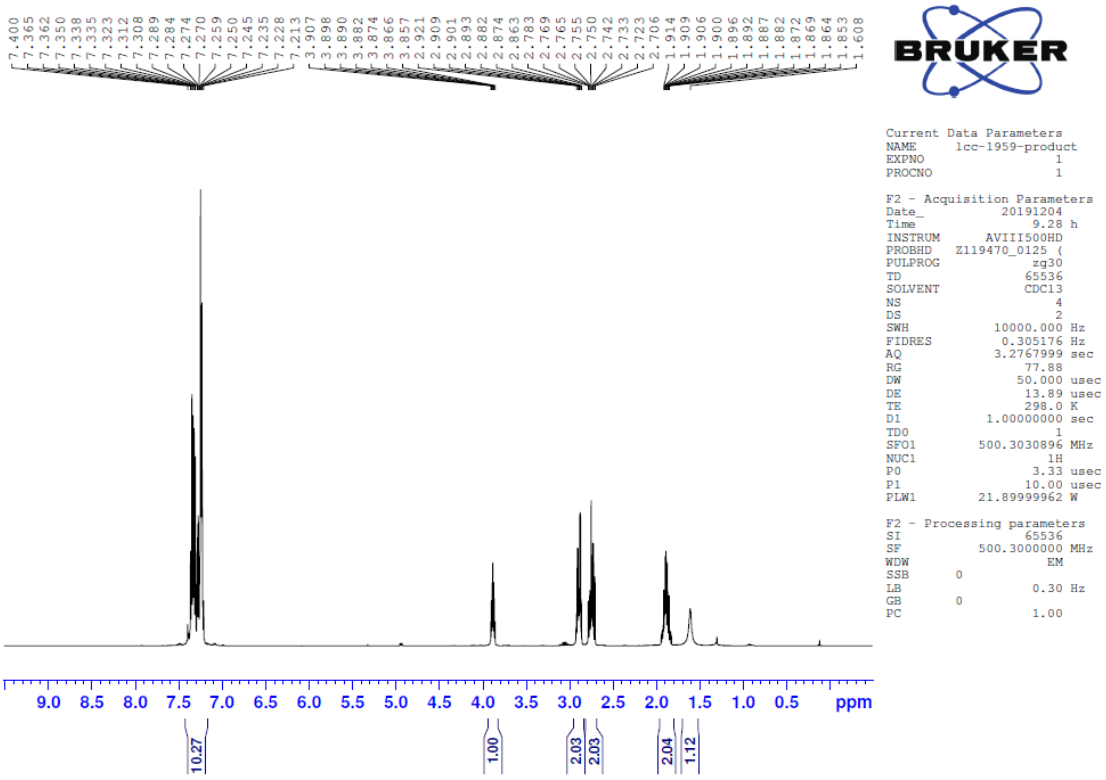
7.400
7.365
7.362
7.350
7.338
7.335
7.323
7.312
7.308
7.289
7.284
7.274
7.270
7.259
7.250
7.245
7.235
7.228
7.213
3.907
3.898
3.890
3.882
3.874
3.866
3.857
2.921
2.909
2.901
2.893
2.882
2.874
2.863
2.783
2.769
2.765
2.755
2.750
2.742
2.733
2.723
2.706
1.914
1.909
1.906
1.900
1.896
1.892
1.887
1.882
1.872
1.869
1.864
1.853
1.608
BRUKER
Current Data Parameters
NAME 1cc-1959-product
EXPNO 1
PROCNO 1
F2 - Acquisition Parameters
Date_ 20191204
Time 9.28 h
INSTRUM AVIII500HD
PROBHD Z119470_0125 (
PULPROG zg30
TD 65536
SOLVENT CDCl3
NS 4
DS 2
SWH 10000.000 Hz
FIDRES 0.305176 Hz
AQ 3.2767999 sec
RG 77.88
DW 50.000 usec
DE 13.89 usec
TE 298.0 K
D1 1.00000000 sec
TD0 1
SFO1 500.3030896 MHz
NUC1 1H
P0 3.33 usec
P1 10.00 usec
PLW1 21.89999962 W
F2 - Processing parameters
SI 65536
SF 500.3000000 MHz
WDW EM
SSB 0
LB 0.30 Hz
GB 0
PC 1.00
9.0 8.5 8.0 7.5 7.0 6.5 6.0 5.5 5.0 4.5 4.0 3.5 3.0 2.5 2.0 1.5 1.0 0.5 ppm
10.27
1.00
2.03
2.03
2.04
1.12

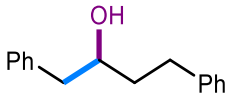

4.3.3ad

^{13}C NMR

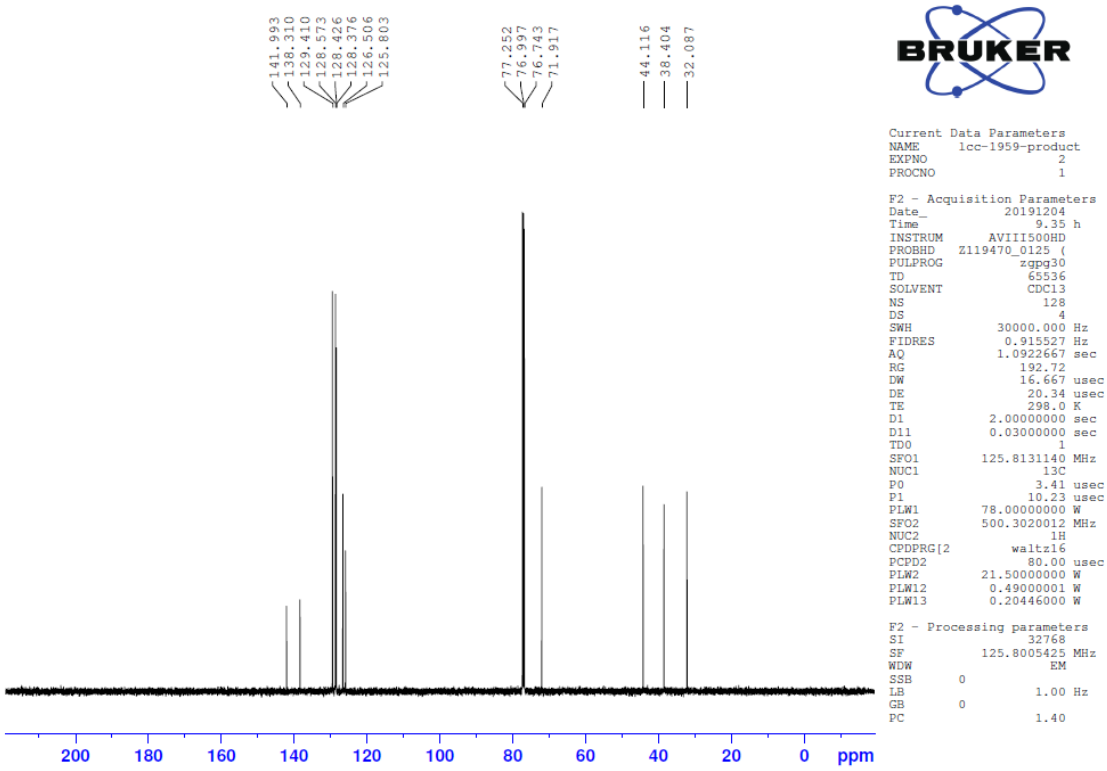


```
Current Data Parameters
NAME      1cc-1959-product
EXPNO                    2
PROCNO                   1

F2 - Acquisition Parameters
Date_           20191204
Time                9.35 h
INSTRUM       AVIII500HD
PROBHD    Z119470_0125 (
PULPROG          zgpg30
TD                65536
SOLVENT           CDCl3
NS                  128
DS                    4
SWH           30000.000 Hz
FIDRES         0.915527 Hz
AQ             1.0922667 sec
RG                192.72
DW                16.667 usec
DE                20.34 usec
TE                298.0 K
D1             2.00000000 sec
D11            0.03000000 sec
TD0                   1
SFO1        125.8131140 MHz
NUC1                 13C
P0                 3.41 usec
P1                10.23 usec
PLW1        78.00000000 W
SFO2        500.3020012 MHz
NUC2                 1H
CPDPRG[2         waltz16
PCPD2             80.00 usec
PLW2        21.50000000 W
PLW12        0.49000001 W
PLW13        0.20446000 W

F2 - Processing parameters
SI                32768
SF          125.8005425 MHz
WDW                  EM
SSB       0
LB                1.00 Hz
GB        0
PC                1.40
```

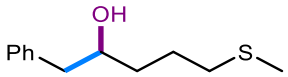
OH
Ph
S

4.3.3ae

^{1}H NMR

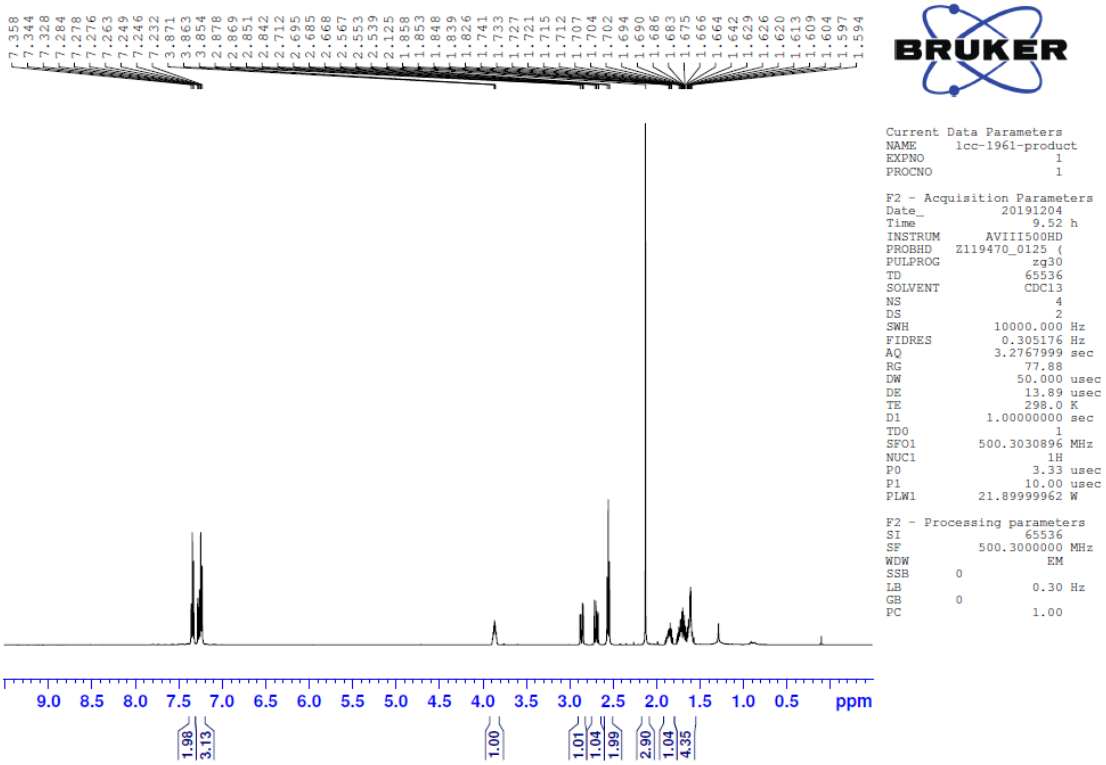
7.358
7.344
7.328
7.284
7.278
7.276
7.263
7.249
7.246
7.232
3.871
3.863
3.854
2.878
2.869
2.851
2.842
2.712
2.695
2.685
2.668
2.567
2.553
2.539
2.125
1.858
1.853
1.848
1.839
1.826
1.741
1.733
1.727
1.721
1.715
1.712
1.707
1.704
1.702
1.694
1.690
1.686
1.683
1.675
1.666
1.664
1.642
1.629
1.626
1.620
1.613
1.609
1.604
1.597
1.594
BRUKER
Current Data Parameters
NAME lcc-1961-product
EXPNO 1
PROCNO 1
F2 - Acquisition Parameters
Date_ 20191204
Time 9.52 h
INSTRUM AVIII500HD
PROBHD Z119470_0125 (
PULPROG zg30
TD 65536
SOLVENT CDCl3
NS 4
DS 2
SWH 10000.000 Hz
FIDRES 0.305176 Hz
AQ 3.2767999 sec
RG 77.88
DW 50.000 usec
DE 13.89 usec
TE 298.0 K
D1 1.00000000 sec
TD0 1
SFO1 500.3030896 MHz
NUC1 1H
P0 3.33 usec
P1 10.00 usec
PLW1 21.89999962 W
F2 - Processing parameters
SI 65536
SF 500.3000000 MHz
WDW EM
SSB 0
LB 0.30 Hz
GB 0
PC 1.00
9.0 8.5 8.0 7.5 7.0 6.5 6.0 5.5 5.0 4.5 4.0 3.5 3.0 2.5 2.0 1.5 1.0 0.5 ppm
1.98
3.13
1.00
1.01
1.04
1.99
2.90
1.04
4.35

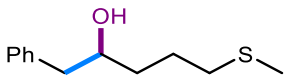

4.3.3ae

^{13}C NMR

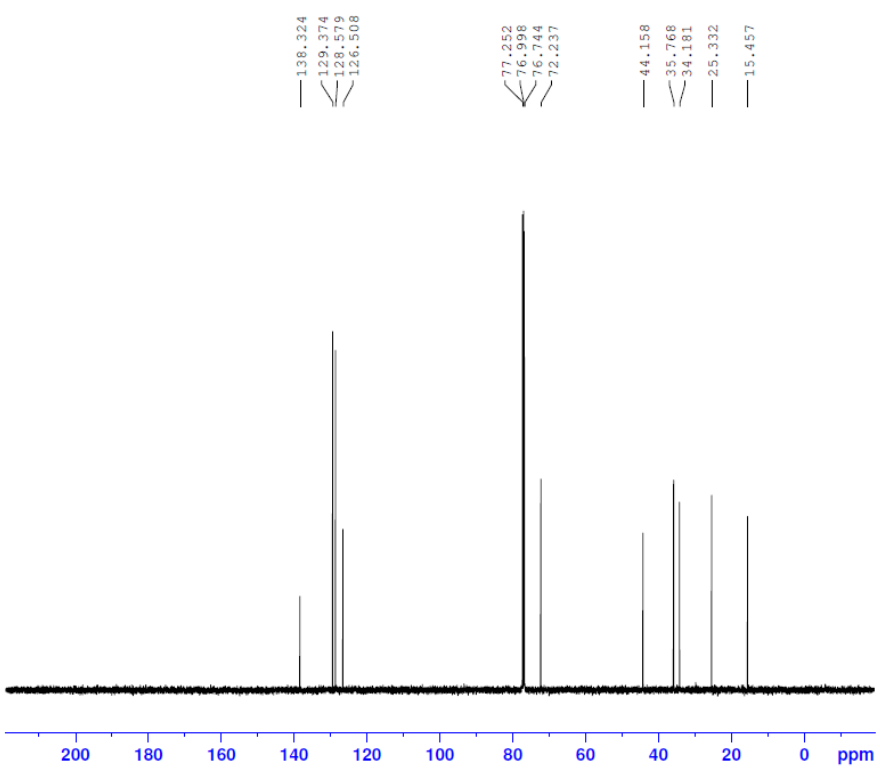


```
Current Data Parameters
NAME      1cc-1961-product
EXPNO                    2
PROCNO                   1

F2 - Acquisition Parameters
Date_             20191204
Time                 9.59 h
INSTRUM       AVIII500HD
PROBHD    Z119470_0125 (
PULPROG              zgpg30
TD                    65536
SOLVENT               CDCl3
NS                      128
DS                        4
SWH               30000.000 Hz
FIDRES                0.915527 Hz
AQ                1.0922667 sec
RG                    192.72
DW                   16.667 usec
DE                    20.34 usec
TE                    298.0 K
D1                2.00000000 sec
D11               0.03000000 sec
TD0                       1
SFO1            125.8131140 MHz
NUC1                    13C
P0                    3.41 usec
P1                   10.23 usec
PLW1           78.00000000 W
SFO2           500.3020012 MHz
NUC2                    1H
CPDPRG[2             waltz16
PCPD2                80.00 usec
PLW2           21.50000000 W
PLW12           0.49000001 W
PLW13           0.20446000 W

F2 - Processing parameters
SI                    32768
SF              125.8005416 MHz
WDW                      EM
SSB          0
LB                    1.00 Hz
GB           0
PC                    1.40
```

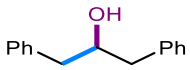

4.3.3af

^{1}H NMR

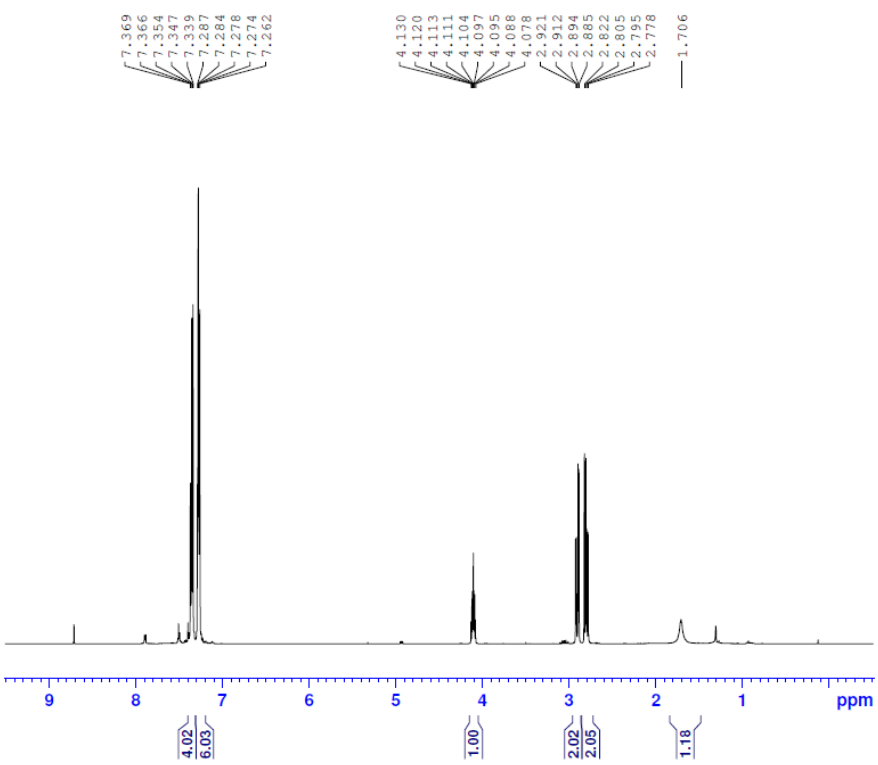


```
Current Data Parameters
NAME      1cc-1964-product
EXPNO                    1
PROCNO                   1

F2 - Acquisition Parameters
Date_             20191213
Time                 6.55 h
INSTRUM        AVIII500HD
PROBHD    Z119470_0125 (
PULPROG              zg30
TD                  65536
SOLVENT             CDCl3
NS                      4
DS                      2
SWH             10000.000 Hz
FIDRES              0.305176 Hz
AQ                3.2767999 sec
RG                   71.03
DW                  50.000 usec
DE                   13.89 usec
TE                  298.0 K
D1              1.00000000 sec
TD0                     1
SFO1           500.3030896 MHz
NUC1                   1H
P0                   3.33 usec
P1                  10.00 usec
PLW1           21.89999962 W

F2 - Processing parameters
SI                  65536
SF             500.3000000 MHz
WDW                    EM
SSB       0
LB                   0.30 Hz
GB        0
PC                   1.00
```

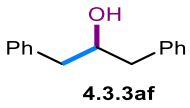

4.3.3af

^{13}C NMR

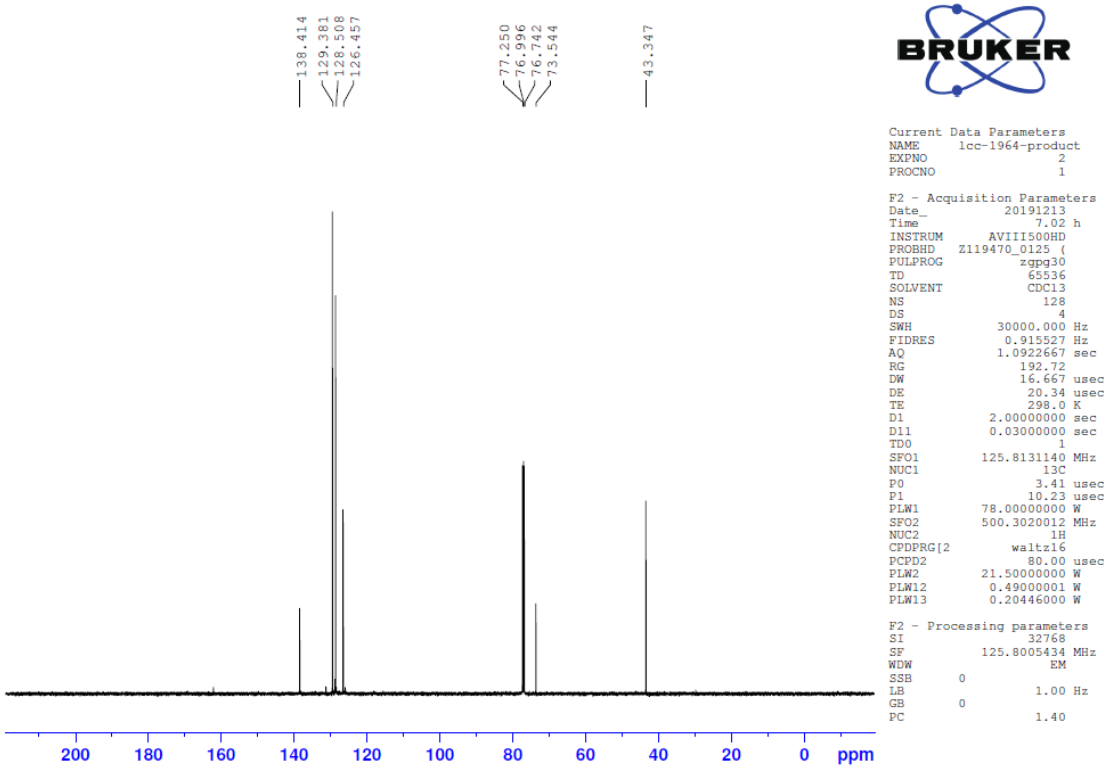


```
Current Data Parameters
NAME      1cc-1964-product
EXPNO                    2
PROCNO                   1

F2 - Acquisition Parameters
Date_             20191213
Time                 7.02 h
INSTRUM       AVIII500HD
PROBHD    Z119470_0125 (
PULPROG           zgpg30
TD                65536
SOLVENT           CDCl3
NS                  128
DS                    4
SWH           30000.000 Hz
FIDRES            0.915527 Hz
AQ                1.0922667 sec
RG                  192.72
DW                 16.667 usec
DE                  20.34 usec
TE                 298.0 K
D1             2.00000000 sec
D11            0.03000000 sec
TD0                   1
SFO1          125.8131140 MHz
NUC1                 13C
P0                  3.41 usec
P1                 10.23 usec
PLW1          78.00000000 W
SFO2          500.3020012 MHz
NUC2                  1H
CPDPRG[2          waltz16
PCPD2               80.00 usec
PLW2          21.50000000 W
PLW12          0.49000001 W
PLW13          0.20446000 W

F2 - Processing parameters
SI                  32768
SF            125.8005434 MHz
WDW                    EM
SSB       0
LB                  1.00 Hz
GB        0
PC                  1.40
```

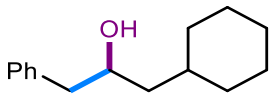
OH
Ph

4.3.3ag

^{1}H NMR

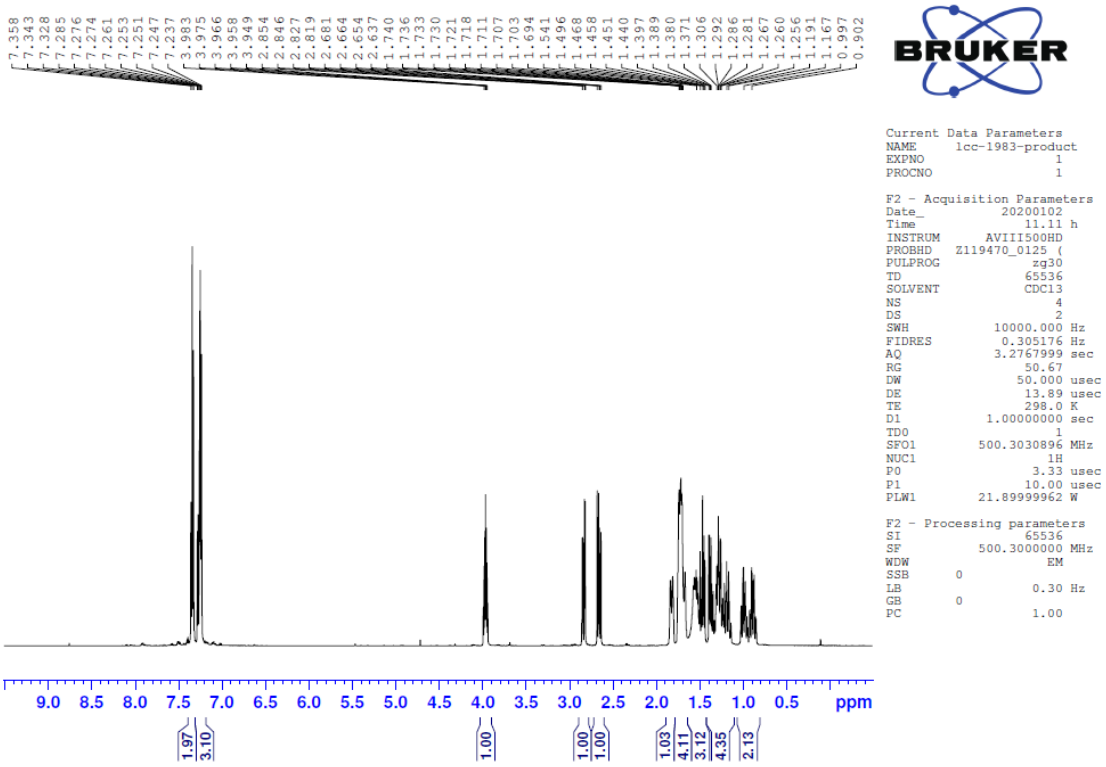
7.358
7.343
7.328
7.285
7.276
7.274
7.261
7.253
7.251
7.247
7.237
3.983
3.975
3.966
3.958
3.949
2.854
2.846
2.827
2.819
2.681
2.664
2.654
2.637
1.740
1.736
1.733
1.730
1.721
1.718
1.711
1.707
1.703
1.694
1.541
1.496
1.468
1.458
1.451
1.440
1.397
1.389
1.380
1.371
1.306
1.292
1.286
1.281
1.267
1.260
1.256
1.191
1.167
0.997
0.902
BRUKER
Current Data Parameters
NAME 1cc-1983-product
EXPNO 1
PROCNO 1
F2 - Acquisition Parameters
Date_ 20200102
Time 11.11 h
INSTRUM AVIII500HD
PROBHD Z119470_0125 (
PULPROG zg30
TD 65536
SOLVENT CDC13
NS 4
DS 2
SWH 10000.000 Hz
FIDRES 0.305176 Hz
AQ 3.2767999 sec
RG 50.67
DW 50.000 usec
DE 13.89 usec
TE 298.0 K
D1 1.00000000 sec
TD0 1
SFO1 500.3030896 MHz
NUC1 1H
P0 3.33 usec
P1 10.00 usec
PLW1 21.89999962 W
F2 - Processing parameters
SI 65536
SF 500.3000000 MHz
WDW EM
SSB 0
LB 0.30 Hz
GB 0
PC 1.00
9.0 8.5 8.0 7.5 7.0 6.5 6.0 5.5 5.0 4.5 4.0 3.5 3.0 2.5 2.0 1.5 1.0 0.5 ppm
1.97
3.10
1.00
1.00
1.00
1.03
4.11
3.12
4.35
2.13

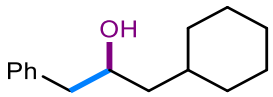

4.3.3ag

^{13}C NMR

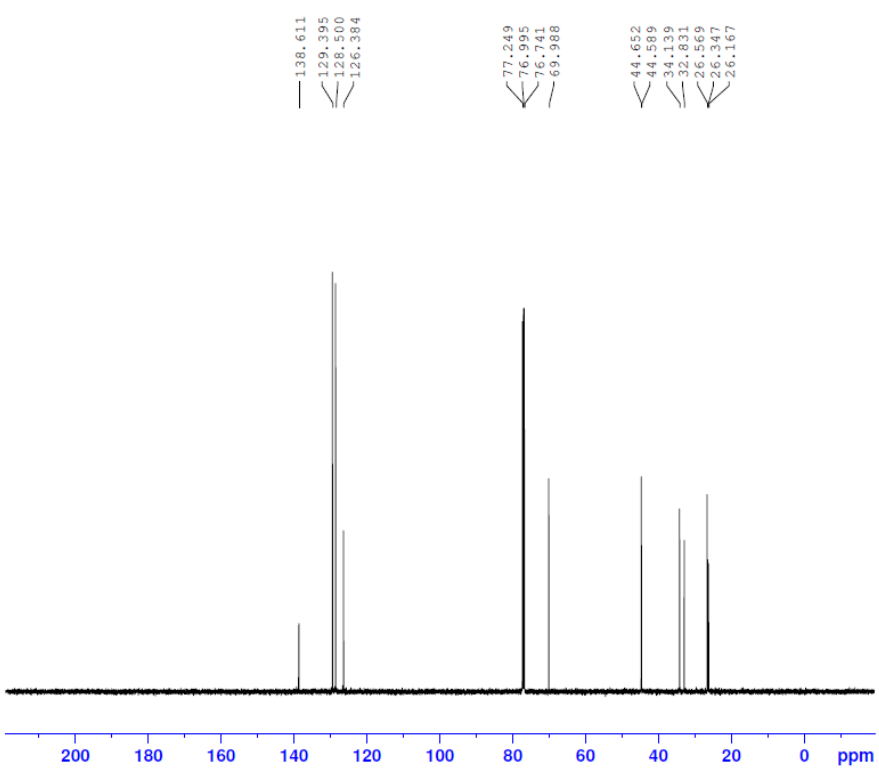


```
Current Data Parameters
NAME      1cc-1983-product
EXPNO                    2
PROCNO                   1

F2 - Acquisition Parameters
Date_           20200102
Time              11.19 h
INSTRUM       AVIII500HD
PROBHD    Z119470_0125 (
PULPROG          zgpg30
TD                65536
SOLVENT            CDCl3
NS                   128
DS                     4
SWH            30000.000 Hz
FIDRES             0.915527 Hz
AQ                 1.0922667 sec
RG                   192.72
DW                  16.667 usec
DE                  20.34 usec
TE                  298.0 K
D1                 2.00000000 sec
D11                0.03000000 sec
TD0                      1
SFO1          125.8131140 MHz
NUC1                   13C
P0                   3.41 usec
P1                  10.23 usec
PLW1          78.00000000 W
SFO2          500.3020012 MHz
NUC2                   1H
CPDPRG[2           waltz16
PCPD2               80.00 usec
PLW2          21.50000000 W
PLW12          0.57543999 W
PLW13          0.20446000 W

F2 - Processing parameters
SI                   32768
SF            125.8005425 MHz
WDW                    EM
SSB       0
LB                  1.00 Hz
GB        0
PC                  1.40
```

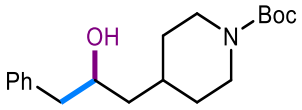

4.3.3ah

^{1}H NMR

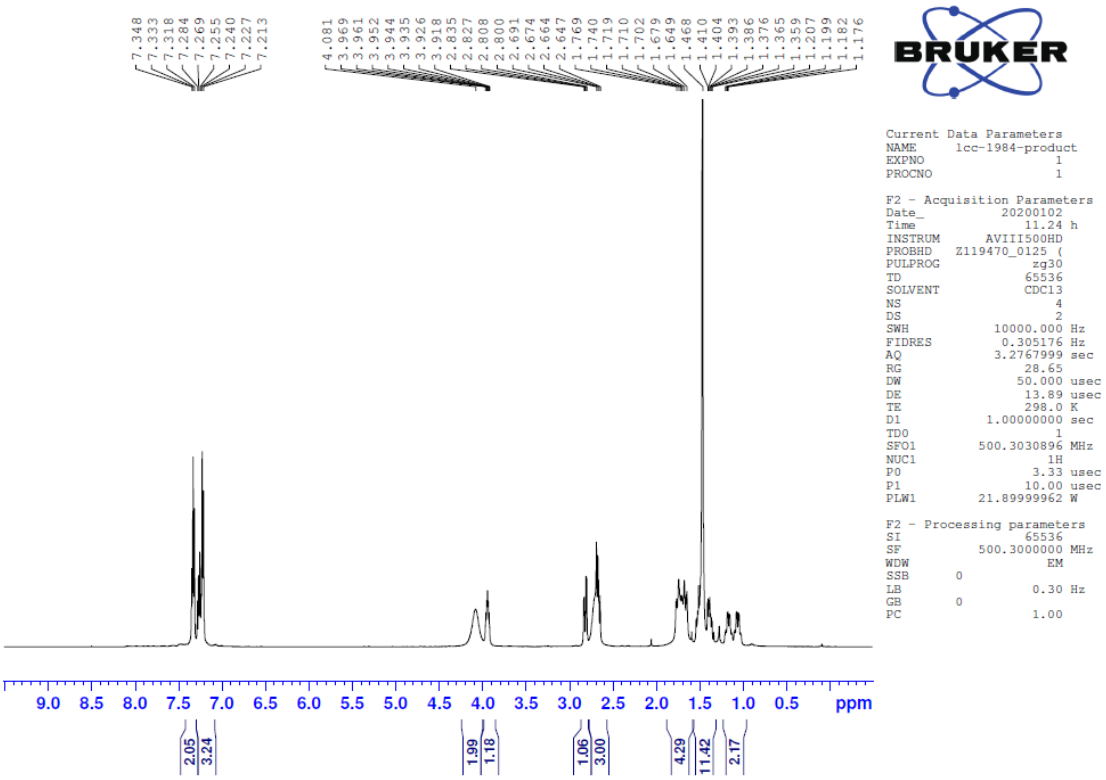


```
Current Data Parameters
NAME      1cc-1984-product
EXPNO                    1
PROCNO                   1

F2 - Acquisition Parameters
Date_             20200102
Time                11.24 h
INSTRUM       AVIII500HD
PROBHD    Z119470_0125 (
PULPROG              zg30
TD                  65536
SOLVENT             CDCl3
NS                      4
DS                      2
SWH             10000.000 Hz
FIDRES              0.305176 Hz
AQ                3.2767999 sec
RG                    28.65
DW                  50.000 usec
DE                  13.89 usec
TE                  298.0 K
D1              1.00000000 sec
TD0                     1
SFO1            500.3030896 MHz
NUC1                   1H
P0                  3.33 usec
P1                 10.00 usec
PLW1           21.89999962 W

F2 - Processing parameters
SI                  65536
SF              500.3000000 MHz
WDW                    EM
SSB       0
LB                  0.30 Hz
GB        0
PC                  1.00
```

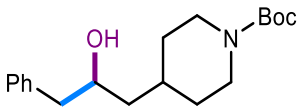

4.3.3ah

^{13}C NMR

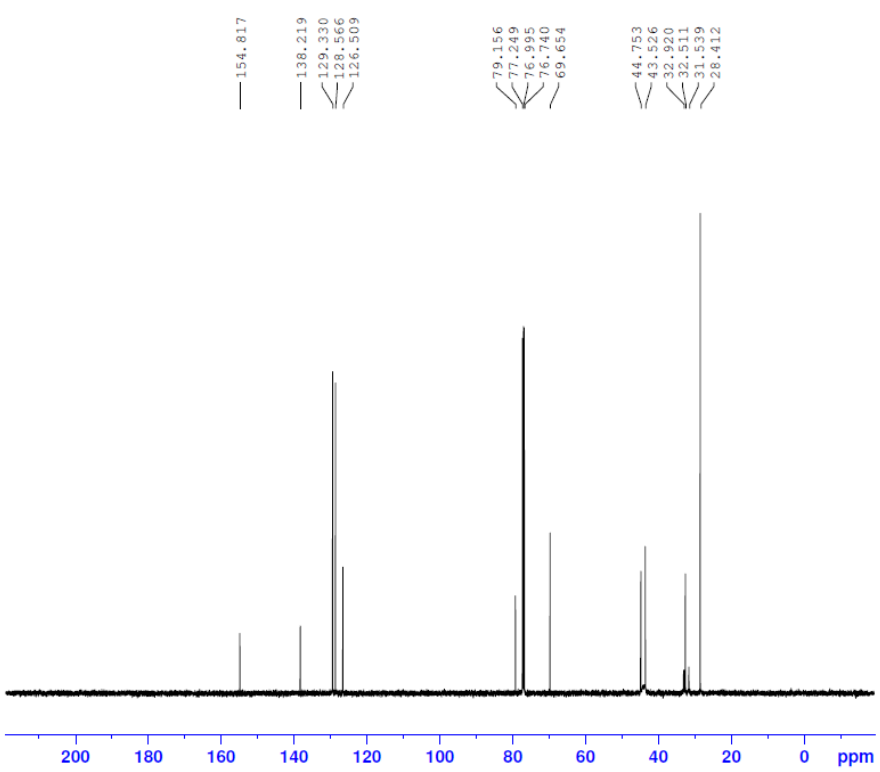

BRUKER

```
Current Data Parameters
NAME      lcc-1984-product
EXPNO                    2
PROCNO                   1

F2 - Acquisition Parameters
Date_           20200102
Time              11.31 h
INSTRUM       AVIII500HD
PROBHD    Z119470_0125 (
PULPROG           zgpg30
TD                65536
SOLVENT           CDCl3
NS                  128
DS                    4
SWH           30000.000 Hz
FIDRES        0.915527 Hz
AQ            1.0922667 sec
RG               192.72
DW               16.667 usec
DE               20.34 usec
TE               298.0 K
D1            2.00000000 sec
D11           0.03000000 sec
TD0                   1
SFO1        125.8131140 MHz
NUC1                13C
P0                3.41 usec
P1               10.23 usec
PLW1        78.00000000 W
SFO2        500.3020012 MHz
NUC2                1H
CPDPRG[2         waltz16
PCPD2            80.00 usec
PLW2        21.50000000 W
PLW12        0.57543999 W
PLW13        0.20446000 W

F2 - Processing parameters
SI                32768
SF          125.8005443 MHz
WDW                EM
SSB       0
LB               1.00 Hz
GB        0
PC               1.40
```

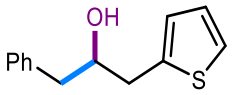

4.3.3ai

^{1}H NMR

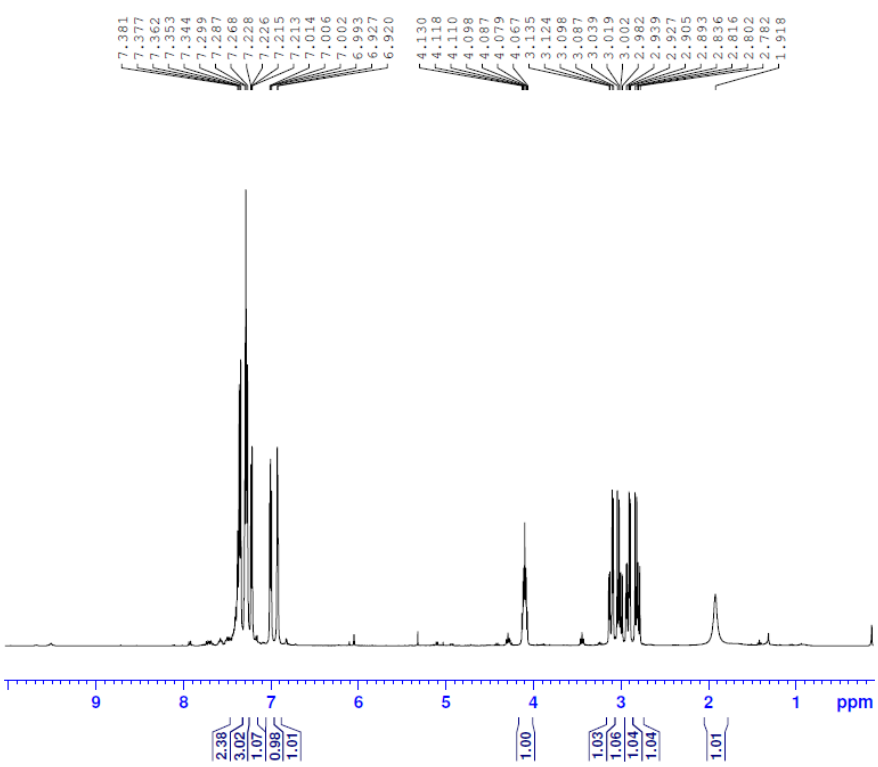


```
Current Data Parameters
NAME      1cc-2113-product
EXPNO                    1
PROCNO                   1

F2 - Acquisition Parameters
Date_             20200229
Time                17.59 h
INSTRUM               B400
PROBHD    Z116098_0217 (
PULPROG               zg30
TD                   65536
SOLVENT              CDCl3
NS                       8
DS                       1
SWH               8012.820 Hz
FIDRES            0.244532 Hz
AQ                4.0894465 sec
RG                   51.41
DW                  62.400 usec
DE                  17.84 usec
TE                  298.0 K
D1              1.00000000 sec
TD0                      1
SFO1           400.3524723 MHz
NUC1                    1H
P0                   3.19 usec
P1                   9.58 usec
PLW1           17.00000000 W

F2 - Processing parameters
SI                   65536
SF            400.3500000 MHz
WDW                     EM
SSB       0
LB                   0.30 Hz
GB        0
PC                   1.00
```

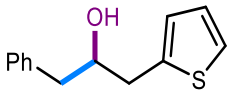

4.3.3ai

^{13}C NMR

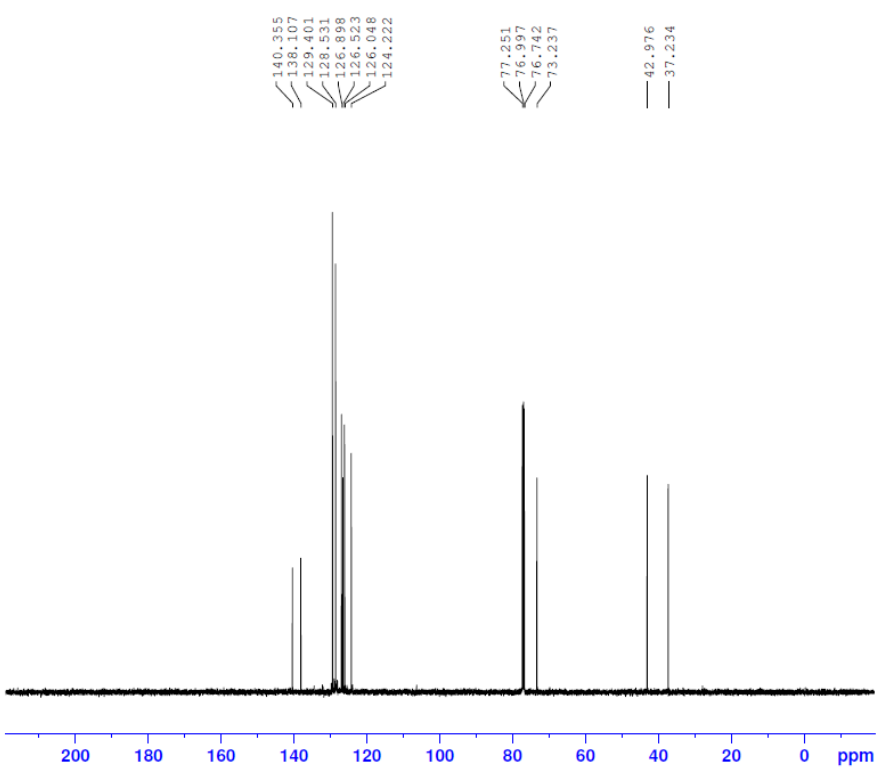


```
Current Data Parameters
NAME      1cc-2113-product
EXPNO                    2
PROCNO                   1

F2 - Acquisition Parameters
Date_           20200229
Time              23.04 h
INSTRUM       AVIII500HD
PROBHD    Z119470_0125 (
PULPROG           zgpg30
TD                65536
SOLVENT           CDCl3
NS                  128
DS                    4
SWH           30000.000 Hz
FIDRES         0.915527 Hz
AQ             1.0922667 sec
RG                192.72
DW                16.667 usec
DE                20.34 usec
TE                298.0 K
D1             2.00000000 sec
D11            0.03000000 sec
TD0                   1
SFO1         125.8131140 MHz
NUC1                 13C
P0                 3.41 usec
P1                10.23 usec
PLW1         78.00000000 W
SFO2         500.3020012 MHz
NUC2                 1H
CPDPRG[2          waltz16
PCPD2             80.00 usec
PLW2         21.50000000 W
PLW12         0.57543999 W
PLW13         0.20446000 W

F2 - Processing parameters
SI                32768
SF           125.8005453 MHz
WDW                  EM
SSB       0
LB                1.00 Hz
GB        0
PC                1.40
```

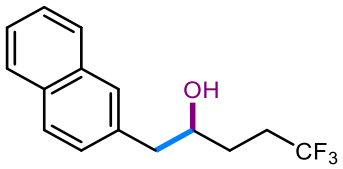
OH
CF3

4.3.3hj

^{1}H NMR

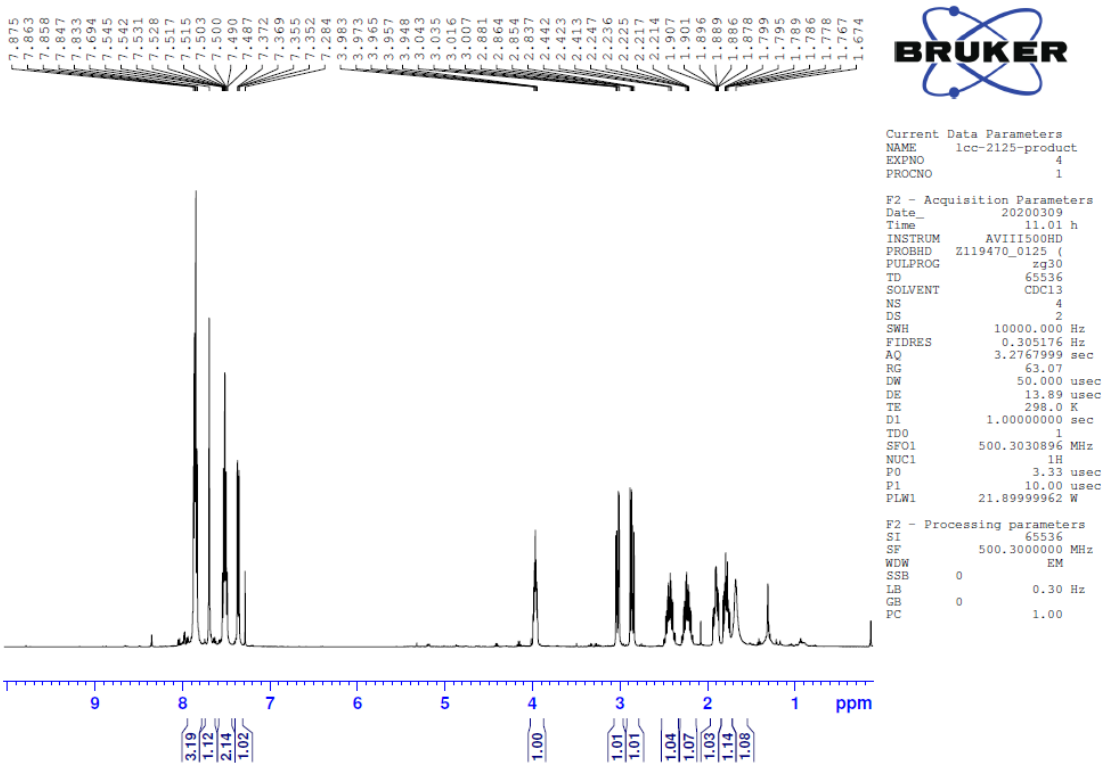
7.875
7.863
7.858
7.847
7.833
7.694
7.545
7.542
7.531
7.528
7.517
7.515
7.503
7.500
7.490
7.487
7.372
7.369
7.355
7.352
7.284
3.983
3.973
3.965
3.957
3.948
3.043
3.035
3.016
3.007
2.881
2.864
2.854
2.837
2.442
2.423
2.413
2.247
2.236
2.225
2.217
2.214
1.907
1.901
1.896
1.889
1.886
1.878
1.799
1.795
1.789
1.786
1.778
1.767
1.674
BRUKER
Current Data Parameters
NAME lcc-2125-product
EXPNO 4
PROCNO 1
F2 - Acquisition Parameters
Date_ 20200309
Time 11.01 h
INSTRUM AVIII500HD
PROBHD Z119470_0125 (
PULPROG zg30
TD 65536
SOLVENT CDCl3
NS 4
DS 2
SWH 10000.000 Hz
FIDRES 0.305176 Hz
AQ 3.2767999 sec
RG 63.07
DW 50.000 usec
DE 13.89 usec
TE 298.0 K
D1 1.00000000 sec
TD0 1
SFO1 500.3030896 MHz
NUC1 1H
P0 3.33 usec
P1 10.00 usec
PLW1 21.89999962 W
F2 - Processing parameters
SI 65536
SF 500.3000000 MHz
WDW EM
SSB 0
LB 0.30 Hz
GB 0
PC 1.00
9
8
7
6
5
4
3
2
1
ppm
3.19
1.12
2.14
1.02
1.00
1.01
1.01
1.04
1.07
1.03
1.14
1.08

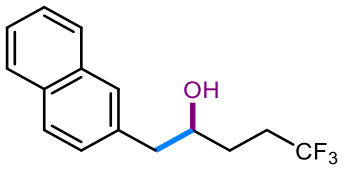

4.3.3hj

^{13}C NMR

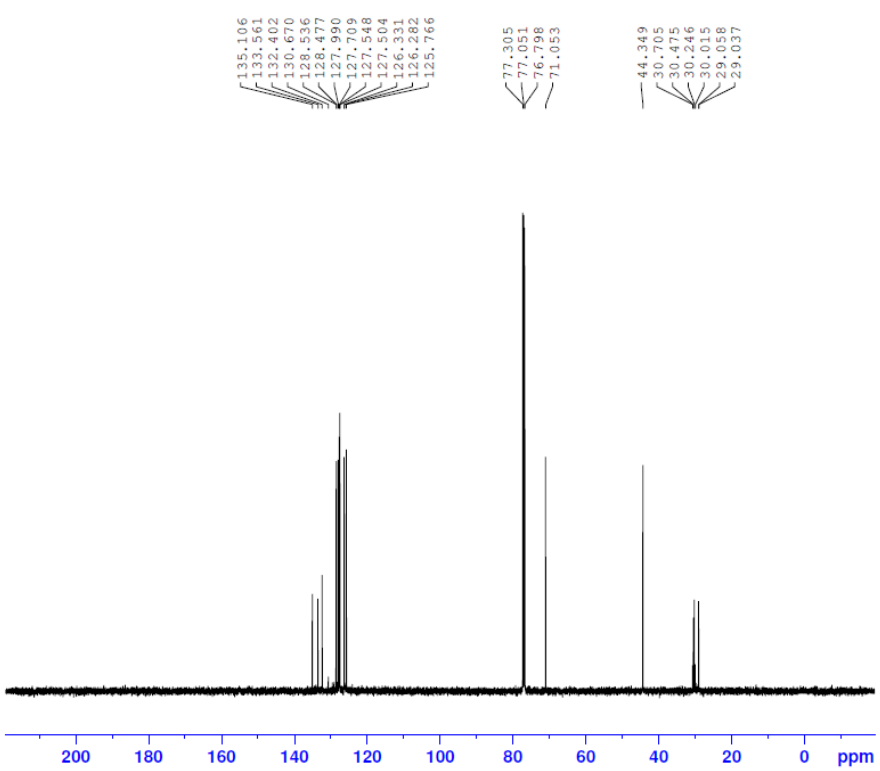


```
Current Data Parameters
NAME      1cc-2125-product
EXPNO                    3
PROCNO                   1

F2 - Acquisition Parameters
Date_           20200309
Time              11.08 h
INSTRUM       AVIII500HD
PROBHD    Z119470_0125 (
PULPROG          zgpg30
TD                65536
SOLVENT           CDCl3
NS                  128
DS                    4
SWH           30000.000 Hz
FIDRES        0.915527 Hz
AQ            1.0922667 sec
RG               192.72
DW               16.667 usec
DE                20.34 usec
TE                298.0 K
D1            2.00000000 sec
D11           0.03000000 sec
TD0                   1
SFO1        125.8131140 MHz
NUC1                 13C
P0                3.41 usec
P1               10.23 usec
PLW1        78.00000000 W
SFO2        500.3020012 MHz
NUC2                 1H
CPDPRG[2         waltz16
PCPD2             80.00 usec
PLW2        21.50000000 W
PLW12        0.57543999 W
PLW13        0.20446000 W

F2 - Processing parameters
SI                32768
SF          125.8005351 MHz
WDW                  EM
SSB       0
LB                1.00 Hz
GB        0
PC                1.40
```

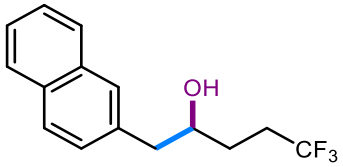

4.3.3hj

^{19}F NMR

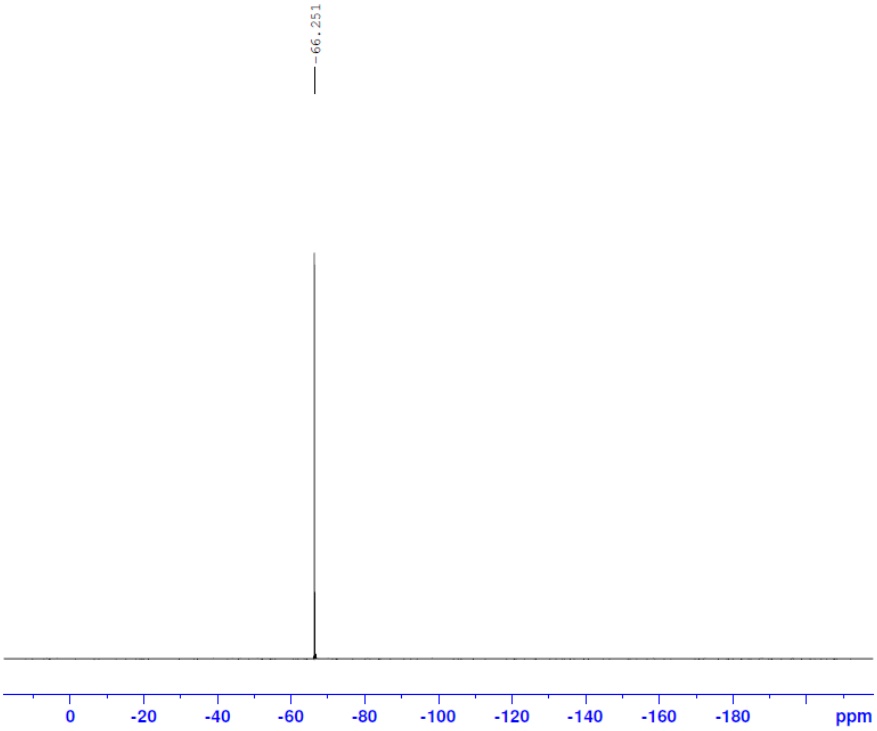


```
Current Data Parameters
NAME      1cc-2017-product
EXPNO                    3
PROCNO                   1

F2 - Acquisition Parameters
Date_           20200119
Time              18.55 h
INSTRUM       AVIII500HD
PROBHD    Z119470_0125 (
PULPROG   zgbsfhiqqn.baseopt
TD                131072
SOLVENT             CDCl3
NS                     16
DS                      4
SWH           111111.109 Hz
FIDRES          1.695421 Hz
AQ              0.5898240 sec
RG                192.72
DW                4.500 usec
DE                35.33 usec
TE                298.0 K
D1             1.00000000 sec
D11            0.03000000 sec
D12            0.00002000 sec
TD0                     1
SFO1         470.7052618 MHz
NUC1                  19F
P1                 15.00 usec
P2                 30.00 usec
PLW1         39.50000000 W
SFO2         500.3025015 MHz
NUC2                  1H
CPDPRG[2          waltz16
PCPD2              80.00 usec
PLW2         21.50000000 W
PLW12         0.57543999 W

F2 - Processing parameters
SI                  65536
SF           470.7523370 MHz
WDW                    EM
SSB       0
LB                  0.30 Hz
GB        0
PC                  1.00
```

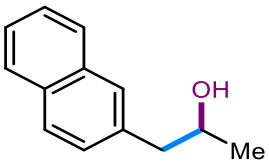

4.3.3hk

^{1}H NMR

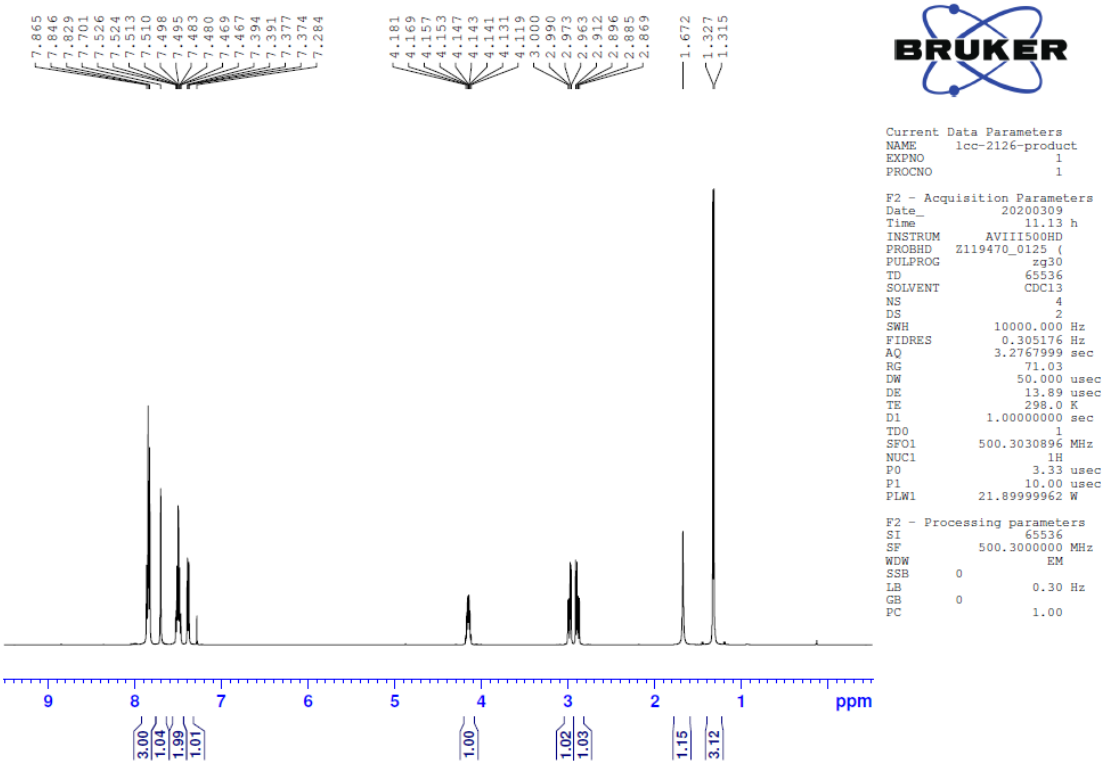

Current Data Parameters
NAME lcc-2126-product
EXPNO 1
PROCNO 1

F2 - Acquisition Parameters
Date_ 20200309
Time 11.13 h
INSTRUM AVIII500HD
PROBHD Z119470_0125 (
PULPROG zg30
TD 65536
SOLVENT CDCl3
NS 4
DS 2
SWH 10000.000 Hz
FIDRES 0.305176 Hz
AQ 3.2767999 sec
RG 71.03
DW 50.000 usec
DE 13.89 usec
TE 298.0 K
D1 1.00000000 sec
TD0 1
SFO1 500.3030896 MHz
NUC1 1H
P0 3.33 usec
P1 10.00 usec
PLW1 21.89999962 W

F2 - Processing parameters
SI 65536
SF 500.3000000 MHz
WDW EM
SSB 0
LB 0.30 Hz
GB 0
PC 1.00

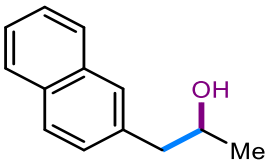

4.3.3hk

^{13}C NMR

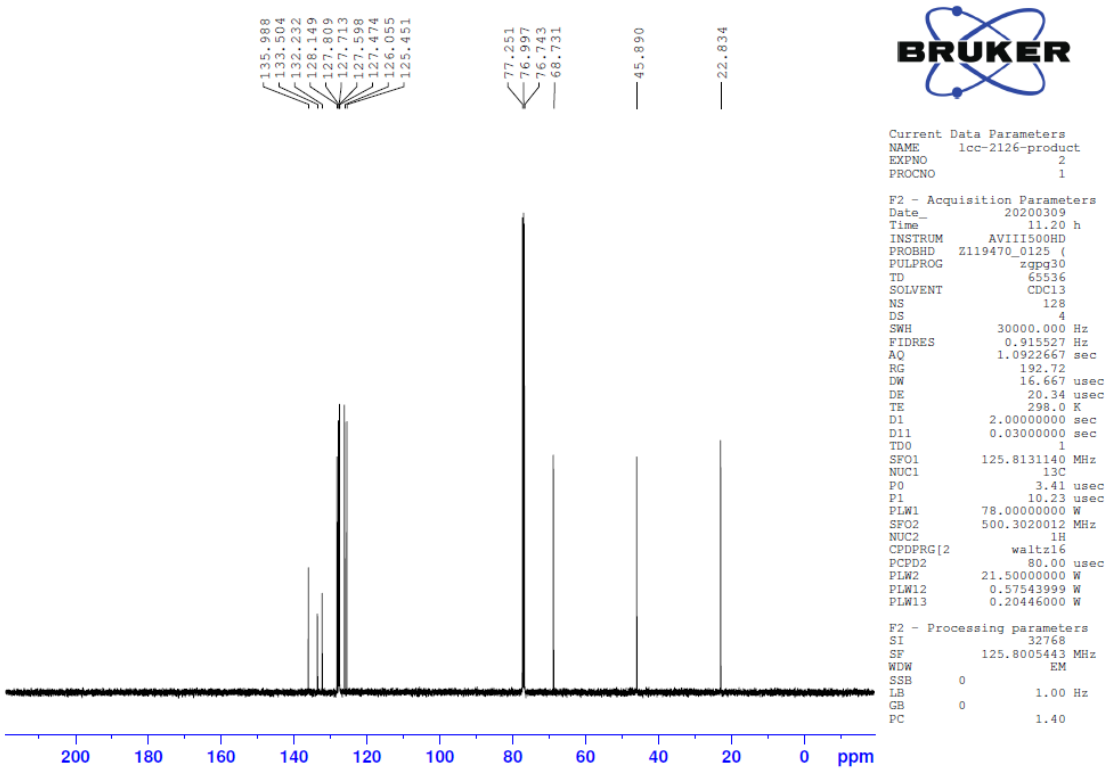


```
Current Data Parameters
NAME      1cc-2126-product
EXPNO                    2
PROCNO                   1

F2 - Acquisition Parameters
Date_           20200309
Time              11.20 h
INSTRUM       AVIII500HD
PROBHD    Z119470_0125 (
PULPROG           zgpg30
TD                65536
SOLVENT           CDCl3
NS                  128
DS                    4
SWH           30000.000 Hz
FIDRES        0.915527 Hz
AQ            1.0922667 sec
RG                192.72
DW               16.667 usec
DE               20.34 usec
TE               298.0 K
D1            2.00000000 sec
D11           0.03000000 sec
TD0                   1
SFO1        125.8131140 MHz
NUC1                13C
P0                3.41 usec
P1               10.23 usec
PLW1        78.00000000 W
SFO2        500.3020012 MHz
NUC2                1H
CPDPRG[2         waltz16
PCPD2             80.00 usec
PLW2        21.50000000 W
PLW12        0.57543999 W
PLW13        0.20446000 W

F2 - Processing parameters
SI                32768
SF          125.8005443 MHz
WDW                  EM
SSB       0
LB                1.00 Hz
GB        0
PC                1.40
```

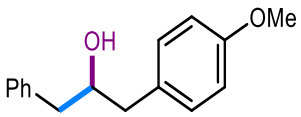

4.3.3al

^{1}H NMR

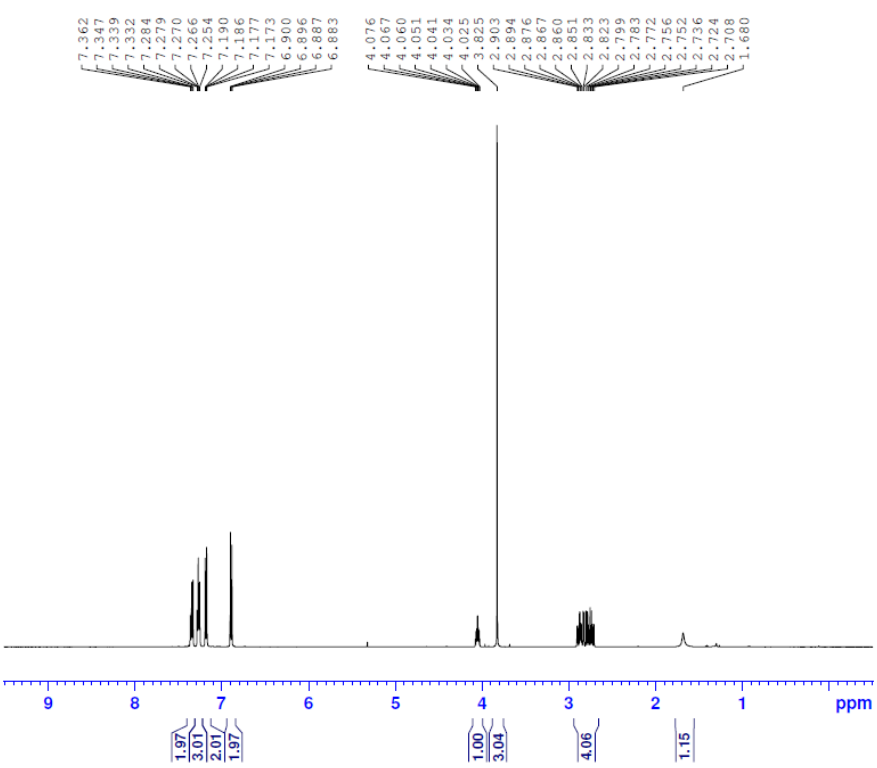


```
Current Data Parameters
NAME      1cc-2139-product
EXPNO                    1
PROCNO                   1

F2 - Acquisition Parameters
Date_             20200313
Time                 8.38 h
INSTRUM       AVIII500HD
PROBHD    Z119470_0125 (
PULPROG              zg30
TD                  65536
SOLVENT             CDCl3
NS                      4
DS                      2
SWH           10000.000 Hz
FIDRES            0.305176 Hz
AQ                3.2767999 sec
RG                   71.03
DW                  50.000 usec
DE                  13.89 usec
TE                  298.0 K
D1              1.00000000 sec
TD0                     1
SFO1          500.3030896 MHz
NUC1                   1H
P0                   3.33 usec
P1                  10.00 usec
PLW1          21.89999962 W

F2 - Processing parameters
SI                  65536
SF            500.3000000 MHz
WDW                    EM
SSB       0
LB                   0.30 Hz
GB        0
PC                   1.00
```

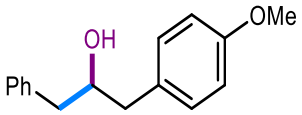

4.3.3al

^{13}C NMR

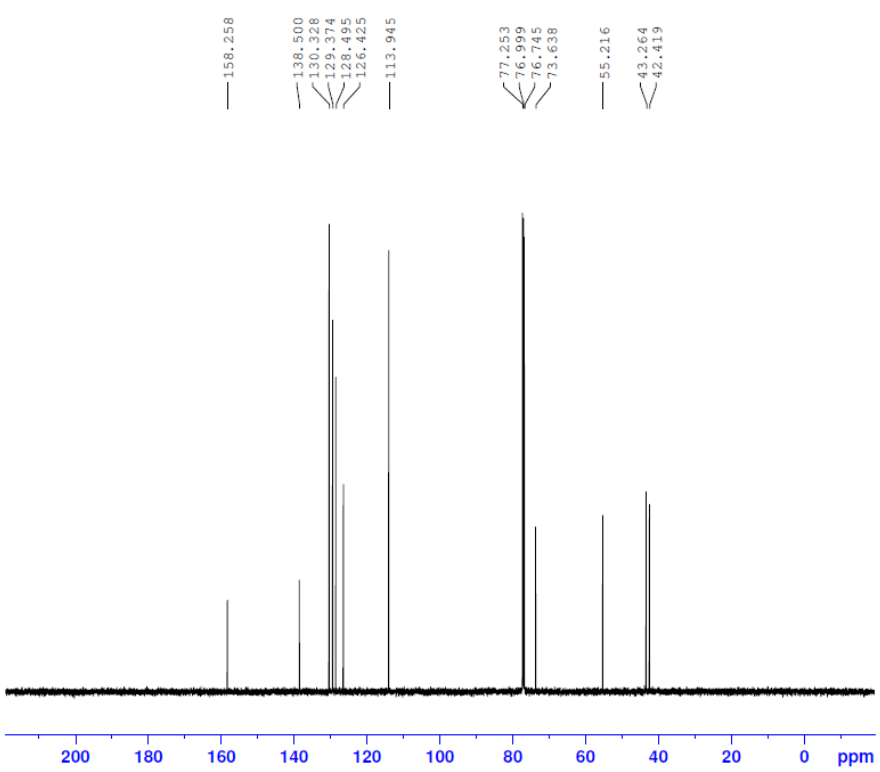

BRUKER

```
Current Data Parameters
NAME      1cc-2139-product
EXPNO                    2
PROCNO                   1

F2 - Acquisition Parameters
Date_             20200313
Time                 8.45 h
INSTRUM       AVIII500HD
PROBHD    Z119470_0125 (
PULPROG             zgpg30
TD                   65536
SOLVENT              CDCl3
NS                     128
DS                       4
SWH              30000.000 Hz
FIDRES               0.915527 Hz
AQ                1.0922667 sec
RG                   192.72
DW                   16.667 usec
DE                   20.34 usec
TE                   298.0 K
D1               2.00000000 sec
D11              0.03000000 sec
TD0                      1
SFO1           125.8131140 MHz
NUC1                   13C
P0                    3.41 usec
P1                   10.23 usec
PLW1           78.00000000 W
SFO2           500.3020012 MHz
NUC2                   1H
CPDPRG[2            waltz16
PCPD2                80.00 usec
PLW2           21.50000000 W
PLW12           0.57543999 W
PLW13           0.20446000 W

F2 - Processing parameters
SI                   32768
SF             125.8005425 MHz
WDW                    EM
SSB       0
LB                    1.00 Hz
GB        0
PC                    1.40
```

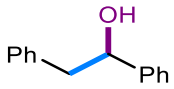

4.3.3am

^{1}H NMR

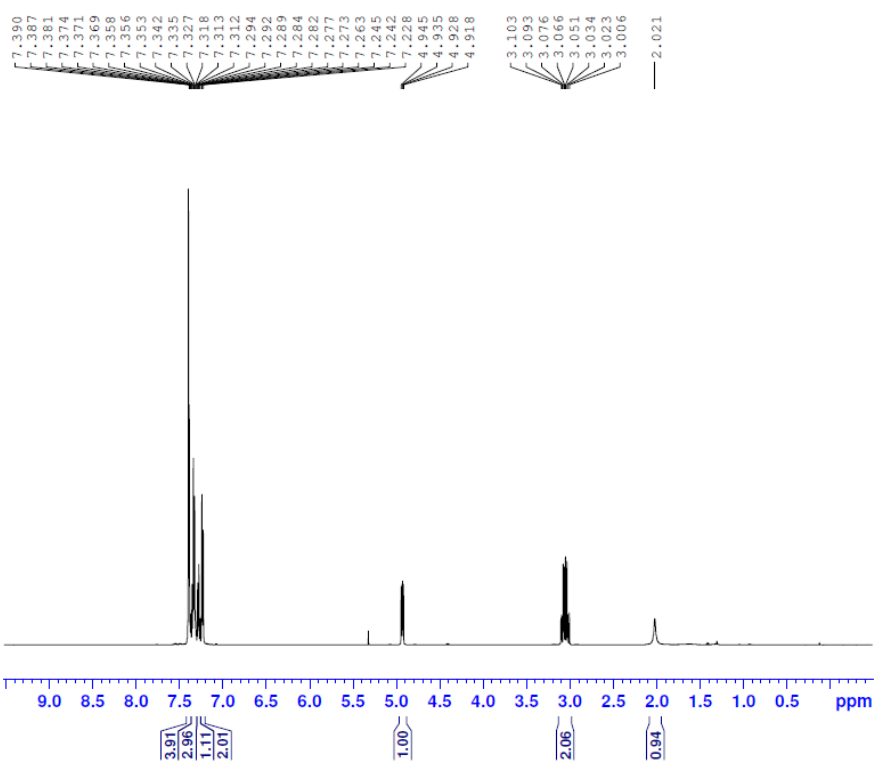


```
Current Data Parameters
NAME      1cc-2114-product
EXPNO                    1
PROCNO                   1

F2 - Acquisition Parameters
Date_             20200229
Time                23.08 h
INSTRUM       AVIII500HD
PROBHD    Z119470_0125 (
PULPROG              zg30
TD                  65536
SOLVENT             CDCl3
NS                      4
DS                      2
SWH             10000.000 Hz
FIDRES              0.305176 Hz
AQ                3.2767999 sec
RG                    77.88
DW                   50.000 usec
DE                   13.89 usec
TE                   298.0 K
D1              1.00000000 sec
TD0                     1
SFO1           500.3030896 MHz
NUC1                   1H
P0                   3.33 usec
P1                  10.00 usec
PLW1           21.89999962 W

F2 - Processing parameters
SI                  65536
SF             500.3000000 MHz
WDW                    EM
SSB       0
LB                   0.30 Hz
GB        0
PC                   1.00
```

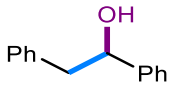

4.3.3am

^{13}C NMR

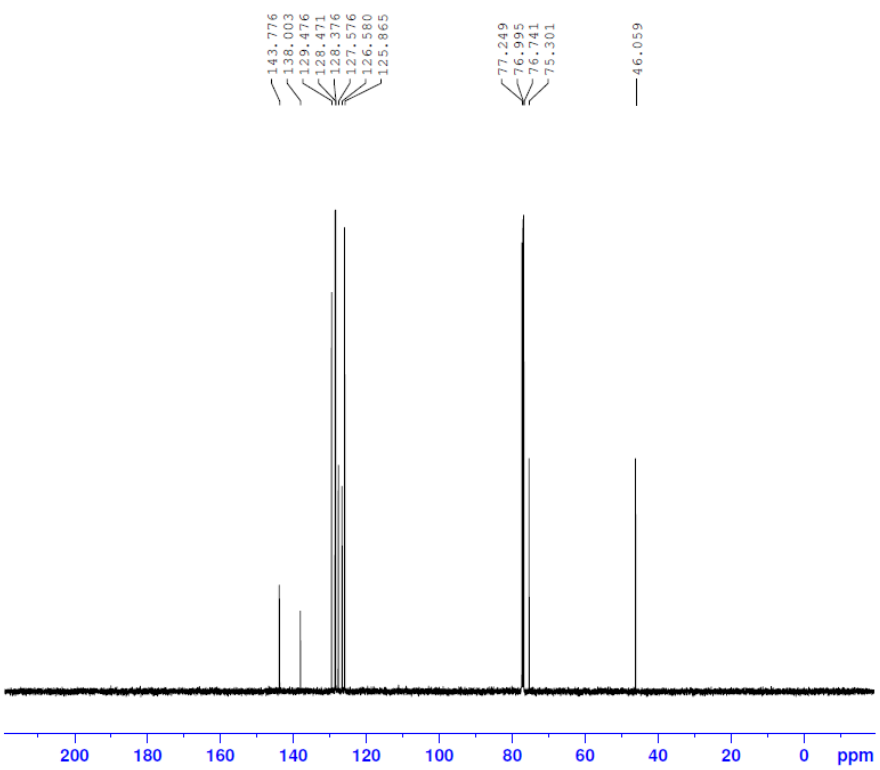


```
Current Data Parameters
NAME      1cc-2114-product
EXPNO                    2
PROCNO                   1

F2 - Acquisition Parameters
Date_           20200229
Time              23.15 h
INSTRUM       AVIII500HD
PROBHD    Z119470_0125 (
PULPROG          zgpg30
TD                65536
SOLVENT           CDCl3
NS                  128
DS                    4
SWH           30000.000 Hz
FIDRES            0.915527 Hz
AQ                1.0922667 sec
RG                  192.72
DW                 16.667 usec
DE                  20.34 usec
TE                 298.0 K
D1             2.00000000 sec
D11            0.03000000 sec
TD0                   1
SFO1          125.8131140 MHz
NUC1                13C
P0                   3.41 usec
P1                  10.23 usec
PLW1          78.00000000 W
SFO2          500.3020012 MHz
NUC2                 1H
CPDPRG[2          waltz16
PCPD2               80.00 usec
PLW2          21.50000000 W
PLW12          0.57543999 W
PLW13          0.20446000 W

F2 - Processing parameters
SI                  32768
SF            125.8005434 MHz
WDW                    EM
SSB       0
LB                   1.00 Hz
GB        0
PC                   1.40
```

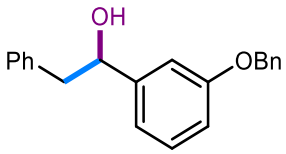

4.3.3an

^{1}H NMR

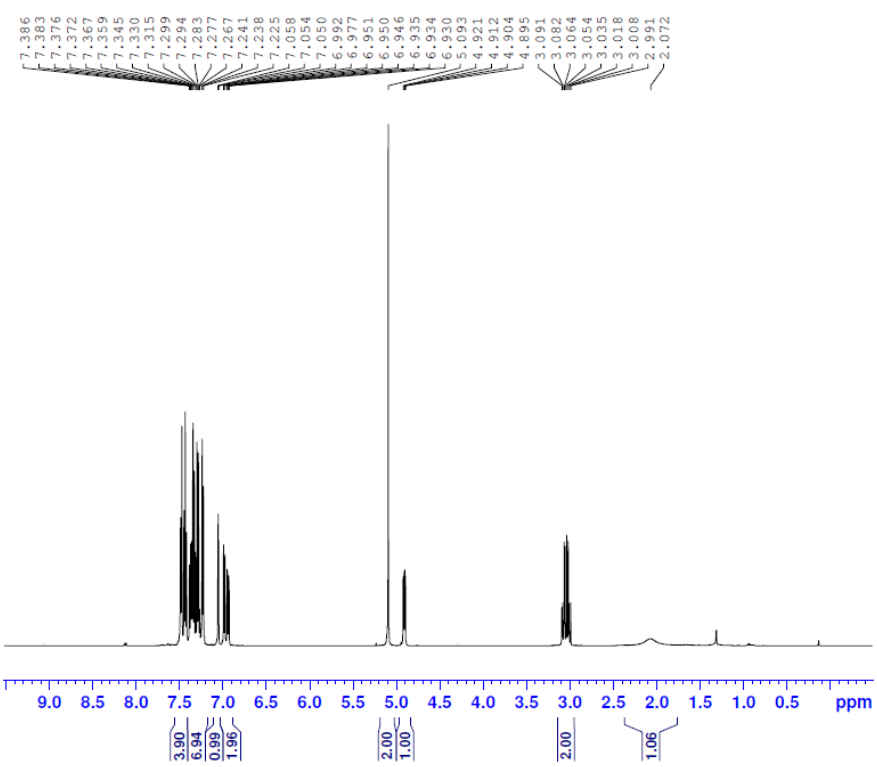


```
Current Data Parameters
NAME      1cc-2121-product
EXPNO                    1
PROCNO                   1

F2 - Acquisition Parameters
Date_           20200307
Time              18.59 h
INSTRUM       AVIII500HD
PROBHD    Z119470_0125 (
PULPROG              zg30
TD                  65536
SOLVENT             CDCl3
NS                      4
DS                      2
SWH           10000.000 Hz
FIDRES            0.305176 Hz
AQ             3.2767999 sec
RG                  71.03
DW                 50.000 usec
DE                 13.89 usec
TE                298.0 K
D1            1.00000000 sec
TD0                     1
SFO1         500.3030896 MHz
NUC1                   1H
P0                  3.33 usec
P1                 10.00 usec
PLW1         21.89999962 W

F2 - Processing parameters
SI                  65536
SF           500.3000000 MHz
WDW                    EM
SSB       0
LB                  0.30 Hz
GB        0
PC                  1.00
```

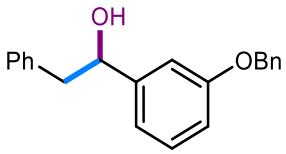

4.3.3an

^{13}C NMR

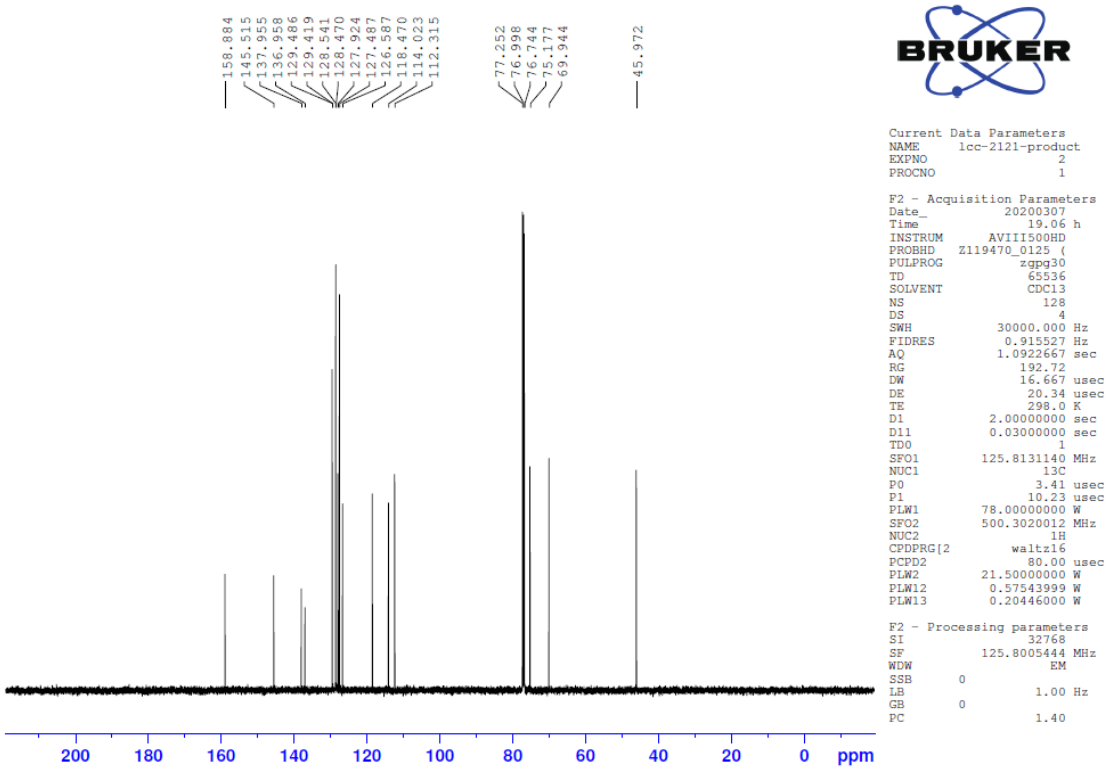

BRUKER

```
Current Data Parameters
NAME      lcc-2121-product
EXPNO                    2
PROCNO                   1

F2 - Acquisition Parameters
Date_           20200307
Time              19.06 h
INSTRUM       AVIII500HD
PROBHD    Z119470_0125 (
PULPROG           zgpg30
TD                65536
SOLVENT           CDCl3
NS                  128
DS                    4
SWH           30000.000 Hz
FIDRES            0.915527 Hz
AQ              1.0922667 sec
RG                192.72
DW                16.667 usec
DE                20.34 usec
TE                298.0 K
D1              2.00000000 sec
D11             0.03000000 sec
TD0                   1
SFO1          125.8131140 MHz
NUC1                13C
P0                  3.41 usec
P1                 10.23 usec
PLW1          78.00000000 W
SFO2          500.3020012 MHz
NUC2                1H
CPDPRG[2          waltz16
PCPD2              80.00 usec
PLW2          21.50000000 W
PLW12          0.57543999 W
PLW13          0.20446000 W

F2 - Processing parameters
SI                32768
SF          125.8005444 MHz
WDW                 EM
SSB       0
LB                1.00 Hz
GB        0
PC                1.40
```

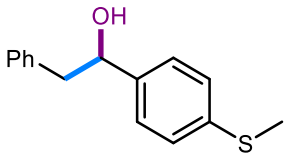

4.3.3ao

^{1}H NMR

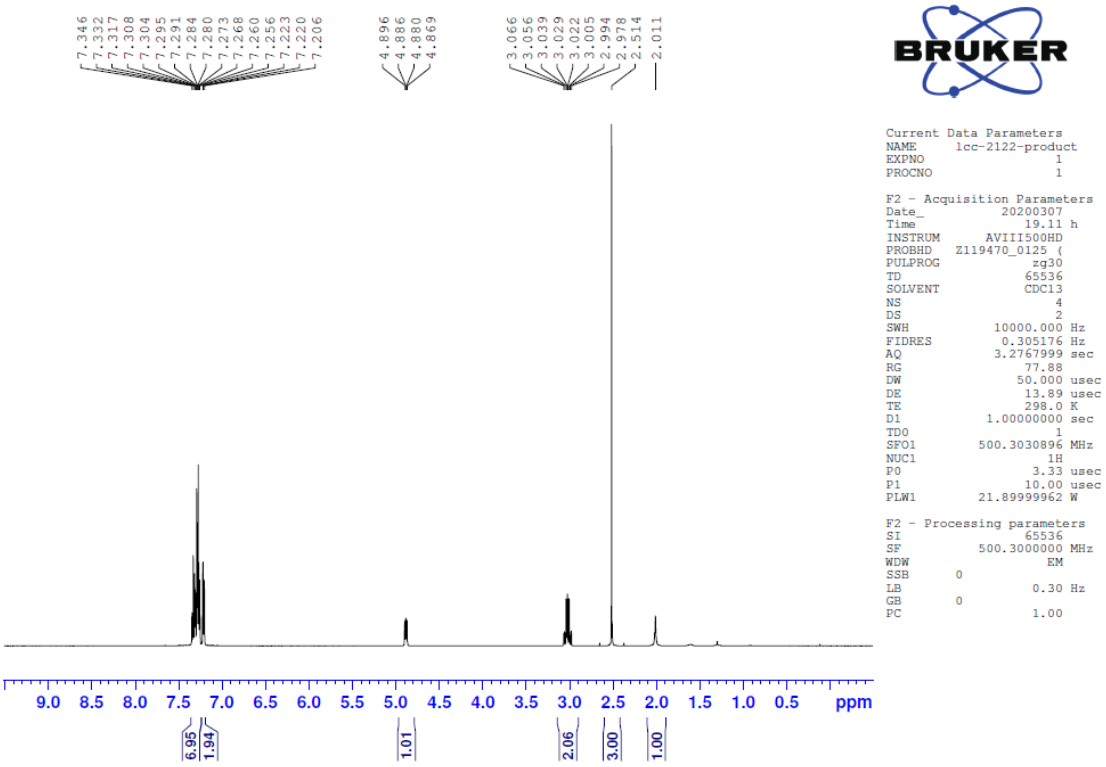

BRUKER

```
Current Data Parameters
NAME      1cc-2122-product
EXPNO                    1
PROCNO                   1

F2 - Acquisition Parameters
Date_             20200307
Time                19.11 h
INSTRUM       AVIII500HD
PROBHD    Z119470_0125 (
PULPROG              zg30
TD                  65536
SOLVENT             CDCl3
NS                      4
DS                      2
SWH             10000.000 Hz
FIDRES              0.305176 Hz
AQ                3.2767999 sec
RG                    77.88
DW                   50.000 usec
DE                   13.89 usec
TE                   298.0 K
D1              1.00000000 sec
TD0                     1
SFO1          500.3030896 MHz
NUC1                   1H
P0                   3.33 usec
P1                  10.00 usec
PLW1          21.89999962 W

F2 - Processing parameters
SI                  65536
SF            500.3000000 MHz
WDW                    EM
SSB       0
LB                   0.30 Hz
GB        0
PC                   1.00
```

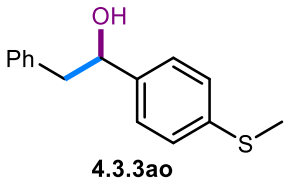

4.3.3ao

^{13}C NMR

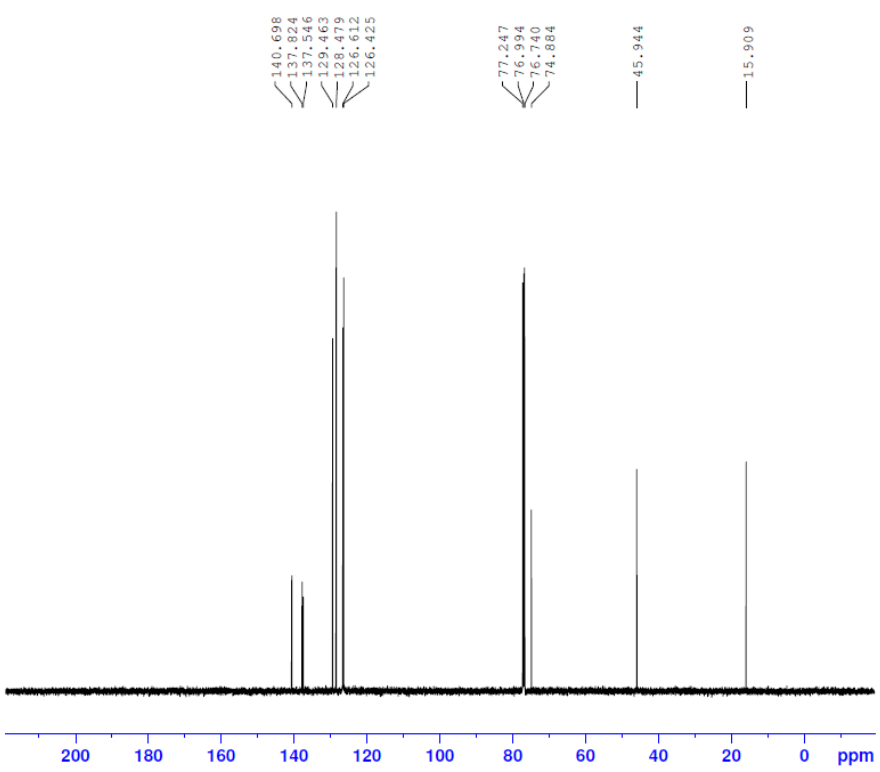

BRUKER

```
Current Data Parameters
NAME      1cc-2122-product
EXPNO                    2
PROCNO                   1

F2 - Acquisition Parameters
Date_           20200307
Time              19.18 h
INSTRUM       AVIII500HD
PROBHD    Z119470_0125 (
PULPROG           zgpg30
TD                65536
SOLVENT           CDCl3
NS                  128
DS                    4
SWH           30000.000 Hz
FIDRES            0.915527 Hz
AQ                1.0922667 sec
RG                  192.72
DW                 16.667 usec
DE                 20.34 usec
TE                 298.0 K
D1              2.00000000 sec
D11             0.03000000 sec
TD0                   1
SFO1          125.8131140 MHz
NUC1                 13C
P0                  3.41 usec
P1                 10.23 usec
PLW1          78.00000000 W
SFO2          500.3020012 MHz
NUC2                 1H
CPDPRG[2          waltz16
PCPD2               80.00 usec
PLW2          21.50000000 W
PLW12          0.57543999 W
PLW13          0.20446000 W

F2 - Processing parameters
SI                  32768
SF            125.8005443 MHz
WDW                   EM
SSB       0
LB                  1.00 Hz
GB        0
PC                  1.40
```

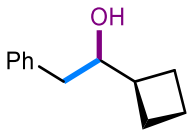

4.3.3ap

^{1}H NMR

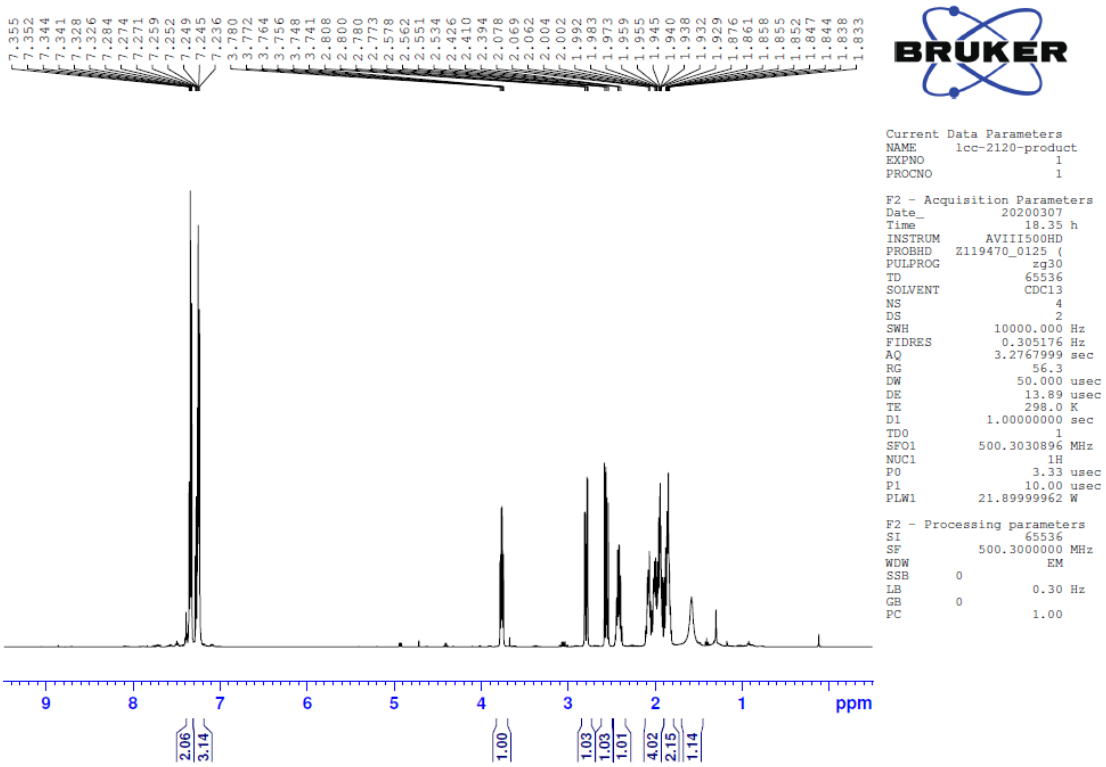

CV

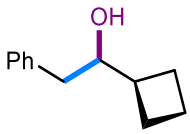

4.3.3ap

^{13}C NMR

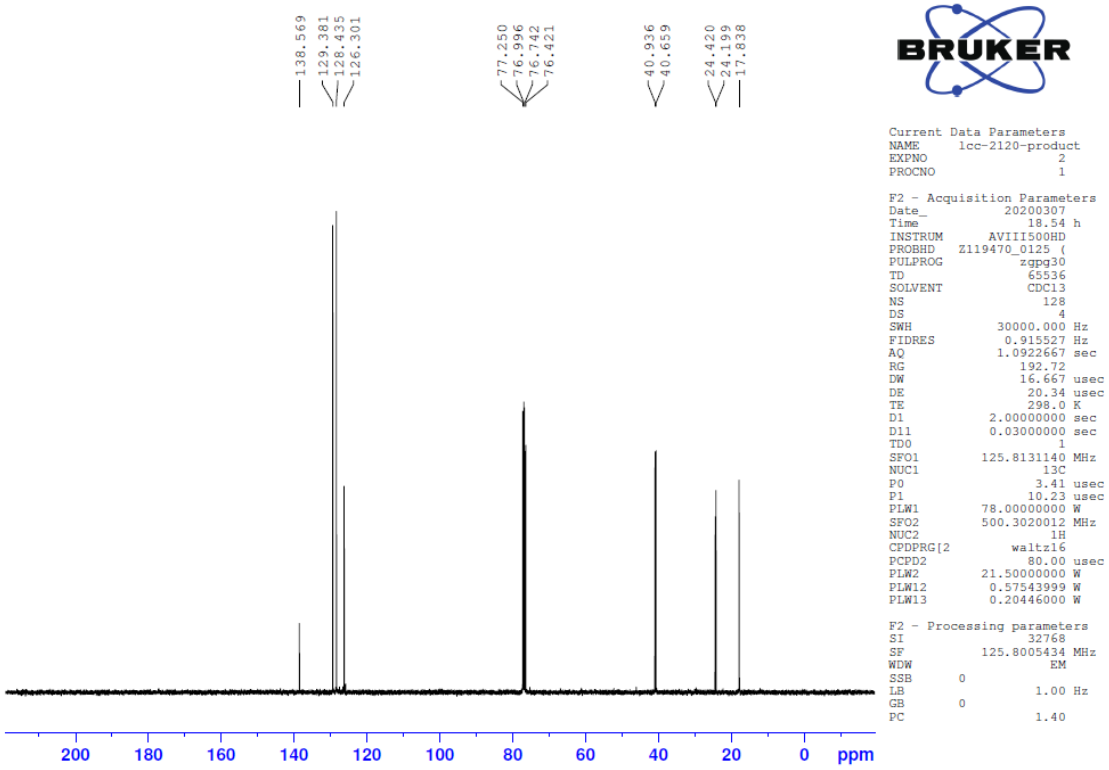


```
Current Data Parameters
NAME      1cc-2120-product
EXPNO                    2
PROCNO                   1

F2 - Acquisition Parameters
Date_             20200307
Time                 18.54 h
INSTRUM       AVIII500HD
PROBHD    Z119470_0125 (
PULPROG           zgpg30
TD                65536
SOLVENT           CDCl3
NS                  128
DS                    4
SWH           30000.000 Hz
FIDRES            0.915527 Hz
AQ                1.0922667 sec
RG                  192.72
DW                 16.667 usec
DE                 20.34 usec
TE                 298.0 K
D1             2.00000000 sec
D11            0.03000000 sec
TD0                   1
SFO1         125.8131140 MHz
NUC1                 13C
P0                 3.41 usec
P1                10.23 usec
PLW1         78.00000000 W
SFO2         500.3020012 MHz
NUC2                 1H
CPDPRG[2          waltz16
PCPD2              80.00 usec
PLW2         21.50000000 W
PLW12         0.57543999 W
PLW13         0.20446000 W

F2 - Processing parameters
SI                32768
SF           125.8005434 MHz
WDW                  EM
SSB       0
LB                1.00 Hz
GB        0
PC                1.40
```

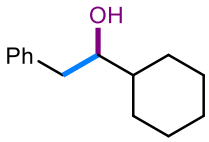
OH
Ph

4.3.3aq

^{1}H NMR

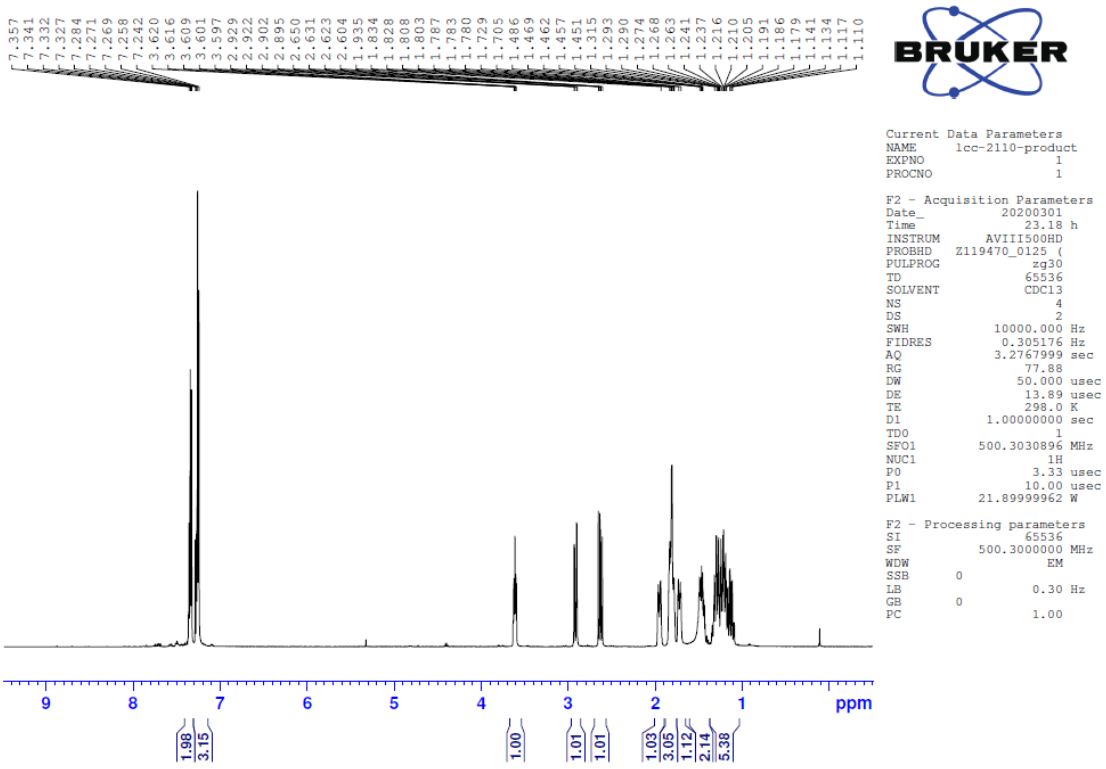
7.357
7.341
7.332
7.327
7.284
7.271
7.269
7.258
7.242
3.620
3.616
3.609
3.601
3.597
2.929
2.922
2.902
2.895
2.650
2.631
2.623
2.604
1.935
1.834
1.828
1.808
1.803
1.787
1.783
1.780
1.729
1.705
1.486
1.469
1.462
1.457
1.451
1.315
1.293
1.290
1.274
1.268
1.263
1.241
1.237
1.216
1.210
1.205
1.191
1.186
1.179
1.141
1.134
1.117
1.110
BRUKER
Current Data Parameters
NAME lcc-2110-product
EXPNO 1
PROCNO 1
F2 - Acquisition Parameters
Date_ 20200301
Time 23.18 h
INSTRUM AVIII500HD
PROBHD Z119470_0125 (
PULPROG zg30
TD 65536
SOLVENT CDCl3
NS 4
DS 2
SWH 10000.000 Hz
FIDRES 0.305176 Hz
AQ 3.2767999 sec
RG 77.88
DW 50.000 usec
DE 13.89 usec
TE 298.0 K
D1 1.00000000 sec
TD0 1
SFO1 500.3030896 MHz
NUC1 1H
P0 3.33 usec
P1 10.00 usec
PLW1 21.89999962 W
F2 - Processing parameters
SI 65536
SF 500.3000000 MHz
WDW EM
SSB 0
LB 0.30 Hz
GB 0
PC 1.00
9
8
7
6
5
4
3
2
1
ppm
1.98
3.15
1.00
1.01
1.01
1.03
3.05
1.12
2.14
5.38

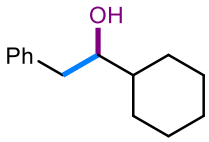

4.3.3aq

^{13}C NMR

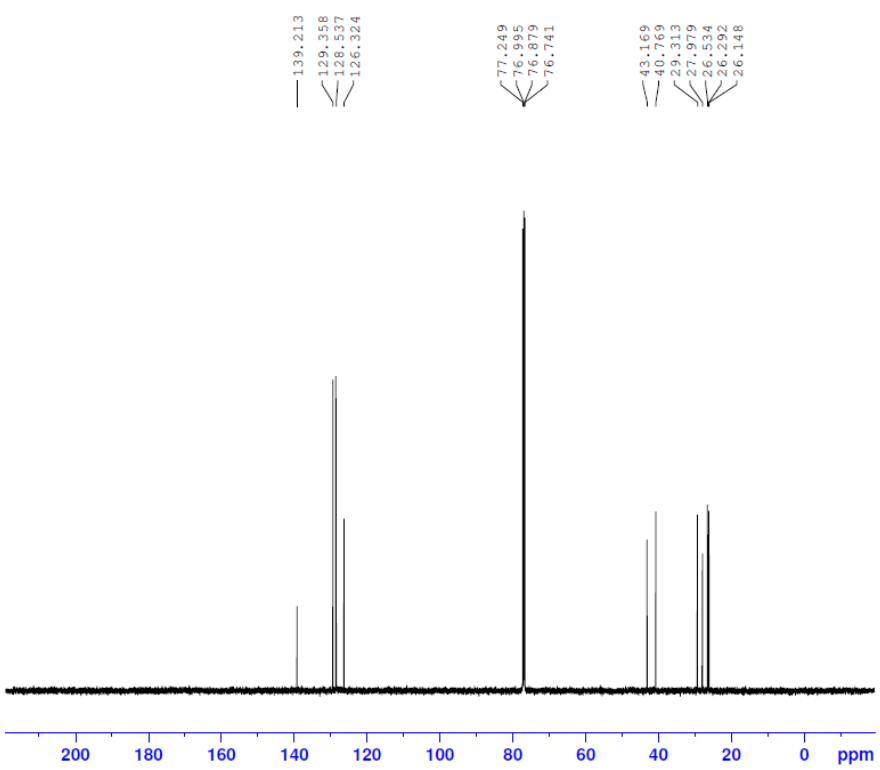

BRUKER

```
Current Data Parameters
NAME      lcc-2110-product
EXPNO                    2
PROCNO                   1

F2 - Acquisition Parameters
Date_             20200301
Time                23.25 h
INSTRUM       AVIII500HD
PROBHD    Z119470_0125 (
PULPROG           zgpg30
TD                 65536
SOLVENT            CDCl3
NS                   128
DS                     4
SWH            30000.000 Hz
FIDRES             0.915527 Hz
AQ                 1.0922667 sec
RG                   192.72
DW                  16.667 usec
DE                  20.34 usec
TE                  298.0 K
D1              2.00000000 sec
D11             0.03000000 sec
TD0                    1
SFO1          125.8131140 MHz
NUC1                  13C
P0                   3.41 usec
P1                  10.23 usec
PLW1           78.00000000 W
SFO2          500.3020012 MHz
NUC2                   1H
CPDPRG[2           waltz16
PCPD2                80.00 usec
PLW2           21.50000000 W
PLW12           0.57543999 W
PLW13           0.20446000 W

F2 - Processing parameters
SI                   32768
SF            125.8005407 MHz
WDW                     EM
SSB       0
LB                    1.00 Hz
GB        0
PC                    1.40
```

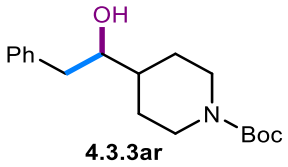
OH
Ph
N
Boc

4.3.3ar

^{1}H NMR

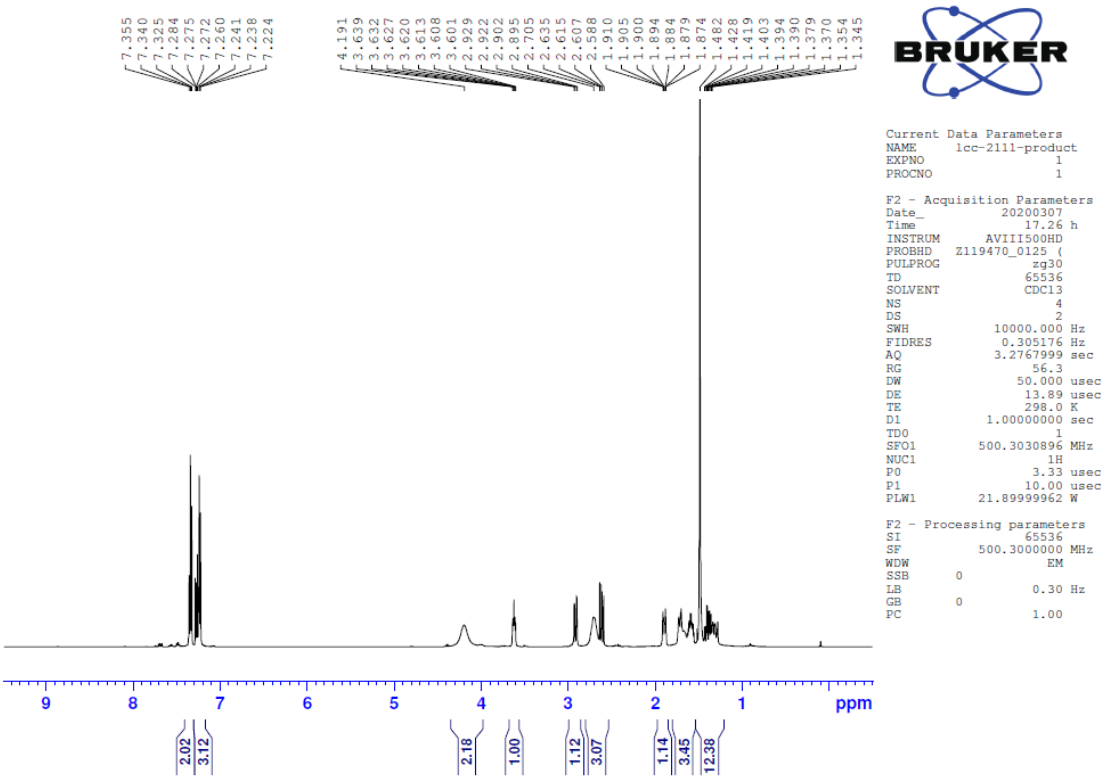
7.355
7.340
7.325
7.284
7.275
7.272
7.260
7.241
7.238
7.224
4.191
3.639
3.632
3.627
3.620
3.613
3.608
3.601
2.929
2.922
2.902
2.895
2.705
2.635
2.615
2.607
2.588
1.910
1.905
1.900
1.894
1.884
1.879
1.874
1.462
1.428
1.419
1.403
1.394
1.390
1.379
1.370
1.354
1.345
BRUKER
Current Data Parameters
NAME lcc-2111-product
EXPNO 1
PROCNO 1
F2 - Acquisition Parameters
Date_ 20200307
Time 17.26 h
INSTRUM AVIII500HD
PROBHD Z119470_0125 (
PULPROG zg30
TD 65536
SOLVENT CDCl3
NS 4
DS 2
SWH 10000.000 Hz
FIDRES 0.305176 Hz
AQ 3.2767999 sec
RG 56.3
DW 50.000 usec
DE 13.89 usec
TE 298.0 K
D1 1.00000000 sec
TD0 1
SFO1 500.3030896 MHz
NUC1 1H
P0 3.33 usec
P1 10.00 usec
PLW1 21.89999962 W
F2 - Processing parameters
SI 65536
SF 500.3000000 MHz
WDW EM
SSB 0
LB 0.30 Hz
GB 0
PC 1.00
9
8
7
6
5
4
3
2
1
ppm
2.02
3.12
2.18
1.00
1.12
3.07
1.14
3.45
12.38

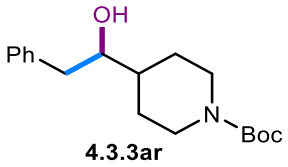

4.3.3ar

^{13}C NMR

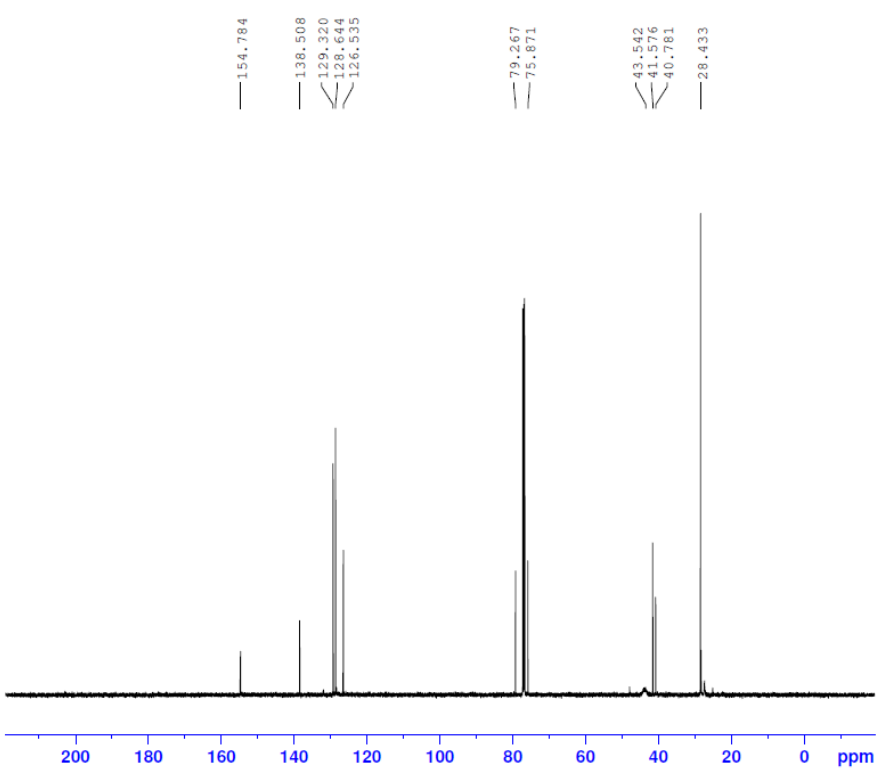

BRUKER

```
Current Data Parameters
NAME      1cc-2111-product
EXPNO                    2
PROCNO                   1

F2 - Acquisition Parameters
Date_             20200307
Time                18.31 h
INSTRUM       AVIII500HD
PROBHD    Z119470_0125 (
PULPROG           zgpg30
TD                 65536
SOLVENT            CDCl3
NS                   256
DS                     4
SWH            30000.000 Hz
FIDRES         0.915527 Hz
AQ             1.0922667 sec
RG                192.72
DW                16.667 usec
DE                20.34 usec
TE                298.0 K
D1            2.00000000 sec
D11           0.03000000 sec
TD0                    1
SFO1         125.8131140 MHz
NUC1                 13C
P0                 3.41 usec
P1                10.23 usec
PLW1         78.00000000 W
SFO2         500.3020012 MHz
NUC2                 1H
CPDPRG[2          waltz16
PCPD2             80.00 usec
PLW2         21.50000000 W
PLW12         0.57543999 W
PLW13         0.20446000 W

F2 - Processing parameters
SI                 32768
SF           125.8005424 MHz
WDW                   EM
SSB       0
LB                 1.00 Hz
GB        0
PC                 1.40
```

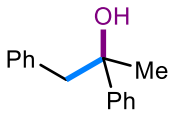

4.3.3as

^{1}H NMR

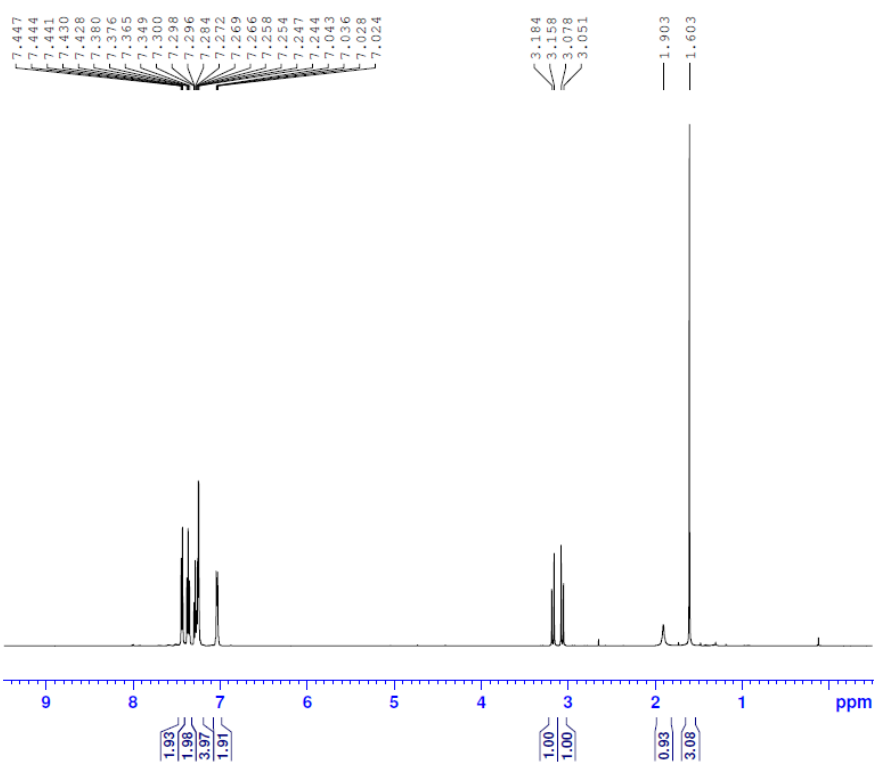


```
Current Data Parameters
NAME      1cc-2128-product
EXPNO                    1
PROCNO                   1

F2 - Acquisition Parameters
Date_             20200309
Time                11.25 h
INSTRUM       AVIII500HD
PROBHD    Z119470_0125 (
PULPROG              zg30
TD                  65536
SOLVENT             CDCl3
NS                      4
DS                      2
SWH             10000.000 Hz
FIDRES              0.305176 Hz
AQ                3.2767999 sec
RG                    77.88
DW                   50.000 usec
DE                   13.89 usec
TE                   298.0 K
D1              1.00000000 sec
TD0                     1
SFO1           500.3030896 MHz
NUC1                   1H
P0                    3.33 usec
P1                   10.00 usec
PLW1          21.89999962 W

F2 - Processing parameters
SI                  65536
SF             500.3000000 MHz
WDW                    EM
SSB       0
LB                    0.30 Hz
GB        0
PC                    1.00
```

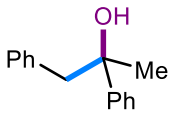

4.3.3as

^{13}C NMR

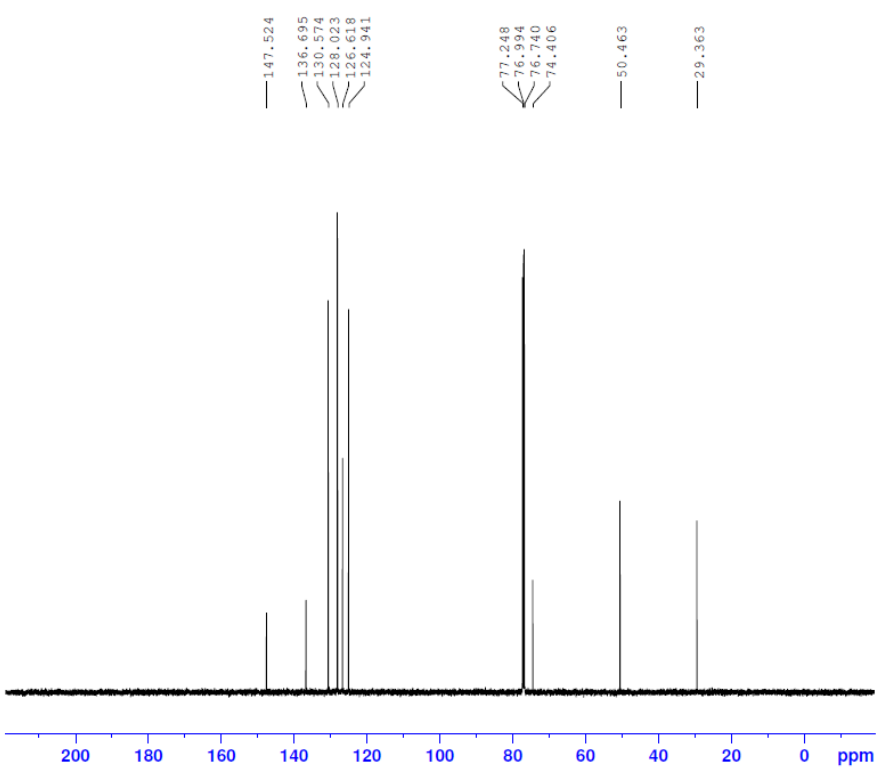


```
Current Data Parameters
NAME      1cc-2128-product
EXPNO                    2
PROCNO                   1

F2 - Acquisition Parameters
Date_             20200309
Time                11.32 h
INSTRUM       AVIII500HD
PROBHD    Z119470_0125 (
PULPROG            zgpg30
TD                  65536
SOLVENT             CDCl3
NS                    128
DS                      4
SWH             30000.000 Hz
FIDRES          0.915527 Hz
AQ              1.0922667 sec
RG                 192.72
DW                 16.667 usec
DE                 20.34 usec
TE                 298.0 K
D1            2.00000000 sec
D11           0.03000000 sec
TD0                     1
SFO1         125.8131140 MHz
NUC1                  13C
P0                  3.41 usec
P1                 10.23 usec
PLW1         78.00000000 W
SFO2         500.3020012 MHz
NUC2                  1H
CPDPRG[2         waltz16
PCPD2              80.00 usec
PLW2         21.50000000 W
PLW12         0.57543999 W
PLW13         0.20446000 W

F2 - Processing parameters
SI                  32768
SF           125.8005425 MHz
WDW                    EM
SSB       0
LB                  1.00 Hz
GB        0
PC                  1.40
```

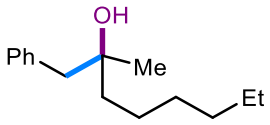
OH
Ph
Me
Et

4.3.3at

^{1}H NMR

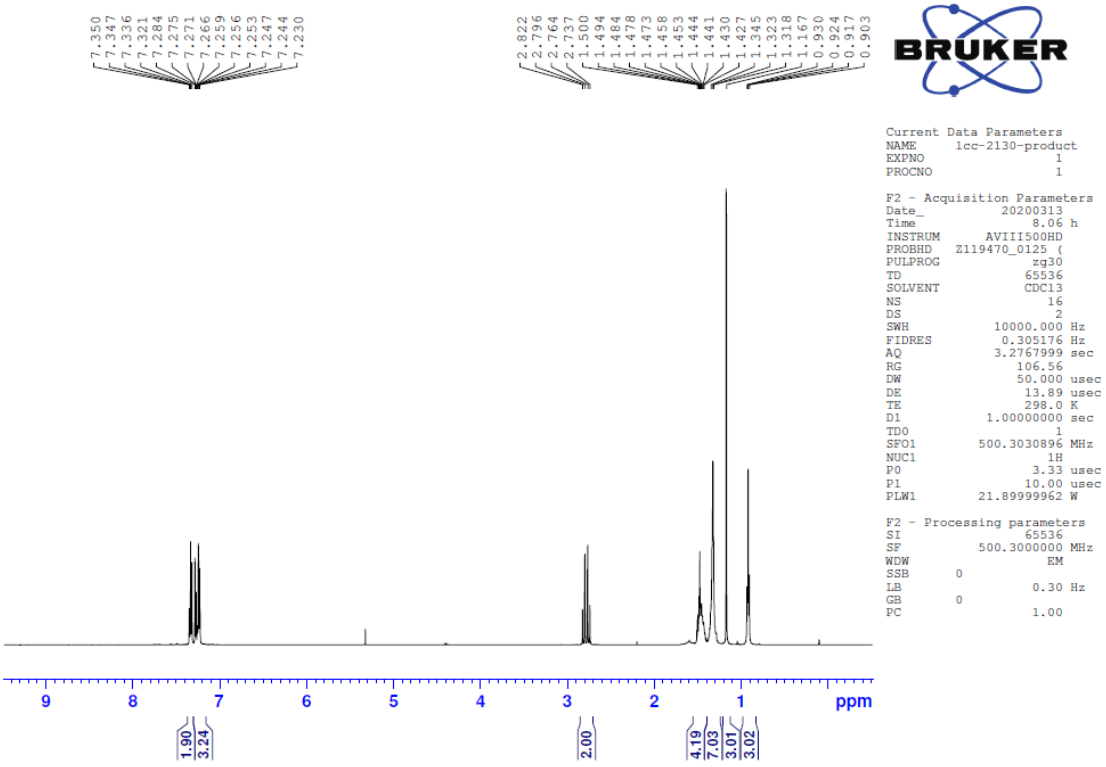
7.350
7.347
7.336
7.321
7.284
7.275
7.271
7.266
7.259
7.256
7.253
7.247
7.244
7.230
2.822
2.796
2.764
2.737
1.500
1.494
1.484
1.478
1.473
1.458
1.453
1.444
1.441
1.430
1.427
1.345
1.323
1.318
1.167
0.930
0.924
0.917
0.903
BRUKER
Current Data Parameters
NAME 1cc-2130-product
EXPNO 1
PROCNO 1
F2 - Acquisition Parameters
Date_ 20200313
Time 8.06 h
INSTRUM AVIII500HD
PROBHD Z119470_0125 (
PULPROG zg30
TD 65536
SOLVENT CDC13
NS 16
DS 2
SWH 10000.000 Hz
FIDRES 0.305176 Hz
AQ 3.2767999 sec
RG 106.56
DW 50.000 usec
DE 13.89 usec
TE 298.0 K
D1 1.00000000 sec
TD0 1
SFO1 500.3030896 MHz
NUC1 1H
P0 3.33 usec
P1 10.00 usec
PLW1 21.89999962 W
F2 - Processing parameters
SI 65536
SF 500.3000000 MHz
WDW EM
SSB 0
LB 0.30 Hz
GB 0
PC 1.00
9
8
7
6
5
4
3
2
1
ppm
1.90
3.24
2.00
4.19
7.03
3.01
3.02

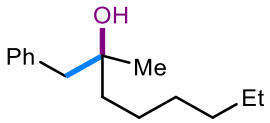

4.3.3at

^{13}C NMR

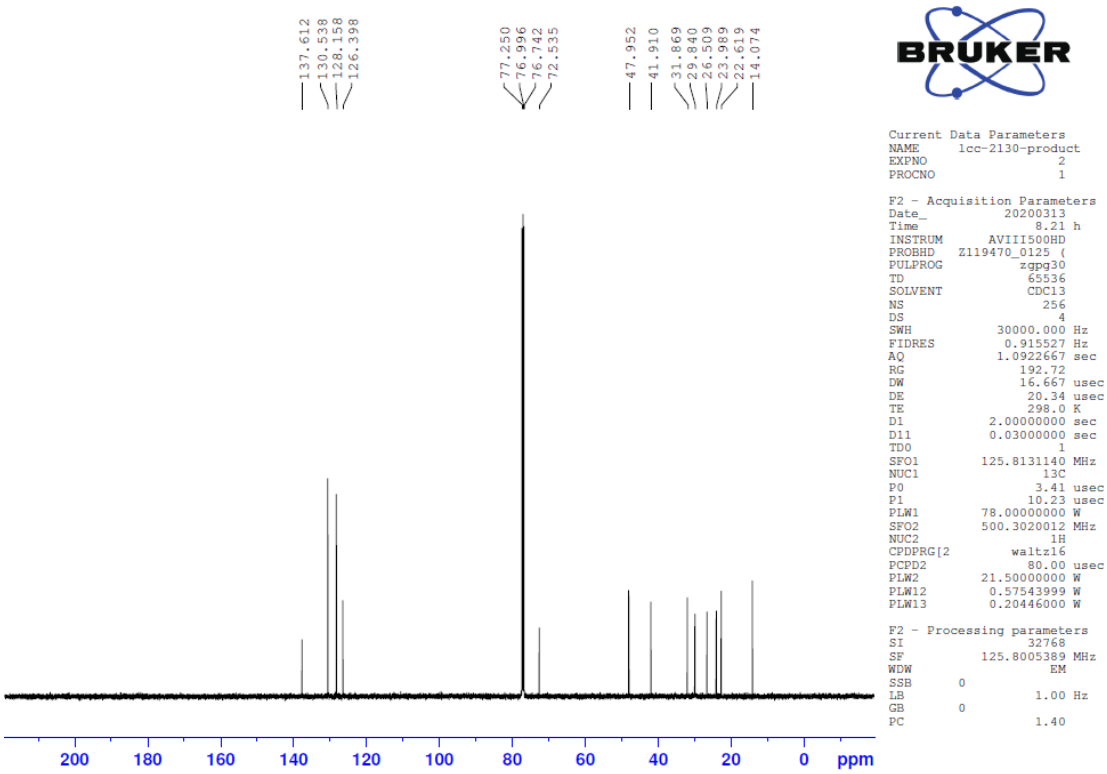

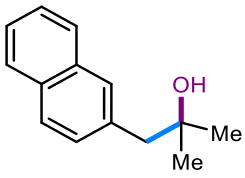
OH
Me
Me

4.3.3hv

^{1}H NMR

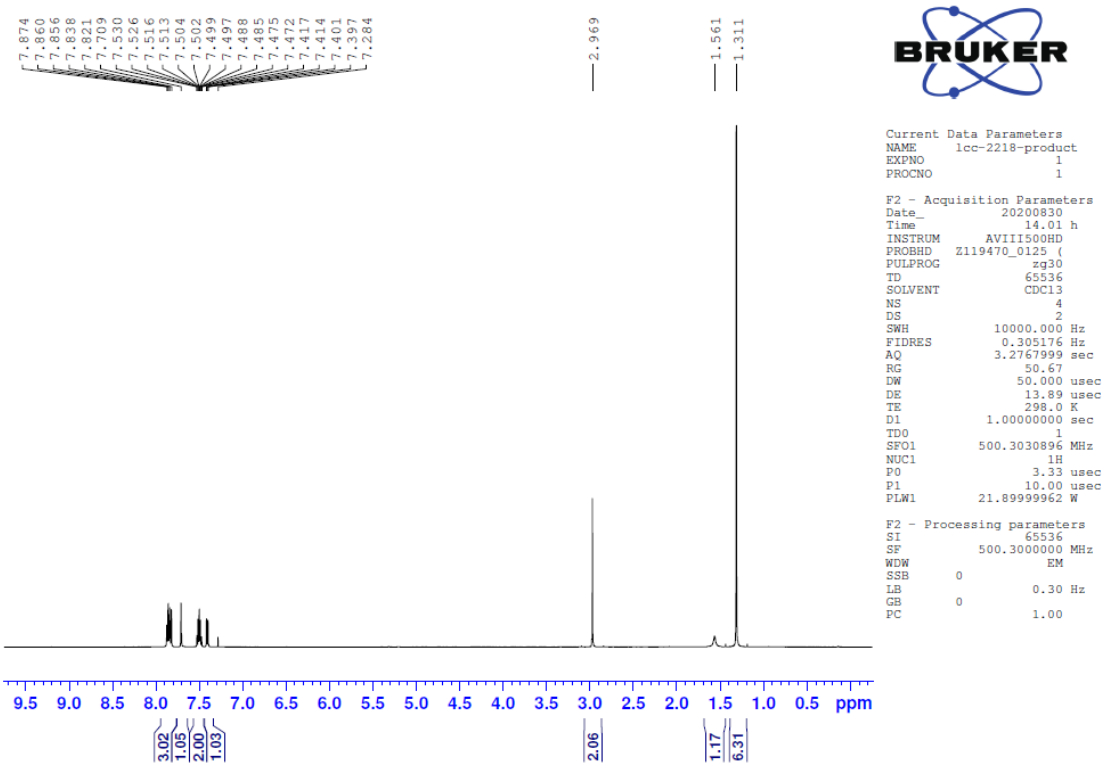
7.874
7.860
7.856
7.838
7.821
7.709
7.530
7.526
7.516
7.513
7.504
7.502
7.499
7.497
7.488
7.485
7.475
7.472
7.417
7.414
7.401
7.397
7.284
2.969
1.561
1.311
BRUKER
Current Data Parameters
NAME 1cc-2218-product
EXPNO 1
PROCNO 1
F2 - Acquisition Parameters
Date_ 20200830
Time 14.01 h
INSTRUM AVIII500HD
PROBHD Z119470_0125 (
PULPROG zg30
TD 65536
SOLVENT CDCl3
NS 4
DS 2
SWH 10000.000 Hz
FIDRES 0.305176 Hz
AQ 3.2767999 sec
RG 50.67
DW 50.000 usec
DE 13.89 usec
TE 298.0 K
D1 1.00000000 sec
TD0 1
SFO1 500.3030896 MHz
NUC1 1H
P0 3.33 usec
P1 10.00 usec
PLW1 21.89999962 W
F2 - Processing parameters
SI 65536
SF 500.3000000 MHz
WDW EM
SSB 0
LB 0.30 Hz
GB 0
PC 1.00
9.5 9.0 8.5 8.0 7.5 7.0 6.5 6.0 5.5 5.0 4.5 4.0 3.5 3.0 2.5 2.0 1.5 1.0 0.5 ppm
3.02
1.05
2.00
1.03
2.06
1.17
6.31

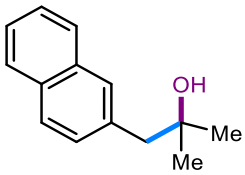

4.3.3hv

^{13}C NMR

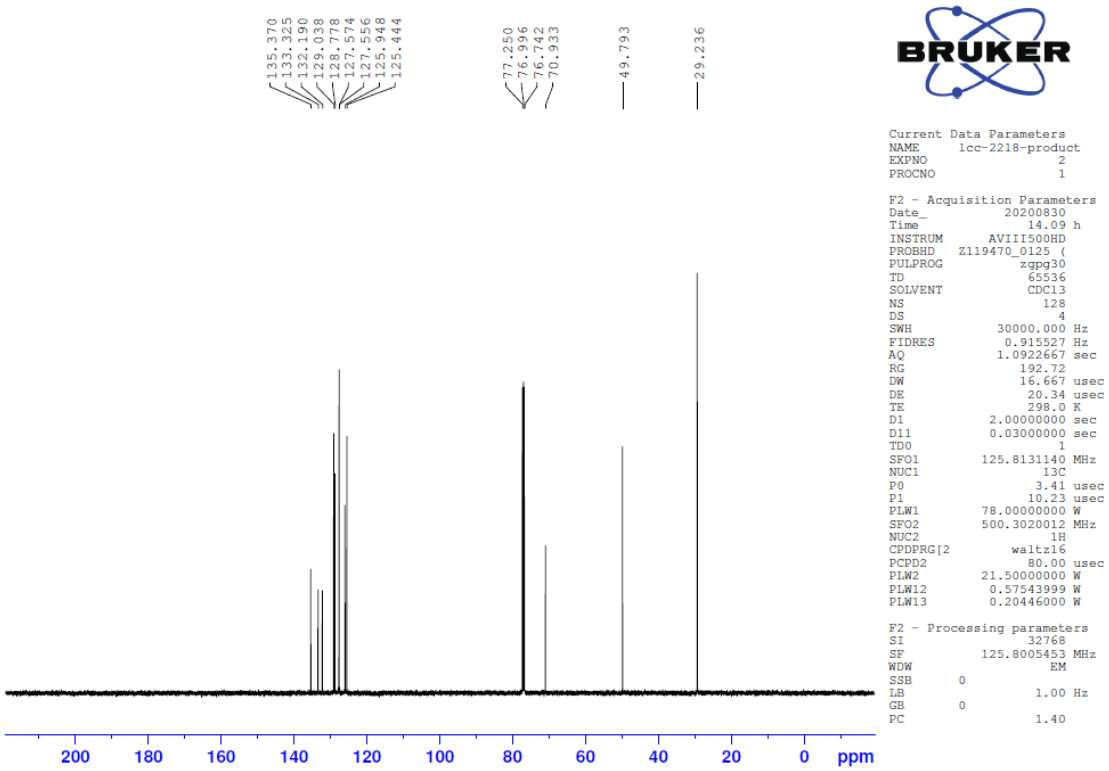


```
Current Data Parameters
NAME      1cc-2218-product
EXPNO                    2
PROCNO                   1

F2 - Acquisition Parameters
Date_           20200830
Time              14.09 h
INSTRUM       AVIII500HD
PROBHD    Z119470_0125 (
PULPROG           zgpg30
TD                65536
SOLVENT           CDCl3
NS                  128
DS                    4
SWH           30000.000 Hz
FIDRES         0.915527 Hz
AQ             1.0922667 sec
RG                192.72
DW                16.667 usec
DE                20.34 usec
TE                298.0 K
D1             2.00000000 sec
D11            0.03000000 sec
TD0                   1
SFO1         125.8131140 MHz
NUC1                 13C
P0                 3.41 usec
P1                10.23 usec
PLW1         78.00000000 W
SFO2         500.3020012 MHz
NUC2                 1H
CPDPRG[2         waltz16
PCPD2             80.00 usec
PLW2         21.50000000 W
PLW12         0.57543999 W
PLW13         0.20446000 W

F2 - Processing parameters
SI                32768
SF           125.8005453 MHz
WDW                  EM
SSB       0
LB                1.00 Hz
GB        0
PC                1.40
```

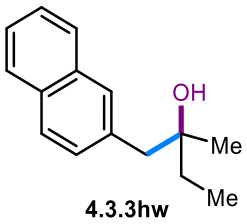
OH
Me
Me

4.3.3hw

^{1}H NMR

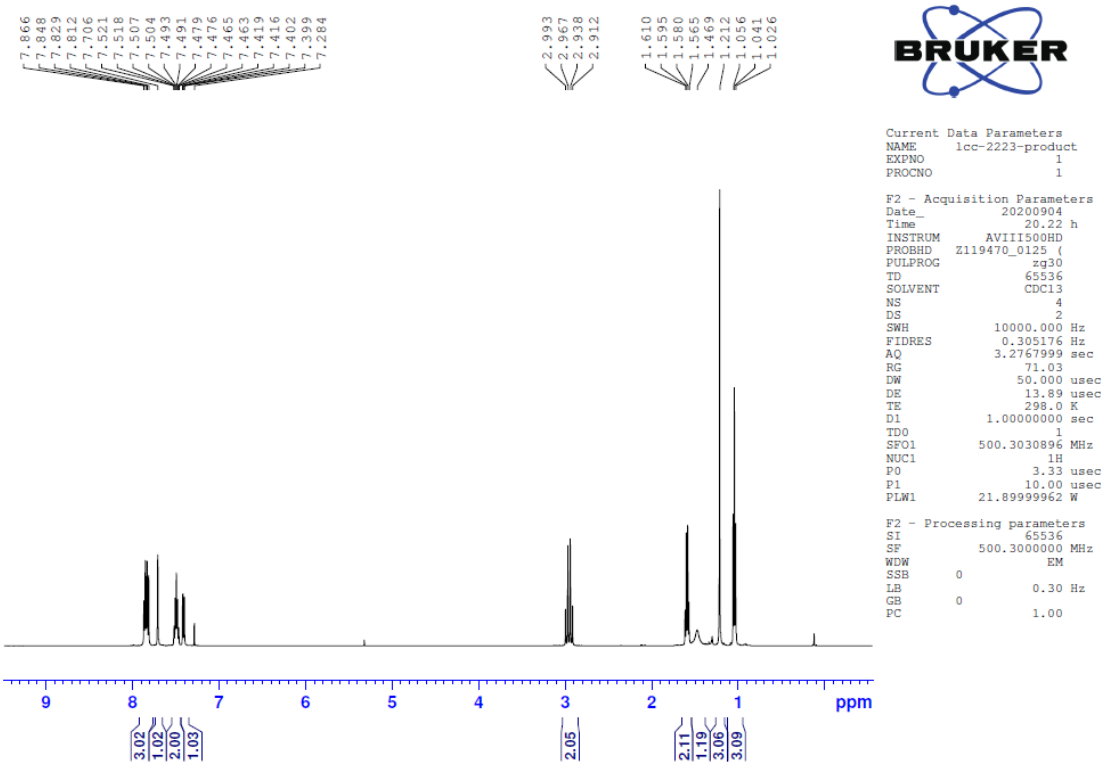
7.866
7.848
7.829
7.812
7.706
7.521
7.518
7.507
7.504
7.493
7.491
7.479
7.476
7.465
7.463
7.419
7.416
7.402
7.399
7.284
2.993
2.967
2.938
2.912
1.610
1.595
1.580
1.565
1.469
1.212
1.056
1.041
1.026
BRUKER
Current Data Parameters
NAME 1cc-2223-product
EXPNO 1
PROCNO 1
F2 - Acquisition Parameters
Date_ 20200904
Time 20.22 h
INSTRUM AVIII500HD
PROBHD Z119470_0125 (
PULPROG zg30
TD 65536
SOLVENT CDC13
NS 4
DS 2
SWH 10000.000 Hz
FIDRES 0.305176 Hz
AQ 3.2767999 sec
RG 71.03
DW 50.000 usec
DE 13.89 usec
TE 298.0 K
D1 1.00000000 sec
TD0 1
SFO1 500.3030896 MHz
NUC1 1H
P0 3.33 usec
P1 10.00 usec
PLW1 21.89999962 W
F2 - Processing parameters
SI 65536
SF 500.3000000 MHz
WDW EM
SSB 0
LB 0.30 Hz
GB 0
PC 1.00
9
8
7
6
5
4
3
2
1
ppm
3.02
1.02
2.00
1.03
2.05
2.11
1.19
3.06
3.09

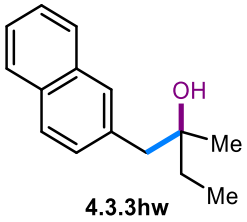

4.3.3hw

^{13}C NMR

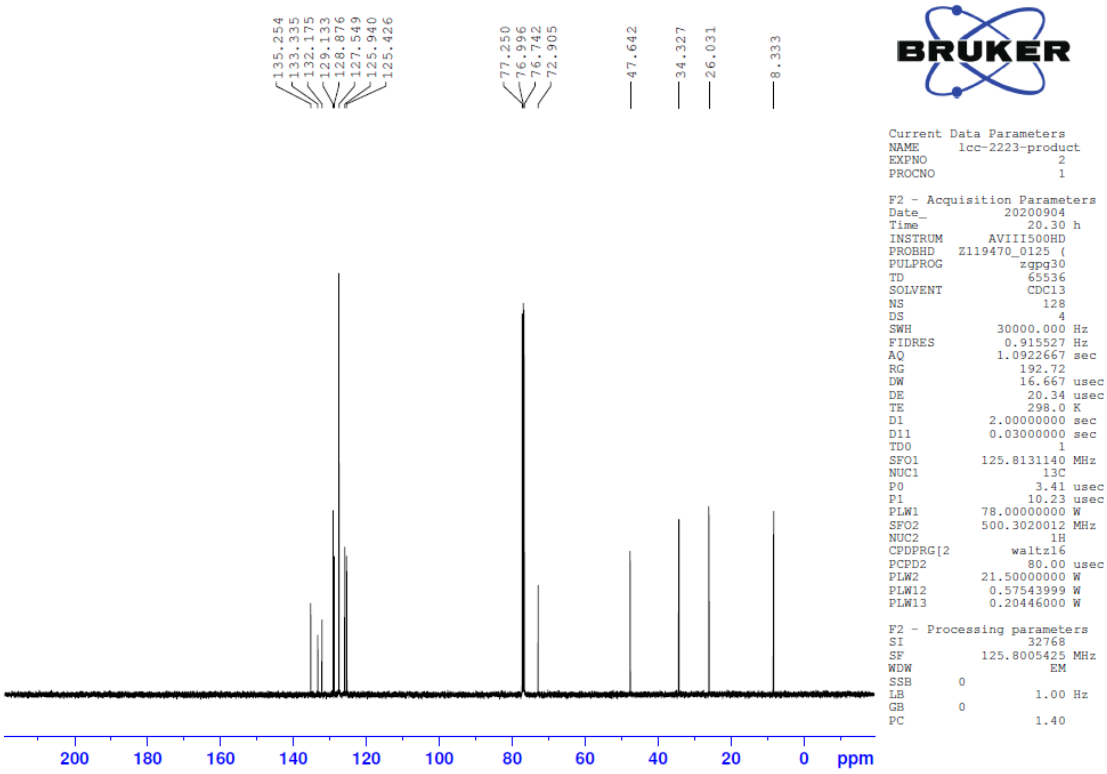


```
Current Data Parameters
NAME      lcc-2223-product
EXPNO                    2
PROCNO                   1

F2 - Acquisition Parameters
Date_           20200904
Time              20.30 h
INSTRUM       AVIII500HD
PROBHD    Z119470_0125 (
PULPROG          zgpg30
TD                65536
SOLVENT           CDCl3
NS                  128
DS                    4
SWH           30000.000 Hz
FIDRES            0.915527 Hz
AQ            1.0922667 sec
RG                192.72
DW                16.667 usec
DE                20.34 usec
TE                298.0 K
D1            2.00000000 sec
D11           0.03000000 sec
TD0                   1
SFO1         125.8131140 MHz
NUC1                 13C
P0                 3.41 usec
P1                10.23 usec
PLW1         78.00000000 W
SFO2         500.3020012 MHz
NUC2                 1H
CPDPRG[2          waltz16
PCPD2             80.00 usec
PLW2         21.50000000 W
PLW12         0.57543999 W
PLW13         0.20446000 W

F2 - Processing parameters
SI                32768
SF           125.8005425 MHz
WDW                  EM
SSB       0
LB                1.00 Hz
GB        0
PC                1.40
```

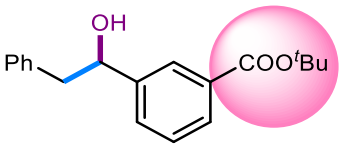

4.3.3ax

^{1}H NMR

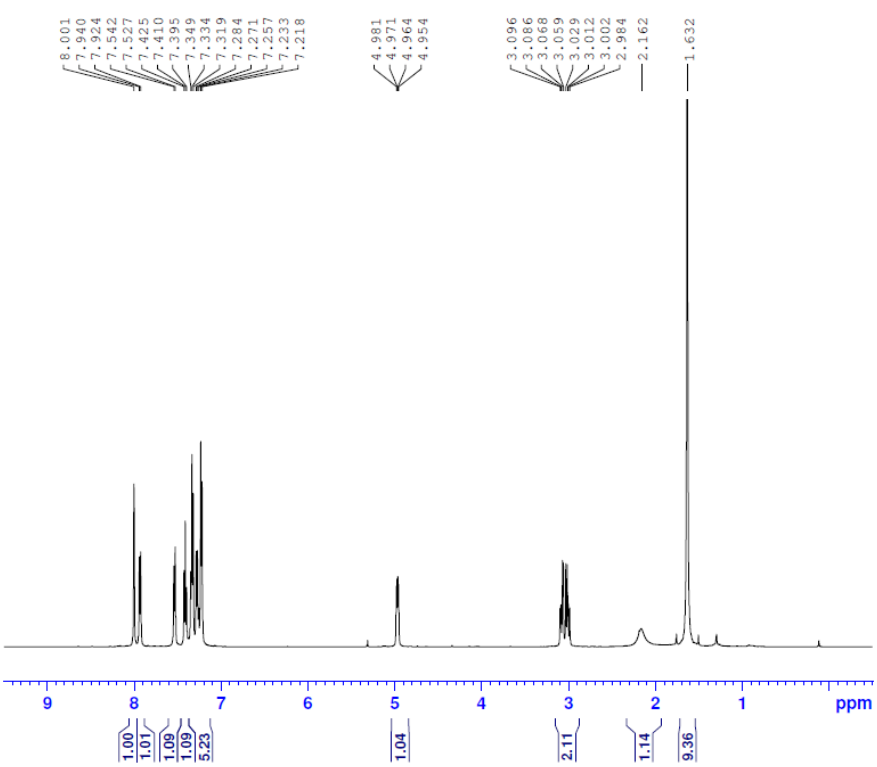


```
Current Data Parameters
NAME      1cc-2174-product
EXPNO                    1
PROCNO                   1

F2 - Acquisition Parameters
Date_             20200718
Time                20.05 h
INSTRUM       AVIII500HD
PROBHD    Z119470_0125 (
PULPROG              zg30
TD                  65536
SOLVENT             CDCl3
NS                      4
DS                      2
SWH             10000.000 Hz
FIDRES              0.305176 Hz
AQ                3.2767999 sec
RG                   32.48
DW                  50.000 usec
DE                  13.89 usec
TE                  298.0 K
D1              1.00000000 sec
TD0                     1
SFO1           500.3030896 MHz
NUC1                   1H
P0                   3.33 usec
P1                  10.00 usec
PLW1           21.89999962 W

F2 - Processing parameters
SI                  65536
SF             500.3000000 MHz
WDW                    EM
SSB       0
LB                   0.30 Hz
GB        0
PC                   1.00
```

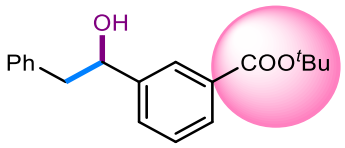

4.3.3ax

^{13}C NMR

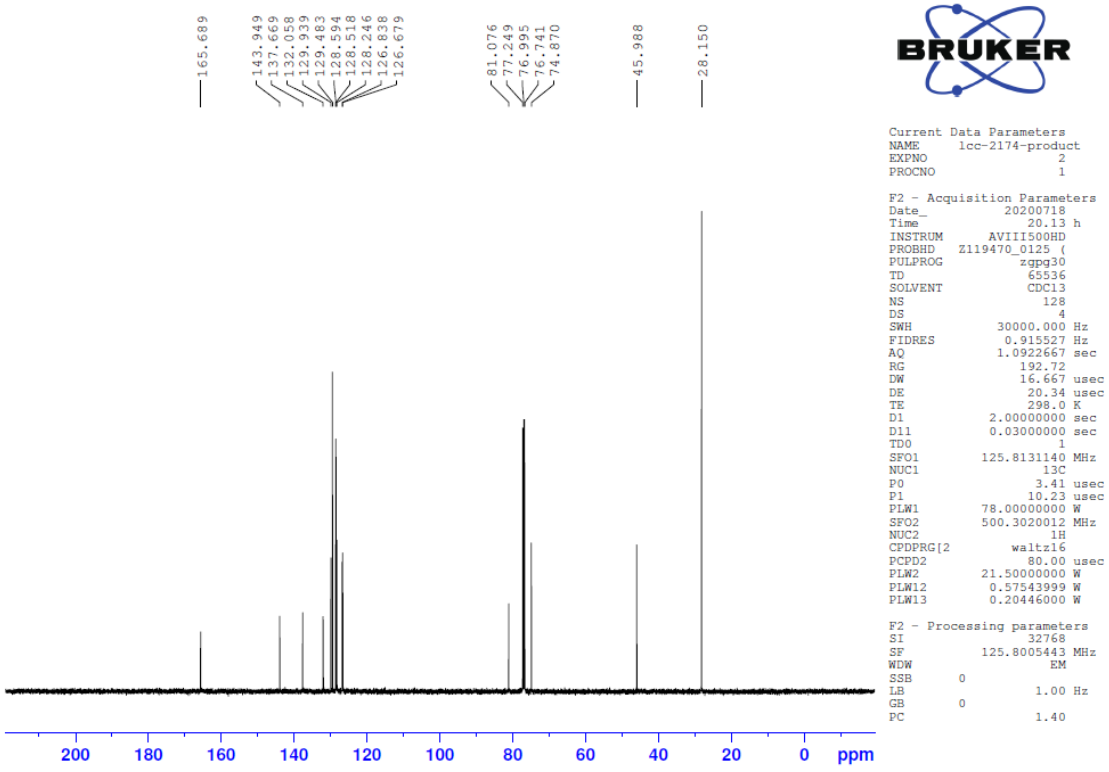

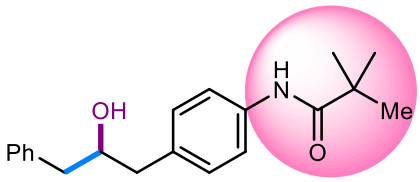

4.3.3az

^{1}H NMR

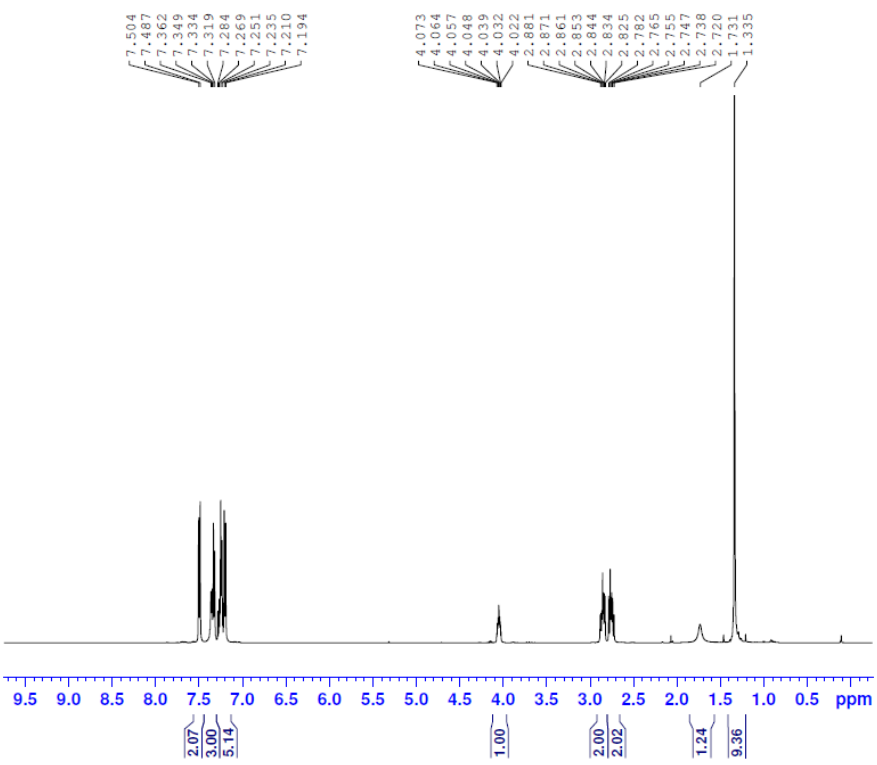


```
Current Data Parameters
NAME      1cc-2245-product
EXPNO                    1
PROCNO                   1

F2 - Acquisition Parameters
Date_             20200915
Time                10.36 h
INSTRUM       AVIII500HD
PROBHD   Z119470_0125 (
PULPROG             zg30
TD                 65536
SOLVENT            CDCl3
NS                     4
DS                     2
SWH            10000.000 Hz
FIDRES             0.305176 Hz
AQ                 3.2767999 sec
RG                    63.07
DW                 50.000 usec
DE                 13.89 usec
TE                 298.0 K
D1              1.00000000 sec
TD0                    1
SFO1          500.3030896 MHz
NUC1                  1H
P0                  3.33 usec
P1                 10.00 usec
PLW1          21.89999962 W

F2 - Processing parameters
SI                 65536
SF            500.3000000 MHz
WDW                   EM
SSB       0
LB                 0.30 Hz
GB        0
PC                 1.00
```

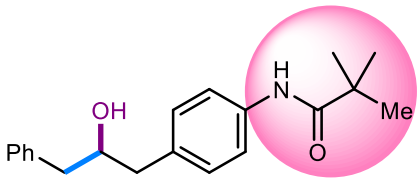

4.3.3az

^{13}C NMR

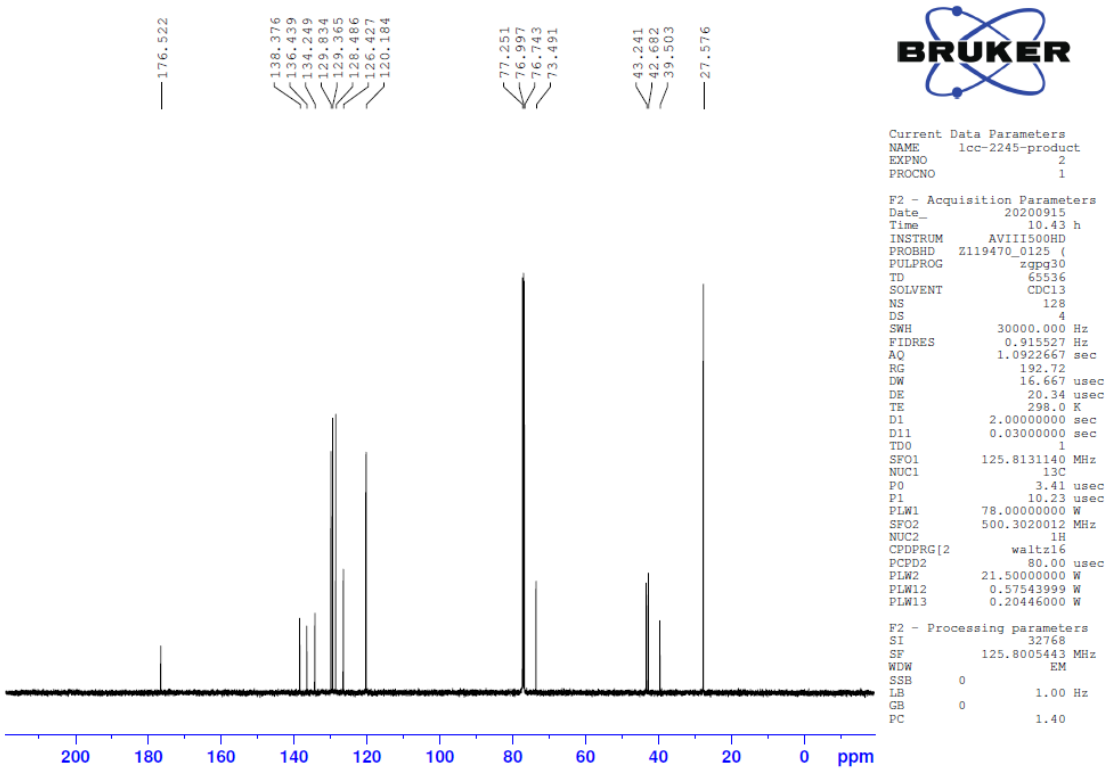


```
Current Data Parameters
NAME      1cc-2245-product
EXPNO                    2
PROCNO                   1

F2 - Acquisition Parameters
Date_           20200915
Time              10.43 h
INSTRUM       AVIII500HD
PROBHD   Z119470_0125 (
PULPROG          zgpg30
TD                65536
SOLVENT           CDCl3
NS                  128
DS                    4
SWH           30000.000 Hz
FIDRES        0.915527 Hz
AQ            1.0922667 sec
RG                192.72
DW                16.667 usec
DE                20.34 usec
TE                298.0 K
D1            2.00000000 sec
D11           0.03000000 sec
TD0                   1
SFO1        125.8131140 MHz
NUC1                13C
P0                 3.41 usec
P1                10.23 usec
PLW1        78.00000000 W
SFO2        500.3020012 MHz
NUC2                1H
CPDPRG[2         waltz16
PCPD2             80.00 usec
PLW2        21.50000000 W
PLW12        0.57543999 W
PLW13        0.20446000 W

F2 - Processing parameters
SI                32768
SF          125.8005443 MHz
WDW                  EM
SSB       0
LB                1.00 Hz
GB        0
PC                1.40
```

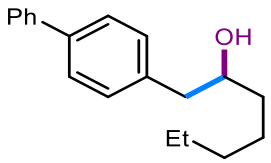
Ph
OH
Et

4.3.3ba

^{1}H NMR

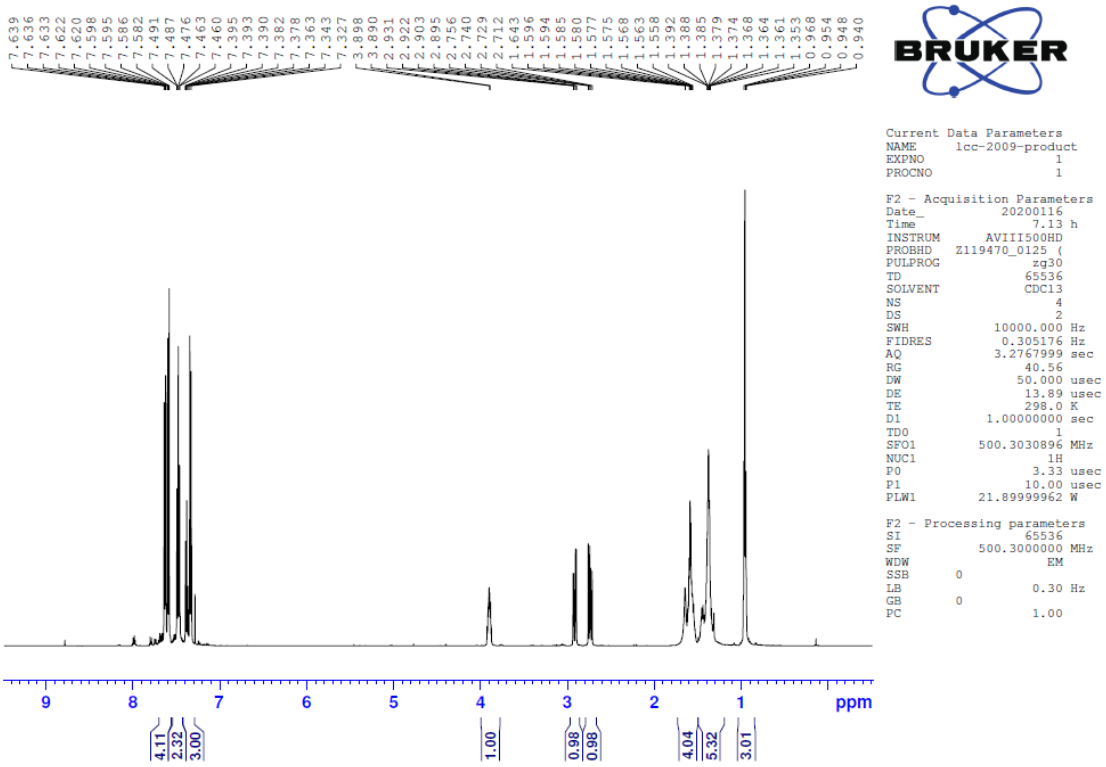
7.639
7.636
7.633
7.622
7.620
7.598
7.595
7.586
7.582
7.491
7.487
7.476
7.463
7.460
7.395
7.393
7.390
7.382
7.378
7.363
7.343
7.327
3.898
3.890
2.931
2.922
2.903
2.895
2.756
2.740
2.729
2.712
1.643
1.596
1.594
1.585
1.580
1.577
1.575
1.568
1.563
1.558
1.392
1.388
1.385
1.379
1.374
1.368
1.364
1.361
1.353
0.968
0.954
0.948
0.940
BRUKER
Current Data Parameters
NAME 1cc-2009-product
EXPNO 1
PROCNO 1
F2 - Acquisition Parameters
Date_ 20200116
Time 7.13 h
INSTRUM AVIII500HD
PROBHD Z119470_0125 (
PULPROG zg30
TD 65536
SOLVENT CDCl3
NS 4
DS 2
SWH 10000.000 Hz
FIDRES 0.305176 Hz
AQ 3.2767999 sec
RG 40.56
DW 50.000 usec
DE 13.89 usec
TE 298.0 K
D1 1.00000000 sec
TD0 1
SFO1 500.3030896 MHz
NUC1 1H
P0 3.33 usec
P1 10.00 usec
PLW1 21.89999962 W
F2 - Processing parameters
SI 65536
SF 500.3000000 MHz
WDW EM
SSB 0
LB 0.30 Hz
GB 0
PC 1.00
9
8
7
6
5
4
3
2
1
ppm
4.11
2.32
3.00
1.00
0.98
0.98
4.04
5.32
3.01

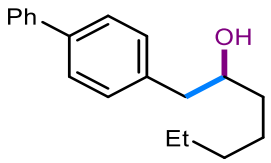

4.3.3ba

^{13}C NMR

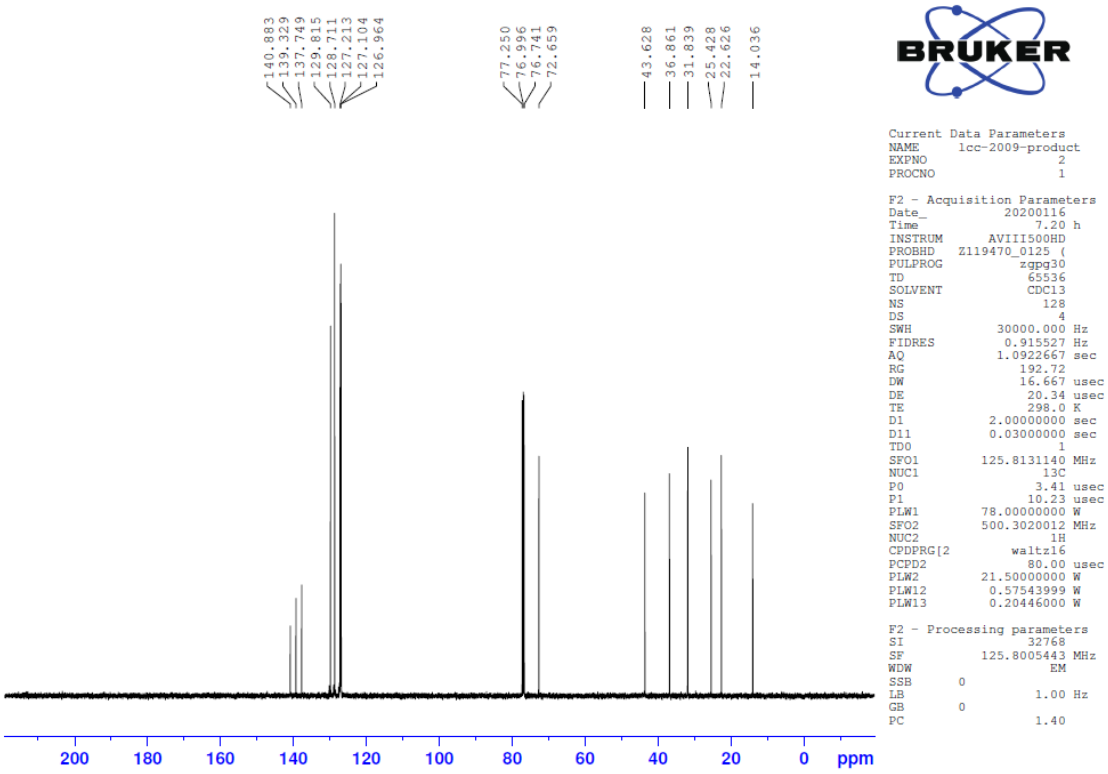


```
Current Data Parameters
NAME      lcc-2009-product
EXPNO                    2
PROCNO                   1

F2 - Acquisition Parameters
Date_           20200116
Time                7.20 h
INSTRUM       AVIII500HD
PROBHD   Z119470_0125 (
PULPROG           zgpg30
TD                65536
SOLVENT           CDCl3
NS                  128
DS                    4
SWH           30000.000 Hz
FIDRES            0.915527 Hz
AQ                1.0922667 sec
RG                  192.72
DW                  16.667 usec
DE                  20.34 usec
TE                 298.0 K
D1              2.00000000 sec
D11             0.03000000 sec
TD0                   1
SFO1          125.8131140 MHz
NUC1                 13C
P0                  3.41 usec
P1                 10.23 usec
PLW1          78.00000000 W
SFO2          500.3020012 MHz
NUC2                 1H
CPDPRG[2          waltz16
PCPD2               80.00 usec
PLW2          21.50000000 W
PLW12          0.57543999 W
PLW13          0.20446000 W

F2 - Processing parameters
SI                32768
SF          125.8005443 MHz
WDW                  EM
SSB       0
LB                  1.00 Hz
GB        0
PC                  1.40
```

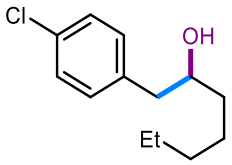
Cl
OH
Et

4.3.3ca

^{1}H NMR

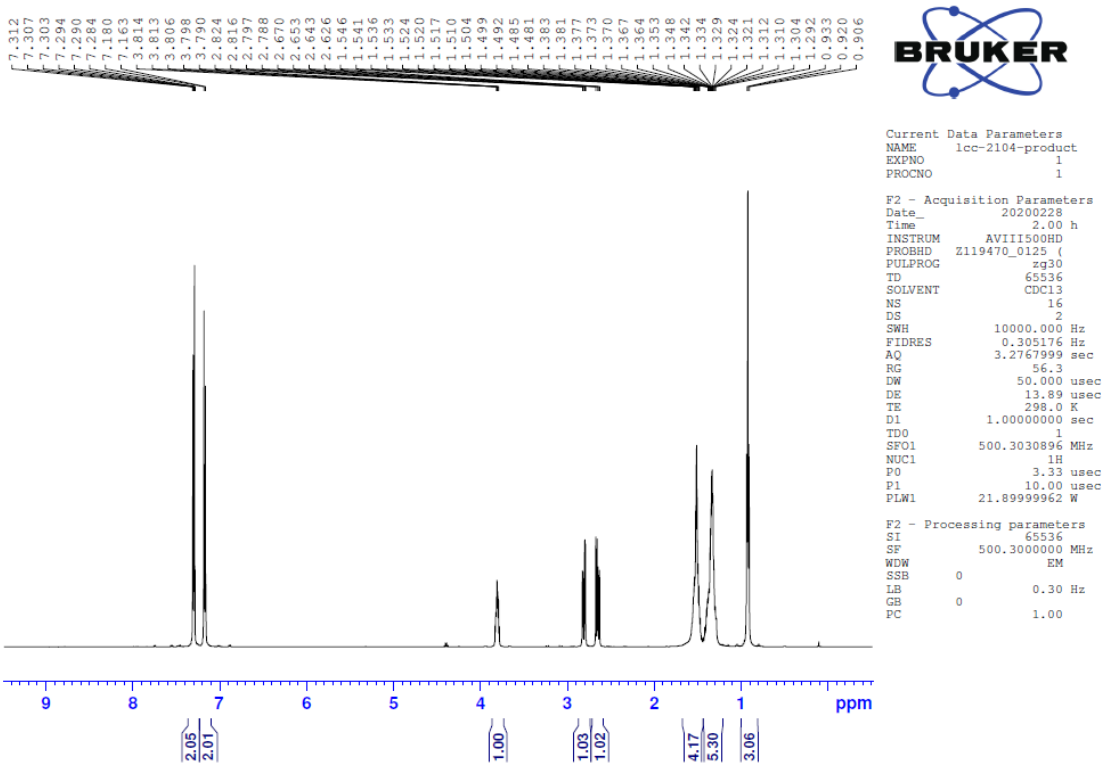
7.312
7.307
7.303
7.294
7.290
7.284
7.180
7.163
3.814
3.813
3.806
3.798
3.790
2.824
2.816
2.797
2.788
2.670
2.653
2.643
2.626
1.546
1.541
1.536
1.533
1.524
1.520
1.517
1.510
1.504
1.499
1.492
1.485
1.481
1.383
1.381
1.377
1.373
1.370
1.367
1.364
1.353
1.348
1.342
1.334
1.329
1.324
1.321
1.312
1.310
1.304
1.292
0.933
0.920
0.906
BRUKER
Current Data Parameters
NAME 1cc-2104-product
EXPNO 1
PROCNO 1
F2 - Acquisition Parameters
Date_ 20200228
Time 2.00 h
INSTRUM AVIII500HD
PROBHD Z119470_0125 (
PULPROG zg30
TD 65536
SOLVENT CDCl3
NS 16
DS 2
SWH 10000.000 Hz
FIDRES 0.305176 Hz
AQ 3.2767999 sec
RG 56.3
DW 50.000 usec
DE 13.89 usec
TE 298.0 K
D1 1.00000000 sec
TD0 1
SFO1 500.3030896 MHz
NUC1 1H
P0 3.33 usec
P1 10.00 usec
PLW1 21.89999962 W
F2 - Processing parameters
SI 65536
SF 500.3000000 MHz
WDW EM
SSB 0
LB 0.30 Hz
GB 0
PC 1.00
9
8
7
6
5
4
3
2
1
ppm
2.05
2.01
1.00
1.03
1.02
4.17
5.30
3.06

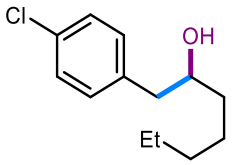

4.3.3ca

^{13}C NMR

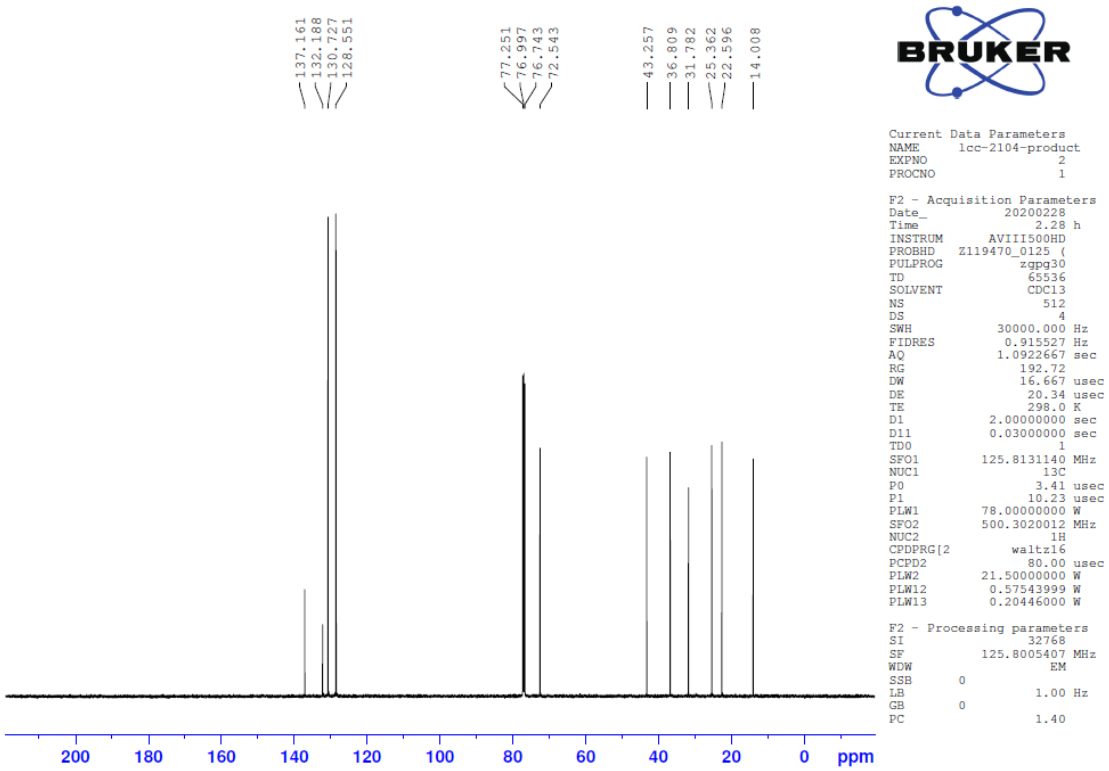


```
Current Data Parameters
NAME      1cc-2104-product
EXPNO                    2
PROCNO                   1

F2 - Acquisition Parameters
Date_           20200228
Time                2.28 h
INSTRUM       AVIII500HD
PROBHD    Z119470_0125 (
PULPROG           zgpg30
TD                65536
SOLVENT           CDCl3
NS                  512
DS                    4
SWH           30000.000 Hz
FIDRES         0.915527 Hz
AQ             1.0922667 sec
RG                192.72
DW                16.667 usec
DE                20.34 usec
TE                298.0 K
D1             2.00000000 sec
D11            0.03000000 sec
TD0                   1
SFO1         125.8131140 MHz
NUC1                 13C
P0                 3.41 usec
P1                10.23 usec
PLW1         78.00000000 W
SFO2         500.3020012 MHz
NUC2                 1H
CPDPRG[2         waltz16
PCPD2             80.00 usec
PLW2         21.50000000 W
PLW12         0.57543999 W
PLW13         0.20446000 W

F2 - Processing parameters
SI                32768
SF           125.8005407 MHz
WDW                  EM
SSB       0
LB                1.00 Hz
GB        0
PC                1.40
```

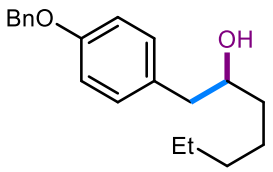
BnO
OH
Et

4.3.3da

^{1}H NMR

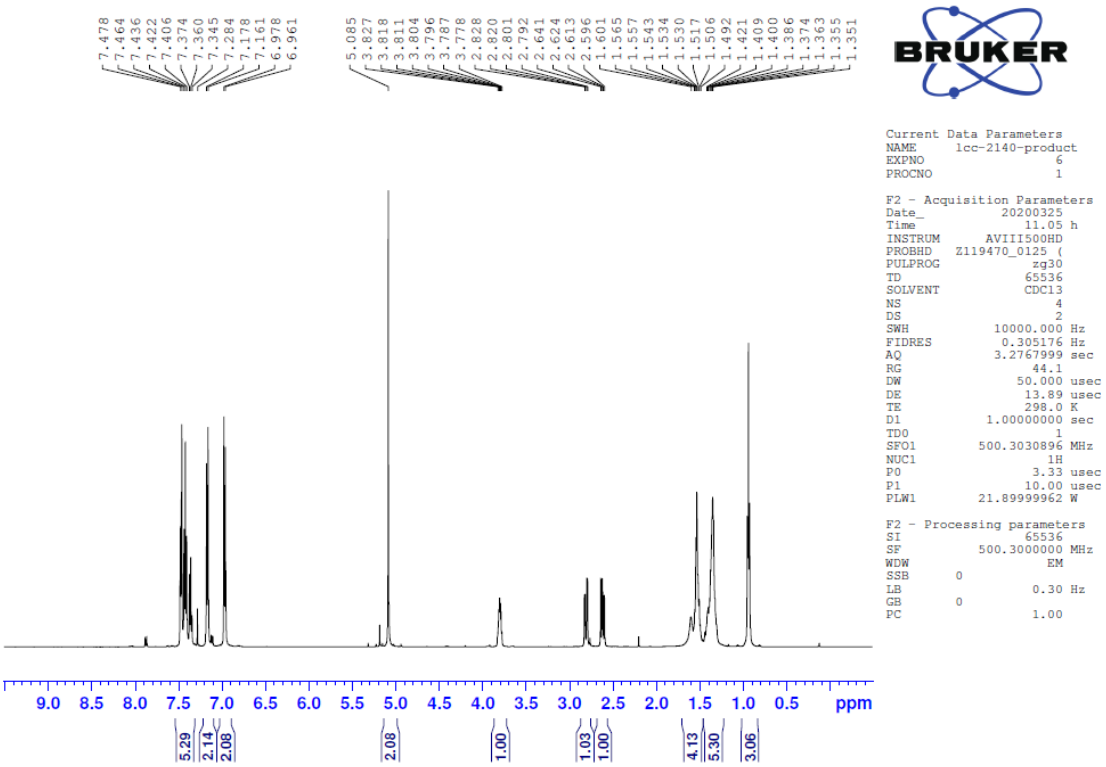
7.478
7.464
7.436
7.422
7.406
7.374
7.360
7.345
7.284
7.178
7.161
6.978
6.961
5.085
3.827
3.818
3.811
3.804
3.796
3.787
3.778
2.828
2.820
2.801
2.792
2.641
2.624
2.613
2.596
1.601
1.565
1.557
1.543
1.534
1.530
1.517
1.506
1.492
1.421
1.409
1.400
1.386
1.374
1.363
1.355
1.351
BRUKER
Current Data Parameters
NAME 1cc-2140-product
EXPNO 6
PROCNO 1
F2 - Acquisition Parameters
Date_ 20200325
Time 11.05 h
INSTRUM AVIII500HD
PROBHD Z119470_0125 (
PULPROG zg30
TD 65536
SOLVENT CDCl3
NS 4
DS 2
SWH 10000.000 Hz
FIDRES 0.305176 Hz
AQ 3.2767999 sec
RG 44.1
DW 50.000 usec
DE 13.89 usec
TE 298.0 K
D1 1.00000000 sec
TD0 1
SFO1 500.3030896 MHz
NUC1 1H
P0 3.33 usec
P1 10.00 usec
PLW1 21.89999962 W
F2 - Processing parameters
SI 65536
SF 500.3000000 MHz
WDW EM
SSB 0
LB 0.30 Hz
GB 0
PC 1.00
9.0 8.5 8.0 7.5 7.0 6.5 6.0 5.5 5.0 4.5 4.0 3.5 3.0 2.5 2.0 1.5 1.0 0.5 ppm
5.29
2.14
2.08
2.08
1.00
1.03
1.00
4.13
5.30
3.06

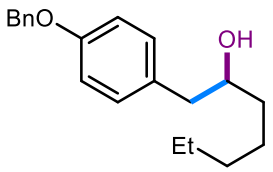

4.3.3da

^{13}C NMR

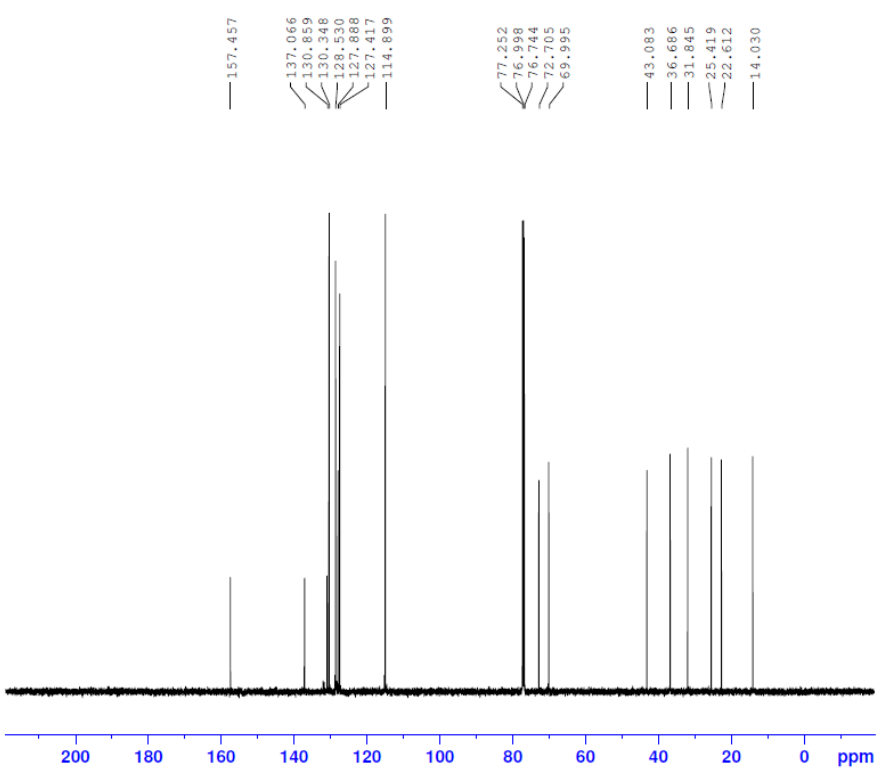


```
Current Data Parameters
NAME      1cc-2140-product
EXPNO                    7
PROCNO                   1

F2 - Acquisition Parameters
Date_           20200325
Time              11.04 h
INSTRUM       AVIII500HD
PROBHD    Z119470_0125 (
PULPROG          zgpg30
TD                65536
SOLVENT           CDCl3
NS                  128
DS                    4
SWH           30000.000 Hz
FIDRES        0.915527 Hz
AQ            1.0922667 sec
RG               192.72
DW               16.667 usec
DE               20.34 usec
TE               298.0 K
D1            2.00000000 sec
D11           0.03000000 sec
TD0                   1
SFO1        125.8131140 MHz
NUC1                13C
P0                3.41 usec
P1               10.23 usec
PLW1         78.00000000 W
SFO2         500.3020012 MHz
NUC2                1H
CPDPRG[2         waltz16
PCPD2            80.00 usec
PLW2         21.50000000 W
PLW12         0.57543999 W
PLW13         0.20446000 W

F2 - Processing parameters
SI                32768
SF          125.8005443 MHz
WDW                  EM
SSB       0
LB                1.00 Hz
GB        0
PC                1.40
```

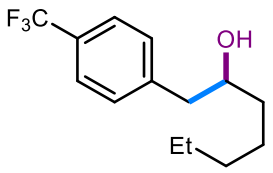
F3C
OH
Et

4.3.3ea

^{1}H NMR

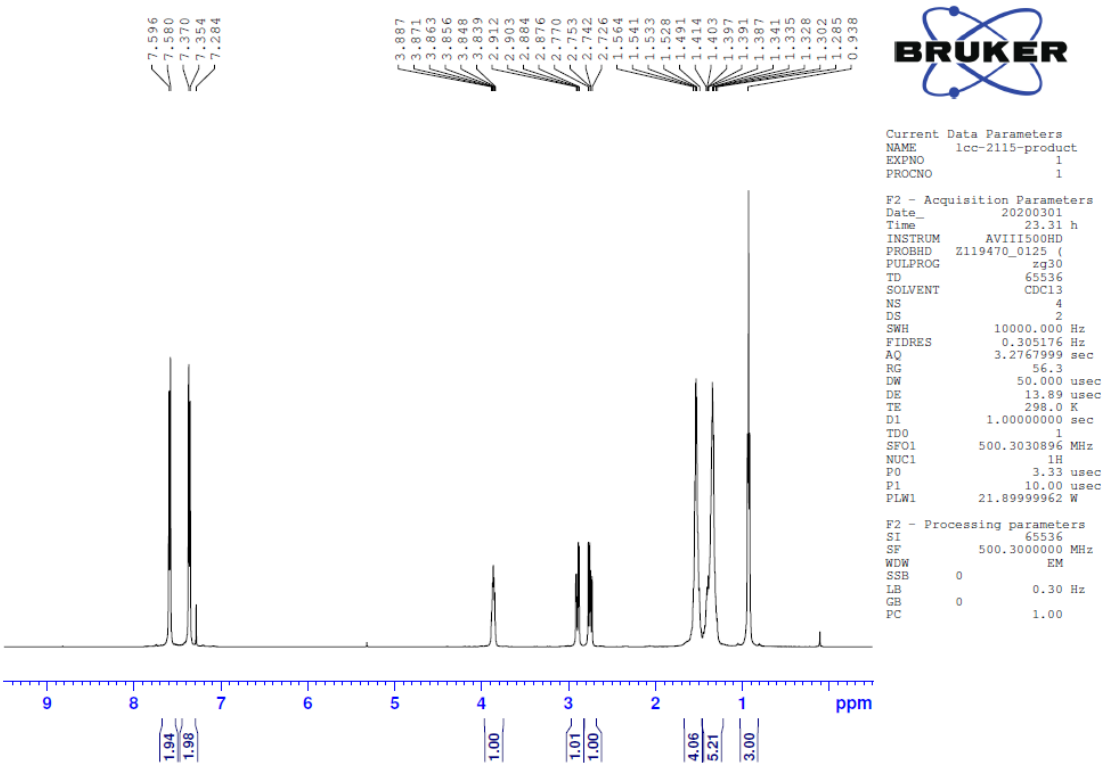
7.596
7.580
7.370
7.354
7.284
3.887
3.871
3.863
3.856
3.848
3.839
2.912
2.903
2.884
2.876
2.770
2.753
2.742
2.726
1.564
1.541
1.533
1.528
1.491
1.414
1.403
1.397
1.391
1.387
1.341
1.335
1.328
1.302
1.285
0.938
BRUKER
Current Data Parameters
NAME 1cc-2115-product
EXPNO 1
PROCNO 1
F2 - Acquisition Parameters
Date_ 20200301
Time 23.31 h
INSTRUM AVIII500HD
PROBHD Z119470_0125 (
PULPROG zg30
TD 65536
SOLVENT CDCl3
NS 4
DS 2
SWH 10000.000 Hz
FIDRES 0.305176 Hz
AQ 3.2767999 sec
RG 56.3
DW 50.000 usec
DE 13.89 usec
TE 298.0 K
D1 1.00000000 sec
TD0 1
SFO1 500.3030896 MHz
NUC1 1H
P0 3.33 usec
P1 10.00 usec
PLW1 21.89999962 W
F2 - Processing parameters
SI 65536
SF 500.3000000 MHz
WDW EM
SSB 0
LB 0.30 Hz
GB 0
PC 1.00
9
8
7
6
5
4
3
2
1
ppm
1.94
1.98
1.00
1.01
1.00
4.06
5.21
3.00

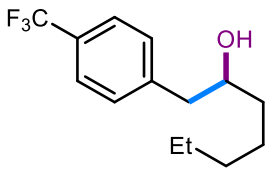

4.3.3ea

^{13}C NMR

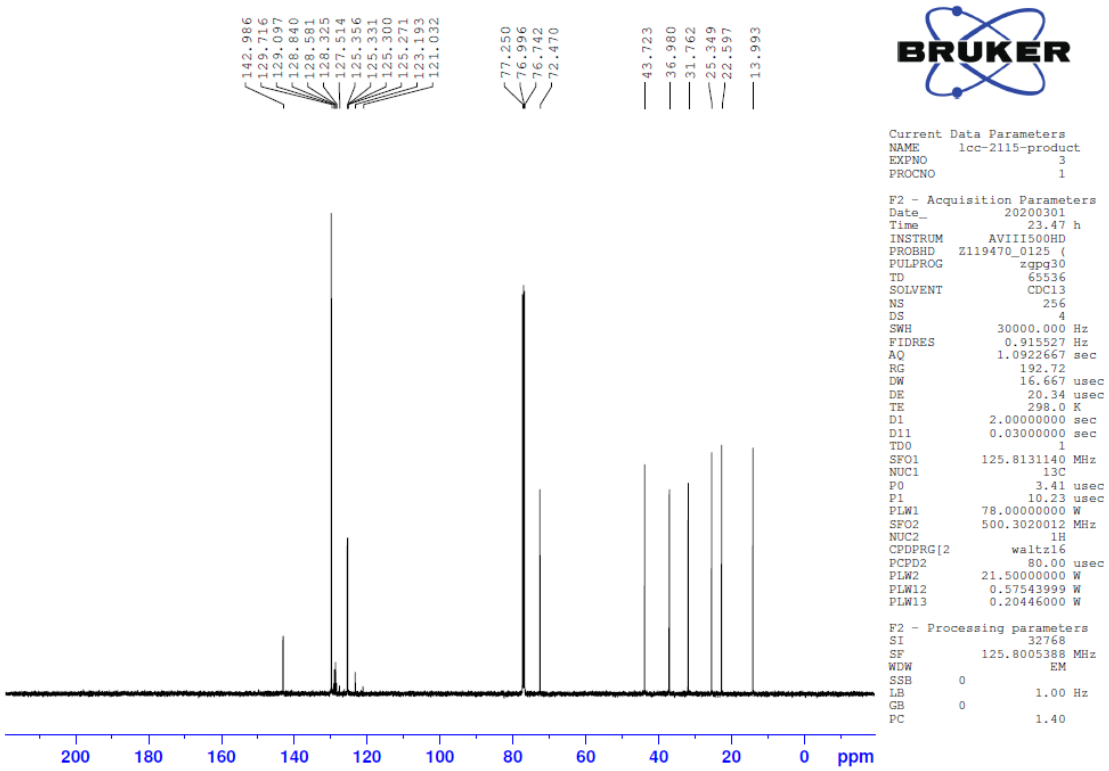


```
Current Data Parameters
NAME      1cc-2115-product
EXPNO                    3
PROCNO                   1

F2 - Acquisition Parameters
Date_           20200301
Time              23.47 h
INSTRUM       AVIII500HD
PROBHD    Z119470_0125 (
PULPROG           zgpg30
TD                65536
SOLVENT           CDCl3
NS                  256
DS                    4
SWH           30000.000 Hz
FIDRES            0.915527 Hz
AQ              1.0922667 sec
RG                192.72
DW                16.667 usec
DE                20.34 usec
TE                298.0 K
D1             2.00000000 sec
D11            0.03000000 sec
TD0                   1
SFO1         125.8131140 MHz
NUC1                 13C
P0                 3.41 usec
P1                10.23 usec
PLW1         78.00000000 W
SFO2         500.3020012 MHz
NUC2                 1H
CPDPRG[2          waltz16
PCPD2             80.00 usec
PLW2         21.50000000 W
PLW12         0.57543999 W
PLW13         0.20446000 W

F2 - Processing parameters
SI                32768
SF           125.8005388 MHz
WDW                  EM
SSB       0
LB                1.00 Hz
GB        0
PC                1.40
```

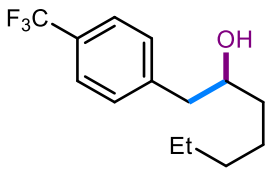

4.3.3ea

^{19}F NMR

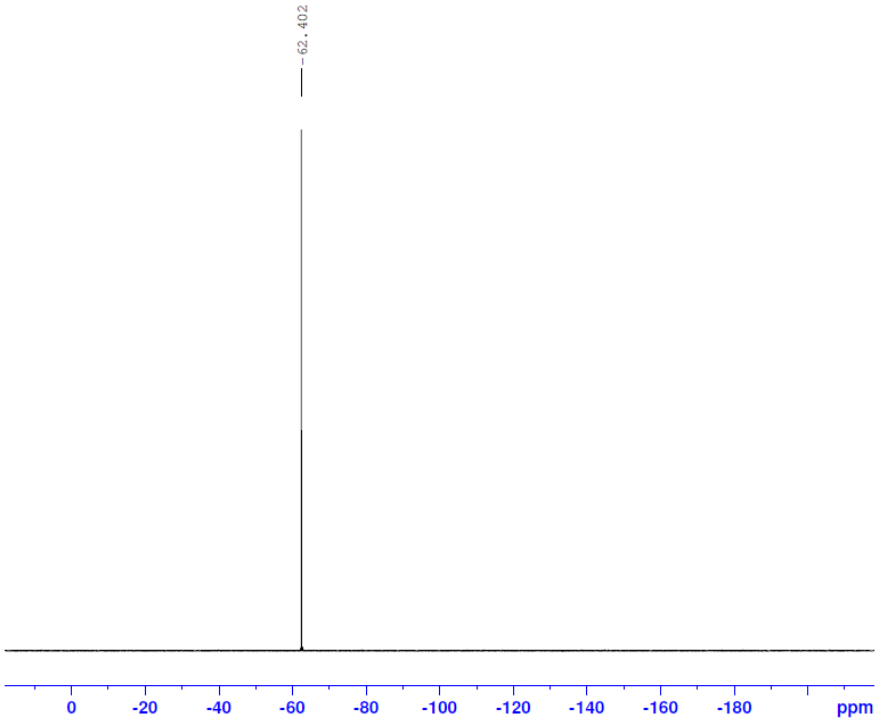


```
Current Data Parameters
NAME      1cc-2115-product
EXPNO                    2
PROCNO                   1

F2 - Acquisition Parameters
Date_           20200301
Time              23.32 h
INSTRUM       AVIII500HD
PROBHD    Z119470_0125 (
PULPROG   zgbsfhiqqn.baseopt
TD               131072
SOLVENT            CDCl3
NS                    16
DS                     4
SWH           111111.109 Hz
FIDRES          1.695421 Hz
AQ              0.5898240 sec
RG                192.72
DW                 4.500 usec
DE                35.33 usec
TE                298.0 K
D1             1.00000000 sec
D11            0.03000000 sec
D12            0.00002000 sec
TD0                    1
SFO1         470.7052618 MHz
NUC1                 19F
P1                15.00 usec
P2                30.00 usec
PLW1         39.50000000 W
SFO2         500.3025015 MHz
NUC2                 1H
CPDPRG[2         waltz16
PCPD2             80.00 usec
PLW2         21.50000000 W
PLW12         0.57543999 W

F2 - Processing parameters
SI                 65536
SF           470.7523370 MHz
WDW                   EM
SSB       0
LB                 0.30 Hz
GB        0
PC                 1.00
```

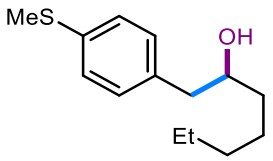
MeS
OH
Et

4.3.3fa

^{1}H NMR

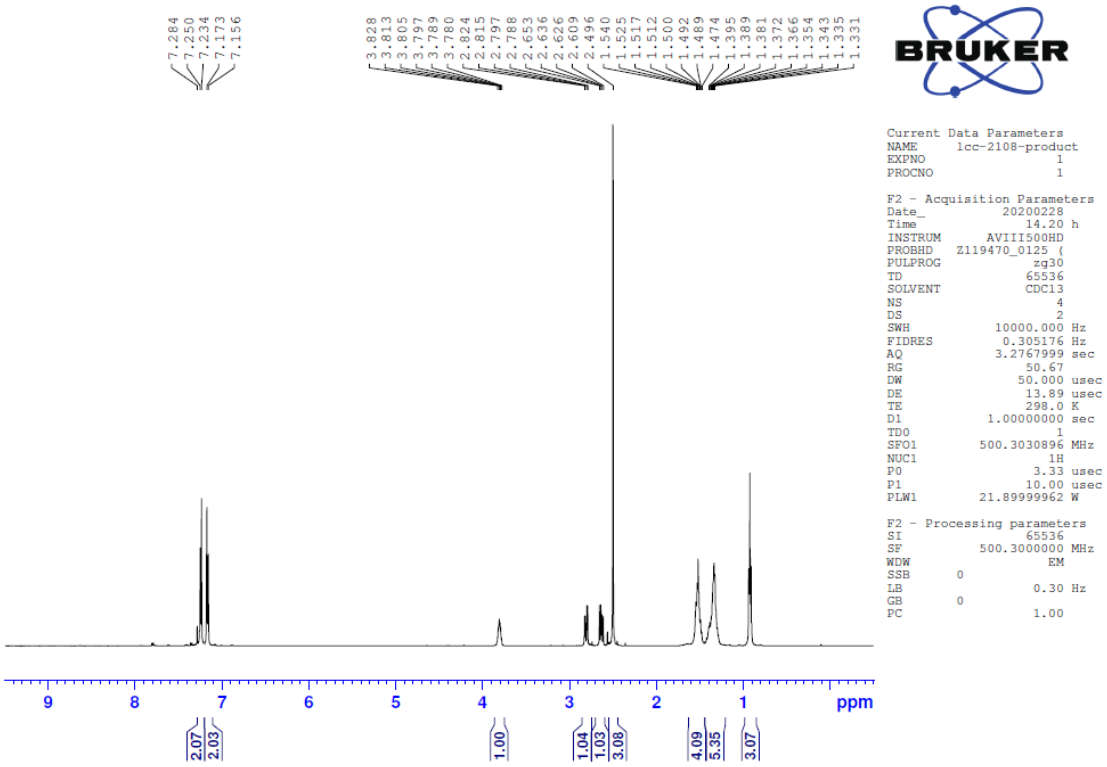
7.284
7.250
7.234
7.173
7.156
3.828
3.813
3.805
3.797
3.789
3.780
2.824
2.815
2.797
2.788
2.653
2.636
2.626
2.609
2.496
1.540
1.525
1.517
1.512
1.500
1.492
1.489
1.474
1.395
1.389
1.381
1.372
1.366
1.354
1.343
1.335
1.331
BRUKER
Current Data Parameters
NAME 1cc-2108-product
EXPNO 1
PROCNO 1
F2 - Acquisition Parameters
Date_ 20200228
Time 14.20 h
INSTRUM AVIII500HD
PROBHD Z119470_0125 (
PULPROG zg30
TD 65536
SOLVENT CDCl3
NS 4
DS 2
SWH 10000.000 Hz
FIDRES 0.305176 Hz
AQ 3.2767999 sec
RG 50.67
DW 50.000 usec
DE 13.89 usec
TE 298.0 K
D1 1.00000000 sec
TD0 1
SFO1 500.3030896 MHz
NUC1 1H
P0 3.33 usec
P1 10.00 usec
PLW1 21.89999962 W
F2 - Processing parameters
SI 65536
SF 500.3000000 MHz
WDW EM
SSB 0
LB 0.30 Hz
GB 0
PC 1.00
9
8
7
6
5
4
3
2
1
ppm
2.07
2.03
1.00
1.04
1.03
3.08
4.09
5.35
3.07

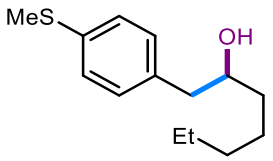

4.3.3fa

^{13}C NMR

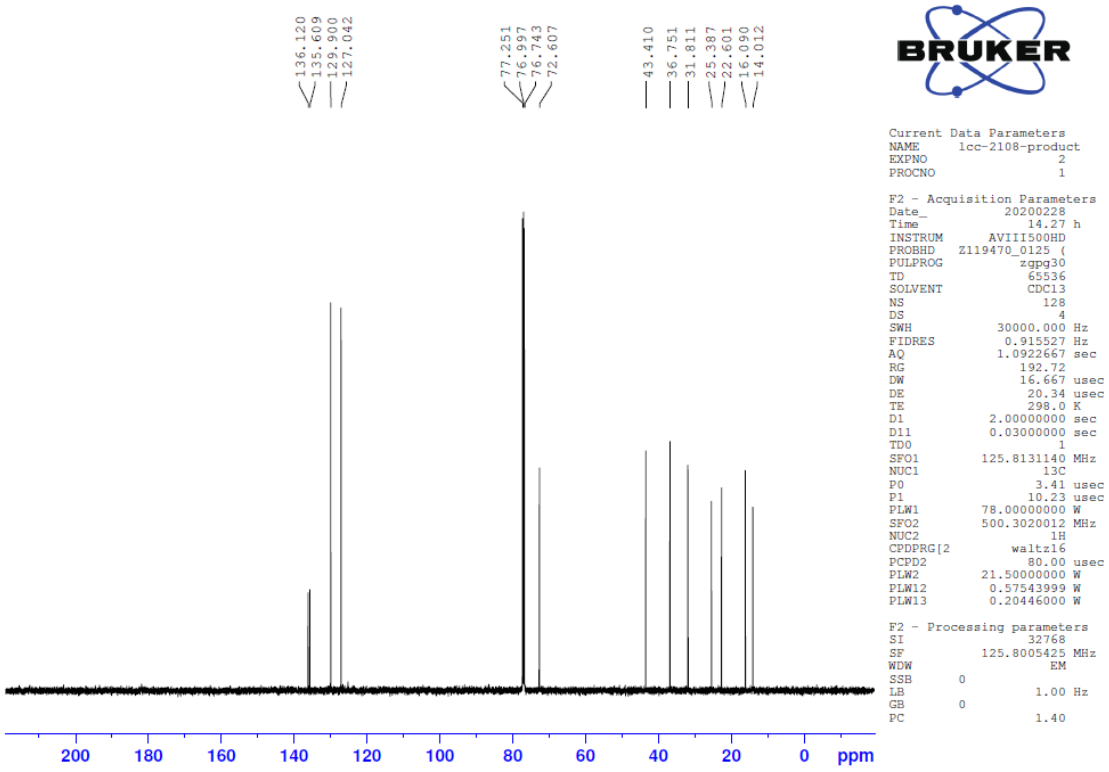


```
Current Data Parameters
NAME      1cc-2108-product
EXPNO                    2
PROCNO                   1

F2 - Acquisition Parameters
Date_           20200228
Time              14.27 h
INSTRUM       AVIII500HD
PROBHD    Z119470_0125 (
PULPROG          zgpg30
TD                65536
SOLVENT           CDCl3
NS                  128
DS                    4
SWH           30000.000 Hz
FIDRES            0.915527 Hz
AQ              1.0922667 sec
RG                192.72
DW                16.667 usec
DE                20.34 usec
TE                298.0 K
D1              2.00000000 sec
D11             0.03000000 sec
TD0                   1
SFO1          125.8131140 MHz
NUC1                 13C
P0                  3.41 usec
P1                 10.23 usec
PLW1          78.00000000 W
SFO2          500.3020012 MHz
NUC2                 1H
CPDPRG[2          waltz16
PCPD2               80.00 usec
PLW2          21.50000000 W
PLW12          0.57543999 W
PLW13          0.20446000 W

F2 - Processing parameters
SI                32768
SF            125.8005425 MHz
WDW                  EM
SSB       0
LB                1.00 Hz
GB        0
PC                1.40
```

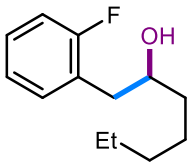
F
OH
Et

4.3.3ga

^{1}H NMR

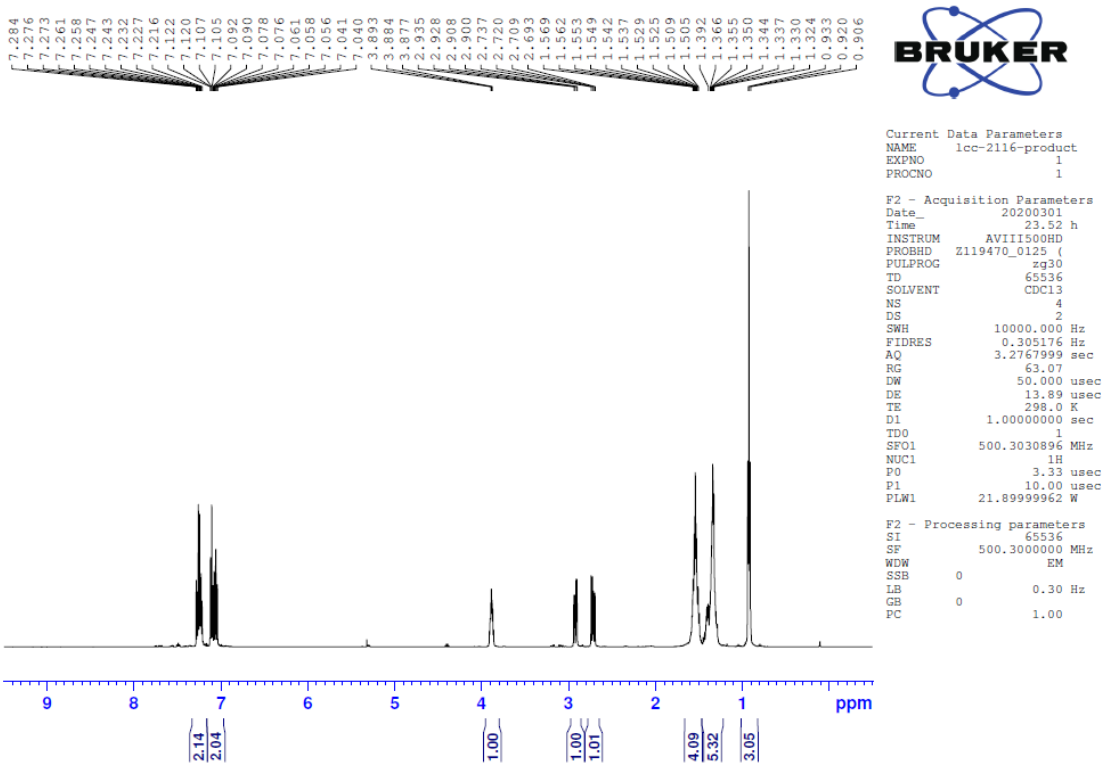
7.284
7.276
7.273
7.261
7.258
7.247
7.243
7.232
7.227
7.216
7.122
7.120
7.107
7.105
7.092
7.090
7.078
7.076
7.061
7.058
7.056
7.041
7.040
3.893
3.884
3.877
2.935
2.928
2.908
2.900
2.737
2.720
2.709
2.693
1.569
1.562
1.553
1.549
1.542
1.537
1.529
1.525
1.509
1.505
1.392
1.366
1.355
1.350
1.344
1.337
1.330
1.324
0.933
0.920
0.906
BRUKER
Current Data Parameters
NAME 1cc-2116-product
EXPNO 1
PROCNO 1
F2 - Acquisition Parameters
Date_ 20200301
Time 23.52 h
INSTRUM AVIII500HD
PROBHD Z119470_0125 (
PULPROG zg30
TD 65536
SOLVENT CDCl3
NS 4
DS 2
SWH 10000.000 Hz
FIDRES 0.305176 Hz
AQ 3.2767999 sec
RG 63.07
DW 50.000 usec
DE 13.89 usec
TE 298.0 K
D1 1.00000000 sec
TD0 1
SFO1 500.3030896 MHz
NUC1 1H
P0 3.33 usec
P1 10.00 usec
PLW1 21.89999962 W
F2 - Processing parameters
SI 65536
SF 500.3000000 MHz
WDW EM
SSB 0
LB 0.30 Hz
GB 0
PC 1.00
9
8
7
6
5
4
3
2
1
ppm
2.14
2.04
1.00
1.00
1.01
4.09
5.32
3.05

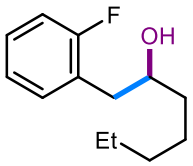

4.3.3ga

^{13}C NMR

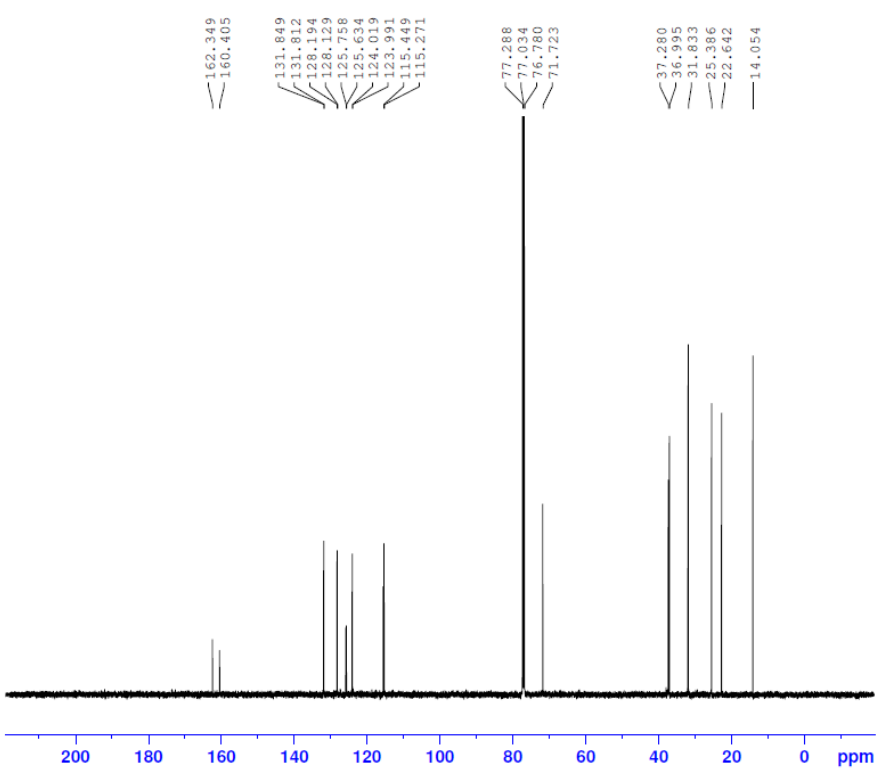


```
Current Data Parameters
NAME      1cc-2116-product
EXPNO                    3
PROCNO                   1

F2 - Acquisition Parameters
Date_           20200302
Time                0.08 h
INSTRUM       AVIII500HD
PROBHD    Z119470_0125 (
PULPROG           zgpg30
TD                65536
SOLVENT           CDCl3
NS                  256
DS                    4
SWH           30000.000 Hz
FIDRES            0.915527 Hz
AQ                1.0922667 sec
RG                  192.72
DW                  16.667 usec
DE                  20.34 usec
TE                  298.0 K
D1              2.00000000 sec
D11             0.03000000 sec
TD0                   1
SFO1          125.8131140 MHz
NUC1                 13C
P0                  3.41 usec
P1                 10.23 usec
PLW1          78.00000000 W
SFO2          500.3020012 MHz
NUC2                 1H
CPDPRG[2          waltz16
PCPD2               80.00 usec
PLW2          21.50000000 W
PLW12          0.57543999 W
PLW13          0.20446000 W

F2 - Processing parameters
SI                  32768
SF            125.8005351 MHz
WDW                    EM
SSB       0
LB                  1.00 Hz
GB        0
PC                  1.40
```

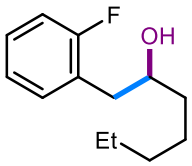

4.3.3ga

^{19}F NMR

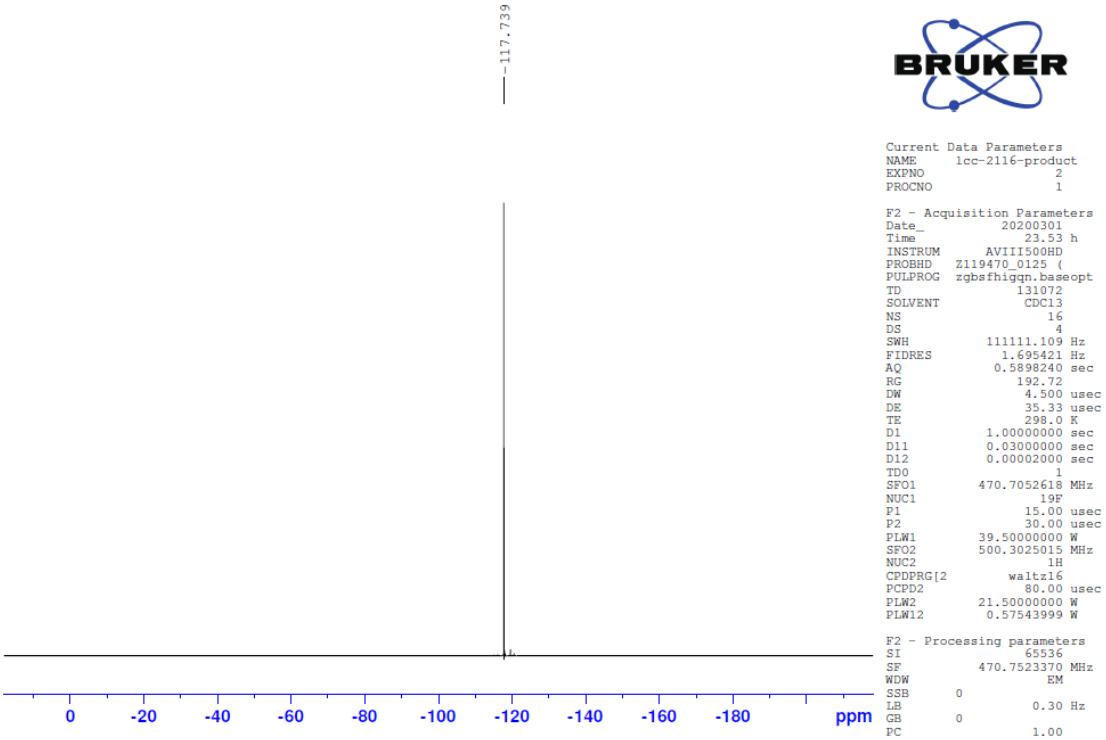

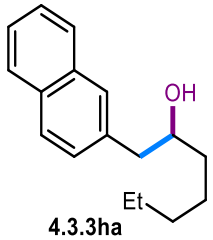
OH
Et

4.3.3ha

^{1}H NMR

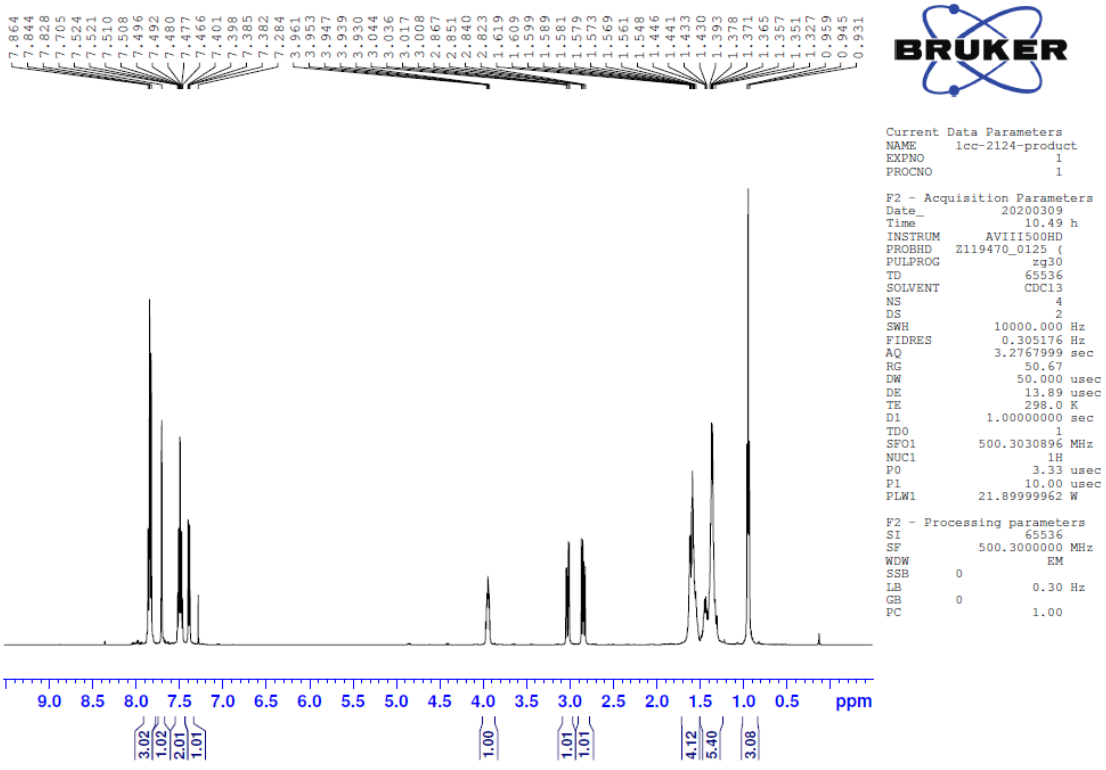
7.864
7.844
7.828
7.705
7.524
7.521
7.510
7.508
7.496
7.492
7.480
7.477
7.466
7.401
7.398
7.385
7.382
7.284
3.961
3.953
3.947
3.939
3.930
3.044
3.036
3.017
3.008
2.867
2.851
2.840
2.823
1.619
1.609
1.599
1.589
1.581
1.579
1.573
1.569
1.561
1.548
1.446
1.441
1.433
1.430
1.393
1.378
1.371
1.365
1.357
1.351
1.327
0.959
0.945
0.931
BRUKER
Current Data Parameters
NAME 1cc-2124-product
EXPNO 1
PROCNO 1
F2 - Acquisition Parameters
Date_ 20200309
Time 10.49 h
INSTRUM AVIII500HD
PROBHD Z119470_0125 (
PULPROG zg30
TD 65536
SOLVENT CDCl3
NS 4
DS 2
SWH 10000.000 Hz
FIDRES 0.305176 Hz
AQ 3.2767999 sec
RG 50.67
DW 50.000 usec
DE 13.89 usec
TE 298.0 K
D1 1.00000000 sec
TD0 1
SFO1 500.3030896 MHz
NUC1 1H
P0 3.33 usec
P1 10.00 usec
PLW1 21.89999962 W
F2 - Processing parameters
SI 65536
SF 500.3000000 MHz
WDW EM
SSB 0
LB 0.30 Hz
GB 0
PC 1.00
9.0 8.5 8.0 7.5 7.0 6.5 6.0 5.5 5.0 4.5 4.0 3.5 3.0 2.5 2.0 1.5 1.0 0.5 ppm
3.02
1.02
2.01
1.01
1.00
1.01
1.01
4.12
5.40
3.08

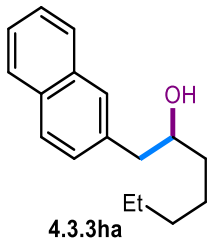

4.3.3ha

^{13}C NMR

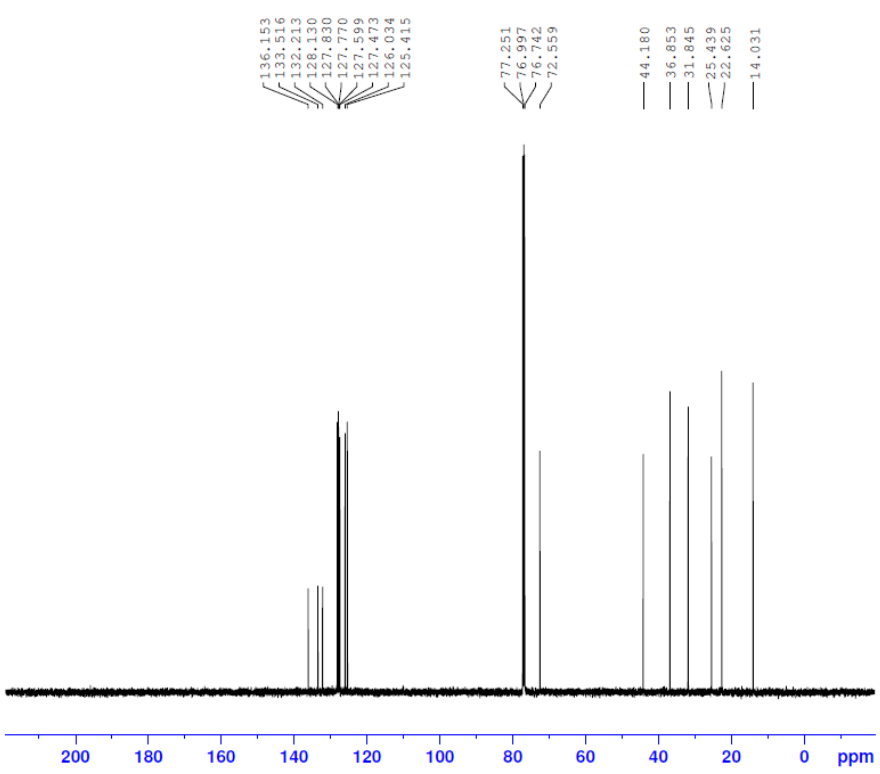

BRUKER

```
Current Data Parameters
NAME      1cc-2124-product
EXPNO                    2
PROCNO                   1

F2 - Acquisition Parameters
Date_           20200309
Time              10.57 h
INSTRUM       AVIII500HD
PROBHD   Z119470_0125 (
PULPROG          zgpg30
TD                65536
SOLVENT           CDCl3
NS                  128
DS                    4
SWH           30000.000 Hz
FIDRES            0.915527 Hz
AQ                1.0922667 sec
RG                  192.72
DW                  16.667 usec
DE                  20.34 usec
TE                  298.0 K
D1                2.00000000 sec
D11               0.03000000 sec
TD0                       1
SFO1         125.8131140 MHz
NUC1                    13C
P0                    3.41 usec
P1                   10.23 usec
PLW1         78.00000000 W
SFO2         500.3020012 MHz
NUC2                    1H
CPDPRG[2          waltz16
PCPD2                80.00 usec
PLW2         21.50000000 W
PLW12         0.57543999 W
PLW13         0.20446000 W

F2 - Processing parameters
SI                   32768
SF           125.8005434 MHz
WDW                     EM
SSB       0
LB                    1.00 Hz
GB        0
PC                    1.40
```

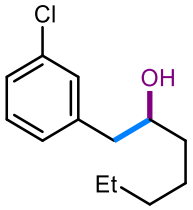
Cl
OH
Et

4.3.3ia

^{1}H NMR

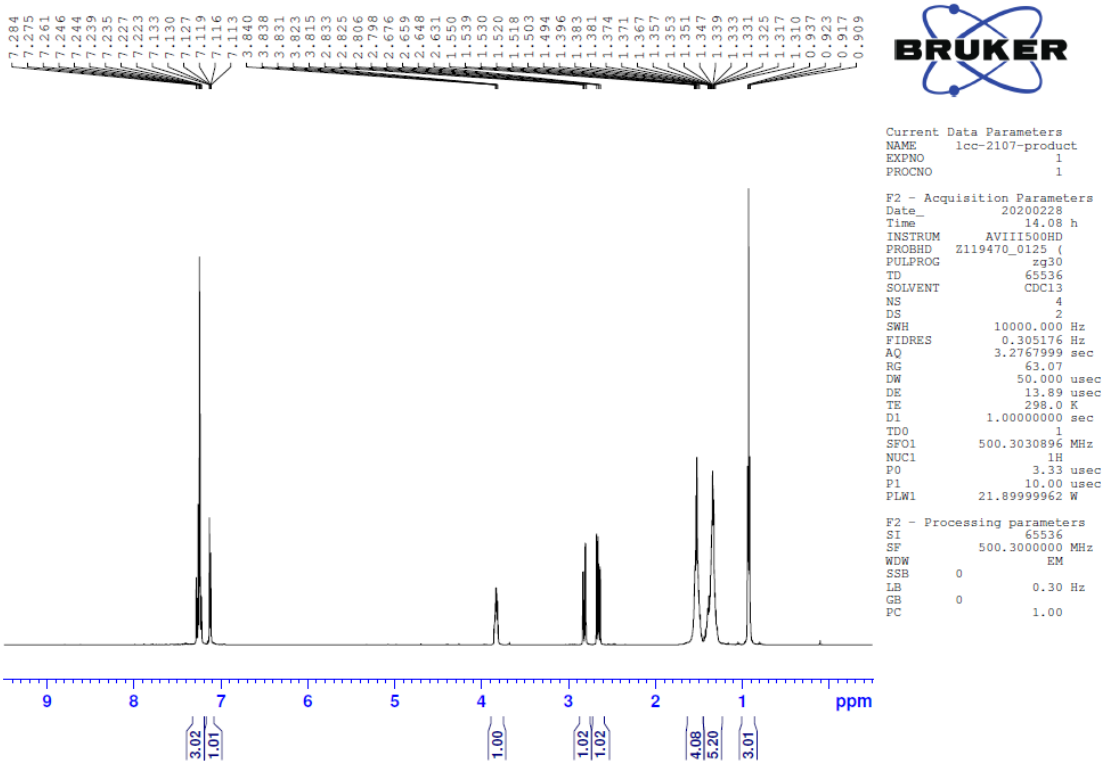
7.284
7.275
7.261
7.246
7.244
7.239
7.235
7.227
7.223
7.133
7.130
7.127
7.119
7.116
7.113
3.840
3.838
3.831
3.823
3.815
3.833
2.825
2.806
2.798
2.676
2.659
2.648
2.631
1.550
1.539
1.530
1.520
1.518
1.503
1.494
1.396
1.383
1.381
1.374
1.371
1.367
1.357
1.353
1.351
1.347
1.339
1.333
1.331
1.325
1.317
1.310
0.937
0.923
0.917
0.909
BRUKER
Current Data Parameters
NAME 1cc-2107-product
EXPNO 1
PROCNO 1
F2 - Acquisition Parameters
Date_ 20200228
Time 14.08 h
INSTRUM AVIII500HD
PROBHD Z119470_0125 (
PULPROG zg30
TD 65536
SOLVENT CDCl3
NS 4
DS 2
SWH 10000.000 Hz
FIDRES 0.305176 Hz
AQ 3.2767999 sec
RG 63.07
DW 50.000 usec
DE 13.89 usec
TE 298.0 K
D1 1.00000000 sec
TD0 1
SFO1 500.3030896 MHz
NUC1 1H
P0 3.33 usec
P1 10.00 usec
PLW1 21.89999962 W
F2 - Processing parameters
SI 65536
SF 500.3000000 MHz
WDW EM
SSB 0
LB 0.30 Hz
GB 0
PC 1.00
9
8
7
6
5
4
3
2
1
ppm
3.02
1.01
1.00
1.02
1.02
4.08
5.20
3.01

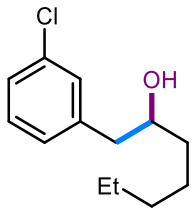

4.3.3ia

^{13}C NMR

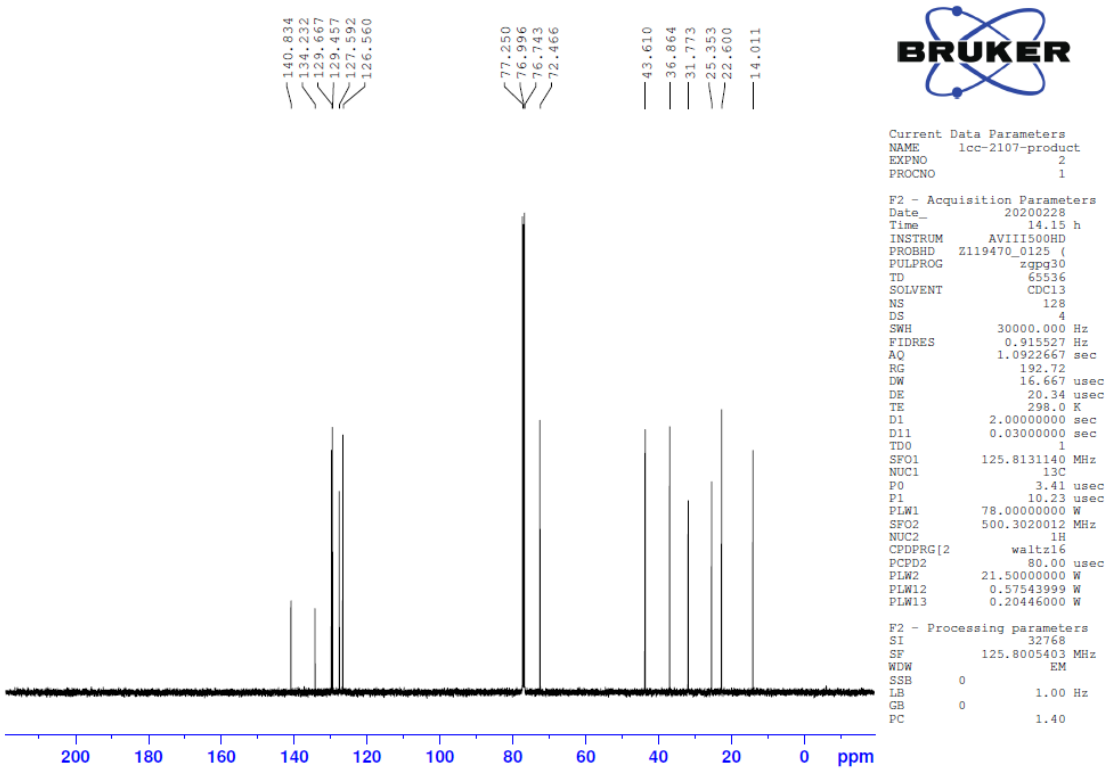


```
Current Data Parameters
NAME      1cc-2107-product
EXPNO                    2
PROCNO                   1

F2 - Acquisition Parameters
Date_           20200228
Time              14.15 h
INSTRUM       AVIII500HD
PROBHD    Z119470_0125 (
PULPROG           zgpg30
TD                65536
SOLVENT           CDCl3
NS                  128
DS                    4
SWH           30000.000 Hz
FIDRES        0.915527 Hz
AQ            1.0922667 sec
RG               192.72
DW               16.667 usec
DE                20.34 usec
TE                298.0 K
D1            2.00000000 sec
D11           0.03000000 sec
TD0                   1
SFO1        125.8131140 MHz
NUC1                13C
P0                 3.41 usec
P1                10.23 usec
PLW1         78.00000000 W
SFO2        500.3020012 MHz
NUC2                1H
CPDPRG[2         waltz16
PCPD2             80.00 usec
PLW2         21.50000000 W
PLW12         0.57543999 W
PLW13         0.20446000 W

F2 - Processing parameters
SI                32768
SF          125.8005403 MHz
WDW                  EM
SSB       0
LB                1.00 Hz
GB        0
PC                1.40
```

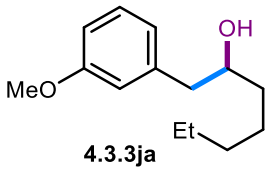
OH
MeO
Et

4.3.3ja

^{1}H NMR

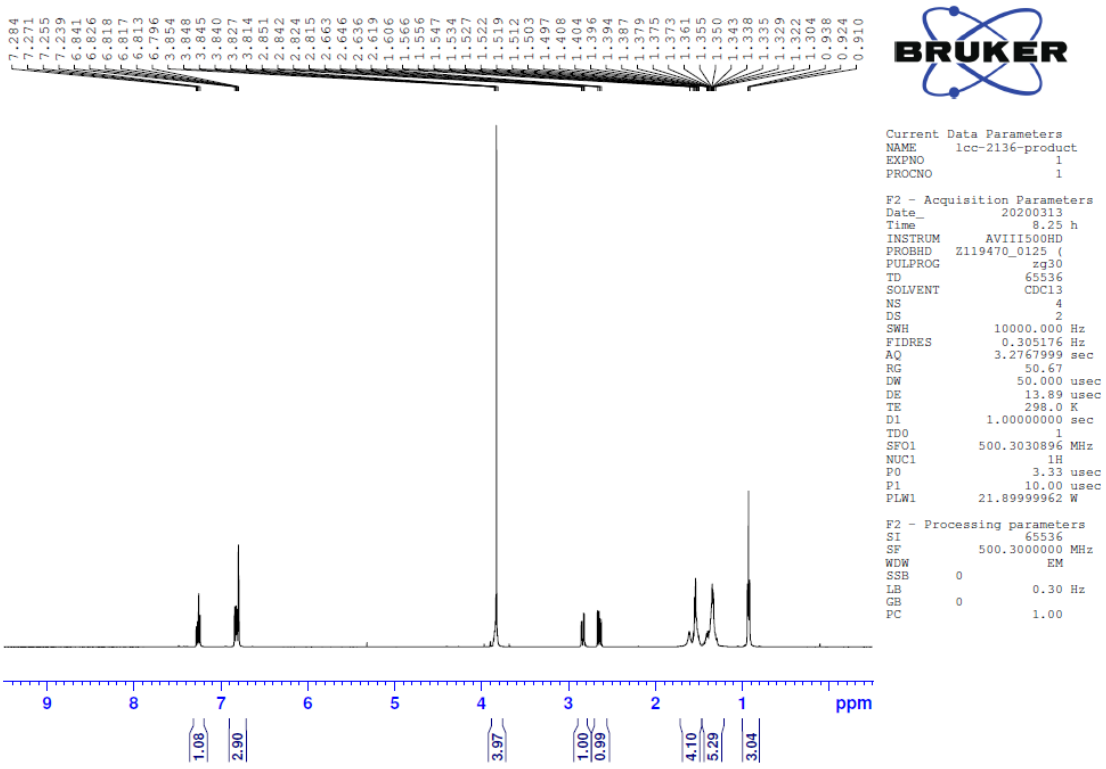
7.284
7.271
7.255
7.239
6.841
6.826
6.818
6.817
6.813
6.796
3.854
3.848
3.845
3.840
3.827
3.814
2.851
2.842
2.824
2.815
2.663
2.646
2.636
2.619
1.606
1.566
1.556
1.547
1.534
1.527
1.522
1.519
1.512
1.503
1.497
1.408
1.404
1.396
1.394
1.387
1.379
1.375
1.373
1.361
1.355
1.350
1.343
1.338
1.335
1.329
1.322
1.304
0.938
0.924
0.910
BRUKER
Current Data Parameters
NAME 1cc-2136-product
EXPNO 1
PROCNO 1
F2 - Acquisition Parameters
Date_ 20200313
Time 8.25 h
INSTRUM AVIII500HD
PROBHD Z119470_0125 (
PULPROG zg30
TD 65536
SOLVENT CDC13
NS 4
DS 2
SWH 10000.000 Hz
FIDRES 0.305176 Hz
AQ 3.2767999 sec
RG 50.67
DW 50.000 usec
DE 13.89 usec
TE 298.0 K
D1 1.00000000 sec
TD0 1
SFO1 500.3030896 MHz
NUC1 1H
P0 3.33 usec
P1 10.00 usec
PLW1 21.89999962 W
F2 - Processing parameters
SI 65536
SF 500.3000000 MHz
WDW EM
SSB 0
LB 0.30 Hz
GB 0
PC 1.00
9
8
7
6
5
4
3
2
1
ppm
1.08
2.90
3.97
1.00
0.99
4.10
5.29
3.04

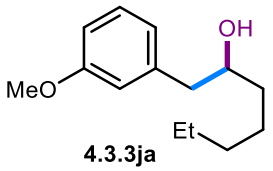

4.3.3ja

^{13}C NMR

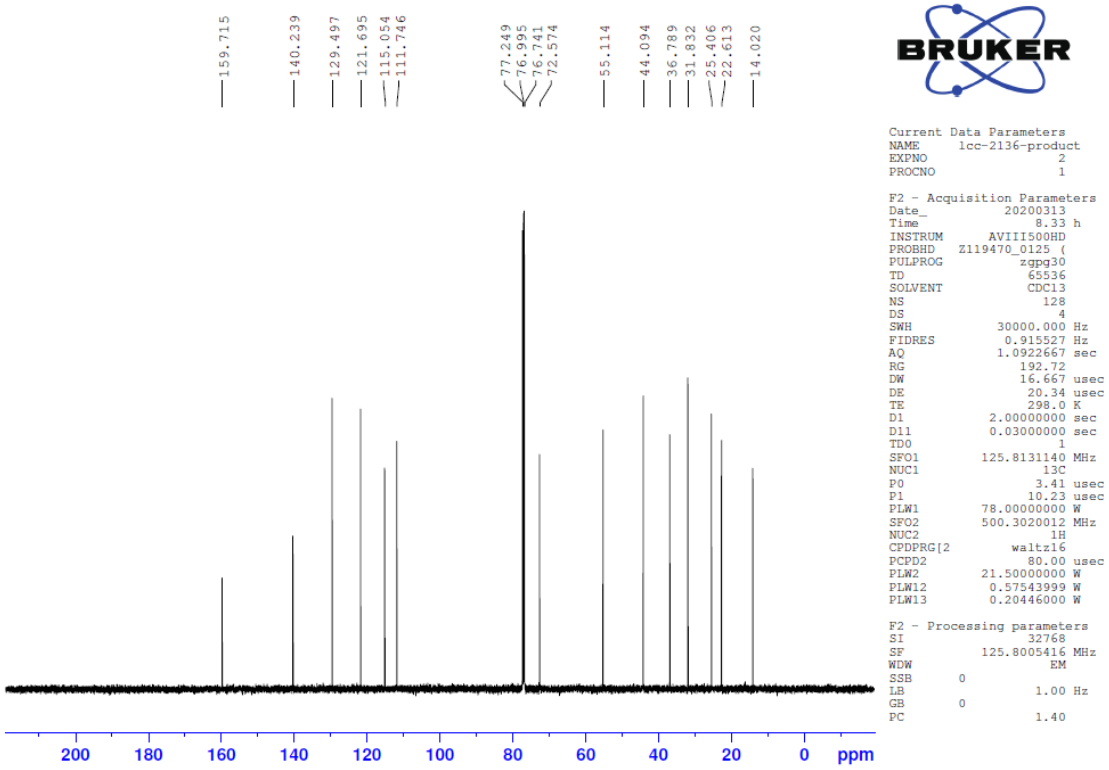


```
Current Data Parameters
NAME      1cc-2136-product
EXPNO                    2
PROCNO                   1

F2 - Acquisition Parameters
Date_             20200313
Time                 8.33 h
INSTRUM       AVIII500HD
PROBHD    Z119470_0125 (
PULPROG          zgpg30
TD                65536
SOLVENT           CDCl3
NS                  128
DS                    4
SWH           30000.000 Hz
FIDRES            0.915527 Hz
AQ                1.0922667 sec
RG                  192.72
DW                 16.667 usec
DE                 20.34 usec
TE                 298.0 K
D1             2.00000000 sec
D11            0.03000000 sec
TD0                   1
SFO1          125.8131140 MHz
NUC1                 13C
P0                 3.41 usec
P1                10.23 usec
PLW1          78.00000000 W
SFO2          500.3020012 MHz
NUC2                 1H
CPDPRG[2          waltz16
PCPD2              80.00 usec
PLW2          21.50000000 W
PLW12          0.57543999 W
PLW13          0.20446000 W

F2 - Processing parameters
SI                  32768
SF            125.8005416 MHz
WDW                  EM
SSB       0
LB                 1.00 Hz
GB        0
PC                 1.40
```

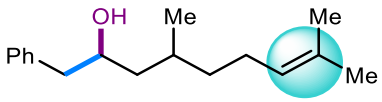
OH
Me
Me
Ph
Me

4.3.5aa

^{1}H NMR

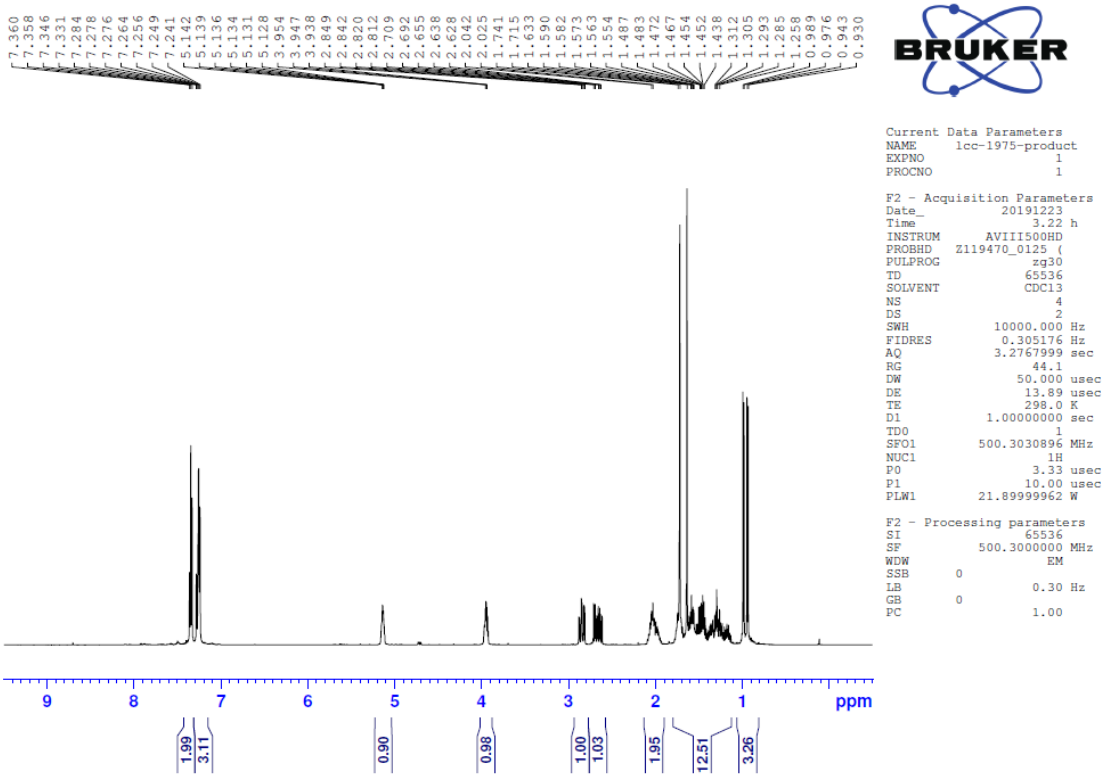
7.360
7.358
7.346
7.331
7.284
7.278
7.276
7.264
7.256
7.249
7.241
5.142
5.139
5.136
5.134
5.131
5.128
3.954
3.947
3.938
2.849
2.842
2.820
2.812
2.709
2.692
2.655
2.638
2.628
2.042
2.025
1.741
1.715
1.633
1.590
1.582
1.573
1.563
1.554
1.487
1.483
1.472
1.467
1.454
1.452
1.438
1.312
1.305
1.293
1.285
1.258
0.989
0.976
0.943
0.930
BRUKER
Current Data Parameters
NAME 1cc-1975-product
EXPNO 1
PROCNO 1
F2 - Acquisition Parameters
Date_ 20191223
Time 3.22 h
INSTRUM AVIII500HD
PROBHD Z119470_0125 (
PULPROG zg30
TD 65536
SOLVENT CDCl3
NS 4
DS 2
SWH 10000.000 Hz
FIDRES 0.305176 Hz
AQ 3.2767999 sec
RG 44.1
DW 50.000 usec
DE 13.89 usec
TE 298.0 K
D1 1.00000000 sec
TD0 1
SFO1 500.3030896 MHz
NUC1 1H
P0 3.33 usec
P1 10.00 usec
PLW1 21.89999962 W
F2 - Processing parameters
SI 65536
SF 500.3000000 MHz
WDW EM
SSB 0
LB 0.30 Hz
GB 0
PC 1.00
9
8
7
6
5
4
3
2
1
ppm
1.99
3.11
0.90
0.98
1.00
1.03
1.95
12.51
3.26

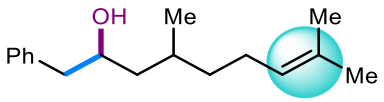

4.3.5aa

^{13}C NMR

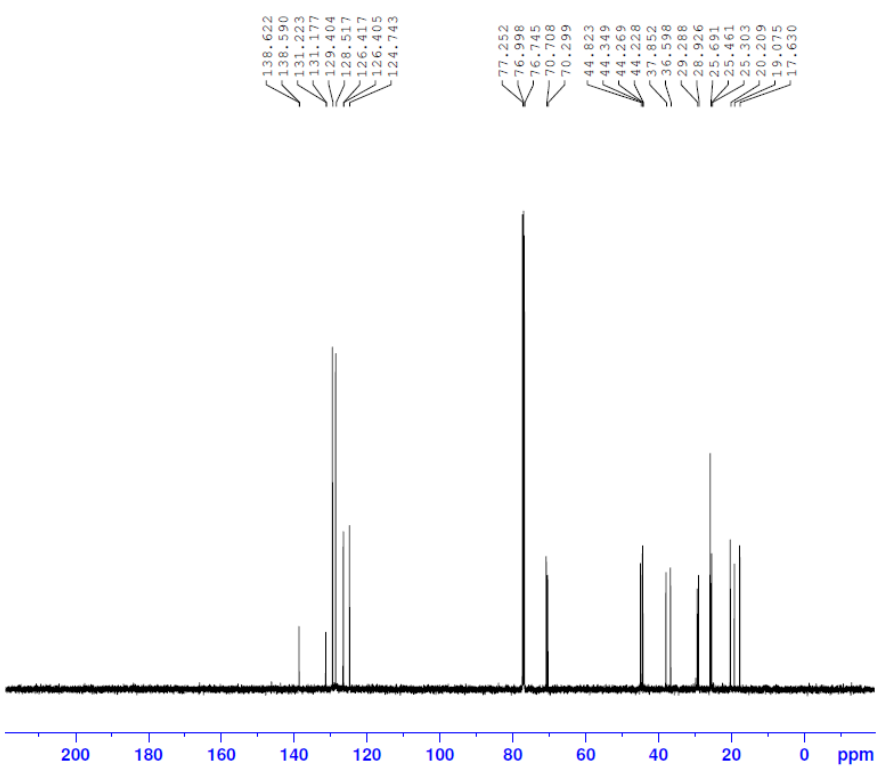

BRUKER

```
Current Data Parameters
NAME      1cc-1975-product
EXPNO                    2
PROCNO                   1

F2 - Acquisition Parameters
Date_             20191223
Time                 3.29 h
INSTRUM       AVIII500HD
PROBHD    Z119470_0125 (
PULPROG              zgpg30
TD                    65536
SOLVENT               CDCl3
NS                      128
DS                        4
SWH               30000.000 Hz
FIDRES            0.915527 Hz
AQ                1.0922667 sec
RG                   192.72
DW                  16.667 usec
DE                   20.34 usec
TE                   298.0 K
D1                2.00000000 sec
D11               0.03000000 sec
TD0                       1
SFO1            125.8131140 MHz
NUC1                    13C
P0                   3.41 usec
P1                  10.23 usec
PLW1            78.00000000 W
SFO2            500.3020012 MHz
NUC2                    1H
CPDPRG[2             waltz16
PCPD2                80.00 usec
PLW2            21.50000000 W
PLW12            0.49000001 W
PLW13            0.20446000 W

F2 - Processing parameters
SI                    32768
SF              125.8005416 MHz
WDW                      EM
SSB       0
LB                    1.00 Hz
GB        0
PC                    1.40
```

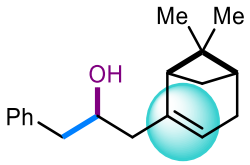
Me
Me
OH
Ph

4.3.5ab

^{1}H NMR

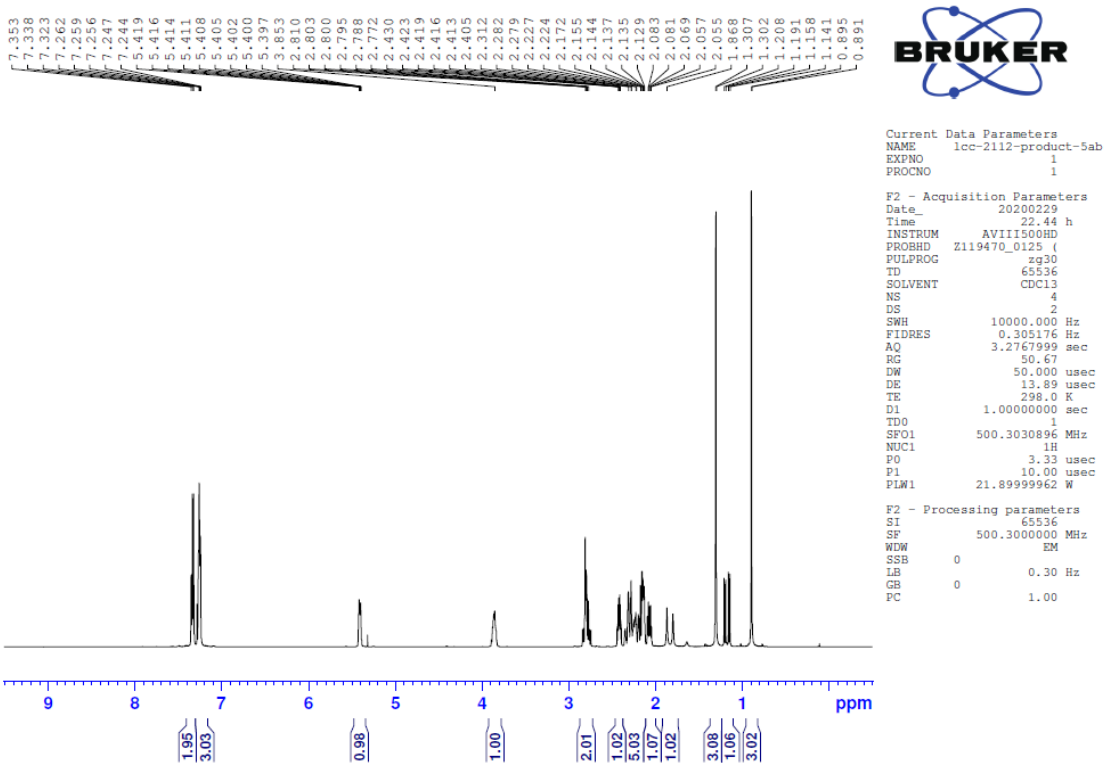
7.353
7.338
7.323
7.262
7.259
7.256
7.247
7.244
5.419
5.416
5.414
5.411
5.408
5.405
5.402
5.400
5.397
3.853
2.810
2.803
2.800
2.795
2.788
2.772
2.430
2.423
2.419
2.416
2.413
2.405
2.312
2.282
2.279
2.227
2.224
2.172
2.155
2.144
2.137
2.135
2.129
2.083
2.081
2.069
2.057
2.055
1.868
1.307
1.302
1.208
1.191
1.158
1.141
0.895
0.891
BRUKER
Current Data Parameters
NAME lcc-2112-product-5ab
EXPNO 1
PROCNO 1
F2 - Acquisition Parameters
Date_ 20200229
Time 22.44 h
INSTRUM AVIII500HD
PROBHD Z119470_0125 (
PULPROG zg30
TD 65536
SOLVENT CDCl3
NS 4
DS 2
SWH 10000.000 Hz
FIDRES 0.305176 Hz
AQ 3.2767999 sec
RG 50.67
DW 50.000 usec
DE 13.89 usec
TE 298.0 K
D1 1.00000000 sec
TD0 1
SFO1 500.3030896 MHz
NUC1 1H
P0 3.33 usec
P1 10.00 usec
PLW1 21.89999962 W
F2 - Processing parameters
SI 65536
SF 500.3000000 MHz
WDW EM
SSB 0
LB 0.30 Hz
GB 0
PC 1.00
9
8
7
6
5
4
3
2
1
ppm
1.95
3.03
0.98
1.00
2.01
1.02
5.03
1.07
1.02
3.08
1.06
3.02

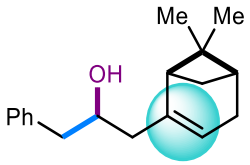

4.3.5ab

^{13}C NMR

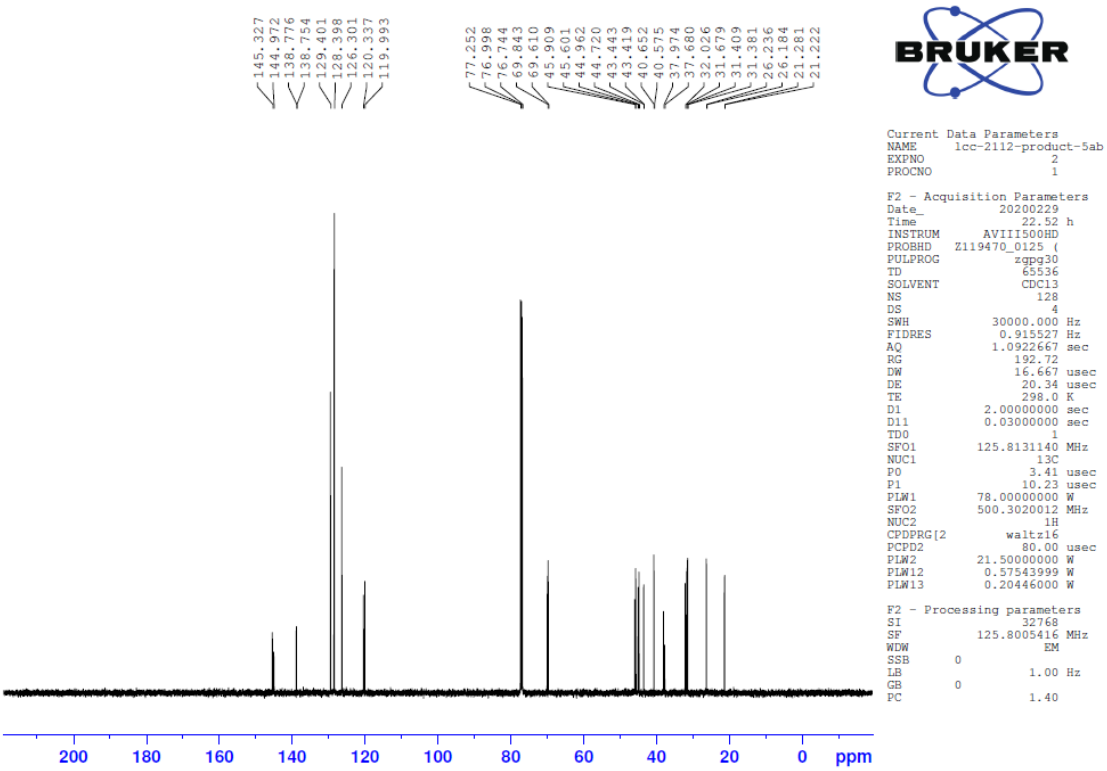


```
Current Data Parameters
NAME      1cc-2112-product-5ab
EXPNO                        2
PROCNO                       1

F2 - Acquisition Parameters
Date_              20200229
Time                 22.52 h
INSTRUM         AVIII500HD
PROBHD    Z119470_0125 (
PULPROG             zgpg30
TD                   65536
SOLVENT              CDCl3
NS                     128
DS                       4
SWH              30000.000 Hz
FIDRES               0.915527 Hz
AQ                1.0922667 sec
RG                   192.72
DW                  16.667 usec
DE                   20.34 usec
TE                   298.0 K
D1               2.00000000 sec
D11              0.03000000 sec
TD0                      1
SFO1           125.8131140 MHz
NUC1                   13C
P0                    3.41 usec
P1                   10.23 usec
PLW1            78.00000000 W
SFO2            500.3020012 MHz
NUC2                   1H
CPDPRG[2            waltz16
PCPD2                80.00 usec
PLW2            21.50000000 W
PLW12            0.57543999 W
PLW13            0.20446000 W

F2 - Processing parameters
SI                   32768
SF             125.8005416 MHz
WDW                     EM
SSB          0
LB                    1.00 Hz
GB           0
PC                    1.40
```

II. NMR spectra of products in Chapter 5

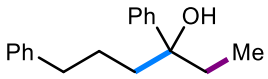

5.6aa

^{1}H NMR

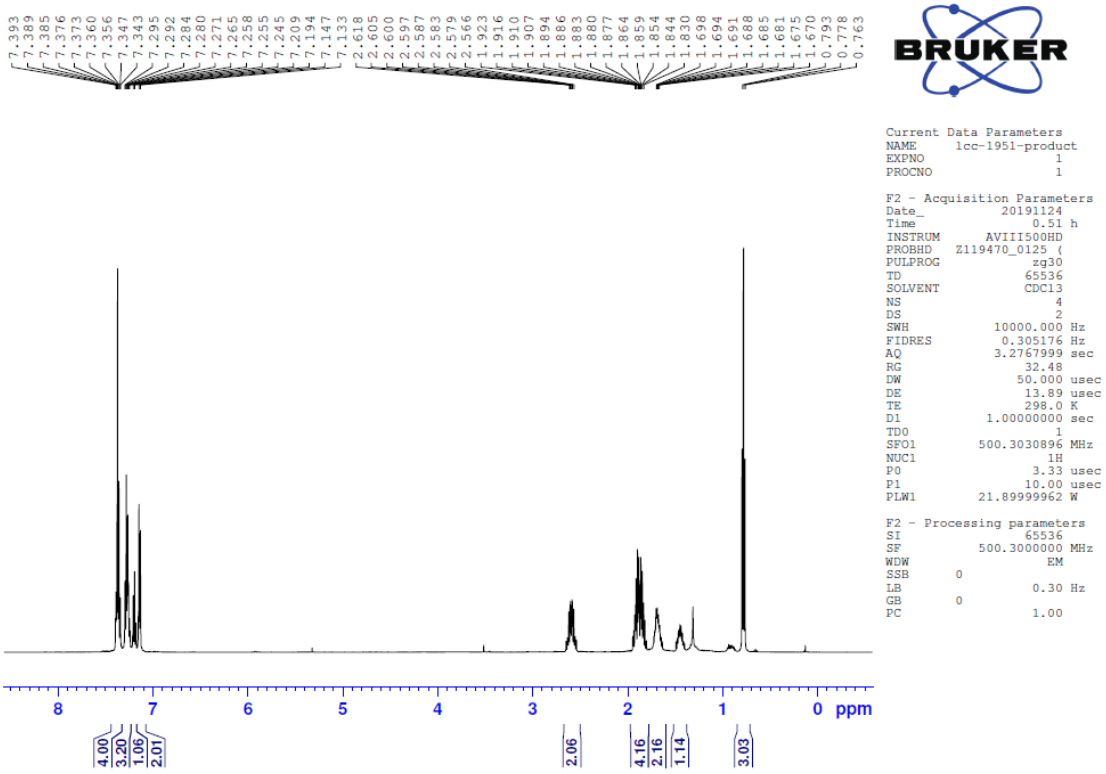

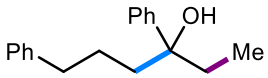

5.6aa

^{13}C NMR

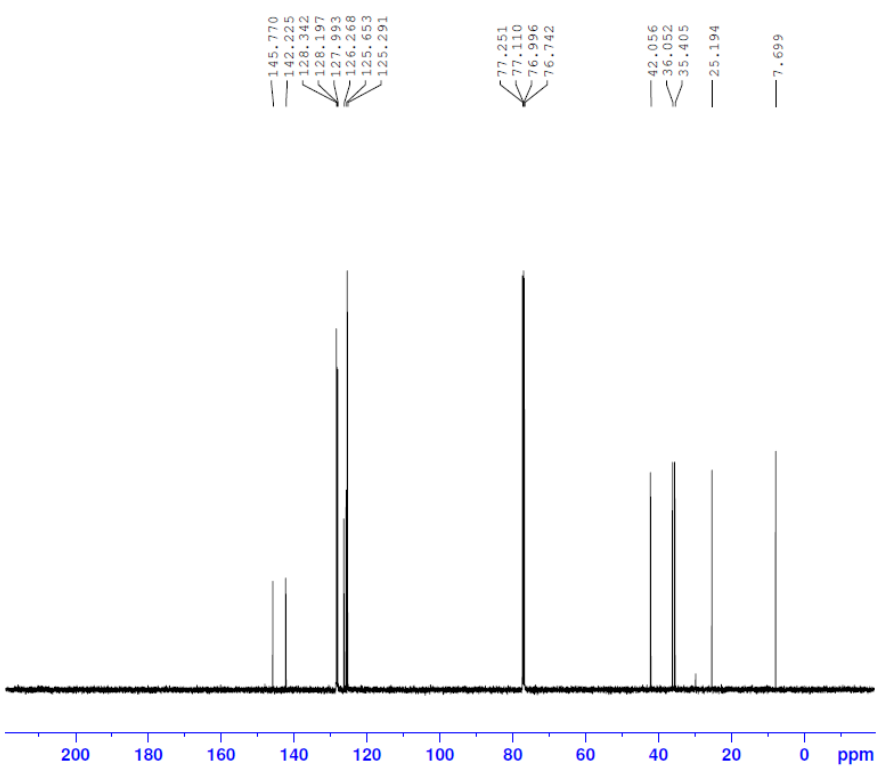


```
Current Data Parameters
NAME      1cc-1951-product
EXPNO                    2
PROCNO                   1

F2 - Acquisition Parameters
Date_           20191124
Time                0.58 h
INSTRUM       AVIII500HD
PROBHD    Z119470_0125 (
PULPROG             zgpg30
TD                  65536
SOLVENT             CDCl3
NS                    128
DS                      4
SWH             30000.000 Hz
FIDRES          0.915527 Hz
AQ              1.0922667 sec
RG                 192.72
DW                16.667 usec
DE                20.34 usec
TE                298.0 K
D1              2.00000000 sec
D11             0.03000000 sec
TD0                     1
SFO1          125.8131140 MHz
NUC1                  13C
P0                  3.41 usec
P1                 10.23 usec
PLW1          78.00000000 W
SFO2          500.3020012 MHz
NUC2                  1H
CPDPRG[2          waltz16
PCPD2              80.00 usec
PLW2          21.50000000 W
PLW12          0.49000001 W
PLW13          0.20446000 W

F2 - Processing parameters
SI                  32768
SF            125.8005434 MHz
WDW                    EM
SSB       0
LB                  1.00 Hz
GB        0
PC                  1.40
```

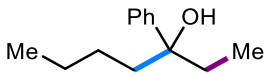
Ph
OH
Me
Me

5.6ba

^{1}H NMR

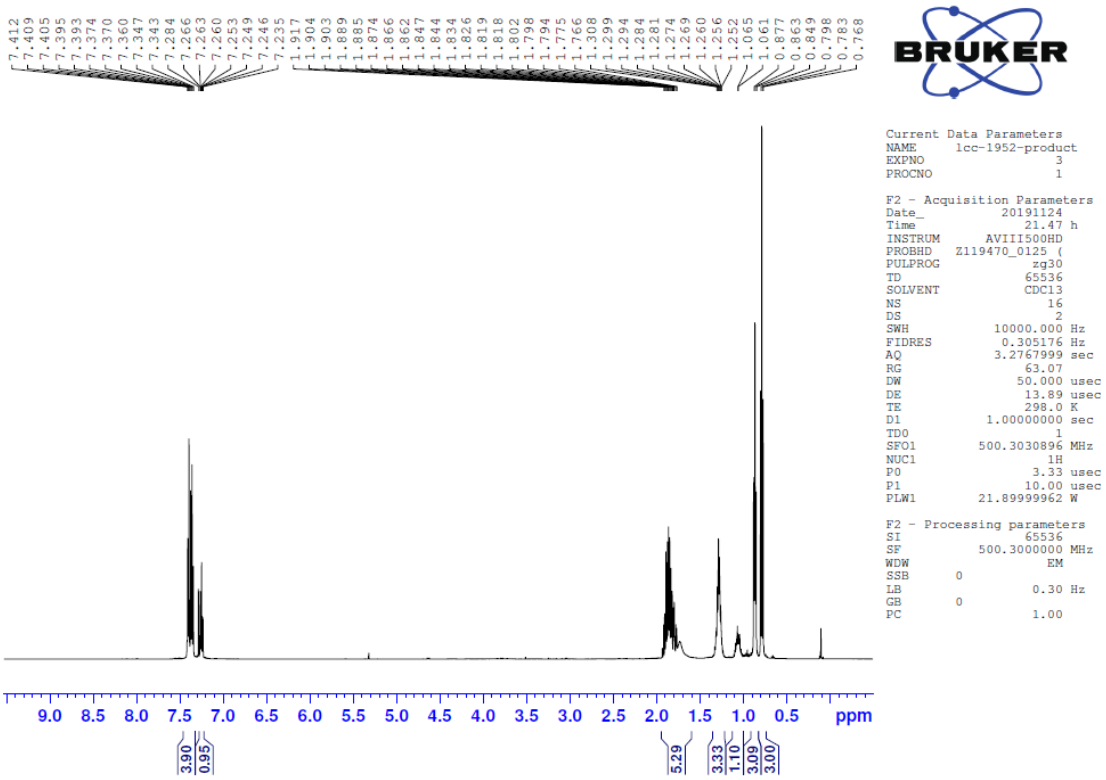
7.412
7.409
7.405
7.395
7.393
7.374
7.370
7.360
7.347
7.343
7.284
7.266
7.263
7.260
7.253
7.249
7.246
7.235
1.917
1.904
1.903
1.889
1.885
1.874
1.866
1.862
1.847
1.844
1.834
1.826
1.819
1.818
1.802
1.798
1.794
1.775
1.766
1.308
1.299
1.294
1.284
1.281
1.274
1.269
1.260
1.256
1.252
1.065
1.061
0.877
0.863
0.849
0.798
0.783
0.768
BRUKER
Current Data Parameters
NAME 1cc-1952-product
EXPNO 3
PROCNO 1
F2 - Acquisition Parameters
Date_ 20191124
Time 21.47 h
INSTRUM AVIII500HD
PROBHD Z119470_0125 (
PULPROG zg30
TD 65536
SOLVENT CDCl3
NS 16
DS 2
SWH 10000.000 Hz
FIDRES 0.305176 Hz
AQ 3.2767999 sec
RG 63.07
DW 50.000 usec
DE 13.89 usec
TE 298.0 K
D1 1.00000000 sec
TD0 1
SFO1 500.3030896 MHz
NUC1 1H
P0 3.33 usec
P1 10.00 usec
PLW1 21.89999962 W
F2 - Processing parameters
SI 65536
SF 500.3000000 MHz
WDW EM
SSB 0
LB 0.30 Hz
GB 0
PC 1.00
9.0 8.5 8.0 7.5 7.0 6.5 6.0 5.5 5.0 4.5 4.0 3.5 3.0 2.5 2.0 1.5 1.0 0.5 ppm
3.90
0.95
5.29
3.33
1.10
3.09
3.00

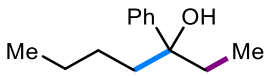

5.6ba

^{13}C NMR

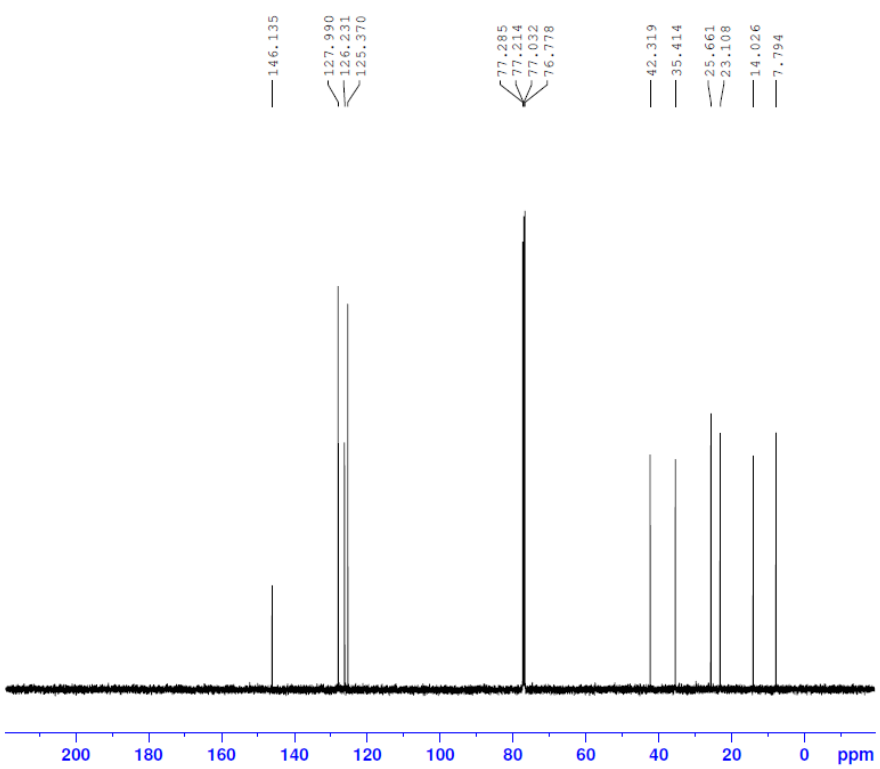


```
Current Data Parameters
NAME      1cc-1952-product
EXPNO                    5
PROCNO                   1

F2 - Acquisition Parameters
Date_             20191125
Time                  2.17 h
INSTRUM       AVIII500HD
PROBHD    Z119470_0125 (
PULPROG             zgpg30
TD                   65536
SOLVENT              CDCl3
NS                     128
DS                       4
SWH              30000.000 Hz
FIDRES               0.915527 Hz
AQ                1.0922667 sec
RG                   192.72
DW                   16.667 usec
DE                    20.34 usec
TE                   298.0 K
D1               2.00000000 sec
D11              0.03000000 sec
TD0                      1
SFO1            125.8131140 MHz
NUC1                    13C
P0                    3.41 usec
P1                   10.23 usec
PLW1            78.00000000 W
SFO2            500.3020012 MHz
NUC2                    1H
CPDPRG[2             waltz16
PCPD2                80.00 usec
PLW2            21.50000000 W
PLW12            0.49000001 W
PLW13            0.20446000 W

F2 - Processing parameters
SI                   32768
SF              125.8005351 MHz
WDW                     EM
SSB          0
LB                    1.00 Hz
GB           0
PC                    1.40
```

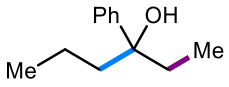

5.6ca

^{1}H NMR

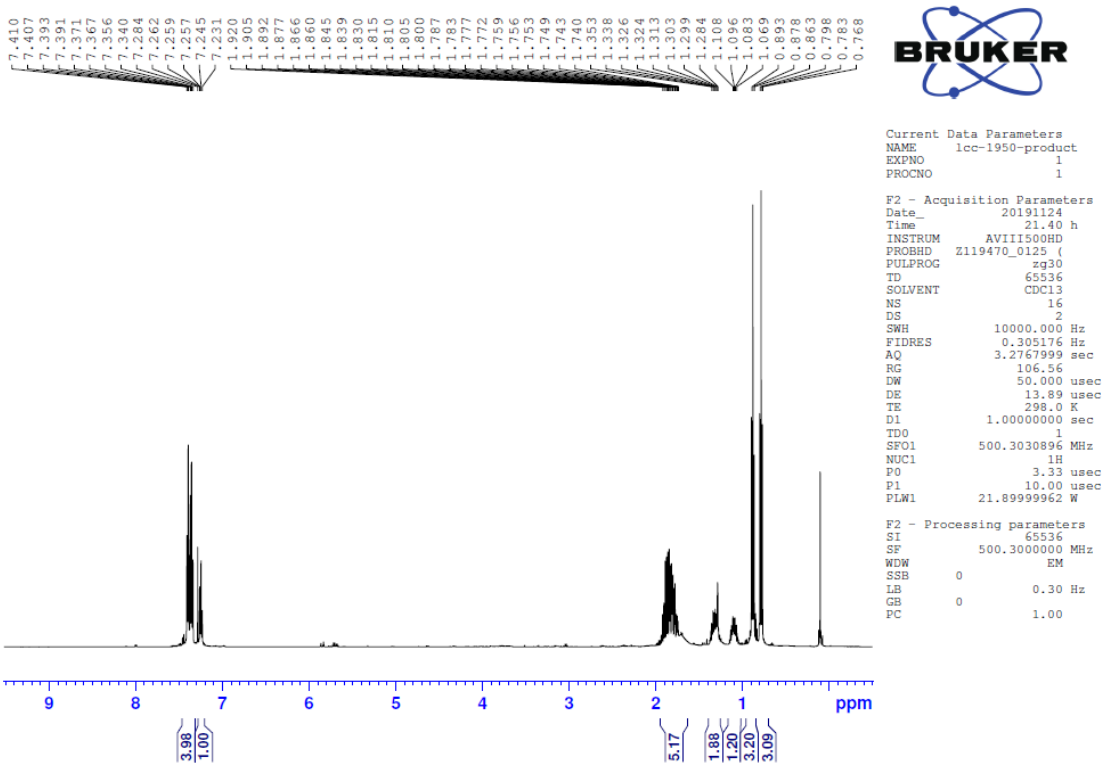

cli

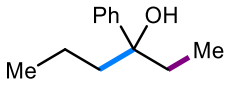

5.6ca

^{13}C NMR

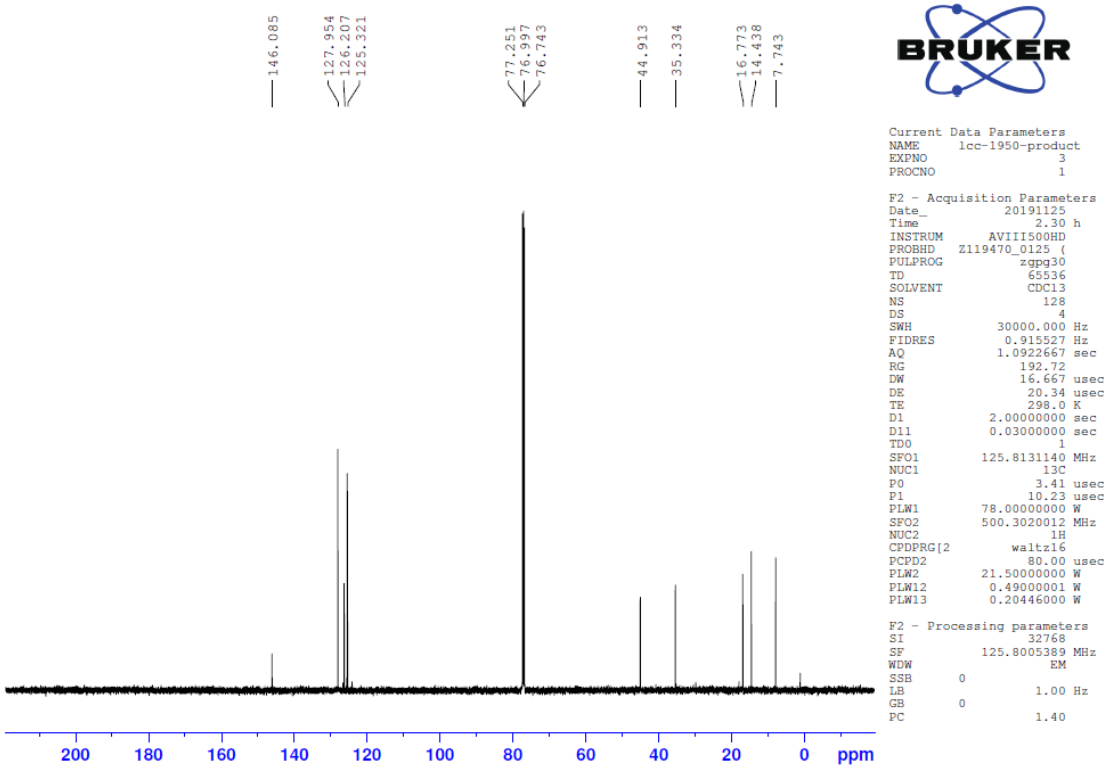


```
Current Data Parameters
NAME      1cc-1950-product
EXPNO                    3
PROCNO                   1

F2 - Acquisition Parameters
Date_             20191125
Time                 2.30 h
INSTRUM       AVIII500HD
PROBHD    Z119470_0125 (
PULPROG           zgpg30
TD                65536
SOLVENT           CDCl3
NS                  128
DS                    4
SWH           30000.000 Hz
FIDRES            0.915527 Hz
AQ                1.0922667 sec
RG                  192.72
DW                 16.667 usec
DE                 20.34 usec
TE                 298.0 K
D1             2.00000000 sec
D11            0.03000000 sec
TD0                   1
SFO1          125.8131140 MHz
NUC1                 13C
P0                  3.41 usec
P1                 10.23 usec
PLW1          78.00000000 W
SFO2          500.3020012 MHz
NUC2                 1H
CPDPRG[2          waltz16
PCPD2               80.00 usec
PLW2          21.50000000 W
PLW12          0.49000001 W
PLW13          0.20446000 W

F2 - Processing parameters
SI                  32768
SF            125.8005389 MHz
WDW                   EM
SSB       0
LB                  1.00 Hz
GB        0
PC                  1.40
```

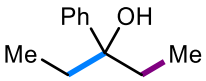
Ph
OH
Me
Me

5.6da

^{1}H NMR

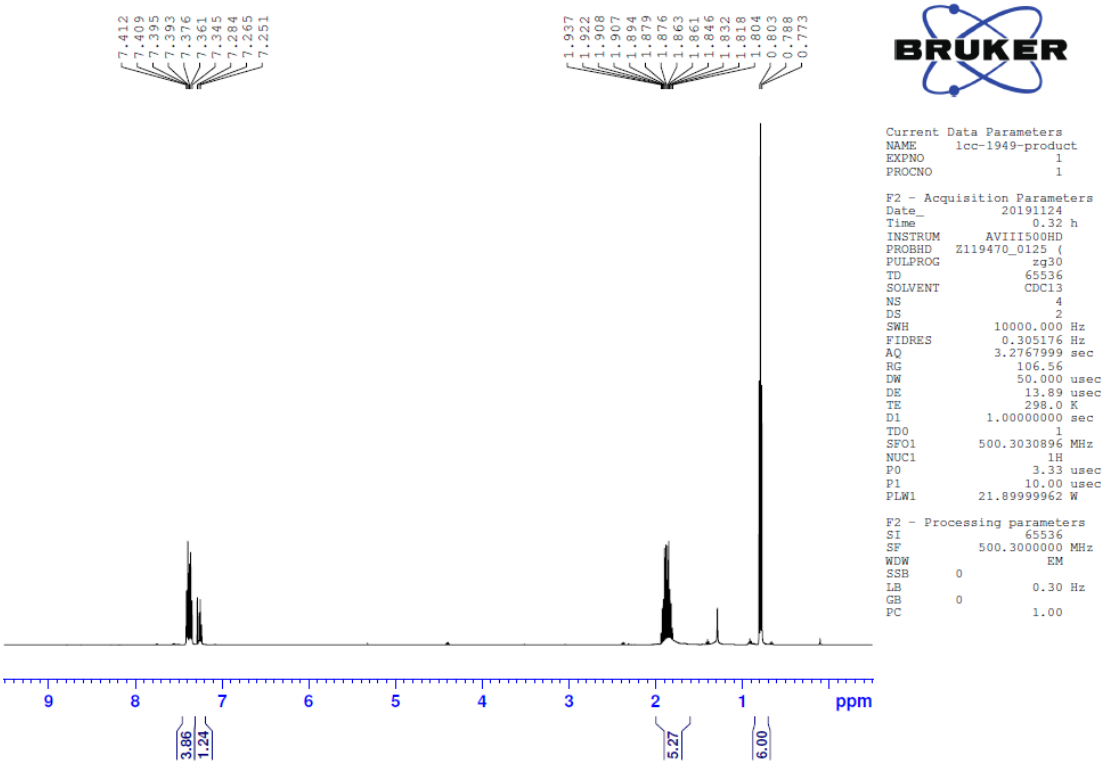
7.412
7.409
7.395
7.393
7.376
7.361
7.345
7.284
7.265
7.251
1.937
1.922
1.908
1.907
1.894
1.879
1.876
1.863
1.861
1.846
1.832
1.818
1.804
0.803
0.788
0.773
BRUKER
Current Data Parameters
NAME 1cc-1949-product
EXPNO 1
PROCNO 1
F2 - Acquisition Parameters
Date_ 20191124
Time 0.32 h
INSTRUM AVIII500HD
PROBHD Z119470_0125 (
PULPROG zg30
TD 65536
SOLVENT CDCl3
NS 4
DS 2
SWH 10000.000 Hz
FIDRES 0.305176 Hz
AQ 3.2767999 sec
RG 106.56
DW 50.000 usec
DE 13.89 usec
TE 298.0 K
D1 1.00000000 sec
TD0 1
SFO1 500.3030896 MHz
NUC1 1H
P0 3.33 usec
P1 10.00 usec
PLW1 21.89999962 W
F2 - Processing parameters
SI 65536
SF 500.3000000 MHz
WDW EM
SSB 0
LB 0.30 Hz
GB 0
PC 1.00
9
8
7
6
5
4
3
2
1
ppm
3.86
1.24
5.27
6.00

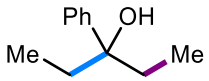

5.6da

^{13}C NMR

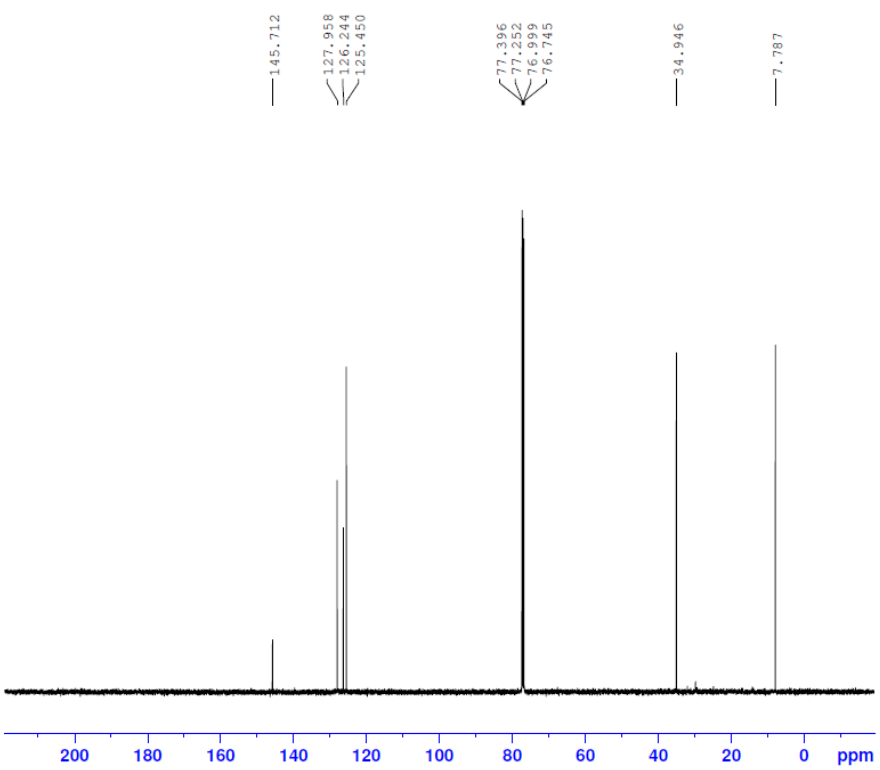


```
Current Data Parameters
NAME      lcc-1949-product
EXPNO                    2
PROCNO                   1

F2 - Acquisition Parameters
Date_           20191124
Time                0.46 h
INSTRUM       AVIII500HD
PROBHD    Z119470_0125 (
PULPROG           zgpg30
TD                65536
SOLVENT           CDCl3
NS                  256
DS                    4
SWH           30000.000 Hz
FIDRES            0.915527 Hz
AQ                1.0922667 sec
RG                  192.72
DW                 16.667 usec
DE                 20.34 usec
TE                298.0 K
D1             2.00000000 sec
D11            0.03000000 sec
TD0                   1
SFO1          125.8131140 MHz
NUC1                 13C
P0                  3.41 usec
P1                 10.23 usec
PLW1          78.00000000 W
SFO2          500.3020012 MHz
NUC2                 1H
CPDPRG[2          waltz16
PCPD2               80.00 usec
PLW2          21.50000000 W
PLW12          0.49000001 W
PLW13          0.20446000 W

F2 - Processing parameters
SI                  32768
SF            125.8005389 MHz
WDW                   EM
SSB       0
LB                  1.00 Hz
GB        0
PC                  1.40
```

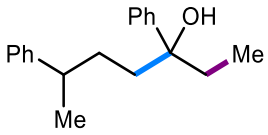
Ph
OH
Ph
Me
Me

5.6ea

^{1}H NMR

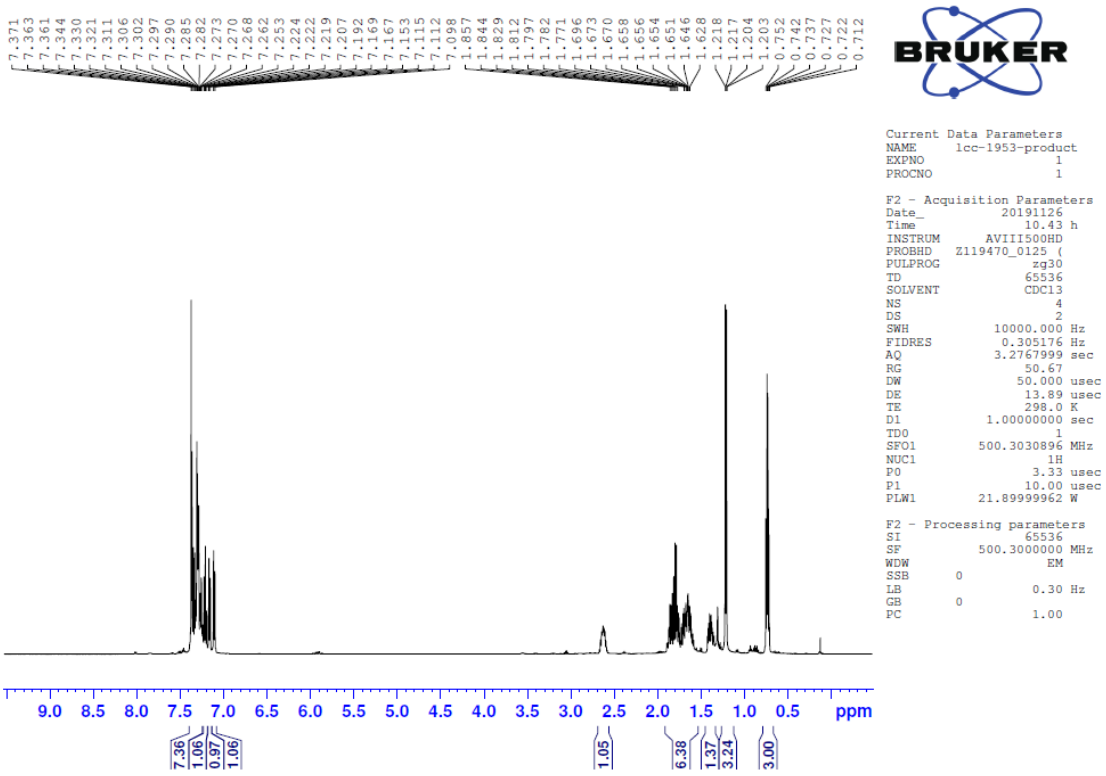
7.371
7.363
7.361
7.344
7.330
7.321
7.311
7.306
7.302
7.297
7.290
7.285
7.282
7.273
7.270
7.268
7.262
7.253
7.224
7.222
7.219
7.207
7.192
7.169
7.167
7.153
7.115
7.112
7.098
1.857
1.844
1.829
1.812
1.797
1.782
1.771
1.666
1.673
1.670
1.658
1.656
1.654
1.651
1.646
1.628
1.218
1.217
1.204
1.203
0.752
0.742
0.737
0.727
0.722
0.712
BRUKER
Current Data Parameters
NAME 1cc-1953-product
EXPNO 1
PROCNO 1
F2 - Acquisition Parameters
Date_ 20191126
Time 10.43 h
INSTRUM AVIII500HD
PROBHD Z119470_0125 (
PULPROG zg30
TD 65536
SOLVENT CDCl3
NS 4
DS 2
SWH 10000.000 Hz
FIDRES 0.305176 Hz
AQ 3.2767999 sec
RG 50.67
DW 50.000 usec
DE 13.89 usec
TE 298.0 K
D1 1.00000000 sec
TD0 1
SFO1 500.3030896 MHz
NUC1 1H
P0 3.33 usec
P1 10.00 usec
PLW1 21.89999962 W
F2 - Processing parameters
SI 65536
SF 500.3000000 MHz
WDW EM
SSB 0
LB 0.30 Hz
GB 0
PC 1.00
9.0 8.5 8.0 7.5 7.0 6.5 6.0 5.5 5.0 4.5 4.0 3.5 3.0 2.5 2.0 1.5 1.0 0.5 ppm
7.36
1.06
0.97
1.06
1.05
6.38
1.37
3.24
3.00

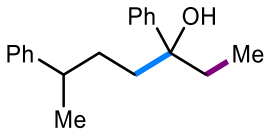

5.6ea

^{13}C NMR

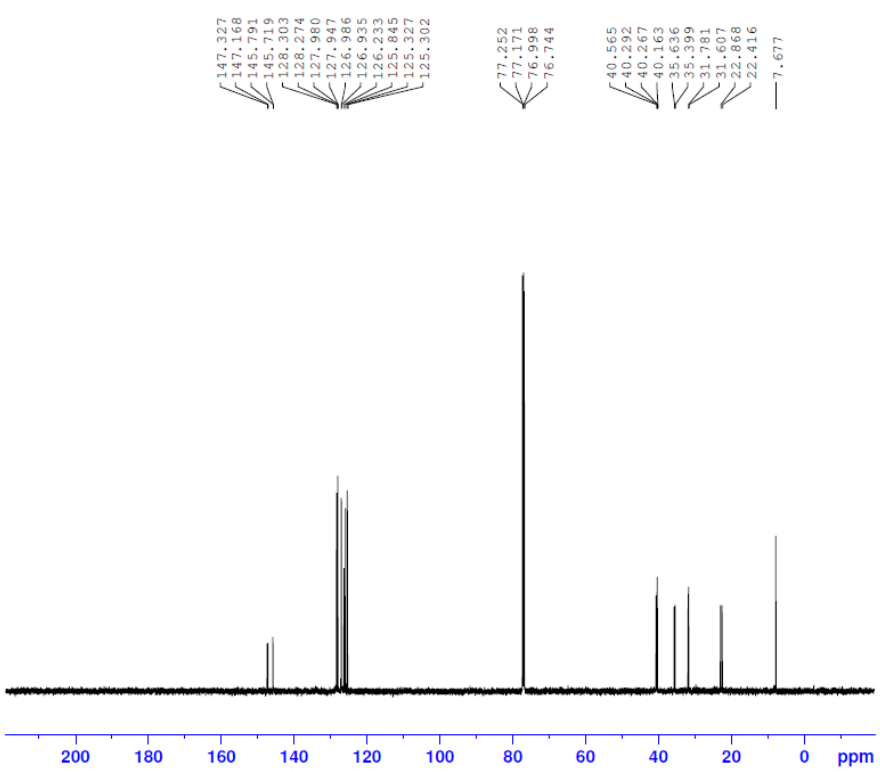

BRUKER

```
Current Data Parameters
NAME      1cc-1953-product
EXPNO                    2
PROCNO                   1

F2 - Acquisition Parameters
Date_             20191126
Time                10.51 h
INSTRUM       AVIII500HD
PROBHD    Z119470_0125 (
PULPROG           zgpg30
TD                65536
SOLVENT           CDCl3
NS                  128
DS                    4
SWH           30000.000 Hz
FIDRES            0.915527 Hz
AQ                1.0922667 sec
RG                  192.72
DW                 16.667 usec
DE                 20.34 usec
TE                 298.0 K
D1             2.00000000 sec
D11            0.03000000 sec
TD0                   1
SFO1         125.8131140 MHz
NUC1                 13C
P0                 3.41 usec
P1                10.23 usec
PLW1          78.00000000 W
SFO2         500.3020012 MHz
NUC2                 1H
CPDPRG[2          waltz16
PCPD2              80.00 usec
PLW2          21.50000000 W
PLW12          0.49000001 W
PLW13          0.20446000 W

F2 - Processing parameters
SI                32768
SF           125.8005425 MHz
WDW                  EM
SSB       0
LB                1.00 Hz
GB        0
PC                1.40
```

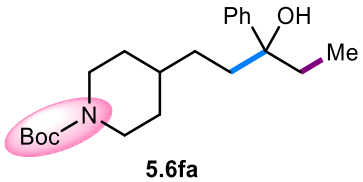
Ph
OH
Me
N
Boc

5.6fa

^{1}H NMR

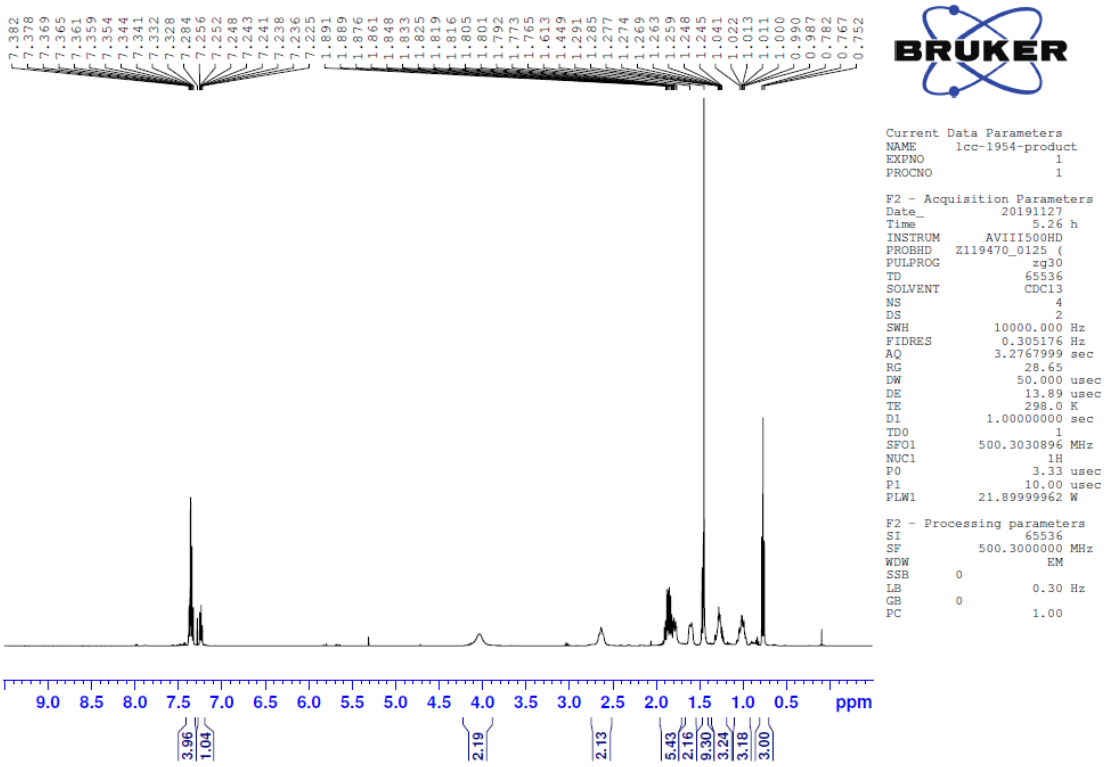
7.382
7.378
7.369
7.365
7.361
7.359
7.354
7.344
7.341
7.332
7.328
7.284
7.256
7.252
7.248
7.243
7.241
7.238
7.236
7.225
1.891
1.889
1.876
1.861
1.848
1.833
1.825
1.819
1.816
1.805
1.801
1.792
1.773
1.765
1.613
1.449
1.291
1.285
1.277
1.274
1.269
1.263
1.259
1.248
1.245
1.041
1.022
1.013
1.011
1.000
0.990
0.987
0.782
0.767
0.752
BRUKER
Current Data Parameters
NAME lcc-1954-product
EXPNO 1
PROCNO 1
F2 - Acquisition Parameters
Date_ 20191127
Time 5.26 h
INSTRUM AVIII500HD
PROBHD Z119470_0125 (
PULPROG zg30
TD 65536
SOLVENT CDCl3
NS 4
DS 2
SWH 10000.000 Hz
FIDRES 0.305176 Hz
AQ 3.2767999 sec
RG 28.65
DW 50.000 usec
DE 13.89 usec
TE 298.0 K
D1 1.00000000 sec
TD0 1
SFO1 500.3030896 MHz
NUC1 1H
P0 3.33 usec
P1 10.00 usec
PLW1 21.89999962 W
F2 - Processing parameters
SI 65536
SF 500.3000000 MHz
WDW EM
SSB 0
LB 0.30 Hz
GB 0
PC 1.00
9.0 8.5 8.0 7.5 7.0 6.5 6.0 5.5 5.0 4.5 4.0 3.5 3.0 2.5 2.0 1.5 1.0 0.5 ppm
3.96
1.04
2.19
2.13
5.43
2.16
9.30
3.24
3.18
3.00

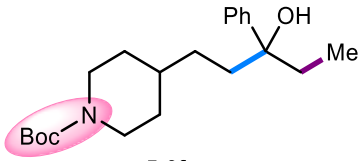

5.6fa

^{13}C NMR

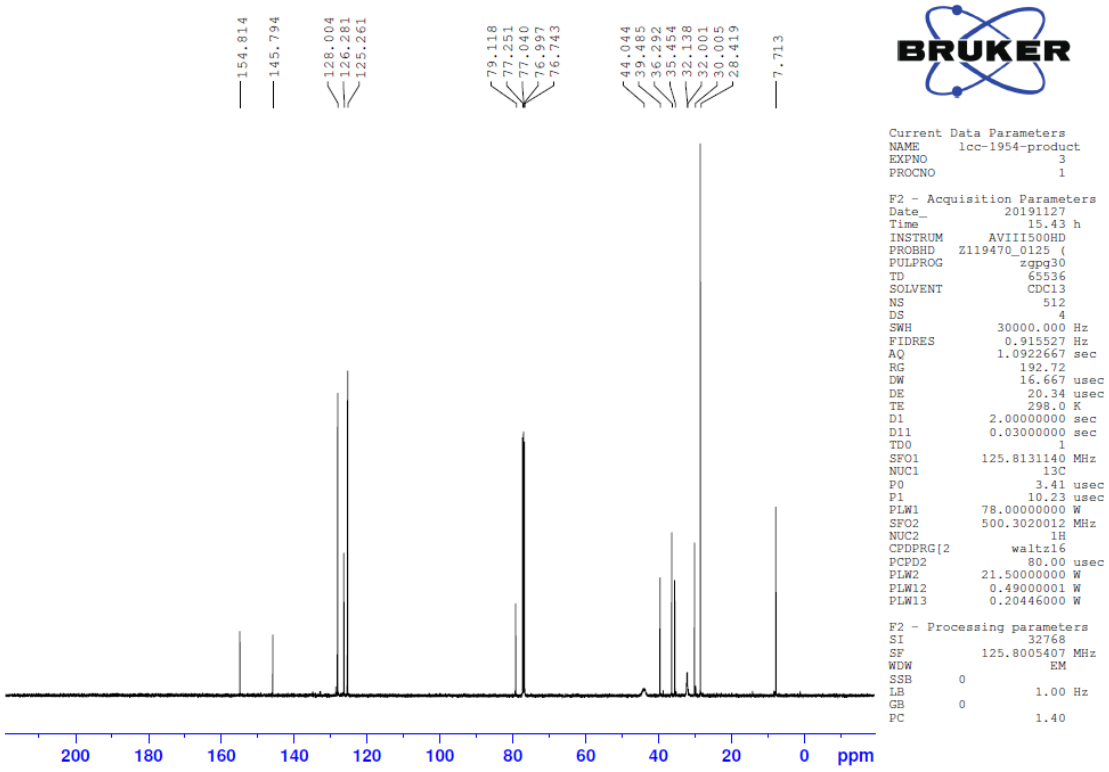


```
Current Data Parameters
NAME      1cc-1954-product
EXPNO                    3
PROCNO                   1

F2 - Acquisition Parameters
Date_           20191127
Time              15.43 h
INSTRUM       AVIII500HD
PROBHD    Z119470_0125 (
PULPROG           zgpg30
TD                65536
SOLVENT           CDCl3
NS                  512
DS                    4
SWH           30000.000 Hz
FIDRES            0.915527 Hz
AQ              1.0922667 sec
RG                192.72
DW                16.667 usec
DE                20.34 usec
TE                298.0 K
D1              2.00000000 sec
D11             0.03000000 sec
TD0                   1
SFO1          125.8131140 MHz
NUC1                 13C
P0                  3.41 usec
P1                 10.23 usec
PLW1          78.00000000 W
SFO2          500.3020012 MHz
NUC2                 1H
CPDPRG[2          waltz16
PCPD2               80.00 usec
PLW2          21.50000000 W
PLW12          0.49000001 W
PLW13          0.20446000 W

F2 - Processing parameters
SI                  32768
SF            125.8005407 MHz
WDW                  EM
SSB       0
LB                1.00 Hz
GB        0
PC                1.40
```

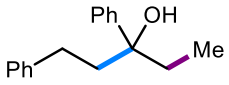

5.6ga

^{1}H NMR

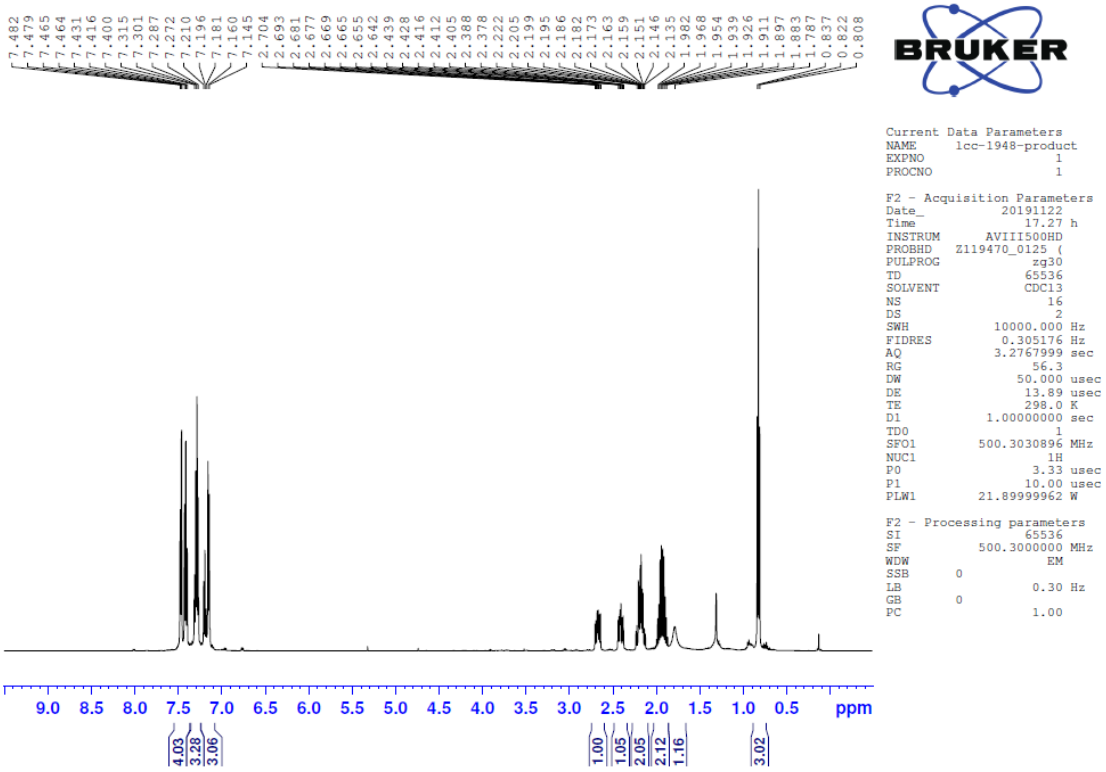


```
Current Data Parameters
NAME      1cc-1948-product
EXPNO                    1
PROCNO                   1

F2 - Acquisition Parameters
Date_           20191122
Time              17.27 h
INSTRUM       AVIII500HD
PROBHD    Z119470_0125 (
PULPROG              zg30
TD                  65536
SOLVENT             CDCl3
NS                     16
DS                      2
SWH           10000.000 Hz
FIDRES            0.305176 Hz
AQ                3.2767999 sec
RG                    56.3
DW                  50.000 usec
DE                  13.89 usec
TE                  298.0 K
D1              1.00000000 sec
TD0                     1
SFO1          500.3030896 MHz
NUC1                   1H
P0                  3.33 usec
P1                 10.00 usec
PLW1          21.89999962 W

F2 - Processing parameters
SI                  65536
SF            500.3000000 MHz
WDW                    EM
SSB       0
LB                  0.30 Hz
GB        0
PC                  1.00
```

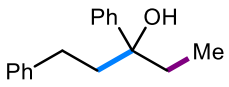

5.6ga

^{13}C NMR

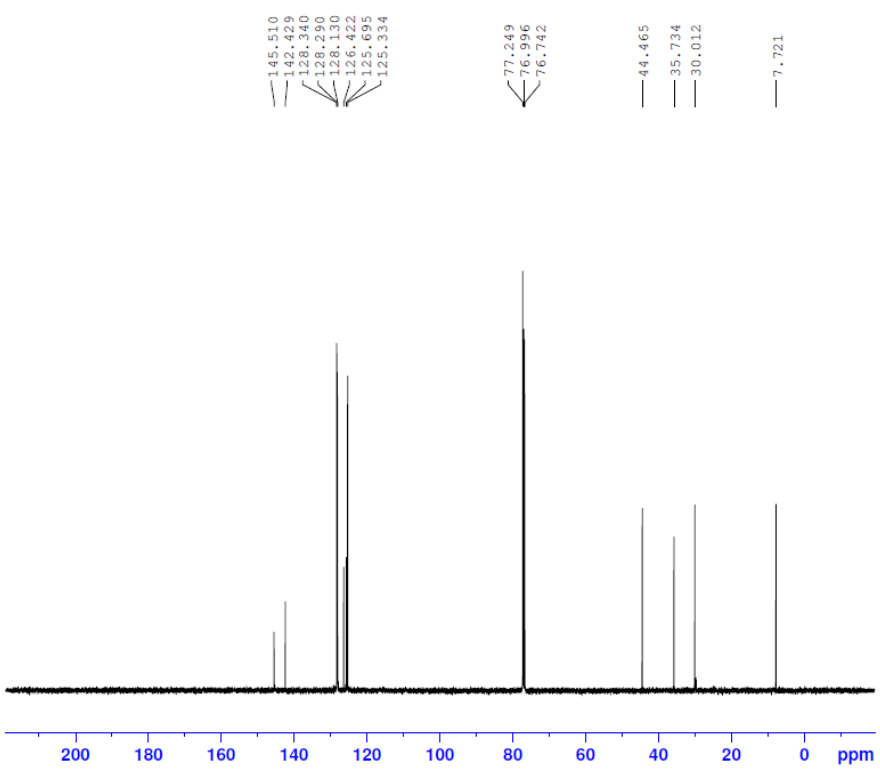

BRUKER

```
Current Data Parameters
NAME      lcc-1948-product
EXPNO                    2
PROCNO                   1

F2 - Acquisition Parameters
Date_           20191122
Time              17.35 h
INSTRUM       AVIII500HD
PROBHD    Z119470_0125 (
PULPROG           zgpg30
TD                65536
SOLVENT           CDCl3
NS                  128
DS                    4
SWH           30000.000 Hz
FIDRES         0.915527 Hz
AQ             1.0922667 sec
RG                192.72
DW                16.667 usec
DE                20.34 usec
TE                298.0 K
D1             2.00000000 sec
D11            0.03000000 sec
TD0                   1
SFO1         125.8131140 MHz
NUC1                13C
P0                 3.41 usec
P1                10.23 usec
PLW1         78.00000000 W
SFO2         500.3020012 MHz
NUC2                1H
CPDPRG[2         waltz16
PCPD2             80.00 usec
PLW2         21.50000000 W
PLW12         0.49000001 W
PLW13         0.20446000 W

F2 - Processing parameters
SI                32768
SF           125.8005434 MHz
WDW                  EM
SSB       0
LB                1.00 Hz
GB        0
PC                1.40
```

III. NMR spectra of products in Chapter 6

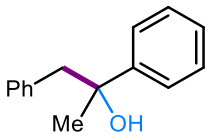

6.3aa

^{1}H NMR

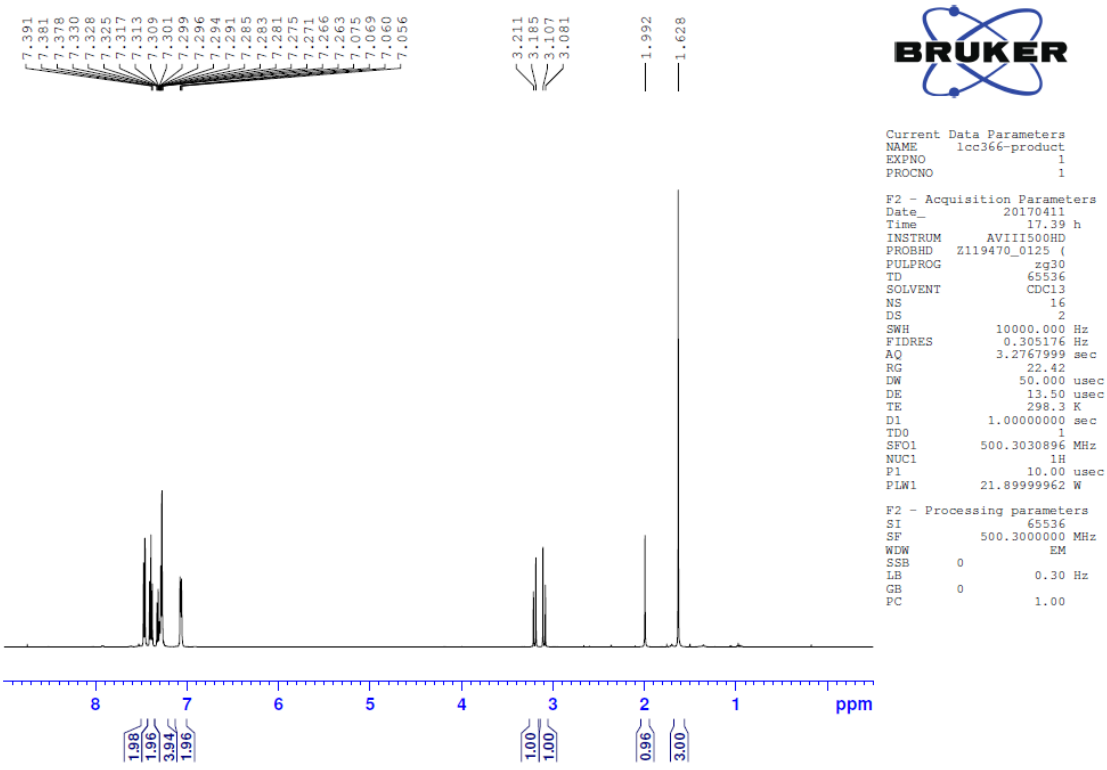

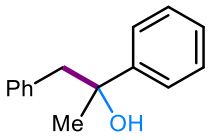

6.3aa

^{13}C NMR

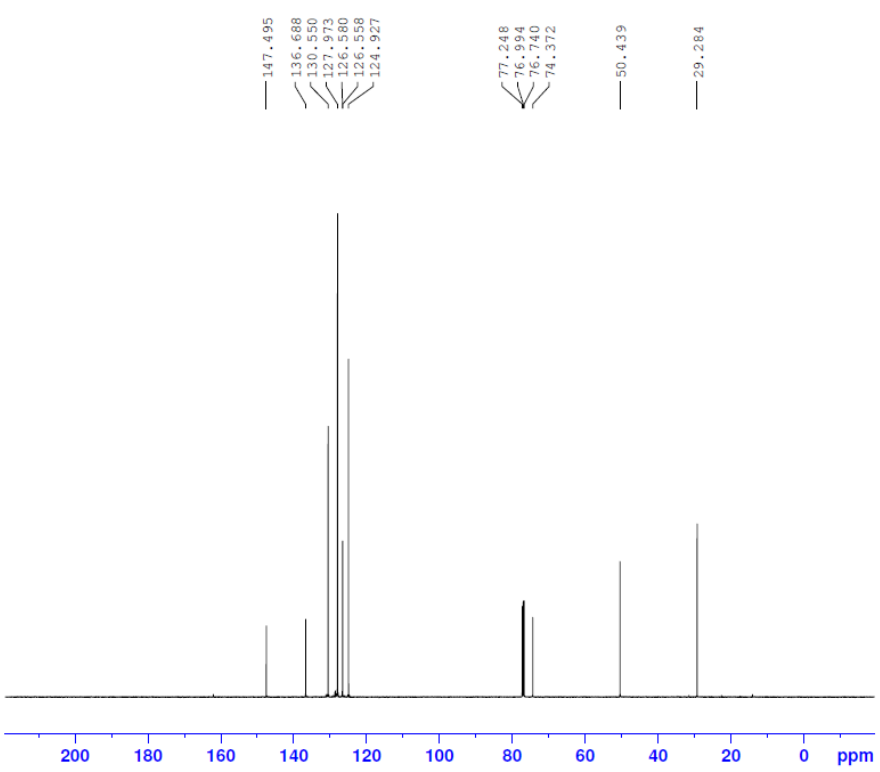


```
Current Data Parameters
NAME      1cc366-product
EXPNO                  2
PROCNO                 1

F2 - Acquisition Parameters
Date_           20170411
Time              18.07 h
INSTRUM       AVIII500HD
PROBHD   Z119470_0125 (
PULPROG           zgpg30
TD                65536
SOLVENT           CDCl3
NS                  512
DS                    4
SWH           30000.000 Hz
FIDRES         0.915527 Hz
AQ             1.0922667 sec
RG                192.72
DW                16.667 usec
DE                 7.43 usec
TE                298.3 K
D1             2.00000000 sec
D11            0.03000000 sec
TD0                   1
SFO1         125.8131140 MHz
NUC1                 13C
P1                 10.23 usec
PLW1         78.00000000 W
SFO2         500.3020012 MHz
NUC2                  1H
CPDPRG[2          waltz16
PCPD2              80.00 usec
PLW2         21.50000000 W
PLW12         0.40648001 W
PLW13         0.20446000 W

F2 - Processing parameters
SI                32768
SF           125.8005526 MHz
WDW                  EM
SSB       0
LB                 1.00 Hz
GB        0
PC                 1.40
```

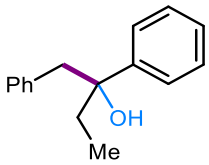

6.3ba

^{1}H NMR

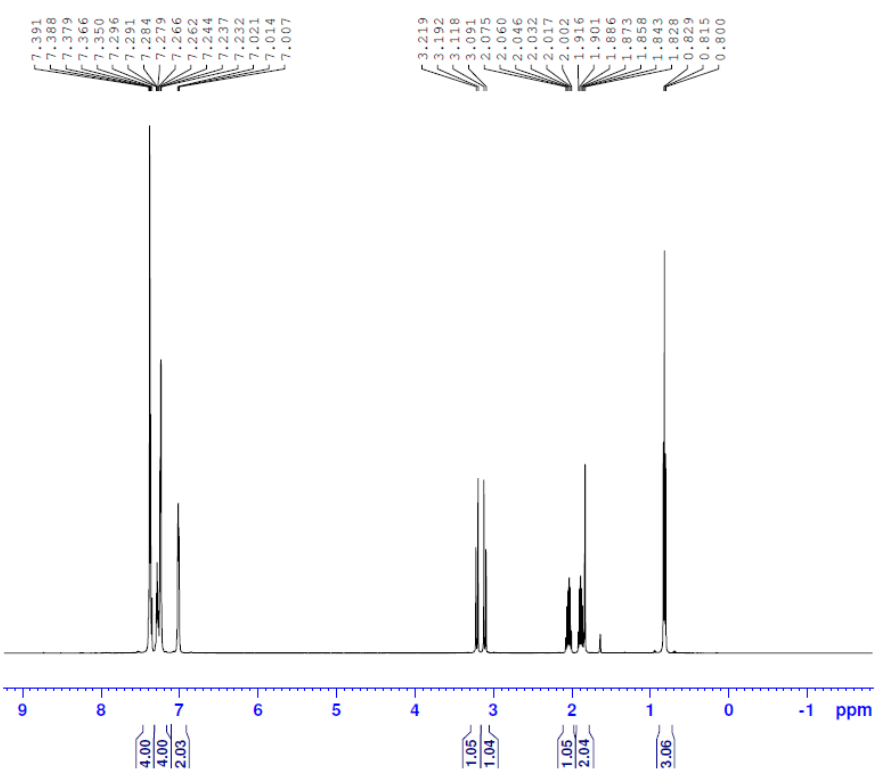


```
Current Data Parameters
NAME      1cc-491-product-H
EXPNO                   1
PROCNO                  1

F2 - Acquisition Parameters
Date_           20170603
Time              20.20 h
INSTRUM       AVIII500HD
PROBHD    Z119470_0125 (
PULPROG             zg30
TD                 65536
SOLVENT            CDCl3
NS                    16
DS                     2
SWH           10000.000 Hz
FIDRES            0.305176 Hz
AQ             3.2767999 sec
RG                 25.23
DW                50.000 usec
DE                13.50 usec
TE                298.3 K
D1             1.00000000 sec
TD0                    1
SFO1          500.3030896 MHz
NUC1                  1H
P1                10.00 usec
PLW1          21.89999962 W

F2 - Processing parameters
SI                 65536
SF            500.3000000 MHz
WDW                   EM
SSB       0
LB                 0.30 Hz
GB        0
PC                 1.00
```

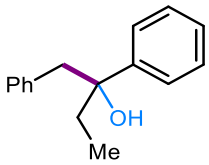

6.3ba

^{13}C NMR

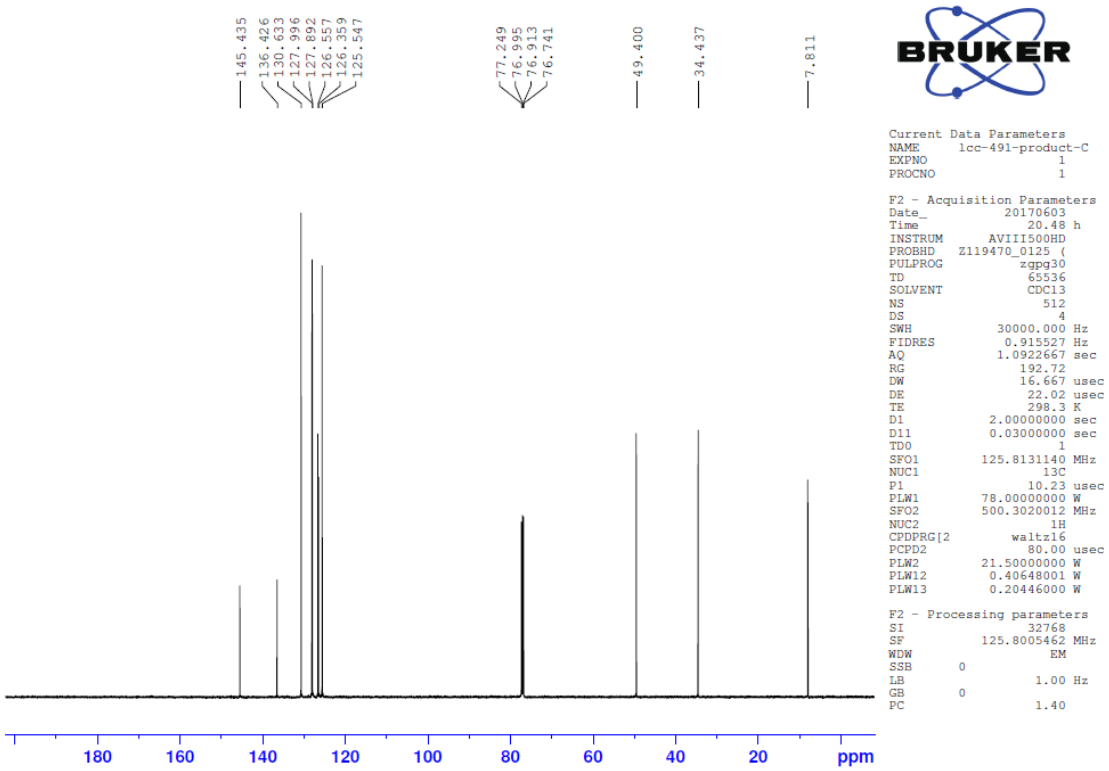


```
Current Data Parameters
NAME      1cc-491-product-C
EXPNO                    1
PROCNO                   1

F2 - Acquisition Parameters
Date_           20170603
Time              20.48 h
INSTRUM       AVIII500HD
PROBHD    Z119470_0125 (
PULPROG           zgpg30
TD                65536
SOLVENT           CDCl3
NS                  512
DS                    4
SWH           30000.000 Hz
FIDRES         0.915527 Hz
AQ             1.0922667 sec
RG                192.72
DW                16.667 usec
DE                22.02 usec
TE                298.3 K
D1             2.00000000 sec
D11            0.03000000 sec
TD0                   1
SFO1         125.8131140 MHz
NUC1                 13C
P1                10.23 usec
PLW1         78.00000000 W
SFO2         500.3020012 MHz
NUC2                  1H
CPDPRG[2          waltz16
PCPD2             80.00 usec
PLW2         21.50000000 W
PLW12         0.40648001 W
PLW13         0.20446000 W

F2 - Processing parameters
SI                32768
SF          125.8005462 MHz
WDW                  EM
SSB       0
LB                1.00 Hz
GB        0
PC                1.40
```

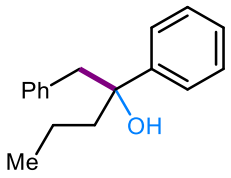
Ph
OH
Me

6.3ca

^{1}H NMR

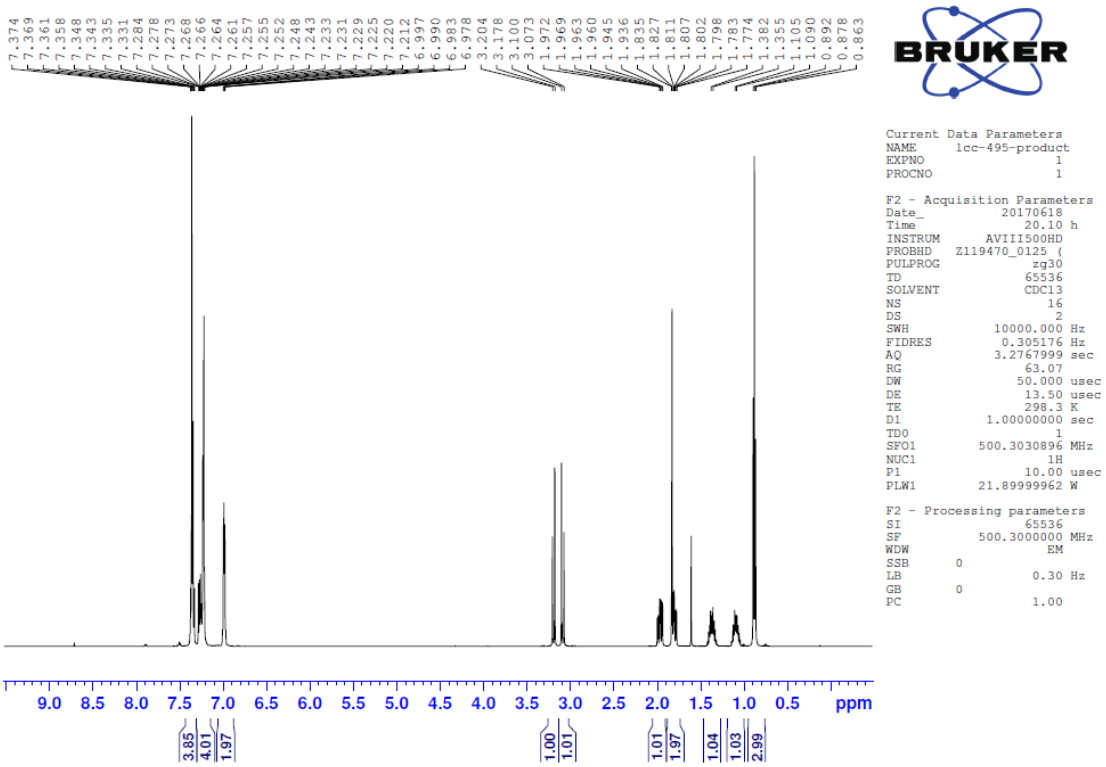
7.374
7.369
7.361
7.358
7.348
7.343
7.335
7.331
7.284
7.278
7.273
7.268
7.266
7.264
7.261
7.257
7.255
7.252
7.248
7.243
7.233
7.231
7.229
7.225
7.220
7.212
6.997
6.990
6.983
6.978
3.204
3.178
3.100
3.073
1.972
1.969
1.963
1.960
1.945
1.936
1.835
1.827
1.811
1.807
1.802
1.798
1.783
1.774
1.382
1.355
1.105
1.090
0.892
0.878
0.863
BRUKER
Current Data Parameters
NAME 1cc-495-product
EXPNO 1
PROCNO 1
F2 - Acquisition Parameters
Date_ 20170618
Time 20.10 h
INSTRUM AVIII500HD
PROBHD Z119470_0125 (
PULPROG zg30
TD 65536
SOLVENT CDCl3
NS 16
DS 2
SWH 10000.000 Hz
FIDRES 0.305176 Hz
AQ 3.2767999 sec
RG 63.07
DW 50.000 usec
DE 13.50 usec
TE 298.3 K
D1 1.00000000 sec
TD0 1
SFO1 500.3030896 MHz
NUC1 1H
P1 10.00 usec
PLW1 21.89999962 W
F2 - Processing parameters
SI 65536
SF 500.3000000 MHz
WDW EM
SSB 0
LB 0.30 Hz
GB 0
PC 1.00
9.0 8.5 8.0 7.5 7.0 6.5 6.0 5.5 5.0 4.5 4.0 3.5 3.0 2.5 2.0 1.5 1.0 0.5 ppm
3.85
4.01
1.97
1.00
1.01
1.01
1.97
1.04
1.03
2.99

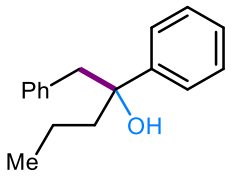

6.3ca

^{13}C NMR

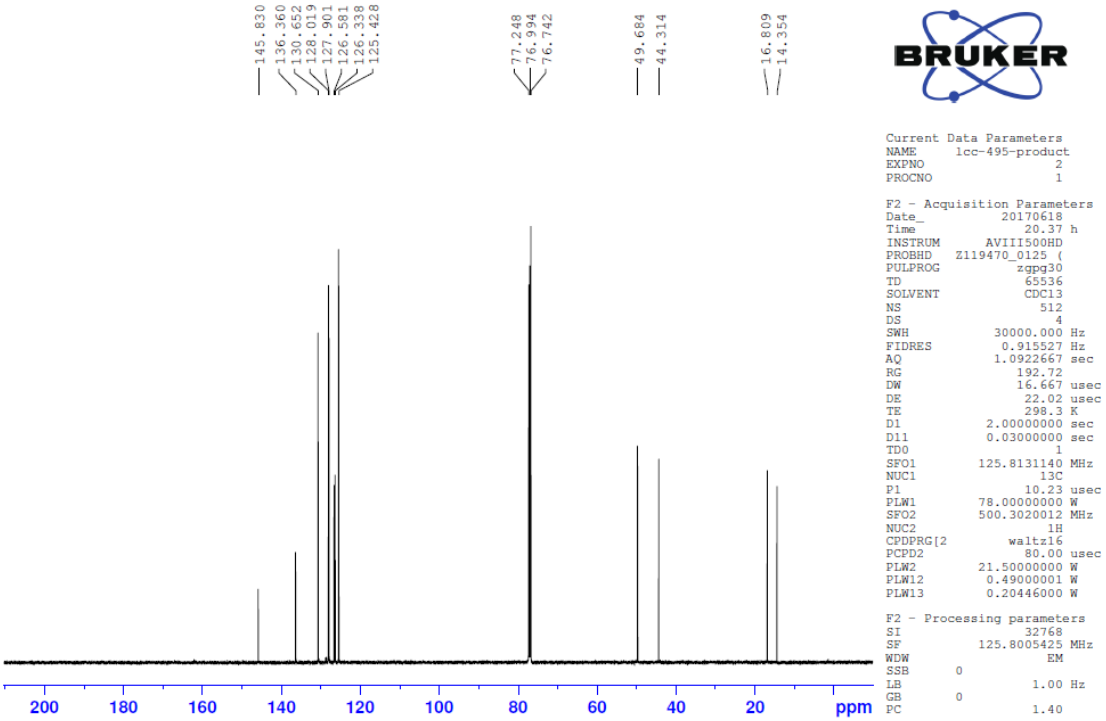


```
Current Data Parameters
NAME      1cc-495-product
EXPNO                   2
PROCNO                  1

F2 - Acquisition Parameters
Date_           20170618
Time              20.37 h
INSTRUM       AVIII500HD
PROBHD    Z119470_0125 (
PULPROG          zgpg30
TD                65536
SOLVENT           CDCl3
NS                  512
DS                    4
SWH           30000.000 Hz
FIDRES         0.915527 Hz
AQ             1.0922667 sec
RG                192.72
DW                16.667 usec
DE                22.02 usec
TE                298.3 K
D1             2.00000000 sec
D11            0.03000000 sec
TD0                   1
SFO1         125.8131140 MHz
NUC1                 13C
P1                10.23 usec
PLW1         78.00000000 W
SFO2         500.3020012 MHz
NUC2                 1H
CPDPRG[2         waltz16
PCPD2             80.00 usec
PLW2         21.50000000 W
PLW12         0.49000001 W
PLW13         0.20446000 W

F2 - Processing parameters
SI                32768
SF           125.8005425 MHz
WDW                  EM
SSB       0
LB                1.00 Hz
GB        0
PC                1.40
```

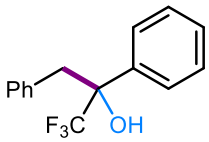

6.3da

^{1}H NMR

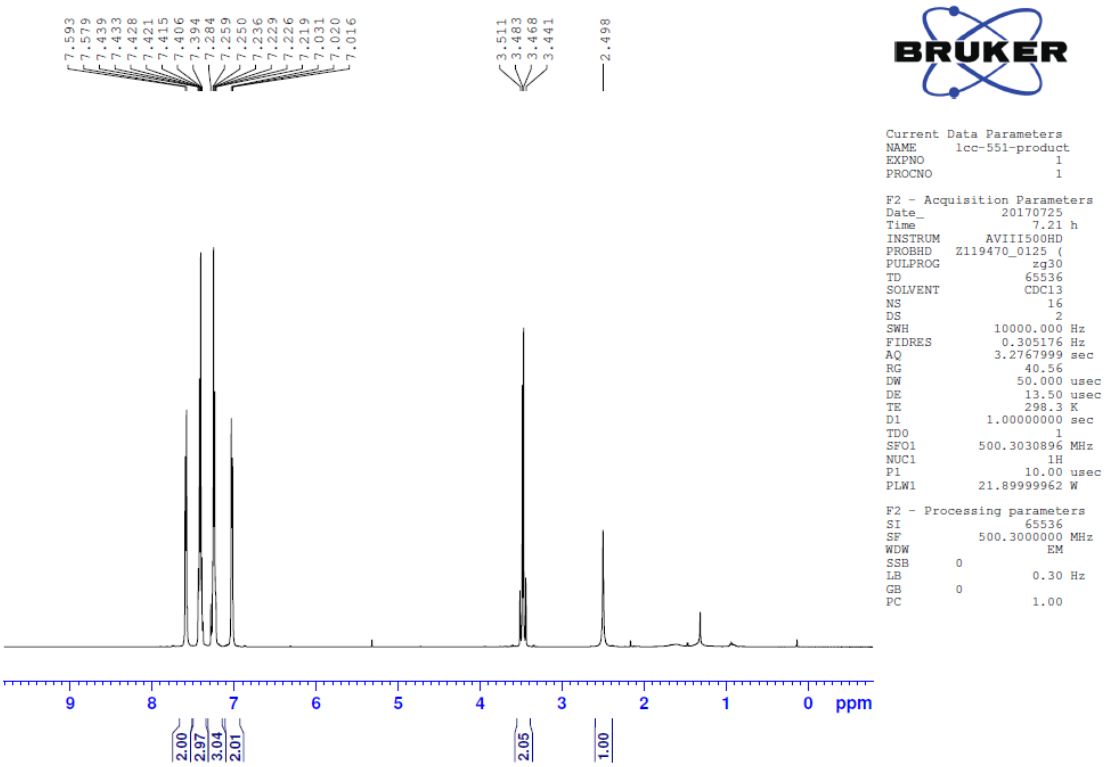


```
Current Data Parameters
NAME      1cc-551-product
EXPNO                   1
PROCNO                  1

F2 - Acquisition Parameters
Date_           20170725
Time                7.21 h
INSTRUM       AVIII500HD
PROBHD    Z119470_0125 (
PULPROG             zg30
TD                 65536
SOLVENT            CDCl3
NS                    16
DS                     2
SWH            10000.000 Hz
FIDRES             0.305176 Hz
AQ              3.2767999 sec
RG                 40.56
DW                 50.000 usec
DE                 13.50 usec
TE                 298.3 K
D1              1.00000000 sec
TD0                    1
SFO1          500.3030896 MHz
NUC1                  1H
P1                 10.00 usec
PLW1          21.89999962 W

F2 - Processing parameters
SI                 65536
SF            500.3000000 MHz
WDW                   EM
SSB       0
LB                 0.30 Hz
GB        0
PC                 1.00
```

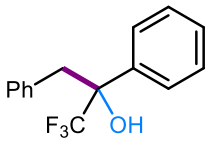

6.3da

^{13}C NMR

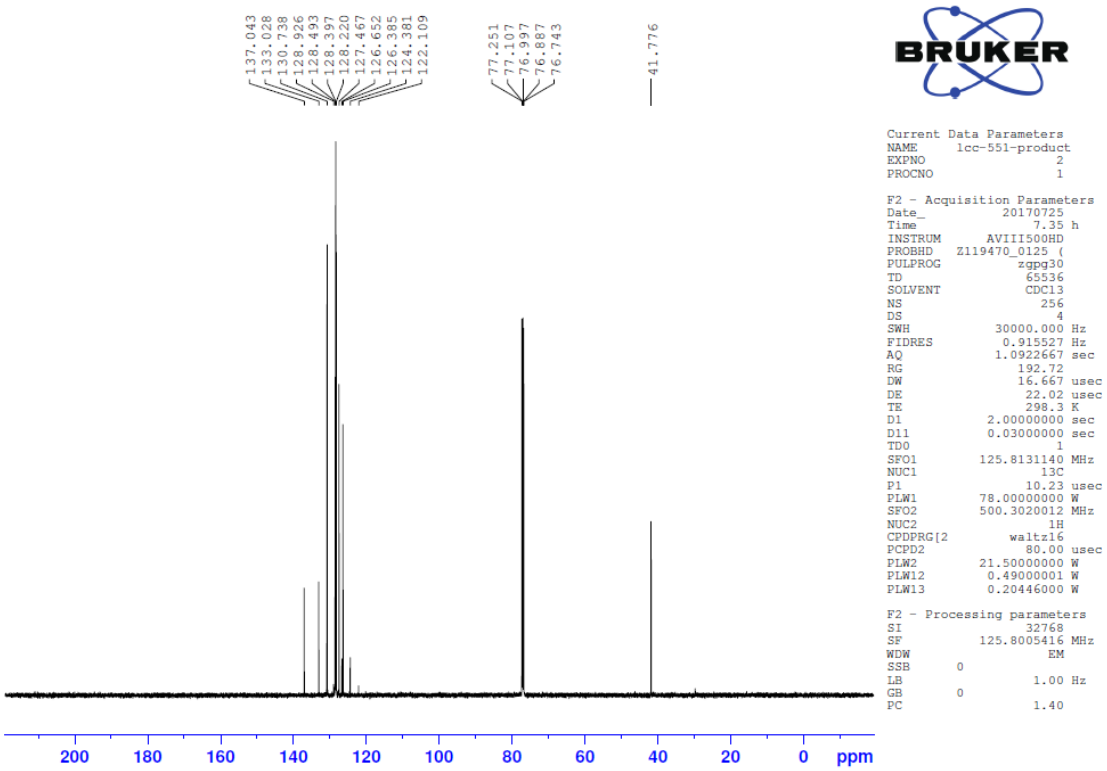

BRUKER

```
Current Data Parameters
NAME      1cc-551-product
EXPNO                   2
PROCNO                  1

F2 - Acquisition Parameters
Date_           20170725
Time                7.35 h
INSTRUM       AVIII500HD
PROBHD    Z119470_0125 (
PULPROG           zgpg30
TD                65536
SOLVENT           CDCl3
NS                  256
DS                    4
SWH           30000.000 Hz
FIDRES            0.915527 Hz
AQ                1.0922667 sec
RG                  192.72
DW                  16.667 usec
DE                  22.02 usec
TE                  298.3 K
D1              2.00000000 sec
D11             0.03000000 sec
TD0                     1
SFO1          125.8131140 MHz
NUC1                  13C
P1                  10.23 usec
PLW1          78.00000000 W
SFO2          500.3020012 MHz
NUC2                  1H
CPDPRG[2          waltz16
PCPD2               80.00 usec
PLW2          21.50000000 W
PLW12          0.49000001 W
PLW13          0.20446000 W

F2 - Processing parameters
SI                  32768
SF          125.8005416 MHz
WDW                   EM
SSB       0
LB                  1.00 Hz
GB        0
PC                  1.40
```

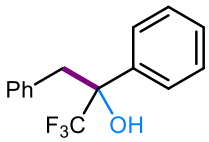

6.3da

^{19}F NMR

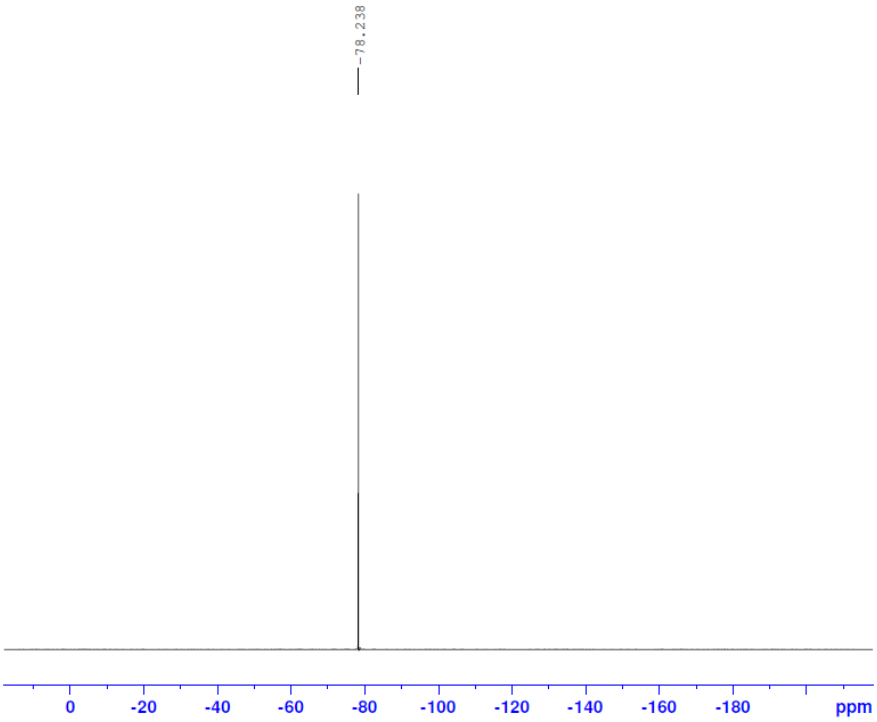


```
Current Data Parameters
NAME      1cc-551-product
EXPNO                   3
PROCNO                  1

F2 - Acquisition Parameters
Date_           20170725
Time                7.36 h
INSTRUM       AVIII500HD
PROBHD    Z119470_0125 (
PULPROG   zgbsfhiqqn.baseopt
TD                 131072
SOLVENT             CDCl3
NS                     16
DS                      4
SWH           111111.109 Hz
FIDRES          1.695421 Hz
AQ              0.5898240 sec
RG                 192.72
DW                  4.500 usec
DE                 35.33 usec
TE                 298.3 K
D1              1.00000000 sec
D11             0.03000000 sec
D12             0.00002000 sec
TD0                     1
SFO1          470.7052618 MHz
NUC1                  19F
P1                  15.00 usec
P2                  30.00 usec
PLW1          39.50000000 W
SFO2          500.3025015 MHz
NUC2                  1H
CPDPRG[2          waltz16
PCPD2               80.00 usec
PLW2          21.50000000 W
PLW12          0.49000001 W

F2 - Processing parameters
SI                  65536
SF            470.7523370 MHz
WDW                    EM
SSB       0
LB                  0.30 Hz
GB        0
PC                  1.00
```

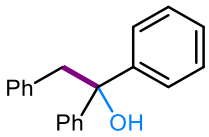

6.3ea

^{1}H NMR

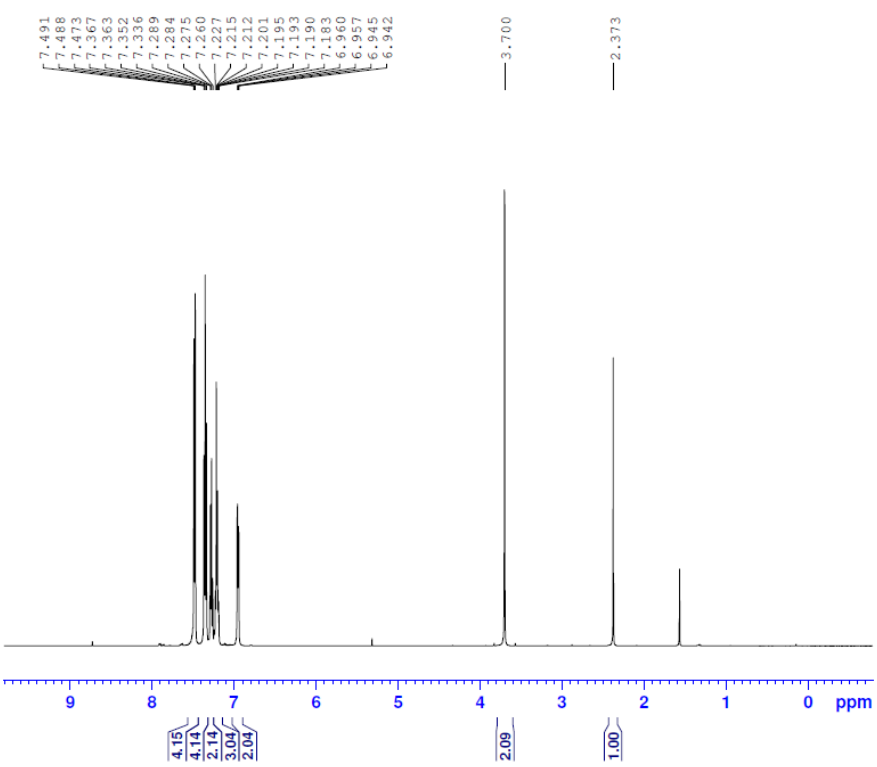


```
Current Data Parameters
NAME      lcc-552-product
EXPNO                   1
PROCNO                  1

F2 - Acquisition Parameters
Date_           20170630
Time               9.12 h
INSTRUM       AVIII500HD
PROBHD    Z119470_0125 (
PULPROG             zg30
TD                 65536
SOLVENT            CDCl3
NS                    16
DS                     2
SWH            10000.000 Hz
FIDRES             0.305176 Hz
AQ             3.2767999 sec
RG                 40.56
DW                 50.000 usec
DE                 13.50 usec
TE                 298.3 K
D1             1.00000000 sec
TD0                    1
SFO1          500.3030896 MHz
NUC1                  1H
P1                 10.00 usec
PLW1          21.89999962 W

F2 - Processing parameters
SI                 65536
SF            500.3000000 MHz
WDW                   EM
SSB       0
LB                 0.30 Hz
GB        0
PC                 1.00
```

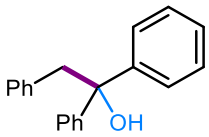

6.3ea

^{13}C NMR

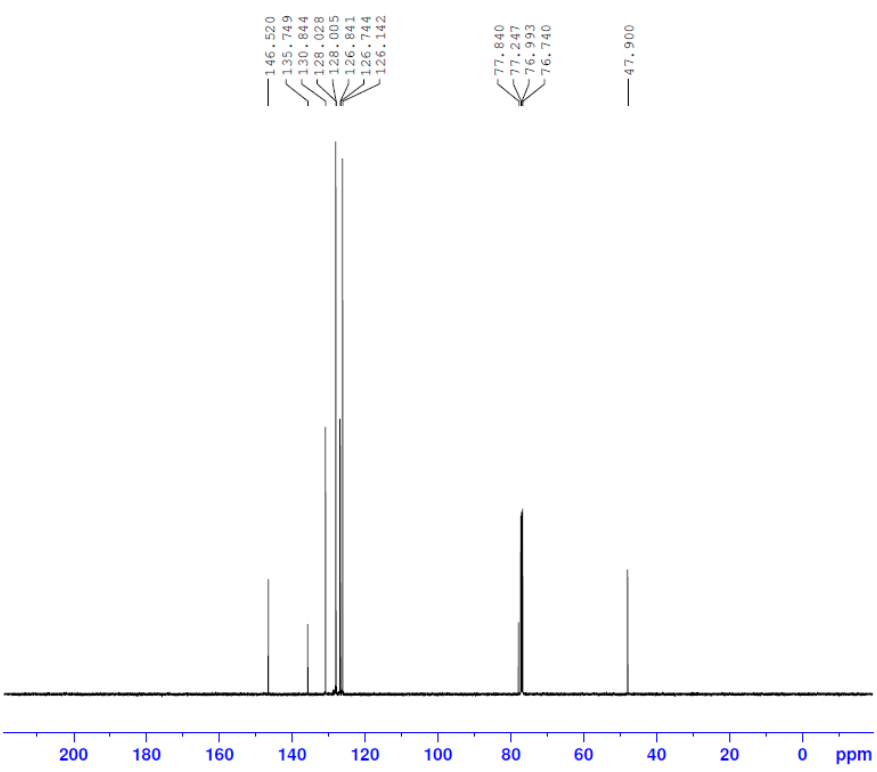


```
Current Data Parameters
NAME      lcc-552-product
EXPNO                   2
PROCNO                  1

F2 - Acquisition Parameters
Date_           20170630
Time              13.03 h
INSTRUM       AVIII500HD
PROBHD    Z119470_0125 (
PULPROG           zgpg30
TD                65536
SOLVENT           CDCl3
NS                  256
DS                    4
SWH           30000.000 Hz
FIDRES            0.915527 Hz
AQ                1.0922667 sec
RG                192.72
DW                16.667 usec
DE                22.02 usec
TE                298.3 K
D1             2.00000000 sec
D11            0.03000000 sec
TD0                   1
SFO1          125.8131140 MHz
NUC1                 13C
P1                10.23 usec
PLW1          78.00000000 W
SFO2          500.3020012 MHz
NUC2                  1H
CPDPRG[2          waltz16
PCPD2             80.00 usec
PLW2          21.50000000 W
PLW12          0.49000001 W
PLW13          0.20446000 W

F2 - Processing parameters
SI                32768
SF            125.8005462 MHz
WDW                  EM
SSB       0
LB                1.00 Hz
GB        0
PC                1.40
```

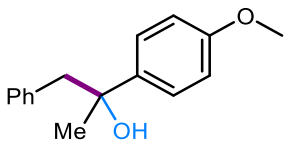

6.3fa

^{1}H NMR

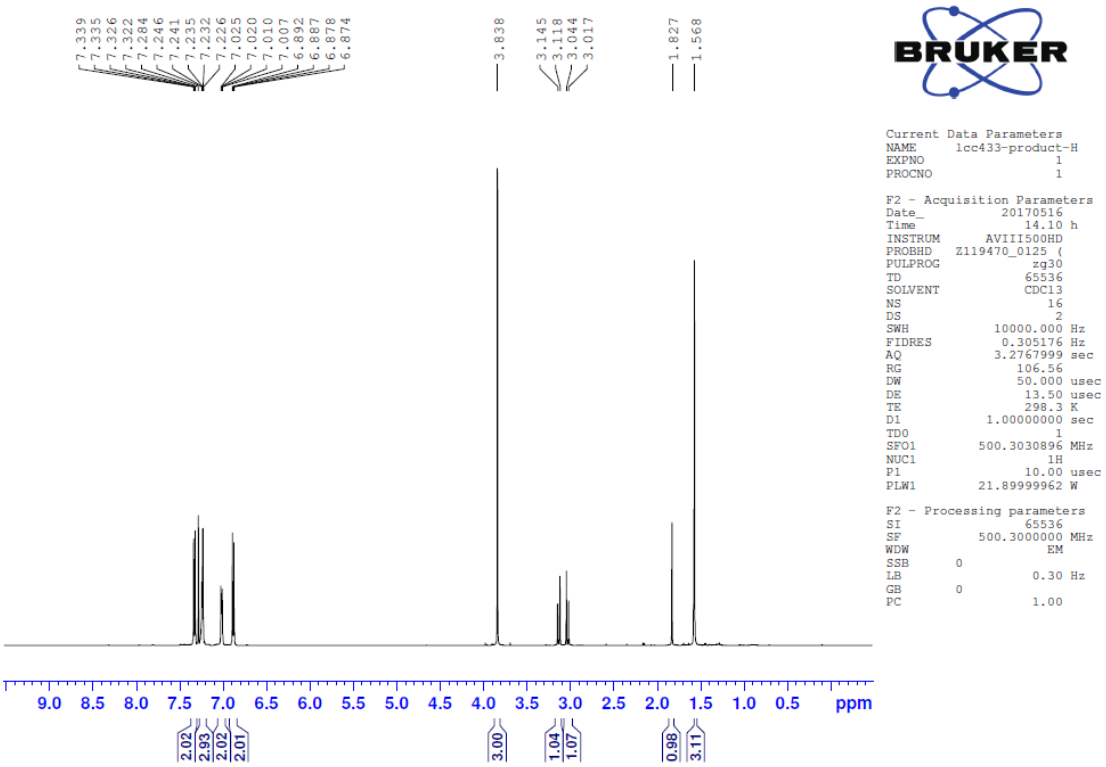

BRUKER

```
Current Data Parameters
NAME      1cc433-product-H
EXPNO                    1
PROCNO                   1

F2 - Acquisition Parameters
Date_           20170516
Time              14.10 h
INSTRUM       AVIII500HD
PROBHD    Z119470_0125 (
PULPROG              zg30
TD                  65536
SOLVENT             CDCl3
NS                     16
DS                      2
SWH             10000.000 Hz
FIDRES          0.305176 Hz
AQ              3.2767999 sec
RG                 106.56
DW                 50.000 usec
DE                 13.50 usec
TE                 298.3 K
D1              1.00000000 sec
TD0                     1
SFO1          500.3030896 MHz
NUC1                   1H
P1                 10.00 usec
PLW1          21.89999962 W

F2 - Processing parameters
SI                  65536
SF            500.3000000 MHz
WDW                    EM
SSB       0
LB                0.30 Hz
GB        0
PC                1.00
```

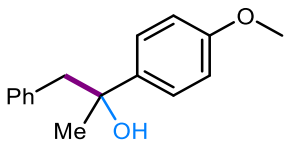
Ph
Me
OH
O

6.3fa

^{13}C NMR

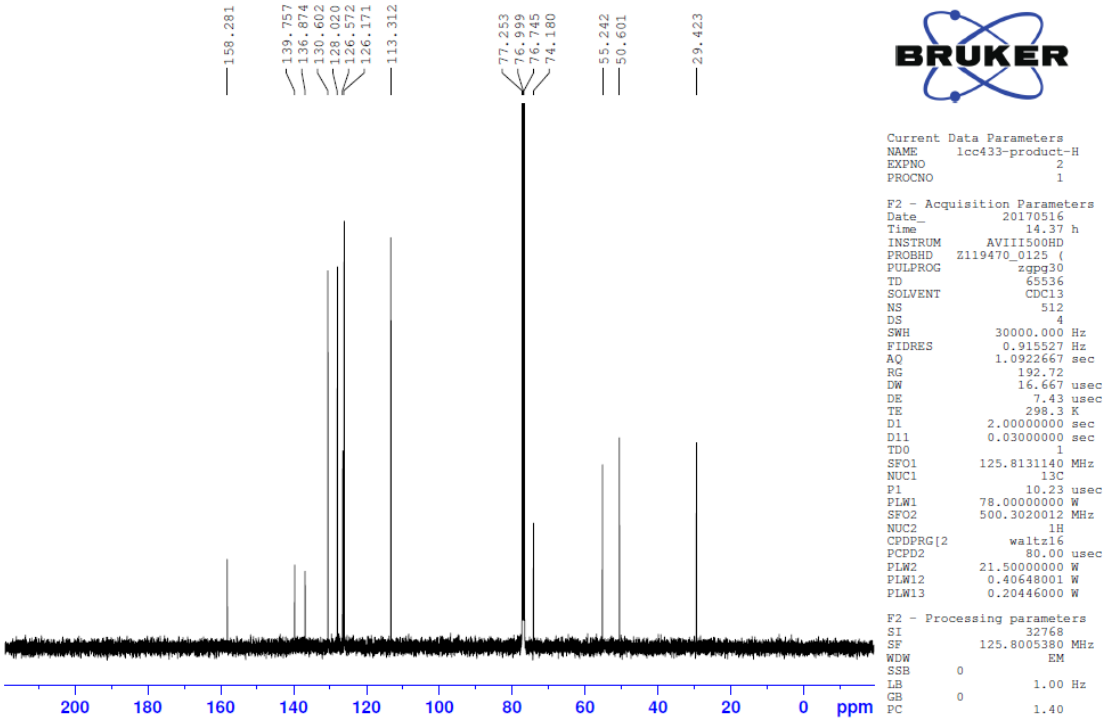
158.281
139.757
136.874
130.602
128.020
126.572
126.171
113.312
77.253
76.999
76.745
74.180
55.242
50.601
29.423
200
180
160
140
120
100
80
60
40
20
0
ppm
BRUKER
Current Data Parameters
NAME 1cc433-product-H
EXPNO 2
PROCNO 1
F2 - Acquisition Parameters
Date_ 20170516
Time 14.37 h
INSTRUM AVIII500HD
PROBHD Z119470_0125 (
PULPROG zgpg30
TD 65536
SOLVENT CDCl3
NS 512
DS 4
SWH 30000.000 Hz
FIDRES 0.915527 Hz
AQ 1.0922667 sec
RG 192.72
DW 16.667 usec
DE 7.43 usec
TE 298.3 K
D1 2.00000000 sec
D11 0.03000000 sec
TD0 1
SFO1 125.8131140 MHz
NUC1 13C
P1 10.23 usec
PLW1 78.00000000 W
SFO2 500.3020012 MHz
NUC2 1H
CPDPRG[2 waltz16
PCPD2 80.00 usec
PLW2 21.50000000 W
PLW12 0.40648001 W
PLW13 0.20446000 W
F2 - Processing parameters
SI 32768
SF 125.8005380 MHz
WDW EM
SSB 0
LB 1.00 Hz
GB 0
PC 1.40

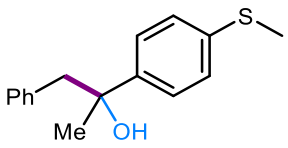

6.3ga

^{1}H NMR

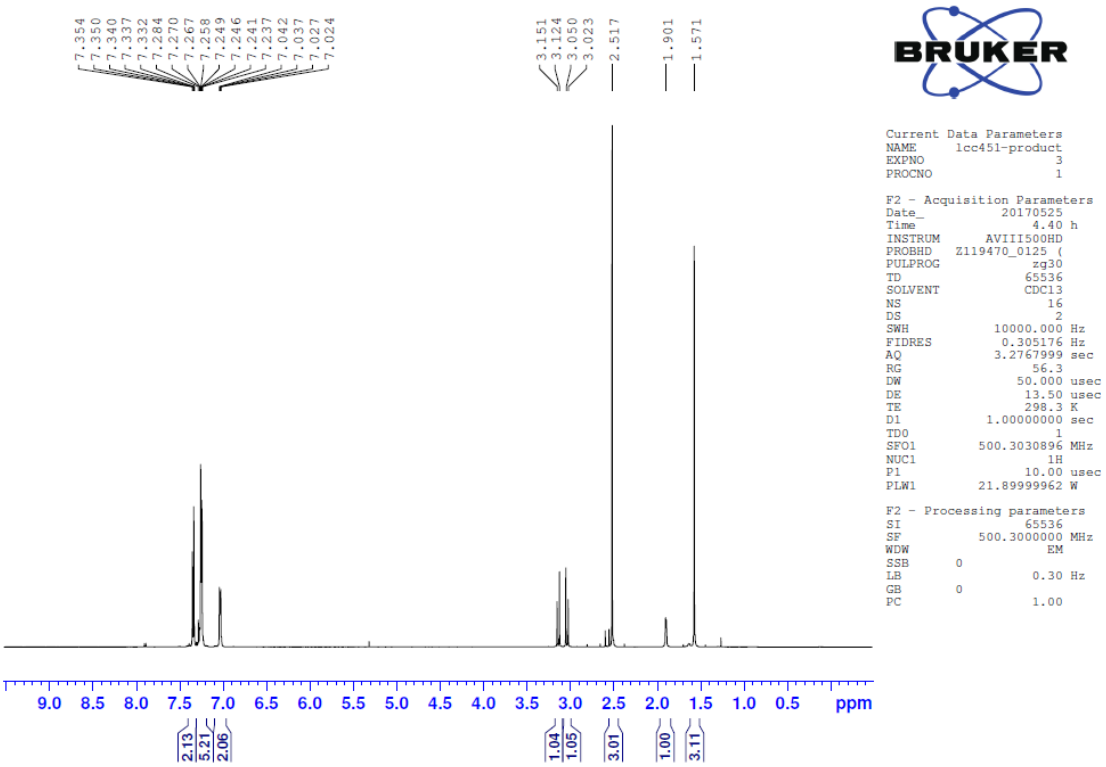

BRUKER

```
Current Data Parameters
NAME      1cc451-product
EXPNO                  3
PROCNO                 1

F2 - Acquisition Parameters
Date_           20170525
Time                4.40 h
INSTRUM       AVIII500HD
PROBHD    Z119470_0125 (
PULPROG             zg30
TD                 65536
SOLVENT            CDCl3
NS                    16
DS                     2
SWH             10000.000 Hz
FIDRES          0.305176 Hz
AQ              3.2767999 sec
RG                  56.3
DW                50.000 usec
DE                13.50 usec
TE                298.3 K
D1             1.00000000 sec
TD0                    1
SFO1          500.3030896 MHz
NUC1                  1H
P1                 10.00 usec
PLW1          21.89999962 W

F2 - Processing parameters
SI                 65536
SF            500.3000000 MHz
WDW                   EM
SSB       0
LB                 0.30 Hz
GB        0
PC                 1.00
```

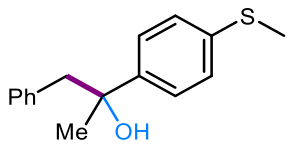
S
Ph
Me
OH

6.3ga

^{13}C NMR

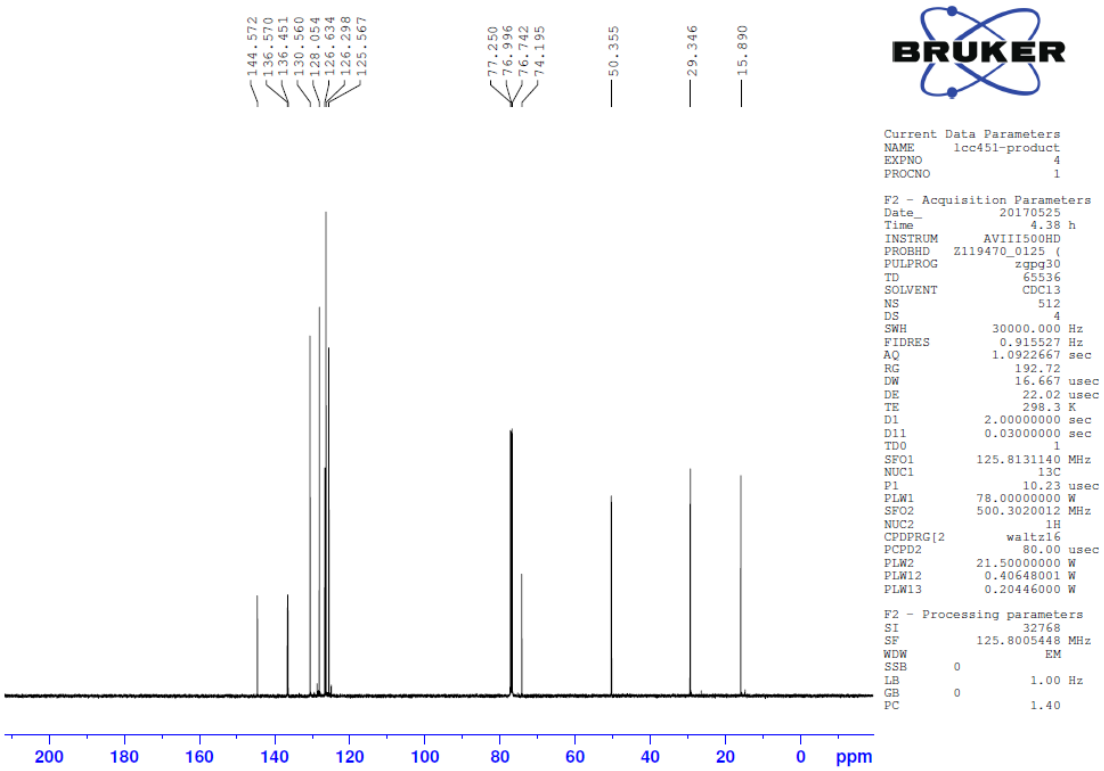
144.572
136.570
136.451
130.560
128.054
126.634
126.298
125.567
77.250
76.996
76.742
74.195
50.355
29.346
15.890
200
180
160
140
120
100
80
60
40
20
0
ppm
BRUKER
Current Data Parameters
NAME 1cc451-product
EXPNO 4
PROCNO 1
F2 - Acquisition Parameters
Date_ 20170525
Time 4.38 h
INSTRUM AVIII500HD
PROBHD Z119470_0125 (
PULPROG zgpg30
TD 65536
SOLVENT CDCl3
NS 512
DS 4
SWH 30000.000 Hz
FIDRES 0.915527 Hz
AQ 1.0922667 sec
RG 192.72
DW 16.667 usec
DE 22.02 usec
TE 298.3 K
D1 2.00000000 sec
D11 0.03000000 sec
TD0 1
SFO1 125.8131140 MHz
NUC1 13C
P1 10.23 usec
PLW1 78.00000000 W
SFO2 500.3020012 MHz
NUC2 1H
CPDPRG[2 waltz16
PCPD2 80.00 usec
PLW2 21.50000000 W
PLW12 0.40648001 W
PLW13 0.20446000 W
F2 - Processing parameters
SI 32768
SF 125.8005448 MHz
WDW EM
SSB 0
LB 1.00 Hz
GB 0
PC 1.40

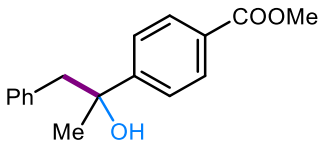

6.3ha

^{1}H NMR

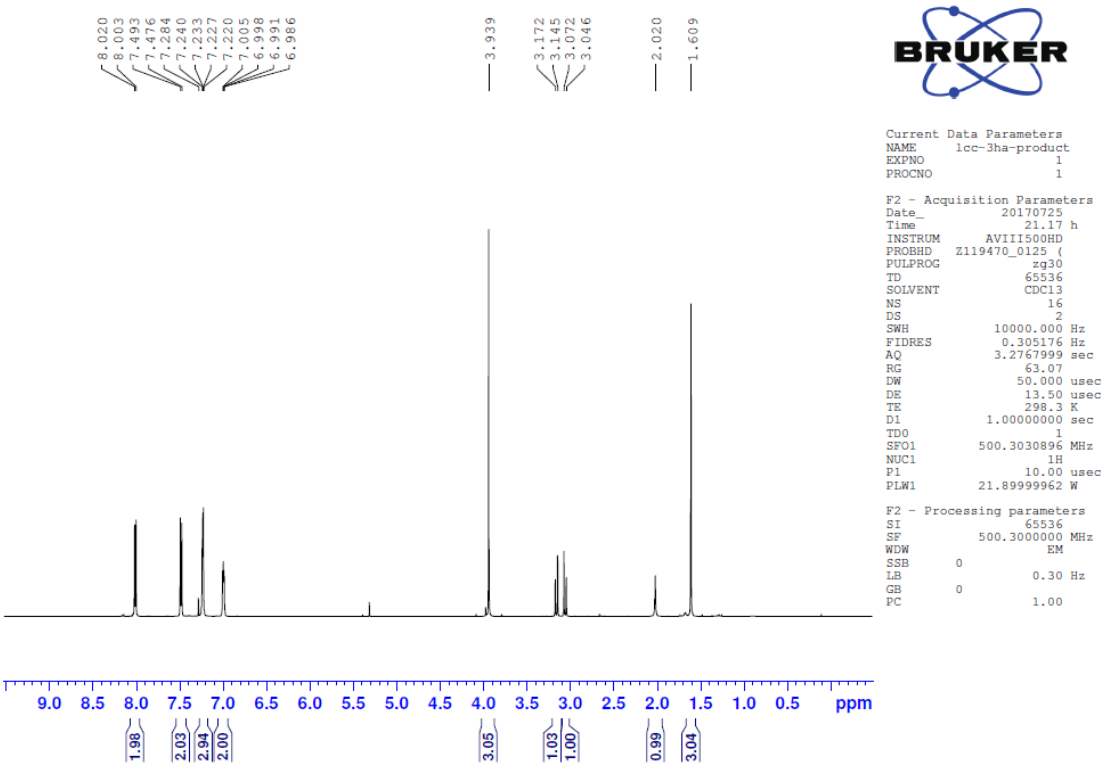


```
Current Data Parameters
NAME      1cc-3ha-product
EXPNO                   1
PROCNO                  1

F2 - Acquisition Parameters
Date_           20170725
Time              21.17 h
INSTRUM       AVIII500HD
PROBHD    Z119470_0125 (
PULPROG             zg30
TD                 65536
SOLVENT            CDCl3
NS                    16
DS                     2
SWH           10000.000 Hz
FIDRES         0.305176 Hz
AQ             3.2767999 sec
RG                63.07
DW               50.000 usec
DE               13.50 usec
TE                298.3 K
D1            1.00000000 sec
TD0                    1
SFO1         500.3030896 MHz
NUC1                  1H
P1                10.00 usec
PLW1         21.89999962 W

F2 - Processing parameters
SI                 65536
SF            500.3000000 MHz
WDW                   EM
SSB       0
LB                 0.30 Hz
GB        0
PC                 1.00
```

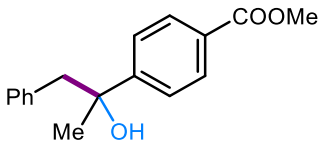
COOMe
Ph
Me
OH

6.3ha

^{13}C NMR

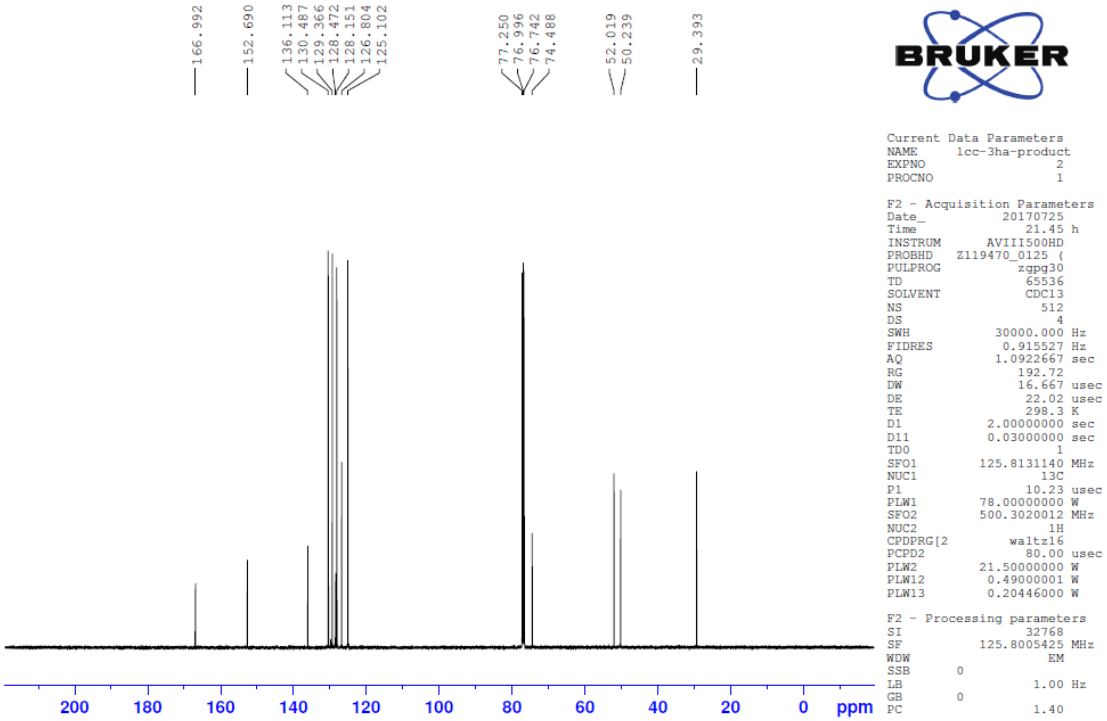
166.992
152.690
136.113
130.487
129.366
128.472
128.151
126.804
125.102
77.250
76.996
76.742
74.488
52.019
50.239
29.393
200
180
160
140
120
100
80
60
40
20
0
ppm
BRUKER
Current Data Parameters
NAME 1cc-3ha-product
EXPNO 2
PROCNO 1
F2 - Acquisition Parameters
Date_ 20170725
Time 21.45 h
INSTRUM AVIII500HD
PROBHD Z119470_0125 (
PULPROG zgpg30
TD 65536
SOLVENT CDCl3
NS 512
DS 4
SWH 30000.000 Hz
FIDRES 0.915527 Hz
AQ 1.0922667 sec
RG 192.72
DW 16.667 usec
DE 22.02 usec
TE 298.3 K
D1 2.00000000 sec
D11 0.03000000 sec
TD0 1
SFO1 125.8131140 MHz
NUC1 13C
P1 10.23 usec
PLW1 78.00000000 W
SFO2 500.3020012 MHz
NUC2 1H
CPDPRG[2 waltz16
PCPD2 80.00 usec
PLW2 21.50000000 W
PLW12 0.49000001 W
PLW13 0.20446000 W
F2 - Processing parameters
SI 32768
SF 125.8005425 MHz
WDW EM
SSB 0
LB 1.00 Hz
GB 0
PC 1.40

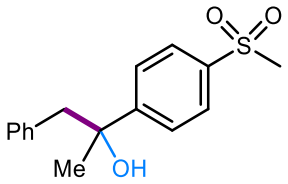

6.3ia

^{1}H NMR

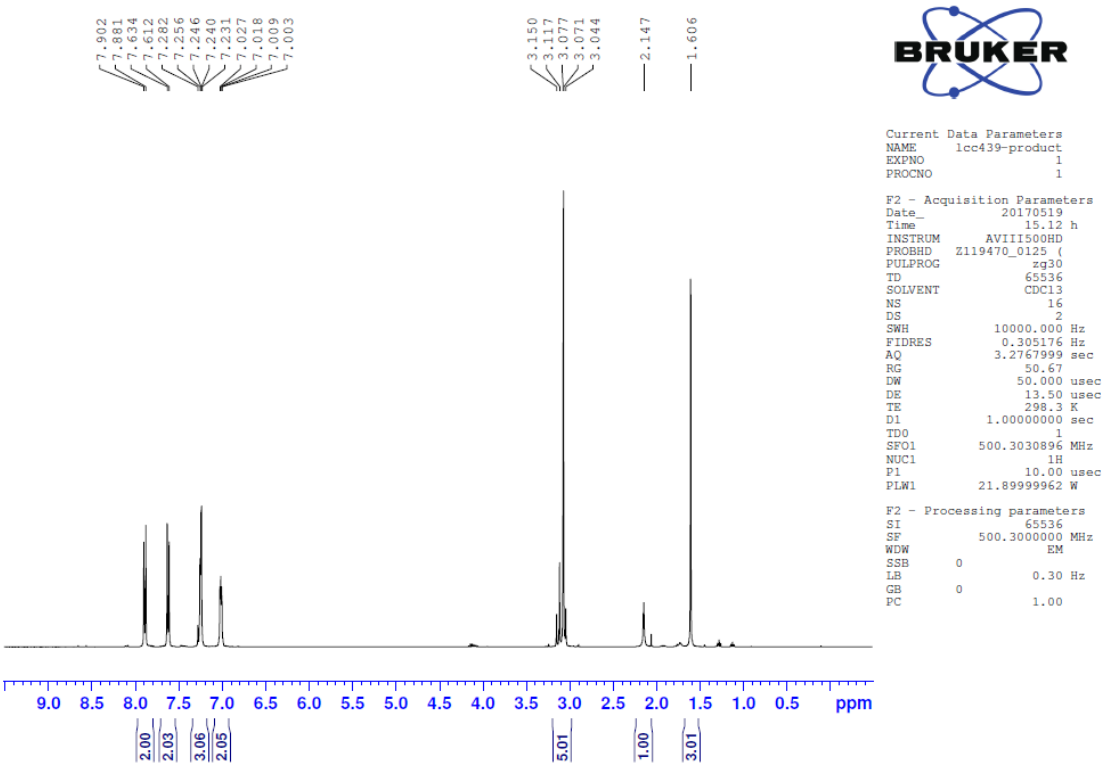

BRUKER

```
Current Data Parameters
NAME      1cc439-product
EXPNO                  1
PROCNO                 1

F2 - Acquisition Parameters
Date_           20170519
Time               15.12 h
INSTRUM       AVIII500HD
PROBHD   Z119470_0125 (
PULPROG             zg30
TD                 65536
SOLVENT             CDCl3
NS                    16
DS                     2
SWH            10000.000 Hz
FIDRES             0.305176 Hz
AQ                 3.2767999 sec
RG                    50.67
DW                 50.000 usec
DE                 13.50 usec
TE                 298.3 K
D1              1.00000000 sec
TD0                    1
SFO1          500.3030896 MHz
NUC1                  1H
P1                 10.00 usec
PLW1          21.89999962 W

F2 - Processing parameters
SI                 65536
SF            500.3000000 MHz
WDW                   EM
SSB       0
LB                 0.30 Hz
GB        0
PC                 1.00
```

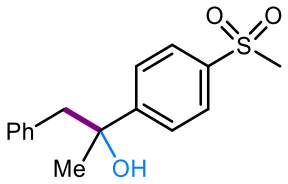

6.3ia

^{13}C NMR

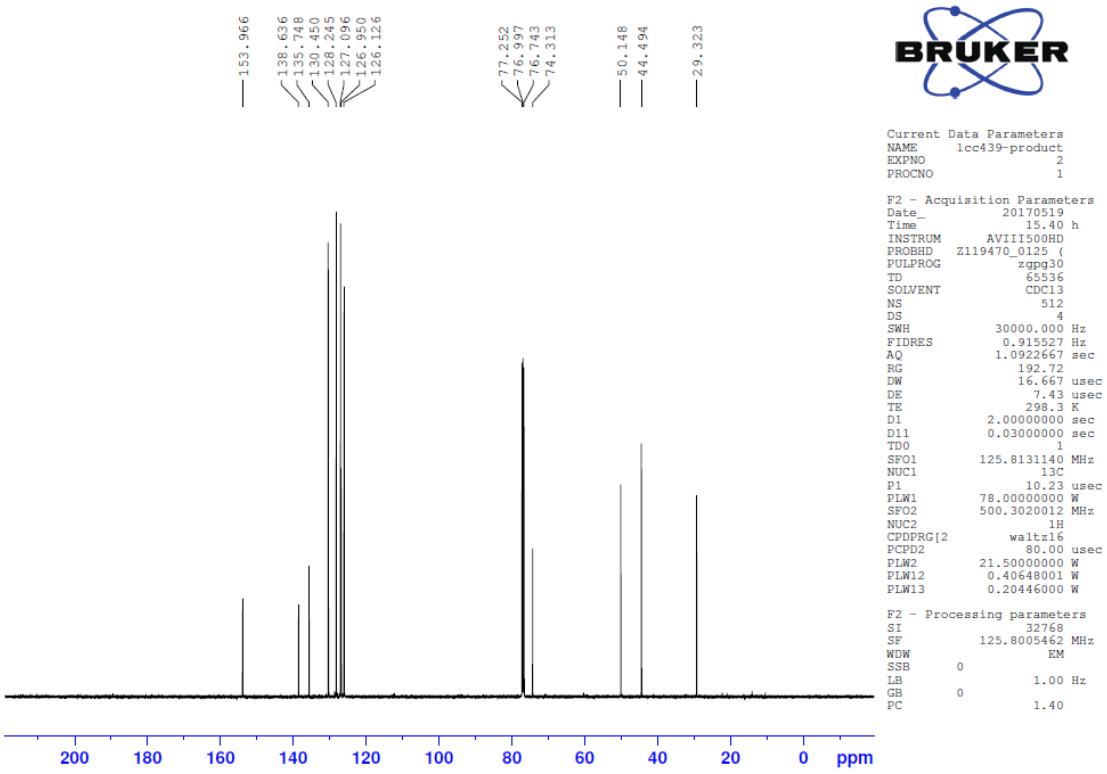


```
Current Data Parameters
NAME      1cc439-product
EXPNO                  2
PROCNO                 1

F2 - Acquisition Parameters
Date_           20170519
Time              15.40 h
INSTRUM       AVIII500HD
PROBHD   Z119470_0125 (
PULPROG          zgpg30
TD                65536
SOLVENT           CDCl3
NS                  512
DS                    4
SWH           30000.000 Hz
FIDRES            0.915527 Hz
AQ                1.0922667 sec
RG                  192.72
DW                  16.667 usec
DE                   7.43 usec
TE                 298.3 K
D1            2.00000000 sec
D11           0.03000000 sec
TD0                   1
SFO1         125.8131140 MHz
NUC1                 13C
P1                 10.23 usec
PLW1         78.00000000 W
SFO2         500.3020012 MHz
NUC2                 1H
CPDPRG[2          waltz16
PCPD2              80.00 usec
PLW2         21.50000000 W
PLW12         0.40648001 W
PLW13         0.20446000 W

F2 - Processing parameters
SI                 32768
SF           125.8005462 MHz
WDW                   EM
SSB       0
LB                 1.00 Hz
GB        0
PC                 1.40
```

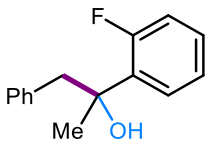
F
Ph
Me
OH

6.3ja

^{1}H NMR

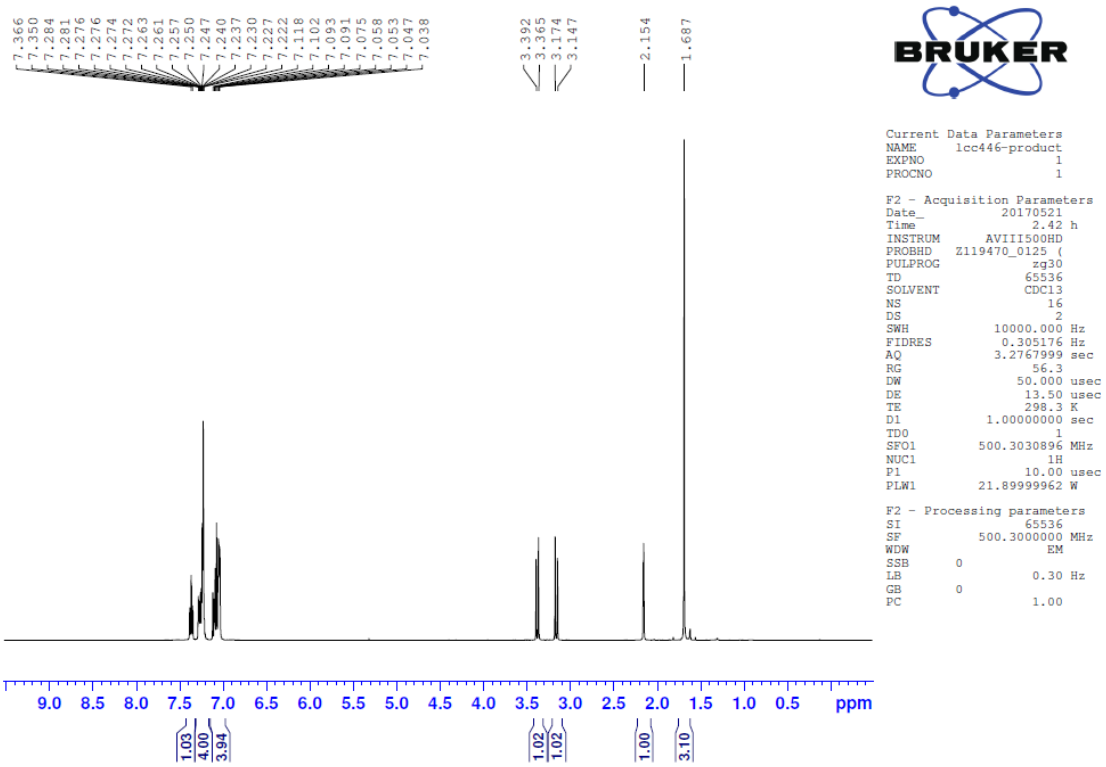
7.366
7.350
7.284
7.281
7.276
7.276
7.274
7.272
7.263
7.261
7.257
7.250
7.247
7.240
7.237
7.230
7.227
7.222
7.118
7.102
7.093
7.091
7.075
7.058
7.053
7.047
7.038
3.392
3.365
3.174
3.147
2.154
1.687
BRUKER
Current Data Parameters
NAME 1cc446-product
EXPNO 1
PROCNO 1
F2 - Acquisition Parameters
Date_ 20170521
Time 2.42 h
INSTRUM AVIII500HD
PROBHD Z119470_0125 (
PULPROG zg30
TD 65536
SOLVENT CDCl3
NS 16
DS 2
SWH 10000.000 Hz
FIDRES 0.305176 Hz
AQ 3.2767999 sec
RG 56.3
DW 50.000 usec
DE 13.50 usec
TE 298.3 K
D1 1.00000000 sec
TD0 1
SFO1 500.3030896 MHz
NUC1 1H
P1 10.00 usec
PLW1 21.89999962 W
F2 - Processing parameters
SI 65536
SF 500.3000000 MHz
WDW EM
SSB 0
LB 0.30 Hz
GB 0
PC 1.00
9.0 8.5 8.0 7.5 7.0 6.5 6.0 5.5 5.0 4.5 4.0 3.5 3.0 2.5 2.0 1.5 1.0 0.5 ppm
1.03
4.00
3.94
1.02
1.02
1.00
3.10

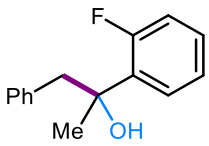

6.3ja

^{13}C NMR

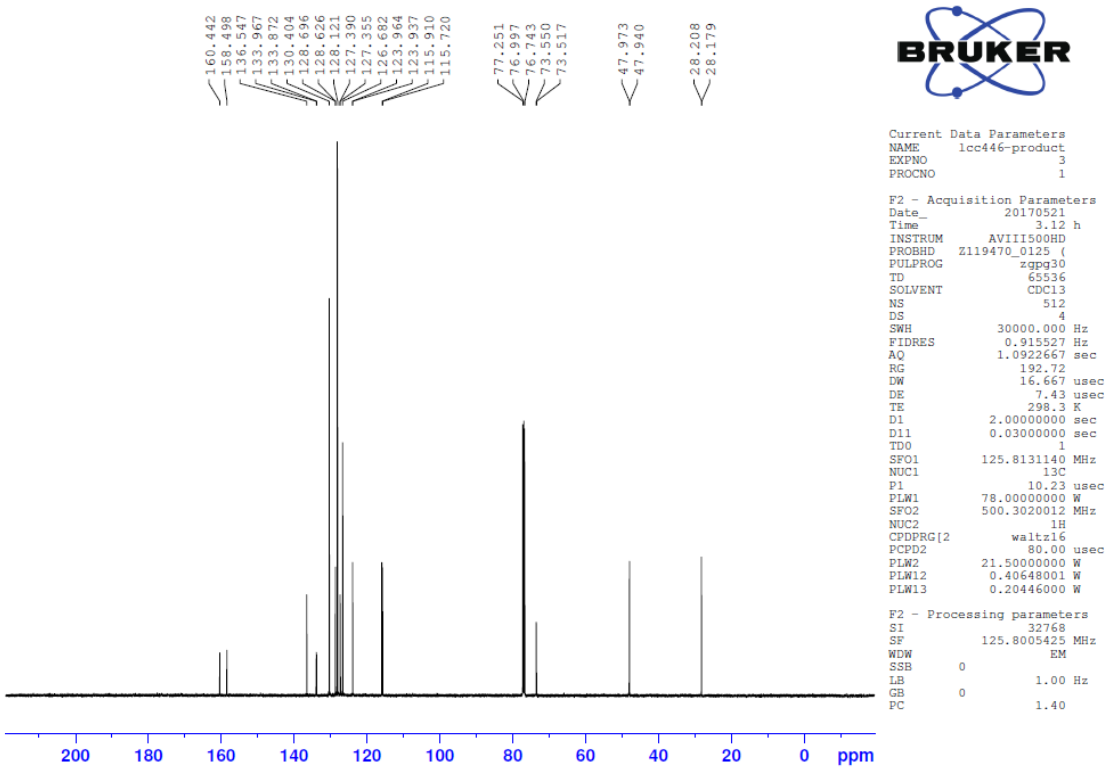


```
Current Data Parameters
NAME      1cc446-product
EXPNO                  3
PROCNO                 1

F2 - Acquisition Parameters
Date_           20170521
Time                3.12 h
INSTRUM       AVIII500HD
PROBHD    Z119470_0125 (
PULPROG           zgpg30
TD                65536
SOLVENT           CDCl3
NS                  512
DS                    4
SWH           30000.000 Hz
FIDRES            0.915527 Hz
AQ                1.0922667 sec
RG                  192.72
DW                  16.667 usec
DE                   7.43 usec
TE                 298.3 K
D1              2.00000000 sec
D11             0.03000000 sec
TD0                   1
SFO1          125.8131140 MHz
NUC1                 13C
P1                  10.23 usec
PLW1          78.00000000 W
SFO2          500.3020012 MHz
NUC2                  1H
CPDPRG[2          waltz16
PCPD2               80.00 usec
PLW2          21.50000000 W
PLW12          0.40648001 W
PLW13          0.20446000 W

F2 - Processing parameters
SI                 32768
SF            125.8005425 MHz
WDW                   EM
SSB       0
LB                  1.00 Hz
GB        0
PC                  1.40
```

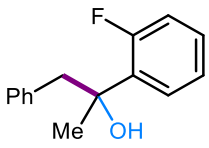

6.3ja

^{19}F NMR

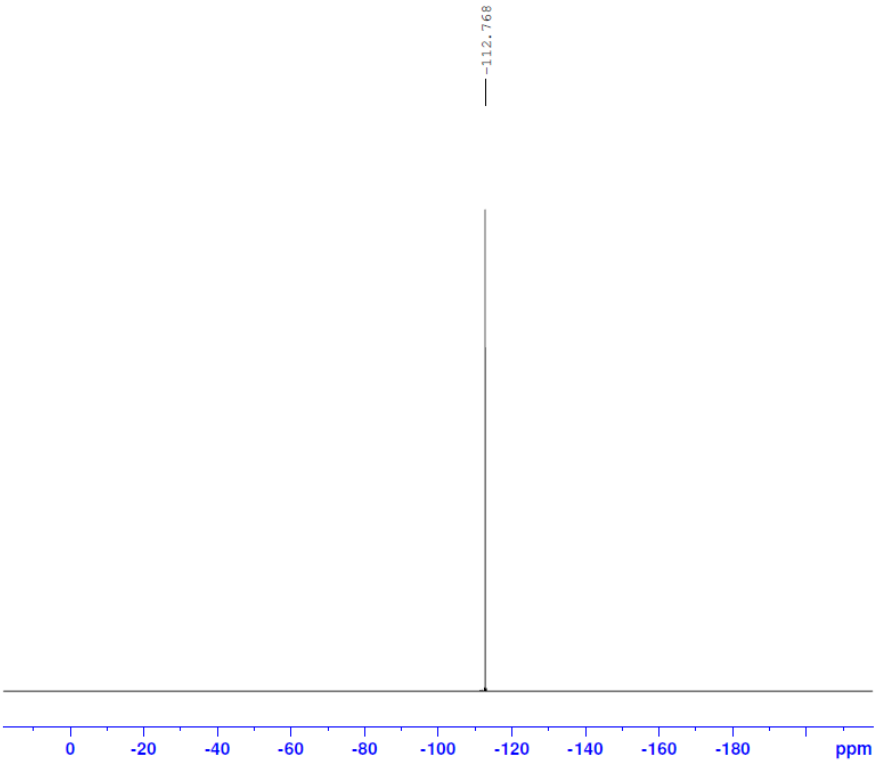


```
Current Data Parameters
NAME      1cc446-product
EXPNO                  2
PROCNO                 1

F2 - Acquisition Parameters
Date_           20170521
Time                2.44 h
INSTRUM       AVIII500HD
PROBHD    Z119470_0125 (
PULPROG   zgbsfhiqqn.baseopt
TD                 131072
SOLVENT              CDCl3
NS                      16
DS                       4
SWH           111111.109 Hz
FIDRES          1.695421 Hz
AQ              0.5898240 sec
RG                 192.72
DW                  4.500 usec
DE                 35.33 usec
TE                 298.3 K
D1              1.00000000 sec
D11             0.03000000 sec
D12             0.00002000 sec
TD0                     1
SFO1          470.7052618 MHz
NUC1                  19F
P1                  15.00 usec
P2                  30.00 usec
PLW1          39.50000000 W
SFO2          500.3025015 MHz
NUC2                  1H
CPDPRG[2          waltz16
PCPD2               80.00 usec
PLW2          21.50000000 W
PLW12          0.40648001 W

F2 - Processing parameters
SI                   65536
SF            470.7523370 MHz
WDW                     EM
SSB       0
LB                   0.30 Hz
GB        0
PC                   1.00
```

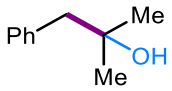

6.3ka

^{1}H NMR

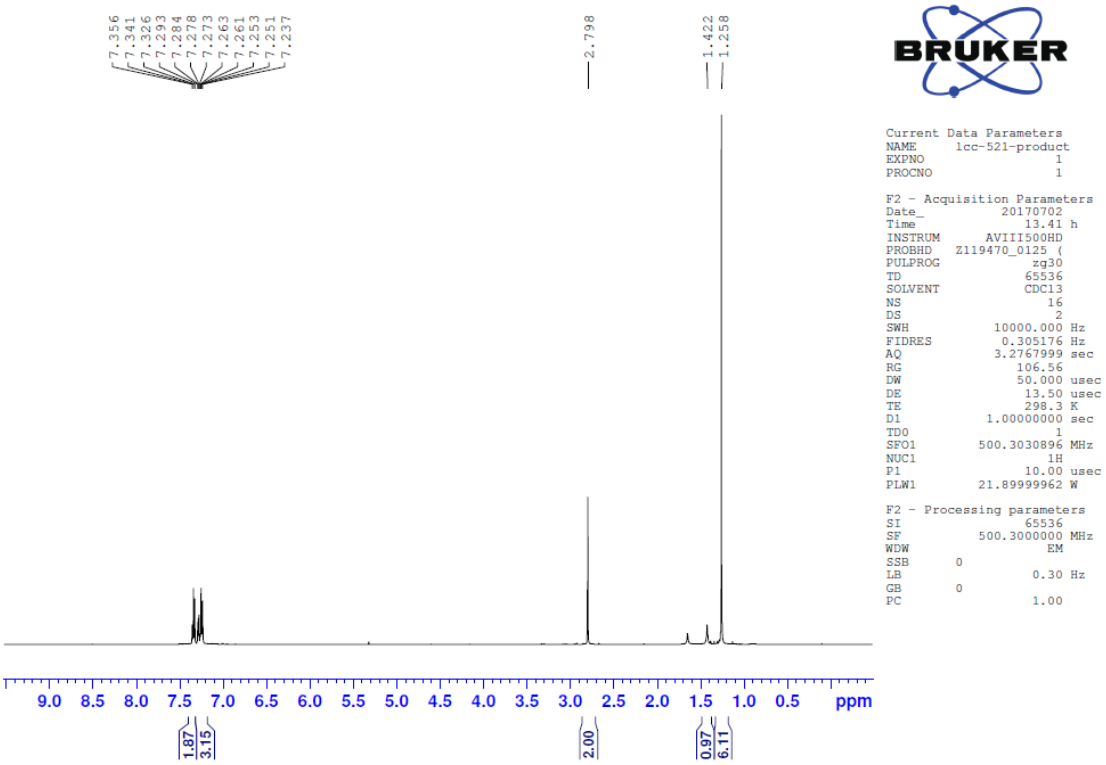

BRUKER

```
Current Data Parameters
NAME      1cc-521-product
EXPNO                   1
PROCNO                  1

F2 - Acquisition Parameters
Date_           20170702
Time              13.41 h
INSTRUM       AVIII500HD
PROBHD    Z119470_0125 (
PULPROG             zg30
TD                 65536
SOLVENT            CDCl3
NS                    16
DS                     2
SWH           10000.000 Hz
FIDRES         0.305176 Hz
AQ             3.2767999 sec
RG                106.56
DW                50.000 usec
DE                13.50 usec
TE                298.3 K
D1            1.00000000 sec
TD0                    1
SFO1         500.3030896 MHz
NUC1                  1H
P1                 10.00 usec
PLW1        21.89999962 W

F2 - Processing parameters
SI                 65536
SF           500.3000000 MHz
WDW                   EM
SSB       0
LB                 0.30 Hz
GB        0
PC                 1.00
```

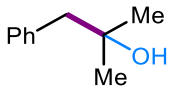

6.3ka

^{13}C NMR

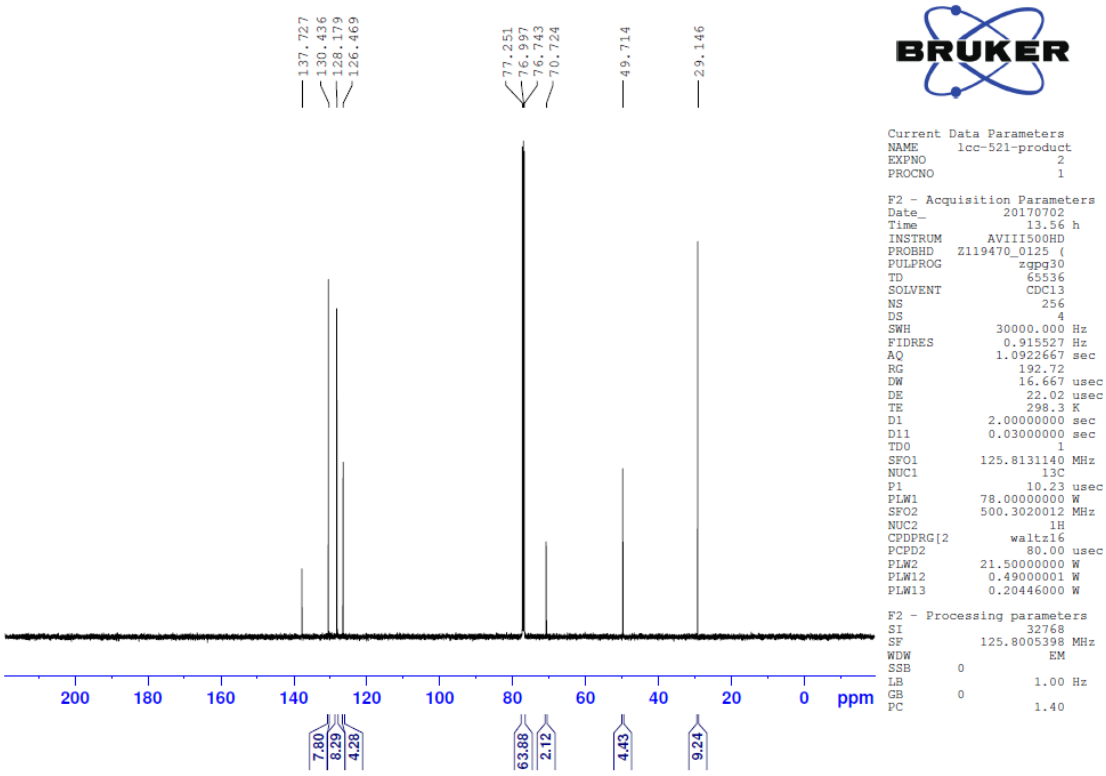


```
Current Data Parameters
NAME      lcc-521-product
EXPNO                   2
PROCNO                  1

F2 - Acquisition Parameters
Date_           20170702
Time              13.56 h
INSTRUM       AVIII500HD
PROBHD   Z119470_0125 (
PULPROG           zgpg30
TD                65536
SOLVENT           CDCl3
NS                  256
DS                    4
SWH           30000.000 Hz
FIDRES         0.915527 Hz
AQ             1.0922667 sec
RG                192.72
DW                16.667 usec
DE                22.02 usec
TE                298.3 K
D1            2.00000000 sec
D11           0.03000000 sec
TD0                   1
SFO1         125.8131140 MHz
NUC1                 13C
P1                10.23 usec
PLW1         78.00000000 W
SFO2         500.3020012 MHz
NUC2                 1H
CPDPRG[2          waltz16
PCPD2             80.00 usec
PLW2         21.50000000 W
PLW12         0.49000001 W
PLW13         0.20446000 W

F2 - Processing parameters
SI                32768
SF           125.8005398 MHz
WDW                  EM
SSB       0
LB                1.00 Hz
GB        0
PC                1.40
```

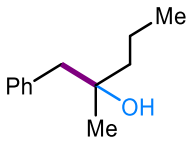
Me
Ph
OH
Me

6.3la

^{1}H NMR

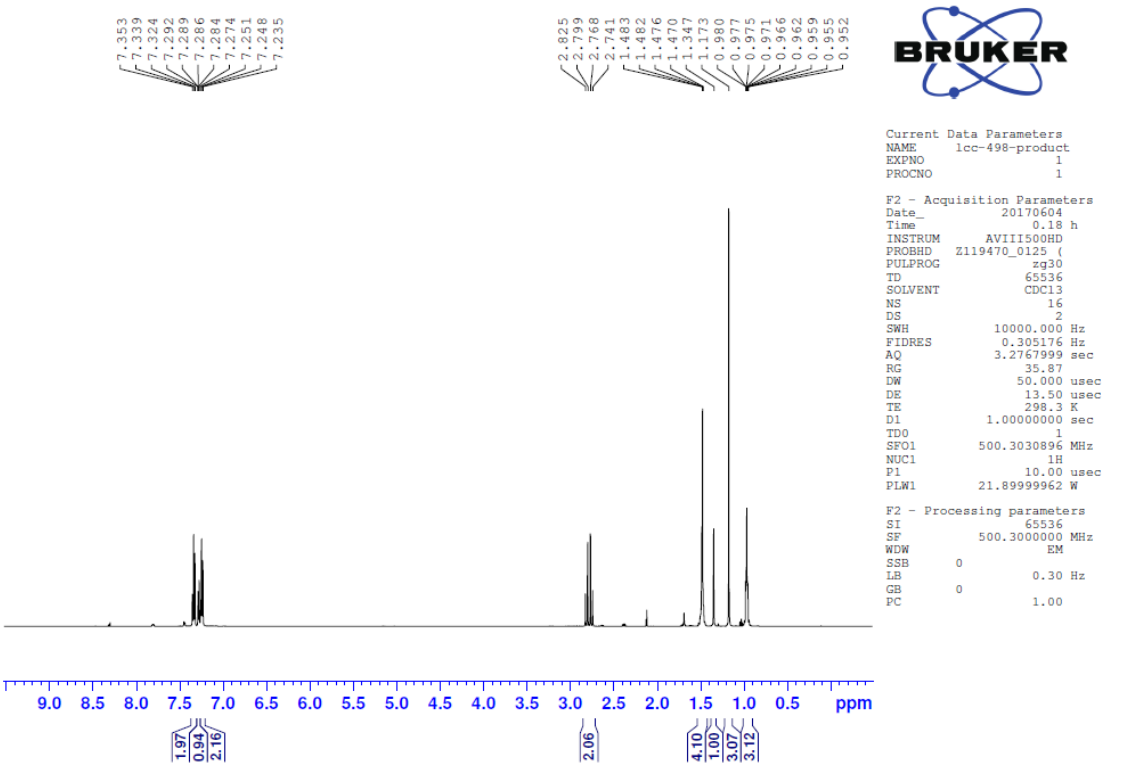
7.353
7.339
7.324
7.292
7.289
7.286
7.284
7.274
7.251
7.248
7.235
2.825
2.799
2.768
2.741
1.483
1.482
1.476
1.470
1.347
1.173
0.980
0.977
0.975
0.971
0.966
0.962
0.959
0.955
0.952
BRUKER
Current Data Parameters
NAME 1cc-498-product
EXPNO 1
PROCNO 1
F2 - Acquisition Parameters
Date_ 20170604
Time 0.18 h
INSTRUM AVIII500HD
PROBHD Z119470_0125 (
PULPROG zg30
TD 65536
SOLVENT CDCl3
NS 16
DS 2
SWH 10000.000 Hz
FIDRES 0.305176 Hz
AQ 3.2767999 sec
RG 35.87
DW 50.000 usec
DE 13.50 usec
TE 298.3 K
D1 1.00000000 sec
TD0 1
SFO1 500.3030896 MHz
NUC1 1H
P1 10.00 usec
PLW1 21.89999962 W
F2 - Processing parameters
SI 65536
SF 500.3000000 MHz
WDW EM
SSB 0
LB 0.30 Hz
GB 0
PC 1.00
9.0 8.5 8.0 7.5 7.0 6.5 6.0 5.5 5.0 4.5 4.0 3.5 3.0 2.5 2.0 1.5 1.0 0.5 ppm
1.97
0.94
2.16
2.06
4.10
1.00
3.07
3.12

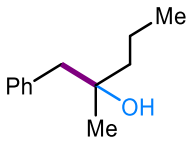

6.3la

^{13}C NMR

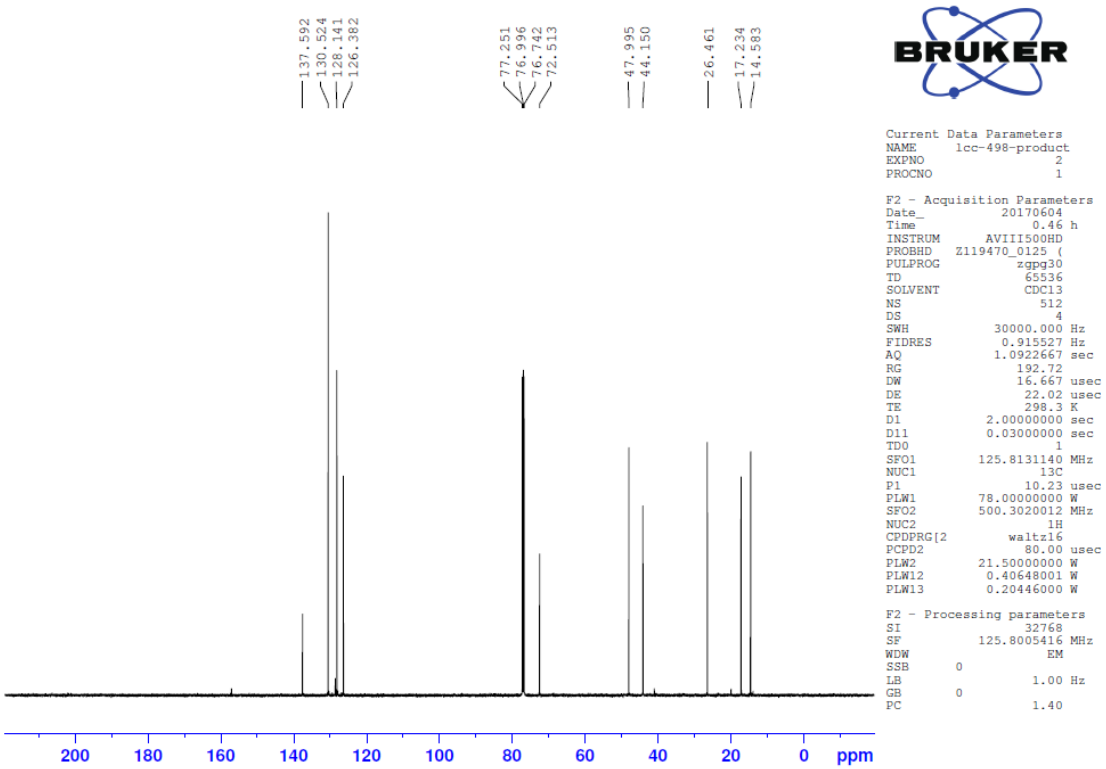


```
Current Data Parameters
NAME      1cc-498-product
EXPNO                   2
PROCNO                  1

F2 - Acquisition Parameters
Date_           20170604
Time                0.46 h
INSTRUM       AVIII500HD
PROBHD    Z119470_0125 (
PULPROG           zgpg30
TD                65536
SOLVENT           CDCl3
NS                  512
DS                    4
SWH           30000.000 Hz
FIDRES         0.915527 Hz
AQ             1.0922667 sec
RG                192.72
DW                16.667 usec
DE                22.02 usec
TE                298.3 K
D1            2.00000000 sec
D11           0.03000000 sec
TD0                   1
SFO1        125.8131140 MHz
NUC1                13C
P1                10.23 usec
PLW1         78.00000000 W
SFO2        500.3020012 MHz
NUC2                1H
CPDPRG[2         waltz16
PCPD2             80.00 usec
PLW2         21.50000000 W
PLW12         0.40648001 W
PLW13         0.20446000 W

F2 - Processing parameters
SI                32768
SF          125.8005416 MHz
WDW                 EM
SSB       0
LB                1.00 Hz
GB        0
PC                1.40
```

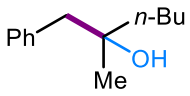
Ph
n-Bu
OH
Me

6.3ma

^{1}H NMR

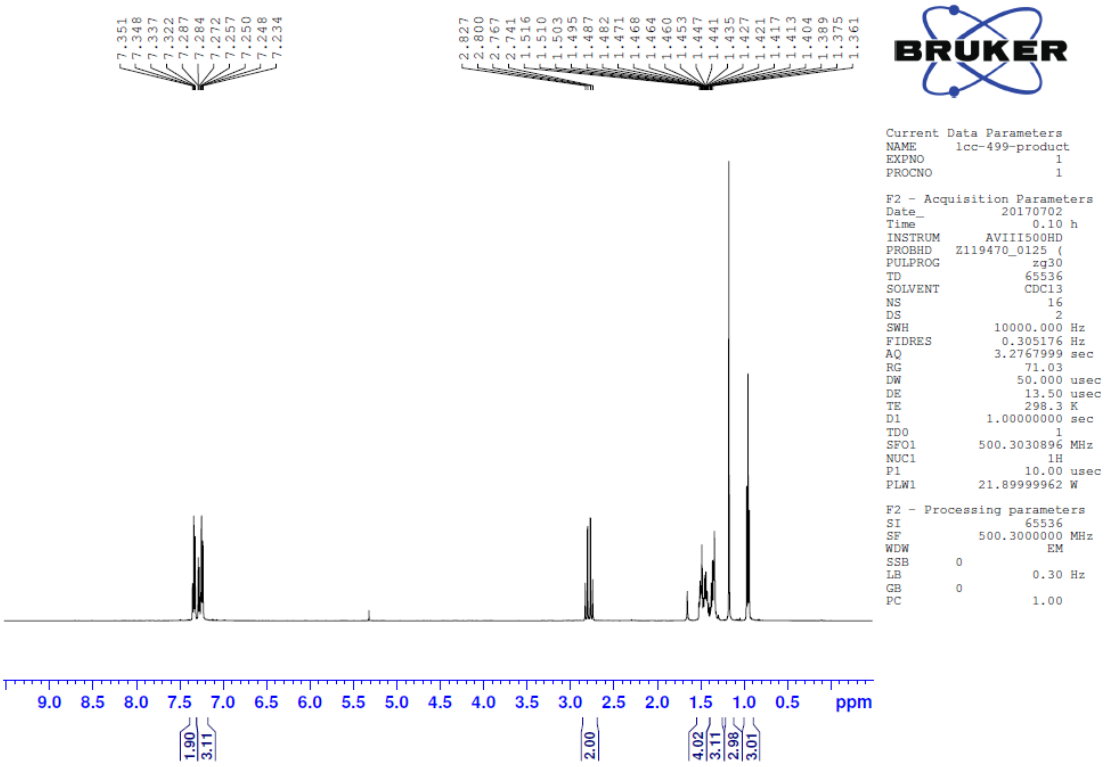
7.351
7.348
7.337
7.322
7.287
7.284
7.272
7.257
7.250
7.248
7.234
2.827
2.800
2.767
2.741
1.516
1.510
1.503
1.495
1.487
1.482
1.471
1.468
1.464
1.460
1.453
1.447
1.441
1.435
1.427
1.421
1.417
1.413
1.404
1.389
1.375
1.361
BRUKER
Current Data Parameters
NAME 1cc-499-product
EXPNO 1
PROCNO 1
F2 - Acquisition Parameters
Date_ 20170702
Time 0.10 h
INSTRUM AVIII500HD
PROBHD Z119470_0125 (
PULPROG zg30
TD 65536
SOLVENT CDCl3
NS 16
DS 2
SWH 10000.000 Hz
FIDRES 0.305176 Hz
AQ 3.2767999 sec
RG 71.03
DW 50.000 usec
DE 13.50 usec
TE 298.3 K
D1 1.00000000 sec
TD0 1
SFO1 500.3030896 MHz
NUC1 1H
P1 10.00 usec
PLW1 21.89999962 W
F2 - Processing parameters
SI 65536
SF 500.3000000 MHz
WDW EM
SSB 0
LB 0.30 Hz
GB 0
PC 1.00
9.0 8.5 8.0 7.5 7.0 6.5 6.0 5.5 5.0 4.5 4.0 3.5 3.0 2.5 2.0 1.5 1.0 0.5 ppm
1.90
3.11
2.00
4.02
3.11
2.98
3.01

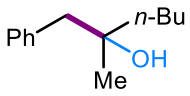

6.3ma

^{13}C NMR

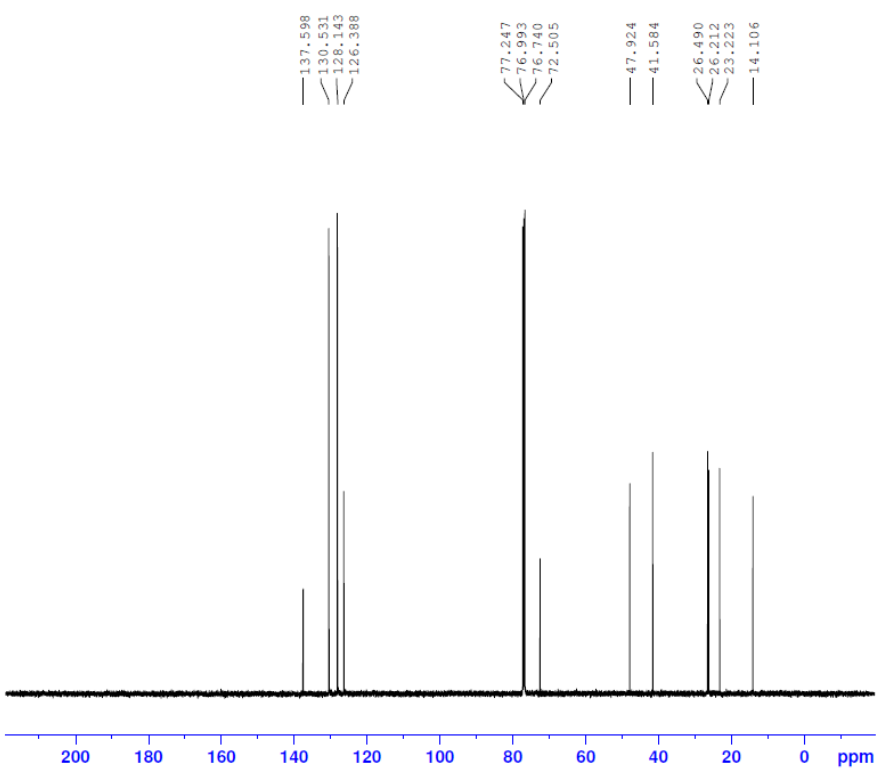


```
Current Data Parameters
NAME      lcc-499-product
EXPNO                   2
PROCNO                  1

F2 - Acquisition Parameters
Date_           20170702
Time                0.24 h
INSTRUM       AVIII500HD
PROBHD    Z119470_0125 (
PULPROG           zgpg30
TD                65536
SOLVENT           CDCl3
NS                  256
DS                    4
SWH           30000.000 Hz
FIDRES         0.915527 Hz
AQ             1.0922667 sec
RG                192.72
DW                16.667 usec
DE                22.02 usec
TE                298.3 K
D1             2.00000000 sec
D11            0.03000000 sec
TD0                   1
SFO1         125.8131140 MHz
NUC1                 13C
P1                10.23 usec
PLW1         78.00000000 W
SFO2         500.3020012 MHz
NUC2                 1H
CPDPRG[2          waltz16
PCPD2             80.00 usec
PLW2         21.50000000 W
PLW12         0.49000001 W
PLW13         0.20446000 W

F2 - Processing parameters
SI                32768
SF           125.8005407 MHz
WDW                  EM
SSB       0
LB                1.00 Hz
GB        0
PC                1.40
```

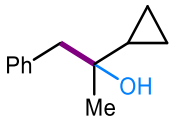
Ph
OH
Me

6.3na

^{1}H NMR

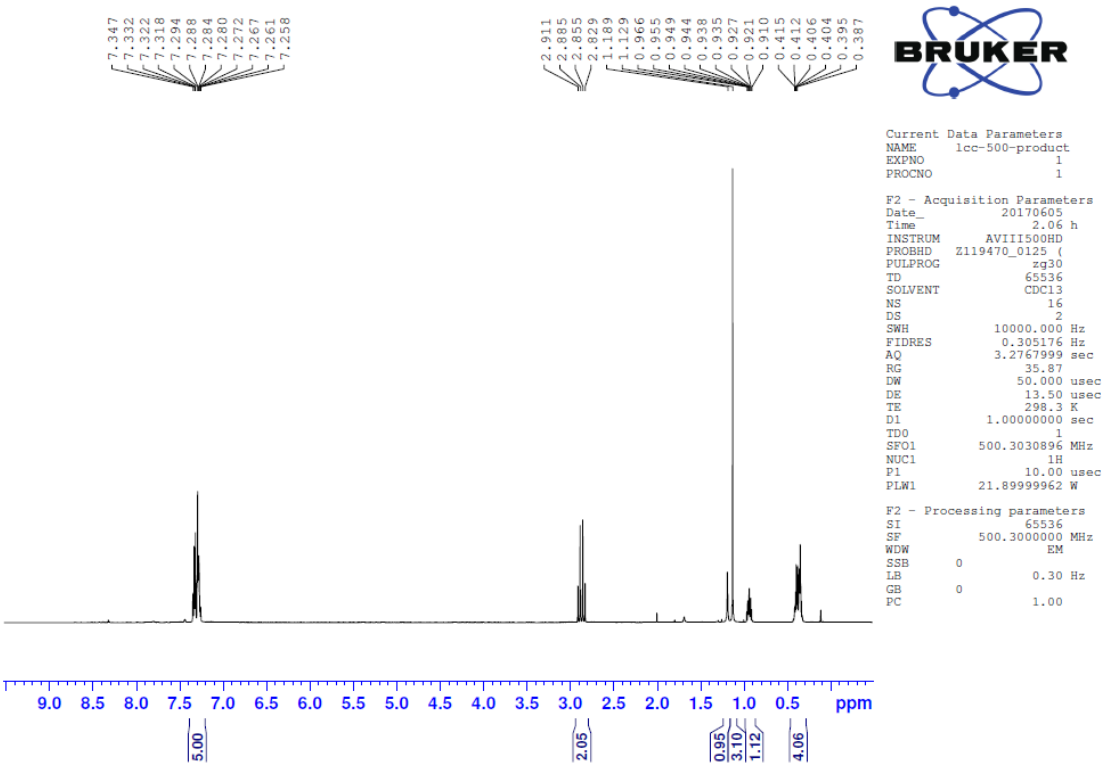
7.347
7.332
7.322
7.318
7.294
7.288
7.284
7.280
7.272
7.267
7.261
7.258
2.911
2.885
2.855
2.829
1.189
1.129
0.966
0.955
0.949
0.944
0.938
0.935
0.927
0.921
0.910
0.415
0.412
0.406
0.404
0.395
0.387
BRUKER
Current Data Parameters
NAME 1cc-500-product
EXPNO 1
PROCNO 1
F2 - Acquisition Parameters
Date_ 20170605
Time 2.06 h
INSTRUM AVIII500HD
PROBHD Z119470_0125 (
PULPROG zg30
TD 65536
SOLVENT CDCl3
NS 16
DS 2
SWH 10000.000 Hz
FIDRES 0.305176 Hz
AQ 3.2767999 sec
RG 35.87
DW 50.000 usec
DE 13.50 usec
TE 298.3 K
D1 1.00000000 sec
TD0 1
SFO1 500.3030896 MHz
NUC1 1H
P1 10.00 usec
PLW1 21.89999962 W
F2 - Processing parameters
SI 65536
SF 500.3000000 MHz
WDW EM
SSB 0
LB 0.30 Hz
GB 0
PC 1.00
9.0 8.5 8.0 7.5 7.0 6.5 6.0 5.5 5.0 4.5 4.0 3.5 3.0 2.5 2.0 1.5 1.0 0.5 ppm
5.00
2.05
0.95
3.10
1.12
4.06

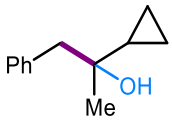

6.3na

^{13}C NMR

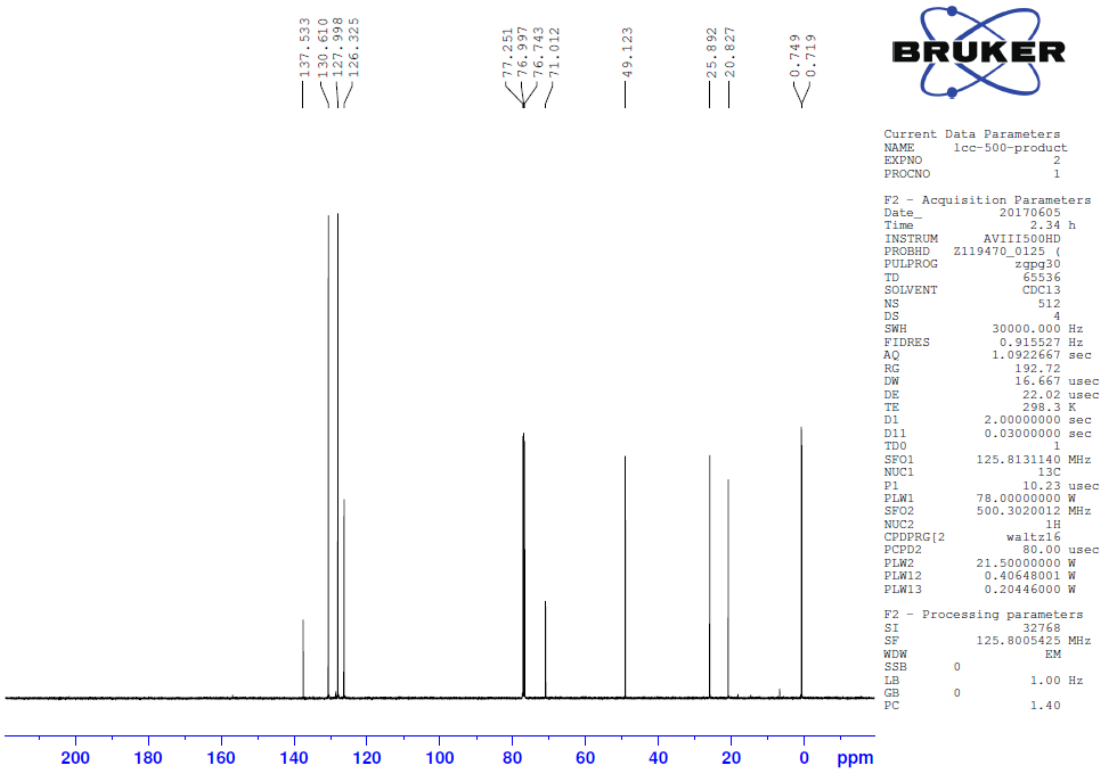


```
Current Data Parameters
NAME      1cc-500-product
EXPNO                   2
PROCNO                  1

F2 - Acquisition Parameters
Date_            20170605
Time                2.34 h
INSTRUM       AVIII500HD
PROBHD    Z119470_0125 (
PULPROG          zgpg30
TD                65536
SOLVENT           CDCl3
NS                  512
DS                    4
SWH           30000.000 Hz
FIDRES            0.915527 Hz
AQ                1.0922667 sec
RG                  192.72
DW                 16.667 usec
DE                 22.02 usec
TE                 298.3 K
D1             2.00000000 sec
D11            0.03000000 sec
TD0                   1
SFO1         125.8131140 MHz
NUC1                 13C
P1                 10.23 usec
PLW1          78.00000000 W
SFO2         500.3020012 MHz
NUC2                 1H
CPDPRG[2          waltz16
PCPD2              80.00 usec
PLW2          21.50000000 W
PLW12          0.40648001 W
PLW13          0.20446000 W

F2 - Processing parameters
SI                32768
SF           125.8005425 MHz
WDW                  EM
SSB       0
LB                1.00 Hz
GB        0
PC                1.40
```

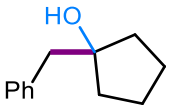
HO
Ph

6.3oa

^{1}H NMR

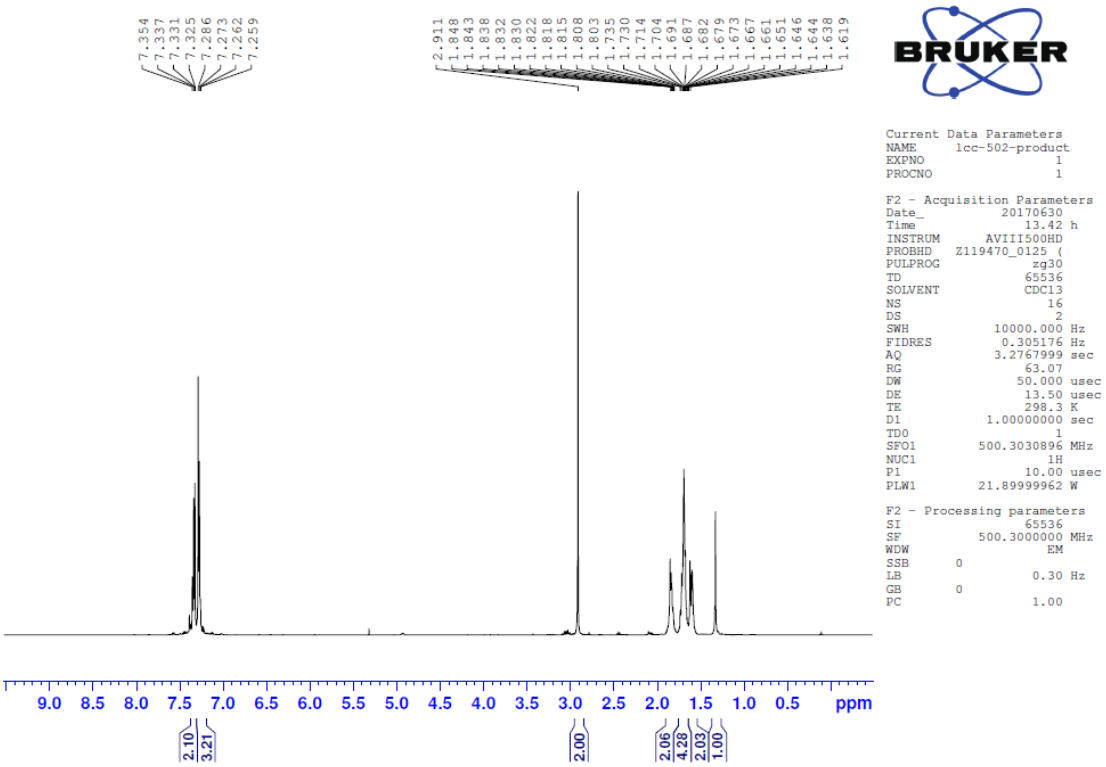
7.354
7.337
7.331
7.325
7.286
7.273
7.262
7.259
2.911
1.848
1.843
1.838
1.832
1.830
1.822
1.818
1.815
1.808
1.803
1.735
1.730
1.714
1.704
1.691
1.687
1.682
1.679
1.673
1.667
1.661
1.651
1.646
1.644
1.638
1.619
BRUKER
Current Data Parameters
NAME lcc-502-product
EXPNO 1
PROCNO 1
F2 - Acquisition Parameters
Date_ 20170630
Time 13.42 h
INSTRUM AVIII500HD
PROBHD Z119470_0125 (
PULPROG zg30
TD 65536
SOLVENT CDCl3
NS 16
DS 2
SWH 10000.000 Hz
FIDRES 0.305176 Hz
AQ 3.2767999 sec
RG 63.07
DW 50.000 usec
DE 13.50 usec
TE 298.3 K
D1 1.00000000 sec
TD0 1
SFO1 500.3030896 MHz
NUC1 1H
P1 10.00 usec
PLW1 21.89999962 W
F2 - Processing parameters
SI 65536
SF 500.3000000 MHz
WDW EM
SSB 0
LB 0.30 Hz
GB 0
PC 1.00
9.0 8.5 8.0 7.5 7.0 6.5 6.0 5.5 5.0 4.5 4.0 3.5 3.0 2.5 2.0 1.5 1.0 0.5 ppm
2.10
3.21
2.00
2.06
4.28
2.03
1.00

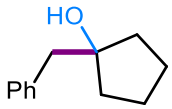

6.3oa

^{13}C NMR

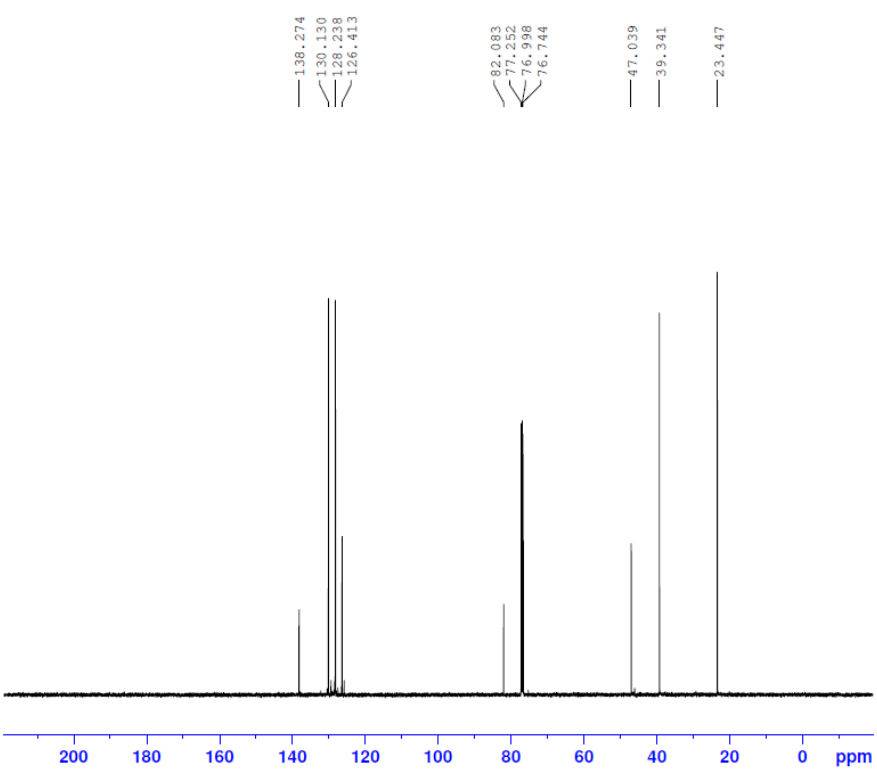


```
Current Data Parameters
NAME      1cc-502-product
EXPNO                   2
PROCNO                  1

F2 - Acquisition Parameters
Date_            20170630
Time                14.33 h
INSTRUM       AVIII500HD
PROBHD    Z119470_0125 (
PULPROG          zgpg30
TD                65536
SOLVENT           CDCl3
NS                  256
DS                    4
SWH           30000.000 Hz
FIDRES            0.915527 Hz
AQ                1.0922667 sec
RG                  192.72
DW                 16.667 usec
DE                 22.02 usec
TE                 298.3 K
D1             2.00000000 sec
D11            0.03000000 sec
TD0                   1
SFO1         125.8131140 MHz
NUC1                 13C
P1                 10.23 usec
PLW1          78.00000000 W
SFO2         500.3020012 MHz
NUC2                 1H
CPDPRG[2          waltz16
PCPD2              80.00 usec
PLW2          21.50000000 W
PLW12          0.49000001 W
PLW13          0.20446000 W

F2 - Processing parameters
SI                32768
SF           125.8005416 MHz
WDW                  EM
SSB       0
LB                 1.00 Hz
GB        0
PC                 1.40
```

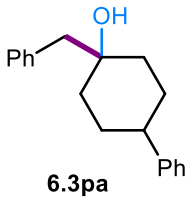
OH
Ph
Ph

6.3pa

^{1}H NMR

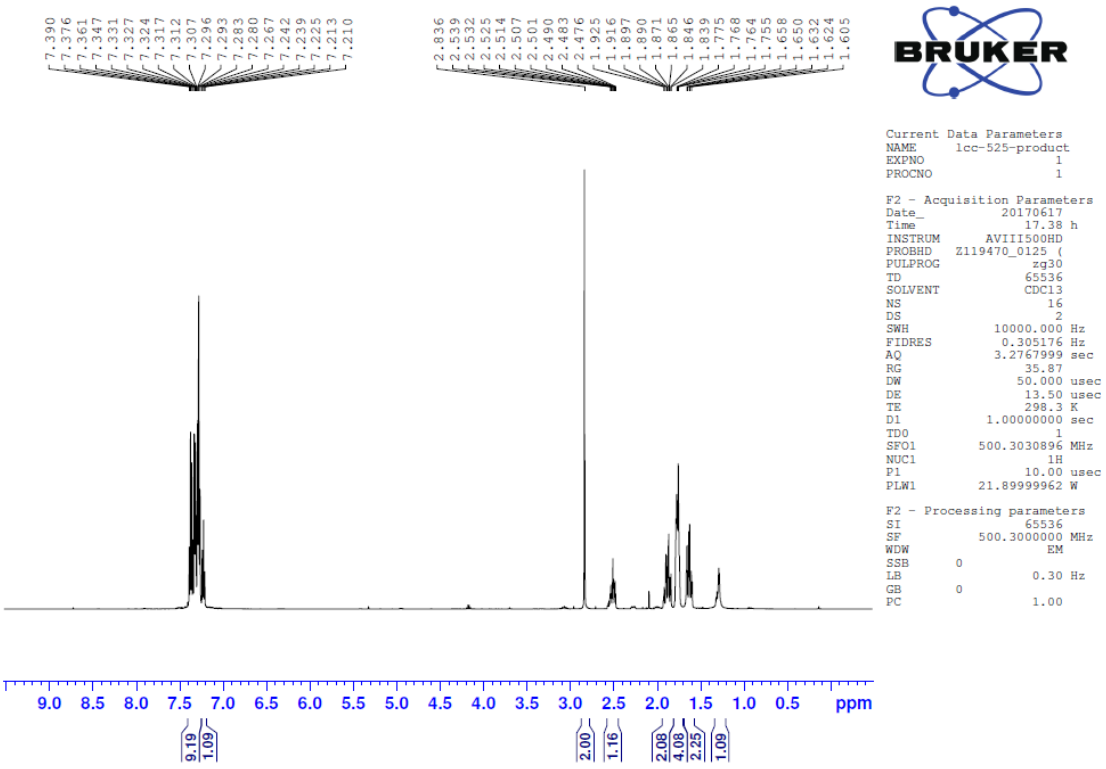
7.390
7.376
7.361
7.347
7.331
7.327
7.324
7.317
7.312
7.307
7.296
7.293
7.283
7.280
7.267
7.242
7.239
7.225
7.213
7.210
2.836
2.539
2.532
2.525
2.514
2.507
2.501
2.490
2.483
2.476
1.925
1.916
1.897
1.890
1.871
1.865
1.846
1.839
1.775
1.768
1.764
1.755
1.658
1.650
1.632
1.624
1.605
BRUKER
Current Data Parameters
NAME 1cc-525-product
EXPNO 1
PROCNO 1
F2 - Acquisition Parameters
Date_ 20170617
Time 17.38 h
INSTRUM AVIII500HD
PROBHD Z119470_0125 (
PULPROG zg30
TD 65536
SOLVENT CDCl3
NS 16
DS 2
SWH 10000.000 Hz
FIDRES 0.305176 Hz
AQ 3.2767999 sec
RG 35.87
DW 50.000 usec
DE 13.50 usec
TE 298.3 K
D1 1.00000000 sec
TD0 1
SFO1 500.3030896 MHz
NUC1 1H
P1 10.00 usec
PLW1 21.89999962 W
F2 - Processing parameters
SI 65536
SF 500.3000000 MHz
WDW EM
SSB 0
LB 0.30 Hz
GB 0
PC 1.00
9.0 8.5 8.0 7.5 7.0 6.5 6.0 5.5 5.0 4.5 4.0 3.5 3.0 2.5 2.0 1.5 1.0 0.5 ppm
9.19
1.09
2.00
1.16
2.08
4.08
2.25
1.09

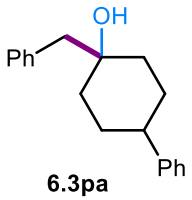

6.3pa

^{13}C NMR

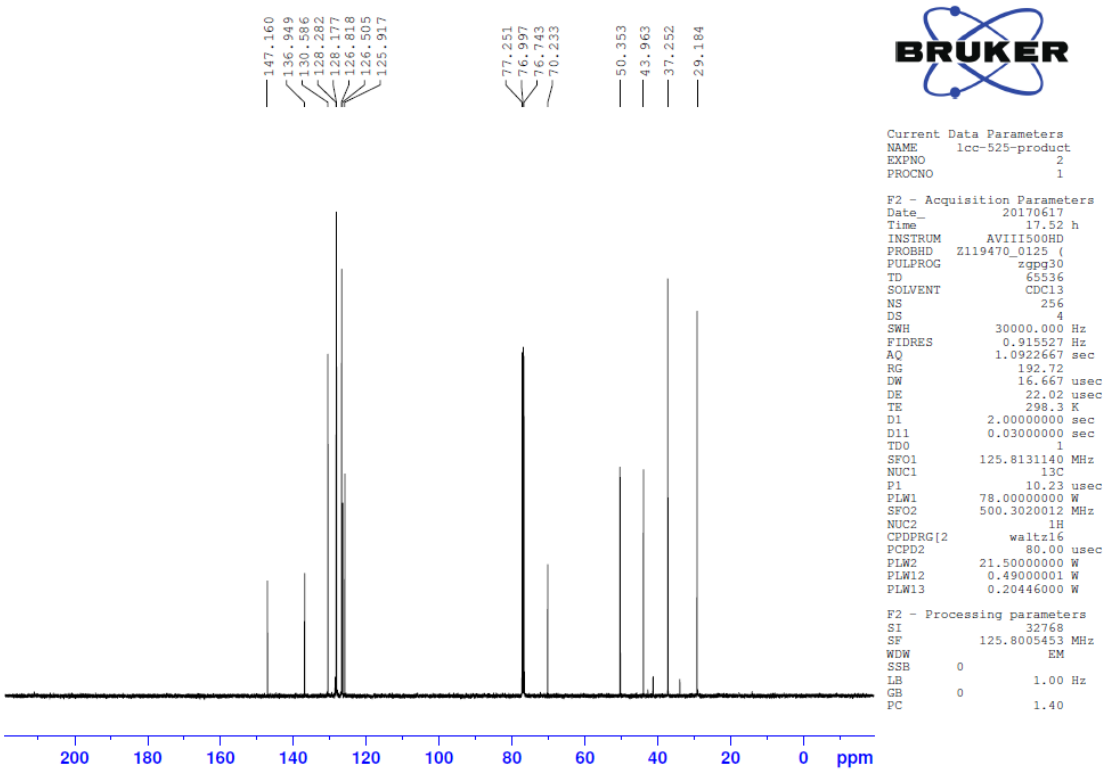


```
Current Data Parameters
NAME      lcc-525-product
EXPNO                   2
PROCNO                  1

F2 - Acquisition Parameters
Date_           20170617
Time              17.52 h
INSTRUM       AVIII500HD
PROBHD    Z119470_0125 (
PULPROG           zgpg30
TD                65536
SOLVENT           CDCl3
NS                  256
DS                    4
SWH           30000.000 Hz
FIDRES         0.915527 Hz
AQ             1.0922667 sec
RG                192.72
DW                16.667 usec
DE                22.02 usec
TE                298.3 K
D1           2.00000000 sec
D11          0.03000000 sec
TD0                   1
SFO1        125.8131140 MHz
NUC1                13C
P1                10.23 usec
PLW1         78.00000000 W
SFO2         500.3020012 MHz
NUC2                1H
CPDPRG[2         waltz16
PCPD2             80.00 usec
PLW2         21.50000000 W
PLW12         0.49000001 W
PLW13         0.20446000 W

F2 - Processing parameters
SI                32768
SF          125.8005453 MHz
WDW                  EM
SSB       0
LB                1.00 Hz
GB        0
PC                1.40
```

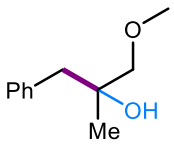
O
Ph
OH
Me

6.3qa

^{1}H NMR

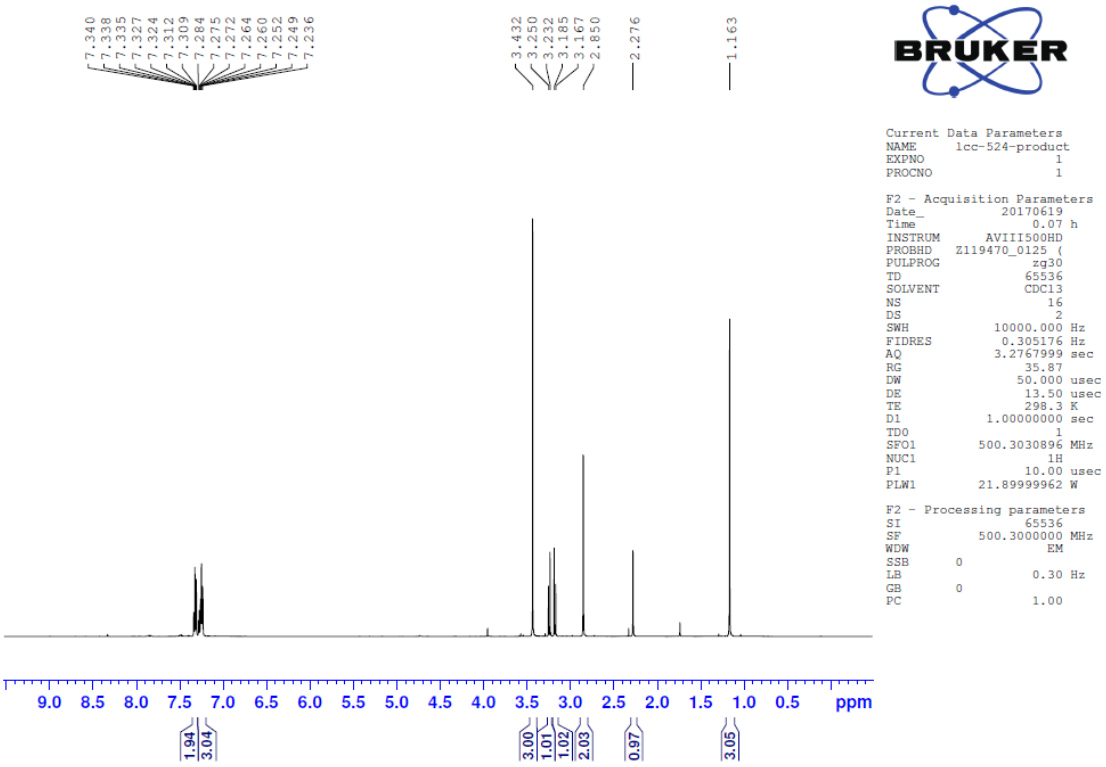
7.340
7.338
7.335
7.327
7.324
7.312
7.309
7.284
7.275
7.272
7.264
7.260
7.252
7.249
7.236
3.432
3.250
3.232
3.185
3.167
2.850
2.276
1.163
BRUKER
Current Data Parameters
NAME lcc-524-product
EXPNO 1
PROCNO 1
F2 - Acquisition Parameters
Date_ 20170619
Time 0.07 h
INSTRUM AVIII500HD
PROBHD Z119470_0125 (
PULPROG zg30
TD 65536
SOLVENT CDCl3
NS 16
DS 2
SWH 10000.000 Hz
FIDRES 0.305176 Hz
AQ 3.2767999 sec
RG 35.87
DW 50.000 usec
DE 13.50 usec
TE 298.3 K
D1 1.00000000 sec
TD0 1
SFO1 500.3030896 MHz
NUC1 1H
P1 10.00 usec
PLW1 21.89999962 W
F2 - Processing parameters
SI 65536
SF 500.3000000 MHz
WDW EM
SSB 0
LB 0.30 Hz
GB 0
PC 1.00
9.0 8.5 8.0 7.5 7.0 6.5 6.0 5.5 5.0 4.5 4.0 3.5 3.0 2.5 2.0 1.5 1.0 0.5 ppm
1.94
3.04
3.00
1.01
1.02
2.03
0.97
3.05

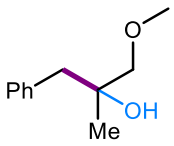

6.3qa

^{13}C NMR

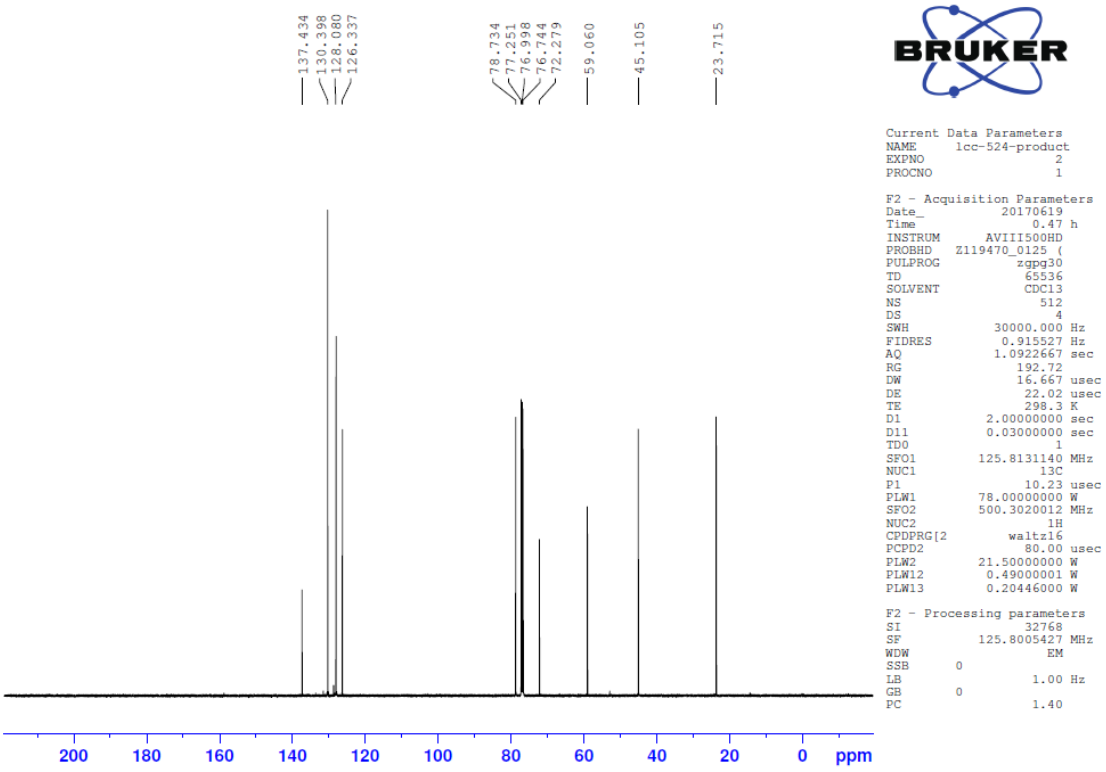


```
Current Data Parameters
NAME      lcc-524-product
EXPNO                   2
PROCNO                  1

F2 - Acquisition Parameters
Date_           20170619
Time                0.47 h
INSTRUM       AVIII500HD
PROBHD    Z119470_0125 (
PULPROG          zgpg30
TD                65536
SOLVENT           CDCl3
NS                  512
DS                    4
SWH           30000.000 Hz
FIDRES         0.915527 Hz
AQ             1.0922667 sec
RG                192.72
DW                16.667 usec
DE                22.02 usec
TE                298.3 K
D1             2.00000000 sec
D11            0.03000000 sec
TD0                   1
SFO1         125.8131140 MHz
NUC1                 13C
P1                 10.23 usec
PLW1         78.00000000 W
SFO2         500.3020012 MHz
NUC2                  1H
CPDPRG[2          waltz16
PCPD2              80.00 usec
PLW2         21.50000000 W
PLW12         0.49000001 W
PLW13         0.20446000 W

F2 - Processing parameters
SI                 32768
SF           125.8005427 MHz
WDW                   EM
SSB       0
LB                 1.00 Hz
GB        0
PC                 1.40
```

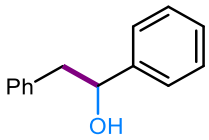
Ph
OH

6.3ra

^{1}H NMR

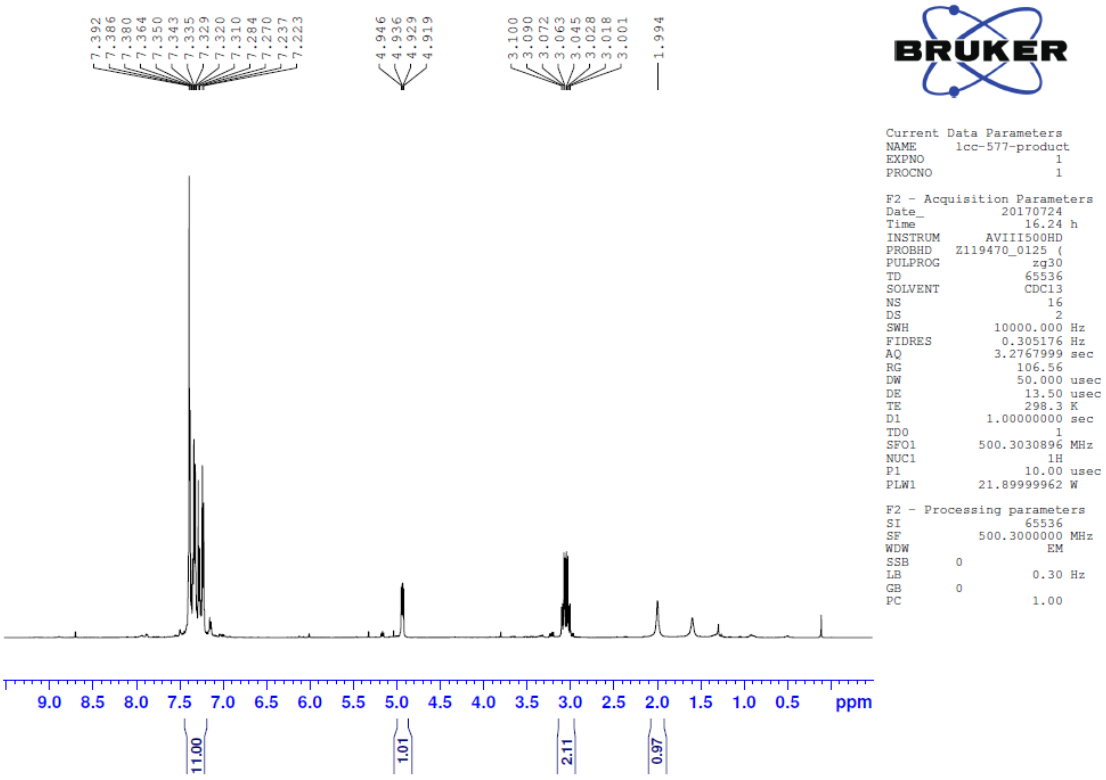
7.392
7.386
7.380
7.364
7.350
7.343
7.335
7.329
7.320
7.310
7.284
7.270
7.237
7.223
4.946
4.936
4.929
4.919
3.100
3.090
3.072
3.063
3.045
3.028
3.018
3.001
1.994
BRUKER
Current Data Parameters
NAME lcc-577-product
EXPNO 1
PROCNO 1
F2 - Acquisition Parameters
Date_ 20170724
Time 16.24 h
INSTRUM AVIII500HD
PROBHD Z119470_0125 (
PULPROG zg30
TD 65536
SOLVENT CDCl3
NS 16
DS 2
SWH 10000.000 Hz
FIDRES 0.305176 Hz
AQ 3.2767999 sec
RG 106.56
DW 50.000 usec
DE 13.50 usec
TE 298.3 K
D1 1.00000000 sec
TD0 1
SFO1 500.3030896 MHz
NUC1 1H
P1 10.00 usec
PLW1 21.89999962 W
F2 - Processing parameters
SI 65536
SF 500.3000000 MHz
WDW EM
SSB 0
LB 0.30 Hz
GB 0
PC 1.00
9.0 8.5 8.0 7.5 7.0 6.5 6.0 5.5 5.0 4.5 4.0 3.5 3.0 2.5 2.0 1.5 1.0 0.5 ppm
11.00
1.01
2.11
0.97

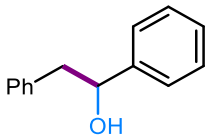

6.3ra

^{13}C NMR

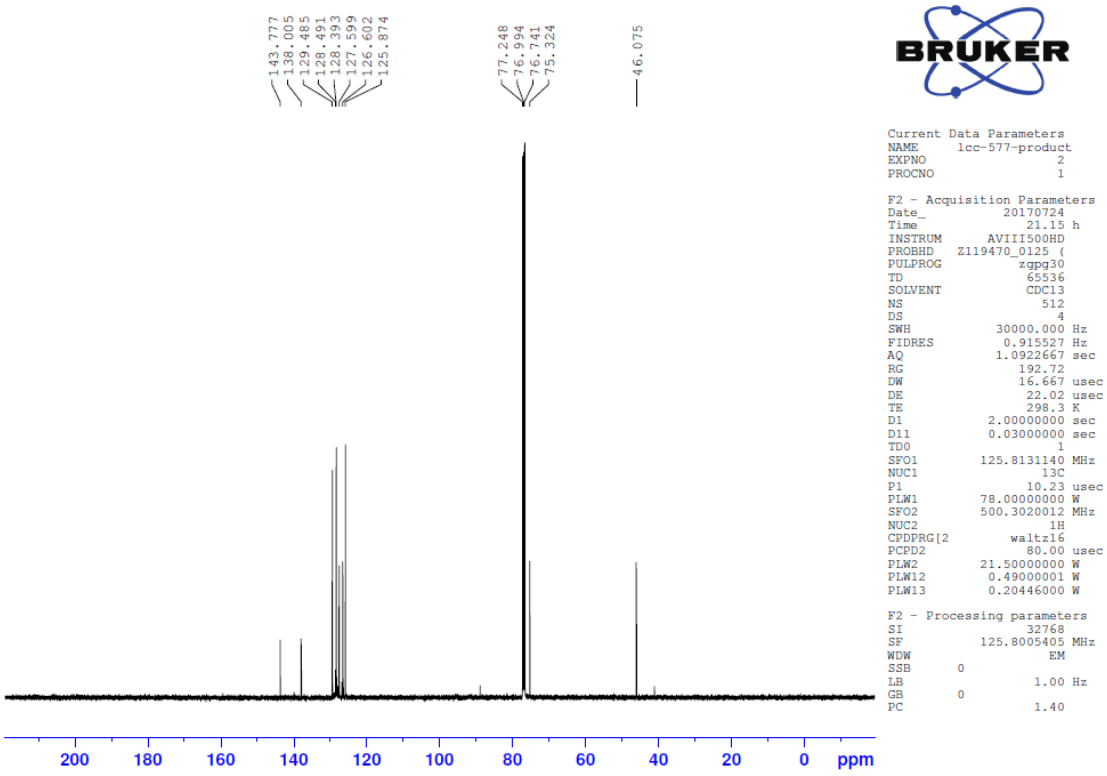


```
Current Data Parameters
NAME      lcc-577-product
EXPNO                   2
PROCNO                  1

F2 - Acquisition Parameters
Date_           20170724
Time              21.15 h
INSTRUM       AVIII500HD
PROBHD   Z119470_0125 (
PULPROG           zgpg30
TD                65536
SOLVENT           CDCl3
NS                  512
DS                    4
SWH           30000.000 Hz
FIDRES        0.915527 Hz
AQ            1.0922667 sec
RG                192.72
DW               16.667 usec
DE               22.02 usec
TE               298.3 K
D1            2.00000000 sec
D11           0.03000000 sec
TD0                   1
SFO1        125.8131140 MHz
NUC1               13C
P1                10.23 usec
PLW1        78.00000000 W
SFO2        500.3020012 MHz
NUC2               1H
CPDPRG[2        waltz16
PCPD2             80.00 usec
PLW2        21.50000000 W
PLW12        0.49000001 W
PLW13        0.20446000 W

F2 - Processing parameters
SI                32768
SF          125.8005405 MHz
WDW                EM
SSB       0
LB                1.00 Hz
GB        0
PC                1.40
```

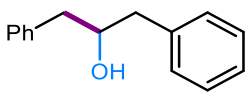

6.3sa

^{1}H NMR

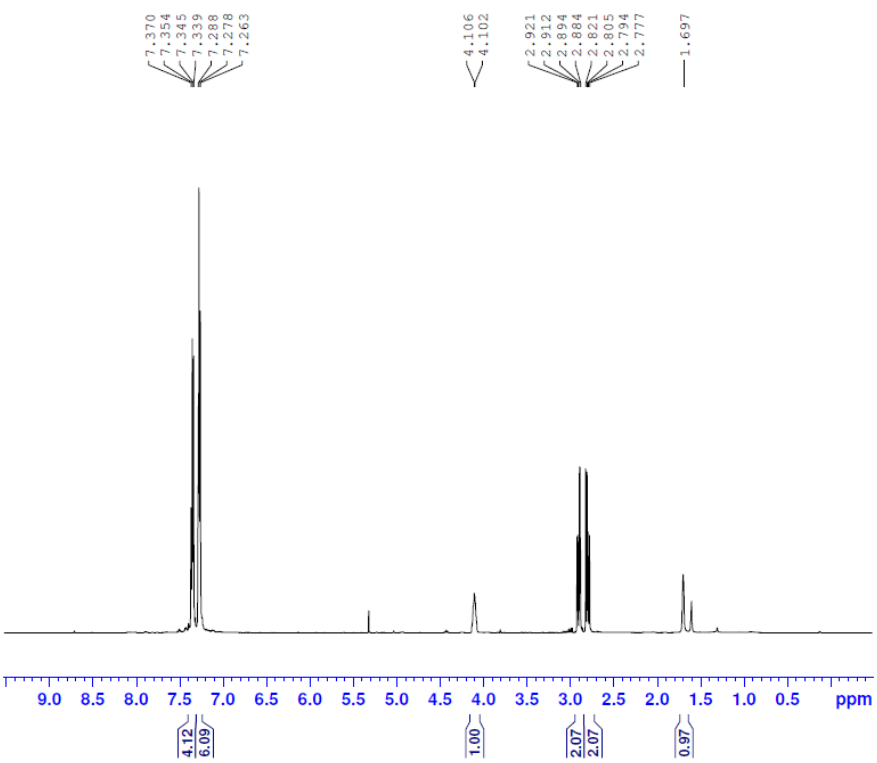


```
Current Data Parameters
NAME      1cc-578-product
EXPNO                   1
PROCNO                  1

F2 - Acquisition Parameters
Date_            20170725
Time                2.09 h
INSTRUM       AVIII500HD
PROBHD    Z119470_0125 (
PULPROG             zg30
TD                 65536
SOLVENT            CDCl3
NS                    16
DS                     2
SWH            10000.000 Hz
FIDRES             0.305176 Hz
AQ                 3.2767999 sec
RG                    77.88
DW                  50.000 usec
DE                  13.50 usec
TE                  298.3 K
D1              1.00000000 sec
TD0                    1
SFO1           500.3030896 MHz
NUC1                   1H
P1                  10.00 usec
PLW1           21.89999962 W

F2 - Processing parameters
SI                 65536
SF            500.3000000 MHz
WDW                   EM
SSB       0
LB                  0.30 Hz
GB        0
PC                  1.00
```

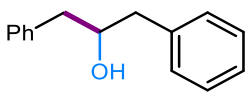

6.3sa

^{13}C NMR

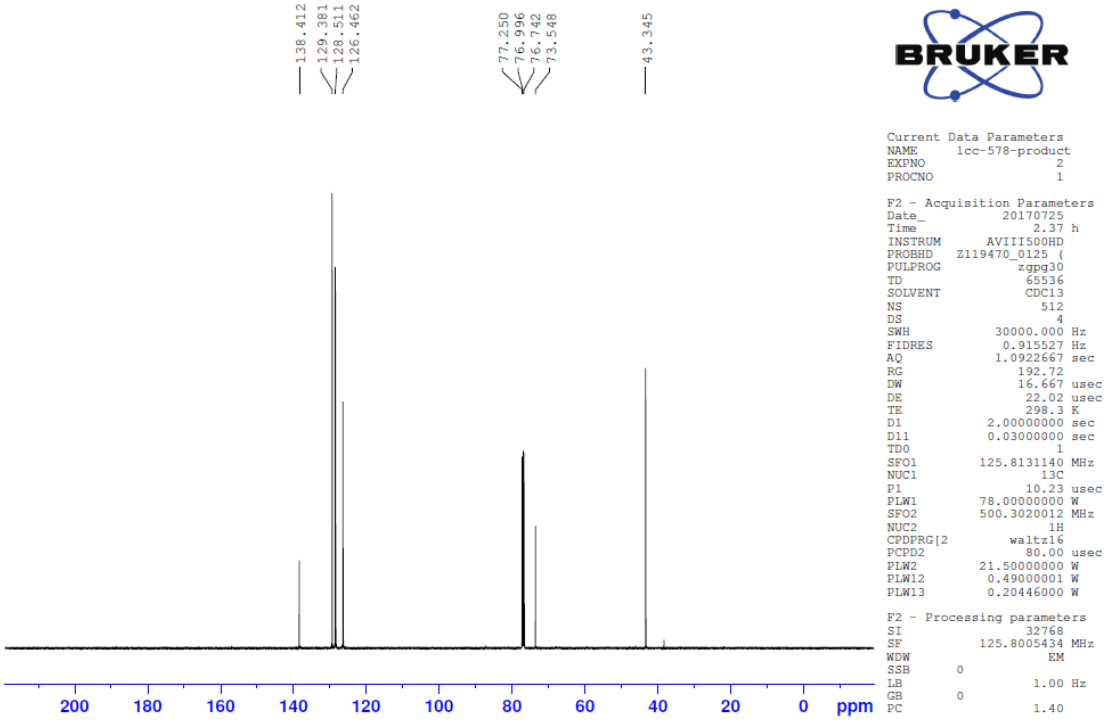


```
Current Data Parameters
NAME      1cc-578-product
EXPNO                   2
PROCNO                  1

F2 - Acquisition Parameters
Date_            20170725
Time                2.37 h
INSTRUM       AVIII500HD
PROBHD    Z119470_0125 (
PULPROG           zgpg30
TD                65536
SOLVENT           CDCl3
NS                  512
DS                    4
SWH           30000.000 Hz
FIDRES            0.915527 Hz
AQ              1.0922667 sec
RG                192.72
DW                16.667 usec
DE                22.02 usec
TE                298.3 K
D1             2.00000000 sec
D11            0.03000000 sec
TD0                   1
SFO1          125.8131140 MHz
NUC1                13C
P1                10.23 usec
PLW1          78.00000000 W
SFO2          500.3020012 MHz
NUC2                1H
CPDPRG[2         waltz16
PCPD2             80.00 usec
PLW2          21.50000000 W
PLW12          0.49000001 W
PLW13          0.20446000 W

F2 - Processing parameters
SI                32768
SF          125.8005434 MHz
WDW                EM
SSB       0
LB                1.00 Hz
GB        0
PC                1.40
```

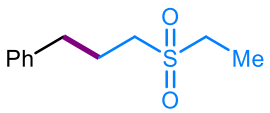

6.3ta

^{1}H NMR

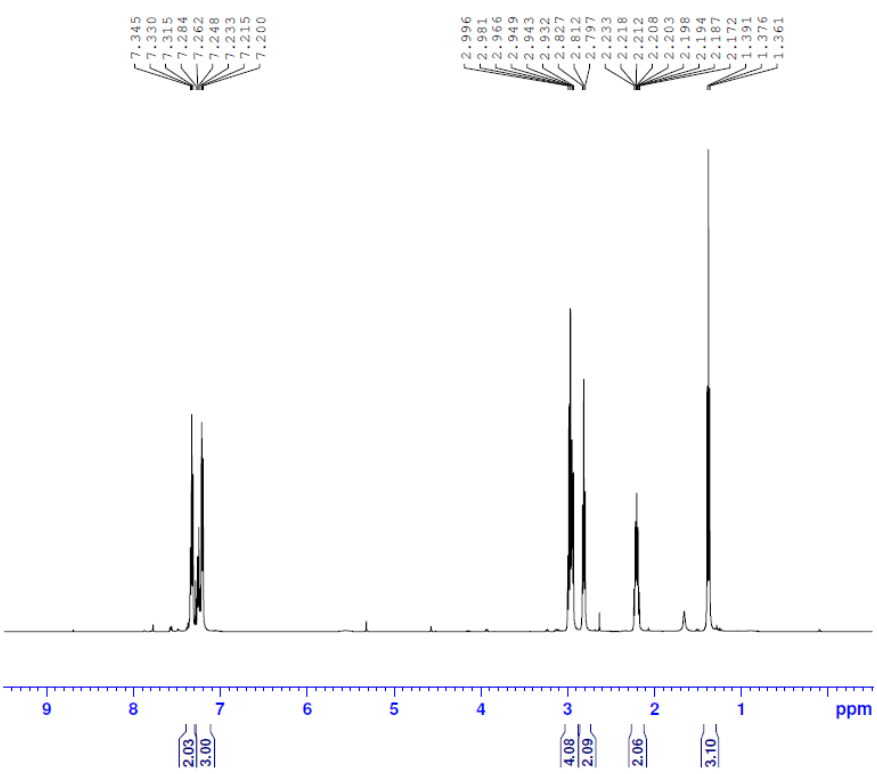

BRUKER

```
Current Data Parameters
NAME      lcc-609-product
EXPNO                   1
PROCNO                  1

F2 - Acquisition Parameters
Date_           20170805
Time              14.57 h
INSTRUM       AVIII500HD
PROBHD    Z119470_0125 (
PULPROG             zg30
TD                 65536
SOLVENT            CDCl3
NS                    16
DS                     2
SWH           10000.000 Hz
FIDRES        0.305176 Hz
AQ            3.2767999 sec
RG                 77.88
DW                50.000 usec
DE                13.50 usec
TE                298.3 K
D1            1.00000000 sec
TD0                    1
SFO1         500.3030896 MHz
NUC1                  1H
P1                10.00 usec
PLW1         21.89999962 W

F2 - Processing parameters
SI                 65536
SF            500.3000000 MHz
WDW                   EM
SSB       0
LB                 0.30 Hz
GB        0
PC                 1.00
```

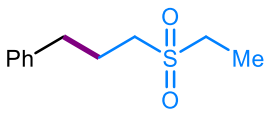

6.3ta

^{13}C NMR

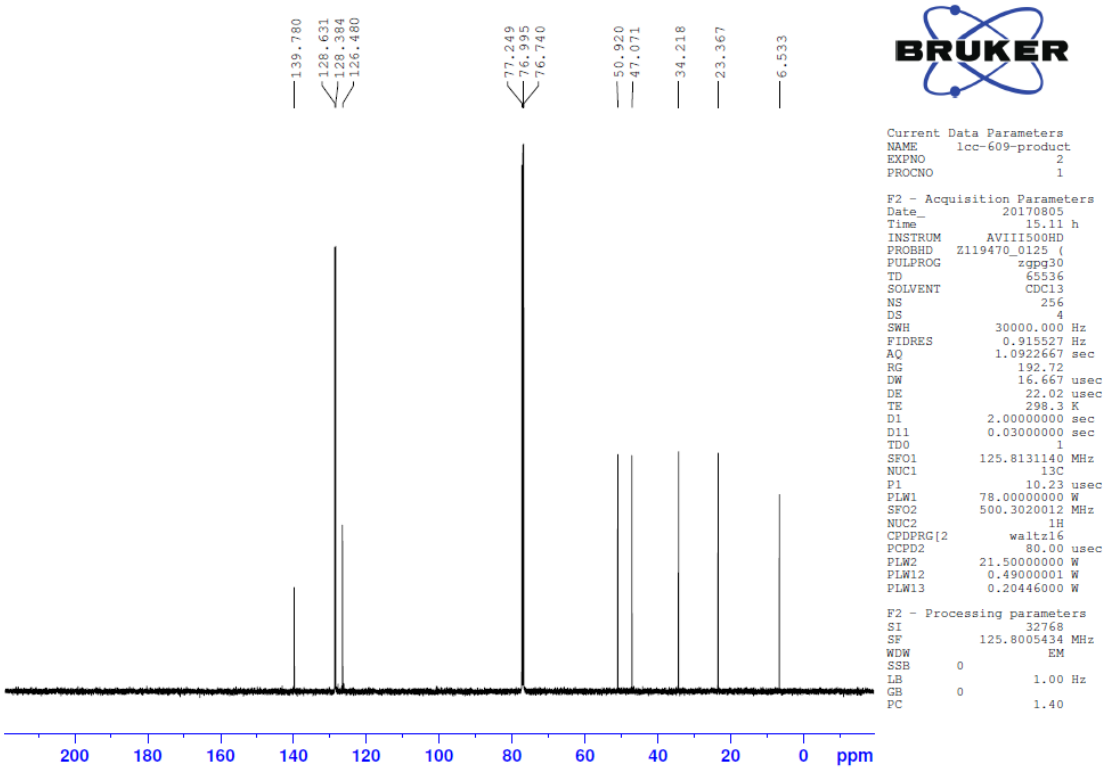


```
Current Data Parameters
NAME      lcc-609-product
EXPNO                   2
PROCNO                  1

F2 - Acquisition Parameters
Date_           20170805
Time              15.11 h
INSTRUM       AVIII500HD
PROBHD    Z119470_0125 (
PULPROG           zgpg30
TD                65536
SOLVENT           CDCl3
NS                  256
DS                    4
SWH           30000.000 Hz
FIDRES         0.915527 Hz
AQ             1.0922667 sec
RG                192.72
DW                16.667 usec
DE                22.02 usec
TE                298.3 K
D1             2.00000000 sec
D11            0.03000000 sec
TD0                   1
SFO1         125.8131140 MHz
NUC1                13C
P1                10.23 usec
PLW1         78.00000000 W
SFO2         500.3020012 MHz
NUC2                1H
CPDPRG[2         waltz16
PCPD2             80.00 usec
PLW2         21.50000000 W
PLW12         0.49000001 W
PLW13         0.20446000 W

F2 - Processing parameters
SI                32768
SF           125.8005434 MHz
WDW                EM
SSB       0
LB                1.00 Hz
GB        0
PC                1.40
```

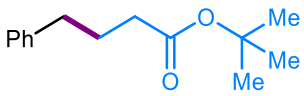
Ph
O
O
Me
Me
Me

6.3ua

^{1}H NMR

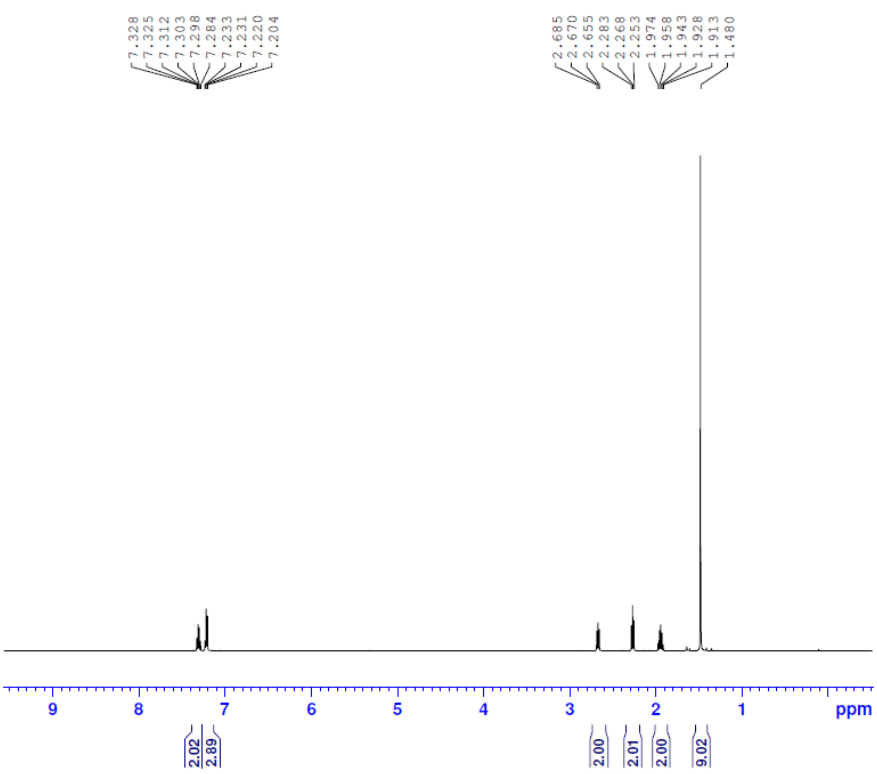
7.328
7.325
7.312
7.303
7.298
7.264
7.233
7.231
7.220
7.204
2.685
2.670
2.655
2.283
2.268
2.253
1.974
1.958
1.943
1.928
1.913
1.480
9
8
7
6
5
4
3
2
1
ppm
2.02
2.89
2.00
2.01
2.00
9.02

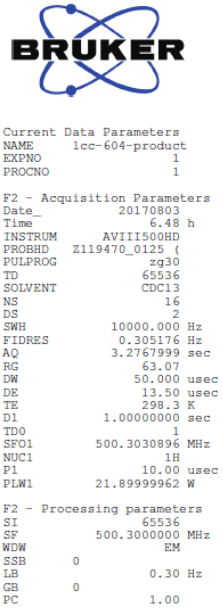
BRUKER
Current Data Parameters
NAME 1cc-604-product
EXPNO 1
PROCNO 1
F2 - Acquisition Parameters
Date_ 20170803
Time 6.48 h
INSTRUM AVIII500HD
PROBHD Z119470_0125 (
PULPROG zg30
TD 65536
SOLVENT CDCl3
NS 16
DS 2
SWH 10000.000 Hz
FIDRES 0.305176 Hz
AQ 3.2767999 sec
RG 63.07
DW 50.000 usec
DE 13.50 usec
TE 298.3 K
D1 1.00000000 sec
TD0 1
SFO1 500.3030896 MHz
NUC1 1H
P1 10.00 usec
PLW1 21.89999962 W
F2 - Processing parameters
SI 65536
SF 500.3000000 MHz
WDW EM
SSB 0
LB 0.30 Hz
GB 0
PC 1.00

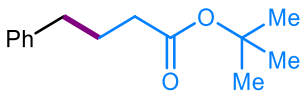

6.3ua

^{13}C NMR

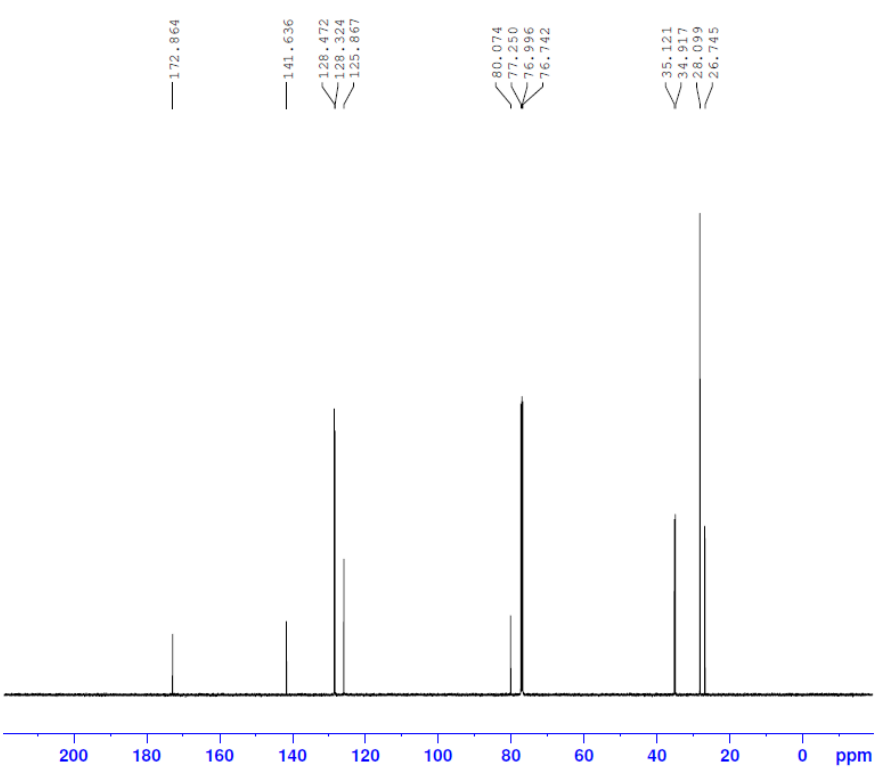

BRUKER

```
Current Data Parameters
NAME      lcc-604-product
EXPNO                   2
PROCNO                  1

F2 - Acquisition Parameters
Date_            20170803
Time                7.16 h
INSTRUM       AVIII500HD
PROBHD    Z119470_0125 (
PULPROG          zgpg30
TD                65536
SOLVENT           CDCl3
NS                  512
DS                    4
SWH           30000.000 Hz
FIDRES            0.915527 Hz
AQ                1.0922667 sec
RG                  192.72
DW                 16.667 usec
DE                 22.02 usec
TE                 298.3 K
D1             2.00000000 sec
D11            0.03000000 sec
TD0                   1
SFO1         125.8131140 MHz
NUC1                 13C
P1                 10.23 usec
PLW1          78.00000000 W
SFO2         500.3020012 MHz
NUC2                  1H
CPDPRG[2          waltz16
PCPD2              80.00 usec
PLW2          21.50000000 W
PLW12          0.49000001 W
PLW13          0.20446000 W

F2 - Processing parameters
SI                32768
SF           125.8005407 MHz
WDW                  EM
SSB       0
LB                1.00 Hz
GB        0
PC                1.40
```

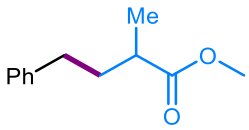
Me
Ph
O
O

6.3va

^{1}H NMR

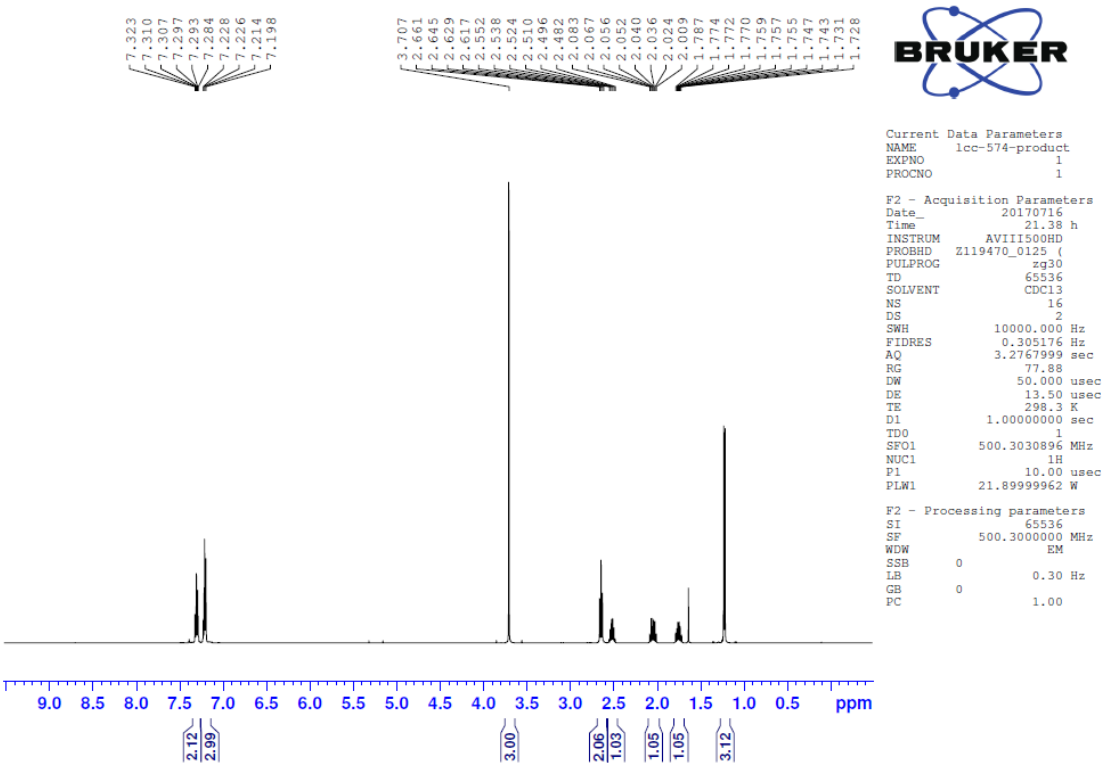
7.323
7.310
7.307
7.297
7.293
7.284
7.228
7.226
7.214
7.198
3.707
2.661
2.645
2.629
2.617
2.552
2.538
2.524
2.510
2.496
2.482
2.083
2.067
2.056
2.052
2.040
2.036
2.024
2.009
1.787
1.774
1.772
1.770
1.759
1.757
1.755
1.747
1.743
1.731
1.728
BRUKER
Current Data Parameters
NAME 1cc-574-product
EXPNO 1
PROCNO 1
F2 - Acquisition Parameters
Date_ 20170716
Time 21.38 h
INSTRUM AVIII500HD
PROBHD Z119470_0125 (
PULPROG zg30
TD 65536
SOLVENT CDCl3
NS 16
DS 2
SWH 10000.000 Hz
FIDRES 0.305176 Hz
AQ 3.2767999 sec
RG 77.88
DW 50.000 usec
DE 13.50 usec
TE 298.3 K
D1 1.00000000 sec
TD0 1
SFO1 500.3030896 MHz
NUC1 1H
P1 10.00 usec
PLW1 21.89999962 W
F2 - Processing parameters
SI 65536
SF 500.3000000 MHz
WDW EM
SSB 0
LB 0.30 Hz
GB 0
PC 1.00
9.0 8.5 8.0 7.5 7.0 6.5 6.0 5.5 5.0 4.5 4.0 3.5 3.0 2.5 2.0 1.5 1.0 0.5 ppm
2.12
2.99
3.00
2.06
1.03
1.05
1.05
3.12

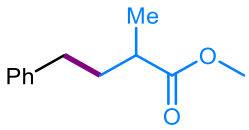

6.3va

^{13}C NMR

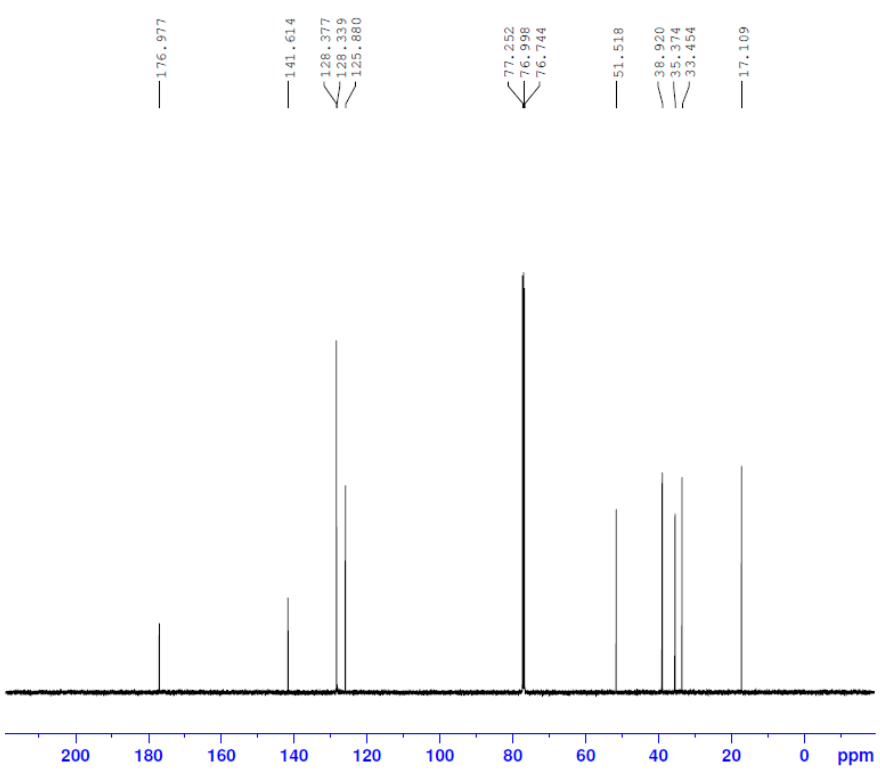


```
Current Data Parameters
NAME      1cc-574-product
EXPNO                   2
PROCNO                  1

F2 - Acquisition Parameters
Date_           20170716
Time              21.52 h
INSTRUM       AVIII500HD
PROBHD    Z119470_0125 (
PULPROG           zgpg30
TD                65536
SOLVENT           CDCl3
NS                  256
DS                    4
SWH           30000.000 Hz
FIDRES         0.915527 Hz
AQ             1.0922667 sec
RG                192.72
DW                16.667 usec
DE                 7.43 usec
TE                298.3 K
D1           2.00000000 sec
D11          0.03000000 sec
TD0                   1
SFO1        125.8131140 MHz
NUC1                13C
P1                10.23 usec
PLW1        78.00000000 W
SFO2        500.3020012 MHz
NUC2                1H
CPDPRG[2         waltz16
PCPD2             80.00 usec
PLW2        21.50000000 W
PLW12        0.40648001 W
PLW13        0.20446000 W

F2 - Processing parameters
SI                32768
SF          125.8005407 MHz
WDW                 EM
SSB       0
LB                1.00 Hz
GB        0
PC                1.40
```


Ph
CN

6.3wa

^{1}H NMR

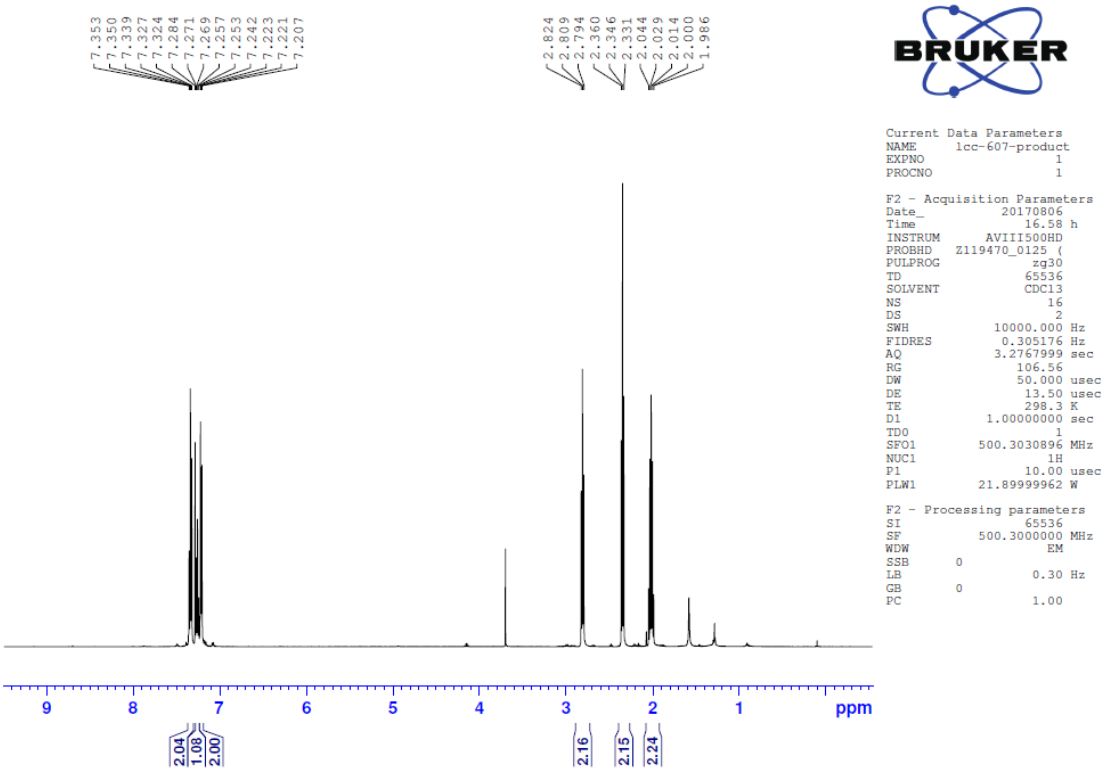
7.353
7.350
7.339
7.327
7.324
7.284
7.271
7.269
7.257
7.253
7.242
7.223
7.221
7.207
2.824
2.809
2.794
2.360
2.346
2.331
2.044
2.029
2.014
2.000
1.986
BRUKER
Current Data Parameters
NAME lcc-607-product
EXPNO 1
PROCNO 1
F2 - Acquisition Parameters
Date_ 20170806
Time 16.58 h
INSTRUM AVIII500HD
PROBHD Z119470_0125 (
PULPROG zg30
TD 65536
SOLVENT CDCl3
NS 16
DS 2
SWH 10000.000 Hz
FIDRES 0.305176 Hz
AQ 3.2767999 sec
RG 106.56
DW 50.000 usec
DE 13.50 usec
TE 298.3 K
D1 1.00000000 sec
TD0 1
SFO1 500.3030896 MHz
NUC1 1H
P1 10.00 usec
PLW1 21.89999962 W
F2 - Processing parameters
SI 65536
SF 500.3000000 MHz
WDW EM
SSB 0
LB 0.30 Hz
GB 0
PC 1.00
9
8
7
6
5
4
3
2
1
ppm
2.04
1.08
2.00
2.16
2.15
2.24

6.3wa

^{13}C NMR

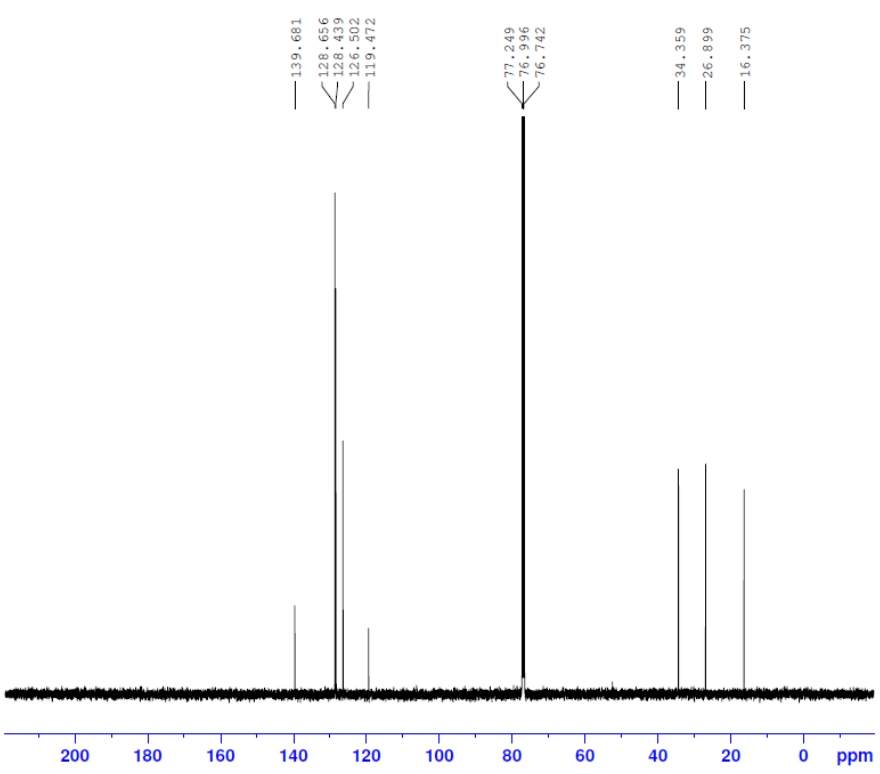

BRUKER

```
Current Data Parameters
NAME      lcc-607-product
EXPNO                   2
PROCNO                  1

F2 - Acquisition Parameters
Date_            20170806
Time                17.26 h
INSTRUM       AVIII500HD
PROBHD    Z119470_0125 (
PULPROG           zgpg30
TD                 65536
SOLVENT            CDCl3
NS                   512
DS                     4
SWH            30000.000 Hz
FIDRES             0.915527 Hz
AQ              1.0922667 sec
RG                 192.72
DW                 16.667 usec
DE                 22.02 usec
TE                 298.3 K
D1             2.00000000 sec
D11            0.03000000 sec
TD0                    1
SFO1          125.8131140 MHz
NUC1                  13C
P1                 10.23 usec
PLW1          78.00000000 W
SFO2          500.3020012 MHz
NUC2                   1H
CPDPRG[2          waltz16
PCPD2              80.00 usec
PLW2          21.50000000 W
PLW12          0.49000001 W
PLW13          0.20446000 W

F2 - Processing parameters
SI                 32768
SF            125.8005393 MHz
WDW                   EM
SSB       0
LB                  1.00 Hz
GB        0
PC                  1.40
```

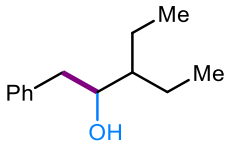
Me
Me
Ph
OH

6.3xa

^{1}H NMR

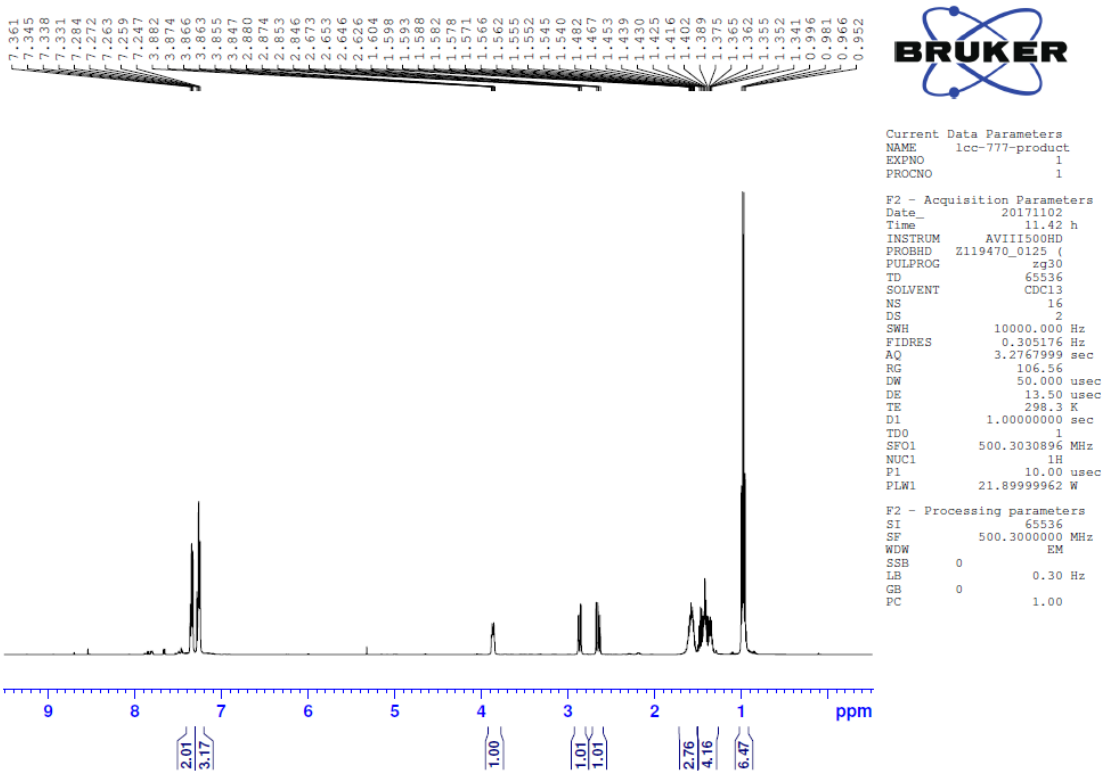
7.361
7.345
7.338
7.331
7.284
7.272
7.263
7.259
7.247
3.882
3.874
3.866
3.863
3.855
3.847
2.880
2.874
2.853
2.846
2.673
2.653
2.646
2.626
1.604
1.598
1.593
1.588
1.582
1.578
1.571
1.566
1.562
1.555
1.552
1.545
1.540
1.482
1.467
1.453
1.439
1.430
1.425
1.416
1.402
1.389
1.375
1.365
1.362
1.355
1.352
1.341
0.996
0.981
0.966
0.952
BRUKER
Current Data Parameters
NAME 1cc-777-product
EXPNO 1
PROCNO 1
F2 - Acquisition Parameters
Date_ 20171102
Time 11.42 h
INSTRUM AVIII500HD
PROBHD Z119470_0125 (
PULPROG zg30
TD 65536
SOLVENT CDCl3
NS 16
DS 2
SWH 10000.000 Hz
FIDRES 0.305176 Hz
AQ 3.2767999 sec
RG 106.56
DW 50.000 usec
DE 13.50 usec
TE 298.3 K
D1 1.00000000 sec
TD0 1
SFO1 500.3030896 MHz
NUC1 1H
P1 10.00 usec
PLW1 21.89999962 W
F2 - Processing parameters
SI 65536
SF 500.3000000 MHz
WDW EM
SSB 0
LB 0.30 Hz
GB 0
PC 1.00
9
8
7
6
5
4
3
2
1
ppm
2.01
3.17
1.00
1.01
1.01
2.76
4.16
6.47

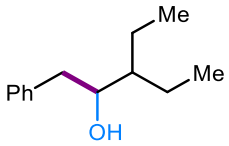

6.3xa

^{13}C NMR

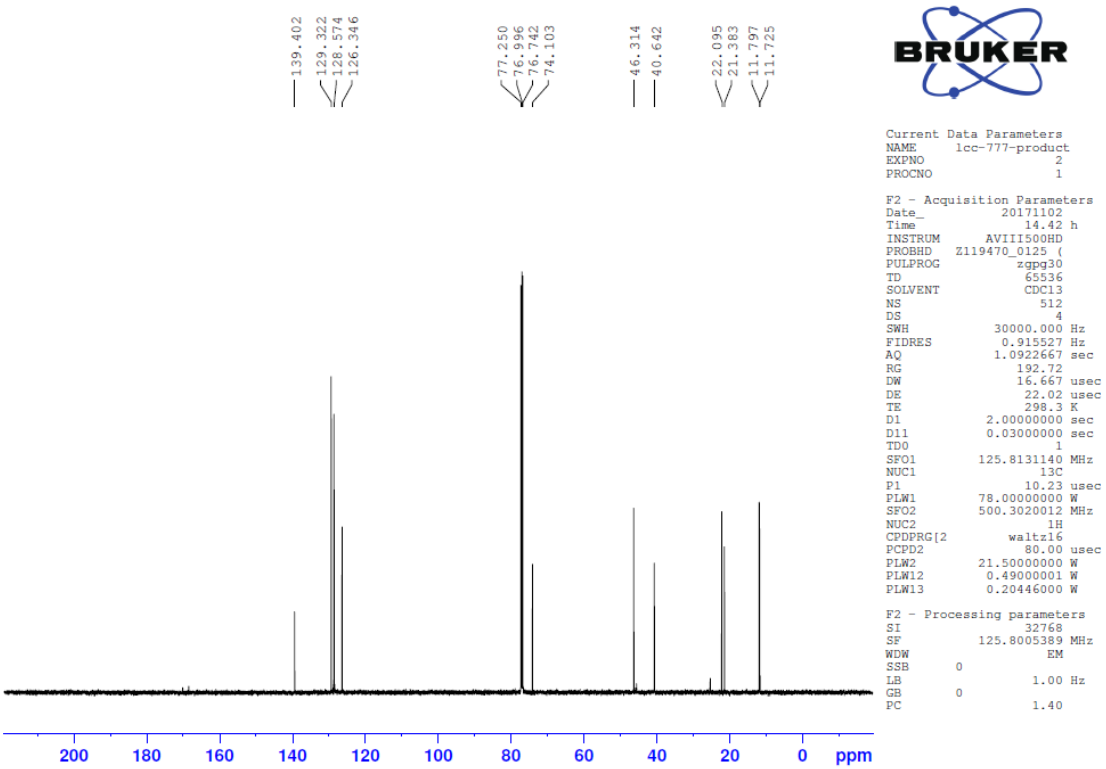


```
Current Data Parameters
NAME      1cc-777-product
EXPNO                   2
PROCNO                  1

F2 - Acquisition Parameters
Date_           20171102
Time              14.42 h
INSTRUM       AVIII500HD
PROBHD    Z119470_0125 (
PULPROG           zgpg30
TD                65536
SOLVENT           CDCl3
NS                  512
DS                    4
SWH           30000.000 Hz
FIDRES         0.915527 Hz
AQ             1.0922667 sec
RG                192.72
DW                16.667 usec
DE                22.02 usec
TE                298.3 K
D1             2.00000000 sec
D11            0.03000000 sec
TD0                   1
SFO1        125.8131140 MHz
NUC1                13C
P1                10.23 usec
PLW1         78.00000000 W
SFO2        500.3020012 MHz
NUC2                1H
CPDPRG[2         waltz16
PCPD2             80.00 usec
PLW2         21.50000000 W
PLW12         0.49000001 W
PLW13         0.20446000 W

F2 - Processing parameters
SI                32768
SF          125.8005389 MHz
WDW                 EM
SSB       0
LB                1.00 Hz
GB        0
PC                1.40
```

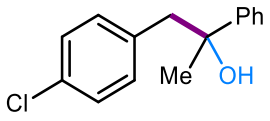
Ph
Me
OH
Cl

6.3ab

^{1}H NMR

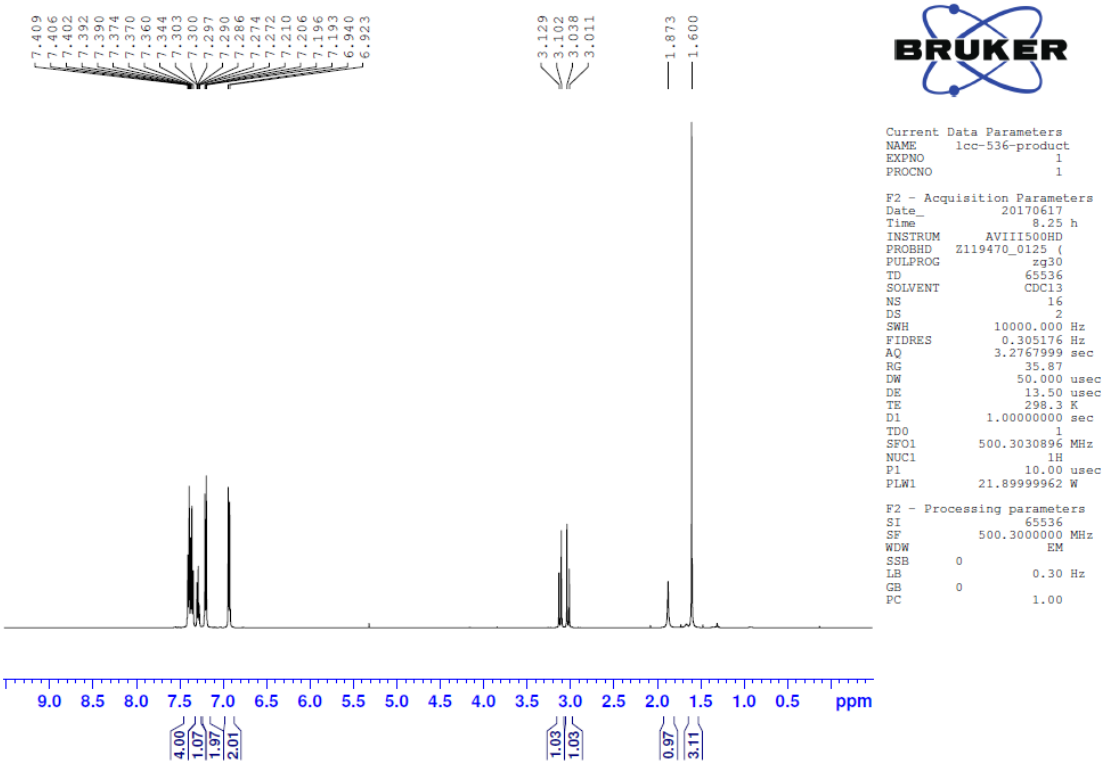
7.409
7.406
7.402
7.392
7.390
7.374
7.370
7.360
7.344
7.303
7.300
7.297
7.290
7.286
7.274
7.272
7.210
7.206
7.196
7.193
6.940
6.923
3.129
3.102
3.038
3.011
1.873
1.600
BRUKER
Current Data Parameters
NAME 1cc-536-product
EXPNO 1
PROCNO 1
F2 - Acquisition Parameters
Date_ 20170617
Time 8.25 h
INSTRUM AVIII500HD
PROBHD Z119470_0125 (
PULPROG zg30
TD 65536
SOLVENT CDC13
NS 16
DS 2
SWH 10000.000 Hz
FIDRES 0.305176 Hz
AQ 3.2767999 sec
RG 35.87
DW 50.000 usec
DE 13.50 usec
TE 298.3 K
D1 1.00000000 sec
TD0 1
SFO1 500.3030896 MHz
NUC1 1H
P1 10.00 usec
PLW1 21.89999962 W
F2 - Processing parameters
SI 65536
SF 500.3000000 MHz
WDW EM
SSB 0
LB 0.30 Hz
GB 0
PC 1.00
9.0 8.5 8.0 7.5 7.0 6.5 6.0 5.5 5.0 4.5 4.0 3.5 3.0 2.5 2.0 1.5 1.0 0.5 ppm
4.00
1.07
1.97
2.01
1.03
1.03
0.97
3.11

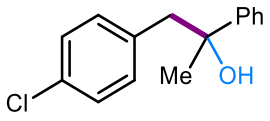

6.3ab

^{13}C NMR

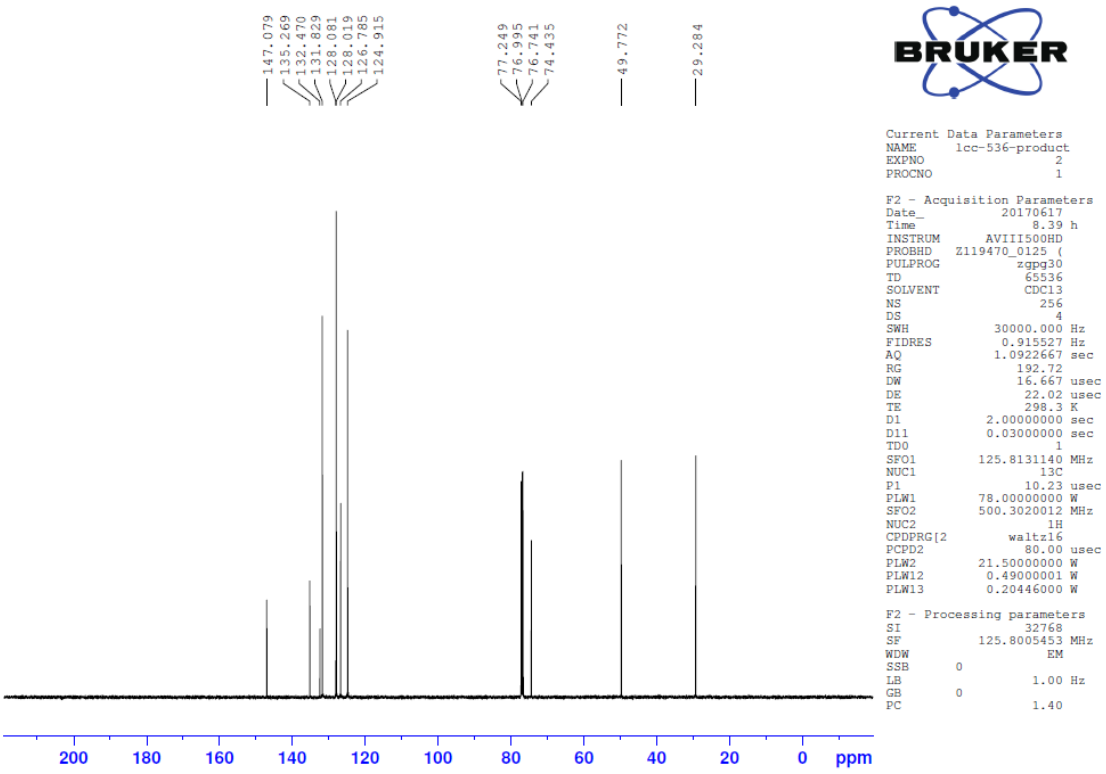


```
Current Data Parameters
NAME      lcc-536-product
EXPNO                   2
PROCNO                  1

F2 - Acquisition Parameters
Date_            20170617
Time                8.39 h
INSTRUM       AVIII500HD
PROBHD    Z119470_0125 (
PULPROG          zgpg30
TD                65536
SOLVENT           CDCl3
NS                  256
DS                    4
SWH           30000.000 Hz
FIDRES            0.915527 Hz
AQ                1.0922667 sec
RG                  192.72
DW                 16.667 usec
DE                 22.02 usec
TE                 298.3 K
D1             2.00000000 sec
D11            0.03000000 sec
TD0                   1
SFO1         125.8131140 MHz
NUC1                 13C
P1                 10.23 usec
PLW1          78.00000000 W
SFO2         500.3020012 MHz
NUC2                  1H
CPDPRG[2          waltz16
PCPD2              80.00 usec
PLW2          21.50000000 W
PLW12          0.49000001 W
PLW13          0.20446000 W

F2 - Processing parameters
SI                32768
SF           125.8005453 MHz
WDW                  EM
SSB       0
LB                1.00 Hz
GB        0
PC                1.40
```

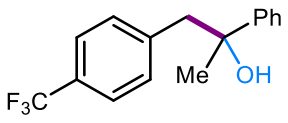

6.3ac

^{1}H NMR

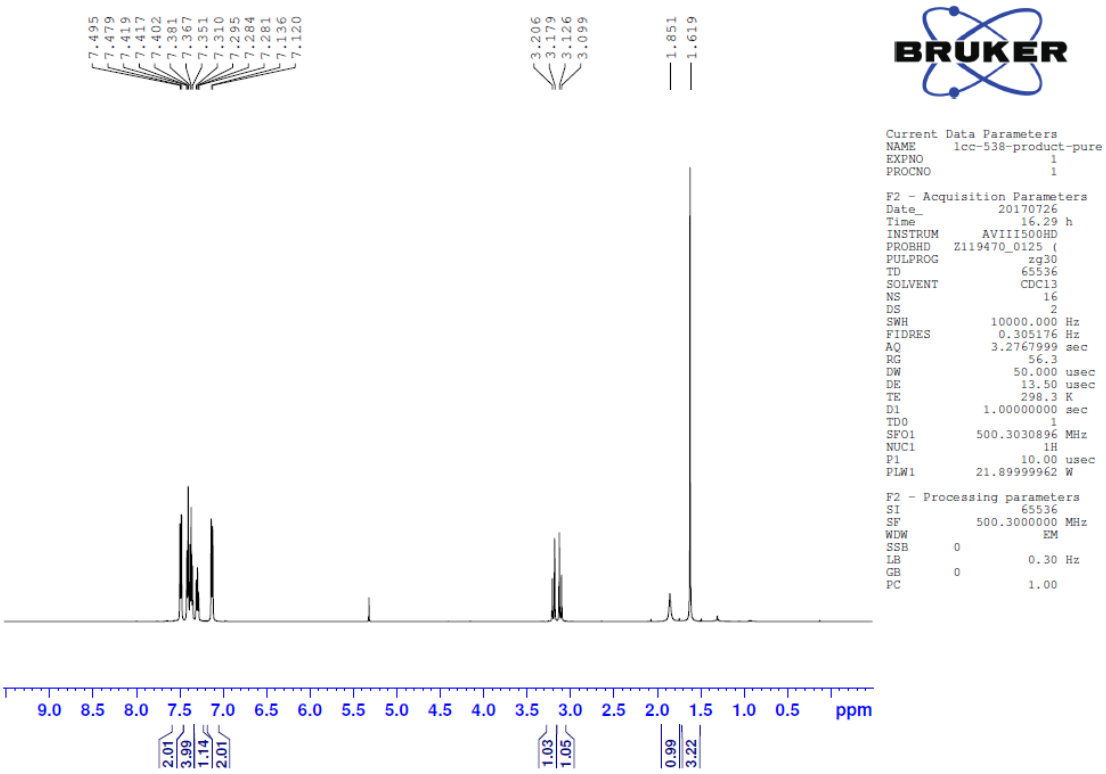

BRUKER

```
Current Data Parameters
NAME        1cc-538-product-pure
EXPNO                          1
PROCNO                         1

F2 - Acquisition Parameters
Date_                   20170726
Time                       16.29 h
INSTRUM              AVIII500HD
PROBHD           Z119470_0125 (
PULPROG                    zg30
TD                        65536
SOLVENT                   CDCl3
NS                           16
DS                            2
SWH                   10000.000 Hz
FIDRES                    0.305176 Hz
AQ                        3.2767999 sec
RG                           56.3
DW                        50.000 usec
DE                        13.50 usec
TE                        298.3 K
D1                    1.00000000 sec
TD0                           1
SFO1                500.3030896 MHz
NUC1                         1H
P1                        10.00 usec
PLW1                21.89999962 W

F2 - Processing parameters
SI                        65536
SF                  500.3000000 MHz
WDW                          EM
SSB                 0
LB                        0.30 Hz
GB                  0
PC                        1.00
```

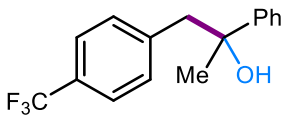
Ph
Me
OH
F3C

6.3ac

^{13}C NMR

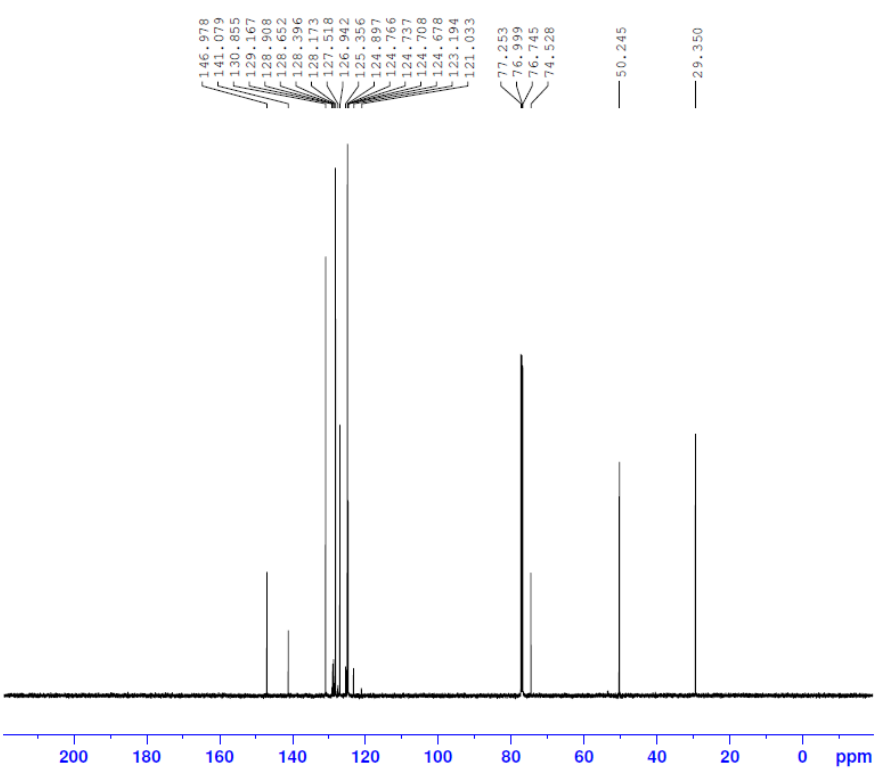
146.978
141.079
130.855
129.167
128.908
128.652
128.396
128.173
127.518
126.942
125.356
124.897
124.766
124.737
124.708
124.678
123.194
121.033
77.253
76.999
76.745
74.528
50.245
29.350
200
180
160
140
120
100
80
60
40
20
0
ppm

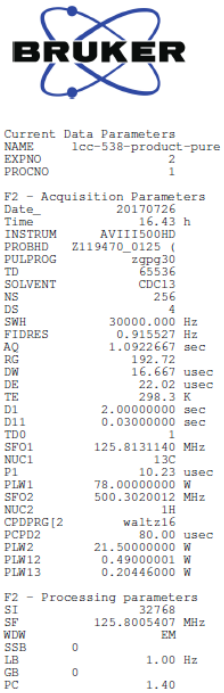
BRUKER
Current Data Parameters
NAME lcc-538-product-pure
EXPNO 2
PROCNO 1
F2 - Acquisition Parameters
Date_ 20170726
Time 16.43 h
INSTRUM AVIII500HD
PROBHD Z119470_0125 (
PULPROG zgpg30
TD 65536
SOLVENT CDCl3
NS 256
DS 4
SWH 30000.000 Hz
FIDRES 0.915527 Hz
AQ 1.0922667 sec
RG 192.72
DW 16.667 usec
DE 22.02 usec
TE 298.3 K
D1 2.00000000 sec
D11 0.03000000 sec
TD0 1
SFO1 125.8131140 MHz
NUC1 13C
P1 10.23 usec
PLW1 78.00000000 W
SFO2 500.3020012 MHz
NUC2 1H
CPDPRG[2 waltz16
PCPD2 80.00 usec
PLW2 21.50000000 W
PLW12 0.49000001 W
PLW13 0.20446000 W
F2 - Processing parameters
SI 32768
SF 125.8005407 MHz
WDW EM
SSB 0
LB 1.00 Hz
GB 0
PC 1.40

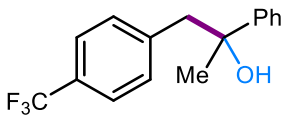

6.3ac

^{19}F NMR

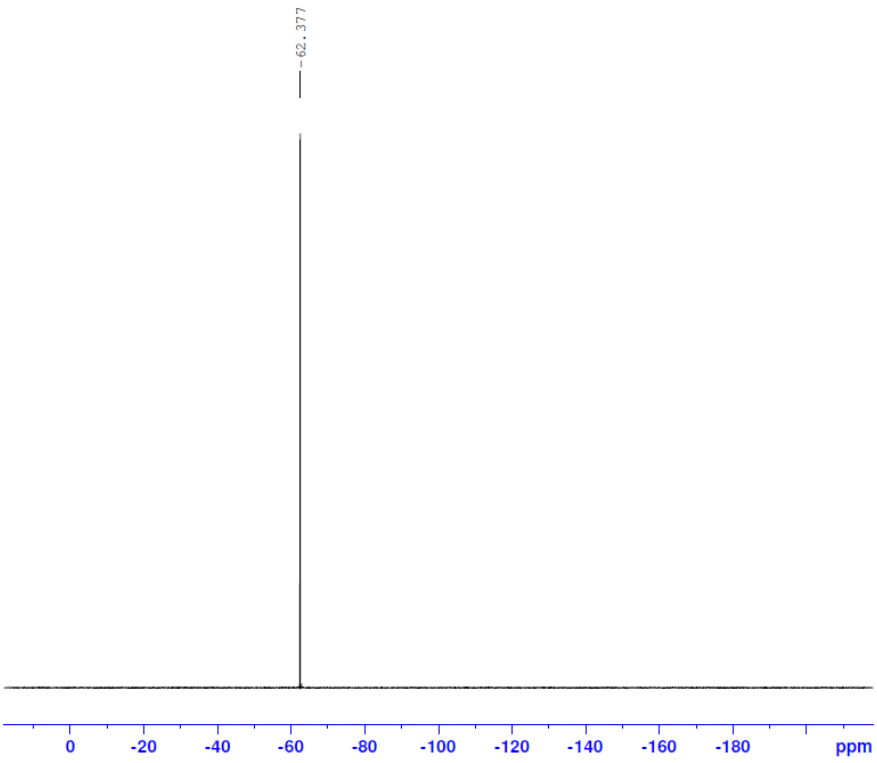


```
Current Data Parameters
NAME      1cc-538-product-pure
EXPNO                        3
PROCNO                       1

F2 - Acquisition Parameters
Date_              20170726
Time                  16.45 h
INSTRUM       AVIII500HD
PROBHD    Z119470_0125 (
PULPROG   zgbsfhigqn.baseopt
TD                    131072
SOLVENT                CDC13
NS                        16
DS                         4
SWH              111111.109 Hz
FIDRES             1.695421 Hz
AQ                 0.5898240 sec
RG                    192.72
DW                     4.500 usec
DE                    35.33 usec
TE                    298.3 K
D1                 1.00000000 sec
D11                0.03000000 sec
D12                0.00002000 sec
TD0                        1
SFO1            470.7052618 MHz
NUC1                     19F
P1                    15.00 usec
P2                    30.00 usec
PLW1            39.50000000 W
SFO2            500.3025015 MHz
NUC2                     1H
CPDPRG[2             waltz16
PCPD2                 80.00 usec
PLW2            21.50000000 W
PLW12            0.49000001 W

F2 - Processing parameters
SI                        65536
SF              470.7523370 MHz
WDW                          EM
SSB       0
LB                     0.30 Hz
GB        0
PC                     1.00
```

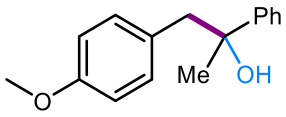

6.3ad

^{1}H NMR

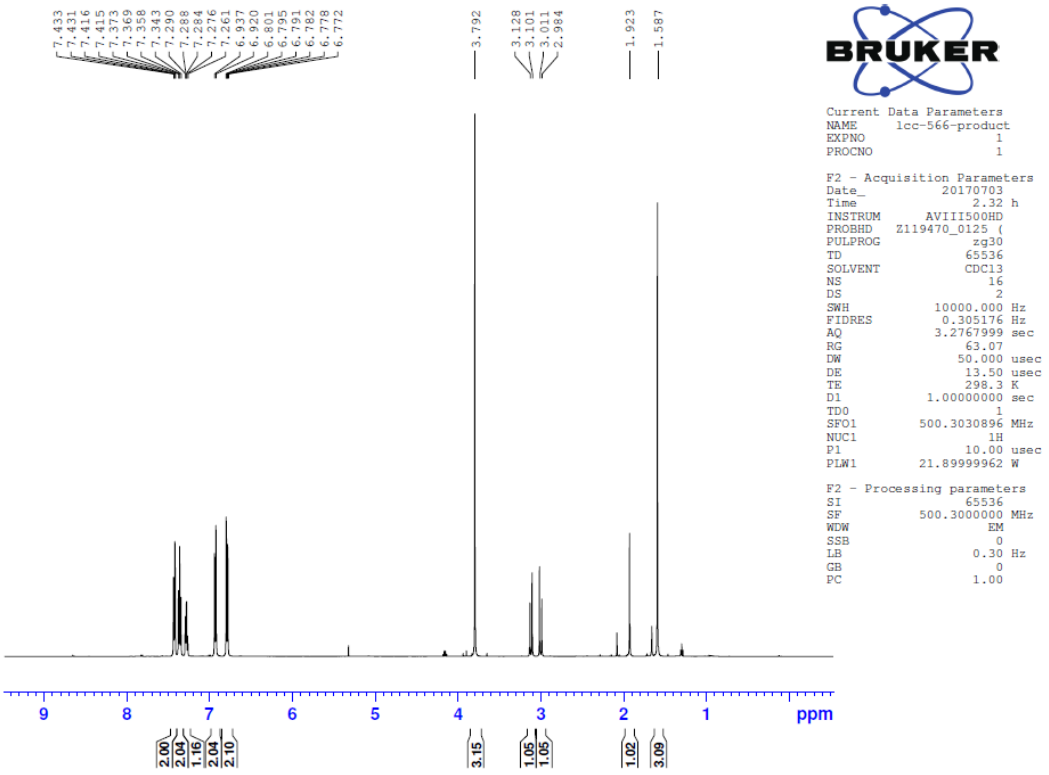

BRUKER

```
Current Data Parameters
NAME        1cc-566-product
EXPNO                     1
PROCNO                    1

F2 - Acquisition Parameters
Date_              20170703
Time                  2.32 h
INSTRUM         AVIII500HD
PROBHD     Z119470_0125 (
PULPROG                zg30
TD                    65536
SOLVENT               CDCl3
NS                       16
DS                        2
SWH               10000.000 Hz
FIDRES                0.305176 Hz
AQ                    3.2767999 sec
RG                       63.07
DW                    50.000 usec
DE                    13.50 usec
TE                    298.3 K
D1                1.00000000 sec
TD0                       1
SFO1           500.3030896 MHz
NUC1                     1H
P1                    10.00 usec
PLW1          21.89999962 W

F2 - Processing parameters
SI                    65536
SF             500.3000000 MHz
WDW                      EM
SSB                       0
LB                    0.30 Hz
GB                        0
PC                    1.00
```

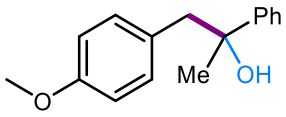

6.3ad

^{13}C NMR

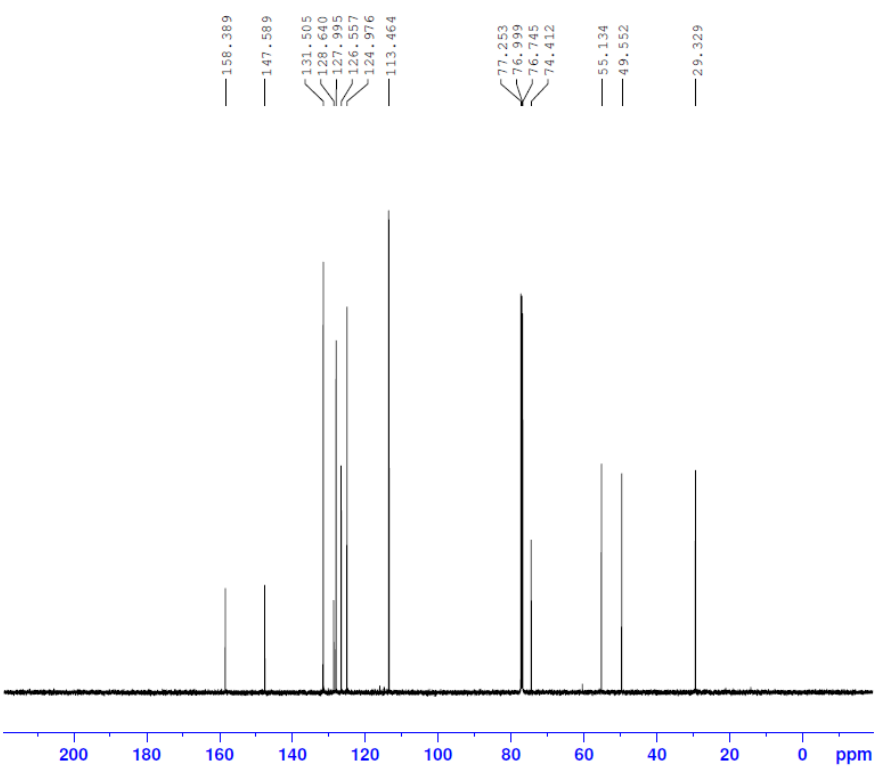


```
Current Data Parameters
NAME      lcc-566-product
EXPNO                   2
PROCNO                  1

F2 - Acquisition Parameters
Date_           20170703
Time              2.47 h
INSTRUM       AVIII500HD
PROBHD    Z119470_0125 (
PULPROG           zgpg30
TD                65536
SOLVENT           CDCl3
NS                  256
DS                    4
SWH           30000.000 Hz
FIDRES         0.915527 Hz
AQ             1.0922667 sec
RG                192.72
DW                16.667 usec
DE                22.02 usec
TE                298.3 K
D1             2.00000000 sec
D11            0.03000000 sec
TD0                   1
SFO1         125.8131140 MHz
NUC1                 13C
P1                10.23 usec
PLW1         78.00000000 W
SFO2         500.3020012 MHz
NUC2                 1H
CPDPRG[2          waltz16
PCPD2             80.00 usec
PLW2         21.50000000 W
PLW12         0.49000001 W
PLW13         0.20446000 W

F2 - Processing parameters
SI                32768
SF           125.8005425 MHz
WDW                  EM
SSB       0
LB                 1.00 Hz
GB        0
PC                 1.40
```

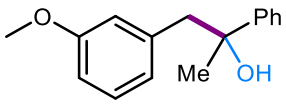
O
Ph
Me
OH

6.3ae

^{1}H NMR

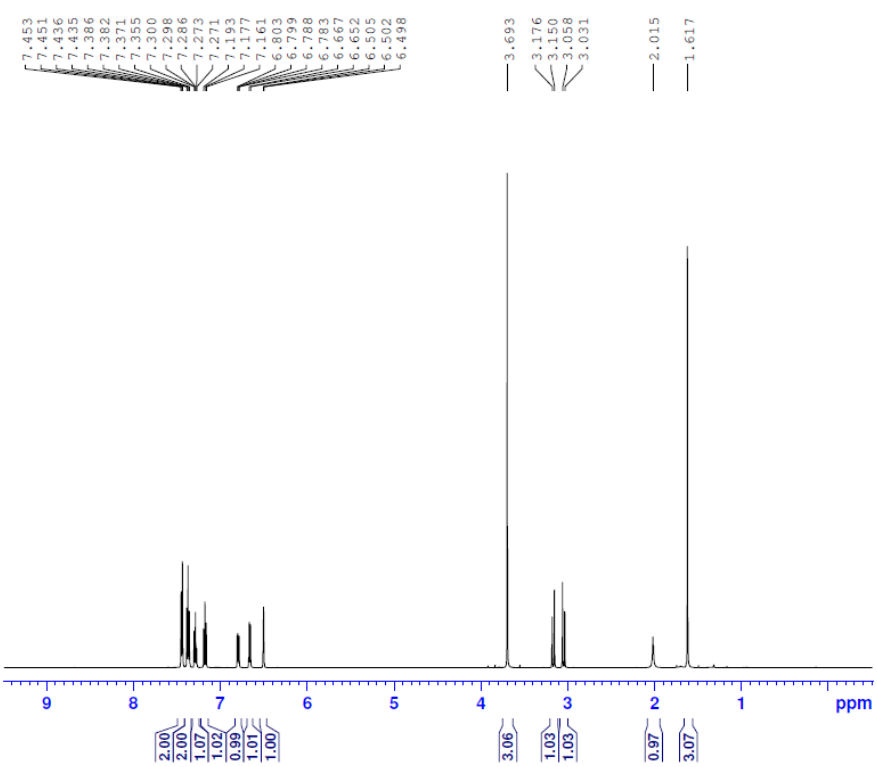
7.453
7.451
7.436
7.435
7.386
7.382
7.371
7.355
7.300
7.298
7.286
7.273
7.271
7.193
7.177
7.161
6.803
6.799
6.788
6.783
6.667
6.652
6.505
6.502
6.498
3.693
3.176
3.150
3.058
3.031
2.015
1.617
9
8
7
6
5
4
3
2
1
ppm
2.00
2.00
1.07
1.02
0.99
1.01
1.00
3.06
1.03
1.03
0.97
3.07

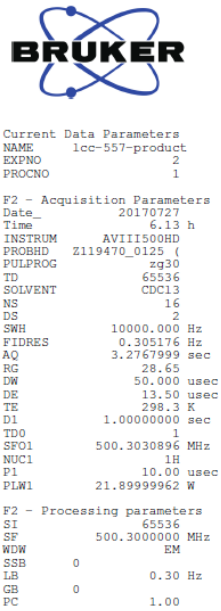
BRUKER
Current Data Parameters
NAME lcc-557-product
EXPNO 2
PROCNO 1
F2 - Acquisition Parameters
Date_ 20170727
Time 6.13 h
INSTRUM AVIII500HD
PROBHD Z119470_0125 (
PULPROG zg30
TD 65536
SOLVENT CDCl3
NS 16
DS 2
SWH 10000.000 Hz
FIDRES 0.305176 Hz
AQ 3.2767999 sec
RG 28.65
DW 50.000 usec
DE 13.50 usec
TE 298.3 K
D1 1.00000000 sec
TD0 1
SFO1 500.3030896 MHz
NUC1 1H
P1 10.00 usec
PLW1 21.89999962 W
F2 - Processing parameters
SI 65536
SF 500.3000000 MHz
WDW EM
SSB 0
LB 0.30 Hz
GB 0
PC 1.00

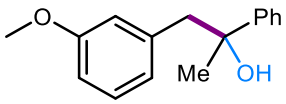
O
Ph
Me
OH

6.3ae

^{13}C NMR

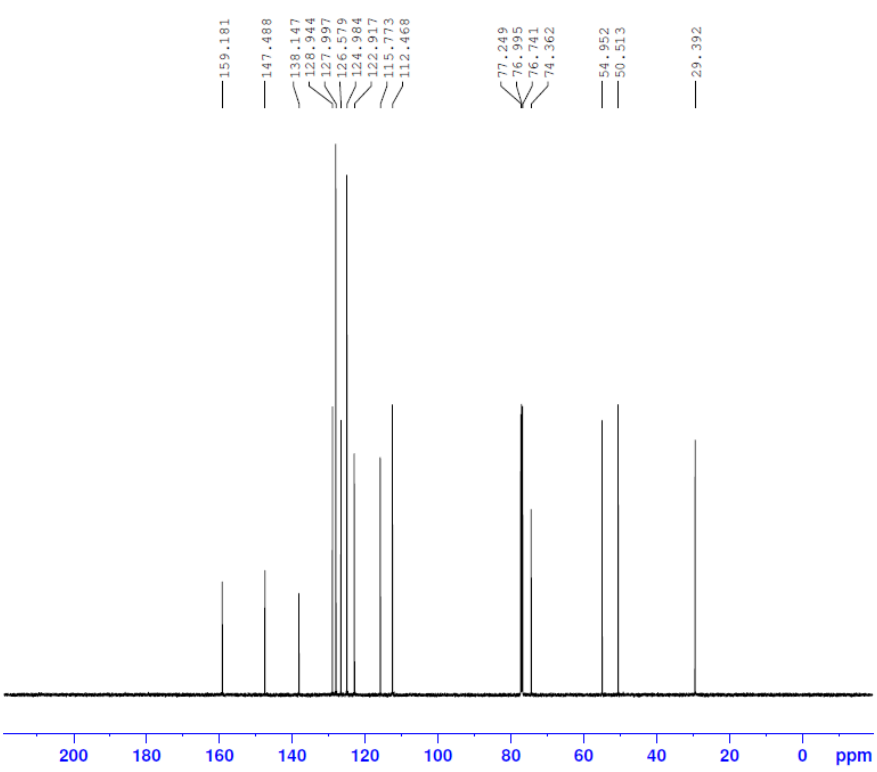
159.181
147.488
138.147
128.944
127.997
126.579
124.984
122.917
115.773
112.468
77.249
76.995
76.741
74.362
54.952
50.513
29.392
200
180
160
140
120
100
80
60
40
20
0
ppm

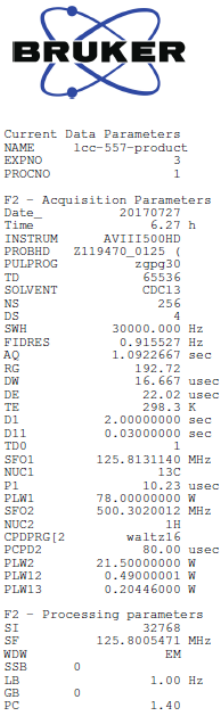
BRUKER
Current Data Parameters
NAME lcc-557-product
EXPNO 3
PROCNO 1
F2 - Acquisition Parameters
Date_ 20170727
Time 6.27 h
INSTRUM AVIII500HD
PROBHD Z119470_0125 (
PULPROG zgpg30
TD 65536
SOLVENT CDCl3
NS 256
DS 4
SWH 30000.000 Hz
FIDRES 0.915527 Hz
AQ 1.0922667 sec
RG 192.72
DW 16.667 usec
DE 22.02 usec
TE 298.3 K
D1 2.00000000 sec
D11 0.03000000 sec
TD0 1
SFO1 125.8131140 MHz
NUC1 13C
P1 10.23 usec
PLW1 78.00000000 W
SFO2 500.3020012 MHz
NUC2 1H
CPDPRG[2 waltz16
PCPD2 80.00 usec
PLW2 21.50000000 W
PLW12 0.49000001 W
PLW13 0.20446000 W
F2 - Processing parameters
SI 32768
SF 125.8005471 MHz
WDW EM
SSB 0
LB 1.00 Hz
GB 0
PC 1.40

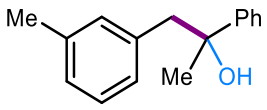
Me
Ph
Me
OH

6.3af

^{1}H NMR

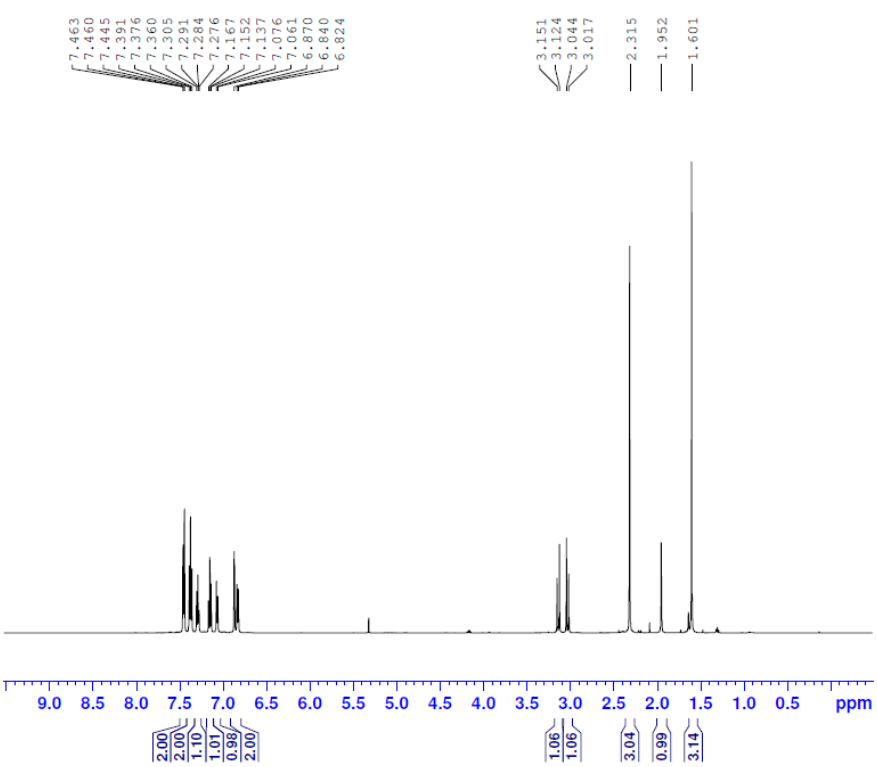
7.463
7.460
7.445
7.391
7.376
7.360
7.305
7.291
7.284
7.276
7.167
7.152
7.137
7.076
7.061
6.870
6.840
6.824
3.151
3.124
3.044
3.017
2.315
1.952
1.601
9.0 8.5 8.0 7.5 7.0 6.5 6.0 5.5 5.0 4.5 4.0 3.5 3.0 2.5 2.0 1.5 1.0 0.5 ppm
2.00
2.00
1.10
1.01
0.98
2.00
1.06
1.06
3.04
0.99
3.14

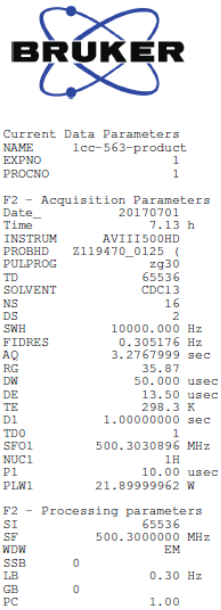
BRUKER
Current Data Parameters
NAME lcc-563-product
EXPNO 1
PROCNO 1
F2 - Acquisition Parameters
Date_ 20170701
Time 7.13 h
INSTRUM AVIII500HD
PROBHD Z119470_0125 (
PULPROG zg30
TD 65536
SOLVENT CDC13
NS 16
DS 2
SWH 10000.000 Hz
FIDRES 0.305176 Hz
AQ 3.2767999 sec
RG 35.87
DW 50.000 usec
DE 13.50 usec
TE 298.3 K
D1 1.00000000 sec
TD0 1
SFO1 500.3030896 MHz
NUC1 1H
P1 10.00 usec
PLW1 21.89999962 W
F2 - Processing parameters
SI 65536
SF 500.3000000 MHz
WDW EM
SSB 0
LB 0.30 Hz
GB 0
PC 1.00

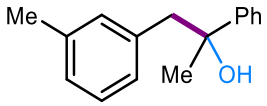

6.3af

^{13}C NMR

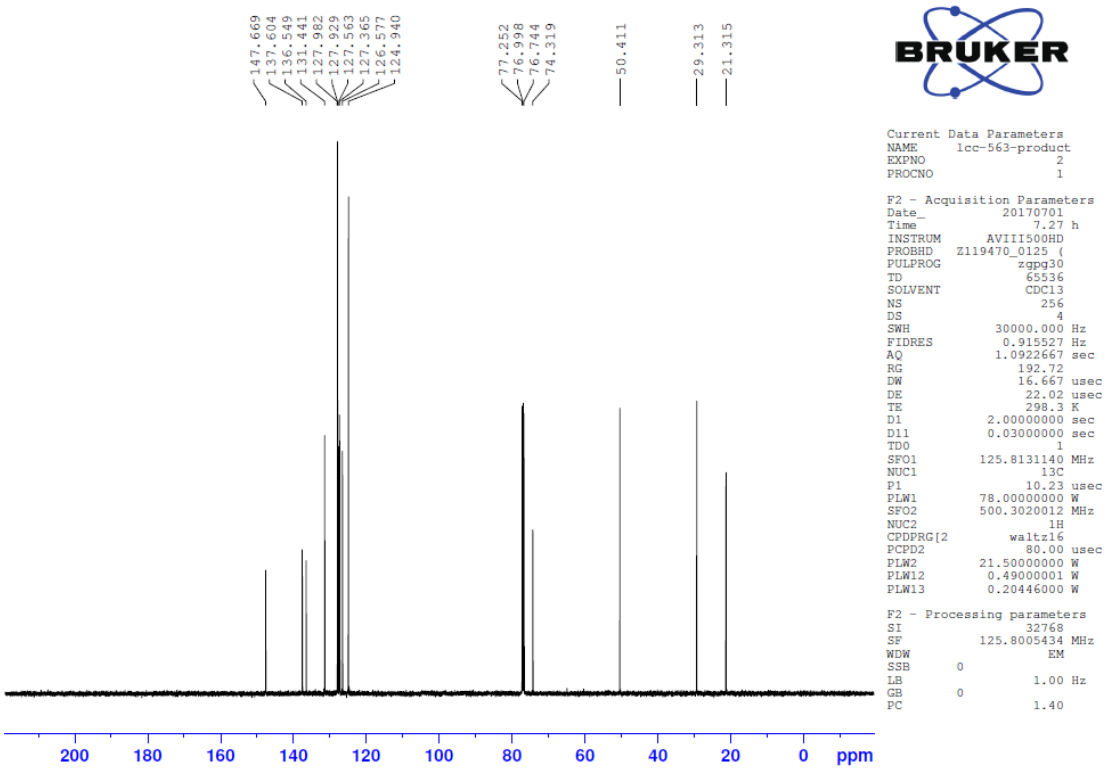

BRUKER

```
Current Data Parameters
NAME      lcc-563-product
EXPNO                   2
PROCNO                  1

F2 - Acquisition Parameters
Date_            20170701
Time                7.27 h
INSTRUM       AVIII500HD
PROBHD    Z119470_0125 (
PULPROG          zgpg30
TD                65536
SOLVENT           CDCl3
NS                  256
DS                    4
SWH           30000.000 Hz
FIDRES        0.915527 Hz
AQ            1.0922667 sec
RG               192.72
DW               16.667 usec
DE                22.02 usec
TE                298.3 K
D1           2.00000000 sec
D11          0.03000000 sec
TD0                   1
SFO1        125.8131140 MHz
NUC1                13C
P1                10.23 usec
PLW1        78.00000000 W
SFO2        500.3020012 MHz
NUC2                1H
CPDPRG[2        waltz16
PCPD2             80.00 usec
PLW2        21.50000000 W
PLW12        0.49000001 W
PLW13        0.20446000 W

F2 - Processing parameters
SI                32768
SF          125.8005434 MHz
WDW                  EM
SSB       0
LB                1.00 Hz
GB        0
PC                1.40
```

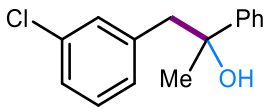
Cl
Ph
Me
OH

6.3ag

^{1}H NMR

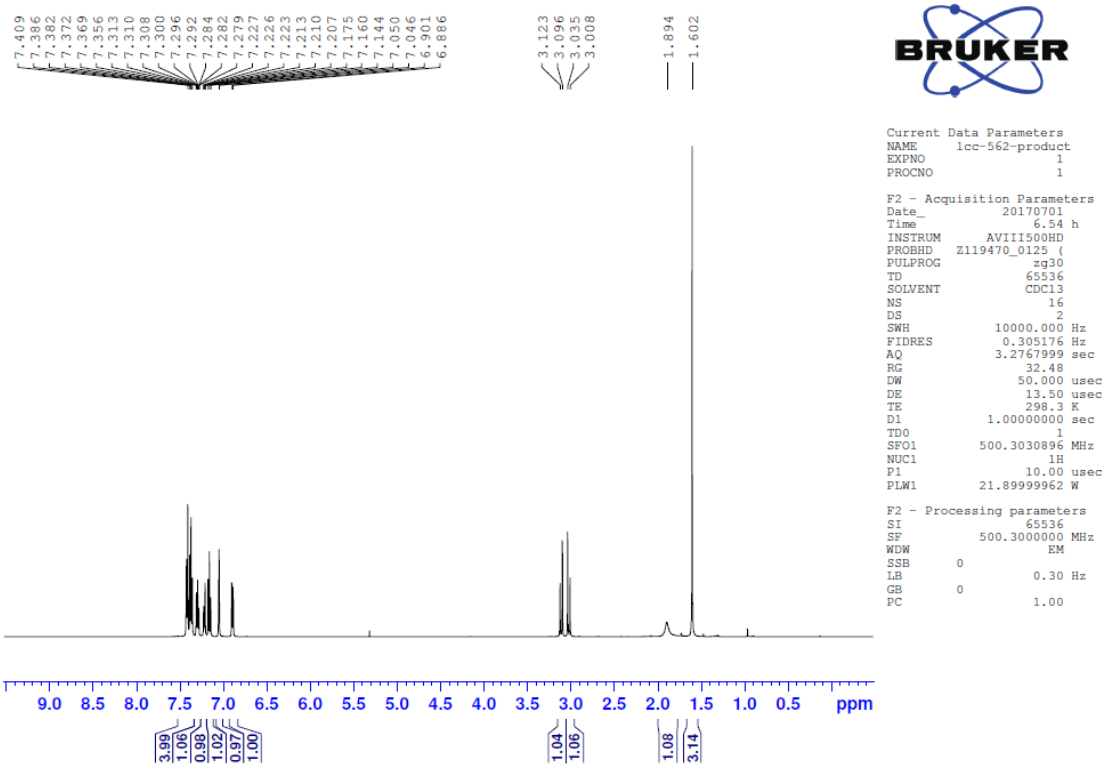
7.409
7.386
7.382
7.372
7.369
7.356
7.313
7.310
7.308
7.300
7.296
7.292
7.284
7.282
7.279
7.227
7.226
7.223
7.213
7.210
7.207
7.175
7.160
7.144
7.050
7.046
6.901
6.886
3.123
3.096
3.035
3.008
1.894
1.602
BRUKER
Current Data Parameters
NAME 1cc-562-product
EXPNO 1
PROCNO 1
F2 - Acquisition Parameters
Date_ 20170701
Time 6.54 h
INSTRUM AVIII500HD
PROBHD Z119470_0125 (
PULPROG zg30
TD 65536
SOLVENT CDCl3
NS 16
DS 2
SWH 10000.000 Hz
FIDRES 0.305176 Hz
AQ 3.2767999 sec
RG 32.48
DW 50.000 usec
DE 13.50 usec
TE 298.3 K
D1 1.00000000 sec
TD0 1
SFO1 500.3030896 MHz
NUC1 1H
P1 10.00 usec
PLW1 21.89999962 W
F2 - Processing parameters
SI 65536
SF 500.3000000 MHz
WDW EM
SSB 0
LB 0.30 Hz
GB 0
PC 1.00
9.0 8.5 8.0 7.5 7.0 6.5 6.0 5.5 5.0 4.5 4.0 3.5 3.0 2.5 2.0 1.5 1.0 0.5 ppm
3.99
1.06
0.98
1.02
0.97
1.00
1.04
1.06
1.08
3.14

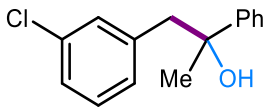

6.3ag

^{13}C NMR

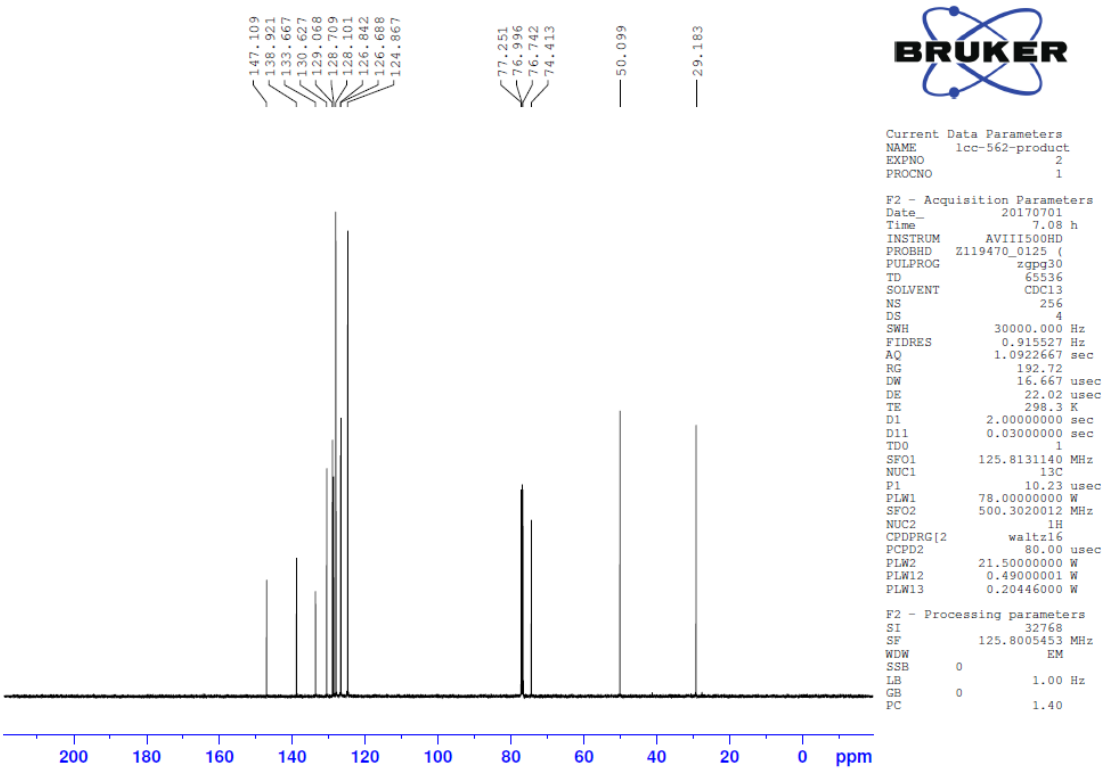


```
Current Data Parameters
NAME      1cc-562-product
EXPNO                   2
PROCNO                  1

F2 - Acquisition Parameters
Date_            20170701
Time                7.08 h
INSTRUM       AVIII500HD
PROBHD    Z119470_0125 (
PULPROG          zgpg30
TD                65536
SOLVENT           CDCl3
NS                  256
DS                    4
SWH           30000.000 Hz
FIDRES            0.915527 Hz
AQ                1.0922667 sec
RG                  192.72
DW                 16.667 usec
DE                 22.02 usec
TE                 298.3 K
D1             2.00000000 sec
D11            0.03000000 sec
TD0                   1
SFO1         125.8131140 MHz
NUC1                 13C
P1                 10.23 usec
PLW1          78.00000000 W
SFO2         500.3020012 MHz
NUC2                 1H
CPDPRG[2          waltz16
PCPD2              80.00 usec
PLW2          21.50000000 W
PLW12          0.49000001 W
PLW13          0.20446000 W

F2 - Processing parameters
SI                  32768
SF           125.8005453 MHz
WDW                   EM
SSB       0
LB                 1.00 Hz
GB        0
PC                 1.40
```

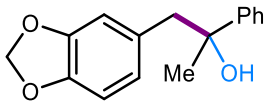

6.3ah

^{1}H NMR

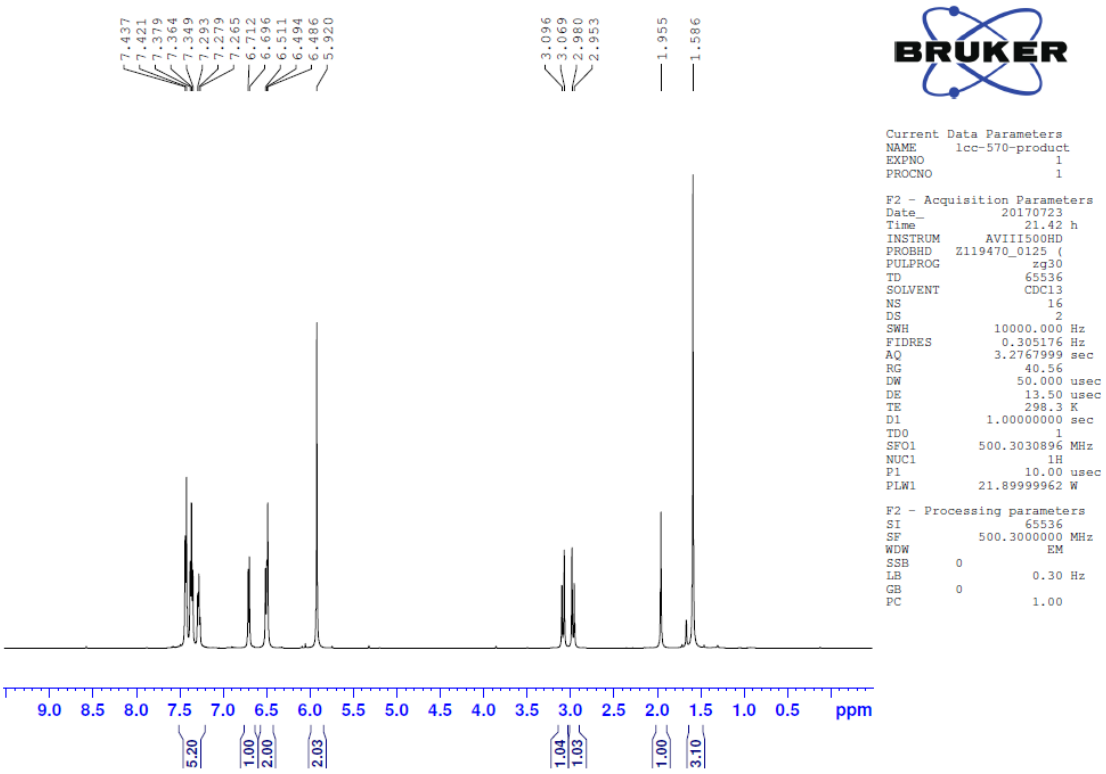

BRUKER

```
Current Data Parameters
NAME      1cc-570-product
EXPNO                   1
PROCNO                  1

F2 - Acquisition Parameters
Date_            20170723
Time                21.42 h
INSTRUM       AVIII500HD
PROBHD    Z119470_0125 (
PULPROG             zg30
TD                 65536
SOLVENT            CDCl3
NS                    16
DS                     2
SWH            10000.000 Hz
FIDRES             0.305176 Hz
AQ                 3.2767999 sec
RG                    40.56
DW                 50.000 usec
DE                 13.50 usec
TE                 298.3 K
D1              1.00000000 sec
TD0                    1
SFO1          500.3030896 MHz
NUC1                  1H
P1                 10.00 usec
PLW1          21.89999962 W

F2 - Processing parameters
SI                 65536
SF            500.3000000 MHz
WDW                   EM
SSB       0
LB                 0.30 Hz
GB        0
PC                 1.00
```

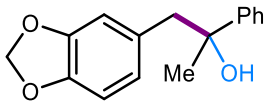

6.3ah

^{13}C NMR

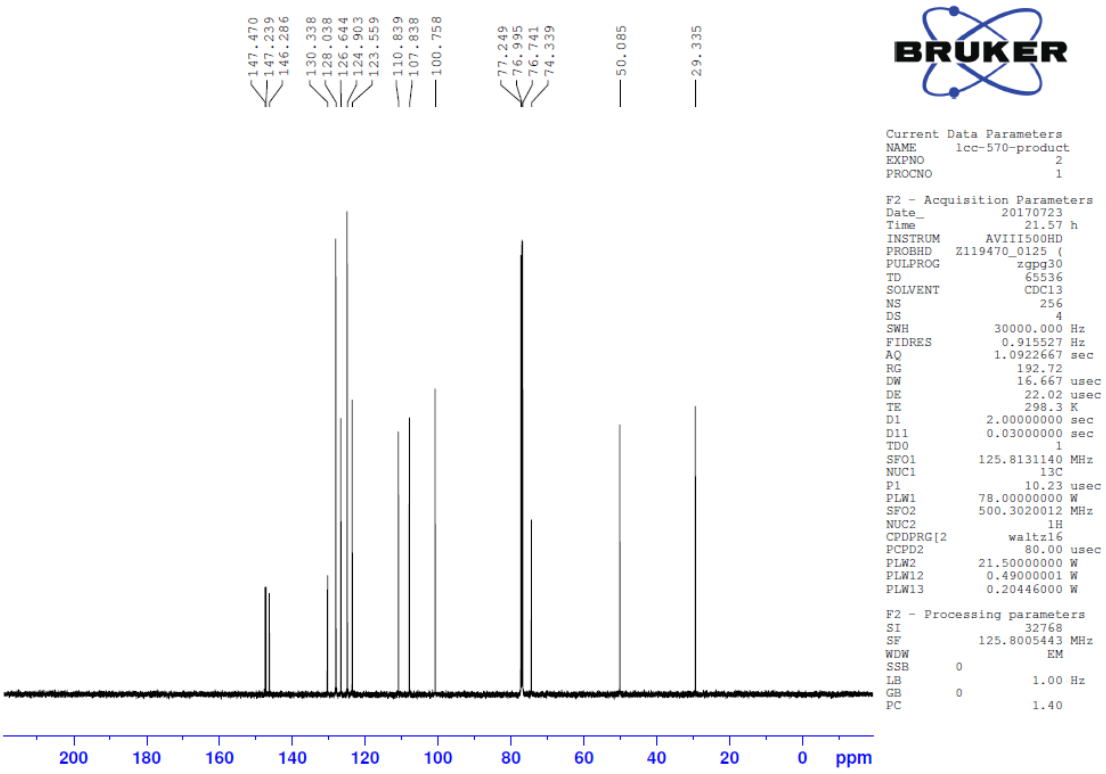


```
Current Data Parameters
NAME      1cc-570-product
EXPNO                   2
PROCNO                  1

F2 - Acquisition Parameters
Date_            20170723
Time                21.57 h
INSTRUM       AVIII500HD
PROBHD    Z119470_0125 (
PULPROG          zgpg30
TD                65536
SOLVENT           CDCl3
NS                  256
DS                    4
SWH           30000.000 Hz
FIDRES            0.915527 Hz
AQ                1.0922667 sec
RG                  192.72
DW                 16.667 usec
DE                 22.02 usec
TE                 298.3 K
D1             2.00000000 sec
D11            0.03000000 sec
TD0                   1
SFO1         125.8131140 MHz
NUC1                 13C
P1                 10.23 usec
PLW1          78.00000000 W
SFO2         500.3020012 MHz
NUC2                 1H
CPDPRG[2          waltz16
PCPD2              80.00 usec
PLW2          21.50000000 W
PLW12          0.49000001 W
PLW13          0.20446000 W

F2 - Processing parameters
SI                32768
SF           125.8005443 MHz
WDW                  EM
SSB       0
LB                1.00 Hz
GB        0
PC                1.40
```

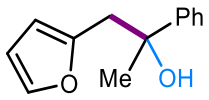
Ph
Me
OH
O

6.3ai

^{1}H NMR

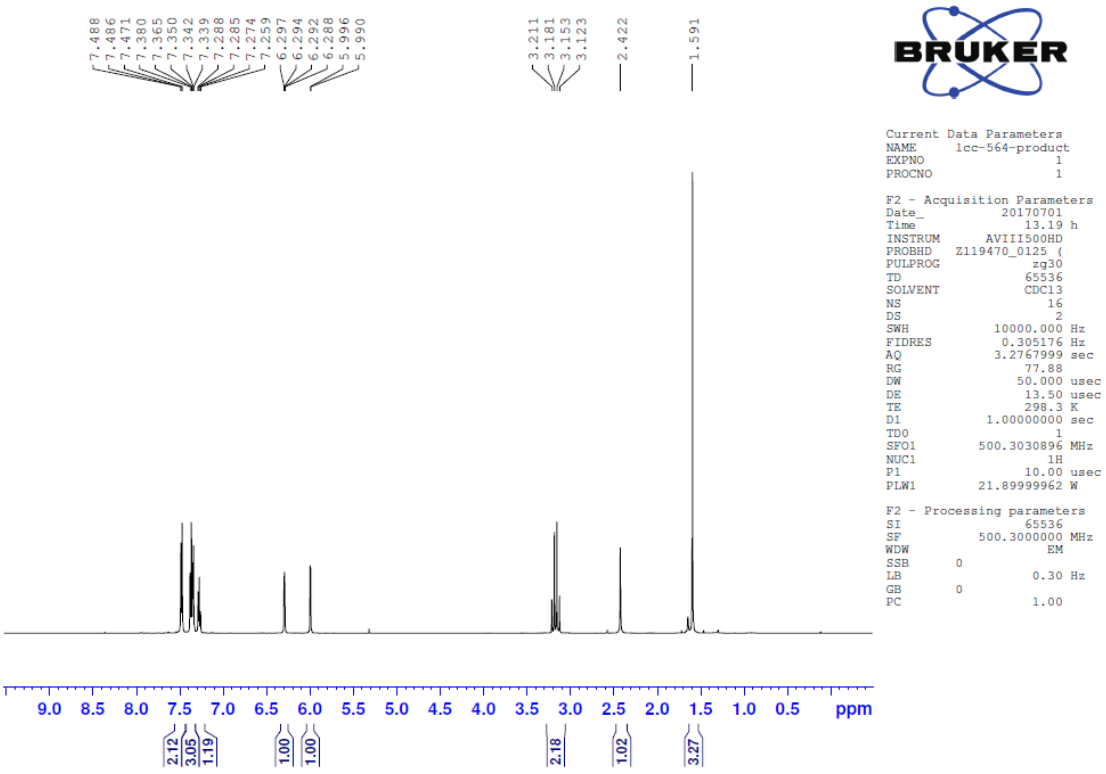
7.488
7.486
7.471
7.380
7.365
7.350
7.342
7.339
7.288
7.285
7.274
7.259
6.297
6.294
6.292
6.288
5.996
5.990
3.211
3.181
3.153
3.123
2.422
1.591
BRUKER
Current Data Parameters
NAME lcc-564-product
EXPNO 1
PROCNO 1
F2 - Acquisition Parameters
Date_ 20170701
Time 13.19 h
INSTRUM AVIII500HD
PROBHD Z119470_0125 (
PULPROG zg30
TD 65536
SOLVENT CDCl3
NS 16
DS 2
SWH 10000.000 Hz
FIDRES 0.305176 Hz
AQ 3.2767999 sec
RG 77.88
DW 50.000 usec
DE 13.50 usec
TE 298.3 K
D1 1.00000000 sec
TD0 1
SFO1 500.3030896 MHz
NUC1 1H
P1 10.00 usec
PLW1 21.89999962 W
F2 - Processing parameters
SI 65536
SF 500.3000000 MHz
WDW EM
SSB 0
LB 0.30 Hz
GB 0
PC 1.00
9.0 8.5 8.0 7.5 7.0 6.5 6.0 5.5 5.0 4.5 4.0 3.5 3.0 2.5 2.0 1.5 1.0 0.5 ppm
2.12
3.05
1.19
1.00
1.00
2.18
1.02
3.27

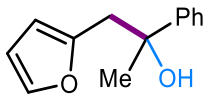

6.3ai

^{13}C NMR

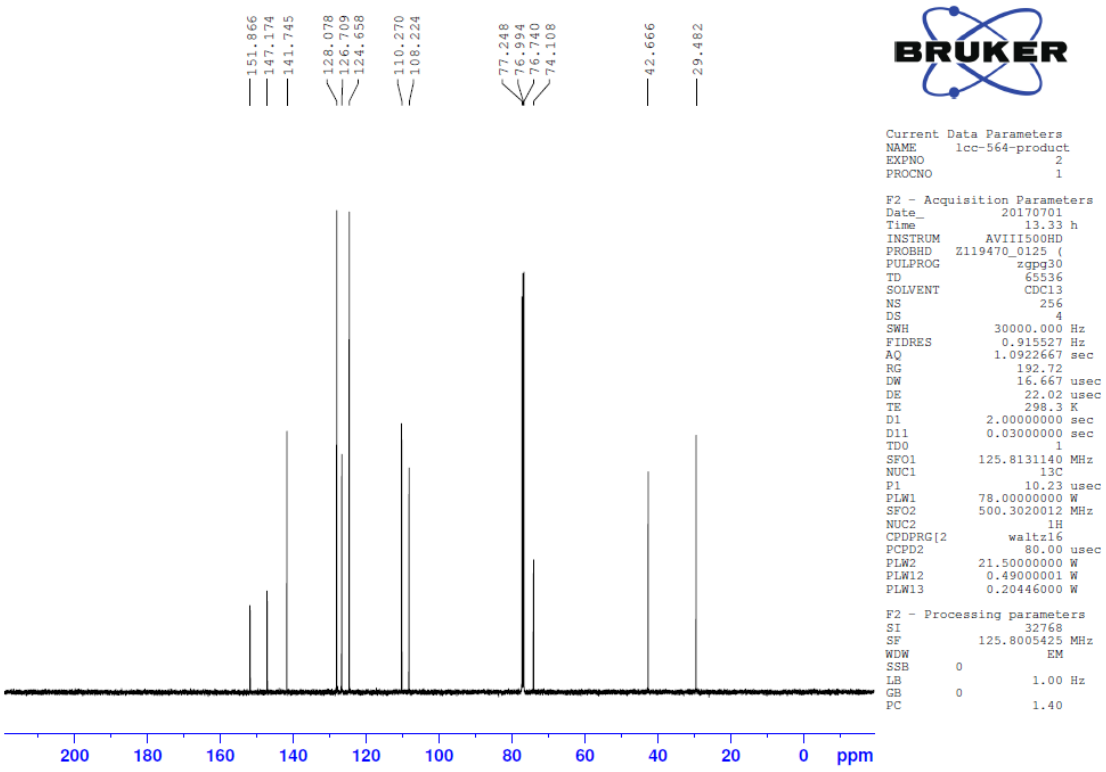


```
Current Data Parameters
NAME      1cc-564-product
EXPNO                   2
PROCNO                  1

F2 - Acquisition Parameters
Date_            20170701
Time                13.33 h
INSTRUM       AVIII500HD
PROBHD    Z119470_0125 (
PULPROG          zgpg30
TD                65536
SOLVENT           CDCl3
NS                  256
DS                    4
SWH           30000.000 Hz
FIDRES            0.915527 Hz
AQ                1.0922667 sec
RG                  192.72
DW                 16.667 usec
DE                 22.02 usec
TE                 298.3 K
D1             2.00000000 sec
D11            0.03000000 sec
TD0                   1
SFO1         125.8131140 MHz
NUC1                 13C
P1                 10.23 usec
PLW1          78.00000000 W
SFO2         500.3020012 MHz
NUC2                 1H
CPDPRG[2          waltz16
PCPD2              80.00 usec
PLW2          21.50000000 W
PLW12          0.49000001 W
PLW13          0.20446000 W

F2 - Processing parameters
SI                32768
SF           125.8005425 MHz
WDW                  EM
SSB       0
LB                 1.00 Hz
GB        0
PC                 1.40
```

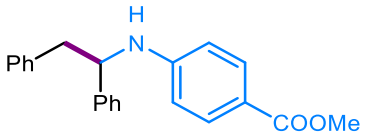

6.4aa

^{1}H NMR

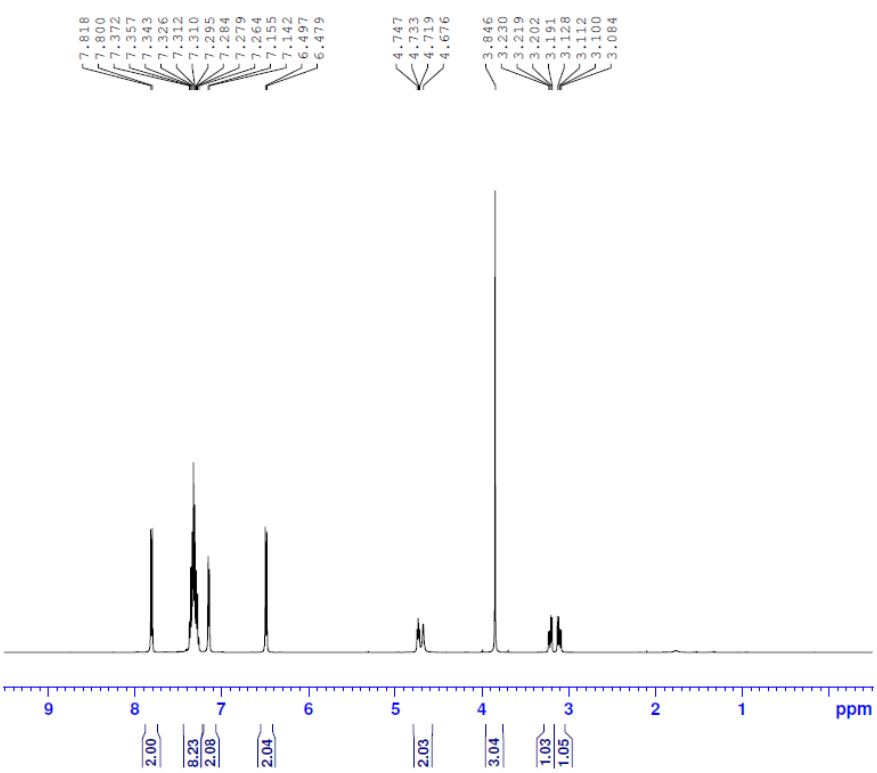


```
Current Data Parameters
NAME      1cc-758-product
EXPNO                   1
PROCNO                  1

F2 - Acquisition Parameters
Date_           20171022
Time              14.55 h
INSTRUM       AVIII500HD
PROBHD    Z119470_0125 (
PULPROG             zg30
TD                 65536
SOLVENT            CDCl3
NS                    16
DS                     2
SWH           10000.000 Hz
FIDRES            0.305176 Hz
AQ                3.2767999 sec
RG                   25.23
DW                  50.000 usec
DE                  13.50 usec
TE                  298.3 K
D1              1.00000000 sec
TD0                    1
SFO1          500.3030896 MHz
NUC1                  1H
P1                  10.00 usec
PLW1          21.89999962 W

F2 - Processing parameters
SI                 65536
SF            500.3000000 MHz
WDW                   EM
SSB       0
LB                 0.30 Hz
GB        0
PC                 1.00
```

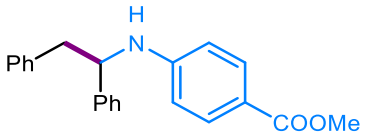

6.4aa

^{13}C NMR

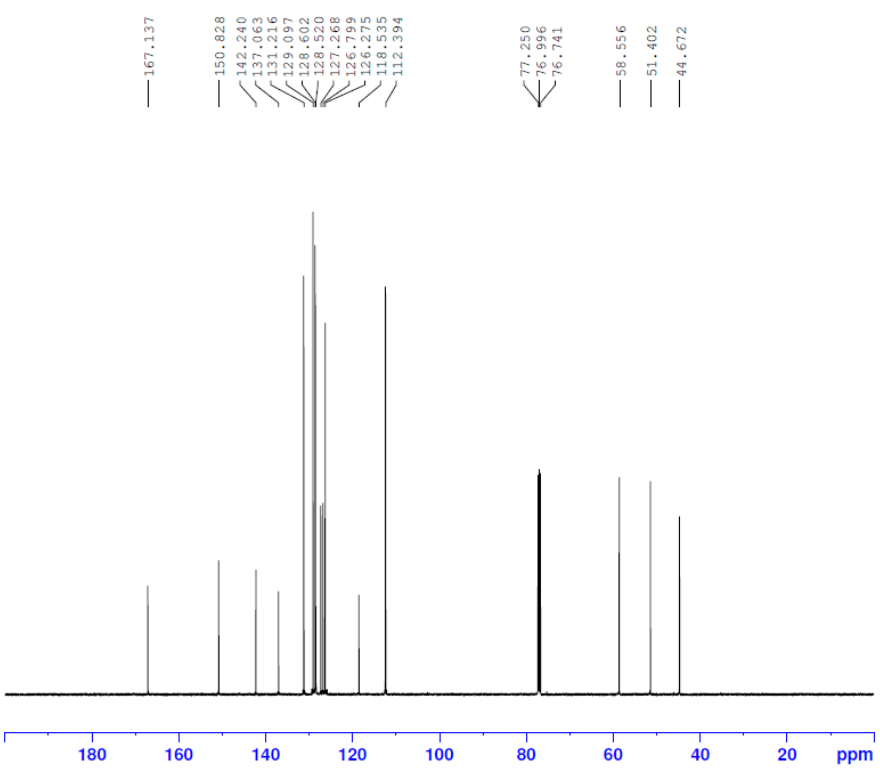


```
Current Data Parameters
NAME      lcc-758-product
EXPNO                   2
PROCNO                  1

F2 - Acquisition Parameters
Date_           20171022
Time              15.23 h
INSTRUM       AVIII500HD
PROBHD    Z119470_0125 (
PULPROG           zgpg30
TD                65536
SOLVENT           CDCl3
NS                  512
DS                    4
SWH           30000.000 Hz
FIDRES         0.915527 Hz
AQ             1.0922667 sec
RG                192.72
DW              16.667 usec
DE              22.02 usec
TE                298.3 K
D1            2.00000000 sec
D11           0.03000000 sec
TD0                   1
SFO1         125.8131140 MHz
NUC1                13C
P1                10.23 usec
PLW1         78.00000000 W
SFO2         500.3020012 MHz
NUC2                1H
CPDPRG[2         waltz16
PCPD2             80.00 usec
PLW2         21.50000000 W
PLW12         0.49000001 W
PLW13         0.20446000 W

F2 - Processing parameters
SI                32768
SF           125.8005526 MHz
WDW                  EM
SSB       0
LB                1.00 Hz
GB        0
PC                1.40
```

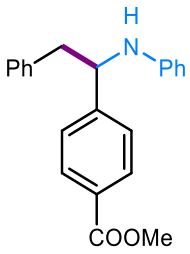
H
N
Ph
Ph
COOMe

6.4ba

^{1}H NMR

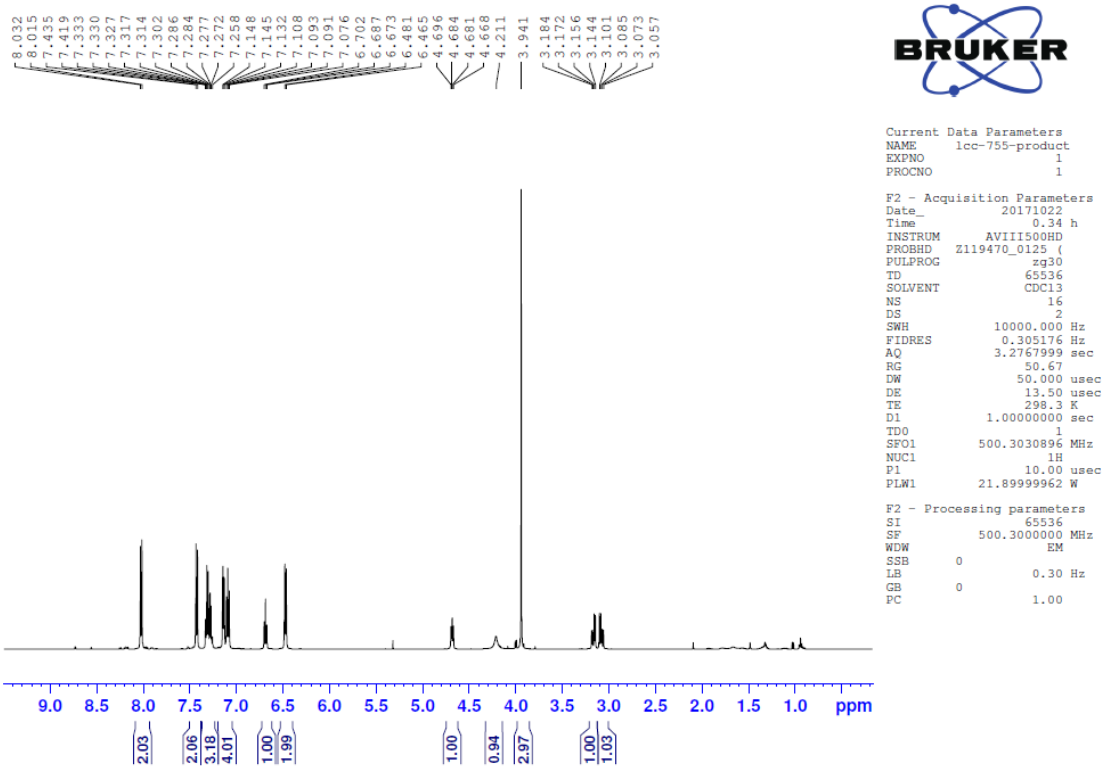
8.032
8.015
7.435
7.419
7.333
7.330
7.327
7.317
7.314
7.302
7.286
7.284
7.277
7.272
7.258
7.148
7.145
7.132
7.108
7.093
7.091
7.076
6.702
6.687
6.673
6.481
6.465
4.696
4.684
4.681
4.668
4.211
3.941
3.184
3.172
3.156
3.144
3.101
3.085
3.073
3.057
BRUKER
Current Data Parameters
NAME 1cc-755-product
EXPNO 1
PROCNO 1
F2 - Acquisition Parameters
Date_ 20171022
Time 0.34 h
INSTRUM AVIII500HD
PROBHD Z119470_0125 (
PULPROG zg30
TD 65536
SOLVENT CDCl3
NS 16
DS 2
SWH 10000.000 Hz
FIDRES 0.305176 Hz
AQ 3.2767999 sec
RG 50.67
DW 50.000 usec
DE 13.50 usec
TE 298.3 K
D1 1.00000000 sec
TD0 1
SFO1 500.3030896 MHz
NUC1 1H
P1 10.00 usec
PLW1 21.89999962 W
F2 - Processing parameters
SI 65536
SF 500.3000000 MHz
WDW EM
SSB 0
LB 0.30 Hz
GB 0
PC 1.00
9.0 8.5 8.0 7.5 7.0 6.5 6.0 5.5 5.0 4.5 4.0 3.5 3.0 2.5 2.0 1.5 1.0 ppm
2.03
2.06
3.18
4.01
1.00
1.99
1.00
0.94
2.97
1.00
1.03

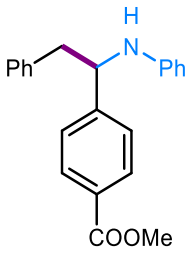

6.4ba

^{13}C NMR

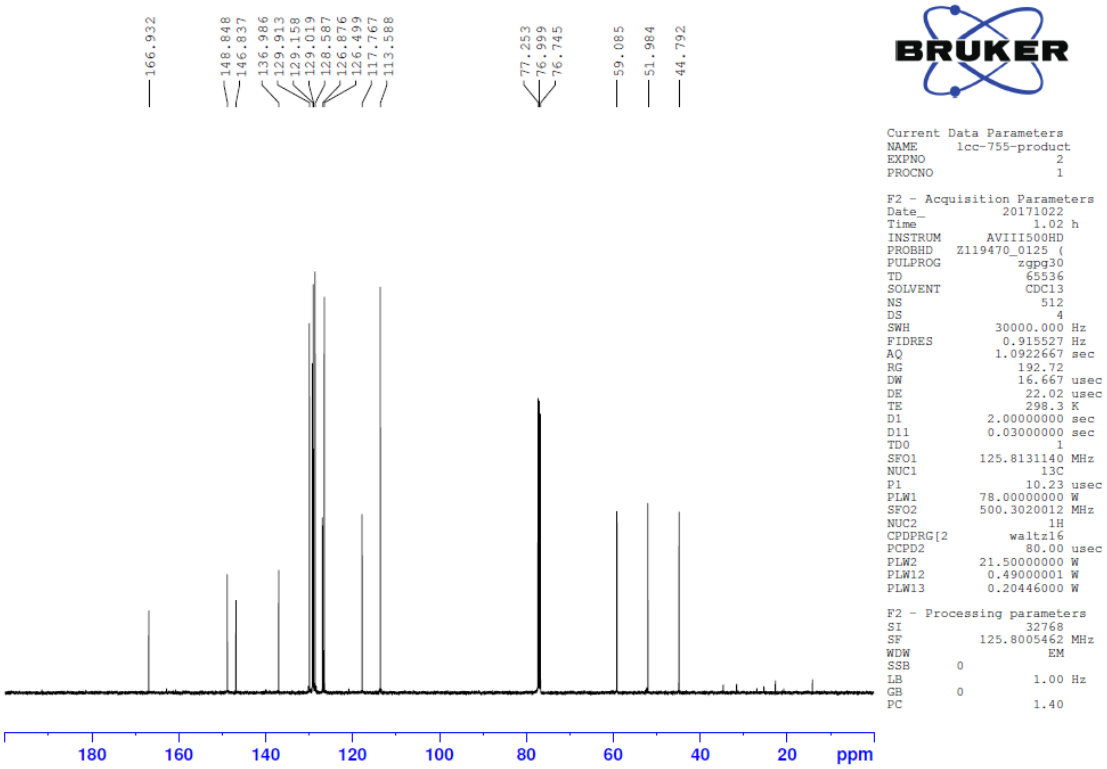

BRUKER

```
Current Data Parameters
NAME      1cc-755-product
EXPNO                   2
PROCNO                  1

F2 - Acquisition Parameters
Date_           20171022
Time                1.02 h
INSTRUM       AVIII500HD
PROBHD    Z119470_0125 (
PULPROG          zgpg30
TD                65536
SOLVENT           CDCl3
NS                  512
DS                    4
SWH           30000.000 Hz
FIDRES            0.915527 Hz
AQ                1.0922667 sec
RG                  192.72
DW                  16.667 usec
DE                  22.02 usec
TE                  298.3 K
D1                2.00000000 sec
D11               0.03000000 sec
TD0                     1
SFO1         125.8131140 MHz
NUC1                  13C
P1                  10.23 usec
PLW1         78.00000000 W
SFO2         500.3020012 MHz
NUC2                  1H
CPDPRG[2          waltz16
PCPD2               80.00 usec
PLW2         21.50000000 W
PLW12         0.49000001 W
PLW13         0.20446000 W

F2 - Processing parameters
SI                  32768
SF           125.8005462 MHz
WDW                   EM
SSB       0
LB                  1.00 Hz
GB        0
PC                  1.40
```

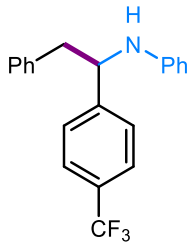

6.4ca

^{1}H NMR

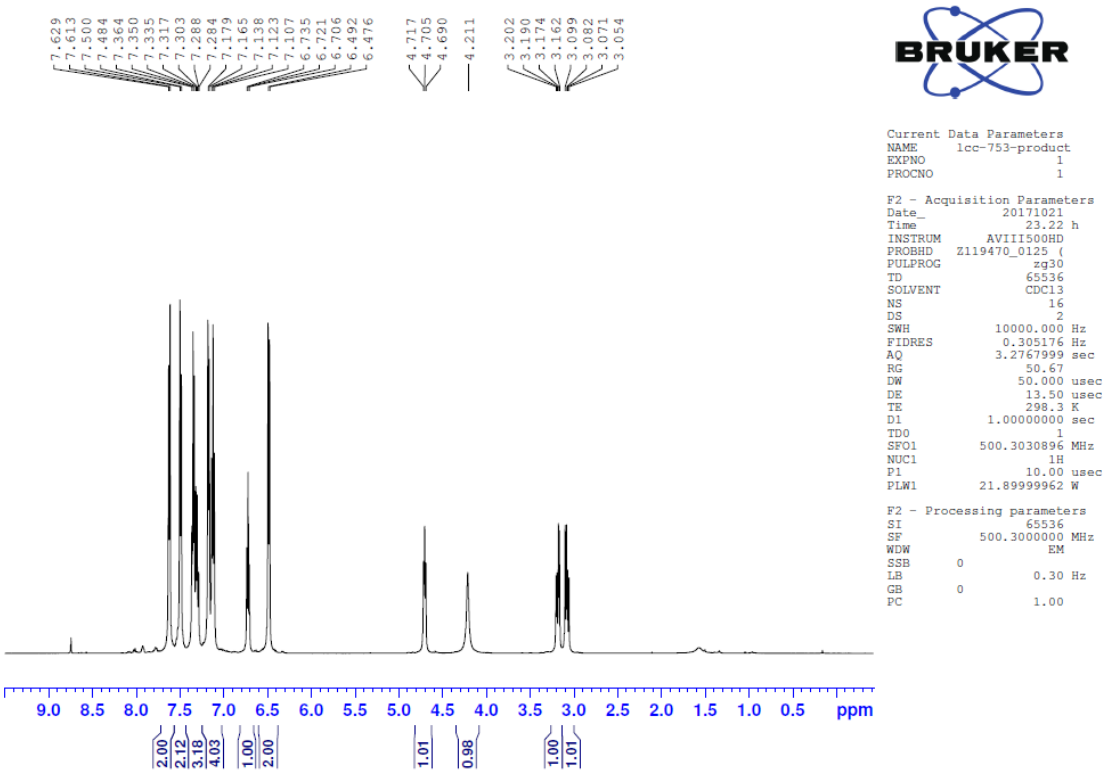


```
Current Data Parameters
NAME      1cc-753-product
EXPNO                   1
PROCNO                  1

F2 - Acquisition Parameters
Date_           20171021
Time              23.22 h
INSTRUM       AVIII500HD
PROBHD   Z119470_0125 (
PULPROG             zg30
TD                 65536
SOLVENT            CDCl3
NS                    16
DS                     2
SWH            10000.000 Hz
FIDRES         0.305176 Hz
AQ             3.2767999 sec
RG                 50.67
DW                50.000 usec
DE                13.50 usec
TE                298.3 K
D1             1.00000000 sec
TD0                    1
SFO1         500.3030896 MHz
NUC1                  1H
P1                10.00 usec
PLW1         21.89999962 W

F2 - Processing parameters
SI                 65536
SF            500.3000000 MHz
WDW                   EM
SSB       0
LB                 0.30 Hz
GB        0
PC                 1.00
```

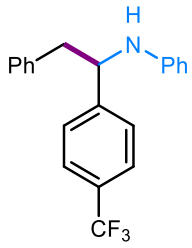

6.4ca

^{13}C NMR

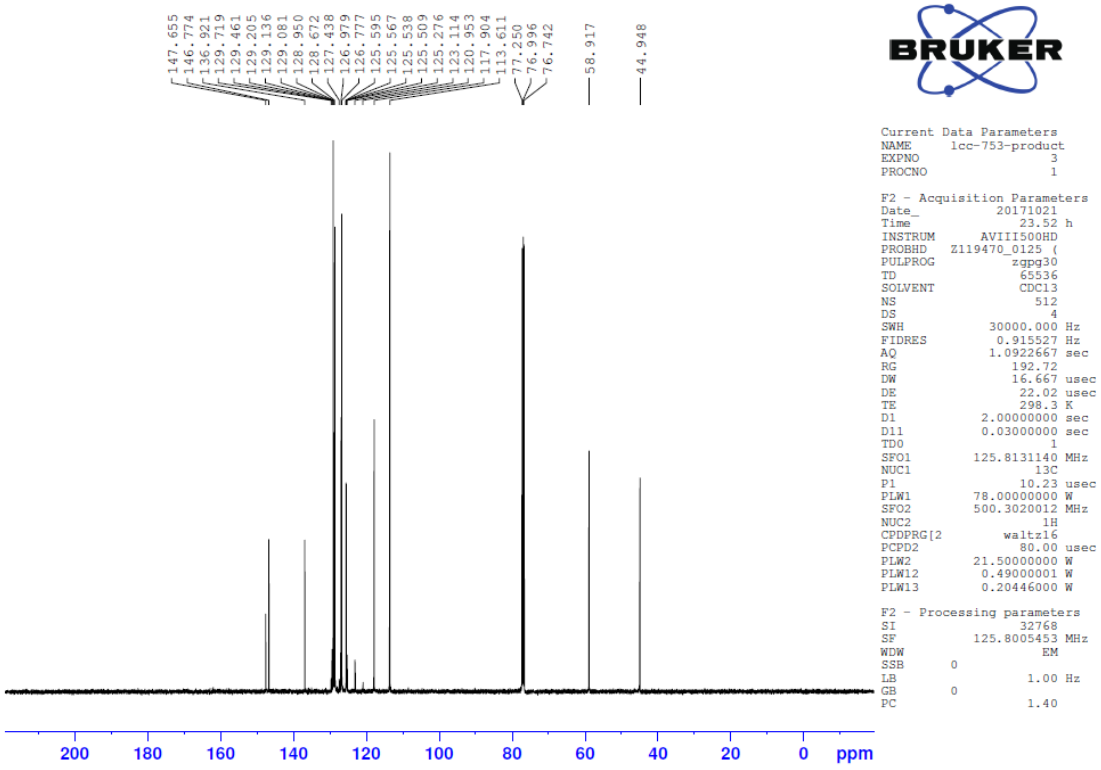


```
Current Data Parameters
NAME      1cc-753-product
EXPNO                   3
PROCNO                  1

F2 - Acquisition Parameters
Date_           20171021
Time              23.52 h
INSTRUM       AVIII500HD
PROBHD    Z119470_0125 (
PULPROG          zgpg30
TD                65536
SOLVENT           CDC13
NS                  512
DS                    4
SWH           30000.000 Hz
FIDRES        0.915527 Hz
AQ            1.0922667 sec
RG               192.72
DW               16.667 usec
DE               22.02 usec
TE               298.3 K
D1            2.00000000 sec
D11           0.03000000 sec
TD0                   1
SFO1        125.8131140 MHz
NUC1                13C
P1               10.23 usec
PLW1         78.00000000 W
SFO2        500.3020012 MHz
NUC2                1H
CPDPRG[2        waltz16
PCPD2             80.00 usec
PLW2         21.50000000 W
PLW12         0.49000001 W
PLW13         0.20446000 W

F2 - Processing parameters
SI                32768
SF          125.8005453 MHz
WDW                  EM
SSB       0
LB                1.00 Hz
GB        0
PC                1.40
```

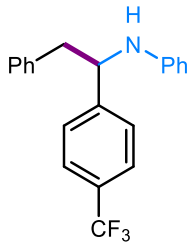

6.4ca

^{19}F NMR

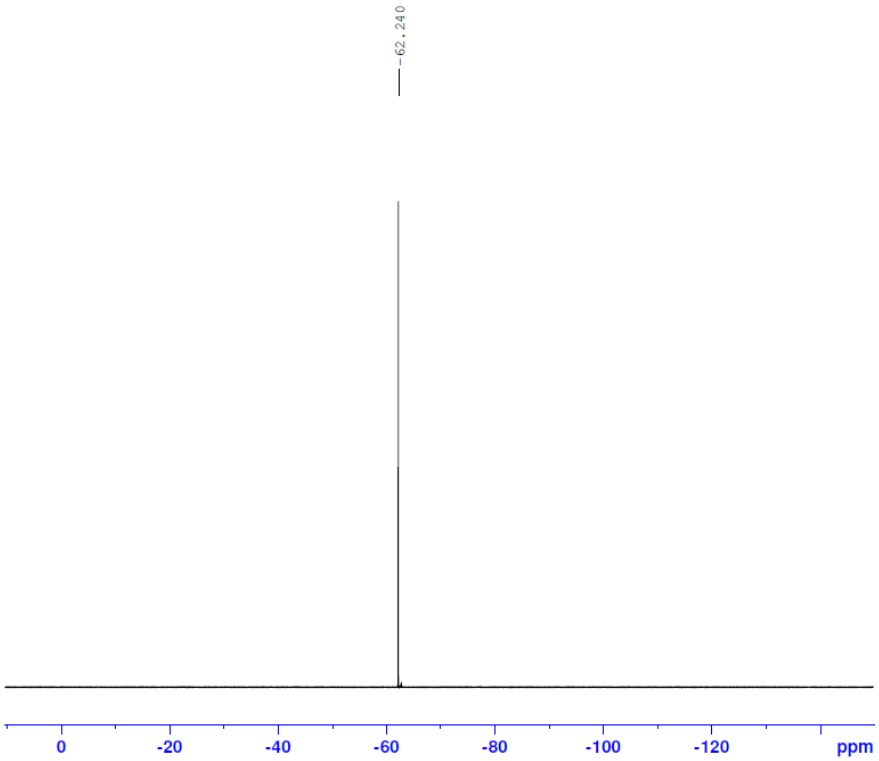


```
Current Data Parameters
NAME      1cc-753-product
EXPNO                   2
PROCNO                  1

F2 - Acquisition Parameters
Date_           20171021
Time              23.24 h
INSTRUM       AVIII500HD
PROBHD   Z119470_0125 (
PULPROG  zgbsfhiqqn.baseopt
TD              131072
SOLVENT           CDCl3
NS                   16
DS                    4
SWH          111111.109 Hz
FIDRES         1.695421 Hz
AQ             0.5898240 sec
RG                192.72
DW                 4.500 usec
DE                35.33 usec
TE                298.3 K
D1             1.00000000 sec
D11            0.03000000 sec
D12            0.00002000 sec
TD0                   1
SFO1         470.7052618 MHz
NUC1                 19F
P1                15.00 usec
P2                30.00 usec
PLW1         39.50000000 W
SFO2         500.3025015 MHz
NUC2                 1H
CPDPRG[2          waltz16
PCPD2             80.00 usec
PLW2         21.50000000 W
PLW12         0.49000001 W

F2 - Processing parameters
SI                  65536
SF           470.7523370 MHz
WDW                    EM
SSB       0
LB                  0.30 Hz
GB        0
PC                  1.00
```

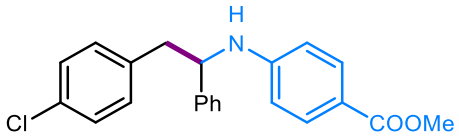

6.4ab

^{1}H NMR

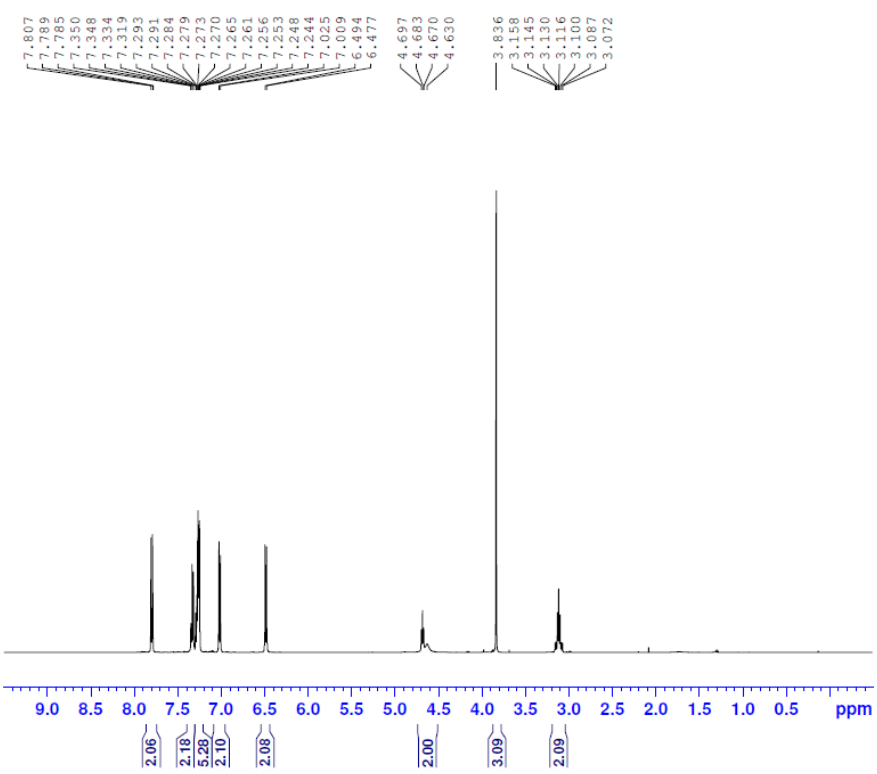


```
Current Data Parameters
NAME      lcc-770-product
EXPNO                   3
PROCNO                  1

F2 - Acquisition Parameters
Date_           20171101
Time               3.58 h
INSTRUM       AVIII500HD
PROBHD    Z119470_0125 (
PULPROG             zg30
TD                 65536
SOLVENT            CDCl3
NS                    16
DS                     2
SWH            10000.000 Hz
FIDRES             0.305176 Hz
AQ                 3.2767999 sec
RG                    44.1
DW                 50.000 usec
DE                 13.50 usec
TE                 298.3 K
D1              1.00000000 sec
TD0                    1
SFO1          500.3030896 MHz
NUC1                  1H
P1                 10.00 usec
PLW1          21.89999962 W

F2 - Processing parameters
SI                 65536
SF            500.3000000 MHz
WDW                   EM
SSB       0
LB                 0.30 Hz
GB        0
PC                 1.00
```

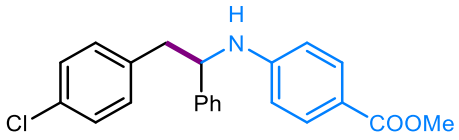

6.4ab

^{13}C NMR

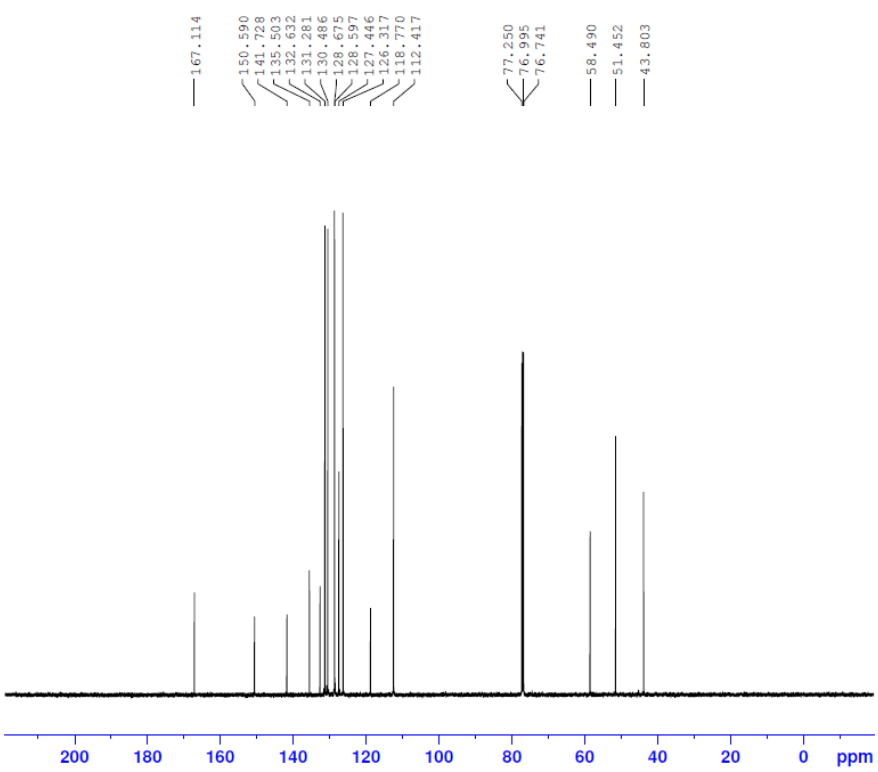


```
Current Data Parameters
NAME      lcc-770-product
EXPNO                   4
PROCNO                  1

F2 - Acquisition Parameters
Date_           20171101
Time                4.12 h
INSTRUM       AVIII500HD
PROBHD    Z119470_0125 (
PULPROG           zgpg30
TD                65536
SOLVENT           CDCl3
NS                  256
DS                    4
SWH           30000.000 Hz
FIDRES            0.915527 Hz
AQ                1.0922667 sec
RG                  192.72
DW                  16.667 usec
DE                  22.02 usec
TE                  298.3 K
D1                2.00000000 sec
D11               0.03000000 sec
TD0                     1
SFO1          125.8131140 MHz
NUC1                  13C
P1                  10.23 usec
PLW1          78.00000000 W
SFO2          500.3020012 MHz
NUC2                  1H
CPDPRG[2          waltz16
PCPD2               80.00 usec
PLW2          21.50000000 W
PLW12          0.49000001 W
PLW13          0.20446000 W

F2 - Processing parameters
SI                  32768
SF            125.8005480 MHz
WDW                   EM
SSB       0
LB                  1.00 Hz
GB        0
PC                  1.40
```

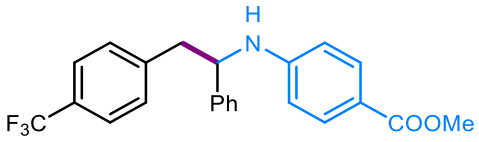
H
N
Ph
F3C
COOMe

6.4ac

^{1}H NMR

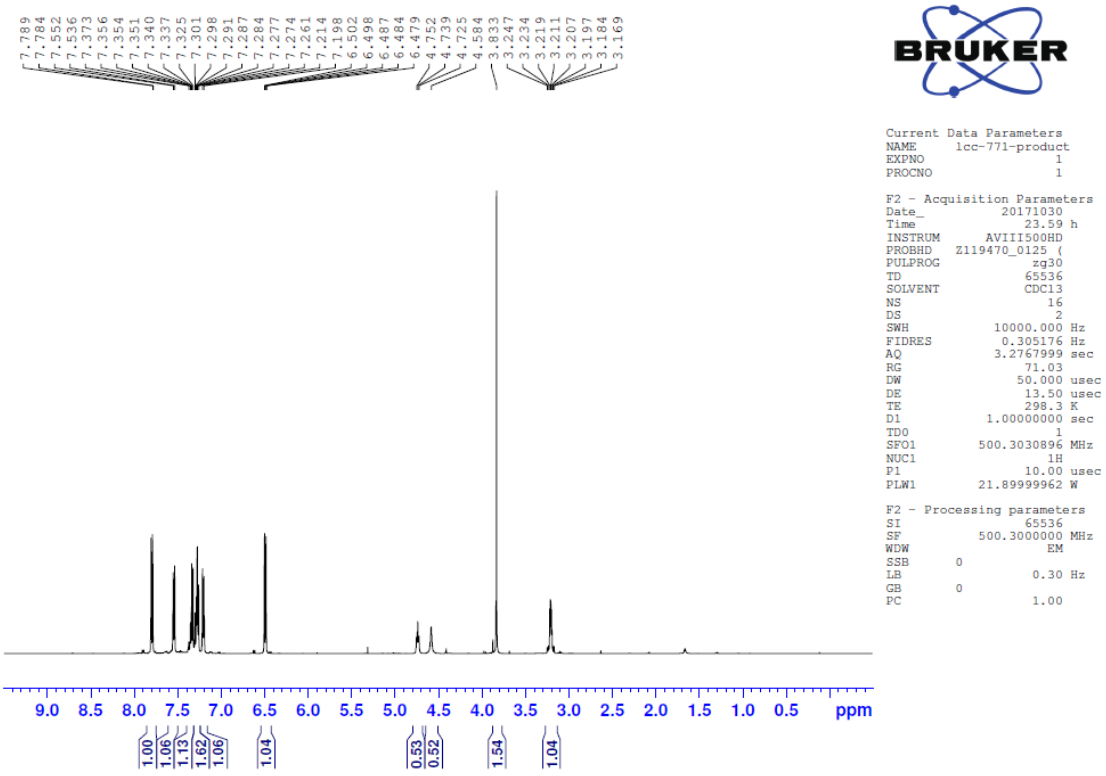
7.789
7.784
7.552
7.536
7.373
7.356
7.354
7.351
7.340
7.337
7.325
7.301
7.298
7.291
7.287
7.284
7.277
7.274
7.261
7.214
7.198
6.502
6.498
6.487
6.484
6.479
4.752
4.739
4.725
4.584
3.833
3.667
3.247
3.234
3.219
3.211
3.207
3.197
3.184
3.169
BRUKER
Current Data Parameters
NAME lcc-771-product
EXPNO 1
PROCNO 1
F2 - Acquisition Parameters
Date_ 20171030
Time 23.59 h
INSTRUM AVIII500HD
PROBHD Z119470_0125 (
PULPROG zg30
TD 65536
SOLVENT CDCl3
NS 16
DS 2
SWH 10000.000 Hz
FIDRES 0.305176 Hz
AQ 3.2767999 sec
RG 71.03
DW 50.000 usec
DE 13.50 usec
TE 298.3 K
D1 1.00000000 sec
TD0 1
SFO1 500.3030896 MHz
NUC1 1H
P1 10.00 usec
PLW1 21.89999962 W
F2 - Processing parameters
SI 65536
SF 500.3000000 MHz
WDW EM
SSB 0
LB 0.30 Hz
GB 0
PC 1.00
9.0 8.5 8.0 7.5 7.0 6.5 6.0 5.5 5.0 4.5 4.0 3.5 3.0 2.5 2.0 1.5 1.0 0.5 ppm
1.00
1.06
1.13
1.62
1.06
1.04
0.53
0.52
1.54
1.04

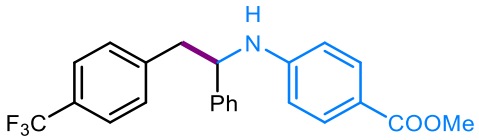

6.4ac

^{13}C NMR

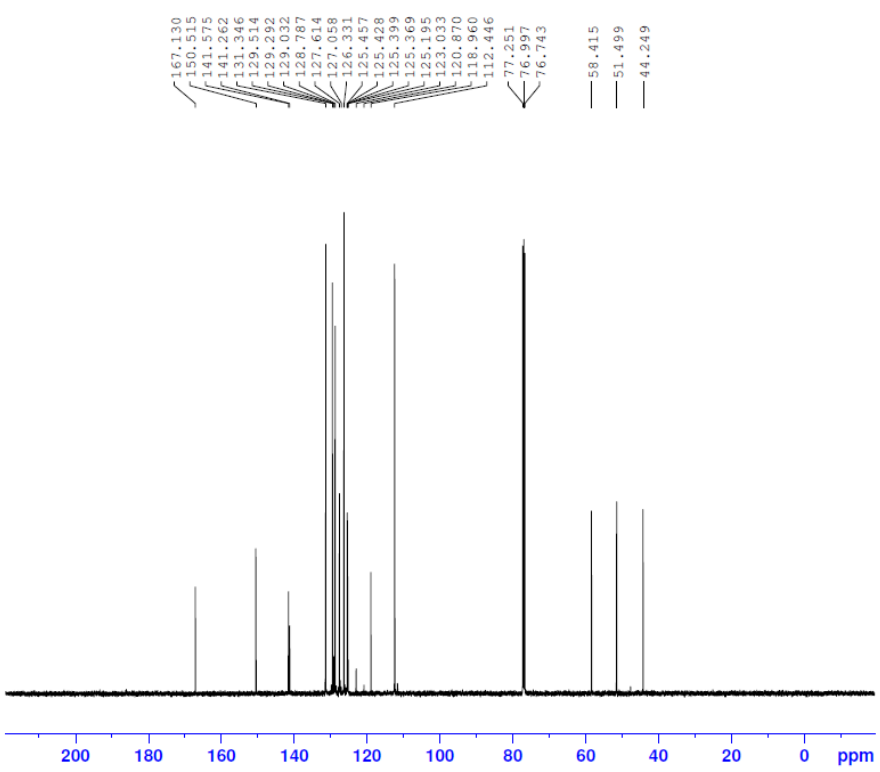

BRUKER

```
Current Data Parameters
NAME      lcc-771-product
EXPNO                   3
PROCNO                  1

F2 - Acquisition Parameters
Date_           20171031
Time                0.29 h
INSTRUM       AVIII500HD
PROBHD    Z119470_0125 (
PULPROG           zgpg30
TD                65536
SOLVENT           CDCl3
NS                  512
DS                    4
SWH           30000.000 Hz
FIDRES            0.915527 Hz
AQ                1.0922667 sec
RG                  192.72
DW                  16.667 usec
DE                  22.02 usec
TE                  298.3 K
D1                2.00000000 sec
D11               0.03000000 sec
TD0                     1
SFO1          125.8131140 MHz
NUC1                  13C
P1                  10.23 usec
PLW1          78.00000000 W
SFO2          500.3020012 MHz
NUC2                  1H
CPDPRG[2          waltz16
PCPD2               80.00 usec
PLW2          21.50000000 W
PLW12          0.49000001 W
PLW13          0.20446000 W

F2 - Processing parameters
SI                  32768
SF            125.8005407 MHz
WDW                   EM
SSB       0
LB                  1.00 Hz
GB        0
PC                  1.40
```

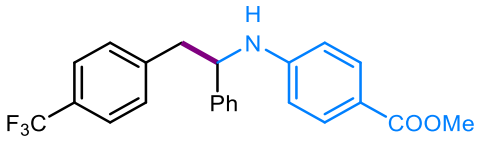

6.4ac

^{19}F NMR

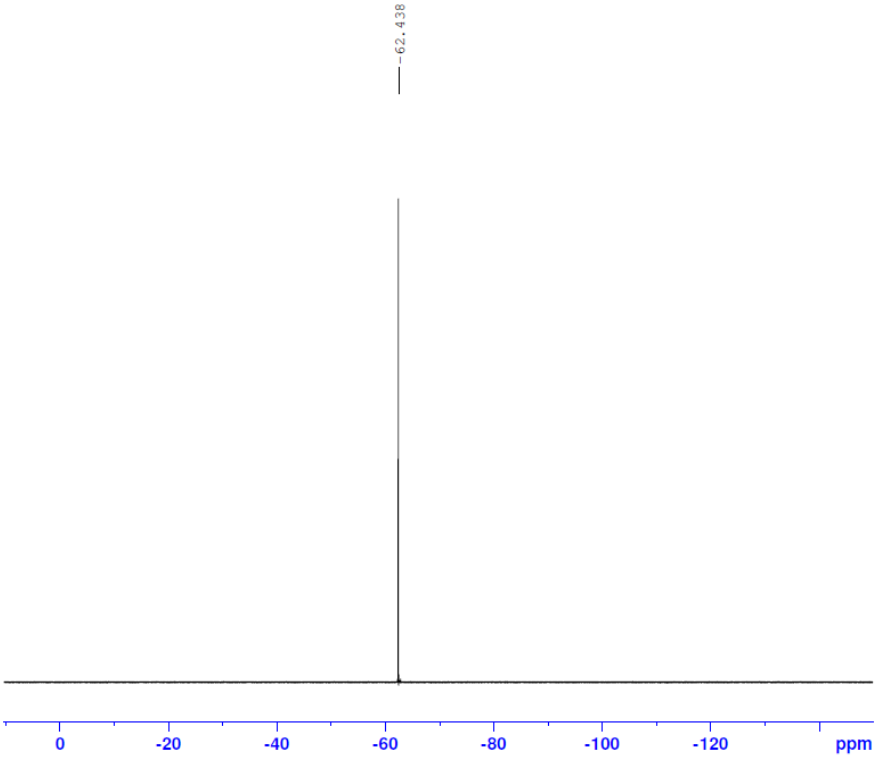

BRUKER

```
Current Data Parameters
NAME      lcc-771-product
EXPNO                   2
PROCNO                  1

F2 - Acquisition Parameters
Date_          20171031
Time       0 h
INSTRUM       AVIII500HD
PROBHD    Z119470_0125 (
PULPROG   zgbsfhiqqn.baseopt
TD                131072
SOLVENT            CDCl3
NS                    16
DS                     4
SWH           111111.109 Hz
FIDRES          1.695421 Hz
AQ              0.5898240 sec
RG                192.72
DW                 4.500 usec
DE                35.33 usec
TE                298.3 K
D1             1.00000000 sec
D11            0.03000000 sec
D12            0.00002000 sec
TD0                    1
SFO1         470.7052618 MHz
NUC1                 19F
P1                15.00 usec
P2                30.00 usec
PLW1         39.50000000 W
SFO2         500.3025015 MHz
NUC2                 1H
CPDPRG[2          waltz16
PCPD2             80.00 usec
PLW2         21.50000000 W
PLW12         0.49000001 W

F2 - Processing parameters
SI                 65536
SF           470.7523370 MHz
WDW                   EM
SSB       0
LB                 0.30 Hz
GB        0
PC                 1.00
```

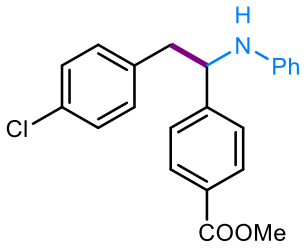

6.4bb

^{1}H NMR

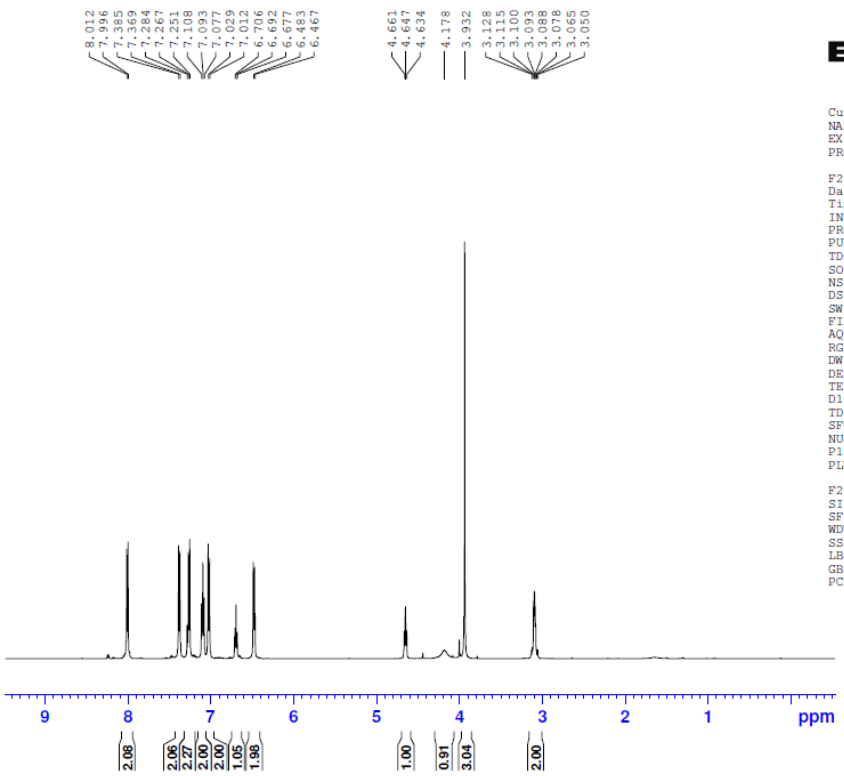


```
Current Data Parameters
NAME      1cc-764-product
EXPNO                   3
PROCNO                  1

F2 - Acquisition Parameters
Date_            20171029
Time               21.50 h
INSTRUM       AVIII500HD
PROBHD    Z119470_0125 (
PULPROG             zg30
TD                 65536
SOLVENT            CDCl3
NS                    16
DS                     2
SWH            10000.000 Hz
FIDRES             0.305176 Hz
AQ                 3.2767999 sec
RG                    71.03
DW                 50.000 usec
DE                 13.50 usec
TE                 298.3 K
D1              1.00000000 sec
TD0                    1
SFO1           500.3030896 MHz
NUC1                   1H
P1                 10.00 usec
PLW1           21.89999962 W

F2 - Processing parameters
SI                 65536
SF            500.3000000 MHz
WDW                   EM
SSB                    0
LB                  0.30 Hz
GB                     0
PC                  1.00
```

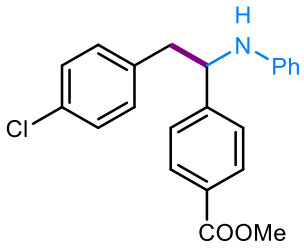

6.4bb

^{13}C NMR

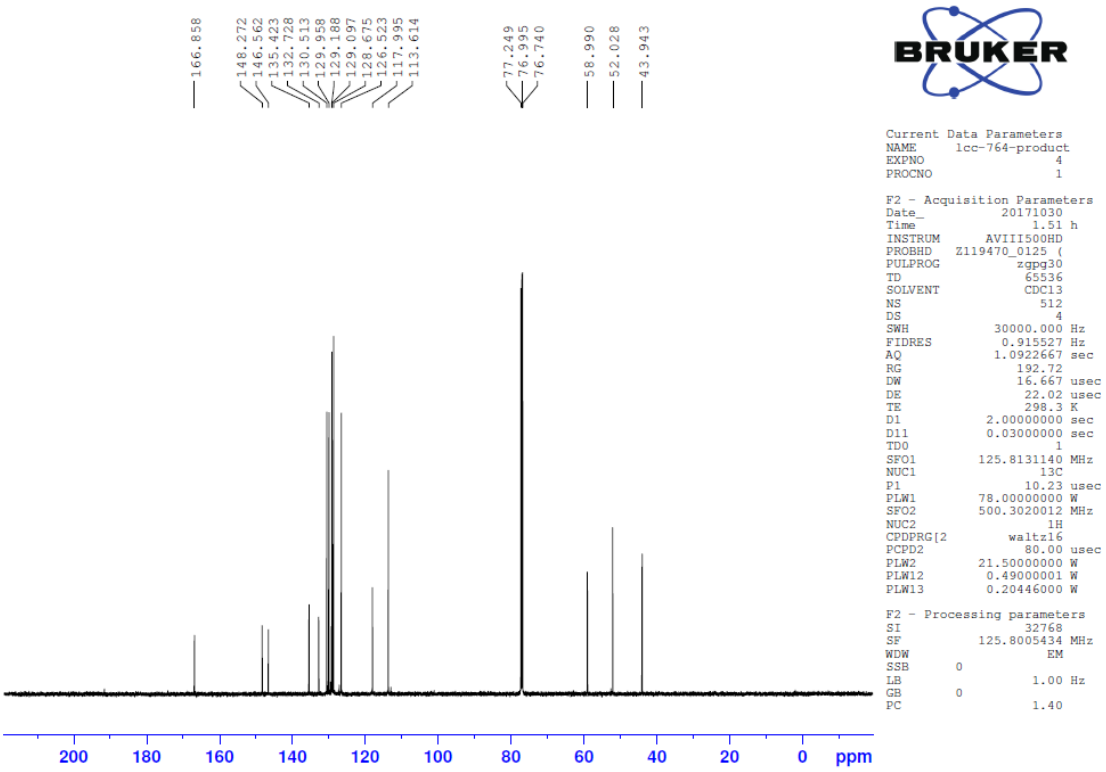

BRUKER

```
Current Data Parameters
NAME      1cc-764-product
EXPNO                   4
PROCNO                  1

F2 - Acquisition Parameters
Date_           20171030
Time               1.51 h
INSTRUM       AVIII500HD
PROBHD    Z119470_0125 (
PULPROG          zgpg30
TD                65536
SOLVENT           CDCl3
NS                  512
DS                    4
SWH           30000.000 Hz
FIDRES        0.915527 Hz
AQ            1.0922667 sec
RG               192.72
DW               16.667 usec
DE               22.02 usec
TE               298.3 K
D1            2.00000000 sec
D11           0.03000000 sec
TD0                   1
SFO1        125.8131140 MHz
NUC1                13C
P1               10.23 usec
PLW1         78.00000000 W
SFO2        500.3020012 MHz
NUC2                1H
CPDPRG[2         waltz16
PCPD2             80.00 usec
PLW2         21.50000000 W
PLW12         0.49000001 W
PLW13         0.20446000 W

F2 - Processing parameters
SI                32768
SF          125.8005434 MHz
WDW                  EM
SSB       0
LB                1.00 Hz
GB        0
PC                1.40
```